DISPLAY

Studies Related to the Charleston, South Carolina, Earthquake of 1886—Tectonics and Seismicity

GEOLOGICAL SURVEY PROFESSIONAL PAPER 1313

STUDIES RELATED TO THE CHARLESTON, SOUTH CAROLINA, EARTHQUAKE OF 1886—TECTONICS AND SEISMICITY

Craterlet produced by the 1886 earthquake at Ten-mile Hill between Charleston and Summerville, S. C.

Cover: Buildings in the vicinity of the Charleston Port Society, Charleston, S. C. Picture taken the day after the 1886 Charleston earthquake. Photograph from the collection of the Charleston Museum.

Studies Related to the Charleston, South Carolina, Earthquake of 1886—Tectonics and Seismicity

Edited by Gregory S. Gohn

GEOLOGICAL SURVEY PROFESSIONAL PAPER 1313

Prepared in cooperation with
the U.S. Nuclear Regulatory Commission

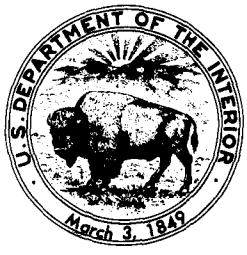

UNITED STATES GOVERNMENT PRINTING OFFICE, WASHINGTON: 1983

UNITED STATES DEPARTMENT OF THE INTERIOR

JAMES G. WATT, *Secretary*

GEOLOGICAL SURVEY

Dallas L. Peck, *Director*

Library of Congress Cataloging in Publication Data
Main entry under title:

Studies related to the Charleston, South Carolina earthquake of 1886–tectonics and seismicity.

(U.S. Geological Survey professional paper ; 1313)
Prepared in cooperation with the U.S. Nuclear Regulatory Commission.
Bibliography: p.
Supt. of Docs. no: I 19.16:1313
1. Charleston (S.C.)–Earthquake, 1886. 2. Geology, Structural. I. Gohn, Gregory S. II. U.S. Nuclear Regulatory Commission. III. Series: Geological Survey professional paper ; 1313.
QE535.2.U6S825 1983 551.2'2'0975791 83-600005

For sale by the Distribution Branch, U.S. Geological Survey,
604 South Pickett Street, Alexandria, VA 22304

CONTENTS

EDITOR'S PREFACE

Since 1973, the U.S. Geological Survey (USGS), with support from the Nuclear Regulatory Commission, has conducted extensive investigations of the tectonic and seismic history of the Charleston, S. C., earthquake zone and surrounding areas. The goal of these investigations has been to discover the cause of the large intraplate Charleston earthquake of 1886, which dominates the record of seismicity in the Southeastern United States, through an understanding of the historic and modern seismicity at Charleston and of the tectonic setting of the seismicity. This goal is being pursued to evaluate the potential for additional large earthquakes in the Charleston area and surrounding regions and to determine whether the Charleston area differs tectonically in any significant fashion from other parts of the Southeastern United States. An understanding of the specific cause for the 1886 event and of the regional distribution of any structures that are generically related to or geometrically and mechanically similar to the source structure is essential for evaluation of seismic hazards throughout the Southeast.

Investigations by the USGS began with the installation of a temporary seismograph network in March 1973, followed by the installation of the permanent South Carolina seismograph network in May 1974. Major geological and geophysical field investigations began in 1975 with drilling of the first of three deep stratigraphic test holes northwest of Charleston, at Clubhouse Crossroads in Dorchester County, and the initiation of several seismic-refraction and electrical-resistivity surveys. Preliminary results of these and other seismological, geophysical, and geological studies were given in 1977 in USGS Professional Paper 1028 (edited by D. W. Rankin) and in other reports and abstracts in the geological literature.

Since the publication of Professional Paper 1028, investigations by USGS scientists and by affiliated and nonaffiliated scientists in other institutions have continued in the Charleston area and throughout the Southeast. Important among the recent investigations have been multidisciplinary studies of the material recovered from the three Clubhouse Crossroads test holes; seismic-reflection and seismic-refraction surveys in the Charleston area and on the Continental Shelf offshore from South Carolina; regional studies of radiometric, aeromagnetic, gravity, and deep-well data; and continued monitoring and analysis of the seismicity in the greater Charleston area. This volume presents the results of 20 of these investigations.

The results given herein represent significant progress toward understanding the tectonic setting of the Charleston-area seismicity. Several chapters in the volume address the distribution and origin of pre-Cretaceous rocks and structures beneath Coastal Plain sediments in the Charleston area and regionally beneath the southern Atlantic Coastal Plain and adjacent Continental Shelf. The modern seismicity at Charleston is occurring at depths equal to or greater than the known extent of these older structures, and rejuvenation of an older fault in the modern stress field is a possible cause of the seismicity. Accordingly, several chapters discuss the possible relationships of the various pre-Cretaceous structures to faults identified near Charleston that have a known Cretaceous and Cenozoic movement history and to the historic and instrumentally recorded seismicity. However, at the present time, none of the young structures can be related unequivocally to the seismicity because earthquake fault-plane solutions and hypocenter distributions do not agree with the locations and orientations of these structures. Therefore, a major emphasis of continuing USGS investigations near Charleston will be to identify additional faults, if any exist, to delineate fault movement histories, and to further refine earthquake locations, focal mechanisms, and related seismological interpretations.

The editor is grateful to the authors, technical editors, and many other individuals and institutions that contributed to the completion of the scientific investigations reported herein and to the preparation of the report itself. The U.S. Nuclear Regulatory Commission, Office of Nuclear Research, principally funded [Agreement No. AT(49-25)-1000] the seismograph network and the deep drilling, several of the seismic surveys, and other related investigations conducted by the USGS in the Charleston area. The USGS is grateful to the Westvaco Company for the use of their land for deep drilling and many of the geophysical surveys.

Geochemistry and Tectonic Significance of Subsurface Basalts Near Charleston, South Carolina: Clubhouse Crossroads Test Holes #2 and #3

By DAVID GOTTFRIED, C. S. ANNELL, and G. R. BYERLY

STUDIES RELATED TO THE CHARLESTON, SOUTH CAROLINA, EARTHQUAKE OF 1886—TECTONICS AND SEISMICITY

GEOLOGICAL SURVEY PROFESSIONAL PAPER 1313-A

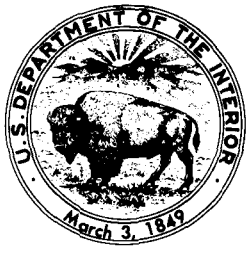

UNITED STATES GOVERNMENT PRINTING OFFICE, WASHINGTON: 1983

CONTENTS

ILLUSTRATIONS

TABLES

STUDIES RELATED TO THE CHARLESTON, SOUTH CAROLINA, EARTHQUAKE OF 1886—
TECTONICS AND SEISMICITY

GEOCHEMISTRY AND TECTONIC SIGNIFICANCE OF SUBSURFACE BASALTS FROM CHARLESTON, SOUTH CAROLINA: CLUBHOUSE CROSSROADS TEST HOLES #2 AND #3

By DAVID GOTTFRIED, C. S. ANNELL, and G. R. BYERLY[1]

ABSTRACT

Major-, minor-, and trace-element compositions of lower Mesozoic basalts from three deep test holes near Charleston, S. C., are used to characterize magma type and to determine the tectonic setting of the volcanic rocks at the time of their eruption. Chemical and petrographic evidence indicates that slight to extreme oxidation and hydration in nearly all samples has caused widespread mobility of K, Na, and related trace elements. The minor elements P and Ti, the trace elements Th, Nb, Ta, Zr, and Hf, and the rare-earth elements (REE) show little or no variation regardless of the degree of alteration. The contents of these stable elements and the patterns of light-REE enrichment in basalts from the deepest of the test holes clearly show the presence of two chemical types that are strikingly similar to lower Mesozoic high-Ti, quartz-normative tholeiites and lower Mesozoic olivine-normative tholeiites exposed in eastern North America.

The olivine-normative basalt is stratigraphically intercalated within a sequence of quartz-normative tholeiitic basalts. Quartz-normative basalts above and below the olivine basalt have nearly identical contents of most of the stable minor and trace elements, but the lower basalts have significantly more Cu and Ni and higher Ni/Co ratios. These differences are ascribed to preeruption separation of an immiscible sulfide melt into which Cu and Ni were strongly partitioned.

The new chemical data clearly show that the olivine tholeiitic magma type does not necessarily represent the earliest stage of volcanism in the eastern North American, early Mesozoic tholeiite province and that the spatial distribution of olivine-normative magma types in the province is not related to any significant change in tectonic environment.

INTRODUCTION

As part of a multidisciplinary study of modern seismicity near Charleston, S. C., three deep test holes were drilled in the meizoseismal area of the 1886 earthquake. The recovery from these holes of core samples of pre-Upper Cretaceous mafic volcanic rocks provided an excellent opportunity for conducting geochemical and geochronological studies for the purpose of characterizing the magmatic affinities and tectonic environment of these rocks. The three test holes were drilled near Clubhouse Crossroads in southern Dorchester County, S. C., between Summerville and the Edisto River (Gohn and others, 1983, fig. 1). Clubhouse Crossroads #1 (CC#1) and Clubhouse Crossroads #2 (CC#2) penetrated a 750- to 776-m-thick Coastal Plain section of Upper Cretaceous and Cenozoic sediments and bottomed in a sequence of subaerial basalt flows. Clubhouse Crossroads #3 (CC#3) also penetrated the Coastal Plain section and bottomed in a sequence of lower Mesozoic(?) sedimentary red beds (Gohn and others, 1983). A generalized section of the cored intervals of lower Mesozoic volcanic rocks and associated sedimentary rocks is shown in figure 1.

The results of a geochemical study of eleven samples of basalt from two flows in CC#1 were discussed in detail in a previous report (Gottfried and others, 1977) and are briefly summarized here. Petrographic observations and major-, minor-, and trace-element data indicated that the two flows were affected by post-crystallization processes, including hydration, oxidation, and hydrothermal alteration, that modified the original magmatic chemistry to varying degrees. However, the minor elements P and Ti, the trace elements Th, Nb, Ta, Zr, and Hf, and the rare-earth elements (REE) were essentially stable and showed that the two flows were identical in composition. The major-element composition of the least altered basalts and the stable trace elements showed that the basalts are of the quartz-normative tholeiitic magma type and are remarkably similar to the

[1]Louisiana State University, Baton Rouge, La.

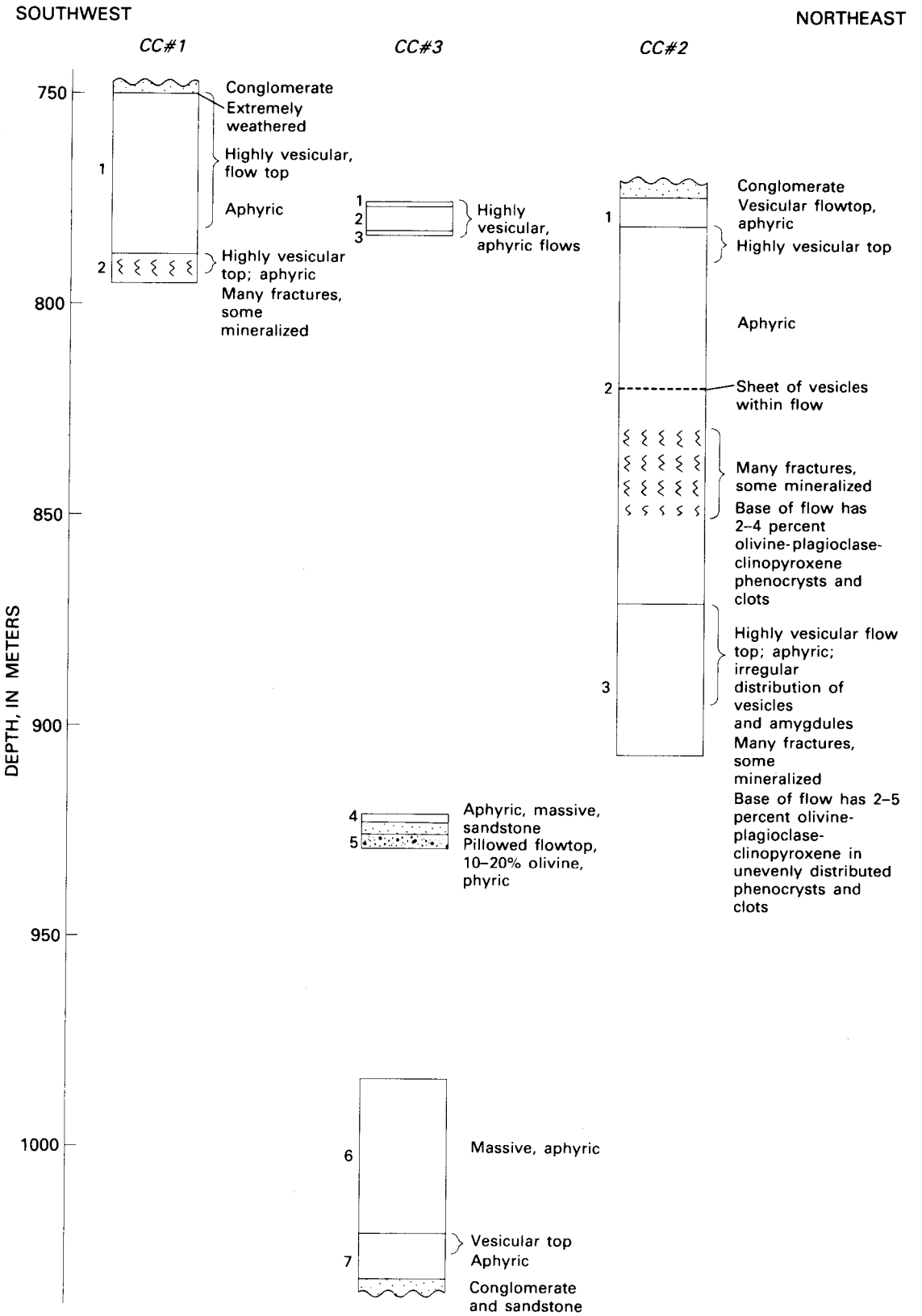

FIGURE 1.—Generalized sections of CC#1, CC#2, and CC#3, near Charleston, S. C., showing lower Mesozoic mafic volcanic rocks and other lithologic units. Circled numbers beside sections correspond to numbered basalt flows described in text.

Upper Triassic or Lower Jurassic high-Ti, quartz-normative tholeiitic rocks of eastern North America.

Whole-rock potassium-argon measurements of two samples from CC#1, however, gave ages of 94.8 and 109 m.y. (million years) (middle Cretaceous), which were considered minimum ages and were ascribed to the effects of secondary processes (Gottfried and others, 1977). Subsequently conventional whole-rock potassium-argon analysis of three samples of basalt from CC#2 yielded ages of 204, 162, and 186 m.y. (Gohn and others, 1978), which are in the range of ages determined for other Upper Triassic–Lower Jurassic basalts and diabase of eastern North America. However, these three ages are out of order with regard to the relative stratigraphic position of the samples in the drill hole, and this lack of vertical age continuity is attributed to the somewhat altered nature of the samples. Lanphere (1983) carried out incremental heating and total fusion $^{40}Ar/^{39}Ar$ experiments on the three samples and found that only one sample was suitable for establishing a meaningful crystallization age. He concluded that the most reliable age for the basaltic volcanism is 184 ± 3.3 m.y. (Early Jurassic).

This paper is a continuation of our geochemical study of the subsurface basalts from the Clubhouse Crossroads drill holes. Major-, minor-, and trace-element data are presented for samples representing 131 m of basalt from CC#2 and 256 m of basalt from CC#3.

Analytical methods.—Major, minor, and trace elements in CC#2 and CC#3 samples were determined by means of the same methods used for the CC#1 samples (Gottfried and others, 1977). In addition to thermal radiation for instrumental neutron activation analysis (INAA), epithermal neutron activation analysis (ENAA) was used for several selected elements from CC#3 samples because of its increased accuracy and ability to detect small amounts (Baedecker and others, 1977). Th, U, Hf, and Ta are reported by this method, along with the rare-earth elements La, Ce, Sm, Tb, and Ho. The U, Sm, and Ho were counted by means of low-energy photon detectors, and the other elements by means of Ge(Li) detectors.

Acknowledgments.—All samples for ENAA were irradiated in Norway at the Institutt for Atomenergi, Isotope Laboratories, Kjeller. We are grateful to E. Steinnes for making this technique available to us for supplementing and substantiating data obtained from thermal irradiation at the National Bureau of Standards reactor, Gaithersburg, Md. Deep drilling and related investigations by the U.S. Geological Survey in the Charleston, S. C., area are supported by the U.S. Nuclear Regulatory Commission, Office of Nuclear Research, under Agreement No. AT(49-25)-1000.

DESCRIPTION OF BASALT FLOWS

CC#1 Basalt

At a depth of 750 m, basalt was encountered beneath a conglomeratic sand. A total thickness of 42 m of basalt was recovered before drilling was terminated. Two flow units are recognized, which do not necessarily correlate with flows having the same numbers in the two nearby holes.

FLOW 1

The top of flow 1 occurs at 750 m and the base is at 785 m; hence, this flow has a thickness of 35 m. Much of the flow is highly vesicular; the upper 32 m contain up to 20 percent vesicles and amygdules. The basalt is fine grained and nearly aphyric. Alteration is very intense within the upper 3 m of the flow and gives the basalt a greasy appearance and feel. The basalt is bright red in the highly altered top but grades to gray with depth. These color changes also correspond to a decrease in vesicularity and an increase in grain size. The groundmass texture ranges from hyalophitic to intersertal. At 759 m, a few 2- to 3-mm olivine phenocrysts are replaced by smectite pseudomorphs. Within several meters of the base, gash veins occur and contain coarser plagioclase crystals and chalcedony. These appear to be segregation veins formed during late stages of crystallization.

The uppermost portion of this flow contains the most altered basalt cored in the Clubhouse Crossroads holes. In the upper 3 m, large amygdules contain white expandable clay pseudomorphs, which replace aggregates of bladed zeolite. The basalt is now broken into pieces by the expansion of this clay by as much as 15 percent. Below the upper 3 m, a pink laumontite is dominant in amygdules. Minor chalcedony occurs with the zeolite. Groundmass plagioclase and pyroxene are partially replaced by zeolite. Residual glassy patches are opaque black to red. As depth increases, the basalt appears much fresher; plagioclase and pyroxene are unaltered, and chalcedony, quartz, and smectite dominate the secondary mineral assemblage. Sulfides are rare and are found only in the lower portion of the flow.

FLOW 2

The top of flow 2 is directly beneath flow 1 at 785 m. The total thickness is unknown because drilling was terminated within this flow at 792 m. The vesicular top extends down to 790 m depth and is significantly less altered than is the top of flow 1. The basalt is aphyric throughout. The upper 0.5 m and the deepest 1 m drilled are streaked red and green. This lowest zone is highly fractured and probably quite permeable. Textures range from hyalophitic to intersertal. The plagioclase and

pyroxene are partially altered to zeolite near the top but are quite fresh throughout the remainder of the unit. Residual glassy patches are altered to smectite. Amygdules are commonly filled by zeolite, but calcite, chalcedony, and smectite also occur. The fractured zone in the lowermost 1 m contains many thin veins of smectite.

CC#2 Basalt

At a depth of 776 m, basalt was encountered beneath a conglomerate in a sequence similar to the sequence in CC#1. A total thickness of 131 m of basalt was recovered before drilling was terminated. Three flows are distinguished in this hole.

FLOW 1

The top is at 776 m and the base at 782 m. The upper 3 m are highly vesicular and moderately altered in appearance. Vesicles and amygdules constitute as much as 25 percent of the upper portion of the flow. Amygdules are commonly filled by coarse aggregates of a pink, bladed zeolite and amorphous, green smectite. Many amygdules are very complex with several different generations of zeolite and (or) smectite. This flow is aphyric throughout. The upper part is altered and greenish but grades to a gray-green color in the lower, fresher part of the flow. The groundmass texture grades from hyalophitic to intersertal. Common segregation veins have a coarser texture and more vesicles than the surrounding basalt and consequently have more associated zeolite, chalcedony, quartz, and smectite. Sulfides are also preferentially associated with the segregations. Some segregation veins are brecciated and filled by a matrix of chalcedony. Pipe vesicles occur in the base of the flow. In the upper part of the flow, plagioclase is partially altered to zeolite.

FLOW 2

A 4-cm layer of green smectite, zeolite, and calcite separates flow 1 from flow 2. Flow 2 is 89 m thick between 782 m and 871 m depth. The upper 8 m are highly vesicular with 10–20 percent vesicles, which are found in sheeted horizontal layers that were produced as a result of flow. At about 6 m below the top, bands of fine-grained and coarser grained basalt occur, which are commonly oriented as much as 3° from the horizontal plane. The coarser grained basalt is always more vesicular. The vesicular zone has a greenish cast and appears somewhat more altered than material below. No phenocrysts are observed in the upper 8 m of the flow. The flow is massive from 790 to 820 m. This basalt is gray, appears fresh, and has less than 2 percent vesicles. At 820 m, another horizontal vesicle sheet about 1 m thick occurs within the flow. A few plagioclase phenocrysts are observed at 825 m. Between 830 and 850 m, the basalt is highly fractured; these fractures are often associated with thin smectite veins. Recovery of core in this interval was locally poor, although there was no indication of any flow boundary. At 860 m, a few plagioclase phenocrysts and a few pseudomorphs of smectite after olivine phenocrysts are found. Glomerocrysts of plagioclase, pyroxene, and olivine (replaced by smectite pseudomorphs) may also be found. The phenocrysts are generally less than 5 mm in diameter. The base of the flow has about 5 percent amygdules, most of which are filled by zeolite.

The groundmass texture generally varies from hyalophitic to subophitic, but several zones within the flow display unusual textures related to flow segregation during crystallization. A mottled texture at 790 m is produced by swirls of oriented plagioclase microlites. Amygdules are commonly filled by basalts having one of two types of texture. One filling displays coarse, flow-alined plagioclase microlites. The other is a very fine-grained, dark, quench-textured material.

In the upper 12 m of the flow, zeolite and smectite are the dominant secondary minerals in vesicles. Between 794 and 867 m, calcite, chalcedony, and smectite are dominant. Below 867 m, zeolite again becomes an important secondary mineral. In the massive basalt, sulfide is commonly found in fine veins, often with smectite, and as disseminated grains. Groundmass minerals are mostly fresh throughout the flow; areas of former residual glass are altered to smectite.

FLOW 3

A 5-cm layer of calcite and zeolite occurs between flows 2 and 3. The top of flow 3 is at 871 m; however, the total thickness is unknown because drilling was terminated at 907 m. The upper 24 m is highly amygdaloidal, although the amygdules are irregularly distributed. The amygdules tend to be alined in horizontal sheets, and most are filled with zeolite or smectite. At 877 m, the basalt is coarsely amygdaloidal; these amygdules are mostly filled by zeolite. As depth increases, the number of vesicles increase, and amygdules are filled by light green, fibrous prehnite, or, more commonly, by pink, bladed zeolite; together, vesicles and amygdules constitute up to 20 percent of the rock. At 895 m and below the basalt is massive with few vesicles and has a much fresher overall appearance. The upper portion of the flow is aphyric, but, at 902 m, phenocrysts of plagioclase and pyroxene occur along with pseudomorphs of smectite after olivine phenocrysts. Some horizontal sheets of vesicles occur near the bottom of the core at 904 m. Phenocrysts do not occur within these vesicle sheets. Clots with the same three types of

phenocrysts also occur in this zone. The groundmass textures range from hyalophitic to intergranular.

At the top of flow 3 the groundmass has been largely altered to a highly birefringent, fine-grained aggregate that may be prehnite. At greater depths the groundmass minerals are fresh and the patches of former residual glass are replaced by smectite.

CC#3 Basalt

Coring began in basalt at 775 m, immediately after cuttings had indicated a change from the overlying sediments. The basalt extends down to 1,031 m, although much of the interval between was not cored. A minimum thickness of 256 m is therefore recorded for the Clubhouse Crossroads basalt. A total of seven basalt flows are recognized, though it is likely some were missed in the uncored intervals.

FLOWS 1, 2, AND 3

These are very thin, highly vesicular flows that are similar to each other in most respects. All are aphyric, and they may represent flow lobes of a single eruption. Flow 1 is 2.7 m thick; its top is at 775 m and its base at 777.7 m. Flow 2 is beneath a 5-cm layer of smectite and zeolite that contains angular fragments of basalt. The base of flow 2 is at 782.5 m. Flow 3 is also beneath a 5-cm layer of smectite and zeolite that contains angular fragments of basalt. Coring was terminated at 784.6 m, within this flow. Vesicles and amygdules compose as much as 25 percent of these flows, commonly are flattened and in horizontal sheets, and commonly are filled by zeolite and smectite. The texture of the groundmass is hyalophitic throughout. Alteration is moderate to intense; in the upper flow, most plagioclase has been altered to zeolite, though some secondary chalcedony and potassium feldspar are also found. Calcite occurs in minor veins throughout the flows.

FLOW 4

Coring was resumed at 921 m. Because of the long uncored interval, the basalt encountered at 921 m was assigned to a new unit. The base of this unit is at 924 m. The basalt of flow 4 is medium grained, massive, gray, and relatively fresh. The base of the flow is very fine-grained and black and contains considerable smectite. In appearance, it is quite similar to the sandstone that underlies it. Rare microphenocrysts of olivine are replaced by smectite pseudomorphs. The rock is essentially free of vesicles. The textures range from hyalophitic to subophitic. Zeolite is rare in this flow. Smectite replaces the residual glassy material. Sulfides occur as fine disseminated grains and in veins with smectite.

SEDIMENTARY BED

A thin sedimentary unit between flows 4 and 5 grades from a fine-grained black sandstone at its top (924 m) to a coarse-grained red sandstone at its base (926 m). Angular fragments of phyric olivine basalt occur in the upper black sediments, and the lower meter of red sandstone contains rounded, irregular pieces of phyric olivine basalt. Quartz and potassium feldspar occur as common detrital grains in the sedimentary bed.

FLOW 5

Coring of flow 5 was stopped at 930 m and thus only 4 m were recovered. The top of flow 5 is sparsely vesicular (less than 5 percent); its very-fine-grained quench texture suggests that the basalt may have intruded into unconsolidated sediment as a sill or invasive flow. The flow contains 10–20 percent olivine phenocrysts that were unevenly distributed in sheets apparently by segregation during flow. All olivine is replaced by smectite or rarely by calcite. Below the quenched top, the basalt is visibly coarser grained. One meter below the top, the groundmass is ophitic. The upper part of the flow is red, but the flow grades with depth to a dark green. Amygdules contain smectite and calcite.

FLOW 6

Coring was resumed at 984 m. Because the recovered basalt was aphyric, it was assigned to a new unit whose base is at 1,021 m. The basalt is fine grained with few vesicles or amygdules. The texture is mostly hyalophitic to intergranular, and the rock appears to be quite fresh. Several small segregation veins of coarser plagioclase and pyroxene, which occur between 995 and 1,000 m depth, commonly have vugs filled with chalcedony and smectite. A few veins have calcite, chalcedony, and smectite. Zeolite is present in the few amygdules which occur in the base of the flow between 1,015 and 1,020 m. The formerly glassy base of this flow is altered to smectite.

FLOW 7

A layer of calcite, smectite, and angular basalt fragments occurs between flows 6 and 7. The top of flow 7 is at 1,021 m. The base of the flow overlies an arkosic sandstone at 1,031 m. The top of the flow is an altered selvedge having amygdules filled by zeolite and calcite. The basalt is aphyric and dark gray to black. Very large vugs and amygdules occur near the top. The amygdules are filled by very coarse, bladed aggregates of zeolite or by quartz crystals, whereas the vugs remain empty. Pipe vesicles are found at the base of the flow. The texture varies from hyalophitic to intersertal. Sulfides and native copper occur but are rare.

CC#2

Major-Element Chemistry

Chemical analyses were made on eight core samples selected from CC#2 to represent the different flow units encountered in that hole. The major oxide and normative compositions of these basalts are presented in table 1. The data indicate that all the samples have undergone hydration; total H_2O contents range from 2 to 5 percent. Contents of the mobile element K_2O show a six-fold variation, whereas the contents of the relatively stable minor elements TiO_2 (1.0 percent) and P_2O_5 (0.15 percent) are essentially the same in all the rocks. A plot of the normative compositions of the samples in the normative diopside-hypersthene-olivine-nepheline-quartz diagram is shown in figure 2. Normative calculations were made on a water-free basis and an assumed $Fe_2O_3/(FeO + Fe_2O_3)$ ratio of 0.15 to standardize the effects of hydration and oxidation.

Six of the eight samples cluster in the quartz-normative tholeiite field and have essentially the same composition as do the basalts from CC#1. Sample 786, which has the highest H_2O and Na_2O contents, is slightly nepheline normative, and sample 878, which has the highest K_2O and high H_2O contents, plots in the olivine-normative tholeiite field. The departure of these two samples from the cluster of samples in the quartz-normative field reflects the mobility of the alkalies,

TABLE 1.—*Major-oxide and normative mineral composition, in weight percent, of basalts from CC#2, near Charleston, S. C.*

[Analyses by Z. A. Hamlin and F. W. Brown]

Depth below surface (meters)	780	786	819	836	842	869	878	908
Major-oxide composition								
SiO_2	53.1	49.4	53.2	53.8	53.6	53.3	51.2	53.0
Al_2O_3	14.3	14.0	14.3	14.2	14.4	14.4	13.4	14.5
Fe_2O_3	2.3	3.1	3.1	2.4	2.8	1.8	4.3	2.2
FeO	8.6	7.8	7.8	8.5	8.6	8.7	6.5	8.6
MgO	6.0	6.3	6.2	5.9	5.9	6.1	6.4	6.3
CaO	9.5	7.4	9.6	9.5	9.7	8.9	7.2	10.2
Na_2O	2.5	4.7	2.3	2.2	2.3	2.3	3.4	2.3
K_2O	.25	.87	.57	.35	.33	.81	1.5	.23
H_2O+	2.3	4.6	1.2	1.5	1.2	1.9	3.0	1.2
H_2O-	1.1	1.0	1.2	.95	1.0	.90	1.7	.64
TiO_2	1.0	.97	1.0	1.0	.99	.99	.99	1.1
P_2O_5	.15	.14	.16	.15	.15	.15	.13	.14
MnO	.15	.17	.16	.16	.16	.17	.17	.17
CO_2	.02	.02	.02	.04	.13	.01	.01	.01
Total	101	100	101	99	101	100	100	101
Major-oxide composition recalculated volatile-free[1]								
SiO_2	54.3	52.2	54.2	54.9	54.3	54.6	53.9	53.7
Al_2O_3	14.6	14.8	14.6	14.5	14.6	14.8	14.1	14.7
Fe_2O_3	1.8	1.9	1.8	1.8	1.9	1.8	1.8	1.8
FeO	9.3	9.5	9.2	9.2	9.6	9.0	9.3	9.1
MgO	6.1	6.7	6.3	6.0	6.0	6.3	6.7	6.4
CaO	9.7	7.8	9.7	9.6	9.7	9.1	7.6	10.3
Na_2O	2.6	5.0	2.3	2.2	2.3	2.4	3.6	2.3
K_2O	.26	.92	.58	.36	.33	.83	1.6	.23
TiO_2	1.0	1.0	1.0	1.0	1.0	1.0	1.0	1.1
P_2O_5	.15	.15	.16	.15	.15	.15	.14	.14
MnO	.15	.18	.16	.16	.16	.17	.18	.17
Total	100	100	100	100	100	100	100	100
Normative mineral composition[1]								
Q	6.73	---	6.40	8.83	7.63	6.75	---	6.37
Or	1.51	5.42	3.42	2.11	1.97	4.90	9.33	1.37
Ab	21.63	36.87	19.81	18.98	19.72	19.94	30.31	19.72
An	27.67	15.34	27.49	28.39	28.37	27.22	17.77	28.94
Ne	---	2.77	---	---	---	---	---	---
Wo	8.09	9.31	8.25	7.68	7.72	7.07	7.88	8.91
En	15.28	4.82	15.72	14.98	14.89	15.56	14.35	15.90
Fs	14.12	4.23	13.96	14.09	14.68	13.69	12.10	13.73
Fo	---	8.23	---	---	---	---	1.70	---
Fa	---	7.97	---	---	---	---	1.58	---
Mt	2.63	2.70	2.60	2.62	2.72	2.55	2.64	2.59
Il	1.94	1.94	1.93	1.93	1.90	1.92	1.98	2.11
Ap	.36	.35	.38	.36	.36	.36	.32	.33
Total	100	100	100	100	100	100	100	100

[1]Based on analyses recalculated to 100 percent volatile-free oxides; $Fe_2O_3/(FeO+Fe_2O_3)$ ratio assumed to be 0.15.

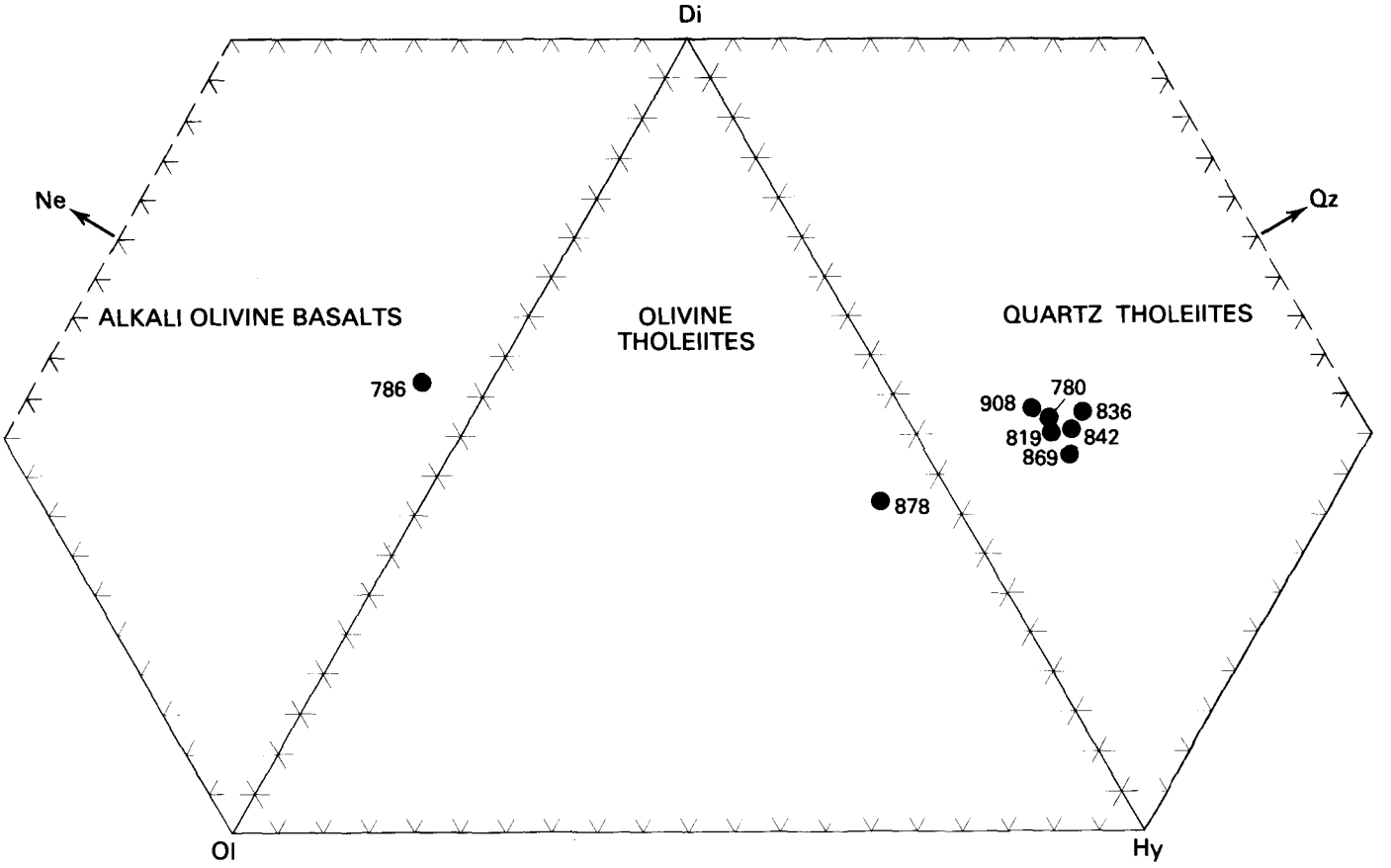

FIGURE 2.—Normative mineralogy of basalts from CC#2 plotted on diopside (Di)-hypersthene (Hy)-olivine (Ol)-nepheline (Ne)-quartz (Qz) diagram. Data are from table 1.

caused by alteration processes, rather than original magma composition.

Trace-Element Chemistry

Trace-element contents and selected interelement ratios in samples from CC#2 are given in table 2. The presentation of the data is similar to that proposed by Taylor (1965) whereby elements are grouped mainly on the basis of ionic radii and charges and hence similar geochemical behavior. Twenty-nine trace elements were determined for the eight samples selected for major-element chemistry. Selected trace elements were determined for 16 additional samples in order to detect possible variations in composition among individual eruptions and to assess on a more refined scale the extent and degree of alteration.

The elements of large ionic radii (Rb, Ba, and K), which are highly susceptible to remobilization by postcrystallization processes, show the widest ranges in abundance. In our study of basalts from CC#1 (Gottfried and others, 1977), Rb was found to be the most sensitive indicator of alteration. The same appears to be true for the suite of samples from CC#2. The range of variation of Rb (more than fiftyfold: 1.1–59 ppm) is greater than that found for Ba and Sr. The only K-related element that appears relatively stable is Pb, which varies for the most part within a factor of two.

In contrast to the wide range of variation in large-cation abundances, the high-valence cations (Th, U, Zr, Hf, Nb, Ta) show striking uniformity in abundance throughout the suite. The limited scatter in the abundance data may be due primarily to analytical uncertainties rather than to alteration processes. Th and U contents range from about 1.5 to 2.3 ppm and 0.5 to 0.8 ppm, respectively. With one exception, the Th/U ratios fall in the narrow range of 3.0 to 3.8. The uniformity in U contents is somewhat surprising; studies of other rocks that have undergone hydration and oxidation have indicated that U is extremely mobile.

TABLE 2.—*Trace-element abundances, in parts per million, and selected interelement*

Depth below surface (meters)	776.5	780	783.3	786	790	798	803.4	808.9	814	819	829
Large cations											
Rb^{+}	10	3.4	1.6	34	6.0	10	8.4	37	59	10	17
Ba^{2+}	270	80	14	110	45	72	57	89	370	140	140
K^{+}	---	2,200	---	7,600	---	---	---	---	---	4,800	---
Sr^{2+}	380	180	64	170	61	210	160	170	160	160	180
Ca^{2+}	---	69,000	---	56,000	---	---	---	---	---	70,000	---
Pb^{2+}	7.4	5.1	7.7	5.5	9.1	4.8	5.4	5.6	7.6	4.9	5.3
K/Rb	---	650	---	220	---	---	---	---	---	480	---
Ba/Rb	27	24	8.8	3.2	7.5	7.2	6.8	2.4	6.3	14	8.2
K/Ba	---	28	---	69	---	---	---	---	---	34	---
High-valence cations											
Th^{4+}	---	2.0	---	1.9	---	---	---	---	---	2.1	---
U^{4+}	---	.6	---	.5	---	---	---	---	---	.7	---
Zr^{4+}	78	90	83	78	100	77	87	77	78	90	90
Hf^{4+}	---	2.1	---	2.1	---	---	---	---	---	2.1	---
Nb^{5+}	4.9	6.1	---	5.9	5.3	---	5.6	5.2	6.2	6.5	4.9
Ta^{5+}	---	.34	---	.45	---	---	---	---	---	.53	---
Th/U	---	3.3	---	3.8	---	---	---	---	---	3.0	---
Zr/Hf	---	43	---	37	---	---	---	---	---	43	---
(Nb×100)/Ti	---	.10	---	.10	---	---	---	---	---	.11	---
Nb/Ta	---	18	---	13	---	---	---	---	---	12	---
Ferromagnesian elements											
Co^{2+}	36	50	44	49	50	39	44	34	37	48	45
Cu^{2+}	16	19	18	20	22	17	17	18	24	20	20
Li^{+}	3.9	7.4	2.2	5.2	8.2	19	12	20	20	10	4.8
Ni^{2+}	19	21	22	23	25	20	23	20	22	21	25
Zn^{2+}	88	93	89	76	93	90	85	93	87	94	89
Cr^{3+}	50	68	56	68	66	50	54	50	51	63	66
Ga^{3+}	12	15	20	17	15	15	17	16	15	15	17
Sc^{3+}	39	39	42	37	50	40	46	40	40	41	46
V^{3+}	230	270	280	300	370	270	270	280	260	250	290
Ni/Co	.53	.42	.50	.47	.50	.51	.52	.59	.59	.44	.56
Rare-earth elements											
La	---	10	---	9	---	---	---	---	---	9	---
Ce	---	20	---	20	---	---	---	---	---	21	---
Nd	---	14	---	12	---	---	---	---	---	14	---
Sm	---	3.2	---	3.1	---	---	---	---	---	3.2	---
Eu	---	.93	---	.94	---	---	---	---	---	.99	---
Gd	---	3.0	---	2.8	---	---	---	---	---	3.4	---
Tb	---	.77	---	.71	---	---	---	---	---	.84	---
Ho	---	.5	---	.7	---	---	---	---	---	.6	---
Tm	---	.33	---	.32	---	---	---	---	---	.36	---
Yb	---	2.7	---	2.6	---	---	---	---	---	3.1	---
Lu	---	.42	---	.44	---	---	---	---	---	.44	---
Y	---	29	---	25	---	---	---	---	---	28	---

Zr and Hf contents range from 78 to 100 ppm and 1.9 to 2.1 ppm, respectively; these ranges are similar to those in CC#1 basalts. Nb contents (4.9–6.8 ppm) are somewhat lower than those found in CC#1 (6.8–7.7 ppm). The Nb/Ta ratios in CC#2 samples range from 12 to 18 and average 14; these are significantly lower than the average ratio of 25 found in CC#1.

Except for Li, the elements of ferromagnesian affinity (Co, Ni, Zn, Cr, Sc, and V) are quite uniform in abundance. The low Cu contents, generally in the range 16–20 ppm, are an unusual feature of the test-hole basalts, as are the rather low Ni/Co ratios of 0.42–0.63 (Gottfried and others, 1977).

The uniformity in abundance of the REE and Y provide further confirmation of the generally recognized stability of these elements during alteration (Gottfried and others, 1977). The chondrite-normalized REE pattern, based on analysis of eight samples of basalt, shows enrichment of the light REE relative to the heavy REE (fig. 3). Omitted from the pattern are the Tb and Ho data, which have rather large analytical uncertainties.

CC#3

Major-Element Chemistry

Studies of the volcanic and underlying lower Mesozoic(?) sedimentary rocks encountered in CC#3 permit a more complete and detailed interpretation of the volcanic-tectonic evolution and pre-Cretaceous geologic history of the Charleston area than do analyses of the basalt sections in CC#1 and CC#2. The sedimentary beds and their implications for tectonism are discussed

ratios in basalt from Clubhouse Crossroads test hole #2, near Charleston, South Carolina

836	842	853.7	858.5	864	869	872	878	888	889	899	905	908
Large cations—Continued												
19	24	8.6	17	14	21	24	54	2.5	1.1	1.6	18	17
190	140	160	150	170	150	180	200	83	7	91	150	130
3,000	2,700	---	---	---	6,900	---	12,000	---	---	---	---	1,900
170	170	240	220	260	170	210	210	250	95	200	190	180
69,000	70,000	---	---	---	65,000	---	54,000	---	---	---	---	74,000
6.2	4.5	7.8	5.4	5.4	4.5	7.1	4.1	4.7	5.1	5.5	4.5	3.8
160	110	---	---	---	330	---	220	---	---	---	---	110
10	5.8	19	8.8	12	7.1	7.5	3.7	33	6.4	57	8.3	7.6
16	19	---	---	---	46	---	60	---	---	---	---	15
High-valence cations—Continued												
2.0	2.1	---	---	---	2.3	---	1.7	---	---	---	---	1.5
.6	---	---	---	---	.7	---	.8	---	---	---	---	.5
91	93	91	85	82	85	86	82	85	84	89	90	89
2.1	2.0	---	---	---	2.0	---	1.9	---	---	---	---	2.0
6.5	5.9	6.4	---	6.3	6.8	6.0	6.0	6.0	6.7	6.1	6.3	5.9
49	.49	---	---	---	.43	---	.42	---	---	---	---	.39
3.3	---	---	---	---	3.3	---	2.1	---	---	---	---	3.0
44	47	---	---	---	43	---	43	---	---	---	---	45
.11	.099	---	---	---	.11	---	.10	---	---	---	---	.090
13	12	---	---	---	16	---	14	---	---	---	---	15
Ferromagnesian elements—Continued												
48	47	46	47	43	44	53	43	42	45	49	49	54
20	21	21	20	19	19	22	30	23	22	24	38	43
5.8	6.2	15	17	25	9.8	16	15	17	8.1	6.6	2.7	1.8
22	23	24	24	21	21	24	25	20	25	24	31	34
97	85	93	90	88	89	100	75	87	79	89	93	82
69	76	74	59	58	72	62	97	56	62	71	130	170
16	17	18	18	15	16	15	12	17	18	18	18	18
44	45	50	49	46	40	38	37	40	39	41	42	43
270	280	290	290	270	290	280	300	290	300	300	300	300
.46	.49	.52	.49	.49	.48	.45	.58	.48	.56	.49	.63	.63
Rare-earth elements—Continued												
10	9	---	---	---	10	---	9	---	---	---	---	9
20	20	---	---	---	20	---	18	---	---	---	---	17
12	12	---	---	---	12	---	11	---	---	---	---	9
3.1	3.2	---	---	---	3.2	---	3.0	---	---	---	---	3.1
.93	.93	---	---	---	.95	---	.87	---	---	---	---	.94
3.4	3.1	---	---	---	3.1	---	2.9	---	---	---	---	3.2
.71	.77	---	---	---	.76	---	.73	---	---	---	---	.86
.7	.6	---	---	---	.5	---	---	---	---	---	---	.7
.31	.31	---	---	---	.33	---	.32	---	---	---	---	.34
2.6	2.5	---	---	---	2.8	---	2.5	---	---	---	---	2.8
.41	.41	---	---	---	.42	---	.39	---	---	---	---	.44
29	30	---	---	---	26	---	25	---	---	---	---	29

elsewhere in this volume (Gohn and others, 1983). In addition to the underlying sedimentary rocks, CC#3 contains a thin sandstone bed at about 925 m between an underlying strongly altered olivine-rich flow and an overlying aphyric flow (fig. 1); these rocks document a brief cessation of volcanism and a distinct change in magma chemistry.

The major-element chemistry and normative composition of 14 samples from CC#3 are presented in table 3. Evidence of alteration of the cored basalt from the top of the section (777–785 m) is clearly shown by the high and variable contents of H_2O and CO_2. Uniformity in TiO_2 and P_2O_5 contents in these samples suggests that the original major-element composition of these samples was the same. The threefold range in K_2O is thus ascribed to its mobility during alteration. Major-oxide analyses of basalts from the next cored interval (921–930 m) indicate that the sample at 921 m is similar to the overlying samples. However, these analyses also confirm petrographic observations of basalt of a significantly different magma type in the interval from 926 to 930 m. Three samples (from 926.3, 928, and 930 m) representing different textural variants of this olivine-rich flow have been analyzed. Rather intense alteration of these samples is indicated by high H_2O, CO_2, and Fe_2O_3/FeO ratios. The high MgO contents (11.5–16.6 percent) are consistent with high modal olivine contents, although some of the variation in MgO could be due to alteration. The nearly constant and relatively low amounts of TiO_2 (0.52 to 0.56 percent) and P_2O_5 (0.08 to

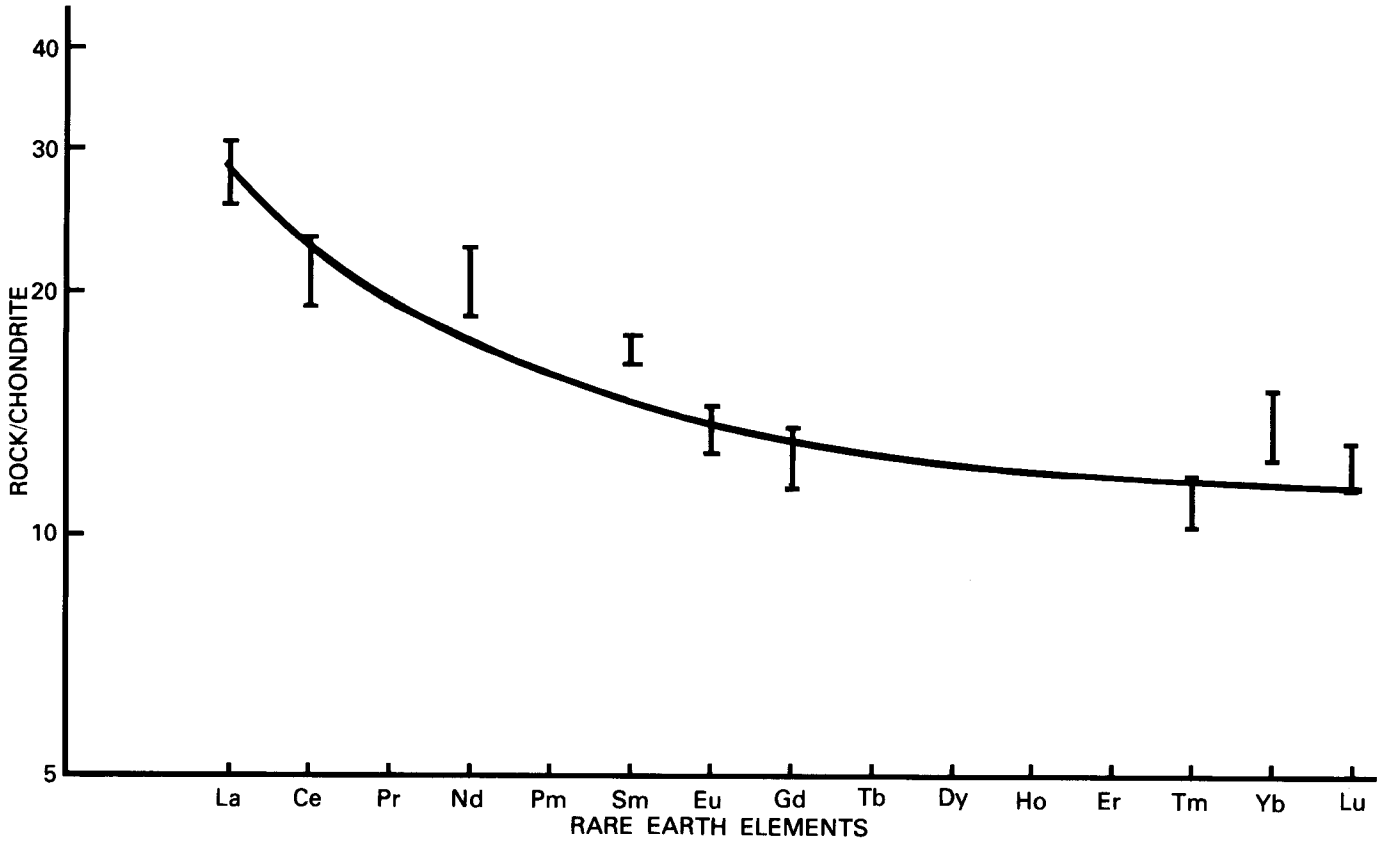

FIGURE 3.—Average abundances of REE in basalts from CC#2. Data are from table 2. Each vertical bar indicates the range of normalized values of eight samples.

0.10 percent) indicate that the samples were originally of rather similar compositions and that this flow unit represents a relatively primitive magma.

The six samples of basalt from 984 m to the base of the basalt section at 1,031 m, though showing variable degrees of alteration, are virtually indistinguishable, on the basis of their stable minor elements (P_2O_5 and TiO_2), from the basalts from the top of the section.

A plot of the normative compositions of the 14 samples from CC#3 is shown in figure 4. As expected, the normative data show a rather wide scatter of points extending from the quartz-tholeiite field to the olivine-tholeiite and alkali-olivine fields. In contrast, the immobile minor elements indicate the presence of two distinct magma types, each of which shows little if any recognizable range in composition. Comparison of the major-oxide chemistry, especially the stable TiO_2 contents, of the CC#3 samples to the chemistry of exposed eastern North American, lower Mesozoic tholeiites (Weigand and Ragland, 1970) and quartz-normative tholeiites in CC#1 (Gottfried and others, 1977) suggests that only high-Ti, quartz-normative tholeiites occur between 777 and 921 m and between 984 and 1,030 m. Apparent olivine-normative compositions for rocks in those intervals are ascribed to chemical alteration of the samples. Olivine-normative compositions that reflect original magma chemistry and not alteration effects are found only in samples from 926.3 to 930 m.

Trace-Element Chemistry

Although petrographic and stable minor-element data indicate the presence of two magma types, additional data are required to effectively distinguish the magmatic affinities of the two suites. The immobile trace elements listed in table 4 make possible the recognition of diagnostic geochemical features on a more refined scale and also have implications for the tectonic setting.

In the CC#3 samples, extensive redistribution of Rb resulted in overlapping of Rb contents, at low concentration levels, between the olivine-rich unit and the more evolved tholeiitic rocks in the section. Contents of high-valence cations are virtually the same, within analytical error, in samples from the top of the section (777 to 921 m) and those from the basal flows (984 to 1,030 m). They

TABLE 3.—*Major-oxide and normative mineral compositions, in weight percent, of basalts from CC#3, near Charleston, S. C.*

[Analyses by Z. A. Hamlin and F. W. Brown]

Depth below surface (meters)	777	779	782	784.4	921	926.3	928	930	984	1002.2	1014	1020.4	1024	1030
Major-oxide composition														
SiO_2	47.8	47.8	46.2	55.1	52.1	42.9	44.3	43.2	52.9	52.2	53.7	52.8	52.5	47.8
Al_2O_3	14.2	14.0	14.8	13.3	14.3	14.6	13.2	13.4	14.1	13.8	14.1	14.3	14.1	14.6
Fe_2O_3	5.6	3.9	4.7	4.5	3.4	6.6	4.9	3.8	3.8	2.4	3.7	2.9	3.7	3.9
FeO	6.4	7.0	7.0	5.3	7.8	3.8	5.4	6.9	8.0	9.7	8.3	8.4	7.9	8.0
MgO	5.9	6.4	6.5	6.0	6.7	10.6	12.8	15.3	5.6	5.9	5.3	5.7	6.3	8.3
CaO	5.0	6.5	5.8	5.8	10.6	11.4	8.5	7.4	8.7	9.7	9.3	9.2	5.7	6.9
Na_2O	3.6	4.5	5.0	4.2	2.3	1.6	1.2	1.2	2.8	2.5	2.6	3.3	5.5	3.3
K_2O	1.3	.44	.93	.74	.16	.05	.27	.15	.64	.64	.74	.34	.05	.05
H_2O^+	5.9	5.8	5.5	3.4	1.1	2.7	4.9	5.4	1.2	1.3	.52	1.4	2.4	2.9
H_2O^-	2.3	2.2	1.7	1.5	1.5	3.3	4.5	2.8	.41	.34	.53	.99	.92	2.0
TiO_2	1.1	.92	1.1	.89	1.1	.52	.47	.49	1.1	.96	1.1	1.1	.97	.99
P_2O_5	.16	.15	.16	.15	.14	.09	.07	.08	.18	.16	.18	.18	.16	.16
MnO	.30	.21	.24	.19	.17	.18	.14	.22	.24	.22	.21	.21	.21	.22
CO_2	.24	.09	.08	.36	.04	.90	.82	.10	.02	.24	.14	.02	.13	.02
Total	100	100	100	101	101	99	101	100	100	100	101	101	100	99
Major-oxide composition recalculated volatile-free														
SiO_2	52.2	52.0	50.0	57.3	52.8	46.5	48.6	47.0	53.9	53.2	54.1	53.6	54.1	50.8
Al_2O_3	15.5	15.3	16.0	13.8	14.5	15.8	14.5	14.5	14.4	14.1	14.2	14.5	14.5	15.5
Fe_2O_3	6.1	4.2	5.1	4.7	3.4	7.1	5.4	4.1	3.9	2.4	3.7	3.0	3.8	4.1
FeO	7.0	7.6	7.5	5.5	7.9	4.1	6.0	7.5	8.2	9.9	8.4	8.5	8.1	8.5
MgO	6.4	7.0	7.1	6.2	6.8	11.5	14.0	16.6	5.7	6.0	5.4	5.8	6.5	8.8
CaO	5.4	7.1	6.2	6.0	10.7	12.4	9.3	8.0	8.9	9.8	9.4	9.4	5.8	7.3
Na_2O	4.0	4.9	5.4	4.3	2.3	1.7	1.3	1.3	2.9	2.6	2.6	3.4	5.7	3.5
K_2O	1.4	.48	1.0	.77	.16	.05	.30	.16	.65	.65	.74	.35	.05	.05
TiO_2	1.2	1.0	1.2	.93	1.1	.56	.52	.53	1.1	.98	1.1	1.1	1.0	1.1
P_2O_5	.17	.16	.17	.16	.14	.10	.08	.09	.18	.16	.18	.18	.17	.17
MnO	.33	.23	.26	.20	.17	.20	.15	.24	.24	.22	.21	.21	.22	.23
Total	100	100	100	100	100	100	100	100	100	100	100	100	100	100
Normative mineral composition[1]														
Q	---	---	---	4.81	4.64	---	---	---	4.92	4.25	6.21	2.78	---	---
Or	9.75	2.84	5.97	4.58	.95	.32	1.77	.96	3.86	3.86	4.42	2.04	.30	.31
Ab	33.52	41.71	33.98	37.26	19.74	14.94	11.31	11.06	24.21	21.63	22.25	28.40	48.11	29.70
An	19.98	18.29	16.50	15.99	28.63	35.88	33.23	33.48	24.54	25.09	24.90	23.60	14.09	26.46
Ne	---	---	6.49	---	---	---	---	---	---	---	---	---	---	---
Wo	1.80	6.37	5.43	4.39	9.81	7.92	2.87	2.16	7.60	8.90	8.18	8.97	5.47	3.62
En	9.53	3.52	2.78	15.66	16.93	12.54	26.67	18.94	14.25	15.02	13.35	14.44	7.30	14.30
Fs	9.75	3.05	2.51	12.78	14.16	6.34	11.25	7.10	15.21	16.05	15.30	14.49	6.87	10.48
Fo	4.65	9.76	10.37	---	---	11.63	6.19	15.81	---	---	---	---	6.25	5.38
Fa	5.24	9.33	10.32	---	---	6.47	2.87	6.53	---	---	---	---	6.48	4.35
Mt	3.04	2.78	2.94	2.36	2.66	2.59	2.64	2.71	2.82	2.93	2.84	2.70	2.80	2.95
Il	2.29	1.91	2.27	1.77	2.12	1.09	.99	1.01	2.13	1.86	2.11	2.12	1.90	2.00
Ap	.41	.38	.41	.37	.33	.23	.18	.20	.43	.38	.43	.43	.39	.40
Total	100	100	100	100	100	100	100	100	100	100	100	100	100	100

[1] Based on analyses recalculated to 100 percent volatile-free oxides; $Fe_2O_3/(FeO+Fe_2O_3)$ ratio assumed to be 0.15.

are also the same as those in samples from CC#2 and CC#1. The concentrations of Th, Zr, and Hf in the three olivine-rich samples are about half those found in the quartz-normative tholeiitic flows. Nb contents, although slightly lower than those in the tholeiites, appear to be relatively enriched in the olivine-rich samples as compared to the relative abundances of the other high-valence cations. The relatively high (Nb × 100)/Ti ratio (0.18) and Nb/Ta ratio (32) in one of the olivine-rich samples (from 926.3 m) may be due mainly to analytical error in the Nb determination rather than to low Ti and Ta contents. Previous studies of suites of tholeiitic basalts and diabases from widely different regions have shown that Nb/Ta ratios are quite similar: 13.5 in the Dillsburg, Pa., sill; 14.4 in diabases of Tasmania; and 16 in upper Paleozoic diabase dikes from Scotland (Gottfried and others, 1968; Macdonald and others, 1981).

The Th/U ratios in the CC#3 samples are quite uniform, and are mostly in the range from 3 to 4. These ratios, like the results for CC#2, suggest that the original U contents have not been seriously modified. Similar Th and U contents and similar Th/U ratios were found in samples of Triassic-Jurassic tholeiitic diabases from Fairfax County, Va. (Larsen and Gottfried, 1960) and the Palisades sill, New Jersey (Heier and Rogers, 1963).

The chondrite-normalized REE patterns of the olivine- and quartz-normative basalts are shown on figure 5. The light REE pattern for the quartz-normative basalts of CC#3 is similar to that for the

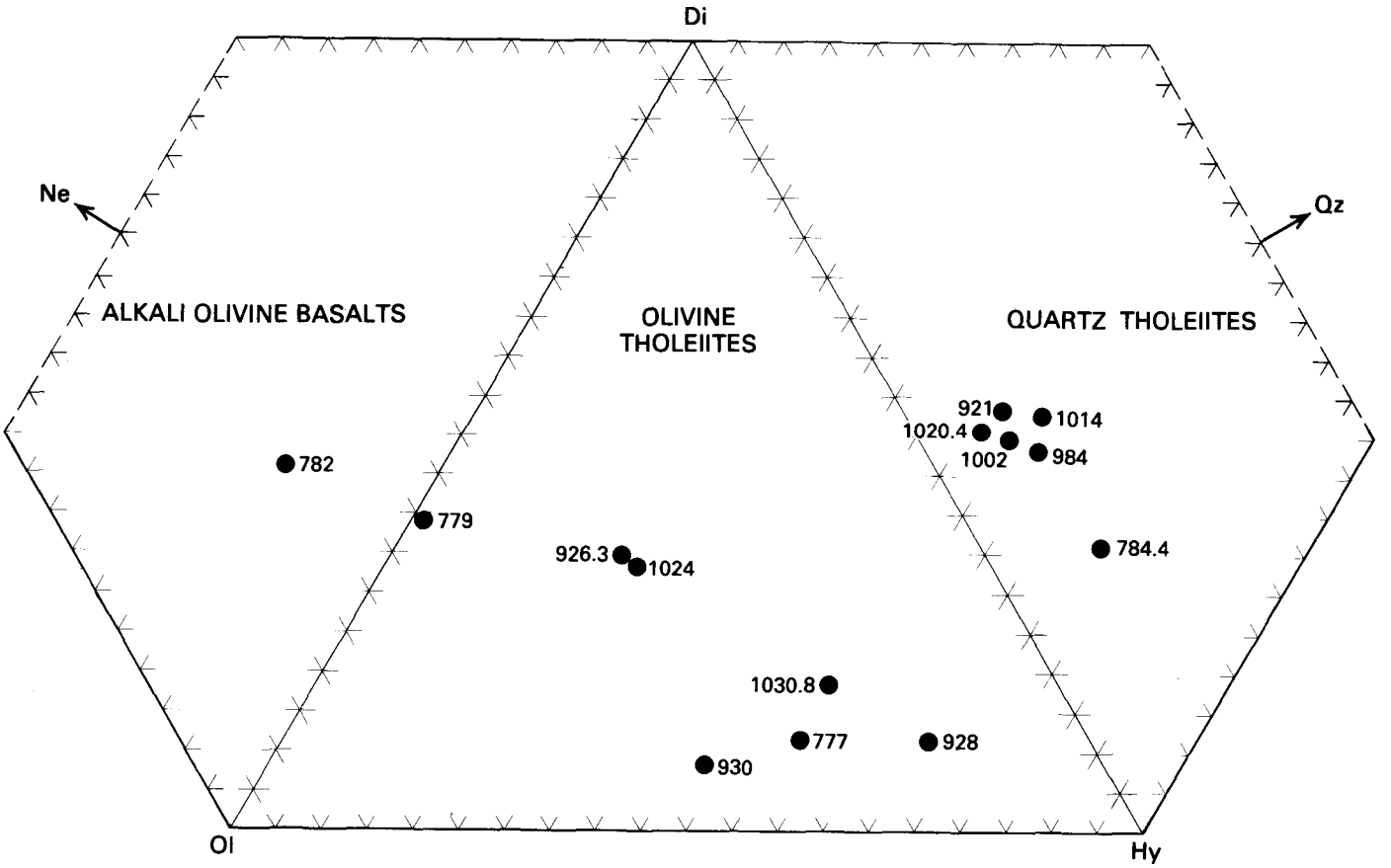

FIGURE 4.—Normative mineralogy of basalts from CC#3 plotted on diopside (Di)-hypersthene (Hy)-olivine (Ol)-nepheline (Ne)-quartz (Qz) diagram. Data are from table 4.

quartz-normative basalts from CC#2 and CC#1 (Gottfried and others, 1977). The patterns for olivine- and quartz-normative basalts in CC#3 are subparallel, which stresses their close chemical relationship even though the abundances of the REE in the olivine-normative type are one-half of those of the quartz-normative type.

Variations in the abundance of some elements in the ferromagnesian group have important petrographic implications and also provide a means of "fingerprinting" units which are otherwise indistinguishable. As noted above, flows from the top of the section (777 to 921 m) have virtually the same contents of stable minor elements (P and Ti) and trace elements (Th, U, Nb, Zr, Hf) as do those from the base of the section (984 to 1,030 m). However, the lower flows contain 3 to 4 times as much Cu and nearly twice as much Ni and have higher Ni/Co ratios than do the upper flows. The average Cu content in the upper flows (20 ppm) is similar to that in flows from CC#2 (22 ppm) and CC#1 (25 ppm) but contrasts with the average of 75 ppm in the lower flows in CC#3. The low and relatively uniform Cu contents in most of the samples of the upper flows suggest that low Cu is for the most part an intrinsic feature of these evolved basalts. Low Cu contents have also been noted by Weigand and Ragland (1970) in some Mesozoic high-Ti, quartz-normative diabases. The low Cu contents and low Ni/Co ratios in CC#1 basalts were previously ascribed to the preeruption separation of an immiscible sulfide melt into which Cu and Ni had been strongly partitioned (Gottfried and others, 1977). Recent experimental studies on the partitioning of Ni, Co, and Cu and the solubility of sulfur in silicate melts provide valuable insight into the nature of the processes that control the observed abundance variations of these elements in the Clubhouse Crossroads basalts. The solubility of sulfur in silicate melts at high temperature and pressure has been shown by Mysen and Popp (1980) to be strongly pressure dependent; that is, solubility decreases with decreasing pressure. They found that a melt at 10 kbar has 50 percent less sulfur than does the same melt at 20 kbar. Thus a decrease in pressure would cause excess sulfur to separate as an immiscible sulfide melt. A strong

TABLE 4.—*Trace-element abundances, in parts per million, and selected interelement ratios in basalt from Clubhouse Crossroads test hole #3, near Charleston, S. C.*

[Y determined by emission spectrography; La, Ce, Sm, Eu, Tb, and Ho determined by epithermal neutron activation analysis (NAA); other elements, including all elements of samples from 926.3 m and 930 m, determined by thermal NAA. __, not determined]

Depth below surface (meters)	777	779	782	784.4	921	924	926.3	928	930	984	1002.2	1014	1020.4	1024	1030
Large cations															
Rb^{+}	44	8.5	36	9.8	1.5	270	1.5	4.1	2.3	17	19	27	7.5	2.0	2.1
Ba^{2+}	550	240	180	74	110	250	70	69	64	170	180	210	200	54	61
K^{+}	12,000	4,000	8,300	6,400	1,300	49,000	400	2,500	1,300	5,400	5,400	6,100	2,900	400	400
Sr^{2+}	410	360	260	150	150	76	110	83	60	230	240	220	310	260	220
Ca^{2+}	39,000	51,000	44,000	43,000	77,000	___	89,000	66,000	57,000	64,000	70,000	67,000	67,000	41,000	52,000
Pb^{2+}	5.5	6.1	6.0	4.8	4.0	16	3.0	2.1	2.2	5.5	7.0	6.6	5.1	4.2	2.5
K/Rb	270	470	230	650	870	180	270	610	570	320	280	230	390	200	190
Ba/Rb	13	28	5.0	7.6	73	.93	47	17	28	10	9.5	7.8	27	27	29
K/Ba	22	17	46	86	12	200	5.7	35	20	32	30	29	15	7.4	6.6
High-valence cations															
Th^{4+}	2.6	2.1	2.4	2.1	1.7	___	1.0	1.0	1.0	2.4	2.2	2.2	2.1	1.8	1.9
U^{4+}	.7	.6	.6	.6	.5	___	___	.3	___	.7	.7	.7	.7	.5	.6
Zr^{4+}	87	77	87	82	85	110	53	46	45	100	110	94	94	84	77
Hf^{4+}	2.5	2.0	2.2	2.1	2.2	___	1.1	1.1	1.2	2.6	2.4	2.3	2.4	2.2	2.0
Nb^{5+}	6.8	5.9	6.9	5.8	5.9	___	5.5	4.5	4.1	6.2	5.6	6.4	5.9	5.7	6.4
Ta^{5+}	.42	.27	.47	.26	.28	___	.17	.21	___	.41	.36	.37	.39	.28	.33
Th/U	3.7	3.5	4.0	3.5	3.4	___	___	3.3	___	3.4	3.1	3.1	3.0	3.6	3.2
Zr/Hf	35	39	40	39	39	___	48	42	38	38	46	41	39	38	39
(Nb×100)/Ti	.10	.11	.10	.11	.09	___	.18	.16	.14	.09	.10	.10	.09	.10	.11
Nb/Ta	16	22	15	22	21	___	32	21	___	15	16	17	15	20	19
Ferromagnesian elements															
Co^{2+}	67	44	43	38	49	33	69	70	68	43	42	42	48	46	51
Cu^{2+}	20	18	22	19	48	37	150	120	98	66	73	64	82	79	85
Li^{+}	7.5	6.0	8.9	27	2.0	5.3	11	7.8	33	8.4	19	13	12	22	26
Ni^{2+}	26	22	20	20	33	200	530	530	530	33	27	35	37	42	35
Zn^{2+}	50	62	68	69	81	63	56	62	74	92	94	110	91	80	82
Cr^{3+}	57	52	50	48	190	370	790	800	650	32	25	36	27	35	28
Ga^{3+}	14	16	14	13	17	12	13	11	12	17	17	16	15	14	14
Sc^{3+}	44	44	41	41	43	19	43	33	39	41	39	43	42	40	37
V^{3+}	290	280	290	250	300	82	230	180	230	320	330	300	290	290	240
Ni/Co	.39	.50	.47	.53	.67	6.1	7.7	7.6	7.8	.77	.64	.83	.77	.91	.69
Rare-earth elements															
La	11	10	10	10	8	___	5.5	5	5	12	11	11	11	9	10
Ce	20	23	20	20	20	___	14	12	12	22	24	26	32	27	23
Nd	14	10	13	12	12	___	9	___	6.5	15	13	15	13	14	13
Sm	3.4	3.0	3.4	3.0	3.2	___	1.8	1.6	1.7	3.8	3.5	3.6	3.5	3.3	3.4
Eu	1.07	.94	1.09	1.10	1.10	___	.62	.57	.51	1.32	1.18	1.06	1.20	.90	1.20
Tb	.76	.78	.75	.67	.81	___	___	.41	___	.83	.79	.69	.81	.74	.69
Ho	.8	.7	.8	.7	.8	___	.7	.6	.6	.8	.8	.9	.8	.8	.8
Yb	2.9	2.5	2.6	2.6	2.7	___	2.5	2.0	2.3	3.0	3.0	2.9	3.0	2.8	2.9
Lu	.44	.35	.38	.35	.43	___	.36	.34	.34	.43	.43	.43	.43	.43	.41
Y	24	23	25	25	29	20	23	17	20	28	28	29	29	26	25

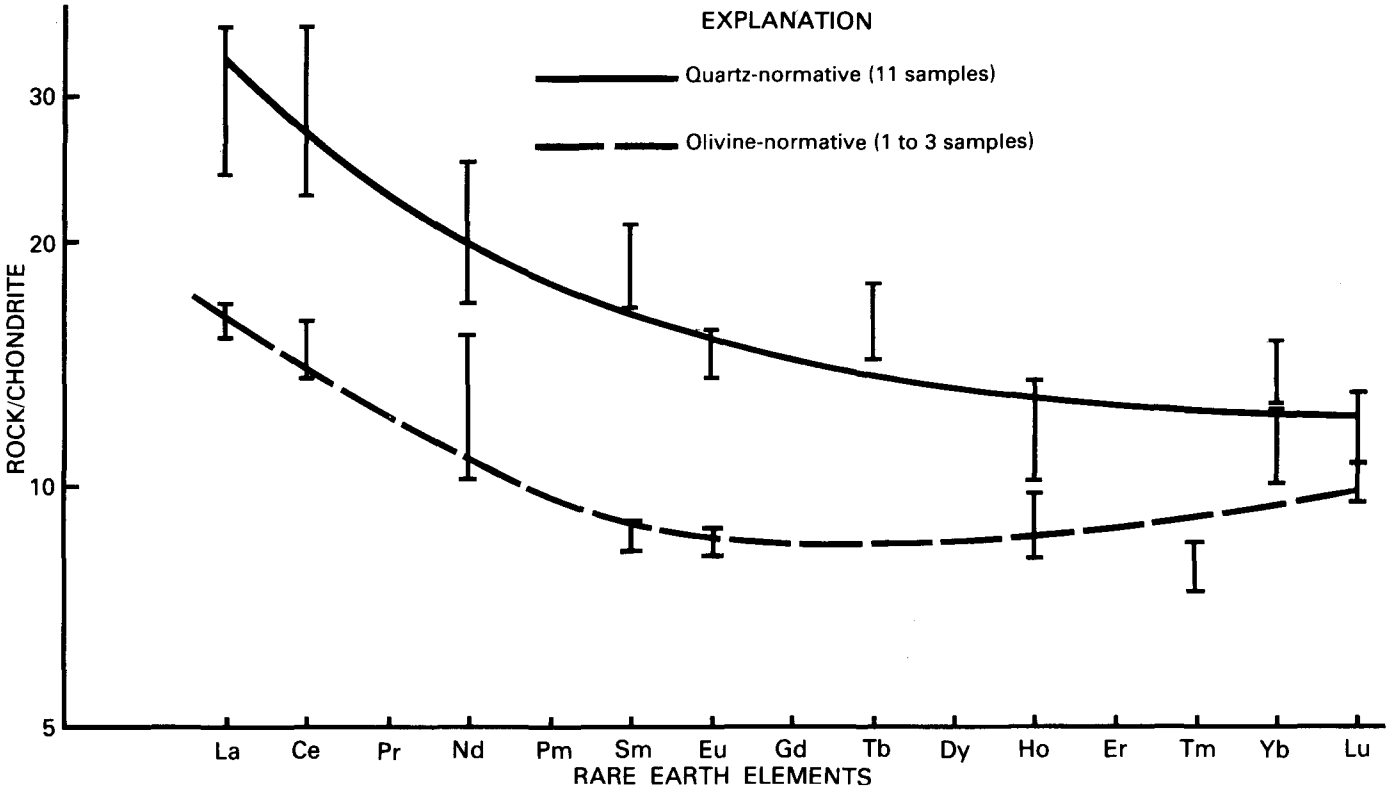

FIGURE 5.–Average abundances of REE in basalts from CC#3. Data are from table 4. Each vertical bar indicates the range of normalized values of 11 quartz-normative samples or 1–3 olivine-normative samples.

preference of Ni, Cu, and Co for the sulfide liquid is clearly indicated by the large partition coefficients that were experimentally determined by Rajamani and Naldrett (1978) between sulfide liquid and a basalt liquid with 8.3 percent MgO. Their values for the partition coefficient D [D = (weight percent metal in sulfide liquid)/(weight percent metal in basalt liquid)] at 1235°C for Ni, Cu, and Co are 274, 245, and 80 respectively. Although the process of separation of a sulfide melt could drastically deplete these elements in residual liquids, the effect on the major-element composition would be negligible if, as suggested by Mysen and Popp (1980), the immiscible sulfide melt amounts to only 0.5 weight percent. The threefold difference in Cu contents among the CC#3 basalts, in which other elements are mainly isochemical, is thus probably the result of differences in physical-chemical conditions during separation of the immiscible sulfide melts.

As noted above, the olivine-rich basalts contain about half the abundances of the stable incompatible minor and trace elements (P, Ti, Zr, Hf, Th, U, and Ta) of the quartz-normative varieties. Olivine-rich basalts are also marked by high Ni and Cr contents and high Ni/Co ratios. The chemistry of the olivine basalts is consistent with their being parental to the quartz-normative type to which they evolved by a crystal-fractionation process. The two-fold enrichment of the incompatible elements indicates that at least 50 percent crystallization and separation of olivine ± pyroxene from parental melts is necessary to produce quartz-normative tholeiites. In addition, the Cu and Ni/Co data point to some sulfide fractionation. Experimental studies suggest that quartz-normative tholeiites evolve from olivine-tholeiite magma by crystal fractionation at crustal pressures of less than 8 to 10 kbar (Yoder, 1976).

The olivine-normative basalts are stratigraphically intercalated between quartz-normative flows. This precludes the sampled olivine-normative rocks from being directly parental to the underlying quartz-normative flows. They may, however, have the composition of such parents. The high MgO (11.5–16.6 percent), Ni (530 ppm), and Cr (650–800 ppm) contents and high Ni/Co ratios (7.7) may be particularly significant; Mysen (1978) and Mysen and Popp (1980) have suggested that partial melting of peridotite at about 20 kbar would result in a tholeiitic liquid that contains 600–700 ppm Ni. The olivine basalts may represent near-primary magmas that have been little modified by crystal fractionation

during ascent from the mantle. The low Ni/Co ratios of the quartz-normative basalts preclude the possibility that they were in equilibrium with mantle peridotite.

Thus a polybaric evolutionary history involving silicate and sulfide fractionation must be envisioned for these flows. The geochemical data are consistent with the possibility that the parental melt for both the olivine-normative and the quartz-normative basalts was generated within a relatively homogeneous peridotite source.

The trace-element chemistry of the sedimentary bed at 924–926 m (table 4, sample 924) reflects the mineralogic composition of this detrital unit. Very high K (49,000 ppm) and Rb (270 ppm) contents reflect the presence of potassium feldspar and illite that almost certainly were not derived from the enclosing basalt flows. High Ni (200 ppm) and Cr (370 ppm) contents agree with the observation of olivine-basalt clasts in the sedimentary bed.

TECTONIC SETTING AND MAGMATIC HISTORY

A particularly valuable result of the geochemical study of the test-hole basalts is the use of their geochemical features to characterize their tectonic setting. Gottfried and others (1977) attempted such a characterization of the CC#1 basalts by using the Ti-Zr, Ti-Zr-Y, and Ti-Zr-Sr discriminant diagrams of Pearce and Cann (1973). The results obtained were mutually contradictory; the basalts were described on various plots as calc-alkalic basalts of the island-arc series, as ocean-floor basalts, and as island-arc tholeiitic basalts. Gottfried and others (1977) concluded that the available plots were inappropriate for tectonic characterization of CC#1 basalts.

More recently, Wood and others (1979) and Wood (1980) have proposed the use of a Th-Hf-Ta triangular diagram for tectonomagmatic classification. A plot of several Clubhouse Crossroads basalts and, for comparison, a typical ocean-ridge basalt and two Paleozoic continental tholeiitic diabases from Scotland is shown in figure 6. The Clubhouse Crossroads basalts plot in the field of basalts from destructive plate margins. However, the test-hole basalts are closely analogous chemically to basalts that occur in Atlantic-type passive continental margins and that represent the early cycles of magmatism that precede or accompany rifting and continental separation. Thus, either the diagram is inappropriately classifying the Clubhouse Crossroads basalts or the comparisons with basalts of rifted continental margins made in our previous study (Gottfried and others, 1977) are spurious.

We suggest that the geochemical characteristics of the subsurface basalts of the Charleston area produce the inappropriate classification on the Th-Hf-Ta plot. The Clubhouse Crossroads basalts are characterized by low abundances of the relatively small ions Ti, Zr, Hf, and Ta. Macdonald and others (1981, their table 10) have shown that the Triassic-Jurassic passive-margin basalts of eastern North America, and presumably the test-hole basalts, belong to a type of intraplate tholeiite that is relatively enriched in Th. Thus, on the Th-Hf-Ta diagram (fig. 6), the test-hole basalts are displaced towards the Th apex and plot in the destructive-plate-margin field. The data base used by Wood (1980) for delineation of his field did not adequately account for tholeiitic basalts of passive continental margins that are chemically similar to those of eastern North America.

Although published discriminant diagrams do not appear appropriate for interpretation of the studied rocks, the results of this extensive geochemical study (tables 5, 6) of the basalts from CC#2 and CC#3 confirm our previous interpretation (Gottfried and others, 1977) regarding the magmatic affinities and tectonic setting of the basalt rocks. Recent radiometric ages determined by refined techniques (Lanphere, 1983) substantiate the correlation by stable minor and trace elements of the Clubhouse Crossroads quartz-normative basalts with the lower Mesozoic high-Ti, quartz-normative diabases of eastern North America. The olivine-normative basalt intercalated with the quartz-normative basalts in CC#3 shows close geochemical similarities to the common olivine-normative diabases from the eastern North American province. Thus two of the three main chemical types of the eastern North American province have been recognized in the Clubhouse Crossroads basalts. In addition, the quartz-normative basalts from Clubhouse Crossroads are virtually indistinguishable from the quartz-normative tholeiitic rocks from eastern North America on the basis of their REE patterns and REE absolute abundances (fig. 7). The REE pattern for the olivine basalt from CC#3 "fingerprints" this rock as belonging to the olivine-normative type of eastern North America (Ragland and others, 1971). The wide ranges in contents of most of the major elements in the quartz-normative rocks (table 5) reflect postmagmatic chemical changes. The average TiO_2 and P_2O_5 contents in all of the quartz-normative basalts are virtually identical, as is the case for Th and Hf and some other stable trace elements. However, Cu and, to a lesser extent, Ni contents in the lower quartz-normative basalts from CC#3 are significantly greater than those encountered in the quartz-normative rocks at higher levels in the test holes. These differences can reasonably be attributed to differences in preeruptional history; namely, during magmatic ascent, the separation of an immiscible sulfide liquid into which Ni, Cu, and Co are strongly partitioned. In addition to providing important clues to the petrogenetic history of these basalts, the abundance

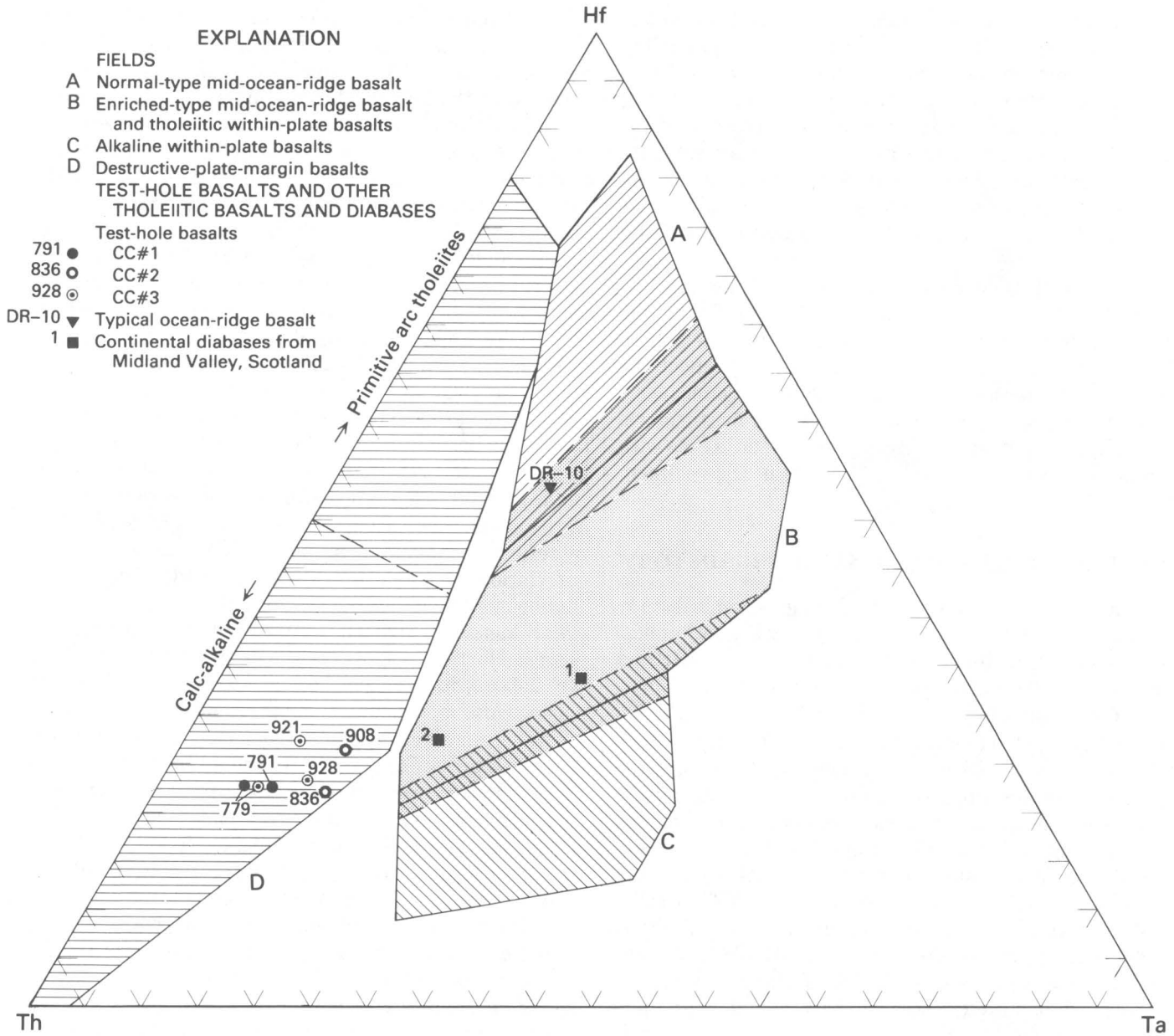

FIGURE 6.—Th-Hf-Ta data for samples of Clubhouse Crossroads basalt, ocean-ridge basalt, and continental tholeiitic diabase plotted on tectonomagmatic discrimination diagram of Wood (1980). Data sources: CC#1 (Gottfried and others, 1977); CC#2 and CC#3 (tables 2 and 4, this paper); ocean-ridge basalt from Juan de Fuca Ridge (David Gottfried, unpub. data, 1979); continental tholeiitic diabase from Scotland (Macdonald and others, 1981).

relations of these elements have potential economic application to further our understanding of the formation of Ni and Ni-Cu sulfide deposits that are associated with similar mafic volcanic rocks.

Previously, studies have proposed that the tholeiitic olivine diabases and flows of the eastern North American province represented the earliest stage of volcanism in that province. Whole-rock K-Ar measurements of undeformed diabase dikes in east-central Alabama yielded ages of 161–168 m.y. for quartz-normative diabase and 184–193 m.y. for olivine-normative diabases (Deininger and others, 1975). Field studies of a swarm of olivine-normative diabase dikes (Smith and others, 1975) in Pennsylvania showed the presence of fracture cleavage in many of the olivine-tholeiitic dikes, which was not observed in quartz-normative dikes. This suggested that the olivine-normative magma was the earliest erupted type.

TABLE 5.—*Average major-oxide composition, in weight percent, of subsurface basalts from Clubhouse Crossroads test holes CC#1, CC#2, and CC#3, near Charleston, S. C.*

[Recalculated volatile-free. Range is given in parentheses after average. Averages derived as follows: CC#1, averages are for 5 least altered samples, from 771, 774, 779, 782, and 791 m below surface; ranges are for all samples. CC#2, averages are for 8 samples, from depths of 780, 786, 879, 836, 842, 869, 878, and 908 m below surface. CC#3 upper quartz-normative, averages are for 4 samples, from depths of 777, 779, 782, and 784.4 m below surface. CC#3 lower quartz-normative, averages are for 6 samples, from depths of 984, 1002.2, 1014, 1020.4, 1024, and 1030 m below surface. CC#3 olivine-normative, averages are for 3 samples, from depths of 926.3, 928, and 930 m below surface.]

Sample location	CC#1	CC#2	CC#3 Upper quartz-normative	CC#3 Lower quartz-normative	CC#3 Olivine normative
SiO_2	54.0 (53.1–68.5)	53.9 (52.1–54.8)	52.9 (50.0–57.3)	53.3 (50.8–54.1)	47.4 (46.5–48.6)
Al_2O_3	14.0 (7.3–16.7)	14.6 (14.1–14.8)	15.2 (13.8–16.0)	14.5 (14.1–15.5)	14.9 (14.5–15.8)
Fe_2O_3	3.1 (2.5–9.5)	2.9 (1.8–4.6)	5.0 (4.2–6.1)	3.5 (2.4–4.1)	5.5 (4.1–7.1)
FeO	8.6 (.79–9.0)	8.4 (6.8–8.9)	6.9 (5.5–7.6)	8.5 (8.1–9.9)	5.9 (4.1–7.5)
MgO	6.0 (2.6–6.9)	6.3 (6.0–6.7)	6.7 (6.2–7.1)	6.4 (5.4–8.8)	14.0 (11.5–16.6)
CaO	9.0 (7.1–9.6)	9.2 (7.6–10.3)	6.2 (5.4–7.1)	8.4 (5.8–9.8)	9.9 (8.0–12.4)
Na_2O	2.8 (.51–3.6)	2.8 (2.2–5.0)	4.7 (4.0–5.4)	3.5 (2.6–5.7)	1.4 (1.3–1.7)
K_2O	.54 (.02–1.4)	.63 (.23–1.6)	.99 (.48–1.4)	.42 (.05–.74)	.17 (.05–.30)
TiO_2	.97 (.82–1.1)	1.0 (1.0–1.1)	1.1 (.93–1.2)	1.1 (.98–1.1)	.54 (.52–.56)
P_2O_5	.14 (.12–.15)	.15 (.14–.16)	.17 (.16–.17)	.17 (.16–.18)	.08 (.08–.10)
MnO_2	.23 (.14–.27)	.17 (.16–.18)	.26 (.20–.33)	.22 (.21–.24)	.20 (.15–.24)

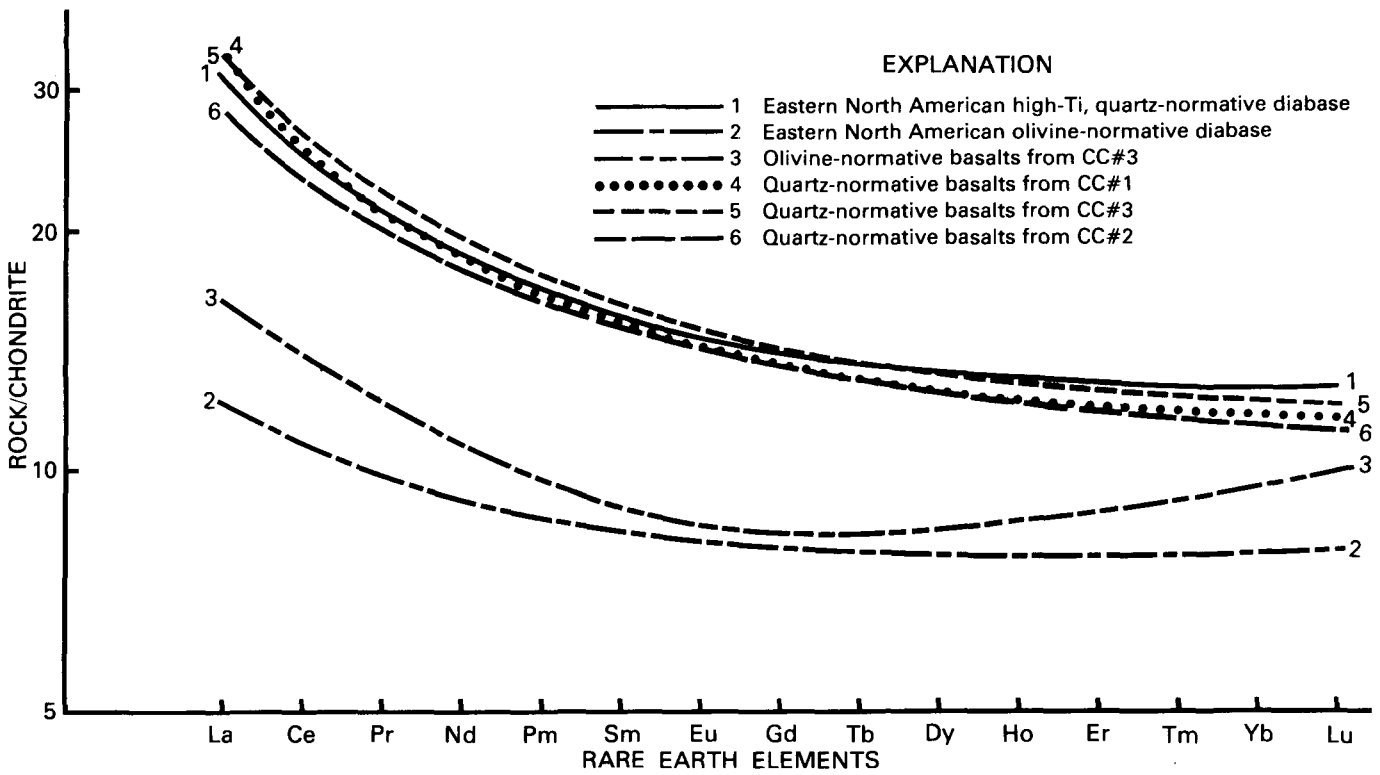

FIGURE 7.—Comparison of average abundances of REE in tholeiitic basalts of eastern North America and subsurface basalts from Clubhouse Crossroads test holes. Data sources: eastern North American high-Ti, quartz-normative diabase and eastern North American olivine-normative diabase (Ragland and others, 1971); CC#1 (Gottfried and others, 1977); CC#2 and CC#3 (tables 2 and 4, this paper).

TABLE 6.—*Average trace-element abundances in subsurface basalts from Clubhouse Crossroads test holes CC#1, CC#2, and CC#3, near Charleston, S. C.*

[Range given in parentheses after average. n.d., not determined]

Sample location	CC#1		CC#2		CC#3 Upper quartz-normative		CC#3 Lower quartz-normative		CC#3 Olivine normative	
Large cations										
Rb^{+}	16	(10–19)	17	(1.1–59)	25	(9–44)	12	(2–27)	2.7	(1.5–4.1)
Ba^{2+}	130	(100–140)	130	(7–370)	260	(74–550)	150	(54–210)	68	(64–70)
K^{+}	4,500	(4,100–5,300)	5,200	(1,900–12,000)	8,200	(3,700–11,000)	3,500	(400–6,100)	1,400	(600–2,200)
Sr^{2+}	190	(160–220)	190	(61–380)	300	(50–410)	250	(220–310)	84	(60–110)
Ca^{2+}	64,000	(62,000–66,000)	66,000	(51,000–73,000)	44,000	(36,000–50,000)	60,000	(41,000–69,000)	71,000	(53,000–82,000)
Pb^{2+}	4.5	(3.9–5)	5.7	(3.8–9.1)	5.6	(4.8–6.1)	5.2	(2.5–7)	2.4	(2.1–3.0)
K/Rb	300	(220–410)	290	(110–650)	410	(230–650)	270	(190–390)	480	(270–610)
Ba/Rb	8.1	(5.8–14)	9.4	(3.2–24)	10	(5–28)	18	(7.8–29)	31	(17–47)
K/Ba	35	(29–39)	36	(15–69)	43	(17–86)	20	(5.7–35)	20	(6.6–32)
High-valence cations										
Th^{4+}	2.1	(2.0–2.2)	2.0	(1.5–2.1)	2.3	(1.7–2.6)	2.1	(1.8–2.4)	1.0	1.0
U^{4+}			0.6	(.5–.8)	0.6	(.5–.7)	0.65	(.5–.7)	.3	
Zr^{4+}	76	(69–82)	86	(78–100)	83	(77–87)	93	(77–100)	48	(45–53)
Hf^{4+}	2.1	(2.0–2.1)	2.0	(1.9–2.1)	2.2	(2.0–2.5)	2.3	(2.0–2.6)	1.1	(1.1–1.2)
Nb^{5+}	7.3	(6.8–7.7)	6.0	(4.9–6.8)	6.4	(5.8–6.9)	6.0	(5.6–6.4)	4.7	(4.1–5.5)
Ta^{5+}	0.29	(.26–.32)	0.44	(.34–.53)	0.36	(.26–.47)	.36	(.28–.41)	[1].19	(.17–.21)
Th/U			3.1	(2.1–3.8)	3.7	(3.4–4.0)	3.2	(3.0–3.6)	3.3	
Zr/Hf	36	(35–39)	43	(37–47)	38	(35–40)	40	(38–46)	44	(38–48)
(Nb×100)/Ti	0.13	(.12–.14)	0.10	(.09–.11)	0.11	(.10–.11)	.098	(.09–.11)	.16	(.14–.18)
Nb/Ta	25	(23–26)	14	(12–18)	19	(15–22)	17	(15–20)	[1]27	(21–32)
Ferromagnesian elements										
Co^{2+}	46	(40–52)	45	(34–54)	48	(38–67)	45	(42–51)	69	(68–70)
Cu^{2+}	25.	(16–34)	22	(16–43)	20	(18–22)	75	(64–85)	120	(98–150)
Li^{+}	9.4	(5–14)	11	(1.8–25)	12	(6–27)	17	(8.4–26)	17	(7.8–33)
Ni^{2+}	17	(14–20)	23	(19–34)	22	(20–26)	35	(27–42)	530	(530)
Zn^{2+}	88	(82–96)	89	(75–100)	62	(50–69)	92	(80–110)	64	(56–74)
Cr^{3+}	33	(28–36)	71	(50–170)	52	(48–57)	31	(25–36)	750	(650–800)
Ca^{3+}	16	(15–18)	16	(12–20)	14	(13–16)	16	(14–17)	12	(11–13)
Sc^{3+}	51	(46–56)	42	(37–50)	43	(41–44)	40	(37–43)	38	(33–43)
V^{3+}	320	(250–400)	280	(230–370)	280	(250–290)	300	(240–330)	210	(180–230)
Ni/Co	.38	(.31–.48)	.52	(.42–.63)	.47	(.39–.53)	.77	(.64–.91)	7.7	(7.6–7.8)
Rare-earth elements										
La	[2]10	(9–11)	[4]9.4	(9–10)	10	[5](10–11)	11	[6](9–12)	5.2	[7](5–5.5)
Ce	19	(18–19)	20	(17–21)	21	(20–23)	26	(22–32)	13	(12–14)
Nd	[3]10		12	(9–14)	12	(10–14)	14	(13–15)	7.8	(6.5–9)
Sm	3.0	(3.0–3.1)	3.1	(3.0–3.2)	3.2	(3.0–3.4)	3.5	(3.3–3.8)	1.7	(1.6–1.8)
Eu	.99	(.95–1.02)	.94	(.87–.99)	1.05	(.94–1.10)	1.14	(.90–1.32)	.57	(.51–.62)
Gd	n.d.	n.d.	3.1	(2.8–3.4)	n.d.	n.d.	n.d.	n.d.	n.d.	n.d.
Tb	.70	(.68–.73)	.77	(.71–.86)	.74	(.67–.78)	.76	(.69–.83)	.41	n.d.
Ho	n.d.	n.d.	.6	(.5–.7)	.8	(.7–.8)	.8	(.8–.9)	.6	(.6–.7)
Tm	n.d.	n.d.	.33	(.31–.36)	n.d.	n.d.	n.d.	n.d.	n.d.	n.d.
Yb	2.2	(2.1–2.3)	2.7	(2.5–3.1)	2.7	(2.5–2.9)	2.9	(2.8–3.0)	2.3	(2.0–2.5)
Lu	.45	(.44–.47)	.42	(.39–.44)	.38		.43		.36	n.d.
Y	32	(28–34)	28	(25–30)	24	(23–25)	28	(25–29)	20	(17–23)

[1] Derived from two samples, from 926.3 and 928 m below surface.
[2] REE averages derived from three samples, from 771, 779, and 791 m below surface.
[3] Derived from one sample, from 779 m below surface.
[4] REE derived from eight samples, from 780, 786, 819, 836, 842, 869, 878, and 908 m below surface.
[5] Derived from four samples, from 777, 779, 782, and 784.4 m below surface.
[6] Derived from six samples, from 984, 1002.2, 1014, 1030.4, 1024, and 1030 m below surface.
[7] Derived from three samples, from 926.3, 928, and 930 m below surface.

However, the extensive geochronologic study of exposed lower Mesozoic dikes in Georgia by Dooley and Wampler (1983) indicates that excess ^{40}Ar in most of these dikes resulted in variable and highly discordant K-Ar ages. Further, several of their samples that contained little excess ^{40}Ar included both olivine- and quartz-normative tholeiites having apparent ages of 190–195 m.y. The new data from CC#3 unequivocally show the presence of an olivine-tholeiite flow intercalated within a sequence of quartz-normative tholeiites. It thus appears that there were repetitive cycles and possibly penecontemporaneous eruptions of olivine-normative and quartz-normative magmas. Weigand and Ragland (1970) discussed the geographic distribution of

the main chemical magma types in the eastern North American province. They proposed that differences in tectonic environment could account for the absence of the olivine-normative magma type in the northeast part of the province. The close association in space and time of these contrasting magmas at Clubhouse Crossroads suggests that the olivine-tholeiitic magma may represent merely a greater degree of melting, hence differences in the thermal regime in the mantle, rather than any significant change in tectonic environment.

REFERENCES CITED

Baedecker, P. A., Rowe, J. J., and Steinnes, Eiliv, 1977, Application of epithermal neutron activation in multi-element analysis of silicate rocks employing both coaxial Ge(Li) and low energy photon detector systems: Journal of Radioanalytical Chemistry, v. 40, p. 115–146.

Deininger, R. W., Dallmeyer, R. D., and Neathery, T. L., 1975, Chemical variations and K-Ar ages of diabase dikes in east-central Alabama [abs.]: Geological Society of America Abstracts with Programs, v. 7, no. 4, p. 482.

Dooley, R. E., and Wampler, J. M., 1983, Potassium-argon relations in diabase dikes of Georgia: the influence of excess ^{40}Ar on the geochronology of early Mesozoic igneous and tectonic events, *in* Gohn, G. S., ed., Studies related to the Charleston, South Carolina, earthquake of 1886–Tectonics and seismicity: U.S. Geological Survey Professional Paper 1313, p. M1–M24.

Gohn, G. S., Gottfried, David, Lanphere, M. A., and Higgins, B. B., 1978, Regional implications of Triassic or Jurassic age for basalt and sedimentary red beds in the South Carolina Coastal Plain: Science, v. 202, no. 4370, p. 887–890.

Gohn, G. S., Houser, B. B., and Schneider, R. R., 1983, Geology of the lower Mesozoic(?) sedimentary rocks in Clubhouse Crossroads test hole #3, Dorchester County, South Carolina, *in* Gohn, G. S., ed., Studies related to the Charleston, South Carolina, earthquake of 1886–Tectonics and seismicity: U.S. Geological Survey Professional Paper 1313, p. D1–D17.

Gottfried, David, Annell, C. S., and Schwarz, L. J., 1977, Geochemistry of subsurface basalt from the deep corehole (Clubhouse Crossroads corehole 1) near Charleston, South Carolina–Magma type and tectonic implications, *in* Rankin, D. W., ed., Studies related to the Charleston, South Carolina, earthquake of 1886–A preliminary report: U.S. Geological Survey Professional Paper 1028, p. 91–113.

Gottfried, David, Greenland, L. P., and Campbell, E. Y., 1968, Variation of Nb-Ta, Zr-Hf, Th-U and K-Cs in two diabase-granophyre suites: Geochimica et Cosmochimica Acta, v. 32, no. 9, p. 925–947.

Heier, K. S., and Rogers, J. J. W., 1963, Radiometric determination of thorium, uranium and potassium in basalts and in two magmatic differentiation series: Geochimica et Cosmochimica Acta, v. 27, no. 2, p. 137–154.

Lanphere, M. A., 1983, $^{40}Ar/^{39}Ar$ ages of basalt from Clubhouse Crossroads test hole #2, near Charleston, South Carolina, *in* Gohn, G. S., ed., Studies related to the Charleston, South Carolina, earthquake of 1886–Tectonics and seismicity: U.S. Geological Survey Professional Paper 1313, p. B1–B8.

Larsen, E. S., III, and Gottfried, David, 1960, Uranium and thorium in selected suites of igneous rocks: American Journal of Science, v. 258-A, p. 151–169.

Macdonald, R., Gottfried, David, Farrington, M. J., Brown, F. W., and Skinner, N. G., 1981, Geochemistry of a continental tholeiite suite: late Paleozoic quartz dolerite dykes of Scotland: Royal Society of Edinburgh Transactions, Earth Sciences, v. 72, p. 57–74.

Mysen, B. O., 1978, Experimental determination of nickel partition coefficients between liquid, pargasite, and garnet peridotite minerals and concentration limits of behavior according to Henry's law at high pressure and temperature: American Journal of Science, v. 278, no. 2, p. 217–243.

Mysen, B. O., and Popp, R. K., 1980, Solubility of sulfur in $CaMgSi_2O_6$ and $NaAlSi_3O_8$ melts at high pressure and temperature with controlled fO_2 and fS_2: American Journal of Science, v. 280, no. 1, p. 78–92.

Pearce, J. A., and Cann, J. R., 1973, Tectonic setting of basic volcanic rocks determined using trace element analyses: Earth and Planetary Science Letters, v. 19, no. 2, p. 290–300.

Ragland, P. C., Brunfelt, A. O., and Weigand, P. W., 1971, Rare-earth abundances in Mesozoic dolerite dikes from eastern United States, *in* Brunfelt, A. O., and Steinnes, Eiliv, eds., Activation analysis in geochemistry and cosmochemistry: Oslo, Universitetsforlaget, p. 227–235.

Rajamani, V., and Naldrett, A. J., 1978, Partitioning of Fe, Co, Ni, and Cu between sulfide liquid and basaltic melts and the composition of Ni-Cu sulfide deposits: Economic Geology, v. 73, no. 1, p. 82–93.

Smith, R. C., II, Rose, A. W., and Lanning, R. M., 1975, Geology and geochemistry of Triassic diabase in Pennsylvania: Geological Society of America Bulletin, v. 86, no. 7, p. 943–955.

Taylor, S. R., 1965, Geochemical analysis by spark source mass spectrometry: Geochimica et Cosmochimica Acta, v. 29, no. 12, p. 1243–1261.

Weigand, P. W., and Ragland, P. C., 1970, Geochemistry of Mesozoic dolerite dikes from eastern North America: Contributions to Mineralogy and Petrology, v. 29, no. 3, p. 195–214.

Wood, D. A., 1980, The application of a Th-Hf-Ta diagram to problems of tectonomagmatic classification and to establishing the nature of crustal contamination of basaltic lavas of the British Tertiary volcanic province: Earth and Planetary Science Letters, v. 50, no. 1, p. 11–30.

Wood, D. A., Joron, J. L., and Treuil, M., 1979, A reappraisal of the use of trace elements to classify and discriminate between magma series erupted in different tectonic settings: Earth and Planetary Science Letters, v. 45, no. 2, p. 326–336.

Yoder, H. S., Jr., 1976, Generation of basaltic magma: Washington, D.C., National Academy of Sciences, 265 p.

$^{40}Ar/^{39}Ar$ Ages of Basalt From Clubhouse Crossroads Test Hole #2, Near Charleston, South Carolina

By MARVIN A. LANPHERE

STUDIES RELATED TO THE CHARLESTON, SOUTH CAROLINA, EARTHQUAKE OF 1886—TECTONICS AND SEISMICITY

GEOLOGICAL SURVEY PROFESSIONAL PAPER 1313-B

UNITED STATES GOVERNMENT PRINTING OFFICE, WASHINGTON: 1983

CONTENTS

ILLUSTRATIONS

TABLES

STUDIES RELATED TO THE CHARLESTON, SOUTH CAROLINA, EARTHQUAKE OF 1886—TECTONICS AND SEISMICITY

$^{40}Ar/^{39}Ar$ AGES OF BASALT FROM CLUBHOUSE CROSSROADS TEST HOLE #2, NEAR CHARLESTON, SOUTH CAROLINA

By MARVIN A. LANPHERE

ABSTRACT

$^{40}Ar/^{39}Ar$ total-fusion ages of three samples of basalt from Clubhouse Crossroads test hole #2, near Charleston, S.C., range from 182 to 236 m.y. (million years); only one of the total-fusion ages agrees within analytical uncertainty with conventional K-Ar ages of the same samples. Data from $^{40}Ar/^{39}Ar$ incremental heating experiments indicate that only one sample meets the criteria for a reliable crystallization age. The $^{40}Ar/^{36}Ar$ versus $^{39}Ar/^{36}Ar$ isochron age for this basalt is 184 ± 3.3 m.y. This age is in good agreement with reliable ages of tectonically related lower Mesozoic diabase intrusions in eastern North America and Liberia. The ages of all these intrusions are consistent with their emplacement shortly after initiation of central Atlantic rifting about 190 m.y. ago.

INTRODUCTION

Many workers believe that the separation of the African and North American plates and the formation of the Atlantic Ocean were the initial events in the breakup of Pangea (Dietz and Holden, 1970; Pitman and Talwani, 1972; Phillips and Forsyth, 1972; Larson and Pitman, 1972; Smith and others, 1973). Basaltic igneous activity of Triassic to Jurassic age in northeastern North America and northwestern Africa is probably related to the extensional tectonics that produced rifting of the continent (Dietz and Holden, 1970; Dalrymple and others, 1975). Triassic or Jurassic basalt flows in deep test wells near Charleston, S. C., indicate that the early Mesozoic tectonic framework of the Southeastern United States is the same as that of northeastern North America (Gohn and others, 1978). The current study is an extension of isotopic dating work on the basalts near Charleston.

Acknowledgments.—I thank S. E. Sims and J. C. Von Essen of the U.S. Geological Survey (USGS) for the argon measurements and D. H. Rusling and the staff of the USGS reactor facility for fast-neutron irradiation of samples. Deep drilling and related investigations by the USGS in the Charleston, S. C., area are supported by the U.S. Nuclear Regulatory Commission, Office of Nuclear Research, under Agreement No. AT(49-25)-1000.

GEOLOGIC SETTING

Fault-bounded basins filled primarily with clastic sedimentary rocks of Triassic and Jurassic age are a characteristic geologic feature of the eastern seaboard of North America. Some basins contain interbedded basalt flows and diabase dikes and sills. The dikes typically extend outside individual basins. Such basins are exposed in the Piedmont from North Carolina on the southeast to Nova Scotia on the northeast. Sediments of the Atlantic Coastal Plain conceal subsurface lower Mesozoic rocks in South Carolina, Georgia, Florida, and Alabama, which have been documented from deep wells or inferred from geophysical surveys.

Three deep test wells drilled by the USGS at Clubhouse Crossroads, Dorchester County, S. C., penetrated a pre-Upper Cretaceous sequence of subaerial, tholeiitic basalt flows underlain by red sandstone, mudstone, and conglomerate (Gohn and others, 1978). Two basalt samples from Clubhouse Crossroads test hole 1 (CC#1) yielded K-Ar ages of 97.0 ± 4.2 and 111 ± 4 m.y. (million years). These ages have been recalculated from those originally reported by Gottfried and others (1977) by using the isotopic abundance and decay constants for ^{40}K recommended by Steiger and Jäger (1977). These ages must be considered minimum, however, because the basalts have been somewhat altered. The basalts unconformably underlie strata of Cretaceous (Cenomanian) age (Hazel and others, 1977) in the test hole; no direct stratigraphic evidence for a maximum age for the basalts is available.

Petrographic and major-element chemical data obtained from samples of basalt from CC#1 (Gottfried and others, 1977) indicate that the rocks have undergone slight to extreme oxidation, hydration, and hydrother-

mal alteration; H_2O and CO_2 contents are relatively high and variable. Secondary minerals resulting from hydrothermal alteration include laumontite, calcite, chlorite, and stilbite. I examined thin sections of the two samples from CC#1 on which K-Ar ages had been measured, and I concluded that these samples were too altered to yield reliable ages.

Conventional K-Ar ages were subsequently measured on three additional samples of basalt from Clubhouse Crossroads test hole 2 (CC#2) (Gohn and others, 1978). Location of the test hole is shown in Gohn and others (1983, fig. 1). The 132-m-thick section of basalt in CC#2 was divided into 3 flow units by Gottfried and others (1983); Phillips (1983) further divided these 3 units into 10 subflows on the basis of paleomagnetic measurements. The three basalt samples used for K-Ar measurements—BBH#1 (818.7 m), BBH#3 (842.3 m), and BBH#5 (907.4 m)—are from flows designated by Phillips as 2–2b, 2–2d, and 2–3d, respectively. The samples are slightly altered but, on the basis of thin-section examination, were considered suitable for dating.

Duplicate analyses of the three basalt samples from CC#2 yielded ages of 204 ± 4.1, 162 ± 3.2, and 186 ± 3.7 m.y. for BBH#1, BBH#3, and BBH#5, respectively. These data confirmed that the basalts, and presumably the underlying sedimentary red beds, are Triassic or Jurassic in age and are equivalent to rocks in the exposed early Mesozoic basins along the Atlantic seaboard; however, the poor agreement of these ages (Gohn and others, 1978) was disturbing. The ages are not in correct stratigraphic order, and it seems unlikely that basalt was erupted over a period exceeding 40 m.y. Therefore, $^{40}Ar/^{39}Ar$ analyses were made on the same three samples of basalt in an attempt to refine the age determinations.

TECHNIQUES

Samples for $^{40}Ar/^{39}Ar$ analysis were small cores (6 mm in diameter and 1 cm long) taken from the same slices of core from CC#2 as were the samples for conventional K-Ar analysis. The samples for $^{40}Ar/^{39}Ar$ dating were sealed in air in flat-bottomed fused silica vials and were irradiated at 1 megawatt for 25 to 30 hours in the USGS TRIGA[1] reactor, where they received a neutron dose of approximately $2.5–3 \times 10^{18}$ nvt (neutron density–velocity–time). Further details of the reactor flux characteristics, the flux monitor mineral, and the corrections for interfering K- and Ca-derived Ar isotopes have been given by Dalrymple and Lanphere (1971) and by Dalrymple and others (1981).

Irradiated samples were fused by induction heating, and the Ar was purified in a standard extraction line. Temperatures for incremental heating experiments were measured by means of a platinum/platinum-rhodium thermocouple inserted into a small hole in the bottom of a machined molybdenum crucible and are accurate within about $\pm 20°C$ (Lanphere and Dalrymple, 1971). Samples were maintained for 30 minutes at each temperature during incremental heating experiments. Ar analyses were made by means of a Nier-type, 15.24-cm radius, 60°-sector magnet, single-collector mass spectrometer, and analog data acquisition.

RESULTS OF AGE DETERMINATIONS ON BASALT SAMPLES

Data for total-fusion and incremental heating $^{40}Ar/^{39}Ar$ experiments are presented in table 1. Errors given for ages of individual samples or gas increments are estimates of one standard deviation of analytical precision. These errors were calculated by using formulas derived by differentiation of the $^{40}Ar/^{39}Ar$ and age equations (Dalrymple and Lanphere, 1971).

The agreement between total-fusion $^{40}Ar/^{39}Ar$ and conventional K-Ar age determinations for the three basalt samples is not particularly good. For only one sample, BBH#5, do the two ages agree within analytical uncertainty. The ages for BBH#3 differ by slightly more than analytical uncertainty, and the total-fusion and conventional ages of BBH#1 differ by nearly 15 percent. The discordance in ages probably reflects the effect of alteration of the K-Ar system.

A considerable body of data on the effects of alteration on K-Ar age determinations has been obtained from studies of Hawaiian-type basalts altered in the submarine environment. No comparable data exist for continental tholeiites such as those in the Clubhouse Crossroads drill holes. The general pattern of the Hawaiian data may be similar, however. Clague and others (1975) and Dalrymple and Clague (1976) found that the total-fusion $^{40}Ar/^{39}Ar$ ages of altered Hawaiian basalts generally were greater than conventional K-Ar ages for the same rocks. They proposed that this pattern was due to proportional loss of radiogenic ^{40}Ar and K-derived ^{39}Ar from K-bearing clays. Dalrymple and others (1980) devised a parameter to portray this discordance in age. This parameter, δ, is the total-fusion age less the conventional age and is expressed as a percentage of the total-fusion age. Dalrymple and others (1980) have suggested that for samples having δ values that are less than +5, the total-fusion $^{40}Ar/^{39}Ar$ and conventional K-Ar ages probably are quite close to crystallization ages. Only BBH#5, which has a δ value of −2.4, fits this criterion for crystallization age, though

[1]The use of trade names in this publication is for descriptive purposes only and does not constitute endorsement by the U.S. Geological Survey.

TABLE 1.—*Analytical data for $^{40}Ar/^{39}Ar$ total fusion and incremental heating experiments on three basalt samples from CC#2, near Charleston, S. C.*

[Subscripts in columns 9-12 indicate radiogenic (*R*), calcium-derived (*Ca*), and potassium-derived (*K*) argon]

Sample no.	Depth below surface (meters)	Temperature (°C)	J[1]	$^{40}Ar/^{39}Ar$	$^{37}Ar/^{39}Ar$[2]	$^{36}Ar/^{39}Ar$	^{39}Ar (percent of total Ar)	$^{36}Ar_{Ca}$ (percent)	$^{39}Ar_{Ca}$ (percent)	$^{40}Ar_R$ (percent)	$^{40}Ar_R$ (percent)	Calculated age[3] (m.y.)
Total fusion experiments												
BBH#1	818.7	----	0.005600	29.10	4.466	0.01550	----	7.8	0.3	85.5	<0.1	236 ± 2.9[4]
BBH#3	842.3	----	.005600	52.65	12.85	.1216	----	2.9	.8	33.7	<.1	172 ± 4.5[4]
BBH#5	907.4	----	.006821	24.54	18.28	.003608	----	13.8	1.2	62.5	<.1	182 ± 2.8[4]
Incremental heating experiments												
BBH#1	818.7	500	0.005600	34.02	0.8163	0.006458	43.1	3.4	<0.1	94.6	<0.1	299 ± 3.5
		600		21.53	4.755	.005877	17.5	22.0	.3	93.7	<.1	194 ± 2.4
		700		23.07	6.759	.01539	8.7	11.9	.4	82.6	<.1	184 ± 3.1
		800		24.31	2.550	.01499	10.3	4.6	.2	82.6	<.1	193 ± 2.7
		900		19.94	1.531	.005252	15.2	7.9	.1	92.8	<.1	178 ± 2.3
		975		23.14	6.960	.04734	1.8	4.0	.4	41.9	<.1	95.8 ± 7.2
		1050		38.78	20.86	.1213	.8	4.7	1.3	11.9	<.1	46.6 ± 18.5
		FUSE		34.68	58.47	.09643	2.6	16.5	3.7	31.4	<.1	111 ± 9.0
							100.0					
BBH#3	842.3	500	0.005600	54.04	1.828	0.1321	14.3	0.4	0.1	28.0	<0.1	147 ± 6.3
		600		45.80	3.831	.09457	14.1	1.1	.2	39.6	<.1	175 ± 6.3
		700		29.84	6.360	.04573	25.7	3.8	.4	56.4	<.1	163 ± 4.3
		800		28.78	8.853	.04266	17.9	5.6	.6	58.6	<.1	164 ± 4.3
		900		35.18	9.406	.06867	7.0	3.7	.6	44.4	<.1	152 ± 10.3
		975		26.29	11.78	.03694	13.8	8.7	.7	62.0	<.1	159 ± 3.8
		1050		34.14	6.987	.07551	3.6	25.2	4.4	51.1	<.1	176 ± 10.9
		FUSE		41.82	7.325	.1135	3.6	17.5	4.6	33.8	<.1	144 ± 16.3
							100.0					
BBH#5	907.4	500	0.006821	57.99	22.05	0.1409	6.4	0.4	0.1	28.5	<0.1	193 ± 10.7
		600		26.98	3.260	.03939	10.0	2.3	.2	57.8	<.1	183 ± 7.1
		700		27.99	6.113	.04059	16.8	4.1	.4	58.9	<.1	193 ± 5.3
		800		22.56	8.063	.02457	27.2	8.9	.5	70.7	<.1	187 ± 3.5
		900		23.04	11.18	.02814	10.2	10.8	.7	67.8	<.1	184 ± 5.3
		975		26.72	12.10	.04445	5.5	7.4	.8	54.5	<.1	172 ± 8.0
		1050		21.14	17.80	.02853	12.4	17.0	1.1	66.9	<.1	168 ± 5.3
		FUSE		19.53	79.93	.03358	11.5	64.7	5.1	82.1	<.1	197 ± 6.0
							100.0					

[1] A function of the age of the monitor mineral and of the integrated fast-neutron flux.
[2] Corrected for ^{37}Ar decay; half-life = 35.1 days.
[3] $\lambda_e = 0.581 \times 10^{-10}$ yr^{-1}, $\lambda_\beta = 4.962 \times 10^{-10}$ yr^{-1}. The ± figures are estimated standard deviation of analytical precision at the 68 percent level of confidence.
[4] Conventional K-Ar ages of BBH#1, BBH#3, and BBH#5 are 204 ± 4.1, 162 ± 3.2, and 186 ± 3.7, respectively (Gohn and others, 1978).

BBH#3, which has a δ value of +5.8, is close. BBH#1 has a δ value of +13.6.

$^{40}Ar/^{39}Ar$ incremental heating experiments were done on all three samples of basalt, and the analytical data are presented in table 1. The data are treated in two different ways: (1) as an age-spectrum diagram in which the apparent age of each gas increment is plotted as a function of the cumulative percentage of ^{39}Ar released and (2) as an $^{40}Ar/^{36}Ar$ versus $^{39}Ar/^{36}Ar$ correlation diagram in which the slope of the line (isochron) fitted to the data points indicates the age of the sample and the intercept on the ordinate indicates the composition of nonradiogenic Ar in the sample.

The age of each gas increment (table 1) is calculated by assuming that the nonradiogenic Ar has the composition of atmospheric Ar ($^{40}Ar/^{36}Ar = 295.5$). The interpretation of age spectra is based on shape; in the ideal case of an undisturbed sample, all gas increments will have the same apparent age (Turner, 1968; Dalrymple and Lanphere, 1974). The interpretation of age spectra for disturbed or altered samples is not straightforward, but workers generally agree that, for igneous rocks, a crystallization age may be represented by a plateau, which is a plotted set of adjacent gas increments having the same apparent age and representing a significant proportion of the ^{39}Ar released from the sample.

No assumption about the isotopic composition of nonradiogenic Ar in a sample is made for an isochron diagram. For each gas increment, the $^{40}Ar/^{36}Ar$ ratio is plotted versus the $^{39}Ar/^{36}Ar$ ratio after the ratios have been corrected for interfering Ar isotopes produced during irradiation. In an unaltered and undisturbed sample, all gas increments will form a straight line (isochron) having an $^{40}Ar/^{36}Ar$ intercept of 295.5 and a slope that is proportional to the age of the sample. For disturbed samples, the interpretation may be more complicated because decisions have to be made on which points to include in fitting an isochron. Isochrons are fitted by using the York 2 least-squares cubic fit and correlated errors (York, 1969), and by using the formula recommended by York (quoted in Ozima and others, 1977) for the linear-regression correlation coefficient, r.

To make the interpretation of age spectra and isochrons as objective as possible, Lanphere and Dalrymple (1978) suggested a set of conservative criteria for an acceptable crystallization age. These criteria are:

1. A well-defined plateau in an age-spectrum diagram formed by three or more contiguous gas increments representing at least 50 percent of the ^{39}Ar released.
2. A well-defined isochron for the plateau points having a York 2 fit index [SUMS/(N − 2)][2] of less than 2.5

[2] SUMS/(N − 2) is a goodness-of-fit parameter of a straight line to a set of data; SUMS is the weighted sum of the squares of the residuals, and N is the number of data.

TABLE 2.—*Summary of age-spectrum and isochron data from $^{40}Ar/^{39}Ar$ incremental heating experiments on three basalt samples from CC#2, near Charleston, S. C.*

Sample no.	Depth below surface (meters)	Temperature increments used (°C)	Age spectrum: Weighted mean age (m.y.)	Age spectrum: ^{39}Ar (percent)	Isochron: Age (m.y.)	Isochron: $^{40}Ar/^{36}Ar$ intercept	Isochron: SUMS/(N−2)[1]
BBH#1	818.7	600–900	187±1.3	51.7	192±15.4	−4±330	1445
BBH#3	842.3	700–975	161±3.1	64.4	167± 2.0	281± 28	1.7
BBH#5	907.4	500–900	187±3.1	70.5	184± 3.3	302± 6	1.6
		500–1050	183±2.6	88.5	175± 1.0	309± 14	8.8

[1] See footnote, p. B3.

(Brooks and others, 1972; Dalrymple and Lanphere, 1974).

3. Concordant isochron and plateau ages.
4. An $^{40}Ar/^{36}Ar$ intercept for the isochron that is not significantly different from the atmospheric value of 295.5.

Samples that do not meet these criteria are considered too disturbed or altered to yield reliable crystallization ages. The age-spectrum and isochron data (table 2) show that only one sample from this study, BBH#5, meets the criteria for a reliable crystallization age. The results for each sample are discussed below.

BBH#1 Analyses

The most disturbed of the three samples is BBH#1 (figs. 1, 2). The initial gas increment removed at 500°C has an apparent age of 299 m.y., more than 50 percent older than the succeeding four gas increments. The 600°–900°C gas increments contain about 52 percent of the ^{39}Ar released and define a reasonably good plateau that has a weighted mean age of 187±1.3 m.y.; each datum was weighted by the inverse of its estimated variance. The first 95 percent of the ^{39}Ar released produces an age spectrum (fig. 1) that resembles those for igneous rocks known to contain excess ^{40}Ar (Lanphere and Dalrymple, 1971; Brereton, 1972; Ozima and Saito,

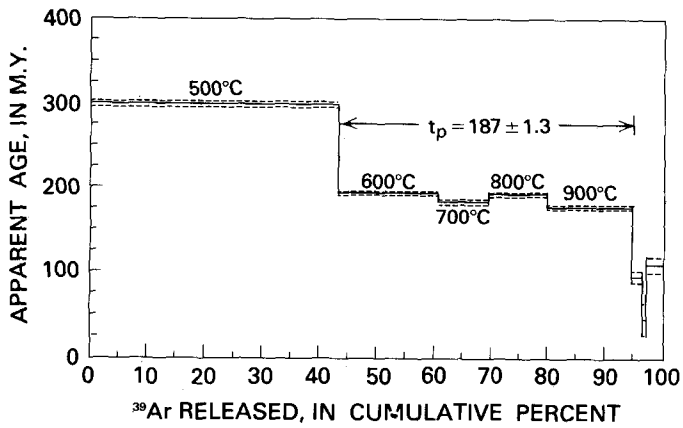

FIGURE 1.—Age-spectrum diagram for $^{40}Ar/^{39}Ar$ incremental heating experiment on BBH#1 basalt. t_p is the weighted mean plateau age.

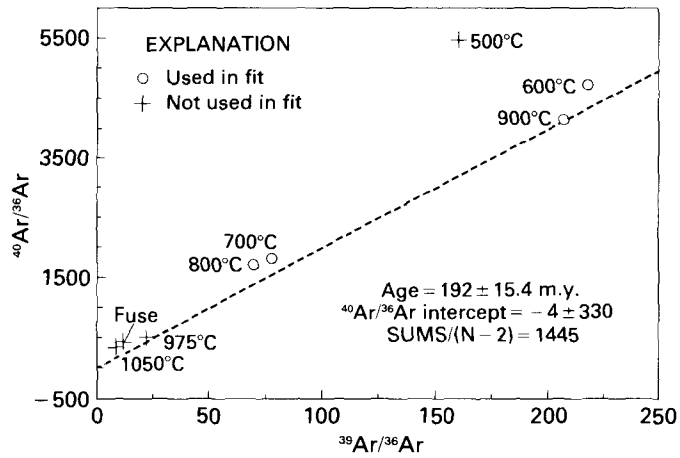

FIGURE 2.—Isochron diagram for $^{40}Ar/^{39}Ar$ incremental heating experiment on BBH#1 basalt.

1973; Kaneoka, 1974; Dalrymple and others, 1975; Lanphere and Dalrymple, 1976). The high-temperature gas increments from BBH#1, however, do not show an increase in age to produce the typical "saddle-shaped" spectrum. Dallmeyer (1975) did not believe that a saddle-shaped spectrum indicates the presence of excess ^{40}Ar; he suggested that for samples containing excess ^{40}Ar, anomalously older apparent ages are found only in the low-temperature fractions.

The isochron diagram for BBH#1 (fig. 2) shows the scatter of data typical of isochron diagrams for samples known to contain excess ^{40}Ar (Brereton, 1972; Dalrymple and others, 1975; Lanphere and Dalrymple, 1976). This scatter is shown very clearly by the large uncertainty in the $^{40}Ar/^{36}Ar$ intercept and the extremely large value of SUMS/(N−2) (table 2). The 192±15.4 m.y. age indicated by an isochron drawn through the points that define the age-spectrum plateau agrees with the plateau age, though the agreement may be fortuitous because the isochron age has a large uncertainty.

BBH#3 Analyses

The 700°–975°C gas increments for BBH#3 contain about 64 percent of the ^{39}Ar released, and the age-spectrum diagram shows a well-defined plateau that has an age of 161±3.1 m.y. (fig. 3). The initial fraction

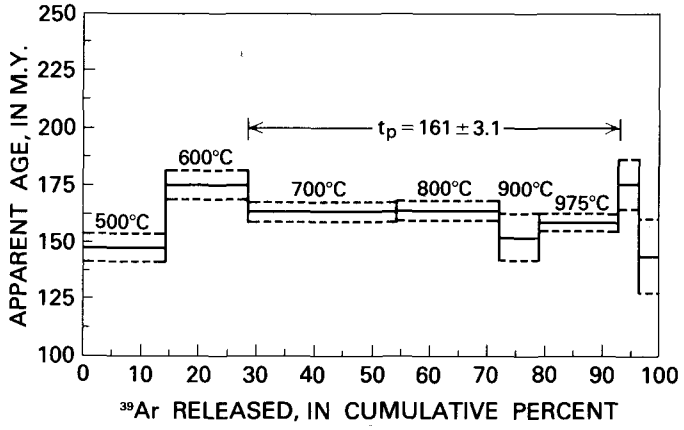

FIGURE 3.—Age-spectrum diagram for $^{40}Ar/^{39}Ar$ incremental heating experiment on BBH#3 basalt. t_p is the weighted mean plateau age.

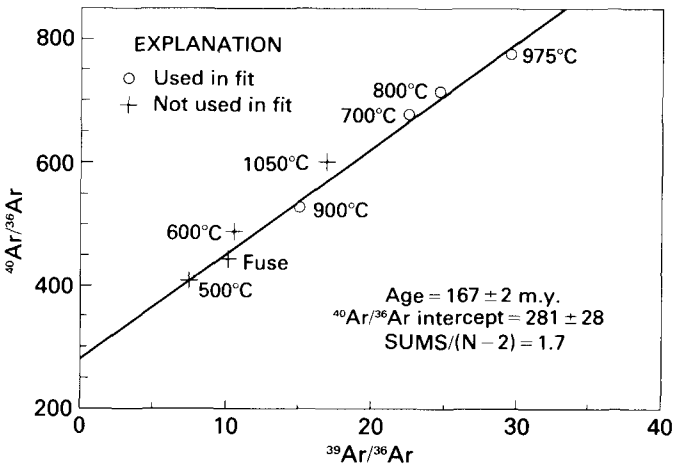

FIGURE 4.—Isochron diagram for $^{40}Ar/^{39}Ar$ incremental heating experiment on BBH#3 basalt.

released at 500°C has an apparent age that is significantly younger than the plateau age. An age spectrum having this shape is characteristic of postcrystallization argon loss (Turner, 1968; Lanphere and Dalrymple, 1971). The isochron age of 167 ± 2.0 m.y. for BBH#3 (fig. 4) differs from the plateau age by slightly more than the analytical uncertainties. The intercept of the isochron (table 2) agrees with the atmospheric $^{40}Ar/^{36}Ar$ ratio but has a large uncertainty. The isochron statistics (table 2) indicate that the fit does not have excessive scatter.

BBH#5 Analyses

The most straightforward age spectrum is that of BBH#5 (fig. 5). The 500°–900°C gas increments contain about 70 percent of the ^{39}Ar released and define a good plateau that has an apparent age of 187 ± 3.1 m.y. If the 500°–1050°C gas increments, which contain about 88 percent of the ^{39}Ar released, are used, the plateau age is 183 ± 2.6 m.y. The isochron (fig. 6) and plateau ages are concordant for the 500°–900°C gas increments, but the two ages are discordant for the 500°–1050°C gas increments (table 2). The fit of the isochron and the precision of the intercept are better for the 500°–900°C gas increments.

DISCUSSION

The objective of this study was to refine the age of basalt in CC#2, and I believe that this objective has been achieved. The incremental heating experiments show that two of the basalt samples are markedly disturbed; the age spectra give evidence for excess ^{40}Ar in one sample and for loss of ^{40}Ar in the other. The 40-m.y. spread in the conventional K-Ar ages, therefore, is not real. The only sample that meets all the given criteria for a reliable crystallization age is BBH#5. The age-spectrum and isochron ages for the gas increments released between 500°C and 900°C are concordant for this sample. If the 975°C and 1050°C increments are included, however, the age-spectrum and isochron ages are discordant. Thus, the 500°–900°C increments yield the best available information on the age of BBH#5. The isochron age of 184 ± 3.3 m.y. is preferred because no assumption needs to be made about the isotopic composition of nonradiogenic argon in the sample. The conventional age of 186 ± 3.7 m.y. and the total-fusion $^{40}Ar/^{39}Ar$ age of 182 ± 2.8 m.y. are concordant with the incremental heating data. Taken collectively, these data indicate that 184 m.y. is a good estimate for the crystallization age of sample BBH#5.

The $^{40}Ar/^{39}Ar$ incremental heating data for sample BBH#3 show that the sample is slightly but definitely disturbed; it meets all the criteria for a reliable crystallization age except concordance of age-spectrum and isochron ages. However, the shape of the age spectrum is typical of postcrystallization argon loss. The isochron age of 167 m.y. for BBH#3 is about 9 percent younger than the preferred age for BBH#5. BBH#3 overlies BBH#5 by 65 m, but there is no way to estimate the time interval between eruption of the two flow units.

Sample BBH#1 clearly is the most disturbed of the three samples of basalt. In the age-spectrum diagram (fig. 1), the low-temperature (500°C) gas increment is significantly older than succeeding fractions. In the high-temperature increments, the age spectrum does not show older apparent ages typical of samples known to contain excess ^{40}Ar. An alternative interpretation for the high apparent age of the 500°C fraction is that it reflects recoil of ^{39}Ar out of the basalt following the $^{39}K(n,p)^{39}Ar$ reaction. Turner and Cadogan (1974) calculated that the recoil energy of ^{39}Ar typically will be

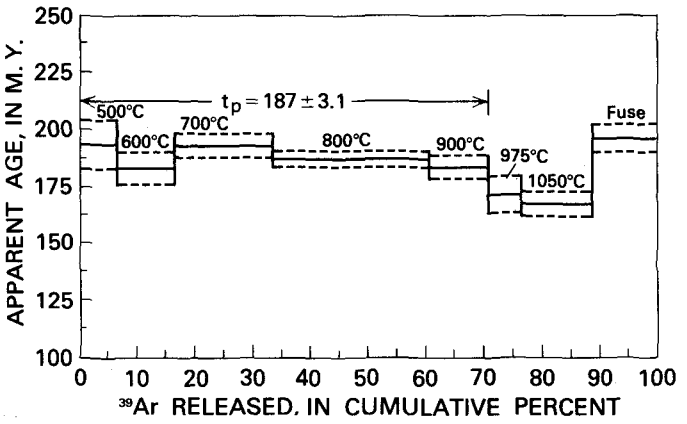

FIGURE 5.—Age-spectrum diagram for $^{40}Ar/^{39}Ar$ incremental heating experiment on BBH#5 basalt. t_p is the weighted mean plateau age.

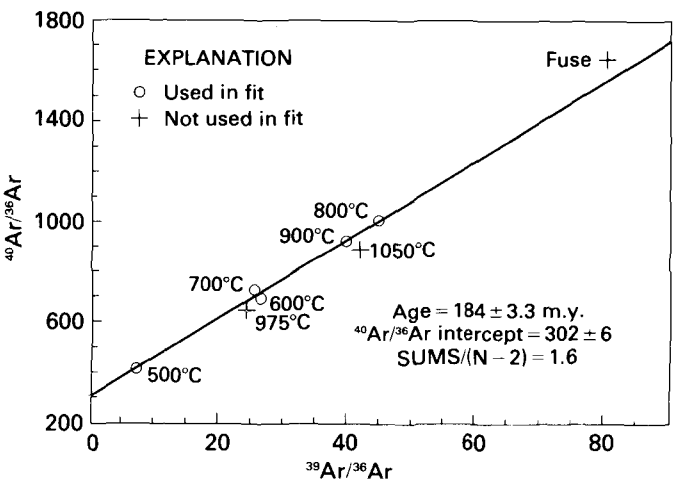

FIGURE 6.—Isochron diagram for $^{40}Ar/^{39}Ar$ incremental heating experiment on BBH#5 basalt.

approximately 200 kiloelectron volts (keV), which would cause a recoil distance of 0.08 μm on the average. This recoil could easily cause loss of K-derived ^{39}Ar from fine-grained alteration products in the basalt. Loss of ^{39}Ar would result in an anomalously high $^{40}Ar/^{39}Ar$ age. Loss of ^{39}Ar by recoil, however, is not a factor in the conventional age determination of BBH#1, 204 ± 4.1 m.y., which is more than 10 percent higher than the preferred age of BBH#5. The latter sample, on the basis of stratigraphy, must be the oldest of the three. Therefore, BBH#1 must contain some excess ^{40}Ar that was loosely bound and removed in the 500°C gas increment (table 1, fig. 5). The 600° – 900°C gas increments of BBH#1 have age-spectrum and isochron ages that agree with those of BBH#5. However, in the absence of the independent data provided by sample BBH#5, a reliable crystallization age cannot be inferred from the analytical data for BBH#1.

The most reliable age for the Clubhouse Crossroads basalt is the preferred age of 184 ± 3.3 m.y. for sample BBH#5. Phillips (1983) estimated an age for the basalt unit as a whole from the paleoinclination of samples from all three drill holes at Clubhouse Crossroads. He compared the paleoinclination with a paleoinclination-versus-time curve produced from the pole positions of Irving (1977). From his paleoinclination data, Phillips suggested that the most probable age of the basalt is 170 m.y; probability that the age is between 110 and 196 m.y. is 95 percent. Given the uncertainty in the paleoinclination-versus-time curve (Phillips, 1983), the agreement in the age inferred from the paleomagnetic data and the K-Ar age measured on BBH#5 is good.

Most workers believe that the basaltic igneous activity in eastern North America and northwestern Africa is related to rifting and separation of the African and North American plates (Dietz and Holden, 1970; Dalrymple and others, 1975). The consensus is that this separation began 180 to 200 m.y. ago. The principal evidence for this conclusion includes the age of the basaltic rocks (Dalrymple and others, 1975; Sutter and Smith, 1979), analysis of the magnetic-anomaly pattern in the North Atlantic Ocean (Pitman and Talwani, 1972; Phillips and Forsyth, 1972; Larson and Pitman, 1972), and extrapolation of the sea-floor spreading rate in the northwestern Atlantic Ocean to the Continental Rise (Geotimes, 1970).

The coincidence of paleomagnetic poles derived from mafic volcanic rocks from eastern North America (Pennsylvania to Nova Scotia) and northwestern Africa (Liberia, Sierra Leone, and Morocco) indicates that the two continents could not have been separated very far before latest Triassic to earliest Jurassic time (Larson and LaFountain, 1970; Dalrymple and others, 1975). Reliable K-Ar ages for diabase dikes in Liberia range from 177 to 196 m.y. (Dalrymple and others, 1975). K-Ar ages of basalt flows and diabase intrusive rocks in eastern North America from Massachusetts to Maryland show considerable scatter, which Armstrong and Besancon (1970) have attributed to potassium inhomogeneity and (or) loss of radiogenic ^{40}Ar during superimposed low-grade metamorphism. For the basalt in the Clubhouse Crossroads drill holes, the alteration appears to be deuteric; no independent evidence exists for a later metamorphic event in the region.

Sutter and Smith (1979) subsequently made $^{40}Ar/^{39}Ar$ incremental heating experiments on diabase intrusive rocks from Connecticut and Maryland. Four of six samples from diabase intrusive rocks in Connecticut and two of four samples from intrusive rocks in Maryland yielded data that meet the criteria outlined for a reliable crystallization age. The four samples from Connecticut have $^{40}Ar/^{36}Ar$ versus $^{39}Ar/^{36}Ar$ isochron ages ranging

from 182 to 192 m.y., and the two samples from Maryland have isochron ages ranging from 186 to 189 m.y.

In conclusion, the most reliable age for the Clubhouse Crossroads basalt is 184 ± 3.3 m.y. This age is in good agreement with the reliable ages of diabase intrusive rocks farther north in eastern North America and in Liberia. All these data are consistent with the initiation of central Atlantic rifting about 190 m.y. ago.

REFERENCES CITED

Armstrong, R. L., and Besancon, James, 1970, A Triassic time scale dilemma–K-Ar dating of Upper Triassic mafic igneous rocks, eastern U.S.A. and Canada and post-Upper Triassic plutons, western Idaho, U.S.A.: Eclogae Geologicae Helvetiae, v. 63, no. 1, p. 15–28.

Brereton, N. R., 1972, A reappraisal of the $^{40}Ar/^{39}Ar$ stepwise degassing technique: Royal Astronomical Society Geophysical Journal, v. 27, no. 5, p. 449–478.

Brooks, C., Hart, S. R., and Wendt, I., 1972, Realistic use of two-error regression treatments as applied to rubidium-strontium data: Reviews of Geophysics and Space Physics, v. 10, no. 2, p. 551–577.

Clague, D. A., Dalrymple, G. B., and Moberly, Ralph, 1975, Petrography and K-Ar ages of dredged volcanic rocks from the western Hawaiian Ridge and the southern Emperor Seamount Chain: Geological Society of America Bulletin, v. 86, no. 7, p. 991–998.

Dallmeyer, R. D., 1975, $^{40}Ar/^{39}Ar$ release spectra of biotite and hornblende from the Cortlandt and Rosetown plutons, New York, and their regional implications: Journal of Geology, v. 83, no. 5, p. 629–643.

Dalrymple, G. B., Alexander, E. C., Jr., Lanphere, M. A., and Kraker, G. P., 1981, Irradiation of samples for $^{40}Ar/^{39}Ar$ dating using the Geological Survey TRIGA reactor: U.S. Geological Survey Professional Paper 1176, 55 p.

Dalrymple, G. B., and Clague, D. A., 1976, Age of the Hawaiian-Emperor Bend: Earth and Planetary Science Letters, v. 31, no. 3, p. 313–329.

Dalrymple, G. B., Grommé, C. S., and White, R. W., 1975, Potassium-argon age and paleomagnetism of diabase dikes in Liberia–Initiation of central Atlantic rifting: Geological Society of America Bulletin, v. 86, no. 3, p. 399–411.

Dalrymple, G. B., and Lanphere, M. A., 1971, $^{40}Ar/^{39}Ar$ technique of K-Ar dating: A comparison with the conventional technique: Earth and Planetary Science Letters, v. 12, no. 3, p. 300–308.

———1974, $^{40}Ar/^{39}Ar$ age spectra of some undisturbed terrestrial samples: Geochimica et Cosmochimica Acta, v. 38, no. 5, p. 715–738.

Dalrymple, G. B., Lanphere, M. A., and Clague, D. A., 1980, Conventional and $^{40}Ar/^{39}Ar$ K-Ar ages of volcanic rocks from Ojin (Site 430), Nintoku (Site 432), and Suiko (Site 433) seamounts and the chronology of volcanic propagation along the Hawaiian-Emperor Chain, *in* California University, Scripps Institution of Oceanography, La Jolla, Initial reports of the Deep Sea Drilling Project, Volume 55: Washington, D. C., National Science Foundation, p. 659–693.

Dietz, R. S., and Holden, J. C., 1970, Reconstruction of Pangaea–Breakup and dispersion of continents, Permian to present: Journal of Geophysical Research, v. 75, no. 26, p. 4939–4956.

Geotimes, 1970, Deep Sea Drilling Project–Leg 12: v. 15, no. 9, p. 14–16.

Gohn, G. S., Gottfried, David, Lanphere, M. A., and Higgins, B. B., 1978, Regional implications of Triassic or Jurassic age for basalt and sedimentary red beds in the South Carolina coastal plain: Science, v. 202, no. 4370, p. 887–890.

Gohn, G. S., Houser, B. B., and Schneider, R. R., 1983, Geology of the lower Mesozoic(?) sedimentary rocks in Clubhouse Crossroads test hole #3, near Charleston, South Carolina, *in* Gohn, G. S., ed., Studies related to the Charleston, South Carolina, earthquake of 1886–Tectonics and seismicity: U.S. Geological Survey Professional Paper 1313, p. D1–D17.

Gottfried, David, Annell, C. S., and Byerly, G. R., 1983, Geochemistry and tectonic significance of subsurface basalts from Charleston, South Carolina–Clubhouse Crossroads test holes #2 and #3, *in* Gohn, G. S., ed., Studies related to the Charleston, South Carolina, earthquake of 1886–Tectonics and seismicity: U.S. Geological Survey Professional Paper 1313, p. A1–A19.

Gottfried, David, Annell, C. S., and Schwarz, L. J., 1977, Geochemistry of subsurface basalt from the deep corehole (Clubhouse Crossroads corehole 1) near Charleston, South Carolina–Magma type and tectonic implications, *in* Rankin, D. W., ed., Studies related to the Charleston, South Carolina, earthquake of 1886–A preliminary report: U.S. Geological Survey Professional Paper 1028, p. 91–113.

Hazel, J. E., Bybell, L. M., Christopher, R. A., Frederiksen, N. O., May, F. E., McLean, D. M., Poore, R. Z., Smith, C. C., Sohl, N. F., Valentine, P. C., and Witmer, R. J., 1977, Biostratigraphy of the deep corehole (Clubhouse Crossroads corehole 1) near Charleston, South Carolina, *in* Rankin, D. W., ed., Studies related to the Charleston, South Carolina, earthquake of 1886–A preliminary report: U.S. Geological Survey Professional Paper 1028, p. 71–89.

Irving, Edward, 1977, Drift of the major continental blocks since the Devonian: Nature, v. 270, no. 5635, p. 304–309.

Kaneoka, Ichiro, 1974, Investigation of excess argon in ultramafic rocks from the Kola Peninsula by the $^{40}Ar/^{39}Ar$ method: Earth and Planetary Science Letters, v. 22, no. 2, p. 145–156.

Lanphere, M. A., and Dalrymple, G. B., 1971, A test of the $^{40}Ar/^{39}Ar$ age spectrum technique on some terrestrial materials: Earth and Planetary Science Letters, v. 12, no. 4, p. 359–372.

———1976, Identification of excess ^{40}Ar by the $^{40}Ar/^{39}Ar$ age spectrum technique: Earth and Planetary Science Letters, v. 32, no. 2, p. 141–148.

———1978, The use of $^{40}Ar/^{39}Ar$ data in evaluation of disturbed K-Ar systems, *in* Zartman, R. E., ed., Short papers of the Fourth International Conference, Geochronology, Cosmochronology, and Isotope Geology: U.S. Geological Survey Open-File Report 78-701, p. 241–243.

Larson, E. E., and LaFountain, L., 1970, Timing of the breakup of the continents around the Atlantic as determined by paleomagnetism: Earth and Planetary Science Letters, v. 8, no. 5, p. 341–351.

Larson, R. L., and Pitman, W. C., III, 1972, World-wide correlation of Mesozoic magnetic anomalies, and its implications: Geological Society of America Bulletin, v. 83, no. 12, p. 3645–3662.

Ozima, Minoru, Honda, Masahiko, and Saito, Kazuo, 1977, $^{40}Ar/^{39}Ar$ ages of guyots in the western Pacific and discussion of their evolution: Royal Astronomical Society Geophysical Journal, v. 51, no. 2, p. 475–485.

Ozima, Minoru, and Saito, Kazuo, 1973, $^{40}Ar/^{39}Ar$ stepwise degassing experiments on some submarine rocks: Earth and Planetary Science Letters, v. 20, no. 1, p. 77–87.

Phillips, J. D., 1983, Paleomagnetic investigations of the Clubhouse Crossroads basalt, *in* Gohn, G. S., ed., Studies related to the Charleston, South Carolina, earthquake of 1886–Tectonics and seismicity: U.S. Geological Survey Professional Paper 1313, p. C1–C18.

Phillips, J. D., and Forsyth, D., 1972, Plate tectonics, paleomagnetism, and the opening of the Atlantic: Geological Society of America Bulletin, v. 83, no. 6, p. 1579–1600.

Pitman, W. C., III, and Talwani, Manik, 1972, Sea-floor spreading in the North Atlantic: Geological Society of America Bulletin, v. 83, no. 3, p. 619–646.

Smith, A. G., Briden, J. C., and Drewry, G. E., 1973, Phanerozoic world maps: Special Papers in Paleontology, no. 12, p. 1–42.

Steiger, R. H., and Jäger, E., 1977, Subcommission of geochronology–Convention on the use of decay constants in geo- and cosmochronology: Earth and Planetary Science Letters, v. 36, no. 3, p. 359–362.

Sutter, J. F., and Smith, T. E., 1979, $^{40}Ar/^{39}Ar$ ages of diabase intrusions from Newark trend basins in Connecticut and Maryland–Initiation of central Atlantic rifting: American Journal of Science, v. 279, no. 7, p. 808–831.

Turner, G., 1968, The distribution of potassium and argon in chondrites, *in* Ahrens, L. H., ed., Origin and distribution of the elements: New York, Pergamon Press, p. 387–398.

Turner, G., and Cadogan, P. H., 1974, Possible effects of ^{39}Ar recoil in $^{40}Ar/^{39}Ar$ dating, *in* Proceeding of the Fifth Lunar Science Conference: Geochimica et Cosmochimica Acta Supplement 5, v. 2, p. 1601–1615.

York, Derek, 1969, Least squares fitting of a straight line with correlated errors: Earth and Planetary Science Letters, v. 5, p. 320–324.

Paleomagnetic Investigations of the Clubhouse Crossroads Basalt

By JEFFREY D. PHILLIPS

STUDIES RELATED TO THE CHARLESTON, SOUTH CAROLINA, EARTHQUAKE OF 1886—TECTONICS AND SEISMICITY

GEOLOGICAL SURVEY PROFESSIONAL PAPER 1313-C

UNITED STATES GOVERNMENT PRINTING OFFICE, WASHINGTON: 1983

CONTENTS

ILLUSTRATIONS

TABLES

STUDIES RELATED TO THE CHARLESTON, SOUTH CAROLINA, EARTHQUAKE OF 1886—TECTONICS AND SEISMICITY

PALEOMAGNETIC INVESTIGATIONS OF THE CLUBHOUSE CROSSROADS BASALT

By JEFFREY D. PHILLIPS

ABSTRACT

Paleomagnetic investigations have been undertaken on partially oriented basalt samples recovered from three USGS (U.S. Geological Survey) deep test holes at Clubhouse Crossroads near Charleston, S. C. The basalt unit lies at the base of the Coastal Plain sedimentary section; it is 256 m thick in test hole #3. It overlies and is partially interbedded with a sedimentary red-bed unit of probable Triassic or Early Jurassic age. On the basis of the paleomagnetic evidence and the geologic descriptions of the cores, 23 flows can be identified. Six of the flows have negative magnetic inclinations, which are interpreted as indicating periods of reversed polarity; one test hole contains a definite sequence of five reversed-polarity intervals separated by four normal-polarity intervals. The mean thermal remanent-magnetization (TRM) inclination for the 23 flows after magnetic cleaning is 35.4±3.2°. Comparison of this value with a paleoinclination curve for the Charleston area reveals that the age of the basalt has a 95-percent chance of being in the range 110–196 m.y. Comparison of the Clubhouse Crossroads basalt with other eastern North American basalts and diabases suggests that the true age is more likely to be in the older part of this range.

INTRODUCTION

Between 1975 and 1977, the U.S. Geological Survey drilled three deep test holes (CC#1, CC#2, and CC#3) near the hamlet of Clubhouse Crossroads, Dorchester County, S. C. (fig. 1) as part of a study of the epicentral area of the 1886 Charleston earthquake. All three penetrated the Coastal Plain sedimentary section, and two of them, CC#1 and CC#2, bottomed in a thick basalt unit underlying the Coastal Plain section. The third test hole, CC#3, penetrated 256 m of basalt and bottomed in a 121-m-thick sedimentary red-bed section of probable Triassic or Early Jurassic age (Gohn and others, 1978).

Paleomagnetic investigations of the basalt were undertaken with two goals in mind. First, flow boundaries within each core were to be detected paleomagnetically, and flows were to be correlated among the three holes. Such a correlation might indicate faults or other tectonic features in the area. Second, the mean inclination of the paleomagnetic samples was to be compared to the paleoinclination curve for the site, as predicted from other North American paleomagnetic studies, in order to estimate the age of the basalts. This would serve as a check on the early Mesozoic radiometric ages obtained for the basalts and aid in the geochronological interpretation of the cores.

Earlier paleomagnetic studies of eastern North American Mesozoic basalts and diabases as summarized by de Boer (1968), Beck (1972), and Smith (1976) have established the following:

1. The igneous rocks associated with eastern North American early Mesozoic basins are all normally magnetized, which suggests that they formed during the Late Triassic–Early Jurassic interval of predominantly normal polarity.
2. Most radiometric ages for eastern North American Mesozoic basalts and diabases fall within the range 180–200 million years (m.y.), which supports a Late Triassic–Early Jurassic age.
3. The position of the magnetic pole relative to North America changed rapidly during the Triassic and Early Jurassic. This permits paleomagnetic studies to be used to determine relative ages of lower Mesozoic units and to correlate these units over large areas.
4. The basalts and diabases associated with eastern North American early Mesozoic basins are of an age similar to that of the associated sedimentary basin-fill materials.

Acknowledgments.—W. E. Huff, Jr., provided laboratory assistance, and S. H. Perlman and D. Gottfried provided geologic descriptions of test holes 2 and 3. Reviewers were D. Watson, R. Reynolds, and R. Simpson. Deep drilling and related investigations by the U.S. Geological Survey in the Charleston, S. C., area are supported by the U.S. Nuclear Regulatory Commission, Office of Nuclear Research, under Agreement No. AT(49-25)-1000.

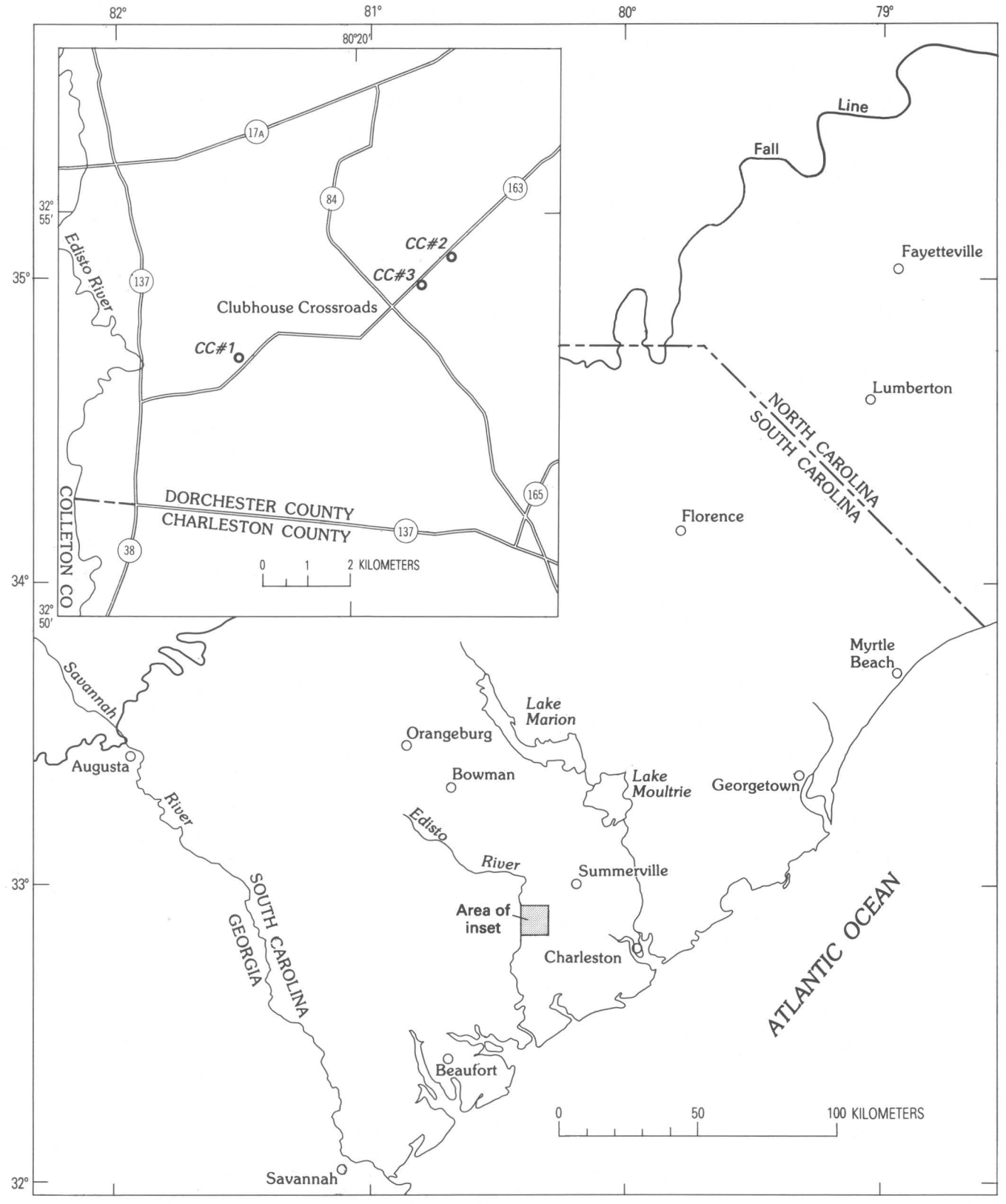

FIGURE 1.–Index map showing the location of the Clubhouse Crossroads test holes CC#1, CC#2, and CC#3, near Charleston, S. C.

TECHNIQUE

A total of 240 m of basalt core was available for study. In CC#1, the basalt was cored continuously from its top at 750 m depth to the bottom of the hole at 792 m, a total of 42 m. In CC#2, the basalt was cored continuously from its top at 776 m to the bottom of the hole at 907 m, a total of 131 m. In CC#3, the basalt was cored in three discontinuous sections. These extended from the top of the basalt at 775 m to 785 m (10 m), from 921 m to 930 m (9 m), and from 983 m to the base of the basalt unit at 1,031 m (48 m). The basalt core is 8 cm in diameter and is fractured into segments 3–50 cm long. Each piece of the core is oriented with respect to the vertical, but there is no azimuthal control.

Samples of the cores were gathered at depths where field descriptions of the cores indicated the possibility of a new flow, and paleomagnetic specimens were prepared. Each sample of core was drilled down its axis with a 2.5-cm-diameter core drill. The resulting 2.5-cm-diameter core was cut into two to four 2.3-cm-long cylindrical specimens. Each specimen was oriented with respect to the vertical, and usually all specimens from a single 2.5-cm-diameter core were assigned the same arbitrary azimuth.

Paleomagnetic directions and intensities of all specimens were measured on high-speed spinner magnetometers (Doell and Cox, 1965), and two magnetic-cleaning techniques were tried (Tarling, 1971, p. 66–69). In a preliminary study, alternating field (af) demagnetization in a two-axis tumbler with peak fields of 30, 60, and 80 mT (millitesla) was attempted on samples from CC#1 and 2. Although samples from CC#1 retained stable magnetization directions throughout the af cleaning process, all samples from CC#2 became unstable as a result of the cleaning. An alternative cleaning method, thermal demagnetization, was therefore tried. CC#1 and 2 were resampled, and the new specimens were cleaned in a magnetically shielded furnace. Thermal demagnetization at a range of temperatures from 100° C to 550° C resulted in greater stability for samples from CC#2 than did af demagnetization. The natural remanent magnetization (NRM) measurements presented here are for samples from both the preliminary and the subsequent studies. However, only the thermally cleaned samples are considered in defining the thermal remanent magnetization (TRM) acquired by the basalts during their initial cooling.

Magnetic stability was assessed on the basis of clustering of paleomagnetic inclinations (Tarling, 1971, p. 85–86). For example, specimen NRM inclinations of a particular sample might cluster loosely. Low-temperature demagnetization might cause the specimen inclinations to diverge somewhat, but at higher temperatures the demagnetization process should bring the inclinations together again. The mean inclination at the demagnetization step that produces the greatest clustering of the specimen inclinations is taken as a measure of the TRM inclination of the sample. An unstable sample is one for which the specimen inclinations fail to converge during the demagnetization process.

THERMOMAGNETIC ANALYSIS

Prior to an extensive program of thermal cleaning and remanence measurement, thermomagnetic curves for several specimens were produced on a Curie balance (Doell and Cox, 1967). These curves helped in designing the thermal cleaning process and in identifying the magnetic minerals present in the samples through their Curie temperatures.

Figure 2 shows thermomagnetic curves (saturation magnetization against temperature) for four different basalt specimens. Curie points and transition temperatures are indicated by inflections in the curves. The heating and cooling were done in air at a slow rate (typically just under 1 hour for an entire heating and cooling cycle) to insure that the sample was always close to thermal equilibrium. A strong magnetic field (~180 mT) was applied to the sample during the entire cycle. The cooling curves do not reproduce the heating curves, which indicates that some of the magnetic minerals were altered during laboratory heating in air. Although the magnetic minerals have not been examined in polished section, we can make inferences about the magnetic mineralogy from the thermomagnetic curves.

The dominant magnetic mineral in fresh basalts is titanomagnetite, a solid-solution-series mineral having a composition intermediate between that of ulvöspinel (Fe_3TiO_4) and that of magnetite (Fe_3O_4). The Curie temperature of titanomagnetite ranges from −153° C for ulvöspinel to 580° C for magnetite (Akimoto and others, 1957). Initial titanomagnetite compositions in basalts must contain more than 50 mole percent ulvöspinel (Carmichael and Nicholls, 1967; Merrill, 1975). However, oxidation can reduce the proportion of ulvöspinel. At high temperatures (250–700° C), such as might exist during the initial cooling of the basalt, titanomagnetite can undergo oxidation to form magnetite and ilmenite ($FeTiO_3$) lamellae. The product will have a Curie temperature between 500° C and 580° C and a strong TRM recording the local direction of the earth's magnetic field at the time of cooling (Grommé and others, 1969).

The specimens used to produce the curves in figures 2*B*, *C*, and *D* have Curie points at around 580° C, suggesting that the magnetic remanence in these specimens is carried by nearly pure magnetite. This is most likely

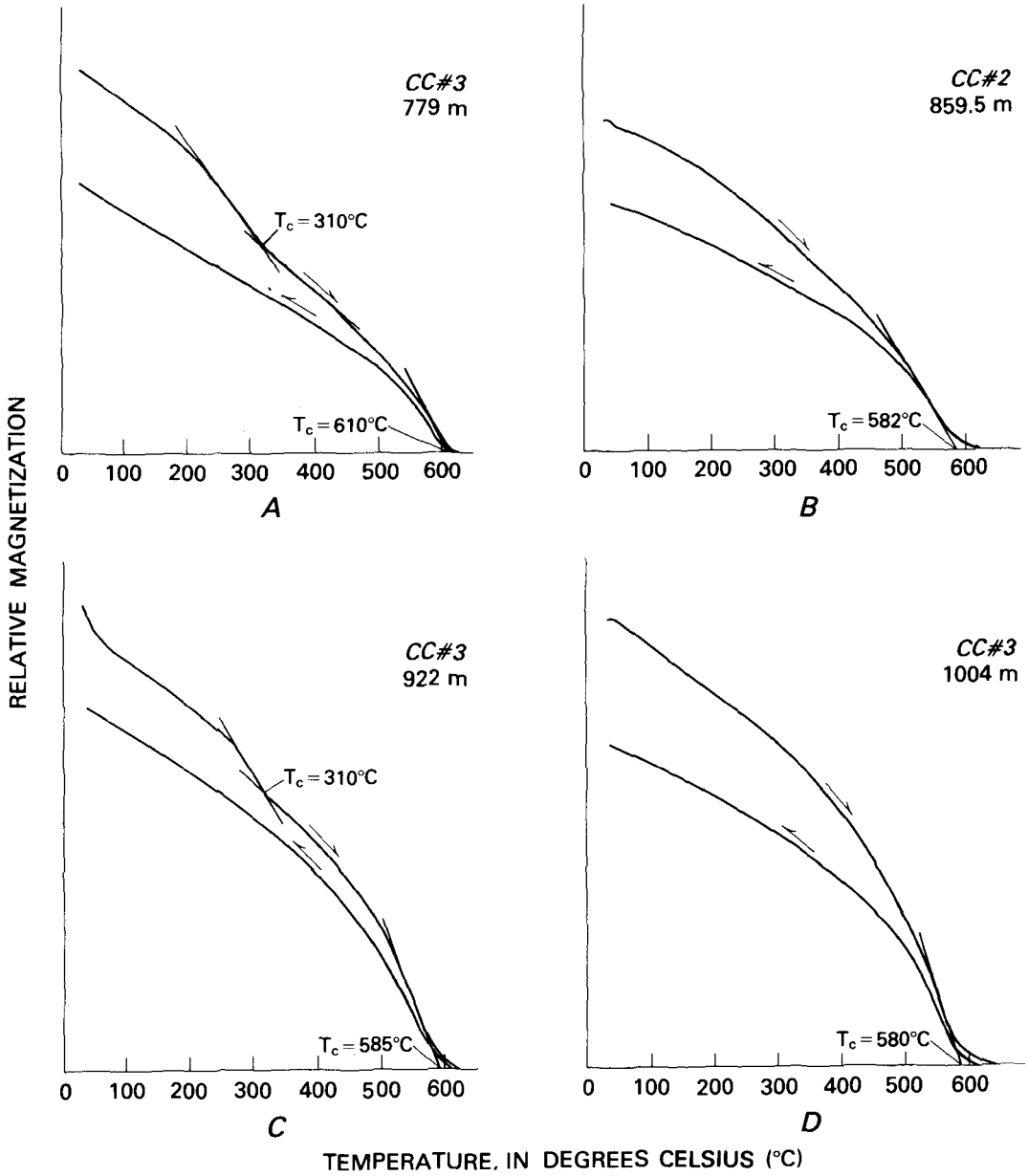

FIGURE 2.—Thermomagnetic curves for four basalt specimens from CC#2 (859.5 m depth) and CC#3 (779, 922, and 1,004 m depth). Curie points (T_c) estimated from the intersections of tangent lines with one another are indicated. Arrows on curves indicate which is the heating curve and which is the cooling curve.

the primary magnetic mineral produced during the initial cooling of the Clubhouse Crossroads basalt. It should be a reliable recorder of the paleomagnetic field directions at the time of cooling.

Magnetite can also form at times other than during the initial cooling of a basalt. For example, it can form through high-temperature oxidation of titanomagnetite during a reheating event, such as the emplacement of a nearby intrusion. In this case the basalt would tend to be uniformly remagnetized in the direction of the earth's field at the time of reheating. As will be seen later, the TRM directions of the Clubhouse Crossroads basalts are far from uniform. Thus a reheating event is an unlikely explanation for the 580° C Curie temperatures.

At low temperatures (50–135° C) and under oxidizing conditions, an original titanomagnetite in a basalt will oxidize to the metastable iron oxide titanomaghemite. At slightly higher temperatures (135° C to the Curie point of the titanomagnetite), this oxidation is accompanied by unmixing of the titanomaghemite into mag-

netite, hematite-ilmenite, and rutile (Johnson and Merrill, 1973). Magnetite formed in this way will contain a strong chemical remanent magnetization (CRM), which could easily be mistaken for a stable TRM.

Although it is difficult to rule out CRM entirely as a source of the stable remanence in the Clubhouse Crossroads basalts, two factors suggest that most of the stable remanence is TRM. First, the present temperature near the top of the basalt is about 40° C (Sass and Ziagos, 1977). Barring much deeper burial, much higher radiogenic heating, or a local reheating event, it is unlikely that the Clubhouse Crossroads basalt has experienced temperatures in excess of 135° C since its initial cooling. Second, there is no evidence in the thermomagnetic curves for the presence of residual titanomagnetite or titanomaghemite. If titanomaghemite were present in the samples, the cooling curves would probably lie above the heating curves (Ozima and Larson, 1970), whereas just the opposite behavior is observed in figure 2.

The curves of figures 2*A* and *C* contain inflections near 310° C. These inflections probably result from the decomposition of maghemite into hematite. Maghemite (γFe_2O_3) is a low-temperature (50–250° C) oxidation product of magnetite (Johnson and Merrill, 1972; Stacey and Banerjee, 1974, p. 30). Depending upon the grain size of the magnetite, the chemical remanence acquired during maghemitization can be parallel either to the original TRM or to the ambient field at the time of oxidation (Johnson and Merrill, 1972, 1974). Fortunately, in most cases, thermal cleaning in a field-free space at temperatures above 350° C can be used to reduce the effect of the CRM and to recover the original TRM directions. Thus the presence of maghemite partially explains the need for thermal cleaning of the samples.

The presence of a third magnetic mineral is indicated in the thermomagnetic curve of figure 2*A*. The Curie point of 610° C is too high for magnetite; most likely it is due to an ilmeno-hematite of composition $Fe_{1.92}Ti_{0.08}O_3$ (Stacey and Banerjee, 1974, p. 37). The presence of titanium suggests that the ilmeno-hematite, like the magnetite, is a primary magnetic mineral. [If the titanium were absent, the resulting hematite could be explained as a byproduct of maghemitization (Johnson and Merrill, 1972).] At this composition, the ilmeno-hematite should be weakly magnetic and may be a carrier of primary remanence.

It should be noted that minerals of the hematite-ilmenite solid-solution series are the best documented self-reversing minerals (Stacey and Banerjee, 1974, p. 166). Thus the presence of ilmeno-hematite in one sample of the Clubhouse Crossroads basalt raises the remote possibility of stable self-reversals. However, at this particular composition, ilmeno-hematite is not known to self-reverse, and in general self-reversals are rarely observed in subaerial basalts (Merrill, 1975).

Thermomagnetic analysis has indicated that three magnetic minerals are present in the Clubhouse Crossroads basalts. Magnetite is probably the carrier of primary remanence. Maghemite is present as a low-temperature oxidation product of the magnetite. Ilmeno-hematite, perhaps rarely present, is another probable carrier of primary remanence. The magnetic mineralogy is consistent with the hypothesis of a subaerial basalt that cooled in a highly oxidizing environment and has not been reheated above 135° C since its initial cooling.

The thermomagnetic curves were considered in the design of the thermal demagnetization experiment. Owing to the apparent range of magnetic minerals present in the samples, cleaning at a single temperature or within a small range of temperatures was deemed inappropriate. Thorough cleaning in small temperature steps, although desirable, was impractical because of the large number of samples. Therefore a procedure was chosen in which large temperature steps were used in cleaning all samples. In addition to the NRM measurements, measurements were taken after heating in air and in zero magnetic field to 100 or 150° C, 300° C, 500°, and 550° C. At low temperatures the samples were heated rapidly and allowed to equilibrate at the desired temperature for 10 minutes prior to cooling and measurement. At higher temperatures, the heating rate was slowed to prevent the samples from exploding from expansion of trapped moisture. Despite these precautions, some samples were destroyed during heating.

MEASUREMENTS

The complete set of paleomagnetic measurements is presented in table 1. Because the azimuth of each specimen is arbitrary, the declinations in this table are unrelated to geomagnetic field directions. Only the changes in declination seen during demagnetization may have some significance. Although every precaution was taken to ensure that the specimens were correctly oriented with respect to the vertical, inconsistencies in the table suggest that one specimen at 858.3 m depth in CC#2 was inverted. In the following analysis the signs of the inclinations have been changed for this specimen. In addition to measurements made on basalt specimens, table 1 contains measurements made on red-bed specimens from two depths near the bottom of CC#3.

During the course of the study, the density and magnetic susceptibility of 60 randomly selected specimens were measured. These results (table 2) are useful for estimating the contribution of the basalt to the gravity and magnetic fields at the ground surface (Daniels and others, 1983).

TABLE 1.—*Paleomagnetic measurements—natural remanent magnetization (NRM) and remanent magnetization after thermal cleaning at various temperatures*

[Inc, inclination; Dec, declination; J, intensity (in ampere/meter). Each sample contained several specimens]

Depth of sample below surface (meters)	NRM			150°C			300°C			500°C			550°C		
	Inc	Dec	J	Inc	Dec	J	Inc	Dec	J	Inc	Dec	J	Inc	Dec	J
CC#1															
756.5	54.2	318.6	3.19×10^{-1}												
760.5	41.1	23.7	1.36												
	42.2	16.0	1.05												
762.9	34.9	355.0	1.82												
	39.3	359.0	1.57	36.3	358.8	1.49	36.7	356.8	1.35	36.0	356.1	9.85×10^{-1}			
	50.2	94.3	6.50×10^{-1}	39.4	92.3	6.97×10^{-1}	38.4	90.4	7.03×10^{-1}						
766.9	48.7	188.9	6.50×10^{-1}												
	49.1	124.2	2.31×10^{-1}	49.1	118.3	1.79×10^{-1}	48.0	115.7	1.78×10^{-1}	47.8	118.4	1.63×10^{-1}			
	37.7	110.8	1.75×10^{-1}	37.0	122.3	1.55×10^{-1}	35.8	123.8	1.70×10^{-1}	38.8	124.7	1.59×10^{-1}			
770.2	39.9	156.3	1.02												
	42.3	144.9	9.22×10^{-1}	38.3	147.0	8.71×10^{-1}	36.2	147.8	8.70×10^{-1}						
772.4	41.8	339.7	4.24												
	40.6	344.4	4.07	36.3	340.7	3.99	35.7	345.1	3.51	36.3	342.5	2.58			
780.0	37.2	268.5	8.33												
	37.8	304.8	7.69	35.7	305.2	7.23	35.5	302.6	7.22	34.4	310.5	5.07			
	68.5	105.9	1.78×10^{-1}	67.1	86.0	1.16×10^{-1}	71.2	74.5	1.29×10^{-1}	49.3	82.4	1.06×10^{-1}			
787.3	49.8	327.1	6.80×10^{-1}												
	60.1	18.4	1.13×10^{-1}	34.6	9.5	5.97×10^{-2}	31.0	350.2	4.42×10^{-2}	29.7	331.7	3.52×10^{-2}			
789.4	36.1	146.3	2.82												
	36.8	149.5	3.02	35.0	149.2	2.94	33.7	144.4	2.85	33.4	145.0	1.87			
790.7	58.5	102.8	1.02												
	56.5	91.7	1.33	48.1	90.2	9.29×10^{-1}	40.7	85.0	8.39×10^{-1}	38.4	89.3	5.09×10^{-1}			
CC#2															
776.0	−32.4	300.6	9.64×10^{-1}	−42.4	296.0	9.00×10^{-1}	−45.8	292.3	6.37×10^{-1}	−48.7	291.1	3.33×10^{-1}	−47.1	300.8	2.58×10^{-1}
	−15.0	281.4	1.38	−22.4	284.2	1.28	−27.3	284.4	6.42×10^{-1}	−31.3	288.6	2.56×10^{-1}	−23.5	292.4	1.83×10^{-1}
	−18.4	284.1	1.10	6.0	242.5	5.17×10^{-1}	−13.2	266.5	2.55×10^{-1}	−16.1	274.2	8.95×10^{-2}	−38.0	285.1	6.36×10^{-2}
777.8	28.6	288.1	1.60×10^{-1}	–	–	–	23.3	280.8	1.12×10^{-1}	46.7	308.0	3.58×10^{-2}	31.3	316.0	3.07×10^{-2}
	30.9	321.3	2.29×10^{-1}	–	–	–	26.5	291.3	1.13×10^{-1}	51.5	300.5	3.97×10^{-2}	23.7	300.4	3.25×10^{-2}
	−19.7	324.8	2.41×10^{-1}	–	–	–	−15.7	321.0	1.72×10^{-1}	−16.9	333.0	5.39×10^{-2}	−31.2	319.8	2.82×10^{-2}
	2.1	305.6	3.14×10^{-1}	–	–	–	−14.8	322.3	1.76×10^{-1}	−18.2	338.4	6.95×10^{-2}	− 9.0	343.1	3.46×10^{-2}
	77.6	159.4	2.01×10^{-1}												
778.2	15.2	185.2	1.05×10^{-1}	−10.4	166.9	1.68×10^{-1}	−21.5	160.9	1.52×10^{-1}	−26.3	158.9	7.51×10^{-2}			
	56.2	185.7	1.61×10^{-1}	23.3	192.4	1.02×10^{-1}	1.6	198.4	7.25×10^{-2}	−13.0	203.7	3.56×10^{-2}			
	70.3	189.5	8.06×10^{-2}	44.2	180.0	4.48×10^{-2}	25.6	184.2	2.18×10^{-2}	24.7	182.1	8.70×10^{-3}			
779.1	5.9	275.9	2.62×10^{-1}	−11.6	284.7	1.38×10^{-1}	11.9	307.0	5.67×10^{-2}	14.1	320.4	2.76×10^{-2}			
	3.5	253.4	2.19×10^{-1}	− 6.0	290.3	8.14×10^{-2}	37.2	315.6	4.92×10^{-2}	36.6	324.7	2.49×10^{-2}			
	49.1	344.2	4.25×10^{-1}	24.2	9.3	2.37×10^{-1}	31.0	15.3	1.19×10^{-1}	28.2	18.6	5.20×10^{-2}			
779.7	21.3	27.3	7.36×10^{-1}												
	20.0	42.8	7.96×10^{-1}												
	20.9	71.0	7.85×10^{-1}												
782.1	19.6	168.6	7.66×10^{-1}												
	44.5	174.5	8.03×10^{-1}												
	44.1	204.7	9.51×10^{-1}												
783.3	−13.4	113.3	6.95×10^{-3}	−30.4	115.7	6.09×10^{-3}	−46.9	116.2	5.04×10^{-3}	−56.6	114.5	3.03×10^{-3}	−53.9	127.7	3.25×10^{-3}
	9.0	99.1	4.58×10^{-3}	−11.4	104.8	3.39×10^{-3}	−25.4	108.6	2.38×10^{-3}	−42.3	108.7	1.06×10^{-3}	−38.5	103.7	1.23×10^{-3}
	16.2	89.1	6.23×10^{-3}	− 9.9	94.4	4.14×10^{-3}	−25.3	96.5	2.97×10^{-3}	−61.6	92.3	1.69×10^{-3}	−53.8	110.5	2.58×10^{-3}
785.1	50.2	94.4	2.73×10^{-3}	5.8	127.7	1.76×10^{-3}	−18.3	133.0	1.41×10^{-3}	−46.5	143.7	1.25×10^{-3}			
	−80.8	124.4	1.83×10^{-3}	−30.0	141.1	4.11×10^{-3}	−37.4	145.3	4.10×10^{-3}	−48.4	144.1	3.58×10^{-3}			
	−54.9	82.0	5.57×10^{-3}	−29.3	93.1	3.74×10^{-3}	−43.6	97.0	3.64×10^{-3}	−56.4	100.2	2.20×10^{-3}			
785.5	5.7	71.3	4.70×10^{-1}												
	66.8	249.5	4.70×10^{-1}												
	40.8	265.4	6.60×10^{-1}												
786.3	55.8	117.0	4.37×10^{-3}	49.4	103.5	1.76×10^{-3}	23.3	46.8	4.40×10^{-4}	−43.4	67.7	3.89×10^{-4}			
	57.2	115.6	2.28×10^{-3}	45.3	108.4	1.00×10^{-3}	36.5	99.5	4.05×10^{-4}	−38.0	88.4	2.39×10^{-4}			
	44.0	114.6	3.28×10^{-3}	24.6	100.1	1.40×10^{-3}	12.7	96.3	7.13×10^{-4}	−44.4	42.8	6.09×10^{-4}			
789.4	− 3.7	131.7	2.14×10^{-2}	−29.6	128.6	1.76×10^{-2}	−44.5	129.7	1.64×10^{-2}	−48.8	128.6	1.27×10^{-2}			
	17.1	116.1	1.07×10^{-1}	3.0	123.3	5.93×10^{-2}	−26.4	133.5	5.06×10^{-2}	−42.7	129.4	3.81×10^{-2}			
	34.3	131.7	5.23×10^{-2}	1.6	138.8	4.21×10^{-2}	−15.5	136.5	3.14×10^{-2}	−27.4	131.9	2.08×10^{-2}			
	15.8	114.0	2.62×10^{-3}												
	15.8	117.7	1.97×10^{-3}												
790.7	47.6	117.3	3.98×10^{-1}												
	67.7	171.9	4.62×10^{-1}												
	71.6	200.7	6.04×10^{-1}												
	62.3	168.0	7.61×10^{-1}												
794.3	−21.1	85.6	1.63												
	−20.4	106.2	8.74×10^{-1}												
	−13.4	122.8	7.02×10^{-1}												
	37.5	82.3	5.44×10^{-1}												

TABLE 1.—*Paleomagnetic measurements—natural remanent magnetization (NRM) and remanent magnetization after thermal cleaning at various temperatures*—Continued

[Inc, inclination; Dec, declination; J, intensity (in ampere/meter). Each sample contained several specimens]

Depth of sample below surface (meters)	NRM			150°C			300°C			500°C			550°C		
	Inc	Dec	J	Inc	Dec	J	Inc	Dec	J	Inc	Dec	J	Inc	Dec	J
CC#2—Continued															
795.5	−32.9	213.8	1.69	−43.5	209.3	1.81	−47.5	207.3	1.52	−46.1	207.6	1.03			
	−41.2	10.0	2.69	−47.3	6.3	2.70	−49.9	4.0	2.19	−51.8	5.2	1.54			
	−30.7	210.8	1.68	−42.6	208.3	1.74	−46.7	205.9	1.36	−44.8	206.6	9.22×10^{-1}			
798.0	−45.0	297.0	2.03	−48.3	300.2	2.42									
	−46.9	294.9	2.56	−49.4	296.8	2.63	−51.3	301.1	2.27	−51.2	302.4	1.52			
	−42.7	27.5	2.39	−47.0	30.2	2.50	−49.9	34.0	2.25	−50.0	33.8	1.65			
801.0	−21.0	96.2	2.04												
	− 1.8	114.5	1.22												
	7.1	122.1	1.04												
	24.7	126.2	9.73×10^{-1}												
801.6	37.7	68.4	9.88×10^{-1}	15.8	56.3	7.69×10^{-1}	3.8	52.9	6.75×10^{-1}	4.2	53.2	4.22×10^{-1}			
	14.3	75.6	1.30	− 0.5	65.3	1.10	− 4.9	61.9	8.59×10^{-1}	− 4.4	59.5	5.59×10^{-1}			
	26.1	51.9	1.10	3.5	48.1	9.42×10^{-1}	− 8.9	56.3	6.55×10^{-1}	− 8.9	55.1	4.17×10^{-1}			
802.5	−40.9	35.7	1.83												
	−53.5	24.4	8.87×10^{-1}												
	−37.5	113.0	8.85×10^{-1}												
	30.6	293.6	5.58×10^{-1}												
	−16.9	323.2	9.83×10^{-1}												
802.8	−22.7	63.3	1.53	−32.2	60.6	1.62	–	–	–	−41.8	299.5	6.56×10^{-1}			
	−28.5	64.1	1.57	−36.4	65.0	1.65	−41.6	64.4	1.52	−39.7	61.1	8.46×10^{-1}			
	−43.3	138.6	1.94	−47.7	137.1	2.01	−49.9	137.1	1.97	−51.0	137.1	1.16			
804.6	− 6.7	318.5	9.84×10^{-1}	−26.5	317.6	9.54×10^{-1}	−38.8	317.6	8.16×10^{-1}	−42.2	318.4	4.68×10^{-1}			
	− 6.1	144.0	8.77×10^{-1}	−26.8	149.6	8.23×10^{-1}	−38.0	155.7	6.98×10^{-1}	−39.9	156.2	4.06×10^{-1}			
	− 5.3	301.2	1.50	−24.5	308.4	1.14	−35.3	310.1	8.44×10^{-1}	−36.7	310.5	5.54×10^{-1}			
808.9	4.6	111.8	1.15	− 9.4	96.0	6.67×10^{-1}									
	− 6.3	122.1	1.66	−15.2	114.1	7.88×10^{-1}	−23.2	98.1	4.09×10^{-1}	−26.7	85.1	2.34×10^{-1}			
	− 4.0	36.5	1.58	−18.0	22.6	8.96×10^{-1}	−26.6	10.0	5.22×10^{-1}	−30.1	1.4	3.18×10^{-1}			
[1]813.8	−43.9	154.5	2.29	−43.0	153.4	3.24	−49.3	160.2	2.29	−48.1	163.5	1.15	−49.1	163.5	9.73×10^{-1}
	−46.1	165.1	2.98	−51.9	158.7	3.05	−51.9	168.1	2.33	−52.5	168.7	1.38	−53.0	169.1	1.17
	−38.4	161.9	2.18	−36.6	160.5	2.23	−47.7	166.3	1.27	−49.7	168.4	7.00×10^{-1}	−50.8	168.6	5.98×10^{-1}
	−38.1	156.0	2.55	−39.9	153.2	2.61	−46.7	157.9	1.81	−43.4	161.2	9.25×10^{-1}	−44.1	160.2	7.79×10^{-1}
814.4	29.6	196.8	3.72×10^{-1}												
	49.7	263.1	2.95×10^{-1}												
	21.3	210.7	6.73×10^{-1}												
	36.5	203.4	1.36												
819.0	9.3	139.8	1.09												
	21.9	171.7	1.06												
	32.1	193.5	6.83×10^{-1}												
	39.0	192.3	1.11												
	48.7	48.9	6.64×10^{-1}												
	42.1	283.6	6.60×10^{-1}												
[1]819.3	32.6	18.5	1.53	32.9	26.6	1.29	17.8	30.2	6.66×10^{-1}						
	40.2	1.4	1.18	43.1	16.7	1.00	22.8	26.5	5.95×10^{-1}	19.4	27.4	2.75×10^{-1}	39.7	14.0	1.30×10^{-1}
	34.9	23.0	1.76	33.2	21.6	1.44	20.7	27.6	7.54×10^{-1}						
823.0	45.5	73.6	2.03	38.9	284.0	2.09	36.1	286.5	1.64	35.1	289.2	3.90×10^{-1}			
	22.5	222.4	2.15	17.9	234.8	2.13	14.7	226.0	1.74	19.2	231.9	2.44×10^{-1}			
	27.4	230.5	2.69	18.7	235.5	2.67	18.0	226.8	1.87	16.8	234.9	2.13×10^{-1}			
	− 4.1	84.7	2.56												
	− 3.4	83.1	3.64												
	− 2.7	98.2	3.68												
[1]825.7	− 9.8	242.1	6.00	−10.3	245.1	5.41	−13.5	244.9	4.52	31.9	240.8	1.67×10^{-1}	− 8.3	132.4	4.64×10^{-2}
	−11.1	239.0	4.81	− 8.9	245.1	5.19	−11.2	244.2	4.46	75.9	130.8	1.03×10^{-1}	− 3.4	72.0	8.92×10^{-2}
	−12.2	284.4	5.54	−14.7	280.2	5.59	−17.3	281.8	4.88	30.2	54.6	1.43×10^{-1}	−10.2	256.4	7.47×10^{-2}
	−10.8	280.0	3.59	−13.1	282.7	5.45	−15.4	282.2	4.64	8.9	66.7	1.79×10^{-1}	24.1	241.7	9.13×10^{-2}
828.8	− 1.7	235.1	4.90												
	2.4	243.8	4.62												
	− 3.9	146.3	4.61												
835.8	− 6.1	139.9	6.25	− 7.0	141.9	5.94	− 6.2	140.2	4.71	2.1	144.8	3.31×10^{-2}			
	− 9.8	138.8	5.23	−10.1	140.0	4.96	− 9.1	141.1	4.23	−23.0	188.7	3.60×10^{-2}			
	2.1	298.7	5.47	− 2.9	296.6	5.27	− 3.8	296.3	4.51	−12.7	221.3	4.31×10^{-2}			
838.8	−39.1	103.2	3.97	−41.2	106.1	4.07	−42.3	107.1	3.78	−65.5	94.9	2.40×10^{-1}			
	−41.0	108.8	3.92	−43.1	111.4	4.02	−43.7	111.8	3.70	−68.6	92.4	1.60×10^{-1}			
	−42.7	326.4	4.32	−44.6	327.4	4.42	−46.0	324.7	3.86	−66.3	346.3	1.36×10^{-1}			
840.9	0.2	170.7	4.90												
	− 2.5	170.1	4.70												
	−10.2	172.9	4.68												
	−19.8	177.9	4.46												
842.8	25.1	280.6	4.49												
	30.6	277.1	4.14												
	28.2	276.2	4.10												

TABLE 1.—*Paleomagnetic measurements—natural remanent magnetization (NRM) and remanent magnetization after thermal cleaning at various temperatures*—Continued

[Inc, inclination; Dec, declination; J, intensity (in ampere/meter). Each sample contained several specimens]

Depth of sample below surface (meters)	NRM			150°C			300°C			500°C			550°C		
	Inc	Dec	J	Inc	Dec	J	Inc	Dec	J	Inc	Dec	J	Inc	Dec	J
CC#2—Continued															
846.7	39.0	44.7	2.51	32.8	41.4	1.85	27.8	36.3	9.83×10^{-1}	23.2	36.7	2.94×10^{-1}	19.8	44.9	4.10×10^{-2}
	45.5	23.2	2.40	38.4	27.2	1.70	33.1	26.6	1.07	28.3	31.6	2.08×10^{-1}	19.7	40.9	2.25×10^{-2}
	45.3	304.1	1.78	38.3	315.2	1.53	32.2	319.3	1.10	23.8	336.2	1.17×10^{-1}	19.1	284.7	9.30×10^{-3}
853.7	34.9	9.0	1.76												
	35.4	1.2	1.94												
	32.8	343.2	1.62												
	49.9	308.9	2.15	41.0	311.2	1.51	31.7	315.3	1.01	27.3	320.7	2.74×10^{-1}	- 3.8	320.4	2.13×10^{-2}
	67.1	323.2	1.53	50.6	320.4	1.10	36.1	317.6	7.65×10^{-1}	30.3	320.9	2.00×10^{-1}	-74.7	250.6	1.17×10^{-2}
	57.8	263.3	1.95	45.5	264.6	1.42	29.6	262.5	7.72×10^{-1}	25.8	263.5	2.41×10^{-1}	-73.6	339.3	1.46×10^{-2}
858.3	11.5	298.0	1.28												
	20.2	267.8	1.69												
	18.5	245.2	2.58												
	[2]-15.4	23.6	1.87	-20.4	27.1	1.81	-26.7	26.8	1.44	-28.3	26.3	4.71×10^{-1}			
[1]859.5	55.0	116.3	2.10	48.5	123.5	2.10	42.8	146.8	1.08	25.9	132.5	2.97×10^{-1}	50.0	128.7	7.06×10^{-2}
	49.4	108.1	2.29	43.6	115.4	2.16	31.9	122.8	1.33	25.4	125.2	3.42×10^{-1}	27.2	99.9	9.37×10^{-2}
	39.7	352.0	2.16	43.2	350.5	1.95	29.3	352.6	1.10	23.0	356.2	2.60×10^{-1}	16.1	46.6	7.33×10^{-2}
	44.2	352.8	2.52	42.2	355.6	1.89	29.9	355.4	1.21	20.2	352.3	1.82×10^{-1}	41.5	48.0	3.44×10^{-2}
863.8	79.2	91.1	9.05×10^{-1}												
	63.6	31.4	9.90×10^{-1}												
	62.0	4.8	8.69×10^{-1}												
	68.2	304.9	1.03												
	-56.7	217.1	1.46×10^{-1}	-43.4	188.1	2.59×10^{-2}	-17.0	242.3	2.70×10^{-2}	50.4	93.8	7.62×10^{-2}			
	-60.5	178.2	1.42×10^{-1}	- 0.7	210.8	7.23×10^{-2}	4.1	220.2	8.13×10^{-2}	56.4	176.6	5.85×10^{-2}			
	-76.0	104.5	1.03	81.1	223.0	8.07×10^{-1}	67.7	166.5	4.34×10^{-1}	53.3	144.9	2.26×10^{-1}			
	72.6	150.6	7.12×10^{-1}	72.7	177.9	8.03×10^{-1}	57.7	150.4	5.07×10^{-1}	49.5	148.6	2.83×10^{-1}			
869.0	71.6	42.8	5.71×10^{-1}												
	51.8	10.6	6.47×10^{-1}												
	48.9	8.0	5.30×10^{-1}												
[1]869.3	59.9	15.0	7.03×10^{-1}	64.4	359.8	6.44×10^{-1}	38.3	345.0	2.79×10^{-1}	17.5	339.4	1.08×10^{-1}	17.8	322.1	6.08×10^{-2}
	58.9	359.7	7.19×10^{-1}	60.3	358.8	6.39×10^{-1}	34.9	344.7	2.93×10^{-1}	11.9	347.7	1.26×10^{-1}	9.5	344.4	6.93×10^{-2}
	38.0	357.9	7.74×10^{-1}	–	–	–	37.9	21.5	3.38×10^{-1}	23.0	29.6	1.57×10^{-1}	23.7	31.8	1.13×10^{-1}
	36.3	3.0	7.87×10^{-1}	45.3	3.9	5.81×10^{-1}	32.2	19.6	3.39×10^{-1}	25.6	35.3	1.14×10^{-1}	10.5	29.4	8.48×10^{-2}
870.5	-59.9	337.6	2.48×10^{-1}												
	38.1	282.8	4.21×10^{-1}												
	48.9	8.0	5.30×10^{-1}												
[1]873.3	50.3	235.6	1.55×10^{-2}	29.3	238.7	2.00×10^{-2}	17.2	238.9	1.13×10^{-2}	9.0	238.0	2.86×10^{-3}	12.7	232.2	2.12×10^{-3}
	36.5	245.2	2.59×10^{-2}	–	–	–	10.6	249.1	1.25×10^{-2}	14.1	241.7	3.17×10^{-3}	-18.5	242.0	2.90×10^{-3}
	–	–	–	22.4	241.4	2.16×10^{-2}	7.6	239.9	1.33×10^{-2}	-15.7	245.5	2.79×10^{-3}	-25.9	83.6	1.03×10^{-3}
878.1	-20.9	19.8	3.22×10^{-1}												
	42.2	344.9	3.46×10^{-1}												
	53.7	46.9	4.31×10^{-1}												
883.9	-24.2	127.3	1.20	-37.8	144.1	1.04	-45.2	146.5	6.29×10^{-1}	-48.4	147.2	3.55×10^{-1}			
	-24.9	102.5	1.27	-38.9	117.7	1.05	-46.3	121.7	7.74×10^{-1}	-49.2	122.4	4.84×10^{-1}			
	-19.4	118.0	1.53	-32.6	132.8	1.24	-39.1	135.2	8.61×10^{-1}	-43.7	137.6	4.65×10^{-1}			
885.4	-40.4	55.2	2.96												
	-38.7	47.8	2.78												
	-34.3	52.3	2.58												
887.6	-44.7	20.4	2.58												
	-47.6	12.0	2.39												
	-48.4	71.9	2.04												
888.8	- 8.9	215.8	1.36×10^{-1}												
	51.4	247.3	3.21×10^{-1}												
	52.1	249.8	2.48×10^{-1}												
890.0	46.2	205.6	1.14×10^{-1}	-17.3	326.0	9.88×10^{-2}	-28.1	334.0	6.19×10^{-2}	-38.3	331.3	3.68×10^{-2}			
	30.7	267.7	2.38×10^{-1}	-31.1	.3	1.88×10^{-1}	-42.2	11.5	1.61×10^{-1}	-53.6	15.8	8.75×10^{-2}			
894.0	18.5	116.8	1.82×10^{-1}	24.1	119.9	7.05×10^{-2}	29.0	121.4	2.98×10^{-2}	38.4	116.9	1.39×10^{-2}			
	24.5	120.6	1.78×10^{-1}	30.8	121.7	7.22×10^{-2}	36.3	122.9	3.08×10^{-2}	40.1	123.7	1.39×10^{-2}			
896.1	-17.1	10.9	6.36×10^{-1}	-57.9	286.6	3.77×10^{-1}	-55.1	253.3	3.17×10^{-1}	-53.8	244.8	2.21×10^{-1}			
	-13.8	86.9	5.07×10^{-1}	-68.7	337.9	2.64×10^{-1}	-55.9	305.5	2.19×10^{-1}	-54.4	297.0	1.61×10^{-1}			
	-18.3	76.1	6.94	-65.4	354.6	3.54×10^{-1}	-58.8	310.6	2.39×10^{-1}	-58.3	300.3	1.55×10^{-1}			
897.3	-34.7	355.6	6.75×10^{-1}												
	-42.7	358.5	1.11												
	7.1	39.2	3.37×10^{-1}												
	82.3	124.9	2.62×10^{-1}												
	71.4	80.5	1.78×10^{-1}												
902.8	36.0	51.6	1.29												
	77.3	140.6	7.21×10^{-1}												
	75.8	115.0	7.71×10^{-1}												

TABLE 1.—*Paleomagnetic measurements—natural remanent magnetization (NRM) and remanent magnetization after thermal cleaning at various temperatures*—Continued

[Inc, inclination; Dec, declination; J, intensity (in ampere/meter). Each sample contained several specimens]

Depth of sample below surface (meters)	NRM			150°C			300°C			500°C			550°C		
	Inc	Dec	J	Inc	Dec	J	Inc	Dec	J	Inc	Dec	J	Inc	Dec	J
CC#2—Continued															
904.3	5.5	20.6	2.26												
	10.0	10.9	3.06												
	5.6	0.1	3.04												
	34.8	93.7	2.01	17.7	92.5	1.53	1.4	96.2	1.16	−23.1	102.1	1.64×10^{-1}			
	14.5	15.4	2.04	3.3	13.2	1.78	−13.5	11.8	1.46	−49.7	9.3	1.89×10^{-1}			
	10.9	131.0	2.20	6.8	133.1	2.04	− 7.6	137.4	1.49	−15.9	152.0	1.47×10^{-1}			
905.3	2.5	145.5	4.19												
	51.5	62.3	1.58												
CC#3															
777	61.2	134.8	6.53×10^{-1}	51.4	104.5	3.21×10^{-1}	38.9	105.8	1.95×10^{-1}	24.9	112.3	8.12×10^{-2}			
	84.3	151.9	9.53×10^{-1}	50.3	110.6	6.00×10^{-1}	41.2	110.0	3.88×10^{-1}	31.0	114.9	1.32×10^{-1}			
	51.1	59.5	1.41	44.2	64.0	8.46×10^{-1}	34.5	60.9	5.05×10^{-1}	28.7	74.8	1.55×10^{-1}			
	61.8	88.8	1.02												
779	11.9	159.8	8.59×10^{-2}	−17.3	152.6	9.56×10^{-2}	−31.6	152.0	8.14×10^{-2}	−39.1	153.8	5.74×10^{-2}			
	−17.3	140.0	1.19	−24.4	143.2	1.27	−29.2	143.9	1.13	−34.5	142.9	5.80×10^{-1}			
	−32.5	146.7	2.72	−35.7	148.4	2.75	−38.9	149.5	2.44	−42.6	150.4	8.28×10^{-1}			
[1]781	67.6	312.2	1.06	66.3	306.4	9.24×10^{-1}	54.0	248.8	5.64×10^{-1}	45.1	237.2	3.18×10^{-1}	47.9	225.0	2.61×10^{-1}
	68.5	341.9	7.73×10^{-1}	65.9	334.9	6.68×10^{-1}	52.2	251.5	3.28×10^{-1}	38.8	237.4	1.65×10^{-1}	56.8	230.7	7.28×10^{-2}
	64.0	338.3	7.13×10^{-1}	61.5	333.7	6.26×10^{-1}	52.7	255.7	2.98×10^{-1}	38.0	237.7	1.67×10^{-1}	57.7	239.4	8.58×10^{-2}
782	24.5	73.0	1.33	20.3	72.5	1.21	16.3	73.7	8.75×10^{-1}	15.0	73.8	3.53×10^{-1}			
	33.5	82.4	1.67	20.1	81.8	1.41	12.9	80.2	1.00	11.2	79.8	3.93×10^{-1}			
	31.2	92.8	1.35	17.5	90.9	1.08	9.0	88.2	6.76×10^{-1}	8.5	86.4	3.07×10^{-1}			
784	21.9	91.1	2.64×10^{-1}	13.2	277.3	1.47×10^{-1}	14.6	281.0	8.42×10^{-2}	12.1	283.9	3.63×10^{-2}			
	53.2	89.1	1.41×10^{-1}	25.9	279.0	1.13×10^{-1}	18.9	284.5	7.05×10^{-2}	8.0	286.4	2.71×10^{-2}			
921	65.8	51.1	5.33×10^{-1}												
	71.3	54.5	5.85×10^{-1}												
922	60.8	48.9	6.16×10^{-1}	55.0	57.8	3.63×10^{-1}	36.4	61.7	1.70×10^{-2}	34.0	64.3	6.27×10^{-2}			
	46.0	57.9	3.25×10^{-1}	36.4	69.9	2.32×10^{-1}	12.7	75.2	1.35×10^{-1}	6.6	69.8	4.49×10^{-2}			
	70.1	.3	4.39×10^{-1}	–	–	–	53.9	246.3	1.18×10^{-1}	55.6	257.2	4.82×10^{-2}	42.4	244.2	2.57×10^{-2}
	21.6	225.5	1.93×10^{-1}	–	–	–	–	–	–	15.7	266.7	4.49×10^{-2}	47.3	194.6	1.68×10^{-2}
	2.1	252.7	2.85×10^{-1}	–	–	–	–	–	–	−17.7	266.4	5.75×10^{-2}	−13.3	180.4	1.08×10^{-2}
[1]60.2	353.4	4.94×10^{-1}	77.5	100.1	5.19×10^{-1}	73.9	253.1	1.63×10^{-1}	56.6	246.4	5.04×10^{-2}	58.9	123.2	2.25×10^{-2}	
[1]927	49.2	284.4	3.06×10^{-1}	50.0	283.5	2.73×10^{-1}	52.5	283.1	2.53×10^{-1}	51.1	283.5	1.68×10^{-1}	50.7	282.9	1.20×10^{-1}
	52.9	277.9	3.58×10^{-1}	51.3	277.3	3.29×10^{-1}	53.4	277.8	3.08×10^{-1}	49.8	279.3	1.87×10^{-1}	48.8	277.5	1.55×10^{-1}
	48.2	282.2	2.33×10^{-1}	46.9	283.0	2.15×10^{-1}	50.3	283.7	2.09×10^{-1}	49.1	283.5	1.30×10^{-1}	50.2	283.2	9.36×10^{-2}
928	46.9	226.6	2.34×10^{-1}	45.6	228.4	2.19×10^{-1}	45.6	228.5	2.06×10^{-1}	44.7	232.1	6.81×10^{-2}			
	52.5	229.1	2.89×10^{-1}	48.8	227.6	2.78×10^{-1}	48.4	227.4	2.62×10^{-1}	50.3	221.6	6.18×10^{-2}			
984	19.9	275.7	5.24	12.2	276.8	5.55	9.7	277.9	5.42	8.1	277.8	4.17			
	15.7	281.1	6.58	10.5	277.9	6.85	8.4	277.9	6.65	7.2	278.8	5.12			
[1]987	67.5	292.0	1.03	66.7	271.3	9.89×10^{-1}	58.1	264.7	5.87×10^{-1}	45.9	266.2	2.32×10^{-1}	41.4	264.4	1.34×10^{-1}
	59.0	306.4	8.99×10^{-1}	64.7	283.0	8.33×10^{-1}	55.1	267.5	5.87×10^{-1}	42.0	268.9	2.10×10^{-1}	32.6	265.4	1.02×10^{-1}
	59.9	304.3	9.31×10^{-1}	66.6	265.6	1.04	56.6	251.1	6.29×10^{-1}	47.4	258.6	2.77×10^{-1}	46.7	262.5	1.48×10^{-1}
[1]989	64.7	20.9	9.13×10^{-1}	72.6	11.1	8.28×10^{-1}	–	–	–	50.1	323.0	1.69×10^{-1}	43.3	343.3	7.42×10^{-2}
	69.9	356.0	7.11×10^{-1}	76.0	265.7	7.37×10^{-1}	–	–	–	41.3	245.7	2.05×10^{-1}	34.7	243.3	1.09×10^{-1}
	54.0	18.8	1.10	63.3	3.0	9.06×10^{-1}	59.9	346.3	4.35×10^{-1}	51.6	329.8	1.96×10^{-1}	27.6	348.9	9.90×10^{-2}
[1]994	38.1	227.0	7.07×10^{-1}	35.6	224.0	6.04×10^{-1}	19.2	221.5	6.45×10^{-1}	16.3	221.9	4.06×10^{-1}	9.3	220.7	2.33×10^{-1}
	67.4	213.4	8.76×10^{-1}	58.5	216.9	7.64×10^{-1}	34.0	213.9	6.24×10^{-1}	21.7	216.2	3.67×10^{-1}	12.2	219.3	2.19×10^{-1}
	62.2	220.9	8.20×10^{-1}	50.1	213.7	8.96×10^{-1}	31.4	215.6	7.08×10^{-1}	18.1	217.1	4.59×10^{-1}	11.9	217.0	3.17×10^{-1}
	51.6	225.6	1.03	51.5	208.7	1.01	32.7	214.9	7.37×10^{-1}	19.8	217.1	4.38×10^{-1}	14.3	216.8	2.74×10^{-1}
[1]1004	47.1	324.3	3.80×10^{-1}	79.3	314.4	6.15×10^{-1}									
	47.9	349.2	5.18×10^{-1}	–	–	–	72.7	181.2	3.99×10^{-1}	43.0	161.8	1.68×10^{-1}	33.0	168.2	1.22×10^{-1}
	63.4	92.3	1.13	59.0	105.4	8.95×10^{-1}	41.3	122.3	6.04×10^{-1}	21.6	125.5	3.06×10^{-1}	18.8	127.7	2.02×10^{-1}
	60.7	108.0	9.01×10^{-1}	57.0	111.8	7.78×10^{-1}	34.9	125.6	5.47×10^{-1}	15.2	134.9	3.10×10^{-1}	15.8	129.3	1.99×10^{-1}
[1]1012	78.6	292.9	8.99×10^{-1}	70.8	230.7	8.03×10^{-1}	60.6	233.5	4.71×10^{-1}						
	79.1	257.6	9.05×10^{-1}	68.2	229.0	8.00×10^{-1}	58.0	231.4	4.62×10^{-1}						
	84.8	183.6	9.81×10^{-1}	65.5	201.0	8.51×10^{-1}	60.3	218.7	4.28×10^{-1}						
1014	75.3	203.4	1.08	65.5	212.2	7.56×10^{-1}	57.2	216.4	5.09×10^{-1}	48.6	227.1	2.67×10^{-1}			
	66.5	235.9	1.03	63.4	228.4	7.48×10^{-1}	55.5	231.5	5.13×10^{-1}	42.9	238.9	2.44×10^{-1}			
	65.5	218.2	7.56×10^{-1}	57.6	223.0	7.33×10^{-1}	53.0	227.9	5.34×10^{-1}	43.8	233.7	2.68×10^{-1}			
1024	14.3	270.3	2.92×10^{-1}												
	30.4	272.3	3.55×10^{-1}												
	45.2	56.7	5.89×10^{-1}	29.9	56.2	3.91×10^{-1}	21.4	55.0	3.01×10^{-1}	17.0	56.4	2.14×10^{-1}			
	52.6	57.1	6.15×10^{-1}	35.3	57.3	3.52×10^{-1}	25.4	59.0	2.45×10^{-1}	21.6	58.1	1.62×10^{-1}			
1031	38.1	152.1	4.25×10^{-1}	27.1	168.7	3.91×10^{-1}	24.9	168.6	2.85×10^{-1}						
	35.9	152.2	4.68×10^{-1}	23.4	157.6	3.63×10^{-1}	23.0	165.0	2.88×10^{-1}						
	22.4	178.9	4.82×10^{-1}	20.0	186.5	3.68×10^{-1}	17.6	179.6	3.34×10^{-1}						
[2][3]1047	17.2	157.0	2.72×10^{-2}	9.8	159.6	2.72×10^{-2}	5.2	159.9	2.74×10^{-2}	4.9	159.3	2.57×10^{-2}			
	14.8	163.7	1.68×10^{-2}	8.6	165.0	1.83×10^{-2}	9.6	163.4	1.83×10^{-2}	8.7	164.0	1.75×10^{-2}			
[3]1146	77.7	3.4	3.95×10^{-3}	71.3	32.2	2.70×10^{-3}	84.4	86.4	1.88×10^{-3}	73.2	168.4	1.40×10^{-3}			
	75.4	93.3	3.13×10^{-3}	69.1	50.2	2.33×10^{-3}	63.5	16.1	1.80×10^{-3}	31.3	26.9	1.81×10^{-3}			
	71.3	**13.6**	$\mathbf{3.25\times10^{-3}}$	59.2	356.8	2.76×10^{-3}	46.9	357.7	2.44×10^{-3}	31.1	2.5	2.58×10^{-3}			

[1] Samples cleaned at 100°C rather than 150°C.
[2] Sample probably inverted.
[3] Red-bed sample.

TABLE 2.—*Measured physical properties*
[Density not available for samples from CC#1]

Depth below surface (meters)	Number of samples	Remanent magnetization (Am^{-1})	Magnetic susceptibility (SI)	Density (g/cm^3)
		CC#1		
756.5	1	3.19×10^{-1}	3.41×10^{-3}	
766.9	1	6.50×10^{-1}	1.02×10^{-2}	
772.4	1	4.24	2.84×10^{-2}	
780.0	1	8.33	3.14×10^{-2}	
787.3	1	6.80×10^{-1}	1.75×10^{-2}	
789.4	1	2.82	2.98×10^{-2}	
790.7	1	1.02	3.83×10^{-2}	
		CC#2		
777.8	4	2.29×10^{-1}	3.43×10^{-2}	2.788
813.8	4	2.48	1.43×10^{-2}	2.669
819.3	3	1.47	6.40×10^{-2}	2.892
825.7	4	4.89	1.73×10^{-2}	2.852
859.5	4	2.26	4.64×10^{-2}	2.901
869.3	4	7.45×10^{-1}	2.94×10^{-2}	2.872
873.3	3	2.00×10^{-2}	1.22×10^{-3}	2.598
		CC#3		
781	3	8.36×10^{-1}	1.57×10^{-2}	2.585
922	4	3.30×10^{-1}	3.38×10^{-2}	2.895
927	3	2.94×10^{-1}	2.92×10^{-2}	2.658
987	3	9.52×10^{-1}	4.64×10^{-2}	2.886
989	3	8.94×10^{-1}	3.97×10^{-2}	2.884
994	4	8.69×10^{-1}	3.38×10^{-2}	2.851
1004	4	6.69×10^{-1}	3.09×10^{-2}	2.885
1012	3	9.28×10^{-1}	4.07×10^{-2}	2.917

In the usual statistical analysis of paleomagnetic data, remanent directions are assumed to have a Fisherian distribution (Tarling, 1971, p. 75). Briden and Ward (1966) and Kono (1980) have developed a method for determining Fisherian statistics when only inclination measurements are available. Use of their technique was attempted in this study, but unfortunately it often failed to converge to a solution, apparently owing to the small number of specimens at each sample depth. Accordingly, in this study statistical analyses assume a normal distribution for the inclination measurements. When comparison could be made with the more exact method, the results were found to be in good agreement. This study has also adopted the standard assumption that the magnetization intensities have a log-normal distribution (Tarling, 1971, p. 87).

RESULTS

Location of Flow Boundaries

As a first step in the interpretation of the paleomagnetic measurements, TRM parameters as a function of depth were estimated. From the information in table 1, the mean inclination and its standard deviation were calculated as a function of depth and demagnetization temperature. At each depth, the mean inclination at the demagnetization temperature that minimized the standard deviation was chosen as the best estimate of the TRM inclination. The resulting parameters are given in table 3.

Flow boundaries for the three test holes were then chosen on the basis of the existing geologic descriptions and the TRM inclinations. (Further details are provided in the following section.) For CC#1, the paleomagnetic results do not disagree with the presence of a single flow boundary as described by Gohn and others (1977). Although sample TRM inclinations were not determined for the lower flow (flow 1-2), specimen inclinations appear indistinguishable across the flow boundary; therefore it is likely that the two flows are close in age. For CC#2, the locations of the two major flow boundaries described by Gottfried and others (1983) are in agreement with the NRM intensities, which show a marked decrease at the top of each major flow. This decrease in NRM intensity may be due to a combination of flow surface weathering immediately following emplacement and hydrothermal alteration during burial. However, more than two flow boundaries are required to explain the paleomagnetic measurements. For this reason, each of the three major flows in CC#2 has been divided into subflows at depths where the sign of the TRM inclination changes. Where lithologic evidence was lacking, NRM inclination changes were sometimes used in an attempt to pin down the flow boundary more precisely than was possible by using the relatively sparse TRM measurements. Most of the required additional flow boundaries are located near lithologic changes identified by Gottfried and others (1983) and S. H. Perlman (unpubl. data, 1977). A similar procedure was used on the data from CC#3. The complete basis for choosing flow boundaries is given in table 4.

There will always be some uncertainty in the locations of flow boundaries. For example, many thin flows may have been missed by the paleomagnetic sampling. This is particularly true near the bottom of CC#2, where the sampling is sparse and the lithologic description indicates many possible disruptions. On the other hand, some of the chosen flow boundaries may be superfluous. For example, the flows labeled 2-3a and 2-3b originally may have been the top and bottom parts of a single flow, but when flow 2-2d was emplaced above it, the top part (2-3a) was reheated and remagnetized so that its polarity is now different from that of the lower part (2-3b). Despite these uncertainties, the flow boundaries given in table 4 should provide a good basis for geologic correlation and paleomagnetic dating.

The next step in the interpretation was to determine the mean TRM inclination for each flow. This was done by averaging sample mean TRM inclinations. The results (table 5) can be used to correlate flows among the three test holes and to estimate the age of the basalt.

TABLE 3.—*Means of inclination and intensity as a function of depth*

[Flows are categorized by the number of the test hole, number of the major flow within the test hole, and letter of the subflow within the major flow. Queries (?) indicate anomalous samples, which are not included in flow averages. N, number of specimens; Inc, inclination; S.D., standard deviation; J, intensity (in ampere/meter).]

Flow	Depth below surface (meters)	Natural remanent magnetization				Thermal remanent magnetization				
		N	Inc	S.D.	J	N	Inc	S.D.	J	T(°C)[1]
					CC#1					
1-1	756.5	1	54.2	–	3.19×10^{-1}					
	760.5	2	41.7	0.8	1.19					
	762.9	3	41.5	7.9	1.23	2	37.6	1.2	9.74×10^{-1}	300
	766.9	3	45.2	6.5	2.97×10^{-1}	2	43.3	6.4	1.61×10^{-1}	500
	770.2	2	41.1	1.7	9.70×10^{-1}					
	772.4	2	41.2	.9	4.15					
	780.0	3	47.8	17.9	2.25	2	41.9	10.5	7.40×10^{-1}	500
1-2	787.3	2	55.0	7.3	2.77×10^{-1}					
	789.4	2	36.5	.5	2.92					
	790.7	2	57.5	1.4	1.16					
					CC#2					
2-1a	776.0	3	−21.9	9.2	1.14	3	−36.2	11.9	1.44×10^{-1}	550
?	777.8	5	23.9	36.5	2.23×10^{-1}	4	4.8	23.2	1.40×10^{-1}	300
?	778.2	3	47.2	28.6	1.11×10^{-1}	3	1.9	23.6	6.22×10^{-2}	300
2-1b	779.1	3	19.5	25.7	2.90×10^{-1}	3	26.3	11.4	3.29×10^{-2}	500
	779.7	3	20.7	.7	7.72×10^{-1}					
2-2a	782.1	3	36.1	14.3	8.36×10^{-1}					
	783.3	3	3.9	15.4	5.83×10^{-3}	3	−48.7	8.9	2.18×10^{-3}	550
	785.1	3	−28.5	69.4	3.03×10^{-3}	3	−50.4	5.3	2.14×10^{-3}	500
	785.5	3	37.8	30.7	5.26×10^{-1}					
	786.3	3	52.3	7.3	3.20×10^{-3}	3	−41.9	3.4	3.84×10^{-4}	500
	789.4	5	15.9	13.5	1.44×10^{-2}	3	−39.6	11.0	2.16×10^{-2}	500
	790.7	4	62.3	10.5	5.39×10^{-1}					
	794.3	4	−4.4	28.1	8.59×10^{-1}					
	795.5	3	−34.9	5.5	1.97	3	−48.0	1.7	1.65	300
	798.0	3	−44.9	2.1	2.32	2	−50.6	.9	1.58	500
	801.0	4	2.3	19.0	1.26					
?	801.6	3	26.0	11.7	1.12	3	−3.3	6.5	7.24×10^{-1}	300
	802.5	5	−23.6	33.0	9.53×10^{-1}					
	802.8	3	−31.5	10.6	1.67	2	−45.8	5.9	1.73	300
	804.6	3	−6.0	.7	1.09					
	808.9	3	−1.9	5.8	1.44	2	−28.4	2.4	2.73×10^{-1}	500
	813.8	4	−41.6	4.0	2.48	4	−48.9	2.3	1.87	300
2-2b	814.4	4	34.3	12.0	5.63×10^{-1}					
	819.0	6	32.2	14.5	8.53×10^{-1}					
	819.3	3	35.9	3.9	1.47	3	20.4	2.5	6.69×10^{-1}	300
	823.0	6	14.2	20.8	2.72	3	23.7	10.0	2.73×10^{-1}	500
2-2c	825.7	4	−11.0	1.0	4.89	4	−14.4	2.6	4.62×10^{-2}	300
	828.8	3	−1.1	3.2	4.71					
?	835.8	3	−4.5	6.0	5.63	3	−6.4	2.7	4.48	300
?	838.8	3	−40.9	1.8	4.07	3	−66.8	1.6	1.73×10^{-1}	500
	840.9	4	−8.1	9.0	4.68					
2-2d	842.8	3	28.0	2.8	4.24					
	846.7	3	43.3	3.7	2.21	3	19.5	.4	2.05×10^{-2}	550
	853.7	6	46.3	14.2	1.81	3	27.8	2.3	2.36×10^{-1}	500
	858.3	4	16.4	3.8	1.80					
	859.5	4	47.1	6.6	2.26	4	23.6	2.6	2.63×10^{-1}	500
?	863.8	8	19.1	69.5	5.76×10^{-1}	4	52.4	3.1	1.30×10^{-1}	500
	869.0	3	57.4	12.4	5.81×10^{-1}					
	869.3	4	48.3	12.9	7.45×10^{-1}	4	35.8	2.9	3.11×10^{-1}	300
	870.5	3	9.0	59.9	3.81×10^{-1}					
2-3a	873.3	2	43.4	9.8	2.00×10^{-2}	2	25.9	4.9	2.08×10^{-2}	100
	878.1	3	38.9	16.6	3.63×10^{-1}					
2-3b	883.9	3	−22.8	3.0	1.33	3	−47.1	3.0	4.31×10^{-1}	500
	885.4	3	−37.8	3.2	2.77					
	887.6	3	−46.9	2.0	2.33					
	888.8	3	31.5	35.0	2.21×10^{-1}					
	890.0	2	38.5	11.0	1.65×10^{-1}	2	−24.2	9.8	1.36×10^{-1}	150

TABLE 3.—*Means of inclination and intensity as a function of depth*—Continued

[Flows are categorized by the number of the test hole, number of the major flow within the test hole, and letter of the subflow within the major flow. Queries (?) indicate anomalous samples, which are not included in flow averages. N, number of specimens; Inc, inclination; S.D., standard deviation; J, intensity (in ampere/meter).]

Flow	Depth below surface (meters)	Natural remanent magnetization				Thermal remanent magnetization				
		N	Inc	S.D.	J	N	Inc	S.D.	J	T(°C)[1]
CC#2—Continued										
2-3c	894.0	2	21.5	4.2	1.80×10^{-1}	2	39.3	1.2	1.39×10^{-2}	500
2-3d	896.1	3	−16.4	2.3	1.31	3	−56.6	2.0	2.55×10^{-1}	300
	897.3	5	16.7	58.2	4.11×10^{-1}					
	902.8	3	63.0	23.4	8.95×10^{-1}					
?	904.3	6	13.6	11.0	2.40	3	−6.6	7.5	1.36	300
	905.3	2	27.0	34.7	2.57					
CC#3										
3-1	777	4	64.6	14.0	9.73×10^{-1}	3	28.2	3.1	1.18×10^{-1}	500
3-2a	779	3	−12.6	22.6	6.53×10^{-1}	3	−38.7	4.1	3.02×10^{-1}	500
3-2b	781	3	66.7	2.4	8.36×10^{-1}	3	53.0	.9	3.81×10^{-1}	300
3-2c	782	3	29.7	4.7	1.44	3	19.3	1.6	1.23	150
3-3	784	2	37.6	22.1	1.93×10^{-1}	2	10.1	2.9	3.14×10^{-2}	500
3-4	921	2	68.6	3.9	5.58×10^{-1}					
	922	6	43.5	26.4	3.66×10^{-1}	3	56.3	20.6	3.52×10^{-1}	150
3-5	927	3	50.1	2.5	2.94×10^{-1}	3	49.9	1.0	1.20×10^{-1}	550
	928	2	49.7	4.0	2.60×10^{-1}	2	47.0	2.0	2.32×10^{-1}	300
?	984	2	17.8	3.0	5.87	2	7.7	.6	4.62	500
3-6a	987	3	62.1	4.7	9.52×10^{-1}	3	66.0	1.1	9.50×10^{-1}	100
	989	3	62.9	8.1	8.94×10^{-1}	3	47.7	5.6	1.89×10^{-1}	500
3-6b	994	4	54.8	12.9	8.69×10^{-1}	4	11.9	2.1	2.58×10^{-1}	550
	1004	4	44.0	27.0	6.69×10^{-1}	3	22.5	9.2	1.70×10^{-1}	550
3-6c	1012	3	80.8	3.4	9.28×10^{-1}	3	59.6	1.4	4.53×10^{-1}	300
	1014	3	69.1	5.4	9.44×10^{-1}	3	55.2	2.1	5.19×10^{-1}	300
3-7	1024	4	35.6	17.0	4.40×10^{-1}	2	23.4	2.8	2.72×10^{-1}	300
	1031	3	32.1	8.5	4.58×10^{-1}	3	23.5	3.6	3.74×10^{-1}	150
sed	1047	2	16.0	1.7	2.14×10^{-2}	2	9.2	.8	2.23×10^{-2}	150
sed	1146	3	74.8	3.2	3.44×10^{-3}					

[1]Thermomagnetic cleaning temperature.

Details on flow determinations.—To aid in the determination of flow boundaries, a statistical test was used to compare pairs of sample mean TRM inclinations. The test statistic is given by

$$U = \frac{|\, m_i - m_j \,|}{\sqrt{(\Delta m_i)^2 + (\Delta m_j)^2}}, \qquad (1)$$

where m_k is the mean TRM inclination at depth k, and Δm_k is the standard error in the mean

$$\Delta m_k = \frac{\sigma_k}{\sqrt{n_k}}. \qquad (2)$$

Here σ_k is the standard deviation of the TRM inclinations at depth k, and n_k is the number of specimens used to estimate m_k and σ_k. The test statistic U is used to test the hypothesis that the mean TRM inclinations at the two depths are identical. If the value of U is greater than 2.0, then the hypothesis is rejected at the 95-percent confidence level.

For each test hole, the test statistic was computed for every possible pairing of samples. Pairs for which the hypothesis of equivalent mean inclinations could not be rejected at the 95-percent confidence level were found to be linked together into groups of samples. Note that paired adjacent samples need not have satisfied the statistical test in order to be classified in the same group. Rather they were only required to satisfy the test when each was paired with a third sample elsewhere in the hole. Due to the large scatter in the inclinations, the more rigorous approach would have yielded nearly as many groupings (flows) as there are samples in test holes 2 and 3.

CC#1 was found to have a single group of samples having a mean TRM inclination of 40.9°. Results for CC#2 were equivocal until the two samples with standard errors in the mean greater than 10° were rejected from the analysis. Three groupings were then found having mean TRM inclinations of 26.9°, −41.2°, and −5.4°. The latter grouping contained three isolated samples that were rejected from further analysis as being anomalous. Two samples found to belong to no grouping were also rejected from further analysis. Rejected samples are indicated by question marks in the flow col-

TABLE 4.—*Evidence for flow boundaries*

Flow	Depth below surface (m) to flow top	Depth below surface (m) to feature	Paleomagnetic evidence	Lithologic evidence
		CC#1		
1-1	750.0			Top of basalt
1-2	784.7			Sharp contact
		792.0		Base of core
		CC#2		
2-1a	775.3			Top of basalt
		776.0		Top of core
2-1b	777.8		Mixed TRM inclinations	
		778.2	Mixed TRM inclinations	
2-2a	781.6		TRM inclination changes from + at 779.1 to − at 783.3	Sharp contact
		793.5		Gradational contact
		801.6	Shallow TRM inclination	
		804.6	Unstable sample	
2-2b	814.0		TRM inclination changes from − at 813.8 to + at 819.3	
			NRM inclination changes from − at 813.8 to + at 814.4	
2-2c	824.0		TRM inclination changes from + at 823.0 to − at 825.7	
		835.8	Shallow TRM inclination	
		838.8	Steep TRM inclination	Sheet of vesicles
2-2d	842.0		TRM inclination changes from − at 838.8 to + at 846.7	
			NRM inclination changes from − at 840.9 to + at 842.8	
2-3a	871.3			Breccia zone
2-3b	883.0		TRM inclination changes from + at 873.3 to − at 883.9	Gradational zone
			NRM inclination changes from + at 878.1 to − at 883.9	
		888.0		Gradational contact
2-3c	892.0		TRM inclination changes from − at 890.0 to + at 894.0	
2-3d	895.0		TRM inclination changes from + at 894.0 to − at 896.1	Gradational contact
		899.3		Gradational contact
		901.3		Sharp contact
		903.0		Gradational contact
		904.3	Shallow TRM inclination	
		907.0		Base of core
		CC#3		
3-1	775.0			Top of core
3-2a	777.7		TRM inclination changes from + at 777 to − at 779	Sharp contact
3-2b	780.0		TRM inclination changes from − at 779 to + at 781	
3-2c	781.5		TRM inclination shallows by 33.7° between 781 and 782	
3-3	782.6			Sharp contact
		785.0		Base of core
3-4	921.0			Top of core
3-5	925.5			Sedimentary wedge
		930.0		Base of core
3-6a	983.0			Top of core
3-6b	992.0		TRM inclination steepens by 35.8° between 989 and 994	
3-6c	1008.0		TRM inclination steepens by 37.1° between 1004 and 1012	
3-7	1021.3		TRM inclination shallows by 39.0° between 1014 and 1024	Sharp contact
		1031.0		Base of basalt

umn of table 3. CC#3 also produced three groupings, having mean TRM inclinations of 54.3°, 18.3°, and −38.7°.

Flow boundaries were located on the basis of the following criteria, listed in order of their importance:

1. Geological description of the core provided unequivocal evidence for a flow boundary;
2. Sample TRM inclinations changed groupings across a probable flow boundary mentioned in the geologic description;
3. Sample TRM inclinations changed groupings without geologic evidence for a flow boundary.

Flows determined using criterion 1 are designated by numbers. Criteria 2 and 3 are used to subdivide the numbered flows into alphabetized subflows.

Correlation of Flows

Correlation of flows among the three test holes is hindered by the limited amount of vertical overlap among the cored sections of the holes and by the horizontal distance between the holes. However, CC#2 and 3 are only about 760 meters apart, and it appears likely either that flow 2-1b (TRM inclination 26.3°) and flow 3-1 (TRM inclination 28.2°) represent the same

TABLE 5.—*Means of inclination and intensity as a function of flow*

[ND, number of depths from which samples for analysis were taken; Inc, inclination; S.D., standard deviation; J, intensity (in ampere/meter)]

Flow	Natural remanent magnetization				Thermal remanent magnetization			
	ND	Inc	S.D.	J	ND	Inc	S.D.	J
CC#1								
1-1	7	44.7	4.9	1.03	3	40.9	3.0	4.88×10^{-1}
1-2	3	49.7	11.5	9.79×10^{-1}				
CC#2								
2-1a	1	−21.9	–	1.14	1	−36.2	–	1.44×10^{-1}
2-1b	2	20.1	.8	4.73×10^{-1}	1	26.3	–	3.29×10^{-2}
2-2a	16	−0.4	33.7	3.06×10^{-1}	9	−44.7	7.2	7.64×10^{-2}
2-2b	4	29.2	10.1	1.18	2	22.1	2.3	4.27×10^{-1}
2-2c	3	−5.4	5.1	4.76	1	−14.4	–	4.62×10^{-2}
2-2d	8	36.6	17.0	1.36	4	26.7	7.0	1.41×10^{-1}
2-3a	2	41.2	3.2	8.52×10^{-2}	1	25.9	–	2.08×10^{-2}
2-3b	5	−7.5	39.8	7.93×10^{-1}	2	−35.7	16.2	2.42×10^{-1}
2-3c	1	21.5	-	1.80×10^{-1}	1	39.3	–	1.39×10^{-2}
2-3d	4	22.6	32.7	1.05	1	−56.6	–	2.55×10^{-1}
CC#3								
3-1	1	64.6	–	4.97×10^{-1}	1	28.2	–	1.18×10^{-1}
3-2a	1	−12.6	–	6.53×10^{-1}	1	−38.7	–	3.02×10^{-1}
3-2b	1	66.7	–	8.36×10^{-1}	1	53.0	–	3.81×10^{-1}
3-2c	1	29.7	–	1.44	1	19.3	–	1.23
3-3	1	37.6	–	1.93×10^{-1}	1	10.1	–	3.14×10^{-2}
3-4	2	56.1	17.8	4.52×10^{-1}	1	56.3	–	3.52×10^{-1}
3-5	2	49.9	.3	2.76×10^{-1}	2	48.5	2.1	1.67×10^{-1}
3-6a	2	62.5	.6	9.23×10^{-1}	2	56.9	12.9	4.24×10^{-1}
3-6b	2	49.4	7.6	7.62×10^{-1}	2	17.2	7.4	2.09×10^{-1}
3-6c	2	75.0	8.3	9.34×10^{-1}	2	57.4	3.1	4.85×10^{-1}
3-7	2	33.9	2.5	4.49×10^{-1}	2	23.5	.1	3.19×10^{-1}

flow or that flow 2-1a (TRM inclination −36.2°) and flow 3-2a (TRM inclination of −38.7°) represent the same flow. In the former case, the major flow boundary at 777.7 m in CC#3 corresponds to the major flow boundary at 781.6 m in CC#2, and flows 3-2b, 3-2c, and 3-3 are absent in CC#2. In the latter case, the major flow boundary at 777.7 m in CC#3 corresponds to the top of the basalt in CC#2, and the major flow boundary at 782.6 m in CC#3 corresponds to the major flow boundary at 781.6 m in CC#2. In this interpretation, flows 3-2b, 3-2c and 2-1b become independent thin flows, and flow 3-3 could be the remagnetized top of flow 2-2a, the remagnetization having occurred at the time of emplacement of flow 3-2c. In either case, the flow boundaries at the top of CC#2 and 3 have a near-horizontal apparent dip, which indicates little tilting since extrusion.

Because CC#1 extends to only 792 m, it is possible that the basalt flows sampled in CC#1 lie entirely above the section sampled in CC#2 and 3. Alternatively, the top flow in CC#3 could correspond to the lower flow in CC#1. Thus the paleomagnetic measurements in the three test holes can be reconciled without requiring the presence of faults or other tectonic elements.

Age of the Basalt

After the basalt unit has been divided into flows and the mean TRM inclination has been estimated for each flow (except flow 1-2), the mean inclination of the basalt unit as a whole can be estimated. This number can be compared to a graph of paleoinclination against time for the Charleston area in order to estimate the age of the basalt. The unit mean inclination is determined by averaging the absolute values of the flow means. Possible correlations of flows among the three holes were not considered in the averaging process; therefore some flows may have been sampled twice. The mean inclination computed from the 22 flow means is $35.4°\pm3.2°$. Ignoring possible errors in the flow averages and assuming a normal distribution for the sample means, the unit mean inclination has a 95-percent chance of falling in the range $35.4°\pm6.4°$.

In figure 3 this mean inclination and its 95-percent confidence band have been superimposed on a paleoinclination curve that shows the mean inclination at Charleston (lat 33° N., long 80° W.) as a function of time for the past 300 million years. The paleoinclination curve was generated by using the pole positions of Irving (1977). The dashed lines in the figure show the 95-percent confidence region about the mean paleoinclination curve.

On the basis of the present study, the most probable age of the basalts corresponds to the time at which the paleoinclination curve crosses 35.4 degrees. This turns out to be 170 m.y. ago. The actual intersection of the two curves, however, has a 95-percent chance of falling anywhere within the ruled area. Thus we can be 95-percent certain that the true age of the basalts lies between 110 m.y. and 196 m.y. This time range runs from the end of the Triassic, through the Jurassic, and into the Early Cretaceous. For comparison with radiometric age dates (fig. 4), we also have computed the one-standard-error range (68-percent confidence interval) on the paleomagnetic age to be 120 m.y. to 188 m.y.

The large uncertainty in the age of the basalts is a result of both the uncertainty in the paleoinclination curve and the uncertainty in the mean magnetic inclination of the Clubhouse Crossroads basalt unit. It is likely that a more precise age could have been determined if completely oriented cores had been available to provide azimuthal information.

Figure 4 is a time line comparing paleomagnetic and radiometric ages of the Clubhouse Crossroads basalt with the geomagnetic reversal history and with radiometric ages for other eastern North American Mesozoic igneous rocks. The figure shows that neither the paleomagnetic data nor the radiometric age measurements provide sufficient constraints on the age of the Clubhouse Crossroads basalt to permit comparison with the other Mesozoic units. However, the presence of normal and reversely magnetized flows in the basalt unit suggests either that the age of the basalt may differ from the age of other early Mesozoic basalts and diabases or that certain periods of lower Mesozoic magnetic reversals are inadequately documented within the paleomagnetic record.

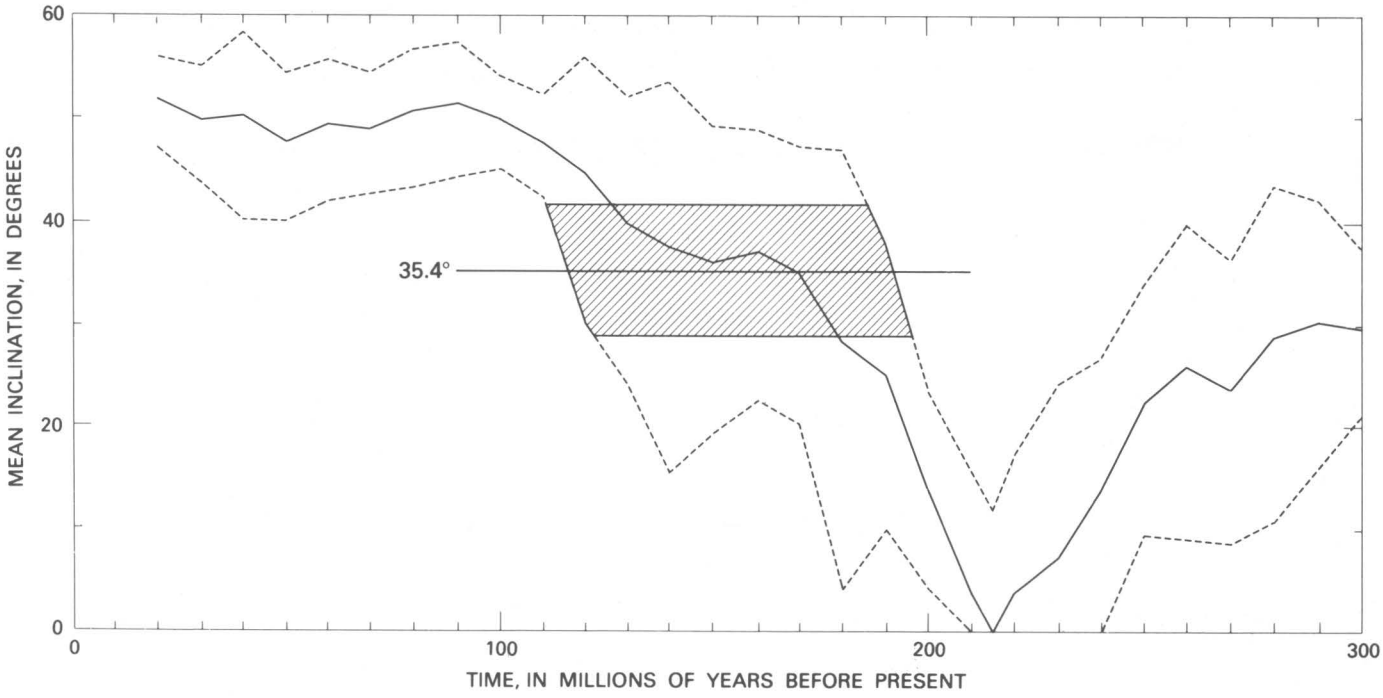

FIGURE 3.—Paleoinclination and age of the basalt. The solid curve shows the mean inclination at Charleston (lat 33° N., long 80°W.) as a function of past time. The dashed curves represent 95-percent confidence limits about the mean. These curves were computed from pole positions given by Irving (1977). The horizontal line at 35.4° represents the mean TRM inclination of the Clubhouse Crossroads basalt, as computed from 22 flow means. The intersection of this line with the solid curve gives the most probable age of the basalt as 170 m.y. The ruled area is the 95-percent confidence region about this intersection. Thus the actual age of the basalt has a 95-percent chance of falling in the range 110–196 m.y.

From the marine magnetic record, frequent magnetic reversals are known to have occurred during the Late Jurassic and Early Cretaceous (Larson and Hilde, 1975). From paleomagnetic measurements made on land, another period of frequent reversals is known to have occurred in the Early Triassic (McElhinny, 1971). These two periods of frequent reversals are separated by a long period of normal polarity, containing few reversed-polarity intervals. It is during this long period of predominantly normal polarity that most of the Mesozoic igneous rocks of eastern North America apparently were formed.

Regional tectonics suggest that the Clubhouse Crossroads basalts probably are not old enough to have formed during the Early Triassic interval of frequent reversals. On the other hand, the initial Cretaceous radiometric ages for the CC#1 basalt (Gottfried and others, 1977) suggest that they may have formed during the Late Jurassic–Early Cretaceous reversal sequence. In that case, the Clubhouse Crossroads basalts would be much younger than the other eastern North American basalts and diabases associated with early Mesozoic basins. Instead their age would be similar to the youngest intrusive rocks of the White Mountain Plutonic-Volcanic Suite of New England (Foland and others, 1971; Armstrong and Stump, 1971). There are three problems with this interpretation. First, like the other eastern North American Mesozoic basalts and diabases, the Clubhouse Crossroads basalts are found close to a probable Triassic-Jurassic basin. Secondly, the presence of a thin sedimentary red-bed unit between flows 3-4 and 3-5 of CC#3 (Gottfried and others, 1983) indicates that the Clubhouse Crossroads basalts, like the other eastern North American basalts and diabases of Mesozoic age, are closely associated in time with the sedimentary rocks they intrude or overlie. Thirdly, geochemical analyses indicate that the Clubhouse Crossroads basalt is of the same chemical type as other eastern North American Triassic-Jurassic basalts (Gottfried and others, 1977, 1983). Thus it is likely that the Clubhouse Crossroads basalts are similar in age to the igneous rocks of other eastern North American early Mesozoic basins. That is, they are of Late Triassic and Early Jurassic age. As a corollary, the reversely magnetized flows of the Clubhouse Crossroads basalt are evidence for a period of frequent reversals during the Late Triassic or Early Jurassic.

Opdyke and McElhinny (1965) and Brock (1968) present evidence for short reversed-polarity intervals within the Late Triassic–Early Jurassic normal-polarity

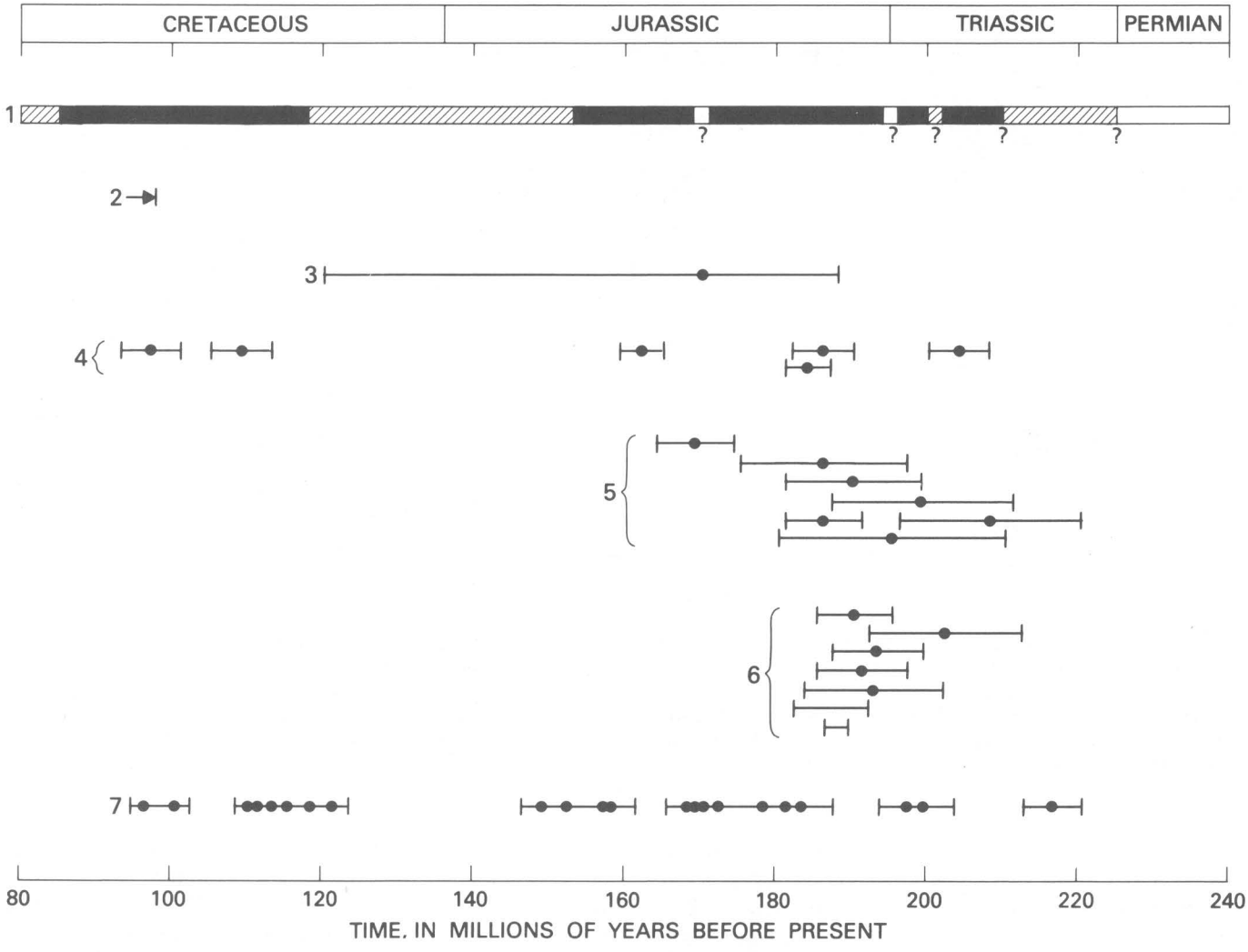

FIGURE 4.—A time line comparing the paleomagnetic and radiometric ages for the Clubhouse Crossroads basalt with geomagnetic field behavior and with radiometric ages for other eastern North American Mesozoic igneous rocks. The following features are shown:

1. Geomagnetic field behavior. Dark bands represent normal polarity. Light bands represent reversed polarity. Shaded bands represent mixed polarity (Larson and Hilde, 1975; McElhinny, 1971; Opdyke and McElhinny, 1965; Brock, 1968; Reeve and Helsley, 1972; Steiner and Helsley, 1974).
2. Biostratigraphic age of the oldest Cretaceous sediment in CC#1 (Hazel and others, 1977).
3. Paleomagnetic age of the Clubhouse Crossroads basalt (this study).
4. Radiometric ages of the Clubhouse Crossroads basalt (Gohn and others, 1978; Lanphere, 1983).
5. Radiometric ages of other southeastern North American Mesozoic basalt and diabase (Gohn and others, 1978; Watts and Noltimier, 1974).
6. Radiometric ages of northeastern North American Mesozoic basalt and diabase (de Boer, 1968; Dallmeyer, 1975; Sutter and Smith, 1979).
7. Radiometric ages of the rocks of the White Mountain Plutonic-Volcanic Suite (Foland and others, 1971; Armstrong and Stump, 1971: Hurley and others, 1960).

interval. Apparently two such reversed intervals can be identified from paleomagnetic studies of South African igneous rocks, one at 195 m.y. near the Triassic-Jurassic boundary and the other around 170 m.y. The reversed flows seen in the Clubhouse Crossroads basalt could date from either of these times, although the younger date corresponds well to the most probable age of the basalt as determined by this study and might therefore be preferred. The presence of five distinct reversed intervals in CC#2 indicates that, if the correlation with the 170-m.y. reversed event is correct, this event is actually a sequence of reversals, similar in form to the short Late Triassic reversal sequences seen by Reeve and Helsley (1972) and Steiner and Helsley (1974) in the Chinle (New Mexico) and Kayenta (Africa) formations.

It should be mentioned that Opdyke and Wensink (1966) found reversely magnetized samples at three sites in the White Mountains; samples from two of the sites were thought to be of Early Jurassic age, whereas samples from the third site were radiometrically dated (K-Ar) as Early Cretaceous. However, K-Ar dating by Foland and others (1971) has since established that one set of the "Jurassic" samples is indeed Early Cretaceous. The other site is undated, but similar paleomagnetic directions in all samples suggest a similar Cretaceous age for all three.

CONCLUSIONS

Although hampered by the lack of completely oriented cores and by the relatively small amount of overlap in the depth ranges of the cored sections of the three test holes, paleomagnetic investigations of the Clubhouse Crossroads basalt have yielded worthwhile results. The age of the basalt has been confirmed as Mesozoic and probably Early Jurassic. No faults are required to correlate flows among the three holes. Reversed polarities and a definite polarity sequence have been found for the first time in eastern North American igneous rocks associated with early Mesozoic basins. In addition, the description of the basalt unit itself has been expanded.

Thermomagnetic analysis indicates that the main carrier of the remanence in the basalt is nearly pure magnetite. In some samples having high Curie points, the remanence may be carried by primary ilmenohematite. Low Curie points are also seen, providing evidence for maghemite. The inference is that all the original unoxidized titanomagnetite in the basalt underwent high-temperature oxidation during the initial cooling to form nearly pure magnetite. Some of the magnetite has undergone low-temperature oxidation since cooling, which has resulted in the production of maghemite. Both the magnetite and the ilmenohematite can be expected to provide reliable paleomagnetic remanent directions.

On the basis of the paleomagnetic measurements and the geologic descriptions of the cores, 23 flows have been identified. These are divided as follows: 2 flows in CC#1, 10 flows in CC#2, and 11 flows in CC#3. One of the top two flows in CC#2 may correspond to one of the top two flows in CC#3. The flow boundaries are essentially horizontal.

The mean TRM inclination of the flows is $35.4° \pm 3.2°$. Comparing this figure with a paleoinclination curve for the Charleston area indicates that the most probable age of the basalt is 170 m.y. and that the actual age has a 95-percent chance of falling in the range 110–196 m.y. Similarities between the Clubhouse Crossroads basalt and other lower Mesozoic eastern North American basalts and diabases suggests that the true age is more likely to fall in the older end of this range.

The flow inclinations in CC#2 exhibit a definite polarity sequence. Five reversed-polarity intervals are separated by four normal-polarity intervals. Reversed polarities are not seen in other eastern North American Mesozoic basalts and diabases. However, reversed polarities and polarity sequences are known from other studies of Upper Triassic and Lower Jurassic rocks in the Southwestern United States and in southern Africa.

REFERENCES CITED

Akimoto, Syun-iti, Katsura, Tukashi, and Yoshida, Minoru, 1957, Magnetic properties of $TiFe_2O_4$–Fe_3O_4 system and their change with oxidation: Journal of Geomagnetism and Geoelectricity, v. 9, no. 4, p. 165–178.

Armstrong, R. L., and Stump, Edmund, 1971, Additional K-Ar dates, White Mountain magma series, New England: American Journal of Science, v. 270, no. 5, p. 331–333.

Beck, M. E., Jr., 1972, Paleomagnetism of Upper Triassic diabase from southeastern Pennsylvania: further results: Journal of Geophysical Research, v. 77, no. 29, p. 5673–5687.

Briden, J. C., and Ward, M. A., 1966, Analysis of magnetic inclination in borecores: Pure and Applied Geophysics, v. 63, no. 1, p. 133–152.

Brock, A., 1968, Paleomagnetism of the Nuanetsi igneous province and its bearing upon the sequence of Karroo igneous activity in southern Africa: Journal of Geophysical Research, v. 73, no. 4, p. 1389–1397.

Carmichael, I.S.E., and Nicholls, J., 1967, Iron-titanium oxides and oxygen fugacities in volcanic rocks: Journal of Geophysical Research, v. 72, no. 18, p. 4665–4687.

Dallmeyer, R. D., 1975, The Palisades sill: a Jurassic intrusion? Evidence from $^{40}Ar/^{39}Ar$ incremental release ages: Geology, v. 3, no. 5, p. 243–245.

Daniels, D. L., Zietz, Isidore, and Popenoe, Peter, 1983, Distribution of subsurface lower Mesozoic rocks in the Southeastern United States as interpreted from regional aeromagnetic and gravity maps, *in* Gohn, G. S., ed., Studies related to the Charleston, South Carolina, earthquake of 1886–Tectonics and seismicity: U.S. Geological Survey Professional Paper 1313, p. K1–K24.

de Boer, Jelle, 1968, Paleomagnetic differentiation and correlation of the Late Triassic volcanic rocks in the central Appalachians (with special reference to the Connecticut Valley): Geological Society of America Bulletin, v. 79, no. 5, p. 609–626.

Doell, R. R., and Cox, Allan, 1965, Measurement of the remanent magnetization of igneous rocks: U.S. Geological Survey Bulletin 1203-A, p. A1–A32.

———1967, Recording magnetic balance, *in* Collinson, D. W., Creer, K. M., and Runcorn, S. K., eds., Methods in paleomagnetism: New York, Elsevier, p. 440–444.

Foland, K. A., Quinn, A. W., and Giletti, B. J., 1971, K-Ar and Rb-Sr Jurassic and Cretaceous ages for intrusives of the White Mountain magma series, northern New England: American Journal of Science, v. 270, no. 5, p. 321–330.

Gohn, G. S., Gottfried, David, Lanphere, M. A., and Higgins, B. B., 1978, Regional implications of Triassic or Jurassic age for basalt and sedimentary red beds in the South Carolina Coastal Plain: Science, v. 202, no. 4370, p. 887–890.

Gohn, G. S., Higgins, B. B., Smith, C. C., and Owens, J. P., 1977, Lithostratigraphy of the deep corehole (Clubhouse Crossroads corehole 1) near Charleston, South Carolina, *in* Rankin, D. W., ed., Studies related to the Charleston, South Carolina, earthquake of 1886–A preliminary report: U.S. Geological Survey Professional Paper 1028, p. 58–70.

Gottfried, David, Annell, C. S., and Byerly, G. R., 1983, Geochemistry and tectonic significance of subsurface basalts near Charleston, South Carolina; Clubhouse Crossroads test holes #2 and #3, *in* Gohn, G. S., ed., Studies related to the Charleston, South Carolina, earthquake of 1886–Tectonics and seismicity: U.S. Geological Survey Professional Paper 1313, p. A1–A19.

Gottfried, David, Annell, C. S., and Schwarz, L. J., 1977, Geochemistry of subsurface basalt from the deep corehole (Clubhouse Crossroads corehole 1) near Charleston, South Carolina–Magma type and tectonic implications, *in* Rankin, D. W., ed., Studies related to the Charleston, South Carolina, earthquake of 1886–A preliminary report: U.S. Geological Survey Professional Paper 1028, p. 91–113.

Grommé, C. S., Wright, T. L., and Peck, D. L., 1969, Magnetic properties and oxidation of iron-titanium oxide minerals in Alae and Makaopuhi lava lakes, Hawaii: Journal of Geophysical Research, v. 74, no. 22, p. 5277–5293.

Hazel, J. E., Bybell, L. M., Christopher, R. A., Frederiksen, N. O., May, F. E., McLean, D. M., Poore, R. Z., Smith, C. C., Sohl, N. F., Valentine, P. C., and Witmer, R. J., 1977, Biostratigraphy of the deep corehole (Clubhouse Crossroads corehole 1) near Charleston, South Carolina, *in* Rankin, D. W., ed., Studies related to the Charleston, South Carolina, earthquake of 1886–A preliminary report: U.S. Geological Survey Professional Paper 1028, p. 71–89.

Hurley, P. M., Fairbairn, H. W., Pinson, W. H., and Faure, G., 1960, K-Ar and Rb-Sr minimum ages for the Pennsylvanian section in the Narragansett Basin: Geochimica et Cosmochimica Acta, v. 18, nos. 3/4, p. 247–258.

Irving, E., 1977, Drift of the major continental blocks since the Devonian: Nature, v. 270, no. 5635, p. 304–309.

Johnson, H. P., and Merrill, R. T., 1972, Magnetic and mineralogical changes associated with low-temperature oxidation of magnetite: Journal of Geophysical Research, v. 77, no. 2, p. 334–341.

——— 1973, Low temperature oxidation of a titanomagnetite and the implications for paleomagnetism: Journal of Geophysical Research, v. 78, no. 23, p. 4938–4949.

———1974, Low-temperature oxidation of a single-domain magnetite: Journal of Geophysical Research, v. 79, no. 35, p. 5533–5534.

Kono, M., 1980, Statistics of paleomagnetic inclination data: Journal of Geophysical Research, v. 85, no. B7, p. 3878–3882.

Lanphere, M. A., 1983, $^{40}Ar/^{39}Ar$ ages of basalt from Clubhouse Crossroads test hole #2, near Charleston, South Carolina, *in* Gohn, G. S., ed., Studies related to the Charleston, South Carolina, earthquake of 1886–Tectonics and seismicity: U.S. Geological Survey Professional Paper 1313, p. B1–B8.

Larson, R. L., and Hilde, T. W. C., 1975, A revised time scale of magnetic reversals for the Early Cretaceous and Late Jurassic: Journal of Geophysical Research, v. 80, no. 17, p. 2586–2594.

McElhinny, M. W., 1971, Geomagnetic reversals during the Phanerozoic: Science, v. 172, no. 3979, p. 157–159.

Merrill, R. T., 1975, Magnetic effects associated with chemical changes in igneous rocks: Geophysical Surveys, v. 2, no. 3, p. 277–311.

Opdyke, [N.] D., and McElhinny, M. W., 1965, The reversal at the Triassic Jurassic boundary and its bearing on the correlation of Karroo igneous activity in Southern Africa [abs.]: EOS, American Geophysical Union Transactions, v. 46, no. 1, p. 65.

Opdyke, N. D., and Wensink, H., 1966, Paleomagnetism of rocks from the White Mountain plutonic-volcanic series in New Hampshire and Vermont: Journal of Geophysical Research, v. 71, no. 12, p. 3045–3051.

Ozima, Mituko, and Larson, E. E., 1970, Low- and high-temperature oxidation of titanomagnetite in relation to irreversible changes in the magnetic properties of submarine basalts: Journal of Geophysical Research, v. 75, no. 5, p. 1003–1017.

Reeve, S. C., and Helsley, C. E., 1972, Magnetic reversal sequence in the upper portion of the Chinle Formation, Montoya, New Mexico: Geological Society of America Bulletin, v. 83, no. 12, p. 3795–3811.

Sass, J. H., and Ziagos, J. P., 1977, Heat flow from a corehole near Charleston, South Carolina, *in* Rankin, D. W., ed., Studies related to the Charleston, South Carolina, earthquake of 1886–A preliminary report: U.S. Geological Survey Professional Paper 1028, p. 115–118.

Smith, T. E., 1976, Paleomagnetic study of lower Mesozoic diabase dikes and sills of Connecticut and Maryland: Canadian Journal of Earth Sciences, v. 13, no. 4, p. 597–609.

Stacey, F. D., and Banerjee, S. K., 1974, The physical principles of rock magnetism: Amsterdam, Elsevier, 195 p.

Steiner, M. B., and Helsley, C. E., 1974, Magnetic polarity sequence of the Upper Triassic Kayenta Formation: Geology, v. 2, no. 4, p. 191–194.

Sutter, J. F., and Smith, T. E., 1979, $^{40}Ar/^{39}Ar$ ages of diabase intrusions from Newark trend basins in Connecticut and Maryland; initiation of central Atlantic rifting: American Journal of Science, v. 279, no. 7, p. 808–831.

Tarling, D. H., 1971, Principles and applications of paleomagnetism: London, Chapman and Hall, 164 p.

Watts, Doyle, and Noltimier, H. C., 1974, Paleomagnetic study of diabase dikes in the inner Piedmont of N. Carolina and Georgia [abs.]: EOS, American Geophysical Union Transactions, v. 55, no. 7, p. 675.

Geology of the Lower Mesozoic(?) Sedimentary Rocks in Clubhouse Crossroads Test Hole #3, Near Charleston, South Carolina

By GREGORY S. GOHN, BRENDA B. HOUSER, and RAY R. SCHNEIDER

STUDIES RELATED TO THE CHARLESTON, SOUTH CAROLINA, EARTHQUAKE OF 1886—TECTONICS AND SEISMICITY

GEOLOGICAL SURVEY PROFESSIONAL PAPER 1313-D

UNITED STATES GOVERNMENT PRINTING OFFICE, WASHINGTON: 1983

CONTENTS

ILLUSTRATIONS

TABLES

STUDIES RELATED TO THE CHARLESTON, SOUTH CAROLINA, EARTHQUAKE OF 1886–TECTONICS AND SEISMICITY

GEOLOGY OF THE LOWER MESOZOIC(?) SEDIMENTARY ROCKS IN CLUBHOUSE CROSSROADS TEST HOLE #3, NEAR CHARLESTON, SOUTH CAROLINA

By GREGORY S. GOHN, BRENDA B. HOUSER, and RAY R. SCHNEIDER

ABSTRACT

In Clubhouse Crossroads drill hole #3, near Charleston, S. C., a minimum of 121 m of well-consolidated sedimentary red beds underlies 256 m of subaerial basalt flows. The basalt flows are of Early Jurassic age and underlie 775 m of Cretaceous and Cenozoic Coastal Plain deposits. The red beds are of probable Late Triassic and (or) Early Jurassic age, on the basis of the age of the basalt and the lithologic similarity of the red beds to lower Mesozoic red beds exposed elsewhere in the Eastern United States.

The red-bed section is divided into an upper fine-grained facies (39 m) consisting of mudstones, siltstones, and argillaceous sandstones and a lower coarse-grained facies (82 m) consisting of mudstones and conglomeratic sandstones. Sandstones in the fine-grained facies show several types of low-amplitude cross-stratification, whereas conglomeratic beds in the coarse-grained facies are inversely and normally graded. The predominant sandstones in both facies are arkosic wackes that contain abundant quartz-feldspar lithic fragments as well as abundant feldspar. Detrital lithic fragments and heavy minerals indicate that the red beds' provenance consisted primarily of granitic rocks. Microbrecciated granitic rock, basalt, and mylonite are additional types of detrital rock fragments found in the deposit. Comparison of the red-bed section with exposed Triassic-Jurassic red beds and modern continental sediments suggests that the Clubhouse Crossroads rocks were deposited in fluvial and alluvial-fan environments.

INTRODUCTION

Between January 1975 and May 1977, the U.S. Geological Survey drilled three deep stratigraphic test holes near Clubhouse Crossroads, Dorchester County, S. C. (fig. 1). Clubhouse Crossroads #1 and #2 penetrated a poorly consolidated Coastal Plain section and bottomed in a sequence of basalt flows. Clubhouse Crossroads #3 (CC#3) penetrated the basalt and bottomed in a sequence of well-indurated sedimentary red beds that is the subject of this report.

CC#3 is located at lat 32°54.18′ N., long 80°18.95′ W., in the south-central part of the Clubhouse Crossroads 7.5-minute quadrangle, 0.8 km northeast of Clubhouse Crossroads and about 40 km west-northwest of Charleston, S. C. CC#3 was drilled to a total depth of 1,152 m below a surface elevation of 6.7 m. Field descriptions of cuttings collected from the Coastal Plain section and of cuttings and cores recovered from the basalt and red-bed sections have been published by Schneider and others (1979). Geophysical logs were run only in the Coastal Plain section because the hole was blocked at the top of the basalt.

Acknowledgments.—Deep drilling and other phases of the investigations conducted by the U.S. Geological Survey near Charleston, S. C., were supported by the U.S. Nuclear Regulatory Commission, Office of Nuclear Research, under Agreement No. AT(49–25)–1000. Melodie Hess performed the X-ray diffraction analyses of the red-bed samples; R. Wayne Burrow and Sharon L. King assisted in other laboratory analyses of the samples. The Clubhouse Crossroads test holes were drilled by a U.S. Army Corps of Engineers team from the Mobile, Ala., district. We express our appreciation to the Westvaco Company for use of their land for drilling sites.

STRATIGRAPHY

The Clubhouse Crossroads test holes encountered three major subsurface stratigraphic sequences: Coastal Plain sediments of Late Cretaceous and Cenozoic age, subaerial basalt flows of Early Jurassic age, and sedimentary red beds of presumed Triassic and (or) Jurassic age (fig. 2). Stratigraphic data from studies of the basalt and the younger sediments are reviewed in this section as ancillary data for a discussion of the stratigraphy of the red-bed section.

Coastal Plain Section

The Upper Cretaceous and Cenozoic section in the Clubhouse Crossroads test holes ranges in thickness from 750 m in CC#1 to 776 and 775 m in CC#2 and #3,

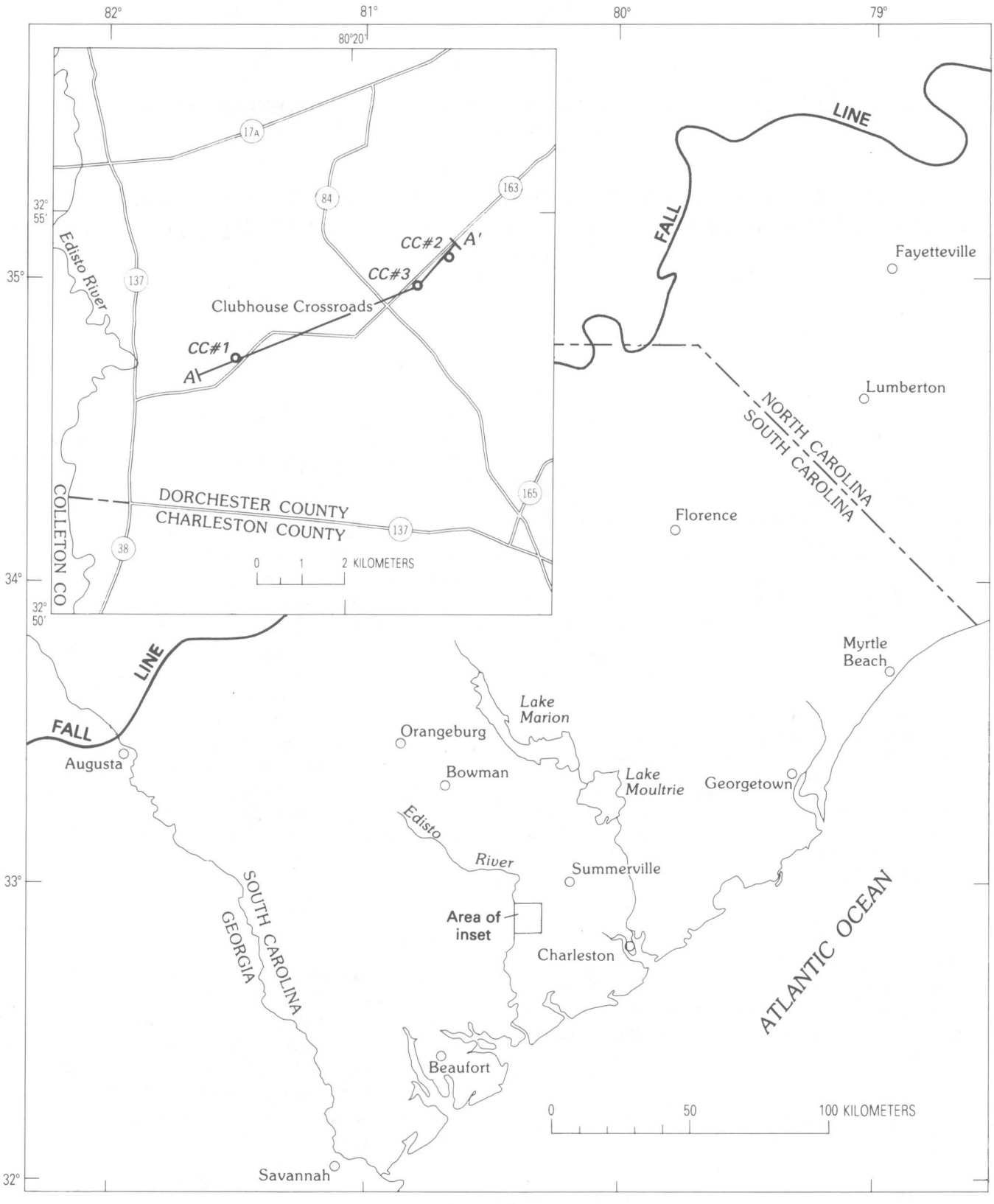

FIGURE 1.—Index map showing the location of the Clubhouse Crossroads stratigraphic test holes near Charleston, S. C. Cross section A–A' is shown in figure 2. Route numbers of roads are shown in inset.

respectively. The Coastal Plain section was continuously cored in CC#1, and preliminary reports on the lithostratigraphy (Gohn and others, 1977) and biostratigraphy (Hazel and others, 1977) of this section have been published. Early Late Cretaceous (late Cenomanian) fossils (Hazel and others, 1977; Hattner and Wise, 1980) in sediments 18 m above the top of the basalt provide a minimum age for the underlying rocks (fig. 2).

Basalt

The basalt unit contains numerous individual subaerial flows of massive to amygdaloidal, moderately to strongly altered basalt (Gottfried and others, 1983; Phillips, 1983). Both the top (775 m) and bottom (1,031 m) contacts of the 256-m-thick basalt unit were penetrated in CC#3 (fig. 2).

Whole-rock K-Ar ages for heavily altered samples of basalt from CC#1 (Gohn and others, 1977; Gottfried and others, 1977) initially suggested a middle Cretaceous age for the basalt flows. Subsequent whole-rock K-Ar and $^{40}Ar/^{39}Ar$ ages and paleomagnetic data for less altered samples from the other holes indicate an older and presently accepted Early Jurassic age (Gohn and others, 1978; Lanphere, 1983; Phillips, 1983). An initial geochemical study of the basalt by Gottfried and others (1977) provided insight into the age, origin, and inferred tectonic affinities of the basalt that have been supported by the additional radiometric ages and by additional geochemical and petrologic studies (Gottfried and others, 1983). The principal conclusions of the basalt studies to date are that the basalt in the Clubhouse Crossroads test holes has geochemical and inferred tectonic affinities with mafic igneous rocks from rifted passive continental margins in general and the eastern North American, lower Mesozoic tholeiitic diabases and basalts in particular.

A 2-m-thick bed of argillaceous red sandstone within the basalt sequence was cored at a depth of about 925 m, and other thin sedimentary beds may exist undetected in uncored sections of the basalt. The sandstone at 925 m contains abundant basalt fragments and quartz and minor microcline and perthite. The quartz and potassium feldspar suggest that the source of the sediment was not limited to the enclosing basalt. The presence of red sediments within the basalt section also suggests that the basalt has some temporal affinity with the underlying red-bed section.

Red-bed Section

In CC#3, 121 m of well-indurated sedimentary rocks were penetrated between depths of 1,031 and 1,152 m (fig. 3) before drilling was terminated because of mechanical problems. Of the 121 m of red beds, the top 23 m and the bottom 7.8 m were cored with moderate recovery, whereas only cuttings were obtained from the remaining 90.2 m.

From the top of the red-bed sequence at 1,031 m to a depth of about 1,070 m, the section consists of red-colored mudstone and smaller amounts of siltstone and

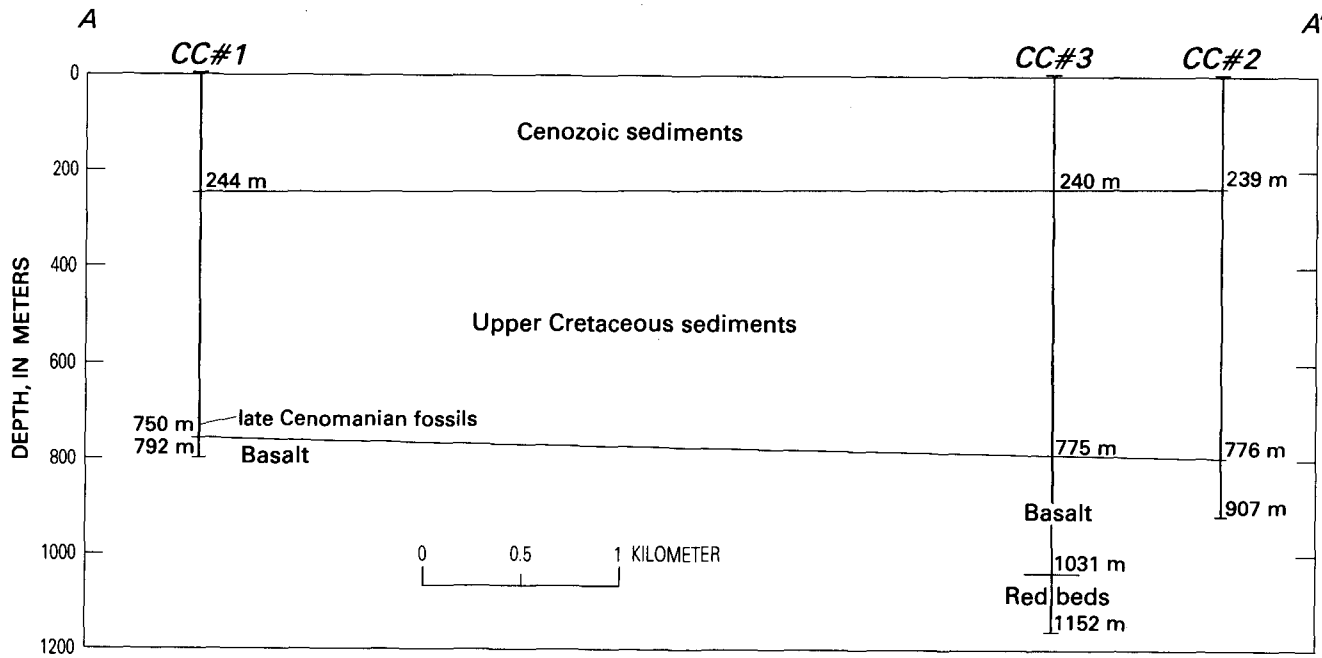

FIGURE 2.—Generalized stratigraphic cross section through the Clubhouse Crossroads test holes. Location of section shown in figure 1. Approximate altitudes of the tops of the drill holes are: 6 m (#1), 6 m (#2), and 7 m (#3).

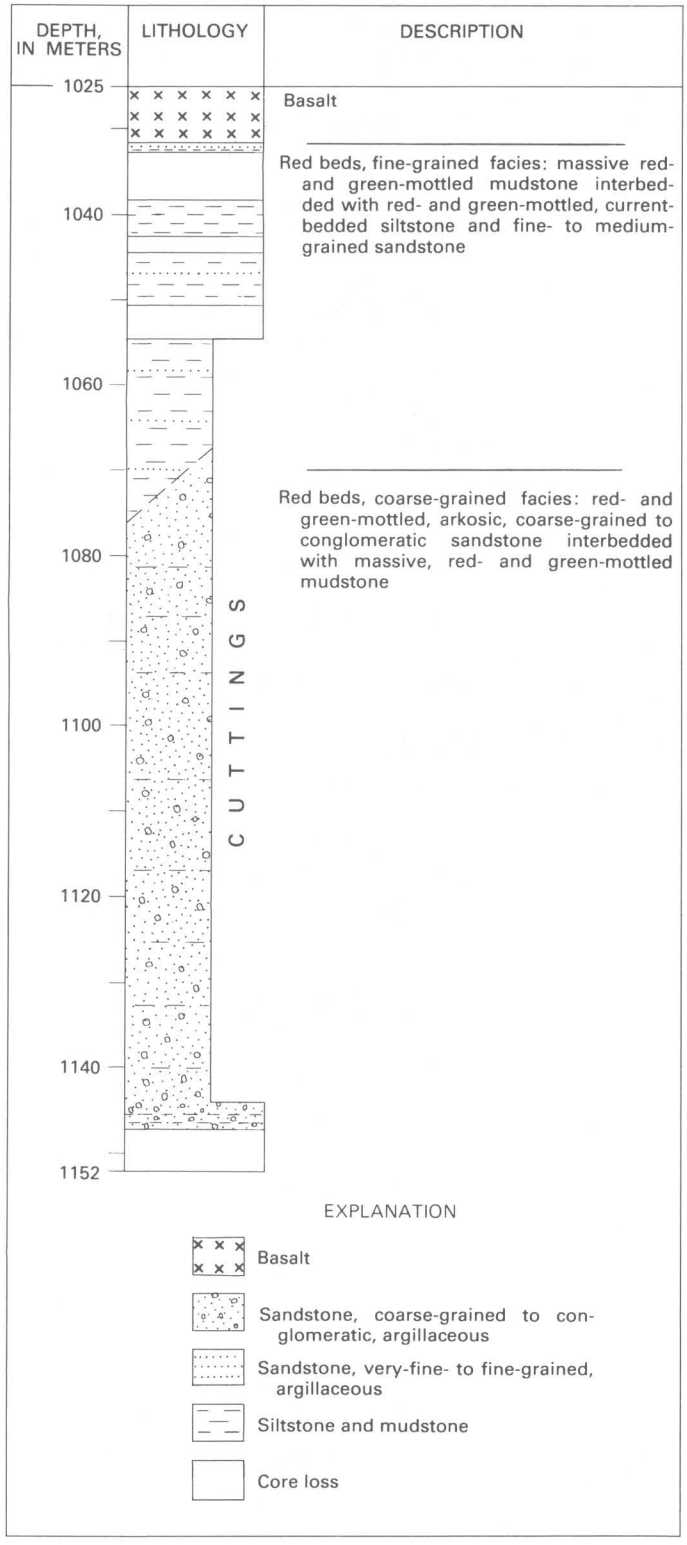

FIGURE 3.—Stratigraphic column for the lower Mesozoic(?) red-bed sequence in CC#3.

fine-grained sandstone. Cuttings from the interval between 1,066.8 and 1,075.9 m indicate that the lithology changes to coarse-grained or conglomeratic sandstone and minor amounts of red mudstone. Therefore, an upper fine-grained facies and a lower coarse-grained facies are defined, and the boundary is placed, somewhat arbitrarily, at 1,070 m.

Although plant debris was observed, no biostratigraphically useful macro- or microfossils were found in the red-bed cores. Nine samples processed for palynomorphs were barren (R. A. Christopher, oral commun., 1977). Age estimates for the red-bed sequence can be based, therefore, only upon the limits imposed by the age of the overlying unit and the uncertain regional lithostratigraphic correlation of this sequence with other similar rock units. The Early Jurassic age for the basalt imposes a minimum age limit of Early Jurassic for the red beds; an additional constraining age of early Late Cretaceous is supplied by the fossils in the basal Coastal Plain sediments. Gohn and others (1978) noted the lithologic similarity of the Clubhouse Crossroads red beds to the exposed fossiliferous Triassic and Jurassic Newark Group of the Eastern United States (Cornet and others, 1973; Cornet and Traverse, 1975) and the association of both exposed and buried rock sequences with radiometrically dated lower Mesozoic basaltic rocks. Although no age-specific data can be cited, these similarities provide some basis for provisionally assigning a Late Triassic and (or) Early Jurassic age to the red-bed sequence below the basalt in CC#3.

Lower Mesozoic red-bed sequences also are associated with basaltic rocks in fault-bounded basins below parts of the Georgia and Florida Coastal Plain and parts of the South Carolina Coastal Plain other than those discussed here (Marine and Siple, 1974; Popenoe and Zietz, 1977; Chowns and Williams, 1983; Daniels and others, 1983). Gohn and others (1978) interpreted the presence of lower Mesozoic basalt and lower Mesozoic(?) red beds in the Clubhouse Crossroads section to represent an extension of this lower Mesozoic(?) sub-Coastal Plain sequence into the Charleston, S. C., area.

DESCRIPTION OF THE RED-BED SECTION

Fine-grained Facies

LITHOLOGY AND PRIMARY SEDIMENTARY STRUCTURES

The fine-grained facies of the red-bed section consists of about 39 m of color-mottled mudstones, siltstones, and argillaceous very-fine- to medium-grained sandstones. Sandstones and siltstones are current-bedded; these beds are grouped in 1- to 2-m-thick sections concentrated near the top of the section (fig. 4). Mudstones typically occur in 1- to 4-m-thick sections. Carbonaceous plant debris is common as finely comminuted grains

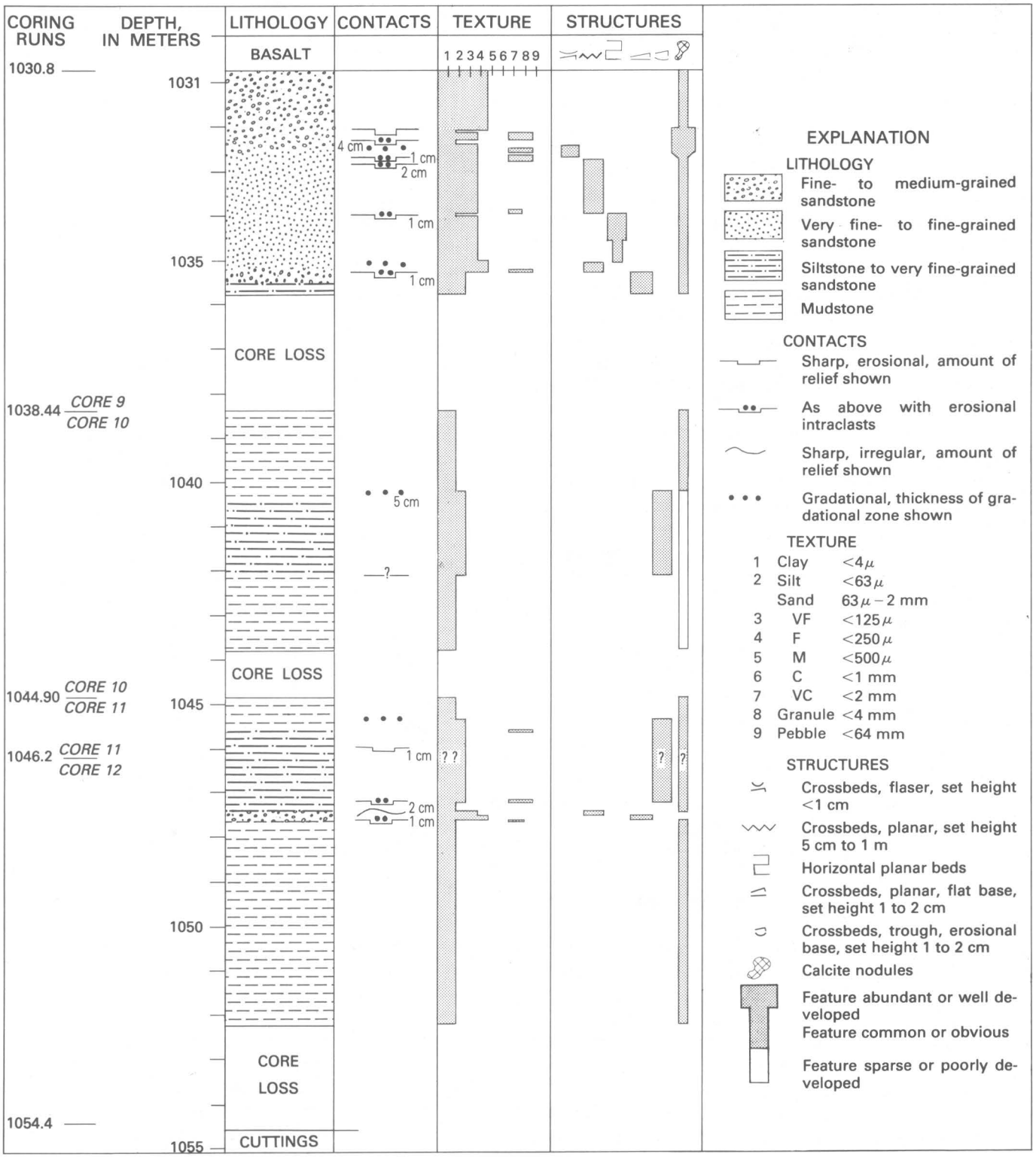

FIGURE 4. – Graphic log for the fine-grained facies of the red-bed section showing rock types, contact relationships, textures (determined from core with hand lens), and sedimentary structures.

along bedding and crossbedding in sandstones and as larger fragments throughout mudstones.

The sandstones and siltstones show a variety of small-scale (low-amplitude) primary sedimentary structures (figs. 4, 5). Cosets of trough crossbeds having individual set heights of less than 2 cm are typical of the siltstone; similarly small sets of planar cross lamination and flaser bedding, in addition to horizontal bedding, characterize the sandstones. A 1-m-thick set of planar crossbeds occurs in a fine-grained sandstone bed near the top of the section. The lower contacts of the sandstone beds typically are erosional and show several centimeters of relief. Mudstone and siltstone intraclasts and quartz granules overlie the erosional surfaces.

Near the top of the core, at about 1,032.0 to 1,032.8 m, there is a broad and irregular contact zone between an upper poorly sorted medium-grained sandstone and a lower sequence of fine-grained sandstone and mudstone that contains abundant calcite nodules (fig. 5*A*). Within the contact zone as seen in the core, the medium-grained sandstone occurs in irregular patches that are not vertically continuous with the main body of this rock type at the top of the section (figs. 4, 5*A*). These structures are interpreted to be soft-sediment deformation features, possibly ball-and-pillow structure, produced by sediment loading on a water-saturated, unstable substrate. As additional evidence of sediment loading, a possible flame structure occurs at the principal contact between the two units at 1032.4 m.

The mudstones in the fine-grained facies are typically massive, nonfissile, fine-grained rocks lacking primary stratification. However, numerous secondary features and zones of disrupted fabrics are common.

DIAGENETIC FEATURES

Calcite occurs in irregularly shaped nodules as large as 6 cm and irregular blebs as small as 1 mm. The nodules consist of microspar in submicroscopic to 100-μ grains. In thin sections, the nodule interiors show a wide range of organization; some have fine-grained rims and coarser grained interiors, whereas others have a translucent clotted fabric. Most nodules contain at least a few relict detrital grains or small patches of matrix. A continuum in the replacement of detrital material can be seen in the thin sections, from areas devoid of calcite to areas where detrital matrix and framework grains are partially replaced to areas showing well-formed nodules. The nodules occur in all lithologies, but the large nodules tend to be concentrated at specific horizons, particularly the calcareous interval near the top of the section (figs. 4, 5*A*).

The color-mottling of the red-bed section is a secondary feature that cross-cuts primary stratification. Most of the rocks of the fine-grained facies are grayish red (5*R*4/2, 10*R*4/2) or pale reddish brown (10*R*5/4) (Goddard and others, 1948). Non-red parts of the core are grayish green (10*GY*5/2, 5*G*5/2, 5*G*6/1) or grayish yellow green (5*GY*7/2). The occurrence of colors other than red is related to depositional and diagenetic features of the core. Green is found in halos around carbonized plant material in fine-grained beds (fig. 5*F*), in halos around calcite nodules, in sandstones containing fine-grained carbonized material (fig. 5*C*), and in mudstones that occur just below carbonaceous sandstones or as intraclasts within those sandstones (figs. 5*B*, *C*, *D*).

Curving, irregular slickensided surfaces pervade the mudstones and occur at all orientations, including horizontal (fig. 5*G*). The thicker mudstone sections of the core typically are broken and partly disaggregated due to breakage along the slickensided surfaces. The absence of a preferred orientation of the slickensides may have resulted from random particle orientation in the massive mudstone. These surfaces indicate that considerable mechanical deformation of the mudstone has occurred. This deformation may have been caused by lithostatic loading, by volumetric mineralogic changes during diagenesis, or by tectonic stress.

MINERALOGY AND PETROLOGY

Clay mineralogy.—Two distinct clay-mineral suites occur in the fine-grained facies (table 1). Samples above 1,035 m contain mostly interlayered illite-smectite, which was found to consist of 100 percent expandable layers and is, therefore, true montmorillonite. Only minor amounts of kaolinite-group minerals or chlorite and moderate amounts of illite are present. In samples from 1,039.24 m to 1,066.8 m, the dominant mineral is discrete illite with lesser amounts of illite-smectite and minor kaolinite and chlorite. The illite-smectite is of relatively low expandability (40 to 62 percent). The two clay-mineral suites correlate with specific rock types in the core. The upper suite, dominated by mixed-layer clay, is contained within sandstones, whereas the lower, illite-dominated suite is contained within mudstones and siltstones.

Sand mineralogy—light-mineral fraction.—The light-mineral fraction of sand samples (63–125 μ) isolated from sandstones of the fine-grained facies were studied by means of refractive index oils in grain mounts (table 2). In all studied samples, feldspar predominated over quartz; plagioclase was more abundant than potassium feldspar. Albite and oligoclase, in subequal amounts, were the only plagioclase minerals recognized.

Sandstone petrology.—Sandstones in the fine-grained facies are compositionally and texturally immature rocks characterized by high matrix contents and abundant unstable detrital grains, including polycrystalline quartz, feldspar, and quartz-feldspar lithic fragments

TABLE 1.—*Mineralogy of the <2-μ, clay-sized fraction of 23 samples from the red-bed section*

[Determined by X-ray diffraction. Samples were sieved and centrifuged after removal of the carbonate fraction by means of acetic acid. Semiquantitative determinations of the types and amounts of the minerals present follow the methods of Reynolds and Hower (1970) and Perry and Hower (1970). Tr, trace.]

Depth of sample below surface (m)	Constituent minerals (percent)			Percent expandable layers in illite-smectite	Lithology
	Kaolinite group	Illite	Mixed-layer illite-smectite		
1,032.74	0	50	50	100	sandstone
1,033.03	14	36	50	100	sandstone
1,033.80	0	10	90	100	sandstone
1,034.23	8	19	73	100	sandstone
1,039.23	18*	76	6	45	mudstone
1,040.03	20*	72	8	40	mudstone
1,040.45	15*	77	8	49	siltstone
1,042.00	8*	35	57	40	mudstone
1,043.25	14*	46	40	49	mudstone
1,047.02	19*	70	11	62	siltstone
1,050.94	14*	76	10	45	mudstone
1,051.78	16*	71	13	49	mudstone
1,052.03	20*	61	19	50	mudstone
1,052.20	13*	60	27	45	mudstone
1,060.7–1,066.8	14*	43	43	40	mudstone cuttings
1,094.2–1,104.0	7*	47	46	45	mudstone and conglomerate cuttings
1,122.3–1,131.4	62	38	Tr	--	granitic rock fragment
1,122.3–1,131.4	8*	77	15	40	mudstone cuttings
1,145.34	Tr	24	76	64	conglomerate
1,145.67	9*	20	71	90	mudstone
1,146.67	10*	40	50	82	conglomerate
1,146.95	Tr	11	89	93	conglomerate
1,147.40	10*	37	53	62	conglomerate

* Also contains chlorite.

(table 3). The framework grains are only moderately rounded. These rocks typically contain at least 10 percent argillaceous matrix, which consists of detrital mica and chlorite, fine-grained quartz and feldspar, and clay minerals, all of which are iron stained. Locally the detrital matrix is partly to completely replaced by secondary calcite.

Using the classification of Williams and others (1954, p. 292–293), we classified most of the studied sandstones as arkosic or feldspathic wackes. Sandstones containing abundant locally derived siltstone and mudstone intraclasts are lithic wackes (sample from 1,032.0 m, table 3).

Coarse-grained Facies

LITHOLOGY AND SEDIMENTARY STRUCTURES

The coarse-grained facies consists of 82 m of very poorly sorted, argillaceous, coarse-grained to conglomeratic sandstones and interbedded mudstones (figs. 6, 7). The sandstones in the cored interval are in 0.5- to 1.0-m-thick beds that alternate with 0.25- to 0.5-m-thick mudstones (fig. 6). The upper contacts of sandstone beds typically are sharp and slightly undulating; as much as 1 cm of relief is visible in the core. Basal contacts of sandstone beds are also sharp. However, recognizing exact basal contacts is difficult because the lower part of each sandstone bed has a high matrix content and resembles the underlying mudstone bed. Each basal sandstone contact is best delineated by the abundance of large calcite nodules in the upper part of the underlying mudstone (figs. 6, 7*D*). Sedimentary structures in the sandstone beds consist of inverse or inverse-to-normal size grading (fig. 6). Pebbles and granules occur in the center or top of each bed, whereas sand-sized grains and fine-grained matrix are distributed throughout each bed ("coarse-tail grading"). Other forms of stratification and ordered fabrics are difficult to discern but are probably present. For example, in figure 7*A*, the top half of the core shows faint inclined bedding (upper left to lower right), and there is a tendency toward subhorizontal alinement of the larger, flat clasts.

TABLE 2.—*Mineralogy of the light-mineral fraction of sand-sized grains (63–125 μ) from sandstones*

[Determined by means of refractive index oils and the central-focal-masking technique. 100 grains were counted per sample. Analyses are given as percentages]

Depth of sample below surface (m)	Quartz	Potassium feldspar	Albite	Oligoclase
1,032.7	45	15	29	11
1,033.0	23	4	26	47
1,033.8	25	4	17	54
1,034.2	24	6	45	25
1,047.0	14	2	32	52

Mudstones in the coarse-grained facies are similar to those in the fine-grained facies and typically are massive, red- and green-mottled rocks. No primary sedimentary structures were observed in the mudstones; their most obvious features are common calcite nodules and veinlets (figs. 7*C*, 7*D*).

Rocks of the coarse-grained facies are dominantly grayish red (5*R*4/2 or 10*R*4/2). Nonred color mottling is typically yellowish gray (5*Y*7/2) or pale greenish yellow (10*Y*8/2) and occurs within and around carbonate nodules and veinlets and plant debris.

MINERALOGY AND PETROLOGY

Clay mineralogy.—The clay-mineral suite found in samples between depths of 1,094.2 m and the bottom of the section differs from both clay suites found in the fine-grained facies (table 1). In the coarse-grained facies, mixed-layer illite-smectite of moderate expandability (64 to 93 percent) is the dominant mineral. Illite is common but in relatively smaller percentages than above; chlorite and a kaolinite-group mineral are present in amounts from trace to 10 percent. A kaolinite-group mineral (62 percent) and illite (38 percent) constitute the clay-sized fraction of a chip of granitic rock from the interval between 1,122.3 and 1,131.4 m. In that sample, these two minerals are interpreted to represent the principal alteration minerals of the feldspars in the granitic rock.

Sandstone petrology.—Argillaceous conglomeratic sandstones in the coarse-grained facies are extremely immature rocks characterized by high matrix content and large amounts of unstable polycrystalline grains, particularly quartz-feldspar lithic fragments (table 3;

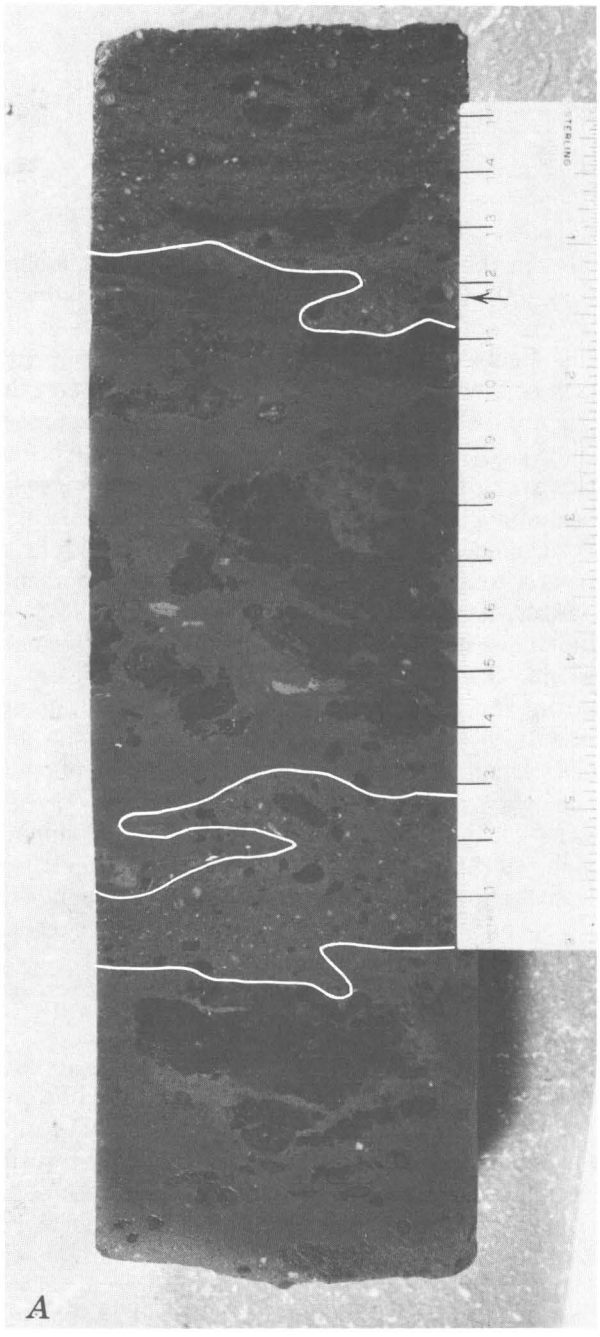

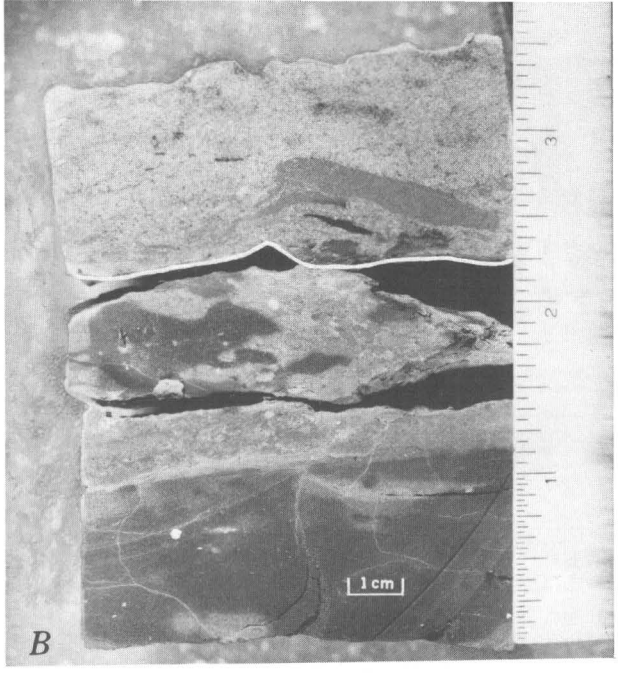

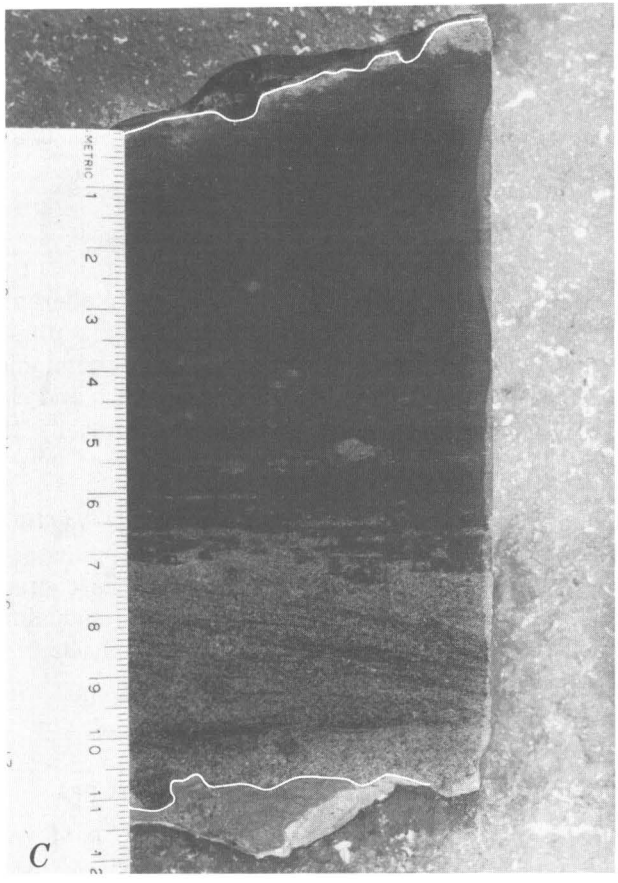

FIGURE 5.—Core segments showing sedimentary features of the fine-grained facies. *A*, Medium-grained sandstone overlies (upper highlighted contact) and is interlayered with (at base of ruler) argillaceous fine-grained sandstone. Lower irregular lens of the coarser lithology and a possible flame structure at the upper contact (arrow) may be due to sediment loading. Calcite nodules (dark) occur in both lithologies. Length of ruler is 15 cm. Upper contact is from a depth of about 1,032.1 m. *B*, Fine- to medium-grained sandstone (upper third of sample) contains numerous grayish-green (light) and grayish-red (dark) siltstone clasts. Sandstone overlies (highlighted contact) the eroded top of red- and green-mottled siltstone containing numerous 1- to 5-mm calcite nodules. Mottled siltstone grades downward into dominantly red siltstone that lacks nodules. Scale in inches; bar equals one cm. Base of sandstone is from depth of 1,035.30 m. *C*, Medium-grained, cross-laminated sandstone overlies the eroded top of grayish-green mudstone at lower highlighted contact (11-cm mark). Quartz granules and small mudstone clasts occur in base of sandstone, and carbonaceous debris is concentrated along cross laminations. Medium-grained sandstone grades upward into fine-grained sandstone with planar, horizontal laminations. Horizontal laminations are truncated at top along moderately dipping erosional surface that displays several hemispherical pits (burrows?). Dipping erosional surface is overlain by mudstone. Base of sample is from 1,047.7 m depth. Scale in centimeters.

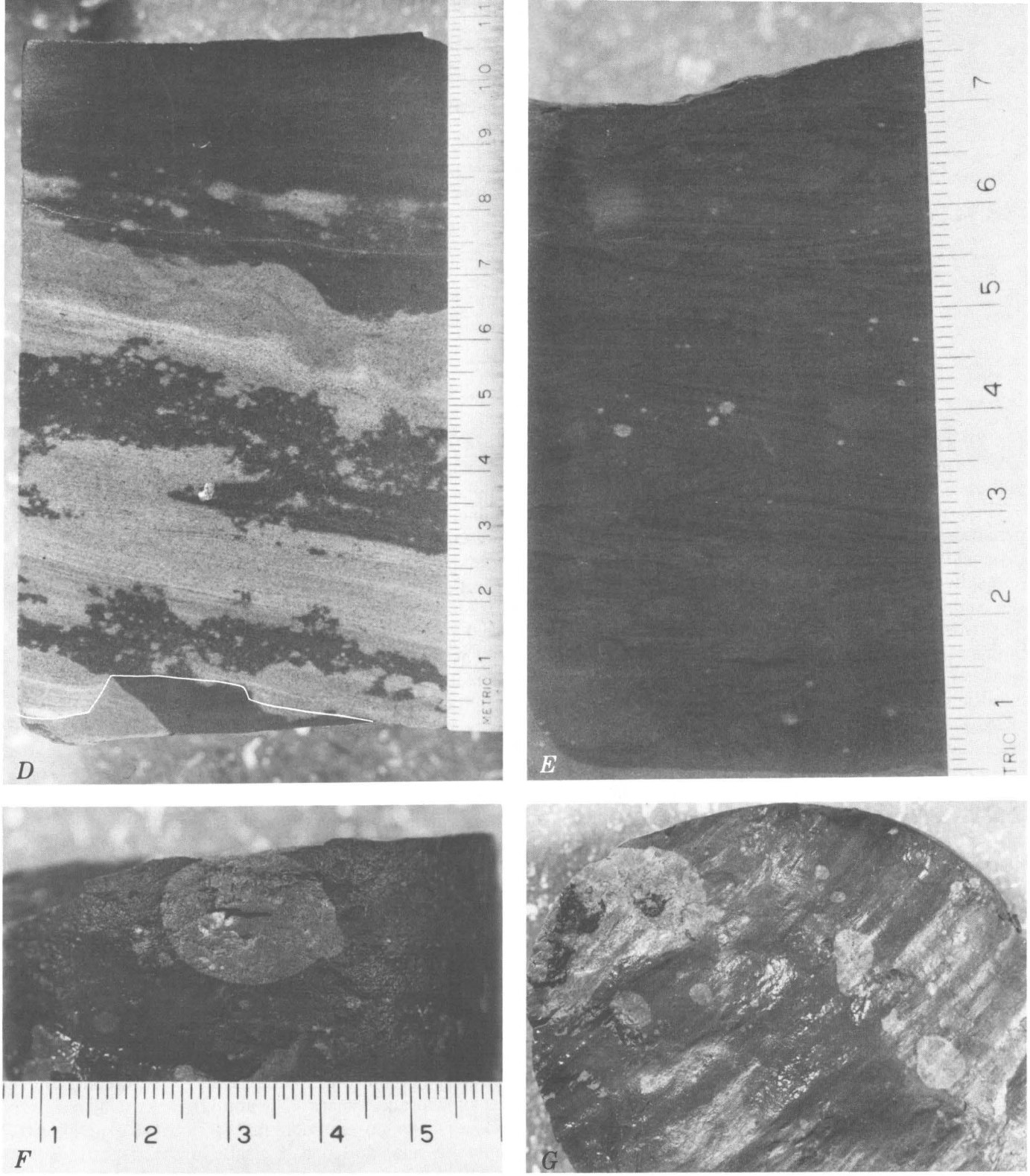

Figure 5.–Continued.–*D*, Contact (highlighted) between an upper color-mottled fine-grained sandstone and a lower color-mottled mudstone. The mudstone is mottled grayish red (dark) and grayish green (light). The sandstone is mottled grayish red and light olive gray and displays several small sets of planar to gently curving cross laminations. The bases of the sets and the sandstone-mudstone contact are erosional; the latter contact has about one centimeter of relief. Cross lamination is disrupted by the presence of thin mudstone clasts at about the 6-cm mark (foreset slumping?). The cross-laminated sandstone grades upward (above the 8-cm mark) into wavy laminated (not visible) red siltstone. Scale in centimeters. Base of sample is from a depth of 1,046.0 m. *E*, Dominantly red siltstone displaying faint sets of trough cross laminations. Scale in centimeters. Sample is from a depth of about 1,046.6 m. *F*, Grayish-green halo around carbonized plant fragment in dominantly grayish-red mudstone. Scale in centimeters. Sample from a depth of 1,050.8 m. *G*, Slickensided horizontal surface in mudstone from a depth of about 1,047.9 m (wet for photograph). Green mottles and carbonaceous material are also visible. Diameter of core is about 6.7 cm.

TABLE 3.—*Modal analyses (in percent) and petrologic classifications of sandstones from the red-bed section*

[250 grains were counted per slide. The sandstone classification is from Williams and others (1954, p. 292–293)]

Depth of sample (m)	Quartz			Feldspar			Lithic fragments			Matrix	Calcite	Other and unknown minerals	Sandstone classification
	Monocrystalline	Polycrystalline	Total	Potassium[1]	Plagioclase[2]	Total	Quartz-feldspar plutonic rock	Fine-grained sedimentary rock	Total				
Fine-grained facies:													
1,032.0	22.4	6.0	28.4	4.8	3.6	8.4	2.0	14.8	16.8	36.4	8.4	1.6	lithic wacke
1,035.3	24.0	15.6	39.6	12.0	5.6	17.6	12.4	1.2	13.6	13.6	14.8	.8	arkose or arkosic wacke
1,046.0	32.4	6.8	39.2	2.4	2.8	5.2	2.4	--	2.4	24.0	27.6	1.6	feldspathic wacke
Coarse-grained facies:													
1,144.7	3.2	4.8	8.0	2.4	8.0	10.4	65.6	--	65.6	10.4	5.2	.4	arkose
1,146.7	8.0	7.4	15.4	9.2	7.8	17.0	25.6	--	25.6	39.6	1.2	1.2	arkosic wacke
1,146.9	2.8	11.2	14.0	12.4	5.6	18.0	34.0	--	34.0	29.2	4.8	--	arkosic wacke

[1] Includes perthite.
[2] Includes myrmekite.

fig. 7). The conglomeratic sandstones are classified as arkoses or arkosic wackes (Williams and others, 1954, p. 292–293).

The quartz-feldspar lithic fragments represent granitic rocks composed of plagioclase, perthite, myrmekite, quartz, chlorite, epidote, opaque minerals, and sphene. Feldspar and quartz also compose most of the single-crystal sand-sized grains in the unit and display the same microstructures and types of alteration both as single grains and in granitic clasts (Gohn, 1983). Less common types of lithic fragments include altered basaltic rocks, mylonite, and microbreccia.

Sediment provenance.—Gohn (1983) discusses in detail the mineralogy and petrology of the rock fragments in the conglomeratic sandstones and concludes that the sediment source area consisted primarily of granitic plutonic rocks. Because the granitic clasts are contained within beds interpreted to have been deposited close to their source area (see following section on depositional environments), at least part of the pre-Mesozoic basement in the greater Charleston area must consist of these granitic rocks (Gohn, 1983). In addition, the microbreccia and mylonite clasts indicate that two styles (and times?) of deformation have affected the local basement. The basalt clasts indicate that a period of basaltic magmatism older than the one represented by the basalt above the red-bed section in CC#3 occurred in the area.

Nonopaque, heavy-mineral suites present in both the fine-grained and the coarse-grained units (table 4) are characterized by low diversity of mineral species and a dominance of epidote. Heavy-mineral fractions separated from samples at the top of the section (samples at 1,034.3 m and above) and at the bottom of the section (samples at 1,145.7 m and below) consist of more than 85 percent epidote. Zircon, tourmaline, apatite, biotite(?), chlorite, and garnet are the only other minerals present in significant amounts. The samples at 1,042 m and 1,047 m contain more diverse suites but are dominated by zircon (1,042 m) or phyllosilicates (1,047 m). Samples consisting of rotary cuttings between depths of 1,061 and 1,131 m contain more diverse suites than do the cored samples, although epidote and biotite (or stained chlorite) remain the most common minerals. Because the cuttings unavoidably contain cavings from higher stratigraphic levels, the relatively high mineralogic diversity of these samples was attributed to contamination. Epidote, zircon, tourmaline, white mica, and iron-stained chlorite were also seen as detrital grains in thin sections, as was detrital sphene. Chlorite flakes as large as 1.0 mm and white mica flakes as large as 0.2 mm were observed.

The low diversity of the heavy-mineral suites in the core samples is interpreted to indicate that the sediments were derived from a limited variety of source-rock types. In addition, the lack of dilution of this limited suite by other minerals from other sources suggests that the source rocks were close to the site of deposition. The abundance of epidote suggests that selective diagenetic removal of mineral species by intrastratal solution is not the cause of the low diversity.

In general, the composition of the heavy-mineral suite supports the interpretation made from the rock-fragment data that the source area was dominantly granitic. Epidote is a common to abundant secondary mineral within all types of rock fragments in the deposit, including the granitic clasts (Gohn, 1983), and its abundance as individual detrital grains in the heavy-mineral suite, therefore, is to be expected. The remainder of the observed heavy minerals that are common in the samples (zircon, tourmaline, apatite, mica, sphene) are all typical accessories in granitoid rocks. Chlorite was observed to be common in the detrital granodiorite, microbreccia, and basalt clasts in the deposit (Gohn, 1983).

DEPOSITIONAL ENVIRONMENTS

The depositional history and environments represented by the red-bed section are interpreted herein through comparison with sediments found in exposed early Mesozoic basins of the Eastern United States and through comparison with modern deposits in Israel and the Southwestern United States. The basis for comparison with the Mesozoic rocks is the general lithologic

TABLE 4.—*Percentages of heavy minerals in red-bed samples (very fine sand fraction)*

[The heavy minerals were studied in refractive index oils; 200–500 grains were counted per slide. Tr, noted but not counted or less than 1 percent. *, cuttings]

Depth of sample below surface (m)	1032.8	1033.0	1034.0	1034.3	1042.0	1047.0	1061–1067*	1094–1104*	1122–1131*	1145.7	1146.7	1147.0
Zircon	5	Tr	1	Tr	78	Tr	4	2	6	7	5	4
Tourmaline	5	0	Tr	Tr	1	Tr	14	5	3	Tr	0	Tr
Rutile	Tr	0	0	0	1	0	0	0	Tr	Tr	0	0
Apatite	1	1	3	Tr	4	2	19	10	7	0	0	0
Muscovite	Tr	0	0	2	Tr	36	7	5	5	Tr	0	0
Biotite	1	0	0	0	Tr	47	28	38	53	1	2	2
Epidote	86	98	95	97	5	11	14	31	16	90	92	94
Chlorite	Tr	1	Tr	Tr	1	3	0	2	5	Tr	0	0
Garnet	1	0	0	0	10	0	10	4	5	0	0	0
Sillimanite	0	0	0	0	0	Tr	1	0	0	0	0	0
Amphibole	0	0	0	0	0	0	2	3	0	Tr	Tr	0
Pyroxene	0	0	0	0	0	0	0	Tr	Tr	0	0	0

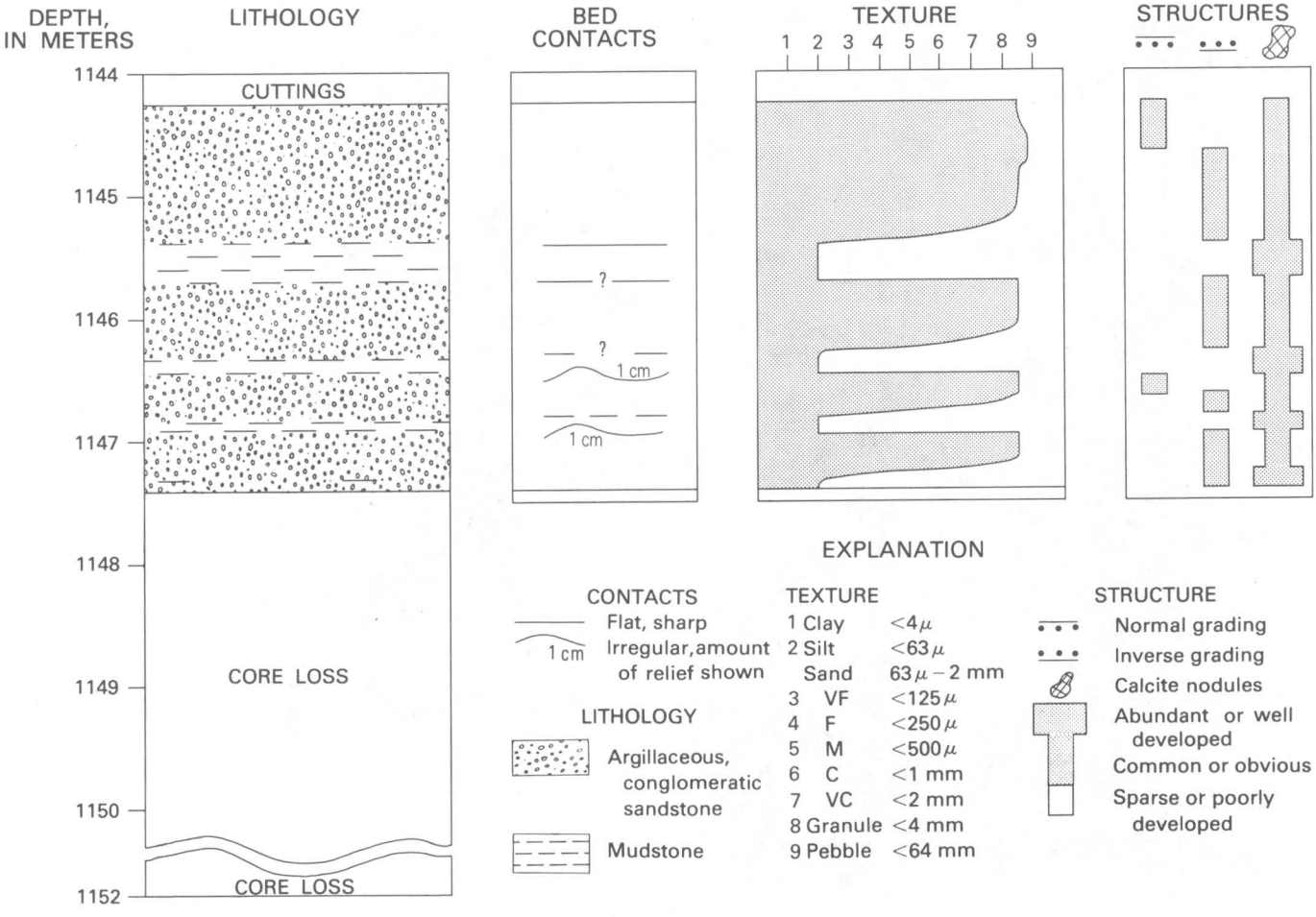

FIGURE 6.—Graphic log for the coarse-grained facies of the red-bed section showing rock types, contact relationships, textures (determined from core with hand lens), and sedimentary structures.

similarity and probable correlation of the Clubhouse Crossroads red-bed section with the exposed Triassic and Jurassic red beds. However, inherent limitations exist in studying a discontinuously cored section and comparing it with exposed sections. These limitations include the lack of information on the large-scale geometries of beds and the limited information on the vertical sequence of units and structures in the cores.

The exposed Triassic-Jurassic red beds and associated igneous rocks, and their tectonic setting, have been extensively researched. The general conclusion of most authors is that exposed Triassic-Jurassic sedimentary

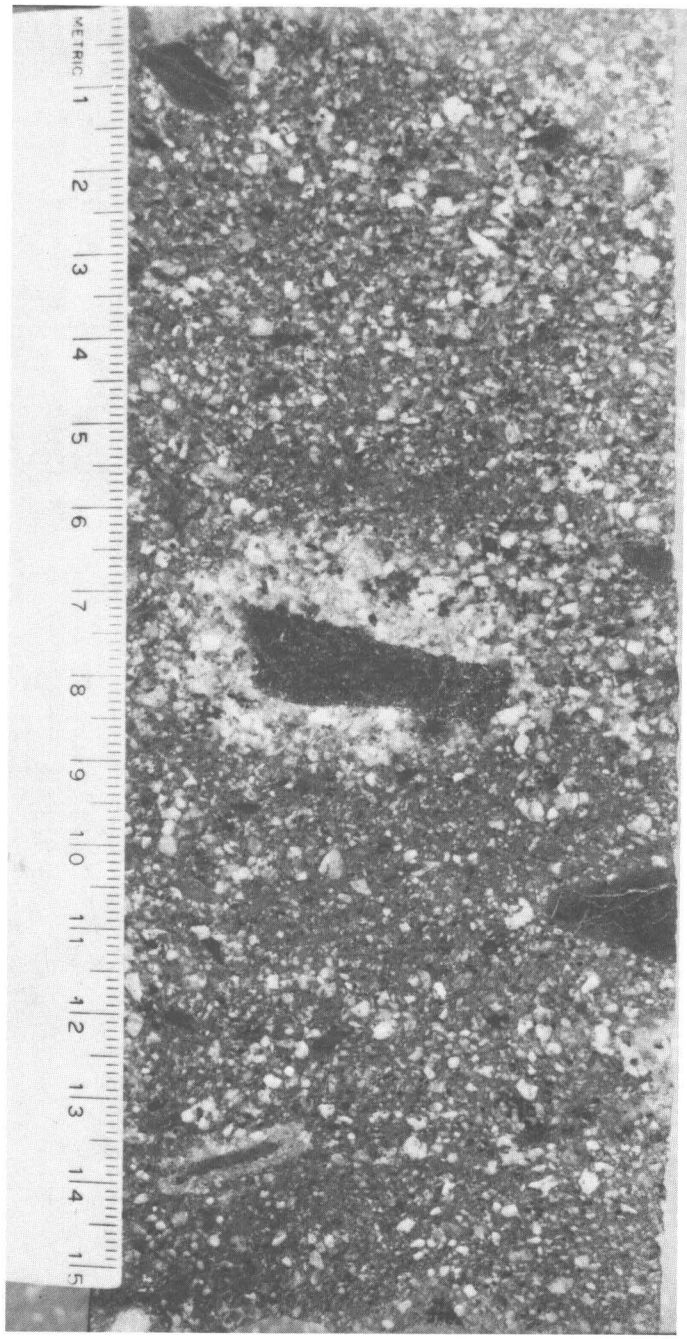

A

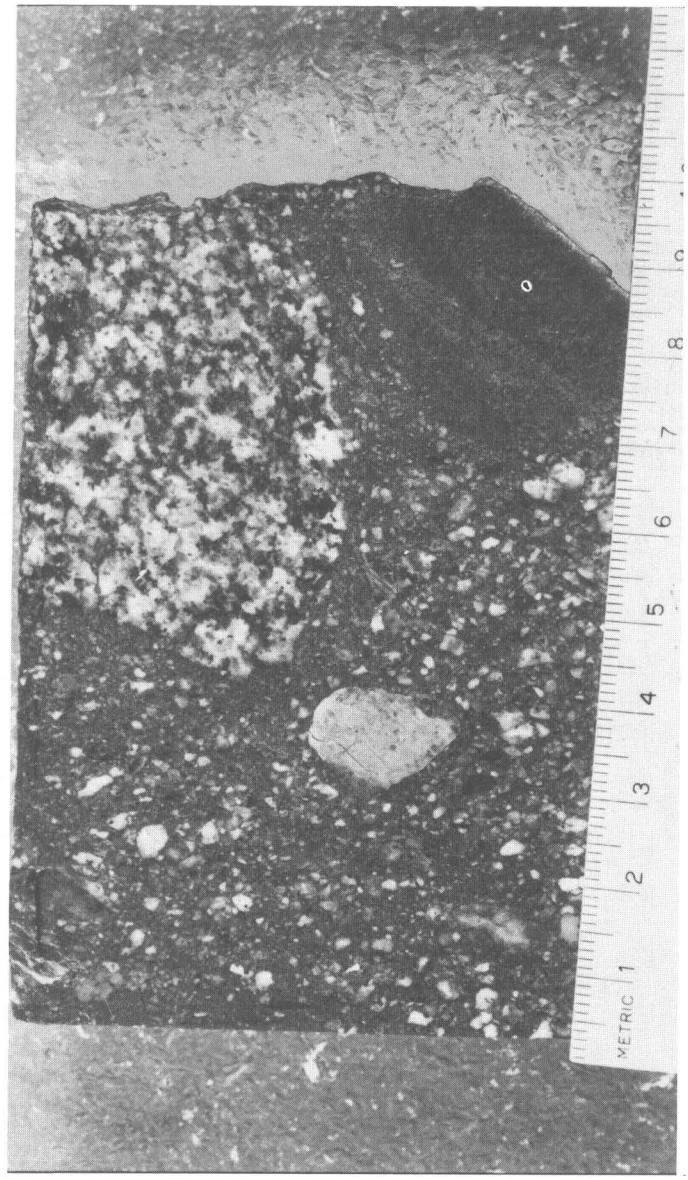

B

FIGURE 7.—Sedimentary features of the coarse-grained facies. *A*, Typical conglomeratic sandstone showing dominance of granitic (light-colored) debris in the sand- and granule-sized fraction. Large (dark) rock fragments are basalt. Note the poor sorting, local variations in matrix content, and possible inclined stratification (in upper third of sample). Sample from a depth of 1,144.7 m. Scale = 15 cm. *B*, Rock fragments in conglomeratic bed. Largest clast is granite. Dark fine-grained clast at upper right is basalt. Smaller light-colored clast near center is epidote-rich cataclastic rock. Note the poor sorting and lack of an ordered fabric. Core segment illustrates local inverse size grading of clasts. Sample from a depth of 1,144.6 m. Scale in cm. *C*, Red mudstone containing green-rimmed calcite nodules and veinlets. Sample from a depth of 1,145.5 m. Scale in cm. *D*, Slabbed section showing contact (highlighted) between sandstone bed and underlying mudstone containing large calcite nodules. Smaller white grains are granitic material in sandstone and calcite in mudstone. Sample from a depth of 1,146.8 m. Inverted scale in cm.

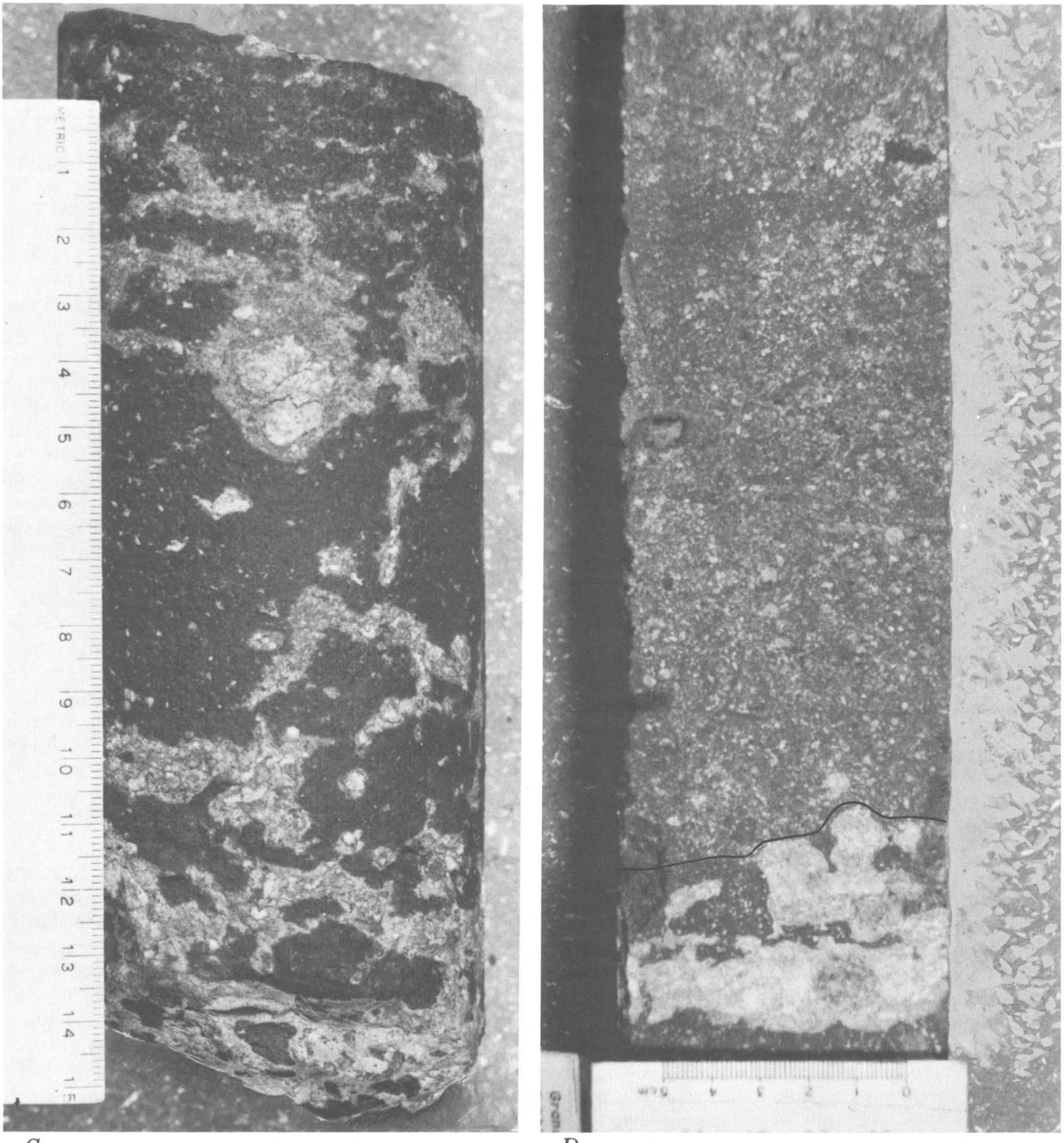

C *D*

FIGURE 7.–Continued.

rocks represent deposition in a variety of continental environments within closed rift basins (grabens). Interpreted environments typically include alluvial fans, braided and meandering streams and associated floodplains, and permanent and intermittent lakes (for example, Van Houten, 1969, 1980; Hubert and others, 1978; Manspeizer, 1980).

Fine-grained Facies

Generally, active sedimentary processes during deposition of the fine-grained facies were relatively low energy. This characteristic is suggested by the fine grain size of the facies as a whole, the moderate sorting of the sandstones, and the small amplitude of the cross stratification. However, several of the sandstones shown in figure 5 contain mudstone intraclasts, which illustrates that energy levels were occasionally high enough to erode partially consolidated, stable substrates. Rapid deposition on unstable, water-saturated substrates also occurred, as suggested by the deformed and intermixed lithologies shown in figure 5*A*. The flaser bedding (fig. 4) indicates that occasionally traction movement of sand alternated with settling of fine sediments from slack water. The absence of body fossils and the rare occurrence of possible biogenic structures (fig. 5*C*) suggest deposition in an environment lacking an abundant fauna.

The lithologies, sedimentary structures, and inferred depositional processes of the fine-grained facies in CC#3 are generally similar to those documented in sections of grayish-red mudstones and associated thin sandstones and siltstones in exposed sequences of Triassic-Jurassic rocks. These exposed rocks are generally interpreted to represent vertically accreting floodplain (overbank) deposits associated with fluvial systems or the distal ends of alluvial fans (Hubert and others, 1978, p. 104, figs. 18, 35; Manspeizer, 1980, p. 331, 334, 343).

However, some sedimentary features considered to be diagnostic of typical fluvial floodplain deposits (Reineck and Singh, 1975, p. 244–253) are absent in the fine-grained facies of the Clubhouse Crossroads section. Specifically, climbing-ripple lamination in sandstones and horizontal lamination in mudstones were not found. In addition, channel-sand deposits, a necessary element in fluvial systems, are not represented in the Clubhouse Crossroads core unless the rocks between 1,035.5 m and the top of the red-bed section (fig. 4) represent one or more truncated, relatively fine-grained, channel-bar deposits. Plant root casts, mud cracks, and raindrop impressions also were not observed in the mudstones. The absence of these features may indicate that the fine-grained facies was deposited in an environment somewhat different from the generally recognized fluvial floodplain environment associated with perennial streams.

Because of the massive character of the dominant mudstone and the paucity of structures and vertical sedimentary sequences typical of fluvial channel deposits, the fine-grained facies bears a close resemblance to sedimentary sequences in the semi-arid southern Basin and Range province, which have been deposited on the floors of dry closed basins (B. Houser, unpub. data, 1981). A dry-basin floor is defined topographically as the relatively flat, generally elongate axial part of a sediment-filled closed basin, flanked by alluvial fans or pediments and exclusive of the parts of the basin occupied by lakes or playas. A key element of the dry-basin floor environment is the high ratio of the volume of transported sediment to the volume of water available to transport this material. Gerson (1977) has described sediment transport by ephemeral streams in an analogous environment near the Dead Sea in Israel.

Dry-basin floors are environments that contain fine-grained alluvium derived from the distal parts of adjacent alluvial fans and also reworked from the basin floor itself. The sediment is transported episodically by overloaded streams during floods, chiefly in the form of slurries and less commonly as mudflows. Coarse-grained sediment (sand and gravel) is deposited in shallow channels on distal fan surfaces during waning flow or on the largely unchanneled surface of the basin floor in response either to waning flow or to the abrupt decrease in topographic gradient at the alluvial fan–basin floor boundary. After deposition of the coarser grained material, high concentrations of suspended fine-grained sediments remain in the transporting fluid. These sediments ultimately are deposited in beds with characteristics that are either typical of mudflow deposits or intermediate between those of mudflow deposits and water-lain sediments (Bull, 1963; Gerson, 1977).

Hence, the characteristic features of the sedimentary sequences of dry-basin floors are interpreted to result from deposition from slurries and differ from the more commonly noted sedimentary features of floodplains of perennial streams where water budgets are larger and sediment concentrations in channels and floodwaters are relatively lower. In particular, bimodal sorting into massive mudstone beds (lacking horizontal lamination) and thinner lenses of sand or gravel is diagnostic of dry-basin-floor sediments.

The similarity of the sedimentary features seen in the fine-grained facies of the core to those outlined above for deposits of dry-basin floors suggests that this may have been the depositional environment of the fine-grained facies. In addition, the calcite nodules (fig. 5) in the core resemble features in upper Paleozoic and Mesozoic continental rocks that are typically interpreted to represent pedogenic carbonate deposits (caliche) (Van Houten, 1973; Marine and Siple, 1974; Steel, 1974;

Jensen, 1975; Hubert, 1977). Paleosol horizons marked by caliche zones are also common in dry-basin floors of the semi-arid Southwestern United States and are taken as evidence of significantly long periods of subaerial exposure between depositional events, during which time little erosion occurred. Caliche in the Clubhouse Crossroads red beds is incipiently developed (mostly type 1 of Steel, 1974; stage 1 of Hubert, 1977) and consists only of scattered nodules and calcite cement in sandstones. Laterally continuous nodular limestone layers and laminar, brecciated, or pisolitic limestone are absent.

Also compatible with the interpretation of a continental (fluvial-alluvial) environment is the dominantly red color of the fine-grained and coarse-grained facies, which suggests oxidation of these rocks in a subaerial setting except where local reducing conditions (producing colors other than red) were maintained by the presence of plant material (fig. 5*C*, *F*) or were produced by the calcification process.

Coarse-grained Facies

Beds of the coarse-grained facies represent deposition by debris flow (sediment-gravity flow) rather than by water-gravity flow. As discussed by Middleton and Hampton (1973), debris flows are cohesive, high-density mixtures of water, mud, and coarser grained sediment that possess a finite yield strength and buoyancy and that move sluggishly downslope under the influence of gravity. Characteristics of the conglomeratic sandstones of the coarse-grained facies that suggest debris flow include inverse and inverse-to-normal size grading of clasts within beds, matrix-supported textures, limited alinement of large and perhaps small clasts in a fine-grained matrix (indicating shearing of a cohesive sediment-water mixture), and very poor sorting (figs. 6, 7). Although mudstones in the coarse-grained facies show few primary features, they may represent mud flows that moved in a manner similar to the debris flows and hence may be genetically related to the mudstones of the fine-grained facies.

The identification of debris-flow deposits in a sequence of continental rocks is evidence for the interpretation of an alluvial-fan environment. Rust (1979) concluded, in a summary discussion of alluvial fans (p. 12), "that with few exceptions debris flow deposits characterize alluvial fans and can be used (together with other criteria) to recognize ancient fan deposits * * *" although other depositional processes do occur on fans. As examples, exposed sequences of Triassic and Jurassic conglomerates and associated rocks displaying many of the same structures and textures as the coarse-grained facies of the Clubhouse Crossroads section have been interpreted as alluvial fan deposits (Randazzo and others, 1970; Cloos and Pettijohn, 1973; Lindholm and others, 1979; Hubert and others, 1978). Additionally, in modern continental settings, the natural conditions observed to promote debris flow are typical of alluvial fans, particularly those in semi-arid climates (Bull, 1972). Our interpretation is, therefore, that the coarse-grained facies of the Clubhouse Crossroads red beds represents deposition on an ancient alluvial fan and probably, on the basis of the lack of boulders and the proportion of fine-grained beds in the deposit, on the medial to distal part of the fan.

Tectonic Implications

Several corollaries follow from the interpretation of alluvial-fan and related sedimentary environments for the Clubhouse Crossroads red-bed section. Firstly, debris flow (and mud flows) do not transport sediment for long distances. An extremely long transport distance of over 20 km for a 1941 Wrightwood, Calif., flow reported by Sharp and Nobles (1953) can probably be considered an upper limit for movement by a single debris flow. Accordingly, as discussed above, detrital lithic fragments and other sediments in the conglomeratic sandstones can be considered representative of at least some of the pre-Mesozoic rocks underlying the Charleston-Summerville area.

Secondly, late Cenozoic alluvial fans in the Western United States (for example, Hooke, 1967, figs. 2, 3; Bull, 1972, p. 77–81), inferred lower Mesozoic alluvial-fan deposits in the Eastern United States (for example, Hubert and others, 1978, p. 9; Lindholm and others, 1979; Ratcliffe, 1980, p. 288–292; Manspeizer, 1980), and other examples of alluvial-fan deposits (for example, Rust, 1979) are spatially associated with faulted basin margins. In these cases, near-surface faulting produced the topographic relief necessary for accumulation of the alluvial-fan deposits. Therefore, by analogy, the coarse-grained facies of the Clubhouse Crossroads red beds probably records deposition in an area of formerly great topographic relief, which was perhaps produced by faulting. This tentative conclusion, based on sediment-facies analysis, is consistent with interpretations, from seismic surveys, that locally thick (up to 1 km) or thin sequences of red beds occur in a faulted horst-and-graben terrane below Jurassic basalt and (or) Cretaceous sediments in the Charleston-Summerville area (Talwani, 1977; Ackermann, 1983; Hamilton and others, 1983; Schilt and others, 1983).

REFERENCES CITED

Ackermann, H. D., 1983, Seismic-refraction study in the area of the Charleston, South Carolina, 1886 earthquake, *in* Gohn, G. S., ed., Studies related to the Charleston, South Carolina, earthquake of 1886–Tectonics and seismicity: U.S. Geological Survey Professional Paper 1313, p. F1–F20.

Bull, W. B., 1963, Alluvial-fan deposits in western Fresno County, California: Journal of Geology, v. 71, no. 2, p. 243–251.

———1972, Recognition of alluvial-fan deposits in the stratigraphic record, *in* Rigby, J. K., and Hamblin, W. K., eds., Recognition of ancient sedimentary environments: Society of Economic Paleontologists and Mineralogists Special Publication no. 16, p. 63–83.

Chowns, T. M., and Williams, C. T., 1983, Pre-Cretaceous rocks beneath the Georgia Coastal Plain–Regional implications, *in* Gohn, G. S., ed., Studies related to the Charleston, South Carolina, earthquake of 1886–Tectonics and seismicity: U.S. Geological Survey Professional Paper 1313, p. L1–L42.

Cloos, Ernst, and Pettijohn, F. J., 1973, Southern border of the Triassic basin, west of York, Pennsylvania: Fault or overlap?: Geological Society of America Bulletin, v. 84, no. 2, p. 523–535.

Cornet, Bruce, and Traverse, Alfred, 1975, Palynological contributions to the chronology and stratigraphy of the Hartford basin in Connecticut and Massachusetts: Geoscience and Man, v. 11, p. 1–33.

Cornet, Bruce, Traverse, Alfred, and McDonald, N. G., 1973, Fossil spores, pollen, and fishes from Connecticut indicate Early Jurassic age for part of the Newark Group: Science, v. 182, no. 4118, p. 1243–1247.

Daniels, D. L., Zietz, Isidore, and Popenoe, Peter, 1983, Distribution of subsurface lower Mesozoic rocks in the Southeastern United States as interpreted from regional aeromagnetic and gravity maps, *in* Gohn, G. S., ed., Studies related to the Charleston, South Carolina, earthquake of 1886–Tectonics and seismicity: U.S. Geological Survey Professional Paper 1313, p. K1–K24.

Gerson, Ran, 1977, Sediment transport for desert watersheds in erodible materials: Earth Surface Processes, v. 2, no. 4, p. 343–361.

Goddard, E. N., and others, 1948, Rock-color chart: Washington, D.C., National Research Council, 6 p. (republished by Geological Society of America, 1951; reprinted 1975).

Gohn, G. S., 1983, Geology of the basement rocks near Charleston, South Carolina–Data from detrital rock fragments in lower Mesozoic(?) rocks in Clubhouse Crossroads test hole #3, *in* Gohn, G. S., ed., Studies related to the Charleston, South Carolina, earthquake of 1886–Tectonics and seismicity: U.S. Geological Survey Professional Paper 1313, p. E1–E22.

Gohn, G. S., Gottfried, David, Lanphere, M. A., and Higgins, B. B., 1978, Regional implications of Triassic or Jurassic age for basalt and sedimentary red beds in the South Carolina Coastal Plain: Science, v. 202, no. 4370, p. 887–890.

Gohn, G. S., Higgins, B. B., Smith, C. C., and Owens, J. P., 1977, Lithostratigraphy of the deep corehole (Clubhouse Crossroads corehole 1) near Charleston, South Carolina, *in* Rankin, D. W., ed., Studies related to the Charleston, South Carolina, earthquake of 1886–A preliminary report: U.S. Geological Survey Professional Paper 1028, p. 59–70.

Gottfried, David, Annell, C. S., and Byerly, G. R., 1983, Geochemistry and tectonic significance of subsurface basalts near Charleston, South Carolina; Clubhouse Crossroads test holes #2 and #3, *in* Gohn, G. S., ed., Studies related to the Charleston, South Carolina, earthquake of 1886–Tectonics and seismicity: U.S. Geological Survey Professional Paper 1313, p. A1–A19.

Gottfried, David, Annell, C. S., and Schwarz, L. J., 1977, Geochemistry of subsurface basalt from the deep corehole (Clubhouse Crossroads corehole 1) near Charleston, South Carolina–Magma type and tectonic implications, *in* Rankin, D. W., ed., Studies related to the Charleston, South Carolina, earthquake of 1886–A preliminary report: U.S. Geological Survey Professional Paper 1028, p. 91–113.

Hamilton, R. M., Behrendt, J. C., and Ackermann, H. D., 1983, Land multichannel seismic-reflection evidence for tectonic features near Charleston, South Carolina, *in* Gohn, G. S. ed., Studies related to the Charleston, South Carolina, earthquake of 1886–Tectonics and seismicity: U.S. Geological Survey Professional Paper 1313, p. I1–I18.

Hattner, J. G., and Wise, S. W., Jr., 1980, Upper Cretaceous calcareous nannofossil biostratigraphy of South Carolina: South Carolina Geology, v. 24, no. 2, p. 41–117.

Hazel, J. E., Bybell, L. M., Christopher, R. A., Frederiksen, N. O., May, F. E., McLean, D. M., Poore, R. Z., Smith, C. C., Sohl, N. F., Valentine, P. C., and Witmer, R. J., 1977, Biostratigraphy of the deep corehole (Clubhouse Crossroads corehole 1) near Charleston, South Carolina, *in* Rankin, D. W., ed., Studies related to the Charleston, South Carolina, earthquake of 1886–A preliminary report: U.S. Geological Survey Professional Paper 1028, p. 71–89.

Hooke, R. L., 1967, Processes on arid-region alluvial fans: Journal of Geology, v. 75, no. 4, p. 438–460.

Hubert, J. F., 1977, Paleosol caliche in the New Haven Arkose, Connecticut; Record of semiaridity in Late Triassic-Early Jurassic time: Geology, v. 5, no. 5, p. 302–304.

Hubert, J. F., Reed, A. A., Dowdall, W. L., and Gilchrist, J. M., 1978, Guide to the redbeds of central Connecticut: 1978 field trip, eastern section of Society of Economic Paleontologists and Mineralogists, Amherst, Massachusetts, 129 p.

Jensen, L. R., 1975, Late Triassic redbeds, Kingsport area: Maritime Sediments, v. 11, no. 2, p. 77–81.

Lanphere, M. A., 1983, $^{40}Ar/^{39}Ar$ ages of basalt from Clubhouse Crossroads test hole #2, near Charleston, South Carolina, *in* Gohn, G. S., ed., Studies related to the Charleston, South Carolina, earthquake of 1886–Tectonics and seismicity: U.S. Geological Survey Professional Paper 1313, p. B1–B8.

Lindholm, R. C., Hazlett, J. M., and Fagin, S. W., 1979, Petrology of Triassic-Jurassic conglomerates in the Culpeper basin, Virginia: Journal of Sedimentary Petrology, v. 49, no. 4, p. 1245–1261.

Manspeizer, Warren, 1980, Rift tectonics inferred from volcanic and clastic structures, *in* Manspeizer, Warren, ed., Field studies of New Jersey geology and guide to field trips: 52nd Annual Meeting of the New York State Geological Association, Rutgers University, Newark, 1980, p. 314–350.

Marine, I. W., and Siple, G. E., 1974, Buried Triassic basin in the central Savannah River area, South Carolina and Georgia: Geological Society of America Bulletin, v. 85, no. 2, p. 311–320.

Middleton, G. V., and Hampton, M. A., 1973, Sediment gravity flows: Mechanics of flow and deposition, *in* Middleton, G. V., and Bouma, A. H., co-chairmen, Turbidites and deep-water sedimentation: Lecture notes for Short Course, Pacific section, Society of Economic Paleontologists and Mineralogists, Anaheim, 1973, p. 1–38.

Perry, Ed, and Hower, John, 1970, Burial diagenesis of Gulf Coast pelitic sediments: Clays and Clay Minerals, v. 18, no. 3, p. 165–177.

Phillips, J. D., 1983, Paleomagnetic investigations of the Clubhouse Crossroads basalt, *in* Gohn, G. S., ed., Studies related to the Charleston, South Carolina, earthquake of 1886–Tectonics and seismicity: U.S. Geological Survey Professional Paper 1313, p. C1–C18.

Popenoe, Peter, and Zietz, Isidore, 1977, The nature of the geophysical basement beneath the Coastal Plain of South Carolina and northeastern Georgia, *in* Rankin, D. W., ed., Studies related to the Charleston, South Carolina, earthquake of 1886–A preliminary report: U.S. Geological Survey Professional Paper 1028, p. 119–137.

Randazzo, A. F., Swe, Win, and Wheeler, W. H., 1970, A study of tectonic influence on Triassic sedimentation–the Wadesboro basin, central Piedmont: Journal of Sedimentary Petrology, v. 40, no. 3, p. 998–1006.

Ratcliffe, N. M., 1980, Brittle faults (Ramapo fault) and phyllonitic ductile shear zones in the basement rocks of the Ramapo seismic zones, New York and New Jersey, and their relationship to current seismicity, *in* Manspeizer, Warren, ed., Field studies of New Jersey geology and guide to field trips: 52nd Annual Meeting of the New York State Geological Association, Rutgers University, Newark, New Jersey, 1980, p. 278–311.

Reineck, H.-E., and Singh, I. B., 1975, Depositional sedimentary environments, with reference to terrigenous clastics: New York, Springer-Verlag, 439 p.

Reynolds, R. C., and Hower, John, 1970, The nature of interlayering in mixed-layer illite-montmorillonites: Clays and Clay Minerals, v. 18, no. 1, p. 25–36.

Rust, B. R., 1979, Coarse alluvial deposits, *in* Walker, R. G., ed., Facies models: Geoscience Canada Reprint Series 1, Geological Association of Canada, p. 9–21.

Schilt, F. S., Brown, L. D., Oliver, J. E., and Kaufman, Sidney, 1983, Subsurface structure near Charleston, South Carolina: Results of COCORP reflection profiling in the Atlantic Coastal Plain, *in* Gohn, G. S., ed., Studies related to the Charleston, South Carolina, earthquake of 1886–Tectonics and seismicity: U.S. Geological Survey Professional Paper 1313, p. H1–H19.

Schneider, R. R., Gohn, G. S., Force, L. M., and King, S. L., 1979, Lithologic log for a deep stratigraphic test hole, Clubhouse Crossroads No. 3, Dorchester County, South Carolina: U.S. Geological Survey Open-File Report 79-449, 23 p.

Sharp, R. P., and Nobles, L. H., 1953, Mudflow of 1941 at Wrightwood, southern California: Geological Society of America Bulletin, v. 64, no. 5, p. 547–560.

Steel, R. J., 1974, Cornstone (fossil caliche)–Its origin, stratigraphic and sedimentological importance in the New Red Sandstone, western Scotland: Journal of Geology, v. 82, no. 3, p. 351–369.

Talwani, Pradeep, 1977, A preliminary shallow crustal model between Columbia and Charleston, South Carolina, determined from quarry blast monitoring and other geophysical data, *in* Rankin, D. W., ed., Studies related to the Charleston, South Carolina, earthquake of 1886–A preliminary report: U.S. Geological Survey Professional Paper 1028, p. 177–187.

Van Houten, F. B., 1969, Late Triassic Newark Group, north-central New Jersey and adjacent Pennsylvania and New York, *in* Subitzky, Seymour, ed., Geology of selected areas in New Jersey and eastern Pennsylvania and guidebook of excursions: New Brunswick, New Jersey, Rutgers University Press, p. 314–347.

———1973, Origin of red beds, a review–1961–1972, *in* Donath, F. A., Stehli, F. G., and Wetherill, G. W., eds., Annual Review of Earth and Planetary Sciences, v. 1: Palo Alto, Annual Reviews, Inc., p. 39–61.

———1980, Late Triassic part of Newark Supergroup, Delaware River section, west central New Jersey, *in* Manspeizer, Warren, ed., Field studies of New Jersey geology and guide to field trips: 52nd Annual Meeting of the New York State Geological Association, Rutgers University, Newark, New Jersey, 1980, p. 264–276.

Williams, Howel, Turner, F. J., and Gilbert, C. M., 1954, Petrography–An introduction to the study of rocks in thin sections: San Francisco, W. H. Freeman and Company, 406 p.

Geology of the Basement Rocks Near Charleston, South Carolina—Data from Detrital Rock Fragments in Lower Mesozoic(?) Rocks in Clubhouse Crossroads Test Hole #3

By GREGORY S. GOHN

STUDIES RELATED TO THE CHARLESTON, SOUTH CAROLINA, EARTHQUAKE OF 1886—TECTONICS AND SEISMICITY

GEOLOGICAL SURVEY PROFESSIONAL PAPER 1313-E

UNITED STATES GOVERNMENT PRINTING OFFICE, WASHINGTON: 1983

CONTENTS

ILLUSTRATIONS

TABLES

STUDIES RELATED TO THE CHARLESTON, SOUTH CAROLINA, EARTHQUAKE OF 1886—TECTONICS AND SEISMICITY

GEOLOGY OF THE BASEMENT ROCKS NEAR CHARLESTON, SOUTH CAROLINA—DATA FROM DETRITAL ROCK FRAGMENTS IN LOWER MESOZOIC(?) ROCKS IN CLUBHOUSE CROSSROADS TEST HOLE #3

By GREGORY S. GOHN

ABSTRACT

Detrital rock fragments in conglomeratic lower Mesozoic(?) sedimentary rocks in Clubhouse Crossroads drill hole #3 are the only material available for direct geologic study of the pre-Mesozoic crystalline basement in the Charleston, S. C., area. No drill holes in the area have penetrated the pre-Mesozoic section. Many lines of evidence from the core (textures, mineralogy, sedimentary structures) and from local geophysical surveys (basement-surface configuration) suggest that the source area for these compositionally immature, poorly sorted conglomeratic sediments was proximal to their site of deposition.

Four types of basement rocks occur as detrital clasts; in decreasing order of abundance, these types are granodiorite and similar plutonic rocks, microbreccia, basalt, and mylonite. Plutonic igneous-rock fragments grouped as granodiorite have apparent compositions ranging from tonalite or granodiorite to granite. Alteration of the granodiorite has occurred, and the present mineralogy is typically saussuritized plagioclase, perthite, quartz, chlorite, opaque minerals, epidote, and sphene. Microbreccia clasts have a protolith that closely resembles the granodiorite clasts, but the microbreccia shows considerable comminution of grains, fracturing, and secondary epidote, chlorite, quartz, and zeolite(?) mineralization in veinlets. Basalt clasts in the deposit have also been mineralogically altered to saussuritized plagioclase, chlorite, epidote, and other secondary minerals, but they do not show obvious effects of penetrative deformation. Mylonite clasts have a mineralogy similar to that of the granodiorite clasts, but the mylonite clasts have been strongly deformed, and their texture is dominated by fluxion structure and porphyroclasts.

Inferences about the geologic history represented by these detrital rock fragments can be made from the petrologic data. However, the lack of data on the larger geometries of the rock units involved and on their relative and absolute ages limits these interpretations. At least one episode of granodiorite intrusion into an unknown sequence of host rocks has been documented, as has an episode of basaltic volcanism or shallow plutonism. The basalt cannot be temporally related to the younger lower Mesozoic basalt encountered higher in the drill hole. The mylonite and microbreccia may represent relatively ductile and relatively brittle deformation, respectively, within a single fault zone, or they may represent contrasting styles of deformation in different fault zones of different age. Deformation textures are restricted to the interiors of the detrital mylonite and microbreccia clasts and do not extend into the enclosing sedimentary matrix. Therefore, on the basis of the probable age of the sedimentary section, the minimum age of the faulting is established as early Mesozoic. The mylonite and microbreccia are direct evidence of ancient faulting in basement rocks of the Charleston area.

INTRODUCTION

In recent years, studies of the historic and modern seismicity in the Charleston, S. C., area have included efforts to understand the geology of the pre-Cretaceous rocks below the South Carolina Coastal Plain and the tectonic history these rocks encode. Important results of these efforts include the recognition of widespread subsurface lower Mesozoic volcanic rocks and lower Mesozoic(?) sedimentary rocks in the Charleston area and the recognition of their stratigraphic equivalence to similar rocks throughout the subsurface of the Southeastern United States and adjacent offshore areas (for example, Gohn and others, 1978). To date, studies of the older, pre-Mesozoic crystalline basement in the Charleston area have been restricted to geophysical investigations including gravity and aeromagnetic studies (Long and Champion, 1977; Phillips, 1977; Popenoe and Zietz, 1977; Daniels and others, 1983), seismic-refraction surveys (Ackermann, 1977, 1983; Talwani, 1977), electrical resistivity surveys (Campbell, 1977), and seismic-reflection surveys (Hamilton and others, 1983; Schilt and others, 1983). Geologic investigations of pre-Mesozoic rocks in the Charleston area were precluded by the absence of boreholes deep enough to penetrate that section. In other parts of the Southeast, however, geologic data from deep boreholes have been used, in conjunction with regional potential field data, to produce maps of the basement rocks (Popenoe and Zietz, 1977; Chowns and Williams, 1983; Daniels and others, 1983).

The deepest borehole in the Charleston area is Clubhouse Crossroads #3 (CC#3) in southwestern Dorchester County, about 40 km west-northwest of Charleston (fig. 1). A generalized geologic column for CC#3 is given in figure 1, and discussions of the pre-Cretaceous rocks in this section are included in papers by Gottfried and others (1983) and Gohn and others

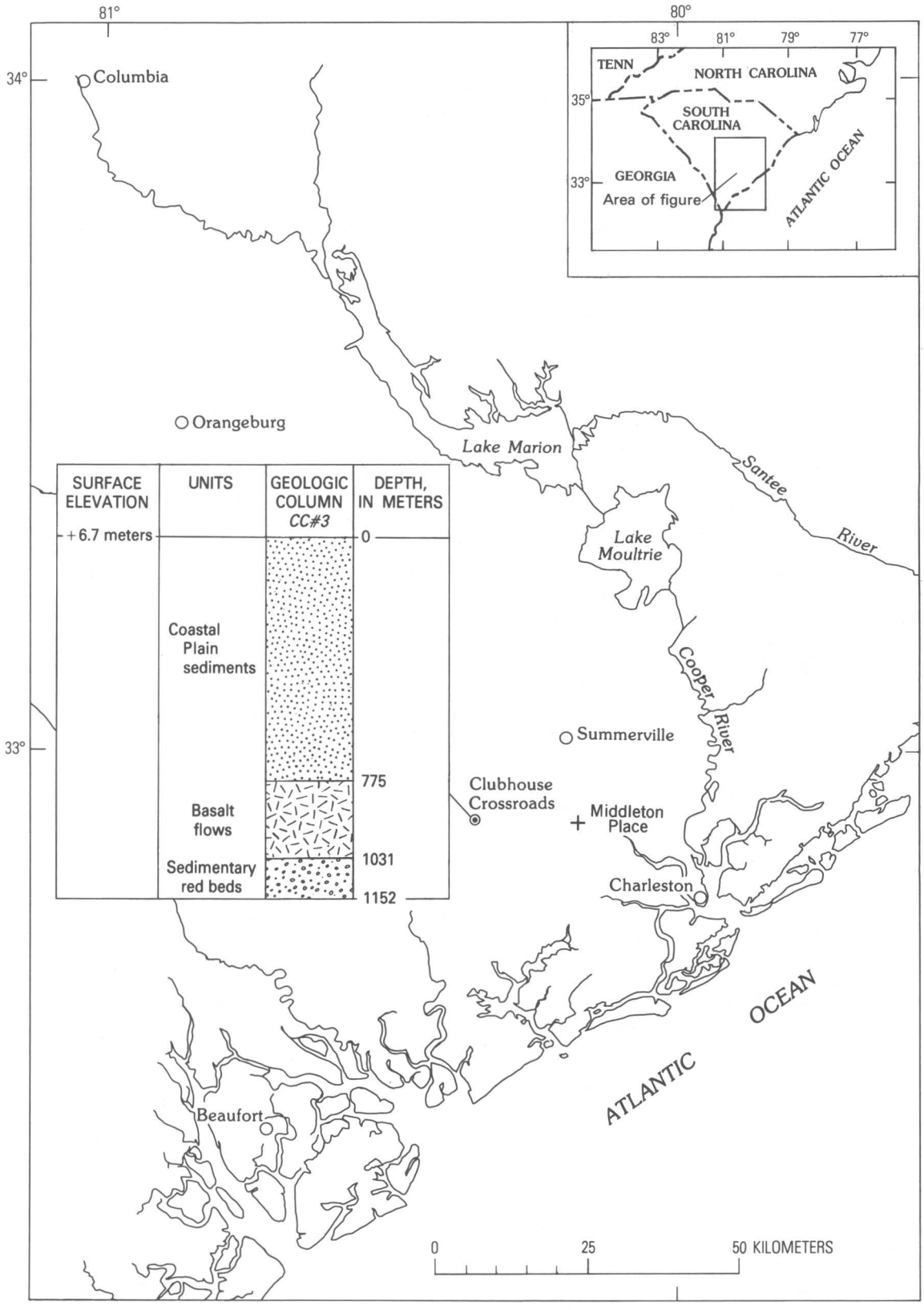

FIGURE 1.–Location map and generalized geologic column for CC#3.

(1978, 1983). In this stratigraphic test hole, below 775 m of Cretaceous and Cenozoic Coastal Plain sediments, 256 m of subaerial basalt flows overlie a minimum of 121 m of sedimentary red beds. On the basis of radiometric ages for the basalt and regional lithostratigraphic relationships of the basalt and red beds, Gohn and others (1978, 1983) assigned a Late Triassic to Early Jurassic age to the combined basalt and red-bed section. Due to mechanical failures, CC#3 did not penetrate the crystalline basement thought to underlie the red-bed sequence. Ackermann (1983) suggests, on the basis of seismic-refraction data, that CC#3 may have stopped only a few tens of meters above that basement.

However, a 3.1-m core recovered from the bottom (1,144–1,147 m) of CC#3 does contribute to our understanding of the basement geology in the Charleston area. Below a depth of about 1,070 m in the hole, the red-bed section consists of interbedded conglomeratic sandstones and mudstones, most of which are represented only by rotary cuttings. The bottom core, however, consists predominantly of conglomeratic sandstone that contains detrital fragments, as large as 4 cm, of crystalline rocks. Numerous lines of evidence suggest that these rock fragments were derived from areas proximal to their site of deposition and that they represent, therefore, the only material available for direct geologic investigation of the crystalline basement near Charleston. For this report, the 2.0- to 40-mm-sized polymineralic fragments were studied petrographically to determine the types of rock present and to provide data from which inferences about the geology of the crystalline basement could be made. Comparisons of the petrologic data with the geophysical interpretations of the basement are also presented.

Acknowledgments.—This work was supported by the U.S. Nuclear Regulatory Commission, Office of Nuclear Research, under Agreement No. AT(49–25)–1000. I thank my colleagues Peter Lyttle, Norman Hatch, Louis Pavlides, David Gottfried, Gilbert Espenshade, Douglas Rankin, Brian Leavy, and especially Nicholas Ratcliffe and J. Wright Horton for their many helpful discussions of igneous and mylonitic rocks.

RED-BED SECTION

Lithofacies

The general geology of the red-bed section in CC#3 is discussed by Gohn and others (1983), and a generalized description of the red-bed lithofacies is given in figure 2. From the base of the overlying basalt, at a depth of 1,030.8 m, to a depth of 1,070 m, the section consists of red and green mudstones, siltstones, and fine-grained sandstones. Due to the fine grain size, these rocks do not lend themselves as readily to studies of sediment

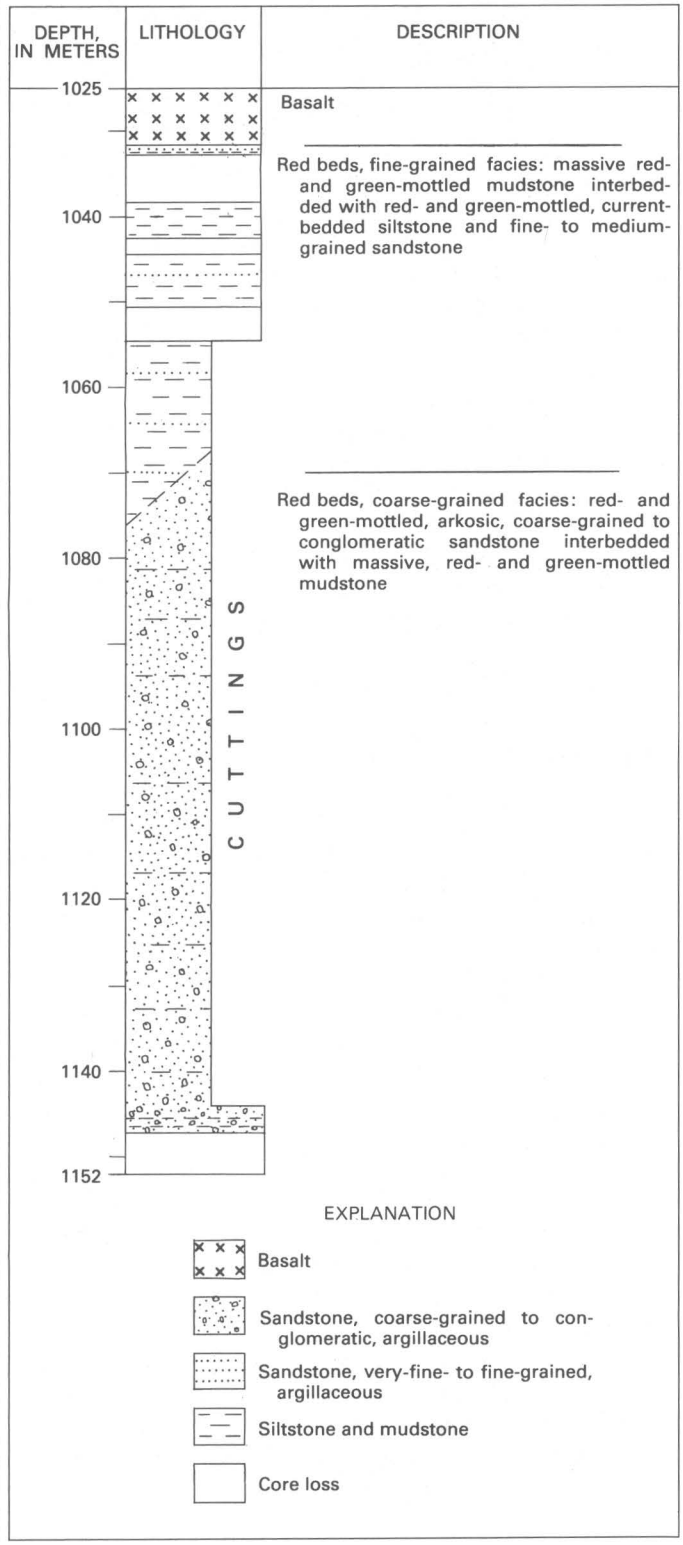

FIGURE 2.—Stratigraphic column showing sedimentary facies of the lower Mesozoic(?) red-bed sequence in CC#3.

provenance and basement geology as do underlying coarser-grained deposits. Beginning with the rotary cuttings from the interval between 1,067 and 1,076 m, drilling chips of conglomeratic sandstone and chips consisting entirely of individual crystalline-rock fragments appear. The depth of 1,070 m has been selected arbitrarily as the top of this conglomeratic unit. This lithology was penetrated to a depth of 1,144 m where a 3.1-m core was recovered.

The conglomeratic beds in the bottom core are divided into seven depositional units (fig. 3). Four inverse-graded or inverse-to-normal-graded beds occur in the core. Starting at the base, each of these beds consists of a matrix-supported conglomeratic mudstone that grades upward into framework-grain-supported argillaceous conglomerate or argillaceous conglomeratic sandstone. Thin mudstone layers intervene between the graded conglomeratic beds. Color-mottling, carbonate nodules, clay mineralogy, and other sedimentary aspects of this core are discussed by Gohn and others (1983). The locations in the core of thin sections examined during the present study are shown by arrows on figure 3.

Evidence for Local Sediment Source

The detrital rock fragments in the conglomerates from the bottom core are relevant to the basement geology of the Charleston area only if their source area was proximal to their site of deposition at Clubhouse Crossroads. Several lines of evidence suggest that such proximity was the case.

DATA FROM CORE

Compositional immaturity.—The conglomeratic beds in the bottom core are poorly sorted deposits containing abundant mineralogically and texturally unstable detrital rock fragments. Although the maturity of a sedimentary deposit may depend on several factors, including intensity of source-rock weathering before transportation and diagenetic alteration after deposition, the interpretation is made here that the time and distance of sediment transport was insufficient to produce appreciable breakdown of polycrystalline grains into texturally stable grains or appreciable chemical alteration of unstable minerals to secondary products. Similarly, the abundance of unstable grains indicates that the pretransportation and postdepositional processes also contributed little to the maturation of the deposit.

The relative maturity of a sediment or sedimentary rock may be represented by a ratio of the stable grains (monocrystalline quartz, chert, orthoquartzite lithic fragments) to the unstable grains (feldspar, polycrystalline quartz, other lithic fragments) in the deposit.

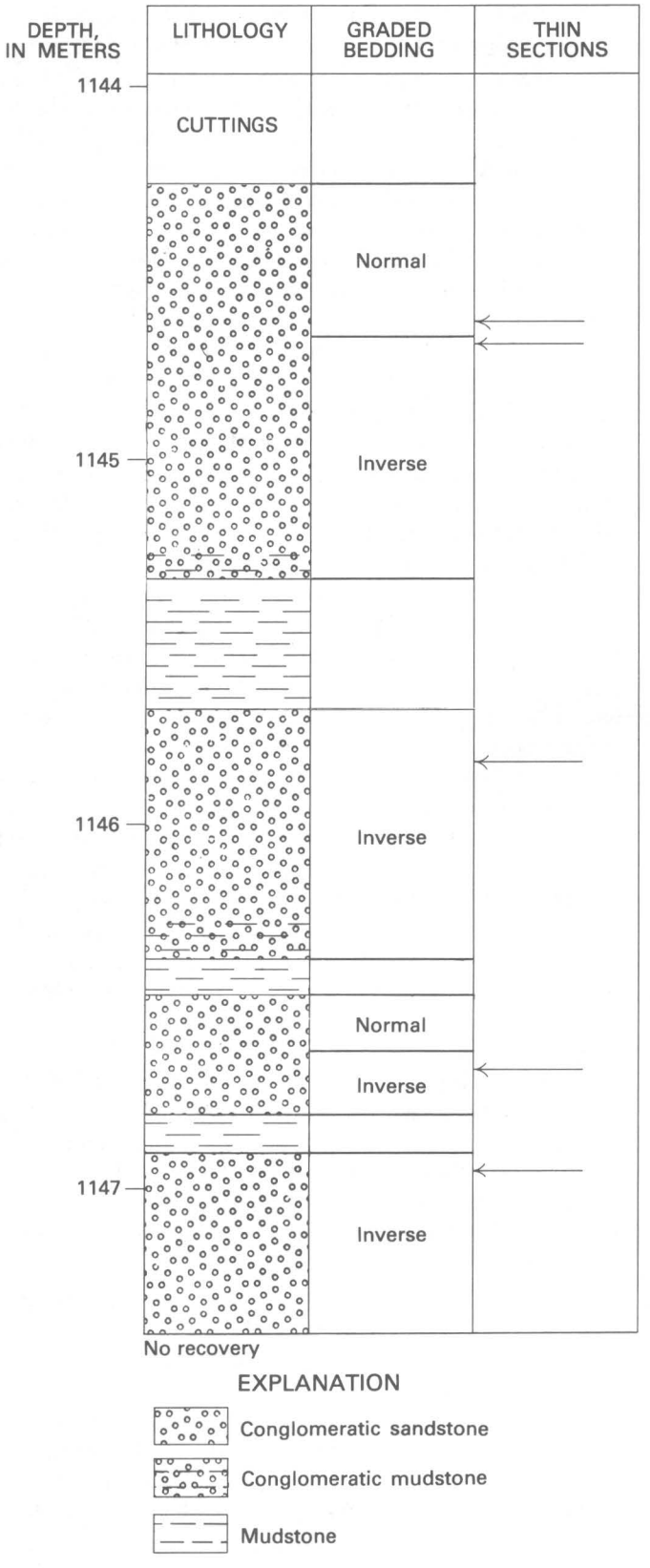

FIGURE 3.—Depositional units recognized in the bottom core from the red-bed sequence. Normally and inversely graded parts of the conglomeratic beds are labeled. Arrows mark locations in the core of samples from which sets of thin sections were cut.

Such a ratio is typically used as a maturity index in sandstone classifications (for example, Pettijohn, 1957, p. 286–293). The greater the percentage of stable grains, the more compositionally mature the sediment has become. In table 1, modal analyses for three representative conglomeratic beds from the core show that the maturity ratio [monocrystalline quartz/(feldspar + polycrystalline quartz + lithic fragments)] is very low (0.4–0.16), and therefore these rocks are considered to be very immature.

Angularity of grains.—As shown in figure 4, the detrital sand-sized and larger grains in the conglomeratic beds are poorly rounded. The framework grains were visually determined to vary in roundness from subrounded to angular on Pettijohn's scale (Pettijohn, 1957, p. 59) and from subangular to very angular on Powers's scale (Powers, 1953); subangular (Pettijohn) or angular (Powers) is the modal class. The relative angularity of the grains, like the other sedimentary parameters, suggests short transport distances.

Sedimentary structures.—Inverse grading and matrix-supported fabrics like those observed in the core (figs. 3, 4, 5) indicate that, during active deposition, the mass of moving sediment and associated fluid possessed sufficient matrix strength and buoyancy to support the larger grains within or on top of the mass. Poorly developed alinement of larger grains within the matrix, visible in some of the conglomeratic beds, also indicates that the depositional mass was sufficiently rigid to be sheared during flow, thereby producing the alinement. The depositional mechanism in which a matrix of interstitial fluid and fine-grained sediment possesses a finite yield strength and internally supports the larger grains is called debris flow (Middleton and Hampton, 1973, p. 2).

Debris flow is a viable mechanism for subaerial deposition of coarse-grained sediments (Sharp and Nobles, 1953; Bull, 1972). The factors necessary to produce subaerial debris flows limit the distances to which sediment may be transported. Bull (1972, p. 69) lists the factors that promote debris flows on subaerial alluvial fans: abundant water supplied over short periods of time at irregular intervals; steep, sparsely vegetated slopes; and a source of material to provide the mud matrix. The distance any debris flow can move is limited, therefore, by the time period of abundant water supply and by any area of very low or reversed slope. A possible transport distance of 20 km for the 1941 Wrightwood, Calif., flow is one of the longest reported examples of subaerial debris flow movement (Sharp and Nobles, 1953). The interpretation of debris flow as a depositional mechanism for the conglomeratic beds in the red-bed section is consistent with the interpretation of alluvial fans and other subaerial environments as the sites of deposition of this sedimentary section (Gohn and others, 1983).

DATA FROM GEOPHYSICAL SURVEYS

Ackermann (1983) presents contour maps based on seismic-refraction surveys that show the configuration of several subsurface horizons in the Charleston area including the pre-Mesozoic(?) basement surface. Conspicuous features on this basement-surface map include a northeast-trending basement ridge (which underlies the Clubhouse Crossroads test holes) separated from a deep basin to the northwest by a steep gradient and from a second basin to the southeast by a less steep gradient. On the basis of several types of seismic evidence and the geologic columns for the Clubhouse Crossroads test holes, Ackermann interprets the two basins to be filled with as much as a kilometer of lower Mesozoic sedimentary rocks (see also Talwani, 1977, fig. 5; Talwani and others, 1979, fig. 14). A thinner section of these sedimentary rocks exists on the basement high, as demonstrated by the red-bed section in CC#3.

The large relief on the basement surface, the interpretation of a fault origin for the steep northwestern slope of the basement high (Ackermann, 1983; Hamilton and others, 1983), and the age, thickness, and compositional immaturity of the associated sedimentary rocks suggest rapid early Mesozoic filling of a graben bounded by active faults. The basement ridge existed as a topographic and structural high (horst) within a larger graben and shed sediment into the adjacent basins. In this setting, sediments in the thin Clubhouse Crossroads

TABLE 1.—*Modal analyses (percent) of representative conglomeratic rocks*

[500 points counted per thin section]

Depth of sample below surface (m)	Quartz			Feldspar			Quartz-feldspar lithic fragments	Matrix	Calcite	Other minerals	Classification[2]	
	Monocrystalline	Polycrystalline	Total	Potassium[1]	Plagioclase	Total					Williams and others[3]	Pettijohn[4]
1,144.7	3.2	4.8	8.0	2.4	8.0	10.4	65.6	10.4	5.2	0.4	arkose or arkosic wacke.	arkose
1,146.6	8.0	7.4	15.4	9.2	7.8	17.0	25.6	39.6	1.2	1.2	arkosic wacke	feldspathic graywacke.
1,146.9	2.8	11.2	14.0	12.4	5.6	18.0	34.0	29.2	4.8	0	do.	Do.

[1] Includes perthite.
[2] Quartz-feldspar lithic fragments grouped with feldspars.
[3] Williams and others (1954).
[4] Pettijohn (1957).

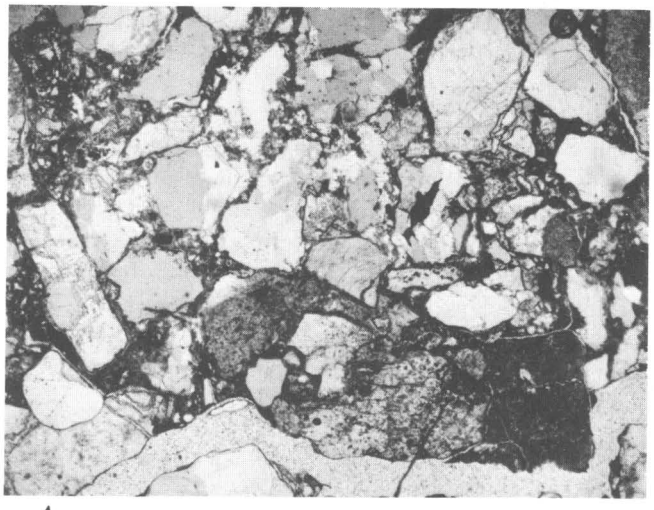

A

500μ

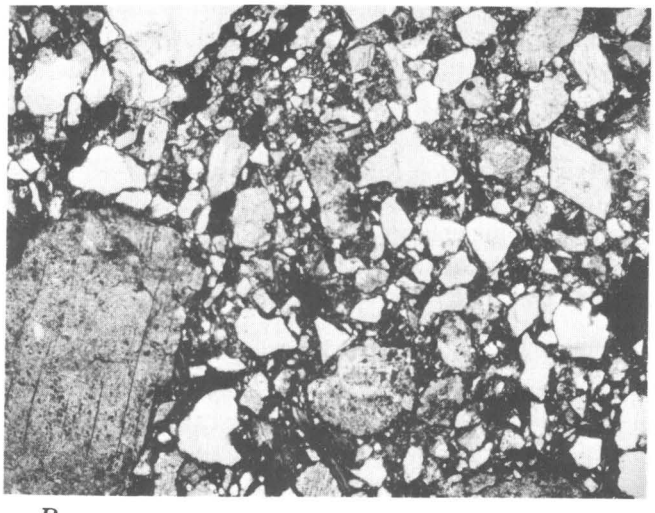

B

500μ

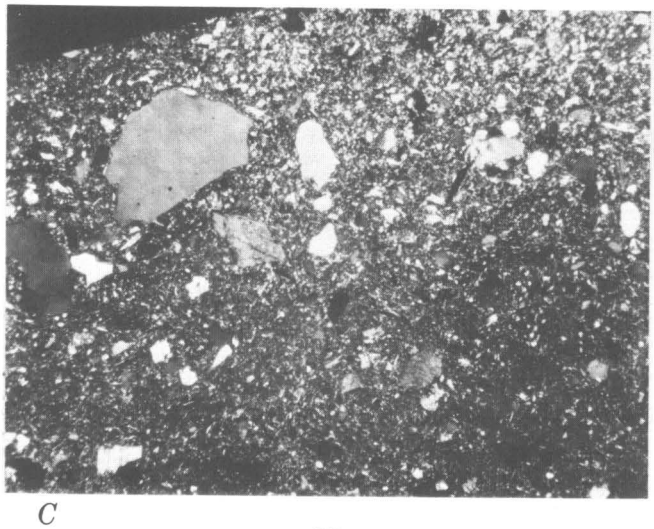

C

500μ

FIGURE 4.—Photomicrographs showing textures of conglomeratic beds. *A*, *B*—plane light; *C*—crossed nicols. *A*, Conglomeratic sandstone from a depth of 1,146.9 m. Sample consists primarily of quartz-feldspar lithic fragments. Note the framework-grain-supported fabric and moderate rounding of grains. Veinlike feature at bottom is epoxy. *B*, Conglomeratic sandstone from a depth of 1,146.6 m. Note possible framework-grain-supported fabric, poor sorting, and moderate to poor rounding of grains. Large, subhedral plagioclase grain at left. *C*, Conglomeratic mudstone from a depth of 1,146.7 m. Note matrix-supported fabric, poor sorting, and moderate rounding of framework grains.

red-bed section, located near the top of the basement ridge, were derived from the older rocks that composed the highest parts of the ridge. Older crystalline rocks in areas adjacent to the ridge would already have been buried by Mesozoic sediments at the time of deposition at Clubhouse Crossroads.

PETROLOGY OF DETRITAL ROCK FRAGMENTS

Study of the basement-rock clasts in the core was concentrated on, but not restricted to, large polymineralic fragments, generally those grains larger than 2 mm. Smaller rock fragments, monomineralic polycrystalline grains, and single-crystal grains, as a group, show minerals, microstructures, and textures similar to those observed in the larger fragments. However, textural relationships within clasts are better displayed in the larger grains, particularly for the coarser-grained rocks. The larger clasts also better display the genetic associations of minerals in the various rock types and, therefore, provide better data for petrologic classification.

The conglomeratic sedimentary rocks in the bottom core were studied by standard petrologic techniques including study of thin sections and rock slabs with binocular and petrographic microscopes. Some slabs and thin sections were stained with sodium cobaltinitrite to aid in the identification and differentiation of plagioclase and potassium feldspars. X-ray diffraction studies aided in the identification of alteration products of the feldspars and mafic minerals. In thin sections, modal analyses of individual rock fragments were made by determining the areal proportions of the minerals present along orthogonal lines in a 0.5-mm grid (line counting). This method, rather than point counting, was used because of the small size of the clasts and the polymodal size of grains within clasts.

Nomenclature used for the textural and optical features of quartz grains follows that of Young (1976) and Bell and Etheridge (1973). The petrologic classifications used for igneous-rock fragments are those of the International Union of Geological Sciences Subcommission (IUGS, 1973; Streckeisen, 1979). Textural nomenclature is taken primarily from Travis (1955). The classification of cataclastic and mylonitic rocks by Hig-

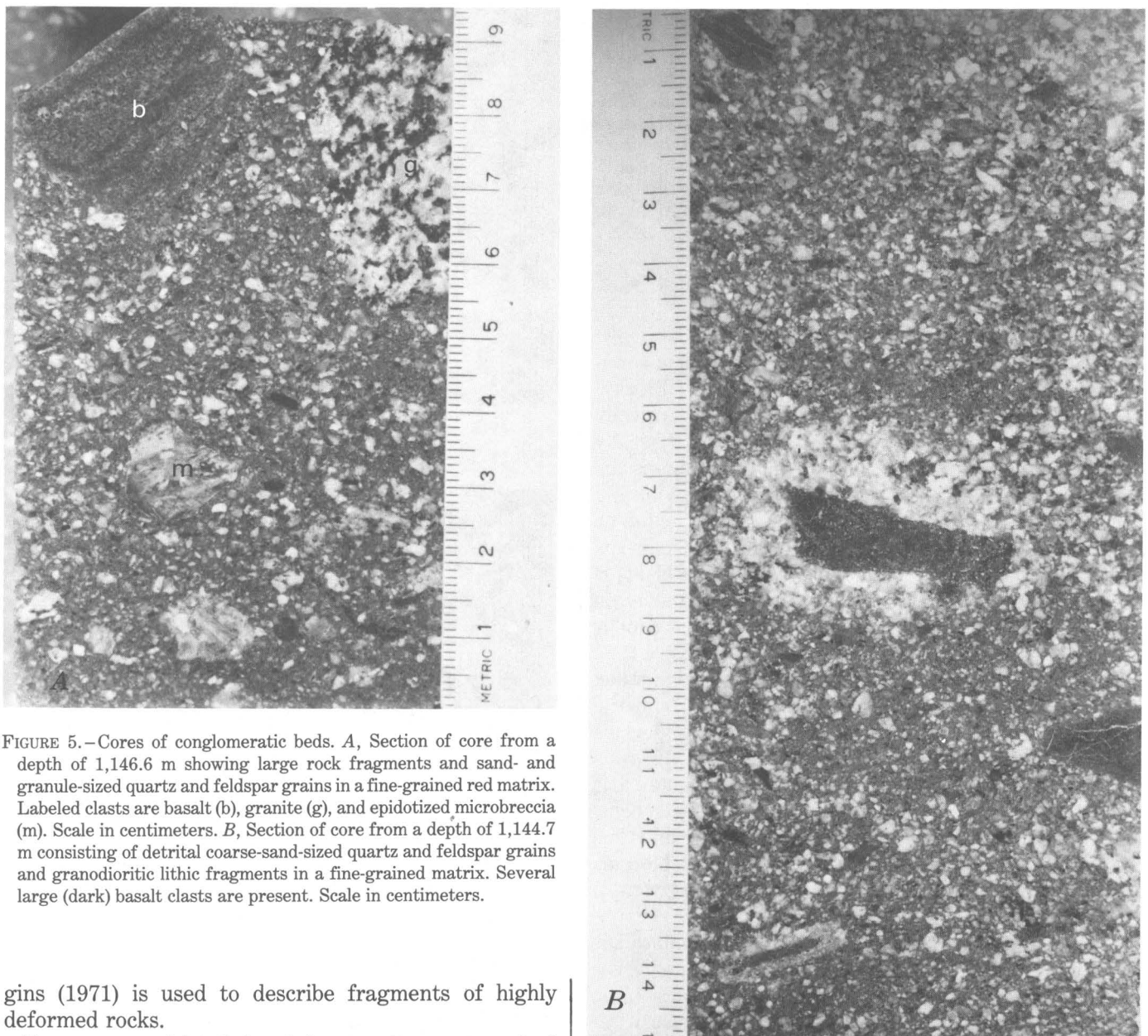

FIGURE 5.—Cores of conglomeratic beds. *A*, Section of core from a depth of 1,146.6 m showing large rock fragments and sand- and granule-sized quartz and feldspar grains in a fine-grained red matrix. Labeled clasts are basalt (b), granite (g), and epidotized microbreccia (m). Scale in centimeters. *B*, Section of core from a depth of 1,144.7 m consisting of detrital coarse-sand-sized quartz and feldspar grains and granodioritic lithic fragments in a fine-grained matrix. Several large (dark) basalt clasts are present. Scale in centimeters.

gins (1971) is used to describe fragments of highly deformed rocks.

Four groups of detrital rock fragments are recognized in the CC#3 conglomeratic rocks: granodiorite, mylonite, microbreccia, and basalt. These groups or their disaggregated constituent minerals compose over 99 percent of the silt-sized and larger detrital grains. Virtually no detrital grains were recognized that could not be related to one of these groups with confidence.

As shown in figure 5, light-colored, coarse-grained crystalline rock fragments, here classified collectively as granodiorite, are the dominant clast type. Individual quartz and feldspar grains interpreted to have been derived from the granodiorite constitute a large part of the sand-sized fraction. Two varieties of strongly deformed rocks, mylonite (sparse) and microbreccia (common), are recognized as small black clasts and light-green epidote-rich clasts, respectively (fig. 5*A*). Basalt clasts are also common in the core and appear as dark, earthy-red clasts that contrast with the leucocratic granodioritic debris (fig. 5*B*).

Granodiorite

The fragments of plutonic rocks described herein as granodiorite represent a compositional range of intermediate to silicic igneous rocks. On the basis of mineral modes, these range in apparent composition from tonalite to granite; granodiorite is the most common rock type. All these plutonic-rock fragments have been assigned to a single category because of the similarities in their primary and secondary mineralogy, texture, and inferred origin.

FIGURE 6.–Photomicrographs of plagioclase and myrmekite in granodioritic clasts. Crossed nicols. *A*, Interior of a large granite clast from a depth of 1,144.6 m. Twinned, moderately to heavily saussuritized plagioclase crystals occur in perthite (dark). Clear, untwinned albitic(?) rims are visible on most plagioclase grains. *B*, Interior of a large granodiorite clast from a depth of 1,144.7 m. Large groundmass plagioclase crystal is bent, broken, and healed by quartz and epidote. Twinning is partially destroyed by saussuritization. *C*, Interior of same clast as in *A*. Myrmekite (grains having vermicular texture) projects from groundmass plagioclase grains into perthite grain at right.

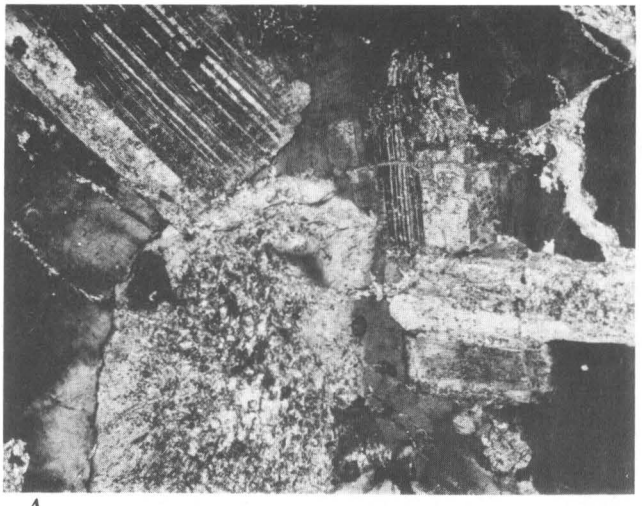

A

500μ

B

500μ

C

500μ

MINERALOGY

Plagioclase.–Plagioclase is the largest and most abundant mineral in the granodioritic clasts. Blocky, euhedral or subhedral plagioclase grains are typically 500 to 6,000 μ in largest dimension and typically polysynthetically twinned (fig. 6). Albite twinning is the most common, along with rare Carlsbad-albite twins and rare combinations of albite twins with either acline or pericline twins. On the basis of maximum albite-twin extinction angles, the typical plagioclase in these clasts is probably oligoclase or sodic andesine. The maximum recorded extinction angles indicate An values of An9 or An31; the average extinction angle (20 grains) of 9.5° indicates An values of An13 or An28. Refractive-index studies of individual detrital plagioclase grains in the red-bed section indicate that only albite and oligoclase are present (Gohn and others, 1983). Clear, untwinned rims on plagioclase are probably albite of late magmatic origin. Plagioclase grains in many clasts have been bent, broken, and subsequently healed by quartz and (or) epidote (fig. 6*B*). Plagioclase crystals occur both as enclosed grains in perthite and as groundmass grains in the rock (fig. 6).

Alteration of the plagioclase to secondary minerals is widespread and was observed in all the granodioritic clasts; unaltered plagioclase occurs but is sparse. The plagioclase is replaced partially by epidote (saussuritization), sericite, calcite, and possibly kaolinite (fig. 6); the epidote and sericite are particularly abundant. Crystallographic orientation of the sericite laths was observed in numerous grains. The epidote is locally coarse grained (30–70 μ).

X-ray diffraction study of selected drilling chips containing only granodioritic material indicates that a kaolinite-group mineral is an important alteration product of feldspars in these grains, although this mineral cannot be definitely related to the plagioclase. Calcite replaces feldspars and other grains in certain samples, but the patchy or nodular replacement of matrix as well as of detrital framework grains suggests that the calcite is a postdepositional, diagenetic mineral (see Gohn and others, 1983).

Myrmekite.—Myrmekite, vermicular quartz in plagioclase, occurs as an epitaxial overgrowth on plagioclase at plagioclase-perthite boundaries in numerous clasts. A few individual detrital myrmekite grains were also noted. Myrmekite in the studied clasts typically has a bulbous shape and "penetrates" adjacent perthite (fig. 6*C*). Myrmekite was observed only on groundmass plagioclase, not on plagioclase enclosed in perthite.

Potassium feldspar and perthite.—For this study, three types of potassium-bearing feldspar were defined on a petrographic basis; in increasing order of abundance, these are orthoclase, microcline, and perthite. Microcline was defined solely by the presence of grid twinning. If any microperthitic structures were observed, the grain was classified as perthite. Perthite grains displaying grid twinning in the potassic lamellae or in irregular areas within the grain were classified as perthitic microcline. Potassium feldspars lacking both twinning and microscopically observable perthite lamellae were classified as orthoclase. Orthoclase was identified only as rare, individual detrital grains. The possibility that untwinned triclinic feldspar or undetected cryptoperthitic structure was present was not explored. Therefore, the classification of the potassium feldspars used in this report, although practical, is not rigorous with regard to the structural state of these minerals. Staining, twinning, and differences in the development and mineralogy of alteration products facilitated the distinction between potassium and plagioclase feldspars.

Perthite is the only potassic feldspar in many rock fragments, but it also occurs with microcline or perthitic microcline (fig. 7*A*). String and film textures were observed in the perthites. Complex micropegmatitic intergrowths of potassium feldspar, plagioclase, and quartz were observed in a few small clasts.

All the potassium-bearing feldspars occur as large anhedral or subhedral grains comparable in size to accompanying plagioclase grains. Quartz and plagioclase are common in the perthite.

The potassium feldspar typically is less altered than is the accompanying plagioclase, even in the same clast. The principal alteration products of the potassium feldspars are sericite, identified petrographically, and possibly the kaolinite-group mineral identified by X-ray diffraction.

Quartz.—Quartz occurs in elongate polycrystalline aggregates of grains (fig. 7) that show undulatory extinction, deformation (extinction) lamellae, or polygonization (segmented undulatory extinction). Individual grains within these aggregates typically are equant, although elongate (1:2 to 1:4) grains lacking any obvious preferred crystallographic orientation occur in some aggregates. Quartz-quartz grain boundaries are slightly serrated, and the amplitude of serration increases as grain length increases. Incipient recrystallization of original quartz grains to smaller, strain-free crystals is not common. Trails of minute inclusions are common within individual grains; some trails pass across several grains. Individual quartz grains are typically 300–600 μ in size, although larger and smaller grains occur, and are one-quarter to one-tenth the size of accompanying feldspar. Quartz, with or without epidote and chlorite, occurs in fractures in broken feldspars (fig. 6) and also as grains in perthite.

Accessory minerals.—Minor constituents of the granodioritic clasts all show evidence of a secondary origin. No magmatic mafic minerals, such as biotite, hornblende, or pyroxene, were observed. Several secondary minerals compose equant to elongate mafic patches in the clasts (fig. 7). Chlorite occurs in these patches as reddish-brown, iron-hydroxide-stained sheaves that retain the chlorite pleochroism pattern and rarely retain the typical green color. Epidote is abundant as an alteration product of plagioclase but also occurs as large (as much as 600 μ) grains associated with chlorite. Clinozoisite was observed in one large clast. Apatite is commonly associated with the chlorite and epidote, and zircon and tourmaline are present but sparse. Opaque minerals are associated with the other accessory minerals and are typically polyhedral, which suggests that the original mineral was magnetite or an iron-titanium oxide; the present mineralogy is hematite with iron-hydroxide rims. Sphene occurs as euhedral (500–1,000 μ) grains, in some cases associated with quartz and feldspar but more typically in association with the secondary minerals. The spatial association of chlorite, epidote, and sphene suggests that these minerals may have formed from primary hornblende.

PETROLOGIC COMPOSITION

Modal analyses for some of the studied granodioritic clasts are given in table 2 to illustrate the apparent range of compositions represented in the granodiorite group. Rigorous interpretation of the petrographic data is not attempted, however, because these clasts, by virtue of their small size, may not be strictly representative of the coarse-grained lithologies involved. On table 2, a range in apparent composition from tonalite or granodiorite to granite is indicated, although the largest clasts (best data) are generally in the more calcic end of this range and the smallest clasts have the most silicic compositions. The name "granodiorite" has been selected, therefore, as representative of this range. All the rock types listed are quartz-rich, intermediate to silicic rocks; therefore, they could be genetically related and actually present in the provenance area.

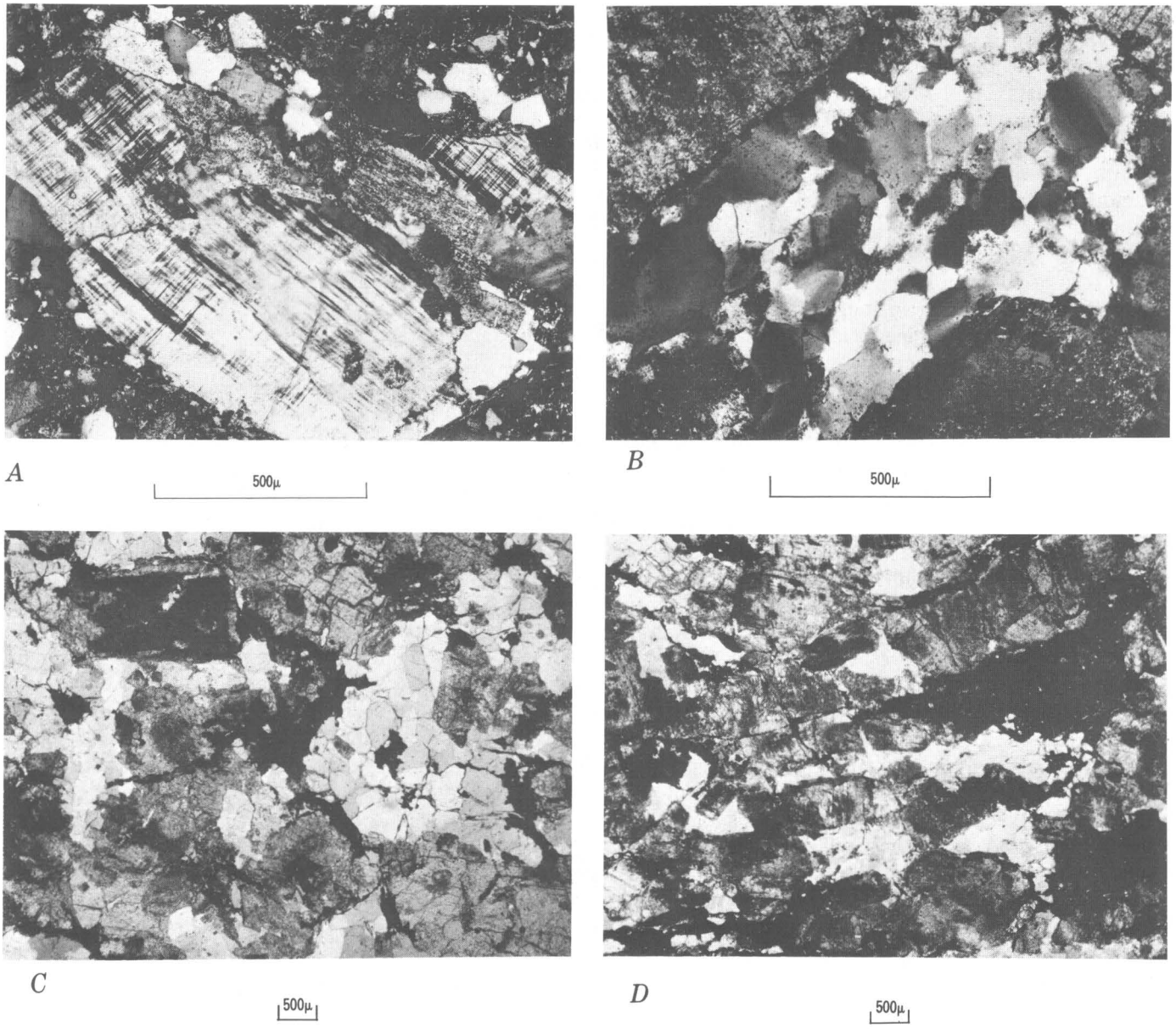

FIGURE 7.—Photomicrographs of feldspars, quartz, and textural features in granodioritic clasts. *A*, *B*—crossed nicols; *C*, *D*—plane light. *A*, Microcline, perthite, and minor quartz and plagioclase in a small granodioritic clast from a depth of 1,146.7 m. Plagioclase is heavily altered. *B*, Interior of granodiorite clast from a depth of 1,144.7 m. Aggregate of quartz grains between altered plagioclase grains. Note the uneven extinction within individual quartz grains. *C*, Interior of granodioritic clast from a depth of 1,144.7 m. Note the hypidiomorphic-granular texture and alteration of the feldspars. *D*, Interior of granodioritic clast from a depth of 1,144.7 m. Directional fabric is defined by oriented plagioclase (turbid), elongate quartz aggregates (white), and elongate mafic patches (black).

TEXTURE

All varieties of the granodiorite clasts are medium-grained (1–5 mm) rocks. An igneous hypidiomorphic-granular texture is suggested by large euhedral to subhedral plagioclase and subhedral to anhedral potassium feldspar grains, but this texture has been somewhat altered. A single clast of granitic composition was observed to have a finer grained (1–1.5 mm) aplitic texture, and several lithic fragments with micropegmatitic textures were encountered. Some clasts appear to have developed an oriented fabric, although observation of this feature is inhibited by the small size of the clasts. This fabric is defined by elongate aggregates of quartz and by elongate patches of chlorite, epidote, and associated secondary minerals (fig. 7*D*). In some clasts, this fabric is more obvious because of the alinement of

TABLE 2.—*Modal analyses (in percent) for granodioritic clasts*
[Analyses 1 through 6 are individual clasts. Analysis 7 is the average for 8 small clasts. tr, trace]

Analysis sample no.	Plagioclase	Myrmekite	Potassium feldspar	Quartz	Chlorite, epidote, apatite, opaque minerals	Sphene	Calcite	Feldspar ratio[1]	Petrologic classification	Maximum clast dimension (mm)
1	53.1	0.6	6.0	24.3	15.1	0.7	0.2	0.90	tonalite or granodiorite.	40
2	62.8	tr	7.1	26.6	3.5	tr	0	.90	leucotonalite or leucogranodiorite.	6
3	51.9	tr	9.8	22.2	15.5	.6	0	.84	granodiorite	20
4	30.7	1.1	28.0	33.9	4.8	.4	1.1	.53	granite	40
5	17.2	3.6	51.6	19.8	6.8	tr	1.0	.29	do.	3
6	13.8	.7	52.2	29.0	3.6	.7	0	.22	do.	3
7	30.0	2.5	28.1	30.6	1.9	0	6.9	.54	leucogranite	2–3.5

[1] (Plagioclase + myrmekite)/(potassium feldspar + plagioclase + myrmekite).

feldspar megacrysts in the elongation direction of quartz aggregates and mafic streaks. The megacrysts are also stretched and broken in the direction parallel to their long-axis alinement, and the resulting fractures are healed by quartz and epidote (fig. 6). This alinement of feldspars could represent, at least in part, an igneous flow texture.

ALTERATION

In addition to the larger scale texture and fabric of the granodioritic clasts, numerous microstructures also indicate that these rocks are somewhat deformed. The characteristic undulose extinction, deformation lamellae, polygonization, and grain elongation of the quartz indicates that some strain and partial strain recovery has occurred in these rocks (Bell and Etheridge, 1973; Young, 1976). The presence of chlorite, epidote, and sphene as the major mafic minerals in the rock also indicates some mineralogic alteration. It is impossible, however, to determine with certainty what processes were responsible for the textural and mineralogic alteration. The relatively low intensity of alteration suggests that magmatic and deuteric processes may have been responsible, although low-grade regional metamorphism and tectonism or fault-zone deformation cannot be unequivocally discounted.

Mylonite

Detrital rock fragments characterized by fluxion structure (mylonitic foliation) and sparse porphyroclasts are classified as mylonite (fig. 8). The only mineral phases recognized with certainty in these clasts are fine-grained quartz, feldspar, and epidote. Quartz occurs in elongate, segmented lenses or stringers of equant to slightly elongate (1:1 to 1:4) grains and as very fine grains in the matrix (fluxion bands). The observed range in quartz grain size was from less than 20 μ to a maximum of 150 μ. Quartz grain boundaries are typically gently curving or microserrate, and most grains show straight or slightly undulatory extinction. Sericitized potassium feldspar and saussuritized plagioclase occur as sparse, subrounded porphyroclasts and as fine grains (less than 20 μ to 150 μ) in the matrix. Albite(?) twinning was observed in some plagioclase porphyroclasts. Dark fluxion lines consist primarily of very-fine-grained epidote that ranges in size from less than 10 μ to 30 μ.

The texture of the mylonite clasts is dominated by the semicontinuous fluxion lines and porphyroclastic quartz and feldspar grains (fig. 8). Fluxion structure is well defined in these clasts by alternating irregular, wavy bands of epidote, similar bands of fine-grained quartz and feldspar, and elongate quartz stringers. The porphyroclasts and quartz stringers are typically 200 to 1,000 μ in longest dimension and typically constitute about one-third of the rock. Small fractures and veinlets of quartz, quartz plus epidote, or calcite cut the mylonitic texture.

The characteristics of the quartz grains in the stringers (polyhedral and serrate grain boundaries, slightly undulatory extinction, small grain size) indicate that considerable, but incomplete, strain recovery has occurred by subgrain growth and subsequent new grain growth. The quartz stringers may represent originally highly strained quartz ribbons in which considerable strain recovery and recrystallization has occurred.

The presence of epidote, quartz, and porphyroclastic feldspar, at least some of which is twinned plagioclase, indicates that the protolith of the mylonite contained quartz and plagioclase and also suggests that the deformation took place under greenschist-grade conditions. The similarity of primary and secondary minerals suggests that the granodiorite recognized as detrital fragments in this deposit could have been the parent rock for the mylonite.

Microbreccia

Many of the granodiorite clasts found in CC#3 have been subjected to moderate to strong cataclasis and associated secondary mineralization. Those granodiorite clasts whose texture and mineralogy are dominated by

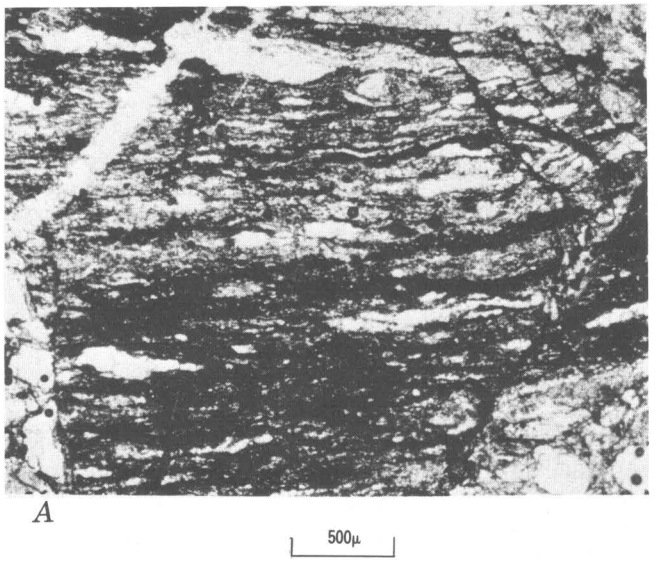

FIGURE 8.—Photomicrographs of mylonite clasts from a depth of 1,144.7 m. Plane light. *A*, Mylonite clast showing early formed mylonitic texture, later fractures (right), and cross-cutting quartz-epidote veinlet (upper left). *B*, Close-up view of part of *A* showing well-defined fluxion structure, oval feldspar porphyroclast, and segmented quartz stringers. Fluxion lines are defined by dark, thin bands dominated by epidote. Numerous bubbles appear in thin section. *C*, Mylonite clast consisting of segmented quartz stringers surrounded by a matrix of fine-grained quartz, epidote, and minor feldspar(?).

fracturing and neomineralization are described here as microbreccia. Most of these clasts retain a recognizable protolith of quartz, plagioclase, potassium feldspar, and associated accessory minerals that is identical to the granodiorite clasts in the deposit. However, the overall texture and fabric of these deformed clasts are produced by secondary processes.

MINERALOGY

Protolith.—The primary mineralogy of the microbreccias is the same as that of the less-fractured granodiorite (fig. 9). Plagioclase, potassium feldspar (chiefly perthite), and quartz are the major minerals, in decreasing order of abundance. The plagioclase is euhedral or subhedral except where crushed, and saussuritization and sericitization of the plagioclase is ubiquitous. Plagioclase is typically very cloudy, and, in many grains, the characteristic polysynthetic twinning is difficult to distinguish. Microcline twinning, perthite structure, and myrmekite are also present, but, where the rock has been crushed or extensive neomineralization has occurred, they are discernible only with difficulty. Accessory minerals of magmatic origin and secondary minerals not associated with the cataclasis occur as lenses or patches; they include chlorite, apatite, sphene, zircon, epidote, and opaque minerals. Quartz occurs in the protolith as aggregates of grains that display the same microstructures as the quartz in the granodiorite clasts.

Vein and fracture-filling minerals.—Chlorite, epidote, and quartz also occur as fracture fillings and veins. A possible zeolite mineral occurs with the epidote in some veins. The chlorite is slightly to heavily iron-hydroxide stained and is the principal mineral in narrow fractures in which little separation normal to the fracture has taken place (fig. 9*A*). Epidote is the most abundant mineral in veinlets and in composite fracture fillings where brecciation has been most intense (fig. 9*B*, *C*).

Several stages of epidote neomineralization can be documented in the microbreccia clasts. Clasts in which little cataclasis has occurred contain only minor amounts of very-fine-grained epidote (for example, the rock in fig. 9*A*). In clasts of rock that are more exten-

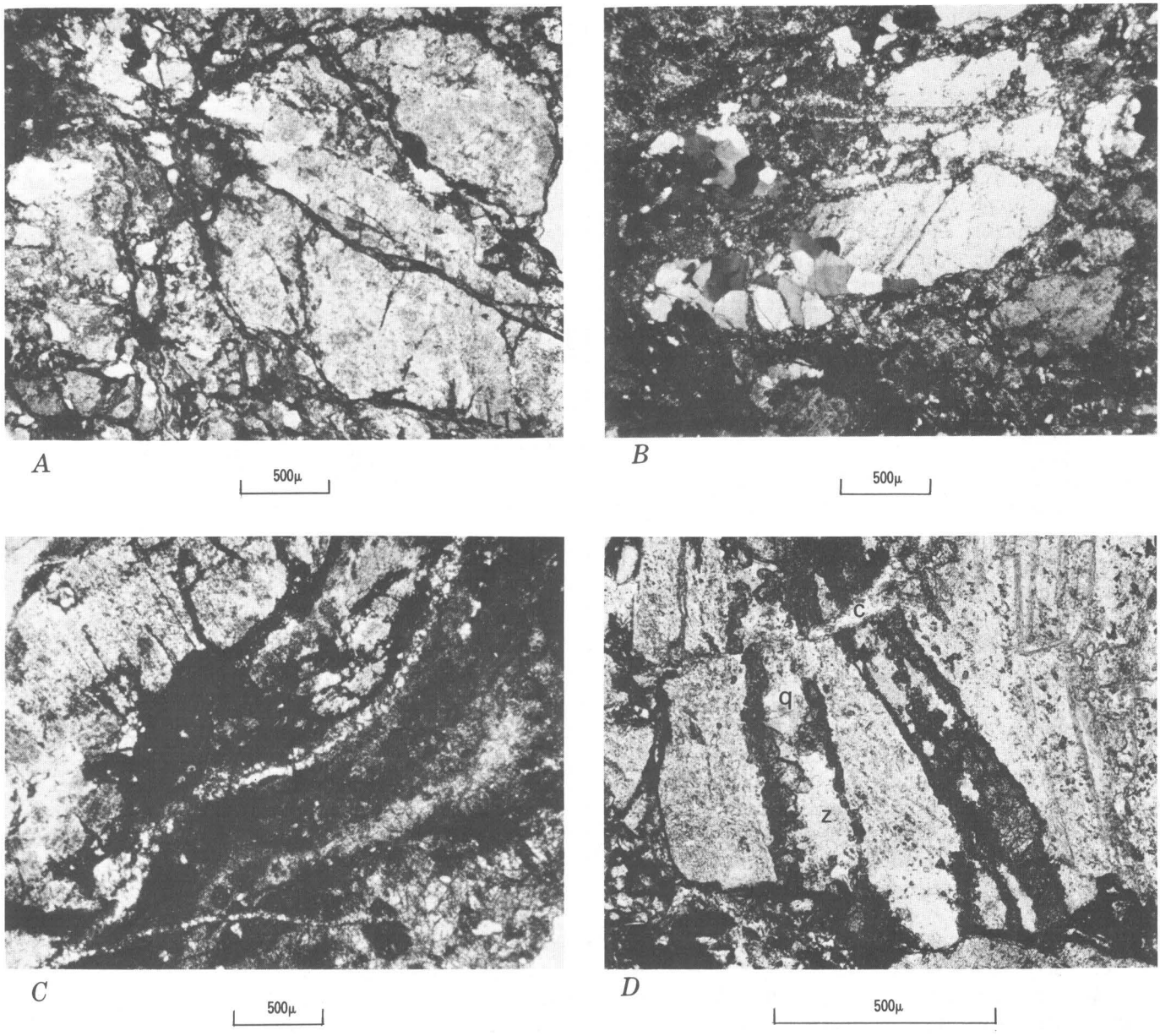

FIGURE 9.—Photomicrographs of microbreccia clasts. Plane light. *A*, Microbreccia clast from a depth of 1,144.7 m. Chlorite-lined fractures and zones of crushing occur in various orientations. Note comminution of quartz and feldspar in crushed zones and turbid appearance of feldspars. Fine-grained epidote (not visible) occurs in crushed zones but not in fractures. Apparent rock composition is granite. *B*, Interior of mineralized microbreccia clast from a depth of 1,144.6 m. Perthite (turbid) and quartz grains "float" in a matrix of fine-grained epidote. Later formed veinlets of epidote cut the perthite and continue into the epidote matrix. Note the closely matching boundaries of the feldspar fragments, *C*, Same clast as *B*. Protolith (upper left) of plagioclase, quartz, and mafic minerals is bordered by a composite quartz and epidote vein. Quartz-rich (lighter and thinner) and epidote-rich (darker and broader) bands parallel the edge of the protolith and alternate from right to left. Coarse-grained epidote at lower right probably formed the center of the vein/fracture filling. *D*, Plagioclase grain at the edge of a granodioritic clast from a depth of 1,146.7 m. Sedimentary matrix is at left and lower left. Composite epidote (dark), quartz (q), and zeolite(?) (z) veins cut the plagioclase and terminate at the clast boundary (bottom). Later compactional fracture (horizontal) offsets the veins and is partially filled by diagenetic calcite (c).

sively crushed, large areas consisting primarily of epidote contain only "floating" quartz or feldspar grains or grain aggregates (fig. 9*B*). Discrete large to small veins of epidote with or without quartz and zeolite(?) crosscut the protolith and the areas of more diffuse epidote mineralization (fig. 9*B*, *D*). Sequential filling of relatively large, open fractures is suggested in figure 9*C* by the mineral zonation parallel to the fracture wall and by the differences in epidote grain size.

Quartz veins without large amounts of epidote also occur in widths from 100 to 1,500 μ. The microstructures of the vein quartz differ considerably from the microstructures of quartz in the protolith. Vein quartz typically is in clear, equant to subrectangular (up to 1:6) grains having straight or broadly curving boundaries. Extinction of these grains is straight to very slightly undulose.

A mineral of uncertain composition, possibly a zeolite, occurs with epidote in certain composite fracture fillings. In figure 9*D*, a veinlet consisting of epidote along its outer edges contains quartz in its center along with another, very-fine-grained, colorless mineral whose relief and birefringence are lower than those of the quartz. The same or an optically similar mineral also occurs in lenticular vugs in large epidote veins.

TEXTURE

Textures of the microbreccia clasts are dramatically different from that of the granodiorite and are divisible into two groups: rocks dominated by broad zones of crushing with some fractures and rocks dominated by fractures and associated mineral veins. Rocks of the first type have bands consisting of large feldspars and aggregates of quartz separated by zones of finely comminuted quartz and feldspars and fine-grained secondary epidote (for example, fig. 9*A*). The epidote in these bands may be the product of plagioclase breakdown. Although this secondary mineralization does occur, crushing and comminution of grains is the dominant process. Discrete fractures with or without associated chlorite also cut these clasts and offset or otherwise disrupt the comminuted zones. Neither the zones of crushing nor the fractures define a directional fabric, nor do the two generations of structures retain any consistent relationship to each other.

Other microbreccia clasts (for example, figs. 9*B–D*) are cut by numerous veins of epidote and associated minerals. These two textural groups are interpreted as representing a continuum of cataclastic textures, the secondary mineralization being most extensive where the granodiorite was most severely deformed. This interpretation implies that this mineralization occurred either during or slightly later than the deformation.

Certain other fractures in the microbreccia clasts are partially filled by calcite and offset other structures (for example, fig. 9*D*). This set of calcite-filled features is interpreted to be diagenetic (compactional) in origin, on the basis of widespread pedogenic(?) calcite (Gohn and others, 1983) in the sedimentary matrix and, in certain examples, the extension of these fractures into the matrix.

EPIDOSITE

The nongenetic term "epidosite" is applied herein to a group of detrital clasts consisting largely or entirely of epidote and minor amounts of quartz and feldspar. With the exception of minor amounts of alteration minerals within feldspars, no other minerals were identified in these clasts. The epidosite clasts are interpreted as fragments of the rocks described as microbreccia, particularly those with large epidote veins. Secondary epidote is a characteristic of these brecciated rocks, and it is expected, because epidote is abundant, that certain clasts randomly derived from the mineralized microbreccia would consist primarily of that mineral. No special significance is attached to the epidosite clasts other than those interpretations of origin that are made for the microbreccia fragments.

Basalt

Common, dusky-red to dark-reddish-brown, earthy clasts as large as 2 cm in maximum dimension have been identified petrographically as altered basalt. These clasts, like the plutonic-rock clasts, record a complex history involving primary magmatic cooling, deuteric or metamorphic alteration, and diagenetic or weathering alteration.

MINERALOGY

Plagioclase.—Plagioclase laths (150–400 μ length) occur in various states of alteration. Most of the plagioclase is polysynthetically twinned (typically albite or less common Carlsbad-albite laws). In some cases it is also compositionally zoned: the (more calcic?) centers of laths are replaced by fine-grained aggregates of epidote and illite and surrounded by clear (more sodic?) rims (fig. 10*B*). In other basalt clasts, twinned but unzoned plagioclase is altered in varying degrees to randomly distributed illite and less common epidote. Altered, zoned plagioclase phenocrysts as large as 500 μ occur in one clast of weathered porphyritic basalt (fig. 10*C*). Feldspar also occurs as untwinned, equant or irregularly shaped interstitial grains (100–200 μ) that are typically free of alteration minerals.

Mafic and accessory minerals.—Chlorite occurs as 100- to 300-μ-sized, iron-hydroxide-stained grains. The chlorite, combined in aggregates with magnetite and very-fine-grained epidote, appears, in some basalt clasts, to be crudely pseudomorphous after pyroxene. In other basalt clasts in which chlorite is less abundant, primary pyroxene and (or) olivine grains have been replaced by aggregates of colorless chlorite (or perhaps serpentine), very-fine-grained epidote, and magnetite (fig. 10*A*). The magnetite in these replaced minerals occurs along the borders of the grains and along fractures and cleavages within the grains, thereby preserving the original grain outlines. The chlorite (serpentine?) is fine grained and has a low birefringence.

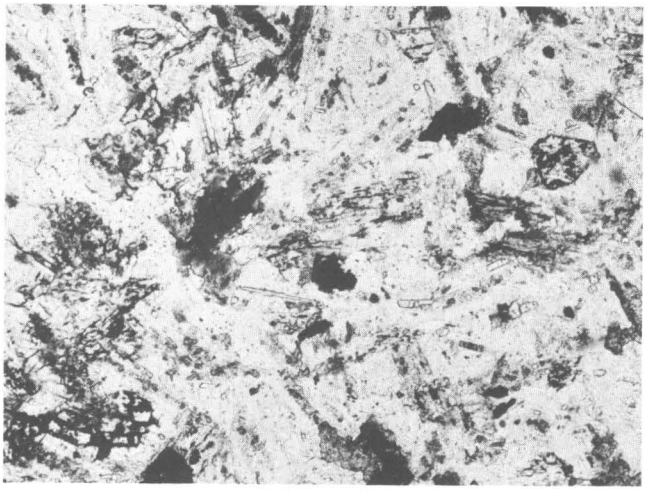

A

500μ

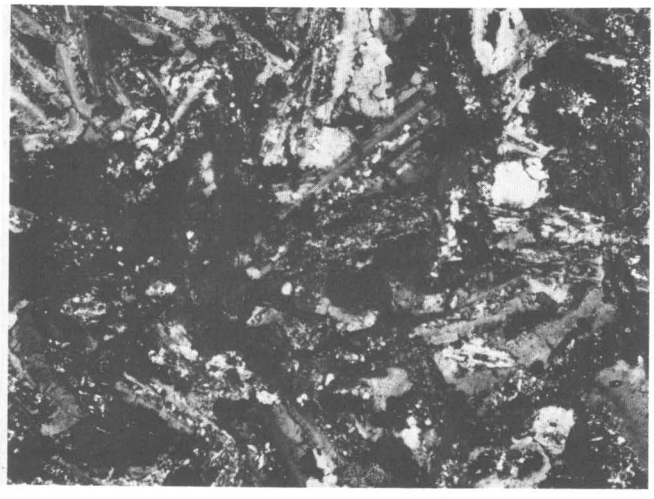

B

500μ

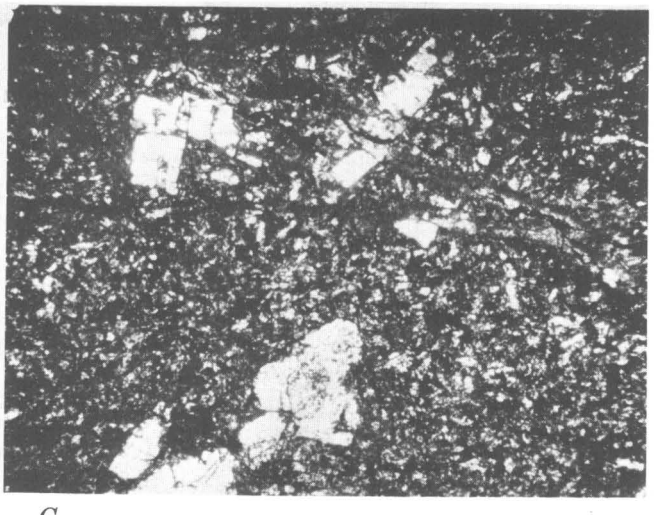

C

500μ

FIGURE 10.—Photomicrographs of basalt clasts. *A*, *C*—plane light. *B*—crossed nicols. *A*, *B*, Altered basalt from a depth of 1,144.6 m. Relict igneous texture is defined by altered plagioclase laths. Plagioclase is zoned with epidote and illite-replaced centers and clear rims. Pyroxene and (or) olivine grains have been replaced by chlorite(?) in their interiors and by magnetite along edges and fractures. Minor chlorite and slender, prismatic apatite crystals are visible in *A*. *C*, Strongly altered, porphyritic basalt from a depth of 1,144.7 m. Iron-hydroxide staining partially obscures igneous texture. Some phenocrysts appear to be aggregates of several plagioclase grains.

In addition to replacing plagioclase and pyroxene, epidote also occurs abundantly as 50- to 100-μ-sized, equant, disseminated grains, and (with minor secondary feldspar) in small veinlets that terminate at the basalt clast boundaries. Magnetite, or a similar iron-titanium oxide (grain size about 100 μ), having pronounced reddish coatings is a common accessory mineral in all the basalt clasts (fig. 10*A*). Apatite needles as large as 70 μ are common (fig. 10*A*). Interstitial calcite was observed in one clast.

TEXTURE

Although the primary igneous texture is partly obscured by the formation of secondary minerals, a relict diabase or subdiabase texture is still suggested by the plagioclase laths. This texture is indicated by the volumetric dominance of the plagioclase laths over the mafic minerals and by the shape and relatively small size of the pyroxene pseudomorphs, which suggest that these grains were isolated interstitial grains or grain aggregates rather than large poikilitic patches (fig. 10*A*). This diabase texture may represent either a diabase or a coarse-grained basalt. Both porphyritic and nonporphyritic basalt clasts are now holocrystalline, although original interstitial glass, if it was ever present, would almost certainly have been replaced.

ALTERATION

Most of the minerals presently observed in the basalt clasts are the result not of primary magmatic crystallization but rather of at least two periods of alteration. Iron hydroxide is widespread as a stain on chlorite, as rims on magnetite, and dispersed in weathering rinds on the clasts, probably because of weathering in the source area or perhaps postdepositional diagenetic processes.

The presence together of chlorite, epidote, and albite(?), however, indicate an earlier period of alteration at pressures and temperatures greater than those of near-surface settings or shallow burial. Albite + epidote + chlorite ± quartz is the classic mineral assemblage for mafic volcanic rocks in the greenschist

facies of regional metamorphism, but these minerals can also be produced under deuteric or hydrothermal (late magmatic) conditions. Serpentine plus magnetite is a common deuteric alteration pair for pyroxene and olivine, apatite forms typically as a late magmatic mineral, and saussuritization and illitization of plagioclase may be deuteric or hydrothermal processes. Chlorite is a common alteration product of the ferromagnesian minerals in altered basalts. Both chlorite and epidote are common alteration minerals in the unmetamorphosed basalt above the red-bed section in the Clubhouse Crossroads drill holes. It is not possible, at present, to choose between a metamorphic and a late magmatic origin for the secondary minerals.

PETROLOGIC CLASSIFICATION

The texture and mineralogy readily categorize this group of clasts as mafic igneous rocks. The virtual absence of quartz and potassium feldspar and the diabase texture suggest that the rock type represented is a basalt or andesite (Streckeisen, 1979). The lack of chemical data for the bulk composition of the rock or for specific minerals and the extensive mineralogic alteration do not permit distinction between basalt and andesite or distinctions among basalt types identifiable from modal or normative mineralogy.

A plutonic rather than volcanic origin for these rocks also cannot be determined with certainty. Moderately coarse-grained diabase textures are produced in both hypabyssal diabases and extruded basalts. Sills, dikes, and flows all may be texturally (and mineralogically) zoned with glassy margins and coarse-grained interiors, thereby making detailed studies of the textural variations among the altered basalt clasts of little value in determining a hypabyssal or volcanic origin. Textures as coarse as those observed in the studied clasts also occur in the subaerial basalt flows encountered higher in the section in the Clubhouse Crossroads holes. Microflow structures were not observed, and micropegmatitic intergrowths of sialic minerals, typical of many diabases, were sparse. This group of igneous-rock clasts is, therefore, loosely classified in this text as basalt, with the understanding that it may represent basaltic or andesitic flows or hypabyssal diabase intrusions.

DISCUSSION

Regional Basement-Rock Provinces

Numerous syntheses of the geology of the pre-Cretaceous rocks below the southern Atlantic Coastal Plain have been published during the past three decades. Recent summaries, which include references to earlier work, are Popenoe and Zietz (1977), Gohn and others (1978), Chowns and Williams (1983), and Daniels and others (1983). In general, three major rock provinces have been recognized in this area. A northern province located near the Fall Line in South Carolina and Georgia (fig. 11) is the extension of the Appalachian Piedmont beneath the sediments of the Coastal Plain. A wide variety of crystalline rocks, including schists, metavolcanic rocks, and mafic and felsic plutonic rocks (Daniels and others, 1983), constitutes this province. Several small early Mesozoic basins containing continental sedimentary rocks and mafic volcanic rocks also occur in this northern province. In eastern and southern Georgia and northern Florida, a southern province consists of relatively undeformed Paleozoic sedimentary rocks that overlie felsic volcanic rocks and granitic plutonic rocks of Paleozoic or Proterozoic age (Chowns and Williams, 1983).

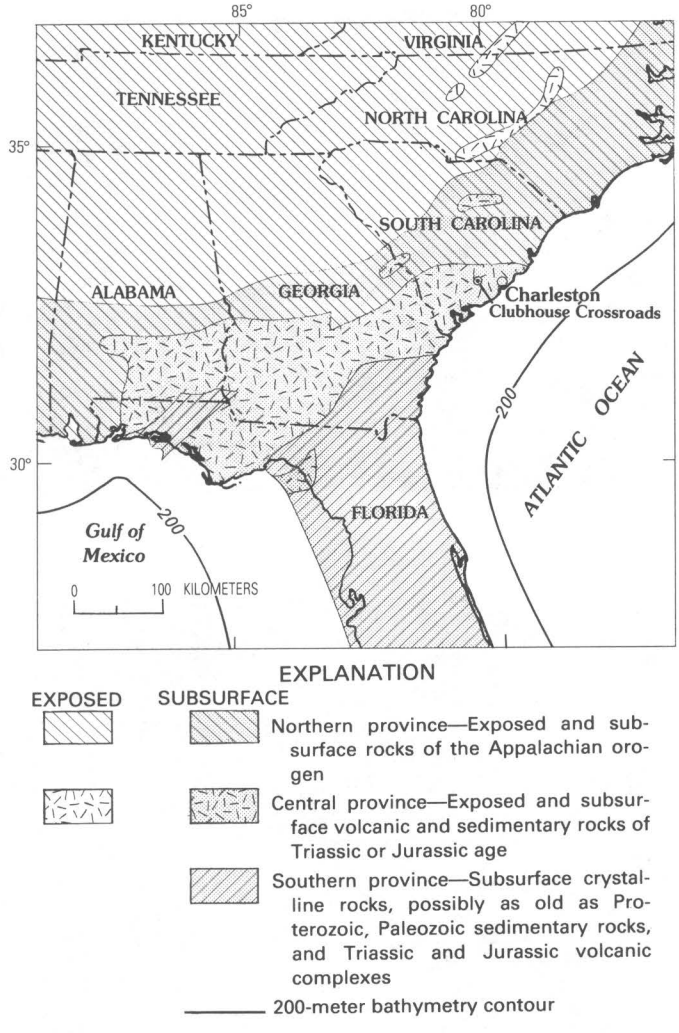

FIGURE 11.—Generalized geologic map of the Southeastern United States showing the subsurface pre-Cretaceous rock provinces. Modified from Gohn and others (1978).

Between the northern and southern provinces is a wide basin filled with lower Mesozoic continental sedimentary rocks and associated mafic igneous rocks. The nature of the pre-Mesozoic rocks below this large basin is poorly understood because of the absence, in most areas, of deep wells that penetrate through the Mesozoic section and into older rocks.

The central early Mesozoic province is represented at Clubhouse Crossroads by the basalt and red beds (Gohn and others, 1978). However, the basement rocks represented by the detrital rock fragments in the Mesozoic section in CC#3 cannot be assigned with any certainty to the northern (Appalachian) or southern (Florida) province. The fragments of granodiorite and basalt in the Clubhouse Crossroads core bear no resemblance to the sandstones, dark shales, and rhyolitic rocks of the southern province; however, a general resemblance exists between the granodiorite clasts and granitic rocks of the southern province in east-central Florida. Similarly, there is a general resemblance of the granodiorite clasts to granitic rocks exposed in the southern Appalachians. As additional conjecture, it is possible that crystalline rocks of the southern province, the basement rocks around Charleston, and some exposed rocks of the southern Appalachians are tectonically and temporally related.

Geologic Events Inferred From Petrographic Data

The studied rock fragments record a complex geologic history of magmatism and deformation that suggests a wide variety of tectonic settings and events. This variety of inferred tectonism in turn suggests that these events occurred across a considerable span of time. Detailed interpretations of this geologic history are severely limited, however, by the lack of data on the large-scale geometries of the rock units involved and on their relative and absolute ages. The presence in the Charleston-area basement of mafic (gabbroic?) plutons, inferred from geophysical data (Popenoe and Zietz, 1977), suggests an additional geologic event that is not recorded by the detrital clasts. The timing of this magmatic event also remains conjectural. A general discussion of inferred geologic events is given below.

GRANODIORITE PLUTONISM

Emplacement of granodioritic magma into an unknown sequence of host rocks is readily inferred from the petrographic data. The textural and mineralogic features of the granodiorite clasts indicate the presence of a magmatic phase, but no evidence was gathered that could address the questions of mechanism or depth of magma emplacement or the size and degree of concordancy of the plutonic bodies. The temporal relationship of the magma emplacement to any particular period of tectonism is similarly unclear.

The hypidiomorphic-granular texture of the granodiorite, although slightly affected by deformation and neomineralization, is typical of granitoid plutonic rocks. A strong long-axis alinement of plagioclase megacrysts in at least one clast suggests an igneous flow foliation, but this alinement is also parallel to the direction of elongation of mafic-mineral and strained-quartz aggregates and could have been produced by late magmatic or regional tectonic forces.

The magmatic nature of the granodiorite clasts is obvious from their primary minerals. Coexisting plagioclase, perthite, myrmekite, and quartz with minor apatite, sphene, zircon, and minor (altered) ferromagnesian minerals are a typically igneous assemblage. In addition, the textural relationships of the feldspars, myrmekite, and quartz show at least a partial record of sequential crystallization of mineral grains that is typical of myrmekite-bearing granitic rocks (for example, the crystallization history described by Hibbard, 1979).

Determination of the age of the granodiorite is impossible from the data at hand. The temporally widespread distribution of plutons in the exposed southern Appalachians, Proterozoic Z to late Paleozoic (Hatcher, 1978; Hatcher and others, 1979; Butler and Fullagar, 1979), precludes any firm conclusions.

BASALT MAGMATISM

The presence of volcanic or hypabyssal basaltic rocks downsection from the basalt flows encountered in the Clubhouse Crossroads drill holes is indicated by the mafic clasts in the bottom core. Geophysical data from two areas northwest of Charleston may be interpreted tentatively as evidence for the presence of deeper, presumably lower Mesozoic basalt flows or sills.

Ackermann (1983) has mapped the high-velocity pre-Mesozoic(?) basement surface in the Charleston area by means of seismic-refraction techniques. In the area west and northwest of Summerville (fig. 1), the deepest refracting horizon observed is characterized by shingled arrivals that indicate the presence of a relatively thin layer. In this area, velocity values for this refractor are only slightly greater than those for the Clubhouse Crossroads basalt flows. Ackermann (1983) suggests that this thin unit could be a lava flow or sill of limited thickness and lateral extent stratigraphically above crystalline basement and below the cored basalt at Clubhouse Crossroads.

Schilt and others (1983) report that reflections near 1.0 seconds (s) (two-way traveltime) on their seismic-reflection line southeast of Middleton Place (fig. 1)

probably represent a stratigraphic unit that does not occur in the Clubhouse Crossroads drill holes. Near Middleton Place, reflections from crystalline basement and the Clubhouse Crossroads basalt are probably about 1.2 to 1.3 s and 0.7 to 0.8 s, respectively (Schilt and others, 1983; Ackermann, 1983), and the reflector near 1.0 s could represent a basalt unit stratigraphically below the Clubhouse Crossroads basalt.

An early Mesozoic age for this deeper (older?) basalt unit is postulated but is based only upon the lack of penetrative deformation in the basalt clasts and the presence of known basalts of this age in the area (Gohn and others, 1978; Lanphere, 1983). If this cryptic basalt unit is of early Mesozoic age, the basalt clasts could have been supplied to the red beds more easily from basalt flows than from subsurface diabase dikes or sills that would have had to be intruded and then exhumed before they could be eroded. However, the possibility of pre-Mesozoic basalt or diabase within the crystalline basement cannot be discounted. Some basalts as old as Proterozoic in the exposed Appalachians are no more altered than are the basalt clasts from the Clubhouse Crossroads red beds (for example, see Reed, 1955).

MAFIC PLUTONISM

Geophysical surveys provide a considerable volume of data on the geometry of the basement surface and the composition of the rocks at or below that surface in the Charleston, S. C., area. Refraction and reflection surveys (Ackermann, 1977, 1983; Hamilton and others, 1983; Schilt and others, 1983; Talwani, 1977) provide most of the information on the depth to crystalline basement in the area, although additional data from magnetic depth estimates supplement the seismic work (Phillips, 1977; Popenoe and Zietz, 1977). As determined by Ackermann (1983), the most striking feature of the basement surface is the northeast-trending basement ridge in the central part of the study area. Seismically determined thick sections of sedimentary rocks that fill basement lows north and south of the ridge are interpreted to be the lateral equivalents of the thinner red-bed section penetrated on top of the ridge in CC#3.

Numerous authors have been in close agreement as to what geophysically defined rock types are to be expected within the basement ridge. At the western end of the ridge, circular to elliptical positive magnetic anomalies of large amplitude coincide spatially with positive gravity anomalies. Together these anomalies indicate the presence of thick cylindrical bodies of dense, magnetic rock. These bodies have been interpreted as gabbroic or ultramafic plutons (Kane, 1977; Phillips, 1977; Popenoe and Zietz, 1977; Daniels and others, 1983).

In the eastern part of the ridge, negative or less positive magnetic anomalies coincide with negative gravity anomalies, which indicates less dense and less magnetic rock (Ackermann, 1983). A two-part geophysically determined composition for the basement ridge is therefore defined; a western terrain of mafic plutons and an eastern terrain of nonmagnetic, less dense rocks. Therefore, the geophysical investigations have identified one rock type, gabbro or a similar rock, that was not recognized as detrital clasts.

Discussions of genetic relationships among the gabbroic plutons and the granodiorite, mylonite, microbreccia, or basalt must remain speculative. The aeromagnetic and residual gravity anomalies associated with the mafic plutons do not suggest a tectonic megafabric for these bodies but rather indicate oval or circular outlines (Long and Champion, 1977; Phillips and others, 1978; Popenoe and Zietz, 1977, p. 134) and, hence, a relatively young, postkinematic age. The mafic plutons must have intruded an older country rock, and it is likely that this country rock is the granodiorite seen as detrital fragments in the core because this rock type could produce the negative potential field anomalies that exist over the eastern part of the basement ridge. The gabbroic plutons could be early Mesozoic plutons associated with the Clubhouse Crossroad tholeiitic basalt flows (Gottfried and others, 1983) and with the other basalt flows or sills whose presence is suggested by the basalt clasts in the red beds. These mafic plutons could also be Mesozoic or younger alkalic plutons as postulated by Sykes (1978, p. 655).

Depths for the top of the gabbroic bodies estimated from magnetic and residual gravity anomalies suggest that many of them have tops at or near the top of the crystalline basement (Popenoe and Zietz, 1977; Long and Champion, 1977; Phillips, 1977). The question of whether the top of the basement at the plutons is a nonconformable or an intrusive contact cannot be presently resolved. The absence of gabbro clasts in the Clubhouse Crossroads red beds suggests a post-Paleozoic age for the mafic plutons. However, the absence of a metamorphic aureole in the red beds, which overlie an inferred mafic pluton at Clubhouse Crossroads, suggests a pre-Mesozoic age for that pluton.

DEFORMATION EVENTS

Two styles of severe rock deformation are recorded by the detrital rock fragments. The microbreccia represents relatively brittle deformation dominated by fracturing and crushing of the rocks. In contrast, the mylonite fragments represent relatively ductile response of a protolith to deformation. The mineralogic similarity of the microbreccia and granodiorite suggests

that the microbreccia almost certainly was produced from the granodiorite. The mineralogy of the mylonite fragments indicates that they also were derived from a granitoid rock and, hence, possibly from the same granodiorite as the microbreccia. If both styles of deformation have affected the same granodioritic rock body, and presumably in the same general geographic area, questions about the relative and absolute ages of the deformations can be discussed.

It is assumed herein that the deformation recorded in the clasts represents movement within a fault zone and not some other tectonic setting. Examples of such discounted tectonic settings would include protoclasis (synkinematic deformation during intrusion) of the borders of granitic plutons and large terranes in which metamorphosed plutonic rocks, including those positioned far from faults, contain pervasive tectonite fabrics such as those found in much of the southern Blue Ridge province (Rankin, 1970; Bryant and Reed, 1970a, 1970b). These settings are discounted because strong penetrative deformational fabrics are lacking in the granodioritic clasts from which the mylonite and microbreccia are believed to have been derived and because microbreccia clasts are much more abundant than mylonite clasts.

Two generations of faults that could cause the deformational fabrics seen in the detrital clasts are: Paleozoic (or Proterozoic) shear zones with predominately thrust or strike-slip movements produced during compressional orogenesis, and early Mesozoic extensional faults produced during continental rifting. Younger fault generations are not discussed, because the observed deformational fabrics do not extend from the clasts into the sedimentary matrix of the enclosing lower Mesozoic(?) sedimentary rocks.

Major fault zones typically described as mylonitic ductile shear zones are important tectonic elements in the southern Appalachian Piedmont (Higgins, 1971; Hatcher and others, 1977; Bobyarchick and Glover, 1979; Horton, 1981; and others). These features are narrow, linear to broadly curving zones of highly strained rocks. Mylonitic, phyllonitic, and blastomylonitic rocks are characteristic of these zones and are interpreted to represent deformation under relatively ductile conditions and commonly at (retrograde) greenschist-grade temperatures and pressures (for example, Hatcher, 1978; Bobyarchick and Glover, 1979; Horton, 1981; Nelson, 1981). The mylonite fragments studied for this report resemble similar rocks described from the exposed shear zones, and the presence of such a zone in the crystalline basement near Charleston is possible. Intuitively, a Paleozoic or older age seems likely for the fault movements that produced the Charleston-area mylonite, on the basis of the age of the exposed Appalachian shear zones. Textures indicative of dynamic recovery (subgrains), a high degree of dynamic recrystallization, and neomineralization of epidote along mylonitic foliation (fluxion) surfaces suggest a dominantly ductile style of deformation for the Charleston-area mylonites, probably at lower greenschist-facies conditions.

In contrast to the mylonite, the fractures and crush zones of the microbreccia clasts indicate deformation under dominantly brittle conditions, although strain-induced microstructures in quartz in these rocks may indicate unrecovered strain produced before brittle failure. Because the microbreccia clasts are enclosed in red beds of probable early Mesozoic age, which fix a minimum age for the faulting, the preferred origin of the microbreccia is in a normal-fault zone of early Mesozoic age that bounds or is within a Triassic-Jurassic basin containing the red beds and basalt encountered in the Clubhouse Crossroads drill holes. This faulting may not be much older than the deposition of the red beds. Numerous examples of multiple and syndepositional movements of border faults of exposed Triassic-Jurassic basins are documented by such data as cataclastic red beds and basalt at these faults and other examples of fault breccia as detrital clasts in the basin sediments (Reinemund, 1955; Randazzo and others, 1970; Ratcliffe, 1980, 1982; Bain and Harvey, 1977; Leavy, 1980).

An alternative to the origin of microbreccia and mylonite in spatially isolated, tectonically different fault zones is worthy of brief consideration. There is an increasingly well documented occurrence of late-kinematic, relatively brittle faults within major Appalachian ductile shear zones (Hatcher and others, 1977; Horton, 1979, 1981; Nelson, 1981; Bobyarchick and Glover, 1979; and others). The possibility exists, therefore, that the mylonite and microbreccia clasts represent different styles and times of deformation within a single fault zone. Horton pointed out (1981, p. 32) that late-stage brittle deformation such as he described in the Kings Mountain shear zone of the Carolinas could be attributed to reactivation (of Taconic or Acadian shear zones) by Alleghanian thrusting or to early Mesozoic rifting. An association of early Mesozoic normal faults with Paleozoic shear zones is readily confirmed in other areas where lower Mesozoic red beds and basalt occur with the faults (Glover and others, 1980). Good examples in the southern Appalachian include the Hylas shear zone along the western margin of the Richmond and Taylorsville Mesozoic basins in Virginia (Weems, 1980; Bobyarchick and Glover, 1979), shear zones along the Dan River Mesozoic basin in Virginia and North Carolina (Henika and Thayer, 1977; Robinson, 1979; Butler and Dunn, 1968), and a shear

zone associated with the Davie County Mesozoic basin in North Carolina (Milton, 1980). Ratcliffe (1971, 1980) also has proposed a tectonic heredity of faults in the Ramapo seismic zone of New Jersey.

Whatever the age(s) of formation of the microbreccia and mylonite might be, the fact that no unequivocal examples of brecciated mylonite were observed is negative evidence that the zone of brecciation was not directly superimposed on the zone of mylonitization, at least locally. However, if more information was available than could be gained from the small detrital fragments, a more complex fault zone with a more complex movement history might be apparent.

The most important conclusion to be drawn from this discussion of the mylonite and microbreccia clasts is that fault-zone materials exist in the crystalline basement. If the arguments about the local derivation of these materials in the Charleston-Summerville area are accepted, then one or more faults in crystalline rock must occur at depths of about 1.15 km or greater in the Charleston earthquake zone. Known movement on these faults is limited by the existing petrologic data to early Mesozoic or before; however, their presence is important to any synthesis of the tectonic and seismic history of the Charleston area because reactivation of Mesozoic and (or) older faults may be a major factor in the localization of modern-day seismic activity in the Eastern United States (Ratcliffe, 1981).

REFERENCES CITED

Ackermann, H. D., 1977, Exploring the Charleston, South Carolina, earthquake area with seismic refraction–A preliminary study, *in* Rankin, D. W., ed., Studies related to the Charleston, South Carolina, earthquake of 1886–A preliminary report: U.S. Geological Survey Professional Paper 1028, p. 167–175.

———1983, Seismic-refraction study in the area of the Charleston, South Carolina, 1886 earthquake, *in* Gohn, G. S., ed., Studies related to the Charleston, South Carolina, earthquake of 1886–Tectonics and seismicity: U.S. Geological Survey Professional Paper 1313, p. F1–F20.

Bain, G. L., and Harvey, B. W., 1977, Field guide to the geology of the Durham Triassic basin: Carolina Geological Society Guidebook, 40th annual meeting, October 1977, 83 p.

Bell, T. H., and Etheridge, M. A., 1973, Microstructure of mylonites and their descriptive terminology: Lithos, v. 6, no. 4, p. 337–348.

Bobyarchick, A. R., and Glover, Lynn, III, 1979, Deformation and metamorphism in the Hylas zone and adjacent parts of the eastern Piedmont in Virginia: Geological Society of America Bulletin, v. 90, no. 8, p. 739–752.

Bryant, Bruce, and Reed, J. C., Jr., 1970a, The Blue Ridge and the Reading Prong–Structural and metamorphic history of the southern Blue Ridge, *in* Fisher, G. W., Pettijohn, F. J., Reed, J. C., Jr., and Weaver, K. N., eds., Studies of Appalachian geology–Central and southern: New York, Interscience, p. 213–225.

———1970b, Geology of the Grandfather Mountain window and vicinity, North Carolina and Tennessee: U.S. Geological Survey Professional Paper 615, 190 p.

Bull, W. B., 1972, Recognition of alluvial-fan deposits in the stratigraphic record, *in* Rigby, J. K., and Hamblin, W. K., eds., Recognition of ancient sedimentary environments: Society of Economic Paleontologists and Mineralogists Special Publication no. 16, p. 63–83.

Butler, J. R., and Dunn, D. E., 1968, Geology of the Sauratown Mountains anticlinorium and vicinity, North Carolina: Southeastern Geology, Special Publication no. 1, p. 19–47.

Butler, J. R., and Fullagar, P. D., 1979, Review of plutonic rocks in the Carolinas, *in* Wones, D. R., ed., Abstracts–The Caledonides in the USA; International Geological Correlation Program, Caledonide Orogen Project, Second Symposium: Blacksburg, Virginia, September 1979, p. A9.

Campbell, D. L., 1977, Electric and electromagnetic soundings near Charleston, South Carolina–A preliminary report, *in* Rankin, D. W., ed., Studies related to the Charleston, South Carolina, earthquake of 1886–A preliminary report: U.S. Geological Survey Professional Paper 1028, p. 189–198.

Chowns, T. M., and Williams, C. T., 1983, Pre-Cretaceous rocks beneath the Georgia Coastal Plain–Regional implications, *in* Gohn, G. S., ed., Studies related to the Charleston, South Carolina, earthquake of 1886–Tectonics and seismicity: U.S. Geological Survey Professional Paper 1313, p. L1–L42.

Daniels, D. L., Zietz, Isidore, and Popenoe, Peter, 1983, Distribution of subsurface lower Mesozoic rocks in the Southeastern United States as interpreted from regional aeromagnetic and gravity maps, *in* Gohn, G. S., ed., Studies related to the Charleston, South Carolina, earthquake of 1886–Tectonics and seismicity: U.S. Geological Survey Professional Paper 1313, p. K1–K24.

Glover, Lynn, III, Poland, F. B., Tucker, R. D., and Bourland, W. C., 1980, Diachronous Paleozoic mylonites and structural heredity of Triassic-Jurassic basins in Virginia [abs.]: Geological Society of America Abstracts with Programs, v. 12, no. 4, p. 178.

Gohn, G. S., Houser, B. B., and Schneider, R. R., 1983, Geology of the lower Mesozoic(?) rocks in Clubhouse Crossroads test hole #3, near Charleston, South Carolina, *in* Gohn, G. S., ed., Studies related to the Charleston, South Carolina, earthquake of 1886–Tectonics and seismicity: U.S. Geological Survey Professional Paper 1313, p. D1–D17.

Gohn, G. S., Gottfried, David, Lanphere, M. A., and Higgins, B. B., 1978, Regional implications of Triassic or Jurassic age for basalt and sedimentary red beds in the South Carolina Coastal Plain: Science, v. 202, no. 4370, p. 887–890.

Gottfried, David, Annell, C. S., and Byerly, G. R., 1983, Geochemistry and tectonic significance of subsurface basalts near Charleston, South Carolina; Clubhouse Crossroads test holes #2 and #3 *in* Gohn, G. S., ed., Studies related to the Charleston, South Carolina, earthquake of 1886–Tectonics and seismicity: U.S. Geological Survey Professional Paper 1313, p. A1–A19.

Hamilton, R. M., Behrendt, J. C., and Ackermann, H. D., 1983, Land multichannel seismic-reflection evidence for tectonic features near Charleston, South Carolina, *in* Gohn, G. S. ed., Studies related to the Charleston, South Carolina, earthquake of 1886–Tectonics and seismicity: U.S. Geological Survey Professional Paper 1313, p. I1–I18.

Hatcher, R. D., Jr., 1978, Tectonics of the western Piedmont and Blue Ridge, Southern Appalachians–Review and speculation: American Journal of Science, v. 278, no. 3, p. 276–304.

Hatcher, R. D., Jr., Butler, J. R., Fullagar, P. D., Secor, D. T., Jr., and Snoke, A. W., 1979, Geologic synthesis of the Appalachians in the Carolinas, Tennessee and northeastern Georgia, *in* Wones, D. R., ed., Abstracts–The Caledonides in the USA: International Geological Correlation Program, Caledonide Orogen Project, Second Symposium: Blacksburg, Virginia, September 1979, p. A6.

Hatcher, R. D., Jr., Howell, D. E., and Talwani, Pradeep, 1977, Eastern Piedmont fault system–Speculations on its extent: Geology, v. 5, no. 10, p. 636–640.

Henika, W. S., and Thayer, P. A., 1977, Geology of the Blairs, Mount Hermon, Danville, and Ringgold quadrangles, Virginia: Virginia Division of Mineral Resources Publication 2, 45 p.

Hibbard, M. J., 1979, Myrmekite as a marker between preaqueous and postaqueous phase saturation in granitic systems: Geological Society of America Bulletin, v. 90, no. 11, p. 1047–1062.

Higgins, M. W., 1971, Cataclastic rocks: U.S. Geological Survey Professional Paper 687, 97 p.

Horton, J. W., Jr., 1979, Post-mylonitic brittle deformation in the Brevard fault zone, North Carolina, *in* Wones, D. R., ed., Abstracts–The Caledonides in the USA: International Geological Correlation Program, Caledonide Orogen Project, Second Symposium: Blacksburg, Virginia, September 1979, p. A17.

———1981, Shear zone between the Inner Piedmont and Kings Mountains belts in the Carolinas: Geology, v. 9, no. 1, p. 28–33.

International Union of Geological Sciences Subcommission on the Systematics of Igneous Rocks, 1973, Plutonic rocks–Classification and nomenclature . . .; Geotimes, v. 18, no. 10, p. 26–30.

Kane, M. F., 1977, Correlation of major eastern earthquake centers with mafic/ultramafic basement masses, *in* Rankin, D. W., ed., Studies related to the Charleston, South Carolina, earthquake of 1886–A preliminary report: U.S. Geological Survey Professional Paper 1028, p. 199–204.

Lanphere, M. A., 1983, $^{40}Ar/^{39}Ar$ ages of basalt from Clubhouse Crossroads test hole #2, near Charleston, South Carolina, *in* Gohn, G. S., ed., Studies related to the Charleston, South Carolina, earthquake of 1886–Tectonics and seismicity: U.S. Geological Survey Professional Paper 1313, p. B1–B8.

Leavy, B. D., 1980, Tectonic and sedimentary structures along the eastern margin of the Culpeper basin, Va. [abs.]: Geological Society of America Abstracts with Programs, v. 12, no. 4, p. 182.

Long, L. T., and Champion, J. W., Jr., 1977, Bouguer gravity map of the Summerville-Charleston, South Carolina, epicentral zone and tectonic implications, *in* Rankin, D. W., ed., Studies related to the Charleston, South Carolina, earthquake of 1886–A preliminary report: U.S. Geological Survey Professional Paper 1028, p. 151–166.

Middleton, G. V., and Hampton, M. A., 1973, Sediment gravity flows: Mechanics of flow and deposition, *in* Middleton, G. V., and Bouma, A. H., co-chairmen, Turbidites and deep-water sedimentation: Lecture notes for Short Course, Pacific section, Society of Economic Paleontologists and Mineralogists, Anaheim, 1973, p. 1–38.

Milton, D. J., 1980, A cataclastic zone associated with the Davie County Triassic basin, *in* Price, V., Jr., Thayer, P. A., and Ranson, W. A., eds., Geological investigations of Piedmont and Triassic rocks, central North Carolina and Virginia: Carolina Geological Society field trip guidebook, October 1980, p. IX-1–IX-10.

Nelson, A. E., 1981, Polydeformed rocks of the Lowndesville shear zone in the Greenville 2° quadrangle, South Carolina and Georgia, *in* Horton, J. W., Jr., Butler, J. R., and Milton, D. J., eds., Geological investigation of the Kings Mountain belt and adjacent areas in the Carolinas: Carolina Geological Society field trip guidebook, October 1981, p. 181–193.

Pettijohn, F. J., 1957, Sedimentary rocks: New York, Harper and Row, 718 p.

Phillips, J. D., 1977, Magnetic basement near Charleston, South Carolina–A preliminary report, *in* Rankin, D. W., ed., Studies related to the Charleston, South Carolina, earthquake of 1886–A preliminary report: U.S. Geological Survey Professional Paper 1028, p. 139–149.

Phillips, J. D., Daniels, D. L., Zietz, Isidore, and Popenoe, Peter, 1978, Geophysical studies of the Charleston, S. C., area–Onshore aeromagnetic map: U.S. Geological Survey Miscellaneous Field Studies Map MF–1022–A, 1 plate, scale 1:250,000.

Popenoe, Peter and Zietz, Isidore, 1977, The nature of the geophysical basement beneath the Coastal Plain of South Carolina and northeastern Georgia, *in* Rankin, D. W., ed., Studies related to the Charleston, South Carolina, earthquake of 1886–A preliminary report: U.S. Geological Survey Professional Paper 1028, p. 119–137.

Powers, M. C., 1953, A new roundness scale for sedimentary particles: Journal of Sedimentary Petrology, v. 23, no. 2, p. 117–119.

Randazzo, A. F., Swe, Win, and Wheeler, W. H., 1970, A study of tectonic influence on Triassic sedimentation–The Wadesboro basin, central Piedmont: Journal of Sedimentary Petrology, v. 40, no. 3, p. 998–1006.

Rankin, D. W., 1970, The Blue Ridge and the Reading Prong–Stratigraphy and structure of Precambrian rocks in northwestern North Carolina, *in* Fisher, G. W., Pettijohn, F. J., Reed, J. C., Jr., and Weaver, K. N., eds., Studies of Appalachian geology–Central and southern: New York, Interscience, p. 227–245.

Ratcliffe, N. M., 1971, The Ramapo fault system in New York and adjacent northern New Jersey: A case of tectonic heredity: Geological Society of America Bulletin, v. 82, no. 1, p. 125–141.

———1980, Brittle faults (Ramapo fault) and phyllonitic ductile shear zones in the basement rocks of the Ramapo seismic zones, New York and New Jersey, and their relationship to current seismicity, *in* Manspeizer, Warren, ed., Field studies of New Jersey geology and guide to field trips: 52nd Annual Meeting of the New York State Geological Association, Newark, New Jersey, Rutgers University, 1980, p. 278–311.

———1981, Reassessment of the Ramapo fault system as control for current seismicity in the Ramapo seismic zone and the New York recess [abs.]: Geological Society of America Abstracts with Programs, v. 13, no. 3, p. 171.

———1982, Results of core drilling of the Ramapo fault at Sky Meadow Road, Rockland Country, New York: U.S. Geological Survey Miscellaneous Investigations Map I-1401.

Reed, J. C., Jr., 1955, Catoctin Formation near Luray, Virginia: Geological Society of America Bulletin, v. 66, no. 7, p. 871–896.

Reinemund, J. A., 1955, Geology of the Deep River coal field, North Carolina: U.S. Geological Survey Professional Paper 246, 159 p.

Robinson, G. R., Jr., 1979, Pegmatite cutting mylonite–evidence supporting pre-Triassic faulting along the western border of the Danville Triassic basin, southern Virigina [abs.]: Geological Society of America Abstracts with Programs, v. 11, no. 4, p. 210.

Schilt, F. S., Brown, L. D., Oliver, J. E., and Kaufman, Sidney, 1983, Subsurface structure near Charleston, South Carolina–Results of COCORP reflection profiling in the Atlantic Coastal Plain, *in* Gohn, G. S., ed., Studies related to the Charleston, South Carolina, earthquake of 1886–Tectonics and seismicity: U.S. Geological Survey Professional Paper 1313, p. H1–H19.

Sharp, R. P., and Nobles, L. H., 1953, Mudflow of 1941 at Wrightwood, southern California: Geological Society of America Bulletin, v. 64, no. 5, p. 547–560.

Streckeisen, Albert, 1979, Classification and nomenclature of volcanic rocks, lamprophyres, carbonatites, and melilitic rocks–Recommendations and suggestions of the I.U.G.S. Subcommission on the Systematics of Igneous Rocks: Geology, v. 7, no. 7, p. 331–335.

Sykes, L. R., 1978, Intraplate seismicity, reactivation of preexisting zones of weakness, alkaline magmatism, and other tectonism postdating continental fragmentation: Reviews of Geophysics and Space Physics, v. 16, no. 4, p. 621–688.

Talwani, Pradeep, 1977, A preliminary shallow crustal model between Columbia and Charleston, South Carolina, determined from quarry blast monitoring and other geophysical data, *in* Rankin, D. W., ed.,

Studies related to the Charleston, South Carolina, earthquake of 1886–A preliminary report: U.S. Geological Survey Professional Paper 1028, p. 177–187.

Talwani, Pradeep, Amick, David, and Stevenson, Don, 1979, Crustal structure studies in South Carolina Coastal Plain: Ninth technical report to U.S. Geological Survey, Contract no. 14-08-0001-17670, 81 p.

Travis, R. B., 1955, Classification of rocks: Colorado School of Mines Quarterly, v. 50, no. 1, 98 p.

Weems, R. E., 1980, Geology of the Taylorsville basin, Hanover County, Virginia, *in* Contributions to Virginia Geology–IV: Virginia Division of Mineral Resources Publication 27, p. 23–38.

Williams, Howel, Turner, F. J., and Gilbert, C. M., 1954, Petrography–An introduction to the study of rocks in thin sections: San Francisco, W. H. Freeman and Company, 406 p.

Young, S. W., 1976, Petrographic textures of detrital polycrystalline quartz as an aid to interpreting crystalline source rocks: Journal of Sedimentary Petrology, v. 46, no. 3, p. 595–603.

Seismic-Refraction Study in the Area of the Charleston, South Carolina, 1886 Earthquake

By HANS D. ACKERMANN

STUDIES RELATED TO THE CHARLESTON, SOUTH CAROLINA, EARTHQUAKE OF 1886—TECTONICS AND SEISMICITY

GEOLOGICAL SURVEY PROFESSIONAL PAPER 1313-F

UNITED STATES GOVERNMENT PRINTING OFFICE, WASHINGTON: 1983

CONTENTS

ILLUSTRATIONS

TABLE

STUDIES RELATED TO THE CHARLESTON, SOUTH CAROLINA, EARTHQUAKE OF 1886—
TECTONICS AND SEISMICITY

SEISMIC-REFRACTION STUDY IN THE AREA OF THE CHARLESTON, SOUTH CAROLINA, 1886 EARTHQUAKE

By HANS D. ACKERMANN

ABSTRACT

Thirty-five seismic-refraction spreads were recorded in an area near Summerville, S. C., that encloses the zone of intensity-X effects of the Charleston 1886 earthquake. Penetration was to a 6.0- to 6.4-km/s layer at depths ranging from 700 to 2,400 m; this layer is interpreted to represent the pre-Mesozoic crystalline basement complex. The surface of this layer has a northeast-trending ridgelike feature, which the coincident magnetic anomalies suggest contains both mafic and silicic rocks. The ridge is bounded on the northwest by an abrupt 900-m drop in altitude of the basement surface, inferred to represent a Triassic-basin border fault. Recent earthquake epicenters appear to cluster on both sides of this fault; however, fault-plane determinations indicate high-angle faults both parallel and perpendicular to the ridge-boundary fault. Thus, the combined results indicate that the basement complex in the earthquake area contains orthogonal northeast- and northwest-trending faults and rocks of highly contrasting types.

Refraction arrivals were also recorded from a shallower, gently seaward sloping horizon marking the base of the Cretaceous section. Clubhouse Crossroads #3, a test hole about 18 km southwest of Summerville, encountered this horizon at 775 m depth and then penetrated 256 m of lower Mesozoic basalt flows before encountering sedimentary red beds. The seismic interpretations suggest that the flows thin and become increasingly intercalated with sediments away from the test hole.

INTRODUCTION

This report discusses the interpretation of 35 seismic-refraction spreads recorded on the Atlantic Coastal Plain in southeastern South Carolina within an area of approximately 20 km radius centered near Summerville (fig. 1). The study area includes the region of intensity-X (Modified Mercalli) effects of the Charleston 1886 earthquake (Bollinger, 1977). Funding for this seismic-refraction study was provided by the U.S. Nuclear Regulatory Commission, Office of Nuclear Research, under Agreement No. AT(49-25)-1000.

Data were interpreted by using interactive computer programs written by the author. A brief description of them is given in the appendix.

Several other seismic-refraction surveys have been done on the Atlantic Coastal Plain of South Carolina (Bonini, 1956; Pooley, 1959; Talwani, 1977) and its offshore extension (Meyer, 1956; Hersey and others, 1959; Antoine and Henry, 1965; Hales and others, 1968). Onshore reflection surveys are reported by Yantis and others (1983), Hamilton and others (1983), and Schilt and others (1983). Offshore multichannel surveys are reported by Dillon and Paull (1978), Dillon and others (1983), and Behrendt and others (1983).

The Coastal Plain sediments in South Carolina are of Cretaceous and Cenozoic age; they increase in thickness from a feather edge at the Fall Line to approximately 1 km (Popenoe and Zietz, 1977) at the coast. The sonic log from a deep drill hole near Summerville, Clubhouse Crossroads 1 (CC#1), shows that sediment velocities range from approximately 1.8 to 2.6 km/s.

The deepest refracting horizon generally reported is an approximately 3.8- to 6.8-km/s layer interpreted as the gently sloping pre-Cretaceous surface marking the postrift unconformity (Dillon and others, 1983). The large range in velocity implies that this horizon represents a diversity of rock types. The average onshore velocity is 5.6 km/s (Bonini, 1956).

The shot-seismometer arrays for the extensive survey of Bonini (1956) were planned to be just long enough to record arrivals from this pre-Cretaceous surface. Thus they stood no chance of detecting deeper, higher-velocity layers. The survey of Pooley (1959), which used longer spreads and tied the survey of Bonini to near-shore spreads of Meyer (1956), implies a deeper, 6-km/s layer at locations where lower (5.4 km/s) velocities were found for the pre-Cretaceous surface. The offshore refraction surveys near Charleston recorded velocities of 5.8–6.2 km/s for the pre-Cretaceous surface, which is in the range generally expected for crystalline basement rocks.

A salient feature of all the reflection surveys is a strong reflection from the pre-Cretaceous unconformity. Deeper events are also identified; however, they tend to

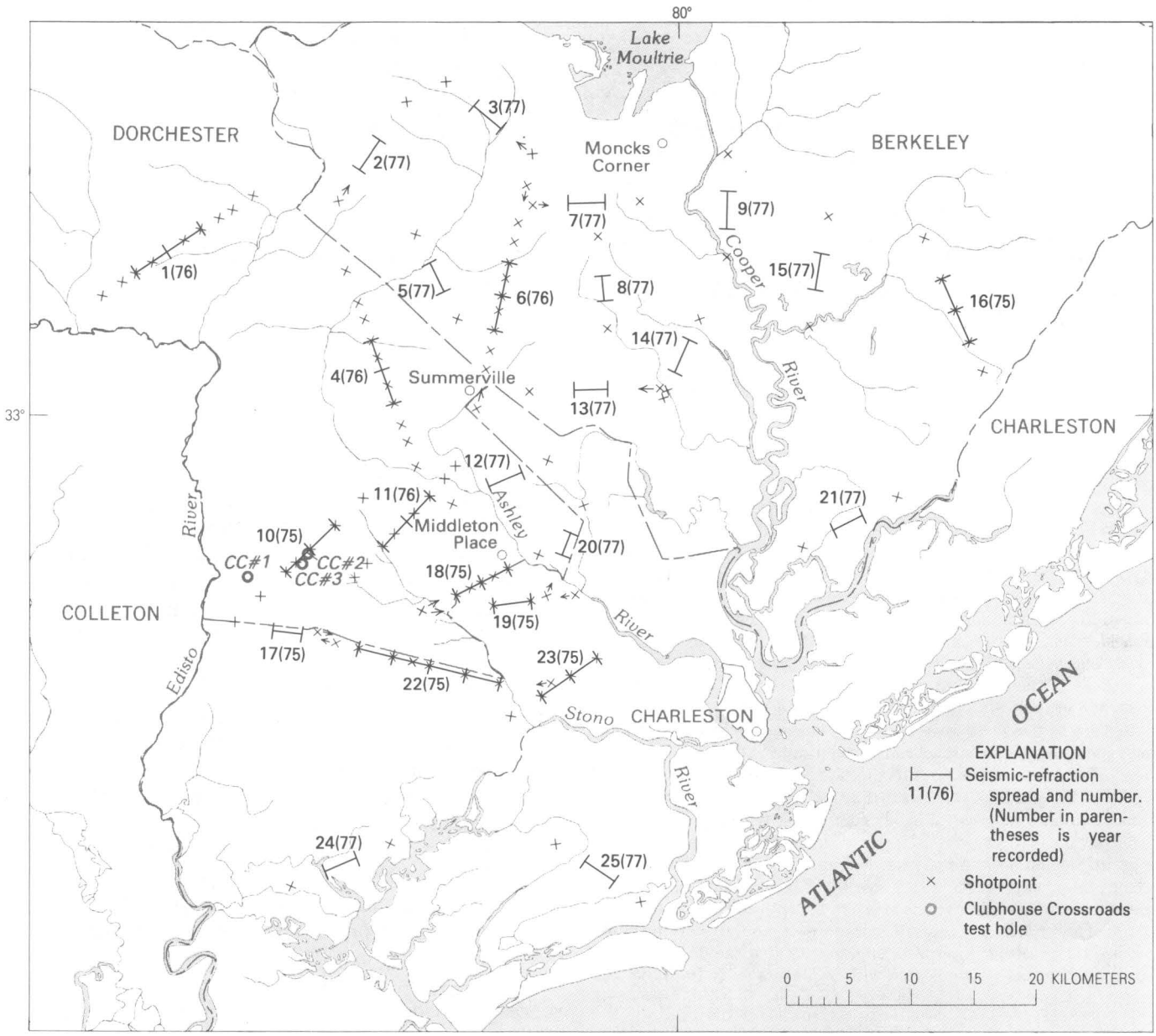

FIGURE 1.—Map of survey area showing location of seismic-refraction spreads and shotpoints for surveys made during 1975, 1976, and 1977. Arrows link shotpoints to the corresponding spreads.

be discontinuous, due to the large reflection coefficient between Cretaceous sediments and underlying dense rocks (Yantis and others, 1983).

Potassium-argon ages from drill samples, and supporting geological and geophysical data (Gohn and others, 1978), imply that the Coastal Plain section in an extensive area across southeastern Alabama, southern Georgia, and southeastern South Carolina is underlain by a basin containing Triassic and Jurassic red beds and basalt produced during crustal extension related to the opening of the modern Atlantic Ocean. A broad range of physical properties of these rocks is indicated by the large variation in their velocities, but the considerable occurrence of values exceeding 6 km/s (Bonini, 1956; Meyer, 1956; Pooley, 1959; Talwani, 1977) indicates that the pre-Cretaceous subcrop in this area may also contain remanents of the crystalline basement rocks that predate continental rifting.

DATA ACQUISITION

Refraction seismic data were acquired during the spring and summer of 1975, 1976, and 1977 (fig. 1). Individual spreads contained 24 single seismometers (4.5 Hz) spaced at approximately 120-m intervals, resulting in a spread length of approximately 2,760 m. Shot-hole depth was from 3 to 20 m, and shot size ranged from 4.5 to 13.6 kg (10 to 30 lb.) of gelatin dynamite. The seismograph was a Texas Instruments Explorer 8000[1] analog unit with magnetic tape and paper oscillograph records. Individual recording channels were set at fixed gain to prevent overdriving of initial arrivals.

The 1975 survey was based on the assumed existence of a single pre-Cretaceous refracting horizon at a depth of 500 to 1,000 m. At most locations, two or more spreads were deployed end to end (fig. 2*A*) and each was recorded by at least four shotpoints: one at each end and one at in-line offset distances of approximately 2,760 m (one spread length) from each end of the spread. Some spreads were recorded at additional closer offset locations. This configuration would have provided complete reversed coverage from the pre-Cretaceous surface at the assumed depth by combining data from adjacent spreads, as shown in figures 2*B* and 2*C*, in addition to providing data from shallower horizons. However, during acquisition of the 1975 data, it was noted that at most locations the pre-Cretaceous rocks yielded arrivals from two distinct layers. The shallower were from the pre-Cretaceous surface and were characterized by highly varying velocities (4.2–5.7 km/s) and by poor transmission properties (both discussed in later sections). The deeper had velocities more representative of crystalline rocks (approximately 6.0–6.4 km/s). Because two distinct pre-Cretaceous layers were recorded, instead of only one as anticipated, complete reversed coverage was obtained from neither.

In an effort to obtain complete reversed coverage from the 6.0- to 6.4-km/s layer, each spread for the 1976 survey was recorded with two additional shots, offset by two spread lengths (5,520 m). Furthermore, half-spread-length offset shots were recorded for better coverage of the pre-Cretaceous surface. Of the four sets of spreads recorded in 1976, however (fig. 1), three obtained few first arrivals from the 6.0- to 6.4-km/s layer, implying a large range in its depth.

In 1977, 14 single spreads were recorded, each using only two shotpoints that were offset between 2,500 and 3,500 m from opposite ends (fig. 1). Most of these, as in 1975, provided data from both the pre-Cretaceous surface and the deeper basement. Inadvertently, three of the four spread locations of 1976 were deployed where the 6.0- to 6.4-km/s layer was anomalously deep.

[1]Use of trade names is for descriptive purposes only and does not constitute endorsement by the U.S. Geological Survey.

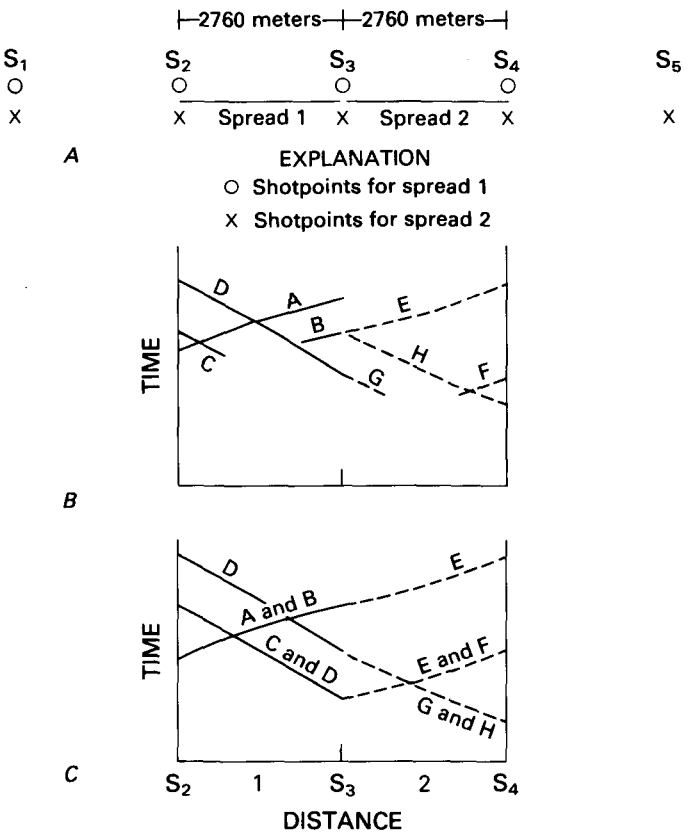

FIGURE 2.—*A*, Typical shot-seismometer configuration used in 1975 for recording end-to-end spreads 1 and 2 with five shotpoints (S_1–S_5). *B*, Hypothetical arrival-time curves (A through H) from a single basement horizon. Solid line segments represent arrivals for spread 1, and dashed line segments represent arrivals for spread 2. Arrival-time segments C, G, B, and F are short because they represent shotpoints at the ends of the spreads and because the arrivals from shallow events are not shown. *C*, Combined data from *B*, resulting in complete reversed coverage between shotpoints 2, 3, and 4.

SHINGLING

Severe attenuation of refracted first arrivals and related shingling (Cassinis and Borgonovi, 1966; Sheriff, 1973, p. 193) were caused by high-velocity beds that are relatively thin compared to the length of the transmitted wave within both the shallow Eocene section and the rocks forming the pre-Cretaceous surface. Shingling is defined by Sheriff as a successive loss of visibility of early cycles as range increases.

The sonic log from CC#1 shows a layer approximately 30 m thick whose upper surface is 111 m below ground. This layer corresponds lithologically to a series of well-cemented Eocene beds having a highly variable velocity that averages 2.5 km/s. The wavelength of the recorded 0.035-s period signal at 2.5 km/s is about 90 m, which is considerably greater than the bed thickness. These beds are underlain by approximately 1.9-km/s rocks to a depth of about 300 m. Except for occasional spikes on

the sonic log, the 2.5-km/s value is close to the maximum velocity for Cenozoic rocks recorded in the drill hole. These Eocene beds form a seismic marker horizon throughout much of the area and were contoured as a 2.5- to 2.7-km/s layer in an earlier report (Ackermann, 1977). The rapid attenuation in this layer is seen in the sample seismogram of figure 3.

Such a high-velocity zone obscures the underlying lower velocity distribution, so that, unless the inversion is properly compensated for, depth calculations to deeper, higher velocity horizons will be too large. Therefore, the velocity function from the CC#1 log was used in this study to calculate all pre-Cretaceous layers. On the other hand, such a highly attenuating marker horizon generally results in a "quiet" seismogram and decreases the effect of interference with later events, which can then be readily identified as second arrivals (fig. 3).

Bonini (1956) makes only one reference to this shingling effect, noted in his spread 53 immediately north of the area of this study. His published arrival-time plots show little evidence for a shallow 2.5-km/s horizon elsewhere in the South Carolina Coastal Plain.

Severe attenuation of arrivals from the pre-Cretaceous surface similarly implies relatively thin high-velocity beds in that position at all spread locations except 6, 9, 15, and 16 (fig. 1), which are underlain by lower velocity rocks. Near CC#3 (Clubhouse Crossroads well 3) (fig. 1, spread location 10), where 256 m of basalt was penetrated, the shingling effect was slight, suggesting that the high-velocity zone beneath the Cretaceous sediments is thicker there than elsewhere. The wavelength of the pre-Cretaceous surface event in the Clubhouse Crossroads area is about 5.7 km/s × 0.045 s or 250 m.

The shingling of this pre-Cretaceous surface event takes two forms. One represents a shift of energy to successively later cycles (figs. 4*A*, 4*B*), in which case the successive cycles have approximately equal phase velocities. The method of picking these data is shown by the tick marks in figures 4*A* and 4*B* and results in a stair-stepped or shingled plot. To facilitate interpretation, a single line is constructed, as shown, by lowering and connecting successive cycles. This process entails personal judgment and, therefore, decreases the likelihood that faults will be identified. It assumes, fur-

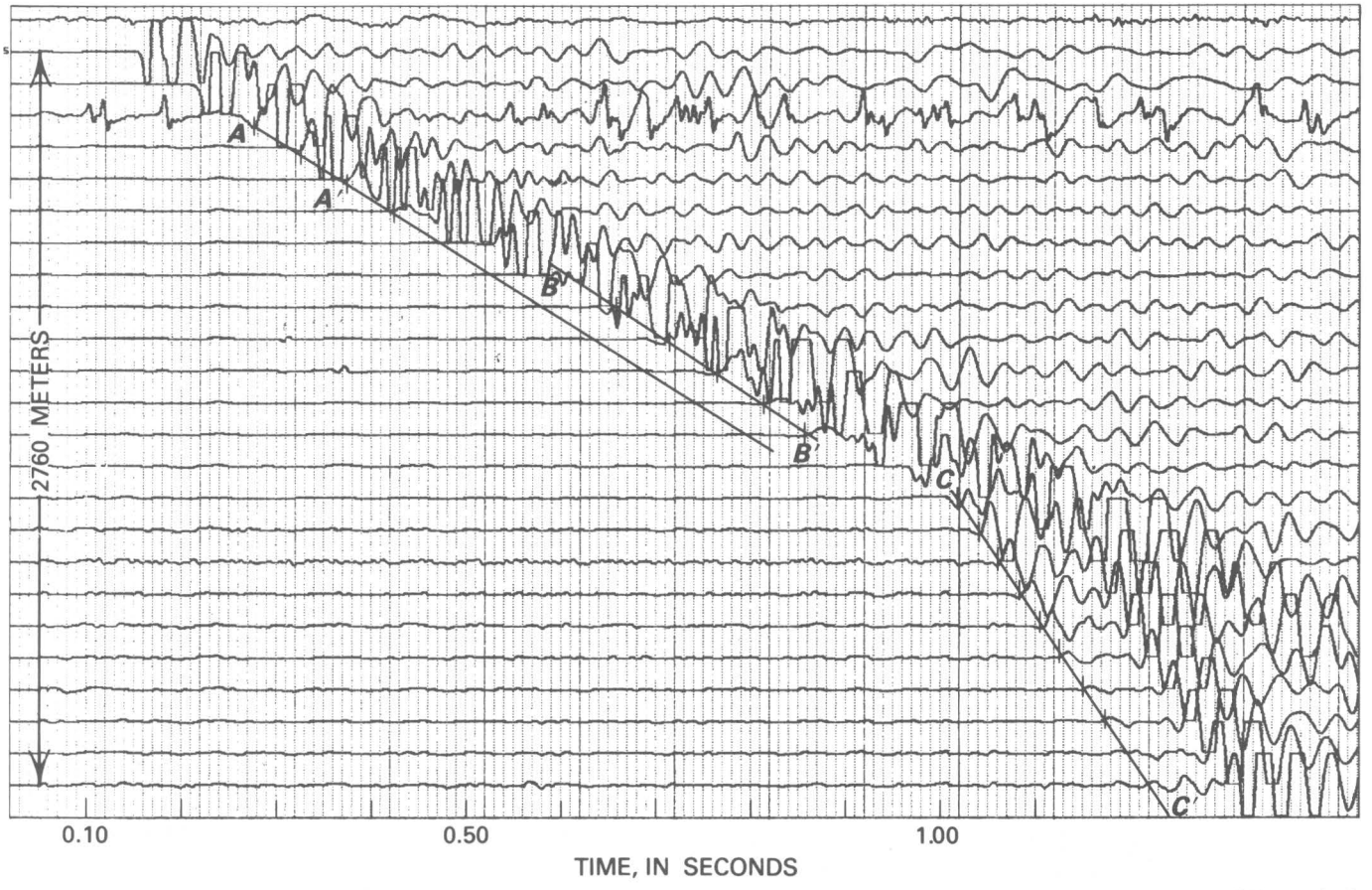

FIGURE 3. – Sample seismogram from spread location 11 showing rapid attenuation of event *A*–*A*′ from relatively thin well-cemented Eocene beds at approximately 100 m depth. The shingled event *B*–*B*′ has the same apparent velocity as *A*–*A*′ but is delayed about 80 milliseconds (ms). Rapid attenuation permits clear identification of the pre-Cretaceous event *C*–*C*′ as a second arrival.

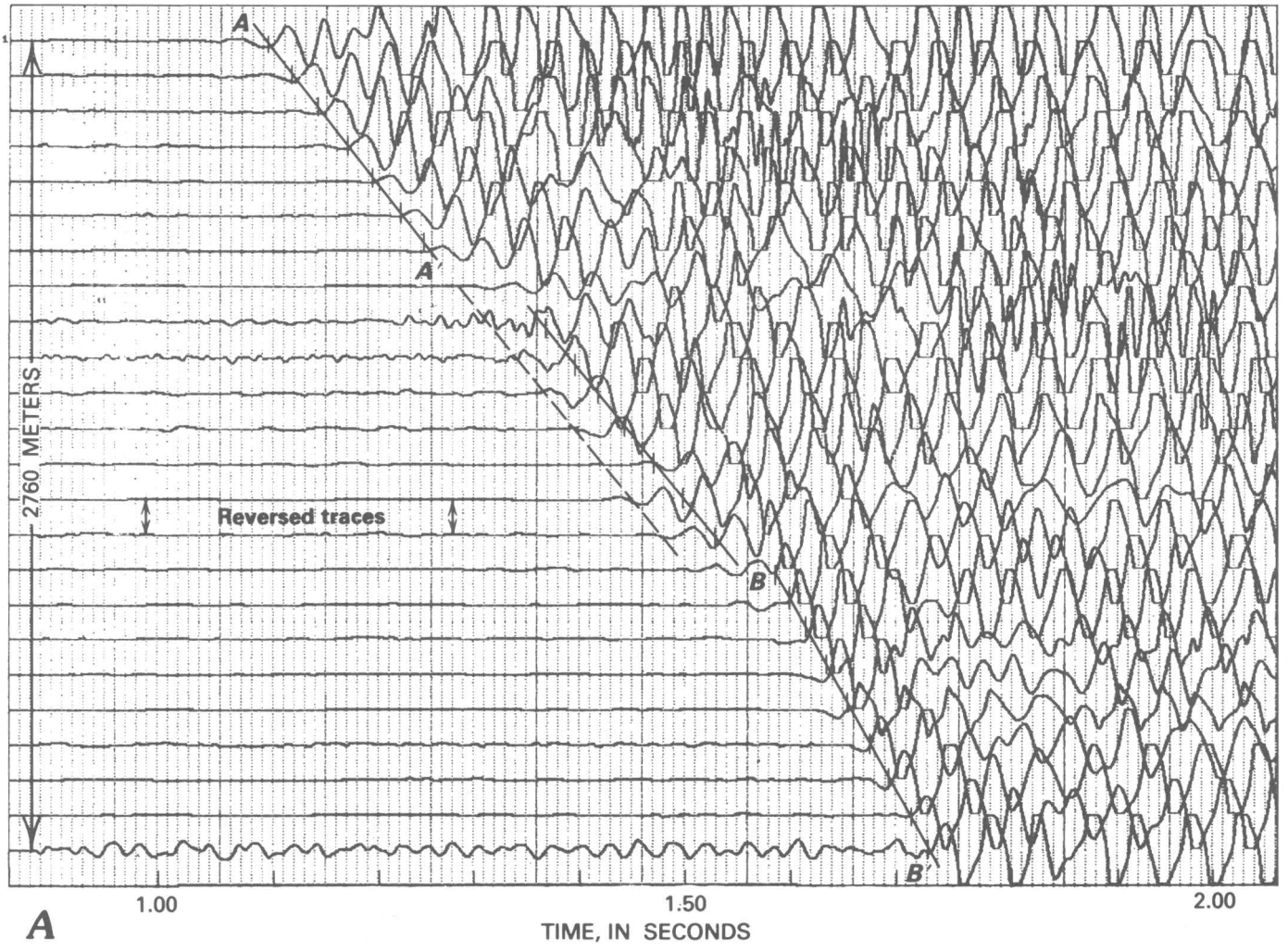

FIGURE 4.—Sample seismograms showing shingling of the pre-Cretaceous event at spread locations 5 (*A*) and 23 (*B*) in the form of cycle skipping. Time-distance plots for this event are made by lowering the shingled arrivals to connect with segment *A*–*A*′, as shown by the dashed lines. In 4*A*, line *B*–*B*′ represents the deeper 6.0- to 6.4-km/s event.

thermore, that the arrivals picked nearest the shotpoint represent an unshingled event. For example, line segments *A*–*A*′ in figures 4*A* and 4*B* might already represent a skipped cycle, which could not have been detected, so that plotted arrival times would be too large and computed depths too deep. Problems of this nature were severe in the 1977 data for which only offset shotpoints were used, and the initial development of shingling could not be clearly identified.

Another form of shingling is illustrated in figure 5. In this case, initial arrivals from the pre-Cretaceous surface (*A*–*A*′) attenuate rapidly but are not followed by later cycles. This permits easy identification of the later, deeper event (*B*–*B*′).

In most cases, the arrivals following the pre-Cretaceous surface event have apparent velocities of about 5.8 to 6.4 km/s and are not themselves shingled, suggesting that they are caused by a thick, continuous, high-velocity layer that underlies the pre-Cretaceous surface. However, at spread locations 1, 2, and 4, these later arrivals also tend to be shingled (fig. 6) and have velocity values only slightly greater than those for the pre-Cretaceous surface. These events may represent some intermediate layer of limited thickness and lateral extent such as a lava flow or sill. Because of uncertainties regarding arrival times, travel paths, and velocity contrasts, depth calculations were not made for these events.

VELOCITY VARIATIONS OF THE PRE-CRETACEOUS SURFACE

Interpretations of the refraction data indicate large areal variations in the velocity of the pre-Cretaceous surface, as shown and contoured in figure 7. Locations at which arrivals from this refractor are not shingled are also indicated. A velocity minimum of 4.2 to 4.5 km/s

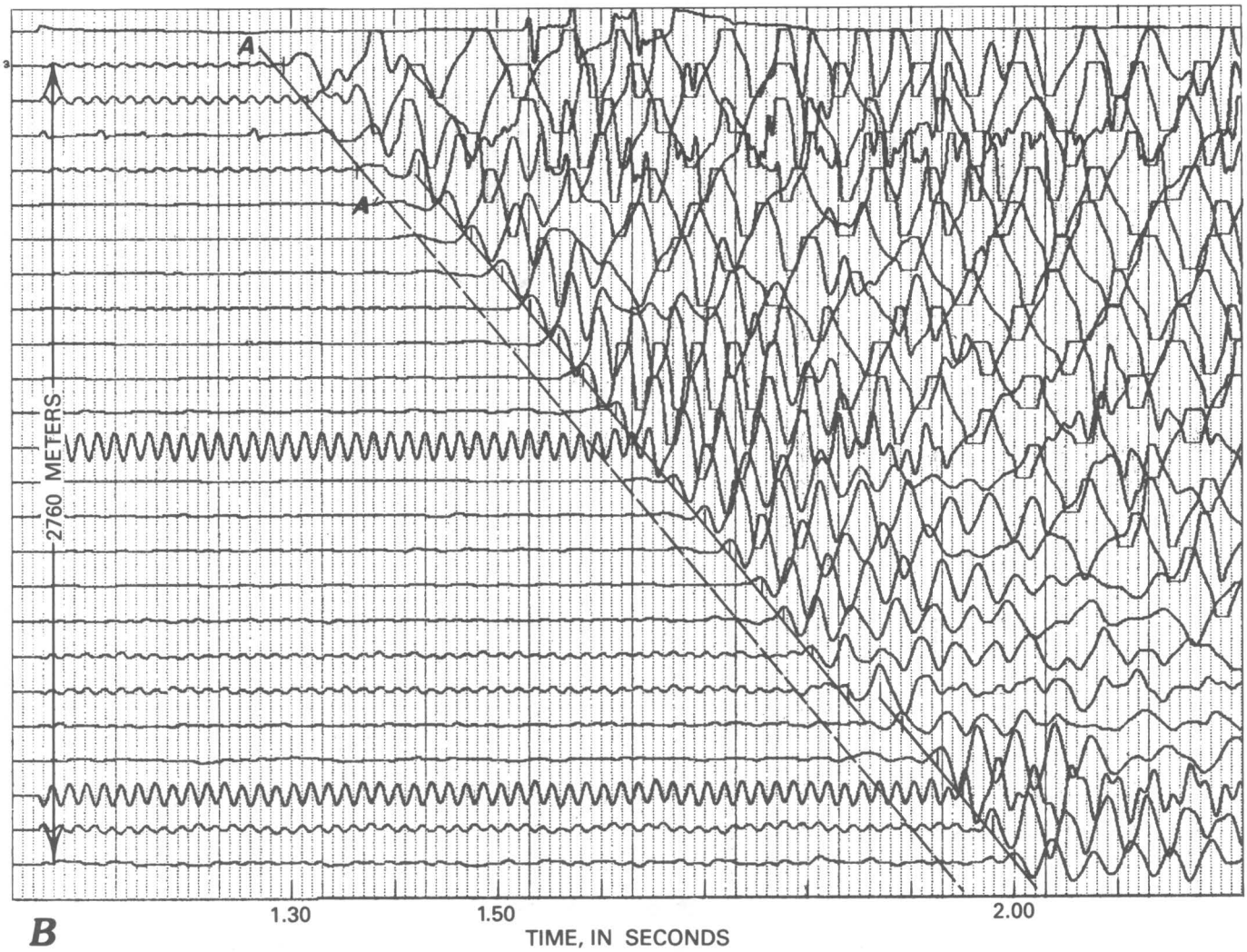

FIGURE 4.—Continued

occurs near the coast and apparently extends approximately 40 km inland along a narrow northwest-trending tongue. Outward from this tongue, velocities increase. The highest velocities occur to the northeast, at spread locations 15 and 16. Because arrivals there are not shingled, they are inferred to represent the 6.0- to 6.4-km/s crystalline basement complex, which, elsewhere in the study area, is considerably deeper and underlies the pre-Cretaceous surface.

Another velocity maximum of 5.7 km/s, known from drill-hole data to represent basalt, occurs at spread location 10 near Clubhouse Crossroads, west of the tongue. Paleomagnetic studies of drill cores (Phillips, 1983) show that the basalt there consists of a sequence of numerous flows. However, the velocity decrease away from this location implies that the physical properties of these flows must change. Ackermann (1977) suggested that this change may be due to increased fracture porosity or simply to termination of the flows. I favor the latter explanation and infer that at spread location 6 within the tongue, where no shingling is observed, the flows are effectively absent, and a horizontally propagating, critically refracted wave sees only the underlying Triassic(?) sediments. One possible explanation for this pattern is that a volcanic vent may have existed in the vicinity of Clubhouse Crossroads. Away from the source, the flows would have thinned and been intercalated with lower velocity sediments, thus accounting for the observed overall velocity decrease and the increased attenuation. The low-velocity tongue would have lain beyond the extent of most, if not all, of these flows. This explanation requires the existence of a second vent or vent system to the north and east of the low-velocity tongue to account for the higher velocities seen again at spread locations 3, 7, 8, and 14. The possibility envisioned here, that lava may have issued from a series

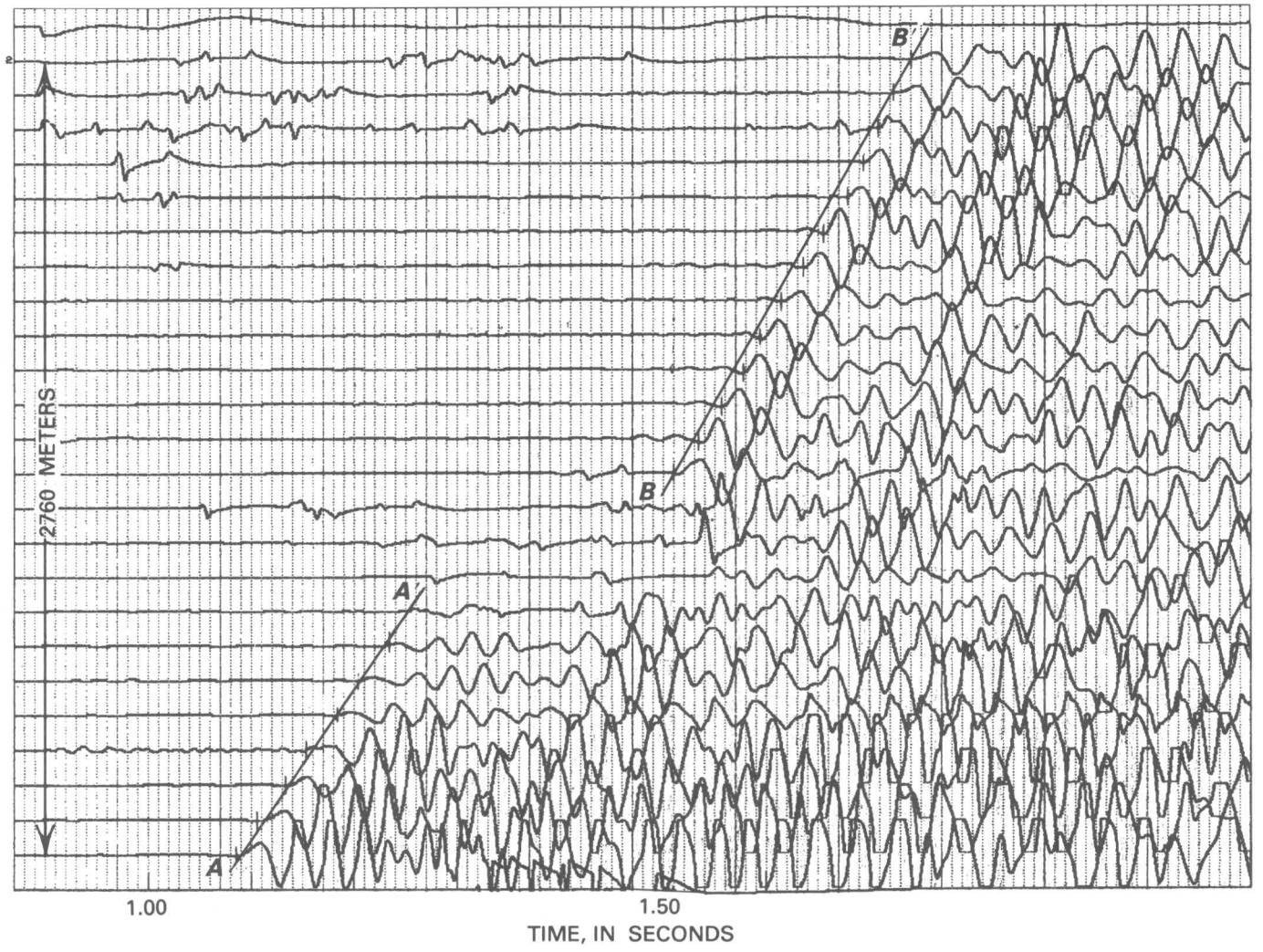

FIGURE 5.—Sample seismogram from spread location 3, showing rapid attenuation of pre-Cretaceous event A–A', without subsequent cycle skipping. The deeper 6.0- to 6.4-km/s event is shown by segment B–B'.

of northwest-trending fissures, is consistent with the northwest-trending system of diabase dikes beneath the Coastal Plain of South Carolina and Georgia, which Popenoe and Zietz (1977) interpreted from aeromagnetic maps.

VELOCITY DISTRIBUTION

The velocity function used for calculating pre-Cretaceous depths consists of six horizontal layers (table 1) derived from the sonic log at CC#1 and augmented by additional refraction data for very shallow depths from which well data were not available.

The function for computing the 6.0- to 6.4-km/s crystalline basement layer below the base of the Cretaceous was approximated by combining results from CC#1, the velocities of the pre-Cretaceous surface layer obtained from the individual seismic spreads, and the results from the spreads at location 6 (fig. 7). The basalt layer at Clubhouse Crossroads is 256 m thick. A thickness of 250 m was thus arbitrarily assumed for the higher velocity pre-Cretaceous subcrop layer that gave rise to shingling. The velocity used for this layer was that determined from the individual refraction results at each site. At spread location 6, pre-Cretaceous surface velocities were 4.4 km/s and were not shingled, implying absence of this relatively thin, high-velocity layer. It was thus assumed that 4.4 km/s represents the underlying Triassic(?) sedimentary rocks throughout the area. Marine (1974) reports Triassic velocities averaging 5.1 km/s, obtained from three closely spaced wells in the Dunbarton Basin in Georgia. Sonic velocities from a well drilled to crystalline basement in the Durham-Wadesboro Triassic basin in North Carolina (Coffey, 1977) average about 4.7 km/s. Using a velocity value actually recorded in the survey area is probably preferable to using those reported from distant wells. If the

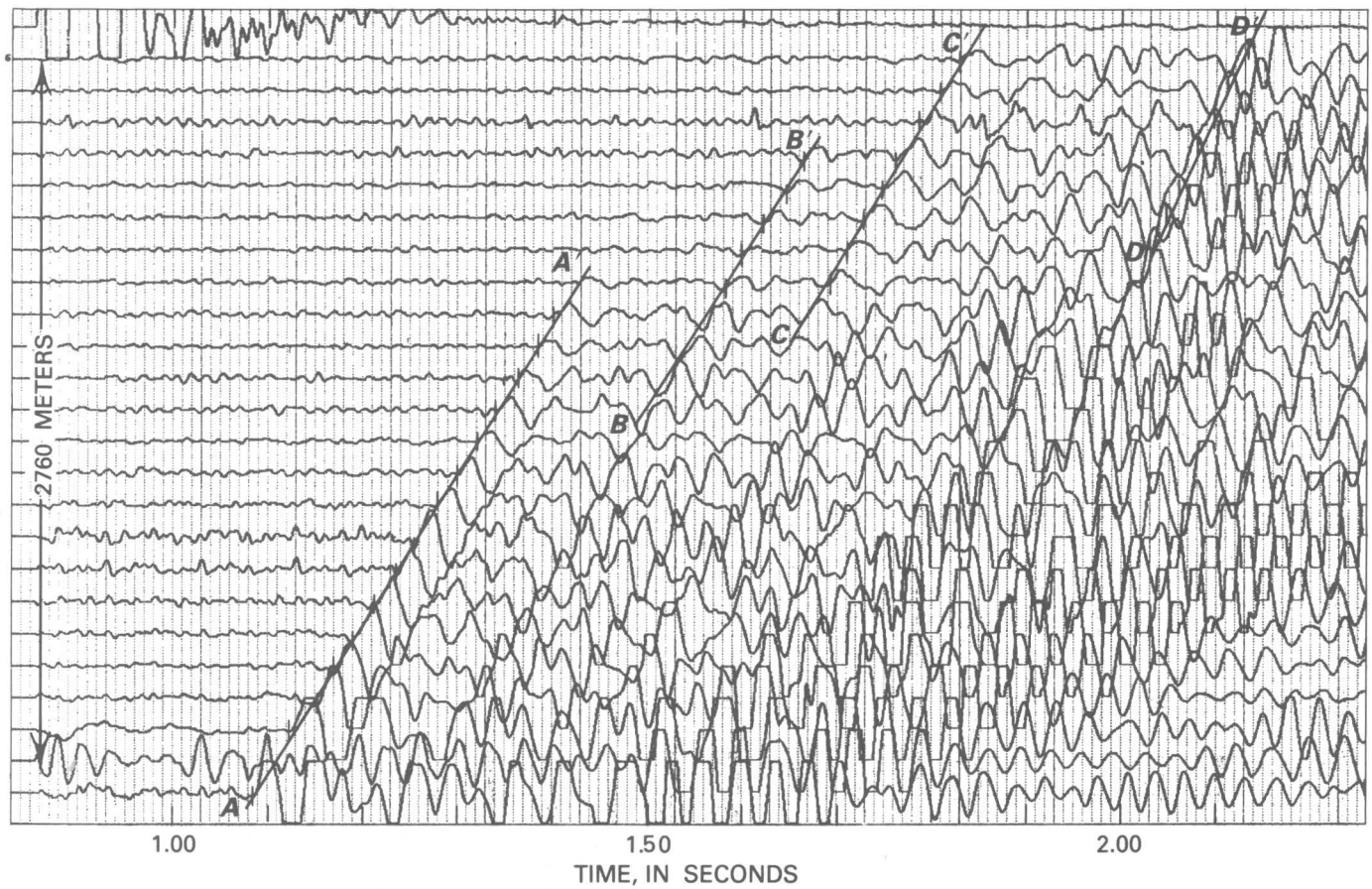

FIGURE 6.—Sample seismogram from spread location 1 showing rapidly attenuating pre-Cretaceous event A–A', followed by later arrivals B–B' and C–C' of approximately equal velocity, inferred to represent some deeper lava flow or sill. The poorly defined event D–D' may represent the 6.0- to 6.4-km/s layer.

adopted velocity of 4.4 km/s is too low, calculated depths to deeper horizons will be too shallow (see discussion of error, next section).

DEPTH TO THE PRE-CRETACEOUS SURFACE

Figure 8 is a contour map of the pre-Cretaceous surface interpreted from the seismic-refraction data of this study. Because the map reflects new data and some changes in interpretations, it differs from an earlier published map (Ackermann, 1977). Therefore, some contours in figure 8 differ from those of the structure map of the pre-Cretaceous surface of the Southeastern United States by Popenoe and Zietz (1977).

Figure 8 shows a gently seaward sloping horizon that has an average gradient of about 7.6 m/km. There are indications of a steeper gradient (26 m/km) between spreads 11 and 18 and between spreads 17 and 22. A slight reverse in dip exists between spreads 22 and 23. Recent reflection profiling (Hamilton and others, 1983) indicates faulting of the pre-Cretaceous surface in this zone of steeper gradients. However, within the limits of interpretation accuracy of this survey, no significant structural features on the pre-Cretaceous surface can be inferred with confidence.

The depth-computation accuracy hinges on the accuracy of the arrival-time picks (here assumed to be good), on the accuracy of the velocity function used for the overlying section, and on the extent of reversed coverage on the critically refracting horizon. Experience has shown that if these criteria are satisfied, depth computations will agree to within a few percent of recorded well depths. If not, errors can be large.

Some error undoubtedly is introduced by the assumption that the velocity function determined at CC#1 applies uniformly throughout the area. Errors caused by this assumption may be particularly serious toward the coast where the depth to the pre-Cretaceous surface is greater than it is at CC#1. Because velocities usually increase with depth, the constant 2.35-km/s velocity used for layer 6 (table 1) may be too small, which would result in depth calculations that are too shallow. For example, if the velocity in the vertical interval ΔZ between the depth of the pre-Cretaceous surface at CC#1 (775 m) and

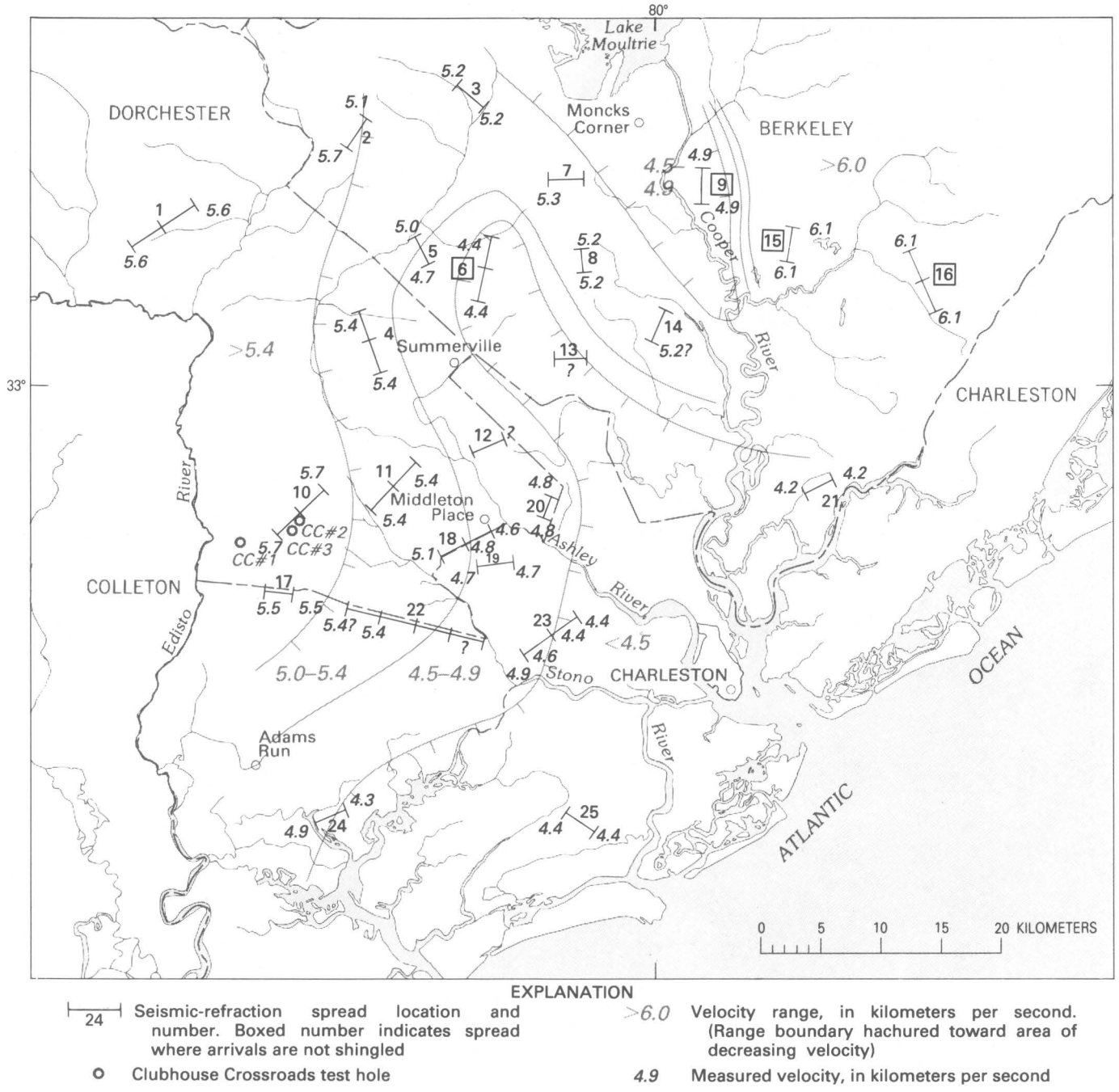

FIGURE 7.—Lateral areal variations in compressional seismic-refraction velocities of the pre-Cretaceous surface, in kilometers per second.

the depth of the same horizon calculated at some other location toward the coast were as large as 3 km/s, the resulting computed depth at the other location would be in error by about $0.5 \times \Delta Z$. Thus, the depth calculation at spread location 25 in the southeast corner of figure 8 would be 140 m too shallow. Of some additional concern are possible differences in the velocities of very shallow beds at different spread locations. Because of the small topographic relief and the shallow depth to the top of the zone of water saturation throughout the area, however, the error introduced by near-surface velocity variations is probably not serious.

Nearly complete reversed coverage from the pre-Cretaceous surface was obtained from the 1975 and 1976 spreads except at locations 19 and 22 (fig. 8). Hence, the condition of sufficient reversed coverage was satisfied for most of these data. For the 1977 survey only two shots were recorded per spread, and they were offset. Due to the lateral velocity variations in the pre-Cretaceous layer (fig. 7), personal judgment had to be

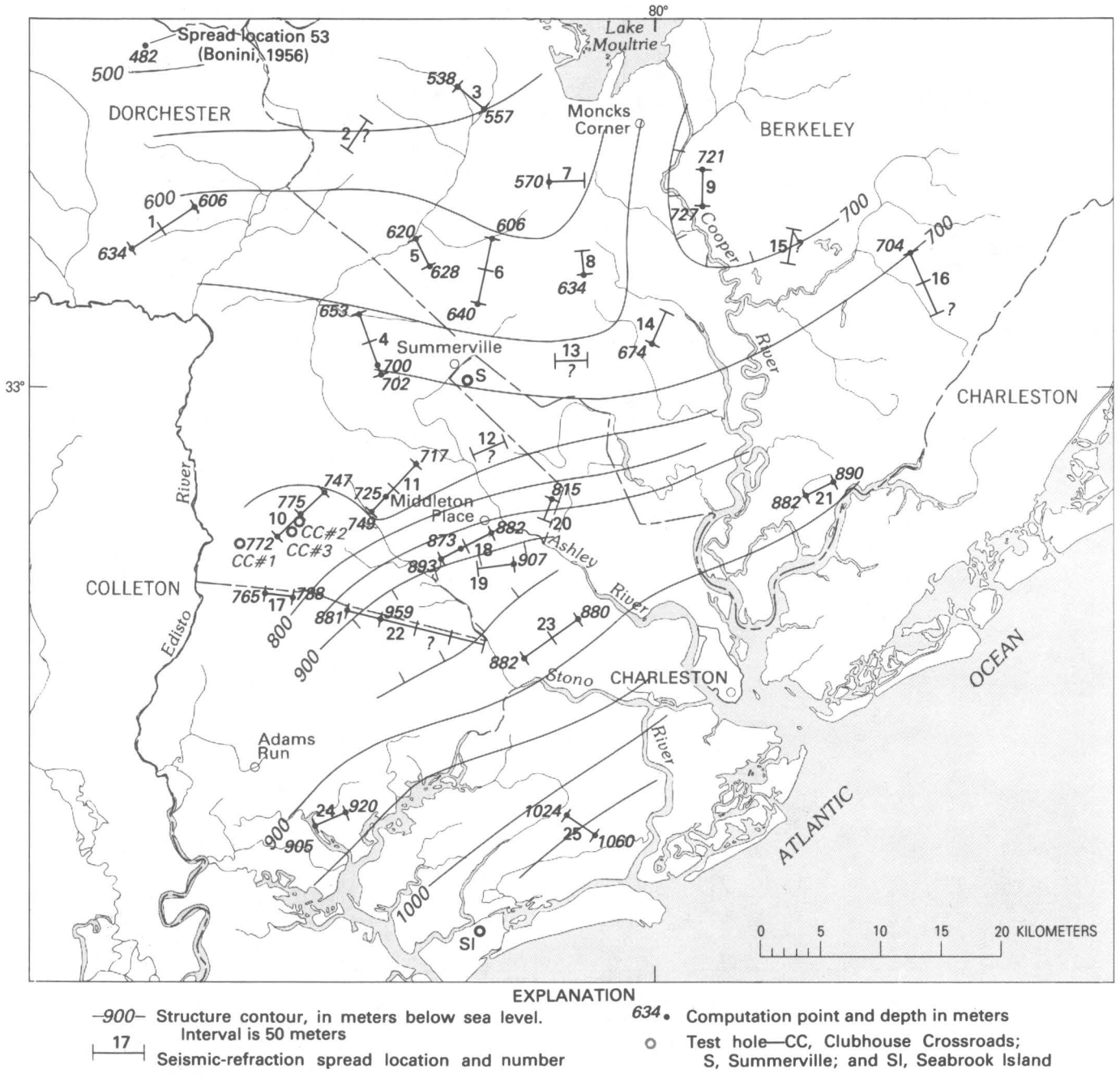

FIGURE 8. – Contour map of the depth below sea level of the pre-Cretaceous surface, in meters, interpreted from seismic-refraction data. Queries mark locations where depths were not computed because of shingling or poor data quality or because no first arrivals were recorded from the pre-Cretaceous surface.

exercised in projecting pre-Cretaceous arrivals either forward to the reciprocal point or back to the intercept point (see interpretation methods in appendix). A difference of only 0.2 km/s in projection velocities results in an approximately 20-m difference in the depth calculations. Finally, possible undetected shingling in the 1977 data was another potential source of error. For this reason, pre-Cretaceous basement depths were not calculated at spread 2 or at the north end of spread 8 (fig. 8).

In the final analysis, the accuracy of depth calculations may best be judged by the degree to which the results agree with other sources of information. At the Clubhouse Crossroads spreads, the depth calculations

TABLE 1.—*Velocity distribution used for depth calculations*

[Layers 1 through 6 were used for determining the pre-Cretaceous surface, and 7 and 8 were used for determining the deeper crystalline basement]

Layer	Thickness (m)	Velocity (km/s)	Depth below surface (m)
1	25	1.50	0– 25
2	71	1.85	25– 96
3	87	2.56	96–183
4	315	1.93	183–498
5	104	2.22	498–602
6	Variable	2.25	
7	250	4.2–5.7	
8	Variable	4.40	
9		6.0–6.4	

agreed exactly with the logged drill hole depth of 775 m, as should be the case, because the velocity function used was derived from the nearby hole.

Comparisons with COCORP (Consortium for Continental Reflection Profiling) reflection data (Schilt and others, 1983) were possible at several places. Between the center of spread location 10 and the east end of location 11 (fig. 8), the pre-Cretaceous reflection time decreases by about 0.025 s (29 m at 2.35 km/s) and the refraction results show a decrease of 58 m: a discrepancy between methods of roughly 30 m. Southeastward, both the present refraction work and the COCORP reflections show increased dip toward the coast. (Note more closely spaced contours in this region in figure 8.) However, the reflection character changes southeastward, rendering further correlation with the refraction interpretations at locations 18 and 23 difficult.

Comparisons were made with reflection results of Yantis and others (1983). Between spread locations 10 and 18, their pre-Cretaceous reflection time increases 0.08 s (94 m at 2.35 km/s) and the refraction results show a change of about 120 m. Between locations 10 and 6, reflection time decreases 0.06 s (70 m at 2.35 km/s) compared with a change of about 130 m for the refraction data. Discrepancies are 26 and 60 m respectively.

A well drilled into the pre-Cretaceous basement at Summerville (Cooke, 1936; Popenoe and Zietz, 1977) has a reported depth below sea level of 740 m for the top of diabase. Although no refraction spread was recorded in Summerville, the pre-Cretaceous surface contour drawn through the town (fig. 8) indicates a 700-m depth. Assuming that the diabase marks the pre-Cretaceous surface, the discrepancy between the two is 40 m.

In a well at Seabrook Island, southwest of Charleston, a depth below sea level of 814 m was reported for the top of a quartzitic sandstone unit (Popenoe and Zietz, 1977). They questioned whether this represented pre-Cretaceous basement but contoured it as such on their basement map. The well is within 15 km, along the regional strike, of spread location 25 (fig. 8), where the computed pre-Cretaceous surface depth is 1,050 m. The well is about 15 km down dip from location 24, which has a computed depth of 900 m for the pre-Cretaceous surface. Thus, the top of the reported sandstone layer is over 200 m shallower than extensions of computed pre-Cretaceous depths would suggest. This 814-m depth also appears too shallow when compared to values computed by Meyer (1956) farther southwest along the coast. I suggest that the Seabrook Island well did not penetrate the pre-Cretaceous surface.

Bonini (1956) reports a depth of 482 m for the pre-Cretaceous surface at his spread 53, approximately 16 km north of our location 1, which agrees well with the results of this survey (fig. 8).

The above comparisons with other sources suggest that, in the northern part of the surveyed area (fig. 8), interpreted pre-Cretaceous depths are accurate within roughly 50 m or one contour interval. Errors for the southern part are difficult to estimate due to the lack of other data for comparison.

THE CRYSTALLINE BASEMENT

At all spread locations except 2 and 9, arrivals were recorded from a refracting layer having a velocity of 6.0 to 6.4 km/s. Interpreted depths below sea level to this layer are contoured in figure 9, which shows several distinct features. A northeast-trending ridge crosses the center of the map. At its northeast end, the ridge broadens and its depth decreases from 1,250 to 700 m where it may form the pre-Cretaceous surface. In the center of the map, the northwest boundary of the ridge is marked by an abrupt 900-m decrease in altitude. Although no spreads actually crossed this boundary, the spreads at locations 4 and 6 (fig. 9), north of the boundary, employed offset shotpoints south of it. Thus, the ridge boundary was determined by comparing delay times for spreads 4 and 6 from shots offset at successively greater distances to the south. The horstlike feature at location 5 (north of the ridge) implies that the generally low area to the northwest of the basement ridge itself contains areas of considerable relief.

Southeast of the ridge, the contours imply a more gently sloping surface. However, the interpretations at spread locations 18 and 19, near Middleton Place, suggest some very abrupt changes in depth southeast of the ridge. Figure 10 shows arrival times from the 6.0- to 6.4-km/s layer at these spread locations, recorded from a common shotpoint offset to the west. Because the delay time at the common shotpoint is the same for both spread locations, differences in arrival time for constant shot-seismometer ranges are due to different delay times below seismometer locations. Differences are between 0.06 and 0.11 s. Figure 10 also shows the computed depth beneath each location. The results suggest a

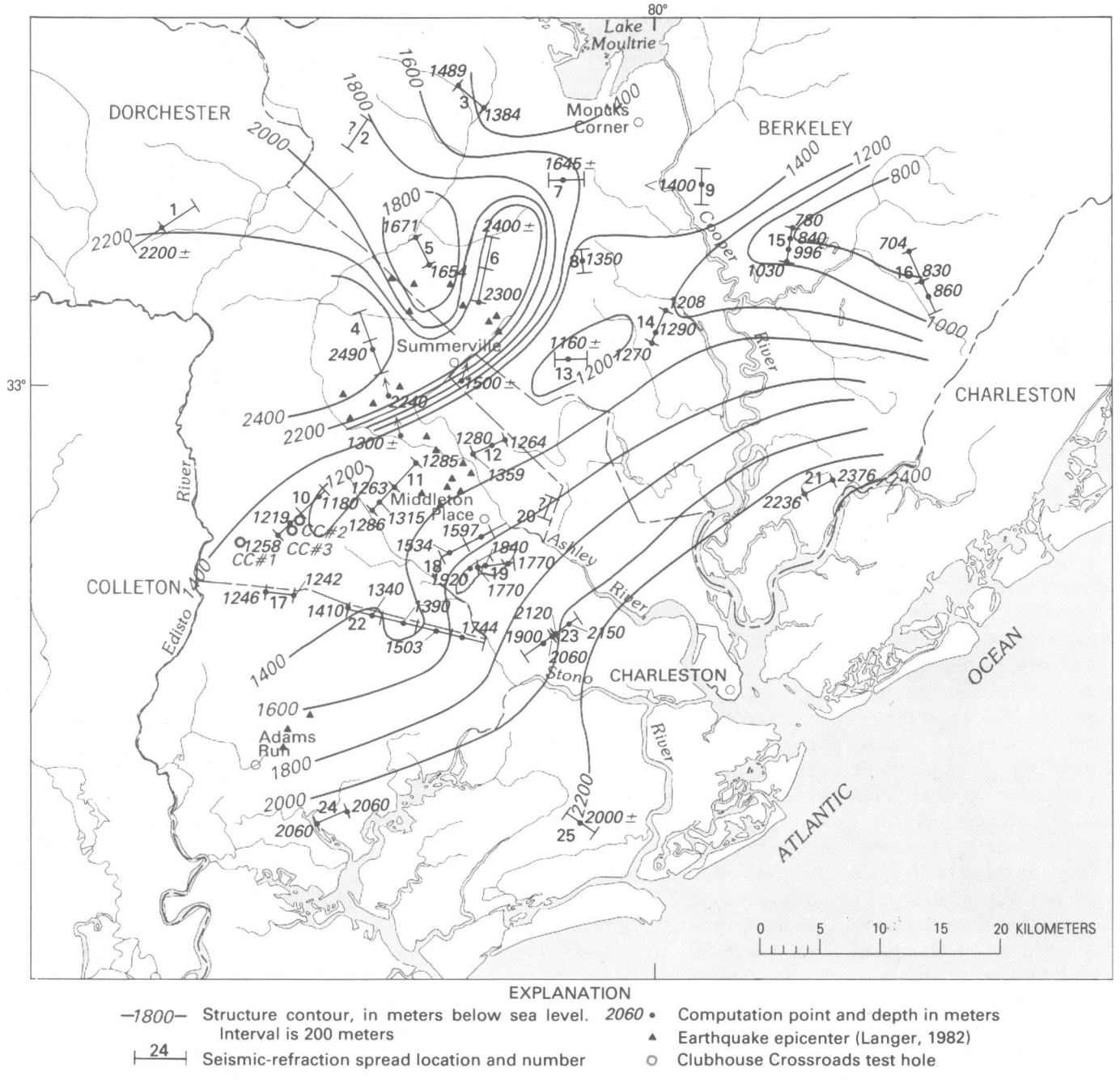

FIGURE 9.—Contour map of the depth below sea level of the 6.0- to 6.4-km/s layer interpreted from seismic-refraction data. This layer is suggested to represent the crystalline basement. Also shown are epicenters of recent earthquakes (Tarr and Rhea, 1983). Depth calculations are based on an assumed velocity function below the base of the Cretaceous; complete reversed coverage was not obtained from most of the spreads. Arrows south of spreads 4 and 6 indicate offset shotpoint locations used to determine the ridge boundary.

fairly constant depth at location 18 but a considerably larger and varying depth at location 19, just 2 to 3 km southward.

The data from the spreads at location 22 (fig. 9) were of poor quality. However, they suggest that the 6.0- to 6.4-km/s layer dips gradually seaward south of the ridge crest.

In the absence of additional information either from drilling or from reflection data beneath the pre-Cretaceous surface, our understanding of the nature of the 6.0- to 6.4-km/s layer is speculative. Unfortunately, CC#3 had to be terminated approximately 100 m short of penetrating the layer as interpreted in this study. I suggest that this layer represents the pre-Mesozoic

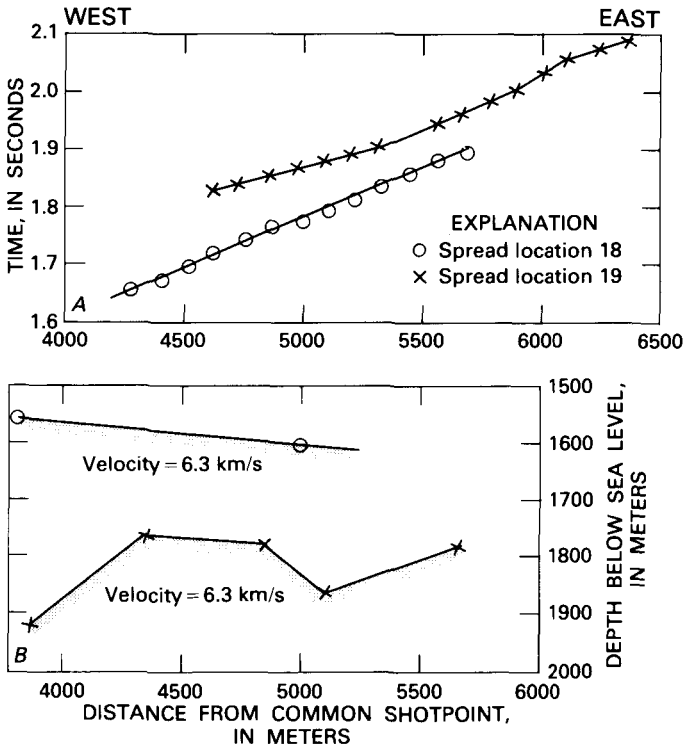

FIGURE 10.—*A*, Arrival times from the 6.0- to 6.4-km/s layer at spread locations 18 and 19, recorded from a common shotpoint offset to the west. *B*, Computed depth of this layer below sea level, beneath spread locations 18 and 19.

crystalline basement complex and thus see its surface as one of large relief; in some places this layer is the pre-Cretaceous subcrop, and in others it is overlain by approximately 1,500 m of Triassic or Jurassic volcanic and sedimentary rocks. The abrupt altitude change northwest of the ridgelike feature (fig. 9) suggests a northeast-trending Triassic border fault similar to border faults in Triassic basins exposed farther inland in the Piedmont.

Another possibility must also be considered regarding the nature of the 6.0- to 6.4-km/s layer. Talwani and others (1975b) suggest that a high-velocity layer underlying the Cretaceous section at Georgetown, S. C. (Bonini, 1956), is either a diabase sill or a basalt flow and that an associated large gravity low represents an underlying 6-km-thick section of Triassic rocks. If very thick (>250 m) units of such high-velocity intrusive or volcanic rocks actually occur within the Triassic and Jurassic sedimentary section, then the horizon mapped in figure 9 may not be continuous but, in places, may represent the upper surface of bodies of dense igneous rock emplaced within the sedimentary section.

The accuracy of figure 9 is difficult to estimate because no holes with which one could compare results have been drilled through the Triassic and Jurassic section into the deeper basement complex. Depth calculations were based on an assumed velocity function below the base of the Cretaceous, and complete reversed coverage was not obtained from most of the spreads. This map probably represents a good approximation of the relief in the crystalline basement surface.

Comparisons with Gravity and Magnetics

Magnetic and gravity data (Popenoe and Zietz, 1977; Phillips, 1977; Long and Champion, 1977; Kane, 1977; Rankin, 1977) show positive anomalies, centered near the Clubhouse Crossroads drill holes, that imply a corresponding mafic pluton in the basement. These highs also lie on the southwestern part of the ridgelike high of the 6.0- to 6.4-km/s crystalline basement layer (fig. 9). However, except for this common feature, the maps compiled from the seismic-refraction, magnetic, and gravity data are noteworthy for their contrasts.

Figure 11 is the map of figure 9 superimposed on the magnetic field contours. The salient feature of the magnetic map is a high presumably caused by the mafic pluton suggested above. The superimposed seismic results suggest that the pluton occurs within a pre-Mesozoic basement ridge bounded on the northwest by a Triassic border fault, which also appears as a steep gradient on the magnetic map. However, the ridge also cuts across magnetic field contours, and the low magnetic field values to the northeast suggest that it contains rocks of low magnetization as well. Thus, I infer that the basement surface has large local relief and that the basement contains rocks having highly contrasting magnetic properties.

Comparing the map of figure 9 with the gravity contours (fig. 12) also shows marked differences. A general lack of correlation would be expected, however, upon considering the small gravity anomaly (4–9 mGal) attributed to Triassic sediments in the exposed Durham-Wadesboro basin in North Carolina (Mann and Zablocki, 1961), which is approximately 2,500 m deep (Ackermann and others, 1976). Assuming similar density contrasts, the resulting gravity anomaly in the area of this study would be even less, not only because of the smaller thickness of Triassic or Jurassic rocks filling the basin but also because of the thick overlying blanket of Cretaceous and Cenozoic rocks. Hence, I suggest that the major gravity features of figure 12 are due not to changes in depth to the crystalline basement but instead to density variations deeper within the crust.

Relationship with Recent Epicenters

Many of the recent instrumentally recorded earthquake epicenters (Tarr and Rhea, 1983) lie above the northeast-trending crystalline-basement ridge crest

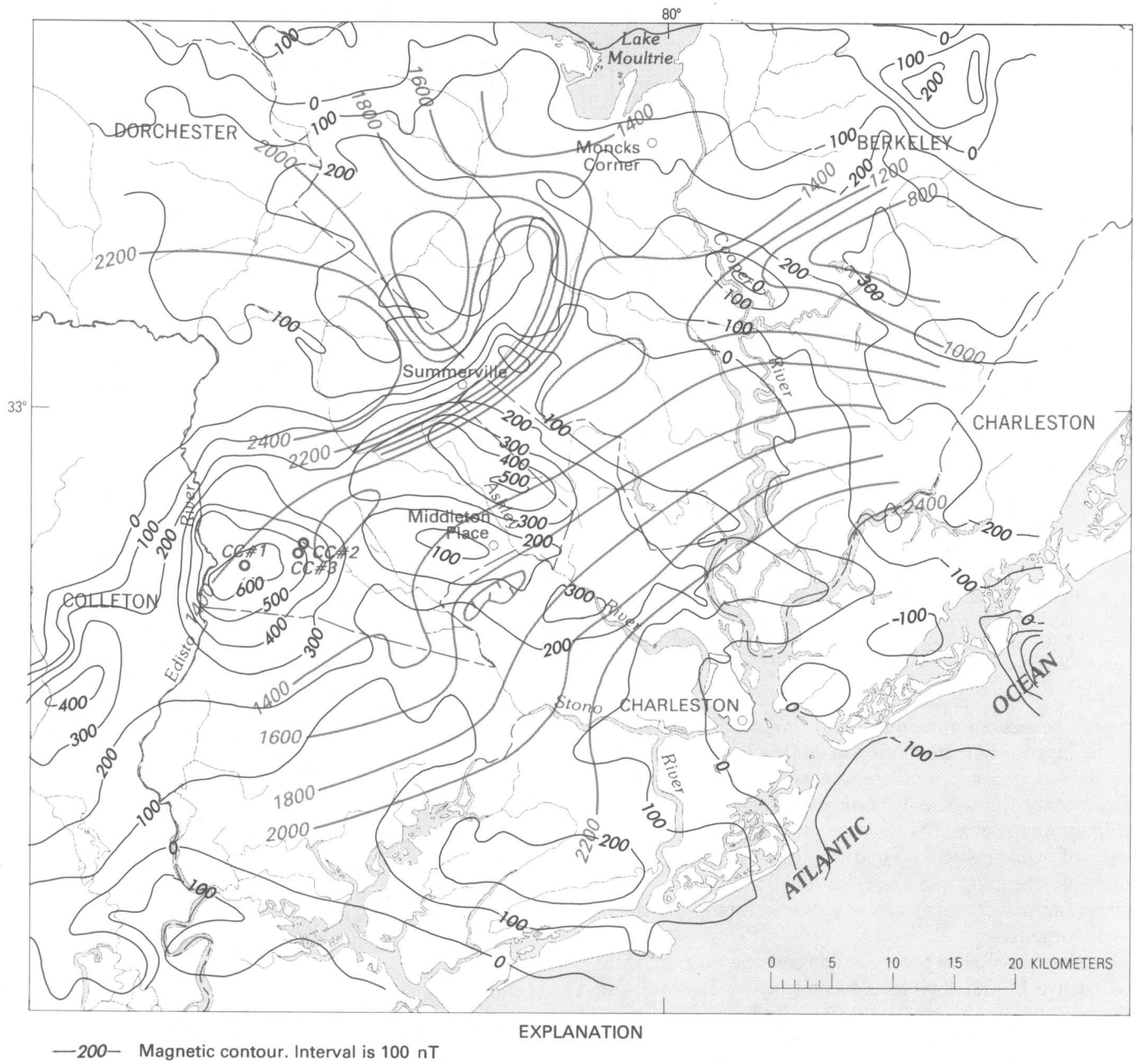

FIGURE 11. – Aeromagnetic map of the study area (Phillips and others, 1978), on which are superimposed contours of interpreted depth of the 6.0- to 6.4-km/s seismic-refracting layer (from fig. 9).

shown in figure 9. Those northwest of the ridge are along the inferred Triassic border fault and the steep gradient of a nearby horstlike feature. A magnitude-3.8 earthquake (Tarr, 1977) at spread location 18 southeast of the ridge crest is near another inferred structure at Middleton Place. Furthermore, the three Adams Run epicenters (Tarr and Rhea, 1983) shown in the southwest part of figure 9 may be displaced southeastward from the ridge crest, analogous to the Middleton Place epicenter. The proximity of the recent seismic activity to these inferred structures suggests reactivation of preexisting faults, analogous to the well-documented modern

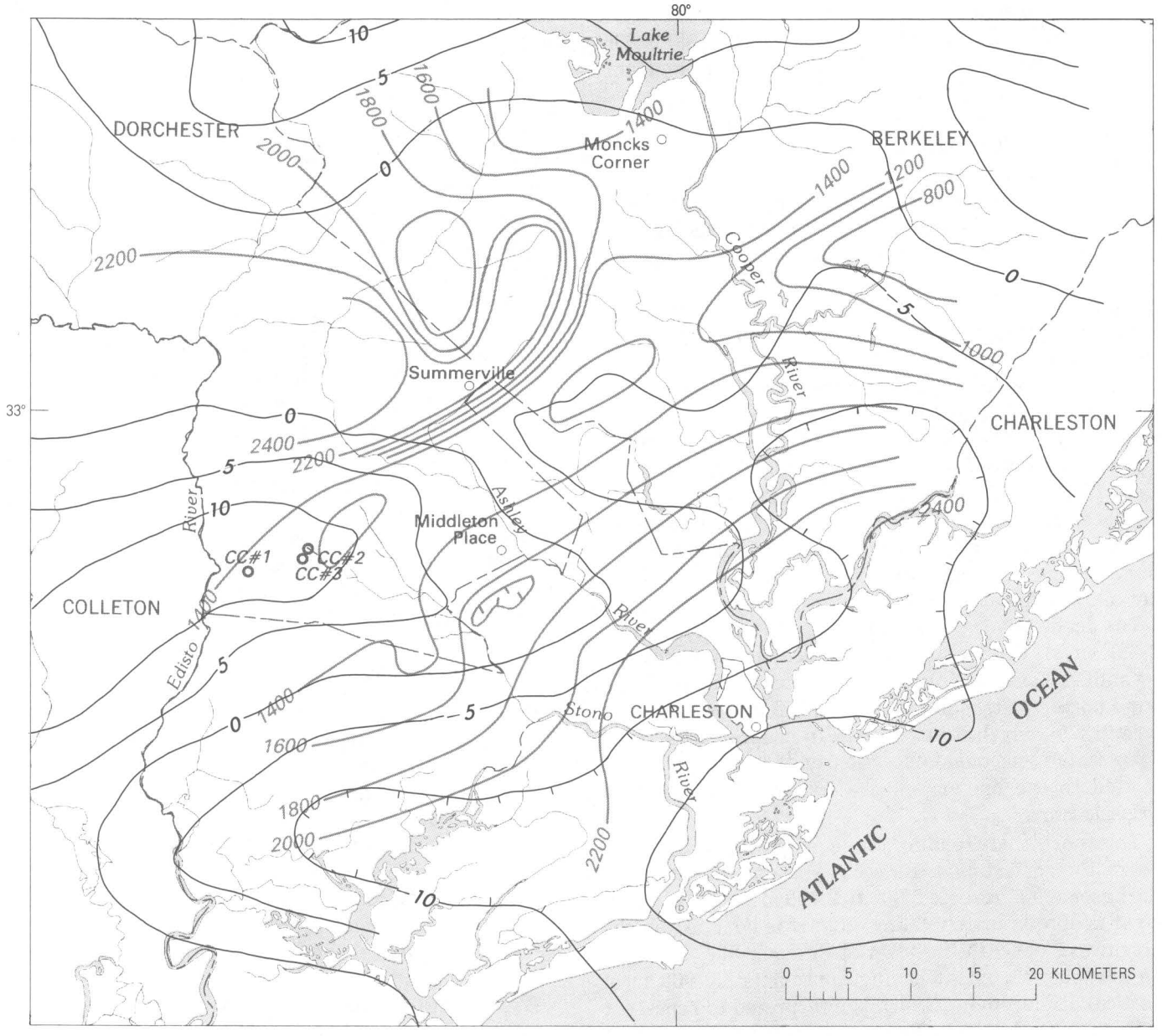

FIGURE 12.—Bouguer gravity anomaly map of the study area (Talwani and others, 1975a), on which are superimposed contours of interpreted depth of the 6.0- to 6.4-km/s seismic-refracting layer (from fig. 9).

activity along the Ramapo fault, which bounds the Newark Triassic and Jurassic basin in southeastern New York and northern New Jersey (Aggarwal and Sykes, 1978). The suggested northwestward regional compressive stress in the Charleston area (Zoback and others, 1978) may also favor reactivation of the northeast-trending structures interpreted here.

DISCUSSION AND CONCLUSIONS

The seismic-refraction survey of this study lies roughly within an area of 20 km radius centered near Summerville, S. C., and includes the meizoseismal zone of the Charleston 1886 earthquake (Bollinger, 1977). Two refracting layers were mapped. The shallower

represents the pre-Cretaceous surface and corresponds to the "J" reflector of the reflection surveys (Behrendt and others, 1983; Hamilton and others, 1983). The deeper represents the crystalline basement and corresponds to the "B" reflector.

The shallower layer (fig. 8) has been identified from the Clubhouse Crossroads drill holes to represent the pre-Cretaceous surface. The refraction results show that this surface dips gently seaward to the southeast and that within the survey area its depth varies from about 500 to 1,000 m. At the Clubhouse Crossroads drill holes, this layer consists of a series of basalt flows, approximately 256 m thick, underlain by red beds of Triassic or Jurassic age (Gohn and others, 1983). The thickness and properties of these flows vary laterally throughout the area, as determined from variations in seismic velocity (4.4 to 5.7 km/s) and attenuation. In some areas of the survey, the basalt flows are probably absent. The reflection data (Hamilton and others, 1983) show faults and flexures having several tens of meters of displacement on the pre-Cretaceous surface; some of these faults and flexures extend into the shallower Tertiary section. The resolution of the refraction data did not allow delineation of structural features of this size.

The deeper layer was identified on the basis of velocity (>6.0 km/s); this velocity is assumed to represent the crystalline-basement surface. This survey delineated a large northeast-trending topographic feature of this surface (fig. 9), which is interpreted to be an expression of deep-seated tensional faults (Behrendt and others, 1983) related to the opening of the Atlantic Ocean during Triassic time.

This northeast-trending ridge is 1,200 to 1,300 m below the surface and transects a region within which the basement surface is 2,000 to 2,400 m deep. The ridge crest is approximately 6 km wide. It is bounded on the northwest, beneath the town of Summerville, S. C., by an abrupt escarpment having approximately 900 m of vertical displacement, which is interpreted to represent a Triassic border fault. The southeast ridge boundary is poorly defined for lack of good data, but data from two spreads near Middleton Place, S. C., suggest that it is a gently southeastward dipping surface broken by a 200- to 300-m faultlike displacement.The area covered by this survey was not sufficient to define the entire faulted ridge structure. As shown in figure 9, the ridge crest and its associated border fault in the northwest are more than 20 km long and extend southeastward beyond the edge of the mapped area. In the northeastern part of the surveyed area, the ridge broadens and the deeper basin portion of the structure is absent. A causal relationship between these bounding faults and the Charleston earthquake is suggested on the basis that the inferred epicenter of the 1886 shock (Tarr, 1977) and epicenters of the instrumentally recorded aftershocks (Tarr and Rhea, 1983) are within or near the edge of this fault zone.

APPENDIX—Interpretation Methods

Interpretations of data were made using interactive computer programs written by the author. The programs have been tested on a large number of real and hypothetical arrival-time curves, and results have demonstrated that computed models satisfy data to a high degree of accuracy. The programs consist of three basic subroutines.

One subroutine, named RECIP, calculates depths and lateral velocity variations for a refraction horizon given the reciprocal time (traveltime between reversed shotpoints) plus overlapping reversed data for that horizon and an overlying velocity distribution. The reversed arrival-time graphs are first lowered, by ray tracing, down to the top of the deepest layer known from the overlying velocity distribution, as though shots and receivers were on that layer. An iterative process, illustrated in figure 13, then calculates successive points such as C_1 and C_2 on the refracting horizon by testing the reciprocity relationship,

$$T_R = (T_{B_1} - T_{B_1C_1}) + (T_{A_1} - T_{A_1C_1}),$$
$$T_R = (T_{B_2} - T_{B_2C_2}) + (T_{A_2} - T_{A_2C_2}),$$

where V = velocity for the deepest known layer of the overlying velocity distribution,
T_R = reciprocal time,
T_{B_1} = arrival time at point B_1,
T_{B_2} = arrival time at point B_2,
T_{A_1} = arrival time at point A_1,
T_{A_2} = arrival time at point A_2,
$T_{B_1C_1}$ = traveltime between points B_1 and C_1 at V,
$T_{B_2C_2}$ = traveltime between points B_2 and C_2 at V,
$T_{A_1C_1}$ = traveltime between points A_1 and C_1 at V, and
$T_{A_2C_2}$ = traveltime between points A_2 and C_2 at V.

C_1, for example, lies on the refracting horizon when two points on reversed curves T_{A_1} and T_{B_1} are found such that the first of the above relationships is satisfied.

After the points C_1 and C_2 are determined, the velocity in the interval between them is calculated from the formula

$$V_{C_1C_2} = \frac{C_1C_2}{(T_{B_2} - T_{B_2C_2}) - (T_{B_1} - T_{B_1C_1})},$$

where C_1C_2 = distance between points C_1 and C_2 and
$V_{C_1C_2}$ = velocity in the interval C_1C_2.

A second subroutine, named CRIT, uses one-way data extended back to the shotpoint to calculate the point of reflection at the critical angle on the refracting horizon by using the inferred velocity of the refracting horizon

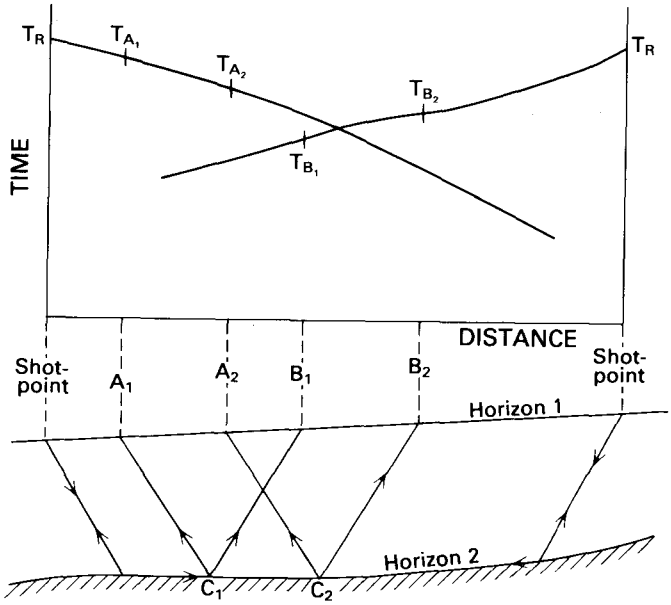

FIGURE 13.—Arrival-time graph, reduced to top of deepest known layer (horizon 1) and showing corresponding ray paths as used in subroutine RECIP. Horizon 2 represents the layer being calculated. Symbols are explained in text.

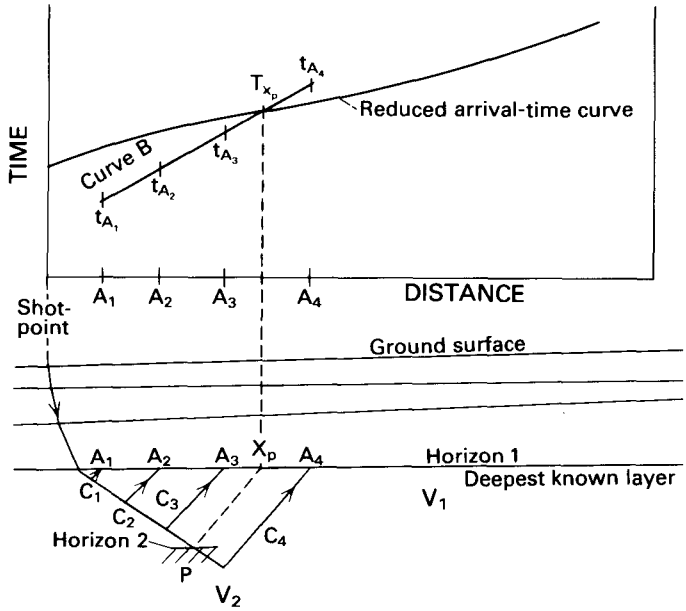

FIGURE 14.—Arrival-time graph, reduced to top of deepest known layer (horizon 1) and showing corresponding ray paths as used in subroutine CRIT. Horizon 2 represents the layer being calculated. Symbols are explained in text. V_1 is the velocity below horizon 1, and V_2 is the inferred velocity below horizon 2.

and the overlying velocity distribution. The one-way arrival-time graph is first lowered down to the top of the deepest layer known, using the overlying velocity distribution, as though the receivers were on that layer. (The shotpoint cannot be lowered because reversed data are not used.) An iterative process follows, as illustrated in figure 14, whereby critical reflecting ray paths are constructed from successive points A_1, A_2,... that intersect the shotpoint. From the computed traveltimes of these ray paths, t_{A_1}, t_{A_2}, a new curve, B, is constructed, which intersects the reduced traveltime curve. From the intersection point T_{X_p}, the subsurface point P is determined by interpolation; P is the critical reflection point on the refracting horizon.

A third subroutine, named ACROSS, uses the results of CRIT and the remaining one-way arrival-time data to calculate the refracting horizon beyond the point of critical reflection. This is illustrated in figure 15. From successive points A_1, A_2,... on horizon 1, emerging rays of velocity V_1 are constructed. (In the following discussion, the ray emerging at A_2 will be used as the general case.) From point P obtained from subroutine CRIT, a ray of velocity V_2 is constructed to intersect the ray emerging at A_2 at the subsurface point C_2 such that the relationship

$$T_{A_2} = T_P + T_{PC_2} + T_{C_2A_2}$$

is satisfied. The point C_2 then lies in the refracting horizon.

T_{A_2} = arrival time at point A_2,

T_P = computed arrival time at P, obtained from subroutine CRIT,

T_{PC_2} = traveltime between points P and C_2 at V_2, and

$T_{C_2A_2}$ = traveltime between points C_2 and A_2 at V_1.

The results of subroutine ACROSS must be used with considerable discretion, because, in the absence of reversed arrival-time data, the value of V_2 could be substantially in error. If V_2 is too small, the computed depth points C_2 will be too shallow; if V_2 is too large, C_2 will be too deep.

Best results are obtained from overlapping reversed data from the refracting horizon and using subroutine RECIP. The surveys of 1975 and 1976 were planned to achieve this goal. However, because of characteristics of the two recorded pre-Cretaceous horizons—shingling of the shallower one and large depth variations of the deeper—this goal was not achieved fully. Where partially overlapping data were obtained, complete reversed time-distance graphs were constructed by "filling in" with pseudo-arrival-time data as illustrated in figure 16. Shown are hypothetical arrival-time data obtained from either of the two basement horizons from two end-to-end spreads A and B and four shotpoints S_1 through S_4. Shotpoints S_1 and S_4 are offset. The solid lines represent actual recorded arrival times, and the dashed lines the constructed pseudo-arrivals. The combined data then

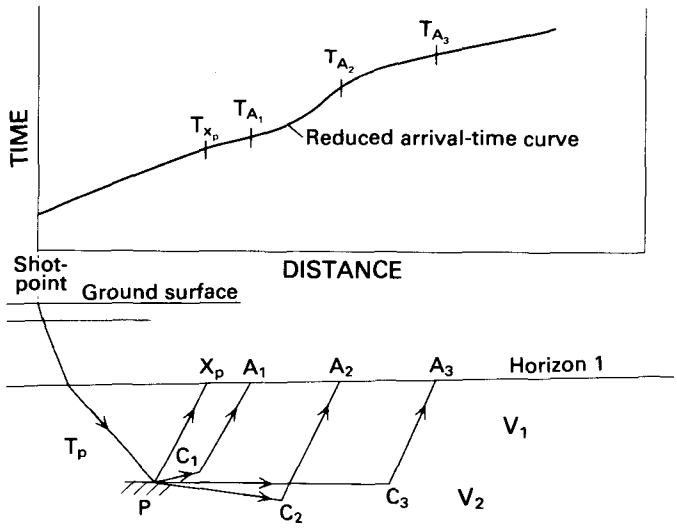

FIGURE 15.—Arrival-time graph, reduced to top of the deepest known layer (horizon 1) and showing corresponding ray paths as used in subroutine ACROSS. Symbols are explained in text. V_1 is the velocity below horizon 1, and V_2 is the inferred velocity of the layer being computed.

represent complete reversed coverage from shotpoints S_2 and S_3, and the subsurface horizon between these shotpoints is computed using subroutine RECIP. Comparing delay times t_1 with t_2 and t_3 with t_4 provides information on structures between the shots at the ends of the spreads (S_2 and S_3) and the offset shotpoints (S_1 and S_4). It was through the analysis of differences in delay times from successively more distant offset shotpoints that the approximate location of the large Triassic border fault was inferred.

Because of the change in the shot-seismometer configuration for the 1977 survey, these data were interpreted differently. Shown in figure 17 is a typical configuration employing a single spread and only two shotpoints, both offset. The offset distance was such that, in most cases, arrivals were obtained from both the pre-Cretaceous surface and the crystalline basement, shown as the two sets of solid line segments. For the shallower event, for which no overlapping reversed arrivals are seen, pseudo-arrivals (dashed in fig. 17) were extended back to the shotpoints S_1 and S_2 with intercept times t_1 and t_2. Depth to this horizon was then computed at both ends of the spread by means of subroutine CRIT. The velocity was estimated from the slopes of the arrival-time curve. For the deeper event, pseudo-arrivals were constructed forward to establish a value for the reciprocal time T_R. In some cases of subsurface changes between the ends of the spread and the offset shotpoints, difficulties arose in forcing reciprocal times to tie (to cause T_R at S_1 to equal T_R at S_2). Pseudo-arrivals were also constructed in the reverse directions

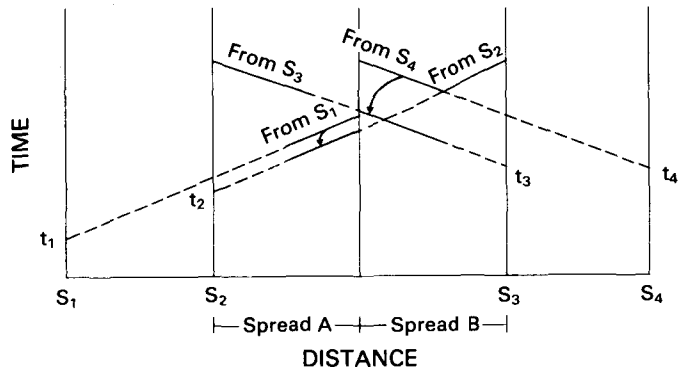

FIGURE 16.—One possible configuration for constructing complete reversed traveltime graphs between shotpoints S_1 and S_4 given partial reversed data. S_1 through S_4 represent shotpoints, t_1 through t_4 are delay times at shotpoints, and dashed lines are inferred pseudo-arrivals.

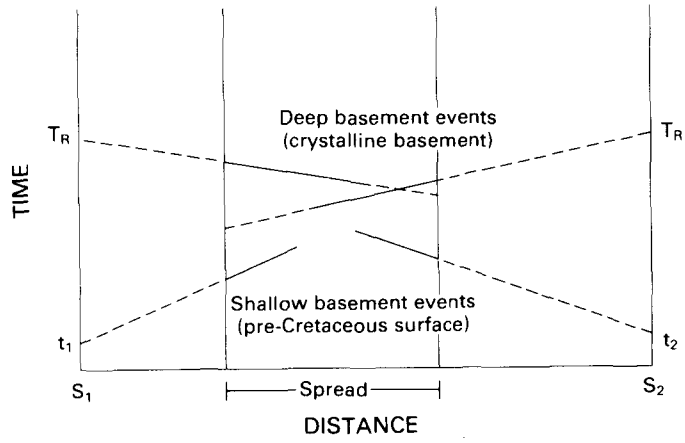

FIGURE 17.—Configuration used for interpreting refraction arrivals by using one spread, two offset shotpoints S_1 and S_2, and arrivals from two horizons. T_R is the reciprocal time, and t_1 and t_2 the delay times at shotpoints. Dashed lines are inferred pseudo-arrivals.

to provide more complete overlap. Subroutine RECIP was then invoked to calculate the configuration of the refracting horizon beneath the spread.

All schemes of refraction interpretation for which complete reversed data are not available involve assumptions, either explicit or implicit, about the nature of the arrival-time curve where data are missing. In the methods used here, the interpreter is forced to face these assumptions head-on by actually constructing a portion of the arrival-time curve where real data are missing. Freedom is restricted, however, because reciprocity must be satisfied and the intercept delay times at the common point of end-to-end spreads must agree. In this study, unless these limitations dictated otherwise, constructions were made by simply continuing plotted arrival times as straight lines having no change in slope.

REFERENCES CITED

Ackermann, H. D., 1977, Exploring the Charleston, South Carolina earthquake area with seismic refraction–A preliminary study, *in* Rankin, D. W., ed., Studies related to the Charleston, South Carolina, earthquake of 1886–A preliminary report: U.S. Geological Survey Professional Paper 1028, p. 167–175.

Ackermann, H. D., Bain, G. L., and Zohdy, A. A. R., 1976, Deep exploration of an east-coast Triassic basin using electrical resistivity: Geology, v. 4, no. 3, p. 137–140.

Aggarwal, Y. P., and Sykes, L. R., 1978, Earthquakes, faults, and nuclear power plants in southern New York and northern New Jersey: Science, v. 200, no. 4340, p. 425–429.

Antoine, J. W., and Henry, V. J., Jr., 1965, Seismic refraction study of shallow part of Continental Shelf off Georgia coast: American Association of Petroleum Geologists Bulletin, v. 49, no. 5, p. 601–609.

Behrendt, J. C., Hamilton, R. M., Ackermann, H. D., Henry, V. J., and Bayer, K. C., 1983, Marine multichannel seismic-reflection evidence for Cenozoic faulting and deep crustal structure near Charleston, South Carolina, *in* Gohn, G. S., ed., Studies related to the Charleston, South Carolina, earthquake of 1886–Tectonics and seismicity: U.S. Geological Survey Professional Paper 1313, p. J1–J29.

Bollinger, G. A., 1977, Reinterpretation of the intensity data for the 1886 Charleston, South Carolina earthquake, *in* Rankin, D. W., ed., Studies related to the Charleston, South Carolina, earthquake of 1886–A preliminary report: U.S. Geological Survey Professional Paper 1028, p. 17–32.

Bonini, W. E., 1956, Subsurface geology in the area of the Cape Fear Arch as determined by seismic-refraction measurements: Madison, University of Wisconsin, Ph.D. thesis, 180 p.

Cassinis, R., and Borgonovi, L., 1966, Significance and implications of shingling in refraction records: Geophysical Prospecting, v. 14, no. 4, p. 547–565.

Coffey, J. C., 1977, Exploratory oil wells of North Carolina, 1925–1976: North Carolina Geology and Mineral Resources Section, Information Circular 22, 52 p.

Cooke, C. W., 1936, Geology of the coastal plain of South Carolina: U.S. Geological Survey Bulletin 867, 196 p.

Dillon, W. P., Klitgord, K. D., and Paull, C. K., 1983, Mesozoic development and structure of the continental margin off South Carolina, *in* Gohn, G. S., ed., Studies related to the Charleston, South Carolina, earthquake of 1886–Tectonics and seismicity: U.S. Geological Survey Professional Paper 1313, p. N1–N16.

Dillon, W. P., and Paull, C. K., 1978, Interpretation of multichannel seismic-reflection profiles of the Atlantic continental margin off the coasts of South Carolina and Georgia: U.S. Geological Survey Miscellaneous Field Studies Map MF–936.

Gohn, G. S., Gottfried, David, Lanphere, M. A., and Higgins, B. B., 1978, Regional implications of Triassic or Jurassic age for basalt and sedimentary red beds in the South Carolina Coastal Plain: Science, v. 202, no. 4370, p. 887–890.

Gohn, G. S., Houser, B. B., and Schneider, R. R., 1983, Geology of the lower Mesozoic(?) sedimentary rocks in Clubhouse Crossroads test hole #3, near Charleston, South Carolina, *in* Gohn, G. S., ed., Studies related to the Charleston, South Carolina, earthquake of 1886–Tectonics and seismicity: U.S. Geological Survey Professional Paper 1313, p. D1–D17.

Hales, A. L., Helsley, C. E., Dowling, J. J., and Nation, J. B., 1968, The East Coast onshore-offshore experiment, [Pt.] I–The first arrival phases: Seismological Society of America Bulletin, v. 58, no. 3, p. 757–819.

Hamilton, R. M., Behrendt, J. C., and Ackermann, H. D., 1983, Land multichannel seismic-reflection evidence for tectonic features near Charleston, South Carolina, *in* Gohn, G. S., ed., Studies related to the Charleston, South Carolina, earthquake of 1886–Tectonics and seismicity: U.S. Geological Survey Professional Paper 1313, p. I1–I18.

Hersey, J. B., Bunce, E. T., Wyrick, R. F., and Dietz, F. T., 1959, Geophysical investigation of the continental margin between Cape Henry, Virginia, and Jacksonville, Florida: Geological Society of America Bulletin, v. 70, no. 4, p. 437–466.

Kane, M. F., 1977, Correlation of major eastern earthquake centers with mafic/ultramafic basement masses, *in* Rankin, D. W., ed., Studies related to the Charleston, South Carolina, earthquake of 1886–A preliminary report: U.S. Geological Survey Professional Paper 1028, p. 199–204.

Long, L. T., and Champion, J. W., Jr., 1977, Bouguer gravity map of the Summerville-Charleston, South Carolina epicentral zone and tectonic implications, *in* Rankin, D. W., ed., Studies related to the Charleston, South Carolina, earthquake of 1886–A preliminary report: U.S. Geological Survey Professional Paper 1028, p. 151–166.

Mann, V. I., and Zablocki, F. S., 1961, Gravity features of the Deep River–Wadesboro Triassic basin of North Carolina: Southeastern Geology, v. 2, no. 4, p. 191–215.

Marine, I. W., 1974, Geohydrology of buried Triassic basin at Savannah River plant, South Carolina: American Association of Petroleum Geologists Bulletin, v. 58, no. 9, p. 1825–1837.

Meyer, R. P., 1956, The geologic structure of the Cape Fear axis as revealed by refraction seismic measurements: Madison, University of Wisconsin, Ph.D. thesis, 85 p.

Phillips, J. D., 1977, Magnetic basement near Charleston, South Carolina–A preliminary report, *in* Rankin, D. W., ed., Studies related to the Charleston, South Carolina, earthquake of 1886–A preliminary report: U.S. Geological Survey Professional Paper 1028, p. 139–150.

———1983, Paleomagnetic investigations of the Clubhouse Crossroads basalt, *in* Gohn, G. S., ed., Studies related to the Charleston, South Carolina, earthquake of 1886–Tectonics and seismicity: U.S. Geological Survey Professional Paper 1313, p. C1–C18.

Phillips, J. D., Daniels, D. L., Zietz, Isidore, and Popenoe, Peter, 1978, Geophysical studies of the Charleston, South Carolina, area–onshore aeromagnetic map: U.S. Geological Survey Miscellaneous Field Studies Map MF–1022–A, scale 1:250,000.

Pooley, R. N., 1959, Basement configuration of subsurface geology of eastern Georgia and southern South Carolina as determined by seismic-refraction measurements: Madison, University of Wisconsin, Masters thesis, 47 p.

Popenoe, Peter, and Zietz, Isidore, 1977, The nature of the geophysical basement beneath the coastal plain of South Carolina and northeastern Georgia, *in* Rankin, D. W., ed., Studies related to the Charleston, South Carolina, earthquake of 1886–A preliminary report: U.S. Geological Survey Professional Paper 1028, p. 119–137.

Rankin, D. W., 1977, Studies related to the Charleston, South Carolina, earthquake of 1886–Introduction and discussion, *in* Rankin, D. W., ed., Studies related to the Charleston, South Carolina, earthquake of 1886–A preliminary report: U.S. Geological Survey Professional Paper 1028, p. 1–15.

Schilt, F. S., Brown, L. D., Oliver, J. E., and Kaufman, Sidney, 1983, Subsurface structure near Charleston, South Carolina; Results of COCORP reflection profiling in the Atlantic Coastal Plain, *in* Gohn, G. S., ed., Studies related to the Charleston, South Carolina, earthquake of 1886–Tectonics and seismicity: U.S. Geological Survey Professional Paper 1313, p. H1–H19.

Sheriff, R. E., 1973, Encyclopedic dictionary of exploration geophysics: Tulsa, Okla., Society of Exploration Geophysicists, 266 p.

Talwani, Pradeep, 1977, A preliminary shallow crustal model between Columbia and Charleston, South Carolina, determined from quarry blast monitoring and other geophysical data, *in* Rankin, D. W., ed., Studies related to the Charleston, South Carolina, earthquake of 1886–A preliminary report: U.S. Geological Survey Professional Paper 1028, p. 177–187.

Talwani, Pradeep, Long, L. T., and Bridges, S. R., 1975a, Simple Bouguer anomaly map of South Carolina: South Carolina State Development Board, Division of Geology, Map Series MS–21, 27 p.

Talwani, Pradeep, Ressetar, Robert, McAleer, Jacqueline, Holmes, Tom, Grothaus, Brian, Findlay, Marsha, Cable, Mark, and Amick, David, 1975b, Gravity and magnetic profiles across the Georgetown gravity low: South Carolina State Development Board, Division of Geology, Geologic Notes, v. 19, no. 2, p. 24–32.

Tarr, A. C., 1977, Recent seismicity near Charleston, South Carolina, and its relationship to the August 31, 1886 earthquake, *in* Rankin, D. W., ed., Studies related to the Charleston, South Carolina, earthquake of 1886–A preliminary report: U.S. Geological Survey Professional Paper 1028, p. 43–58.

Tarr, A. C., and Rhea, Susan, 1983, Seismicity near Charleston, South Carolina, March 1973 to December 1979, *in* Gohn, G. S., ed., Studies related to the Charleston, South Carolina, earthquake of 1886–Tectonics and seismicity: U.S. Geological Survey Professional Paper 1313, p. R1–R17.

Yantis, B. R., Costain, J. K., and Ackermann, H. D., 1983, A reflection seismic study near Charleston, South Carolina, *in* Gohn, G. S., ed., Studies related to the Charleston, South Carolina, earthquake of 1886–Tectonics and seismicity: U.S. Geological Survey Professional Paper 1313, p. G1–G20.

Zoback, M. D., Healy, J. H., Roller, J. C., Gohn, G. S., and Higgins, B. B., 1978, Normal faulting and in situ stress in the South Carolina coastal plain near Charleston: Geology, v. 6, no. 3, p. 147–152.

A Reflection Seismic Study Near Charleston, South Carolina

By B. R. YANTIS, J. K. COSTAIN, and HANS D. ACKERMANN

STUDIES RELATED TO THE CHARLESTON, SOUTH CAROLINA, EARTHQUAKE OF 1886—TECTONICS AND SEISMICITY

GEOLOGICAL SURVEY PROFESSIONAL PAPER 1313-G

UNITED STATES GOVERNMENT PRINTING OFFICE, WASHINGTON: 1983

CONTENTS

ILLUSTRATIONS

STUDIES RELATED TO THE CHARLESTON, SOUTH CAROLINA, EARTHQUAKE OF 1886—TECTONICS AND SEISMICITY

A REFLECTION SEISMIC STUDY NEAR CHARLESTON, SOUTH CAROLINA

By B. R. YANTIS,[1] J. K. COSTAIN,[2] and HANS D. ACKERMANN

ABSTRACT

Three reflection seismic lines were recorded approximately 40 km northwest of Charleston, S. C., by the U.S. Geological Survey. Lines designated Clubhouse Crossroads, Interstate, and Middleton Place are 1.7, 1.0, and 4.3 km long, respectively, and their minimum separation is approximately 20 km. The three lines cover an area of approximately 200 km^2 in the meizoseismal region of the 1886 earthquake. Fourfold and sixfold common-depth-point data were obtained.

The largest amplitude reflection on any of the seismic lines is from the top of a basalt layer at a depth of 750 m in Clubhouse Crossroads test hole #1 (CC #1). Wave shape, amplitude, and arrival time of reflections on individual unprocessed traces indicate that the basalt is present at all three sites. If we assume a planar reflector, the strike and dip of the basalt are approximately N. 55° E. and 0.5° SE. Velocity analyses of some individual seismograms indicate a reflection from the bottom of the basalt layer. From the seismic data, the basalt appears to range from 150 to 230 m in thickness; it may be thinnest at the Interstate line and thickest at the Middleton Place line.

Four reflections above the basalt can be correlated with changes in lithology and (or) degree of induration of the core from CC #1. A reflection from near the top of the Peedee Formation (Upper Cretaceous) can be correlated on all three lines. If we assume a planar structure, the strike and dip of this reflector are N. 45° E. and less than 0.1° SE. No faults were detected on any of the three reflection lines; these lines are not near the Cooke fault, a structural feature defined by other reflection surveys.

INTRODUCTION

The U.S. Geological Survey (USGS), in the spring of 1974, undertook a multidisciplinary study of the Charleston 1886 earthquake region to investigate the cause of the earthquake, to evaluate the future seismicity of the area, and to determine how the area is related tectonically to other parts of the Eastern United States (Rankin, 1977). In particular, seismic-reflection data were used to investigate subsurface structure. In the summer of 1974, three seismic-reflection lines were recorded by the USGS at locations approximately 40 km northwest of Charleston, S. C., on the Atlantic Coastal Plain. The three lines are designated Interstate, Clubhouse Crossroads, and Middleton Place and are 1.0, 1.7, and 4.3 km in length, respectively. Figure 1 shows the location of the three lines, which are separated from each other by at least 20 km but no more than 30 km.

Amoco Production Company digitized the analog magnetic tapes. Computer time for data analysis was provided by the Virginia Polytechnic Institute and State University (VPI&SU) Computing Center. All data processing was done at VPI&SU on an IBM 360.[3]

Purpose of the Study

The modern locus of seismicity near Charleston, designated the Middleton Place–Summerville seismic zone, is a northwest-trending zone that is currently active in the depth range of approximately 2 or 4 to 10 or 12 km on a nearly vertical plane (Tarr and Rhea, 1983).

Subsurface structure within the Coastal Plain and sub-Coastal Plain sections was largely unknown in 1974. The three seismic-reflection lines were recorded in this seismically active area to search for faults that might have been related to the 1886 earthquake. The reflection lines are located over a large area, approximately 200 km^2, centered at Summerville. The longest of the three lines, the Middleton Place line, is about 1 km north of the epicenter of a recent earthquake of Richter magnitude 3.8 that occurred in November 1974 at a depth of about 4 km (Tarr, 1977). The shortest of the lines, the Interstate line, is about 20 km north of this epicenter. The third line, the Clubhouse Crossroads line, is about 20 km west of the epicenter.

[1]Shell Development Corporation, Houston, TX 77025.
[2]Virginia Polytechnic Institute and State University, Blacksburg, VA 24061.

[3]Any use of trade names is for descriptive purposes only and does not imply endorsement by the U.S. Geological Survey.

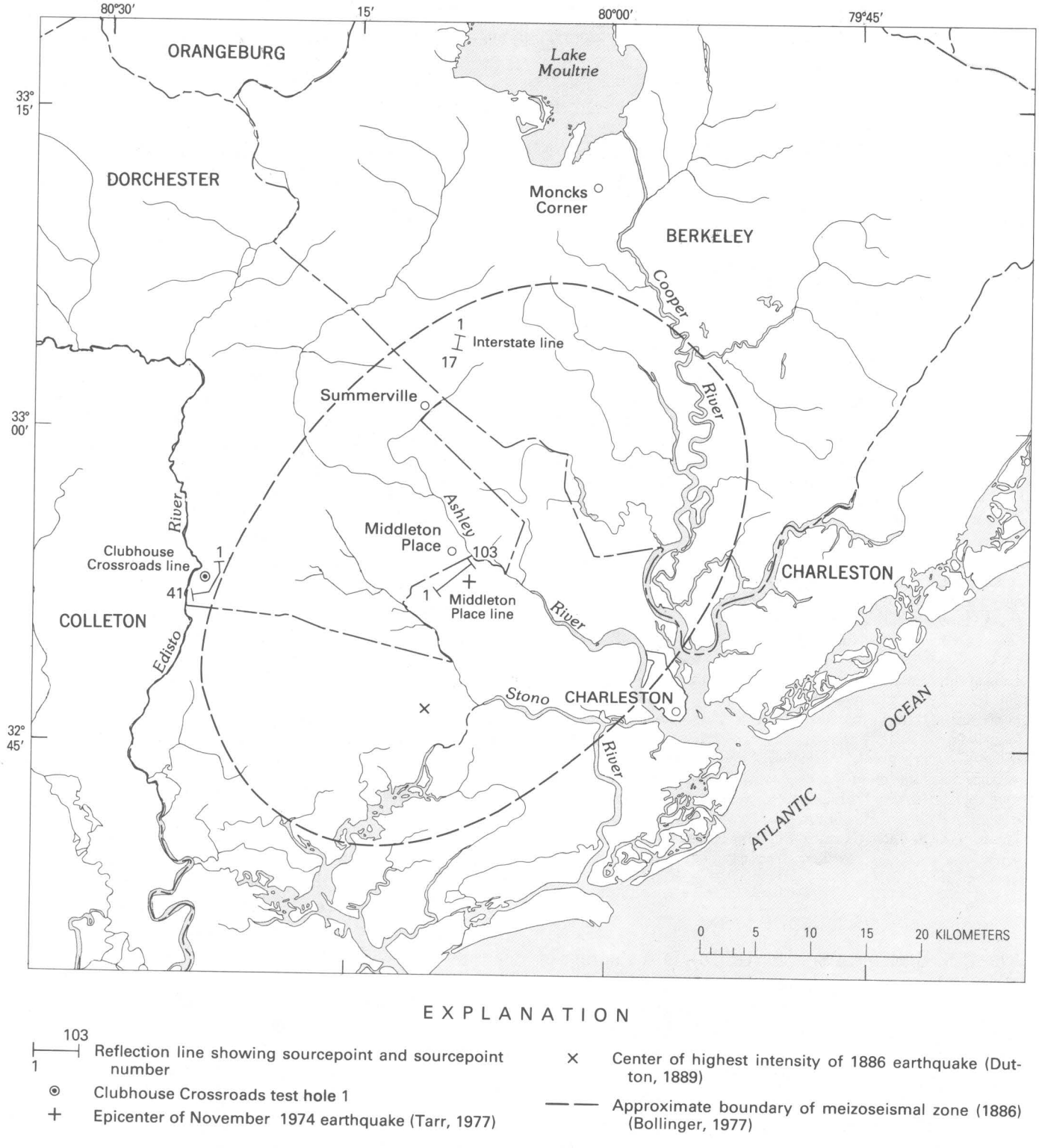

FIGURE 1.—Location map of reflection seismic lines near Charleston, S. C.

Atlantic Coastal Plain Stratigraphy

The crystalline basement beneath the Atlantic Coastal Plain typically is considered to be a southeastward continuation of metamorphic and igneous rocks exposed in the Appalachian Piedmont. However, part of the basement beneath the Coastal Plain sediments in southeastern South Carolina and east-central Georgia does not appear to be an extension of the same Piedmont rocks (Popenoe and Zietz, 1977). Triassic and Jurassic basins, containing red terrestrial sedimentary rocks, are also found in some parts of the basement. Some of the basins contain basalt flows (Gohn and others, 1978).

The Atlantic Coastal Plain is composed of a seaward-thickening wedge of sediments resting upon the crystalline basement. The Coastal Plain extends from the Appalachian Piedmont to the Atlantic Ocean; the sediments dip seaward at angles of less than 1° (Clark and Stearn, 1960, p. 155).

The sedimentary units of the Coastal Plain range in age from Early Cretaceous to Holocene. The ages of the exposed formations decrease in a seaward direction. In eastern Georgia and South Carolina, Lower Cretaceous sediments are thin or absent. The overlying Upper Cretaceous and Cenozoic sediments form a series of poorly to moderately consolidated beds of sand, clay, and limestone (Gohn and others, 1979).

Previous Data

A continuously cored test hole, Clubhouse Crossroads test hole 1 (CC#1), was drilled to a depth of 792 m by the U.S. Army Corps of Engineers at 32° 53.25′ N., 80° 21.41′ W., approximately 40 km northwest of Charleston in 1975. The lithology of the core was described by Gohn and others (1977).

Figure 2 is the lithostratigraphic description of core above the basalt from CC#1 as given by Gohn and others (1977). The Tertiary sediments (239 m) have been divided into four formations: the Cooper Formation (Oligocene and Eocene), the Santee Limestone (Eocene), the Black Mingo Formation (Eocene and Paleocene), and a unit tentatively identified as the Beaufort(?) Formation (Paleocene). The Cretaceous sediments (506 m) are divided into four formations: the Peedee Formation, the Black Creek Formation, the Middendorf Formation, and the Cape Fear Formation. The Santee Limestone (56 m) has a 11-m-thick bed of well-indurated crossbedded calcarenite as its base. An unconformity occurs at the base of the Santee. The Black Mingo Formation (67 m) is the most heterogeneous of the Tertiary formations (Gohn and others, 1977, p. 68). The Beaufort(?) Formation (52 m), as the term is used by Gohn and others in South Carolina, includes a basal unit of nodular glauconitic muddy sand directly overlying an unconformity. The remainder of the formation is primarily a silty clay.

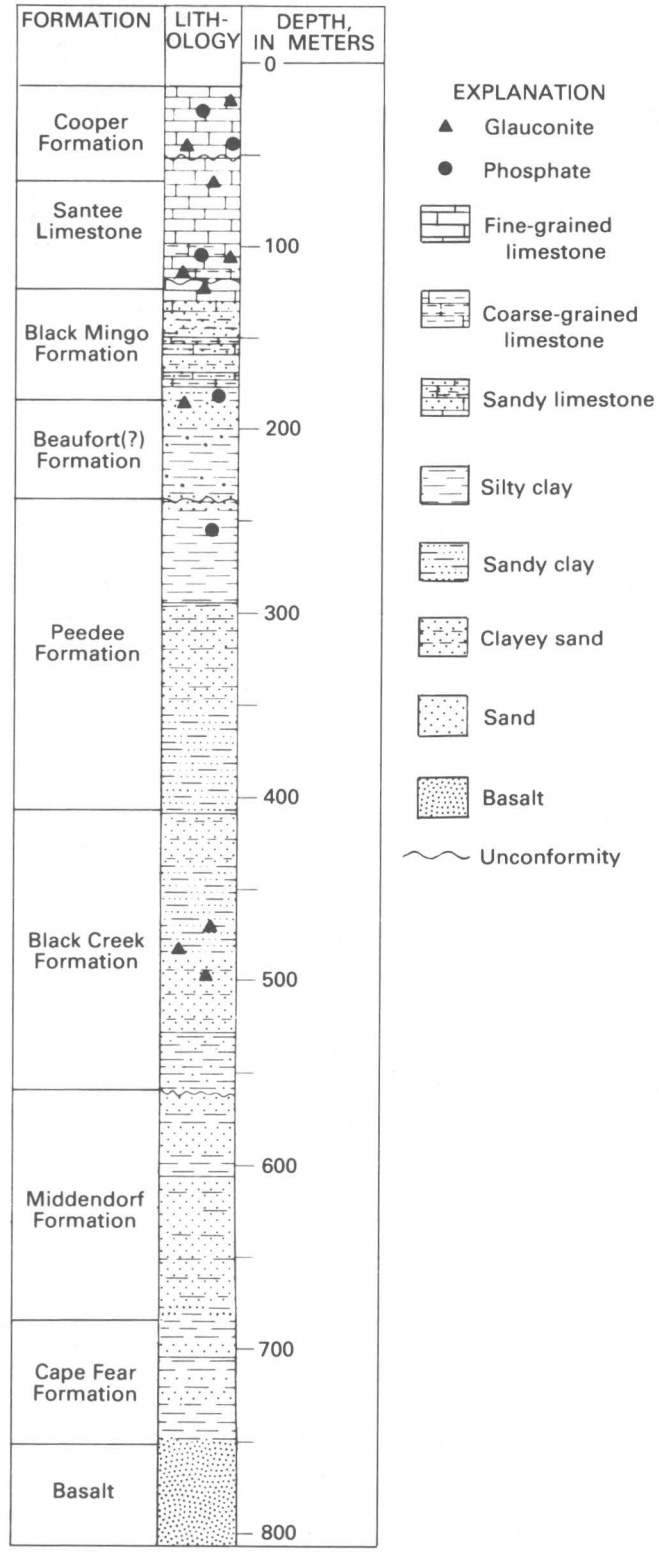

FIGURE 2.—Stratigraphic column of CC#1 (from Gohn and others, 1977).

The Peedee Formation (164 m), the youngest of the Cretaceous formations, consists of a thick sequence of calcareous muddy sand in the lower part and calcareous mud in the upper part. The Black Creek Formation (159 m) is the most heterogeneous of the Upper Cretaceous formations (Gohn and others, 1977, p. 67). An unconformity is present at the base of the formation. The Middendorf Formation (124 m), as the term is used by Gohn and others (1977), is composed of feldspathic sand, clayey silt, and sandy and silty clay. The Cape Fear Formation (59 m) overlies the basalt; its lower part is a basal muddy conglomeratic sand. A 42-m interval of weathered, amygdaloidal, massive basalt was penetrated before drilling was terminated.

After the reflection data discussed herein were acquired, two additional drill holes (CC#2 and CC#3) penetrated the basalt, and one of them (CC#3) bottomed in sedimentary red beds (Gohn and others, 1978).

In addition to the results from CC#1, Ackermann (1977) reported on refraction seismic studies in the Summerville-Charleston area. His data showed three refraction marker horizons throughout the area. The shallowest refractor is the well-indurated calcarenite at the base of the Santee at a depth of about 100 m in CC#1; a second horizon is the top of the basalt at a depth of 750 m in CC#1; the deepest marker horizon is interpreted to be crystalline basement and was not penetrated by CC#1.

REFLECTION SEISMIC DATA ACQUISITION AND PROCESSING

The reflection seismic data discussed herein were recorded on analog magnetic tape and later digitized at a sampling interval of 2 milliseconds (ms). Details of the shooting and recording array and energy source (dynamite) are given by Yantis (1978). Fourfold common-depth-point (CDP) recording configurations were used for the Clubhouse Crossroads line and the Interstate line. At Middleton Place, sixfold CDP configurations were used for the first 25 sourcepoints and fourfold CDP configurations for the remaining 78 sourcepoints. No elevation control for sourcepoints or for receiver arrays was available for correction to a datum.

RMS (root-mean-square) velocity spectra (Taner and Koehler, 1969) computed from individual seismograms were used to determine appropriate stacking velocities to remove normal moveout. Velocity spectra were also useful in the interpretation of the data.

Interval velocities were computed at intervals of 0.61 m in CC#1 from a continuous velocity log (CVL) (fig. 3) obtained by Schlumberger Corporation (Rhodehamel, 1975). Interval velocity as a function of depth is shown in figure 3*A*. RMS velocities were computed at 106 depths (Yantis, 1978). The RMS velocity function was used to generate synthetic data for comparison with real data. RMS velocity, as a function of depth, and reflection coefficients, as a function of time (calculated by means of the logarithmic approximation described by Peterson and others, 1955, and Sengbush and others, 1961), are shown in figures 3*B* and 3*C*, respectively.

A visual inspection of reflection coefficients as a function of time (or depth) is generally not useful in predicting when reflections will occur. Estimates of arrival time of reflections can be done only after convolution of a source wavelet with the reflection coefficient function; that is, after generation of a synthetic seismogram (hereafter referred to as a synthetic). Analysis of synthetic data derived from the CVL and velocity spectra computed from synthetic data were important in arriving at some of the conclusions presented herein.

The velocity determined from seismic surface measurements is a root-mean-square velocity (Dix, 1955; Taner and Koehler, 1969). Under optimum conditions, interval velocities can be computed from RMS velocities (Neidell and Taner, 1971). Interval velocities are more useful for the interpretation of the data.

All seismic techniques used to determine subsurface velocity from surface measurements measure the horizontal component of velocity, whereas a continuous velocity log obtained in a drill hole measures the vertical component of velocity. Anisotropy has not been considered in the interpretation of the Charleston reflection data. Sufficient data to evaluate its importance are not available.

RMS velocity analyses for the three reflection lines were examined for T_0 times (two-way traveltimes) ranging from 0.0 to 1.5 s and for RMS velocities ranging from 1.52 to 3.35 km/s.

Velocity spectra computed from each sourcepoint of the three reflection lines were used to determine the stacking velocities. Normal moveout was removed and CDP traces were summed with and without cross-correlation before stacking. Cross-correlation before stacking commonly improves data quality in areas where there is a severe near-surface statics problem. Cross-correlation windows of different lengths were used. In order to insure that the cross-correlation function would not be overly influenced by the strong reflection from the basalt, tests included windows with and without the reflection from the basalt. Stacked record sections showed no significant difference between cross-correlation windows that included the reflection from the basalt and those that excluded it. There was some improvement in the section, particularly at intermediate times, when cross-correlation was used, but the differences were not significant enough to change any of the conclusions presented herein.

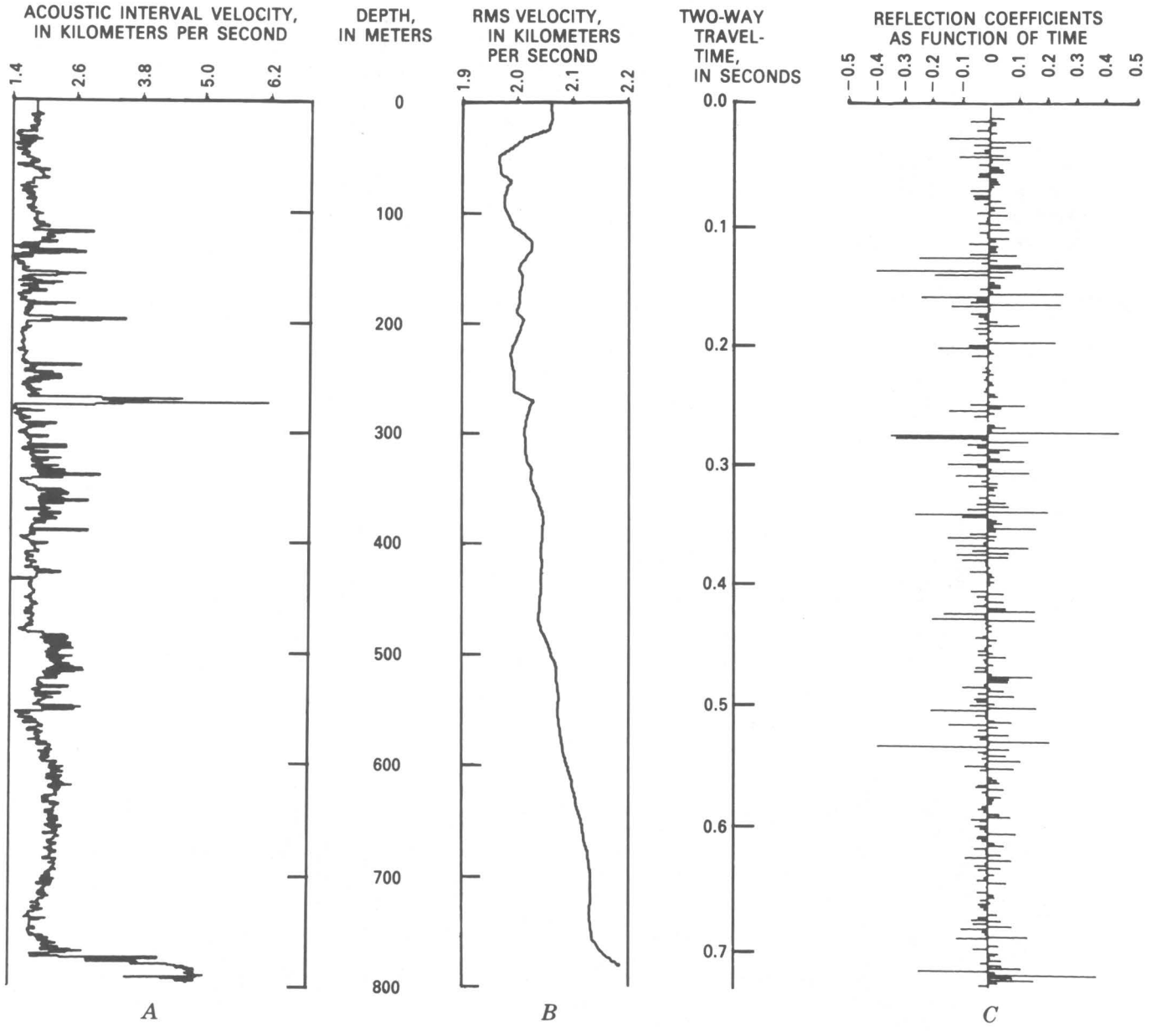

FIGURE 3.—*A*, Continuous velocity log (CVL) recorded in CC#1. *B*, RMS velocity (as a function of depth) calculated from CVL. *C*, Reflection coefficients (as a function of time) calculated from CVL.

INTERPRETATION OF REFLECTION SEISMIC DATA

Individual seismograms, stacked record sections, and velocity analyses of real as well as synthetic data are all useful in the interpretation of reflection data. For the three reflection profiles, all of these techniques were employed. The reflections interpreted from seismograms recorded on the Clubhouse Crossroads line were correlated with the lithologic variations observed in CC#1. The Interstate and Middleton Place seismograms were then correlated with the Clubhouse Crossroads seismograms on the basis of shape, amplitude, and arrival time of reflected events.

Because the discovery of faults was of interest, the expected resolution of the reflection data is important. The dominant period of the source wavelet, the time between the two largest positive (or negative) peaks, was found to be approximately 40 ms (Yantis, 1978). A fault that shifts a positive peak next to the adjacent negative trough of the source wavelet would be easily detectable. For a fault having a time displacement of 20 ms and a velocity of approximately 2.9 km/s, the detectable throw

would be at least $V\Delta t/2 = 29$ m, where Δt is two-way traveltime equal to half the dominant period of the source wavelet.

Clubhouse Crossroads Line

The Clubhouse Crossroads line was recorded approximately 23 km southwest of Summerville, S. C. The approximate elevation of the line was 6 m. Sourcepoints 1 through 19 were along a line approximately 0.8 km long oriented N. 45° E. Sourcepoint 20 through 41 were on a line approximately 0.9 km long oriented N. 85° E. (fig. 1). Sourcepoints 20 through 27 were recorded with split spreads. Figure 4 shows a representative seismogram, from sourcepoint 3 on the Clubhouse Crossroads line. Figure 5 is a velocity analysis of the sourcepoint 3 seismogram.

CORRELATION BETWEEN CLUBHOUSE CROSSROADS REFLECTION SEISMIC DATA AND CC#1

The first distinct arrival on seismograms recorded at Clubhouse Crossroads (fig. 4) begins at approximately 0.13 s and corresponds to the sharp transition, at a depth of about 125 m, from well-indurated calcarenite at the base of the Santee Limestone to fine-grained limestone at the top of the Black Mingo Formation. This is probably the same acoustic contrast responsible for the shallow refraction marker horizon of Ackermann (1977). The reflection at 0.20 s correlates with the boundary at 192 m between the Black Mingo and Beaufort(?) Formations. Near the base of the Black Mingo, as depth increases, there is a change from a calcareous mud to a glauconitic sand to almost entirely glauconite just above the boundary; just below the boundary in the Beaufort(?) is a slightly calcareous silt.

A strong reflection at approximately 0.27 s corresponds to a large acoustic velocity change at a depth of 260 m on a continuous velocity log obtained from CC#1, but Gohn and others (1977) described no distinct lithologic change. This reflection appears to originate from within the top part of the Peedee Formation, but it could mark the Cretaceous-Tertiary boundary.

The reflections in the interval betweeen 0.27 s and 0.71 s can not be positively identified with any formation boundaries; however, there are enough lithologic, cementation, and density changes within the Peedee, Black Creek, and Middendorf Formations to imply the presence of good acoustic impedance contrasts. The event at approximately 0.34 s appears to correspond to a change from friable sediments to carbonate-cemented sediments near the middle of the Peedee Formation at

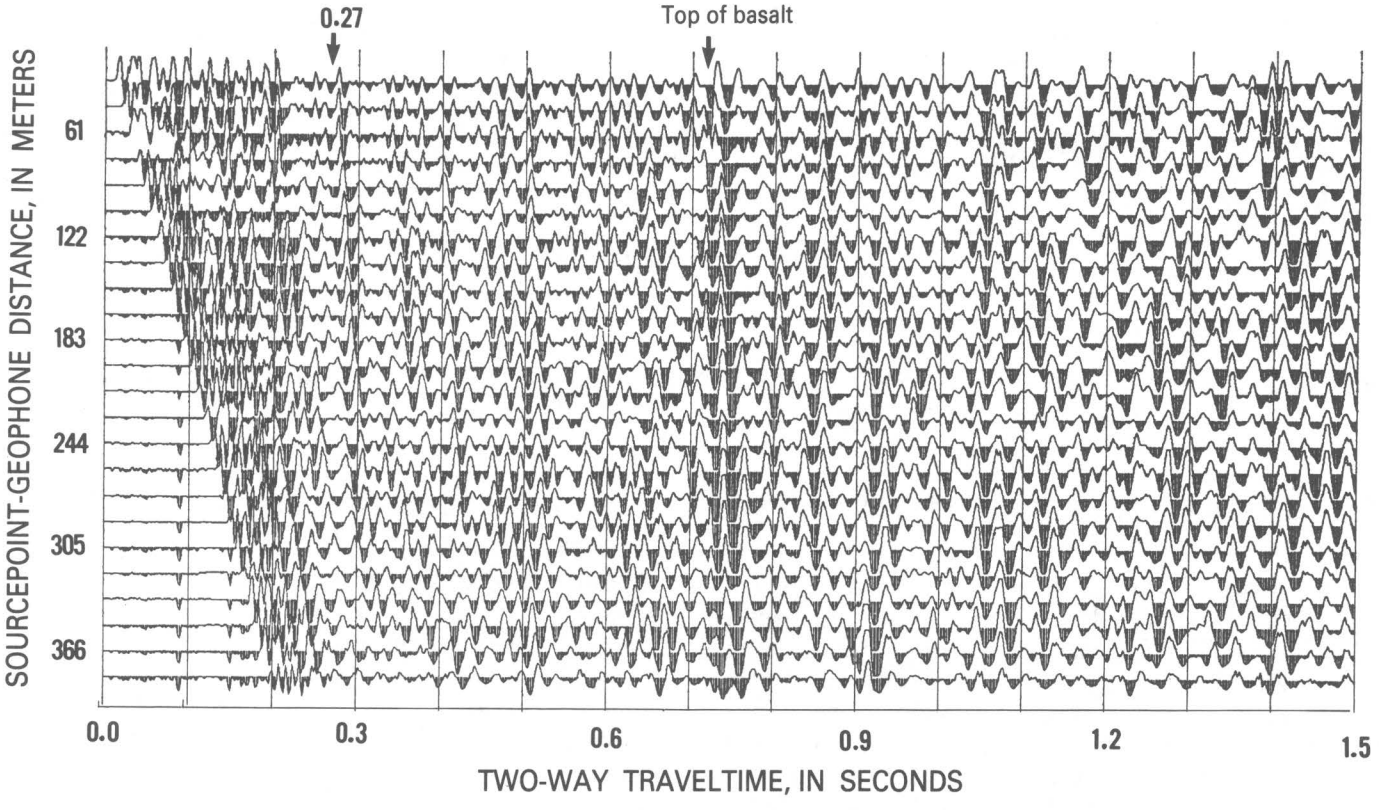

FIGURE 4.—Representative seismogram from Clubhouse Crossroads line, sourcepoint 3.

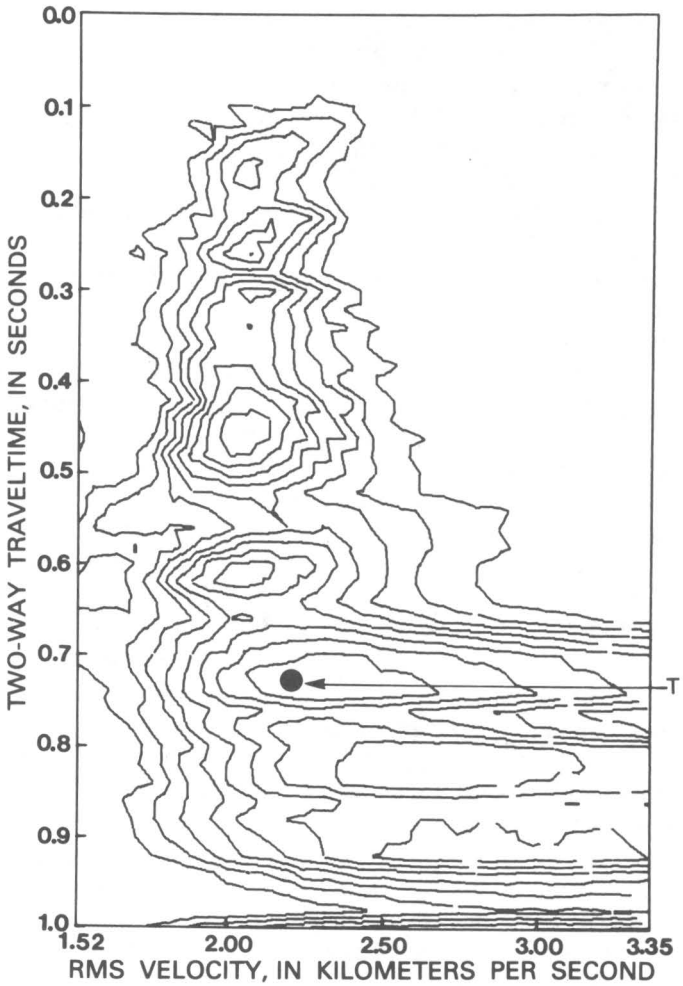

FIGURE 5.—Velocity analysis of sourcepoint 3 seismogram (fig. 4), Clubhouse Crossroads line. T, top of basalt.

335 m (not shown on fig. 2). The event at 0.43 s may be the result of a change in cementation from hard dolomitic cement in tight sandy clay below 425 m to almost no cement in loose sand near the top of the Black Creek Formation. The event at 0.45 s correlates with a change from clay to sand just above the middle of the Black Creek Formation at 475 m. This event merges with one at 0.48 s and appears to correspond to a change from fine quartzose sand to fine quartzose sandy silt, just below the middle of the Black Creek Formation. An event at approximately 0.55 s corresponds to an increase in calcium content and induration with increasing depth in sediments near the bottom of the Black Creek Formation.

The reflection from the top of the basalt, the strongest reflection recorded, arrives at approximately 0.71 s. The basalt was encountered in CC#1 at a depth of 750 m. This reflection is designated as the J reflection (Schilt and others, 1983); the reflection has been observed on seismic profiles more than 200 km seaward over the northern Blake Plateau (Dillon and others, 1979). Dillon and others show the offshore extent to be about 100,000 km^2. Behrendt and others (1981) discuss further the offshore extent of the reflection from the basalt.

Recorded events having traveltimes greater than that from the basalt cannot be directly related to CC#1. Analysis of synthetic data (Yantis, 1978) indicates that reflections at approximately 1.05, 1.25, and 1.4 s might be multiples; the event at 1.05 s is unaffected by basalt depth, the event at 1.25 s could be a combination of first- and second-order multiples, and the event at 1.4 s is the first-order multiple from the basalt. The reflections at approximately 0.90, 1.11, and 1.20 s do not appear to be multiples, on the basis of analyses of synthetic data. These events could be primary reflections from beneath the basalt layer. The event at 0.9 s might be from basement.

On many of the velocity spectra from the Clubhouse Crossroads line, a reflection from the bottom of the basalt flow is strongly indicated (fig. 6). Many of the seismograms show reflected events that arrive about 0.08 s after the reflection from the top of the basalt. This would suggest a thickness of about 232 m if the basalt velocity is approximately 5.8 km/s. This interpretation is confirmed by data from CC#3, in which the thickness of basalt was found to be 256 m.

The reflection from the top of the basalt will incorporate the characteristics of the overlying sediments and the basalt. Reflections from within and, particularly, from the bottom of the basalt flow will be affected also by characteristics such as internal layering, if any, of the basalt. Because of the higher interval velocity for the basalt, approximately 5.8 km/s from the CVL, the largest RMS velocity increase should be between the top and bottom of the basalt. This large increase is found on the velocity analysis between 0.65 and 0.80 s. T_0-times from velocity analyses of the Clubhouse Crossroads line indicate arrival times for the top and bottom of the basalt that agree well with analyses of synthetic seismograms (Yantis, 1978).

When no multiples are included in the synthetic seismogram, the pattern of the velocity analysis of the synthetic between 0.75 and 0.80 s has approximately the same shape as do analyses of real data at earlier times. When multiples are added to the synthetic made with a free-surface reflection coefficient of 0.60, the velocity analyses are similar to some from the Clubhouse Crossroads line (Yantis, 1978). Velocity analyses of synthetic data suggest that the thickness of the basalt could not be determined more accurately than ± 50 m; however, better resolution is theoretically obtainable. An estimate of 165–225 m thickness for the basalt flow is consistent

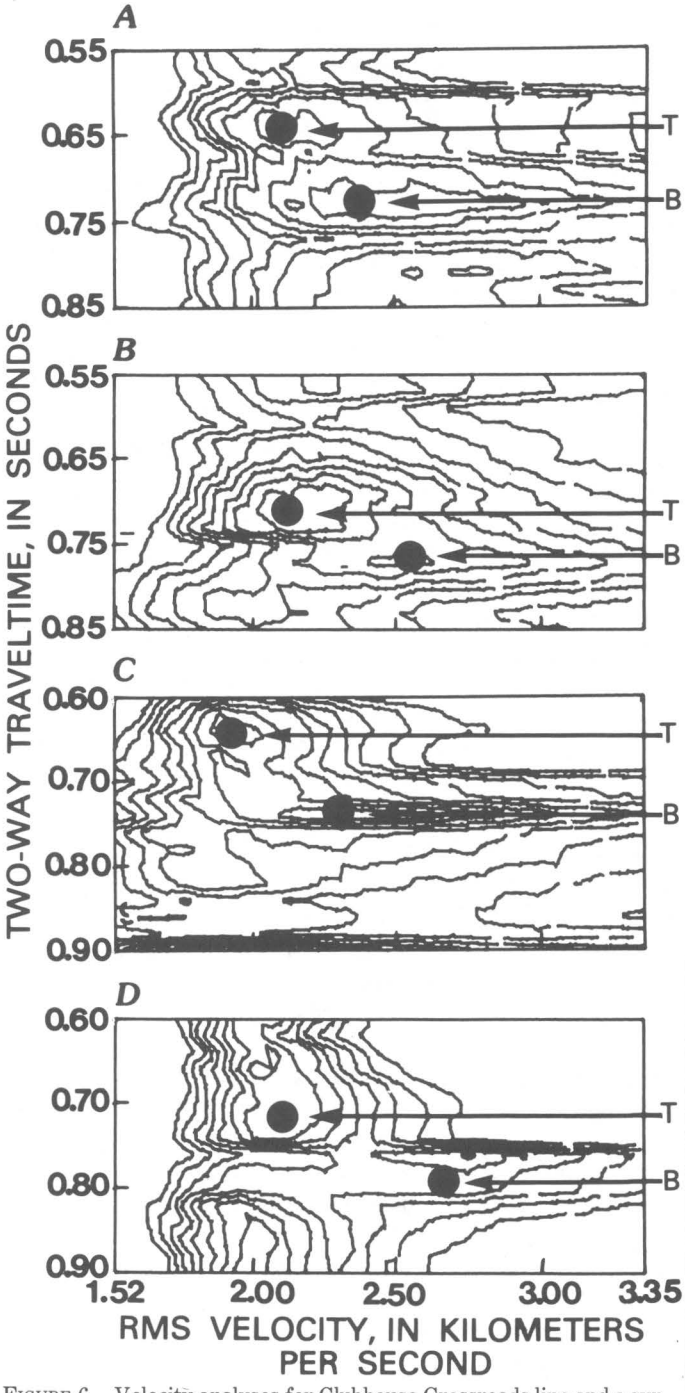

FIGURE 6.—Velocity analyses for Clubhouse Crossroads line and a synthetic seismogram, showing patterns indicating reflections from the top (T) and bottom (B) of the basalt. Note large increase in RMS velocity over time intervals shown. *A*, Sourcepoint 18; *B*, sourcepoint 31; *C*, sourcepoint 37; *D*, synthetic, generated assuming basalt flow is approximately 210 m thick.

with analysis of synthetic data for a basalt velocity of 5.8 km/s.

For reflections below the basalt, the velocity analyses are less conclusive because of the small amount of normal moveout caused by short spread lengths. Some analyses, that of sourcepoint 37, for example (Yantis, 1978, fig. 18), indicated an RMS velocity of 2.3 km/s at approximately 0.74 s and suggest RMS velocities for later times in the 1.7- to 2.3-km/s range. This is the RMS velocity range seen on the analysis of the synthetic, which has only multiples after 0.80 s. A velocity analysis of seismogram 18 (Yantis, 1978, fig. 19) indicates increasing RMS velocities, which suggests that these are associated with reflections from rocks with velocities greater than the velocities (2.1 km /s) of sediment above the basalt.

Type I, II, and III multiples (Ellsworth, 1948) caused by the basalt and strong reflectors above the basalt are to be expected. At sourcepoint 37, at about 0.94 s, there is an event having a low RMS velocity, approximately the same as the velocity of the event at 0.47 s, which suggests that it is a pegleg multiple reflection (Yantis, 1978, fig. 18).

CLUBHOUSE CROSSROADS LINE RECORD SECTION

The first part of the Clubhouse Crossroads record section (fig. 7) is oriented northeast-southwest; the remainder (fig. 8) is oriented almost east-west. The reflections from the basalt, as well as most events from above the basalt, are continuous over the entire line. There is essentially no regional dip evident on the record sections. As previously discussed, reflections corresponding to changes in CC#1 lithologies can be identified on the record sections. The reflection from near the base of the Santee Limestone is more distinct near CC#1 than at the other end of the line.

The events below the basalt are not as continuous as those above the basalt. Because of the generation of surface waves, data quality was poor where the split-spread data were stacked (fig. 8). Relatively strong events are apparent at approximately 0.81 and 0.91 s. Analyses of synthetic data cannot confirm that these are multiple reflections, although they might be. Comparison of the character of arrivals, however, indicates that these events may be related to the basalt and may originate either from the bottom of the basalt (as velocity analyses indicate for the event at 0.81 s), from another basalt layer, or from basement. The reflections at 0.71, 0.81, and 0.91 s were all strong enough to saturate the analog magnetic tape.

Interstate Line

The Interstate line was recorded 3.7 km north of Summerville, S. C. (fig. 1). The elevation was approximately 25 m. The line was oriented N. 10° E. and was approximately 1 km long.

Figure 9 shows a representative seismogram, sourcepoint 2, from the Interstate line. Figure 10 is a velocity analysis of this seismogram.

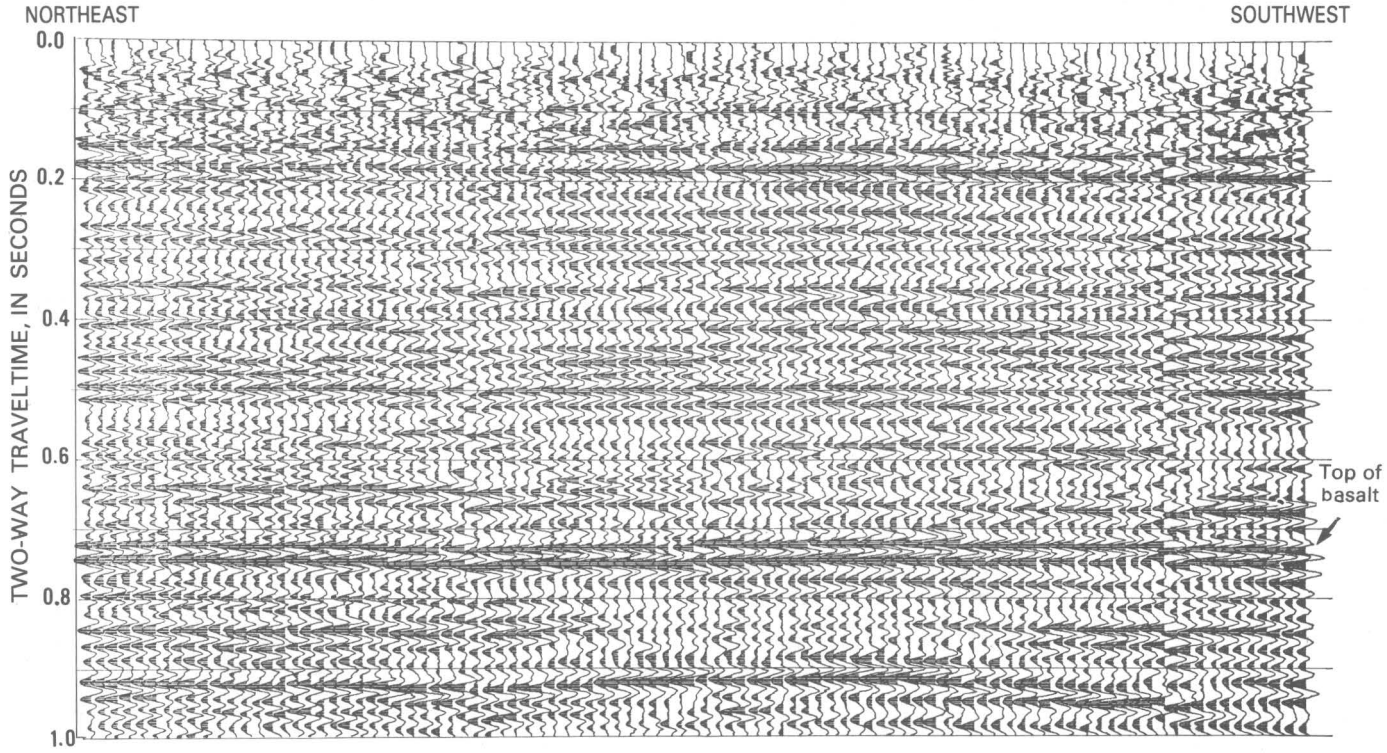

FIGURE 7.—Stacked record section for Clubhouse Crossroads line; data are from sourcepoints 1 (northeast) through 19 (southwest).

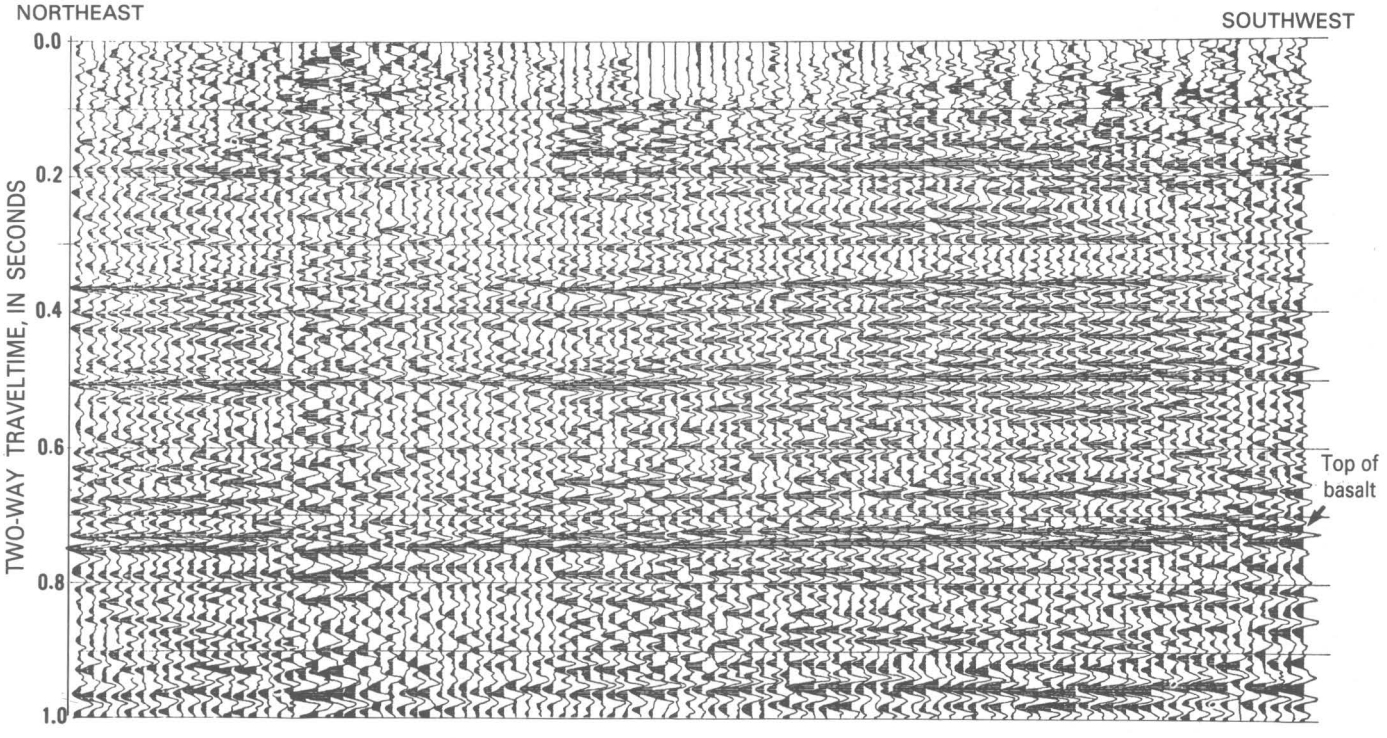

FIGURE 8.—Stacked record section for Clubhouse Crossroads line; data are from sourcepoint 20 (northeast) through 41 (southwest). Split-spread recording used for sourcepoints 20 through 27.

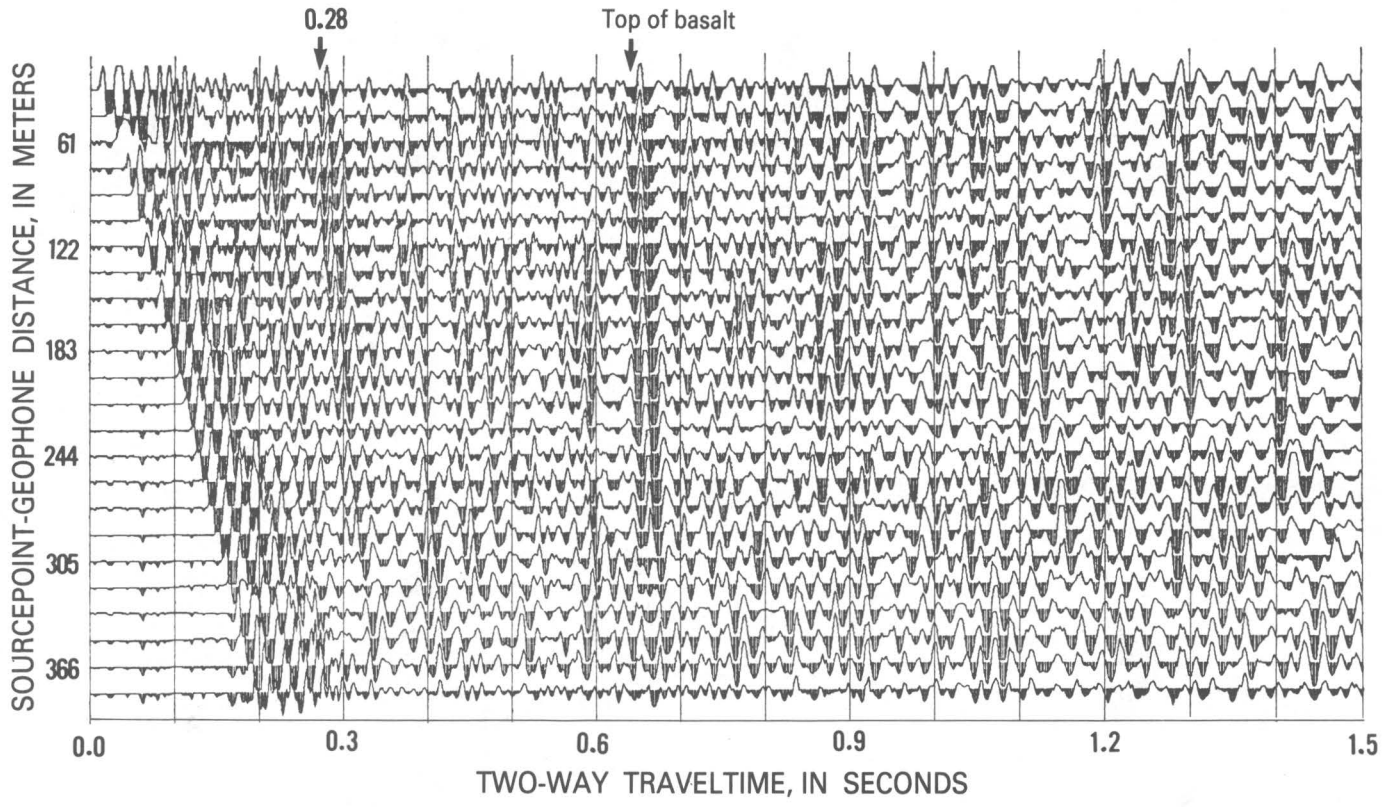

FIGURE 9.—Representative seismogram from Interstate line, sourcepoint 2.

CORRELATION BETWEEN INTERSTATE AND CLUBHOUSE CROSSROADS LINES

The strongest reflection on the seismograms from the Interstate lines arrives at approximately 0.65 s. This reflection is correlated with the reflection from the top of the basalt on the Clubhouse Crossroads line. As seen in figure 11, reflections on both lines saturated the analog magnetic tape and are clipped. The first motion of the event is downward, commonly with a deflection in the downgoing side of the first half-cycle ("a" in fig. 11). The trough of the first half-cycle is not always saturated. A large peak and trough, almost always clipped ("b" in fig. 11), follow. The upward part of the last negative half-cycle has a concave-upward irregularity ("c" in fig. 11). Following the last trough, there is sometimes an additional half-cycle.

The shape and amplitude of the later part of the reflection depend in part on the internal characteristics of the basalt. At these later times, some reflections from within the basalt are being recorded and superimposed on the end of the reflection from the top of the basalt. The similarity in character between reflections on the Clubhouse Crossroads and the Interstate lines persists, which suggests that the reflections are from basalts with the same or similar internal flow characteristics.

The reflection arriving at approximately 0.28 s on the Interstate line (fig. 9) appears to correlate well with the reflection at approximately 0.27 s on the Clubhouse Crossroads line (fig. 4). The reflection is usually clipped ("a" in fig. 12). On both lines, the upgoing side of the peak commonly has a small amplitude irregularity near the base ("b" in fig. 12).

Correlation of other events is less certain. Without isolated reflections and true-amplitude (digital) recording, it is difficult to make a correlation on the basis of wave shape and amplitude.

An event at 0.17 s (fig. 9) that may be a reflection from the calcarenite near the base of the Santee Limestone is not as distinct on the Interstate line as it is on the Clubhouse Crossroads line. An event at 0.21 s may be a reflection from the boundary between the Black Mingo and Beaufort(?) Formations. Between the reflection at approximately 0.28 s and the reflection from the basalt at 0.66 s, the Interstate line appears to be similar to the Clubhouse Crossroads line, although there is a smaller time interval between some of the events. This suggests that the same lithologic sequence is present at both locations; possibly the Middendorf and Cape Fear Formations (Gohn and others, 1977) are thinner at the Interstate line than at the Clubhouse Crossroads line. This

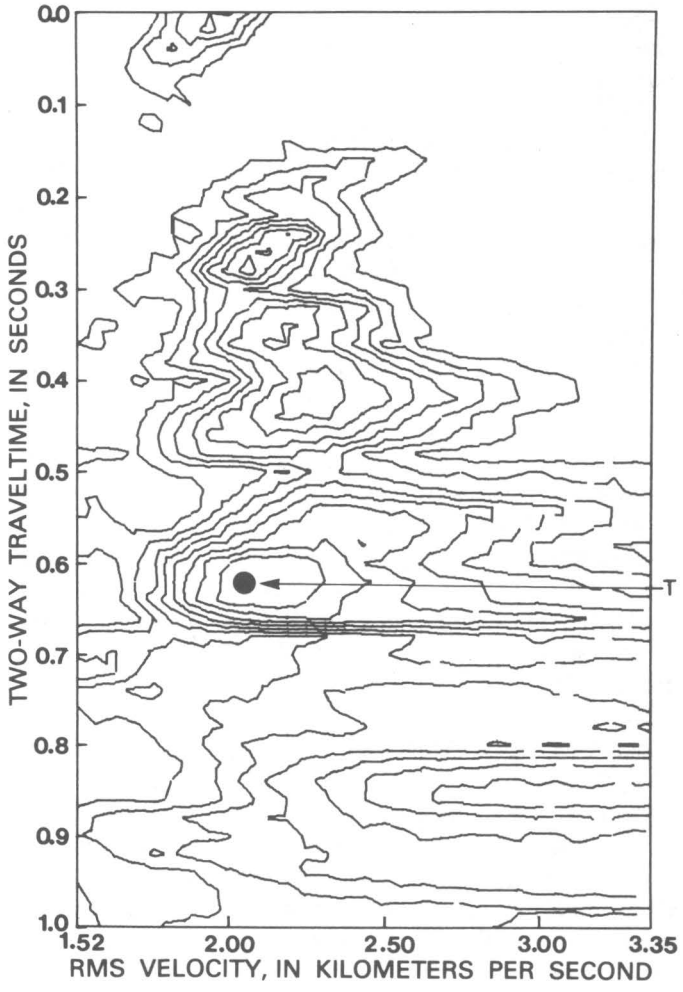

FIGURE 10.—Velocity analysis of sourcepoint 2 seismogram (fig. 9), Interstate line. T, top of basalt.

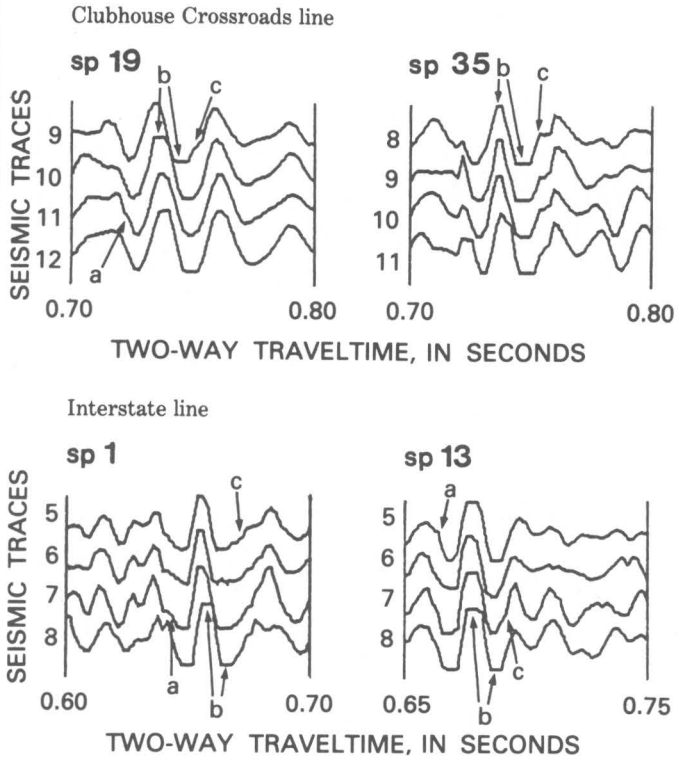

FIGURE 11.—Correlation of reflection from top of basalt flow between the Clubhouse Crossroads and Interstate lines. The correlation was based on the shape and amplitude of the reflections. The label "a" indicates a deflection in the downgoing side of the first trough; "b" indicates the clipped peak and trough; "c" indicates a concave-upward irregularity in the last negative half-cycle. sp, sourcepoint.

interpretation is consistent with the relative location of the lines: the Interstate line is further inland, and the Middendorf and Cape Fear Formations are expected to be thinner there than at Clubhouse Crossroads.

Velocity analyses of data along the Interstate line (fig. 13) also suggest a reflection from the bottom of the basalt. The data suggest that the basalt flow is thinner there, possibly 130–180 m thick, than at the Clubhouse Crossroads line.

INTERSTATE LINE RECORD SECTION

Figure 14 shows the record section for the Interstate line. Most reflections are continuous over the entire line. The reflection from near the base of the Santee Limestone, which would occur before 0.2 s according to other correlations and some individual seismograms, cannot be followed for more than about 1 km, either because of interference from strong early arrivals or because the reflector is less well defined. As was the case at Clubhouse Crossroads, surface waves may cause the poor continuity of some of the reflections, particularly those at later arrival times. A regional dip of approximately 0.5° SE. along the line is indicated by the reflection data. Similar reflection character is apparent between 0.5 and 0.55 s near the northeast end of the line and between 0.52 and 0.57 s at the southwest end of the line.

A flexure may be indicated near the middle of the line. The reflectors in the northeast half of the line appear to be slightly flatter than those to the southwest. The deterioration of data quality near the middle of the line is probably caused by excessive generation of surface waves, perhaps because the energy source was too shallow or was above the water table.

Below the basalt there is only one continuous reflection, at approximately 0.9 s. Analysis of synthetic data suggests that this could be a primary event. Other events below the basalt are continuous over 2 to 12 stacked traces. If the reflection that is most continuous toward the northeast end of the record section at approximately 0.7 s is from the bottom of the basalt, as is suggested by the velocity analysis, then events between

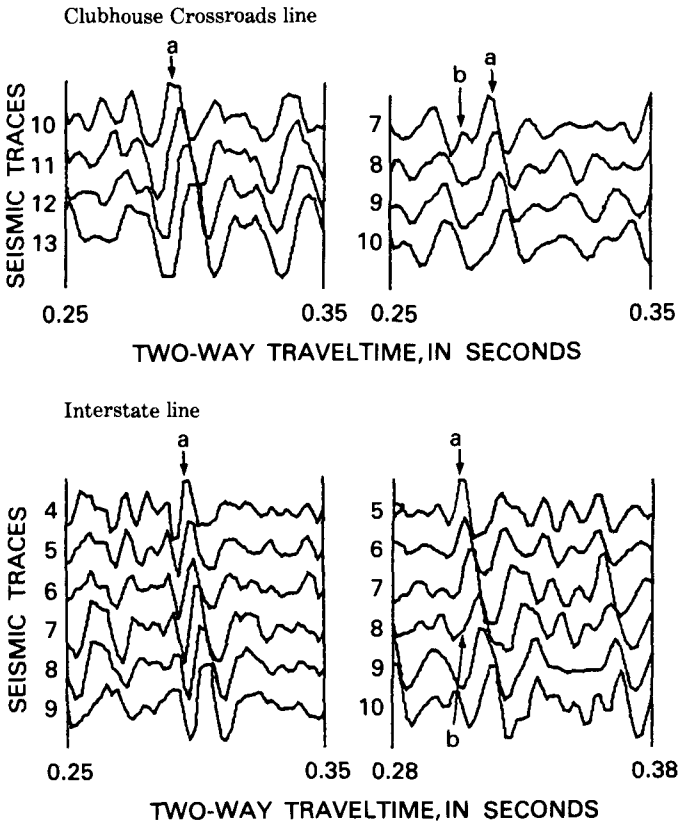

FIGURE 12. – Correlation of reflection at approximately 0.28 s (near top of Peedee Formation) between the Clubhouse Crossroads and Interstate lines. The correlation was based on the shape and amplitude of the reflection. The label "a" indicates the clipped peak; "b" indicates character before the peak.

0.88 and 0.94 s at the northern end of the line may represent reflections from a second basalt layer or from basement.

Middleton Place Line

The Middleton Place line is 15 km south-southeast of Summerville, S. C. (fig. 1). The elevation was approximately 7 m. The line is oriented N. 60° E. and is approximately 4.3 km long.

Figure 15 shows a representative seismogram, sourcepoint 13, from the Middleton Place line. Figure 16 shows a velocity analysis of seismogram 13.

CORRELATION BETWEEN MIDDLETON PLACE AND CLUBHOUSE CROSSROADS LINES

The strongest reflection on the Middleton Place line arrives at approximately 0.79 s. This reflection is correlated with the one from the basalt at Clubhouse Crossroads (labeled "a" on fig. 17). The event did not saturate the analog magnetic tape as commonly or for as long on the Middleton Place line as it did on the Clubhouse Crossroads line. The shape of the reflection is the same as that described for the reflection from the basalt along the Interstate and Clubhouse Crossroads lines.

The strong event arriving at approximately 0.29 s correlates well with the event at approximately 0.27 s on the Clubhouse Crossroads line. As seen in figure 18, for most sourcepoints on both lines the single peak is usually clipped ("a" in fig. 18). At the base or near the peak there is commonly another small-amplitude peak or deflection in the trace ("b" in fig. 18). Some of the negative half-cycles on either side of the peak are clipped, but less commonly than the peaks themselves are.

It is not possible to determine whether the reflections between 0.13 and 0.20 s correlate with the reflection from near the base of the Santee Limestone (0.13 s at Clubhouse Crossroads) or the reflection from the boundary between the Black Mingo Formation and the Beaufort(?) Formation (0.20 s at Clubhouse Crossroads). Noise (surface waves) in the Clubhouse Crossroads line for the first 0.2 s interferes with the character of the reflection from near the base of the Santee Limestone.

Distinct events are recorded between 0.29 s and the basalt reflection at 0.79 s, but the shapes are not distinctive enough to be of use for correlation with reflections on the Clubhouse Crossroads line. There are two likely possibilities for correlation. The section might be the same as that at Clubhouse Crossroads, down to a time of approximately 0.53 s or to near the base of the Black Creek Formation. The time intervals from there to the basalt indicate a thicker section of Black Creek, Middendorf, and Cape Fear Formations. A second possibility is that the section from the base of the Black Creek to the basalt is approximately the same thickness as it is at Clubhouse Crossroads. In that case, the section associated with reflections arriving from 0.30 to 0.55 s (the Peedee and Black Creek Formations) is thicker than the section at Clubhouse Crossroads. Either interpretation is consistent with a seaward-thickening wedge of sediments.

A possible reflection from the bottom of the basalt can be identified on some velocity analyses, for example sourcepoints 43, 52, and 90 (fig. 19). Comparison with synthetic data suggests a basalt thickness of 200 to 250 m.

MIDDLETON PLACE LINE RECORD SECTION

The Middleton Place line (fig. 20) has the lowest signal-to-noise ratio of the three lines, and many of the reflections are discontinuous along the record section. The reflection from the basalt at 0.8 s is continuous enough to define an apparent regional dip of about 0.1° SE. In spite of the relatively low signal/noise ratio,

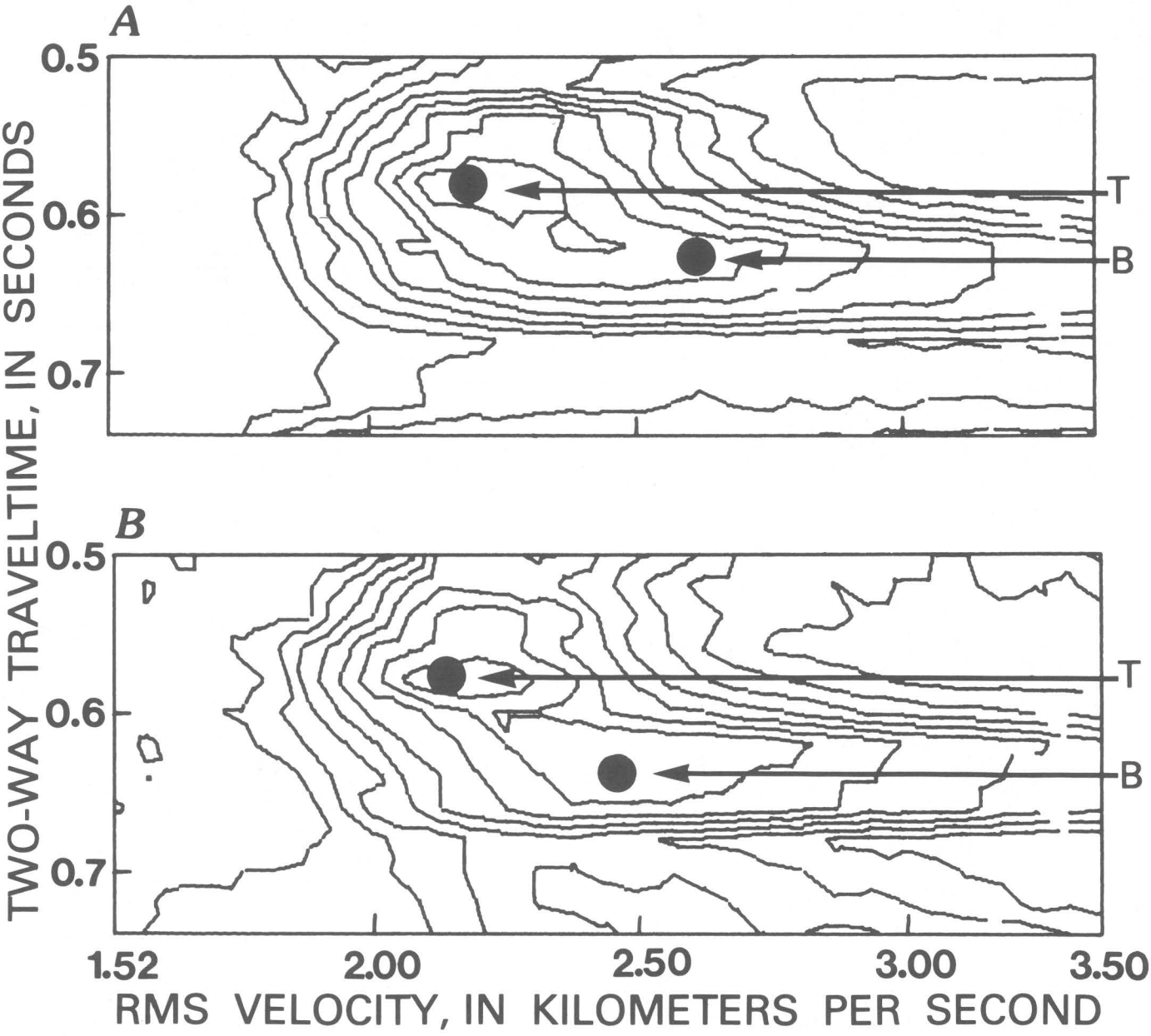

FIGURE 13. – Velocity analyses of seismograms from Interstate line, showing patterns indicating reflections from the top (T) and bottom (B) of the basalt. Note large increase in RMS velocity over the time intervals shown. *A*, Sourcepoint 4: *B*, sourcepoint 5.

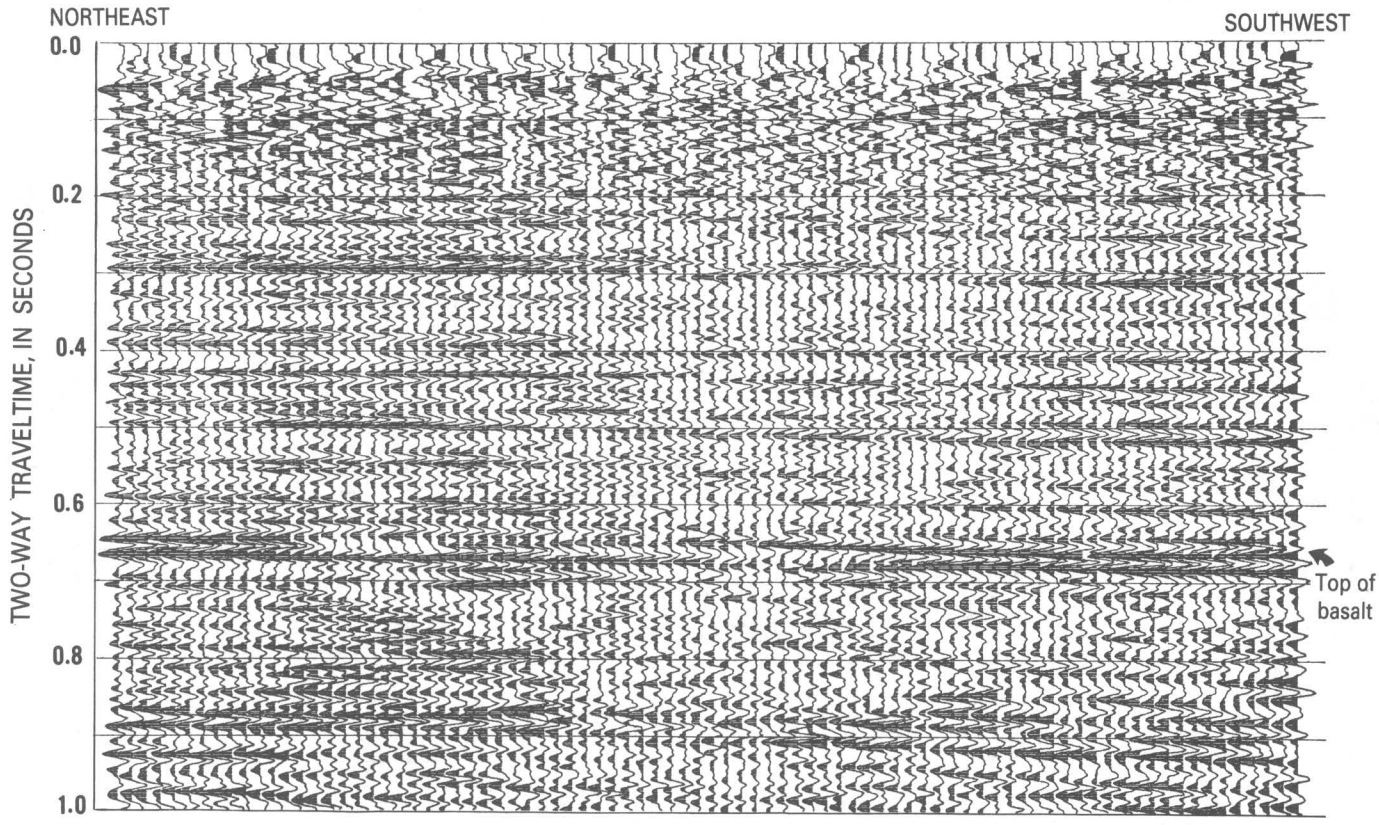

FIGURE 14.—Stacked record section for Interstate line; data are from sourcepoints 1 (northeast) through 17 (southwest).

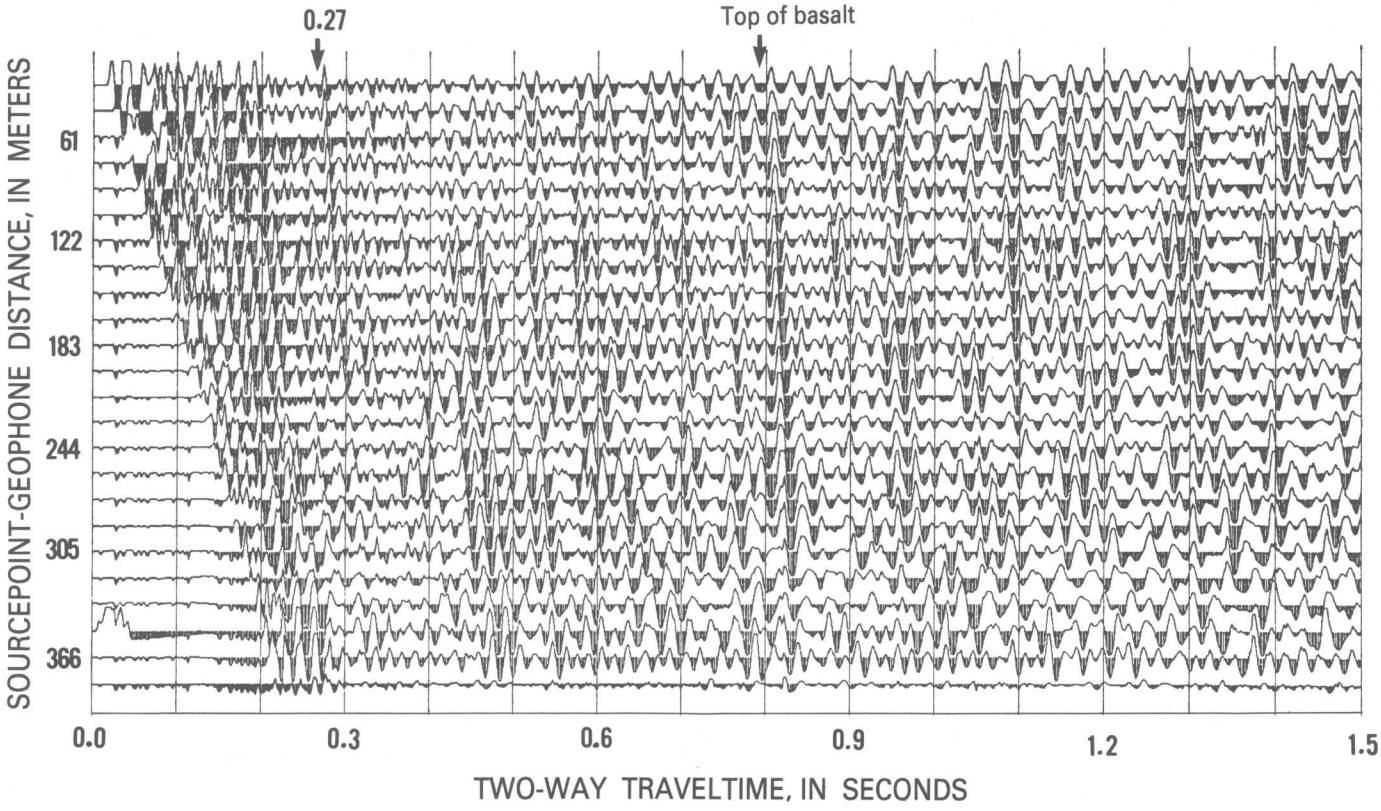

FIGURE 15.—Representative seismogram from Middleton Place line, sourcepoint 13.

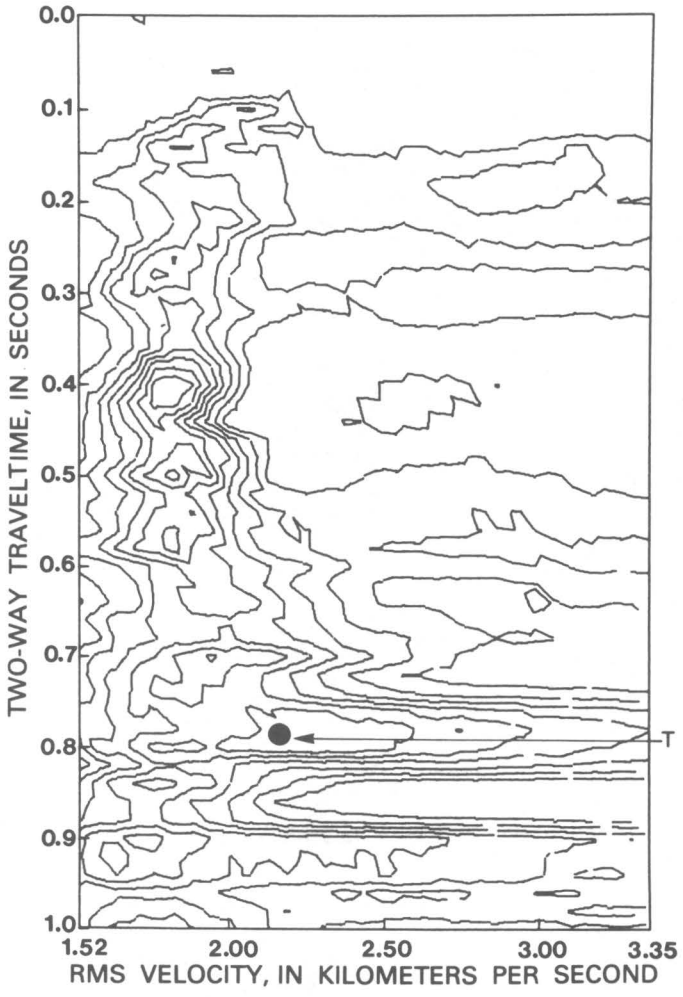

FIGURE 16. – Velocity analysis of sourcepoint 13 seismogram (fig. 15), Middleton Place line. T, top of basalt.

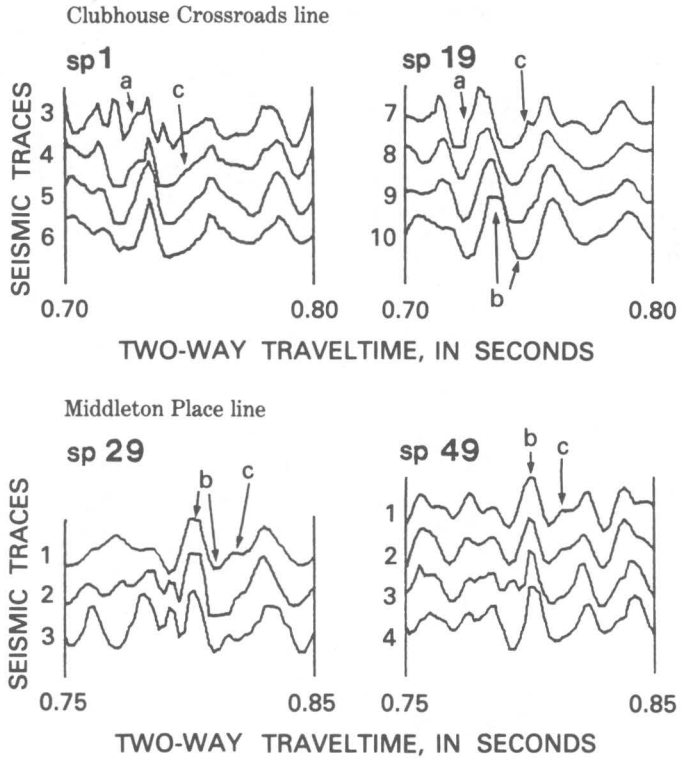

FIGURE 17. – Correlation of reflection from top of basalt flow between the Clubhouse Crossroads and Middleton Place lines. The correlation was based on the shape and amplitude of the reflections. The label "a" indicates a deflection in the upgoing side of the first trough; "b" indicates the clipped peak and trough; "c" indicates "character" in the last negative half-cycle. sp, sourcepoint.

reflected events over the time interval 0.75 s to 0.85 s are similar in character (fig. 20*A* and 20*F*), and therefore we conclude that the basalt is present at each end of the line.

The strong event at 0.30 s is essentially continuous, especially in the northern two-thirds of the line. This reflector appears to be horizontal.

Near the southwest end of the line (southwest of sourcepoint 4) the reflection from the basalt seems to arrive about 20 ms later than it does elsewhere on figure 20*A*; however, there is not enough data coverage to the southwest to confirm this. The reflection character immediately above the basalt does not suggest faulting. A slight doming of the basalt is apparent along the portion of the line shown on figure 20*D*, but no elevation control was available to correct the seismic data to a reference datum.

Below the basalt, the only event that is somewhat continuous occurs at approximately 0.95 s. Synthetic data cannot confirm that this is a multiple, but it might be. The reflection at 0.95 s is commonly clipped. The event arriving at 0.91 to 0.95 s on all of the lines might be from basement.

DISCUSSION AND CONCLUSIONS

Three seismic-reflection lines located in and near the meizoseismal area of the Charleston, S. C., earthquake were studied. A search for faults that might have been associated wih the 1886 earthquake was of special interest. A continuous velocity log and the lithologic log from CC#1 were used to correlate reflected events with changes in lithology.

At least four reflections on seismograms from the Clubhouse Crossroads line can be correlated with confidence with lithologic changes in the core from CC#1. These correlations are the reflection from the contact between the Santee Limestone and underlying Black Mingo Formation, the reflection from the contact between the Black Mingo and Beaufort(?) Formations, the reflection caused by an apparent change in sediment type and induration just below the top of the Peedee Formation, and the reflection from the top of the basalt.

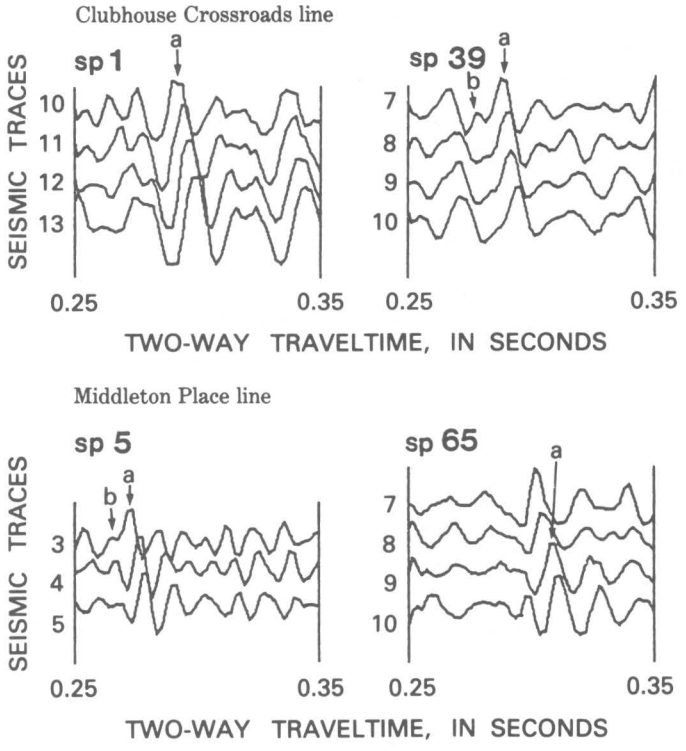

FIGURE 18.—Correlation of reflection at approximately 0.28 s (near top of Peedee Formation) between the Clubhouse Crossroads and Middleton Place lines. The correlation was based on the shape and amplitude of the reflections. The label "a" indicates the clipped peak; "b" indicates character before the peak. sp, sourcepoint.

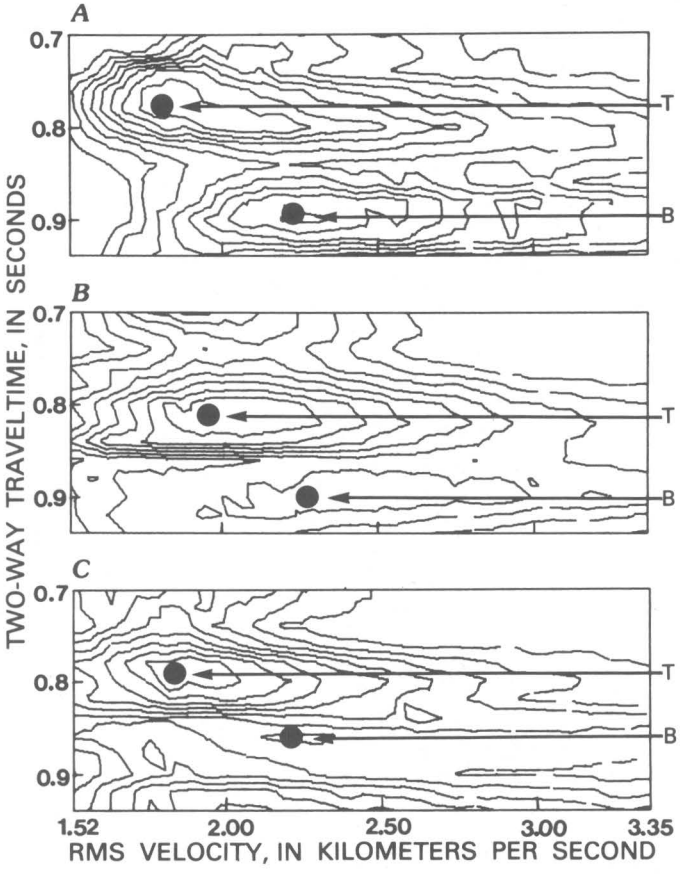

FIGURE 19.—Velocity analyses of seismograms on the Middleton Place line, showing patterns indicating reflections from the top and the bottom of the basalt. Note large increase in RMS velocity in time interval shown. *A*, Sourcepoint 43; *B*, sourcepoint 52; *C*, sourcepoint 90.

Reflections from near the top of the Peedee Formation and from the top of the basalt can be correlated for all three lines.

No faults in rocks of Cretaceous or younger age were detected along the three reflection lines. The reflector from near the top of the Peedee Formation, if assumed to be planar, has an approximate strike of N. 45° E. If the basalt flow, which is present throughout the study area, is assumed to be planar, its approximate strike and dip are N. 55° E. and 0.5° SE. Varying the depth of the basalt at the Interstate line and Middleton Place line by as much as 100 m would cause the strike to change by only 5°. The dip would remain at approximately 0.5° SE.

The possibility of faulting of the basalt at the southwesternmost end of the Middleton Place line is suggested by an apparent offset in reflected energy from the basalt, but additional data are needed. The reflection data immediately above the basalt do not suggest a fault in this area. If elevation and statics corrections do not seriously affect the data, some slight doming of the basalt may be present on the Middleton Place line.

Interpretation of velocity spectra computed from the reflection data indicates that reflections from both the top and the bottom of the basalt were observed. This was subsequently confirmed by drill hole CC#3. On the basis of the reflection data presented herein, the thickness of the basalt flow ranges from 150 to 250 m; however, the determination of thickness is somewhat uncertain because of the relatively short spread lengths used. The basalt flow is apparently thinnest at Interstate and thickest at Middleton Place; the difference in thickness may be as great as 100 m.

The relative thinness of the basalt at the Interstate line may explain the apparent inconsistency of reflection and refraction studies (this study; Talwani, 1977) as to whether or not the basalt is present in the vicinity of the Interstate line. The flow may be thinning in this region and thus be present in some areas but not in others near the edge of the flow. Refraction data involve lower frequencies than those considered in reflection studies. Thus reflection data would be more likely to detect a thinning edge.

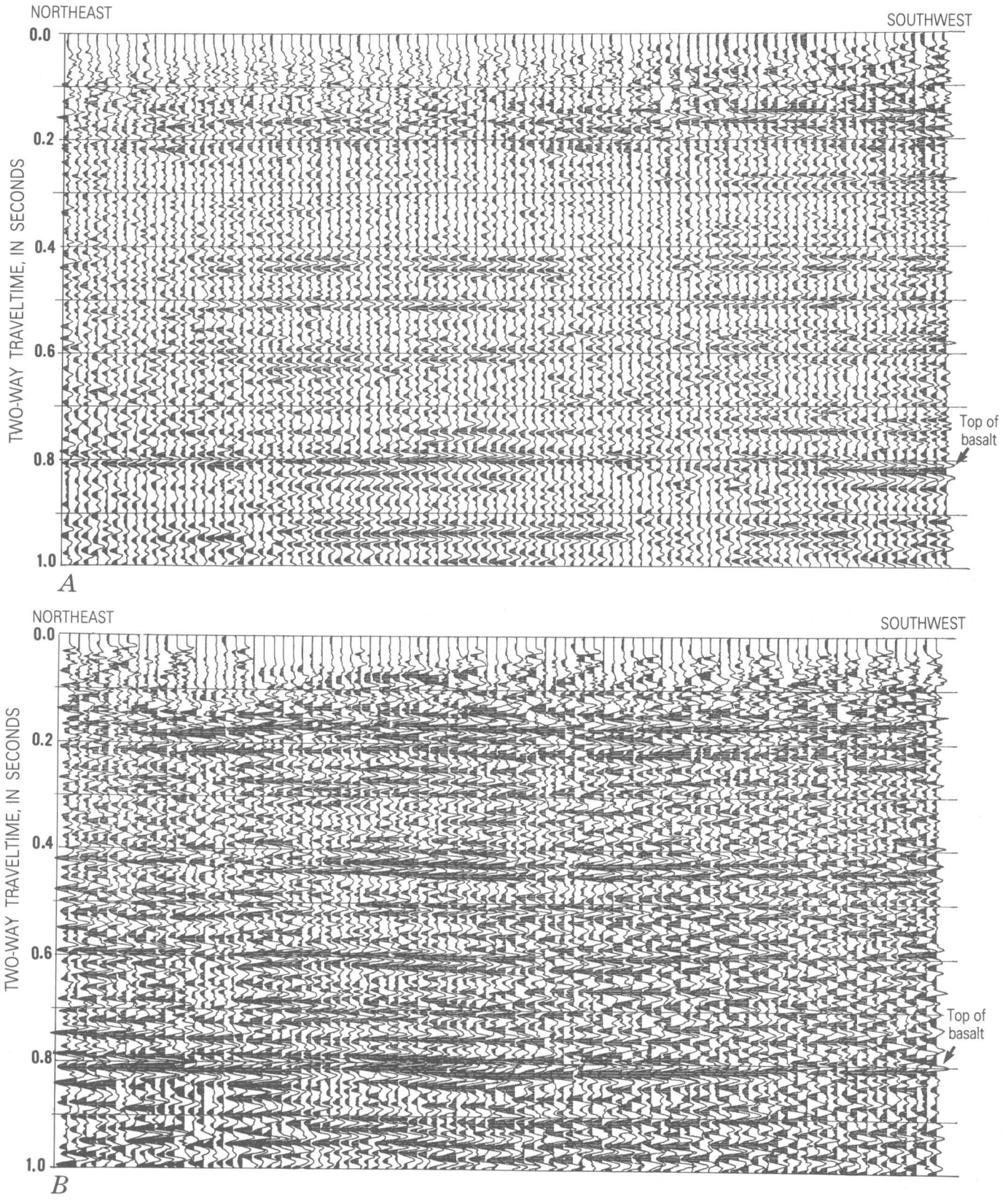

FIGURE 20. – Stacked record section for Middleton Place line. *A*, Data from sourcepoints 1 through 34. *B*, Data from sourcepoints 24 through 42. *C*, Data from sourcepoints 39 through 57. *D*, Data from sourcepoints 55 through 72. *E*, Data from sourcepoints 69 through 87. *F*, Data from sourcepoints 84 through 103.

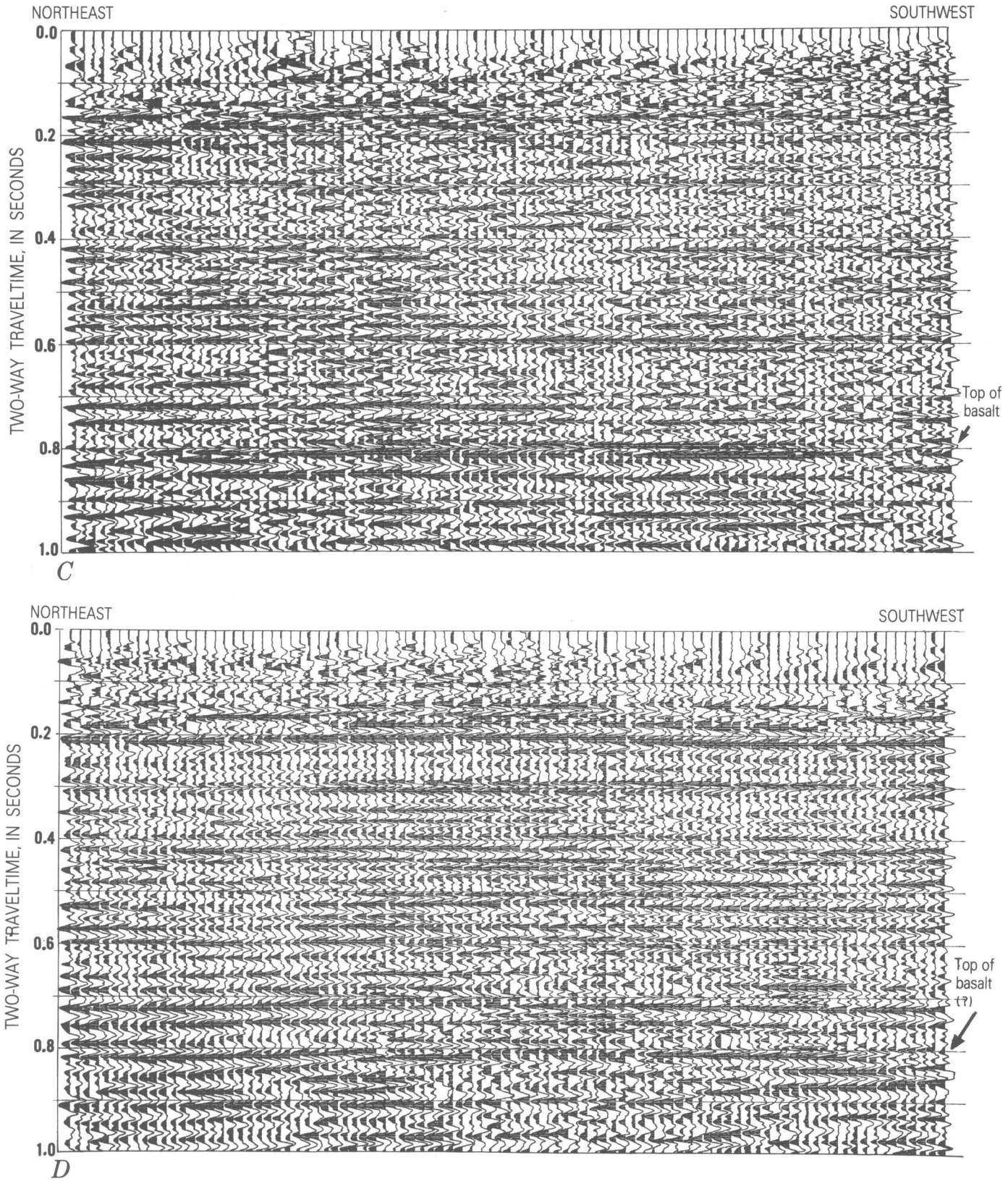

FIGURE 20.—Continued.

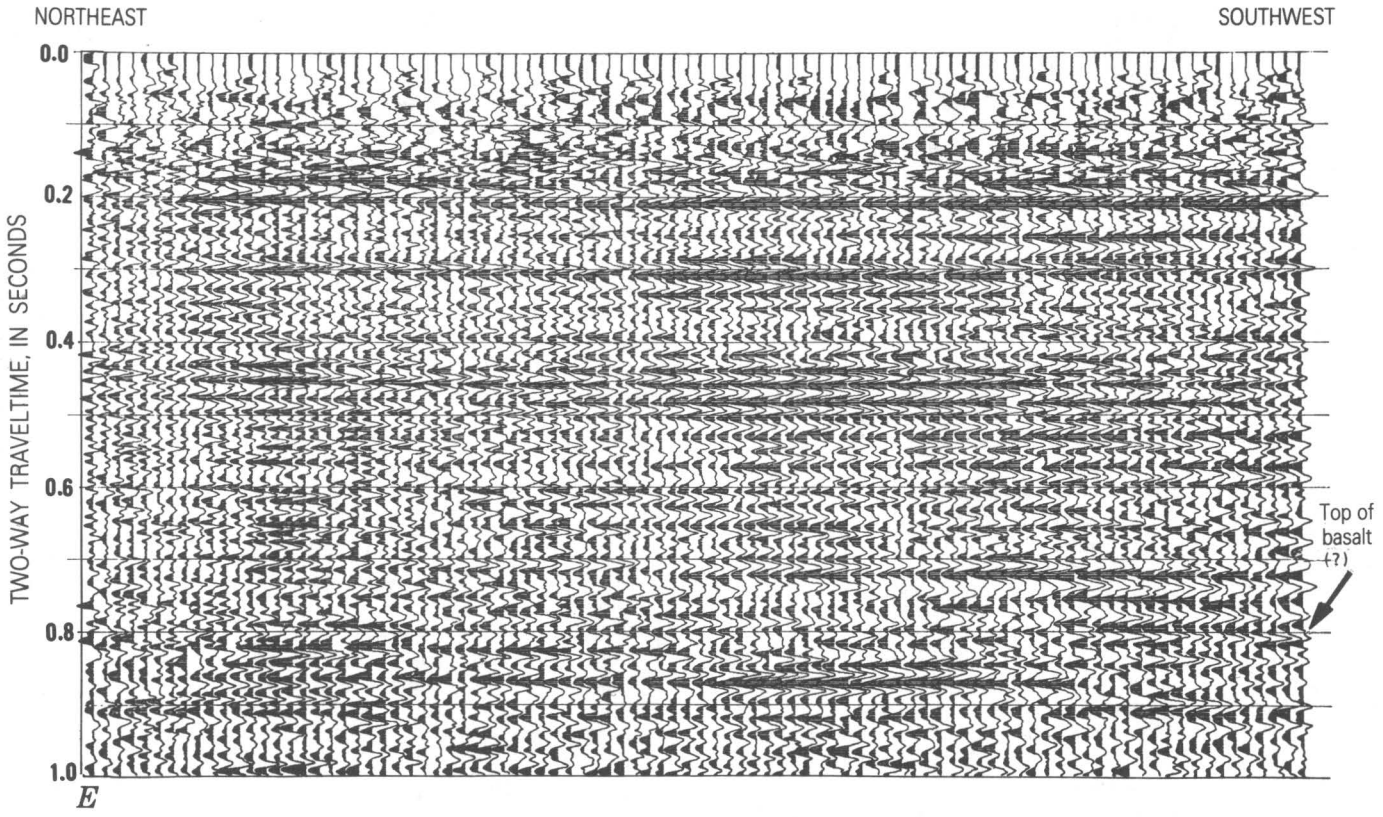

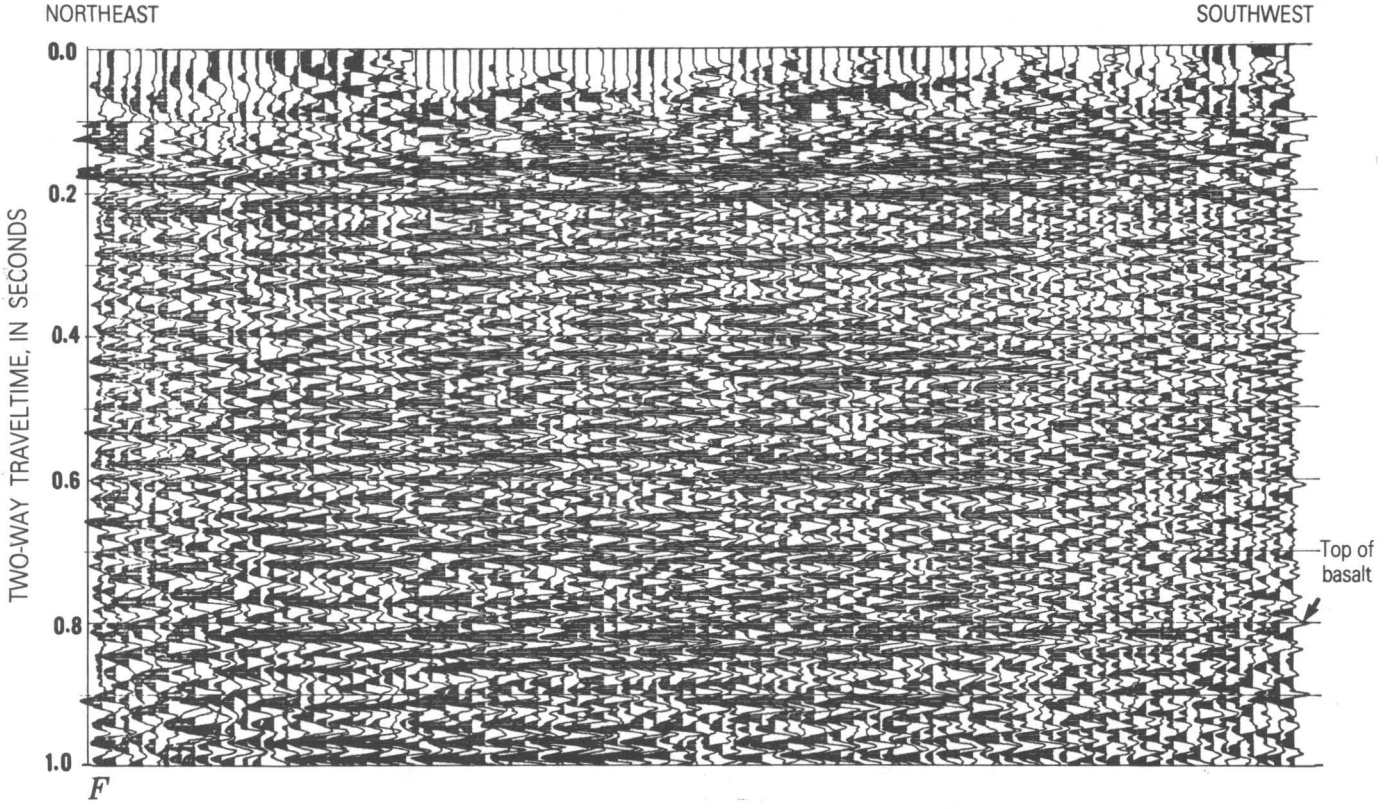

FIGURE 20.—Continued.

REFERENCES CITED

Ackermann, H. D., 1977, Exploring the Charleston, South Carolina, earthquake area with seismic refraction–A preliminary study, *in* Rankin, D. W., ed., Studies related to the Charleston, South Carolina, earthquake of 1886–A preliminary report: U.S. Geological Survey Professional Paper 1028, p. 167–175.

Behrendt, J. C., Hamilton, R. M., Ackermann, H. D., and Henry, V. J., 1981, Cenozoic faulting in the vicinity of the Charleston, South Carolina, 1886 earthquake: Geology, v. 9, no. 3, p. 117–122.

Clark, T. H., and Stearn, C. W., 1960, The geological evolution of North America–A regional approach to historical geology: New York, The Ronald Press Company, 434 p.

Dillon, W. P., Paull, C. K., Buffler, R. T., and Fail, J. P., 1979, Structure and development of the Southeast Georgia Embayment and Northern Blake Plateau–Preliminary analysis, *in* Watkins, J. S., Montadert, Lucien, and Dickerson, P. W., eds., Geological and geophysical investigations of continental margins: American Association of Petroleum Geologists Memoir 29, p. 27–41.

Dix, C. H., 1955, Seismic velocities from surface measurements: Geophysics, v. 20, no. 1, p. 68–86.

Dutton, C. E., 1889, The Charleston earthquake of August 31, 1886: U.S. Geological Survey Ninth Annual Report 1887–88, p. 203–528.

Ellsworth, T. P., 1948, Multiple reflections: Geophysics, v. 13, p. 1–18.

Gohn, G. S., Bybell, L. M., Christopher, R. A., Owens, J. P., and Smith, C. C., 1979, Cretaceous and Paleogene stratigraphic framework of the South Carolina and Georgia coastal margins [abs.]: Program and Abstracts, Second Symposium on the Geology of the Southeastern Coastal Plain, March 5–6, Georgia Southwestern College, Americus, Georgia, p. 11.

Gohn, G. S., Gottfried, David, Lanphere, M. A., and Higgins, B. B., 1978, Regional implications of Triassic or Jurassic age for basalt and sedimentary red beds in the South Carolina Coastal Plain: Science, v. 202, no. 4370, p. 887–890.

Gohn, G. S., Higgins, B. B., Smith, C. C., and Owens, J. P., 1977, Lithostratigraphy of the deep corehole (Clubhouse Crossroads corehole 1) near Charleston, South Carolina, *in* Rankin, D. W., ed., Studies related to the Charleston, South Carolina, earthquake of 1886–A preliminary report: U.S. Geological Survey Professional Paper 1028, p. 59–70.

Neidell, N. S., and Taner, M. T., 1971, Semblance and other coherency measures for multichannel data: Geophysics, v. 36, no. 3, p. 482–497.

Peterson, R. A., Fillippone, W. R., and Coker, F. B., 1955, The synthesis of seismograms from well log data: Geophysics, v. 20, no. 3, p. 516–538.

Popenoe, Peter, and Zietz, Isidore, 1977, The nature of the geophysical basement beneath the Coastal Plain of South Carolina and northeastern Georgia, *in* Rankin, D. W., ed., Studies related to the Charleston, South Carolina, earthquake of 1886–A preliminary report: U.S. Geological Survey Professional Paper 1028, p. 119–137.

Rankin, D. W., 1977, Studies related to the Charleston, South Carolina, earthquake of 1886–Introduction and discussion, *in* Rankin, D. W., ed., Studies related to the Charleston, South Carolina, earthquake of 1886–A preliminary report: U.S. Geological Survey Professional Paper 1028, p. 1–15.

Rhodehamel, E. C., 1975, Geophysical logs from a geologic test hole near Charleston, South Carolina: U.S. Geological Survey Open-File Report 75–247, 1 p.

Schilt, F. S., Brown, L. D., Oliver, J. E., and Kaufman, Sidney, 1983, Surface structure near Charleston, South Carolina: Results of COCORP reflection profiling in the Atlantic Coastal Plain, *in* Gohn, G. S., ed., Studies related to the Charleston, South Carolina, earthquake of 1886–Tectonics and seismicity: U.S. Geological Survey Professional Paper 1313, p. H1–H19.

Sengbush, R. L., Lawrence, P. L., and McDonal, F. J., 1961, Interpretation of synthetic seismograms: Geophysics, v. 26, no. 2, p. 138–157.

Talwani, Pradeep, 1977, A preliminary shallow crustal model between Columbia and Charleston, South Carolina, determined from quarry blast monitoring and other geophysical data, *in* Rankin, D. W., ed., Studies related to the Charleston, South Carolina, earthquake of 1886–A preliminary report: U.S. Geological Survey Professional Paper 1028, p. 177–187.

Taner, M. T., and Koehler, Fulton, 1969, Velocity spectra–digital computer derivation and applications of velocity functions: Geophysics, v. 34, no. 6, p. 859–881.

Tarr, A. C., 1977, Recent seismicity near Charleston, South Carolina, and its relationship to the August 31, 1886 earthquake, *in* Rankin, D. W., ed., Studies related to the Charleston, South Carolina, earthquake of 1886–A preliminary report: U.S. Geological Survey Professional Paper 1028, p. 43–57.

Tarr, A. C., and Rhea, Susan, 1983, Seismicity near Charleston, South Carolina, March 1973 to December 1979, *in* Gohn, G. S., ed., Studies related to the Charleston, South Carolina, earthquake of 1886–Tectonics and seismicity: U.S. Geological Survey Professional Paper 1313, p. R1–R17.

Yantis, B. R., 1978, A reflection seismic study near Charleston, South Carolina: Blacksburg, Virginia Polytechnic Institute and State University, M.S. thesis.

Subsurface Structure Near Charleston, South Carolina—Results of COCORP Reflection Profiling in the Atlantic Coastal Plain

By F. STEVE SCHILT, LARRY D. BROWN, JACK E. OLIVER, and SIDNEY KAUFMAN

STUDIES RELATED TO THE CHARLESTON, SOUTH CAROLINA, EARTHQUAKE OF 1886—TECTONICS AND SEISMICITY

GEOLOGICAL SURVEY PROFESSIONAL PAPER 1313-H

UNITED STATES GOVERNMENT PRINTING OFFICE, WASHINGTON: 1983

CONTENTS

ILLUSTRATIONS

TABLES

SUBSURFACE STRUCTURE NEAR CHARLESTON, SOUTH CAROLINA—RESULTS OF COCORP REFLECTION PROFILING IN THE ATLANTIC COASTAL PLAIN

By F. STEVE SCHILT,[1] LARRY D. BROWN,[1] JACK E. OLIVER,[1] and SIDNEY KAUFMAN[1]

ABSTRACT

In May and June of 1978, the Consortium for Continental Reflection Profiling (COCORP) surveyed four lines totalling 72 km in length in the Charleston-Summerville area of South Carolina. The objective was to map the structure of the entire crust in that area. Some particularly interesting near-surface structures were detected in addition to deeper features. A strong event at 0.7 s (seconds) is present on all profiles and corresponds to the lower Mesozoic basalt layer penetrated at about 750 m in U.S. Geological Survey drill holes. The top of an older basement having as much as 1 km of relief can be seen at about 1.0 s (~1600 m). The Coastal Plain sediments, basalt layer, and basement can all be traced with good continuity over much of the lines; they are cut by a reverse fault and possibly by a small fault-bounded graben, each having an offset of a few tens of meters. A line that crosses a zone of recent seismicity shows noticeable differences in shallow structures on either side, although the shallow section across part of the seismic zone itself was not observed on this line, owing to a gap in the data on either side of the Ashley River. Beneath the Mesozoic and younger strata, the upper crust appears generally transparent to seismic energy down to 6.0 s (~18 km). From about 6.0 to 11.0 s, many short scattered reflections having a laminated appearance suggest a transition from relatively homogeneous igneous rocks to a more anisotropic and metamorphosed lower crust. The crust-mantle transition appears to be represented by a distinct band of short reflection segments at 10.5–11.0 s, whose depth (~32–34 km) agrees with data from a refraction study in the central Appalachian Piedmont. If the gently dipping Appalachian overthrust discovered in Georgia by a COCORP survey extends beneath the Charleston area, it is conceivable (but speculative) that some of the reflections below 6.0 s are metasedimentary layers beneath imbricate thrusts.

INTRODUCTION

As part of the effort to determine the structural setting of the Charleston seismic zone and to investigate proposed extensional structures of a rifted continental margin, the Consortium for Continental Reflection Profiling (COCORP) surveyed four lines near Summerville, S. C. The project was jointly funded by the National Science Foundation, the U.S. Geological Survey (USGS), and the Nuclear Regulatory Commission. A recording time of 20 seconds (s) was used to collect data down to the crust-mantle boundary and deeper if possible. The VIBROSEIS[2] technique was used, and the various seismic parameters (see table 1) were similar to those used in previous COCORP surveys (Oliver and others, 1976; Brown and others, 1979; Schilt and others, 1979; Brewer and Oliver, 1980).

The reflection survey was designed primarily for penetration and resolution of deep crustal features (down to several tens of kilometers). Consequently, reflections shallower than about 0.4 s (~400 m) are not discernible. However, shallow reflections and structures in the range 0.4–1.5 s (~400–2,600 m) are clearly seen, and deep reflections are observed on some records as late as 12.0 s (~36 km). The reflection data are discussed in two parts: the shallow sedimentary section and deep reflections (greater than 1.5 s).

Cretaceous shelf sediments, a lower Mesozoic basalt, and an older basement have been traced over most of the survey area. The older basement has a relief of at least 1 km over the area surveyed. Although no exposed faults have been mapped at the surface, some shallow faults (two apparently normal and one possibly reverse) have been interpreted on the basis of the reflection data. The reverse fault is near the greatest concentration of earthquake epicenters, and another inferred zone of faulting beneath the Ashley River is near the southeastern end of the epicentral pattern. These faults are not necessarily those along which the current seismicity occurs, as most of the hypocenters appear to be deeper than 5 km. However, the spatial correlation of the faults and the epicenters suggests a possible causal relationship.

[1]Department of Geological Sciences, Cornell University, Ithaca, NY 14853.

[2]Any use of trade names is for descriptive purposes only and does not imply endorsement by the USGS.

TABLE 1.—*Seismic survey parameters*

Source	5 VIBROSEIS vibrators, 23 m apart
Sweep frequencies	8–32 Hz (upsweep)
Recording system	96 channels (MDS-10)
Record length	20 s
Sampling interval	8 ms
Distance to nearest station	469 m (1,540 ft)
Station spacing	67 m (220 ft)
Length of receiver array	6,370 m (20,900 ft)
Nominal fold:	
Line 1 (sta. 41–199), line 2, and line 3	24
Line 1 (sta. 948–41) and line 4	16

Nominal fold after muting:

Time (s)	Fold (16 max.)	Fold (24 max.)
0.0	0	0
.5	1	1
1.0	2	3
1.5	4	6
2.0	5	8
3.0	11	16
4.0–20.0	16	24

Deep reflections were recorded; they were especially concentrated in the depth range of 18–33 km. Reflections near 11.0 s (~33 km) are interpreted as representing the Moho (Mohorovicic discontinuity) on the basis of their depth, which is consistent with depths to the Moho derived from a refraction survey in the Piedmont and from offshore multichannel recordings of similar deep reflections.

Acknowledgments.—We thank I. Zietz, P. Popenoe, B. Houser, A. Tarr, H. Ackermann, and B. Morgan for proposing this area to COCORP for reflection profiling. We gratefully acknowledge discussions with many USGS Charleston Project scientists, especially H. Ackermann, J. Behrendt, D. Campbell, G. Gohn, and D. Rankin. Discussions with graduate students and staff of Cornell University influenced parts of this paper. The seismic data were acquired and processed by Petty Ray Geophysical Company. Support for this research came from National Science Foundation grants EAR-7713653 and EAR-7714674, the U.S. Geological Survey, and the Nuclear Regulatory Commission.

SITE OF REFLECTION PROFILES

The regional location of the four reflection profiles, which total 72 km in length, is shown in figure 1. A more detailed map showing the location of the lines and selected station numbers is shown in figure 2. Line 1 begins near the center of the largest magnetic high [>600 nT (nanoteslas)] and proceeds northeast toward Summerville, passing three USGS drill holes (maximum depths of 800–1,150 m). Line 2 crosses line 1 near the northeastern end of the latter; it heads southeast, parallel to the Ashley River, obliquely crossing a northwest-trending group of epicenters south of Summerville. Line 3 also crosses the southern end of the

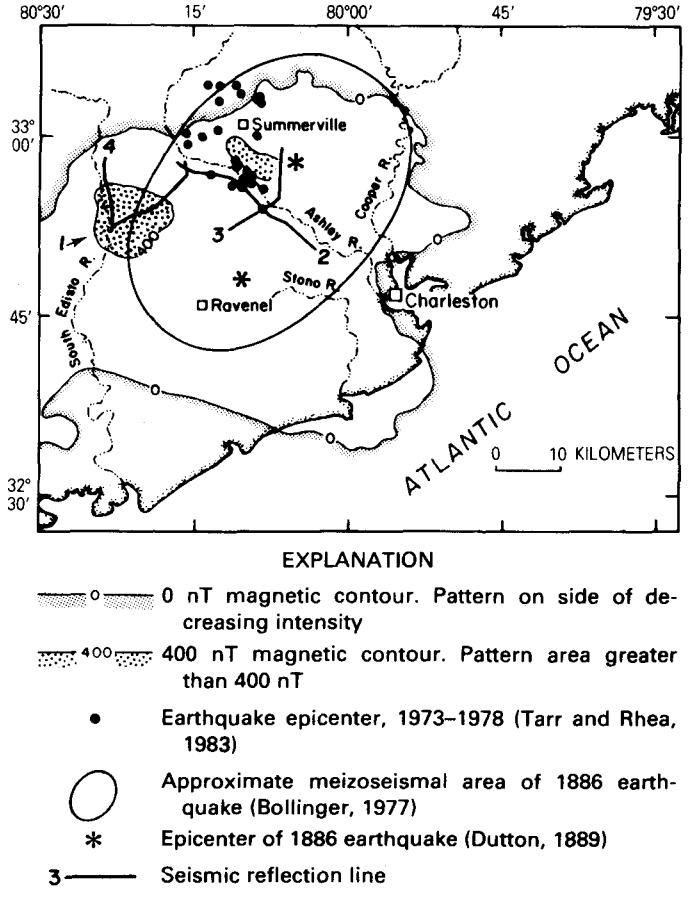

FIGURE 1.—Index map showing location of COCORP lines. Four lines totalling 72 km in length overlap to form a net about 30 km northwest of Charleston.

epicenter trend near the Ashley River; it crosses line 2 and the river at approximately right angles, heading from southwest to northeast, then bends north toward Summerville and passes over a large elliptical magnetic high (>500 nT). The last and shortest line, line 4, starts at the southwestern end of line 1 and heads due north.

PREVIOUSLY KNOWN STRATIGRAPHY

Line 1 passes three deep test holes drilled by the USGS near Clubhouse Crossroads, S. C. All three of the wells (henceforth referred to as CC#1, CC#2, and CC#3) penetrated 750–776 m of Upper Cretaceous and younger sediments and then encountered amygdaloidal basalt, which occurs as multiple subaerial flows. An $^{40}Ar/^{39}Ar$ age of 184±3.3 m.y. for a sample from CC#2 indicates an Early Jurassic age (Lanphere, 1983). Chemical analyses indicate that these basalts are mostly quartz-normative tholeiites, which closely resemble the lower Mesozoic high-Ti quartz-normative diabases of eastern North America (Gottfried and others, 1977, 1983). A seismic-refraction study by Ackermann (1977,

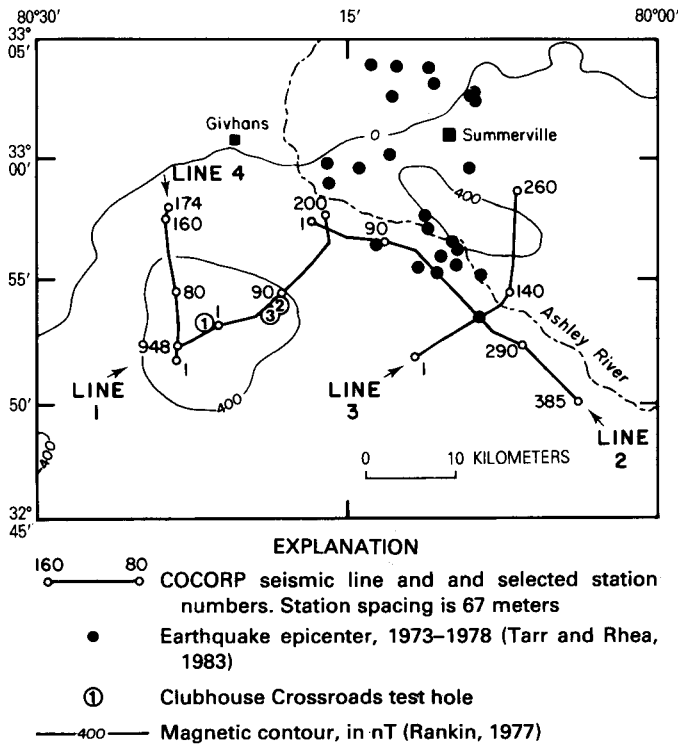

FIGURE 2. – Location of COCORP seismic lines and station numbers.

1983) traced the basalt (or pre-Cretaceous unconformity) as a refracting horizon about 30 km eastward from CC#1. Contours of the depth and velocity of the refractor show a general trend of decreasing velocity and increasing depth to the east.

Although CC#1 and CC#2 (total depths 792 m and 907 m, respectively) bottomed within the basalt, CC#3 (total depth 1,152 m) penetrated over 250 m of basalt and then passed through about 120 m of unfossiliferous sedimentary red beds before stopping. These red beds bear a lithologic similarity to Upper Triassic and Lower Jurassic continent-derived sediments in exposed grabens along eastern North America. An immature conglomerate unit in the red beds contains quartz-feldspar lithic fragments and some basalt clasts, which implies a local erosional source of plutonic granitic rocks as well as an older basalt (Gohn, 1983). None of the three holes penetrated beyond the red beds, but seismic-refraction surveys in the area (Ackermann, 1983) indicate a high-velocity basement (~6 km/s) beneath the red-bed sequence at a depth of about 1,200–1,300 m near CC#1.

The sediments above the basalt are all interpreted to be of marine origin, with the exception of the partly continental Cape Fear Formation (Upper Cretaceous), which immediately overlies the basalt, and the mostly continental Middendorf Formation (Upper Cretaceous), which in turn overlies the Cape Fear (Gohn and others, 1977). The top of the Middendorf represents the last pre-Pleistocene fluvial deposition in the area and is an unconformity marked by an abrupt decrease in the sand/clay ratio.

The subsequent marine sediments are Late Cretaceous through Oligocene in age; an unconformity near the surface separates a thin Pleistocene(?) cover from underlying Eocene or Oligocene limestone. The post-Middendorf strata are interpreted as predominately inner-shelf sediments.

STACKING AND INTERVAL VELOCITY DETERMINATION

The velocity functions used to stack the reflection data were determined primarily by comparison of stacked sections produced by using different constant stacking velocities. The velocities obtained in this way were subsequently checked against selected velocity spectra and constant-velocity common-depth-point (CDP) gathers; they generally agree fairly well with only minor differences.

Although there is some variation in the stacking velocities as a function of position along the profiles, these changes are not major. A representative stacking velocity function obtained by analysis of constant velocity stacks (from line 2) is shown in table 2. Also listed are the corresponding interval velocities and depth estimates. At this point on line 2, an event near 0.94 s is the deepest reflection that is reasonably coherent and continuous over large distances; it probably represents the boundary between lower Mesozoic sediments and crystalline basement or an older basalt. The depth to this boundary at this point is approximately 1,400 m. Velocities below about 3.0 s are not well constrained by normal moveout patterns and were to some extent arbitrarily specified on the basis of probable rock types.

An abrupt increase in the stacking velocity occurs at about 0.7 s, as shown in table 2. Two velocity spectra that clearly illustrate the steep change in velocity past 0.7 s are shown in figure 3. The strong peak at 0.7–0.8 s and the subsequent increase in the stacking velocity were also reported by Yantis and others (1983). Drilling, reflection, and refraction data indicate that this velocity jump is caused by an extensive subsurface basalt layer, as discussed below.

The rapid velocity increase from sediments to basalt or other high-velocity rocks could be expected to cause multiple reflections. Strong multiples were observed on constant-velocity stacks for velocities corresponding to the sediments, but the multiples were strongly attenuated when realistic stacking-velocity functions were used. The rapid velocity increase from sediments to crystalline rocks tends to discriminate against these

TABLE 2.—*Representative stacking velocities, interval velocities, and implied depths*

[Data from station 23, line 2]

Time (s)	Stacking velocity (km/s)	Interval velocity (km/s)	Depth below surface (km)
0.00	1.98		0.
		1.98	
.48	1.98		.475
		2.80	
.72	2.29		.811
		5.23	
.84	2.90		1.13
		5.08	
.94	3.20		1.38
		5.87	
3.00	5.18		7.42
		6.51	
9.00	6.10		26.9
		7.24	
12.00	6.40		37.8
		8.17	
20.00	7.16		70.5

sedimentary multiples during stacking. The multiples are undercorrected by the normal moveout for primary reflections and are stacked out of phase; thus they tend to be cancelled. Faint remnants of multiples are sometimes visible in the 1- to 3-s range.

GENERALIZED SEISMIC STRATIGRAPHY

Three conspicuous reflections or groups of reflections can generally be seen throughout the area surveyed. All three are clearest on line 3 (figs. 8, 9) but are present to a varying degree on almost all the profiles. An especially notable and coherent reflection occurs at about 0.7 s (two-way traveltime) on line 1 (fig. 4) and can be easily traced onto the other three lines. The velocities derived from the reflection data imply a depth of approximately 800 m at 0.7 s. Interval velocities increase from about 2.0–3.0 km/s above this horizon to 4.5 km/s or greater below it (see table 2 and fig. 3). Refraction velocities measured from common-source recordings (an individual source recorded by a linear array of recording stations) show a corresponding jump from 1.9–2.3 km/s to 4.5–5.5 km/s at about the same depth. We interpret this event to represent the top of the Jurassic basalt found at 750–770 m depth in the USGS test holes. (The 0.7-s horizon is referred to hereafter as "J," for brevity.) It is generally consistent with a refractor mapped at similar depths by Ackermann (1977, 1983).

This surface may not necessarily be basalt everywhere. The reflection amplitude and character vary considerably, especially along line 2. An interface of upper Cretaceous sediments over Triassic red beds could be present in some areas and could be expected to produce a good reflection. On the other hand, the 250-m thickness of the basalt observed in CC#3 suggests an area that could easily be as large as or larger than the area covered by the COCORP survey. The Watchung Basalt flows of the Newark basin are of comparable thickness (individual flow units 50–100 m thick) and are estimated to have covered an area of 5,000 km^2 (Faust, 1975), corresponding to a radial dimension of the order of 40 km. The Charleston basalts could have a similar or greater extent.

A high-velocity basalt layer between lower velocity sediments could be expected to produce some seismic resonance (constructive interference between reflections from top and bottom). For a thickness of 250 m and a velocity of 5.0 km/s, the first three resonant frequencies are 5, 15, and 25 Hz. Although the first is below the 8–32 Hz sweep, the second and third fall near the center of this range. The effective pulse duration of an 8–32 Hz Klauder wavelet is about 65 milliseconds (ms) (width of central peak plus one side lobe), and the reflection spacing is about 100 ms; thus even a small resonance effect would tend to mask the bottom of the basalt. This may explain the ringing character along some portions of the survey.

Dillon and others (1979, 1983) have reported a very strong reflection beneath the inner Blake Plateau and Continental Shelf offshore from South Carolina. On the basis of its amplitude, high refraction velocity, and proximity to the Clubhouse Crossroads basalt (~80 km), they interpret this event to represent the seaward portion of a regional volcanic layer and estimate its areal extent offshore to be of the order of 100,000 km^2. Dillon and McGinnis (1983) have observed a corresponding strong refractor (5.8–6.3 km/s) on offshore refraction profiles.

At about 0.45–0.55 s, well above the pre-Cretaceous unconformity, a pair of reflections within the Cretaceous section can be clearly traced across all four lines (see figs. 6, 7). The top of the Black Creek Formation (410 m in CC#1) and the unconformity between the Black Creek and Middendorf (560 m in CC#1) are probably the major contributors to this signature. (This reflection pair will be referred to hereafter as "K.")

The third group of conspicuous reflections shows the greatest variation in time (and depth); arrival times range from about 0.85 to 1.05 s (~1,200–1,700 m). Refracted arrivals on common-source playouts show a refraction crossover corresponding to this reflection boundary. The refraction velocities (unreversed) at this crossover increase from around 4.5–5.5 km/s (a refraction along the top of the basalt layer) to 6.0–7.0 km/s (a refraction along the top of an older high-velocity unit beneath the red beds).

This band of reflections is inferred to correspond to a pre-Late Triassic unconformity on crystalline basement, which probably developed considerably prior to the rifting that generated the modern Atlantic Ocean basin. The basement event is referred to hereafter as "B" in the text and figures. There are no drill holes in the immediate vicinity of the reflection profiles deep enough to sample this pre-Mesozoic basement. Numerous wells west and southwest of Savannah, Ga., have penetrated a variety of basement rock types (rhyolite, volcanic ash,

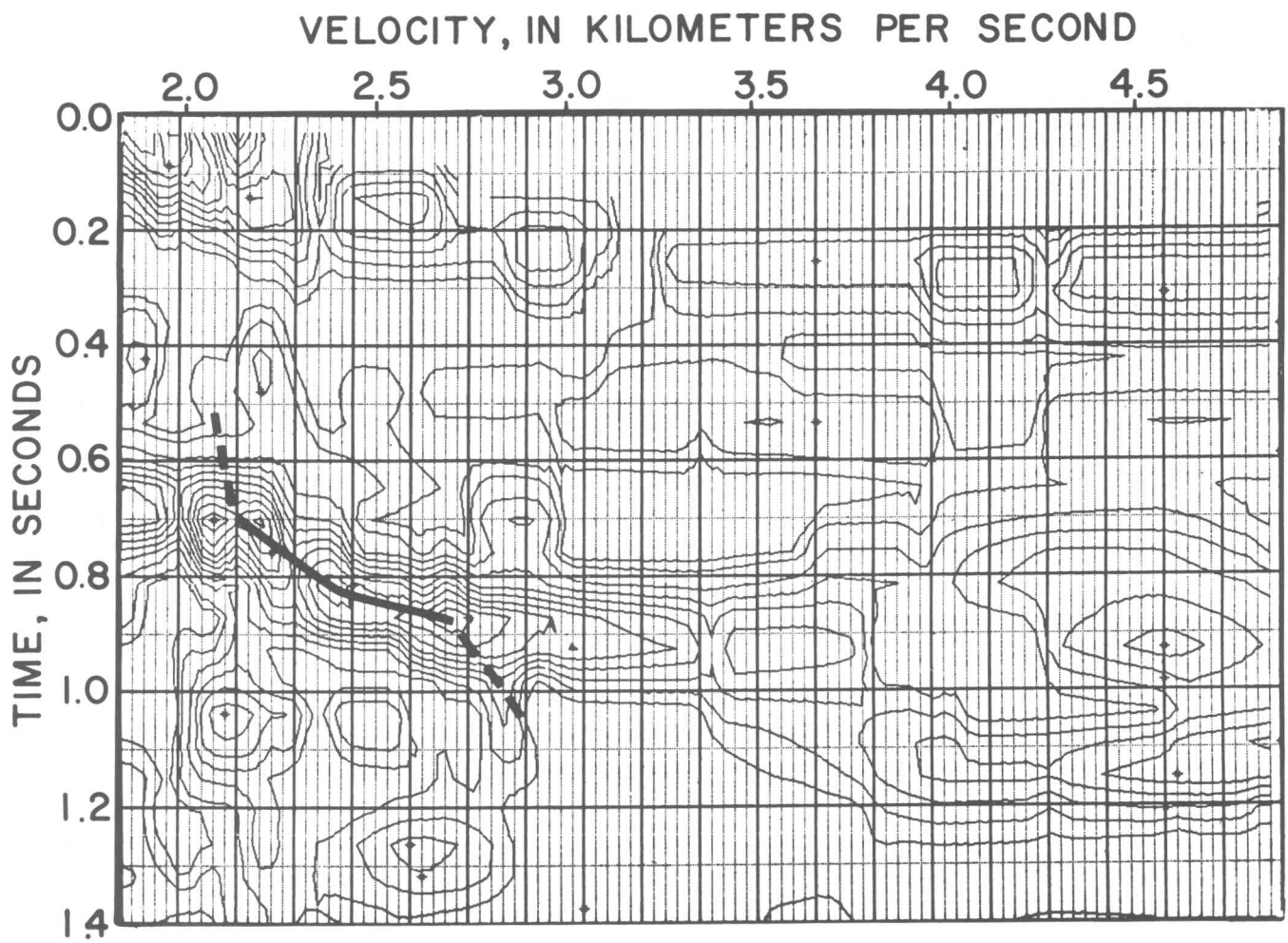

FIGURE 3.—Examples of velocity spectra (stacking velocity against time). *A*, From station 60, line 1. Note rapid increase in velocity below 0.7 s, when basalt layer is encountered. *B*, From station 32, line 3. Reflection peaks occur slightly later, and deeper, than those in *A*.

arkose, granite, diabase, and others) at 1,200–1,400 m depth (Chowns and Williams, 1983). To the north, near the border between North and South Carolina, samples of chlorite schist have been recovered from approximately 400 m depth (Popenoe and Zietz, 1977).

The existence of basalt clasts in the red beds drilled in CC#3 (Gohn and others, 1983) raises the possibility that some of these reflections in the 0.9- to 1.1-s range are from basalt, older than the red beds, which may locally cover still older red beds and (or) a predominantly granitic basement.

SHALLOW FAULTS AND STRATIGRAPHIC VARIATION

Line 1

A line drawing of the seismic section obtained along line 1 and the locations of the adjacent USGS test holes are shown in figure 4. Reflections K and J appear to be offset by about 30 ms between stations 74 and 75, just beyond drill hole CC#2. However, no such feature was observed on USGS reflection profile SC10 (Behrendt and others, 1981), which overlaps COCORP line 1 here. Special reprocessing of this portion of line 1 will be necessary to resolve this question.

The deepest of the three holes (CC#3) ended in red beds at 1,152 m. The drill probably came within 100 m of basement if a reflection segment at 0.89 s near station 50 is interpreted to be basement. If the average velocity of the basalt and red beds is assumed to be 5 km/s, the basement is estimated to occur about 400 m beneath the top of the basalt, or at about 1,170 m total depth. This estimate, of course, depends upon the selected 0.89-s peak in the waveform coinciding with the actual lithologic interface, which interpretation is subject to

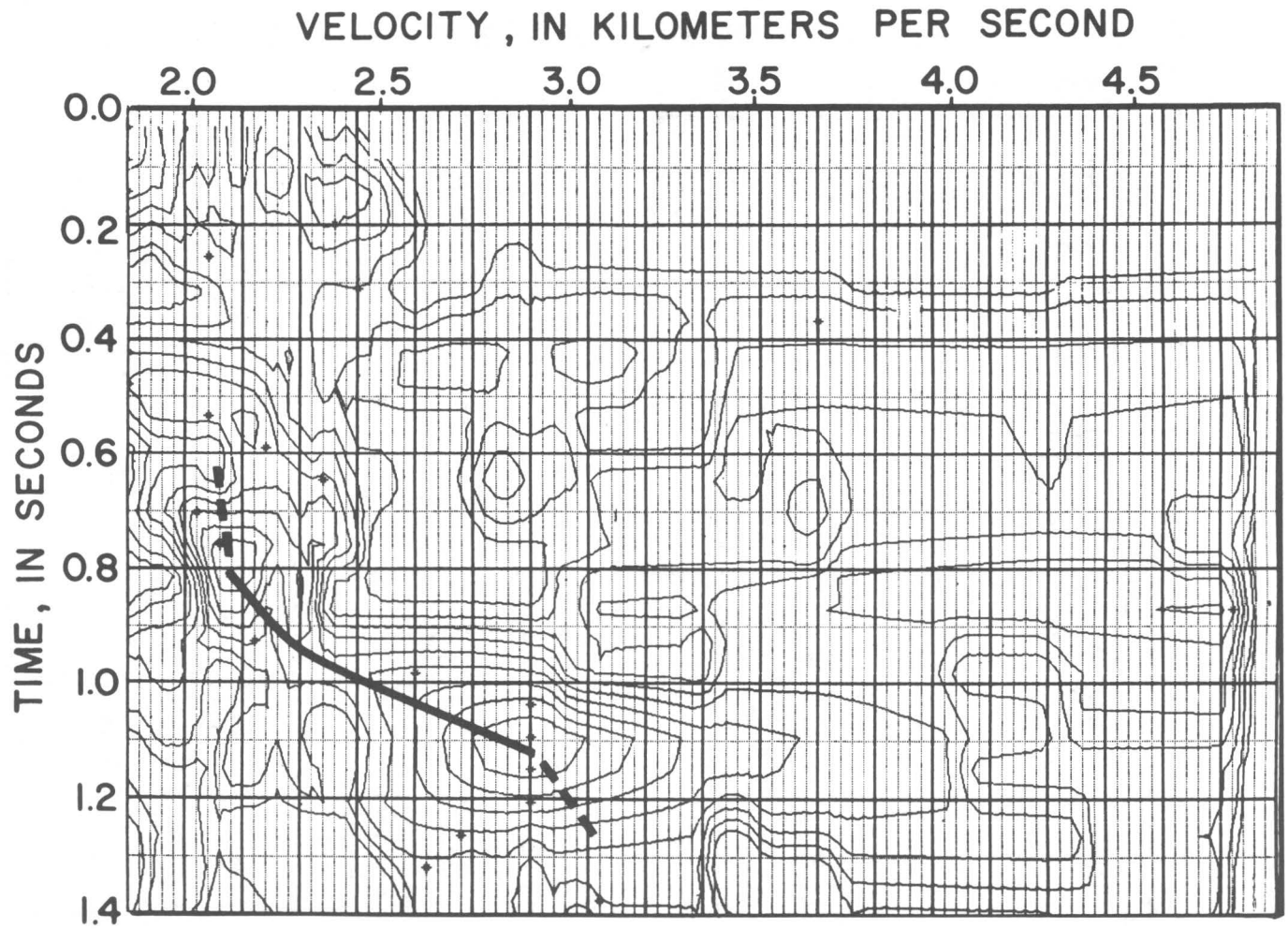

FIGURE 3.—Continued.

uncertainty. However, the estimated depth is consistent with a refraction depth estimate of approximately 1,200 m here (Ackermann, 1983).

All three reflectors, K, J, and B, appear to have very little regional dip along the direction of line 1.

Line 4

Line 4, a north-south line, intersects station 948 of line 1 at station 16 (see fig. 5). Although reflections J and K are still evident, reflection B is not clearly developed, and its discontinuous identification in figure 4 is tentative. Minor irregularities which could be small offsets can be seen along the J horizon but cannot be correlated with breaks in K or B, and thus no faults have been interpreted. As on line 1, the regional dip of these shallow reflectors is very small.

Line 2

Line 2, the longest of the profiles, runs from northwest to southeast and intersects station 177 on line 1 at station 29 (see fig. 6). Much more structural and stratigraphic variation is apparent along lines 2 and 3 than along lines 1 and 4. Lines 2 and 3 do, in fact, cross the northwest-trending seismic zone identified by the South Carolina seismograph net since its installation in 1973 (Tarr, 1977; Tarr and Rhea, 1983).

From stations 5 to 100 on line 2, the three shallow sets of reflections are very similar to the shallow reflections from line 1. Near station 130, however, reflections K and J bow upward slightly into a moderately dipping reverse fault that offsets both horizons (see fig. 7). The basement reflection B cannot be clearly traced through this fault. The offset is approximately 20 ms, which

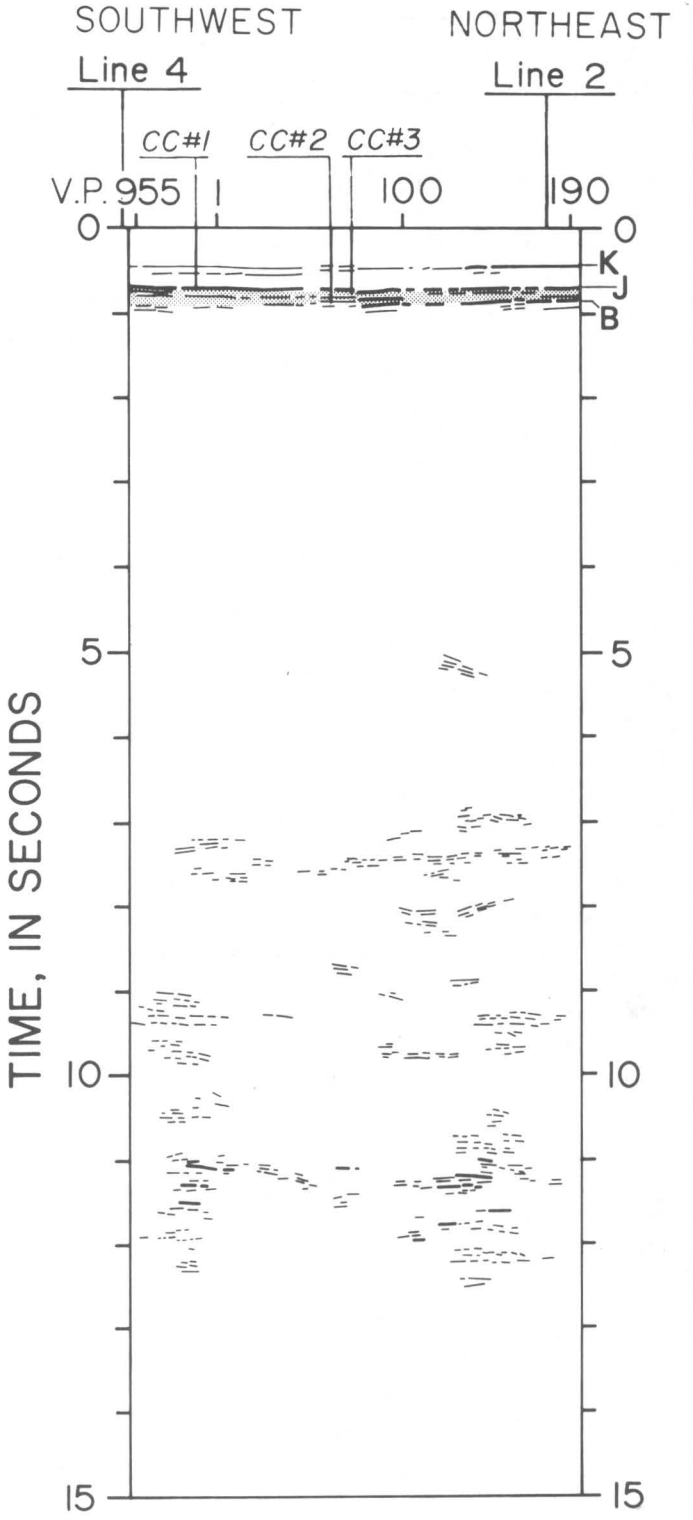

FIGURE 4.—Line drawing of seismic section for line 1, showing the upper 15 s of a 20-s record. Clubhouse Crossroads test holes are projected to line 1. K = reflections near 0.5 s, interpreted to represent reflectors within the Upper Cretaceous Coastal Plain sediments at about 500 m depth. J = reflections near 0.7 s (especially prominent), interpreted to be the top of a Jurassic basalt layer at about 800 m depth, which overlies at least 120 m of red beds (according to USGS drilling results). B = reflections near 1.0 s, inferred to be pre-Mesozoic crystalline basement at 1,200–1,300 m depth. Stippled interval shows inferred basalt layer and underlying Triassic or Jurassic sedimentary rocks.

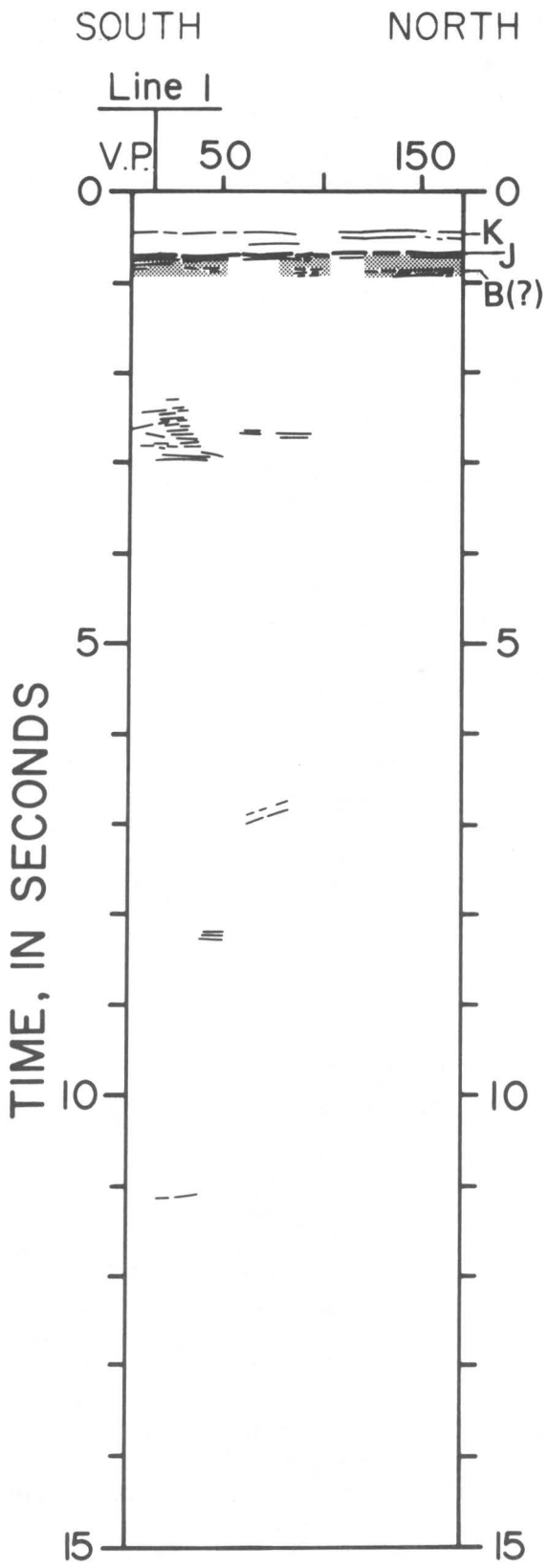

FIGURE 5.—Line drawing of seismic section for line 4. See explanation of figure 4.

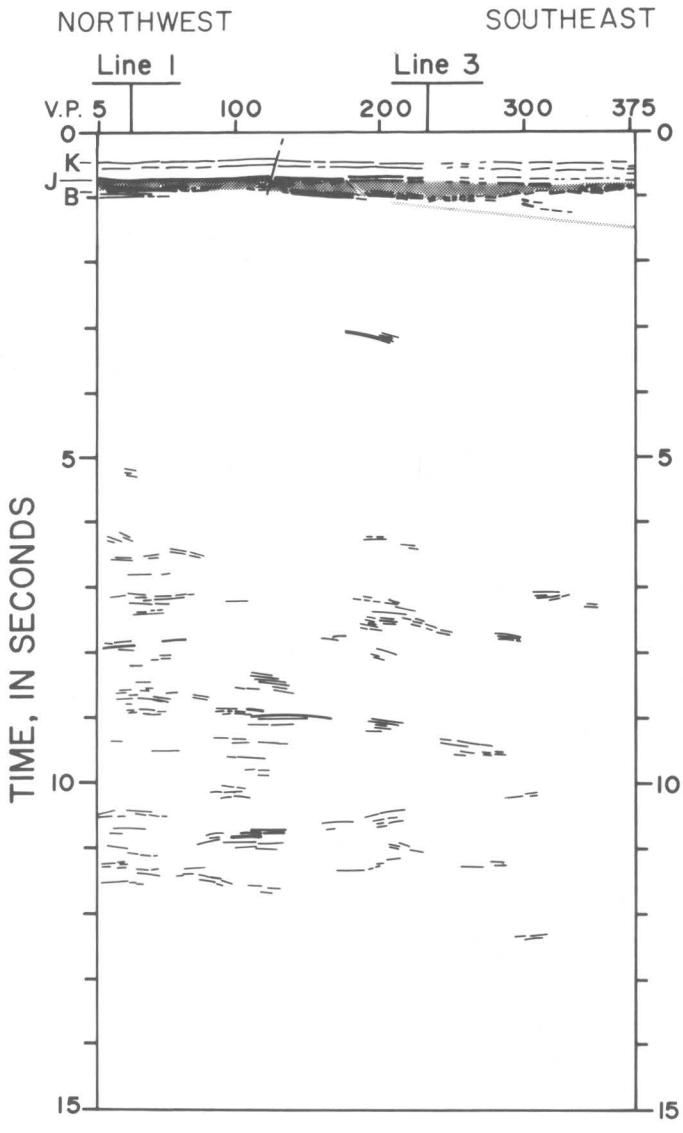

FIGURE 6.—Line drawing of seismic section for line 2. See explanation of figure 4.

implies a displacement of 20–30 m. The angle of dip calculated from the profile (an apparent dip, since the strike of the fault cannot be specified) is 50–60°. Behrendt and others (1981) have correlated this offset with a similar feature on USGS reflection line SC10 and have suggested a northeast strike for the fault, which they have named the Cooke fault. From about station 130 to station 180, all three reflections deepen and dip slightly toward the southeast. The dip is greatest on the basement event B (about 3°), as the estimated depth increases from about 1,200 to 1,400 m.

Continuing southeast beyond this moderate-angle thrust, line 2 passes Middleton Place, located at station 234 and near the center of the 1886 meizoseismal region. Numerous shallow V-shaped gaps from here to the end of line 2 are the result of editing necessitated by noisier data. The shallow reflections from the Upper Cretaceous and younger units may be just as continuous beyond station 230 as before it, but the reflections past station 230 are somewhat weaker and less coherent.

Beyond station 230, the basement reflections appear to become shallower (less than 1.0 s) to the southeast and show an overall dip back toward the northwest. However, refraction studies by Ackermann (1977, 1983) suggest that the basement here is at a depth of approximately 2,000 m, which implies a reflection time of 1.2–1.3 s. This is supported by refraction analysis of first arrivals from a common-source reflection record near the end of line 2. On the basis of these refraction results, the shallower reflections near 1.0 s here probably represent a stratigraphic unit that does not occur in the Clubhouse Crossroads test holes. The velocity of this unidentified unit is not sufficiently great to produce a distinct refracted first arrival on the common-source records. This does not rule out the possibility, however, that these reflections are from a second basalt layer. The presence of such a layer would tend to be masked on refraction records by the uppermost basalt (at 0.7 s two-way traveltime).

A long, gently dipping event is weak but visible below 1.0 s, extending from station 200 (1.0 s) to the end of line 2 (1.5 s); it is shown on the far right of figure 6. It is very planar and might represent the top of the basement here; however, it is much weaker than the basement reflection along the first half of the line. An alternative interpretation is that it is a feature within the basement. This could be a Paleozoic thrust plane developed during the collisional orogenies of the Paleozoic (see discussion below of COCORP Appalachian survey results).

Line 3

Line 3 was designed to cross the seismic zone from southwest to northeast in a more or less orthogonal sense, subject to the constraints of roads and population density. It intersects station 234 on line 2 at station 89 (see fig. 8). Middleton Place is nearly coincident with the intersection of lines 2 and 3. A large gap in the data exists between stations 90 and 135, caused by the Ashley River and its lowlands. The gap is about 3 km wide and divides the line into two segments of different azimuth; south of the Ashley River the line trends southwest-northeast, whereas north of the river it trends north-south.

Reflections K, J, and B are all clearly identifiable over almost all of line 3. There is a noticeable contrast in the apparent structure of the basement reflection B on either side of the gap (figs. 8, 9). To the southwest, the reflections are flat and fairly continuous, showing only minor variations in the reflection waveforms. To the

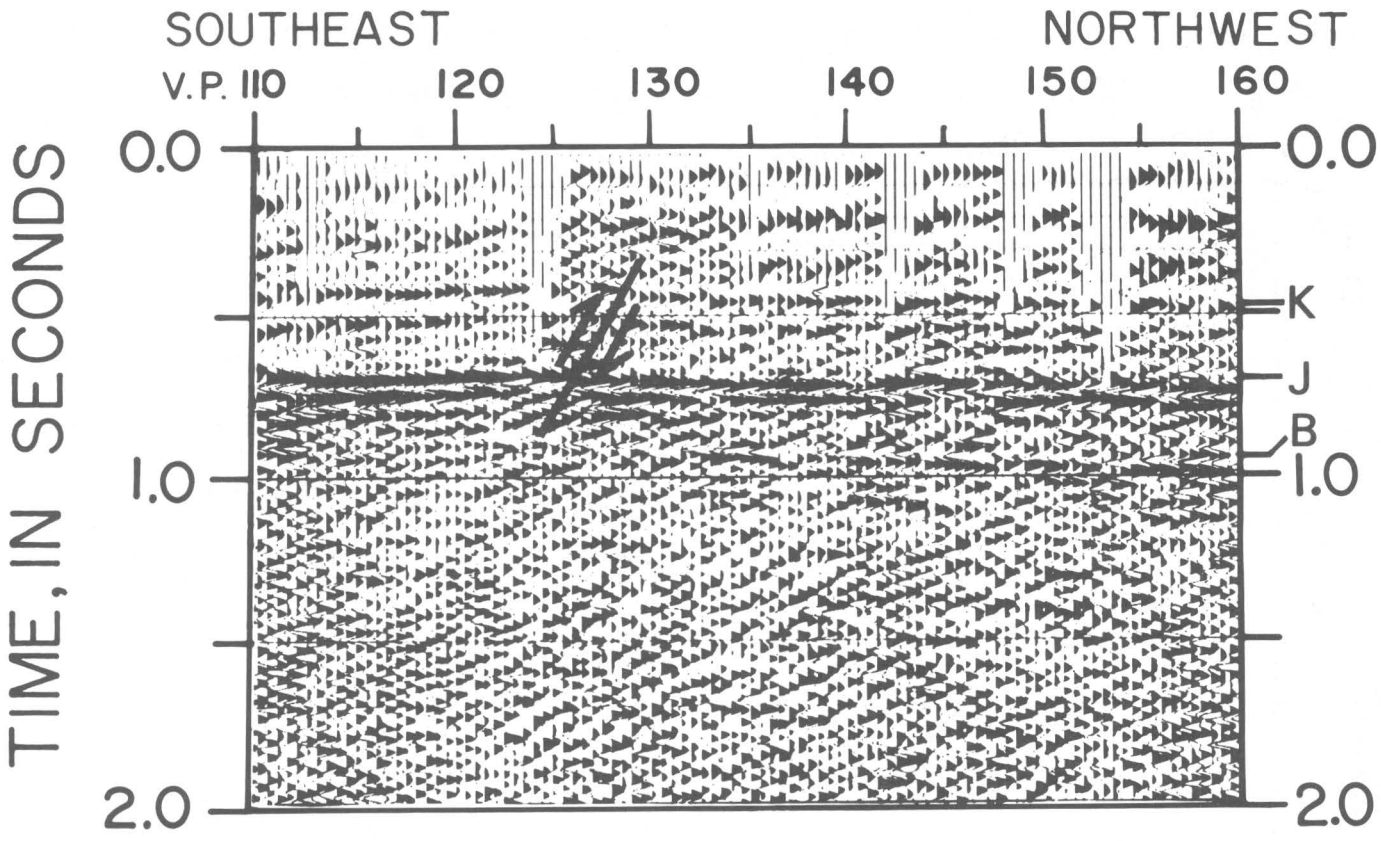

FIGURE 7. – Detail of part of seismic section for line 2, showing reverse fault near station 130. The offset is approximately 20 ms on reflection K, which implies a displacement of 20–30 m.

north, the B horizon is quite variable and discontinuous, showing apparent regional dip to the south of about 3–4°.

The reflections K and J dip downwards near station 160 as they approach the gap and have an apparent dip to the south of about 1°; along the rest of the line they are nearly flat. Thus, although the arrival times of these reflections match across the gap, their apparent dip does not. The difference in dip could result from the two profile segments having slightly different azimuths above southeast-dipping reflectors; however, these events on line 2 show no significant dip as they cross line 3. Alternatively, the dip could be an artifact of a velocity decrease in the overlying sediments, but no such velocity decrease is evident from velocity analyses. (However, velocities above 0.5 s are poorly resolved, as the smallest source-receiver offset is 469 m.)

The arrival time of the basement reflection mismatches by about 0.1 s across the gap. Furthermore, it has a more complex character on the north edge of the gap (fig. 9), and there is an event curving downward away from the gap whose curvature suggests it is a diffraction coming from a discontinuity within the gap.

The mismatch in the local apparent dip of events J and K, the mismatch in arrival time and regional dip of event B, and the possible diffraction suggest structural complexity (perhaps faulting) within the gap. The southeastern cluster of epicenters (Tarr and Rhea, 1983) is locally subparallel to the Ashley River, which is a major drainage system for the region. Perhaps crustal movements associated with the Charleston seismic zone have influenced the drainage pattern.

Another interesting feature of this line is a graben-like offset of the reflection groups between stations 200 and 211. The graben offsets can be traced to the shallowest reflection resolved; that is, the K reflection. This offset pattern is shown in enlargements of a portion of the seismic section for line 3 (figs. 10*A*, 10*B*).

In the graben, reflections J and K are shifted by about 30 ms (~30 m, assuming a velocity of 2.1 km/s). Reflection B shows an asymmetrical offset of about 30 ms near station 200 and about 100 ms near station 209. The asymmetry could be a result of development of the graben along a preexisting basement fault. An abrupt decrease in the velocity of the sediments (possibly due to a buried river channel, for example) overlying reflection K could create the appearance of a graben. Close examination of stacking velocities revealed no such anomaly. However, as stated previously, velocities above 0.5 s are not well constrained, because the angles

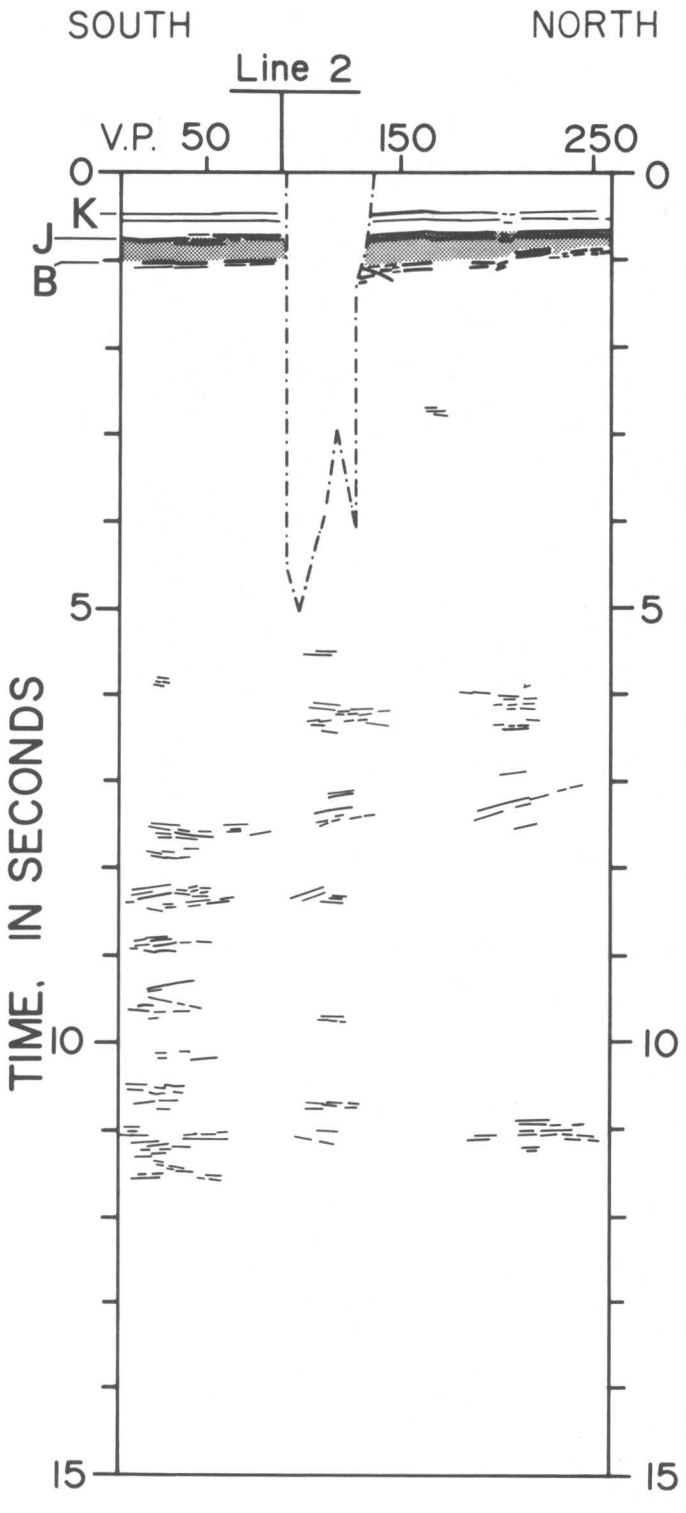

FIGURE 8.—Line drawing of seismic section for line 3. See explanation of figure 4. The large notch between stations 90 and 130 is a data gap caused by the Ashley River, which flows to the Atlantic Ocean through Charleston.

of incidence of these rays become large. If the faults are real, and not the result of a shallow low-velocity region, these suggested normal faults would be at least as young as middle Late Cretaceous.

If the graben feature is an actual structure, it may be genetically related to the 1886 shock; it occurs very near one of the two epicenters designated by Dutton (1889) in his study of intensity patterns (see fig. 1).

Fence Diagram

The reflections and faults discussed above are represented in the fence diagram in figure 11. All faults shown in the fences appear to be distinct from each other; that is, each fault is observed on only one line.

The fences illustrate the relatively smooth and minor variation of the depth to the K and J interfaces. The basement horizon B shows greater variation in its depth, deepening toward the southern half of line 3 (1,500 m) and southeastern end of line 2 (2,300 m) and shallowing towards the northern end of line 3 (1,200 m).

RELATIONSHIP OF FAULTS TO SEISMICITY

No faults have been mapped at the surface within 100 km of the Charleston meizoseismal area (Rankin, 1977). However, three cases of post-Jurassic faults (possibly post-Cretaceous, but the resolution is marginal for strata this shallow) are suggested by the COCORP reflection data: (a) an east-directed reverse (?) fault near station 130 on line 2; (b) two normal faults forming a graben between stations 200 and 211 on line 3; and (c) possible faulting of unknown type near the Ashley River, inferred on the basis of structural differences observed on either side of the river.

All these faults show offsets of a few tens of meters, except (c), which is not directly observed. The offset along (c) could be as much as 200 m. Features (a) and (c) are located within or very near the currently active epicentral zone at Middleton Place (instrumentally located events since 1973), as shown in figure 2. The graben (b) is approximately 5 km northeast of the zone. Items (b) and (c) cannot be unambiguously traced through two different lines, and thus their trends have not been accurately determined.

Tarr (1977) has discussed the recent seismicity near Charleston; he associates instrumentally located events since 1973 with the source volume of the 1886 Charleston earthquake. Tarr and Rhea (1983) identify three clusters of epicenters within this zone. Their hypocenter cross sections and focal mechanisms suggest that most of the current activity is taking place along two near-vertical planes that trend northwest. The sense of motion along the preferred nodal planes is reverse; the fault planes dip nearly vertically or very steeply to the southwest. Hypocentral depths range from about 3 to 13 km for 25 events; six of the best-

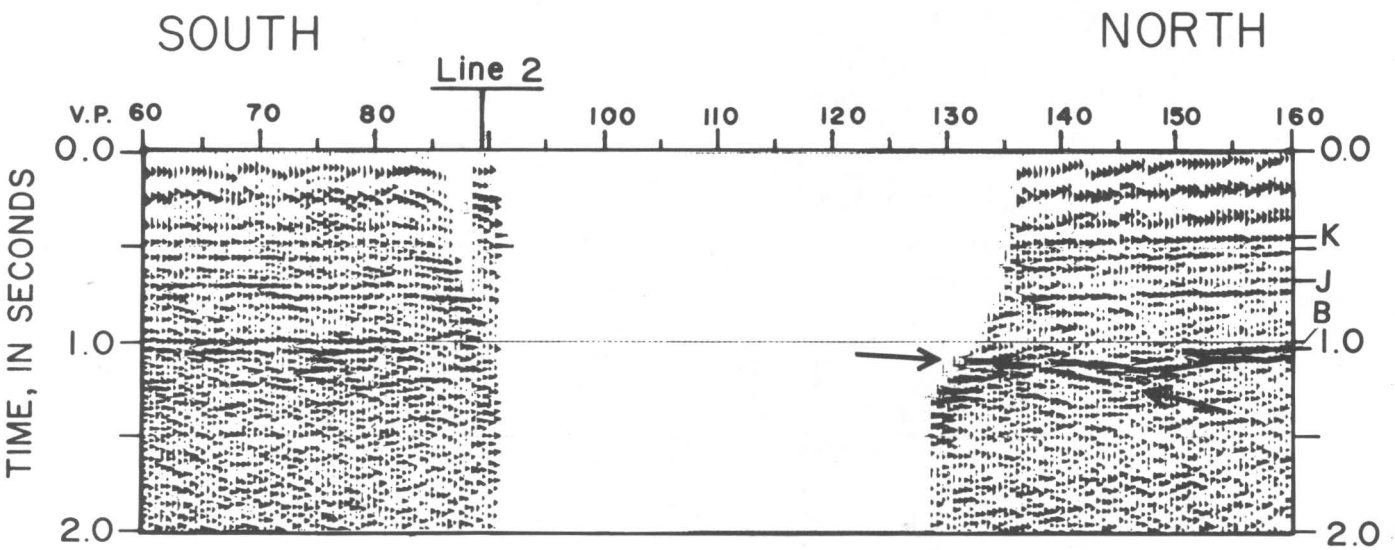

FIGURE 9.—Detail of part of seismic section for line 3 between stations 60 and 160, the region of the data gap caused by the Ashley River. Reflections are more complex near 1.0 s (labelled B) at the north end of the gap than they are at the south end. Arrows indicate diffraction coming from within the gap.

located events in the Middleton Place cluster fall between 4 and 8 km.

Other investigations (Amick and Talwani, 1979; Amick, 1979) that use a refined crustal model have suggested a northwest-trending seismic zone. Their composite focal plane solution suggests a northwest-trending thrust fault (N. 58° W.), with a southwesterly dip (50° SW.). Hypocentral depths, constrained by a seismograph station in operation since 1977 at Middleton Place, are greater than 5 km.

The reverse fault near station 130 on line 2 of the COCORP profiles apparently trends northeast (Behrendt and others, 1981) and thus cannot be readily associated with the main pattern of current seismicity. In addition, seismic slip confined to the upper few kilometers would not be consistent with hypocentral depths below 4 km, although the fault on line 2 could extend deeper than is evident from the reflection data.

Alternatively, the inferred faulting beneath the Ashley River may be the primary zone in which seismicity is occurring. The sense of basement relief there (higher on the southwest side of the gap; see figs. 8, 9) is also consistent with a northwest-trending, southwest-dipping thrust fault. The depth to which such faulting could extend is not well determined by line 3, owing to the depth of the gap. The gap (fig. 8) extends to below 3 s, which corresponds to a depth greater than 7 km.

If the major earthquake fault zone is not a low-angle thrust, some simple speculations on earthquake frequency are possible. Because near-surface faulting is relatively minor (~10–100 m, this study; Behrendt and others, 1981), earthquakes of the size of the 1886 event (magnitude ~7, slip ~1 m; Bollinger, 1983) may have been infrequent in the past. If the seismic zone has been active along a dip-slip fault of moderate to steep dip for the last million years or more, the recurrence interval for major events is of the order of 10,000 years or more. If such events occurred more often during that length of time, they would have resulted in vertical fault movements greater than any presently observed. On the other hand, if seismic slip began as recently as 20,000 years ago, such earthquakes could be as frequent as every 200 years.

If a major fault associated with the large 1886 event is of the order of 10 km deep, then the degree of surface faulting is indirect and less conclusive evidence for constraining earthquake frequency. However, it is difficult to postulate large accumulated displacement on a dip-slip fault at mid-crustal depth that does not have major effects near the surface, which are not observed along these profiles.

Behrendt and others (1983) interpret a major horizontal surface offshore at considerable depth (~10–13 km), on the basis of multichannel reflection profiles near Charleston. They postulate a regional horizontal fault along a décollement as a possible source zone of the seismicity near Charleston. The pattern of recent seismicity does not strongly support this hypothesis, although it does not completely disallow it, as discussed by Behrendt and others (1983). Whether or not the discontinuity is seismically active, it might be an extension of the large-scale Appalachian overthrusts reported by Cook and others (1979), but the connection must be regarded as uncertain. The possibility that the

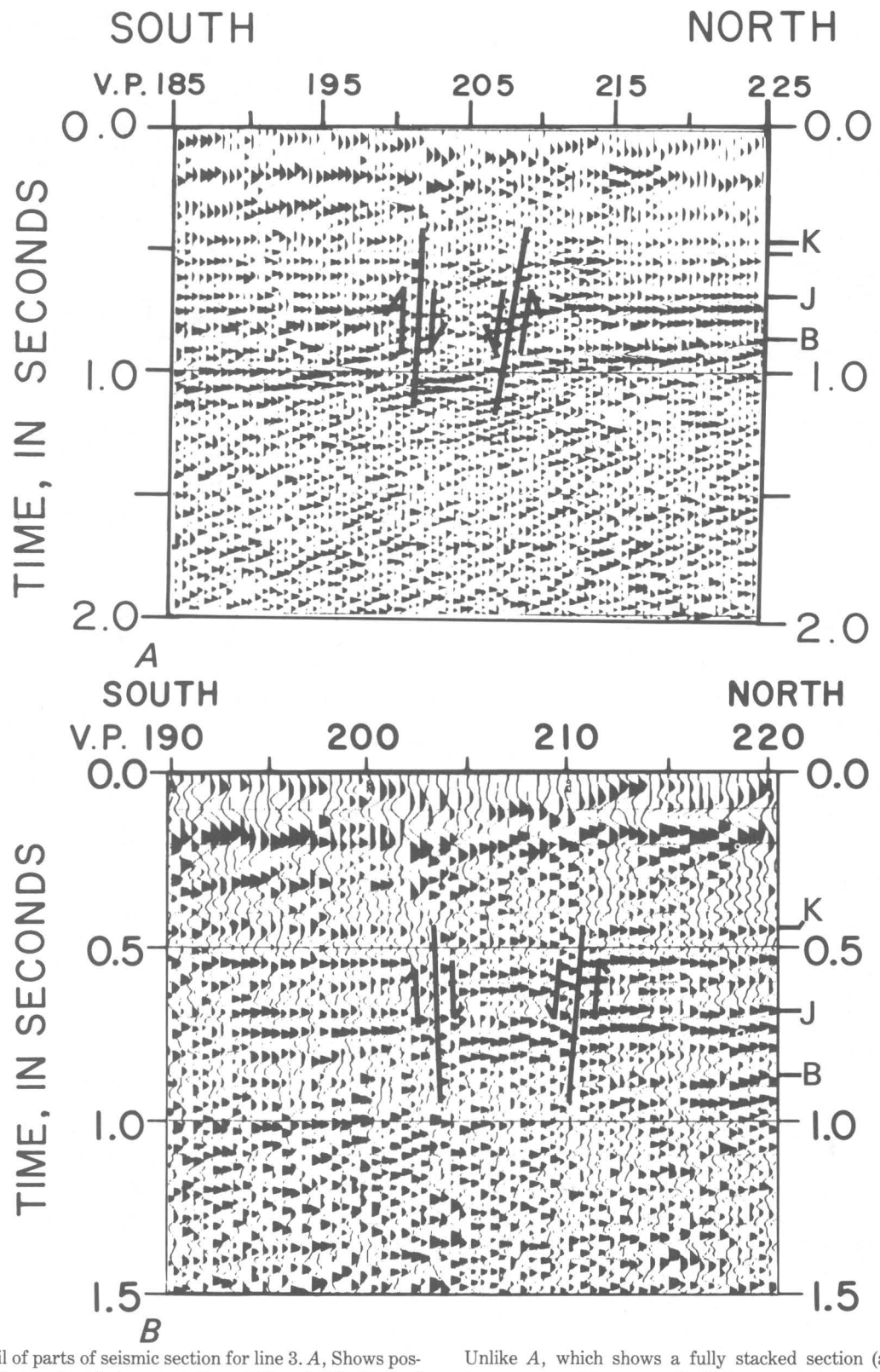

FIGURE 10.—Detail of parts of seismic section for line 3. *A*, Shows possible fault-bounded graben between stations 200 and 210. Normal stack shows paired offsets of basement reflection B. The overlying reflections K and J are also affected but cannot be clearly followed. *B*, Shows possible fault-bounded graben between stations 200 and 210. Reduced stack shows the same area as *A* at a larger scale. Unlike *A*, which shows a fully stacked section (as many seismic traces as possible are used), *B* shows a stack in which only the four traces nearest to each source have been included in the stack. This restricted stack allows the reflections K and J to be traced across the offsets. It does not show reflection B as clearly as does the complete stack, however.

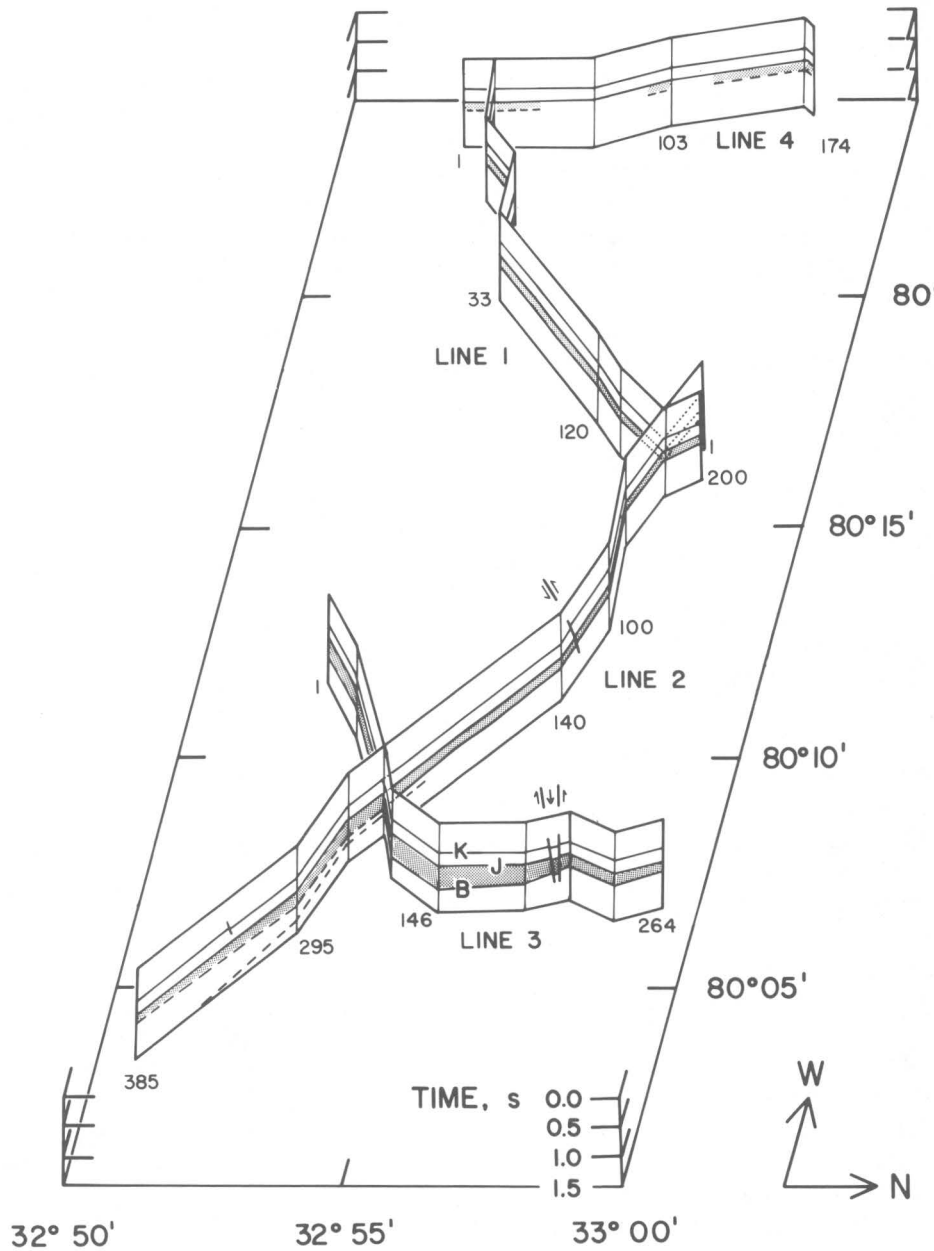

FIGURE 11.—Fence diagram representing reflections and faults from 0.0 to 1.5 s (two-way traveltime). The letters K, J, and B are defined in figure 4. Reflections are dashed where continuity is uncertain.

Appalachian overthrust extends beneath South Carolina is discussed below.

Wentworth and Mergner-Keefer (1983) argue that the 1886 event occurred along a high-angle, northeast-trending reverse fault like the Cooke fault. They emphasize the regional geological evidence for such faulting along the Eastern United States and suggest that the seismicity since the 1886 earthquake has occurred mostly along subsidiary northwest-trending structures. Seeber and Armbruster (1980) hypothesize that the 1886 Charleston earthquake occurred on a shallow-dipping detachment.

Until specific earthquakes can be pinned to specific faults, none of the alternative models are compelling. Additional high-resolution reflection data that cover the epicentral area more completely and uniformly might help to discriminate these hypotheses but, for logistical reasons, may be very difficult to obtain.

STRESS MEASUREMENTS

Stress measurements have been made by means of the hydrofracture technique in sediments at 200–400 m depth in CC#2 and CC#3 (Zoback and others, 1978).

Values for the least principal stress were found to be considerably sublithostatic, perhaps sufficient to activate normal-type fault motion on favorably oriented faults. The azimuth of the hydrofractures suggests relative horizontal extension in a northeast-southwest direction, favoring normal displacement on faults striking northwest. Unfortunately, the trend of the normal faults on line 3 has not been determined. Nothing in the reflection data is inconsistent with a northwest trend for these faults, however.

The existence of normal (b) and reverse (a, c?) faulting in the same region suggests that not all of these faults were formed as a direct result of contemporaneous tectonic stress and that at least some of these reflect adjustments on preexisting faults or zones of weakness. The importance of preexisting zones of weakness for the origin of the Charleston seismic zone has been emphasized by many workers (Bollinger, 1972; Fletcher and others, 1978; Sykes, 1978; Nishenko and Sykes, 1979; Behrendt and others, 1981; Tarr and Rhea, 1983). Amick (1979) points out that the lack of agreement between the stress measurements and the composite focal mechanism may be reconciled by the >5-km depth of the earthquake. If this is the case, the small faults seen at the surface in the reflection data may be minor surficial adjustments to a more deep-seated and intense compressional stress regime in the upper middle crust.

Turcotte and others (1977) suggest that stresses associated with the cooling and subsidence of the oceanic lithosphere and subsequent sedimentary loading may be responsible for the seismicity along the eastern continental margin of the United States. From such a model, one would expect high-angle displacements along faults trending parallel to the margin, rather than the northwest trend suggested by either the stress measurements (normal) or the hypocentral pattern (reverse; Tarr and Rhea, 1983; Amick, 1979). Behrendt and others (1981) identify fault (a) as trending northeast, but the reflector offsets indicate reverse motion, which implies possible reactivation of a Triassic normal fault by a later stress field. Obviously, further work is necessary to resolve better the patterns of shallow faulting and to determine their relationship to stress and seismicity.

RELATIONSHIP OF PROFILES TO GRAVITY AND MAGNETIC DATA

Detailed gravity and aeromagnetic surveys have been made of the Coastal Plain of South Carolina and Georgia, and these indicate that the crust beneath Charleston is considerably different in structure and composition from that exposed in the nearby Piedmont to the northwest (Popenoe and Zietz, 1977; Daniels and others, 1983). In the vicinity of Charleston, both gravity and magnetic data show a broad-wavelength, east-west-trending low between 33° and 33°15′ N., flanked on both sides by complementary regional highs (fig. 2). Superimposed on these regional magnetic and gravity highs are numerous shorter wavelength magnetic highs having magnitudes as high as 650 nT. This pattern of narrow highs on broad ones has been attributed to mafic plutons beneath extensive basalt flows in a rift setting; the broad central low may indicate a down-dropped crustal block flanked by uplifted horsts.

The COCORP profiles and USGS test holes are situated over the regional high just south of the prominent east-west low near 33° N. The strongest gravity and magnetic high in the region occurs at the site of CC#1 (see figs. 2, 4).

The southwestern end of line 1 and the southern end of line 4 converge over this most prominent magnetic high but show few reflections that can be clearly interpreted as the source region for the anomaly. Southwest of station 50 on line 1 are some dipping events whose relatively constant dip, occurrence in successive trains, and sense of dip (away from the source) suggest they are source-generated noise (for example, surface waves, guided waves, and reflected refractions). Similar wave trains having the same dip occur north of station 100 on line 4, dipping towards the south (again, dipping away from the source).

On line 4, there is a cluster of reflections from 2.3 to 3.0 s near station 30. Depths of 4.7–6.5 km are implied by these times, which are probably too deep for these reflections to represent the source of the observed magnetic high (Phillips, 1977). They could, however, be reflections caused by cumulate-type layering near the base of a mafic intrusive body. Few reflections can be seen on line 1 (the cross line in that area), but this might be due to structural asymmetry.

Other magnetic highs occur near the junction of lines 1 and 2 (~300 nT), near stations 300–350 on line 2 (~300 nT), and near stations 200–220 on line 3 (~500 nT). These have no clear seismic expression. Some possible explanations which come to mind are

(1) The primary magnetic sources are shallow basalt flows.
(2) The mafic plutons are difficult to detect seismically because the impedance contrast between the crystalline host rock and the intruded rock is small.
(3) The top of the pluton is coplanar with the top of the crystalline basement, and its sides are too steep to reflect energy.

The first explanation is not consistent with a study of the depth to magnetic sources made by Phillips (1977). His study suggests that most of the power in the anomalies is produced by strongly magnetized sources (interpreted to be mafic intrusive bodies) at depths of

2–4.5 km. Furthermore, thin, extensive basalt flows do not explain the strong gravity peak near CC#1. Thus, some combination of explanations (2) and (3) is more reasonable.

DEEP STRUCTURE

From about 1.5 to 6.0 s, little coherent energy is present on the reflection profiles. Exceptions are the clusters of events at the southern end of line 4 near 3.0 s, discussed previously, and an isolated event at 3.0 s near station 200 on line 2. This zone is apparently a relatively transparent one; many scattered short reflections are present on lines 1–3 from about 6.0–12.0 s. (Line 4 shows a few reflections below 3.0 s, but it seems to have a significantly lower signal-to-noise ratio than the other lines, as suggested by its poorer definition of shallow events.)

The strongest deep reflection occurs at 9.0 s from stations 105 to 165 along line 2 (see fig. 12). Assuming a mean crustal velocity of 6 km/s, the depth is approximately 27 km. The event consists of only two cycles, which implies a rather sharp impedance contrast very deep within the crust. There is no cross line here, so if the reflection were outside the plane of the profile, it might be somewhat shallower. The apparent depth is probably too shallow for this event to represent the Moho discontinuity, since a refraction survey in the central Piedmont of Georgia and South Carolina obtained a crustal thickness of 33 km (Kean and Long, 1978). Furthermore, there is a deeper group of reflections near 11.0–11.5 s (~33–35 km) (fig. 11), which we interpret as the base of the crust on the basis of the agreement with this refraction estimate. The short, discontinuous reflections disappear rather quickly past 11.5–12.0 s. Similar observations of reflections in this time range have been made from USGS multichannel reflection profiles along the eastern Continental Shelf and margin (Hutchinson and Grow, 1979). They interpreted reflections between 9 and 12 s (many in the 10–11 s range) in the area of the Long Island Platform as representing the Moho at depths of 30 to 35 km.

Zones of no reflections in the shallow crust overlying deeper zones having numerous short, discontinuous reflection segments have also been observed on COCORP profiles in the Rio Grande Rift (Brown and others, 1979) and along the northwestern portion of COCORP profiles in the Wind River Basin (Brewer and others, 1980). Brown and others (1979) have suggested that the transparent zones observed on the Rio Grande Rift profiles may indicate homogeneous plutons (granitic) emplaced in the upper crust, and a similar interpretation may apply here.

POSSIBLE RELATIONSHIP TO COCORP SOUTHERN APPALACHIAN TRAVERSE

COCORP surveys across parts of Tennessee, North Carolina, and Georgia have shown that the crystalline rocks of the southern Appalachians constitute an allochthonous thrust sheet 6 to 15 km thick, which thickens to the southeast (Cook and others, 1979). The thrust wedge is interpreted to have moved at least 260 km westward over relatively undisturbed lower Paleozoic sedimentary rocks of the proto-Atlantic continental margin. The thrust plane has been traced as far eastward as the Carolina slate belt near the Coastal Plain overlap in Georgia. Harris and Bayer (1979) have made a palinspastic reconstruction of a cross section across Virginia and North Carolina that is consistent with the crustal shortening proposed by Cook and others (1979). Harris and Bayer (1979) further interpret deep reflections present on USGS marine seismic-reflection profiles near Cape Lookout and Cape Fear as a continuation of the thrust observed on the COCORP Appalachian traverse beneath the Continental Shelf; they postulate a detachment zone consisting of imbricate thrusts at two-way traveltimes of 8.0–11.0 s.

The extension of the fault surface beneath the present continental margin would imply a minimum displacement much greater than that which Cook and others (1979) have interpreted on the basis of the present reflection data. In any case, one might expect to observe similar features in the COCORP lines near Charleston.

In the absence of continuous deep seismic-reflection data from the southeastern end of the Appalachian lines to Charleston, this extrapolation of the southern Appalachian thrust system must be regarded as speculative at this time. However, it is conceivable that some of the events below 6 s (for example, the event near 9 s on Charleston line 2) could occur along such a regional shear zone, and the overall seismic character can be construed as being consistent with the southern Appalachian structure as described by Cook and others (1979).

As discussed earlier, Behrendt and others (1983) have observed a marked seismic discontinuity at 3–4 s (10–13 km) just offshore from Charleston. This surface, which is defined by the tops of several diffractions, is interpreted as a décollement extending landward and projecting into the Charleston seismic zone. No clearly similar group of events in this depth range is evident in the Charleston COCORP data, although there are a few widely scattered returns.

The strength of the reflections defining the Appalachian overthrust (Cook and others, 1979) varies considerably, so it is possible that the reflection strength of

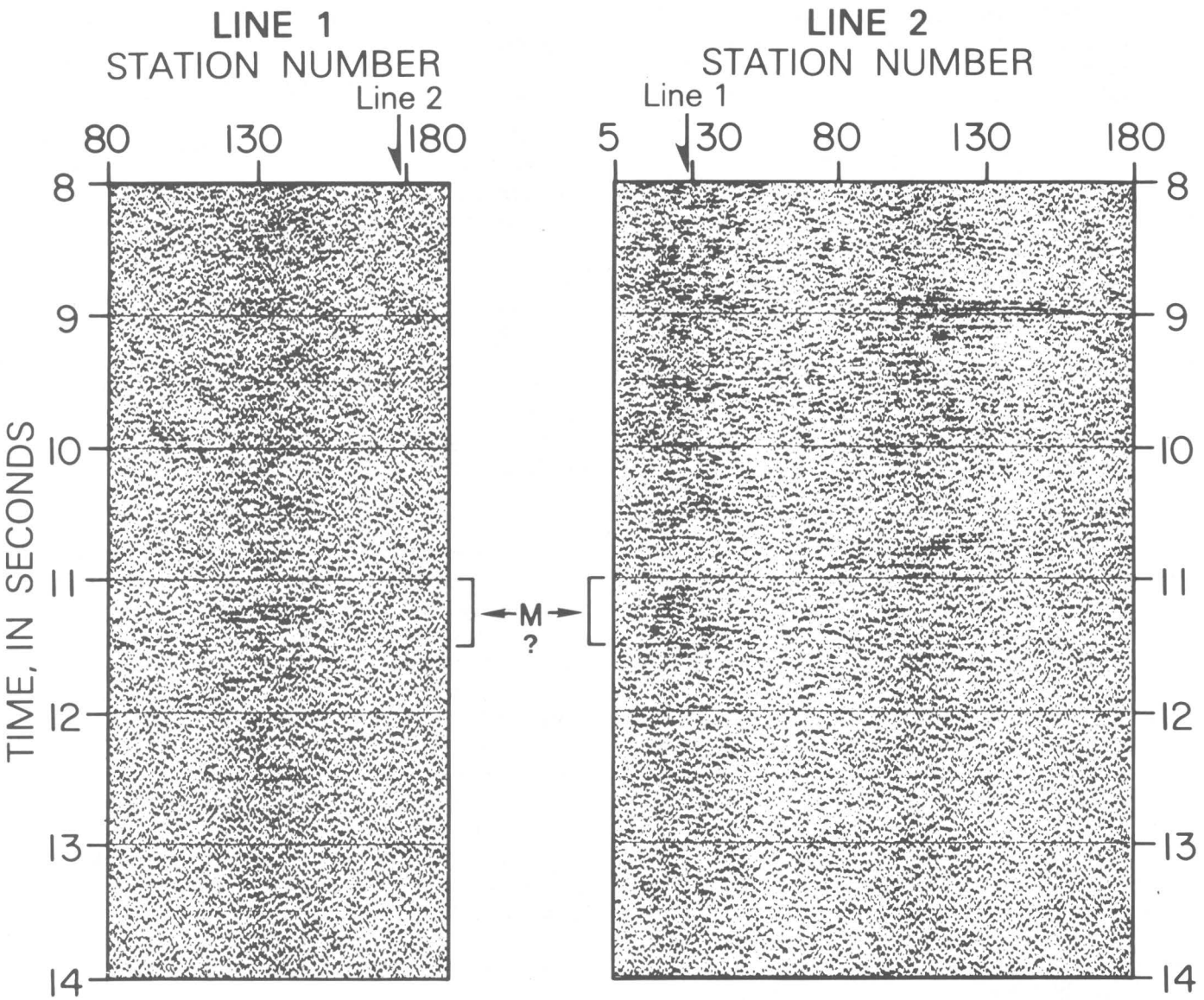

FIGURE 12. – Detail of seismic sections for lines 1 and 2, showing strong reflection at 9.0 s. The reflections near 11.0 s are interpreted as the Moho (M) or crust-mantle transition zone.

this boundary is less beneath the Charleston lines. It is also possible that the marine data are of somewhat better quality than are the land data. A third possibility is that the reflections near 6 s on the Charleston COCORP lines correlate with the 3- to 4-s events offshore, although this would require major relief on the surface over the relatively short distance between the two surveys.

New COCORP Appalachian data in central and southeastern Georgia indicate that the overthrust tectonic pattern is also present there (Cook and others, 1981). The depth to the top of the sediments in southeastern Georgia is variable but is of the order of 10–15 km.

POSSIBLE RELATIONSHIP OF CHARLESTON COCORP DATA TO CONDUCTIVITY STRUCTURE

Edwards and Greenhouse (1975) studied temporal variations in the geomagnetic field along an Appalachian profile extending from the Chesapeake Bay into northern West Virginia. Their data show a surprisingly small geomagnetic "coast effect" and appear to require anomalously low conductivity in the lower crust, especially under the eastern half of their profile. Although the modeling results are nonunique, Edwards and Greenhouse (1975) point out that their results might be explained by the presence of water at considerable depths within the crust.

If the upper crust beneath Charleston is in fact allochthonous with respect to the lower crust, some or most of the numerous reflections from 6–10 s (~18–30 km) might be from water-rich metasedimentary layers pushed tens of kilometers downward as an allochthonous wedge was driven over them. More extensive and detailed conductivity surveys would be of considerable interest to see if these results can be verified at other sites along the Eastern United States.

CONCLUSIONS

Seismic-reflection profiling in the Coastal Plain near Charleston, S. C., has delineated the regional Mesozoic and younger stratigraphy there and has identified faults in these units. Both normal and reverse faults appear to have been active late in the Cretaceous or Tertiary(?), causing displacements of a few tens of meters. Although it cannot be conclusively stated whether any of these faults is responsible for the 1886 Charleston earthquake or the seismicity currently being monitored, at least some of the post-Jurassic faults may be related to the seismicity. The relatively small offsets on these faults suggest either that events the size of the 1886 earthquake have been infrequent, unless the Charleston seismicity developed just a few tens of thousands of years ago, or that the earthquakes are not related to these faults. Additional shallow, higher resolution seismic profiling was undertaken by the USGS and Nuclear Regulatory Commission in light of the COCORP results (Behrendt and others, 1981).

Many deep reflections were recorded by COCORP, most of which occurred in the lower crust (~18–36 km). There appears to be a pronounced difference in the reflectivities of the upper and lower crust. The upper crust is rather featureless at these frequencies (8–32 Hz), whereas the lower crust shows a complex pattern of short, discontinuous reflections not unlike portions of seismic records from other COCORP sites. Some of the reflections from the lower crust may be from metasedimentary rocks deeply buried by Appalachian thrusting (Cook and others, 1979, 1981), a hypothesis that might also help to explain anomalously high conductivity in the lower crust along the Atlantic margin.

A group of deep reflections was observed at 10.5–11.5 s (~33 km); they appear to be more coherent than surrounding events and are postulated to represent reflected energy from the crust-mantle boundary or transition zone. This interpretation is based on compatibility with a nearby refraction profile and supplemented by observations of reflections at similar times on USGS offshore multichannel seismic profiles.

REFERENCES

Ackermann, H. D., 1977, Exploring the Charleston, South Carolina earthquake area with seismic refraction–A preliminary study, *in* Rankin, D. W., ed., Studies related to the Charleston, South Carolina, earthquake of 1886–A preliminary report: U.S. Geological Survey Professional Paper 1028, p. 167–175.

———1983, Seismic-refraction study in the area of the Charleston, South Carolina, 1886 earthquake, *in* Gohn, G. S., ed., Studies related to the Charleston, South Carolina, earthquake of 1886–Tectonics and seismicity: U.S. Geological Survey Professional Paper 1313, p. F1–F20.

Amick, David, 1979, Crustal structure studies in the South Carolina coastal plain: Columbia, University of South Carolina, M.Sc. Thesis, 81 p.

Amick, David, and Talwani, Pradeep, 1979, An examination of Charleston-Summerville seismicity utilizing a new velocity model [abs.]: 74th Annual Meeting of the Seismological Society of America, Golden, Colorado, May 21–23, 1979, p. 18–19.

Behrendt, J. C., Hamilton, R. M., Ackermann, H. D., and Henry, V. J., 1981, Cenozoic faulting in the vicinity of the Charleston, South Carolina, 1886 earthquake zone: Geology, v. 9, no. 3, p. 117–122.

Behrendt, J. C., Hamilton, R. M., Ackermann, H. D., Henry, V. J., and Bayer, K. C., 1983, Marine multichannel seismic-reflection evidence for Cenozoic faulting and deep crustal structure near Charleston, South Carolina, *in* Gohn, G. S., ed., Studies related to the Charleston, South Carolina, earthquake of 1886–Tectonics and seismicity: U.S. Geological Survey Professional Paper 1313, p. J1–J29.

Bollinger, G. A., 1972, Historical and recent seismic activity in South Carolina: Seismological Society of America Bulletin, v. 62, p. 851–864.

———1977, Reinterpretation of the intensity data for the 1886 Charleston, South Carolina earthquake, *in* Rankin, D. W., ed., Studies related to the Charleston, South Carolina, earthquake of 1886–A preliminary report: U.S. Geological Survey Professional Paper 1028, p. 17–32.

———1983, Speculations on the nature of seismicity at Charleston, South Carolina, *in* Gohn, G. S., ed., Studies related to the Charleston, South Carolina, earthquake of 1886–Tectonics and seismicity: U.S. Geological Survey Professional Paper 1313, p. T1–T11.

Brewer, J. A., and Oliver, J. E., 1980, Seismic reflection studies of deep crustal structure: Annual Review of Earth and Planetary Sciences, v. 8, p. 205–230.

Brewer, J. A., Smithson, S. B., Oliver, J. E., Kaufman, Sidney, and Brown, L. D., 1980, The Laramide orogeny: Evidence from COCORP deep crustal reflection profiles in the Wind River Mountains, Wyoming: Tectonophysics, v. 62, no. 3–4, p. 165–189.

Brown, L. D., Chapin, C. E., Sanford, A. R., Kaufman, Sidney, and Oliver, J. E., 1979, Deep structure of the Rio Grande Rift from seismic reflection profiling, *in* Riecker, R. E., ed., Rio Grande Rift: Tectonism and magmatism: American Geophysical Union Special Publication, p. 169–184.

Chowns, T. M., and Williams, C. T., 1983, Pre-Cretaceous rocks beneath the Georgia Coastal Plain–Regional implications, *in* Gohn, G. S., ed., Studies related to the Charleston, South Carolina, earthquake of 1886–Tectonics and seismicity: U.S. Geological Survey Professional Paper 1313, p. L1–L42.

Cook, F. A., Albaugh, D. S., Brown, L. D., Kaufman, Sidney, Oliver, J. E., and Hatcher, R. D., Jr., 1979, Thin-skinned tectonics in the crystalline southern Appalachians; COCORP seismic-reflection profiling of the Blue Ridge and Piedmont: Geology, v. 7, no. 12, p. 563–567.

Cook, F. A., Brown, L. D., Kaufman, Sidney, Oliver, J. E., and Petersen, T. A., 1981, COCORP seismic profiling of the Appalachian Orogen beneath the Coastal Plain of Georgia: Geological Society of America Bulletin, v. 92, p. 738–748.

Daniels, D. L., Zietz, Isidore, and Popoenoe, Peter, 1983, Distribution of subsurface lower Mesozoic rocks in the Southeastern United States as interpreted from regional aeromagnetic and gravity maps, *in* Gohn, G. S., ed., Studies related to the Charleston, South Carolina, earthquake of 1886–Tectonics and seismicity: U.S. Geological Survey Professional Paper 1313, p. K1–K24.

Dillon, W. P., Paull, C. K., Buffler, R. T., and Fail, J. P., 1979, Structure and development of the Southeast Georgia Embayment and Northern Blake Plateau–Preliminary analysis, *in* Watkins, J. S., Montadert, Lucien, and Dickerson, P. W., eds., Geological and geophysical investigations of continental margins: American Association of Petroleum Geologists Memoir 29, p. 27–41.

Dillon, W. P., Klitgord, K. D., and Paull, C. K., 1983, Mesozoic development and structure of the continental margin off South Carolina, *in* Gohn, G. S., ed., Studies related to the Charleston, South Carolina, earthquake of 1886–Tectonics and seismicity: U.S. Geological Survey Professional Paper 1313, p. N1–N16.

Dillon, W. P., and McGinnis, L. D., 1983, Basement structure indicated by seismic-refraction measurements offshore from South Carolina and adjacent areas, *in* Gohn, G. S., ed., Studies related to the Charleston, South Carolina, earthquake of 1886–Tectonics and seismicity: U.S. Geological Survey Professional Paper 1313, p. O1–O7.

Dutton, C. E., 1889, The Charleston earthquake of August 31, 1886: U.S. Geological Survey Ninth Annual Report, p. 203–528.

Edwards, R. N., and Greenhouse, J. P., 1975, Geomagnetic variations in the Eastern United States: Evidence for a highly conducting lower crust?: Science, v. 188, no. 4189, p. 726–728.

Faust, G. T., 1975, A review and interpretation of the geologic setting of the Watchung Basalt flows, New Jersey: U.S. Geological Survey Professional Paper 864–A, 42 p.

Fletcher, J. B., Sbar, M. L., and Sykes, L. R., 1978, Seismic trends and travel-time residuals in eastern North America and their tectonic implications: Geological Society of America Bulletin, v. 89, no. 11, p. 1656–1676.

Gohn, G. S., 1983, Geology of the basement rocks near Charleston, South Carolina–Data from detrital rock fragments in lower Mesozoic(?) rocks in Clubhouse Crossroads test hole #3, *in* Gohn, G. S., ed., Studies related to the Charleston, South Carolina, earthquake of 1886–Tectonics and seismicity: U.S. Geological Survey Professional Paper 1313, p. E1–E22.

Gohn, G. S., Higgins, B. B., Smith, C. C., and Owens, J. P., 1977, Lithostratigraphy of the deep corehole (Clubhouse Crossroads corehole 1) near Charleston, South Carolina, *in* Rankin, D. W., ed., Studies related to the Charleston, South Carolina, earthquake of 1886–A preliminary report: U.S. Geological Survey Professional Paper 1028, p. 59–70.

Gohn, G. S., Houser, B. B., and Schneider, R. R., 1983, Geology of the lower Mesozoic(?) sedimentary rocks in Clubhouse Crossroads test hole #3, near Charleston, South Carolina, *in* Gohn, G. S., ed., Studies related to the Charleston, South Carolina, earthquake of 1886–Tectonics and seismicity: U.S. Geological Survey Professional Paper 1313, p. D1–D17.

Gottfried, David, Annell, C. S., and Byerly, G. R., 1983, Geochemistry and tectonic significance of subsurface basalts near Charleston, South Carolina: Clubhouse Crossroads test holes #2 and #3, *in* Gohn, G. S., ed., Studies related to the Charleston, South Carolina, earthquake of 1886–Tectonics and seismicity: U.S. Geological Survey Professional Paper 1313, p. A1–A19.

Gottfried, David, Annell, C. S., and Schwarz, L. J., 1977, Geochemistry of subsurface basalt from the deep corehole (Clubhouse Crossroads corehole 1) near Charleston, South Carolina–Magma type and tectonic implications, *in* Rankin, D. W., ed., Studies related to the Charleston, South Carolina, earthquake of 1886–A preliminary report: U.S. Geological Survey Professional Paper 1028, p. 91–113.

Harris, L. H., and Bayer, K. C., 1979, Sequential development of the Appalachian orogen above a master décollement–A hypothesis: Geology, v. 7, no. 12, p. 568–572.

Hutchinson, D. R., and Grow, J. A., 1979, Deep crustal reflectors and mantle returns from multichannel seismic profiles on the eastern United States continental shelf [abs.]: EOS, American Geophysical Union Transactions, v. 60, no. 18, p. 374.

Kean, A. E., and Long, L. T., 1978, A crustal seismic refraction study of the southeastern United States [abs.]: Earthquake Notes, v. 49, no. 3, p. 16–17.

Lanphere, M. A., 1983, $^{40}Ar/^{39}Ar$ ages of basalt from Clubhouse Crossroads test hole #2, near Charleston, South Carolina, *in* Gohn, G. S., ed., Studies related to the Charleston, South Carolina, earthquake of 1886–Tectonics and seismicity: U.S. Geological Survey Professional Paper 1313, p. B1–B8.

Nishenko, S. P., and Sykes, L. R., 1979, Fracture zones, Mesozoic rifts, and the tectonic setting of the Charleston, South Carolina earthquake of 1886 [abs.]: EOS, American Geophysical Union Transactions, v. 60, no. 18, p. 310.

Oliver, Jack, Dobrin, Milton, Kaufman, Sidney, Meyer, Robert, and Phinney, Robert, 1976, Continuous reflection profiling of the deep basement, Hardeman County, Texas: Geological Society of America Bulletin, v. 87, p. 1537–1546.

Phillips, J. D., 1977, Magnetic basement near Charleston, South Carolina–A preliminary report, *in* Rankin, D. W., ed., Studies related to the Charleston, South Carolina, earthquake of 1886–A preliminary report: U.S. Geological Survey Professional Paper 1028, p. 139–149.

Popenoe, Peter, and Zietz, Isidore, 1977, The nature of the geophysical basement beneath the Coastal Plain of South Carolina and northeastern Georgia, *in* Rankin, D. W., ed., Studies related to the Charleston, South Carolina, earthquake of 1886–A preliminary report: U.S. Geological Survey Professional Paper 1028, p. 119–137.

Rankin, D. W., 1977, Studies related to the Charleston, South Carolina, earthquake of 1886–Introduction and discussion, *in* Rankin, D. W., ed., Studies related to the Charleston, South Carolina, earthquake of 1886–A preliminary report: U.S. Geological Survey Professional Paper 1028, p. 1–15.

Schilt, F. S., Oliver, J. E., Brown, L. D., Kaufman, Sidney, Albaugh, D. S., Brewer, J., Cook, F., Jensen, L., Krumhansl, P., Long, G., and Steiner, D., 1979, The heterogeneity of the continental crust: Results from deep seismic reflection profiling using the VIBROSEIS technique: Reviews of Geophysics and Space Physics, v. 17, no. 2, p. 354–368.

Seeber, Leonardo, and Armbruster, J. G., 1980, Charleston, South Carolina, 1886: A great earthquake on the Appalachian detachment [abs.]: EOS, American Geophysical Union Transactions, v. 61, no. 32, p. 573.

Sykes, L. R., 1978, Intraplate seismicity, reactivation of preexisting zones of weakness, alkaline magmatism, and other tectonism postdating continental fragmentation: Reviews of Geophysics and Space Physics, v. 16, no. 4, p. 621–688.

Tarr, A. C., 1977, Recent seismicity near Charleston, South Carolina, and its relationship to the August 31, 1886, earthquake, *in* Rankin, D. W., ed., Studies related to the Charleston, South Carolina, earthquake of 1886–A preliminary report: U.S. Geological Survey Professional Paper 1028, p. 43–57.

Tarr, A. C., and Rhea, Susan, 1983, Seismicity near Charleston, South Carolina, March 1973 to December 1979, *in* Gohn, G. S., ed.,

Studies related to the Charleston, South Carolina, earthquake of 1886–Tectonics and seismicity: U.S. Geological Survey Professional Paper 1313, p. R1–R17.

Turcotte, D. L., Ahern, J. L., and Bird, J. M., 1977, The state of stress at continental margins: Tectonophysics, v. 42, no. 1, p. 1–28.

Wentworth, C. M., and Mergner-Keefer, Marcia, 1983, Regenerate faults of small Cenozoic offset–Probable earthquake sources in the Southeastern United States, *in* Gohn, G. S., ed., Studies related to the Charleston, South Carolina, earthquake of 1886–Tectonics and seismicity: U.S. Geological Survey Professional Paper 1313, p. S1–S20.

Yantis, B. R., Costain, J. K., and Ackermann, H. D., 1983, A reflection seismic study near Charleston, South Carolina, *in* Gohn, G. S., ed., Studies related to the Charleston, South Carolina, earthquake of 1886–Tectonics and seismicity: U.S. Geological Survey Professional Paper 1313, p. G1–G20.

Zoback, M. D., Healy, J. H., Roller, J. C., Gohn, G. S., and Higgins, B. B., 1978, Normal faulting and in situ stress in the South Carolina Coastal Plain near Charleston: Geology, v. 6, no. 3, p. 147–152.

Land Multichannel Seismic-Reflection Evidence for Tectonic Features Near Charleston, South Carolina

By ROBERT M. HAMILTON, JOHN C. BEHRENDT, and HANS D. ACKERMANN

STUDIES RELATED TO THE CHARLESTON, SOUTH CAROLINA, EARTHQUAKE OF 1886—TECTONICS AND SEISMICITY

GEOLOGICAL SURVEY PROFESSIONAL PAPER 1313-I

UNITED STATES GOVERNMENT PRINTING OFFICE, WASHINGTON: 1983

CONTENTS

ILLUSTRATIONS

STUDIES RELATED TO THE CHARLESTON, SOUTH CAROLINA, EARTHQUAKE OF 1886—
TECTONICS AND SEISMICITY

LAND MULTICHANNEL SEISMIC-REFLECTION EVIDENCE FOR TECTONIC FEATURES NEAR CHARLESTON, SOUTH CAROLINA

By ROBERT M. HAMILTON, JOHN C. BEHRENDT, and HANS D. ACKERMANN

ABSTRACT

In 1979, 140 km of multichannel seismic-reflection profiles were acquired in the vicinity of the 1886 Charleston earthquake. The strongest reflection is from the pre-Late Cretaceous unconformity, which is generally smooth (local relief less than 50 m) and dips southeast. The smoothness shows that vertical faulting within a kilometer of the surface has not been substantial since at least the Late Cretaceous. Nevertheless, the few places of deformation appear to have tectonic significance. On one profile, a zone of flexure in the Upper Cretaceous and Cenozoic sediments overlies an apparent offset in older rocks, which indicates the presence of a fault zone. Similar deformation on another profile indicates that the strike of the fault zone may be northeast, but, because the line crosses the fault zone at a low angle, the evidence for the strike direction is not strong. The fault zone, named Cooke fault, has about 50 m vertical displacement (southeast side down) on a Jurassic-age basalt layer at 750 m depth. Overlying Upper Cretaceous and Cenozoic beds have decreasing displacement with decreasing depth. The nature of these offsets coupled with the large displacement (190 m) of a reflector below the basalt suggests continuing Cenozoic movement of a post-basalt-flow, pre-Late Cretaceous fault, which may have been formed during Triassic rifting. Another fault zone indicating Cenozoic movement was found; this fault zone, named Gants fault, has a strike and an amount of vertical displacement similar to those of the Cooke fault. The surface projections of these faults extend into clusters of 1973–78 epicenters, possibly indicating that the faults may be the cause of the seismicity; these faults must extend at least into the upper part of the focal depth range of 3–13 km, which supports the causal relationship to seismicity. Also seen is a northeast-striking fault zone, named Drayton fault; it offsets only the basalt (southeast side down) and immediately overlying sediments, an indication of Late Cretaceous movement. In the northern part of the study area, layered reflections are interpreted to be Triassic red beds a few kilometers thick that are bounded on the southeast by a possible Triassic(?) normal fault. The shallow, minor deformation seen on the profiles is interpreted as a second-order manifestation of deep faulting possibly caused by reactivation of ancient thrust faults. Possibly the steep faults are reactivated from older listric normal faults. Future corroboration of the existence of the Cooke and Gants faults, the association of these faults or other faults with seismicity, and determination of the primary mode of current tectonic deformation will be important in assessing the earthquake risk in many areas of similar tectonic setting outside the Charleston region in the Atlantic coastal continental margin area.

INTRODUCTION

A seismic-reflection study was carried out during 1979 in the Charleston, S. C., region; 140 km of common-depth-point, multichannel profiles were obtained by using the VIBROSEIS[1] (Continental Oil Co. trademark) method. The purpose of the study was to investigate the relation between seismicity and geologic structure in and around the meizoseismal area of the 1886 earthquake to gain insight into the cause of that strong shock. Evaluation of future earthquake potential for the Charleston region depends critically on such information, as does the larger question of whether a Charleston-type earthquake could occur elsewhere in the Eastern United States.

Earlier seismic-reflection studies in the Charleston area were done by Yantis and others (1983) and Schilt and others (1983). The study by Yantis and others, a joint effort by Virginia Polytechnic Institute and State University (VPI&SU) and the U.S. Geological Survey (USGS), involved high-resolution profiling on three short lines (total length 7 km) and a record length of 1.5 seconds (s) two-way traveltime. The study by Schilt and others under the Consortium for Continental Reflection Profiling (COCORP) Program involved 72 km of profiling on four lines and a record length of 20 s. Our record length is 3 s on 10 lines. Thus the three studies had somewhat different targets, and the various data are complementary. Comparison of the data is facilitated by having parts of one profile in common among all three studies and parts of two other profiles in common between the COCORP and USGS studies. In 1980 and 1981, additional profiling was done in the area by VPI&SU under a cooperative study with the USGS (Coruh and others, 1981). Also in 1981, the USGS acquired a

[1] Any use of trade names is for descriptive purposes only and does not imply endorsement by the U.S. Geological Survey.

seismic-reflection profile that extends northwest across South Carolina from near Charleston (Behrendt and Hamilton, 1981). Although the new profiles are not discussed in this paper, the preliminary conclusions were known when this paper was being completed and were taken into account.

In conjunction with the land seismic-reflection surveys, marine surveys were also carried out in 1979 and 1981 in the area offshore of Charleston (Behrendt and others, 1983). Preliminary results of both the land and marine surveys were reported in Behrendt and others (1981).

The seismic-reflection surveys add to other types of geophysical surveys of the Charleston region that provide relevant data on regional structure. These include seismic-refraction (Bonini and Woollard, 1960; Ackermann, 1977, 1983; Talwani, 1977), magnetic (Popenoe and Zietz, 1977; Phillips, 1977; Daniels and others, 1983), and gravity (Long and Champion, 1977) surveys, and vertical electrical soundings (Campbell, 1977). In addition, data from three holes drilled in the study area as part of the Charleston program provide critical information on rocks in the upper kilometer of crust (Gohn and others, 1977, 1978; Gohn, 1983).

Acknowledgments. – Investigations by the USGS in the Charleston, S. C., area are partially supported by the U.S. Nuclear Regulatory Commission, Office of Nuclear Research, under Agreement No. AT(49–25)–1000.

TECTONIC SETTING

The only evidence for the epicenter of the 1886 earthquake is intensity data. The meizoseismal area, in which the maximum intensity observed was Modified Mercalli X, is centered on Middleton Place (fig. 1), about 20 km northwest of Charleston (Bollinger, 1977). Recent seismicity in the Charleston region is mostly concentrated in the meizoseismal area near Summerville except for a small cluster of activity to the south near Adams Run and another cluster 60 km to the northwest near Bowman (Tarr and Rhea, 1983; fig. 1). Thus the intensity-X area appears to be the primary target for study.

The focal depth of the 1886 shock is unknown, although the well-defined and relatively small area of intensity-IX and -X effects suggests that the depth was shallow. Focal depths of recent seismicity range from 3 to 13 km (Tarr and Rhea, 1983). Where known, focal depths elsewhere in the Central and Eastern United States are mostly less than 20 km. These factors indicate that the fault system responsible for the 1886 earthquake is most likely in the crust, probably in the upper half.

The crustal structure of the Charleston region could have been affected by at least three major tectonic events: continental rifting and formation of the proto-Atlantic, or Iapetus, Ocean in Proterozoic Z time; closing of the Iapetus Ocean in the Paleozoic; and opening of the Atlantic Ocean in the Triassic and Jurassic (Dillon and others, 1983). The last of these events certainly affected the geologic structure of the Charleston region. Data from the drill holes northwest of Charleston show that Cenozoic and Upper Cretaceous sediments rest on a sequence of Jurassic (Lanphere, 1983) basalt flows, 256 m thick; the flows overlie Triassic or Jurassic red beds at least 121 m thick (Gohn and others, 1978). The basalt layer may extend over much of the onshore and offshore Charleston region (Dillon and others, 1983; Behrendt and others, 1983). Basins filled with red beds underlie the basalt, and numerous mafic or ultramafic intrusive bodies reach to within a few kilometers of the surface (Phillips, 1977; Popenoe and Zietz, 1977; Daniels and others, 1983). Magnetic data suggest that the structural trends of the Charleston region are distinct from Appalachian orogenic trends and that the region is part of the zone of crustal extension formed in the Atlantic coastal area and beneath the Continental Shelf during opening of the Atlantic Ocean (Gohn and others, 1978; Klitgord and others, 1983). The structure of Paleozoic rocks in the Charleston region is unknown, although deep seismic-reflection data offshore have been interpreted by Behrendt and others (1983) to indicate the existence of a décollement. Another décollement, under the Appalachians, is inferred from deep seismic-reflection data (Cook and others, 1979; Harris and Bayer, 1979).

Thus, the Charleston earthquake occurred along the "passive" Atlantic margin in a zone that was the site of extensive rifting during the Mesozoic. The Paleozoic history of the area is largely conjectural. The nature of seismogenic structure in the Charleston region is essentially unknown, as is its relation to other geologic features.

DATA ACQUISITION AND PROCESSING

The USGS contracted to collect the seismic-reflection profiles presented in this report. We chose the parameters of the field operations to obtain good resolution of the upper several kilometers of the crust and, at the same time, to cover as much distance as possible.

We acquired data along ten profiles designated SC1 through SC10 (fig. 1). Figure 1 also shows the locations of the four COCORP profiles (C1 through C4). We located our profiles to obtain regional coverage in and around the meizoseismal area and to investigate features delineated by geophysical and geologic studies. An important consideration in choosing the line locations was that the trucks could not vibrate within 180 m of a building or well; this limitation accounts for the lack of

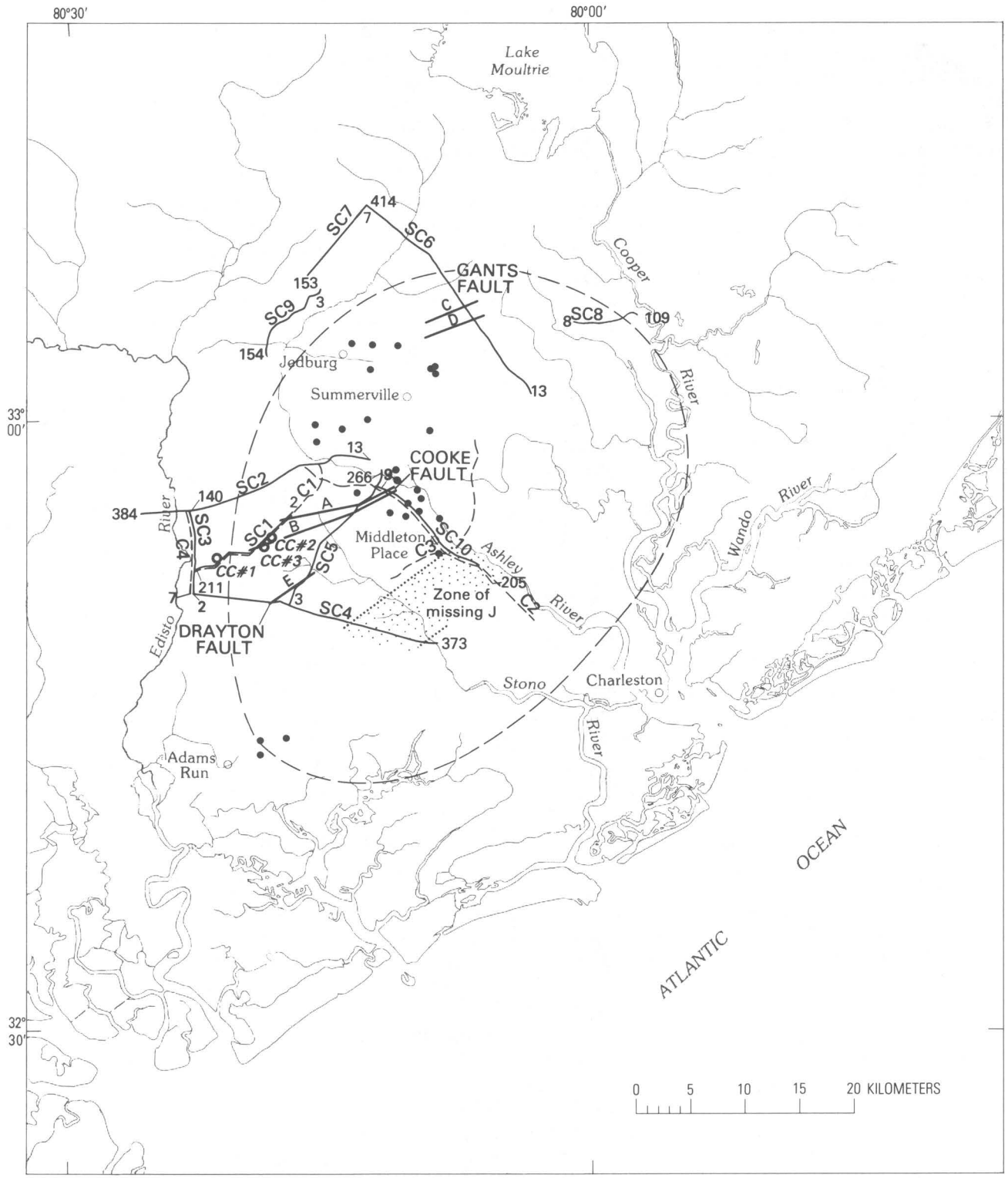

FIGURE 1.—Map of the Charleston, S. C., region showing: meizoseismal area of the 1886 earthquake (Bollinger, 1977)—heavy dashed line; epicenters of recent earthquakes (Tarr and Rhea, 1983)—dots; Clubhouse Crossroads drill holes CC#1, CC#2, and CC#3—circles; seismic-reflection profiles from this study—light solid lines with vibration-point numbers at ends; COCORP profiles (Schilt and others, 1983)—light dashed lines; and inferred faults—heavy solid lines. The zone of missing J, indicated by the pattern, refers to the intervals on SC4 and SC10 (pl. 1) where the J reflection is missing altogether or very weak. Our profiles are labeled SC1 through SC10, and COCORP's C1 through C4. Movement on the Drayton fault is Cretaceous; for the Cooke and Gants faults, movement continued into the Cenozoic. The lines marked A through E refer to features correspondingly marked in figures 2, 4, and 6.

coverage in part of the area of recent seismicity. The orientation of the lines was chosen in part to search specifically for northwest-trending structures previously suggested from various lines of evidence; none was found.

The vibration points were in the middle of the geophone spread (split spreads); the nearest geophone group was 120 m away, and the groups were 60 m apart. Thus, with a total of 48 groups the geophone spread reached to 1,500 m from the vibration point. Three vibrator trucks generated a 7-s sweep from 10 to 60 Hz at alternate geophone groups and made 15 sweeps at each vibration point. The trucks moved up about 3 m between sweeps. The data sample rate was 4 milliseconds (ms).

Standard data processing yielded 12-fold stacked sections. In addition to the final-stack sections, the data include brute-stack sections (before residual statics and residual normal-moveout corrections) and velocity analyses. Velocity analyses provided stacking velocities at intervals of about 3 km. In each velocity analysis, the data for 15 consecutive common-depth points were stacked assuming nine different velocity-depth functions. A measure of the coherency of reflections provided the basis for choosing the final stacking velocities. Velocities were assumed where reflections were poor.

Velocities derived from seismic-refraction data were also used to process line SC10 for the interval below the Upper Cretaceous sediments. This approach provided a significant improvement in record quality, which indicates that much could be gained by reprocessing the data to incorporate more information from other geophysical and geologic studies.

CORRELATION OF REFLECTIONS WITH STRATIGRAPHY

Data from three holes drilled in the Charleston region as part of the program of earthquake investigations provide a basis for correlating reflections in the upper part of the sections with stratigraphy. The holes (CC#1, CC#2, and CC#3) are 40 km west-northwest of Charleston (fig. 1). CC#1 penetrated 750 m of Cenozoic and Upper Cretaceous sediments and then passed through 42 m of basalt to a total depth of 792 m (Gohn and others, 1977). CC#2 reached basalt at 776 m and continued in it to a depth of 907 m (Gohn and others, 1983). The deepest hole, CC#3, passed through 256 m of basalt flows between 775 and 1,031 m, below which it penetrated 121 m of sedimentary red beds to reach a total depth of 1,152 m (Gohn, 1983).

In order to correlate seismic stratigraphy with geology, each of the three seismic-reflection studies included a line past the drill holes: the Clubhouse Crossroads (CC) line from Yantis and others (1983), line C1 from Schilt and others (1983), and our line SC1. The overlap of these lines also permitted correlation of reflections among the three studies. (Note: the polarity of the profiles in Yantis and others is opposite that of the other studies, but because negative amplitudes, instead of positive ones, are blackened, the profiles appear similar.)

The part of line SC1 northeast of CC#1 (fig. 2) shows that the strongest reflection on the section is between 0.70 and 0.75 s. This reflection correlates with the contact, an unconformity, between Upper Cretaceous sediments and basalt at a depth of 750–775 m. The average seismic-wave velocity of the sediments is about 2.0 km/s; therefore, two-way traveltime in seconds is approximately equivalent to depth in kilometers. A plot of velocity against depth in the sediments (Yantis and others, 1983, fig. 3*B*) shows that the root-mean-square velocity increases from 1.97 km/s at 50 m depth to 2.13 km/s at the base of the Upper Cretaceous section. Because this reflection is associated with the Jurassic-age basalt, it is referred to by Schilt and others (1983) as the "J" reflection, a practice we have followed here. Several fairly continuous reflections are seen above the basalt, and numerous discontinuous ones are seen below it.

Yantis and others (1983) analyzed thoroughly the correlation of reflections and stratigraphy for the Cenozoic and Upper Cretaceous section using information from hole CC#1. Their correlations, which are based on a synthetic record section derived from a sonic velocity log, are incorporated in figure 2. The most conspicuous reflection above the basalt at 0.47–0.49 s corresponds to a facies change in the Black Creek Formation of Late Cretaceous age. This reflection could be correlated over most of our profiles. We refer to it as the "K" reflection, again following Schilt and others (1983).

In CC#3, the basalt was found to be 256 m thick. Refraction data indicate a range from less than 4.5 to 5.8 km/s for the seismic velocity of material below the pre-Cretaceous unconformity (Ackermann, 1983), which is probably basalt where the higher velocities were observed but which may be lower Mesozoic red-bed deposits for the lower velocities. If we assume a velocity of 5.0 km/s, this thickness corresponds to a two-way traveltime of 0.10 s. A reflection below CC#3 at 0.86 s (fig. 2), 0.11 s below the basalt, may represent the basalt–red-bed contact. This reflection is similar in character to the one at 0.90 s beneath CC#1. Numerous reflections below 0.90 s in figure 2 could be from red-bed deposits or crystalline basement, but none of them stands out particularly well; some of them may be multiples.

COCORP line C1 (Schilt and others, 1983) shows a strong reflection that dips southwest from 0.85 s at the northeast end of C1 to 0.93 s at VP (vibration point) 78, which corresponds to VP70 on line SC1, where the

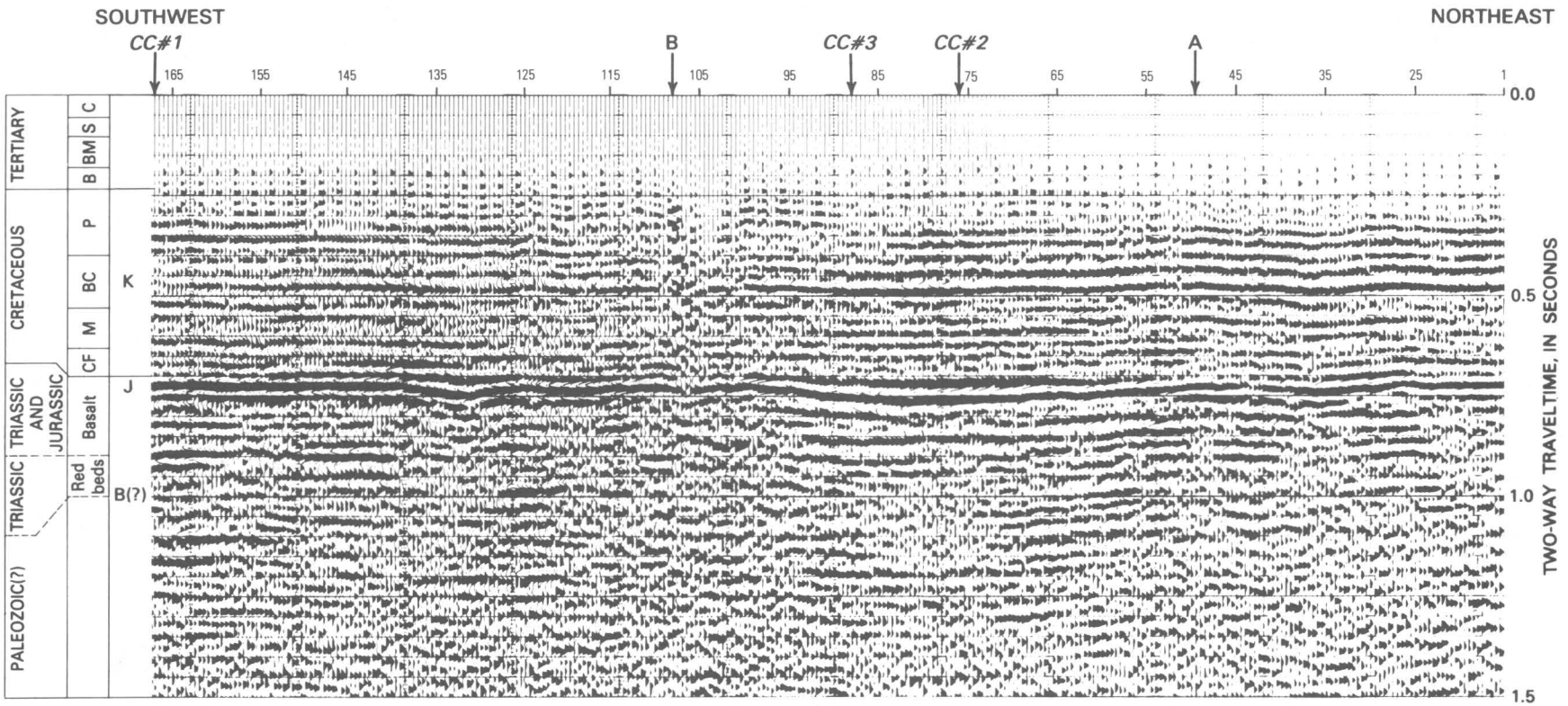

FIGURE 2.—Correlation of stratigraphy in CC#1 (Gohn and others, 1977) with the part of line SC1 northeast of the hole. Abbreviations for rock units in the Tertiary are: C, Cooper Formation; S, Santee Limestone; BM, Black Mingo Formation; and B, Beaufort(?) Formation. In the Cretaceous, they are: P, Peedee Formation; BC, Black Creek Formation; M, Middendorf Formation; and CF, Cape Fear Formation. The correlation is partially based on the analysis by Yantis and others (1983). The K reflection is from a lithologic change within the Black Creek Formation at a depth of about 500 m. The J reflection is from the top of a Jurassic-age basalt layer 750 m deep. The reflection at 0.9 s below CC#1 may be from the base of the basalt at the contact with red-bed deposits. The B reflection, which is weak here, may be crystalline basement about 1.5 km deep. Designation of these reflections follows Schilt and others (1983). The A and B arrows mark features that are correlated with ones on lines SC5 and SC10 (fig. 4).

reflection ends abruptly. This reflection does not appear as clearly on line SC1, although it may be represented by some discontinuous reflections. Seismic-refraction data in the vicinity of the Clubhouse Crossroads drill holes indicate the presence of high-velocity material (greater than 6 km/s) at depths of 1,200–1,300 m (Ackermann, 1983). Phillips (1977) estimated magnetic basement to lie at about this depth. Campbell (1977) computed a depth of 1,300 m for basement from resistivity soundings. These estimates suggest that basement depth would be 450–550 m below the basalt top, or about 0.2 s in two-way time. Thus, the reflection on COCORP line C1 may represent the basement surface – the interpretation made by Schilt and others (1983), who label it the "B" reflection. This reflection is also seen well on COCORP lines C2 and C3 and on SC4, SC5, and SC10 (pl. 1).

INTERPRETATION OF THE SEISMIC-REFLECTION PROFILES

Plate 1 shows the record sections. Discussion of the profiles begins with comments concerning their general characteristics then deals with specific features.

The J reflection, which was identified on line SC1 as corresponding to the contact of Upper Cretaceous sediments and Jurassic basalt, is clearly seen on all profiles. However, one cannot assume that the basalt is everywhere present under the sediments. It may be missing in places, in which case the J reflection would represent the contact with red-bed deposits, intrusive rocks, pre-Mesozoic crystalline rocks, or some other rock type.

Correlation of the J reflection between sections is straightforward. The only places where tracing J is difficult are in the eastern part of line SC4 (pl. 1) and the southeastern part of line SC10 (pl. 1); this zone is shown in figure 1. Where J is relatively weak, the B reflection, at about 1.0 s, is particularly strong. This suggests that the very high reflection coefficient at the J reflector (about 0.5 where basalt is present) effectively screens energy from the lower reflector. At the same time, the use of stacking velocities based on seismic-refraction data achieved considerable improvement in enhancing B on line SC10.

The J reflection is generally smooth, which shows that there has not been substantial vertical deformation of the pre-Late Cretaceous unconformity. Local relief on J is 50 m or less. This smoothness is consistent with the absence of surficial faulting in the 1886 earthquake. Apparently faults associated with the seismicity either do not propagate upward to offset shallower strata substantially or have experienced very little displacement. A contour map of the two-way traveltime to J reveals a southeastward dip of about 0.3° and an increased gradient between the 0.75-s and 0.80-s contours (fig. 3).

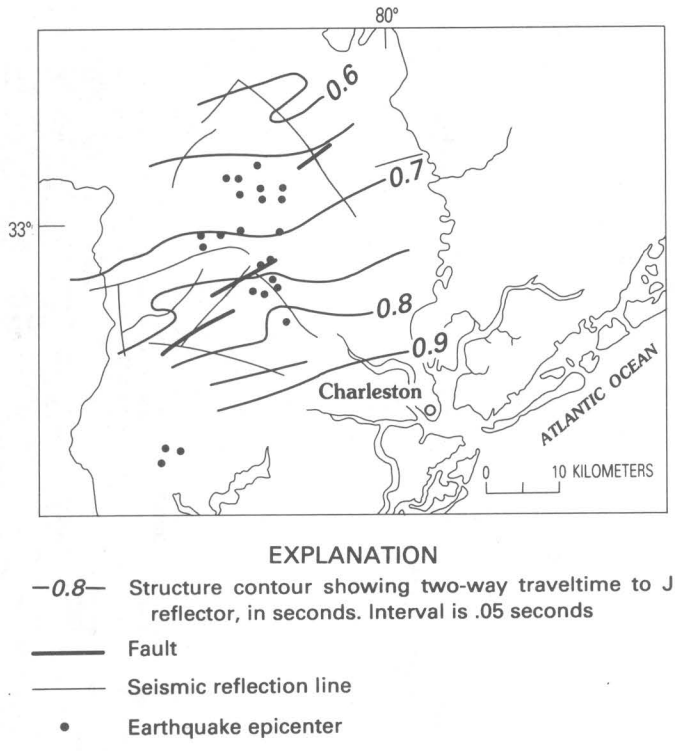

FIGURE 3. – Map of the Charleston region showing contours of the two-way traveltime, in seconds, to the J reflection. Locations of faults, seismic-reflection lines, and epicenters are also shown.

Although the J reflection is generally smooth, there are several places where the local dip is anomalously steep, and in some of these places the J reflection is also disrupted and offset. See, for example, line SC4 between VP95 and 130, line SC6 between VP191 and 160, and line SC10 between VP35 and 45 (pl. 1). As will be discussed in detail, the configuration of reflections in these and other places shows that the effects cannot be attributed to inadequate statics corrections and suggests that they are tectonically significant. Figure 1 shows the main places where J is deformed or disrupted. The K and other reflections above J are generally conformable with J. The K reflection could not be correlated as well between sections as could J, and in some places it is missing. The B reflection is clearly seen only on our lines SC4, SC5, and SC10 and on COCORP lines C1, C2, and C3. Projection to the north of the dip of B on line C3 suggests that B may impinge on J near the southeastern end of line SC6. Dipping reflections are indeed seen southeast of VP55 on SC6 (pl. 1). This interpretation implies that in the middle of SC6 J is underlain by the rocks that underlie B further to the south, which may be basement. B also impinges on J south of the east end of line SC4 (Behrendt and Hamilton, 1981).

The sections show a few reflections below 1.0 s that appear to indicate structure. Some examples are a reflection at about 2.6 s beneath VP185 on line SC1 (pl. 1), and sets of reflections between VP328 and 342 and VP210 and 225 on line SC6 (pl. 1). Numerous subhorizontal reflections may also indicate structure, but they must be viewed with suspicion because they could be multiples.

The following discussion of some features of the sections is organized according to the features' tectonic significance.

Cenozoic Deformation

Of the places where the J and shallower reflections are anomalously deformed, one near the west end of line SC10 (pl. 1) is particularly significant because it appears to provide good evidence for the existence and nature of Cenozoic deformation. Figure 4 shows an enlargement of this part of the section. The critical aspects of the feature seen in figure 4*A* are the deformation in the J and overlying reflections, disruption of the B reflection, and thickening of the interval between J and B. The amount of offset across the deformed zone increases with depth from about 20 m on the shallowest reflection to about 50 m on J; a much larger offset of about 190 m is seen on B (Behrendt and others, 1981).

Although near-surface velocity variations could contribute to the deformation, the increasing offset with depth across the zone indicates that part of the deformation is a flexure in the sediments. Coincidence of the flexure in J and shallower reflections with the disruption in B suggests a fault-related origin for the flexure. There are two possibilities for the timing of fault movement, each having quite different implications. In one case, a scarp would have existed on J when sedimentation began in the Late Cretaceous; the flexure would then be the result of differential compaction of the varying thickness of the sedimentary column. In the other case, the sediments would have been deposited on a smooth surface and the deformation would have occurred during sedimentation. The former case seems unlikely for three reasons. One reason is that at least four unconformities are recognized in the Upper Cretaceous and Tertiary section of the Charleston region (Gohn and others, 1977). An unconformity would smooth the flexure and cause shallower beds to continue more or less flat across it. Another reason is suggested by section SC4 (pl. 1 and fig. 6) between VP100 and 130 where the overlying reflections are not conformable with the deformation of the J reflection. The deformation on SC4 apparently occurred soon before sedimentation, yet there is no draping of sediments across the deformed zone. The final reason is that if significant topographic features existed when sedimentation began there probably should be more of them in evidence. Our conclusion, therefore, is that some faulting occurred during sedimentation.

We have named the zone of deformation on SC10 the Cooke fault because it lies near Cooke Crossroads. The Cooke fault was also identified by Schilt and others on line C2, which is coincident with SC10 (fig. 1); they interpreted it to be a reverse fault. Although the attitude of the fault is difficult to discern in the zone of flexure (fig. 4*A*), the points of inflection on the reflections and the truncation of some of them indicate a reverse fault (fig. 4*B*). Such an attitude is quite significant because it implies a reversal of stress orientation from the extensional regime that prevailed during opening of the Atlantic Ocean. Current northwest compression is indicated in the Southeastern United States by various lines of evidence (Zoback and Zoback, 1980).

The time of onset of reverse fault movement is suggested by the relative deformation of the J and B reflections and by the reflections between them, which appear to be conformable with B (fig. 4*B*). These relations indicate that reverse faulting followed deposition of the material between the basalt and basement, probably Triassic or Jurassic red beds, and the basalt. According to this interpretation, the scarp at the basalt surface would have been eroded before Late Cretaceous sedimentation. The shallowest warped reflection seen on line SC10 (fig. 4*B*) is at 0.15 s. This corresponds to an unconformable contact of Eocene age (Gohn and others, 1977). Thus, faulting continued at least to the Eocene.

Determining the strike of the Cooke fault is important because the orientation carries implications about which geologic structure is active and ultimately about seismic risk. The evidence, however, is not clear. Relevant data are seen on line SC5, whose north end ties with the west end of line SC10 (fig. 1). The characteristics of Cooke fault on line SC5 that would provide a basis for correlation are deformation in the J and shallower reflections, disruption of B, and thickening of the interval between the J and B reflections, approximately by the amounts seen on line SC10. Figure 4*A* shows an enlargement of the critical part of section SC5. The characteristics of the two sections between the arrows marked A and B are in some respects similar, especially when the angle between line and fault is taken into account. If, as shown in figure 1, the angles at which SC5 and SC10 cross the inferred trend of Cooke fault are about 22° and 49°, respectively, the flexure and offset are stretched over a greater distance on SC5 than on SC10, which explains some of the differences between the sections. These characteristics bear sufficient similarity to suggest a possible correlation, which would yield a northeast strike.

Some features on other lines further support delineation of Cooke fault. On line SC1 at A (fig. 2), the J and

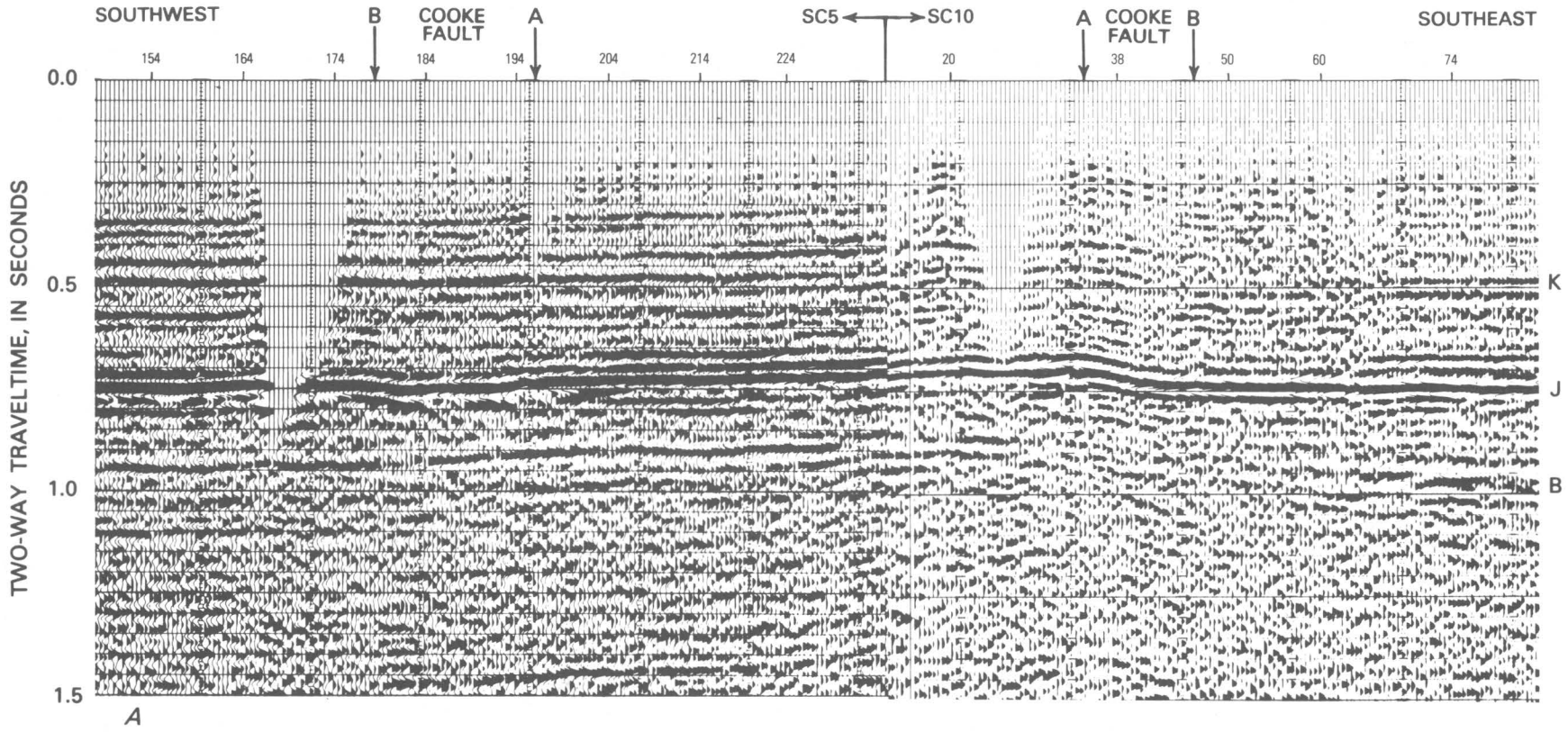

FIGURE 4.—*A*, Parts of profiles SC5 (left) and SC10 (right) showing features that define Cooke fault, the location of which is shown in figure 1. The A and B arrows mark the fault zone and indicate possible corresponding features. Note that all reflections drop across the zone, and that the amount of drop increases with depth (Behrendt and others, 1981). The interval between J and B increases by about 70 ms (140 m) across the zone. Lines SC5 and SC10 cross the fault at angles of 22° and 49°, respectively, which may be the reason the fault zone seems broader and less abrupt on line SC5 than on SC10. See figure 2 for other features that suggest projection of the fault to line SC1. In this figure, gaps in data are the result of vibration points being missed because of buildings and wells, and draping of reflections toward the gap on SC10 is thought to be an artificial effect. *B*, An enlargement of a part of profile SC10 showing the interpretation that defines Cooke fault.

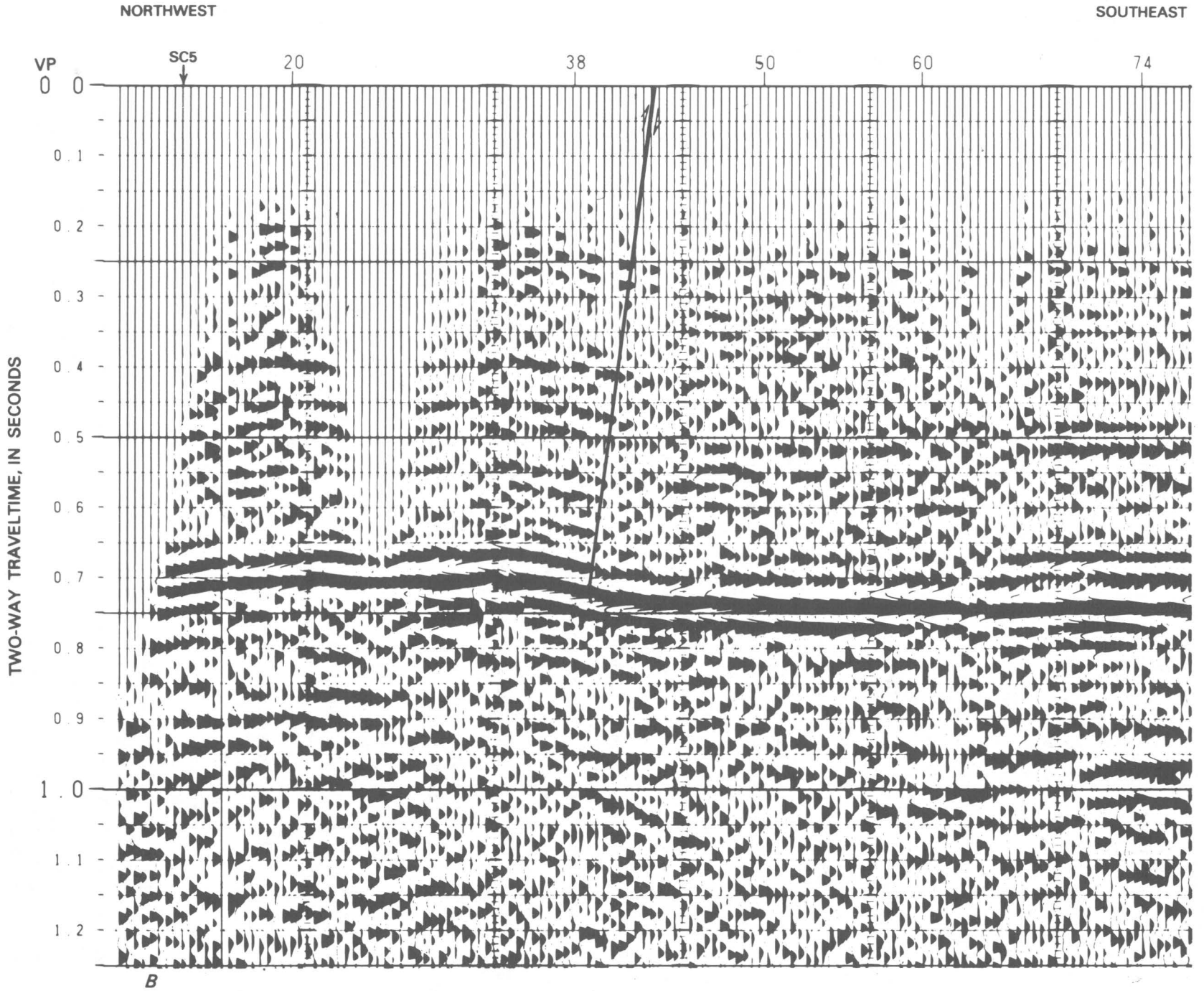

FIGURE 4.—Continued

other reflections drop. They rise to about their previous level at VP95, forming a sag that is unique on the sections; its significance is unclear. However, COCORP line C1 shows termination of B and a small offset in J at VP75, which corresponds to VP74 on SC1 and is about in the middle of the sag. At B on SC1 (fig. 2), there is a thickening between J and the reflection that may represent the base of the basalt. No features on line SC3 (pl. 1) or line C4, which are coincident (fig. 1), indicate the location of Cooke fault except perhaps the gradual increase in time of the reflections south of VP50 on SC3. To the northeast, Cooke fault may be expressed on COCORP line C3 between VP200 and 210 as a drop in B and the associated graben feature described by Schilt and others (1983). However, these possible correlative features are not strong, and Cooke fault may not extend beyond the interval defined.

Another example of apparent Cenozoic deformation is on line SC6 (fig. 5). The J reflection drops about 50 ms across the zone and changes in character. The shallower reflections conform to this flexure. This feature is also seen on the 1980–81 data (Coruh and others, 1981). Together the data define a northeast-striking fault zone, which we have named Gants fault after a creek in the area. We interpret this fault to mark the edge of a Triassic(?) basin, on the basis of line SC6 and our other unpublished data.

A third possible case of Cenozoic deformation is seen near the west end of line SC2 (pl. 1) between VP328 and 313. This place is where the line crosses the Edisto River, which is the reason for the gap in the record section. On each side of the interval, the J and shallower reflections are fairly flat, but on the west side they are about 20 ms higher. The possibility that this offset is of near-surface origin cannot be ruled out; however, if this were the case, the largest effect should be in the gap itself. The strike of this feature is unknown.

Mesozoic Deformation

The feature on line SC4 (pl. 1) between VP100 and 130 that was mentioned above provides evidence of deformation near the beginning of Late Cretaceous sedimentation. Figure 6 shows an enlarged view. The basis for this age estimate is that the J reflection is deformed whereas shallower reflections from Upper Cretaceous and younger rocks are not.

Line SC5 ties with SC4 a little east of the disrupted zone (fig. 1). Between VP48 and 62 on SC5 (fig. 6), the J reflection rises about 30 ms, which is similar to the change on SC4. As is also seen on line SC4, the K and shallower reflections do not show this change, although some reflections near the lower part of the Upper Cretaceous section show it. Correlation of the disrupted zones on lines SC4 and SC5 delineates a northeast-striking fault that we have named the Drayton fault because Drayton Swamp is located above where the fault is seen.

In the eastern part of line SC4 between VP250 and 350, the J reflection becomes weak and in places disappears altogether (pl. 1). In the same interval, the B reflection is unusually strong. Between VP220 and 250 and between VP330 and 350 both J and B can be seen clearly. A dipping reflection and apparent diffractions between J and B and just below B at VP350 indicate a fault. The continuation of B beneath J to the west of VP250 seems to be evidence against a fault at VP250; however, this apparent continuation could be caused by the profile crossing the fault at a low angle and reflections being detected from both the upthrown and downthrown sides of the fault in this part of the record section. In any case, the gap in the J reflection suggests that there is a gap in the basalt and that the gap is filled with material having a velocity similar to that of Coastal Plain sediments, either the same sediments or Jurassic sediments. Weak J and strong B are also characteristics of the southeast part of SC10 (pl. 1).

Structure Below the B Reflection

Few reflections are seen on the record sections that suggest the nature of structure below the B reflection. A major difficulty in analyzing the deeper data is uncertainty about multiple reflections. The velocity analyses are helpful in this regard, but they are often ambiguous.

Numerous reflections that appear to be significant are seen on line SC6 (pl. 1) below about 0.9 s. A set of reflections between VP342 and 328 from about 0.75 to 1.5 s separates a stack of horizontal reflections to the northwest from a zone of numerous diffractions and poor reflections to the southeast. Because these reflections are located below a data gap, they may be a processing artifact. The velocity analysis near the northwest end of SC6 indicates that the reflections from J down to at least 1.35 s are not multiples and shows an interval velocity of 3.6 km/s. The velocity analyses southeast of VP342 indicate significantly higher velocities for the interval. Thus, the set of reflections between VP342 and 328 may indicate the location of a fault that separates lower velocity material to the northwest from higher velocity material to the southeast. The velocity relations, the horizontal layering of the reflections, and the orientation of the fault suggest that it is a boundary fault of a basin. Considering the tectonic history of the Charleston region and the seismic-wave velocity of 3.6 km/s estimated for the basin material, we conclude that the materials are Triassic or Jurassic red-bed deposits. Ackermann (1983) similarly concluded that red-bed deposits are present in this area; however, he located

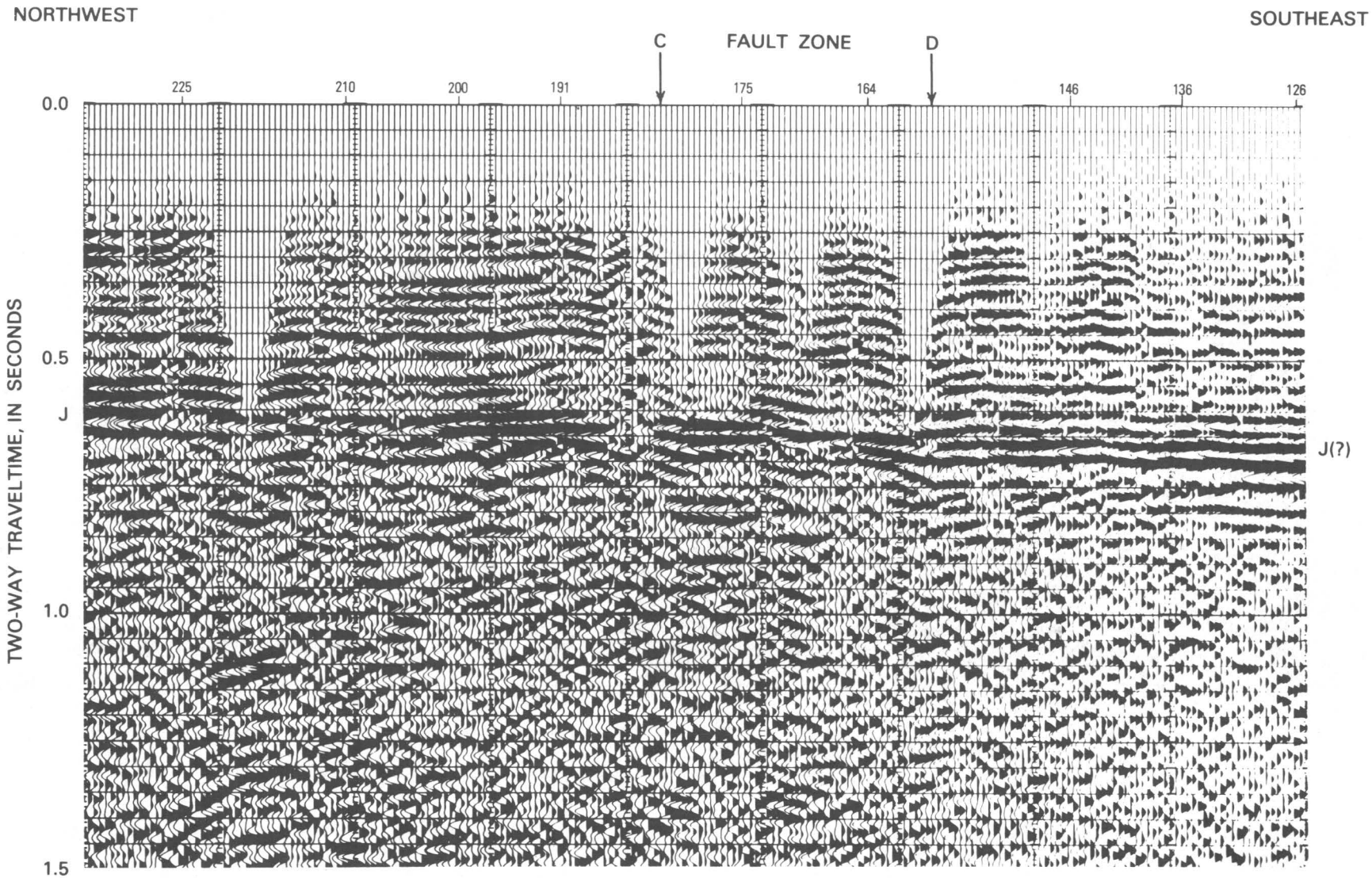

FIGURE 5. – Part of line SC6 showing a flexure in the J and overlying reflections that defines Gants fault. The C and D arrows mark the fault zone. The reflections drop about 50 ms (50 m) across the zone. At the southeast edge of the zone the character of J changes, which makes its identification uncertain.

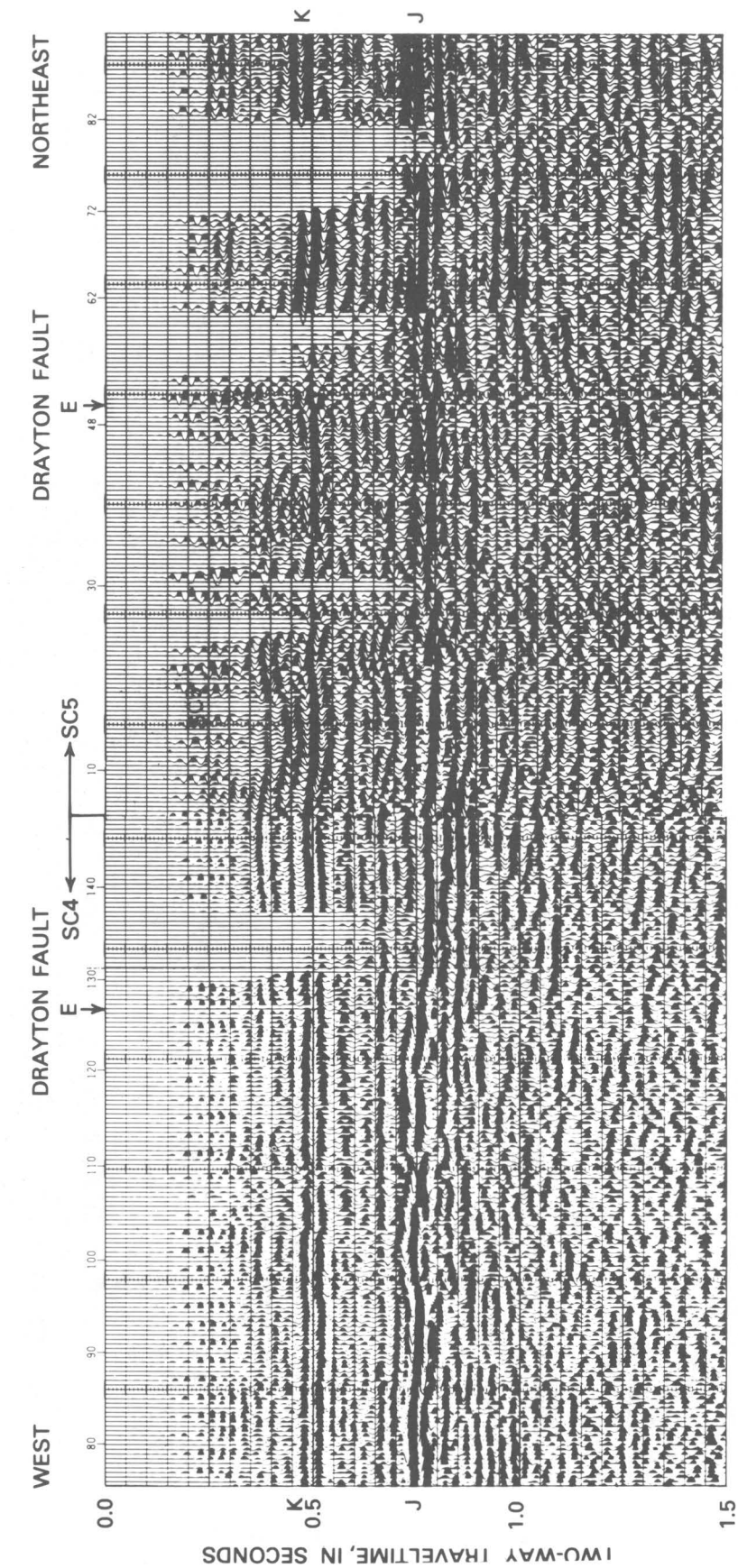

FIGURE 6. – Parts of profiles SC4 (left) and SC5 (right), showing features that define Drayton fault, the location of which is shown in figure 1. The E arrow marks the middle of the zone where the J reflection drops about 30 ms. Overlying reflections on SC4 above 0.66 s do not mirror this deformation, but ones just above J may. On SC5 the K and shallower reflections do not show the change, but deeper ones may. Thus, it appears that the deformation took place in the Late Cretaceous. The J reflection is anomalously disrupted west of the fault zone. The offset at VP60 on SC5 may be an artifact of processing.

the boundary fault 10 km southeast of the one inferred here.

Other deep reflections on line SC6 between VP261 and 210 to about 2.2 s also indicate faulting and possibly the presence of a small basin.

Lines SC7 and SC9 (pl. 1) show many reflections below the J reflection, which may be further evidence for red-bed deposits. The deeper reflections are subparallel with J and shallower reflections, however, so they could be multiples. The velocity analyses show that some of the reflections stack well at higher velocities and may be primary reflections, and some do not and may be multiples.

COMPARISON OF GEOPHYSICAL FEATURES

Other geophysical data in the Charleston region help in interpreting the seismic-reflection data. Figure 7 includes three maps showing the locations of our seismic-reflection profiles and features interpreted from the profiles superimposed on contours of seismic-refraction data from Ackermann (1983) and of magnetic data from Phillips and others (1978).

The pre-Cretaceous unconformity, as defined by refraction data (fig. 7*A*), has a southeasterly regional dip similar to that determined from the reflection data (fig. 3). The most interesting features of the pre-Cretaceous surface are the increased gradient along an east-northeast trend between the 750-m and 900-m contours and the shallow trough southeast of it bounded by the 900-m contour. The strike of this feature is similar to that delineated for the nearby Cooke and Drayton faults. Also, the location of the trough coincides approximately with the places on lines SC4 and SC10 where the J reflection is weak and the B reflection is strong, which suggests that the basalt is missing there. In this area, there are several strong diffractions under B on line SC4 (pl. 1) that are indicative of faulting. Thus the trough defined by refraction data may have tectonic significance. The trough does not have a distinct expression in Cretaceous subcrop velocities (fig. 7*B*), which generally decrease to the southeast except for a northwest-striking reentrant of lower velocity.

In figure 7*C*, the refraction data show a northeast-striking basement ridge, which, at its southwestern end, overlies a magnetic high with which there is a corresponding gravity high (Long and Champion, 1977). The trough seen in figure 7*A* lies over the southeast flank of the ridge. The steep slope of the northwest side of the ridge is interpreted as a boundary fault by Ackermann (1983). Talwani (1977) also places a boundary fault at about this location, on the basis of refraction and gravity data.

Line SC6 crosses the northwest side of the ridge and shows evidence of faulting. However, the Gants fault is considerably northwest of the one defined by refraction data. Also, the Gants fault shows about 50 m offset down to the southeast, which is opposite to the sense of movement on the boundary fault. This may constitute evidence for fault reactivation in an opposite direction of movement.

The epicenters in the study area (fig. 1) are mostly grouped around Summerville and fall in three clusters. The southernmost cluster is located near the Cooke fault. The activity in the northern clusters is loosely centered in the area of Ackermann's boundary fault and Gants fault. The actual relationship between the seismicity and these features, however, is unclear because focal depths range from 3 to 13 km, whereas the structures mentioned are well above 3 km; however, these shallow faults must extend into the focal depth range.

TECTONIC IMPLICATIONS

In several places, the seismic-reflection profiles show evidence of flexure of Upper Cretaceous and Cenozoic rocks (fig. 1) of as much as 50 m in vertical deformation. In one place along the Cooke fault, this deformation is associated with offset in pre-Cretaceous rocks of about 190 m. This is interpreted as evidence of faulting in which movement began during Jurassic or Cretaceous time and continued into Cenozoic time, the most recent deformation occurring in the Eocene or later. Evidence of probable Late Cretaceous faulting, having a northeast strike, is seen on two lines (SC4 and SC5). These two faults coincide with a northeast-striking band of increased dip on the pre-Cretaceous unconformity and lie along the northwest margin of a northeast-striking trough in this unconformity defined by refraction data. These factors and the tectonic setting together suggest reactivation of faulting associated with a Triassic and Jurassic basin. The coincidence of a cluster of epicenters with the Cooke and Gants faults raises the possibility that the faults may be currently active; however, the earthquakes occur as deep as 13 km in the cluster, which is consistent with the interpretation that the Cooke and Gants faults are of tectonic origin and that the deformation observed is only a shallow manifestation of deeper fault movement.

The COCORP data provide some clues as to the deeper structure of the Charleston region (Schilt and others, 1983). A general characteristic of those profiles is that they are quite featureless between 1.5 and 3 s where little coherent energy is seen; below 3 s, and increasingly below 6 s, there are numerous subhorizontal reflections and diffractions. The marine data off Charleston are similar in that good reflections and diffractions begin at about 3 s beneath a similarly transparent zone (Behrendt and others, 1983); these features may correlate

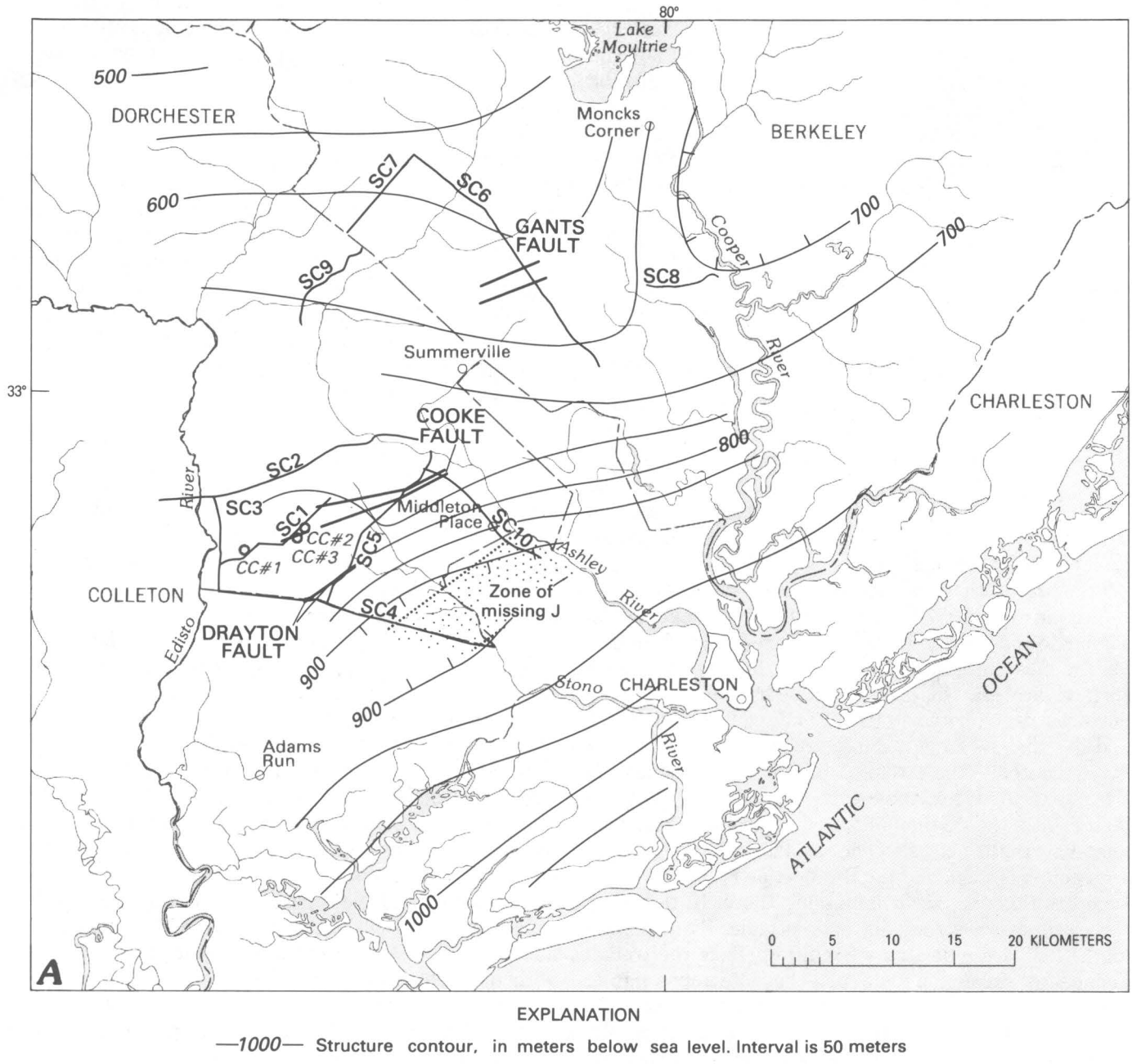

FIGURE 7.—Maps of the Charleston region showing seismic-reflection profiles and inferred tectonic features on contour maps (after Ackermann, 1983) of: *A*, depth to the pre-Cretaceous unconformity, based on seismic-refraction data; *B*, seismic- refraction velocity below the unconformity; and *C*, magnetic intensity and depth to a layer having velocity 6.0–6.4 km/s (Phillips and others, 1978).

with the few coherent features shown by Schilt and others (1983). The earthquakes lie near or above the zone of diffractions; therefore, knowledge of this zone is quite important.

Schilt and others (1983) follow the interpretation of Brown and others (1979) for the Rio Grande rift in concluding that the transparent zone may indicate the presence of homogeneous granite plutons in the upper crust. The magnetic and gravity data clearly indicate the presence of numerous mafic plutons reaching to within a few kilometers of the surface (Popenoe and Zietz, 1977; Phillips, 1977). This zone probably was cut by normal faults during Mesozoic rifting, but nothing is known of fault structure at depth. It is clear from the smoothness of the pre-Cretaceous unconformity that there has been little vertical movement of the faults since the Late Cretaceous. This lack of movement suggests either that fault activity in the Charleston region

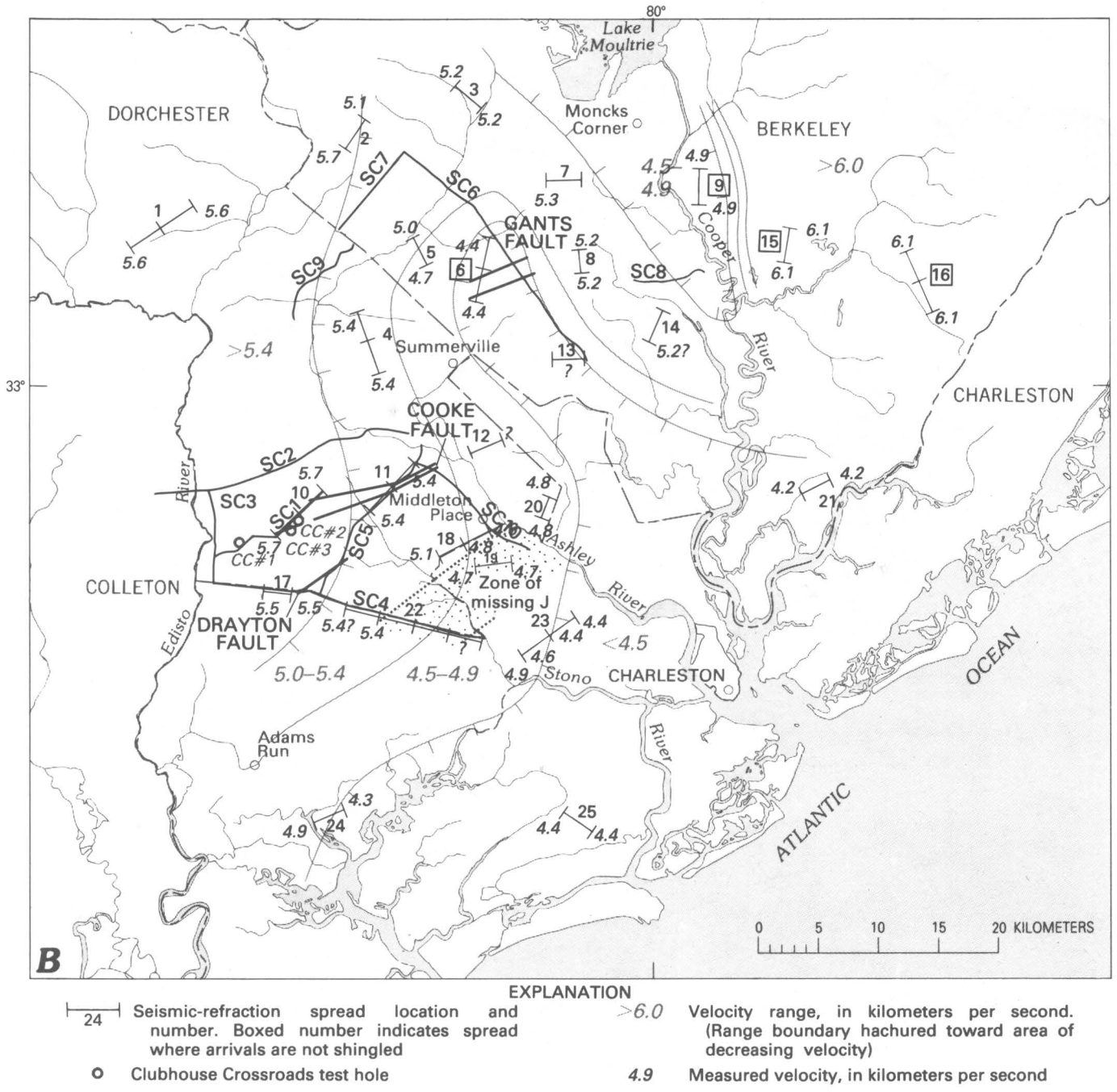

FIGURE 7.–Continued.

is very low or that the predominant mode of deformation involves horizontal movement. Such movement could take place either on low-angle thrust faults formed during continental convergence or on a zone of detachment between brittle failure at shallower depths and regional extension associated with rifting at greater depths. In fact, the same zone could have originated as a thrust fault and at a later time could have served as the detachment zone.

Fault-plane solutions provide evidence of the nature of fault movement that can be critical in assessing the tectonic significance of seismicity. Only one single-earthquake fault-plane solution has been determined in the Charleston area (Tarr, 1977); three composite-fault-plane solutions have been determined, one each for the three clusters of seismicity near Summerville (Tarr and Rhea, 1983). All solutions have one nodal plane that is almost horizontal; the other nodal plane strikes north-

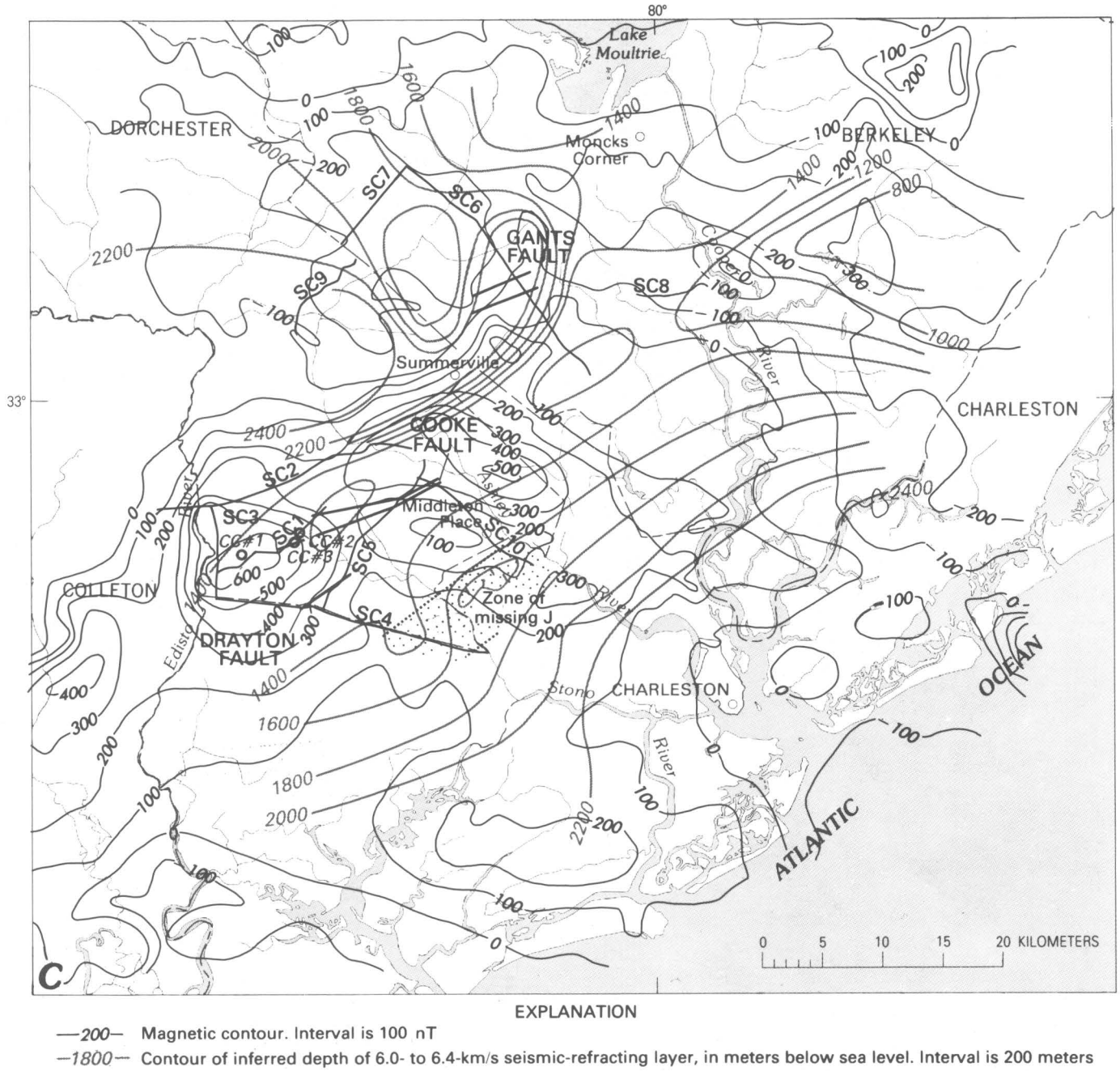

FIGURE 7.—Continued.

west for the single-earthquake solution and two composite solutions (the better two) and northeast for one composite solution. Thus, movement on a subhorizontal plane is consistent with all solutions.

Although focal depths of Charleston seismicity range from 3 to 13 km (Tarr and Rhea, 1983), two-thirds of them lie from 5 to 8 km deep. Considering the difficulties in determining focal depths, particularly in a region such as Charleston where large lateral variations in velocity exist, the data permit interpretation of a horizontal zone of seismicity. Seeber and Armbruster (1980, 1981) interpret intensity data from the Charleston region to indicate horizontal movement.

This evidence for subhorizontal faulting as the cause of Charleston seismicity is certainly not compelling, but it is sufficient to require that the possibilities considered for seismogenic structures be broadened. In fact, the almost complete lack of information about structure at

earthquake depths leaves open a wide range of possibilities. This range can be narrowed to a few likely structures through consideration of the geologic history of the Charleston region.

Closing of the Iapetus Ocean surely compressed the crust of the Charleston region and probably caused extensive thrust faulting there. A décollement associated with westward overthrusting of Paleozoic sedimentary rocks has been proposed to exist under the Appalachians and eastward under the Coastal Plain (Cook and others, 1979; Harris and Bayer, 1979). Whether the décollement extends under the Charleston region is controversial. The later opening of the Atlantic rifted the Charleston area along with the rest of the present continental margin. This extensional episode was apparently followed by a return to weak northwest compression before Late Cretaceous time (possibly in Jurassic time).

Virtually nothing is known of the deep structure of the fault systems at Charleston, but they must constitute a complex zone of highly fractured crust. Fault movement could be of various types. Because it is likely that ancient thrust faults exist in the Charleston area and because the stress field is oriented about the same way now as when the thrust faults developed, it seems reasonable that movement on the thrust faults is the primary cause of modern seismicity. In this hypothesis, movement on other types of faults would be viewed as a second-order effect, accommodating the deeper horizontal movement but also causing earthquakes.

The model envisioned is a complex one in which ancient compressional and extensional fault systems are interlaced. The compressional faults are presently the more active because of the stress-field orientation. The originally extensional faults are less active, and their movement is in a reverse sense. The smoothness of the pre-Late Cretaceous unconformity suggests that this mode of deformation has continued since then.

The implications of this hypothesized origin of Charleston seismicity are several. Seismicity would be confined to the décollement and shallower faults. The types of fault movement would be diverse and could include thrust, reverse, and probably even shear faulting. Because the Charleston area (and possibly the entire Triassic rifted province) actually is composed of numerous fault blocks, the interaction of these blocks above a décollement could give rise to various styles of deformation. One would also expect that, over the long run, seismicity would be dispersed over a broad area, although certain areas could be intermittently active.

The degree to which these implications are applicable elsewhere along the Atlantic margin would depend on the similarity of tectonic setting. That early Mesozoic basins occur along most of the margin, that thrust faulting occurred along the whole margin, and that numerous cases of Cenozoic reverse faulting have been recognized (Wentworth and Mergner-Keefer, 1983) suggest that deformation such as is occurring in the Charleston area may indeed be occurring in other similar areas. Thus, the possibility of a Charleston-type earthquake in other areas of similar tectonic setting must be considered.

REFERENCES CITED

Ackermann, H. D., 1977, Exploring the Charleston, South Carolina, earthquake area with seismic refraction–A preliminary study, *in* Rankin, D. W., ed., Studies related to the Charleston, South Carolina, earthquake of 1886–A preliminary report: U.S. Geological Survey Professional Paper 1028, p. 167–175.

———1983, Seismic-refraction study in the area of the Charleston, South Carolina, 1886 earthquake, *in* Gohn, G. S., ed., Studies related to the Charleston, South Carolina, earthquake of 1886–Tectonics and seismicity: U.S. Geological Survey Professional Paper 1313, p. F1–F20.

Behrendt, J. C., and Hamilton, R. M., 1981, Preliminary interpretation of a seismic reflection profile crossing South Carolina Coastal Plain and Piedmont, and implications concerning the origin of the Charleston, 1886, earthquake [abs.]: EOS, American Geophysical Union Transactions, v. 62, no. 45, p. 954.

Behrendt, J. C., Hamilton, R. M., Ackermann, H. D., and Henry, V. J., 1981, Cenozoic faulting in the vicinity of the Charleston, South Carolina, 1886 earthquake: Geology, v. 9, no. 3, p. 117–122.

Behrendt, J. C., Hamilton, R. M., Ackermann, H. D., Henry, V. J., and Bayer, K. C., 1983, Marine multichannel seismic-reflection evidence for Cenozoic faulting and deep crustal structure near Charleston, South Carolina, *in* Gohn, G. S., ed., Studies related to the Charleston, South Carolina, earthquake of 1886–Tectonics and seismicity: U.S. Geological Survey Professional Paper 1313, p. J1–J29.

Bollinger, G. A., 1977, Reinterpretation of the intensity data for the 1886 Charleston, South Carolina, earthquake, *in* Rankin, D. W., ed., Studies related to the Charleston, South Carolina, earthquake of 1886–A preliminary report: U.S. Geological Survey Professional Paper 1028, p. 17–32.

Bonini, W. E., and Woollard, G. P., 1960, Subsurface geology of North Carolina-South Carolina Coastal Plain from seismic data: American Association of Petroleum Geologists Bulletin, v. 44, no. 3, p. 298–315.

Brown, L. D., Chapin, C. E., Sanford, A. R., Kaufman, Sidney, and Oliver, J. E., 1979, Deep structure of the Rio Grande Rift from seismic reflection profiling, *in* Riecker, R. E., ed., Rio Grande rift–Tectonism and magmatism: American Geophysical Union Special Publication, p. 169–184.

Campbell, D. L., 1977, Electric and electromagnetic soundings near Charleston, South Carolina–A preliminary report, *in* Rankin, D. W., ed., Studies related to the Charleston, South Carolina, earthquake of 1886–A preliminary report: U.S. Geological Survey Professional Paper 1028, p. 189–198.

Cook, F. A., Albaugh, D. S., Brown, L. D., Kaufman, Sidney, Oliver, J. E., and Hatcher, R. D., Jr., 1979, Thin-skinned tectonics in the crystalline southern Appalachians; COCORP seismic-reflection profiling of the Blue Ridge and Piedmont: Geology, v. 7, no. 12, p. 563–567.

Coruh, C., Costain, J. K., Behrendt, J. C., and Hamilton, R. M., 1981, New reflection seismic evidence for deformation of Mesozoic sediments near Charleston, S. C. [abs.]: Geological Society of America Abstracts with Programs, v. 13, no. 7, p. 431.

Daniels, D. L., Zietz, Isidore, and Popenoe, Peter, 1983, Distribution of subsurface early Mesozoic rocks in the southeastern United States as interpreted from regional aeromagnetic and gravity maps, *in* Gohn, G. S., ed., Studies related to the Charleston, South Carolina, earthquake of 1886–Tectonics and seismicity: U.S. Geological Survey Professional Paper 1313, p. K1–K24.

Dillon, W. P., Klitgord, K. D., and Paull, C. K., 1983, Mesozoic development and structure of the continental margin offshore from South Carolina, *in* Gohn, G. S., ed., Studies related to the Charleston, South Carolina, earthquake of 1886–Tectonics and seismicity: U.S. Geological Survey Professional Paper 1313, p. N1–N16.

Gohn, G. S., 1983, Geology of the basement rocks near Charleston, South Carolina–Data from detrital rock fragments in lower Mesozoic(?) rocks in Clubhouse Crossroads test hole #3, *in* Gohn, G. S., ed., Studies related to the Charleston, South Carolina, earthquake of 1886–Tectonics and seismicity: U.S. Geological Survey Professional Paper 1313, p. E1–E22.

Gohn, G. S., Gottfried, David, Lanphere, M. A., and Higgins, B. B., 1978, Regional implications of Triassic or Jurassic age for basalt and sedimentary red beds in the South Carolina Coastal Plain: Science, v. 202, no. 4370, p. 887–890.

Gohn, G. S., Higgins, B. B., Smith, C. C., and Owens, J. P., 1977, Lithostratigraphy of the deep corehole (Clubhouse Crossroads corehole 1) near Charleston, South Carolina, *in* Rankin, D. W., ed., Studies related to the Charleston, South Carolina, earthquake of 1886–A preliminary report: U.S. Geological Survey Professional Paper 1028, p. 59–70.

Gohn, G. S., Houser, B. B., and Schneider, R. R., 1983, Geology of the lower Mesozoic(?) sedimentary rocks in Clubhouse Crossroads test hole #3, near Charleston, South Carolina, *in* Gohn, G. S., ed., Studies related to the Charleston, South Carolina, earthquake of 1886–Tectonics and seismicity: U.S. Geological Survey Professional Paper 1313, p. D1–D17.

Harris, L. D., and Bayer, K. C., 1979, Sequential development of the Appalachian orogen above a master décollement–A hypothesis: Geology, v. 7, no. 12, p. 568–572.

Klitgord, K. D., Dillon, W. P., and Popenoe, Peter, 1983, Mesozoic tectonics of the Southeastern United States Coastal Plain and continental margin, *in* Gohn, G. S., ed., Studies related to the Charleston, South Carolina, earthquake of 1886–Tectonics and seismicity: U.S. Geological Survey Professional Paper 1313, p. P1–P15.

Lanphere, M. A., 1983, $^{40}Ar/^{39}Ar$ ages of basalt from Clubhouse Crossroads test hole #2, near Charleston, South Carolina, *in* Gohn, G. S., ed., Studies related to the Charleston, South Carolina, earthquake of 1886–Tectonics and seismicity: U.S. Geological Survey Professional Paper 1313, p. B1–B8.

Long, L. T., and Champion, J. W., Jr., 1977, Bouguer gravity map of the Summerville-Charleston, South Carolina, epicentral zone and tectonic implications, *in* Rankin, D. W., ed., Studies related to the Charleston, South Carolina, earthquake of 1886–A preliminary report: U.S. Geological Survey Professional Paper 1028, p. 151–166.

Phillips, J. D., 1977, Magnetic basement near Charleston, South Carolina–A preliminary report, *in* Rankin, D. W., ed., Studies related to the Charleston, South Carolina, earthquake of 1886–A preliminary report: U.S. Geological Survey Professional Paper 1028, p. 139–149.

Phillips, J. D., Daniels, D. L., Zietz, Isidore, and Popenoe, Peter, 1978, Geophysical studies of the Charleston, South Carolina, area–Onshore aeromagnetic map: U.S. Geological Survey Miscellaneous Field Studies Map MF–1022–A, 1 sheet, scale 1:250,000.

Popenoe, Peter, and Zietz, Isidore, 1977, The nature of the geophysical basement beneath the Coastal Plain of South Carolina and northeastern Georgia, *in* Rankin, D. W., ed., Studies related to the Charleston, South Carolina, earthquake of 1886–A preliminary report: U.S. Geological Survey Professional Paper 1028, p. 119–137.

Schilt, F. S., Brown, L. D., Oliver, J. E., and Kaufman, Sidney, 1983, Subsurface structure near Charleston, South Carolina; Results of COCORP reflection profiling in the Atlantic Coastal Plain, *in* Gohn, G. S., ed., Studies related to the Charleston, South Carolina, earthquake of 1886–Tectonics and seismicity: U.S. Geological Survey Professional Paper 1313, p. H1–H19.

Seeber, Leonardo, and Armbruster, J. G., 1980, Charleston, South Carolina, 1886–A great earthquake on the Appalachian detachment [abs.]: EOS, American Geophysical Union Transactions, v. 61, no. 32, p. 573.

———1981, The 1886 Charleston, South Carolina, earthquake and the Appalachian detachment: Journal of Geophysical Research, v. 86, no. B9, p. 7874–7894.

Talwani, Pradeep, 1977, A preliminary shallow crustal model between Columbia and Charleston, South Carolina, determined from quarry blast monitoring and other geophysical data, *in* Rankin, D. W., ed., Studies related to the Charleston, South Carolina, earthquake of 1886–A preliminary report: U.S. Geological Survey Professional Paper 1028, p. 177–187.

Tarr, A. C., 1977, Recent seismicity near Charleston, South Carolina, and its relationship to the August 31, 1886, earthquake, *in* Rankin, D. W., ed., Studies related to the Charleston, South Carolina, earthquake of 1886–A preliminary report: U.S. Geological Survey Professional Paper 1028, p. 43–57.

Tarr, A.C., and Rhea, Susan, 1983, Seismicity near Charleston, South Carolina, March 1973 to December 1979, *in* Gohn, G. S., ed., Studies related to the Charleston, South Carolina, earthquake of 1886–Tectonics and seismicity: U.S. Geological Survey Professional Paper 1313, p. R1–R17.

Wentworth, C. M., and Mergner-Keefer, Marcia, 1983, Regenerate faults of small Cenozoic offset–Probable earthquake sources in the Southeastern United States, *in* Gohn, G. S., ed., Studies related to the Charleston, South Carolina, earthquake of 1886–Tectonics and seismicity: U.S. Geological Survey Professional Paper 1313, p. S1–S20.

Yantis, B. R., Costain, J. K., and Ackermann, H. D., 1983, A reflection seismic study near Charleston, South Carolina, *in* Gohn, G. S., ed., Studies related to the Charleston, South Carolina, earthquake of 1886–Tectonics and seismicity: U.S. Geological Survey Professional Paper 1313, p. G1–G20.

Zoback, M. L., and Zoback, Mark, 1980, State of stress in the conterminous United States: Journal of Geophysical Research, v. 85, no. B11, p. 6113–6156.

Marine Multichannel Seismic-Reflection Evidence for Cenozoic Faulting and Deep Crustal Structure Near Charleston, South Carolina

By JOHN C. BEHRENDT, ROBERT M. HAMILTON, HANS D. ACKERMANN, V. JAMES HENRY, and KENNETH C. BAYER

STUDIES RELATED TO THE CHARLESTON, SOUTH CAROLINA, EARTHQUAKE OF 1886—TECTONICS AND SEISMICITY

GEOLOGICAL SURVEY PROFESSIONAL PAPER 1313-J

UNITED STATES GOVERNMENT PRINTING OFFICE, WASHINGTON: 1983

CONTENTS

ILLUSTRATIONS

[Plates are in pocket]

TABLE

STUDIES RELATED TO THE CHARLESTON, SOUTH CAROLINA, EARTHQUAKE OF 1886—
TECTONICS AND SEISMICITY

MARINE MULTICHANNEL SEISMIC-REFLECTION EVIDENCE FOR CENOZOIC FAULTING AND DEEP CRUSTAL STRUCTURE NEAR CHARLESTON, SOUTH CAROLINA

By JOHN C. BEHRENDT, ROBERT M. HAMILTON, HANS D. ACKERMANN, V. JAMES HENRY,[1] and KENNETH C. BAYER

ABSTRACT

Multichannel seismic-reflection data combined with single-channel, high-resolution reflection profiles collected offshore from Charleston in 1979 have allowed us to define the following geologic features.

1. The Helena Banks fault, a northeast-striking, high-angle, west-dipping reverse fault at least 30 and possibly 70 km long, is about 12 km offshore and extends upward to about 10 m from the sea bottom. This fault was probably reactivated in the Cenozoic from a Triassic-age structure; the most recent movement is at least as young as Miocene or Pliocene. The Helena Banks fault is a possible source of seismicity. Other shallow Cenozoic faults were also found.
2. A subhorizontal surface is defined by diffractions at about 11.4 ± 1.5 km depth. The depth range of hypocenters calculated for Charleston-area seismicity during 1973–78 is 3 to 13 km. We interpret the subhorizontal surface as a décollement or zone of detachment and suggest a causal relationship to seismicity.
3. A band of reflections at 9–11 seconds corresponding to a depth of about 29–35 km is interpreted to be from the Mohorovicic discontinuity (Moho); this depth is in agreement with a crustal-refraction determination for the Moho of 29.9 km.
4. A series of west-dipping, north-striking reflecting surfaces(?) or diffracting "edges" lies at or beneath the surface defined by diffractions.
5. A Jurassic-age basalt layer extending onshore and offshore for about 100,000 km^2 deepens seaward from about 1.0 to 1.4 km in the Charleston region. This surface, as defined by a strong reflection, is largely undisturbed except by the Helena Banks and a few other faults showing small vertical displacement.
6. Several Triassic-age or older faults exist; within resolution of the seismic-reflection data, these faults do not show evidence of reactivation since the basalt was extruded.

We suggest that the Charleston seismicity is primarily caused by movement along the décollement and that movement on the high-angle reverse faults may also cause earthquakes. Future corroboration of association of the décollement, or reactivated shallow faults, with seismicity will be important in assessing the earthquake risk in many areas of similar tectonic setting outside the Charleston region in the Atlantic coastal and continental margin area.

[1]Skidaway Institute of Oceanography, Savannah, GA 31406.

INTRODUCTION

A comprehensive program has been underway since 1973 to establish the cause of the 1886 Charleston earthquake and to evaluate the potential for future earthquakes in this and tectonically similar regions. In 1979, we decided to acquire multichannel seismic-reflection data in the offshore Charleston area. Land seismic data were being obtained in the Charleston area at about the same time, which the marine data would complement nicely. Thus, the marine survey provided an economical way to examine the structure over a large area near Charleston.

Various geophysical investigations had been carried out previously on land in an effort to extend the known surface and subsurface geologic information. On the basis of seismic-refraction data, Ackermann (1983) interpreted a northeast-striking structure in the area of modern seismicity to be a Triassic boundary fault. This feature lies roughly along northeast-trending magnetic and gravity lineations (Popenoe and Zietz, 1977). A seismograph network established in 1973 revealed several clusters of epicenters including a tight group in the meizoseismal area of the 1886 shock, and Tarr and Rhea (1983) used these data to define hypocenters of earthquakes since 1973 in the depth range of 3 to 12 km.

Multichannel seismic-reflection profiles on land have been collected in 1977 and 1978 in the area of the

epicenters (Yantis and others, 1983; Schilt and others, 1983). The seismic-reflection survey made in 1979 by the U.S. Geological Survey (USGS) (Hamilton and others, 1983; Behrendt and others, 1981) defined a northeast-trending fault zone, called the Cooke fault (fig. 1), which was interpreted to have been reactivated from an older (Triassic?) structure that moved down to the southeast in Cenozoic time in a high-angle, northwest-dipping reverse sense. Several other faults showing Cenozoic displacement of unknown trend were also observed in the land profiles (fig. 1), as were a Triassic fault zone and one of Cretaceous(?) age.

Although no known seismicity originates in the area offshore of Charleston (fig. 1), the low level observed on the land net and the low sensitivity of the instruments resulting from generally high noise levels suggest that only earthquakes having magnitudes greater than about 2 could have been detected offshore since 1973. Because part of the objective of the Charleston earthquake research program is the understanding of the general

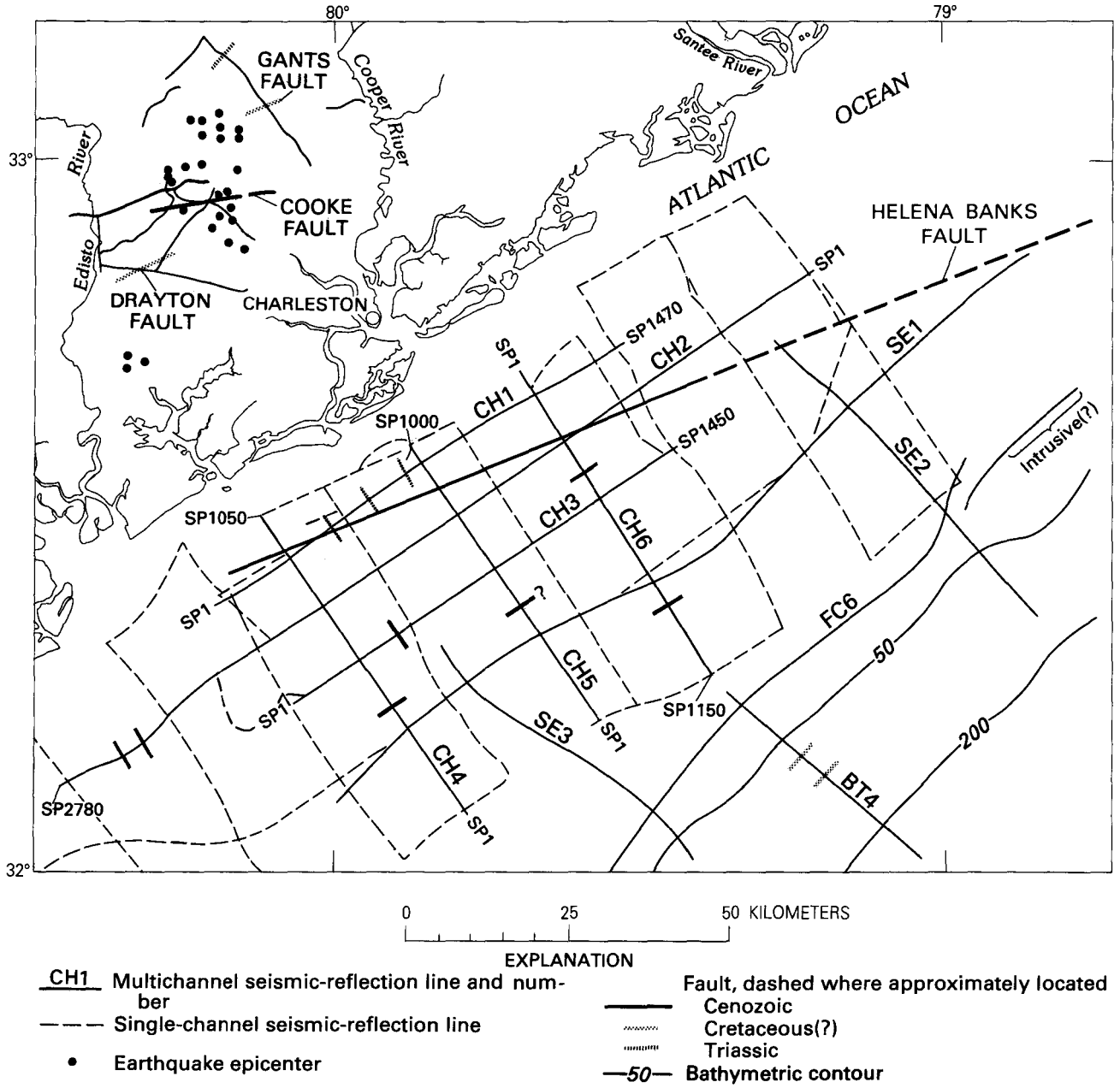

FIGURE 1.—Map showing location of multichannel and single-channel seismic-reflection profiles, earthquake epicenters, and interpreted faults. Lines CH1–CH6 are from this study and record sections for these lines are shown on plates 1 and 2; the SE, FC, and BT lines are from Dillon and others (1979). The single-channel data also overlap lines CH1–CH6. The 50- and 200-m bathymetric contours and shotpoints (SP) are shown.

tectonic structure of the region, the water-covered area could not be ignored. An aeromagnetic survey (Behrendt and Klitgord, 1979) was available, sparse marine gravity data existed (Grow and others, 1979), and a few marine multichannel seismic lines extended into the southeast corner of the area (Dillon and others, 1979).

The Cooke fault zone trends normal to two of the focal-mechanism solutions and parallel to the third (Tarr and Rhea, 1983); it has been discussed by Hamilton and others (1983) and Behrendt and others (1981). Zoback and Zoback (1980) discussed the regional stress pattern in the United States and found a general northwest-southeast direction of maximum compressive stress in the Atlantic Coastal Plain area. Such a stress direction appears to be inconsistent with two of the focal-mechanism solutions of Tarr and Rhea (1983). However, if the horizontal focal-mechanism solutions are considered, rather than the vertical as proposed by Tarr and Rhea (1983), the seismicity may have its source in movement along a low-angle décollement or zone of detachment. On the basis of interpretations of the multichannel seismic data, we present evidence in this paper to support the hypothesis of a subhorizontal surface or surfaces in the depth range of earthquakes found by the seismic net.

Sykes (1978), in a review of intraplate seismicity, suggested that the Blake Spur fracture zone (BSFZ) might have originated from an old zone of weakness near Charleston that could have been reactivated to cause the 1886 earthquake and modern seismicity. Dillon and others (1979), in a map of depth to a Late Triassic–Early Jurassic-age unconformity and to oceanic basement, show a lineation of the contours based on multichannel seismic-reflection data that is on trend with the extension of the BSFZ southeast of about 31° N. 79° W. The aeromagnetic map of Behrendt and Klitgord (1979) shows magnetic contours associated with the BSFZ extending toward the continent to about 31°40′ N. 78°30′ W., and Klitgord and Behrendt (1979) show that the BSFZ is a major boundary between the Carolina trough and the Blake Plateau basin.

The discovery of northwest-striking nodal planes from composite-fault-plane solutions (Tarr and Rhea, 1983) enhances the credibility of some relation between the BSFZ and Charleston seismicity. In any case, suggestions of association of seismicity with a reactivated old zone of weakness that might have defined the location of the BSFZ provided a hypothesis which we examined by means of multichannel seismic surveys on land and over the Continental Shelf offshore from Charleston. The land and marine reflection lines (fig. 1) were planned specifically to obtain evidence of any northwest-trending structures. Neither the land survey (Hamilton and others, 1983) nor the marine multichannel seismic profiles presented in this paper produced information on any structures having northwest trends that might have localized the BSFZ or that might be related to the BSFZ in any way. Instead, we found evidence of a northeast-striking fault that can be traced for at least 30 km and possibly for 70 km. This fault shows clear evidence of Cenozoic and earlier movement on a common Triassic trend; the most recent movement occurred in post-Miocene or post-Pliocene time. We also saw numerous strong, deep reflections that provide insight on deep crustal structure.

Acknowledgments. – We thank J. A. Grow and W. P. Dillon for critically reviewing this manuscript. M. D. Zoback, M. L. Zoback, and H. Schouten contributed through many helpful discussions. The research was supported in part by the U.S. Nuclear Regulatory Commission, Office of Nuclear Research, under Agreement No. AT(49-25)-1000.

MARINE MULTICHANNEL SEISMIC SURVEY

The marine multichannel seismic-reflection survey was carried out by contract along the 450 km of lines CH1–CH6 shown in figure 1. The water was very shallow in the area surveyed; line CH1 and the northwest ends of lines CH4, CH5, and CH6 are all in 10–15 m depths. Note the location of the 50-m bathymetric contour at the southeast corner of figure 1. The data were collected by Whitehall Corporation, by means of a 3,200-m-long, 64-channel streamer and a tuned airgun array with a capacity of ~33 L (~2,000 in^3). Shotpoints were 50 m apart. The recording time was 12 s (seconds) at a 4-ms (millisecond) sample rate. Adjacent traces were summed, and the data were processed 16-fold and displayed in record sections at two scales (6.4 and 19 cm/s), to enable us to study the deep and the shallow structure. The record sections are displayed at reduced scales in plates 1 and 2. Specific examples of the records at larger scales are shown and discussed in the text.

In conjunction with the multichannel survey, the Skidaway Institute collected high-resolution, single-channel reflection data, by means of a 16-cm^3 (1-in^3) airgun along and between the multichannel reflection lines. The single-channel line locations are also shown in figure 1. These data allowed us to follow interpreted structure from the multichannel data into the shallowest sedimentary section in several cases. The multichannel data are useful only below about 150 m depth.

Additional multichannel lines (Dillon and others, 1979) SE1, SE2, SE3, FC6, and BT4 (fig. 1), part of the regional USGS seismic-reflection survey of the U.S. Atlantic continental margin, complement our data and allow us to make further inferences.

RESULTS

Shallow Stratigraphy

The land multichannel profiles (Hamilton and others, 1983) were tied to drill holes, so acoustic stratigraphy was well correlated to a depth of about 1 km. Although the marine data are not tied to the land data as yet, the lines are close enough (fig. 1) that in this paper we can make correlations on the basis of similarities in appearance of the record section and regional dip of the stratigraphic units. A portion of a typical record section is shown in figure 2. The obvious fault (Helena Banks fault) will be discussed below in the section on Cenozoic faulting. The shallowest reflections, at about 0.14–0.17 s, probably are from Eocene-age rocks. The strong reflection at the left at about 0.63 s may correspond to the "K" horizon in rocks of Late Cretaceous age (Hamilton and others, 1983; Schilt and others, 1983), although the reflection is not as continuous in the marine data as it is in the land data.

Basalt Layer

The strongest reflection, at about 1.1 s, is labeled "J" to be consistent with the land data (Schilt and others, 1983; Hamilton and others, 1983). The source of this reflection is the unconformity at 775 m between poorly consolidated basal Upper Cretaceous deposits and a sequence of probably Jurassic-age (184 ± 3.3 m.y.) basalt flows (Lanphere, 1983), which are 256 m thick in a drill hole on one of the land seismic lines (Hamilton and others, 1983). Seismic-refraction velocities associated with the J reflector on land range from less than 4.5 to at least 5.8 km/s (Ackermann, 1983). Beneath the Continental Shelf, seaward of our survey, they range from 5.5 to 6.3 km/s; 9 of 12 measurements are between 5.8 and 6.1 km/s (Dillon and McGinnis, 1983). Because the drill hole on land penetrated interbedded basalt and sedimentary rocks (of Triassic? or Jurassic? age) (Phillips, 1983), we suggest that the range in velocity is presumably the result of a range in the amount of lower velocity sedimentary rock interbedded with the basalt, although Dillon and others (1983) suggested variation in weathering as a possible cause. The increase of velocity seaward probably indicates a decrease in the thickness of interbedded sedimentary rock. Deeper reflections below J are apparent in the land data in many parts of the survey (Hamilton and others, 1983; Schilt and others, 1983), but the marine data only occasionally show clearly identifiable reflection horizons in the 1- to 2-s range below J. Farther seaward, Dillon and others (1979) were rarely able to observe reflections below the basalt. This suggests that the basalt sequence thickens seaward or that it directly overlies crystalline basement. On the basis of velocities from refraction studies (Ackermann, 1983) and from this reflection work, the reflection coefficient at the interface between the overlying sedimentary rock and the basalt is about 0.5, which is one of the highest observed in nature.

The aeromagnetic data over the area (Phillips and others, 1978; Behrendt and Klitgord, 1979) do not show evidence of the basalt layer even though the magnetization measured at an onshore test hole is about 10^{-3} emu (electromagnetic unit)/cm^3 (Phillips, 1983). In fact, because the basalt layer closely approximates a uniformly magnetized thin sheet, an anomaly would be expected only at the edges. Daniels and others (1983) calculated that the basalt should produce an anomaly of about 15 nanoteslas (nT), which would be difficult to observe. Depths to magnetic basement calculated by means of high-sensitivity marine aeromagnetic data (Behrendt and Klitgord, 1980) were reexamined in detail over the area immediately offshore from Charleston, shown in figure 1. We observed small anomalies (5–15 nT) that suggest depths to sources in approximate agreement with depths indicated by the contours on the J reflection shown in figure 3. Generally, however, we conclude, in agreement with Daniels and others (1983), that in effect the basalt layer is magnetically transparent and the obvious anomalies in the aeromagnetic maps (Phillips and others, 1978; Behrendt and Klitgord, 1979) and in figure 4 are from deeper sources at the top of, or within, the magnetic basement, as discussed by Klitgord and Behrendt (1979).

Using the J reflection to define the basalt layer, we contoured the reflection times as shown in figure 3. The average velocity of the sedimentary rock above J is about 2.0 km/s, on the basis of measurements at a test hole in the area of the land survey (fig. 1) (Yantis and others, 1983); therefore, above J, two-way traveltime in seconds is approximately equal to depth in kilometers. However, the average seismic velocity above J probably increases with increasing depth to J, hence the velocity to convert the time contours in figure 3 to depth contours would also increase with increasing time.

The basalt layer is very smooth throughout the area surveyed on land (Hamilton and others, 1983) and over the Continental Shelf (see pls. 1 and 2). From the north end of the land data to the marine line closest to the coast, the average dip is only 0.3° (line CH1, fig. 1), although there is some inflection in the area of the Cooke fault (Hamilton and others, 1983, fig. 3). Offshore the dip increases to about 0.6° from the 1- to the 2-s contour of figure 3 (assuming a velocity of 2.0 km/s). There appears to be an increase seaward of the 1.4-s contour to about 0.8°; this increase corresponds to a slight flexure that is observed in the record sections for lines CH4, CH5, and CH6 (pl. 1).

The area of the basalt layer, if we accept its correlation with the J reflection as delineated by Dillon and

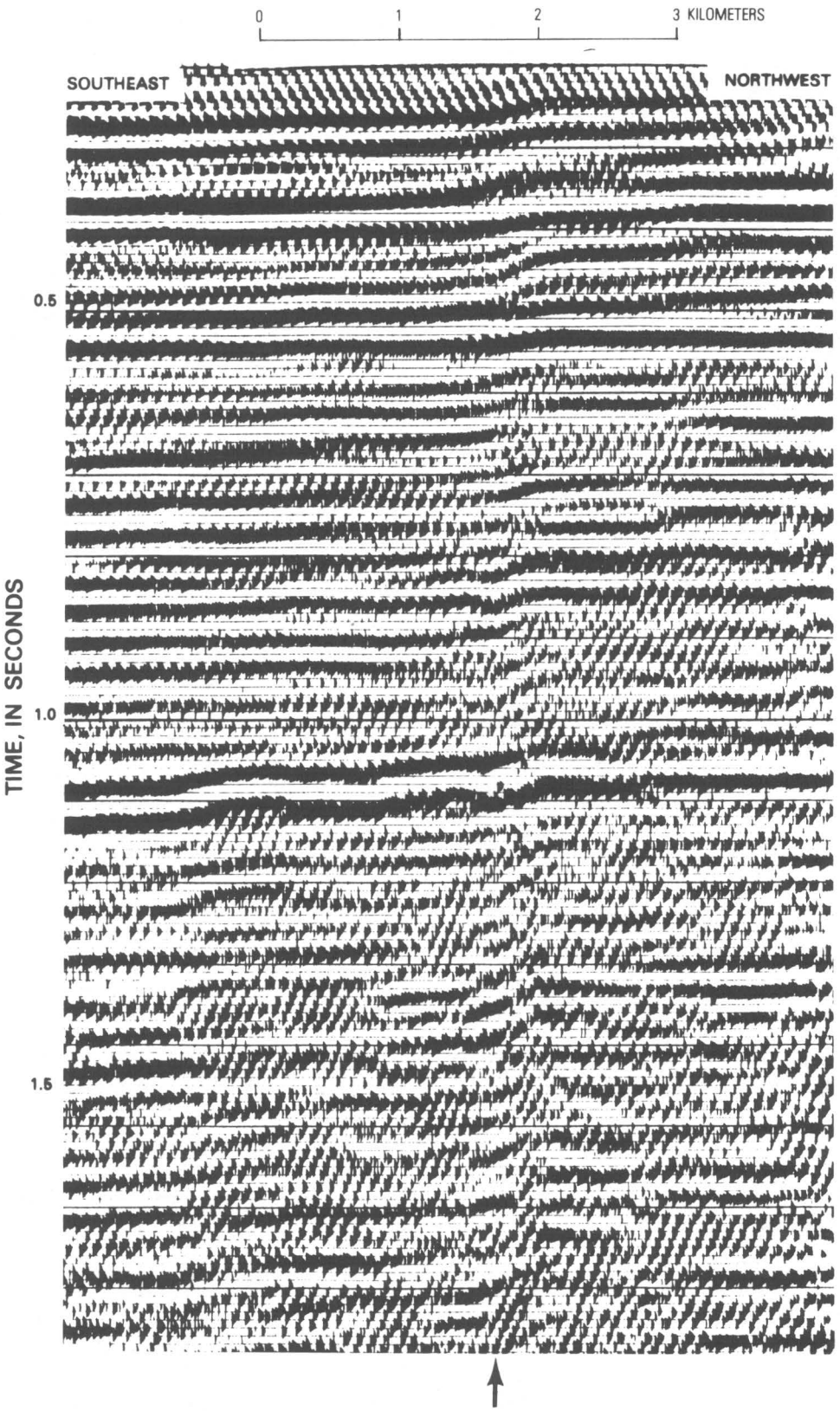

FIGURE 2.—Part of of seismic record section from line CH4. The strong reflection at about 1.1 s is designated "J" and is from a basalt layer. Arrow marks position of inferred Helena Banks fault.

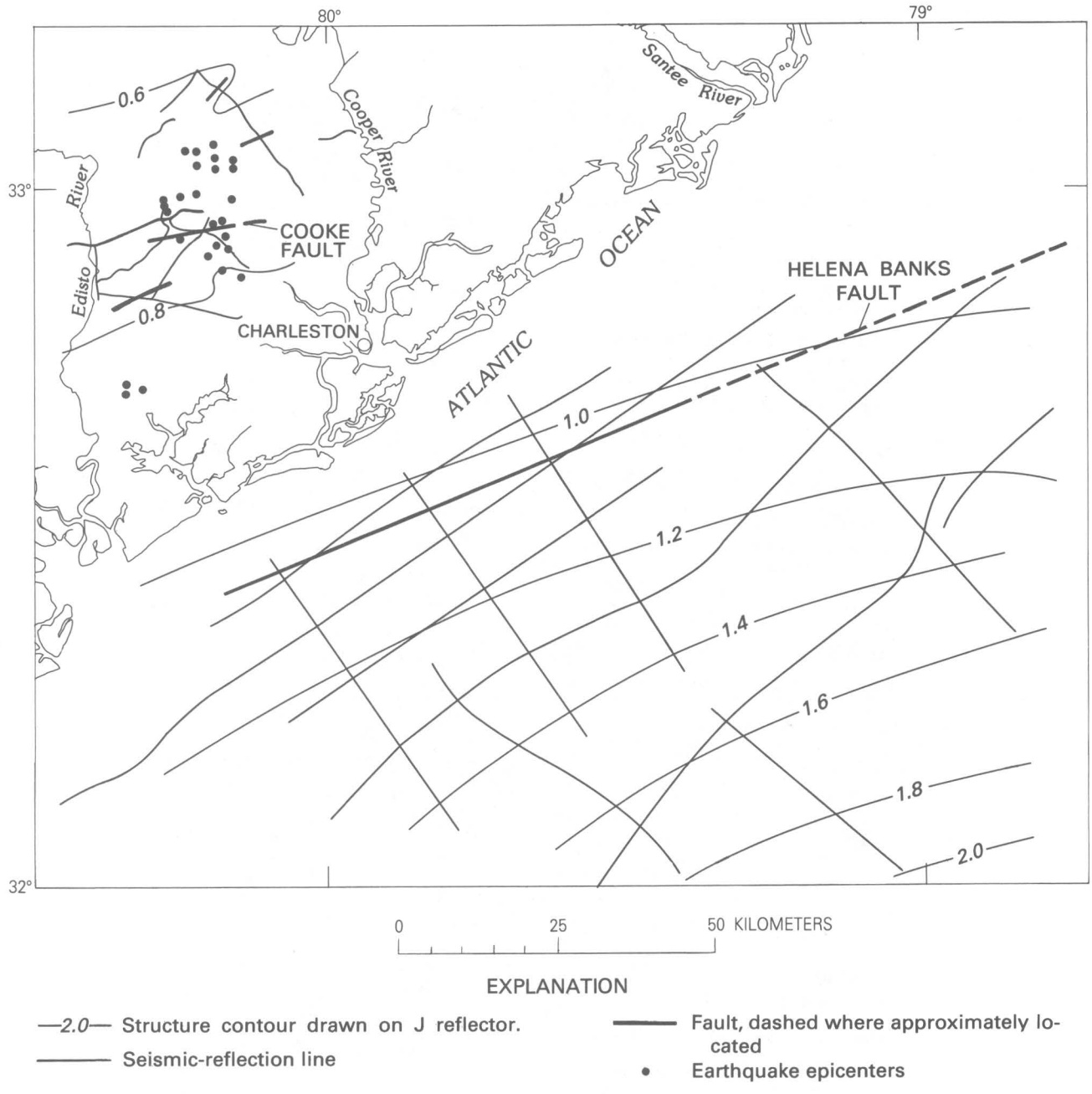

FIGURE 3.—Two-way traveltime to the J reflection; contour interval 0.2 s. Because the seismic velocity above J is about 2.0 km/s, the two-way traveltime in seconds approximately equals the depth in kilometers. The locations of the Helena Banks fault and the multichannel seismic-reflection lines are shown.

others (1979), is about 100,000 km², which makes this one of the smaller of the great basalt fields of the world. Table 1 (P. Lipman, written commun., 1980) indicates the relative size of the basalt field, as defined by the J reflection, compared with the sizes of a number of other basalt areas. The thickness of the basalt at Clubhouse Crossroads drill hole 3 (CC#3) is 256 m, but the area near CC#3 gives lower seismic velocity, less continuity, and better quality reflections below J than are found in the rest of the area surveyed. We therefore expect the average thickness of the basalt to be greater than the 256 m drilled at CC#3.

We can only speculate as to the source of the basalt layer or its significance to the Charleston earthquake problem. A series of mafic intrusions defined by aeromagnetic data (Behrendt and Klitgord, 1979) and

TABLE 1.—*Selected basaltic flows of the world*
[From P. Lipman (written commun., 1980)]

Location	Average thickness (m)	Area (km²)	
		Present	Original
Karroo, S. Africa	1,000	140,000	2,000,000?
Paraná, Brazil	650	1,200,000	2,000,000
Siberia, U.S.S.R.	1,000	>1,500,000	
Lake Superior, U.S.A.	5,000	100,000	125,000
Deccan, India	100–2,000	500,000	1,000,000
Columbia River, U.S.A.	----	200,000	200,000
Brito-Arctic	----	1,000,000	
Blake Plateau, U.S.A.	250	100,000	

gravity data (Grow and others, 1979) trend north-south in the eastern part of the area, as indicated in the aeromagnetic map in figure 4. Possibly these intrusions are related to the basalt, but they could be older. The Triassic-Jurassic age of the basalt (Lanphere, 1983), the fact that it overlies sedimentary rocks of probable Triassic or Jurassic age at the drill hole, and the fact that at its seaward edge it overlies the postrift unconformity (Dillon and others, 1983) all indicate that the basalt postdates the early opening of the Atlantic. Possibly the basalt was produced by tectonism at the time of the jump in the Atlantic spreading center to the location of the Blake Spur magnetic anomaly (Klitgord and Behrendt, 1979). The long hiatus represented by the time interval between the extrusion of the basalt and the deposition of the overlying Upper Cretaceous sedimentary rocks allows sufficient time for significant erosion of the basalt. Probably the extent and thickness were originally much greater than the 100,000 km² remaining today. The generally very smooth character of the J reflection supports the idea that this erosion also would have removed relief associated with any pre-Late Cretaceous tectonic activity.

Triassic Faulting

Reflections from deeper horizons below the basalt are common throughout the area (for example, see fig. 2) but are not easily identified. A reflection, referred to as B, in the area of the Cooke fault on land line SC10, (Schilt and others, 1983; Hamilton and others, 1983) is probably from crystalline basement of Paleozoic or older age. Other deeper reflections on the land data were identified as from possible Triassic sedimentary rock or additional basalt flows. Generally, in the marine data, we cannot easily identify the B reflection.

An example of a probable Triassic graben below the J reflection is shown in figure 5. The J reflection is apparent at about 1.0 s; earlier reflections are from undefined Upper Cretaceous and Tertiary sedimentary strata. Diffractions are quite visible below J; we interpret them to be from boundary faults. Dipping reflections at the left side of the basin appear to flatten at about 1.5 s, which would correspond to a depth of about 2.0 km (assuming a velocity of 4.0 km/s) for the sedimentary rock below the J reflector. In the center of the graben in figure 5 are a number of apparent reflections at still greater depths, but they may be "pegleg" multiple reflections. The lack of deformation of the reflections above the boundary faults indicates that there has been no movement on these faults since Late Cretaceous time when the overlying sedimentary rocks were deposited. The boundary faults observed in the record section of figure 5 are shown in figure 1; the basin is 12 km across. We are not able to correlate this structure with anything similar in appearance on the parallel line CH2 10 km to the southeast, so the structure seen in figure 5 must be of limited extent.

Cretaceous(?) Faulting

We interpret the structure (visible on the interpretation shown by Dillon and others, 1979) shown in figure 6 (location indicated in fig. 1) as possibly the result of Cretaceous(?) faulting. There could be a fault at the left side of the depression, where diffractions are conspicuous, but the evenness and similarity in depth of the J reflection on either side of the depression suggests some form of collapse. In either case, we would expect erosion to have removed evidence of this feature during the long interval between the extrusion of the basalt (~184 million years ago) (Lanphere, 1983) and the deposition of the sediments in Late Cretaceous time. On this basis, we assign a Late Cretaceous(?) age to the origin of the structure. Until additional seismic-reflection profiles indicating trend, length, and other aspects of the feature become available, we will not speculate further as to its origin or tectonic significance.

Cenozoic Faulting

Behrendt and others (1981) and Hamilton and others (1983), in discussing the Cenozoic movement on the Cooke fault (fig. 1), pointed out that future corroboration of the association of the Cooke fault or other faults with seismicity will be important to assessing the earthquake risk in areas of similar tectonic setting. One of the main objectives of the marine multichannel seismic-reflection work was to gather evidence bearing on this problem.

The marine seismic profiles have allowed us to define several faults that show evidence of Cenozoic movement. We have named the best documented fault zone the Helena Banks fault; its location is indicated in figure 1 where it is crossed by the multichannel and single-channel profiles. The fault is seen on an enlargement of a part of the record section from line CH4 in figure 2. Figure 7 is an enlargement of the original 6.4 cm/s display of the same data at one-third the vertical scale of

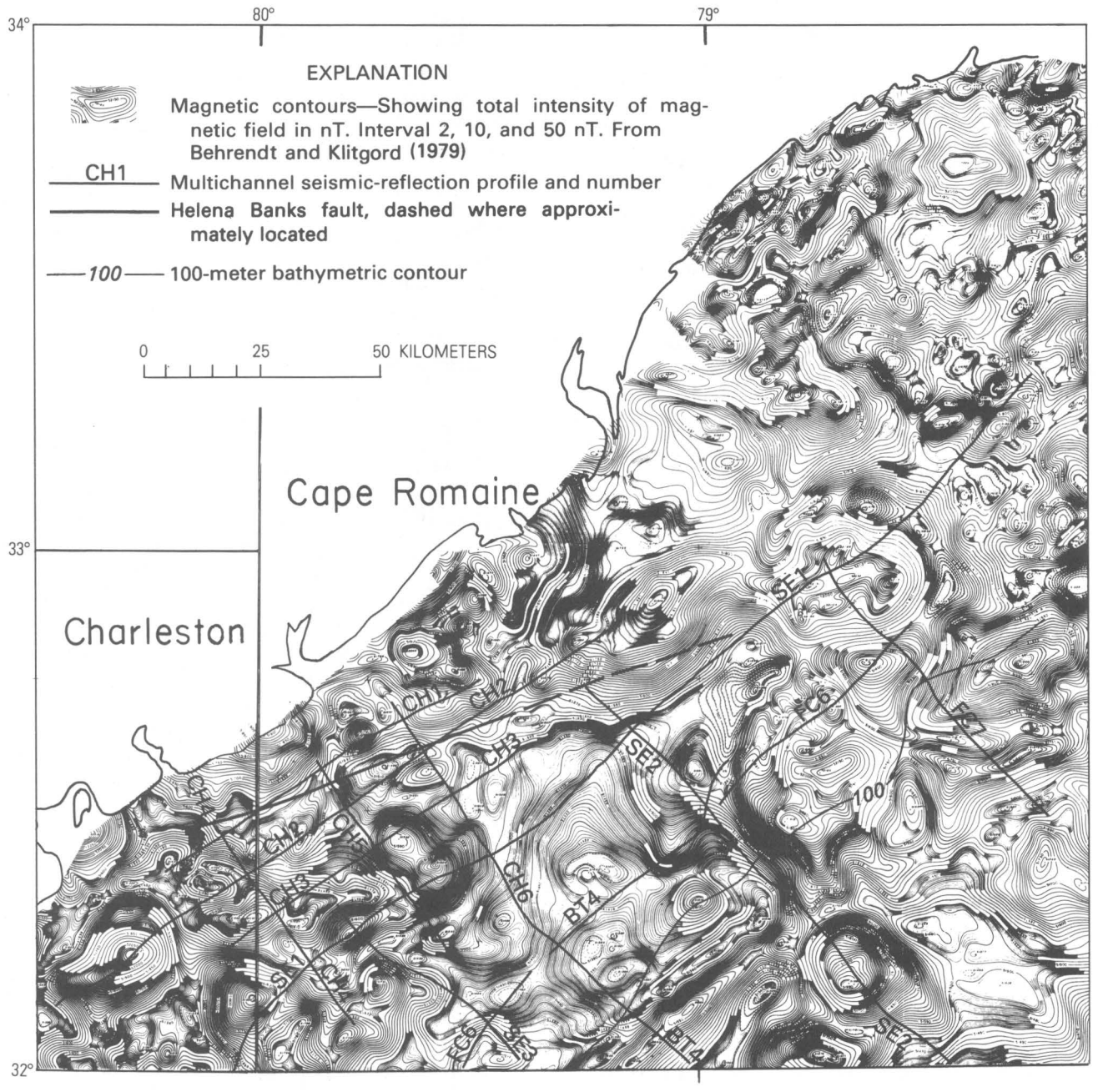

FIGURE 4.—Part of aeromagnetic map over the continental margin, from Behrendt and Klitgord (1979); contour interval 2 nT. Locations of multichannel seismic-reflection profiles and the Helena Banks fault are shown. The 100-m bathymetric contour is indicated.

figure 2. The coincident high-resolution profile over this feature is shown in figure 8. The Helena Banks fault is clearly seen on multichannel lines CH4, 5, and 1 and on the corresponding single-channel lines. Figures 9 and 10 are from line CH5 and the corresponding high-resolution line. Another profile crossing at a low angle to the strike of the fault is shown in figure 11 from line CH1. To the northeast, evidence of the Helena Banks fault is not as clear, but there are features on seismic profiles along the projected strike that may represent the fault; one of these profiles is shown in figure 12.

Displacement on the Helena Banks fault is significantly greater on the reflections below J than on J and shallower reflections; this difference in amount of displacement indicates reactivation of an older, possibly Triassic, structure. The Helena Banks fault is down to the southeast, and the progressive southeastward shift of the inflection in the reflections upward in the record

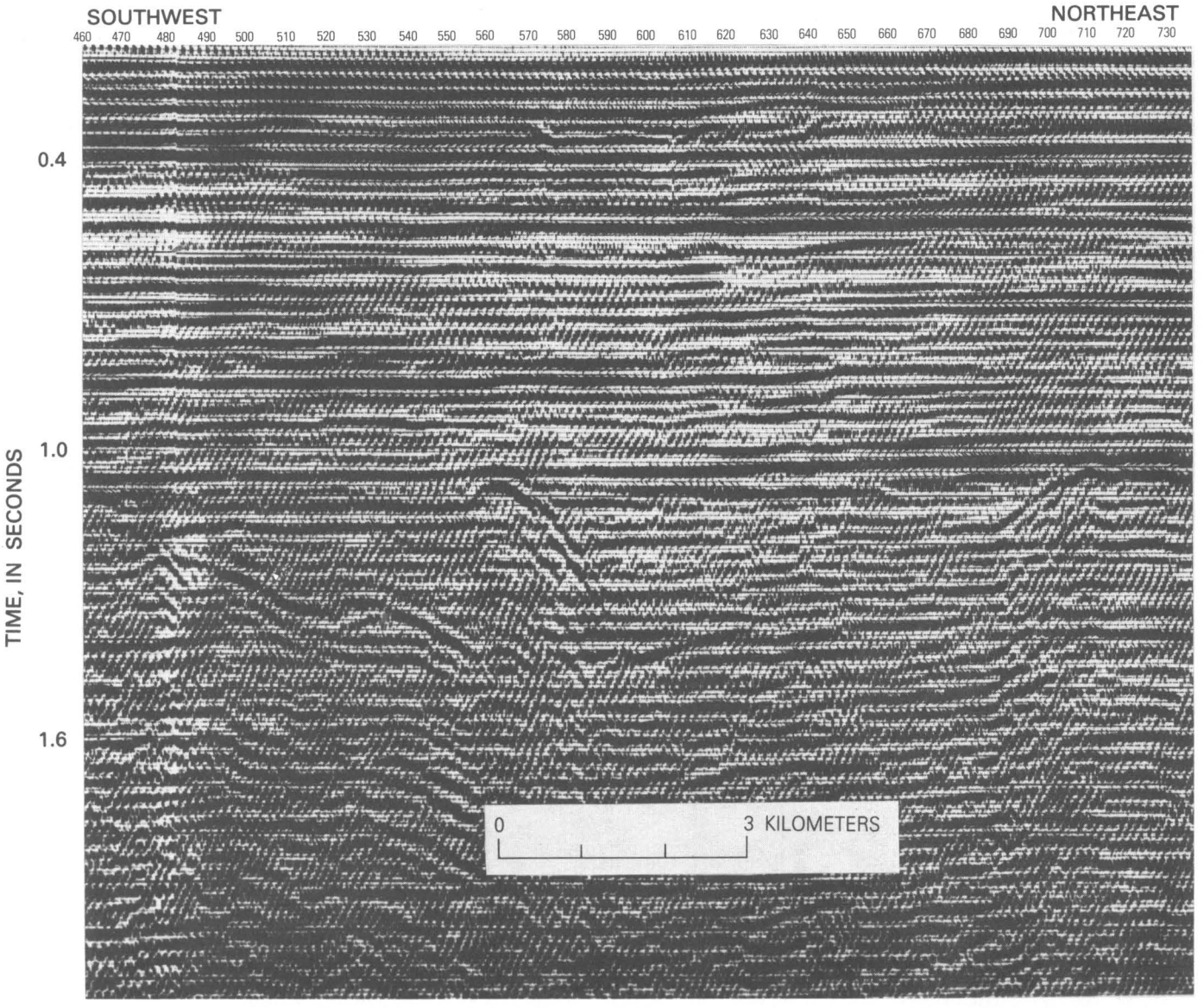

FIGURE 5.—Part of seismic record section from line CH2 over an inferred Triassic graben (fig. 1). The strong reflection at about 1.0 s is J.

section (for example, figs. 2, 7, 9) indicates that it is a high-angle reverse fault. We cannot pick the basement reflection, but reflections (for example, fig. 2) indicate about 80 m displacement below J (assuming 4.0 km/s velocity below J) and about 20 m on the J reflection (assuming 2.0 km/s above J). The shallowest reflections on figure 3 indicate about 15 m displacement. The shallowest displacement in the high-resolution record of figure 6 shows about 10 m or less of warping associated with this fault. Although the displacement on the J reflection suggests an actual break on the basalt layer, deformation of shallow reflections appears as a monoclinal flexure. This type of structure would be expected in poorly consolidated sediments, in association with faulting at depth. The shallowest deformation appears to be about 10 m below the sea bottom (figs. 8, 10). The strata represented by the shallowest observed deformed reflections are probably Miocene clay. Coring by the Skidaway Institute indicates that the shallower, apparently undeformed, acoustically transparent strata are probably unconsolidated sand of Miocene or Pliocene age. We would not expect to see any seismic-reflection evidence for deformation in the sand, even if it were present.

Consequently, we cannot date the most recent movement in the Helena Banks fault as younger than Miocene or Pliocene. No known seismicity is associated with the fault. We have no evidence of any seismicity in the offshore area near Charleston, but, as mentioned previously, the seismic net installed in 1973 cannot detect events

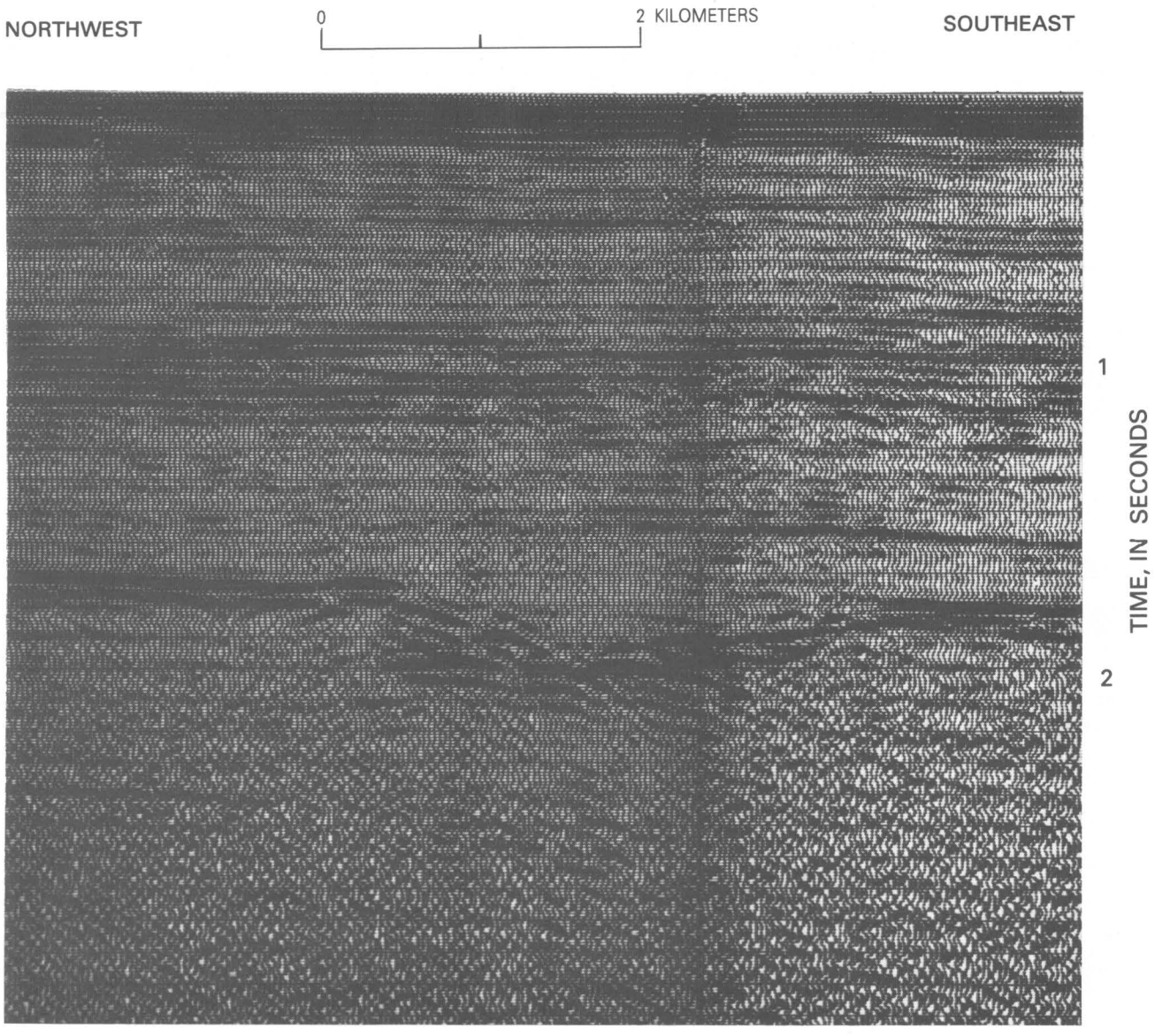

FIGURE 6.—Part of record section along line BT4 showing Cretaceous(?) fault or collapse structure. The conspicuous reflection at about 1.8 s is J.

of magnitude smaller than about 2 in the area of the Helena Banks fault. Prior to 1973, small events would have been undetected, and larger events may have been assigned a location no more precise than the general Charleston area. Nevertheless, the evidence for post-Miocene or post-Pliocene movement and the general seismicity of the Charleston area raises the possibility that the Helena Banks fault is a source of seismic activity.

Other faults of unknown trend displacing Cenozoic rocks were crossed by the seismic lines as indicated in figure 1. Some, but not all, of these faults are similar in appearance to the Helena Banks fault (pl. 1). Part of the reflection record from line CH2 (fig. 13) shows a zone of obvious disruption of the J reflection (fig. 1) about 10 km from the southwestern end of the line. This zone could be interpreted to continue to the southwest end of the line. Evidence of displacement or warping of shallower beds, where indicated by the arrow (fig. 13), is visible as shallow as about 0.2 s depth, which probably corresponds to rocks of Eocene age. We interpret this to mean that the basalt surface was faulted and disturbed in probable Late Cretaceous time (evidence of any earlier movement would probably have been removed by erosion) and that this fault was reactivated in Cenozoic time. A diffraction on the J horizon in the left part of

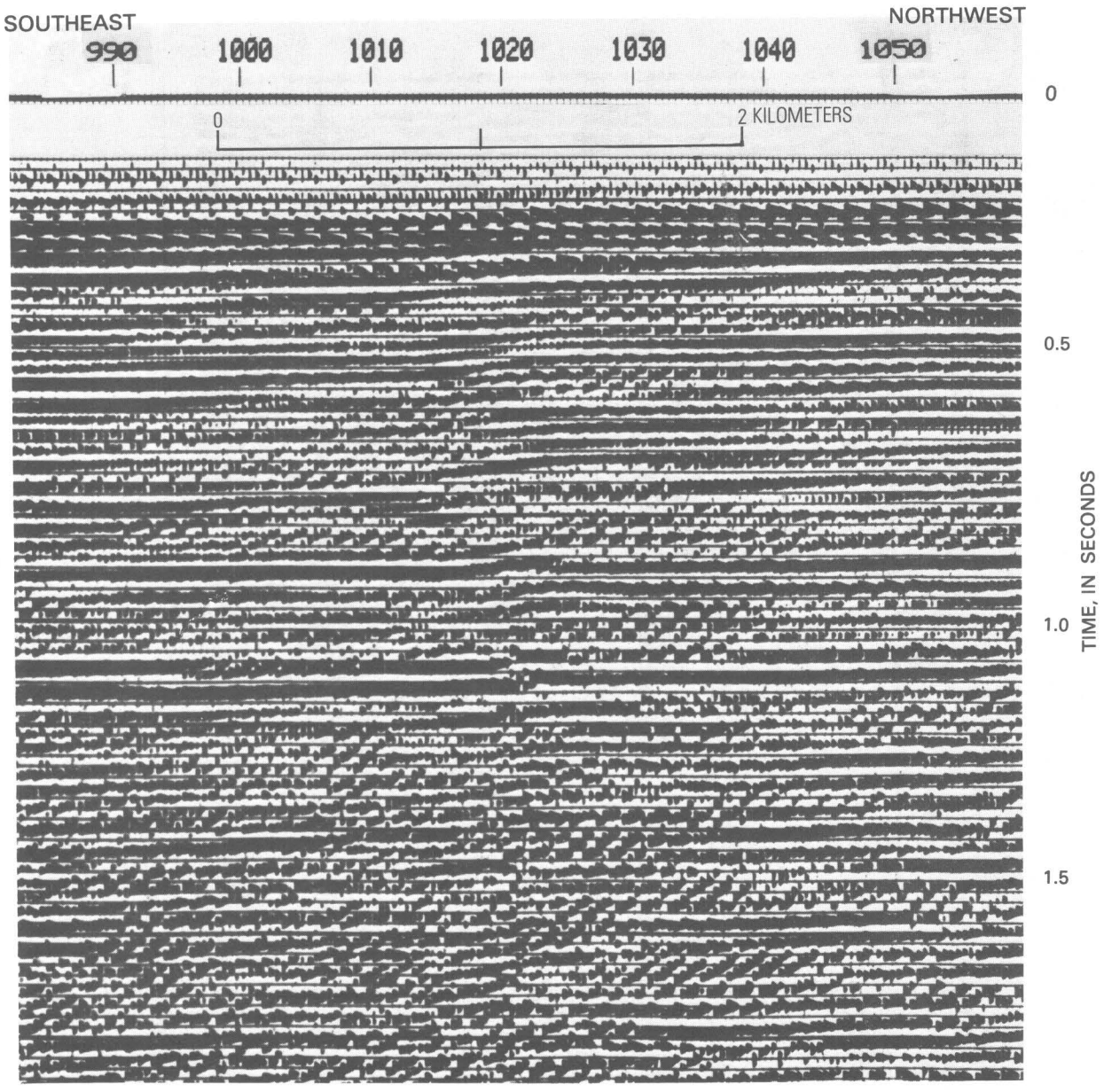

FIGURE 7.—Part of seismic record section from line CH4 crossing Helena Banks fault at about SP1020; one-third the vertical scale of figure 2.

figure 13 indicates a probable fault, but there is no evidence of offset on the shallower beds above this point.

Channel Deposits

Other shallow features observed in the multichannel data are probably not evidence of Cenozoic faulting. A feature shown in figure 14 from near the northwest end of line CH6 shows a velocity pullup of reflections below 0.5 s and a trough structure in shallower reflections. Similar features were also observed on lines CH1 and CH2. The three features define a northwest-striking trend that projects toward the vicinity of Charleston harbor. We interpret these features to be channel deposits filled with sediments of higher velocity than that of the material into which the channel is cut.

We do not interpret the apparent upwarping or doming of the J reflection at 1.0 s and of the other reflections at as shallow as 0.45 s to be evidence of structure or faulting. Rather, we believe that the reflections below 0.45 s were pulled up by higher velocity sediments within the channel-fill deposit. If we assume that the J reflector actually is flat, as it is over most of the region, and assume 2.0 km/s for the velocity from the surface to

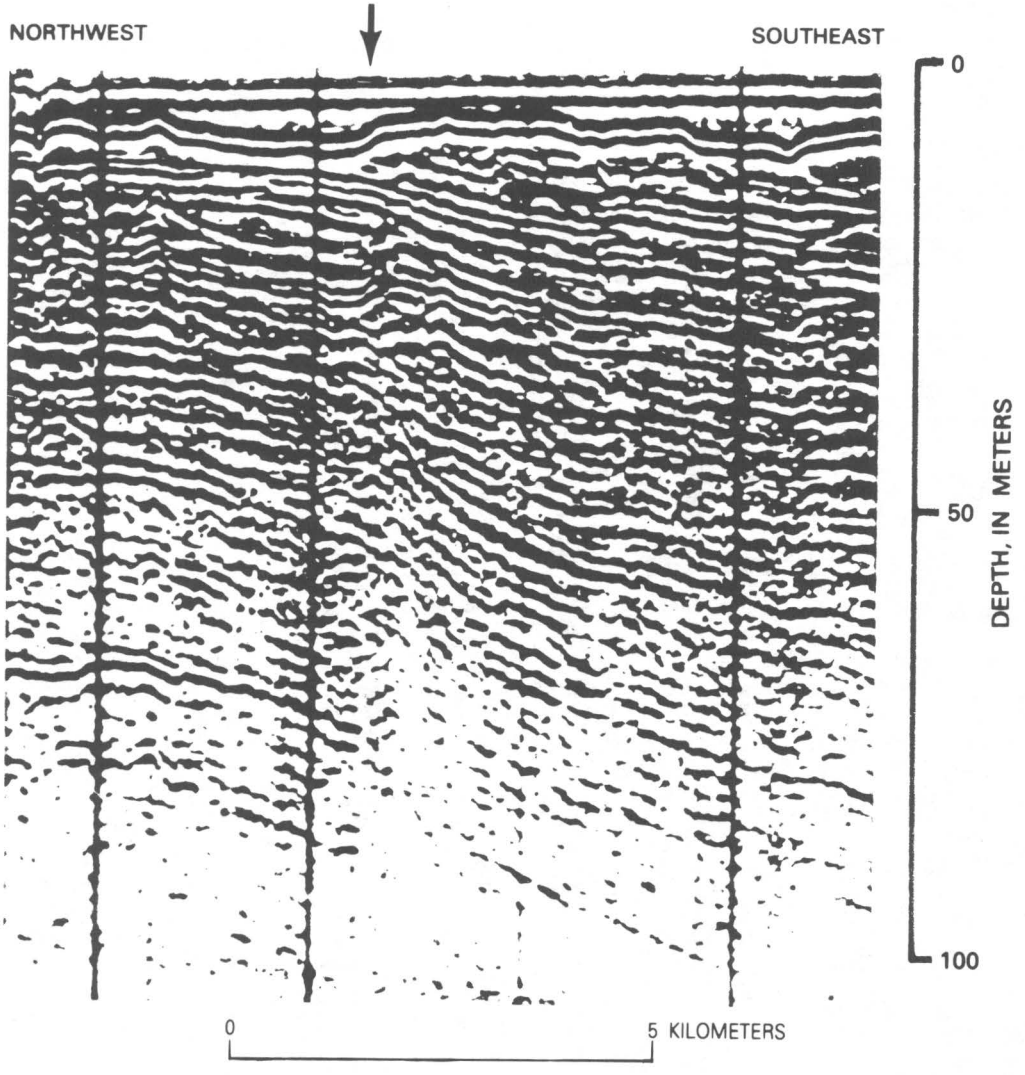

FIGURE 8.—Part of single-channel seismic record section crossing Helena Banks fault (arrow) recorded along multichannel line CH4 (figs. 2 and 7). Note extreme vertical exaggeration compared with figures 2 and 7.

the J reflector just northwest of the channel in figure 14, then the depth to the J horizon is 1.0 km, which corresponds to a reflection time of 1.0 s. Where the channel has a reflection depth of 0.39 s and a corresponding J reflection pullup to 0.97 s, the velocity of the channel fill would need to be 2.15 km/s, or about 8 percent higher than the velocity of sediments on either side.

Many of the Upper Cretaceous units along the coastal margin of South Carolina contain channel-shaped and lens-shaped bodies of deltaic and nearshore-marine sand within dominantly clayey sequences (Gohn and others, 1977). In particular, Campanian sands of restricted lateral extent are found in the area immediately onshore from the seismic grid and in the depth range of the channels seen on the seismic profiles (Gohn and others, 1978). By means of the interval-transit-time log from the Clubhouse Crossroads #1 drill hole (CC#1) located northwest of Charleston, average interval velocities for Campanian sands and clays were calculated. The average velocity for the best sorted sand in the Campanian section was calculated as 2.17 km/s, whereas the average velocity calculated for Campanian marine clays is 1.98 km/s (G.S. Gohn, written commun., 1980), a difference of 0.19 km/s or about 10 percent. It is likely, therefore, that the channels and associated velocity pullups seen in the multichannel data can be attributed to velocity variations between sands and laterally adjacent clays within the Upper Cretaceous sedimentary section.

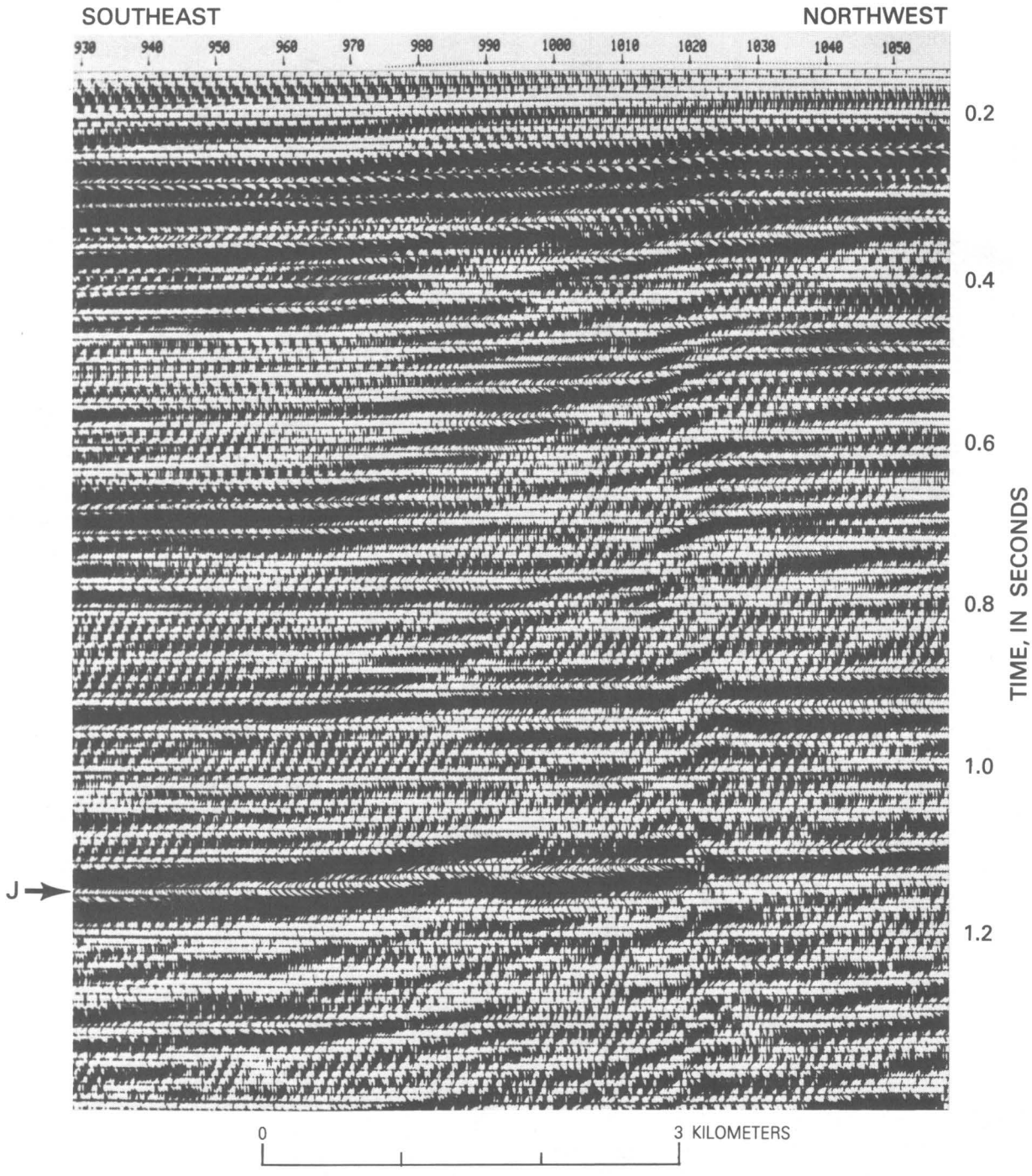

FIGURE 9.–Part of seismic record section from line CH5 crossing Helena Banks fault (arrow).

Intrusive Structures

Figure 4 shows a part of the aeromagnetic map (Behrendt and Klitgord, 1979) covering the area offshore of Charleston; the offshore seismic lines of figure 1 are indicated. A north-south trending group of 300–350 nT amplitude, having three conspicuous circular positive anomalies, suggests a series of magnetic (mafic?) intrusions. Grow and others (1979) briefly discussed the 80–100 mGal associated gravity anomalies and suggested their origin as mafic intrusions within the Paleozoic basement or Triassic rift complexes. We have examined the seismic-reflection data for lines FC6, FC7, and SE1 (Dillon and others, 1979), which cross these anomalies as indicated in figure 4. Figure 15 shows the part of line FC6 crossing one of the intrusions. The J

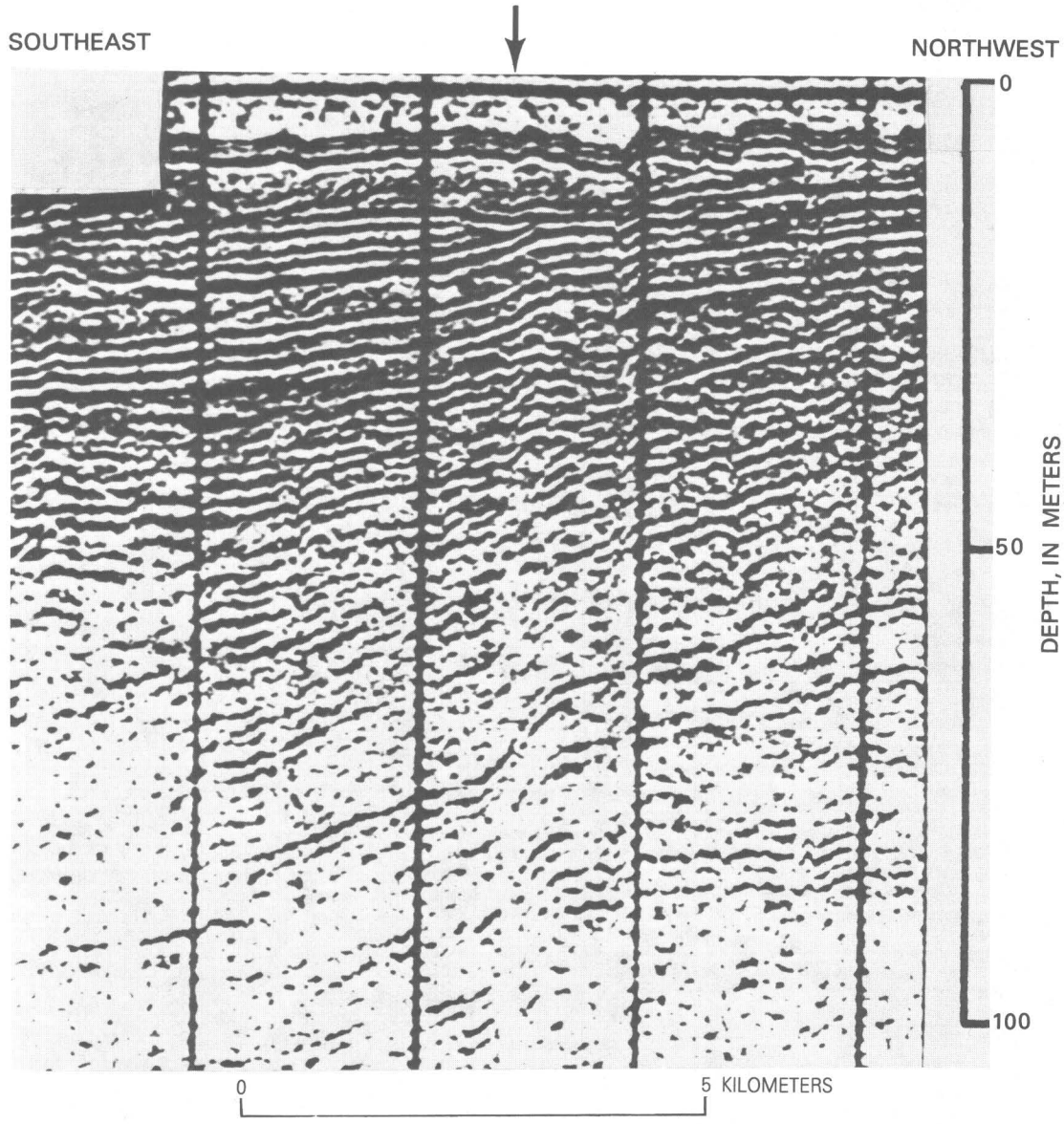

FIGURE 10.—Part of single-channel seismic record section, recorded along multichannel line CH5, crossing Helena Banks fault (arrow).

horizon merges with a disrupted reflection obviously correlated with the intrusion. We cannot distinguish among three possible age relationships: (1) the reflection from the intrusion cuts across the J reflection, which indicates a younger age for the intrusion; (2) the intrusion and the J horizon are syntectonic, which suggests that the intrusion is the source of the basalt layer; or (3) the topography on the intrusion is an erosional remanent around which the basalt flowed when it was extruded.

There is some deformation of the sediments over the intrusion, which is seen as a slight doming of about 20 ms as shallow as 0.5 s reflection time at about SP1790 and the suggestion of a syncline at about SP1860. These effects probably were caused by draping of the sediments over the intrusion at the time (Late Cretaceous and younger) of deposition, but they could be an indication of movement or emplacement subsequent to sedimentary deposition. There should be more obvious effects on the sedimentary rocks as indicated on the seismic section if the plutons were intruded at a later date, as was the Late Cretaceous intrusion in the Baltimore Canyon trough offshore from New Jersey (Schlee and others, 1976). If the buried topography existed when the basalt was extruded, we would expect the long period of erosion between the Triassic-Jurassic basalt extrusion and the deposition of the Upper Cretaceous sedimentary

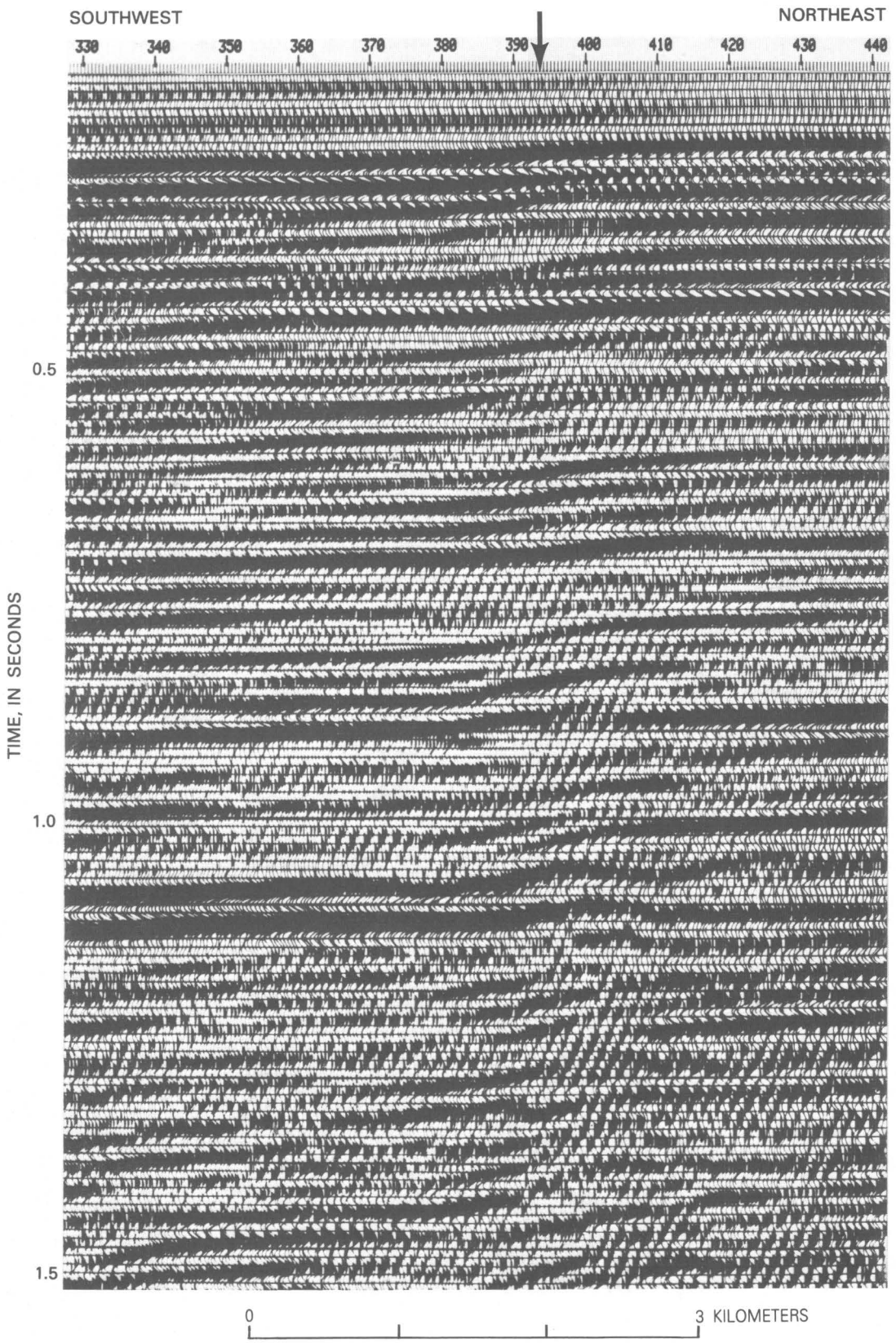

FIGURE 11. – Part of record section along line CH1 crossing Helena Banks fault (arrow).

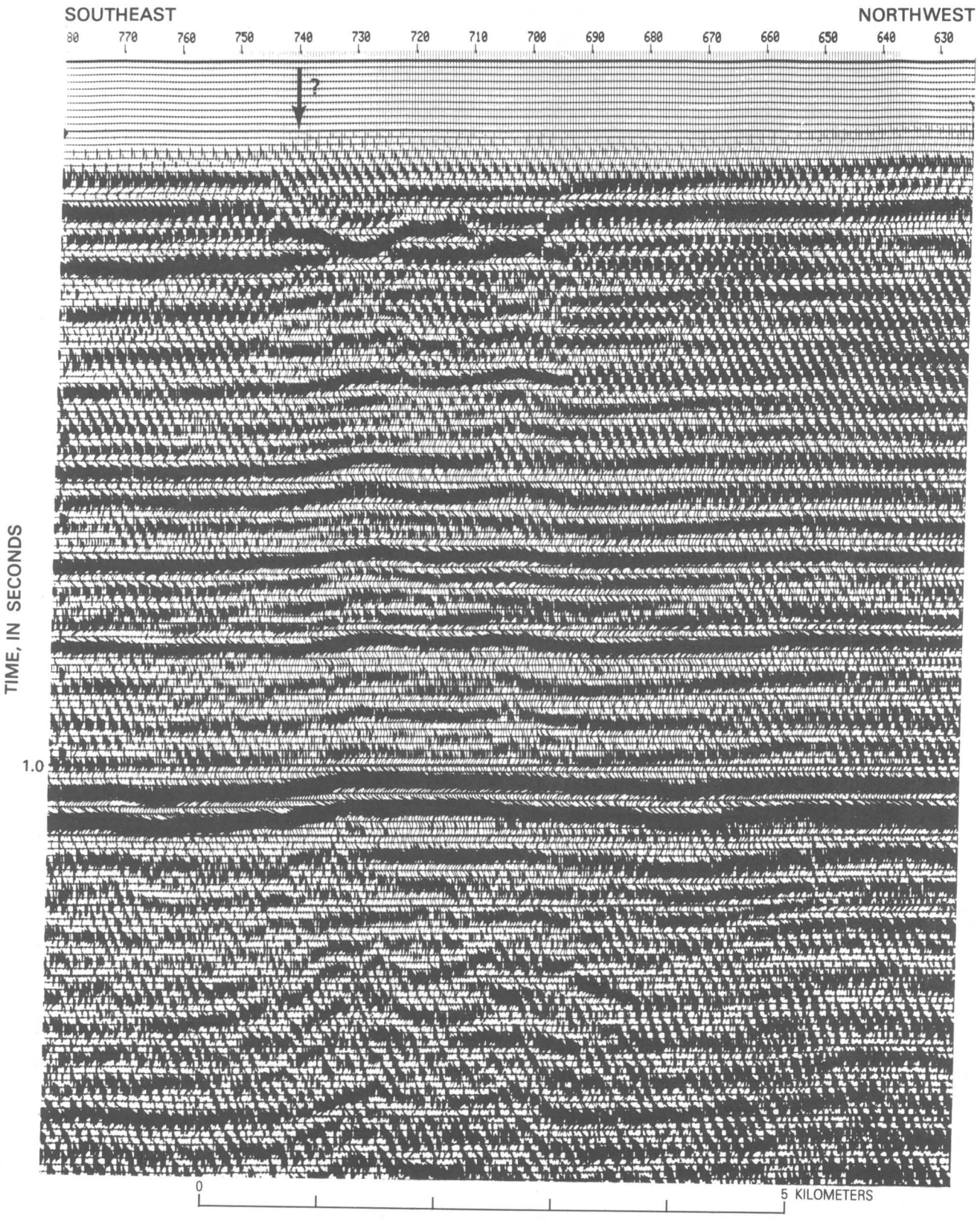

FIGURE 12. – Part of record section along line CH2 crossing projection of Helena Banks fault indicated in figure 1. Arrow indicates possible fault or velocity pullup.

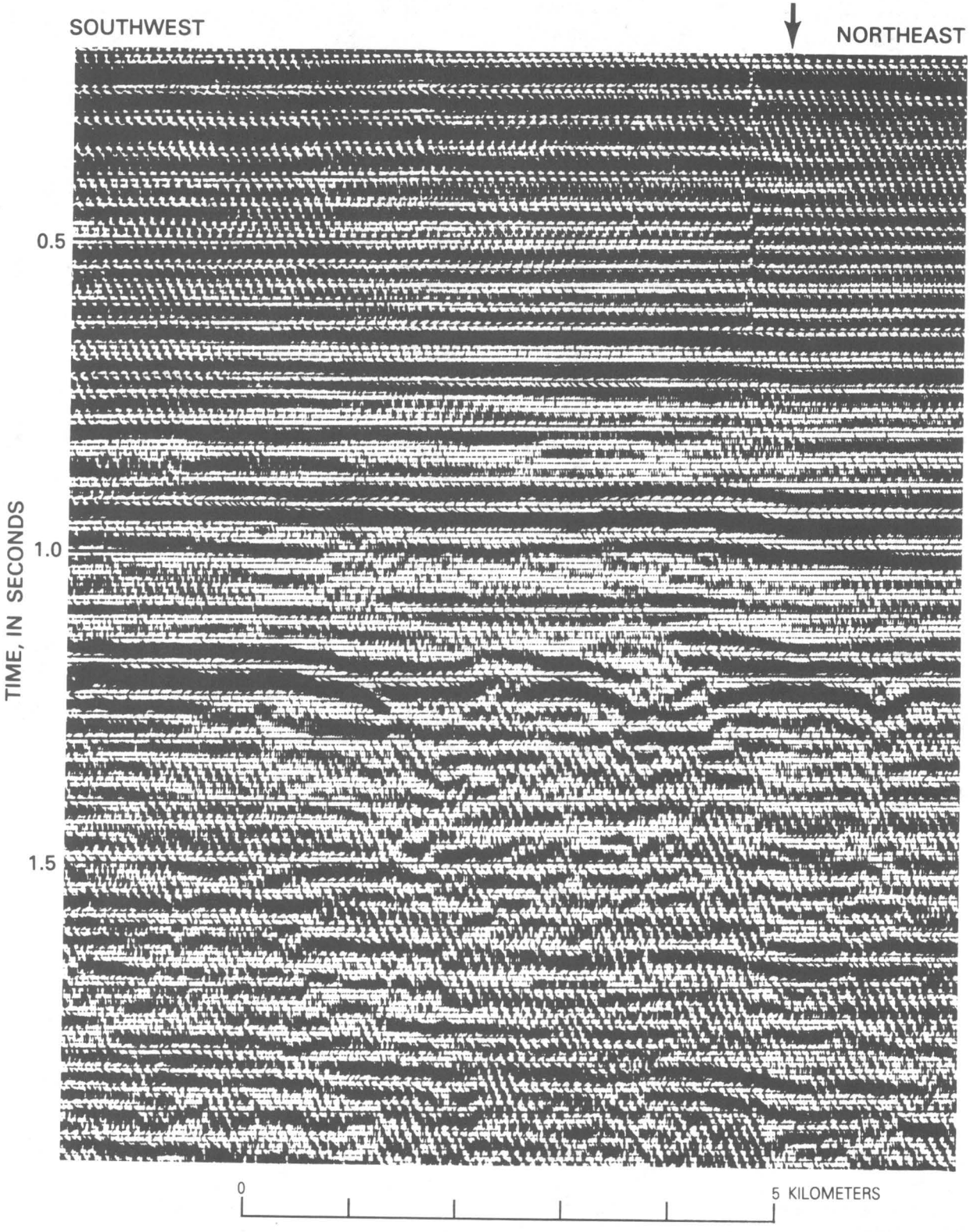

FIGURE 13.–Part of record section along line CH2 crossing inferred fault near southwest end of line indicated in figure 1.

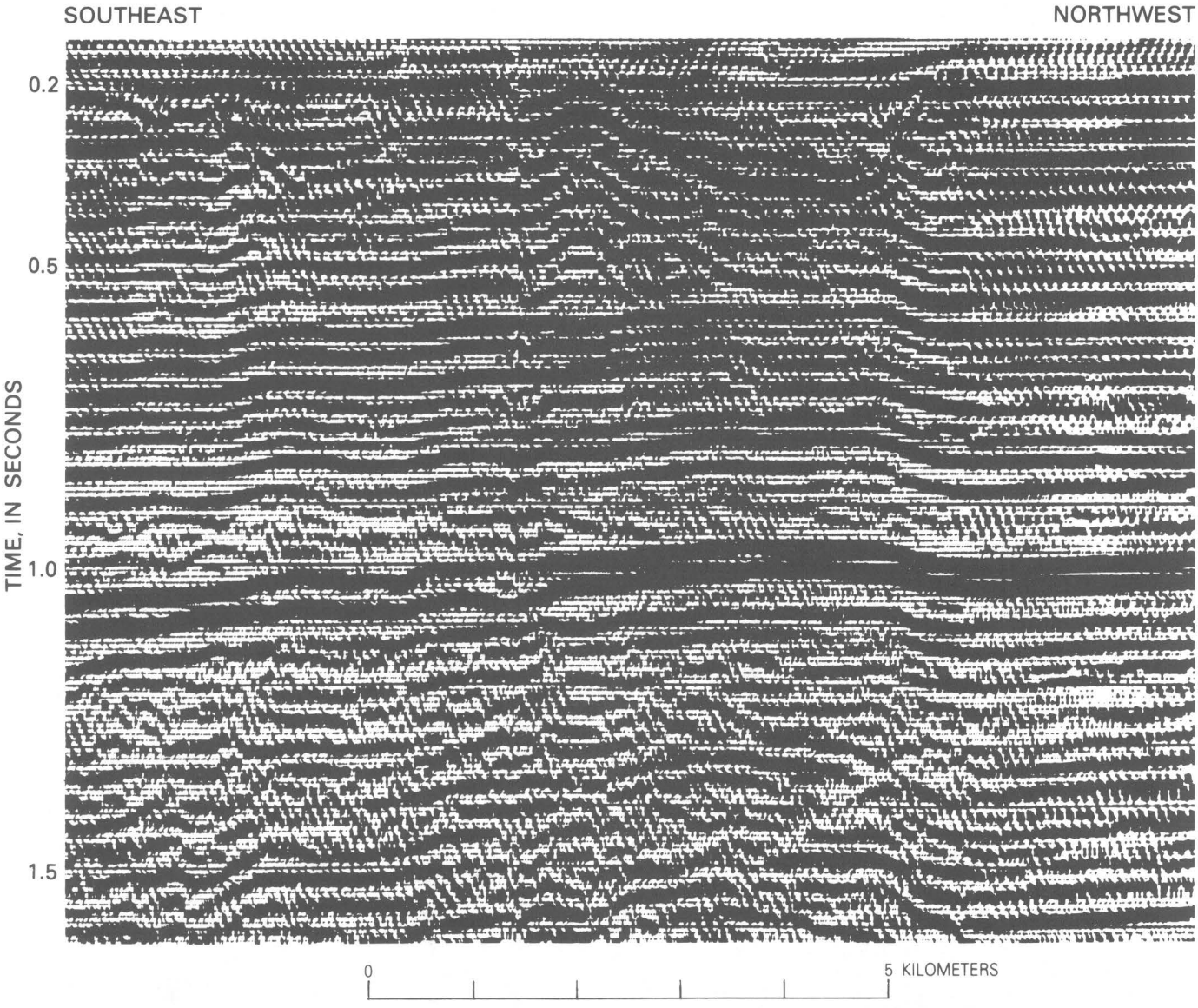

FIGURE 14.—Part of record section along line CH6 crossing inferred channel off Charleston harbor. Note effect of velocity pullup, interpreted to have been caused by higher velocity sediments in channel above 0.4 s.

rocks to have removed the topography associated with the intrusion, but possibly this was not the case.

The question of age of the intrusions is important not only because they might be related to Mesozoic or Cenozoic tectonic activity but also because the north-south trend they define is parallel to and about 50 km east of deep (4–8 s) westward-dipping, north-striking reflections(?) or diffractions discussed in the section on deep crustal reflections. The only other north-south trends in the area are some of the diabase dikes of inferred Triassic or Jurassic age north of the coast between about 79°10′ W. and 79°40′ W. (Popenoe and Zietz, 1977), which are interpreted from magnetic data.

DEEP CRUSTAL REFLECTIONS

The preceding discussion of results is restricted primarily to the basalt layer and shallower sedimentary rocks. Hamilton and others (1983) and Schilt and others (1983) discussed the B reflection beneath the J reflection from the basalt layer observed in the land data and suggested that B is from crystalline basement, Triassic sedimentary rock, or additional basalt flows. We do not see a reflection in our marine data in the second or so below J that we can correlate with B in the land survey. The velocity analyses indicate that a number of the seismic arrivals below J (for example, see fig. 2), are

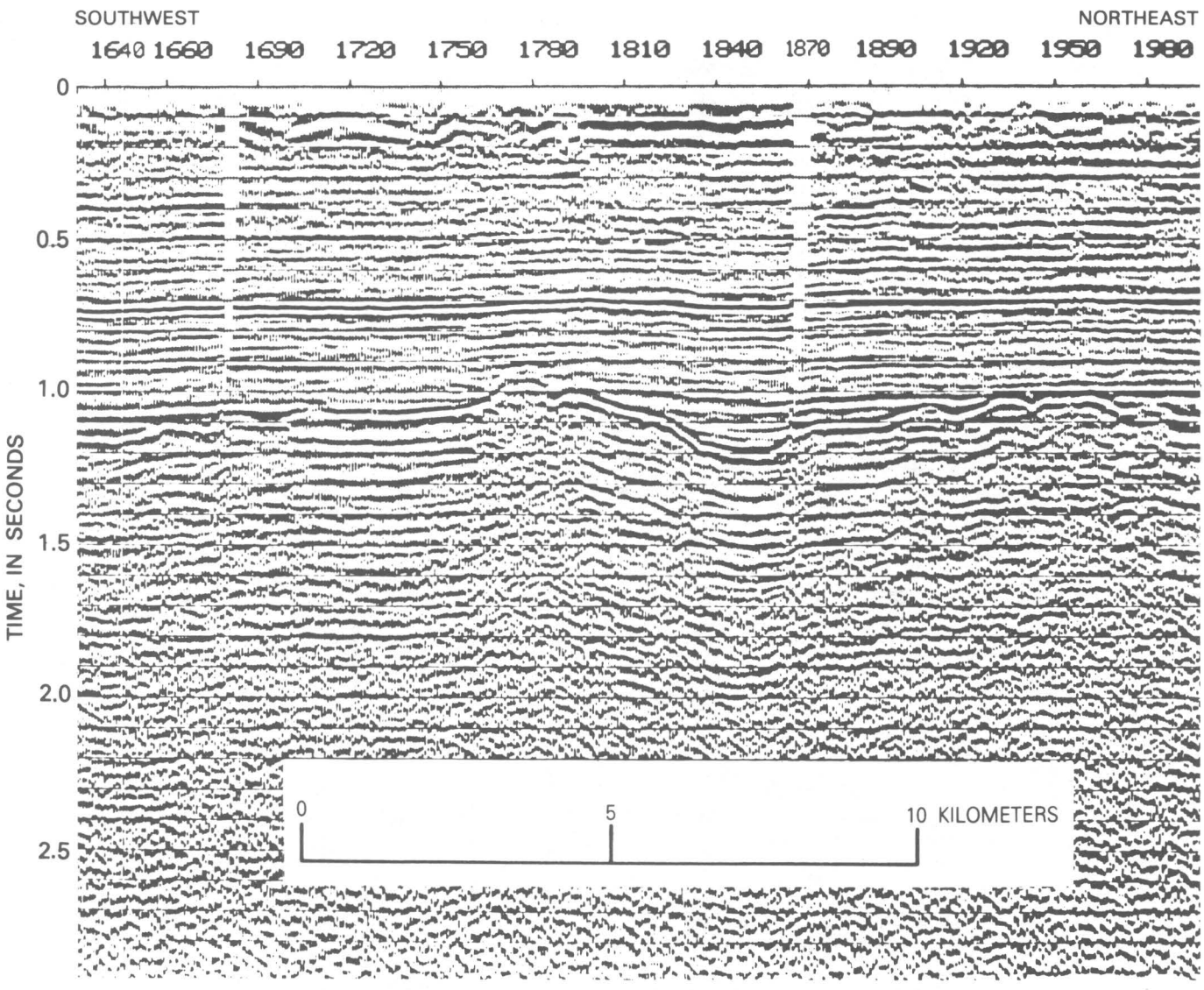

FIGURE 15.—Part of record section along line FC6 over inferred intrusion, shown by magnetic data on figure 4.

reflections from real geologic layers, but we are concerned that many are "pegleg" multiple reflections from within the sedimentary section above and including J. For the most part, Dillon and others (1979) were not able to interpret reliable reflections from other marine data below the basalt layer, although they did identify some on BT4. Therefore, to be conservative, we did not pick reflections from the nearly horizontal arrivals below the J reflection to about 3–4 s, although we believe some to be real.

Figure 16 shows a part of the unmigrated data of line CH2 from the original record section plotted at 6.4 cm/s. The J reflection and shallower reflections from sedimentary rock are seen above 1 s near the top. We will examine three types of events below J, labeled "D," "W," and "M" in the figure. We show examples of each and discuss them in more detail by means of line-drawing interpretations in the following sections.

At about 4 s near the left side of the figure are convex-upward arrivals, which we interpret to be diffractions. We designate such arrivals "D." Figure 17 shows a part of the record section covering the same data from line CH2 as does figure 16. The vertical scale is the same as that of figure 2, which is three times that of figure 16. In an effort to resolve the B reflection, the part of the data below the J reflection were assigned higher stacking velocities, and the data were reprocessed (fig. 17) as was done with the land data (Hamilton and others, 1983). We did not improve resolution of B, but the D diffractions were significantly enhanced above 4.2 s (the data inter-

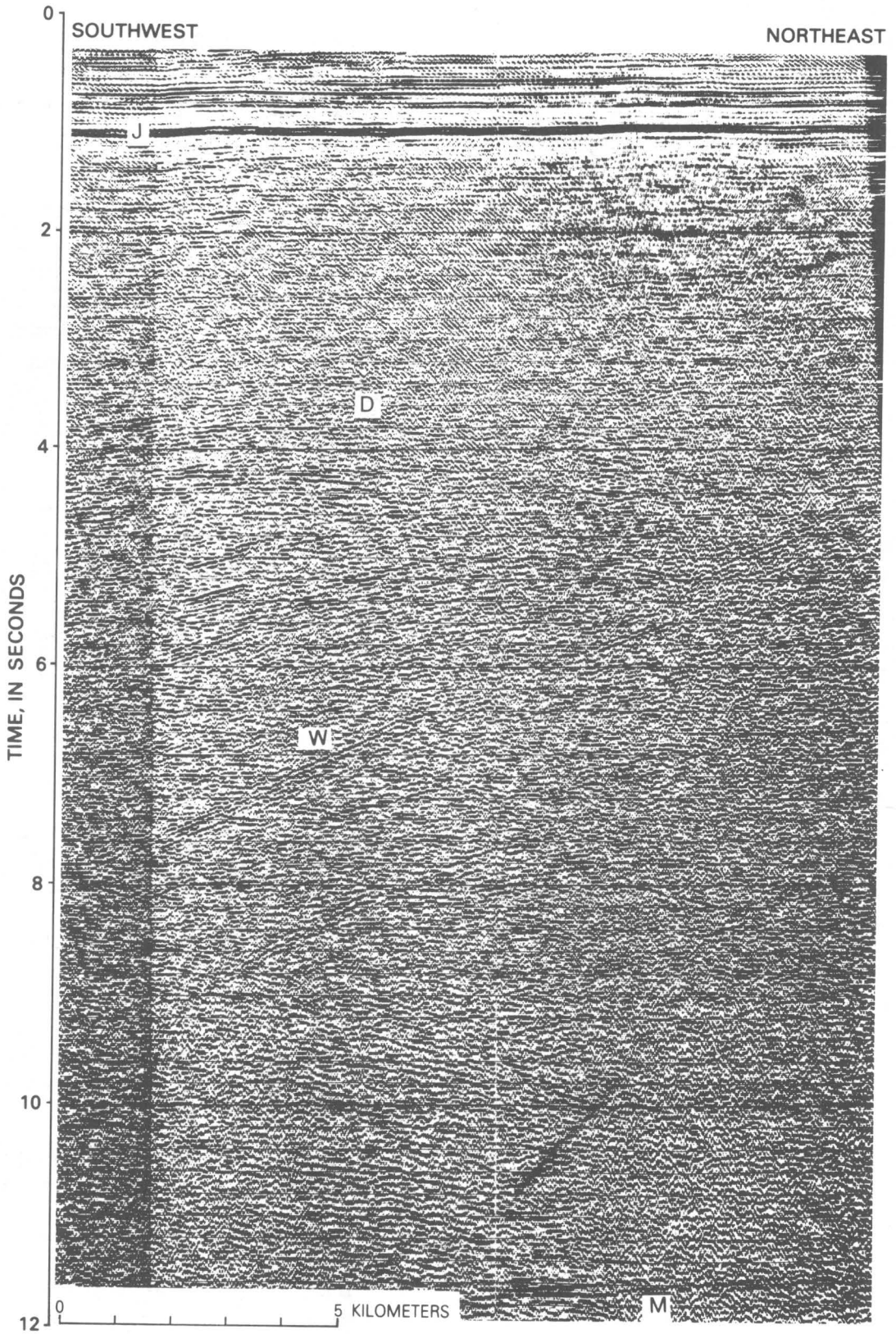

FIGURE 16. – Part of record section along line CH2, shown at one-third vertical scale of figure 2. Note curved diffraction D at about 4 s, W reflection(?) dipping to the left (southwest), and M reflections from the Moho at the bottom of the figure.

val reprocessed). In figure 17, two conspicuous diffractions are visible. The shallower diffraction curves over at about 2.78 s where its northeast part is obscured, and the lower diffraction probably flattens out at about 3.6 s. The lower diffraction may not be deeper than the upper but may be farther out of the plane of the section.

At about 7 s on the left side of figure 16, a series of reflections(?) dipping down to the left can be seen. The reflection marked "W" correlates with one on the cross line CH6 and on line CH3. We will designate this reflection(?) and others of the same trend as "W," for west-dipping. A close-up of a part of the right side of figure 16 is shown in figure 18, which shows part of the W reflection(?) in greater detail.

Another significant group of arrivals in the deepest part of the records (9–11 s on CH5) is probably from the Moho, as shown by an example in figure 19 from the southeast end of line CH5. These reflections are typical of those observed by others (Cook and others, 1979; Hutchinson and Grow, 1979) in the Eastern United States on land and offshore and in the COCORP data at Charleston (Schilt and others, 1983). Note the convex-upward curvature, indicative of diffractions, on some of the arrivals in figure 19.

Plate 2 presents the seismic-reflection profiles in the 1–12 s range but is difficult to interpret at the publication scale. Therefore, we made line drawings to show our interpretation of the data at the 6.4-cm/s vertical scale and reduced these, as shown in plate 3 for lines CH1–CH6. We used a single line weight for each seismic arrival, so the range apparent in the photographs of the record sections has been reduced to a binary code "shown or not shown"; therefore, the bias of the interpreter must be kept in mind by the reader. Several features of the record sections, illustrated as examples in the preceding figures, are clearly visible in the line

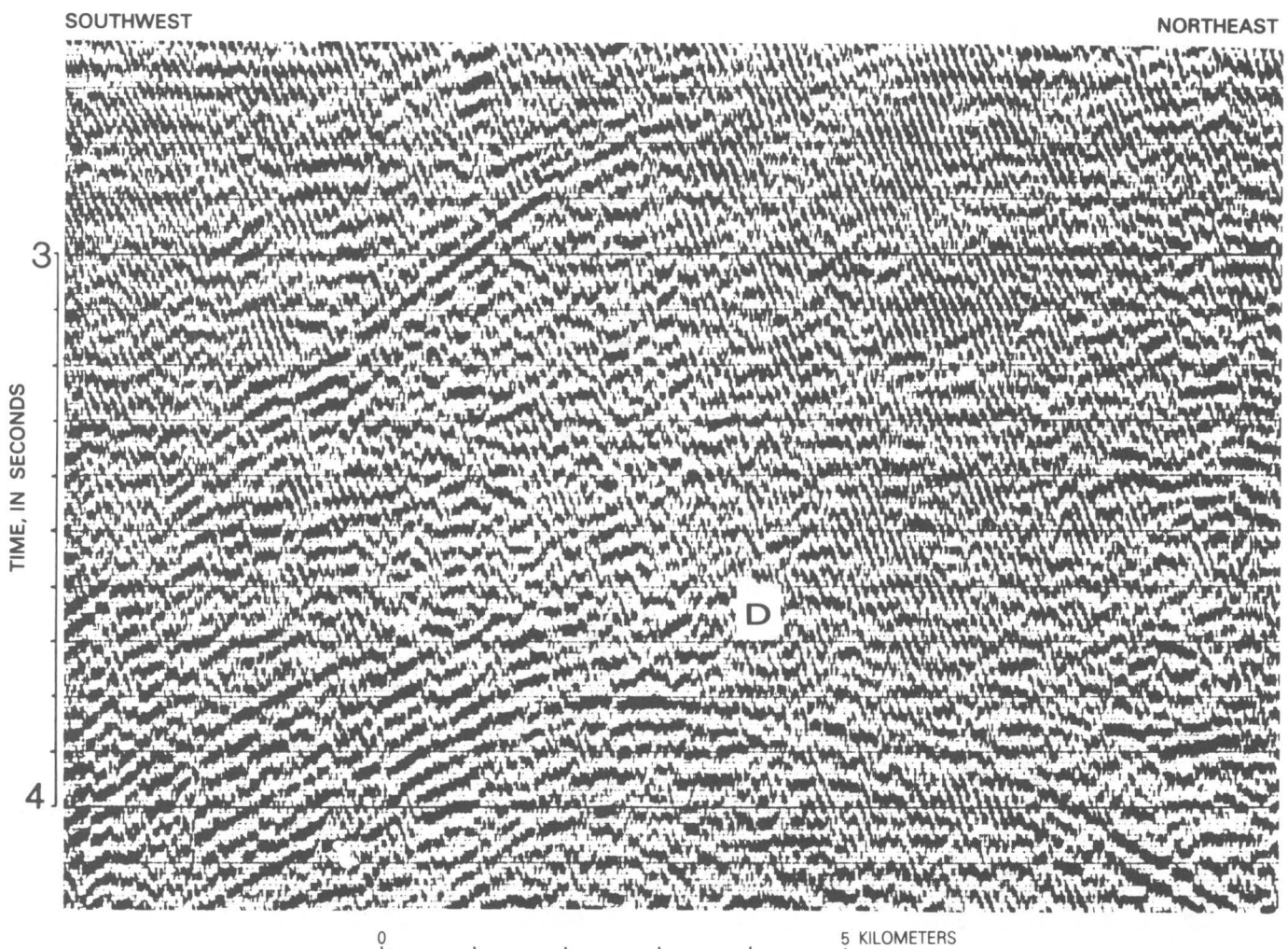

FIGURE 17.—Enlarged part of record section from line CH2 shown in figure 16, reprocessed and displayed at three times the vertical scale of figure 16. Note diffraction, labeled D in figure 16.

drawings. The J reflection, including the Helena Banks fault (lines CH1, CH4, and CH5), and the Triassic basins on a few profiles where obvious are the only shallow features indicated.

Diffractions

The diffractions, some of which we have labeled "D" as discussed previously, are apparent from the convex-upward curves (pl. 3) in the 3–5 s range on all of the lines. We calculated theoretical diffraction curves on the basis of refraction velocities (Ackermann, 1983; Talwani and Amick, 1979); our calculated curves fit these observed curves and support our interpretation that they are diffractions at depth below the seismic profiles. Figure 20 shows a plot of the two-way time in seconds to the shallowest diffraction curves we could pick with confidence from the interpretation shown in plate 3 and from the original records. The mean of the values is 3.7 s; a standard deviation is 0.5 s. If we assume the same velocity function used by Tarr and Rhea (1983) to calculate the focal depths, the average velocity to D is 6.1 km/s; the mean depth thus is about 11.4 ± 1.5 km. Probably, the mean is not as representative of the true minimum depth as is the mean (11.4) – the standard deviation (1.5) = 9.9 km. The diffractions are as shallow as or shallower than measured in the record sections because of the ambiguity due to sources out of the plane of the sections. Therefore, the best estimated depth to the surface defined by the diffractions is about 10 km.

Examination of the D diffractions (pl. 3) shows that the greatest depths for this zone appear to range between 6 and 8 s, which corresponds to depths of 16–22 km. Whether we are looking at several discrete layers or whether there is a more or less continuous zone over the range 9–20 km of structures causing the diffractions

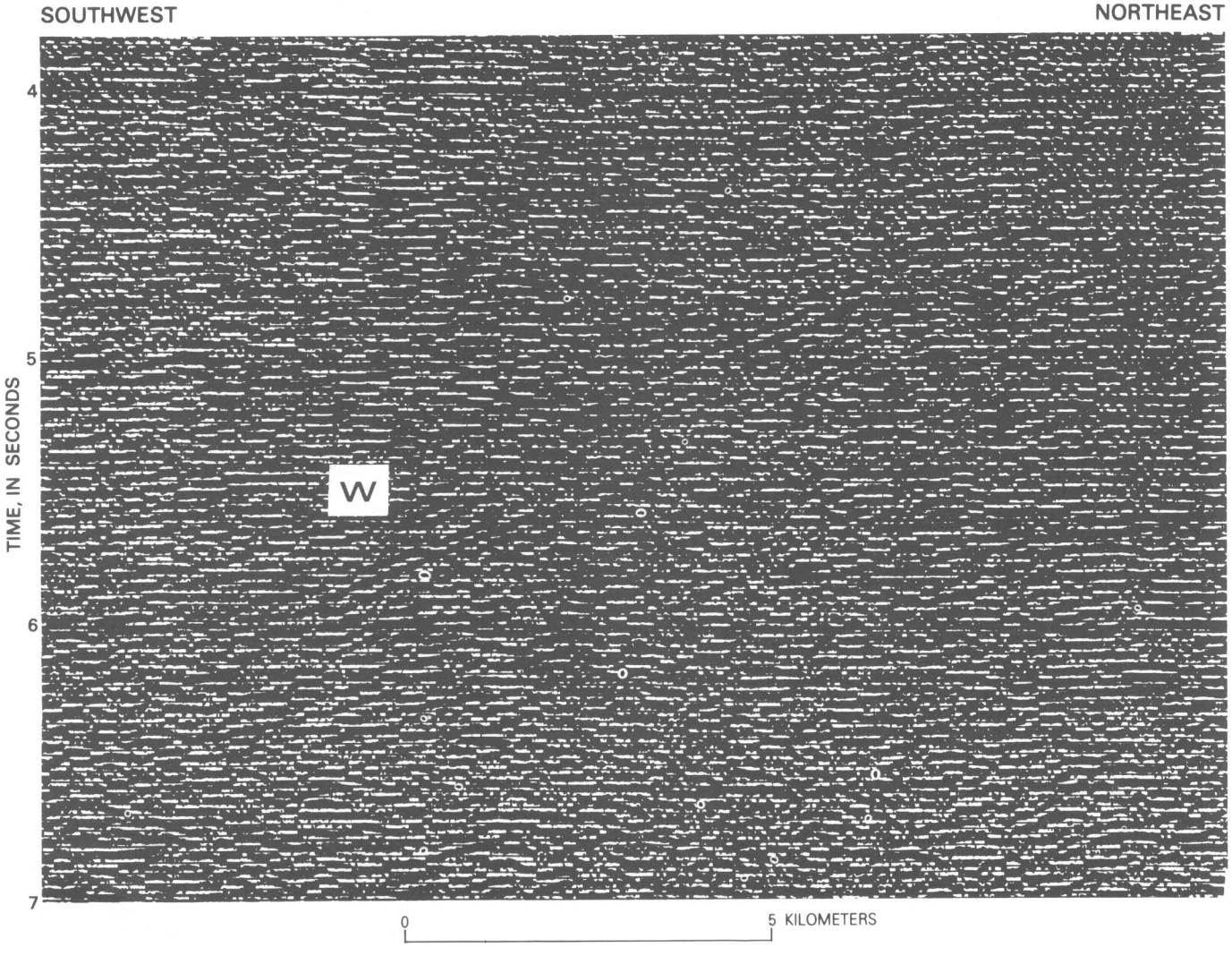

FIGURE 18.–Enlargement of part of record section shown in figure 16. Note W arrival dipping to the left.

cannot be determined from our data. Certainly some of the diffractions at greater times than indicated in figure 20 are from out of the plane of the section, which is the reason we used only the minimum times. We interpret these diffractions as having been caused by "rough spots" (or asperities?), of small dimension relative to the 300- to 500-m seismic wavelength, along a surface or surfaces defined by the shallowest part of the curve, similar to the definition of rough oceanic basement identified by diffractions in seismic-reflection profiles.

Schilt and others (1983) do not interpret any diffractions of this type in the COCORP data, but we reexamined their results and find some evidence of curved arrivals from 3–6 s that could be interpreted as diffractions like those in plate 3. Therefore, we believe that the D surface as defined in figure 20 probably extends beneath the land data (fig. 1).

The hypocenters calculated in the Charleston area range in depth from 3 to 13 km (Tarr and Rhea, 1983). The surface defined by the diffractions would project into the lower part of this range. Therefore, the D surface may represent a tectonic feature associated with the seismicity. Talwani (1982) reported a velocity discontinuity from 5.9 to 6.4 km/s at a depth of 10 km in the area, on the basis of inversion of earthquake and blast data recorded by the local seismograph network. This discontinuity lends supports to the extension onshore of the surface defined offshore by diffractions. This interpretation is treated further below.

Deep West-Dipping Reflections(?)

In the interpretation of plate 3, there is a series of arrivals dipping mostly from right to left but cross-cut by a number of arrivals having the opposite dip. We interpret

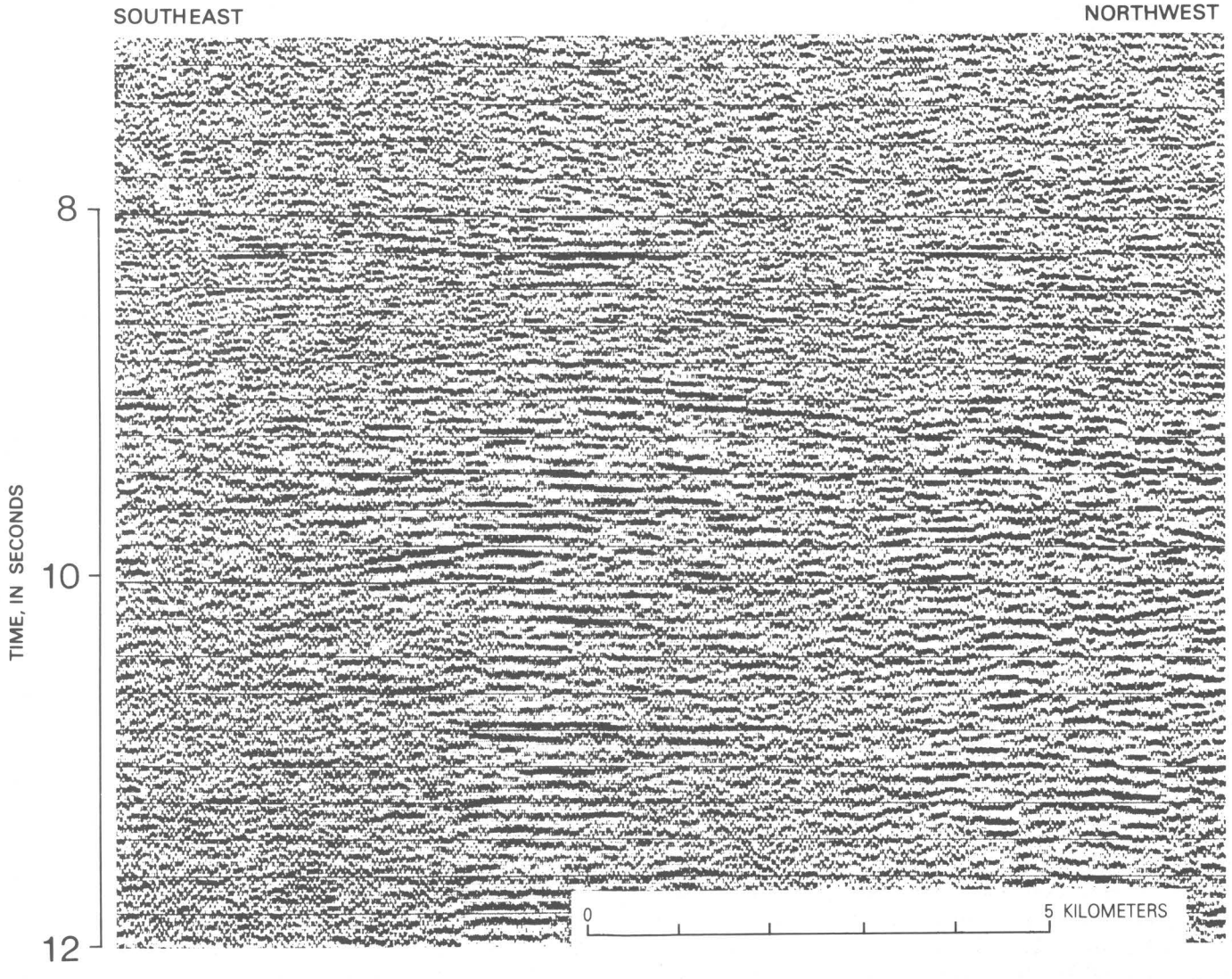

FIGURE 19.—Part of record section at southeast end of line CH5 showing reflections interpreted as having come from the Moho.

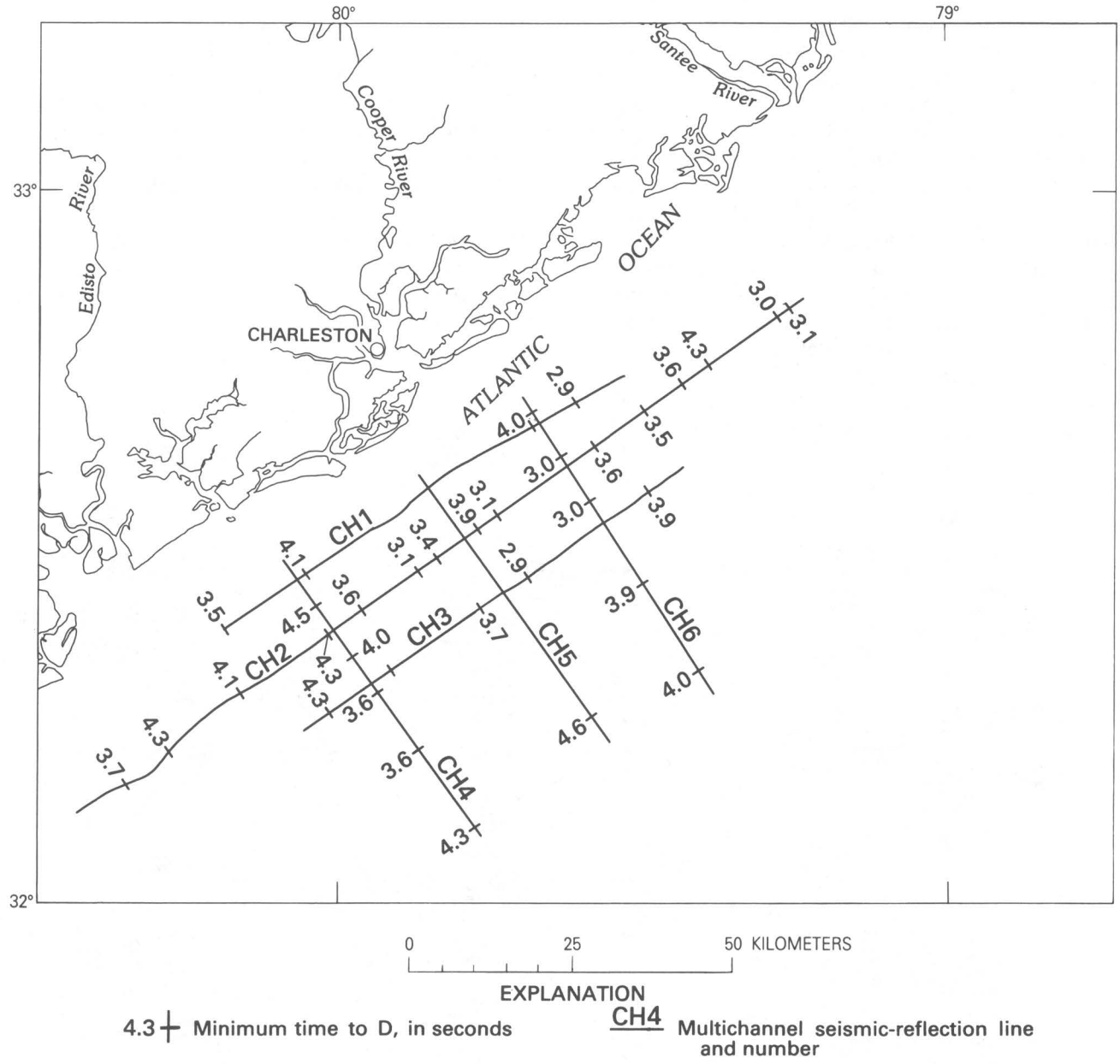

FIGURE 20.—Map showing minimum time in seconds to tops of curves defining diffractions from inferred décollement, which are indicated as D in plate 3. Average time $\bar{t} = 3.7 \pm 0.5$ s, depth $h = 11.4 \pm 1.5$ km.

many of these as the apparently straight "legs" of the diffractions associated with D, discussed above. However, several of these, such as the one shown in the parts of the record section of line CH2 (figs. 16, 18), have a different appearance. We have labeled a particularly conspicuous arrival as W (fig. 16). We have considered several possible sources for W, such as a diffraction or reflected refraction. Lack of curvature could rule out a diffraction as a source, but the line drawings (pl. 3, lines CH1, CH2, and CH5) illustrate that there is some curvature on W so this source possibility must be considered. We eliminated a reflected refraction because parallel lines (CH1, CH2, and CH3, fig. 1) all show these reflections(?) dipping in the same direction, even though the three lines were shot in alternately opposite directions. A reflected refraction would dip in the opposite direction for a line shot in the opposite direction.

We are able to correlate the W arrivals from line to line as indicated in the interpretation of plate 3 (lines CH1, CH2, and CH5) and the simple contour map of apparent reflection time shown in figure 21. The contours indicate a north-striking apparent surface dipping from about 3 to 9 s. Preliminary computer migration of part of line CH2 suggests that the W arrivals such as that

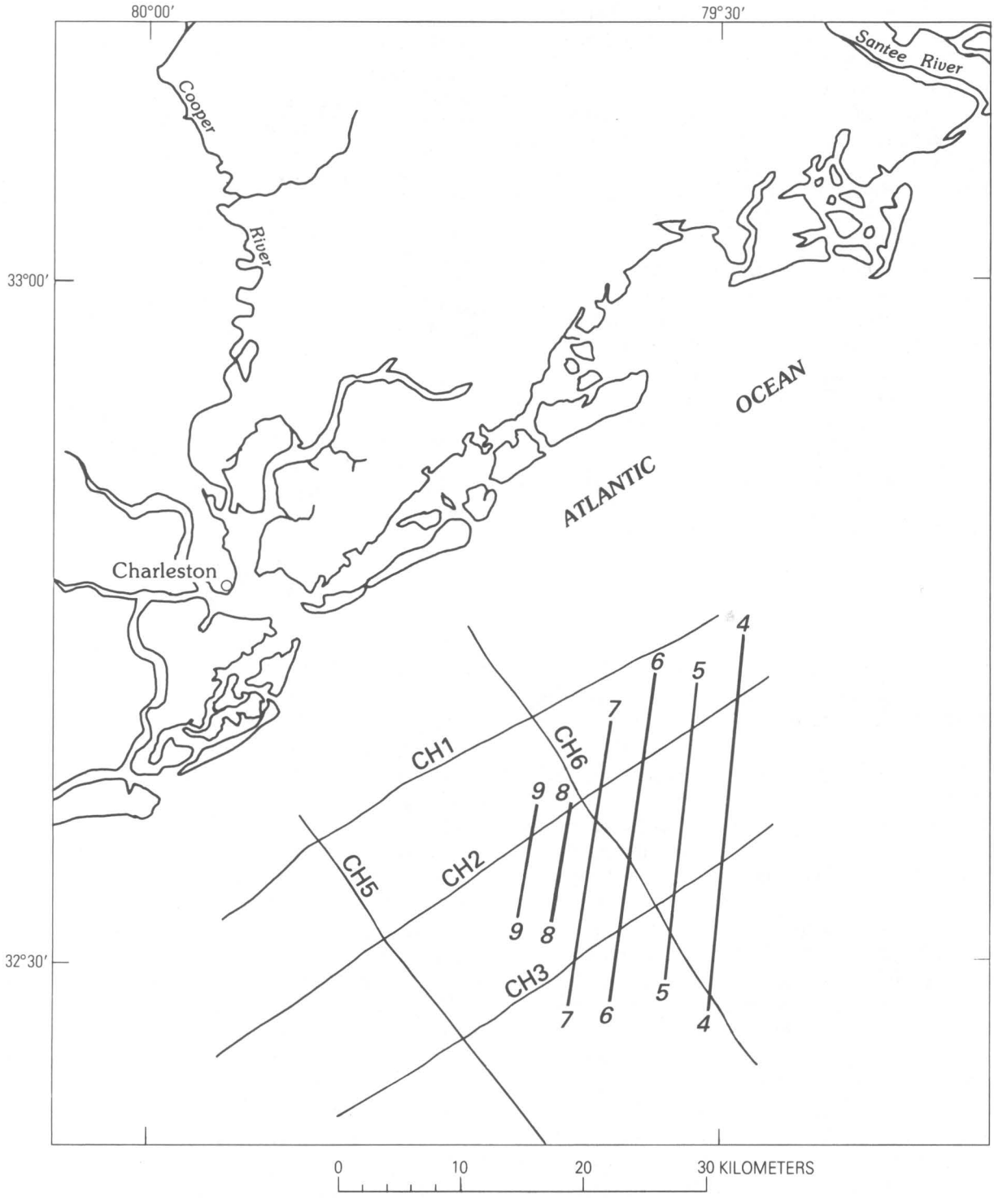

FIGURE 21.—Contour map of apparent reflection time, in seconds, to W arrivals as interpreted from plate 3, lines CH1, CH2, and CH5.

contoured in figure 21 collapse to short subhorizontal segments of reflections and therefore probably are "legs" of diffractions. Proper three-dimensional migration would change the location and dip of the W arrivals, shifting them to the east, but the basic north strike (fig. 21) would not change. Even if the W arrivals and the others of similar parallel appearance in plate 3 are diffractions, they appear different from those defining D (pl. 3, line CH5). The D diffractions show curvature in two directions (for example, pl. 3, line CH1), whereas

the W reflections only dip west and show a linear trend, as indicated by figure 21. The W arrival and those parallel to it were recorded over a much greater horizontal distance than were the individual D diffractions.

The northerly strike defined by W is paralleled by only two other features of the region. These are the line of circular intrusions (figs. 4, 15), about 50 km east of the area where W is observed, and the Triassic diabase dikes (Popenoe and Zietz, 1977) about 100 km to the northeast. We considered the possibility of the W arrival being a side reflection off the intrusions and rejected it because of distance. It is possible, however, that the structure associated with W and the conformable parallel arrivals (for example, see pl. 3, line CH1) to the east and west are related to the line of intrusions, although we have no information as to the relative ages. The surface defined by the D diffractions (fig. 20) appears to be above and to truncate the W arrival and other parallel arrivals, as shown in plate 3. Further speculation on the interpretation of W and related structures must await additional migration of the data.

Mantle Reflections

In figure 19 we showed an example of a group of arrivals that we interpret as having come from the Moho and that we have called "M." These reflections are common throughout the interpretations shown in plate 3. Comparison of the interpretation for lines CH1, CH2, and CH3 (pl. 3) shows that the M reflections are sparse on CH1 and CH2 but are quite common on CH3, which suggests that the reflection quality on M increases seaward. The dip lines CH4–6 (pl. 3) illustrate this change quite clearly. We do not understand the reason for this difference, but we do not believe it is the result of increasing crustal thickness landward, because Schilt and others (1983) reported reflections from the Moho at the same time range in the epicentral area (fig. 1). The character of the M reflections suggests that the transition zone from crust to mantle is not a single sharp boundary but rather a complex zone several kilometers in thickness having a number of reflecting surfaces. The diffractions visible in the M arrivals also attest to the presence of sharp boundaries in the zone. The complexity of the reflections does not permit an exact calculation of depth to the Moho. A rough estimate, based on the range of times, 9–11 s, and an average velocity of 6.39 km/s (Tarr and Rhea, 1983; Talwani and Amick, 1979) is 29–35 km, which is reasonable for a continental-margin area and brackets the refraction depth to the Moho of 29.9 km (Talwani and Amick, 1979) that was measured on land in the area of the epicenters (fig. 1).

DISCUSSION

These results raise several points that appear relevant to the question of the origin of the 1886 Charleston earthquake and subsequent seismicity.

1. The deep reflection data offshore have allowed us to interpret a surface from an envelope defined by diffractions at a depth of about 10 km. We suggest this surface may be a décollement or zone of detachment. The diffractions which define the décollement probably have their origin in "rough spots" (asperities?).

Movement along the décollement may be the source of the Charleston seismicity. The 1886 earthquake may have been only one event on a moving, near-horizontal, thrust plane within the present-day compressive stress regime perpendicular to the coast (Zoback and Zoback, 1980). The seismicity since 1886 may just be an aftershock sequence, as suggested by Bollinger (1983).

2. Shallow, high-angle reverse faults exist, and some (for example, Cooke fault and Helena Banks fault) have northeast trends that may be related to the Triassic basins or to other older structures. Several probably are reactivated pre-basalt-age (Jurassic or older) normal faults associated with rifting. These faults were active at least as recently as Eocene time on land and Miocene or Pliocene time offshore and may have been active to the present. The Cooke fault trends into a cluster of seismic epicenters in the meizoseismal zone of the 1886 earthquake, which suggests a causal relationship. There is no known seismicity associated with the Helena Banks fault. We suggest that the shallow faults flatten with depth and merge with the décollement. These shallow faults may also be the source of earthquakes.

3. Tarr and Rhea (1983) calculated composite focal mechanisms for 12 earthquakes recorded by the U.S. Geological Survey seismic net since 1973. Their solutions suggest vertical planes with northwest and northeast trends. The northeast-trending Cooke fault trends into a cluster having a solution that can be satisfied by a vertical plane with a northwest trend. However, the composite solutions of focal mechanisms can also define a horizontal plane for which the best determined hypocenters of the earthquakes are mostly at depths ranging from about 3 to 12 km, which brackets the depth of the D surface defined by diffractions. We propose that such a horizontal plane may be the preferable choice and that the primary seismicity may result from movement on a subhorizontal décollement, movement on the high-angle reverse faults being a second-order effect.

Figure 22 is a cartoon of the type of structure suggested by our hypothesis. We based this on models presented by Wallace (1980) and Eaton (1980) for the Basin and Range area in the Western United States.

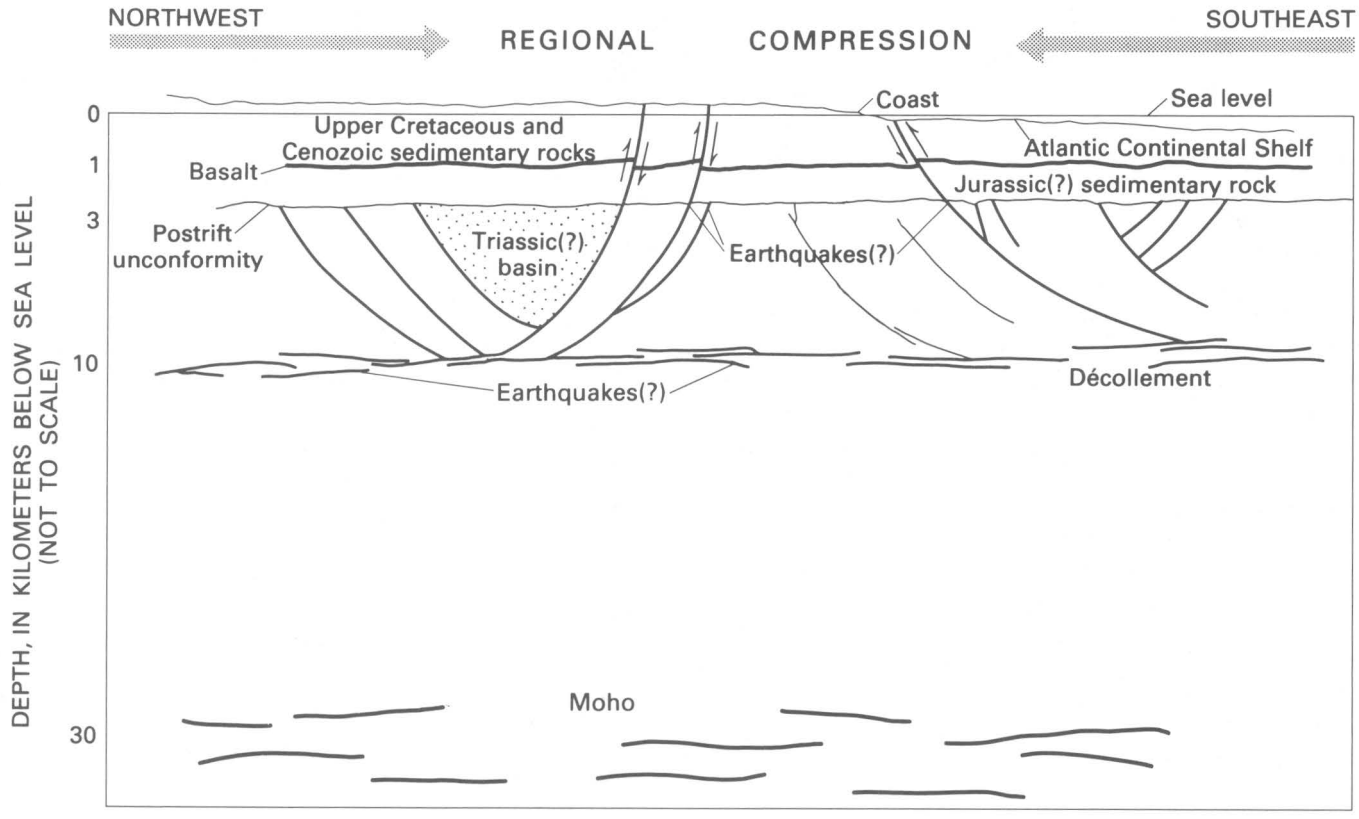

FIGURE 22.—Hypothetical structure based on interpretation of multichannel seismic-reflection profiles and a drill hole into Triassic sedimentary rock. Basalt is Jurassic age; sedimentary rocks above basalt are Late Cretaceous and Cenozoic in age. In this model, horizontal movement along the décollement or zone of decoupling is the primary cause of earthquakes; movement on the high-angle reverse faults is a secondary cause.

Although the driving mechanism in the Basin and Range model is different from that at the time of rifting and opening of the Atlantic, there may be similarities in the style of movement.

In our model, the closing of the Iapetus in one or two episodes during the Paleozoic would have led to a compressive stress regime and establishment of one or several zones of low-angle thrust faulting or décollements. At the opening of the Atlantic in Triassic and Jurassic time, high-angle, northeast-trending normal faults would have formed, some in listric style splaying into the décollement. There would also have been extensional movement on the décollement at this time. Other secondary northeast-trending, high-angle normal faults would also have formed, dipping either northwest or southeast. Triassic basins formed and were later overlain by extensive basalt flows in Jurassic time. Probably shortly after the basalt extrusion, the stress field reversed again, as demonstrated by movement on the Cooke fault (Behrendt and others, 1981), and high-angle reverse faults formed, probably reactivated from the secondary normal faults formed in Triassic time. Movement on the décollement again would have been in the northwest-southeast compressional sense.

During a long hiatus (possibly from the age of the basalt of 184 m.y. to the start of sedimentary deposition in Late Cretaceous time), reverse faulting occurred under a compressional stress regime normal to the coast. Evidence of movement on the shallow faults was removed by erosion, except on the basement as observed for the Cooke fault (Behrendt and others, 1981). Probably there was movement on the décollement at the same time. Compressive stress causing continuation of movement on the high-angle reverse faults and the décollement persisted to the present day, as illustrated in figure 22.

The source of the regional northwest-southeast compressive stress is not known, and various hypotheses such as ridge push, gravity sliding, asthenospheric drag, and others have serious problems (Zoback and Zoback, 1980). Those authors suggest that the regional stress may be from a combination of effects. At any rate, the regional stress has been consistently northwest-southeast for at least 110 m.y. and may date back to Jurassic

time, on the basis of analysis of movement on the Cooke fault (Behrendt and others, 1981).

Cook and others (1979) and Harris and Bayer (1979) have interpreted a décollement or low-angle thrust fault under the Appalachians, which they suggest extends to the coast. Harris and Bayer (1979) interpret deep reflections beneath the Continental Shelf about 200 km to the northeast as the continuation of the décollement; however, the reflections they pick are in the time range of the Moho reflection in our data (fig. 19, pl. 3). Hutchinson and others (1982) also present a considerably different interpretation of the same data used by Harris and Bayer (1979). We prefer the depth of about 10 km for the décollement in the Charleston area as discussed here.

In an earlier paper (Behrendt and others, 1981), we proposed that the Charleston earthquake was caused by movement on a décollement or zone of detachment, on the basis of the data also presented here. Seeber and Armbruster (1981) have also suggested that the 1886 Charleston earthquake was caused by movement along a zone of detachment. They cite various lines of evidence, including the argument of the broad area of MM (Modified Mercalli) intensity-VII and -VIII damage (Bollinger, 1977). However, the source of the Charleston earthquake could have been movement in the Cooke or Helena Banks fault zones, as discussed by Behrendt and others (1981) and Wentworth and Mergner-Keefer (1983). This would also be consistent with the isoseismal contours shown by Bollinger (1977).

Association of Charleston seismicity with reactivated Triassic or older structures, or a décollement, or a combination of the two, as suggested above, means association of seismicity with geologic structure that is or may be prevalent along the Atlantic coastal area and continental margin of the United States. This raises the possibility that future Charleston-type earthquakes may not necessarily be limited to the Charleston region but may occur in other areas where similar reactivated structures exist.

REFERENCES

Ackermann, H. D., 1983, Seismic-refraction study in the area of the Charleston, South Carolina, 1886 earthquake, *in* Gohn, G. S., ed., Studies related to the Charleston, South Carolina, earthquake of 1886–Tectonics and seismicity: U.S. Geological Survey Professional Paper 1313, p. F1–F20.

Behrendt, J. C., and Klitgord, K. D., 1979, High resolution aeromagnetic anomaly map of the U.S. Atlantic continental margin: U.S. Geological Survey Geophysical Investigations Map GP–931, scale 1:1,000,000.

———1980, High sensitivity aeromagnetic survey of the U.S. Atlantic continental margin: Geophysics, v. 45, no. 12, p. 1813–1846.

Behrendt, J. C., Hamilton, R. M., Ackermann, H. D., and Henry, V. J., 1981, Cenozoic faulting in the vicinity of the Charleston, South Carolina, earthquake zone: Geology, v. 9, no. 3, p. 117–122.

Bollinger, G. A., 1977, Reinterpretation of the intensity data for the 1886 Charleston, South Carolina, earthquake, *in* Rankin, D. W., ed., Studies related to the Charleston, South Carolina, earthquake of 1886–A preliminary report: U.S. Geological Survey Professional Paper 1028, p. 17–32.

Cook, F. A., Albaugh, D. S., Brown, L. D., Kaufman, Sidney, Oliver, J. E., and Hatcher, R. D., Jr., 1979, Thin-skinned tectonics in the crystalline southern Appalachians; COCORP seismic reflection profiling of the Blue Ridge and Piedmont: Geology, v. 7, no. 12, p. 563–567.

Daniels, D. L., Zietz, Isidore, and Popenoe, Peter, 1983, Distribution of subsurface lower Mesozoic rocks in the Southeastern United States as interpreted from regional aeromagnetic and gravity maps, *in* Gohn, G. S., ed., Studies related to the Charleston, South Carolina, earthquake of 1886–Tectonics and seismicity: U.S. Geological Survey Professional Paper 1313, p. K1–K24.

Dillon, W. P., Klitgord, K. D., and Paull, C. K., 1983, Mesozoic development and structure of the continental margin offshore from South Carolina, *in* Gohn, G. S., ed., Studies related to the Charleston, South Carolina, earthquake of 1886–Tectonics and seismicity: U.S. Geological Survey Professional Paper 1313, p. N1–N16.

Dillon, W. P., Paull, C. K., Buffler, R. T., and Fail, F. P., 1979, Structure and development of the Southeast Georgia Embayment and northern Blake Plateau–Preliminary analysis, *in* Watkins, J. S., Montadert, Lucien, and Dickerson, P. W., eds., Geological and geophysical investigations of continental margins: American Association of Petroleum Geologists Memoir 29, p. 27–41.

Eaton, G. P., 1980, Geophysical and geological characteristics of the crust of the Basin and Range province, *in* Continental tectonics: Washington, D.C., National Academy of Sciences, p. 96–113.

Gohn, G. S., Christopher, R. A., Smith, C. C., and Owens, J. P., 1978, Preliminary stratigraphic cross sections of Atlantic Coastal Plain sediments of the Southeastern United States–Cretaceous sediments along the South Carolina coastal margin: U.S. Geological Survey Miscellaneous Field Studies Map MF 1015–A, 2 sheets.

Gohn, G. S., Higgins, B. B., Smith, C. C., and Owens, J. P., 1977, Lithostratigraphy of the deep corehole (Clubhouse Crossroads corehole 1) near Charleston, South Carolina, *in* Rankin, D. W., ed., Studies related to the Charleston, South Carolina, earthquake of 1886–A preliminary report: U.S. Geological Survey Professional Paper 1028, p. 59–70.

Grow, J. A., Bowin, C. O., and Hutchinson, D. R., 1979, The gravity field of the U.S. Atlantic continental margin: Tectonophysics, v. 59, p. 27–52.

Hamilton, R. M., Behrendt, J. C., and Ackermann, H. D., 1983, Land multichannel seismic-reflection evidence for tectonic features near Charleston, South Carolina, *in* Gohn, G. S., ed., Studies related to the Charleston, South Carolina, earthquake of 1886–Tectonics and seismicity: U.S. Geological Survey Professional Paper 1313, p. I1–I18.

Harris, L. D., and Bayer, K. C., 1979, Sequential development of the Appalachian orogen above a master décollement–A hypothesis: Geology, v. 7, no. 12, p. 568–572.

Hutchinson, D. R., and Grow, J. A., 1979, Deep crustal reflectors and mantle returns from multichannel seismic profiles on the eastern United States continental shelf [abs.]: EOS, American Geophysical Union Transactions, v. 60, no. 18, p. 374.

Hutchinson, D. R., Grow, J. A., Klitgord, K. D., and Swift, B. A., 1982, Deep structure and evolution of the Carolina trough, *in* Watkins, J. S., and Drake, C. L., eds., Hedburg Symposium: American Association of Petroleum Geologists Memoir, in press.

Klitgord, K. D., and Behrendt, J. C., 1979, Basin structure of the U.S. Atlantic margin, *in* Watkins, J. S., Montadert, Lucien, and Dicker-

son, P. W., eds., Geological and geophysical investigations of continental margins: American Association of Petroleum Geologists Memoir 29, p. 85–112.

Lanphere, M. A., 1983, $^{40}Ar/^{39}Ar$ ages of basalt from Clubhouse Crossroads test hole #2 near Charleston, South Carolina, *in* Gohn, G. S., ed., Studies related to the Charleston, South Carolina, earthquake of 1886–Tectonics and seismicity: U.S. Geological Survey Professional Paper 1313, p. B1–B8.

Phillips, J. D., 1983, Paleomagnetic investigations of the Clubhouse Crossroads basalt, *in* Gohn, G. S., ed., Studies related to the Charleston, South Carolina, earthquake of 1886–Tectonics and seismicity: U.S. Geological Survey Professional Paper 1313, p. C1–C18.

Phillips, J. D., Daniels, D. L., Zietz, Isidore, and Popenoe, Peter, 1978, Geophysical studies of the Charleston, South Carolina, area–Onshore aeromagnetic map: U.S. Geological Survey Miscellaneous Field Studies Map MF-1022-A, scale 1:250,000.

Popenoe, Peter, and Zietz, Isidore, 1977, The nature of the geophysical basement beneath the Coastal Plain of South Carolina and northeastern Georgia, *in* Rankin, D. W., ed., Studies related to the Charleston, South Carolina, earthquake of 1886–A preliminary report: U.S. Geological Survey Professional Paper 1028, p. 119–139.

Schilt, F. S., Brown, L. D., Oliver, J. E., and Kaufman, Sidney, 1983, Subsurface structure near Charleston, South Carolina–Results of COCORP reflection profiling in the Atlantic Coastal Plain, *in* Gohn, G. S., ed., Studies related to the Charleston, South Carolina, earthquake of 1886–Tectonics and seismicity: U.S. Geological Survey Professional Paper 1313, p. H1–H19.

Schlee, J. S., Behrendt, J. C., Grow, J. A., Robb, J. M., Mattick, R. E., Taylor, P. T., and Lawson, B. J., 1976, Regional geologic framework off northeastern United States: American Association of Petroleum Geologists Bulletin, v. 60, no. 6, p. 926–951.

Seeber, Leonardo, and Armbruster, J. G., 1981, The 1886 Charleston, South Carolina earthquake and the Appalachian detachment: Journal of Geophysical Research, v. 86, no. B9, p. 7874–7894.

Sykes, L. R., 1978, Intraplate seismicity, reactivation of preexisting zones of weakness, alkaline magmatism, and other tectonism postdating continental fragmentation: Reviews of Geophysics and Space Physics, v. 16, no. 4, p. 621–688.

Talwani, Pradeep, 1982, The Woodstock fault is alive and ticking near Charleston, S. C. [abs.]: EOS, American Geophysical Union Transactions, v. 63, no. 6, p. 155.

Talwani, Pradeep, and Amick, David, 1979, Crustal structure studies in the South Carolina Coastal Plain: 9th Technical Report to U.S. Geological Survey, contract no. 14-08-0001-17670, 81 p.

Tarr, A. C., and Rhea, Susan, 1983, Seismicity near Charleston, South Carolina, March 1973 to December 1979, *in* Gohn, G. S., ed., Studies related to the Charleston, South Carolina, earthquake of 1886–Tectonics and seismicity: U.S. Geological Survey Professional Paper 1313, p. R1–R17.

Wallace, R. E., 1980, Tectonic analysis of active faults: U.S. Geological Survey National Earthquake Hazards Reduction Program, Summaries of Technical Reports, v. 10, p. 233–235.

Wentworth, C. M., and Mergner-Keefer, Marcia, 1983, Regenerate faults of small Cenozoic offset–Probable earthquake sources in the Southeastern United States, *in* Gohn, G. S., ed., Studies related to the Charleston, South Carolina, earthquake of 1886–Tectonics and seismicity: U.S. Geological Survey Professional Paper 1313, p. S1–S20.

Yantis, B. R., Costain, J. K., and Ackermann, H. D., 1983, A reflection seismic study near Charleston, South Carolina, *in* Gohn, G. S., ed., Studies related to the Charleston, South Carolina, earthquake of 1886–Tectonics and seismicity: U.S. Geological Survey Professional Paper 1313, p. G1–G20.

Zoback, M. L., and Zoback, Mark, 1980, State of stress in the conterminous United States: Journal of Geophysical Research, v. 85, no. B11, p. 6113–6156.

Distribution of Subsurface Lower Mesozoic Rocks in the Southeastern United States, as Interpreted from Regional Aeromagnetic and Gravity Maps

By DAVID L. DANIELS, ISIDORE ZIETZ, and PETER POPENOE

STUDIES RELATED TO THE CHARLESTON, SOUTH CAROLINA, EARTHQUAKE OF 1886—TECTONICS AND SEISMICITY

GEOLOGICAL SURVEY PROFESSIONAL PAPER 1313-K

UNITED STATES GOVERNMENT PRINTING OFFICE, WASHINGTON: 1983

CONTENTS

ILLUSTRATIONS

STUDIES RELATED TO THE CHARLESTON, SOUTH CAROLINA, EARTHQUAKE OF 1886—
TECTONICS AND SEISMICITY

DISTRIBUTION OF SUBSURFACE LOWER MESOZOIC ROCKS IN THE SOUTHEASTERN UNITED STATES, AS INTERPRETED FROM REGIONAL AEROMAGNETIC AND GRAVITY MAPS

By DAVID L. DANIELS, ISIDORE ZIETZ,[1] and PETER POPENOE

ABSTRACT

Aeromagnetic data, in conjunction with data from deep wells, are used to interpret the nature of the pre-Cretaceous "basement" beneath the Coastal Plain in Georgia and South Carolina. These data reveal some of the complexity of the broad early Mesozoic rift basin, which appears to extend at least from the Gulf of Mexico to the Atlantic Ocean. Along the northern edge of this rift, in the Savannah River region, depth-to-magnetic-source calculations delineate two interconnected basins, which are separated from the main rift by a broad horst of crystalline basement. The Riddleville (Ga.) basin appears to contain at least a 2.2-km thickness of basin fill; it is deeper than the Dunbarton (S. C.) basin, which has at least a 1.0 km thickness of fill. A maximum thickness of 3.5 km near Statesboro, Ga., is indicated for the main basin, called here the South Georgia rift.

Abundant lower Mesozoic diabase dikes in the South Carolina Coastal Plain are revealed on the magnetic map by narrow anomalies that have two dominant trends, northwest and north. One set of several north-trending anomalies can be traced continuously northward across the Coastal Plain, Piedmont, and Blue Ridge for 480 km. The two sets, which may represent two episodes of intrusion, have characteristic distributions within the study area: northwesterly trends are to the southwest and northerly trends to the northeast. A broad area of overlap extends from 80° W., in South Carolina, to northern Virginia. Several lower Mesozoic diabase sills within the rift are indicated by circular, low-amplitude magnetic anomalies.

Intense magnetic highs and corresponding gravity highs indicate the presence of abundant large bodies of mafic rocks in the pre-Cretaceous "basement" in addition to the dikes and sills; two groups of mafic rocks are distinguished. Circular or oval anomalies are interpreted as largely gabbroic plutons, which may be as young as early Mesozoic and which are present both within and outside the rift. Elongate anomalies, which form a northeast-trending belt across Georgia and South Carolina, may reflect deformed pre-Mesozoic mafic rocks.

The largest and least understood magnetic feature of the region is the Brunswick anomaly, a long-wavelength anomaly system 1,100 km long, which is mostly offshore but which also bisects the Georgia Coastal Plain. The anomaly divides two regions of differing magnetic character and magnetic trend, which suggests that it is closely related to a Paleozoic suture between a Florida–South Georgia microcontinent and the North American craton.

[1]Phoenix Corporation, McLean, Va.

INTRODUCTION

Detailed aeromagnetic coverage in the Coastal Plain region around Charleston, S. C., reflects the type and distribution of rocks and structures in the pre-Cretaceous basement. This report examines the evidence for subsurface lower Mesozoic rocks in the aeromagnetic data supplemented by gravity and seismic-refraction data, with reference to rocks returned from deep drilling.

Information about the subsurface "basement" rocks in the Coastal Plain of the Southeastern United States has been derived from deep drill samples. Although Alabama and northern Florida have been extensively drilled, the Coastal Plain of South Carolina and eastern Georgia has very few useful wells. Because the samples returned from drilling represent a point source of data, large, horizontally continuous structures, such as sedimentary beds, may be adequately defined by a vertical sample. Many basement structures, however, have steep contacts and are poorly defined by drilling. Further, most deep drilling was performed as oil tests and therefore was terminated shortly after the basement was penetrated.

Existing aeromagnetic surveys (see fig. 1), by contrast, cover the study region (pl. 1) uniformly; flight-line spacing is 1 mi (1.6 km) or less on land and 2 mi (3.2 km) offshore. Magnetic and gravity surveys respond to large volumes of rock and most strongly to structures of large vertical extent. It should be recognized, however, that gravity and magnetic information is subject to multiple interpretations, so the anomalies can never be unequivocally explained unless constrained by other geophysical or geological data.

Therefore, the gravity and magnetic data give us a different, though complementary, picture from that obtained by drilling. Many major features on the magnetic

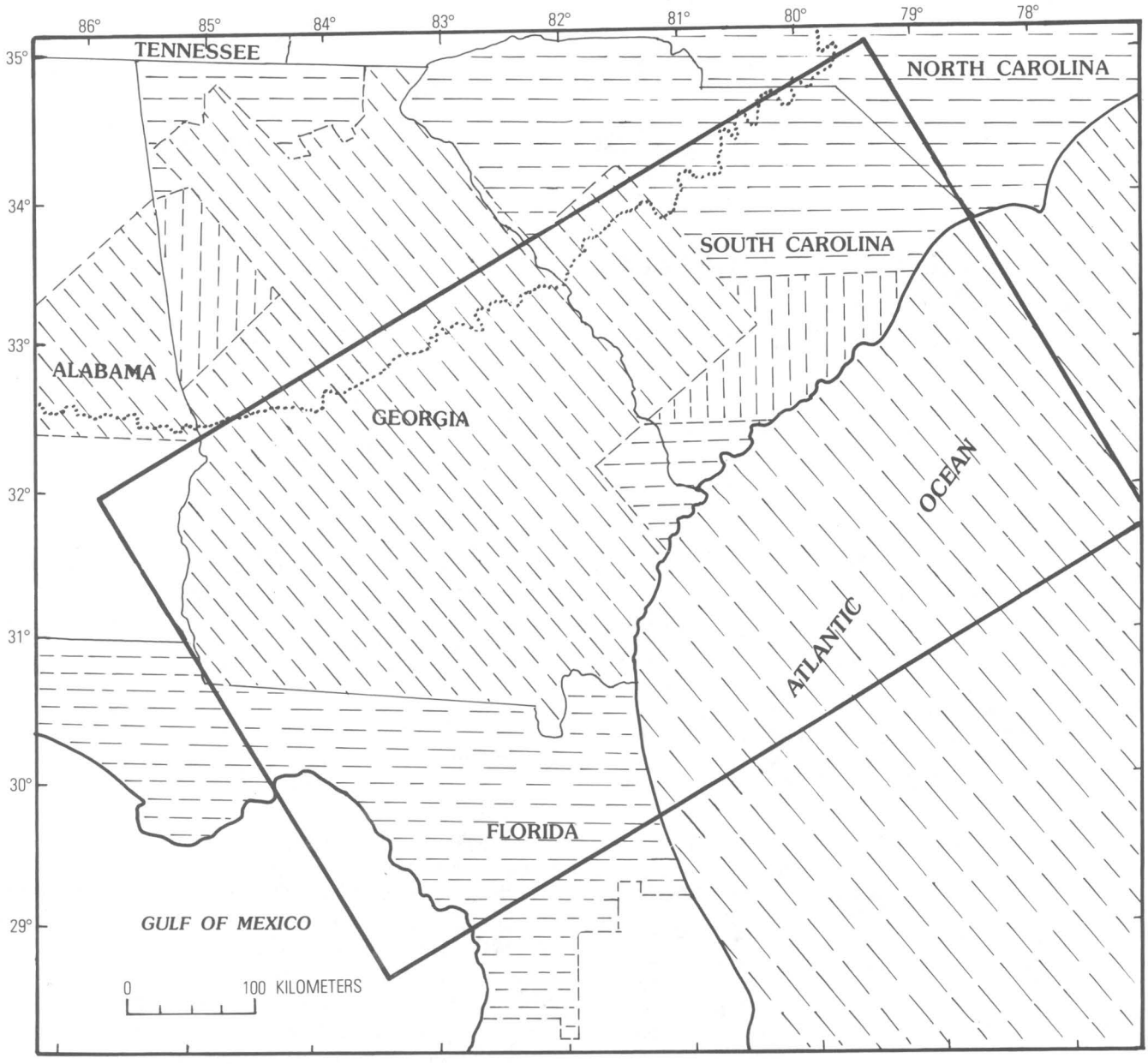

FIGURE 1.—Coverage of aeromagnetic surveys of 1-mi (1.6-km) (land) and 2-mi (3.2-km) (ocean) flight-line spacings in the Southeastern Atlantic States. Dashes indicate directions of flight lines. Dotted line divides Coastal Plain and Piedmont. Rectangle encloses study area.

and gravity maps have not yet been identified by drilling. Nevertheless, the features can be generally identified, and many of them affect strongly the interpreted tectonic history of the region.

Acknowledgments.—Partial support for this research and funding for many of the aeromagnetic surveys of the Coastal Plain of the Southeastern States was provided by the Coastal Plains Regional Commission.

INTERPRETIVE TECHNIQUE

The interpretations in this paper have been based mainly on the aeromagnetic data, because of the greater data uniformity, resolution, and dynamic range of rock magnetic properties (remanent magnetization effects included). Gravity maps, which are more reliable indicators of lithology, were used to further refine the interpretations made from the aeromagnetic maps.

Qualitative Method

Only a limited number of features (six are discussed here) are distinct enough to be recognized on the gravity and magnetic maps of the Southeastern States. These "signatures" are based upon comparison between magnetic and gravity maps of the Piedmont and Blue

Ridge provinces and geologic maps of the same areas. Detailed aeromagnetic maps [flight spacing 1 mi (1.6 km) or less] are now available for more than 95 percent of this region. Many gravity and magnetic features in the Piedmont, however, are currently unexplained geologically and so cannot be used as a guide. The recognizable features may be classified loosely by anomaly shape, orientation, amplitude, and sign (high or low). In order of decreasing confidence in their geologic associations, these six features are:

1. Narrow linear magnetic anomalies with northwest or northerly trends, which are largely correlated with Triassic-Jurassic diabase dikes. Dike anomalies are most easily recognized where they cross nonmagnetic terrain or where they cross the trend of the country rock at an angle greater than about 20 degrees.
2. Circular or oval magnetic anomalies and closely corresponding gravity anomalies. These occur in the following combinations:
   a. Magnetic high–gravity high: Mafic intrusive rocks are indicated where both anomalies are of large amplitude [examples: Concord and Mecklenburg plutons in North Carolina (pluton names from Speer and others, 1980)]. Numerous smaller mafic intrusive bodies having irregular map patterns may also be recognized from the magnetic high–gravity high association, provided the geophysical data have adequate resolution. Metamorphosed mafic rocks may lack the magnetic high.
   b. Magnetic low–gravity low: Many of the cross-cutting, post-metamorphic plutons in the Piedmont correlate with distinct magnetic and gravity lows (examples: Landis and Churchland plutons in North Carolina). Premetamorphic plutons are more difficult to distinguish by means of gravity and magnetic data alone.
   c. Magnetic high–gravity low: A few of the post-metamorphic granitic plutons in the Piedmont have distinct gravity lows but are also moderately magnetic (examples: Liberty Hill and Pageland plutons in South Carolina).
3. Parallel groups of narrow linear magnetic anomalies trending northeast, which characterize folded metamorphic rocks of the Piedmont. The linear pattern is not uniformly developed but seems to be associated with upper greenschist- or lower amphibolite-grade rocks that have undergone tight folding around largely horizontal fold axes and that have the right composition to develop magnetite. Alternatively, some of these anomalies may be attributed to mylonite zones (Hatcher and others, 1977).
4. Elongate regions of low magnetic gradient and intensity and generally small gravity lows, which correlate with parts of many Triassic-Jurassic basins in the Eastern United States. The gravity and magnetic signatures of such basins are quite variable and depend on the thickness of the sedimentary rocks, the presence or absence of diabase intrusive rocks, and the magnetic character of the underlying rocks.
5. Ring-shaped magnetic anomalies, associated with many of the diabase sills in the Gettysburg, Pa. (Bromery and Griscom, 1967), and Culpeper, Va. (Daniels, 1980), Triassic-Jurassic basins. A variety of other, less distinctive shapes is also common. Low-amplitude gravity highs are also associated with these sills but lack the resolution of the magnetic data because of generally wider station spacing.
6. Some straight magnetic or gravity gradients, associated with mapped faults (examples: Jonesboro and Gold Hill faults in North Carolina; Hatcher and others, 1977; Stromquist and Sundelius, 1969).

Note that all or nearly all signatures described above could also arise from pre-Cretaceous intrabasement contrasts in the Coastal Plain region. Since the blanket of Coastal Plain rocks that overlies the pre-Cretaceous basement is weakly magnetic and quite uniform horizontally, its effect on the potential field is one of distance. An increasing thickness of sedimentary cover acts to smoothly decrease the gravity and magnetic gradients. Narrow anomalies decrease in amplitude readily with increasing distance, whereas broad anomalies change little.

Quantitative Method

To supplement the qualitative technique described above, the depth to many magnetic sources in the Coastal Plain was estimated from original profiles and reconstructed profiles, by means of the horizontal-gradient method (Vacquier and others, 1951). The depth estimates were corrected for anomaly-to-flight-line angle, airplane elevation, and approximate ground elevation. In order to smooth the large range in the results, a minimum of three adjacent depth estimates were averaged for each anomaly. In some areas of the Coastal Plain, the magnetic sources are consistently deeper than the average top of the pre-Cretaceous rocks as determined from nearby wells or seismic-refraction measurements, which indicates the existence of an upper layer of nonmagnetic rock within the pre-Cretaceous basement. This nonmagnetic layer is interpreted in most

cases to be Triassic and Jurassic sedimentary rocks. It is necessary to assume that crystalline basement rarely has a nonmagnetic upper layer.

In other areas, many magnetic sources plot close to the expected level of the base of the Cretaceous within an error range of ±25 percent of the total depth. These sources are interpreted to be evidence of either crystalline basement or Mesozoic mafic igneous rocks near the top of a sedimentary sequence. Anomaly amplitude and character were then used to distinguish between the two groups. A number of magnetic sources appear to lie above the projected pre-Cretaceous surface and within the Coastal Plain sedimentary section. Because no rocks capable of producing detectable magnetic anomalies are known to occur within the Coastal Plain sediments, these depth determinations are assumed to be too shallow and incorrect. Only two of these, however, were too shallow by more than 25 percent of the total depth. These may indicate either unsuspected relief on the pre-Cretaceous surface or violation of the assumptions required in the depth technique, such as bodies that have nonvertical contacts or significantly nonuniform magnetic properties.

INTERPRETATION OF COASTAL PLAIN MAGNETIC AND GRAVITY MAPS

Features of Probable Early Mesozoic Age

Continental sedimentary rocks of Triassic and Jurassic age (Van Houten, 1977) crop out along eastern North America in a series of fault-bounded basins, displacing rocks of the Piedmont, Blue Ridge, and Valley and Ridge provinces. Red-brown mudstones, arkoses, and conglomerates are common; basalt flows are found in the upper part of the section, and diabase intrusions (some of which are sills) in the more northerly basins. Diabase dikes also cut both the Piedmont and the basins in a regular pattern from Alabama to Nova Scotia (King, 1971).

The existence of similar sedimentary and igneous rocks beneath the Coastal Plain was recognized very early from deep wells that had penetrated the pre-Cretaceous basement rocks – at Florence, S. C. (Darton, 1896), Summerville, S. C. (Cooke, 1936), Laurens, Appling, and Montgomery Counties, Ga. (Applin, 1951), and Camden County, N. C. (Richards, 1954). These and later reports have correlated these rocks with the Newark Group (Atlantic Coast) or the Eagle Mills Formation (Gulf Coast) on the basis of lithologic similarity and association with diabase and (or) basalt (Applin and Applin, 1964; Maher, 1971; Marine and Siple, 1974; Barnett, 1975; Brown and others, 1979).

Currently the number of wells in the Southeastern States that have returned suspected Triassic and Jurassic rocks has increased to about 60, and, in fact, there appears to be a large, continuous rift basin, nowhere exposed, which traverses western Florida, southern Alabama, Georgia, and South Carolina and extends beneath the Gulf of Mexico and Atlantic Ocean (Popenoe and Zietz, 1977; Popenoe, 1977; Gohn and others, 1978; Chowns, 1979). This basin, called here the South Georgia rift (fig. 2), is longer than the largest exposed Triassic-Jurassic basin in the Eastern States (the Culpeper-Gettysburg-Newark basin) and about four times its width. The east-northeast trend of this basin also distinguishes it from the exposed basins, which generally trend northeast. The sediments of this complex basin have been deposited on Piedmont crystalline rocks at its northern edge and on Paleozoic sedimentary rocks, rhyolitic rocks, and assorted granitic rocks along its southern half.

During the past ten years, isotopic age measurements have confirmed that some of the subsurface diabase and basalt are Triassic and Jurassic in age and have implied that the sedimentary rocks are equivalent to those in the exposed Triassic-Jurassic basins (Milton and Grasty, 1969; Barnett, 1975; Gohn and others, 1978; Lanphere, 1983).

Whereas felsic volcanic rocks are unknown in exposed early Mesozoic basins of the Appalachian orogen, rhyolites interlayered with Mesozoic arkose have been reported from several wells within the rift in southern Alabama (Neathery and Thomas, 1975). Radiometric age dating of unmetamorphosed to slightly metamorphosed felsic pyroclastic units in southeast Georgia has resulted in a wide range of ages which includes the early Mesozoic (Chowns, 1979). However, the Georgia rhyolites have been excluded from the rift shown in figure 2 because of uncertainty about the reliability of these dates.

The South Georgia rift may be an extension of the rift that initiated the opening of the Gulf of Mexico (Rankin and others, 1978), as the North American and South American plates separated (Pilger, 1978). The South Georgia rift accumulated continental clastic sediments and mafic igneous rocks from the Late Triassic through the Early Jurassic, at which time it probably became inactive. The Gulf rift, however, experienced continued crustal thinning and depression and was invaded by Pacific Ocean waters, which entered across the Mexican peninsula in the Middle Jurassic (Salvador, 1979). Thick salt deposits that overlie continental red beds in the Gulf region (fig. 2) indicate that the Gulf rift remained a relatively restricted basin during the Jurassic. The spreading center that developed in the Gulf of Mexico may have been connected to Atlantic spreading centers along a northwest-trending transform fault across south Florida, the Bahamas fracture zone (Klitgord and others, 1983).

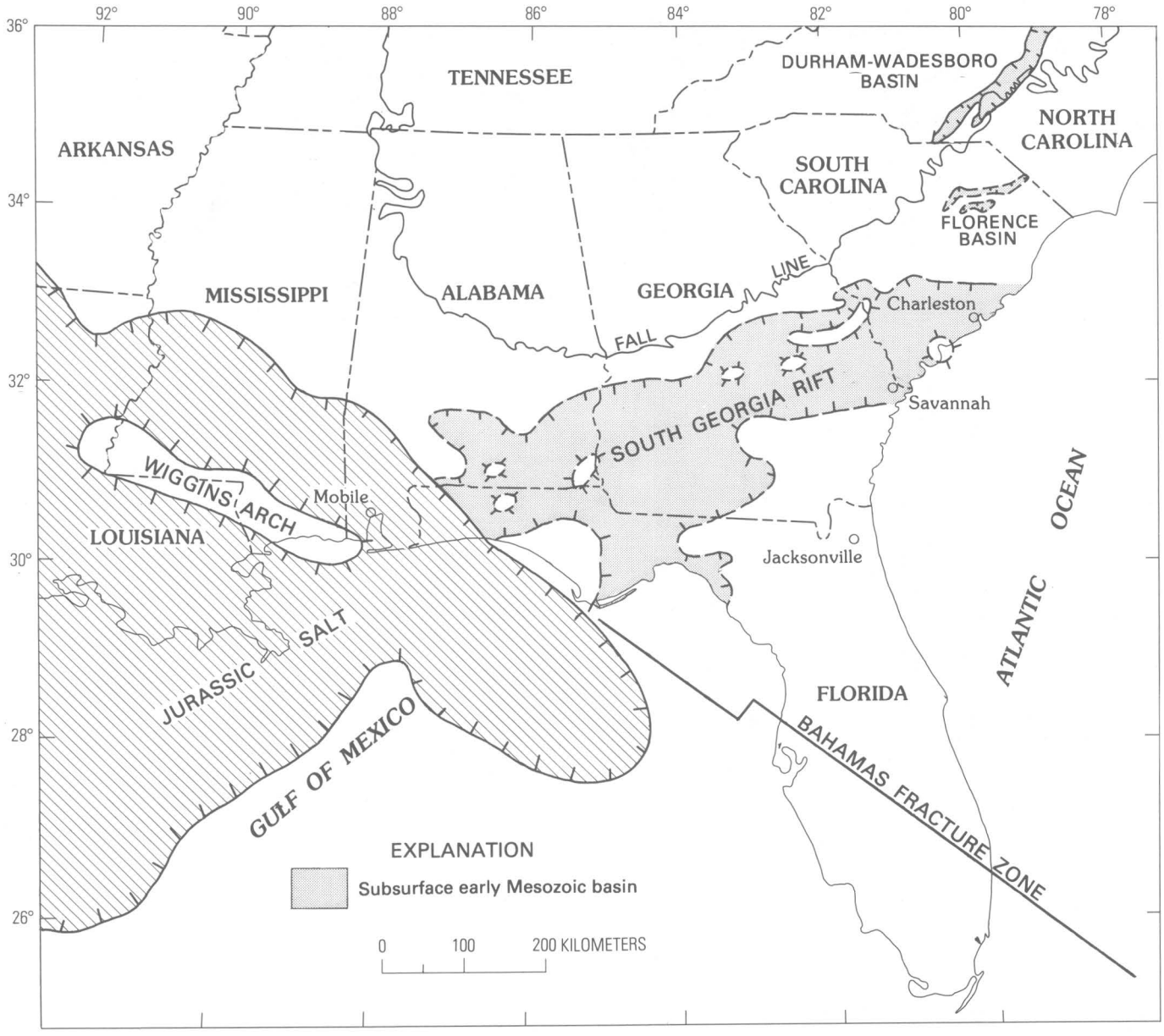

FIGURE 2.—Map of interpreted distribution of subsurface early Mesozoic basins. Boundaries have been generalized from well data and magnetic data. Bahamas fracture zone from Klitgord and others (1982). Extent of Jurassic salt from McGookey (1975). Well data from Applin (1951), Bridge and Berdan (1951), Milton and Hurst (1965), Milton and Grasty (1969), Marine and Siple (1974), Marine (1974), Barnett (1975), Neathery and Thomas (1975), Gohn and others (1978), Daniels and Zietz (1978) and unpublished data. Durham-Wadesboro basin in North Carolina and edge of Coastal Plain (dotted line) from King (1969).

SEDIMENTARY ROCKS

Large areas of the Coastal Plain in Georgia and South Carolina are characterized by low magnetic gradients that may be caused by subsurface lower Mesozoic sedimentary rocks (pl. 1). However, it is known from deep well samples that, although much of this low-gradient area is underlain by rocks of probable early Mesozoic age, some parts are underlain by other rocks: Paleozoic sedimentary rocks, felsic volcanic rocks, felsic plutons, diorite, schist, and felsic gneiss, all of which seem to be weakly magnetic and produce a low-gradient magnetic field. Only in the shallow part of the Coastal Plain, in the region of the Savannah River, where basement crystalline rocks are strongly magnetic, is sufficient contrast available to define the thicker areas of rift sediments. Because northeast-trending anomalies are characteristic of the Piedmont, the presence of these anomalies can identify areas where thick sections of Triassic and Jurassic red beds are probably absent. Narrow linear magnetic anomalies are not equally abundant

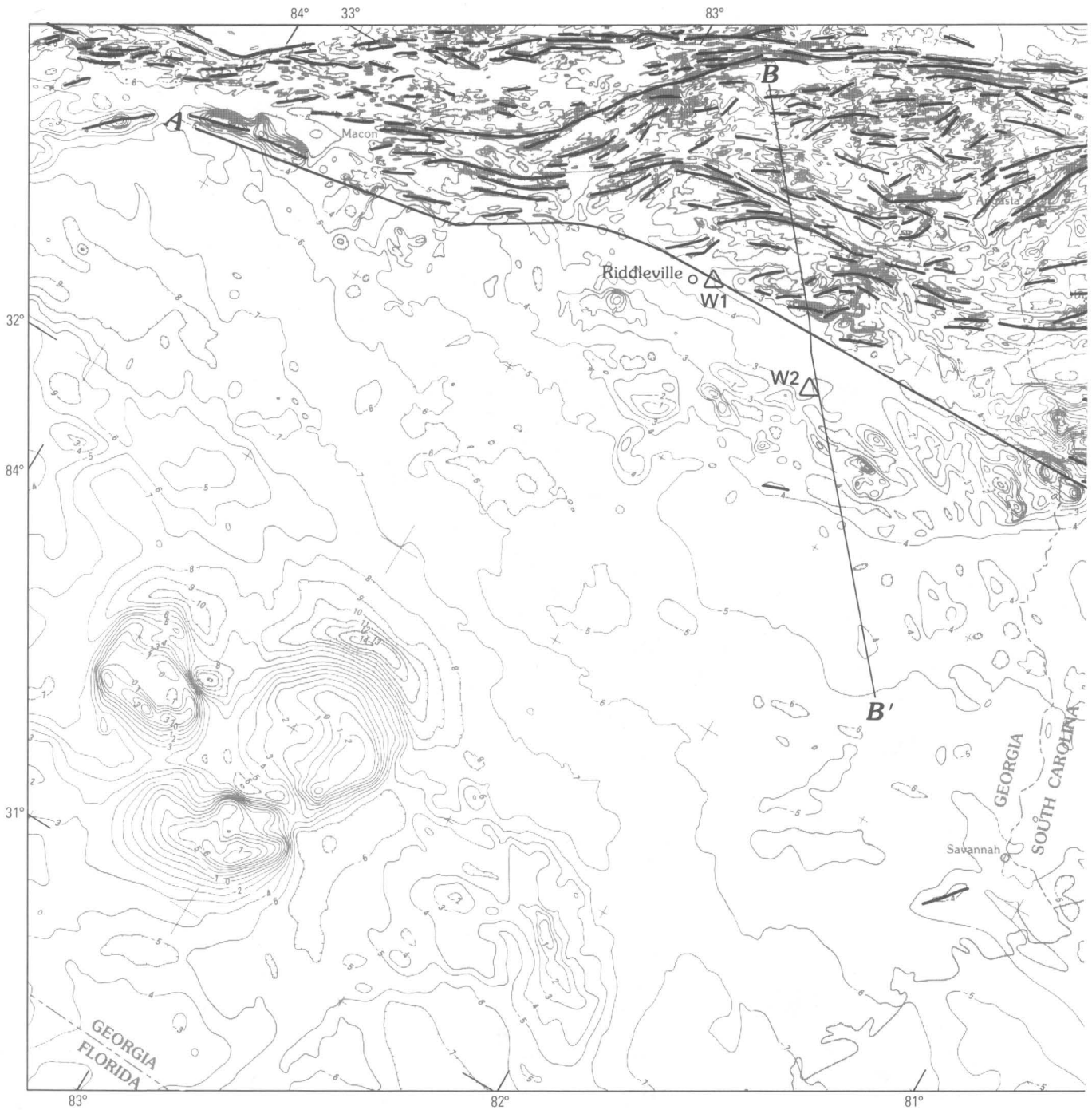

FIGURE 3. – Aeromagnetic map of the Coastal Plain and part of the Piedmont, South Carolina and Georgia. Contour interval 100 nT. Heavy lines trace northeast-trending linear anomalies interpreted as characteristic of Piedmont rocks. Line *A–A′* marks the southern boundary of the region of abundant northeast-trending anomalies. Line *B–B′* marks the location of cross section shown in figure 6. Triangles mark two wells that penetrated red beds in the Riddleville basin.

everywhere in the Piedmont and so can only be used as a general indicator of relatively shallow subsurface extension of Piedmont terrain. Progressively deeper burial of these rocks causes the anomalies to broaden and diminish in amplitude until they lose character.

Instead of a smooth attenuation with distance from the Fall Line, the linear grain ends abruptly in certain areas, indicated by line *A–A′* on figure 3. This line follows several strong linear magnetic trends and may mark the approximate northern edge of the main rift

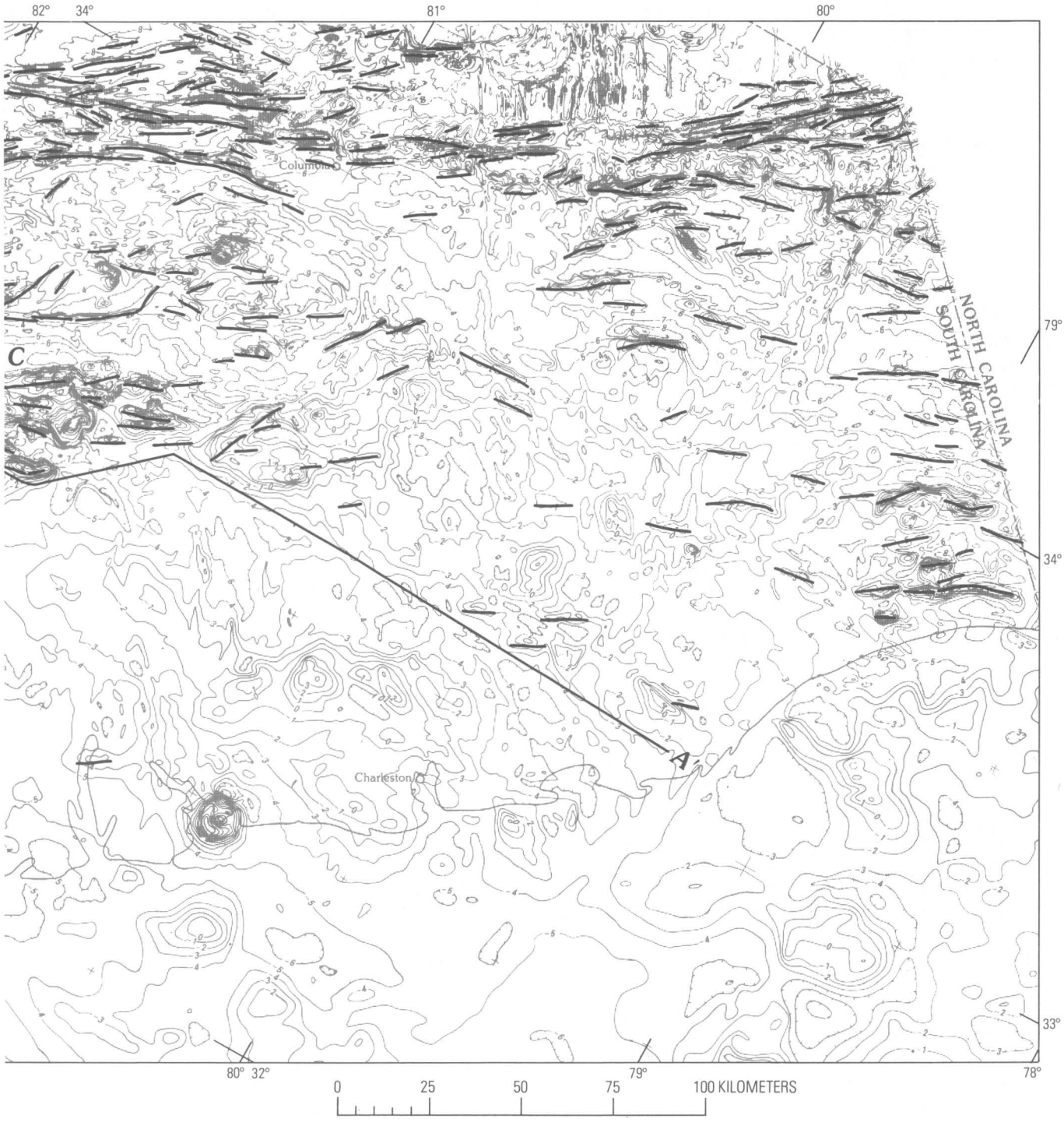

FIGURE 3.—Continued.

zone. A few northeast-trending anomalies lie south of line *A–A′* and may indicate southward continuation of Piedmont crystalline rocks beneath the rift sediments or as horsts of crystalline basement. Comparison with a plot of wells that reached the pre-Cretaceous basement shows that nearly all of the wells that returned foliated metamorphic rocks characteristic of the exposed Piedmont lie north of line *A–A′*. Rocks judged to be of probable Triassic and Jurassic age (red beds, diabase, and basalt) are mostly confined to wells that lie south of this

line. The wells that identified the Dunbarton basin (Marine and Siple, 1974) and the Florence basin (Popenoe and Zietz, 1977) are exceptions.

Riddleville basin

Immediately south of line *A–A'*, an exceptionally featureless magnetic low extends east from Riddleville, Ga. (fig. 3). This feature led Daniels and Zietz (1978) to predict a subsurface Triassic-Jurassic basin there. Recent wells in the area of the magnetic low have confirmed this interpretation. Near Riddleville, Ga., more than 500 meters of red conglomerate and fanglomerate of probable Triassic and Jurassic age were penetrated in a gas test well (T.R. Taylor 1; W1, fig. 3) (R. Bennett, oral commun., 1978). Three other wells in the immediate vicinity also struck red beds (D. Ziegler, oral commun., 1980). Red beds were also recovered beneath the Cretaceous in a U.S. Geological Survey (USGS) hydrologic test well at Midville, Ga. (W2, fig. 3) (Harold Gill, oral commun., 1980). For clarity in this paper we refer to these rocks as the "Riddleville basin." The aeromagnetic contours suggest that this basin trends east-west and that maximum thickness occurs along the axis of the magnetic low. Piedmont crystalline rocks have been recovered from wells on the north side of the basin, and mafic rocks of uncertain character are inferred to lie to the south (Daniels and Zietz, 1978), although none has been identified from drilling.

Depth-to-source estimates on magnetic anomalies in the Savannah River region are shown on figure 4. Approximate structure contours on the pre-Cretaceous basement drawn from depths from deep wells and seismic-refraction measurements are also shown in figure 4. To estimate the thickness of nonmagnetic rocks below the Cretaceous, the magnetic-source depths were subtracted from the basement elevation as interpolated from the structure contours. These thicknesses were contoured where an adequate number of data points was available (fig. 5). The solid lines on figure 5 enclose sources for which the thickness of pre-Cretaceous nonmagnetic rock is zero or less than the probable error range of the magnetic depth technique (±25 percent), including those sources that appear to lie above the base of the Cretaceous. These sources are interpreted to be a subcrop of crystalline basement, and, in the region north of the Riddleville and Dunbarton basins, some are directly associated with wells that returned foliated metamorphic rocks characteristic of the exposed Piedmont. Because of the wide range of shallow depths accepted as evidence of crystalline basement subcrop, the area of these rocks may be smaller than indicated. Some magnetic sources that plot close to the base of the Cretaceous were measured on low-amplitude anomalies, and these were interpreted to be lower Mesozoic diabase or basalt (open squares, fig. 5).

Those sources that indicated a large thickness of nonmagnetic rock (open circles, fig. 5) were interpreted to be evidence of early Mesozoic sedimentary basins. Magnetic sources in the Riddleville basin confirm the east-west elongation and indicate at least 2.2 km of sedimentary fill. The more closely spaced isopach contours along the north edge of the basin (fig. 5) suggest that the Riddleville basin is asymmetrical, bounded by a major east-west fault on the north, and that the sedimentary rocks dip generally north (fig. 6). Cook and others (1980) report seismic-reflection evidence in this location for a possible listric-normal fault that may dip south and join a deep master décollement.

Dunbarton basin

The Dunbarton basin was discovered as a result of a deep corehole in southern Barnwell County, S. C. Continental red beds similar to rocks found in exposed Triassic and Jurassic basins were recovered beneath the Cretaceous (Christl, 1964). Siple (1967) noted that the well was located in a broad, northeast-trending aeromagnetic low (Petty and others, 1965) (C, fig. 3) and inferred that the low defined the limits of a subsurface Triassic and Jurassic basin. A steep, linear magnetic gradient that limits the magnetic low on the southeast suggests this edge of the basin is fault bounded (Daniels, 1974). Four additional coreholes across the northwest half of the magnetic low verified the inferred extent of the basin in that direction. Maximum red-bed penetration of 925 m was achieved at the center of the magnetic low (Marine and Siple, 1974). Additional geophysical data (seismic-reflection, gravity, and ground magnetic surveys) led Marine (1974) to suggest, however, that the basin is not confined to the aeromagnetic low but extends southeast well beyond the linear magnetic gradient. The maximum basin thickness was estimated to be 1,615 m, and a region of high intensity to the southeast of the magnetic low was interpreted to be mafic rocks overlain by a thinner section of Triassic sedimentary rocks (Marine, 1974).

Magnetic depth estimates in the same region in general support the model offered by Marine (1974). Like the Riddleville basin, the Dunbarton basin appears to be nearly enclosed by a subcrop of crystalline rocks but is apparently connected to the main rift basin, to the south, across a saddle of thinner lower Mesozoic rocks (fig. 5). Marine and Siple (1974) have suggested that the general dip of the basin is southeast.

Several factors, although they are not well established at this time, indicate a difference in character between the Riddleville and Dunbarton basins even though the two basins are adjacent and appear to be connected (fig. 5). The indications of northeast elongation, southeast dip, and relatively small thickness of the Dunbarton basin suggest affinity with the nearest exposed early

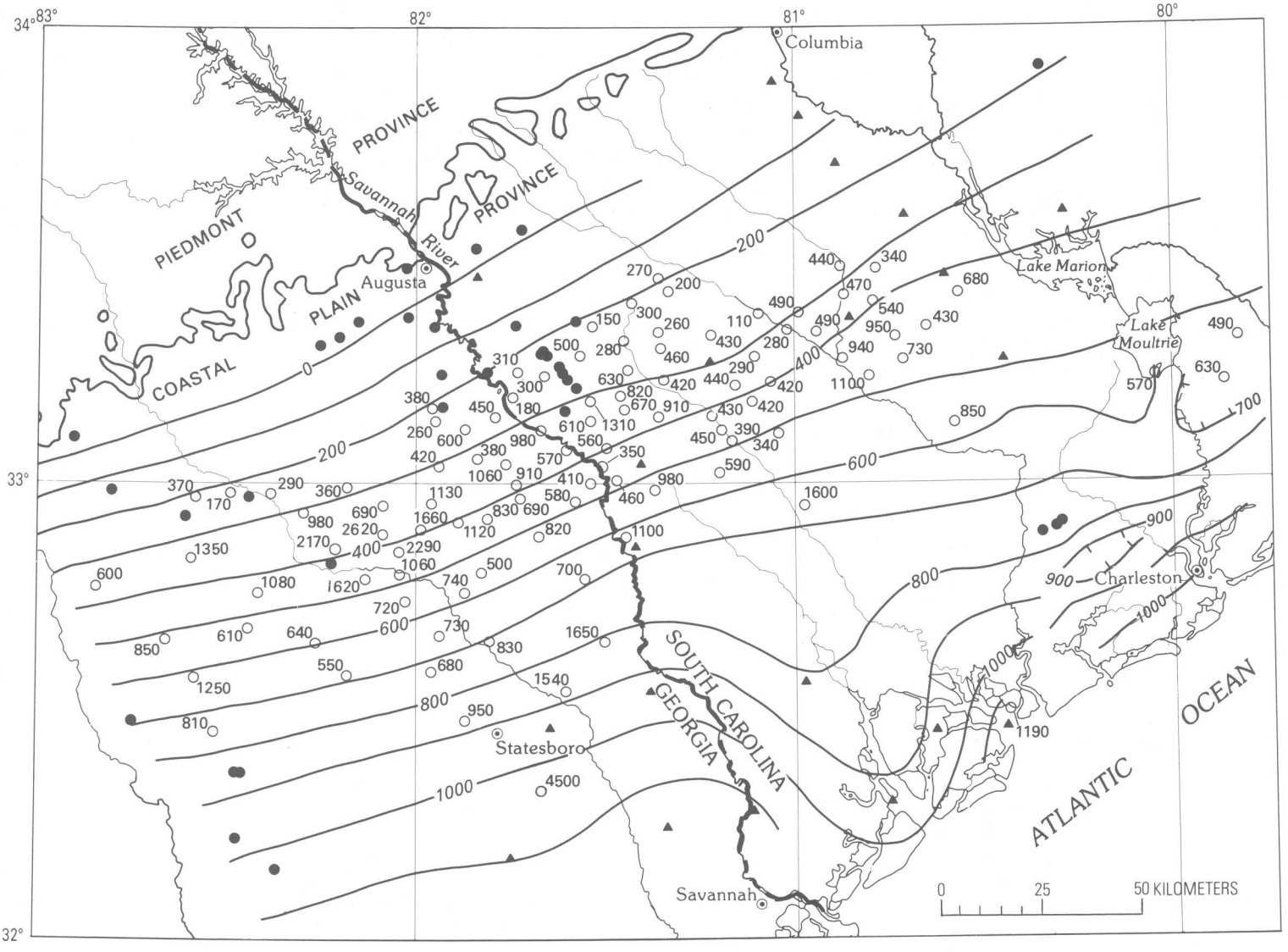

FIGURE 4.—Map of the Savannah River region, Georgia and South Carolina, showing calculated depths to magnetic sources (open circles, in meters), structure contours on the top of the pre-Cretaceous basement surface (contour interval 100 m), and data points from which the contours were derived (solid circles, well data; triangles, seismic-refraction data). Refraction data from Woollard and others (1957), Pooley (1960), and Ackermann (1983).

Mesozoic basin, the Durham-Wadesboro basin in North Carolina. In contrast, the Riddleville basin's east-west elongation, northerly dip, and greater thickness suggest that it is part of the main rift system to the south. The position of line *A–A'* (fig. 3), which divides the two basins, further supports this concept. The Dunbarton basin may be the southernmost basin that parallels the Appalachian trend.

Main rift basin

The deepest magnetic source (4,500 m) found in the area examined is located south of Statesboro, Ga. (fig. 4), where about 3.5 km of pre-Cretaceous nonmagnetic rock is indicated. Because depths were obtained for only a limited part of the main rift basin, this figure might not be typical. For comparison, the maximum thickness of Triassic and Jurassic rocks proven by drilling in this basin is 1.8 km in southwest Georgia (Chowns, 1979). Although the Statesboro area contains no wells to basement and only a few magnetic depth determinations have been made, a deep basin is inferred because of the flat magnetic field.

Florence basin

The rocks retrieved from two wells at Florence, S. C., constitute the major evidence for an early Mesozoic basin in that area. Darton (1896) reported that brown and gray sandstones identified as "Newark Formation"

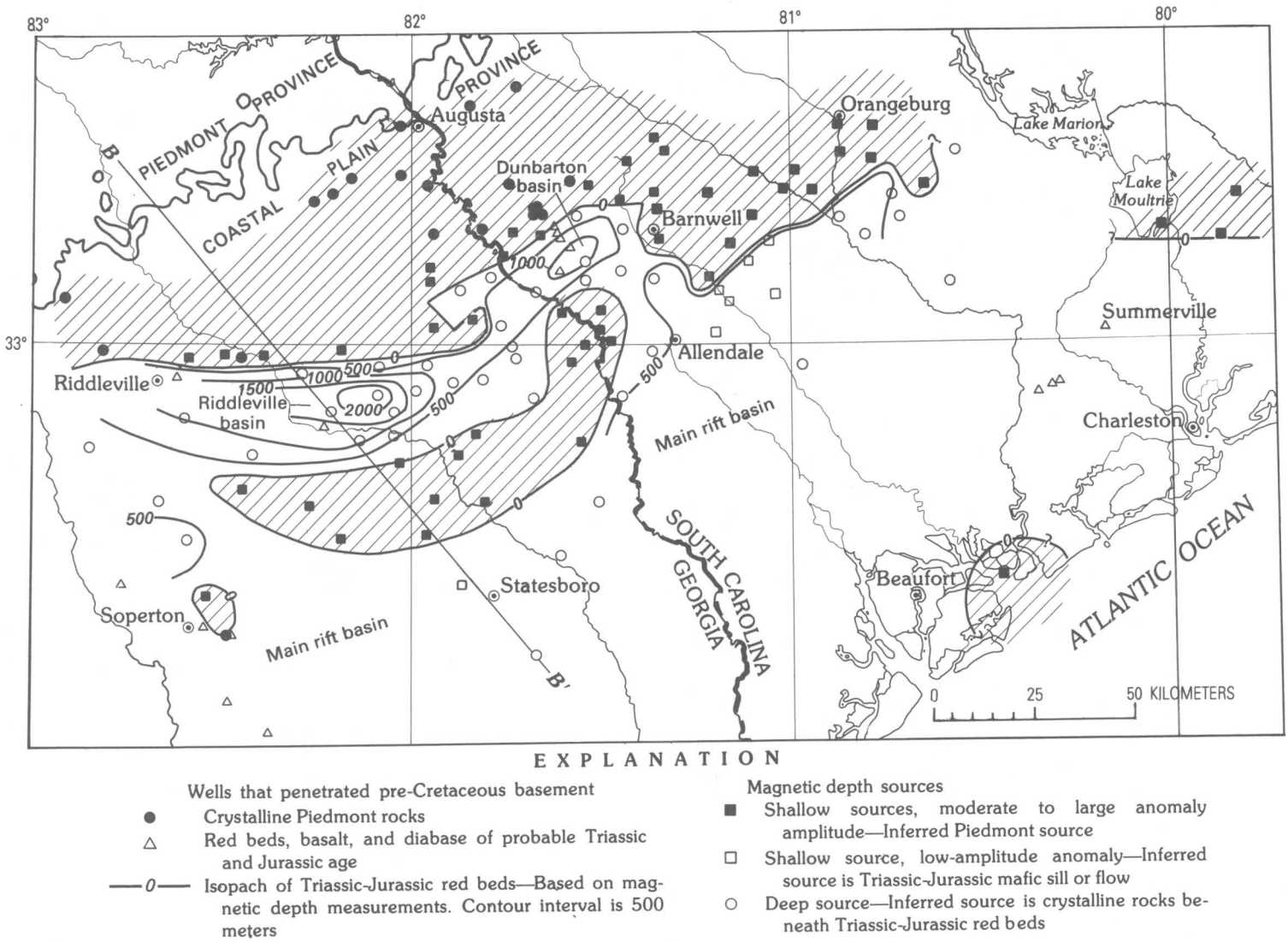

FIGURE 5.—Map showing crystalline basement subcrop (patterned areas) and thickness of lower Mesozoic red beds in the Coastal Plain, Savannah River region, Georgia and South Carolina derived from magnetic depths (fig. 4) and well data.

were terminated by a black trap rock; olivine diabase was recovered from a more recent well there (Siple, 1958). Bonini and Woollard (1960) suggested further that the seismic-refraction measurement 47 km west of Florence, which gave an unusually low basement velocity (3.93 km/s, station 43), may indicate that the basin extends west to include this location. An aeromagnetic low (*A*, fig. 7) is associated with both the well sites and the seismic-refraction site, although the character of this low is less suggestive of a basin than are those of the lows associated with the Riddleville and Dunbarton basins. Popenoe and Zietz (1977) inferred a basin that follows the dimensions of the low. Inspection of the magnetic maps shows magnetic lows of similar character at *B* and *C* (fig. 7). Lows *A* and *B* may be a continuous basin whose center is at Florence, and a separate parallel basin may lie at *C*. Seismic velocities of the pre-Cretaceous rocks of 4.9 and 4.8 km/s (Woollard and others, 1957) within these lows (*B* and *C*, fig. 7) are compatible with velocities for lower Mesozoic sedimentary rocks (Ackermann, 1983). The magnetic lows and low seismic velocities, although supportive of an interpretation of early Mesozoic sedimentary basins, are equally characteristic of predominantly metasedimentary parts of the Carolina slate belt, so the extent of the basin at Florence must remain uncertain at this time.

DIABASE DIKES

The lower Mesozoic rocks most easily recognized from the magnetic maps of the Southeastern States are diabase dikes generally considered to be Late Triassic to Early Jurassic in age (Van Houten, 1977; de Boer and Snider, 1979). Narrow linear magnetic anomalies trend-

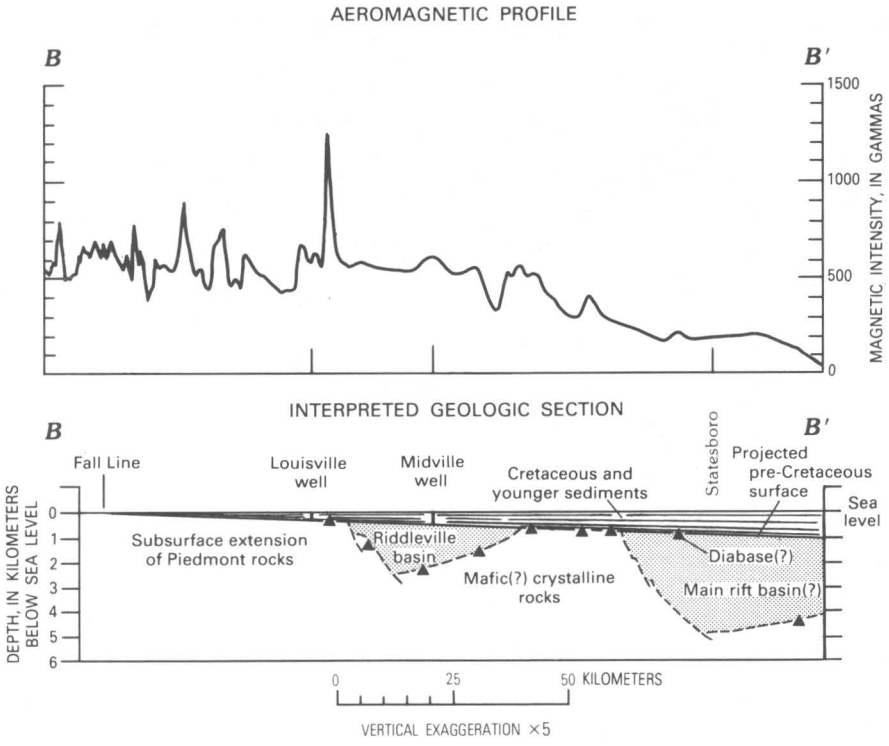

FIGURE 6.—Aeromagnetic profile and interpreted geologic section along line *B–B'* (figs. 3, 5). Magnetic sources shown by triangles, projected onto line of section. Early Mesozoic basins shown by pattern.

ing predominately northwest or north dominate the magnetic maps of central North Carolina and eastern South Carolina and clearly are generated by diabase dikes (Burt and others, 1978). In this region magnetic maps are almost essential tools for mapping dikes in the Piedmont and Coastal Plain. Investigations by Bell and others (1978) have shown that some, and probably many, of the major aeromagnetic anomalies attributed to dikes are caused not by continuous, single, wide dikes but by parallel groups of several narrower dikes of limited continuity. Most of the dikes trend northwest, but in a restricted area of central North Carolina there is a conspicuous swarm of very long dikes trending north, which were largely unknown before magnetic mapping of the region was completed (U.S. Geological Survey, 1974, 1977a, 1977b, 1977c).

Anomalies of both trends can be traced on the magnetic maps of North and South Carolina far out onto the Coastal Plain until increasing depths put the dikes beyond the detection range of the magnetometer. Those anomalies considered to be generated by subsurface dikes are shown in figure 8 (see also Popenoe and Zietz, 1977; Daniels and Zietz, 1978). The north-trending anomalies identify a set of dikes that are unique because of their orientation, length, and continuity. This set can be traced, by means of the magnetic maps, from the vicinity of the Santee River just north of Charleston, S. C., north, across the Piedmont and the Blue Ridge near Buena Vista, Va., a distance of about 480 km (Daniels and Zietz, 1978). The significance of the north-trending dikes in central North Carolina lies with the local coexistence and overlap of the northerly and northwesterly trends. The northerly trends are characteristic of areas to the north (Virginia and Maryland), whereas the northwesterly trends are typical in the southernmost Appalachians (Alabama and Georgia). King (1961, 1971) described a regular change in trend, but there was a conspicuous void for the North Carolina area in his data. The new magnetic data suggest a discontinuity in trend instead of a regular change and imply two distinct ages for the dikes, corresponding to the northern and southern locations. The southern (northwest-trending) set extends from Alabama to northern Virginia, whereas the northern (north-trending) set begins at about 80° W. in eastern South Carolina and central North Carolina and continues northeast (fig. 9). North of Maryland the dikes bend to northeasterly trends. Much of Virginia, North Carolina, and eastern South Carolina contain both trends (overlapping patterns, fig. 9).

The abundance of dikelike magnetic anomalies in the Coastal Plain of eastern South Carolina continues the unusual concentration of dikes found in the immediately

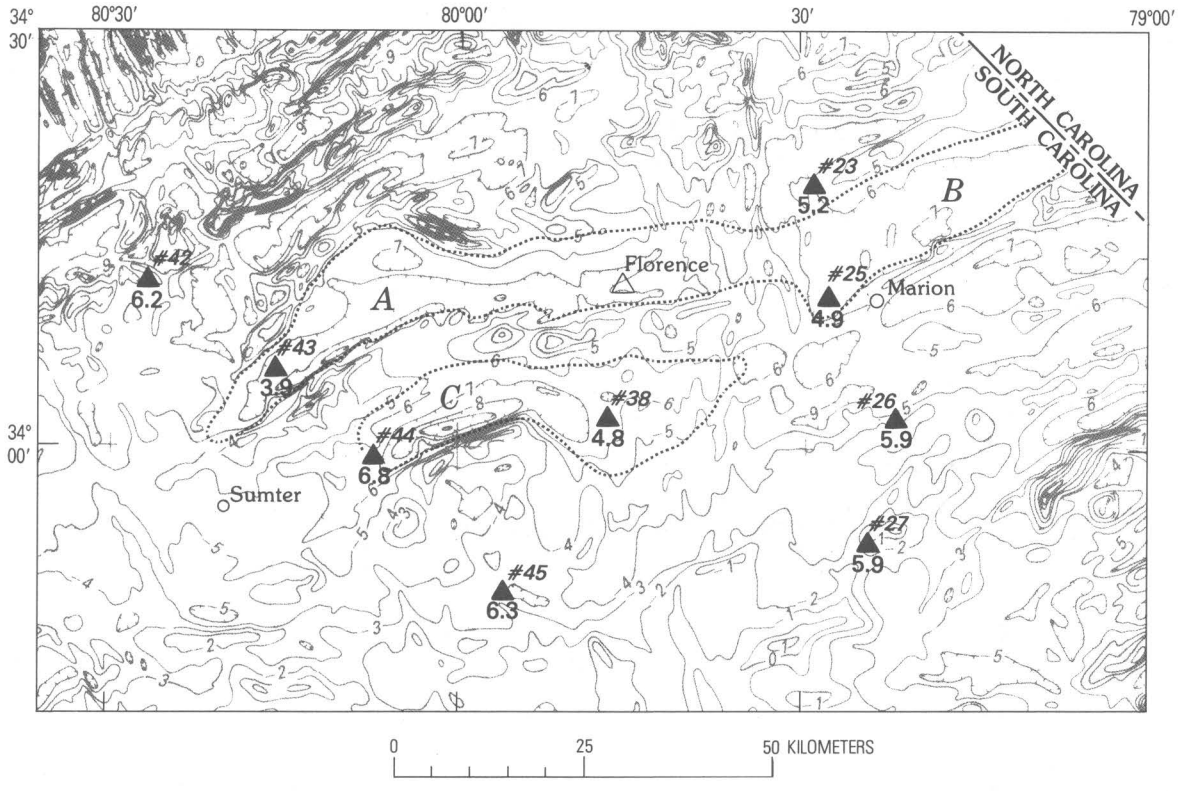

FIGURE 7.—Magnetic map of the Florence, S. C., area, showing magnetic lows that may be underlain by subsurface early Mesozoic basins (areas *A*, *B*, *C*, outlined by dotted lines). Probable Triassic-Jurassic rock recovered from two wells at Florence (open triangle). Sites of seismic-refraction measurements marked by solid triangles [seismic velocity of basement rocks indicated by value below triangles, given in kilometers per second (Woollard and others, 1957)]. Contour interval 100 nT.

adjacent Piedmont. The comparative lack of similar anomalies seen in the Coastal Plain of Georgia (pl. 1), however, is probably related to the similar lack of anomalies over the abundant dikes in the adjacent Piedmont of that area (Pickering and Murray, 1976). De Boer and Snider (1979) have shown that the apparent absence of anomalies there is owing largely to northwest flight lines but also to weaker dike magnetizations. Northwest-trending flight lines in Georgia are nearly parallel to average dike trends in the Piedmont and to the expected trends under the Coastal Plain. Contouring on aeromagnetic maps is usually strongly biased in favor of trends perpendicular to the flight lines, which in this case is the regional Appalachian trend.

It is reasonable to expect, therefore, that a density of diabase dikes similar to that found in the Piedmont exists in the Coastal Plain of Georgia but is not clearly shown by the aeromagnetic maps.

DIABASE SILLS AND BASALT FLOWS

Diabase and basalt, often associated with continental clastic rocks of presumed Triassic and Jurassic age or with Paleozoic marine sedimentary rocks, have been reported from more than 50 wells in the Coastal Plain in South Carolina, Georgia, Alabama, and northern Florida (Applin, 1951; Milton and Hurst, 1965; Milton, 1972; Barnett, 1975; Gohn and others, 1978). In spite of this abundance and the consistent anomalies produced by diabase and basalt in exposed basins, it is difficult to correlate their occurrence in these wells with magnetic anomalies. The magnetic maps of the Coastal Plain were searched for distinctive ring-shaped anomalies indicative of certain diabase sills or basalt flows, and several low-amplitude anomalies, each associated with a low-amplitude gravity high, were located: one near Jeffersonville, Ga., a second near Vidalia, Ga., and a third near Fairfax, S. C. (fig. 10). Magnetic depth estimates place both the Vidalia and Fairfax anomalies level with the base of the Cretaceous. Only the Vidalia anomaly appears to be identified by well samples (diabase in wells GGS 964 and GGS 190, fig. 10; Daniels and Zietz, 1978). The pre-Cretaceous depth control comes from wells near the Vidalia anomaly and from seismic-refraction measurements (Woollard and others, 1957, stations 59 and 60) within 25 km of the Fairfax anomaly. The low-amplitude Vidalia and Fairfax magnetic anomalies are discernible only because they lie in a low-gradient region. Nearby anomalies of other shapes may also be generated by diabase.

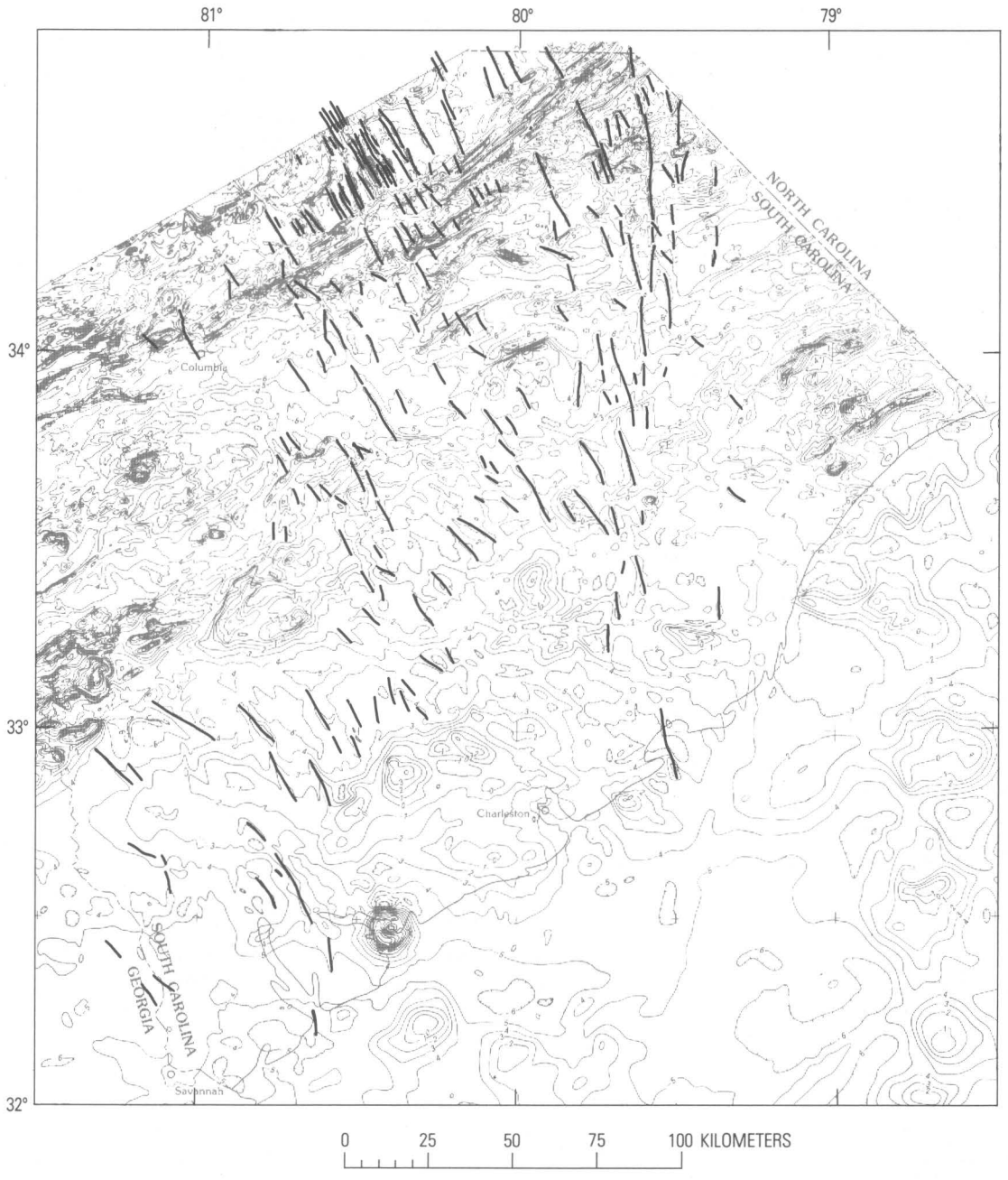

FIGURE 8.—Aeromagnetic map of the South Carolina Coastal Plain. Contour interval 100 nT. Heavy lines trace linear magnetic anomalies that are probably caused by lower Mesozoic diabase dikes. The anomalies interpreted as dikes were picked from larger scale magnetic maps with a 20-nT contour interval. Anomalies having amplitudes of less than 100 nT do not show well on this map.

The lack of magnetic anomalies near most of the wells from which diabase or basalt has been recovered may be due to the size, orientation, and depth of these bodies. Most are probably thin, nearly horizontal sheet structures, which typically do not generate large-amplitude magnetic anomalies, even though moderately magnetized, except at sharp vertical edges. The magnetic intensity of a test model chosen to approximate the dimensions and magnetic properties of the basalt recovered in the Clubhouse Crossroads drill holes near Charleston, S. C. (Phillips, 1983), was calculated to test this effect. The model consisted of a horizontal sheet of basalt 255 m thick at a 775-m depth with 3.5 A/m (amperes/meter) magnetization. Only about 15 nT is produced at a level equivalent to 150 m above ground at the broad center of the model (Daniels and Zietz, 1978).

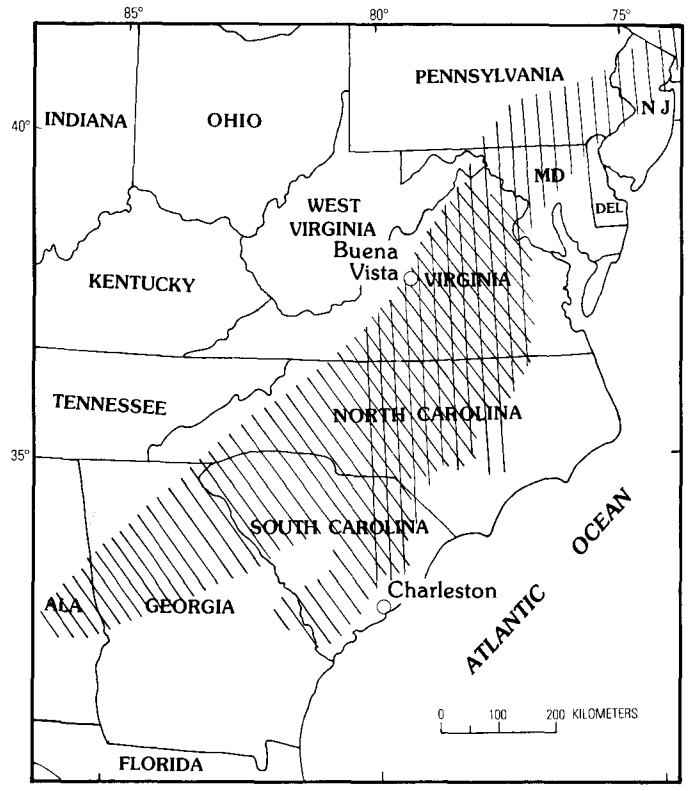

FIGURE 9.—Map of the Southeastern Atlantic States showing two provinces of lower Mesozoic diabase dikes classified on the basis of dike trends. Both trends are present in area of overlap. Dike trends in Virginia and the Carolinas largely determined from magnetic maps. Dike trends elsewhere from King and Beikman (1974).

Anomalies of 150 nT are produced at the vertical edges of the sheet model, but a 255-m vertical edge is probably not typical for a diabase sill or a basalt flow except where faulted. Tapered edges seem more reasonable for basalt flows. Broad anomalies of 15 nT are difficult to discriminate among anomalies of several hundred nT typically produced by contrasts in the crystalline basement, and in fact there does not seem to be a magnetic anomaly clearly associated with any part of the basalt at Charleston.

Features of Possible Early Mesozoic Age

MAFIC INTRUSIVE ROCKS

Three types of mafic rock seem to be present in the pre-Cretaceous basement beneath the Coastal Plain. Lower Mesozoic diabase sills, dikes, and basalt flows have already been discussed. A second type of mafic rock is represented by elongate magnetic anomalies and associated gravity anomalies oriented parallel to magnetic trends in the nearby Piedmont province. These anomalies extend from Alabama near the Fall Line to the vicinity of Cape Fear, N. C. (figs. 11, 12). The Piedmont anomaly trends indicate that the source rocks may be folded mafic metamorphic rocks in an extension of the Piedmont terrain.

A third type of mafic rock is represented by a series of large-amplitude circular or oval magnetic highs and closely matching gravity highs of equally large amplitude (figs. 11, 12). Some of these appear to cut across anomalies of the second type and may, therefore, be younger, perhaps of Mesozoic age. Some are alined along a northerly trend, especially a set of four anomalies off the coast of South Carolina (figs. 11, 12). Several magnetic anomalies of the third type are characterized by an outer ring of higher intensity around a lower intensity core. The most completely developed ring is found on the anomaly at St. Helena Sound near Beaufort, S. C. The St. Helena Sound anomaly is similar in size and shape to an anomaly at Concord, N. C., produced by a gabbro pluton with an outer ring of syenite, which suggests that the ring-shaped anomalies may indicate alkalic-mafic complexes. In general, anomalies of the third group are interpreted as unmetamorphosed mafic-ultramafic intrusive complexes consisting largely of gabbroic rocks (Popenoe and Zietz, 1977; Daniels and Zietz, 1978).

No direct evidence of the age of emplacement of the mafic rocks of the third group is available. Comparison with similar occurrences can suggest approximate ages. The Concord pluton already mentioned is the largest of many gabbroic plutons within the Charlotte belt of North and South Carolina. Although these gabbros currently cannot be dated directly, contact relations show that many are contemporaneous with middle to upper Paleozoic granitic plutons, but there is no direct evidence of Mesozoic age (Speer and others, 1980). Most of the Coastal Plain anomalies differ from the Charlotte belt plutons (other than the Concord pluton) by their larger diameter and the more common ring-shaped anomalies.

Circular mafic plutons as large as the largest in the Coastal Plain occur in the continental interior (as inferred from anomalies on regional magnetic and gravity maps). Two examples in the Mississippi embayment region lie in an environment similar to the Charleston area. One anomaly is associated with exposed alkalic igneous rocks at Magnet Cove, Ark. (Erickson and Blade, 1963). Preliminary lead-alpha measurements on a nepheline syenite dike associated with the complex gave dates of 178 and 184 million years (Jurassic) (Erickson and Blade, 1963). The second example is the Bloomfield anomaly, of possible Mesozoic age, near New Madrid in southeast Missouri, one of several inferred mafic plutons in the region associated with a buried rift system (Hildenbrand and others, 1977).

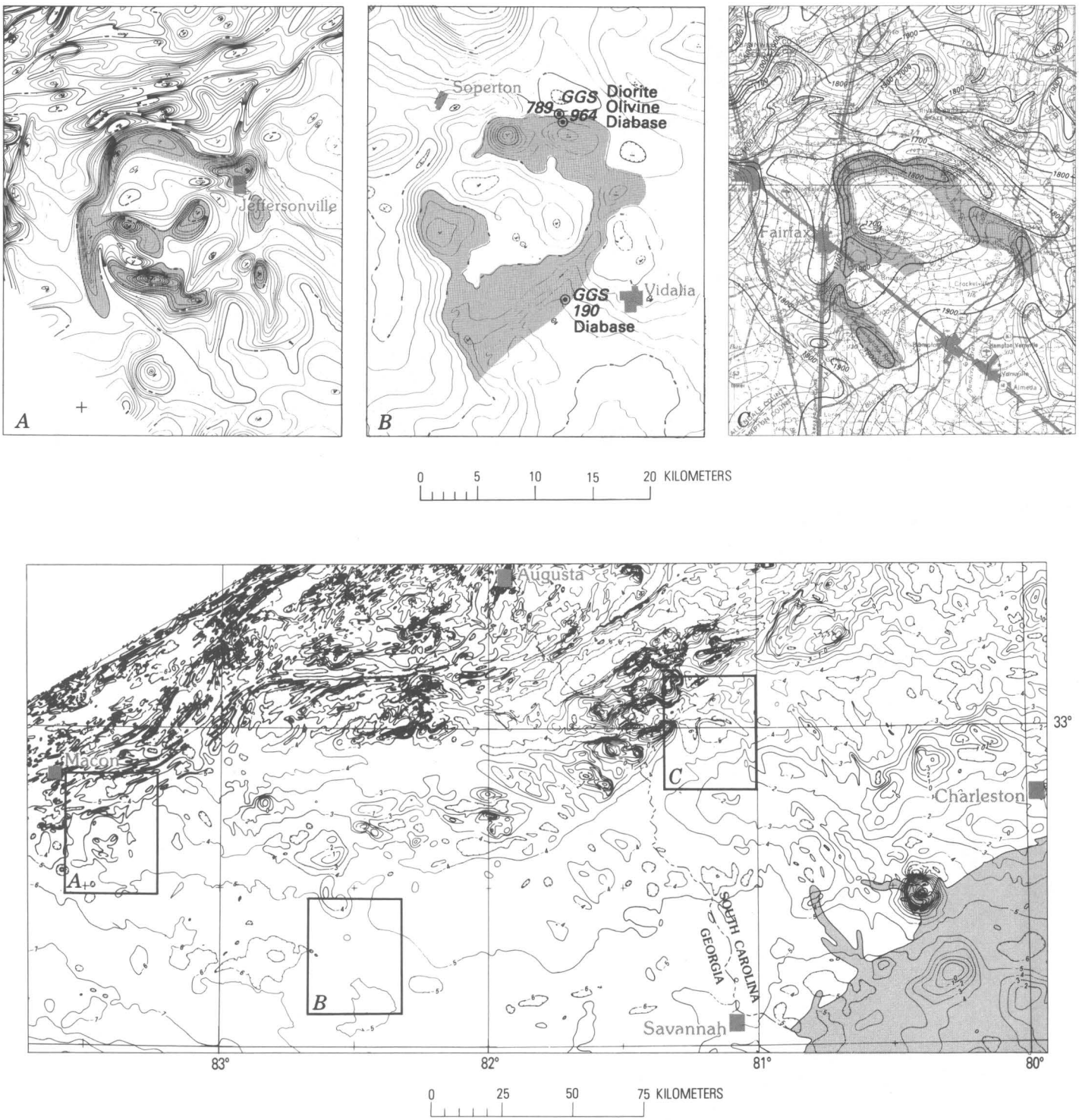

FIGURE 10. – Detailed aeromagnetic maps showing features interpreted as subsurface lower Mesozoic diabase sills (shaded areas in *A*, *B*, and *C*). *A*, Jeffersonville, Ga.; *B*, Vidalia, Ga.; *C*, Fairfax, S. C.; *D*, index aeromagnetic map. Basement rock types from oil tests shown in *B*.

One other example of a large circular mafic intrusive body occurs in the opposite direction, on the edge of the African Coastal Plain at Freetown, Sierra Leone. This location was not as distant in the early Mesozoic, prior to continental separation (Bullard and others, 1965), as it is now. The Freetown layered mafic intrusive body is only partly exposed, but, on the basis of the shape of the gravity anomaly, it is estimated to be circular in outline

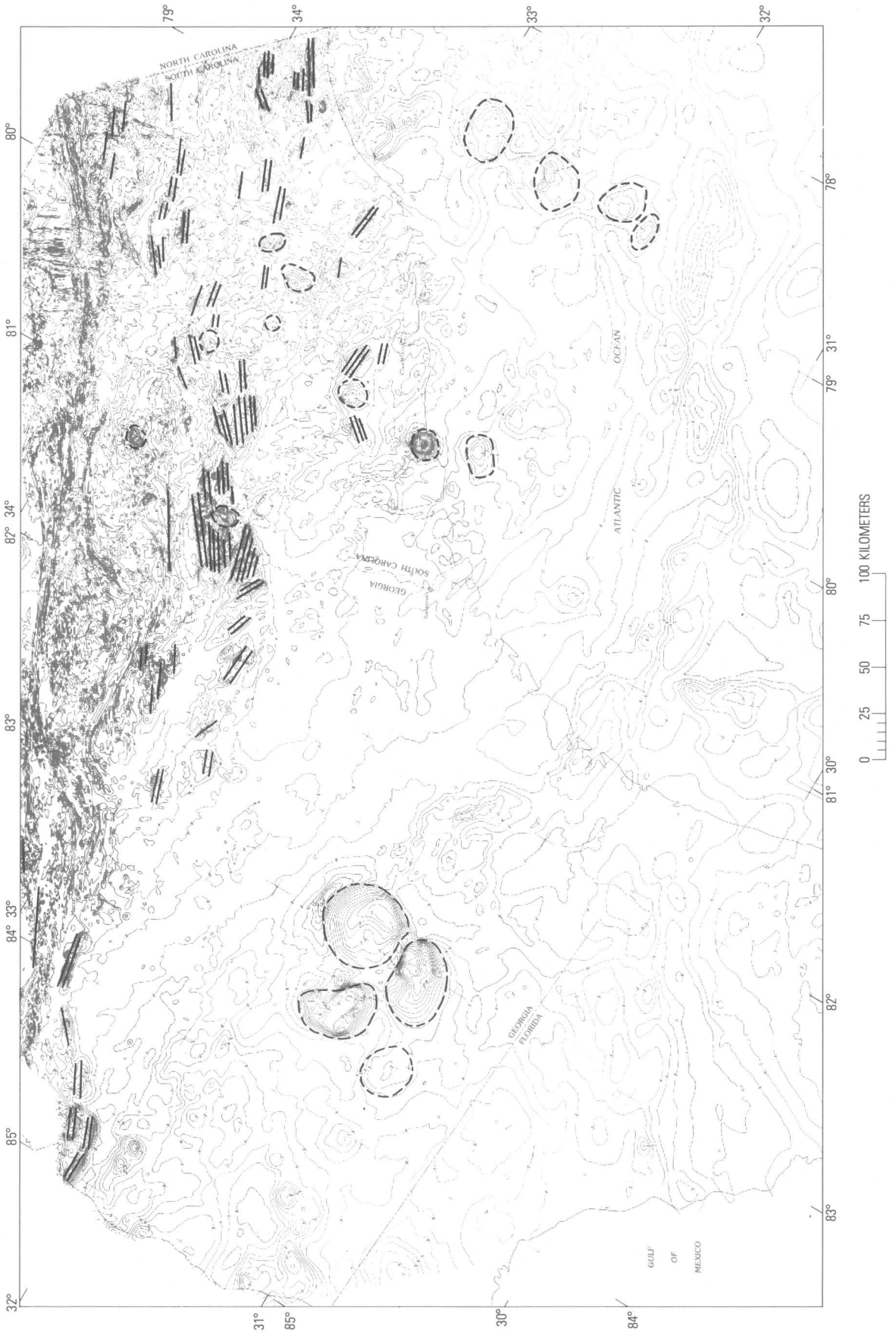

FIGURE 11.—Aeromagnetic map of the Coastal Plain region of the Southeastern United States showing anomalies that may be produced by subsurface mafic rocks. Anomalies marked by lines are thought to reflect deformed mafic metamorphic rocks. Dashed lines enclose roughly circular anomalies interpreted to be cross-cutting gabbroic plutons. Contour interval 100 nT.

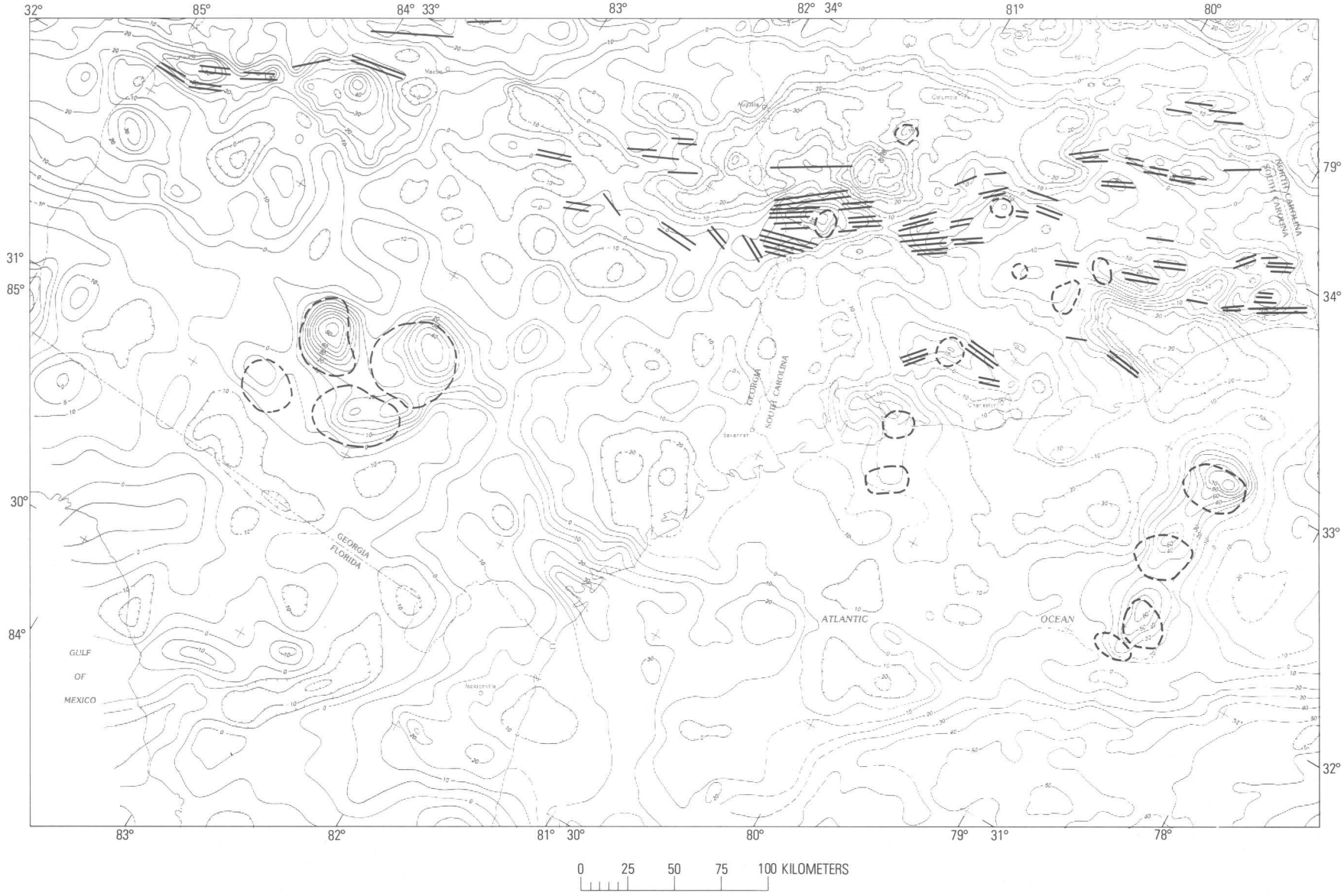

FIGURE 12.—Simple Bouguer gravity anomaly map of part of the Southeastern United States showing correspondence between magnetic interpretation (fig. 11) and gravity anomalies. Gravity data from Krivoy and Eppert (1977), Long and others (1972, 1976), Long and Champion (1977), Oglesby and others (1973), and unpublished data including U.S. Department of Defense gravity file. Contour interval 5 mGal (land), 10 mGal (ocean).

and to have a diameter somewhat larger than those of the Georgia anomalies (Baker and Bott, 1961). The age of the complex has been placed at early Mesozoic on the evidence of paleomagnetic and radiometric measurements (Briden and others, 1971). The occurrence in the African Coastal Plain suggests the geologic setting there is similar to that of the inferred mafic plutons in Georgia and South Carolina.

Circumstantial evidence, based largely on similarity of the anomalies in shape, diameter, and amplitude to anomalies in other regions, suggests that the circular magnetic-gravity anomalies in the Coastal Plain may be generated by lower Mesozoic mafic-ultramafic (alkalic?) complexes or layered mafic complexes.

EAST COAST AND BRUNSWICK MAGNETIC ANOMALIES

The tectonic significance of the East Coast magnetic anomaly (Drake and others, 1968; Taylor and others, 1968) has long been recognized, but the origin is still debated. Taylor and others (1968) used the term "East Coast magnetic anomaly" to include a series of landward, parallel but not continuous magnetic highs and the associated magnetic trough that develop south of Cape Hatteras and cross the coastline at Brunswick, Ga. (fig. 13). Recent workers (Grow and others, 1979; Klitgord and Behrendt, 1979) reserve the name "East Coast anomaly" for the broad, continuous, and larger amplitude magnetic high that terminates close to the shelf edge at 31° N. and apply the term "Brunswick anomaly" to the parallel anomalies, about 1,100 km in length, that continue westward beyond the termination of the East Coast magnetic anomaly. This distinction between the East Coast and Brunswick magnetic anomalies is useful, as several factors suggest that the features are not of the same age even though they are spacially associated. First, the East Coast anomaly coincides with the westernmost edge of Jurassic oceanic crust, on the basis of seismic-reflection data (Klitgord and Behrendt, 1979), whereas the Brunswick anomaly is underlain by crust which is largely continental or transitional in nature (Dillon and others, 1983). Second, the Brunswick anomaly on land is associated with a variety of pre-Cretaceous basement rocks. These include rhyolitic volcanic and pyroclastic rocks near the Georgia coast, granite, probable lower Mesozoic red beds and diabase, and rocks characteristic of the Piedmont (schist, biotite gneiss, granodiorite) near the inner edge of the Coastal Plain. The Brunswick anomaly cannot be related to all these rocks. Further, the anomaly cuts across the trend of the subsurface South Georgia rift (fig. 13), which would tend to rule out a Mesozoic age. The Brunswick anomaly appears to be generated by a structure situated beneath all these rocks, because it does not conform to the distribution of any of these groups. Klitgord and Behrendt (1979) calculated a depth of 2–3 km to the top of the source of this anomaly at the coastline, which places the source at about 0.5–1.5 km below the base of the Cretaceous. The Brunswick anomaly does bound, on their north, the distinctive, flat-lying, Ordovician to Devonian clastic rocks found in numerous wells in northern Florida and southeastern Georgia that may underlie Triassic rocks in southwestern Georgia (Applin, 1951; Bridge and Berdan, 1951; Carroll, 1963; Barnett, 1975). On the basis of palynological evidence, these rocks were separated from the Alabama Valley and Ridge rocks by about 7 degrees of latitude more during the Silurian than they are now (Cramer, 1971). This suggests that a Paleozoic suture between North American rocks and a Florida microcontinent lies somewhere north of the Florida Paleozoic rocks and that the Brunswick magnetic anomaly may mark the position of a structure associated with this suture (Nishenko and Sykes, 1979). Evidence supporting the suture interpretation can be seen by comparing the trends of long-wavelength magnetic anomalies (generated by deep crystalline basement) on either side of the anomaly. North of the Brunswick anomaly the trend is generally east-west, whereas northeast trends predominate south of the anomaly (fig. 13; pl. 1). This suggests that two terrains having different orogenic imprints have been juxtaposed and welded together.

LINEAR FEATURES AND FAULTS

The parallel alinement of numerous individual linear magnetic anomalies into long curvilinear traces is a common feature of the aeromagnetic maps of the Piedmont south of Virginia. The association of some individual anomalies with mylonitic rocks (Daniels, 1974; Casadevall, 1977) led Hatcher and others (1977) to propose an eastern Piedmont fault system along one of these alinements. This and other curvilinear magnetic alinements in the Coastal Plain (Daniels and Zietz, 1978) are probably pre-Mesozoic tectonic features.

Linear magnetic gradients are also abundant on the aeromagnetic maps of the Coastal Plain, especially in the region near the Savannah River, and are largely associated with pre-Cretaceous basement here interpreted to be lower Mesozoic. Our interpretation of lineaments that may be significant is shown in figure 14. Some of these linear gradients may be produced by pre-Mesozoic basement faults, and some of these may have been reactivated during Mesozoic rifting. There are undoubtedly many faults which are not expressed in the magnetic maps. The association of the Orangeburg scarp with one of these gradients has prompted speculation that a basement fault has exerted structural control on the scarp (Popenoe and Zietz, 1977). The alinement of the scarp (*A*–*A'*, fig. 14) (Winkler and Howard, 1977)

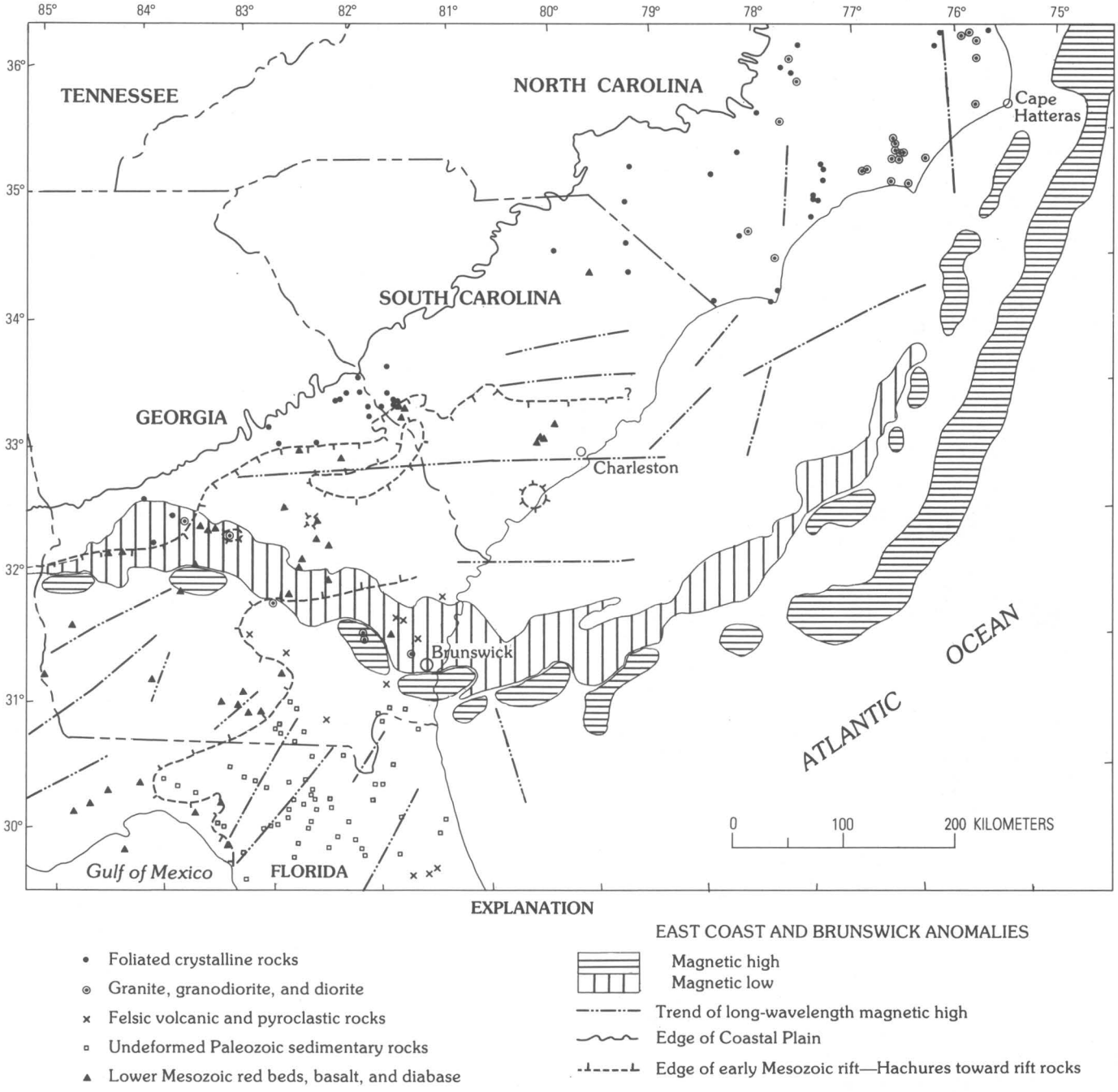

FIGURE 13.—Map showing relation between the Brunswick and East Coast magnetic anomalies and the subsurface early Mesozoic rift, trends of long-wavelength magnetic highs, and rock type in basement wells.

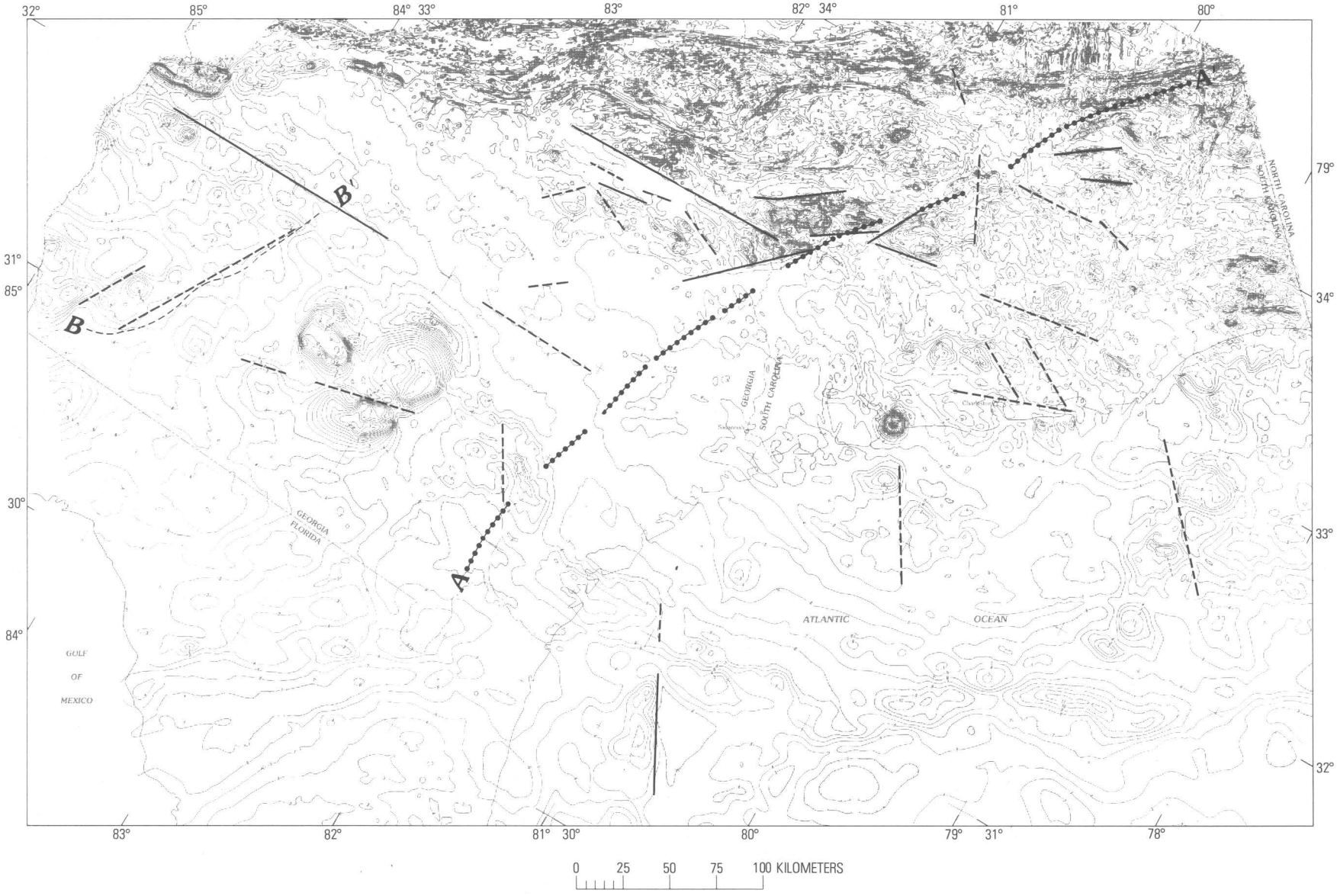

FIGURE 14.—Aeromagnetic map of the Coastal Plain region of the Southeastern United States showing some of the linear magnetic gradients and anomaly alinements that may be related to subsurface faults. Solid lines are judged more significant than dashed lines. Some of these features are more easily seen on maps with a smaller contour interval. The trace of the Orangeburg scarp is shown by a dot-dash line, *A*–*A*′, after Winkler and Howard (1977). Part of the contact between Eocene and younger rocks is shown by the short-dashed line *B*–*B*′, after Pickering and Murray (1976). Magnetic contour interval 100 nT.

with the magnetic gradient, however, is limited to a short segment near Fairfax, S. C., which is only a small fraction of the total length of the scarp.

In southwestern Georgia, a subtle linear gradient that divides areas of high and low magnetic intensity is approximately alined with the contact between Eocene and younger rocks (*B–B'*, fig. 14) (Pickering and Murray, 1976). This relationship suggests that basement structure, as indicated by the magnetic map, has influenced the distribution of Tertiary sediments.

CONCLUSIONS

The evidence from aeromagnetic, regional gravity, seismic-refraction, and deep-well data indicates that the Coastal Plain of Georgia and South Carolina is underlain by abundant lower Mesozoic rocks. Several, and perhaps many, individual basins compose a broad, complex rift system, the South Georgia rift, oriented roughly east-northeast and extending from the Gulf of Mexico to the Atlantic Ocean. This rift is filled with continental, subaerial clastic sedimentary rocks, basalt flows, and numerous interlayered diabase sills. North-trending and northwest-trending diabase dikes intrude both the basins and the flanking crystalline basement. In many respects, these subsurface basins are closely similar to exposed early Mesozoic basins within the Piedmont province of the Appalachian orogen. The major differences are scale and trend. The subsurface rift system is longer than and, at its widest point, four times the width of the largest exposed basin of the Appalachian orogen (Culpeper-Gettysburg-Newark basins combined). The trend and alinement of the South Georgia rift suggest an affinity more with the rift that preceded the opening of the Gulf of Mexico than with the exposed early Mesozoic basins along the Appalachian system.

Mapping the subsurface rift by means of the magnetic maps yields uneven results, owing in part to the highly variable magnetic contrast between the lower Mesozoic rocks and the flanking rocks. Most of the basin analysis in this paper is concentrated on a region of the inner (shallow) Coastal Plain on either side of the Savannah River because of favorable magnetic contrasts in that area. There qualitative and quantitative analysis indicates two interconnected basins that are partly separated from the main rift by a broad subcrop of crystalline (probably mostly mafic) basement. The thickness of nonmagnetic rock beneath the Cretaceous was estimated by subtracting the value for depth to the base of the Cretaceous from the value for the top of the magnetic sources. Isopach contours of the nonmagnetic rock (interpreted to be lower Mesozoic rift sediments) outline the two basins and show areas of maximum sediment accumulation. The Dunbarton basin, which is at least 1.0 km thick and has a northeast trend and probable southeast dip, seems similar to exposed basins. In contrast, the Riddleville basin is at least 2.2 km thick, trends east-west, and probably dips to the north; it appears closer in style to the main rift immediately to the south. The main rift may be as thick as 3.5 km near Statesboro, Ga. Well samples and linear northeast-trending magnetic anomalies indicate that highly magnetic Piedmont rocks flank the rift on the north. A few similar anomalies appear within the rift, which indicate possible Piedmont basement. Nonmagnetic rhyolitic volcanic rocks, granites, and Paleozoic sedimentary rocks flank and underlie the rift on the south, making magnetic discrimination of the south edge of the rift difficult. Sharp linear magnetic gradients partly bound the rift and inliers of crystalline rock and indicate basement faults active in the early Mesozoic.

Lower Mesozoic diabase dikes are clearly present in the basement in South Carolina. Owing to unfavorable flight-line direction and weaker dike magnetization, the dikes in Georgia are not detected by aeromagnetic surveys. In South Carolina, only northwest-trending magnetic anomalies, characteristic of the Alabama-Georgia region, are found west of 80° W. East of 80°, prominent north-trending anomalies, characteristic of more northern States, are mixed with the northwest-trending set. The Charleston earthquake epicentral zone is located near the western edge of the overlap zone. One set of north-south anomalies can be traced northward on magnetic maps continuously for 480 km. The existence of two dike sets suggests that two episodes of intrusion may have occurred.

Several circular, low-amplitude magnetic anomalies, thought to characterize certain diabase sills, are identified within the subsurface rift system.

Other types of major magnetic features are generated by rocks of uncertain age, which have not been penetrated by drilling. Intense circular magnetic-gravity anomalies are interpreted to be mafic plutons similar to but mostly larger than the mafic plutons that occur in the Charlotte belt. Comparison with large circular mafic plutons in the Mississippi embayment region and in Sierra Leone suggests that an early Mesozoic age is reasonable for some or all of these plutons. The circular anomalies in the Coastal Plain are considered to be distinct from a belt of elongated magnetic-gravity anomalies, which may be older, metamorphosed mafic rocks.

The largest magnetic feature of the Coastal Plain region is also the least understood. The Brunswick magnetic anomaly is actually a series of long-wavelength, elongate high-low anomaly pairs arranged in a broad S-shaped curve. The low is the dominant feature; it begins in the Atlantic Ocean, landward of and

parallel to the East Coast magnetic anomaly. The anomaly crosses the coastline at Brunswick, Ga., and passes into Alabama where the magnetic data terminate. The anomaly cannot be explained in terms of the basement rocks returned from deep wells, because these rocks do not form a coherent group. The basement rocks in the path of the anomaly include felsic volcanic rocks, granites, schist, biotite gneiss, and lower Mesozoic rift rocks (red beds and diabase). The most significant feature of the Brunswick anomaly is that it acts as a division between two terrains of differing magnetic character. North of the anomaly the longest wavelength anomalies have an easterly orientation, whereas south of the anomaly a northeast trend is most characteristic at the same wavelengths. This relationship suggests that the Brunswick anomaly may be closely related to a Paleozoic suture between a Florida–South Georgia microcontinent and the North American continent. Thrusting resulting from the collision may have buried the rocks that produce the anomaly.

REFERENCES CITED

Ackermann, H. D., 1983, Seismic-refraction study in the area of the Charleston, South Carolina, 1886 earthquake, *in* Gohn, G. S., ed., Studies related to the Charleston, South Carolina, earthquake of 1886–Tectonics and seismicity: U.S. Geological Survey Professional Paper 1313, p. F1–F20.

Applin, E. R., and Applin, P. L., 1964, Logs of oil tests in the Coastal Plain of Georgia: Georgia Geologic Survey Bulletin 74, 229 p.

Applin, P. L., 1951, Preliminary report on buried pre-Mesozoic rocks in Florida and adjacent States: U.S. Geological Survey Circular 91, 28 p.

Baker, C. O., and Bott, M. H. P., 1961, A gravity survey over the Freetown basic complex of Sierra Leone: Overseas Geology and Mineral Resources, v. 8, no. 3, p. 260–278.

Barnett, R. S., 1975, Basement structure of Florida and its tectonic implications: Gulf Coast Association of Geological Societies Transactions, v. 25, p. 122–142.

Bell, Henry, III, Daniels, D. L., Popenoe, Peter, and Huff, W. E., 1978, Comparison of anomalies detected by airborne and truck-mounted magnetometers in the Haile-Brewer area, South Carolina, *in* Snoke, A. W., ed., Geological investigations of the eastern Piedmont, Southern Appalachians: Carolina Geological Society Guidebook, p. 21–27.

Bonini, W. E., and Woollard, G. P., 1960, Subsurface geology of North Carolina–South Carolina Coastal Plain from seismic data: American Association of Petroleum Geologists Bulletin, v. 44, no. 3, p. 298–315.

Briden, J. C., Henthorn, D. I., and Rex, D. C., 1971, Palaeomagnetic and radiometric evidence for the age of the Freetown igneous complex, Sierra Leone: Earth and Planetary Science Letters, v. 12, no. 4, p. 385–391.

Bridge, Josiah, and Berdan, J. M., 1951, Preliminary correlation of the Paleozoic rocks from test wells in Florida and adjacent parts of Georgia and Alabama: U.S. Geological Survey Open-File Report, 8 p.

Bromery, R. W., and Griscom, Andrew, 1967, Aeromagnetic and generalized geologic map of southeastern Pennsylvania: U.S. Geological Survey Geophysical Investigations Map GP–577, scale 1:125,000.

Brown, P. M., Brown, D. E., Reid, M. S., and Lloyd, O. B., Jr., 1979, Evaluation of the geologic and hydrologic factors related to the waste-storage potential of Mesozoic aquifers in the southern part of the Atlantic Coastal Plain, South Carolina and Georgia: U.S. Geological Survey Professional Paper 1088, 37 p.

Bullard, E. C., Everett, J. E., and Smith, A. G., 1965, The fit of continents around the Atlantic, *in* A symposium on continental drift: Philosophical Transactions of the Royal Society of London, ser. A, v. 258, no. 1088, Mathematical and Physical Sciences, p. 41–51.

Burt, E. R., Carpenter, P. A., III, McDaniel, R. D., and Wilson, W. F., 1978, Diabase dikes of the eastern Piedmont of North Carolina: North Carolina Geological Survey Section, Information Circular 23, 12 p.

Carroll, Dorothy, 1963, Petrography of some sandstones and shales of Paleozoic age from borings in Florida: U.S. Geological Survey Professional Paper 454–A, p. A1–A15.

Casadevall, Tom, 1977, The Nutbush Creek dislocation, Vance County, North Carolina, and Mecklenburg County, Virginia–a probable fault of regional significance [abs.]: Geological Society of America Abstracts with Programs, v. 9, no. 2, p. 127–128.

Chowns, T. M., 1979, Pre-Cretaceous rocks beneath the Georgia Coastal Plain [abs.]: Second symposium on the geology of the southeastern Coastal Plain, March 5–6, Georgia Southwestern College, Americus, Georgia, Program with Abstracts, p. 5.

Christl, R. J., 1964, Storage of radioactive wastes in basement rock beneath the Savannah River Plant: Du Pont de Nemours Savannah River Plant Laboratory Report, DP–844, 39 p., and Appen. A–G.

Cook, F. A., Albaugh, D. S., Brown, L. D., Kaufman, Sidney, Oliver, J. E., and Hatcher, R. D., Jr., 1980, The COCORP seismic reflection transverse in the southern Appalachian orogen–Tennessee to Savannah [abs.]: Geological Society of America Abstracts with Programs, v. 12, no. 7, p. 405.

Cooke, C. W., 1936, Geology of the Coastal Plain of South Carolina: U.S. Geological Survey Bulletin 867, 196 p.

Cramer, F. H., 1971, Position of the North Florida Lower Paleozoic block in Silurian time; phytoplankton evidence: Journal of Geophysical Research, v. 76, no. 20, p. 4754–4757.

Daniels, D. L., 1974 [1975], Geological interpretation of geophysical maps, central Savannah River area, South Carolina and Georgia: U.S. Geological Survey Geophysical Investigations Map GP–893, 9 p.

———1980, Geophysical-geological analysis of Fairfax County, Virginia: U.S. Geological Survey Open-File Report 80–1165, 66 p.

Daniels, D. L., and Zietz, Isidore, 1978, Geologic interpretation of aeromagnetic maps of the Coastal Plain region of South Carolina and parts of North Carolina and Georgia: U.S. Geological Survey Open-File Report 78–261, 62 p., Appendix.

Darton, N. H., 1896, Artesian-well prospects in the Atlantic Coastal Plain region: U.S. Geological Survey Bulletin 138, 232 p.

de Boer, Jelle, and Snider, F. G., 1979, Magnetic and chemical variations of Mesozoic diabase dikes from eastern North America: evidence for a hot spot in the Carolinas?: Geological Society of America Bulletin, pt. 1, v. 90, no. 2, p. 185–198.

Dillon, W. P., Klitgord, K. D., and Paull, C. K., 1983, Mesozoic development and structure of the continental margin off South Carolina, *in* Gohn, G. S., ed., Studies related to the Charleston, South Carolina, earthquake of 1886–Tectonics and seismicity: U.S. Geological Survey Professional Paper 1313, p. N1–N16.

Drake, C. L., Ewing, J. I., and Stockard, Henry, 1968, The continental margin of the eastern United States: Canadian Journal of Earth Sciences, v. 5, no. 4, p. 993–1010.

Erickson, R. L., and Blade, L. V., 1963, Geochemistry and petrology of the alkalic igneous complex at Magnet Cove, Arkansas: U.S. Geological Survey Professional Paper 425, 95 p.

Gohn, G. S., Gottfried, David, Lanphere, M. A., and Higgins, B. B., 1978, Regional implications of Triassic or Jurassic age for basalt and sedimentary red beds in the South Carolina Coastal Plain: Science, v. 202, no. 4370, p. 887–890.

Grow, J. A., Bowin, C. O., and Hutchinson, D. R., 1979, The gravity field of the U.S. Atlantic continental margin: Tectonophysics, v. 59, p. 27–52.

Hatcher, R. D., Jr., Howell, D. E., and Talwani, Pradeep, 1977, Eastern Piedmont fault system: speculations on its extent: Geology, v. 5, no. 10, p. 636–640.

Hildenbrand, T. G., Kane, M. F., and Stauder, W., S. J., 1977 [1978], Magnetic and gravity anomalies in the northern Mississippi Embayment and their spacial relation to seismicity: U.S. Geological Survey Miscellaneous Field Studies Map MF-914, scale 1:1,000,000.

King, P. B., 1961, Systematic pattern of Triassic dikes in the Appalachian region: U.S. Geological Survey Professional Paper 424-B, p. B93–B95.

———1969, Tectonic map of North America: U.S. Geological Survey Map, scale 1:5,000,000, 2 sheets.

———1971, Systematic pattern of Triassic dikes in the Appalachian region–Second report: U.S. Geological Survey Professional Paper 750-D, p. D84–D88.

King, P. B., and Beikman, H. B., 1974 [1975], Geologic map of the United States: U.S. Geological Survey, scale 1:2,500,000.

Klitgord, K. D., and Behrendt, J. C., 1977 [1978], Aeromagnetic anomaly map of the United States Atlantic Continental Margin: U.S. Geological Survey Miscellaneous Field Studies Map MF-913, scale 1:1,000,000, 2 sheets.

———1979, Basin structure of the U.S. Atlantic margin, *in* Watkins, J. S., Montadert, Lucien, and Dickerson, P. W., eds., Geological and geophysical investigations of continental margins: American Association of Petroleum Geologists Memoir 29, p. 85–112.

Klitgord, K. D., Popenoe, Peter, and Schouten, Hans, 1982, Florida: a Jurassic transform plate boundary: Journal of Geophysical Research, in press.

Krivoy, H. L., and Eppert, H. C., Jr., 1977, Simple Bouguer anomaly representation over a part of the Atlantic Continental Shelf and adjacent land areas of Georgia, the Carolinas, and northern Florida: U.S. Geological Survey Open-File Map 77-316, scale 1:1,000,000.

Lanphere, M. A., 1983, $^{40}Ar/^{39}Ar$ ages of basalt from Clubhouse Crossroads test hole #2, near Charleston, South Carolina, *in* Gohn, G. S., ed., Studies related to the Charleston, South Carolina, earthquake of 1886–Tectonics and seismicity: U.S. Geological Survey Professional Paper 1313, p. B1–B8.

Long, L. T., Bridges, S. R., and Dorman, L. M., 1972, Simple Bouguer gravity map of Georgia: Georgia Institute of Technology, scale 1:500,000.

Long, L. T., and Champion, J. W., Jr., 1977, Bouguer gravity map of the Summerville-Charleston, South Carolina epicentral zone and tectonic implications, *in* Rankin, D. W., ed., Studies related to the Charleston, South Carolina, earthquake of 1886–A preliminary report: U.S. Geological Survey Professional Paper 1028, p. 151–166.

Long, L. T., Talwani, Pradeep, and Bridges, S. R., 1976, Simple Bouguer gravity map of South Carolina: South Carolina Development Board, Division of Geology, scale 1:500,000.

Maher, J. C., 1971, Geologic framework and petroleum potential of the Atlantic Coastal Plain and Continental Shelf: U.S. Geological Survey Professional Paper 659, 98 p.

Marine, I. W., 1974, Geohydrology of buried Triassic basin at Savannah River Plant, South Carolina: American Association of Petroleum Geologists Bulletin, v. 58, no. 9, p. 1825–1837.

Marine, I. W., and Siple, G. E., 1974, Buried Triassic basin in the central Savannah River area, South Carolina and Georgia: Geological Society of America Bulletin, v. 85, no. 2, p. 311–320.

McGookey, D. P., 1975, Gulf Coast Cenozoic sediments and structure: an excellent example of extra-continental sedimentation: Gulf Coast Association of Geological Societies Transactions, v. 25, p. 104–120.

Milton, Charles, 1972, Igneous and metamorphic basement rocks of Florida: Florida Bureau of Geology Bulletin 55, 125 p.

Milton, Charles, and Grasty, Robert, 1969, "Basement" rocks of Florida and Georgia: American Association of Petroleum Geologists Bulletin, v. 53, no. 12, p. 2483–2493.

Milton, Charles, and Hurst, V. J., 1965, Subsurface "basement" rocks of Georgia: Georgia Geologic Survey Bulletin 76, 56 p.

Neathery, T. L., and Thomas, W. A., 1975, Pre-Mesozoic basement rocks of the Alabama Coastal Plain: Gulf Coast Association of Geological Societies Transactions, v. 25, p. 86–99.

Nishenko, S. P., and Sykes, L. R., 1979, Fracture zones, Mesozoic rifts and the tectonic setting of the Charleston, South Carolina earthquake of 1886 [abs.]: EOS, American Geophysical Union Transactions, v. 60, no. 18, p. 310.

Oglesby, W. R., Ball, M. M., and Chaki, S. J., 1973, Bouguer anomaly map of the Florida Peninsula and adjoining continental shelves: Florida Bureau of Geology Map Series No. 57, scale 1:1,000,000.

Petty, A. J., Petrafeso, F. A., and Moore, F. C., Jr., 1965, Aeromagnetic map of the Savannah River Plant area, South Carolina and Georgia: U.S. Geological Survey Geophysical Investigations Map GP-489, scale 1:250,000.

Phillips, J. D., 1983, Paleomagnetic investigations of the Clubhouse Crossroads basalt, *in* Gohn, G. S., ed., Studies related to the Charleston, South Carolina, earthquake of 1886–Tectonics and seismicity: U.S. Geological Survey Professional Paper 1313, p. C1–C18.

Pilger, R. H., Jr., 1978, A closed Gulf of Mexico, pre-Atlantic Ocean plate reconstruction and the early rift history of the Gulf and North Atlantic: Gulf Coast Association of Geological Societies Transactions, v. 28, p. 385–393.

Pickering, S. M., Jr., and Murray, J. B., 1976, Geologic map of Georgia: Georgia Geologic Survey, scale 1:500,000.

Pooley, R. N., 1960, Basement configuration of subsurface geology of eastern Georgia and southern South Carolina as determined by seismic refraction measurements: Madison, University of Wisconsin, Masters thesis, 47 p.

Popenoe, Peter, 1977, A probable major Mesozoic rift system in South Carolina and Georgia [abs.]: EOS, American Geophysical Union Transactions, v. 58, no. 6, p. 432.

Popenoe, Peter, and Zietz, Isidore, 1977, The nature of the geophysical basement beneath the Coastal Plain of South Carolina and northeastern Georgia, *in* Rankin, D. W., ed., Studies related to the Charleston, South Carolina, earthquake of 1886–A preliminary report: U.S. Geological Survey Professional Paper 1028, p. 119–137.

Rankin, D. W., Popenoe, Peter, and Klitgord, K. D., 1978, The tectonic setting of Charleston, South Carolina [abs]: Geological Society of America Abstracts with Programs, v. 10, no. 4, p. 195.

Richards, H. G., 1954, Subsurface Triassic in eastern North Carolina: American Association of Petroleum Geologists, v. 38, no. 12, p. 2564–2565.

Salvador, Amos, 1979, Late Triassic-Jurassic paleogeography and origin of the Gulf of Mexico [abs.]: American Association of Petroleum Geologists Bulletin, v. 63, no. 3, p. 520.

Siple, G. E., 1958, Stratigraphic data from selected oil tests and water wells in the South Carolina Coastal Plain: South Carolina Division of Geology, Mineral Industries Laboratory Monthly Bulletin, v. 2, no. 9, p. 62–68.

———1967, Geology and ground water of the Savannah River Plant and vicinity, South Carolina: U.S. Geological Survey Water Supply Paper 1841, 113 p.

Speer, J. A., Becker, S. W., and Farrar, S. S., 1980, Field relations and petrology of the postmetamorphic, coarse-grained granitoids and associated rocks of the southern Appalachian Piedmont, *in* Wones, D. R., ed., The Caledonides in the USA, Proceedings of the second symposium of the International Geological Correlation Program, Caledonide Orogen Project: Virginia Polytechnic Institute and State University Memoir 2, p. 137–148.

Stromquist, A. A., and Sundelius, H. W., 1969, Stratigraphy of the Albemarle Group of the Carolina Slate Belt in central North Carolina: U.S. Geological Survey Bulletin 1274–B, 22 p.

Taylor, P. T., Zietz, Isidore, and Dennis, L. S., 1968, Geologic implications of aeromagnetic data for the eastern continental margin of the United States: Geophysics, v. 33, no. 5, p. 755–780.

U.S. Geological Survey, 1970, Aeromagnetic map of the Camden-Kershaw area, north-central South Carolina: U.S. Geological Survey Open-File Map, scale 1:62,500.

———1973, Aeromagnetic map of north-central Georgia: U.S. Geological Survey Open-File Report, scale 1:250,000.

———1974, Aeromagnetic map of parts of the Greensboro and Raleigh 1 by 2 degree quadrangles, North Carolina: U.S. Geological Survey Open-File Report 74–29, scale 1:250,000.

———1975, Aeromagnetic map of Charleston and vicinity, South Carolina: U.S. Geological Survey Open-File Report 75–590, scale 1:250,000.

———1976a, Aeromagnetic maps of parts of Georgia, South Carolina, and North Carolina: U.S. Geological Survey Open-File Report 76–181, 13 pls.

———1976b, Aeromagnetic map of parts of the Brunswick and Savannah 1° by 2° quadrangles, Georgia and South Carolina: U.S. Geological Survey Open-File Report 76–155.

———1977a, Aeromagnetic map of north-central North Carolina: U.S. Geological Survey Open-File Report 77–192, 1 pl.

———1977b, Aeromagnetic map of south-central North Carolina: U.S. Geological Survey Open-File Report 77–205, 1 pl., scale 1:250,000.

———1977c, Aeromagnetic map of part of southeastern Georgia: U.S. Geological Survey Open-File Report 77–96, 1 pl.

———1978a, Aeromagnetic map of northern Florida: U.S. Geological Survey Open-File Report 78–891, 2 pls., scale 1:250,000.

———1978b, Aeromagnetic map of north-central Florida: U.S. Geological Survey Open-File Report 78–761, 1 pl.

———1978c, Aeromagnetic map of northwestern South Carolina: U.S. Geological Survey Open-File Report 78–847, 2 pls., scale 1:250,000.

———1979, Aeromagnetic map of southwestern Georgia: U.S. Geological Survey Open-File Report 79–756, 3 pls., scale 1:250,000.

Vacquier, Victor, Steenland, N. C., Henderson, R. G., and Zietz, Isidore, 1951, Interpretation of aeromagnetic maps: Geological Society of America Memoir 47, 151 p. (reprinted 1963).

Van Houten, F. B., 1977, Triassic-Liassic deposits of Morocco and eastern North America; comparison: American Association of Petroleum Geologists Bulletin, v. 61, no. 1, p. 79–99.

Winkler, C. D., and Howard, J. D., 1977, Correlation of tectonically deformed shorelines on the southern Atlantic Coastal Plain: Geology v. 5, no. 2, p. 123–127.

Woollard, G. P., Bonini, W. E., and Meyer, R. P., 1957, A seismic refraction study of the sub-surface geology of the Atlantic Coastal Plain and Continental Shelf between Virginia and Florida: University of Wisconsin, Madison, Wisconsin, Department of Geology, Geophysics Section, Technical Report Contract No. N7onr-28512, 128 p.

Pre-Cretaceous Rocks Beneath the Georgia Coastal Plain—Regional Implications

By T. M. CHOWNS and C. T. WILLIAMS

STUDIES RELATED TO THE CHARLESTON, SOUTH CAROLINA, EARTHQUAKE OF 1886—TECTONICS AND SEISMICITY

GEOLOGICAL SURVEY PROFESSIONAL PAPER 1313-L

UNITED STATES GOVERNMENT PRINTING OFFICE, WASHINGTON:1983

CONTENTS

ILLUSTRATIONS

TABLES

STUDIES RELATED TO THE CHARLESTON, SOUTH CAROLINA, EARTHQUAKE OF 1886—TECTONICS AND SEISMICITY

PRE-CRETACEOUS ROCKS BENEATH THE GEORGIA COASTAL PLAIN—REGIONAL IMPLICATIONS

By T. M. CHOWNS[1] and C. T. WILLIAMS[1]

ABSTRACT

The records of 78 wells that have penetrated pre-Upper Jurassic(?) rocks beneath the Georgia Coastal Plain have been analyzed and used as the basis for a regional interpretation of the "basement" of the Southeastern U.S. Coastal Plain. Four major terranes may be recognized. The first consists of medium- to high-grade metamorphic rocks and granitic plutons immediately south of the Fall Line that are the subsurface continuation of the Piedmont province. In south Georgia the "basement" is quite different; it is a terrane of mildly deformed Paleozoic sedimentary rocks underlain by a terrane of felsic volcanic rocks. The total thickness of the Paleozoic sedimentary sequence is around 2,500 m; the sequence consists of Lower Ordovician quartz arenites overlain by fossiliferous shales and sandstones of Middle Ordovician to Middle Devonian age. The felsic volcanic terrane is probably Proterozoic Z to Cambrian in age and consists of porphyritic rhyolites, vitric crystal tuffs, and tuffaceous arkoses intruded by granitic plutons. These two anomalous terranes are separated from the buried Piedmont by a fourth terrane of lower Mesozoic continental red beds, correlated with the Newark Group. The red beds are known to be at least 3,500 m thick and occupy a complex graben, the South Georgia basin. They contain dikes and sills of tholeiitic diabase belonging to the lower Mesozoic eastern North American suite. Basalt flows, possibly related to the intrusives, also occur, although they are not directly associated with the red beds. Where the composition of the red beds is appropriate, well-developed metamorphic aureoles indicative of zeolite-facies alteration are present. Similar alteration minerals are also disseminated in small amounts regionally through the Triassic terrane, suggesting very-low-grade regional metamorphism.

These results have been compared with the results of similar studies in Florida, Alabama, and South Carolina, and, with the aid of regional aeromagnetic data, they allow us to construct a geologic map of the Fall Line unconformity beneath the southeastern Coastal Plain. The Proterozoic Z? to Paleozoic rocks in South Georgia and Florida represent a disjunct fragment of the African craton, which was sutured to North America during the late Paleozoic. The position of the suture is uncertain, but the boundary between Piedmont rocks of the Appalachian orogen and African platform deposits, which is possibly a northwest-dipping thrust fault, may be traced in the subsurface from Alabama to South Carolina. Before the opening of the Atlantic Ocean, this boundary was continuous with the overthrust on the east side of the African Mauritanide orogenic belt. The South Georgia basin formed during the early Mesozoic in response to the opening of the North Atlantic Ocean. The Brunswick magnetic anomaly, which swings through South Georgia, is most probably of late Paleozoic origin. It may be caused by a thick section of African-plate rocks, which was formed by overthrusting during continental collision. The similarity in trend between the early Mesozoic East Coast anomaly at the margin of the Carolina shelf and the Brunswick anomaly suggests that the position of the Atlantic spreading center may have been locally influenced by this Paleozoic structure.

[1]Department of Geology, West Georgia College, Carrollton, GA 30118.

INTRODUCTION

Until about 1950, it was generally assumed that the exposed igneous and metamorphic rocks of the Appalachian Piedmont province extended seawards to form the basement below the entire Georgia Coastal Plain (see, for example, Schuchert, 1935, p. 256). However, largely as a result of work by Applin (1951), it became apparent that large areas of Florida and south Georgia were underlain by a distinctly different province of relatively undeformed Paleozoic sedimentary and felsic volcanic rocks. The southeast flank of the Appalachian orogen had been discovered (King, 1950, p. 656).

Extending this work northwards, Hurst (1965) was able to show that the pre-Cretaceous rocks below the Georgia Coastal Plain could be divided into four general zones, proceeding from north to south as follows:

1. a zone of buried Piedmont rocks,
2. a zone of red beds and diabase inferred to be Triassic in age,
3. a zone of volcanic rocks (basalt, rhyolite, and tuff) intruded by granite, and
4. a zone of Paleozoic sedimentary rocks.

This general pattern was supported by the publication of detailed well logs of the Georgia Coastal Plain by Herrick (1961) and Applin and Applin (1964) as well as by a more complete description of "basement" lithologies given by Milton and Hurst (1965).

Since 1965, additional data, both published (McLaughlin, 1970; Arden, 1974a, b) and unpublished, have confirmed the overall pattern deduced by these

authors and have allowed a more detailed delineation and description of these rocks.

To date, approximately 140 oil test wells (Swanson and Gernazian, 1979) and innumerable water wells have been drilled in the Georgia Coastal Plain. Of these, 78 are known to have penetrated pre-Cretaceous rocks; 53 have been described previously, and the remaining 25 are described here for the first time (pl. 1). The samples from most of these wells consist entirely of cuttings (usually taken at 3-m intervals), and this has placed some restrictions on interpretation. However, these restrictions have been alleviated, in part, by information from geophysical logs and by the study of more than 250 thin sections.

This paper combines the results of both old and new work in an attempt to provide a comprehensive account of the stratigraphy and petrology of the pre-Cretaceous section beneath the Georgia Coastal Plain. It also integrates the results of well-sample studies and geophysical surveys in Florida (Barnett, 1975; Klitgord and others, 1982), Alabama (Neathery and Thomas, 1975), and South Carolina and Georgia (Popenoe and Zietz, 1977; Daniels and others, 1983) to facilitate regional interpretations and to provide a geologic map of the "basement" rocks beneath the southeastern Coastal Plain.

The term "basement" is used in this work to include any terrane that underlies the Coastal Plain sedimentary wedge (Cramer and Arden, 1980). Through most of Georgia, the Coastal Plain consists of Cretaceous to Neogene deposits, but in places Upper Jurassic(?) rocks are thought to occur, so that "basement" includes all pre-Upper Jurassic(?) rocks. Depending on the local situation, the terms "pre-Cretaceous" and "pre-Upper Jurassic(?)" are both used to refer to "basement" rocks in the paper. The youngest rocks included in the "basement" are equated with the Newark Group. In New England, it has been shown that Newark red beds, and associated mafic igneous rocks, range in age from Late Triassic to Early Jurassic (Cornet and others, 1973; Puffer and others, 1981). The precise age of these rocks in Georgia is uncertain. The diabase bodies are probably mainly Early Jurassic (Dooley and Wampler, 1983), and the red beds are clearly older, but paleontologic evidence of age is lacking. For convenience, therefore, the red beds will be referred to simply as Triassic or early Mesozoic in age, although the possibility that some of them are Early Jurassic should be borne in mind. The boundary between the "basement" and the Coastal Plain sequence is a regional unconformity, which emerges at the Fall Line and will be termed the Fall Line unconformity.

Acknowledgments.—The work was supported by a grant to the Georgia Geological Survey from the U.S. Geological Survey (14-08-001-G-232) and is part of a larger study of subsurface geology beneath the Georgia Coastal Plain. The writers are particularly indebted to Sam M. Pickering, former State Geologist of Georgia, for his continual support and encouragement and to Howard R. Cramer of Emory University, who administered and coordinated the larger study. Chemical analyses were provided by Richard P. Sanders of West Georgia College. Numerous students assisted in various stages of sample preparation and well logging; in particular, Burchard D. Carter, Yonnie W. Carter, Robert W. Bolding, S. Claire Crawford, Stephen D. Duncan, J. Bruce Jackson, Keith D. Kribbs, John C. Lumsden, and Charles T. Swann. We gratefully acknowledge all these contributions.

CONFIGURATION OF THE PRE-UPPER JURASSIC(?) SURFACE

As the structure contour map (fig. 1) indicates, the pre-Upper Jurassic(?) surface dips fairly uniformly southeast in the northern part of the Georgia Coastal Plain, whereas the southern part is divided into two distinct basins separated by an intervening saddle. This configuration is well known from the work of previous authors (for example, Pressler, 1947; Applin, 1951; Murray, 1961, p. 103; Maher, 1971, pl. 4) and, although the loci of maximum sedimentation have shifted slightly from epoch to epoch, appears to have maintained a recurrent influence on sedimentation throughout the late Mesozoic and Cenozoic (Herrick and Vorhis, 1963; Vorhis, 1974; Cramer, 1974; Cramer and Arden, 1980).

Several names have been applied in the past to the major features of the pre-Upper Jurassic(?) surface, and their definitions have changed as understanding of the Coastal Plain has evolved (Cramer, 1969; Patterson and Herrick, 1971; Bennison, 1975; May, 1977). Thus, the southwestern basin has been variously referred to as the Chattahoochee embayment (Johnson, 1892), Apalachicola embayment (Pressler, 1947), Southwest Georgia basin (Murray, 1957), Suwannee strait (Dall and Harris, 1892), and Gulf trough of Georgia (Herrick and Vorhis, 1963). The southeastern basin has been called the Okefenokee embayment (Pressler, 1947), Southeast Georgia embayment (Toulmin, 1955), Savannah basin (Murray, 1961, p. 96), and Atlantic embayment of Georgia (Herrick and Vorhis, 1963). The saddle which separates these two basins and isolates the Peninsular arch of Florida was named the Central Georgia uplift by Pressler (1947) and the Suwannee saddle by Applin and Applin (1965, p. 33; 1967, p. 30), the latter being a modification of earlier usage.

The terminology adopted in this paper reflects a consensus of modern usage rather than priority. Hence, the depocenter in the southwest part of Georgia that opens

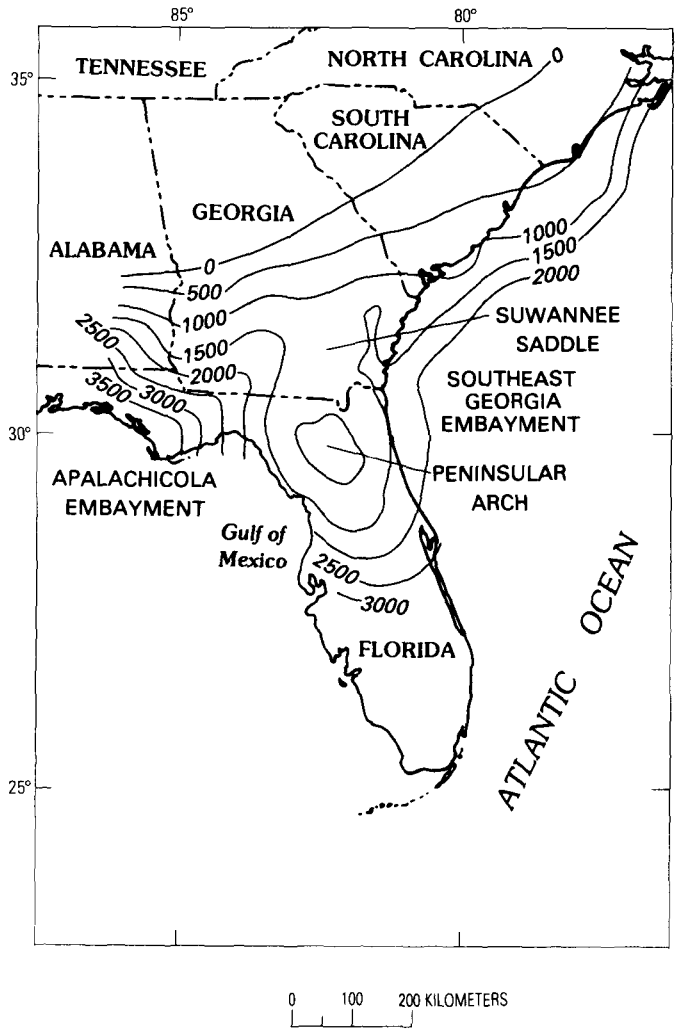

FIGURE 1.—Contour map of depth below sea level (in meters) to the Fall Line unconformity beneath the southeastern Coastal Plain. Based on Popenoe and Zietz (1977, fig. 2).

up into a deeper basin beneath the Florida panhandle is referred to as the Apalachicola embayment, whereas the southeastern depocenter is referred to as the Southeast Georgia embayment. This usage has the advantage of eliminating a possible source of confusion where the terms "Southeast Georgia embayment" and "Southwest Georgia embayment" are used together. The name "Suwannee saddle" is used in preference to "Central Georgia uplift," which does not accurately describe the location of this feature. This terminology represents a modification of the original usage by Dall and Harris (1892) but follows the intent of various recent authors of indicating a throughway between the major embayments (Applin and Applin, 1965, p. 33; 1967, p. 30; Vorhis, 1974; Brown, 1974; Bennison, 1975).

Because the elevation of drill holes in the Coastal Plain is generally less than 100 m, except close to the Fall Line, the structure contour map closely approximates an isopach map of the post-Lower Jurassic Coastal Plain sequence, especially downdip. The total thickness of this sequence in the Apalachicola embayment reaches 2,500 m in Georgia and thickens to 3,700 m under the Florida panhandle; in the Southeast Georgia embayment, it exceeds 1,500 m onshore and continues to thicken beneath the Continental Shelf (Dillon and others, 1983).

RECOGNITION OF THE FALL LINE UNCONFORMITY IN DRILL HOLES

The position of the Fall Line unconformity is generally marked in drill holes by a distinct change in lithology, which is reflected in geophysical logs by higher resistivity, higher sonic velocity, greater neutron density, and less caving from the sides of the hole. The distinction is unclear only in holes where Upper Jurassic(?) red beds rest directly on Triassic red beds, especially if the top of the lower Mesozoic section is highly weathered or if massive caving has occurred in the vicinity of the contact. Under these circumstances, it may be difficult to distinguish shale cuttings of different ages, and the geophysical contrast may be subdued.

Lower Mesozoic and older rocks have undergone more intense diagenesis than have younger rocks, and, as a general rule, sedimentary rocks above and below the unconformity may be distinguished on the basis of their induration. The older sandstones are well lithified by compaction, suturing of grains, and cementation with quartz, calcite, and sometimes laumontite; the older shales are harder than the younger shales. Above the unconformity, most of the sands are unlithified, and the shales are soft and can be plucked easily from thin sections. Where Upper Jurassic(?) or Cretaceous sandstones have been cemented, calcite alone is present, and little or no diagenetic overpacking is evident.

In order to distinguish shales of different ages, X-ray diffractograms of samples from Devonian, Triassic, Upper Jurassic(?), and Cretaceous cuttings were compared (table 1). Each sample, comprising a small, homogeneous group of shale chips, was crushed, sedimented on a glass slide, and X-rayed before and after glycolation. As expected from the difference in induration, younger samples were found to contain appreciably larger quantities of expandable clay mineral than did older samples. Thus, the Devonian shales are predominantly illite and kaolinite; Triassic rocks contain illite, chlorite, and minor kaolinite; and Upper Jurassic(?) and Cretaceous samples contain mixed-layer illite-smectite together with illite and chlorite and (or) kaolinite. These differences are usually sufficient to separate Upper Jurassic(?) and Cretaceous clays from underlying

TABLE 1.—*Mineralogy of Lower Cretaceous, Upper Jurassic(?), Upper Triassic, and Devonian shales from beneath the Georgia Coastal Plain*

[Samples from GGS 3122 between 4,160 and 4,990 ft gave anomalous results, thought to result from a combination of mislabeling and caving, and are therefore not reported]

GGS well no.	Depth (in feet)	Color[1]	Clay Minerals[2]				Other minerals[3]	Comments
			Illite-Smectite	Illite	Chlorite	Kaolinite		
Lower Cretaceous								
719	4,620–4,640	5R4/2	–	t	–	p	Q	
719	4,620–4,640	5R4/2	–	–	–	p	Q	
1145	6,310–6,340	10R6/2	p	p	p	–	Q, K	
1145	6,490–6,520	10R4/2	t	p	p	–	Q, K, D	
3001	6,515–6,530	10R4/2	p	p	p	?	Q, K	
3001	6,815–6,830	10R4/2	t	p	p	p	Q	
3099	4,300–4,310	10R5/4	p	p	p	–	Q, K	
3113	4,450–4,460	10R5/4	t	p	p	p	Q, K	
3114	5,320–5,330	10R4/2	?	p	p	–	Q, K, P	
3114	5,380–5,390	N6	p	p	–	p	Q, K, P, C	
3114	5,380–5,390	10R3/4	p	p	p	–	Q, K, P	
3115	3,960–3,970	N6	–	p	p	–	Q, K, C	
3120	3,690–3,700	N4	?	p	p	t	Q, P, C,	
3137	2,160–2,170	10R4/6	–	p	–	p	Q	
3137	2,170–2,180	10R5/4	p	p	p	–	Q, K, P	
Upper Jurassic(?)								
1145	6,580–6,610	N6	p	p	–	p	Q, P, C	in Devonian section but caved from Jurassic(?) section between 6588 and 6630 ft
1145	6,700–6,730	10R3/4	p	p	?	p	Q, K, P	
3001	6,950–6,965	10R3/4	p	p	p	p	Q, K, P	in basement section but caved from Jurassic(?) section between 6,870 and 7,004 ft
3001	6,995–7,010	10R4/6	p	p	p	?	Q, K, P	
3001	7,090–7,095	10R5/4	p	p	p	p	Q, P, C	
3099	4,600–4,610	10R4/6	t	p	p	–	Q, K, P, D	
3099	4,850–4,860	10R5/4	p	p	p	–	Q	
3113	4,560–4,570	N6	p	p	–	p	Q, C	
3113	4,560–4,570	10R5/4	?	p	p	–	Q	
3113	4,700–4,710	10R4/6	–	p	p	?	Q, C	
3114	5,620–5,630	10R3/4	p	p	p	p	Q, K	
3114	5,890–5,900	10R3/4	p	p	–	p	Q, K	
3114	6,200–6,210	10R3/4	p	p	p	–	Q, K	
3115	4,250–4,260	10R3/4	–	p	–	p	Q, K, P	
3115	4,500–4,510	10R4/2	–	p	p	–	Q	
3120	4,150–4,160	10R5/4	–	p	p	–	Q, K, P	
3120	4,150–4,160	N5	–	p	p	p	Q, K, P, C	

See footnotes at end of table.

Triassic and Paleozoic shales, provided care is taken to eliminate contamination by caved material. This is best accomplished by analyzing replicate samples if there is doubt about the degree of induration.

Because the diabase intrusions in Georgia and elsewhere along the East Coast are Early Jurassic in age or older, the presence of diabase in a sedimentary section, or the presence of metamorphic minerals such

TABLE 1.—*Mineralogy of Lower Cretaceous, Upper Jurassic(?), Upper Triassic, and Devonian shales from beneath the Georgia Coastal Plain*—Continued

[Samples from GGS 3122 between 4,160 and 4,990 ft gave anomalous results, thought to result from a combination of mislabeling and caving, and are therefore not reported]

GGS well no.	Depth (in feet)	Color[1]	Clay Minerals[2]				Other minerals[3]	Comments
			Illite-Smectite	Illite	Chlorite	Kaolinite		
Upper Triassic								
442	3,100–3,110	10R3/4	–	p	p	–	Q, P	
442	3,210–3,220	10R6/2	–	p	p	p	Q, K, P, C	
442	4,770–4,780	10R6/2	–	p	p	–	Q, P	
3099	4,950–4,960	10R3/4	–	p	p	–	Q, P, C	
3099	5,160–5,170	10R3/2	–	p	p	?	Q, C	
3099	5,160–5,170	10R3/4	–	p	t	–	Q	
3099	5,160–5,170	10R2/4	–	p	t	–	Q	
3099	5,230–5,243	10R2/2	–	p	t	–	Q	
3113	4,960–4,970	10R4/2	–	p	p	–	Q, P	
3113	5,310–5,320	10R2/2	–	p	p	–	Q, P, C	
3113	8,260–8,270	10R4/6	–	p	p	–	Q, K, P, C	
3113	8,260–8,270	10R3/4	–	p	p	–	Q, P, C	
3114	6,650–6,660	10R4/6	?	p	p	p	Q	probably caving from Jurassic(?) section between 5,750 and 6,553 ft
3114	6,650–6,660	5R4/2	p	p	p	–	Q	
3114	6,660–6,670	10R3/4	–	p	p	–	Q, C,	
3114	6,660–6,670	10R2/2	–	p	p	–	Q, P, C	probably caving from Jurassic(?) section between 5,750 and 6,553 ft
3114	6,660–6,670	10R3/4	p	p	?	p	Q, P	
3115	4,600–4,610	10R3/4	–	p	p	p	Q	
3115	4,800–4,810	10R3/4	–	p	p	–	Q, P	
3115	4,990–5,000	5R3/4	–	p	p	–	Q, P	
3120	4,250–4,260	10R3/4	–	p	p	–	Q, K	
3120	5,050–5,052	10R3/4	–	p	p	–	Q	
3120	5,050–5,052	10R4/2	–	p	p	p	Q, P	
3137	2,390–2,400	10R4/6	p	p	p	–	Q, K, P	probably caving from Cretaceous section above 2,197
3137	2,390–2,400	10R4/6	t	p	p	–	Q, K, P	
3137	2,390–2,400	10R3/4	p	p	t	–	Q, K, P	
3137	2,400–2,410	10R3/4	p	p	t	–	Q, P	
3137	2,700–2,710	5R4/2	t	p	t	–	Q, P	
3137	2,960–2,970	10R3/4	–	p	p	p	Q, K	
3137	3,970–3,980	5R2/2	–	p	p	p	Q, K, P	
3137	4,470–4,480	5R2/2	–	p	p	–	Q, K, P	
3137	5,500–5,510	10R2/2	–	p	p	p	Q, P	
3137	5,620–5,630	10R3/4	–	p	p	–	Q, K, P	
Middle Devonian								
1145	7,270–7,300	N4	–	p	t	p	Q	
1145	7,338	N4	–	p	–	p	Q	core

[1] Goddard and others (1948).
[2] p, present; t, trace; ?, uncertain; –, absent.
[3] Q, quartz; P, plagioclase; K, potassium feldspar; C, calcite; D, dolomite.

as laumontite and epidote-clinozoisite that are associated with the diabase, serves to indicate a pre-Early Jurassic age for the host rocks.

Finally, when seismic data or dipmeter readings are available, it is possible to separate Upper Jurassic(?) plus Cretaceous strata from Triassic strata and Mesozoic strata from Paleozoic strata by tracing the intervening unconformities (Arden, 1974a, b). Unfortunately, dipmeter readings are available for only two Georgia holes (GGS 3122, 3353), but in GGS 3122 they help establish the position of the angular unconformity at the top of the Triassic section.

UPPER JURASSIC(?) ROCKS

In most holes, the Fall Line unconformity is overlain by a sequence of pink to white conglomeratic sands and medium-gray to grayish-red micaceous shales of Early Cretaceous (Comanchean) or younger age (see, for example, Applin and Applin, 1965; Cramer, 1974; Cramer and Arden, 1980, p. 17). However, in ten holes in the southwest corner of the State, this Cretaceous sequence is underlain by a group of brick-red conglomeratic shales interbedded with medium-gray shales and some fine-grained calcareous sandstone. This group is provisionally assigned to the Jurassic Cotton Valley Formation (Gray, 1978). Granule-sized grains, apparently released from a shaly matrix, are especially abundant in cuttings from this interval and represent a variety of lithologies mainly derived from the underlying terrane of felsic volcanic rocks. The sequence reaches a maximum observed thickness of 245 m in Thomas County and thins both east and west to feather edges in Lowndes and Early Counties (pl. 1, fig. 2).

At first, these beds were believed to be part of the Triassic section because of the similarity in the hue of the shales. However, in GGS 3114 (Thomas County), they rest on weathered diabase, and, in neighboring Lowndes County, cross sections and dipmeter data suggest that they lie unconformably on Triassic rocks. In addition, they are much less indurated than are typical Triassic rocks, and the shales invariably contain large amounts of expandable clay mineral. It appears, therefore, that the group is the basal unit of the Coastal Plain sequence, although it is difficult to ascertain its exact age in the absence of fossils.

Similar conglomeratic red shales have been recorded in several wells in the Florida panhandle (Maher and Applin, 1968, p. 9). Their age has been established as Jurassic by the recovery of spores, in one case from a coal seam (Maher and Applin, 1968, p. 9, pl. 6). Farther south, the base of the Fort Pierce Formation in the Amerada–Cowles Magazines well, St. Lucie County, Fla., also contains conglomeratic red shales having a large proportion of reworked felsic volcanic debris (Applin and Applin, 1965, p. 24–25; Bass, 1969). These shales are dated as either earliest Cretaceous or latest Jurassic (Maher and Applin, *in* Maher, 1971, p. 36).

In the past, the Cotton Valley(?) rocks in Georgia probably have been grouped both with the Cretaceous and with the Triassic, but there appears to be a strong possibility that this basal unit is Late Jurassic in age (Gray, 1978). From its lithologic character and the fact that it passes into marine deposits farther south and west in Florida and Alabama (Maher and Applin, 1968, p. 10–11), it appears to have been deposited on a low-lying coastal plain backed by a hinterland of older felsic volcanic rocks and Triassic red beds.

GEOLOGY OF THE PRE-UPPER JURASSIC(?) SURFACE

The rocks that subcrop below the Fall Line unconformity in Georgia may be subdivided into four different terranes (pl. 1):

1. A terrane of plutons and medium- to high-grade metamorphic rocks representing the subsurface continuation of the Appalachian Piedmont province and extending 50 to 60 km southeast of the Fall Line.
2. A red-bed section, containing numerous diabase intrusions and inferred to be of Late Triassic to Early Jurassic age, which occupies a complex graben underlying large areas of southern Georgia.
3. A group of fossiliferous Lower Ordovician to Middle Devonian sandstones and shales, which forms the nucleus of the Peninsular arch in Florida and extends into the southern part of Georgia.
4. A terrane of Proterozoic Z to lower Paleozoic(?) felsic volcanic rocks and associated granite plutons, which subcrops beneath the Suwannee saddle and Southeast Georgia embayment and appears to correlate with similar rocks in the Apalachicola embayment and on the east side of the Peninsular arch in Florida.

In most cases, the boundaries between these terranes have been drawn on the basis of drill-hole data alone, but, in areas where boundaries are expressed by potential field maps (Popenoe and Zietz, 1977; Klitgord and others, 1982, 1983; Daniels and others, 1983), this information is taken into account. This applies particularly to South Carolina and east-central Georgia where drill holes are sparse and the boundary between the Piedmont and Triassic terranes appears to be defined best on aeromagnetic maps.

Each terrane occupies a fairly distinct area, and hence it is difficult to establish the stratigraphic and structural interrelationships among them. However, stratigraphic ages have been determined on the basis of paleontology (Bridge and Berdan, 1952; Pojeta and others, 1976) and radiometric dating (Bass, 1969; Milton and Grasty, 1969; Georgia Geologic Survey, unpublished data) and directly by superposition in those few holes that have intersected more than one terrane or in areas where seismic-reflection studies have been carried out (Arden, 1974a, b). Structural relationships must be inferred mainly on the basis of outcrop patterns on the geologic map (pl. 1).

Data from Georgia are consistent with previously published information from Florida (Applin, 1951; Barnett, 1975), Alabama (Neathery and Thomas, 1975), and South Carolina (Popenoe and Zietz, 1977). Data from these four States are summarized on plate 1.

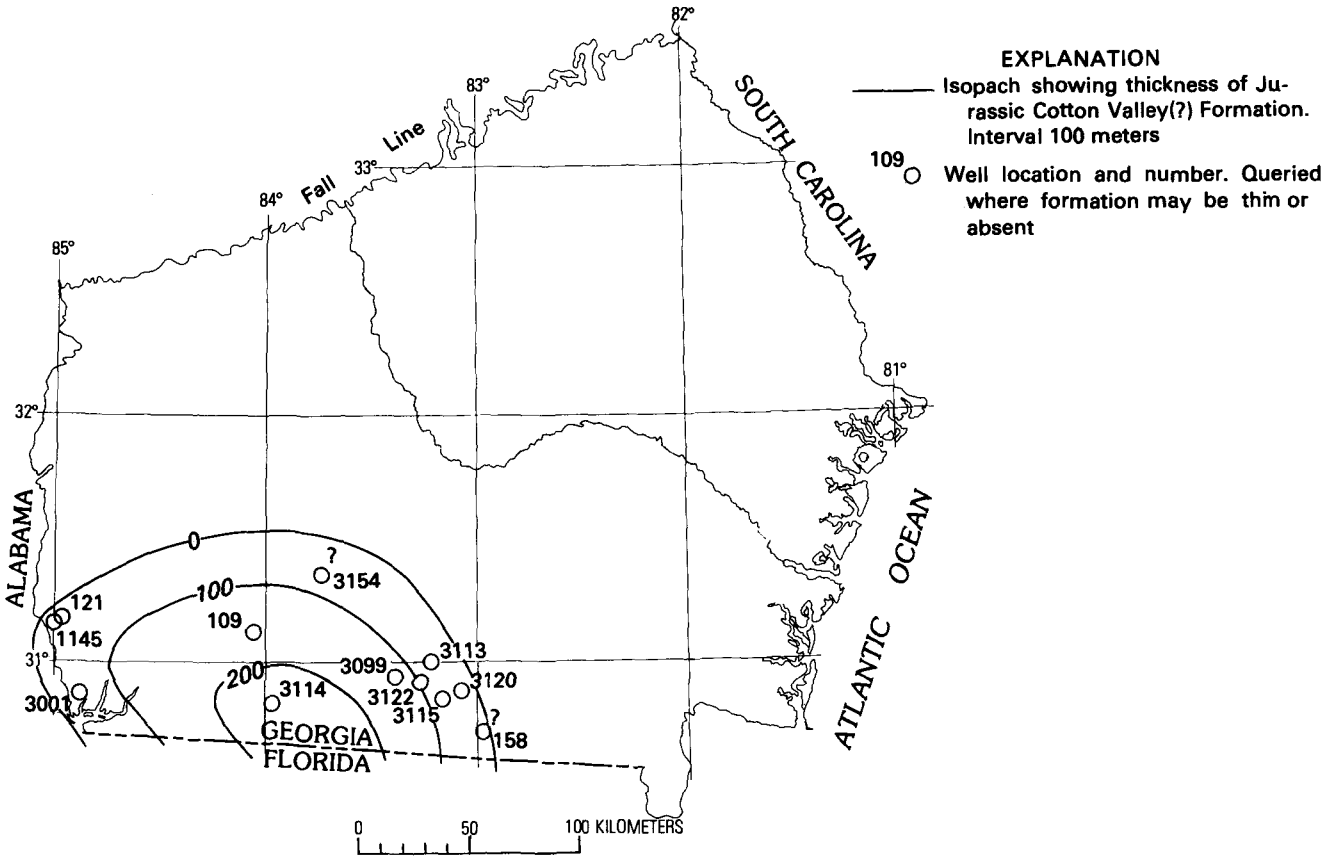

FIGURE 2. – Distribution and thickness, in meters, of the Jurassic Cotton Valley(?) Formation in the Georgia Coastal Plain. Well locations and numbers are shown.

PIEDMONT METAMORPHIC TERRANE

In the northern part of the Coastal Plain, 26 wells have bottomed in medium- to high-grade metamorphic rocks or associated plutons, which are clearly a continuation of the exposed Piedmont province (table 2). Most of these holes are old and have been described briefly by Herrick (1961) and by Milton and Hurst (1965, p. 16–18). Reported rock types include hornblende schist, biotite gneiss, and granite.

The only additional information provided by recent drilling is derived from GGS 3105 (pl. 1), a gas-storage test well, which penetrated 537 m of biotite granite crosscut by one small diabase dike. Because this hole lies several kilometers south of the group of holes containing Triassic rocks in Pulaski County, it indicates that the Piedmont-Triassic contact is displaced to the south on the east side of the Ocmulgee River, possibly owing to faulting (pl. 1).

The geophysical maps suggest that further subdivisions within this area are possible (Daniels, 1974; Popenoe and Zietz, 1977). For example, from a combination of aeromagnetic maps, gravity data, and outcrop and drill-hole information on the east side of the Oconee River (pl. 1), these authors have shown that it is possible to trace belts of high-grade (Kiokee belt) and low-grade (Carolina slate belt) metamorphic rocks into the subsurface (Popenoe and Zietz, 1977). These belts are flanked to the south by the small early Mesozoic Dunbarton basin (Marine and Siple, 1974; Marine, 1974) and by a broken belt of mafic rock that extends from South Carolina (Popenoe and Zietz, 1977) to the Georgia-Alabama border and probably beyond. According to Popenoe and Zietz (1977), these mafic intrusions or flows are of probable early Mesozoic age, and, in fact, circular magnetic anomalies in the Charleston, S. C., area (anomalies 4e, f, g, h, of Popenoe and Zietz, 1977, p. 129) may result from such Mesozoic mafic rocks. However, the northeast-southwest aeromagnetic trend of the discontinuous South Carolina–Georgia–Alabama belt (for example, anomalies 2h, 4b, 4c of Popenoe and Zietz, 1977, p. 129) suggests a tectonic megafabric typical of the Piedmont. Furthermore, in Georgia, this discontinuous belt intersects the lineament that appears to mark the Piedmont-Triassic boundary (Daniels and others, 1983) and lies well to the north, in the Piedmont

TABLE 2.—*Holes bottomed in Piedmont rocks*

County	GGS number	Ground elevation[1]	Elevation of drill platform	Depth to base of Cretaceous	Total depth	Elevation of base of Cretaceous	Thickness of pre-Cretaceous	Comments	References[2]
Richmond	none	–	300 D.F	–	400	–	–	"Crystalline rock"	4, 7
Do.	129	136	–	155	329	−19	174	Water well; low-grade metavolcanic phyllite.	3, 6
Do.	130	136	–	162	1,200	−26	1,038	Water well; low-grade metavolcanic phyllite.	3, 6
Do.	309	330	–	158	480	+172	322	Water well; chlorite schist	3
Do.	3,184	–	–	–	445	–	–	Phyllite	6
Do.	TW1	–	–	–	–	+95	–	Biotite granite	6
Do.	TW2	–	–	–	–	+133	–	Mica phyllite	6
Jefferson	none	445	–	–	1,143	–	–	Diorite schist	4, 6, 7
Macon	DP39	–	290 D.F.	–	2,140	–	–	Schist	4, 7
Bibb	7	358	–	496	509	−138	13	Water well; chloritic gneiss	3, 6
Do.	357	364	–	301	303	+63	2	Water well; hornblende gneiss.	3, 6
Do.	361	305	–	249	253	+56	4	Water well; "crystalline rock."	3
Washington	94	465	–	871	872	−406	1	Granite	3, 4
Do.	223	480	–	392	605	+88	213	Biotite gneiss	3, 4
Burke	131	129	–	602	620	−473	18	USGS test; weathered mica schist.	3
Do.	316	276	–	1,028	1,033	−752	5	"Crystalline"	3, 4
Houston	193	–	419 D.F.	–	1,494	–	–	Biotite gneiss	4, 7
Do.	194	364	–	1,685	1,698	−1,321	13	Biotite gneiss	3, 4
Muscogee	235	250	–	439	445	−189	6	Water well; "crystalline rock."	4
Columbia	264	500	–	135	300	+365	165	Water well; "crystalline rock."	3
Chattahoochee	341	550	–	1,185	1,205	−635	20	Water well; hornblende schist.	3, 4
Marion	476	600	–	1,590	1,770	−990	180	Biotite gneiss?	3, 4
Treutlen	730	351	–	3,053	3,239	−2,702	186	Quartzofeldspathic gneiss (cataclastic).	4, 7, 8
Do.	789	–	349 D.F.	3,166?	3,180	−2,817?	14	Biotite gneiss	4, 7, 8
Screven	855	130	–	2,674	2,677	−2,544	3	Granite?	4, 7
Dodge	3105	302	310 K.B.	2,762	4,526	−2,452	1,764	Biotite granite and small diabase dike.	8

[1] Because oil test wells are logged by depth from the drilling platform, rather than from ground level, it is important to know the elevation of the platform (kelly bushing, K.B., or derrick floor, D.F.), rather than ground level, in computing the absolute elevation of stratigraphic markers in the holes. Wherever available, this information is given in the tables and is used to compute absolute elevations at the base of the Cretaceous [or depth to base of Jurassic(?) where these rocks form the base of the Coastal Plain sequence]. Measurements are given in feet.

[2] Data in the table are drawn from the following references: 1, Applin (1951); 2, Applin and Applin (1964); 3, Herrick (1961); 4, Milton and Hurst (1965); 5, McLaughlin (1970); 6, Daniels and Zietz (1978); 7, Swanson and Gernazian (1979); 8, new data.

terrane, in the western part of the State. Therefore, magnetic anomalies in this mafic belt are interpreted to result from mafic Piedmont rocks perhaps similar to the hornblende schist in GGS 341 (pl. 1), which is on the flank of the belt in west Georgia. The broken trace of this anomaly belt is interpreted to result from a range in depths to the magnetic source rocks; this range in depth is caused by horsts and grabens at the margins of a major early Mesozoic basin (Daniels and others, 1983).

Subsidiary early Mesozoic grabens within the Piedmont terrane in Georgia and South Carolina include the Riddleville basin (Daniels and others, 1983), the Dunbarton basin (Marine and Siple, 1974; Marine, 1974), and the Florence basin (Popenoe and Zietz, 1977; Daniels and others, 1983).

Some question arises as to the nature of the pre-Cretaceous basement southeast of this zone of mafic crust. Popenoe and Zietz (1977) have proposed that this mafic zone marks the edge of a major downfaulted early Mesozoic basin, the so-called South Carolina–Georgia basin of Gohn and others (1978) or South Georgia basin of Daniels and others (1983), and have, therefore, raised doubts about the nature of the bottom-hole lithologies in GGS 730, 789, and 855 (pl. 1). In consequence, these holes were reexamined during this study. No samples were returned from GGS 855 in Screven County, and

thus the designation of granite in that hole by Milton and Hurst (1965, p. 18) must remain in doubt. However, GGS 730 and 789 in Treutlen County both bottomed in metamorphic rock, as reported by Milton and Hurst (1965, p. 18); GGS 730 contains a biotite gneiss, and GGS 789 contains a cataclastic garnetiferous quartz-feldspathic gneiss. Thus, the boundary between Piedmont and Triassic rocks probably lies somewhere between GGS 789 in Treutlen County and GGS 190 in northern Montgomery County and does not appear to be marked by a major magnetic contrast. Perhaps, as suggested by Popenoe and Zietz (1977), the triangular area of Piedmont rocks including the Treutlen wells represents a secondary horst block.

PALEOZOIC SEDIMENTARY ROCKS

The existence of a buried mass of essentially flat-lying Paleozoic sedimentary rocks beneath the Coastal Plain of Florida and Georgia was first clearly demonstrated by Applin (1951) on the basis of early paleontologic work by Richards (1948), Howell and Richards (1949), Swartz (1949), Kjellesvig-Waering (1950), and Bridge and Berdan (1952). These reports suggested a range of ages from Early Ordovician to Middle Devonian, which has since been confirmed by later studies (see, for example, Berdan and Schopf, *in* Puri and Vernon, 1964, p. 19–21; Andress and others, 1969; Goldstein and others, 1969; McLaughlin, 1970; Cramer, 1973; Pojeta and others, 1976). The possibility that some upper Paleozoic rocks may also occur has been suggested by Palmer (1970) and Barnett (1975). However, Palmer's conclusion that the rocks in GGS 121 are Pennsylvanian is disputed by other workers who regard them as Middle Devonian (see, for example, Pojeta and others, 1976, p. 12).

The principal subcrop of Paleozoic rocks is in north Florida on the crest of the Peninsular arch, but there is a second subcrop in the Florida panhandle. Together these form a triangular tract, which was referred to as the Suwannee River basin (Braunstein, 1957); this name was later contracted to "Suwannee basin" (King, 1961). Unfortunately, this has led to confusion with the older name "Suwannee strait," which refers to a different feature of later age (see, for example, Arden, 1974a; May, 1977), and it is therefore recommended that the term "Suwannee basin" be abandoned.

When data from this entire area are combined, the following stratigraphic succession may be assembled (Pojeta and others, 1976):

4. *Middle Devonian*—Dark-gray to dusky-red shales and light-gray siltstones and crossbedded sandstone intervals containing plant debris, bivalves, and ostracodes.
3. *Upper Silurian to Lower Devonian*—Dark-gray to black shales containing pelecypods, gastropods, orthocone cephalopods, tentaculitids, brachiopods, crinoids, ostracodes, and eurypterids, as well as chitinozoans and other microfossils.
2. *Upper or Middle Ordovician*—Dark-gray to black shales and some interbedded sandstones containing inarticulate brachiopods, conularids, trilobites, conodonts, and chitinozoans.
1. *Lower Ordovician*—White quartz arenites and highly micaceous shales, rather unfossiliferous but containing inarticulate brachiopods, graptolites, and *Skolithos* burrows.

The total thickness of this section appears to be about 2,500 m on the basis of results of gravity modelling in peninsular Florida (Wicker and Smith, 1978). Seismic sections from the Florida panhandle (Arden, 1974a) suggest that about 1,900 m should be assigned to the Ordovician and 600 m to the Silurian and Devonian. Because only a small fraction of this thickness has been drilled, it is probable that some stratigraphic gaps are more apparent than real, but there may well be an unconformity between the Ordovician and Silurian.

The 12 wells that have encountered these Paleozoic rocks in Georgia are on the northern margin of this terrane (pl. 1). Most have been described previously (table 3); only three (GGS 876, 1198, 1199) are completely new, and these add little to what is already known. The whole stratigraphic section appears to be present, although not in any one area. The stratigraphic succession from Lower Ordovician through Upper Silurian rocks in wells in Clinch and Echols Counties (GGS 481, 169, and possibly 144: Lower Ordovician; GGS 150, 158, 166: Middle to Upper Ordovician; GGS 189: Upper Silurian) suggests an orderly, west- or southwest-dipping sequence, whereas the two wells in Early County (GGS 121, 1145) contain Middle Devonian strata. The ages of the beds in the three new holes in Charlton and Camden Counties (GGS 876, 1198, 1199) are unknown in the absence of fossils, but their lithology rules out a Lower Ordovician designation.

The petrographically determined lithologies of the Georgia samples resemble those of the Florida samples (Carroll, 1963); three major lithologies are present.

1. Medium- to very-coarse-grained, mature quartz arenites consist of well-rounded grains that are sutured together or cemented by quartz overgrowths or chalcedony.
2. Very-fine-grained, immature quartz arenites and micaceous sublitharenites contain angular grains and may show planar and ripple lamination and bioturbation. These sandstones are commonly interbedded with shale that at places shows flaser bedding.
3. Dark-gray to black shales contain illite, kaolinite, and quartz and may contain microcrystalline siderite and calcite.

TABLE 3.—*Holes bottomed in Paleozoic sandstones and shales*

[*, Age determined by paleontological analysis; otherwise, age inferred from lithologic affinities]

County	GGS number	Ground elevation[1]	Elevation of drill platform	Depth to base of Cretaceous	Total depth	Elevation of base of Cretaceous	Thickness of pre-Cretaceous	Comments	References[2]
Early	121	182	187 D.F	6,635	7,320	−6,448	685	Middle Ordovician* overlain by Jurassic(?) red beds (50 ft).	2, 8
Do.	1145	190	204 K.B.	6,630	7,567	−6,426	937	Devonian* overlain by Jurassic(?) red beds (42 ft).	5, 8
Clinch	144	–	177 D.F.	3,834	3,848	−3,657	14	Lower Ordovician	2
Do.	481	–	147 D.F.	3,953	4,088	−3,806	135	Lower Ordovician	1, 2
Echols	150	–	144 D.F.	3,657	4,003	−3,513	346	Middle Ordovician*	2
Do.	158	–	156 D.F.	3,911	3,916	−3,755	5	Middle Ordovician*	2
Do.	166	148	–	3,782	3,865	−3,634	83	Middle Ordovician*	1, 8
Do.	169	–	142 D.F.	3,730	4,062	−3,588	332	Lower Ordovician	1, 2, 4
Do.	189	–	181 D.F.	4,120	4,185	−3,939	65	Upper Silurian* intruded by diabase.	2, 4
Charlton	876	25	35 D.F.	4,480	4,579	−4,445	99	Apparently unfossiliferous	8
Camden	1198	14	27 K.B.	4,532	4,690	−4,505	158	Apparently unfossiliferous	8
Do.	1199	22	33 K.B.	4,542	4,597	−4,509	55	From electric logs and records of side-wall cores.	8

[1] Because oil test wells are logged by depth from the drilling platform, rather than from ground level, it is important to know the elevation of the platform (kelly bushing, K.B., or derrick floor, D.F.), rather than ground level, in computing the absolute elevation of stratigraphic markers in the holes. Wherever available, this information is given in the tables and is used to compute absolute elevations at the base of the Cretaceous [or depth to base of Jurassic(?) where these rocks form the base of the Coastal Plain sequence]. Measurements are given in feet.

[2] Data in the table are drawn from the following references: 1, Applin (1951); 2, Applin and Applin (1964); 3, Herrick (1961); 4, Milton and Hurst (1965); 5, McLaughlin (1970); 6, Daniels and Zietz (1978); 7, Swanson and Gernazian (1979); 8, new data.

Regionally, mature quartz arenites predominate in the Lower Ordovician, whereas shales and immature sandstones make up the upper part of the section. However, some mature sandstones are known from Upper Silurian (GGS 189) and Middle Devonian (GGS 121, 1145) rocks.

The overall succession suggests a shallow shelf association of littoral or near-shore sandstones (*Skolithos* facies) passing up into fossiliferous offshore shales in the Middle or Late Ordovician. The possibility of an unconformity at the top of the Ordovician, the presence of well-sorted sandstones in the upper part of the section, and the presence of plant fossils alongside marine microfossils in the Middle Devonian (McLaughlin, 1970, p. 7) all indicate regressive intervals.

Several authors have remarked upon the occurrence of red shales at the top of the Paleozoic section (for example, Carroll, 1963; Pojeta and others, 1976, p. 8). In all cases, this red color is clearly related to weathering along the Fall Line unconformity. According to Arden (1974a), seismic velocities suggest that this weathered zone may in places be as much as 300 m thick, but the greatest thickness encountered in this work was 31 m. In one hole (GGS 1145), Devonian shale cuttings have a dusky-red tinge, which is probably original.

FELSIC VOLCANIC ROCKS AND ASSOCIATED LITHOLOGIES

Fourteen wells, mainly within the area of the Southeast Georgia embayment and Suwannee saddle, have bottomed in felsic volcanic rocks, tuffaceous sedimentary rocks, or granite plutons, which are believed to belong to a single petrologic province. These rocks have attracted considerable attention in the past and have been described previously by Applin (1951), Ross (1958), and Milton and Hurst (1965). Six new localities are described in this work (table 4).

The principal lithologies encountered in the Georgia holes are vitric crystal tuff, tuffaceous arkose, porphyritic rhyolite, and granite. Most common are the vitric crystal tuffs (GGS 52, 153, 167, 338, 651, 3146, 3201). These are generally very-fine-grained rocks, ranging in color from light gray to black; they are sometimes confused with shales, especially in cuttings. However, they differ from shale by being much harder and nonfissile. In thin section, they are seen to consist mainly of small (as much as 200 μ), angular grains of quartz and feldspar, sometimes accompanied by flattened devitrified glass shards, set in a matrix of cryptocrystalline material that probably also contains a large amount of devitrified glass. Cores from GGS 338 (Ross, 1958) and GGS 3201 contain beds of spectacular vitric tuff consisting of largely undistorted shards. Together with the presence of delicate graded laminations in some samples, these shards clearly indicate that these are volcanic ash-fall deposits.

Interbedded with these fine-grained tuffs are beds of poorly sorted, medium-grained to very-coarse-grained tuffaceous arkose (GGS 52, 153, 338) consisting of very angular to rounded grains of quartz, plagioclase, and untwinned potassium feldspar(?) and fragments of

TABLE 4.—*Holes bottomed in Paleozoic tuffs and associated granite plutons*

County	GGS well number	Ground elevation[1]	Elevation of drill platform	Depth to base of Cretaceous	Total depth	Elevation of base of Cretaceous	Thickness of pre-Cretaceous	Comments	References[2]
Atkinson	107	217	222 D.F	4,220	4,296	-3,998	76	Rhyolite or felsic tuff	3, 4
Pierce	119	75	–	4,348	4,375	-4,273	27	Granite	3, 4
Do.	120	75	–	4,348	4,355	-4,273	7	Granite	3, 4
Camden	153	52	65 D.F.	4,674	4,955	-4,609	281	Felsic tuff	2, 4
Clinch	338	110	176 D.F.	3,843	4,588	-3,667	745	Felsic vitric crystal tuff	2, 4
Liberty	363	–	26 D.F.	4,250	4,254	-4,224	4	Porphyritic rhyolite	3, 4
Coffee	468	–	317 D.F.	4,110	4,130	-3,793	20	Granite	2
Do.	3127	280	295 K.B.	4,306	4,339	-4,011	33	Porphyritic rhyolite	8
Wayne	651	49	65 D.F.	4,317	4,544	-4,252	227	Felsic vitric crystal tuff	4, 8
Glynn	719	15	25 K.B.	4,700	4,736	-4,675	36	Granite	4, 7
Do.	1197	13	24 K.B.	4,324	4,431	-4,300	107	Porphyritic rhyolite	8
Seminole	3001	98	110 K.B.	7,004	7,098	-6,894	94	Granite overlain by Jurassic(?) red beds (134 ft).	8
Wayne	3146	58	71 K.B.	4,440	4,487	-4,369	47	Felsic vitric crystal tuff	8
Do.	3201	74	84 K.B.	4,290	4,371	-4,206	81	Felsic vitric tuff intruded by diabase.	8

[1] Because oil test wells are logged by depth from the drilling platform, rather than from ground level, it is important to know the elevation of the platform (kelly bushing, K.B., or derrick floor, D.F.), rather than ground level, in computing the absolute elevation of stratigraphic markers in the holes. Wherever available, this information is given in the tables and is used to compute absolute elevations at the base of the Cretaceous [or depth to base of Jurassic(?) where these rocks form the base of the Coastal Plain sequence]. Measurements are given in feet.

[2] Data in the table are drawn from the following references: 1, Applin (1951); 2, Applin and Applin (1964); 3, Herrick (1961); 4, Milton and Hurst (1965); 5, McLaughlin (1970); 6, Daniels and Zietz (1978); 7, Swanson and Gernazian (1979); 8, new data.

andesite, dacite, and pumice as much as 5 mm in diameter (Ross, 1958). Although the texture of these sediments suggests that they have undergone aqueous transport, their immaturity indicates that they were derived from a local volcanic source.

The porphyritic rhyolites (GGS 363, 1197, 3127) are also probably pyroclastic in origin and represent ash-flow deposits rather than lavas. They consist of euhedral to subrounded, corroded phenoclasts of quartz, plagioclase, and perthite in a cryptocrystalline groundmass that shows flow foliation, and elongate lithophysae. The groundmass typically is partially recrystallized as spherulites, especially around lithophysae, and again probably is devitrified glass.

Several granites have been drilled within the volcanic-rock terrane in southeast Georgia (GGS 119, 120, 468, 719), and one has been found in a similar setting in southwest Georgia (GGS 3001). They have a typical granitic texture; the absence of foliation and the presence of granophyric intergrowths (GGS 719, 3001) suggests that they are epizone plutons intruded into the felsic volcanic terrane rather than older basement rocks. Although Milton (in Milton and Hurst, 1965, p. 39–40; Milton and Grasty, 1969, p. 2489; Milton, 1972, p. 8) interprets the granites in Pierce County (GGS 119, 120) as hydrothermally altered sedimentary arkoses, the writers believe that all these granites are magmatic. This was also the opinion of Hurst (in Milton and Hurst, 1965) and Bass (1969, p. 300); it is borne out by an examination of chemical analyses (table 5, fig. 3), which show the granites and rhyolites to be almost identical in composition. By comparison, the tuffs are slightly lower in silica and alkalies.

In general, all these rocks appear relatively fresh in thin section, but the alteration of the feldspars in some of the granites (GGS 119, 120, 719) and the presence of calcite, laumontite, and epidote in the tuffs suggest that late-stage deuteric and hydrothermal alteration as well as low-grade metamorphism may have occurred. Evidence of hydrothermal alteration is especially pronounced in core from GGS 3201. The tuffs in this core contain abundant pyrite both disseminated through the groundmass and as delicate synsedimentary microlaminations. Bedding is interrupted and sometimes even obliterated by numerous finely anastamosing dark veins, which pervade the rock and produce a chaotic brecciation. These features are interpreted to be penecontemporaneous, probably having developed through a combination of hydrothermal alteration and collapse in a welded ash. Several generations of extension fractures filled with calcite, quartz, laumontite, and pyrite are also present.

In the vicinity of the felsic volcanic terrane are two wells that bottomed in basalt (GGS 148, 496). Basalts in both wells are very fine grained and amygdaloidal and, therefore, are probably flows. They are the only lavas encountered during this study, and they might conceivably be interbedded with the felsic tuffs; basalts are found apparently within a similar terrane in peninsular Florida and Alabama. Alternatively, they may be related to the lower Mesozoic diabase and occur within downfaulted basins and (or) lie unconformably on the felsic volcanic rocks.

Fragments of felsic volcanic debris occur very commonly as granules and coarse- to very-coarse-grained sand at the base of the Coastal Plain sequence (see, for

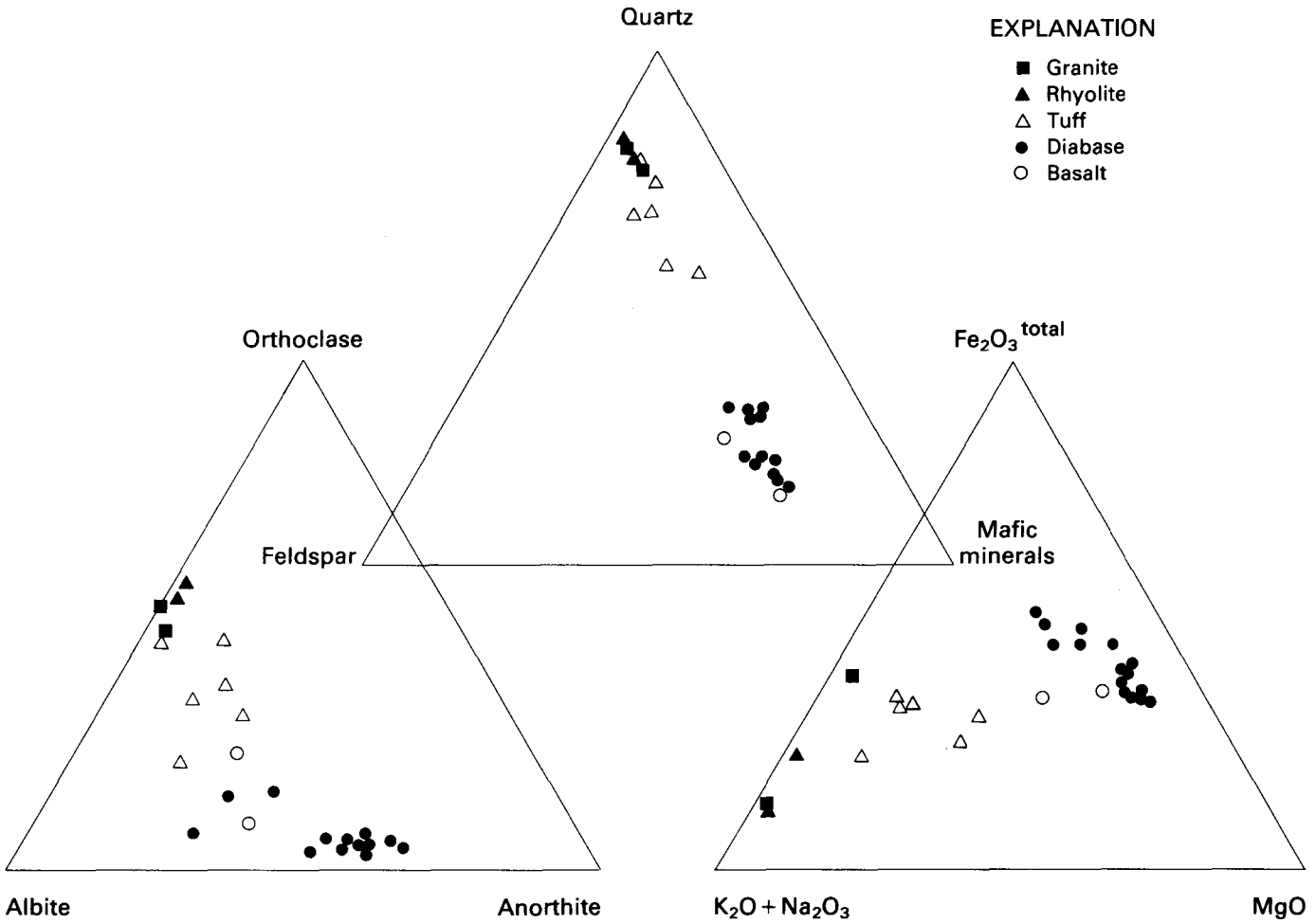

FIGURE 3.—Normative composition of pre-Cretaceous igneous rocks from beneath the Georgia Coastal Plain. $Fe_2O_3/(FeO + Fe_2O_3)$ calculated as 0.30.

example, Bass, 1969) and in the Triassic section. In fact, each of the lithologies described above, perhaps including basalt, is present as detrital grains, thus reinforcing conclusions about the overall makeup of the terrane. As might be expected, these clasts of felsic volcanic rock are most abundant in the southern part of the Georgia Coastal Plain, but they also occur in some of the holes close to the Fall Line (for example, GGS 505). This probably indicates that this felsic volcanic terrane extends farther northwest than is indicated on plate 1, presumably under the cover of Triassic rocks.

Felsic volcanic rocks and associated granites and basalts virtually identical to those in southeast Georgia are found in three other areas in the southeastern Coastal Plain: beneath the Apalachicola embayment in Alabama and the Florida panhandle, on the southeastern flank of the Peninsular arch in central Florida, and in southern Florida. However, opinion is divided on whether these terranes are parts of a single contemporaneous province. Three main possibilities have been suggested:

1. They belong to a single province of early Paleozoic or Proterozoic Z age (Applin, 1951).
2. They are differentiates of the same magma that produced the diabase and are, therefore, Triassic or Early Jurassic in age (Milton and Grasty, 1969; Milton, 1972, p. 2).
3. Proterozoic Z–lower Paleozoic and lower Mesozoic felsic volcanic rocks occur in separate provinces (Bass, 1969). In this case, Barnett (1975) has suggested that, whereas the volcanic rocks in extreme south Florida are Triassic and Lower Jurassic, the remainder are lower Paleozoic.

TABLE 5.—*Chemical analyses and norms for felsic volcanic rocks (porphyritic rhyolites, 1–2; rhyolitic and dacitic crystal tuffs, 3–8) and associated granites (9–10)*

[Analyses by Richard P. Sanders, West Georgia College. $Fe_2O_3/(Fe_2O_3 + FeO)$ in norms calculated as 0.30. LOI, loss on ignition]

	Sample no.	1	2	3	4	5	6	7	8	9	10
	GGS no.	1197	3127	107	153	338	338	651	3146	719	3001
	Depth (ft below surface)	4,380	4,330	4,282	4,779	3,983	4,348	4,450	4,470	4,729	7,090
	Major-oxide composition										
	SiO_2	74.3	76.6	66.4	67.2	73.0	63.9	63.3	71.0	76.8	74.3
	TiO_2	.21	.27	1.2	.73	.24	.61	.85	.55	.12	.31
	Al_2O_3	12.5	11.5	13.4	13.8	12.1	17.3	16.4	14.5	12.3	10.4
	Total Fe as Fe_2O_3	2.5	1.1	4.7	4.4	2.2	5.0	5.7	3.0	1.3	5.1
	MgO	.17	.19	1.0	1.1	.72	1.4	3.0	1.7	.12	.17
	MnO	.03	.03	.04	.07	.04	.12	.07	.05	.02	.10
	CaO	.27	.21	2.2	1.6	1.9	1.6	.34	2.5	.38	.27
	Na_2O	3.1	2.9	3.2	3.6	3.6	3.0	3.3	2.7	3.7	3.4
	K_2O	5.2	5.4	3.7	3.2	1.9	4.8	4.0	2.6	4.8	4.7
	LOI	–	–	2.7	3.5	3.6	2.8	3.3	–	.79	–
	Total	98.3	98.2	98.5	99.2	99.3	100.5	100.3	98.6	100.3	98.8
	Normative mineral composition										
	Qz	32.25	37.99	27.28	28.25	39.58	21.72	23.16	37.28	36.03	35.81
	Co	1.29	.47	.12	1.45	.74	4.18	6.01	2.63	.40	–
	Or	30.67	32.09	21.69	19.15	10.93	28.31	23.67	15.13	28.31	27.66
	Ab	26.40	24.29	27.08	30.46	30.72	25.55	27.59	23.10	31.06	27.29
	An	1.34	1.04	11.01	8.04	9.23	8.04	1.69	12.50	1.89	–
Di	Wo	–	–	–	–	–	–	–	–	–	.56
Di	En	–	–	–	–	–	–	–	–	–	.13
Di	Fs	–	–	–	–	–	–	–	–	–	.47
Hy	En	.42	.47	2.54	2.79	1.79	3.49	7.42	4.33	.30	.30
Hy	Fs	.47	–	.40	1.03	.37	1.60	1.46	.11	.21	1.10
	Ac	–	–	–	–	–	–	–	–	–	1.09
	Mt	1.93	3.47	3.22	3.02	1.75	3.42	3.93	2.35	.99	3.47
	Hn	–	.06	–	–	–	–	–	–	–	–
	Il	.40	.59	2.20	1.39	.46	1.16	1.61	1.05	.23	.59

Leaving the question of the age of the south Florida volcanic rocks open for the present, the writers believe that the weight of evidence strongly favors an early Paleozoic or Proterozoic Z age for each of the other three groups. The reasons are as follows:

1. The similarities of lithology and association suggest a single petrologic province.
2. The symmetrical structural setting of the volcanic rocks on opposing sides of the Paleozoic terrane suggests that they may be correlated.
3. The felsic volcanic terrane is known to lie stratigraphically below Lower Ordovician strata in two places: the Camp No. 1 well in central Florida (Pojeta and others, 1976, p. 10) and, from seismic profiles, in the Florida panhandle (Arden, 1974a). In both places, faulted contacts have been inferred, which complicates the problem. If the felsic volcanic rocks are assumed to be early Mesozoic, large-scale thrust faulting would be required, which is unlikely during Mesozoic time.
4. Clasts of felsic volcanic debris are common in litharenites inferred to be Triassic in age and are even found in Devonian quartz arenites (GGS 1145).
5. The presence of granite plutons in this terrane, but not in the sedimentary Paleozoic and Triassic terranes, suggests that this magmatic terrane is older. Even if these granites are regarded as basement rocks, the argument holds.
6. Radiometric ages for the volcanic rocks show a great deal of scatter but fall into two main groups having modes at about 190 m.y. (million years) and 500 m.y. (fig. 4). Previously, this grouping has been used to support the idea of two distinct provinces (Bass, 1969; Barnett, 1975), but it is possible that the older mode reflects the date of volcanism, whereas the younger records a later period of alteration and low-grade metamorphism. Most of the dates (table 6) were obtained by the K-Ar method, and argon loss is a strong possibility especially if incipient metamorphism has occurred; Rb-Sr ages, when available, are consistently older than the K-Ar dates.

All available dates from the south Florida volcanic rocks suggest that they are of Mesozoic age (see table 6). In addition, they are separated from the volcanic rocks in central Florida by a major northwest-trending magnetic anomaly, which approximately coincides with

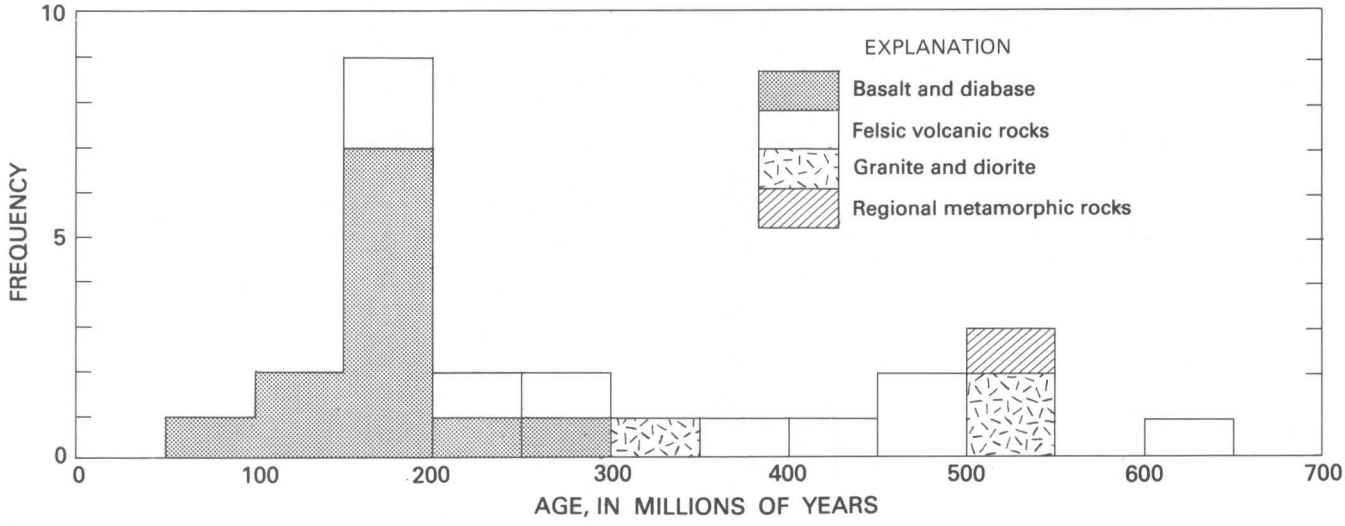

FIGURE 4.—Histogram of radiometric ages for pre-Upper Jurassic(?) rocks, other than Piedmont-province rocks, beneath the southeastern Coastal Plain; data from table 6. Where more than one date is given in the table, only the most reliable date is used in this figure.

the break between the South Florida shelf and the Peninsular arch (Klitgord and others, 1983). This anomaly suggests that the petrogenesis of the south Florida rocks may differ from that of the central Florida rocks, as indicated by Bass (1969) and Barnett (1975). However, the reported lithologies are similar to those in central Florida and Georgia. Milton (1972, p. 2) makes no distinction on the basis of petrology and chemistry, so the possibility that the south Florida rocks are Paleozoic should not be ruled out, in spite of the radiometric dates.

UPPER TRIASSIC–LOWER JURASSIC ROCKS

The most extensive "basement" terrane in the subcrop is a broad basin filled with red beds, associated diabase intrusions, and possibly basalts, which are correlated with the Upper Triassic–Lower Jurassic Newark Group. None of these red beds are found in outcrops in Georgia, but it is estimated that in the subsurface they occupy an area of approximately 50,000–65,000 km² in Georgia and a similar area in contiguous parts of Florida, Alabama, and South Carolina (pl. 1). This area is approximately four times the combined areas of all other early Mesozoic basins onshore in the Appalachian region and at least ten times the size of the next largest, the Newark-Gettysburg-Culpeper basin (10,000 km²). In Georgia, a total of 26 holes have bottomed in the red beds; 14 of the holes encountered diabase intrusions. Of the total, 12 are described here for the first time (table 7).

Although no fossils have ever been recorded from these rocks in Georgia, several lines of evidence may be used to infer their age. Stratigraphic evidence indicates that they predate Lower Cretaceous or Upper Jurassic rocks of the Coastal Plain cover, and a lower limit is suggested by the abundance of rock fragments derived from Proterozoic Z(?) to Devonian formations. Moreover, the close association between red beds and diabase intrusions suggests a structural and genetic relationship reminiscent of the exposed Upper Triassic–Lower Jurassic Newark Group of the Piedmont (Maher and Applin, 1968, p. 8; Van Houten, 1977) and Eagle Mills Formation of the Gulf Coast subsurface (Scott and others, 1961). Dooley and Wampler (1983) suggest that the crosscutting diabase dikes are probably not more than 195 m.y. old and may be contemporaneous with structurally similar dikes in the Northeastern United States that are about 180 m.y. old; Lanphere (1983) gives an age of 184 m.y. B.P. for basalt from Clubhouse Crossroads test hole #2 near Charleston, S. C. It is concluded, therefore, that the diabase and basalts are mainly Early Jurassic in age, whereas the red beds are probably Late Triassic to Early Jurassic. Because their precise age is still uncertain, and for convenience, the red beds will be referred to simply as Triassic.

Sedimentary Rocks

The total thickness of Triassic rocks within Georgia is uncertain. Only one hole, in Washington County near Riddleville (GGS 3353), has penetrated an entire section. According to the operator (C. E. Sherrill, oral commun., 1980), about 2,200 m of red beds and minor diabase were encountered before the hole bottomed in Piedmont rocks. This figure compares favorably with estimates made by Daniels and others (1983) on the basis of depth to magnetic sources in the neighborhood. In Screven County, near Statesboro, Daniels and others (1983) calculated a thickness of about 3,500 m; seismic data in the Florida panhandle (Arden, 1974a) suggest at least

1,830 m of section. Two other deep holes in Pulaski and Lowndes Counties (GGS 3137, 3113), close to the northern and southern boundaries of the terrane, respectively, penetrated at least 1,220 m of Triassic rocks before being abandoned (fig. 5). In earlier work, Applin and Applin (1964, p. 136) and Maher (1971, p. 86, well no. 72) suggested that wells in Early and Mitchell Counties (GGS 121, 109) passed out of Triassic rocks into underlying Paleozoic rocks. However, the rocks labeled Triassic in GGS 121 appear to be Cretaceous and Upper Jurassic(?), whereas GGS 109 appears to have bottomed in a metamorphosed Triassic sedimentary rock close to the contact with a diabase body. Whatever thicknesses are eventually proved, it should be remembered that recorded thicknesses are likely to be highly variable because they are controlled by block faulting and erosional truncation beneath the Fall Line unconformity.

The Triassic section characteristically consists of arkosic sandstones (60 percent) interbedded with red shales and siltstones (40 percent). The sandstones are mainly fine- to medium-grained, immature to submature arkoses, lithic arkoses, and subarkoses, ranging in color from pale red to almost white depending on the amount of matrix present. They are well indurated and commonly have sutured grains, quartz overgrowths, and calcite cements. In composition and texture, they are distinctly different from the mature quartz arenites of the Paleozoic section as well as from the poorly lithified sands of the Coastal Plain sequence.

Sandstone suites from two distinct provenances are recognizable (figs. 6*A*, *B*). In the northern suite, the predominant lithologies are arkose (54 percent), subarkose (23 percent), and lithic arkose (23 percent) that contains a large proportion of metamorphic-rock fragments evidently derived from the Piedmont. The southern suite, on the other hand, contains a smaller proportion of arkose (30 percent) and subarkose (15 percent), a correspondingly larger proportion of lithic arkose, feldspathic litharenite, and sublitharenite (46 percent), and some quartz arenite (9 percent). The lithic sandstones contain a variety of felsic volcanic-rock clasts and some quartz arenite clasts that plainly originated in the felsic volcanic and Paleozoic sedimentary terranes further south.

The shales and siltstones range in color from grayish- to brownish-red, and some contain buff-colored reduction spots. These rocks consist mainly of quartz, feldspar, illite, chlorite or kaolinite, and, in some samples, a small amount of expandable clay mineral. Many samples show evidence of bioturbation, and some contain iron-stained nodules of calcite microspar that are interpreted to be caliche. In some holes, these nodules have been reworked and included as clasts. The lithology of the shales in the northern suite differs from that of the shales in the southern suite. Whereas the shales in the northern suite are thin bedded, are sandy and micaceous, and typically grade into wackes, the southern shales are thicker bedded, contain less sand-sized material, and show sharper contacts with the sandstones.

Because none of the Triassic rocks have been cored, little information on sedimentary structures is available. However, electric logs suggest that fining-upward cycles are present in some holes (for example, GGS 3122, 3137), and dipmeter information indicates channelling and possibly crossbedding in GGS 3122 and GGS 3353.

The preponderance of red beds and the lack of fossil debris in the Triassic section suggest that it was deposited in continental environments. In general, the relative proportions of sandstone and shale combined with the poor sorting and lack of both textural and mineralogical maturity indicate a fluvial origin. This interpretation is supported by the presence of fining-upward cycles and channelling, as well as by the occurrence of caliche horizons in the shales. The fact that fining-upward cycles are not more common suggests a predominance of braided- rather than meandering-stream alluvium.

Other environments that might be expected in this association include alluvial fans, eolian dunes, and playa lakes. Coarse-grained fanglomerates are common in the subsidiary Riddleville (GGS 3353) and Dunbarton (Marine and Siple, 1974) basins, which are flanked by horsts of Piedmont rock, but fanglomerates have not been found in the main South Georgia basin except at the base of Clubhouse Crossroads test hole #3 in South Carolina (Gohn and others, 1983). Although anhydrite occurs as a cement in some sandstones, no bedded or nodular evaporite deposits occur, and the sandstones are generally too poorly sorted to be eolian.

Diabase

Diabase intrusions occur in 15 of the 24 holes within the Triassic sedimentary terrane and comprise an average of 17 percent of the sections logged during this study (table 7). They are also present in five holes located in other terranes (tables 2, 3, 4). All these occurrences probably represent minor intrusions, but it is rarely possible to be certain whether individual bodies are dikes or sills. Nevertheless, the frequency with which they occur suggests that most are gently dipping sills rather than high-angle dikes. This is borne out by dipmeter measurements in one hole (GGS 3122), by seismic data from the neighboring Florida panhandle (Arden, 1974a), and by observations from other Triassic basins in the Eastern United States (Toewe, 1966, p. 12; Reinemund, 1955, p. 55; Rodgers, 1970, p. 208).

TABLE 6.—*Radiometric ages for pre-Upper Jurassic(?) rocks beneath the southeastern Coastal Plain (Georgia, Florida, Alabama, South Carolina)*

[*, K-Ar dates that appear to be too young, perhaps owing to argon loss; †, average of duplicate analyses. Where duplicate dates are given, the more reliable date is underlined]

Well no.	Well name and location	Rock type	Age (m.y.)	Technique	Reference
Applin 6	Humble-Carroll No. 1 Osceola Co., Fla.	quartz monzonite	527	Rb-Sr feldspar	Bass (1969)
			546	do	Do.
Applin 7	Sun-Powell Land No. 1 Volusia Co., Fla.	diorite	480*	K-Ar whole rock	Milton and Grasty (1969)
		do.	524	K-Ar biotite	Bass (1969)
		hornfels	634	Rb-Sr biotite	Do.
Applin 20	Humble-Keen No. 1 Hardee Co., Fla.	altered basalt	145†	K-Ar whole rock	Milton and Grasty (1969)
Applin 21	Humble-Carlton No. 1 Highlands Co., Fla.	basalt	183±10	do.	Do.
Applin 24	Humble-Hayman No. 1 Osceola Co., Fla.	rhyolitic tuff	173±4	do.	Do.
	Amerada-Cowles Magazine No. 1 St. Lucie Co., Fla.	amphibolite	503	K-Ar hornblende	Bass (1969)
		quartz diorite gneiss	530	Rb-Sr biotite	Do.
		do.	226±6*	K-Ar whole rock	Milton and Grasty (1969)
		do.	224±3*	do.	Do.
		do.	308±5*	do.	Do.
		basalt	89±2*	do.	Do.
Barnett 33	Humble-Lehigh Acres Lee Co., Fla.	basalt	163	do.	Barnett (1975)
Barnett 20	Mobil-State Lease 224A, No. 1c, offshore Franklin Co., Fla.	diabase	192†	do.	Do.
		do.	154†	K-Ar pyroxene	Do.
Barnett 6	Mobil-State Lease 224B, No. 1, offshore Charlotte Co., Fla.	rhyolite	170±4†	K-Ar feldspar	Do.
		do.	212±30†	Rb-Sr feldspar	Do.
		do.	228±40†	Rb-Sr whole rock	Do.
	COST GE-1, offshore Nassau Co., Fla.	felsic volcanic rock	374±14	K-Ar whole rock	Simonis (*in* Scholle, 1979, p. 71)
		do.	346±12	do.	Do.
		do.	159±6*	do.	Do.
		do.	355±3†	Rb-Sr	Do.

The apparent thickness of the diabase bodies ranges from 1.5 to 124 m, but it must be remembered that, if nearly vertical dikes are present, some of these values may be excessive. Most of these igneous bodies consist of a single uninterrupted mass of diabase, but a number of intrusions in GGS 3113 appear to be split by intervals of sedimentary rock.

The mineralogy of the diabase is relatively simple; zoned plagioclase (An_{50-70}) and pyroxene (mainly clinopyroxene) are the essential primary constituents. Some intrusions contain small amounts of olivine (for example, GGS 3137, 3,406–3,813 ft; GGS 51) or pseudomorphs after olivine, whereas others have interstitial intergrowths of quartz and potassium feldspar (micropegmatite) (for example, GGS 3137, 5,827–6,180 ft; GGS 3080, 4,019–4,070 ft). Accessories include magnetite-ilmenite, typically showing distinctive skeletal crystals, and interstitial biotite, chlorite, and serpentine, as well as secondary replacement minerals. Olivine is especially prone to alteration and in thin sections is represented by pseudomorphs of serpentine, iddingsite, and magnetite. Clinopyroxene is partially altered to chlorite, serpentine, and uralite. Plagioclase typically is partially albitized (An_{30-45}) and replaced by sericite.

It is difficult to establish mineralogical trends within individual intrusions on the basis of cuttings because of the mixing that occurs during rotary drilling, especially

TABLE 6.—*Radiometric ages for pre-Upper Jurassic(?) rocks beneath the southeastern Coastal Plain (Georgia, Florida, Alabama, South Carolina)*—Continued

[*, K-Ar dates that appear to be too young, perhaps owing to argon loss; †, average of duplicate analyses. Where duplicate dates are given, the more reliable date is underlined]

Well no.	Well name and location	Rock type	Age (m.y.)	Technique	Reference
GGS 109	Stanolind–Pullen No. 1 Mitchell Co., Ga.	diabase	182±5	K-Ar whole rock	Milton and Grasty (1969)
GGS 153	California–Buie No. 1 Camden Co., Ga.	altered felsic tuff	480±17	do.	Georgia Geologic Survey (unpub.)
GGS 189[1]	Humble–Bennett and Langdale No. 1, Echols Co., Ga.	diabase	191±11	do.	Milton and Grasty (1969)
GGS 341	Cusseta waterwell, Chattahoochee Co., Ga.	amphibolite	303±15	K-Ar hornblende	Do.
GGS 338	Pan American–Griffis No. 1, Clinch Co., Ga.	felsic tuff	230±35*	K-Ar whole rock	Georgia Geologic Survey (unpub.)
		do.	425±14	do.	Do.
GGS 651	Humble–Union Bay and Paper No. 1, Wayne Co., Ga.	felsic tuff	460±15	do.	Do.
GGS 3127	Chevron–Fussel No. 1, Coffee Co., Ga.	rhyolite	165±6*	do.	Do.
GGS 3128	Chevron–Sinclair No. 1, Jeff Davis Co., Ga.	diabase	195±11	do.	Do.
GGS 3137	Atlanta Gas Light Griffin–No. 1, Pulaski Co., Ga.	do.	186±12	do.	Dooley and Wampler (1983)
		do.	202±15	do.	Do.
		do.	209±14	do.	Do.
GGS 3201	Davis–Hopkins No. 2, Wayne Co., Ga.	felsic tuff	298†	K-Ar whole rock	Dooley and Wampler (oral commun., 1982).
Neathery and Thomas 35	Shell–Alger Tenants No. 1, Escambia Co., Ala.	granite	334±4.8	K-Ar whole rock	Neathery and Thomas (1975)
Neathery and Thomas 36	Chevron–Neal No. 1, Escambia Co., Ala.	basalt	267±10	K-Ar whole rock(?)	Do.
CC#1	USGS–Clubhouse Crossroads No. 1, Dorchester Co., S.C.	basalt	97±4.2*	K-Ar whole rock	Gohn and others (1978)
		do.	111±4*	do.	Do.
CC#2	USGS–Clubhouse Crossroads No. 2, Dorchester Co., S.C.	do.	204±4.1†	K-Ar whole rock	Do.
		do.	162±3.2†	do.	Do.
		do.	186±3.7†	do.	Do.
		do.	184±3.3	$^{40}Ar/^{39}Ar$	Lanphere (1983)

[1] Milton and Grasty indicate that this analysis is from GGS 169; this is evidently a typographical error because they refer to the well as Humble-Bennett and Langdale No. 1.

when the density of the drilling mud is not properly adjusted. However, in one diabase (GGS 3137, 3,406–3,813 ft), either differentiation has occurred or the sill is a multiple intrusion. Whereas the margins of this intrusion contain calcic plagioclase (An_{52-70}) and olivine, the center carries less calcic plagioclase (An_{40-61}) and small amounts of micropegmatite (fig. 7).

Most of the diabase is phaneritic, having a texture ranging from diabasic (intergranular) to ophitic depending mainly on grain size (Chalcraft, 1978). Aphanitic cuttings containing plagioclase phenocrysts, sometimes arranged in radiating aggregates, are presumed to be derived from marginal chill zones.

The chemistry of similar mafic igneous rocks, referred to as the eastern North American suite, has been described and discussed by Weigand and Ragland (1970), Smith and others (1975), Gottfried and others (1977, 1983), and Dooley and Wampler (1983). These authors recognize three main chemical types: olivine-normative tholeiites (characterized by low TiO_2 values between 0.4 and 0.6 percent), low-TiO_2 quartz-normative tholeiites (0.6–0.9 percent TiO_2). and high-TiO_2 quartz-normative tholeiites (0.9–1.3 percent TiO_2).

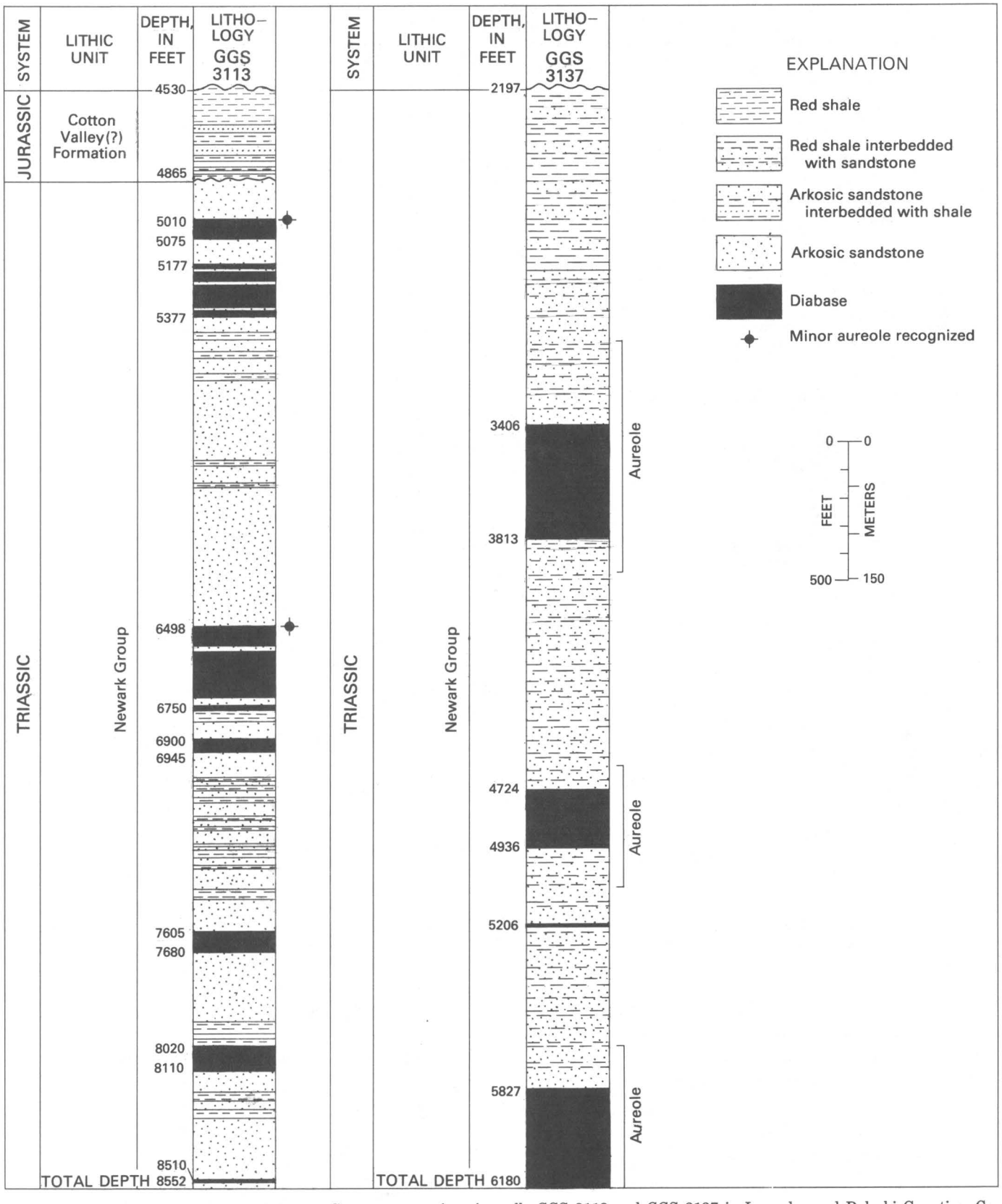

FIGURE 5.—Stratigraphic columns of the pre-Cretaceous sections in wells GGS 3113 and GGS 3137 in Lowndes and Pulaski Counties, Ga.

TABLE 7.—*Holes bottomed in Triassic sediments and diabase*

County	GGS number	Ground elevation[1]	Elevation of drill platform	Depth to base of Cretaceous	Total depth	Elevation of base of Cretaceous	Thickness of pre-Cretaceous	Comments	References[2]
Laurens	51	280	–	2,532	2,548	−2,252	16	Diabase in country rock of unknown age.	1
Wayne	52	–	73 D.F.	4,570	4,626	−4,497	56	Arkosic sandstone	3, 4
Toombs	95	198	–	3,663	3,680	−3,465	17	Conglomeratic arkose	3, 4
Crisp	108	364	–	4,220	5,010	−3,856	790	Sandstone	8
Mitchell	109	338	–	6,220	7,487	−5,882	2,167	Diabase in clastic rocks	4, 7
Appling	148	229	–	4,075	4,098	−3,846	23	Basalt intruded into sandstone of unknown age.	3, 4
Montgomery	190	–	293 D.F.	3,390	3,424	−3,097	34	Diabase in country rock of unknown age.	1, 4, 8
Calhoun	192	345	–	3,850?	5,265	−3,505?	1,415?	Diabase overlain by clastic rock.	1, 4
Sumter	296	509	–	–	–	–	–	Arkosic sandstone containing diabase.	3, 4
Do.	442	431	–	2,935	5,240	−2,504	2,305	Arkosic sandstone, red shale, and diabase.	3, 8
Wheeler	336	190	195 D.F.	–	4,002	–	–	"Ferruginous sandstone"	3, 7
Do.	3080	157	168 K.B.	3,814	4,070	−3,646	256	Arkosic sandstone intruded by diabase.	8
Pulaski	472	280	–	–	2,710 ?	–	–	---	3, 4
Do.	491	328	–	2,350	6,035	−2,022	3,685	Arkosic sandstone, red shale, and diabase.	7, 8
Do.	960	–	305 D.F.	2,500?	2,929	−2,195?	429?	Diabase and "granite wash"	4
Do.	3137	324	332 K.B.	2,197	6,180	−1,865	3,983	Arkosic sandstone, shale, and diabase.	8
Clinch	496	–	214 D.F.	4,155	4,232	−3,941	77	Amygdaloidal basalt of uncertain age.	2, 4
Marion	505	600	–	2,410?	4,010	−1,810?	1,600?	Arkosic sandstone, red shale, and diabase.	8
Dooly	619	442	–	3,512	3,748	−3,070	236	Arkosic sandstone	3, 4
Lowndes	3099	243	254 K.B.	4,896	5,247	−4,642	351	Arkosic sandstone and shale overlain by Jurassic(?) red beds (546 ft).	8
Do.	3113	157	167 K.B.	4,865	8,552	−4,698	3,687	Arkosic sandstone, shale, and diabase overlain by Jurassic(?) red beds (335 ft).	8
Do.	3115	201	212 K.B.	4,532	4,986	−4,320	454	Red shale overlain by Jurassic(?) red beds (336 ft).	8
Do.	3120	171	182 K.B.	4,220	5,053	−4,038	833	Arkosic sandstone, shale, and diabase overlain by Jurassic(?) red beds (126 ft).	8
Do.	3122	191	201 K.B.	4,676	5,004	−4,475	328	Arkosic sandstone, shale and diabase overlain by Jurassic(?) red beds (290 ft).	8
Thomas	3,114	266	279 K.B.	6,553	6,668	−6,274	115	Arkosic sandstone, shale and diabase overlain by Jurassic(?) red beds (803 ft).	8
Jeff Davis	3128	272	287 K.B.	3,932	4,046	−3,645	114	Arkosic sandstone, shale, and diabase.	8
Twiggs	3147	–	–	–	1,545	–	–	Diabase	8
Worth	3154	325	–	5,425?	5,567	−5,100?	142?	Arkosic sandstone and red shale.	8
Wilkinson	3165	480	–	1,232	1,547	−752	315	Red beds	8
Washington	3353	342	348 D.F.	1,105	3,814	−757	2,709	Red fanglomerates	8

[1] Because oil test wells are logged by depth from the drilling platform, rather than from ground level, it is important to know the elevation of the platform (kelly bushing, K.B., or derrick floor, D.F.), rather than ground level, in computing the absolute elevation of stratigraphic markers in the holes. Wherever available, this information is given in the tables and is used to compute absolute elevations at the base of the Cretaceous [or depth to base of Jurassic(?) where these rocks form the base of the Coastal Plain sequence]. Measurements are given in feet.

[2] Data in the table are drawn from the following references: 1, Applin (1951); 2, Applin and Applin (1964); 3, Herrick (1961); 4, Milton and Hurst (1965); 5, McLaughlin (1970); 6, Daniels and Zietz (1978); 7, Swanson and Gernazian (1979); 8, new data.

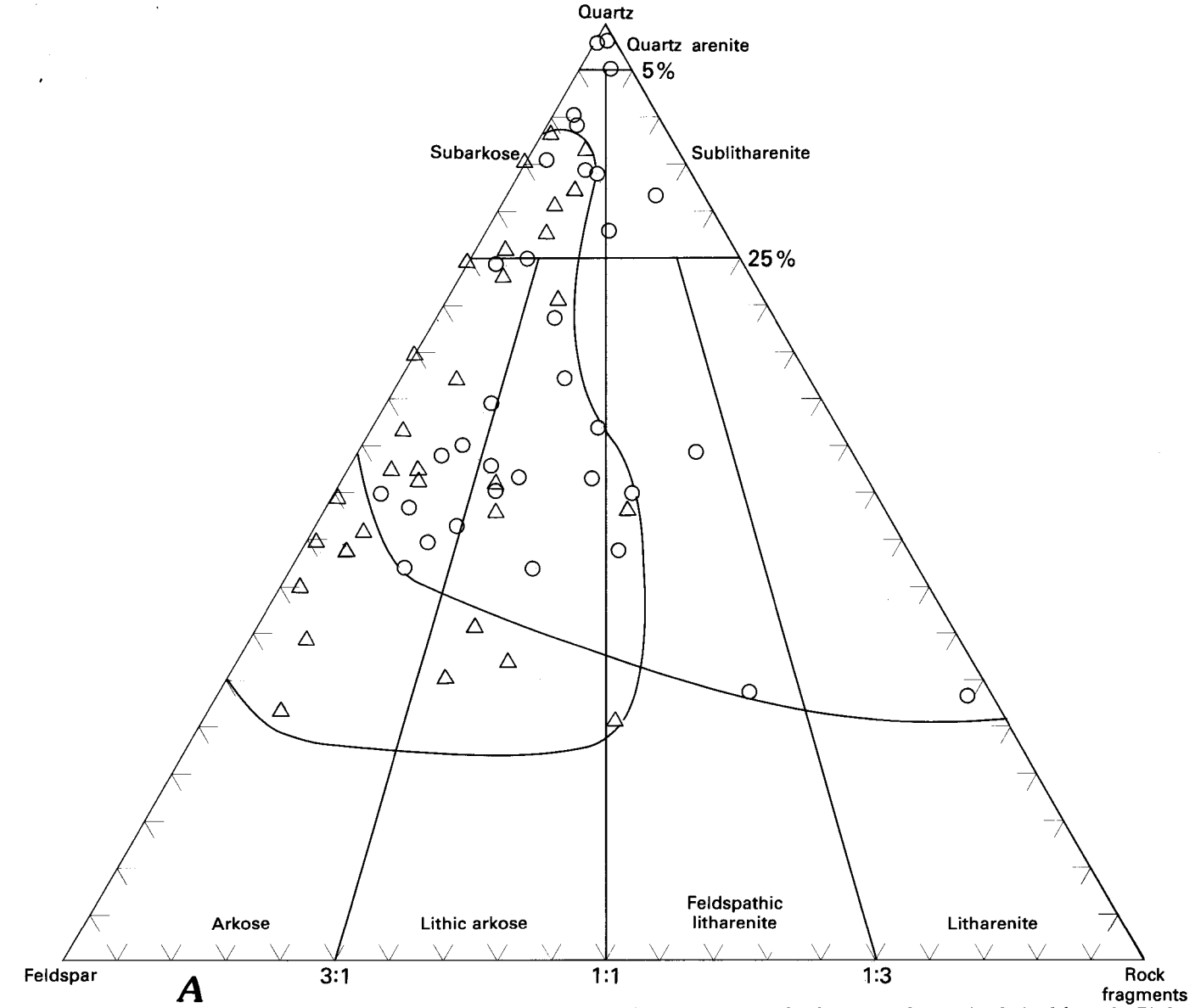

FIGURE 6.—*A*, Petrography of sandstones from the Triassic terrane. Triangles represent samples from a northern suite derived from the Piedmont, and circles represent a southern suite derived from the area of the Peninsular arch and Suwannee saddle. (All Paleozoic sandstones from the south Georgia subsurface fall within the field of quartz arenites. Modal analyses prepared by visual estimation from five random cuttings per sample.) *B*, Distribution of different suites of Triassic sedimentary rocks in the Georgia Coastal Plain.

Chemical analyses and norms from the present study are given in table 8. Because all samples were obtained from cuttings, it was difficult to separate chips of a single rock type from a particular depth. Thus, no attempt was made to isolate material from the chilled margins for analysis, as recommended by Smith and others (1975). However, highly serpentinized cuttings associated with veins were avoided.

The analyses show an apparent range in normative composition from olivine-normative tholeiite to quartz-normative tholeiite roughly corresponding to the petrographic range from olivine diabase to micropegmatitic diabase (fig. 8). Part of the scatter in figure 8 is probably the result of secondary alteration, as suggested by thin-section analyses and confirmed by low An values for the plagioclases and low totals in the analyses (a result of high H_2O) (Gottfried and others, 1977). In particular, the norms for samples 8 and 9 (GGS 3113, 6640 ft, 8070 ft), which show the presence of nepheline, and for sample 6 (GGS 3122, 4730 ft), which shows excess SiO_2 without micropegmatite in thin section, appear to be anomalous. Elimination of these most altered samples leaves a cluster of analyses in the quartz-tholeiite field and a scatter of points in the olivine-tholeiite field.

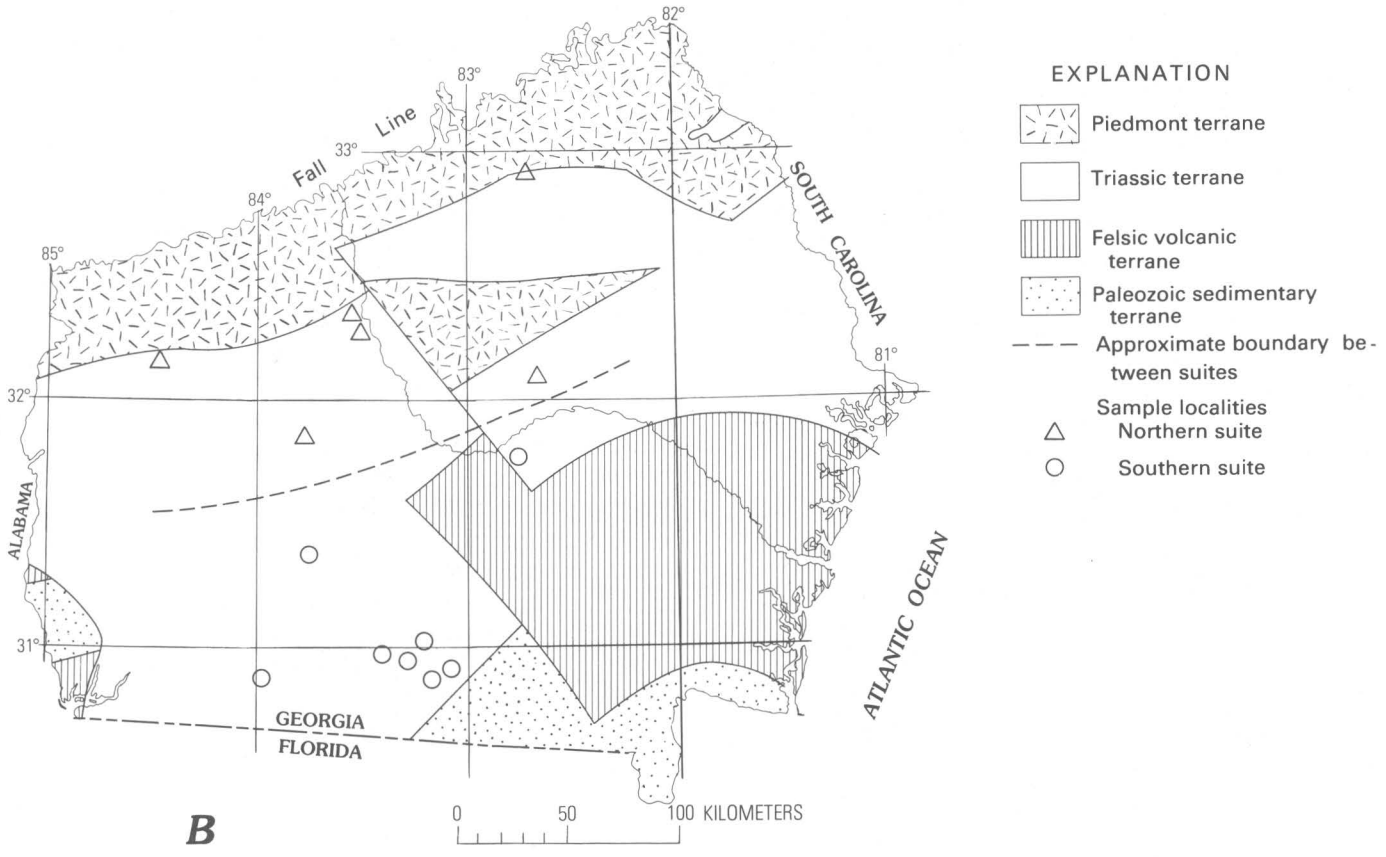

FIGURE 6.—Continued

A plot of TiO_2 against mafic index (Weigand and Ragland, 1970) indicates that our olivine-normative tholeiites contain higher percentages of TiO_2 than do our quartz-normative tholeiites (fig. 9). This result is somewhat surprising in the light of earlier work by Weigand and Ragland (1970), Smith and others (1975), and Gottfried and others (1977, 1983). None of our olivine-normative tholeiites contain TiO_2 percentages as low as those reported by these workers. After the highly altered samples (6, 8, and 9) were eliminated, most of our tholeiites showing olivine in the norm plot within the high-TiO_2 field designated by Weigand and Ragland (1970), while those having quartz in the norm plot mainly in the low-TiO_2 field. A single sample (18) occurs within the high-Fe_2O_3 field (a minor variant described by Weigand and Ragland) but was derived from the same intrusion as were 16 and 17 (low-TiO_2 types).

There are several possible explanations for the apparent discrepancy between normative composition and TiO_2 content.

1. The appearance of olivine in the norms may be the result of alteration, as discussed by Gottfried and others (1983). In this case, the olivine-normative tholeiites in this study might be regarded as altered high-TiO_2 quartz tholeiites. However, most of the samples in question are relatively little altered, and some (10, 12, 13) contain appreciable olivine in the mode as well as in the norm.
2. The diabases in question may be high-TiO_2 quartz tholeiites that have undergone fractional crystallization in place to produce olivine-rich varieties. Local differentiation has been suggested in samples 10–12 (GGS 3137, 3,406–3,813 ft) and is also probable in samples 13–15 (GGS 3137, 4,724–4,936 ft) and samples 16–18 (GGS 3137, 5,827–6,180 ft). However, the fact that olivine occurs so commonly in the present sample suite and is not restricted to narrow zones at the bases of the sills(?) suggests that it is not simply the result of local fractionation.
3. Because the present samples are geographically distinct from samples analyzed by other workers, our samples may be a separate magma type (high-TiO_2, olivine-normative) not previously sampled.

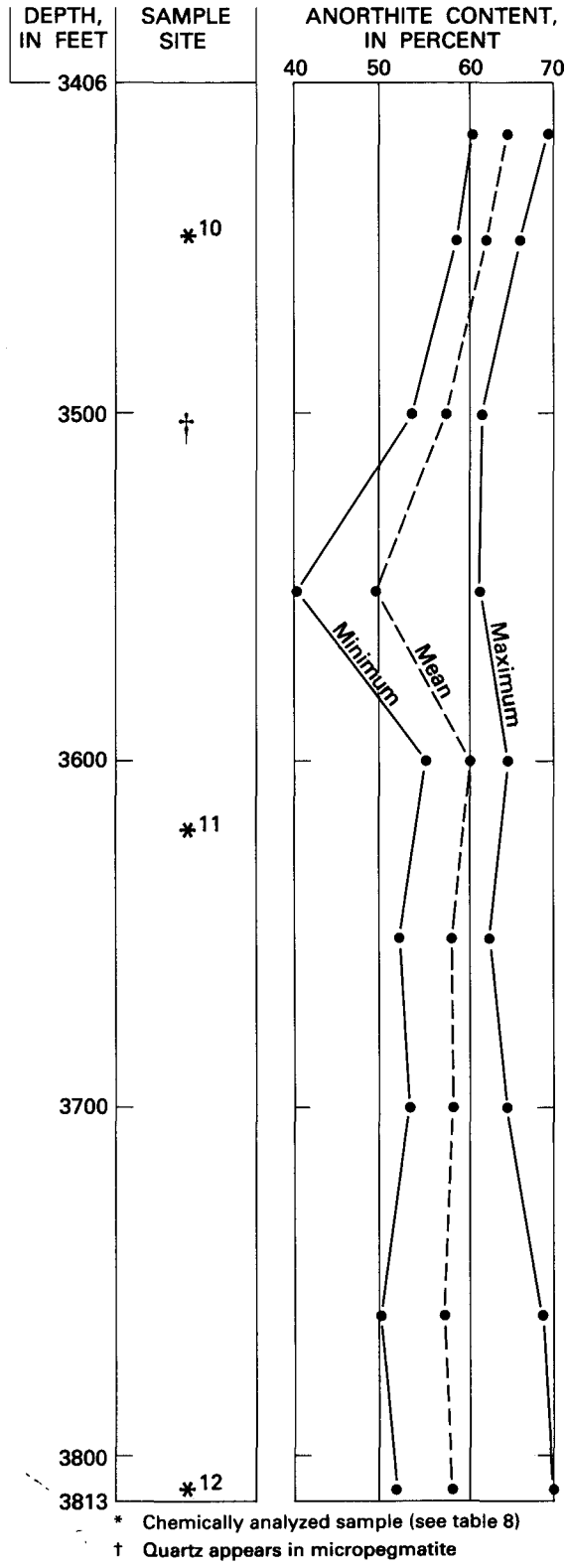

FIGURE 7.—Differentiation in sill from GGS 3137 (3,406–3,813 ft) as indicated by composition of plagioclase. Anorthite values were determined from extinction angles by using duplicate measurements from nine crystals obtained from three different rock chips per sample interval. Because measurements were made from cuttings, some sample mixing is to be expected, especially toward the base of the section.

At present, the writers prefer the third possibility, but more work, especially analysis of stable trace elements, is needed before a firm conclusion is reached.

Basalt

From an examination of the contact relations and texture of the mafic igneous rocks within the Triassic sedimentary rocks, it is clear that all the mafic rocks are intrusive. However, two wells that are not positively associated with the Triassic terrane have bottomed in fine-grained, amygdaloidal basalt (GGS 148) and basaltic andesite (GGS 496), which are probably flows. Unfortunately, their age is uncertain since neither the individual holes nor plate 1 suggest a definite stratigraphic position. They could be contemporaneous with either the felsic volcanic rocks or the diabase intrusions, but no radiometric dates are available.

Chemical analyses and norms (table 8, figs. 8, 9) indicate that the basalts resemble the diabase in chemistry except that they are relatively enriched in alkalies and, in the case of GGS 148, also in silica. In part, these differences may be the result of greater alteration, especially partial albitization of the plagioclase (An_{35-40}).

Metamorphism of Triassic Rocks

Laumontite, epidote, and other low-grade metamorphic minerals are widespread in the Triassic rocks, and it is clear that much of this terrane has undergone zeolite-facies alteration. This alteration is especially noticeable in the northern suite of sections (for example, GGS 3137, 491, 505, 108, 3080) but also occurs in some holes in the southern suite (for example, GGS 3154, 3113). It is most pronounced in the contact aureoles of the diabase bodies but also occurs regionally to a lesser degree in sections that contain no igneous rock.

Contact aureoles affecting all rock types may be recognized around the diabase in GGS 3080, 3113, 3120, and 3137. In most cases, the aureoles are quite narrow (less than one 3-m interval in the cuttings) and are easily overlooked. However, the largest intrusions in GGS 3137 have hornfels zones apparently extending more than 30 m from the contacts; in one case, the zone extends 76 m from a contact (GGS 3137, 3,406 ft) (fig. 5). Field observations from some exposed early Mesozoic basins indicate that aureoles wider than about 9 m are uncommon (see, for example, Reinemund, 1955, p. 60), suggesting the possibility that the diabase dikes in GGS 3137 were intersected at a very acute angle. However, some large sills may have much wider aureoles. For example, detailed studies of the Palisades sill indicate an aureole as much as 135 m wide (Van Houten, 1969), and a sill within the Culpeper basin near Leesburg, Va., has

TABLE 8.—*Chemical analyses and norms for basalt (1–2) and diabase (3–18)*

[Analyses by Richard P. Sanders, West Georgia College. $Fe_2O_3/(Fe_2O_3 + FeO)$ in norms calculated as 0.15. †, highly altered samples. LOI, loss on ignition]

Sample no.	1	2	3	4	5	6†	7	8†	9†	10	11	12	13	14	15	16	17	18
GGS no.	148	496	3120	3120	3120	3122	3080	3113	3113	3137	3137	3137	3137	3137	3137	3137	3137	3137
Depth (ft below surface)	4,090	4,200	4,610	4,670	4,970	4,730	4,065	6,640	8,070	3,430	3,610	3,810	4,750	4,820	4,860	5,850	5,960	6,180
Major-oxide composition																		
SiO_2	54.4	49.1	48.5	47.8	48.5	51.9	52.9	46.6	45.8	48.5	49.1	47.6	48.7	47.8	48.3	51.2	51.2	52.2
TiO_2	1.3	.92	1.3	1.8	1.2	1.8	.55	2.3	2.3	1.0	1.4	.96	1.1	.93	1.2	.85	.70	1.0
Al_2O_3	15.1	14.3	16.1	15.3	16.1	14.5	15.3	14.0	14.0	15.7	16.5	15.1	14.8	15.9	14.6	13.8	14.4	14.8
Total Fe as Fe_2O_3	8.2	11.2	10.6	12.6	10.4	12.9	9.1	13.9	14.7	10.6	10.5	11.2	11.0	10.1	11.3	11.4	10.7	12.8
MnO	.14	.15	.18	.21	.19	.17	.15	.23	.23	.17	.17	.16	.17	.16	.19	.19	.18	.18
MgO	4.9	7.8	7.5	6.6	7.1	3.7	7.0	5.8	4.9	9.0	4.9	10.0	8.2	8.0	7.4	7.4	7.0	5.1
CaO	6.7	7.0	10.8	11.2	12.0	7.3	11.3	6.2	6.8	11.5	11.7	10.7	9.1	11.7	11.9	10.9	10.8	10.6
Na_2O	3.7	3.6	2.5	2.4	2.4	3.2	2.2	4.6	3.9	2.3	2.7	2.3	2.8	1.9	2.4	1.8	2.1	2.5
K_2O	2.5	.84	.43	.28	.28	1.4	.64	.71	1.3	.46	.61	.48	.33	.38	.31	.45	.54	.62
LOI	–	5.1	–	–	–	–	1.6	–	–	–	–	–	–	–	–	–	–	–
Total	96.9	100	97.9	98.2	98.2	96.9	100.7	94.3	93.9	99.2	97.6	98.5	96.2	96.9	97.6	98.0	97.6	99.8
Normative mineral composition																		
Qz	.97	–	–	–	–	4.70	3.72	–	–	–	–	–	–	–	–	4.09	3.13	3.22
Or	15.10	5.29	2.61	1.70	1.70	8.52	3.85	4.51	8.35	2.77	3.73	2.91	1.96	2.34	1.90	2.74	3.29	3.54
Ab	32.87	32.70	21.53	20.73	21.06	27.71	18.68	36.77	30.71	19.56	23.02	19.73	26.14	16.76	21.30	15.53	18.51	22.99
An	17.87	21.44	32.39	31.22	33.10	21.76	30.74	16.97	18.06	31.86	32.41	30.39	27.59	35.13	28.88	29.28	28.96	27.05
Ne	–	–	–	–	–	–	–	2.49	2.83	–	–	–	–	–	–	–	–	–
Di Wo	6.91	6.53	9.51	10.77	11.76	6.55	11.06	6.72	7.69	10.97	11.58	9.99	7.68	10.50	13.41	11.02	10.88	9.91
Di En	3.85	3.70	5.65	5.65	6.70	2.67	6.39	3.24	3.34	6.65	5.79	6.09	4.54	6.23	7.49	6.06	5.98	4.57
Di Fs	2.79	2.55	3.38	4.80	4.56	3.92	4.16	3.37	4.34	3.73	5.55	3.34	2.76	3.74	5.39	4.55	4.50	5.26
Hy En	8.93	5.69	8.24	7.37	5.79	7.23	11.22	–	–	5.08	5.77	4.36	9.12	10.05	5.37	13.00	12.09	8.86
Hy Fs	6.48	3.93	4.93	6.26	3.94	10.60	7.31	–	–	2.85	5.52	2.39	5.53	6.04	3.87	9.74	9.11	10.20
Ol Fo	–	7.93	3.72	2.81	3.98	–	–	8.57	6.95	7.71	.82	10.38	6.10	3.18	4.29	–	–	–
Ol Fa	–	6.03	2.45	2.63	2.98	–	–	9.80	9.96	4.77	.87	6.26	4.08	2.10	3.41	–	–	–
Mt	1.70	2.36	2.16	2.58	2.12	2.63	1.83	2.96	3.14	2.14	2.16	2.29	2.29	2.09	2.33	2.33	2.18	2.53
Il	2.53	1.86	3.55	3.48	2.32	3.72	1.06	4.61	4.63	1.93	2.79	1.87	2.21	1.84	2.36	1.67	1.37	1.86

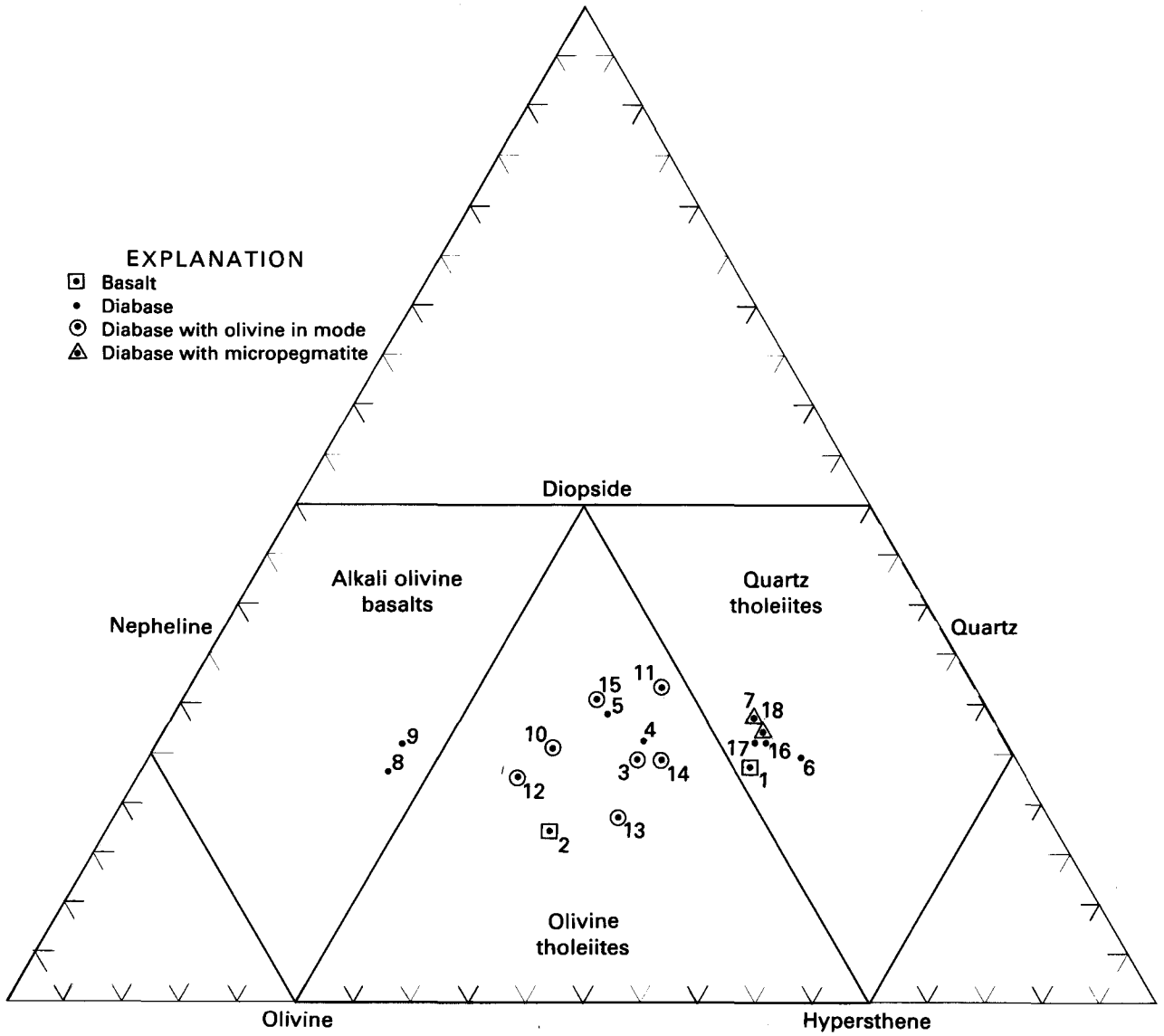

FIGURE 8.–Ternary diagram showing composition of basalt and diabase from pre-Upper Jurassic section. $Fe_2O_3/(FeO+Fe_2O_3) = 0.15$.

a hornfels zone (originally interpreted as pyroclastic deposits by Toewe, 1966, p. 8–12) between 150 and 200 m wide (Froelich and others, 1982).

Although low-grade metamorphic minerals are most common adjacent to the diabase, they are not restricted to these contact zones but occur widely in sandstones throughout much of the Triassic terrane as well as in some of the felsic volcanic rocks bordering it. This indicates that the entire area has undergone some degree of zeolite-facies alteration, as suggested by Armstrong and Besancon (1970).

Apart from quartz overgrowths, calcite cements and replacements, and anhydrite cements, which are probably unrelated to the intrusion of the diabase, the principal authigenic minerals are laumontite, epidote-clinozoisite, magnetite, and sphene, and minor amounts of chlorite, garnet, prehnite, pumpellyite, quartz, and unidentified zeolites. Mineral identifications have been made primarily on the basis of thin sections and confirmed by X-ray powder-diffraction photographs.

The most abundant of these minerals is laumontite, which occurs as a replacement and void filling in the diabase and sedimentary rocks and as cross-cutting veins. It appears to form by the replacement of feldspars, clay matrix, caliche nodules, and possibly earlier formed zeolites. For example, in samples from GGS 3137 at 3,220 ft and 3,950 ft, an acicular zeolite(?) appears to be partially replaced by laumontite. In sandstones, laumontite commonly forms relatively large poikiloblastic crystals (as much as 4 mm), which invade the rock by selectively replacing the feldspar grains and matrix.

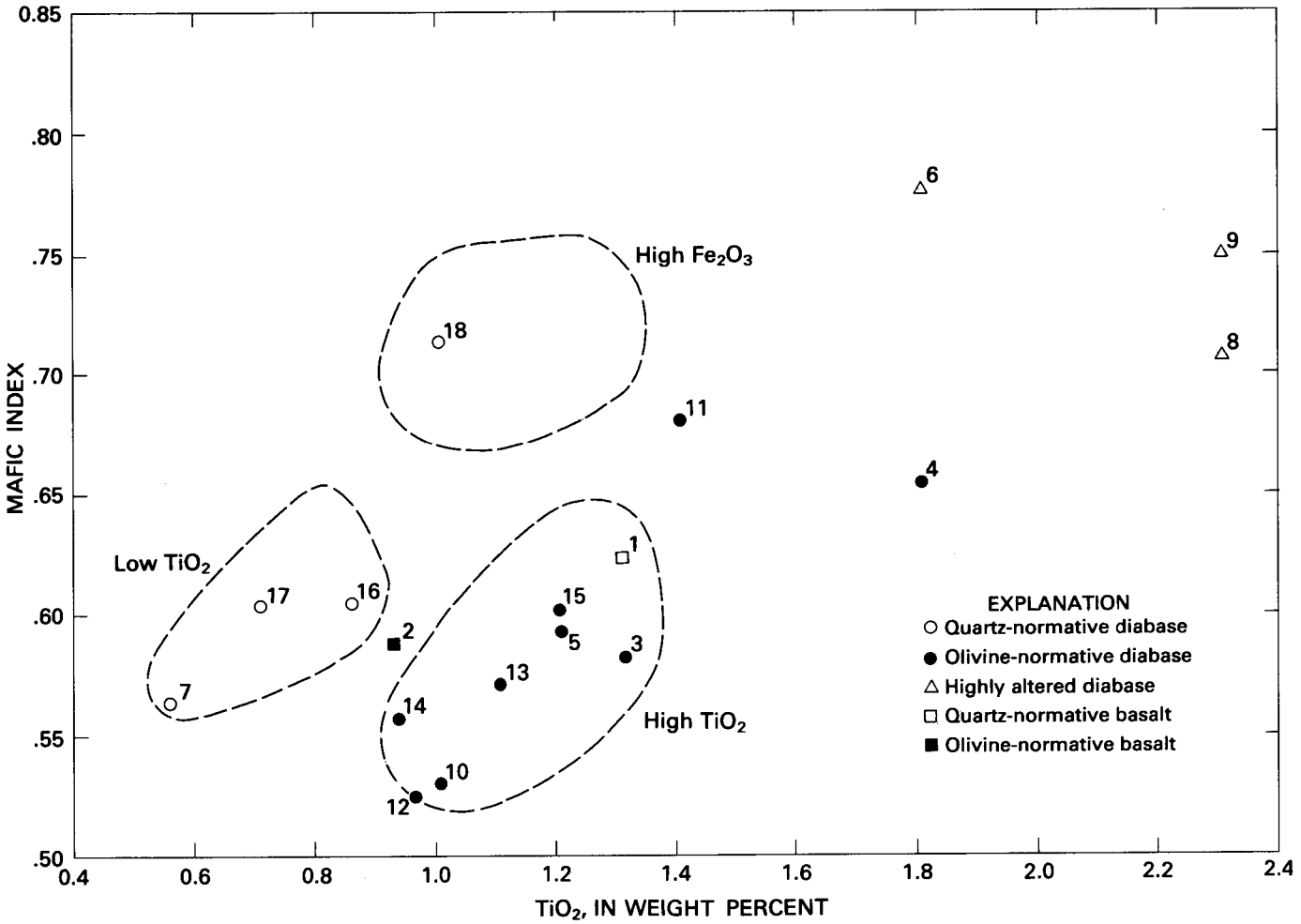

FIGURE 9.—Subdivisions of tholeiites on the basis of TiO_2 versus mafic index. Sample numbers correspond to table 8. The following groups of analyses represent samples from the same intrusions: 3–4; 10–12; 13–15; 16–18. Analyses 1 and 2 are for basalt, the remainder for diabase.

Also widespread are green to colorless crystals of epidote-clinozoisite, which frequently accompany laumonite. They occur as small (20–750 μ) anhedral to euhedral crystals, formed by replacement and secondary void filling in the sedimentary rocks. Much of the epidote-clinozoisite in the sandstones is interstitial and has grown at the expense of the matrix, but it is also common as a replacement of detrital grains and caliche nodules. Unlike laumontite, it is not found filling veins.

Sphene is much less abundant than are laumontite and epidote-clinozoisite but is widely distributed in sandstones and diabase throughout the Triassic area. Like the epidote-clinozoisite, it is largely interstitial in the sandstones and probably grew by a combination of replacement and void filling. In some places, in sandstone and diabase, it appears as a secondary overgrowth on grains of ilmenite.

Finely disseminated magnetite, sometimes forming spots, is abundant in the shales and immature sandstones within the contact aureoles of the diabase bodies (for example, GGS 3137, 3113), and is probably the result of the reduction of the hematitic stain in the argillaceous red beds.

Prehnite, pumpellyite, chlorite, and garnet are all relatively rare and are restricted to the contact aureoles. Prehnite and garnet have been positively identified only from hornfels in GGS 3137 and pumpellyite only from the hornfels in GGS 3080. The garnet (andradite-grossularite), which forms clusters of subhedral crystals showing anomalous birefringence, occurs only as pseudomorphs after caliche nodules.

The fact that the majority of these minerals are calcium-bearing aluminosilicates, combined with the textural evidence of replacement, suggests that the presence of feldspar, calcite, and clay minerals is critical for the formation of this mineral paragenesis. This is supported by a parallel increase in feldspar alteration (albitization?) in rocks containing large amounts of laumontite and epidote-clinozoisite.

As indicated above, it is common for several of these authigenic minerals to occur together, especially in caliche nodules, and it is possible to derive the following paragenetic sequence:

1a. Early diagenetic growth of caliche nodules in shales (often reworked as detrital grains in sandstones);
b. Cementation of sandstone by quartz overgrowths;
2a. Reduction of hematite to magnetite in contact aureoles of diabase;
b. Replacement of matrix, grains, and caliche nodules (especially at margins) by epidote-clinozoisite;
3. Replacement, void filling, and veining by late-stage poikilitic minerals (laumontite and calcite), possibly accompanied by growth of sphene and a second generation of epidote-clinozoisite.

Of these minerals, garnet, chlorite, prehnite, pumpellyite, and magnetite are restricted to the contact aureoles of the diabase; epidote-clinozoisite is most abundant in the aureoles but is also common outside; and quartz, anhydrite, laumontite, and calcite are more generally distributed. This suggests that, whereas stage one presumably represents normal diagenesis prior to the intrusion of the diabase, stage two is the direct result of thermal and hydrothermal alteration associated with the intrusions, and stage three represents later alteration, burial metamorphism, and (or) diagenesis.

In the case of the aureole around the upper diabase in GGS 3137 (3,406–3,813 ft), it is possible to make further subdivisions within stage two as follows:

2a. Reduction of hematite to magnetite;
b. Replacement and minor void filling by epidote-clinozoisite;
c. Growth of euhedral quartz crystals in voids created by solution of caliche nodules [these crystals contain inclusions of epidote-clinozoisite but none of the associated acicular zeolite(?)];
d. Growth of acicular zeolite(?) mainly in secondary voids;
e. Replacement of acicular zeolite by garnet (chlorite and prehnite possibly developed at this stage);
3. Replacement and void filling by laumontite and calcite, which enclose or replace all the minerals in stages 2b–e.

By way of comparison, similar mineral parageneses have been reported from hornfels around diabase in the arkoses of the Connecticut Triassic-Jurassic basin (Heald, 1956) and from the aureole of the Palisades sill in the Newark basin (Van Houten, 1969).

Most Triassic sedimentary rocks retain their original clastic texture and contain only a small percentage (generally less than one percent) of low-grade metamorphic minerals. In two samples, however, close to contacts with diabase (GGS 3137, 3,183 ft; GGS 3080, 4,019 ft), the clastic texture of the arkosic sandstones has been largely obliterated by recrystallization. Grain boundaries between quartz and feldspar become first embayed, then interpenetrative, and finally complexly intergrown in the manner of granophyre. Milton and Hurst (1965, p. 11, 30) suggest that the granophyric granites in Pierce County (GGS 119, 120) were formed by this type of recrystallization. However, as indicated previously, on the basis of texture, grain size, and mineralogy, we suggest that the Pierce County granites are truly igneous.

Figure 10 shows that the regional distribution of zeolite minerals in the Triassic terrane is nonuniform. Although the data are sparse, they suggest that zeolites are most abundant in the northern suite of holes. Laumontite is particularly abundant there and almost absent farther south. There are two possible explanations. Either the northern suite has undergone more alteration as a result of the intrusion of greater volumes of igneous rock, higher heat flow, and (or) greater depth of burial; or the difference in provenance and original mineralogy between the northern and southern suite of sediments is responsible.

To deal with the first possibility, although the width of the aureoles in GGS 3137 and GGS 3080 is undoubtedly related to the size of these intrusions, the data from sample wells do not indicate a great difference in the total percentages of diabase in the northern and southern areas. Furthermore, the available gravity and magnetic data (Long and others, 1972; Zietz and Gilbert, 1980) do not suggest a major difference in the distribution of mafic igneous rocks. If the northern part of the Triassic terrane was more deeply buried than the southern, the amount of overburden stripped from the two areas during the Triassic to Cretaceous interval must have been considerably different. This seems unlikely since it would imply a major difference in epeirogenic uplift.

Turning to the second possibility, Boles and Coombs (1977) have shown that variations in sandstone composition play an important role in determining the mineral parageneses in zeolite-facies rocks in the Southland syncline of New Zealand, the area where zeolite-facies metamorphism was first defined (Coombs, 1954; Fyfe and others, 1958, p. 215). Specifically, sandstones having calcic plagioclase in mafic to intermediate volcanic-rock clasts contain more authigenic calcium-bearing aluminosilicates than do sandstones having sodic plagioclase in felsic volcanic-rock clasts. It is possible, therefore, that because of differences in the plagioclase compositions, sandstones derived from the medium- to high-grade metamorphic terrane of the Piedmont are more susceptible to alteration than are sandstones derived from the felsic volcanic terrane of the Suwannee saddle and neighboring areas.

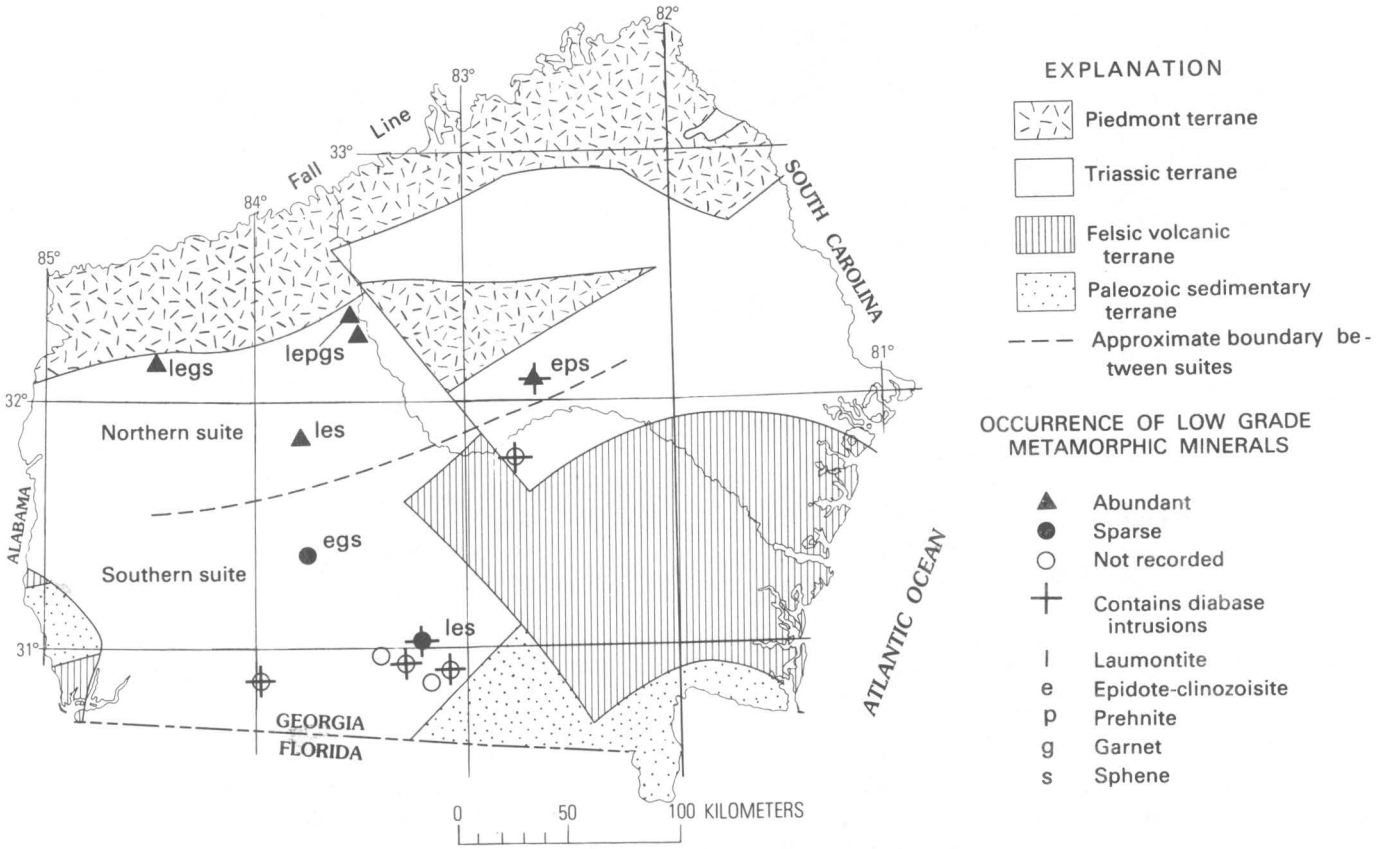

FIGURE 10. Distribution of low-grade metamorphic minerals in Triassic rocks beneath the Georgia Coastal Plain. Crosses indicate sections containing diabase intrusions. Note that distribution of metamorphic minerals is not directly related to the occurrence of diabase but appears to depend on the mineralogy of the Triassic sedimentary rocks (see fig. 6).

It may be recalled that zeolite-facies minerals are not restricted to the Triassic rocks but occur in older felsic volcanic rocks (for example, GGS 3146, 107, 153, 338) on the south side of the Triassic terrane. However, metamorphic minerals are absent in nearby Paleozoic sedimentary rocks, again suggesting that lithology is a major controlling factor.

It is concluded from the above discussion that the most likely cause for the regional variation in metamorphic alteration is the observed variation in bulk composition of the northern and southern suite of Triassic sedimentary rocks. However, it is also possible that broad variations in heat flow, perhaps related to heat generation or conductivity of the underlying basement, may be a contributing cause.

As far as the overall temperature and pressure conditions necessary for zeolite-facies metamorphism are concerned, early work summarized by Winkler (1974, p. 67) suggested pressures less than 3 kbar and temperatures in the range of 200°–350°C. However, more recent work by Castano and Sparks (1974) and Boles and Coombs (1977) shows that pressures around 0.3 kbar and temperatures as low as 50°–100°C may be sufficient for the formation of laumontite; prehnite may appear between 90° and 130°C, and pumpellyite around 190°C.

REGIONAL INTERPRETATIONS

Structure

The regional structural interpretation of the pre-Upper Jurassic(?) rocks beneath the Southeastern U.S. Coastal Plain is shown diagrammatically in figure 11. Unfortunately, the amount of structural data from individual drill holes is minimal. Very few holes intersect more than one major rock group; therefore, few holes provide direct stratigraphic evidence of superposition. With the exception of deep seismic surveys in the Florida panhandle (Arden, 1974a, b) and on the Continental Shelf (for example, Dillon and others, 1983), only a small amount of seismic data has been published, and it is necessary to rely almost entirely on stratigraphy as deduced from subcrop patterns to elucidate structure. Aeromagnetic maps (King, 1959; Zietz and Gilbert, 1980) and gravity maps (Oglesby and others, 1973; Long and others, 1972; Talwani and others, 1976)

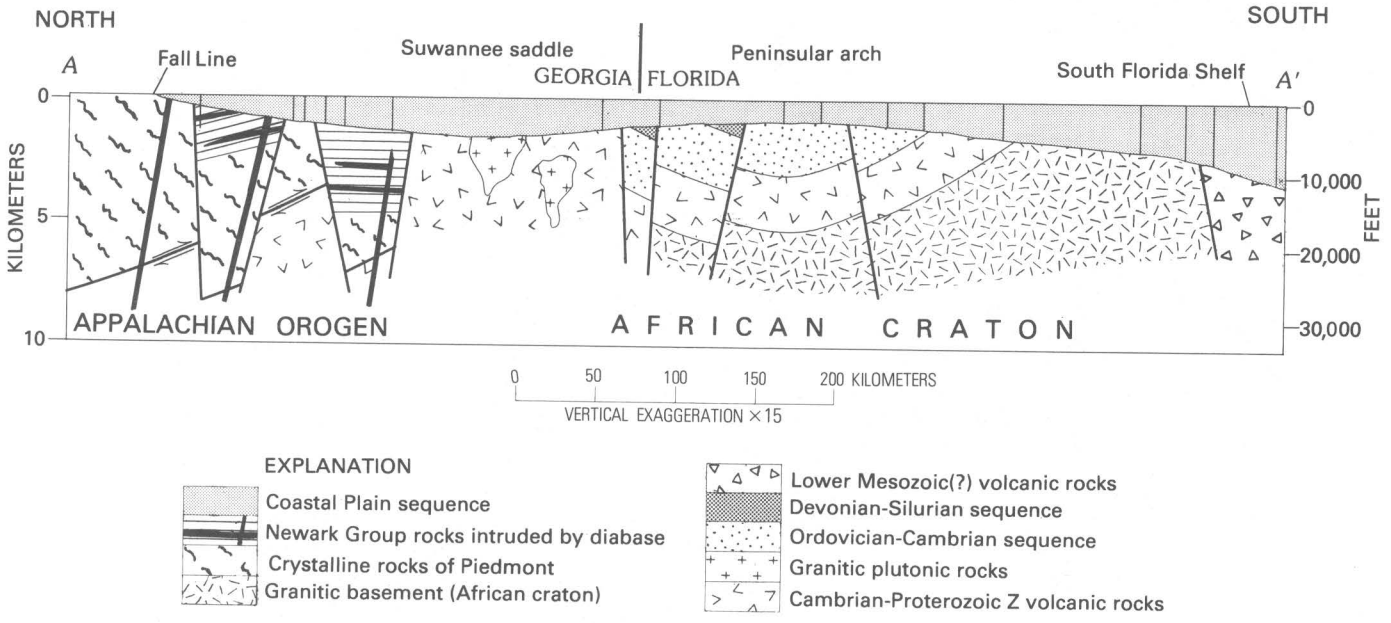

FIGURE 11.—Idealized cross section across Southeastern U.S. Coastal Plain showing regional structural interpretation of pre-Cretaceous rocks. Line of section is north-south from the vicinity of Warrenton, Ga., to Ocheechobee, Fla. (line *A*–*A'*, pl. 1). Vertical exaggeration is × 15.

are available for most of the area except Alabama, and these are useful for locating faults and establishing broad regional trends.

By analogy with other eastern North American Triassic basins, the Triassic deposits beneath the Georgia Coastal Plain and contiguous parts of Florida, Alabama, and South Carolina are assumed to occupy a complex graben structure. Unfortunately, faulting is impossible to prove from drill-hole information alone. In no case is the spacing of drill holes across the boundaries close enough to prove steep, faulted contacts, and the lack of stratigraphic data precludes the recognition of faults within the Triassic terrane. Nevertheless, there are several areas where faulting is suspected. Where control is good, segments of the northern boundary are relatively straight, which suggests faulting; this inference is borne out by aeromagnetic data (Popenoe and Zietz, 1977; Daniels and others, 1983). In particular, aeromagnetic depth estimates by Daniels and others (1983) indicate that Piedmont rocks having high magnetic susceptibility are downthrown south of this boundary. Also, in the vicinity of the Ocmulgee River, the interruption of this northern boundary fault, combined with a break in aeromagnetic contours, indicates a northwest-trending fault approximately along the line of the river. The truncation of pre-Cretaceous rocks along these two faults suggests that the faults are early Mesozoic in origin, but they may have been reactivated during Tertiary time. The post-Eocene Andersonville fault (Zapp, 1965), although it shows downthrow to the north, exactly coincides with the projected position of the northern boundary fault, and Oligocene faulting has been recognized along the Ocmulgee River by Cramer and Arden (1980, p. 78). Additional early Mesozoic faults are suggested by the work of Daniels and others (1983) and Cramer and Arden (1980), but these cannot be confirmed from the present drill-hole information.

In two areas, one beneath the northeastern part of the Georgia Coastal Plain and the other in the Florida panhandle, the continuity of the Triassic terrane is known to be broken by inliers of older rocks that are probably horsts. These are shown in a generalized way on the basis of drill-hole data (pl. 1, fig. 11), but they have been more accurately delineated by means of magnetic depth estimates (in Georgia) (Daniels and others, 1983) and seismic-reflection data (in Florida) (Arden, 1974a, b). The seismic survey in the Florida panhandle (Arden, 1974a, b) shows that the Triassic rocks there are not only faulted but also gently folded and indicates that the structure of these rocks is probably much more complicated than is understood at present. It is probable that they occupy a series of interconnected fault troughs rather than a single downfaulted basin.

The structural interpretation of the Paleozoic rocks, associated felsic volcanic rocks, and granite bodies in south Georgia and peninsular Florida depends on the relative ages assigned to the various units. If the felsic volcanic rocks on the southeast flank of the Peninsular arch are older than the Ordovician sandstones and occur in normal stratigraphic sequence, as suggested earlier on the basis of several lines of evidence, then the

regional dip in this vicinity is towards the northwest. In this case, the granites and metamorphic rocks around St. Lucie County, Fla., probably represent a Precambrian basement complex overlain by Proterozoic Z and (or) lower Paleozoic felsic volcanic rocks and Paleozoic sedimentary rocks. This interpretation is in accord with what is known of the regional distribution of Ordovician and Silurian rocks within the Paleozoic terrane. Given an estimated thickness of about 1,900 m for the Ordovician part of the section (estimated from the data of Wicker and Smith, 1978, and Arden, 1974a), a regional dip of 1–2° to the northwest may be computed between the upper and lower contacts of the Ordovician strata on the south side of the arch. Although the possibility of faulting and small-scale folding hedges this estimate with uncertainty, a relatively low dip is also suggested by the attitude of bedding in the cores (see, for example, Pojeta and others, 1976, p. 10), the width of the subcrop, and the relatively simple subcrop pattern.

The felsic volcanic rocks in southeast Georgia and the Florida panhandle mark the northwest flanks of the Paleozoic terrane and, if they correlate with those in peninsular Florida, as argued previously, indicate that the dip is towards the southeast, thus defining a regional syncline enclosing the Paleozoic section (the East Suwannee basin of Klitgord and others, 1982, 1983). The outcrop pattern suggests that this syncline may close to the northeast in the vicinity of the offshore COST GE–1 well where felsic volcanic rocks have also been reported (Rhodehamel, *in* Scholle, 1979, p. 36; Halley, *in* Scholle, 1979, p. 45). Complications to this relatively simple picture arise from several circumstances:

1. Arden (1974a, b) showed the contact between Lower Ordovician sandstones and felsic volcanic rocks in the Florida panhandle as a northeast-dipping, low-angle thrust fault, and faulting has also been postulated where this contact appears in peninsular Florida (Pojeta and others, 1976, p. 5, 10).
2. The Paleozoic terrane may be segmented by crosscutting faults, as depicted by Barnett (1975).
3. The distribution of Silurian and Devonian rocks within the Paleozoic terrane suggests steeper dips and probably faulting on the northwest flank. It also suggests the presence of a number of small basins rather than a single westerly plunging syncline.
4. Radiometric dates for the felsic volcanic rocks at the base of the COST GE–1 well indicate a Devonian age (Simonis, *in* Scholle, 1979, p. 71), which at first would seem to conflict with the Proterozoic Z–Cambrian age inferred for the felsic volcanic terrane. However, it must be remembered that these rocks have undergone low-grade metamorphism and that they are probably older than their apparent ages.

The contrast between the metamorphic rocks of the Piedmont province and the relatively undeformed rocks of the Florida basement indicates that a major tectonic boundary, perhaps analogous to the overthrust boundary on the northwest side of the Appalachians, lies hidden beneath the cover of Triassic deposits. The approximate position of this boundary is best fixed in southwestern Alabama where felsic volcanic rocks similar to those in Florida and South Georgia occur close to Piedmont rocks without an obscuring cover of Triassic deposits. This interpretation represents a modification of the interpretation by Neathery and Thomas (1975). Whereas those authors assign most wells in Monroe, Conecuh, and Escambia Counties to the Piedmont terrane, we find the volcanic rocks (their wells 33 and 34) and granites (their wells 35, 37, and 38) in the area to be more suggestive of the felsic volcanic terrane and associated plutons. The boundary follows an east-northeasterly trend through Georgia, its position being roughly fixed between the metamorphic rocks in Treutlen County and the felsic volcanic rocks in Coffee County (pl. 1). Farther east its position is less certain. The lithology of detrital clasts in lower Mesozoic(?) red beds from Clubhouse Crossroads test hole #3, near Charleston, S. C. (Gohn, 1983), suggests that Piedmont rocks subcrop nearby beneath a Triassic cover. If these interpretations are correct, then the boundary probably crosses the coast between Charleston and Savannah and passes onto the Continental Shelf.

Comparison of Drill-Hole Data with Regional Aeromagnetic and Gravity Maps

The interpretation of regional aeromagnetic maps (Taylor and others, 1968; Klitgord and Behrendt, 1977; Zietz and Gilbert, 1980) and gravity maps (Long and others, 1972; Talwani and others, 1976) has been discussed by Popenoe and Zietz (1977), Daniels and others (1983), and Klitgord and others (1982, 1983). However, some brief comparisons with plate 1 are in order, because drill holes provide point sources of detailed petrologic information whereas geophysical surveys show regional trends and help establish major terrane boundaries.

In making this comparison, bear in mind that plate 1 is a generalization of the regional geology at the unconformity at the base of the Coastal Plain sequence, whereas the geophysical maps record both areal and vertical variations in physical properties. Thus the geophysical anomalies are influenced by the depth of water on the shelf, the thickness of the Coastal Plain cover, the thickness of lower Mesozoic sedimentary rocks in grabens, and the percentage of Mesozoic mafic igneous rock present, as well as by variations in thickness and physical properties of the "deep basement."

In spite of these differences, several correlations of regional significance can be made.

1. The terrane of shallow-buried Piedmont rocks in the northern part of the Coastal Plain is immediately recognizable by its signature of small-wavelength east-northeast-trending magnetic anomalies. In addition, it is possible to recognize Piedmont rocks that are more deeply buried beneath lower Mesozoic rocks from the presence of attenuated magnetic anomalies of the same type.
2. The felsic volcanic and Paleozoic sedimentary terranes of south Georgia and north Florida generally show a smoother magnetic field having a deep-seated northeasterly grain. Even allowing for depth of burial, this pattern is quite distinct from that seen in the Appalachians. Because drill-hole data indicate a major tectonic boundary between the Piedmont and south Georgia terranes, this contrast is of great significance.
3. The terrane of lower Mesozoic rocks does not have a completely diagnostic anomaly pattern because of variations in stratigraphic thickness, in percentage of mafic igneous rock, and in the underlying basement. Nevertheless, the strong contrast between magnetic Piedmont rocks and less magnetic Triassic deposits has allowed delineation of the northern boundary of the early Mesozoic graben in Georgia and South Carolina (Popenoe and Zietz, 1977; Daniels and others, 1983).
4. In addition to the minor mafic intrusive rocks that have been recognized in drill holes, aeromagnetic and gravity anomalies serve to identify large numbers of mafic bodies that are most probably lower Mesozoic intrusive rocks (Daniels and others, 1983). In Georgia these include a group of stocklike anomalies near Tifton, a large dikelike anomaly west of Brunswick (part of the Brunswick magnetic anomaly), and various smaller anomalies arising from dikes and sills. Unfortunately, aeromagnetic mapping defines dikes much more poorly beneath the Georgia Coastal Plain than in the Carolinas and Virginia, probably mainly because flight lines in Georgia were subparallel to dike trend (Daniels and others, 1983). As might be expected, these intrusions are not restricted to deposits of the Newark Group but occur in all pre-Upper Jurassic(?) terranes. The dikelike Brunswick anomaly and the stocks near Tifton lie too deep to have been intersected by drilling, but they appear to have been intruded into the felsic volcanic terrane.

The main problem in attempting to correlate paleogeologic and geophysical data is accounting for the major magnetic low that sweeps across the South Carolina–Georgia Continental Shelf and bisects the Georgia Coastal Plain (fig. 12). This anomaly was first described in detail by Klitgord and Behrendt (1979) and was equated with the Brunswick magnetic anomaly (Pickering and others, 1977; Popenoe and Zietz, 1977).

As defined by Klitgord and Behrendt (1979), the Brunswick anomaly comprises a series of magnetic troughs and peaks that commences on the Carolina shelf landward of the East Coast magnetic anomaly and then swings across the Georgia coast near Brunswick. Recent aeromagnetic mapping (Zietz and Gilbert, 1980) shows that the principal magnetic low associated with the anomaly continues across the Georgia Coastal Plain into Alabama (fig. 12), flanked to the south and southwest by a discontinuous series of magnetic highs, most of which are also associated with gravity highs (Daniels and others, 1983). Gravity values along the anomaly vary but on average appear to be slightly lower in the crustal block northeast of the anomaly than they are in the block to the southwest. The ridge of gravity highs that crosses the Georgia Coastal Plain (Long and others, 1972) subparallel to the Brunswick anomaly (fig. 12) apparently marks the northeast boundary of the denser block, which extends beneath the Peninsular arch (Oglesby and others, 1973; Klitgord and others, 1982, 1983).

Drill-hole data in the vicinity of the anomaly indicate rocks ranging from presumed Proterozoic Z or Cambrian felsic volcanic rocks and granites to Triassic rocks and even Piedmont metamorphic rocks, but, on the basis of distribution, none of these can be directly related to the source of the anomaly. The broad wavelength and discordant nature of the anomaly, together with magnetic depth estimates by Klitgord and Behrendt (1979), suggest that its source lies below the level currently tested by drilling (Daniels and others, 1983). Because of age and depth relations, it seems most likely that the main magnetic low is associated with the older felsic volcanic rocks (or related rocks) that apparently underlie the Triassic terrane and that coincide with a less pronounced belt of magnetic lows in northeastern Florida (Taylor and others, 1968; Klitgord and others, 1982). However, this does not entirely settle the question of the age and tectonic significance of the anomaly, which will be discussed more fully below.

Geologic Affinities of the Paleozoic Sequence of Northern Florida

Workers have commented on the anomalous nature of the Paleozoic rocks in northern Florida since the time of their first discovery. At first, correlations with the Valley and Ridge province were sought (see, for exam-

ple, Campbell, 1939; Schuchert, 1943, p. 455; Applin and Applin, 1944), but, once a stratigraphic succession emerged (Applin, 1951), it began to appear that the two provinces were unrelated. This was later confirmed by paleontologic work (see, for example, Goldstein and others, 1969; Whittington and Hughes, 1972; Cramer, 1971, 1973; Pojeta and others, 1976, p. 24).

Correlations with the Piedmont province have also been proposed. After examining basement lithologies in Georgia, Milton and Hurst (1965, p. 10) equated the felsic volcanic rocks with the low-grade metavolcanic rocks of the Carolina slate belt, implying a gradual decline in metamorphic grade toward the southeast. Although these rocks are not continuous beneath the Coastal Plain cover, they share similar lithologies and are apparently about the same age, Proterozoic Z–Cambrian (St. Jean, 1973; Cloud and others, 1976; Maher and others, 1981). On a regional scale, Rodgers (1972) and Piqué (1981) have postulated an Avalonian province of Proterozoic Z–Cambrian volcanic and sedimentary rocks extending continuously along the eastern margin of the Appalachians from Newfoundland to Florida. However, with the possible exception of the quartzites of the Pine Mountain belt (Crickmay, 1952, p. 22), there are very few miogeosynclinal lithologies on the east side of the Piedmont that might represent counterparts to the Lower Ordovician quartz arenites in the subsurface of north Florida.

In 1962, Sougy presented evidence that the western rim of Africa between Morocco and Guinea consists of a mainly Hercynian (Alleghenian) orogenic belt similar to the Appalachians in many respects. Wilson (1966), writing of the closing of the Iapetus Ocean, came to the logical conclusion that the anomalous Florida basement might represent a disjunct fragment of the African platform. Such a correlation now appears to be supported by paleontologic, stratigraphic, structural, and paleomagnetic evidence.

Paleontologic affinities between the Paleozoic rocks in Florida and west Africa have been established on the basis of work with trilobites (Whittington, 1953; Whittington and Hughes, 1972), chitinozoans (Andress and others, 1969; Goldstein and others, 1969; Cramer, 1973), phytoplankton (Cramer, 1971), and mollusks (Pojeta and others, 1976, p. 24).

The stratigraphy on the eastern margin of the Mauritanides has been summarized by Furon (1963, p. 3–75), Sougy (1962), Dillon and Sougy (1974), and Grant (1973). Although it is not possible to make exact correlations between the stratigraphic succession in Florida and any one area in west Africa, there are striking similarities in the general succession (table 9). Of particular significance is the occurrence of rhyolites and felsic tuffs in Proterozoic Z and Cambrian time (sequences I and II of Dillon and Sougy, 1974), overlying granitic basement in the Anti-Atlas of Morocco, and the Ougarta ranges of Algeria (Furon, 1963, p. 8; Dillon and Sougy, 1974); the widespread occurrence of burrowed quartz arenites in the Cambrian and Ordovician (sequence II), extending from Morocco in the north at least as far as Guinea in the south and eastwards to the Hoggar of the Central Sahara (Furon, 1963, p. 13, 90–97, 217); and, finally, the preponderance of shaly lithologies in Silurian and Devonian rocks (lower sequence III) over the same area. Absent in Florida are the cherty dolomitic limestones containing stromatolites that occur in Proterozoic Z and Cambrian rocks in west Africa (sequences I and II) and the tillites that are used to divide the Saharan sections into sequences. However, because of unconformities and facies changes, these lithologies also are locally absent in Africa.

In attempting to make a structural correlation between west Africa and eastern North America, the location and continuity of what may be called the Guinea line are important. The Guinea line marks the southern terminus of the Mauritanides, which apparently turn seaward beneath the Coastal Plain of Guinea-Bissau and which are presumably truncated at the continental margin (Sougy, 1962; Rodgers, 1970, p. 201; Templeton, 1971). The contact between undeformed platform rocks of the Bové basin and highly deformed rocks of the Mauritanides is hidden by younger rocks in Guinea-Bissau, and its exact position on the shelf is unknown at present (Dillon and Sougy, 1974), but farther north in Mauritania the boundary has been mapped as a westward-dipping, low-angle thrust, which throws high-grade metamorphic rocks over Paleozoic platform rocks of the Taoudeni basin (Sougy, 1962). The situation in Africa is, therefore, similar to that which has been postulated beneath the Coastal Plain of south Georgia.

On the basis of computer matching at the shelf edge, Bullard and others (1965) placed the Guinea line adjacent to the southern tip of Florida. However, this fit applies specifically to Early Jurassic time. Recent paleomagnetic data (Van der Voo and others, 1976) suggest that, for late Carboniferous reconstruction, Africa and South America should be rotated some 20° north about a pole in the Sahara. This rotation would move South America into the Gulf of Mexico and shift the Guinea line into the region of the Georgia-Carolina shelf, greatly improving the structural fit between the continents (Pilger, 1978). Such a fit would also place the Paleozoic rocks of Florida in juxtaposition to similar rocks in the Bové basin of Guinea (Dillon and Sougy, 1974; Grant, 1973) (see fig. 13).

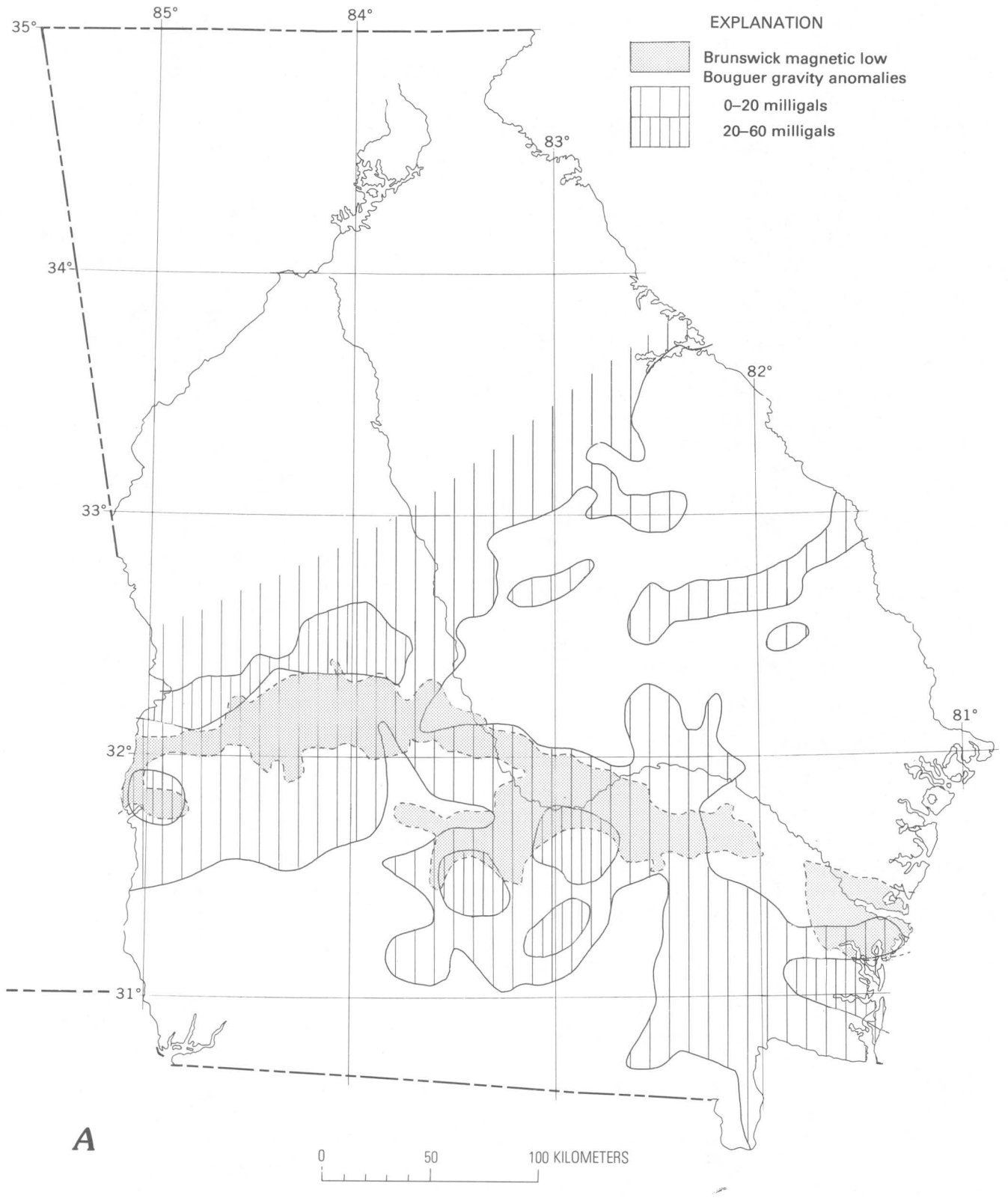

FIGURE 12. *A*, Magnetic and gravity anomalies in the Georgia Coastal Plain. After Zietz and Gilbert (1980) and Long and others (1972). *B*, Geologic terrane boundaries in the Georgia Coastal Plain (for comparison with the geophysical anomalies).

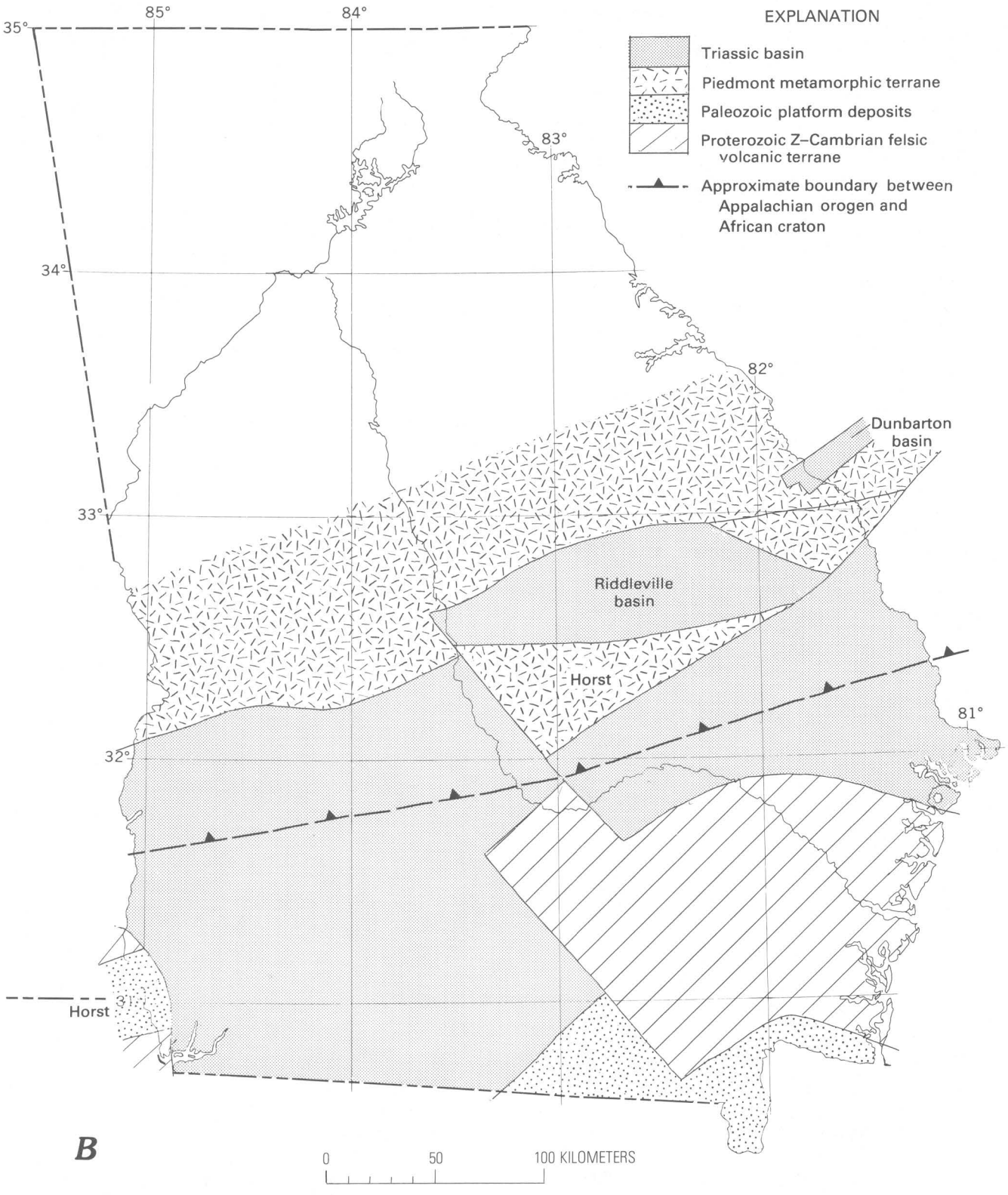

FIGURE 12. Continued.

TABLE 9.—*Comparison between Paleozoic sections in northwest Africa and in the subsurface beneath the southeastern Coastal Plain*

Sequence of Dillon and Sougy (1974)	Anti-Atlas and N. Tindouf basin, Morocco (Furon, 1963, p. 9–11, 106–108) (location 1, fig. 13)	Ougarta Ranges and Saoura, Algeria (Furon, 1963, p. 112) (location 2, fig. 13)	Western Taoudeni basin Mauritania (Furon, 1963, p. 127) (location 3, fig. 13)	Southern Mauritanides, Bové basin; S. Senegal, Guinea-Bissau (Grant, 1973, p. 459; Furon, 1963, p. 217) (location 4, fig. 13)	Florida Platform (location 5, fig. 13)
Sequence III 440–270 m.y. Silurian-Carboniferous.	4. Carboniferous–fossiliferous limestones overlain by interbedded sandstones and shales containing plants.	4. Carboniferous–sandstones, shales, and limestones.	4. Carboniferous–?	4. Carboniferous absent.	4. Carboniferous absent.
	3. Devonian–fossiliferous shales, sandstones, and limestones.	3. Devonian–sandstones and shales and intercalated beds of fossiliferous limestones.	3. Devonian–fossiliferous limestones and sandstones.	3. Devonian–sandstones overlain by fossiliferous, gray shales (300–400 m).	3. Devonian–fossiliferous, gray shales. Devonian + Silurian thickness approx. 600 m.
	2. Silurian–graptolitic shales.	2. Silurian–graptolitic shales; some limestone at top.	2. Silurian–fossiliferous sandstones overlain by gray graptolitic shales (20–50 m)	2. Silurian–black pyritic, graptolitic shales and thin-bedded sandstones (45–100 m).	2. Silurian–dark-gray to black, fossiliferous shales.
(Late Ordovician glaciation)			1. Siliceous sandstones.	1. Crossbedded sandstones containing basal quartz-pebble conglomerate (> 500 m).	
Sequence II 650–440 m.y. Cambrian-Ordovician.	4. Fossiliferous shales containing massive units of quartz sandstone.	Massive Cambrian-Ordovician sandstones with lingulas and other fossils. Arkosic at base (1,000–2,000 m).	4. Massive quartz sandstones containing lingulas and *Skolithos* burrows.		White quartz sandstones containing inarticulate brachiopods and *Skolithos* burrows overlain by fossiliferous, dark-gray shales (approx. 1,900 m).
	3. Shales and sandstones containing beds of volcanic ash (approx. 2,000 m).		3. Red and purple sandstones and shales.	3. Red, feldspathic sandstone.	
	2. Impure limestones containing archaeocyathids (75–450 m) resting on conglomeratic red beds (200–500 m).	?	2. Cherty dolomitic limestones and shales containing algal stromatolites.	2. Pelites, graywackes, cherts, and volcanic ashes (500–1,000 m) underlain by calcareous dolostones (5–10 m).	?
(Eocambrian glaciation)	1. Tillite.		1. Tillite.	1. Tillite, interbedded with volcanic rocks (< 300 m), underlain by spilitic volcano-sedimentary complex in west (approx. 1,000 m).	Felsic tuffs and tuffaceous sediments.
Sequence I 1,000–650 m.y. Middle to Late Proterozoic.	2. Dolomitic limestones containing stromatolites (3,000 m).	Rhyolites and tuffs (> 200 m).	2. Cherty dolomitic limestones and shales containing algal stromatolites (as much as 150 m).	?	?
	1. Rhyolites and andesites overlain by shales (1,000 m).		1. Varicolored sandstones, conglomerates, and shales.		
Precambrian Metamorphic Basement					

The Granitic and Metamorphic Terrane of Central Florida

The only major rock terrane beneath the Southeastern U.S. Coastal Plain that does not appear to be represented in Georgia is the triangular area of granitic and metamorphic rock in central Florida. These rocks were first described by the Applins (Applin, 1951, p. 5; Applin and Applin, 1965, p. 16); further details were provided by Bass (1969), Milton (1972, p. 64, 81), and Barnett (1975). Eight wells have encountered granitic rocks (granite, quartz monzonite, alaskite); one well in St. Lucie County bottomed in amphibolite and quartz diorite gneiss (Amerada–Cowles Magazines, no. 2). Originally, Applin (1951, p. 8) included the hornblende diorite in Volusia County (Sun–Powell Land Co., no. 2) in this terrane, but this diorite has since proved to be a sill within a part of the felsic volcanic terrane (Bass, 1969).

The Cowles well is unique in Florida in having penetrated high-grade regional metamorphic rocks that are quite separate from the Piedmont province.

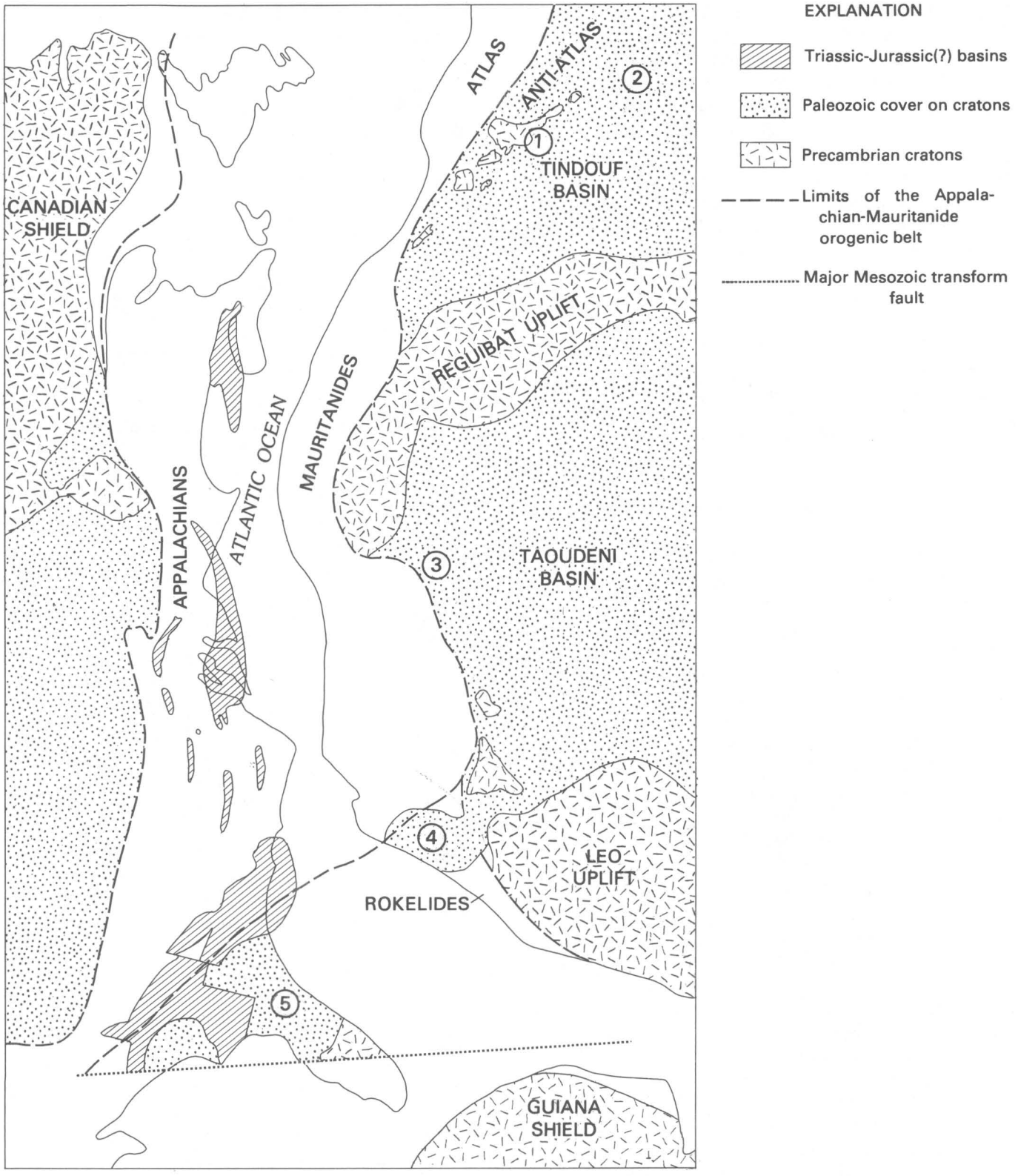

FIGURE 13. - Reconstruction of the Appalachian-Mauritanide orogenic belt in early Mesozoic time. Based on paleomagnetic data of Van der Voo and others (1976) and geologic mapping by Sougy (1962), Dillon and Sougy (1974), and this paper. Circled numbers refer to table 9.

Aeromagnetic mapping (Taylor and others, 1968) suggests that these rocks occupy a rather small area characterized by a conspicuous northwest-trending magnetic lineation. Radiometric dating indicates an age of at least 530 m.y. B.P. (Bass, 1969).

The distribution of wells that have bottomed in granitic rocks in east-central Florida indicates that these rocks comprise a single conterminous group. This interpretation appears to be supported by magnetic and gravity data, which indicate a broad area of low magnetization and low gravity in the region (King, 1959; Klitgord and others, 1982).

As pointed out by Bass (1969), there are several possible interpretations of the age relations among the metamorphic, granitic, and neighboring felsic volcanic rocks. However, the most likely possibility is that the felsic volcanic rocks overlie the granitic and metamorphic rocks and are separated from them by a tectonic boundary, either a northwest-dipping thrust fault or an unconformity (fig. 11). This conclusion is reached firstly because of the relative positions of these rocks on the southeast flank of the major syncline that encloses the Paleozoic sedimentary sequence and secondly because radiometric dates inferred for the granitic and metamorphic rocks are older than those for the felsic volcanic rocks (with one exception; see fig. 4). In addition, the difference in deformation between the felsic volcanic and sedimentary terranes, on one hand, and the metamorphic rocks in the Cowles well, on the other, suggests the presence of a major tectonic boundary. Because of uncertainty about the radiometric dates, a further possibility should be considered. If the boundary is a thrust fault, or if the granitic rocks prove to be intrusive into their surrounding terranes, then the felsic volcanic rocks and the Cowles metamorphic rocks may be approximately equivalent in age.

In a late Paleozoic reconstruction, there are notable similarities between the geology on the southeast side of the Peninsular arch and around the flanks of the Bové basin in southeast Senegal, Guinea, and Sierra Leone (Bassot, 1966, 1970; Allen, 1968, 1969; Grant, 1973). Within west Africa, gently folded sandstones and shales of Ordovician (or possibly Silurian) to Devonian age (sequence III of Dillon and Sougy, 1974) rest unconformably on folded thrust-faulted and partially metamorphosed Proterozoic Z to Cambrian sedimentary and volcanic rocks (sequence I and II of Dillon and Sougy, 1974) and also on remobilized older cratonic rocks (table 9). These deformed rocks constitute a southeastern branch of the Mauritanides in Senegal and continue into Sierra Leone as the Rokelides. Both structural complexity and metamorphic grade increase to the west.

Judging by the magnetic lineation (Taylor and others, 1968), the tectonic grain in the Cowles metamorphic rocks is similar to that in the Rokelides. Furthermore, the 530-m.y. radiometric dates for the granitic and metamorphic rocks in Florida (Bass, 1969) compare favorably with dates of about 550 m.y. obtained for the youngest rocks in the Rokelides (Grant, 1973).

On the basis of these similarities, it seems probable that the granitic and metamorphic terrane of central Florida represents a segment of the western part of the Pan African (Damaran) Rokelide fold belt (Bass, 1969).

The South Georgia Basin and the Opening of the Atlantic

One of the major findings of this work is to substantiate the presence of an extremely large early Mesozoic basin beneath the Southeastern U.S. Coastal Plain. It is estimated to occupy an area of approximately 100,000 km^2 and to contain a thickness of at least 3,500 m of continental sediments ascribed to the Newark Group. This structure has been described by Gohn and others (1978) as the South Carolina–Georgia basin and by Daniels and others (1983) as the South Georgia basin. Although drill-hole data have not revealed the exact form of the basin, analogy with other early Mesozoic basins (Van Houten, 1977) suggests that it is probably a complex graben. This suggestion is supported by geophysical evidence of faulting in Georgia (Daniels and others, 1983), South Carolina (Popenoe and Zietz, 1977), and the Florida panhandle (Arden, 1974a). Like other early Mesozoic grabens, both onshore and offshore, it is believed to have formed during the early stages of opening of the North Atlantic Ocean about 215–175 m.y. B.P. (Van Houten, 1977, p. 83). The southeastern corner of North America lay close to the triple junction between the North Atlantic, South Atlantic, and Gulf of Mexico, in an area where complex rifting and transform faulting might be expected (Pilger, 1978).

Facies variations within the basin fill indicate that the overall geometry of the basin during the early Mesozoic was similar to that of the present subcrop. Alluvial sediments were derived from both northern and southern highlands. Fine-grained sediments accumulated in the center of the basin, while coarser clastic rocks were probably deposited in braided-fan complexes around the margins. The coarsest fanglomerates recognized thus far are in the subsidiary Dunbarton (Marine and Siple, 1974) and Riddleville (GGS 3353) basins. The presence of caliche nodules suggests semiaridity, but, apart from minor occurrences of anhydrite cement in sandstones, no evaporite deposits or eolian sands have been encountered.

Between about 190 and 175 m.y. B.P., rifting was accompanied by the emplacement of large volumes of mafic igneous rock, including basaltic lavas, dikes, sills, and probably stocks (Daniels and others, 1983). Basaltic lavas are believed to extend from the vicinity of

Charleston (Gottfried and others, 1977; Gohn and others, 1978) onto the Continental Shelf (Dillon and others, 1979, 1983). Contours from seismic-reflection profiles (Dillon and others, 1979, fig. 11) indicate that these basalts project into southeastern Georgia approximately at the elevation of the pre-Cretaceous surface, suggesting that isolated occurrences of basalt in GGS 148 and 496 may be part of the same series of flows. Extensive swarms of radial dikes that are now segmented between North America, South America, and Africa (May, 1971) appear to have been centered on the triple junction. There are also a number of larger mafic intrusions, identified by high gravity and magnetic anomalies, that are probably early Mesozoic in age (Long and others, 1972; Talwani and others, 1976; Zietz and Gilbert, 1980; Daniels and others, 1983). These include the dikelike anomaly west of Brunswick and the group of anomalies near Tifton.

Drill holes indicate that some of these larger intrusions have broad metamorphic aureoles and that zeolite-facies metamorphism is widespread throughout the lower Mesozoic terrane. Farther afield, probably contemporaneous zeolite-facies alteration is common in the felsic volcanic terrane of the subsurface and has also been reported in the exposed Piedmont province of Georgia (Ramspott, 1967), the Carolinas, and Virginia (Privett, 1974; Bell and others, 1980). This widespread alteration indicates that large areas of the Southeast may have been subjected to abnormally high heat flow during the early Mesozoic.

The position and size of the South Georgia basin, as well as the large volume of mafic igneous rock and evidence of high heat flow, suggest that, during Late Triassic and Early Jurassic times, incipient spreading centers in the Gulf of Mexico and North Atlantic (Klitgord and others, 1982) may have been linked beneath this basin.

Significance of the Brunswick Magnetic Anomaly

The origin of the Brunswick anomaly is uncertain, but two major hypotheses have been proposed. The first is that the anomaly is related to continental extension during the early Mesozoic (Pickering and others, 1977; Popenoe and Zietz, 1977; Cramer and Arden, 1980, p. 14). The principal evidence in support of this conclusion is the similarity in trend and wavelength of the Brunswick anomaly to the East Coast magnetic anomaly, where the two occur together at the margin of the Carolina shelf. The East Coast anomaly is acknowledged by most recent authors to mark the edge of oceanic basement (Emery and others, 1970; Mayhew, 1974; Uchupi and others, 1976; Grow and other, 1979; Klitgord and Behrendt, 1979). It is dated as Late Triassic to Early Jurassic (Rona, 1980, p. 31; Klitgord and Behrendt, 1979) and marks the spreading center along which the North Atlantic began to open. In addition, Klitgord and Behrendt (1979) point out that on the Carolina shelf, the Brunswick anomaly coincides with a basement high and trough that appear to indicate early Mesozoic block faulting in the continental(?) crust.

Alternatively, Daniels and others (1983) suggest that the Brunswick anomaly may arise from rocks emplaced by underthrusting during the late Paleozoic suturing of the North American and African continents. The principal evidence for this hypothesis is the contrast between the northern part of the Georgia Coastal Plain and the southern part, including Florida, in rock type, structural trend, and geophysical properties of the basement.

The main problem encountered by both hypotheses is that the Brunswick anomaly is discordant with both Mesozoic and Paleozoic structural trends as interpreted from plate 1. Thus, if the anomaly is Mesozoic, it is surprising that it does not conform to the trend of the South Georgia basin. If it arises from a tectonically thickened section of felsic volcanic or related rocks formed during late Paleozoic continental collision, it is necessary to explain the occurrence of felsic volcanic and Piedmont terranes north and south of the anomaly, respectively. The suggestion of underthrusting provides a convenient explanation of the discordance observed between shallow and deep structural trends. Thus, the occurrence of Piedmont rocks overlying the anomaly in the northwest part of the Georgia Coastal Plain may be readily explained as the result of a northwest-dipping thrust fault having Piedmont metamorphic rocks in the upper plate and felsic volcanic rocks in the lower.

It is possible that elements of both hypotheses may be involved and that the Brunswick anomaly is of composite origin. Thus, a major late Paleozoic structure may have influenced the location of early Mesozoic rifting. This would explain the en-echelon relationship between the Brunswick and East Coast magnetic anomalies close to where they terminate, as well as the clustering of presumed early Mesozoic intrusions along the same trend. If this is the case, it lends support to the idea that an incipient spreading center may have existed north of the Florida peninsula but failed to propagate, perhaps as a result of a jump in the spreading center around 175 m.y. B.P. when the source rocks of the Blake Spur magnetic anomaly began to form (Dillon and others, 1979).

CONCLUSIONS

1. The base of the Coastal Plain sequence in the Southeastern United States is marked by the Fall Line unconformity. In the northern part of the Coastal Plain, this surface dips uniformly

southeast, but downdip it is divided into two distinct basins, the Apalachicola and Southeast Georgia embayments. These are separated by an intervening saddle (the Suwannee saddle), which connects with the Peninsular arch in central Florida.

2. The oldest rocks above the Fall Line unconformity are generally Cretaceous, but in the Apalachicola embayment, as well as in southern Florida, Upper Jurassic rocks may be present.
3. The medium- to high-grade metamorphic rocks that underlie the northern part of the Coastal Plain are the subsurface continuation of the Piedmont province; this area is characterized by a pattern of narrow, northeast-trending magnetic anomalies.
4. The terrane of metamorphic rocks and granites mapped in central Florida is the subcrop of a segment of the Pan African Rokelide fold belt, which is part of the west African shield. African Precambrian basement rocks probably extend eastwards and northwards, corresponding to the area of subdued paleomagnetic anomalies in northern Florida and southern Georgia.
5. The central Florida crystalline rocks are mantled by a thick sequence of gently folded and faulted Proterozoic Z to Middle Devonian rocks including felsic volcanic rocks and associated plutons (Proterozoic Z–Cambrian), quartz arenites (Lower Ordovician), and interbedded shales and sandstones (Middle Ordovician to Middle Devonian), which show striking similarities to the cratonic cover in west Africa.
6. The terrane of felsic-mafic volcanic rocks in southern Florida is separated from those rocks in northern Florida by a major crustal anomaly, and the terranes may or may not be related. The evidence to date appears to suggest an early Mesozoic age for the southern Florida rocks, but the possibility that parts of this terrane are Proterozoic Z or Cambrian should be borne in mind.
7. The boundary between Piedmont and African terranes is mainly obscured by younger Triassic–Lower Jurassic deposits but may be located approximately, on the basis of drill-hole data. It can be traced east-northeast from Alabama into South Carolina and may represent a northwest-dipping thrust fault that marks the southeastern side of the Appalachian orogen.
8. This proposed overthrust probably extends beneath the Continental Shelf south of Charleston, S. C., and is truncated at the shelf edge. It correlates with the Guinea line in west Africa, which marks the truncated terminus of the Mauritanides. Where this boundary is exposed in Mauritania, it also appears as a west- or northwest-dipping overthrust where high-grade metamorphic rocks rest on unmetamorphosed Paleozoic sedimentary rocks.
9. An extensive terrane of lower Mesozoic red beds and associated mafic igneous rocks occupies a complex graben, the South Georgia basin, and the rocks therein are assigned to the Newark Group. This graben formed in response to crustal extension during the initiation of the Atlantic Ocean but was not invaded by the sea. Its position appears to have been partially controlled by underlying Paleozoic structures.
10. Mafic igneous rocks in the South Georgia basin include basalt lavas and diabase dikes and sills, which have been encountered in drill holes, as well as larger plutons, which have been detected from aeromagnetic and gravity surveys. Chemical analyses of the minor intrusive rocks suggest that they are tholeiites of the eastern North American suite.
11. Zeolite-facies alteration in Triassic sedimentary rocks and Paleozoic felsic volcanic rocks was a response to high heat flow during the early Mesozoic. Alteration is not restricted to contact aureoles but occurs regionally in rocks of appropriate composition.
12. The Brunswick anomaly is a major, deep-seated crustal feature of uncertain age and tectonic significance. The main magnetic low most likely arises from a tectonically thickened sequence of Proterozoic Z–Cambrian felsic volcanic rocks formed during late Paleozoic continental collision.

REFERENCES

Allen, P. M., 1968, The stratigraphy of a geosynclinal succession in western Sierra Leone, West Africa: Geological Magazine, v. 105, no. 1, p. 62–73.

———1969, The geology of part of an orogenic belt in western Sierra Leone, west Africa: Geologische Rundschau, v. 58, no. 2, p. 588–620.

Andress, N. E., Cramer, F. H., and Goldstein, R. F., 1969, Ordovician chitinozoans from Florida well samples: Gulf Coast Association of Geological Societies Transactions, v. 19, p. 369–375.

Applin, E. R., and Applin, P. L., 1964, Logs of selected wells in the Coastal Plains of Georgia: Georgia Geologic Survey Bulletin 74, 229 p.

Applin, P. L., 1951, Preliminary report on buried pre-Mesozoic rocks in Florida and adjacent states: U.S. Geological Survey Circular 91, 28 p.

Applin, P. L., and Applin, E. R., 1944, Regional subsurface stratigraphy and structure of Florida and southern Georgia: American Association of Petroleum Geologists Bulletin, v. 28, no. 12, p. 1673–1753.

———1965, The Comanche Series and associated rocks in the subsurface in central and south Florida: U.S. Geological Survey Professional Paper 447, 84 p.

———1967, The Gulf Series in the subsurface in northern Florida and southern Georgia: U.S. Geological Survey Professional Paper 524-G, 35 p.

Arden, D. D., Jr., 1974a, A geophysical profile in the Suwannee Basin, north-western Florida, *in* Stafford, L. P., ed., Symposium on the petroleum geology of the Georgia Coastal Plain: Georgia Geologic Survey Bulletin 87, p. 111-122.

———1974b, Geology of the Suwannee Basin interpreted from geophysical profiles: Gulf Coast Association of Geological Societies Transactions, v. 24, p. 223-230.

Armstrong, R. L., and Besancon, James, 1970, A Triassic time scale dilemma-K-Ar dating of Upper Triassic mafic igneous rocks, eastern U.S.A. and Canada and post-Upper Triassic plutons, western Idaho, U.S.A.: Eclogae Geologicae Helvetiae, v. 63, no. 1, p. 15-28.

Barnett, R. S., 1975, Basement structure of Florida and its tectonic implications: Gulf Coast Association of Geological Societies Transactions, v. 25, p. 122-142.

Bass, M. N., 1969, Petrography and ages of crystalline basement rocks in Florida-Some extrapolations: American Association of Petroleum Geologists Memoir 11, p. 283-310.

Bassot, J. P., 1966, Etude géologique du Sénégal oriental et de ses confins guinéo-maliens [Geologic study of Senegal and its borders with Guinea and Mali]: Senegal Direction des Mines et de la Géologie Bulletin 1, 322 p.

———1970, Aperçu sur les formations précambriennes et paléozoïques du Sénégal oriental [Precambrian and Paleozoic formations of eastern Senegal]: Bulletin de la Société Géologique de France, sér. 7, v. 11, no. 2, p. 160-169.

Bell, Henry, III, Carpenter, R. H., and Feiss, P. G., 1980, Volcanogenic ore deposits of the Carolina slate belt, *in* Frey, R. W., ed., Excursions in southeastern geology, v. 1: American Geological Institute, p. 149-178.

Bennison, A. P., 1975, Geological highway map of the Southeastern region: American Association of Petroleum Geologists, U.S. Geological Highway Map 9.

Boles, J. R., and Coombs, D. S., 1977, Zeolite facies alteration of sandstones in the Southland Syncline, New Zealand: American Journal of Science, v. 277, no. 8, p. 982-1012.

Braunstein, Jules, 1957, The habitat of oil in the Cretaceous of Mississippi and Alabama, *in* Frascogna, X. M., ed., Mesozoic-Paleozoic producing areas of Mississippi and Alabama, v. 1: Mississippi Geological Society, p. 1-11.

Bridge, Josiah, and Berdan, J. M., 1952, Preliminary correlation of the Paleozoic rocks from test wells in Florida and adjacent parts of Georgia and Alabama: Florida Geological Survey Guidebook, Association of American State Geologists, 44th Annual Meeting Field Trip, p. 29-38.

Brown, P. M., 1974, Subsurface correlation of Mesozoic rocks in Georgia, *in* Stafford, L. P., ed., Symposium on the petroleum geology of the Georgia Coastal Plain: Georgia Geologic Survey Bulletin 87, p. 45-59.

Bullard, Edward, Everett, J. E., and Smith, A. G., 1965, The fit of the continents around the Atlantic, *in* A symposium on continental drift: Royal Society of London, Philosophical Transactions, ser. A, v. 258, no. 1088, p. 41-51.

Campbell, R. B., 1939, Paleozoic under Florida?: American Association of Petroleum Geologists Bulletin, v. 23, no. 11, p. 1712-1713.

Carroll, Dorothy, 1963, Petrography of some sandstones and shales of Paleozoic age from borings in Florida: U.S. Geological Survey Professional Paper 454-A, 15 p.

Castano, J. R., and Sparks, D. M., 1974, Interpretation of vitrinite reflectance measurements in sedimentary rocks and determination of burial history using vitrinite reflectance and authigenic minerals: Geological Society of America Special Paper 153, p. 31-52.

Chalcraft, R. G., 1978, A textural study of Mesozoic dolerite dikes in eastern North America [abs.]: Geological Society of America Abstracts with Programs, v. 10, no. 4, p. 165.

Cloud, Preston, Wright, James, and Glover, Lynn, III, 1976, Traces of animal life from 620-million-year-old rocks in North Carolina: American Scientist, v. 64, no. 4, p. 396-406.

Coombs, D. S., 1954, The nature and alteration of some Triassic sediments from Southland, New Zealand: Royal Society of New Zealand Transactions, v. 82, pt. 1, p. 65-109.

Cornet, Bruce, Traverse, Alfred, and McDonald, N. G., 1973, Fossil spores, pollen, and fishes from Connecticut indicate Early Jurassic age for part of the Newark Group: Science, v. 182, no. 4118, p. 1243-1247.

Cramer, F. H., 1971, Position of the north Florida lower Paleozoic block in Silurian time-Phytoplankton evidence: Journal of Geophysical Research, v. 76, no. 20, p. 4754- 4757.

———1973, Middle and Upper Silurian chitinozoan succession in Florida subsurface: Journal of Paleontology, v. 47, no. 2, p. 279-288.

Cramer, H. R., 1969, Structural features of the Coastal Plain of Georgia: Southeastern Geology, v. 10, p. 111-123; correction, v. 11, p. 202, 1970.

———1974, Isopach and lithofacies analyses of the Cretaceous and Cenozoic rocks of the Coastal Plain of Georgia, *in* Stafford, L. P., ed., Symposium on the petroleum geology of the Georgia Coastal Plain: Georgia Geologic Survey Bulletin 87, p. 21-44.

Cramer, H. R., and Arden, D. D., 1980, Subsurface Cretaceous and Paleogene geology of the Coastal Plain of Georgia: Georgia Geologic Survey Open-File Report 80-8, 184 p.

Crickmay, G. W., 1952, Geology of the crystalline rocks of Georgia: Georgia Geologic Survey Bulletin 58, 54 p.

Dall, W. H., and Harris, G. D., 1892, Correlation papers-Neocene: U.S. Geological Survey Bulletin 84, 349 p.

Daniels, D. L., 1974 [1975], Geologic interpretation of geophysical maps, central Savannah River area, South Carolina and Georgia: U.S. Geological Survey Geophysical Investigations Map GP-893.

Daniels, D. L., and Zietz, Isidore, 1978, Geologic interpretation of aeromagnetic maps of the Coastal Plain region of South Carolina and parts of North Carolina and Georgia: U.S. Geological Survey Open-File Report 78-261, 47 p.

Daniels, D. L., Zietz, Isidore, and Popenoe, Peter, 1983, Distribution of subsurface lower Mesozoic rocks in the Southeastern United States as interpreted from regional aeromagnetic and gravity maps, *in* Gohn, G. S., ed., Studies related to the Charleston, South Carolina, earthquake of 1886-Tectonics and seismicity: U.S. Geological Survey Professional Paper 1313, p. K1-K24.

Dillon, W. P., Klitgord, K. D., and Paull, C. K., 1983, Mesozoic development and structure of the continental margin off South Carolina, *in* Gohn, G. S., ed., Studies related to the Charleston, South Carolina, earthquake of 1886-Tectonics and seismicity: U.S. Geological Survey Professional Paper 1313, p. N1-N16.

Dillon, W. P., Paull, C. K., Buffler, R. T., and Fail, J. P., 1979, Structure and development of the Southeast Georgia embayment and northern Blake Plateau; preliminary analysis, *in* Watkins, J. S., Montadert, Lucien, and Dickerson, P. W., eds., Geological and geophysical investigations of continental margins: American Association of Petroleum Geologists Memoir 29, p. 27-41.

Dillon, W. P., and Sougy, J. M. A., 1974, Geology of West Africa and Canary and Cape Verde Islands, *in* Nairn, A. E. M., and Stehli, F.

G., eds., The ocean basins and margins; v. 2, The North Atlantic: New York, Plenum Press, p. 315–390.

Dooley, R. E., and Wampler, J. M., 1983, Potassium-argon relations in diabase dikes of Georgia–The influence of excess ^{40}Ar on the geochronology of early Mesozoic igneous and tectonic events, *in* Gohn, G. S., ed., Studies related to the Charleston, South Carolina, earthquake of 1886–Tectonics and seismicity: U.S. Geological Survey Professional Paper 1313, p. M1-M24.

Emery, K. O., Uchupi, Elazar, Phillips, J. D., Bowin, C. O., Bunce, E. T., and Knott, S. T., 1970, Continental rise off eastern North America: American Association of Petroleum Geologists Bulletin, v. 54, no. 1, p. 44–108.

Froelich, A. J., Leavy, B. D., and Lindholm, R. C., 1982, Geologic traverse across the Culpeper basin (Triassic-Jurassic) of northern Virginia, *in* Lyttle, P. T., ed., Central Appalachian Geology, Geological Society of America joint Northeastern-Southeastern section guidebook: Falls Church, Va., American Geological Institute, p. 55–81.

Furon, Raymond, 1963, Geology of Africa: Edinburgh, Oliver & Boyd, 377 p.

Fyfe, W. S., Turner, F. J., and Verhoogen, John, 1958, Metamorphic reactions and metamorphic facies: Geological Society of America Memoir 73, 259 p.

Goddard, E. N., and others, 1948, Rock-color chart: Washington, D. C., National Research Council, 6 p. (republished by Geological Society of America, 1951; reprinted 1975).

Gohn, G. S., 1983, Geology of the basement rocks near Charleston, South Carolina–Data from detrital rock fragments in lower Mesozoic(?) rocks in Clubhouse Crossroads test hole #3, *in* Gohn, G. S., ed., Studies related to the Charleston, South Carolina, earthquake of 1886–Tectonics and seismicity: U.S. Geological Survey Professional Paper 1313, p. E1-E22.

Gohn, G. S., Gottfried, David, Lanphere, M. A., and Higgins, B. B., 1978, Regional implications of Triassic or Jurassic age for basalt and sedimentary red beds in the South Carolina Coastal Plain: Science, v. 202, no. 4370, p. 887–890.

Gohn, G. S., Houser, B. B., and Schneider, R. R., 1983, Geology of the lower Mesozoic(?) sedimentary rocks in Clubhouse Crossroads test hole #3, near Charleston, South Carolina, *in* Gohn, G. S., ed., Studies related to the Charleston, South Carolina, earthquake of 1886–Tectonics and seismicity: U.S. Geological Survey Professional Paper 1313, p. D1-D17.

Goldstein, R. F., Cramer, F. H., and Andress, N. E., 1969, Silurian chitinozoans from Florida well samples: Gulf Coast Association of Geological Societies Transactions, v. 19, p. 377–384.

Gottfried, David, Annell, C. S., and Byerly, G. R., 1983, Geochemistry and tectonic significance of subsurface basalts near Charleston, South Carolina–Clubhouse Crossroads test holes #2 and #3, *in* Gohn, G. S., ed., Studies related to the Charleston, South Carolina, earthquake of 1886–Tectonics and seismicity: U.S. Geological Survey Professional Paper 1313, p. A1-A19.

Gottfried, David, Annell, C. S., and Schwarz, L. J., 1977, Geochemistry of subsurface basalt from the deep corehole (Clubhouse Crossroads corehole 1) near Charleston, South Carolina–Magma type and tectonic implications, *in* Rankin, D. W., ed., Studies related to the Charleston, South Carolina, earthquake of 1886–A preliminary report: U.S. Geological Survey Professional Paper 1028, p. 91–113.

Grant, N. K., 1973, Orogeny and reactivation to the west and southeast of the West African Craton, *in* Nairn, A. E. M., and Stehli, F. G., eds., The ocean basins and margins; v. 1, The South Atlantic: New York, Plenum Press, p. 447–492.

Gray, M. G., III, 1978, Pre-Gulfian rocks of the southeastern Georgia Coastal Plain: Atlanta, Georgia, Emory University, unpublished M.S. thesis.

Grow, J. A., Mattick, R. E., and Schlee, J. S., 1979, Multichannel seismic depth sections and interval velocities over outer continental shelf and upper continental slope between Cape Hatteras and Cape Cod, *in* Watkins, J. S., Montadert, Lucien, and Dickerson, P. W., eds., Geological and geophysical investigations of continental margins: American Association of Petroleum Geologists Memoir 29, p. 65–83.

Heald, M. T., 1956, Cementation of Triassic arkoses in Connecticut and Massachusetts: Geological Society of America Bulletin, v. 67, no. 9, p. 1133–1154.

Herrick, S. M., 1961, Well logs of the Coastal Plain of Georgia: Georgia Geologic Survey Bulletin 70, 461 p.

Herrick, S. M., and Vorhis, R. C., 1963, Subsurface geology of the Georgia Coastal Plain: Georgia Geologic Survey Information Circular 25, 78 p.

Howell, B. F., and Richards, H. G., 1949, New Paleozoic linguloid brachiopod from Florida: Wagner Free Institute of Science Bulletin, v. 24, no. 4, p. 35–37.

Hurst, V. J., 1965, Oil tests in Georgia–A compilation: Georgia Geologic Survey Information Circular 19, 16 p.

Johnson, L. C., 1892, The Chattahoochee embayment: Geological Society of America Bulletin, v. 3, p. 128–132.

King, E. R., 1959, Regional magnetic map of Florida: American Association of Petroleum Geologists Bulletin, v. 43, no. 12, p. 2844–2854.

King, P. B., 1950, Tectonic framework of southeastern United States: American Association of Petroleum Geologists Bulletin, v. 34, no. 4, p. 635–671.

———1961, The subsurface Ouachita structural belt east of the Ouachita Mountains, *in* Flawn, P. T., Goldstein, A., Jr., King, P. B., and Weaver, C. E., eds., The Ouachita System: University of Texas Publication 6120, p. 83–98.

Kjellesvig-Waering, E. M., 1950, A new Silurian eurypterid from Florida: Journal of Paleontology, v. 24, no. 2, p. 229–231.

Klitgord, K. D., and Behrendt, J. C., 1977, Aeromagnetic anomaly map of the United States Atlantic continental margin: U.S. Geological Survey Miscellaneous Field Studies Map MF–913, 2 sheets, scale 1:1,000,000.

———1979, Basin structure of the U.S. Atlantic margin, *in* Watkins, J. S., Montadert, Lucien, and Dickerson, P. W., eds., Geological and geophysical investigations of continental margins: American Association of Petroleum Geologists Memoir 29, p. 85–112.

Klitgord, K. D., Dillon, W. P., and Popenoe, Peter, 1983, Mesozoic tectonics of the Southeastern United States Coastal Plain and continental margin, *in* Gohn, G. S., ed., Studies related to the Charleston, South Carolina, earthquake of 1886–Tectonics and seismicity: U.S. Geological Survey Professional Paper 1313, p. P1-P15.

Klitgord, K. D., Popenoe, Peter, and Schouten, Hans, 1982, Florida; a Jurassic transform plate boundary: Journal of Geophysical Research, in press.

Lanphere, M. A., 1983, $^{40}Ar/^{39}Ar$ ages of basalt from Clubhouse Crossroads test hole #2, near Charleston, South Carolina, *in* Gohn, G. S., ed., Studies related to the Charleston, South Carolina, earthquake of 1886–Tectonics and seismicity: U.S. Geological Survey Professional Paper 1313, p. B1-B8.

Long, L. T., Bridges, S. R., and Dorman, L. M., 1972, Simple Bouguer gravity map of Georgia: Georgia Geologic Survey Map GM-4.

Maher, H. D., Palmer, A. R., Secor, D. T., and Snoke, A. W., 1981, New trilobite locality in the Piedmont of South Carolina, and its regional implications: Geology, v. 9, no. 1, p. 34–36.

Maher, J. C., 1971, Geologic framework and petroleum potential of the Atlantic Coastal Plain and Continental Shelf *with a section on*

Stratigraphy, by J. C. Maher and E. R. Applin: U.S. Geological Survey Professional Paper 659, 98 p.

Maher, J. C., and Applin, E. R., 1968, Correlation of subsurface Mesozoic and Cenozoic rocks along the eastern Gulf Coast: American Association of Petroleum Geologists, Cross Section Publication 6, 29 p.

Marine, I. W., 1974, Geohydrology of buried Triassic basin at Savannah River Plant, South Carolina: American Association of Petroleum Geologists Bulletin, v. 58, no. 9, p. 1825–1837.

Marine, I. W., and Siple, G. E., 1974, Buried Triassic basin in the central Savannah River area, South Carolina and Georgia: Geological Society of America Bulletin, v. 85, no. 2, p. 311–320.

May, J. P., 1977, The Chattahoochee embayment: Southeastern Geology, v. 18, p. 149–156.

May, P. R., 1971, Pattern of Triassic-Jurassic dikes around the North Atlantic in the context of pre-drift positions of the continents: Geological Society of America Bulletin, v. 82, no. 5, p. 1285–1292.

Mayhew, M. A., 1974, Geophysics of Atlantic North America, *in* Burk, C. A., and Drake, C. L., eds., The geology of continental margins: New York, Springer-Verlag, p. 409–427.

McLaughlin, R. E., 1970, Palynology of core samples of Paleozoic sediments from beneath the Coastal Plain of Early County, Georgia: Georgia Geologic Survey Information Circular 40, 27 p.

Milton, Charles, 1972, Igneous and metamorphic basement rocks of Florida: Florida Bureau of Geology Bulletin 55, 125 p.

Milton, Charles, and Grasty, Robert, 1969, "Basement" rocks of Florida and Georgia: American Association of Petroleum Geologists Bulletin, v. 53, no. 12, p. 2483–2493.

Milton, Charles, and Hurst, V. J., 1965, Subsurface "basement" rocks of Georgia: Georgia Geologic Survey Bulletin 76, 56 p.

Murray, G. E., 1957, Geological occurrence of oil and gas in Gulf Coastal province of the United States: Gulf Coast Association of Geological Societies Transactions, v. 7, p. 253–299.

———1961, Geology of the Atlantic and Gulf coastal province of North America: New York, Harper and Brothers, 692 p.

Neathery, T. L., and Thomas, W. A., 1975, Pre-Mesozoic basement rocks of the Alabama coastal plain: Gulf Coast Association of Geological Societies Transactions, v. 25, p. 86–99.

Oglesby, W. R., Ball, M. M., and Chaki, S. J., 1973, Bouguer anomaly map of the Florida peninsula and adjoining continental shelves: Florida Bureau of Geology Map MS 57, scale 1:1,000,000.

Palmer, K. V. W., 1970, Paleozoic nonmarine bivalve from a deep well in Georgia: Georgia Academy of Sciences Bulletin, v. 28, no. 1, p. 45–54.

Patterson, S. H., and Herrick, S. M., 1971, Chattahoochee Anticline, Apalachicola Embayment, Gulf Trough and related structural features, southwestern Georgia; fact or fiction: Georgia Geologic Survey Information Circular 41, 16 p.

Pickering, S. M., Jr., Higgins, M. W., and Zietz, Isidore, 1977, Relationship between the Southeast Georgia Embayment and the onshore extent of the Brunswick Magnetic Anomaly [abs.]: EOS, American Geophysical Union Transactions, v. 58, no. 6, p. 432.

Pilger, R. H., Jr., 1978, A closed Gulf of Mexico, pre-Atlantic Ocean plate reconstruction and the early rift history of the Gulf and North Atlantic: Gulf Coast Association of Geological Societies Transactions, v. 28, pt. 2, p. 385–393.

Piqué, Alain, 1981, Northwestern Africa and the Avalonian plate–Relations during late Precambrian and late Paleozoic time: Geology, v. 9, no. 7, p. 319–322.

Pojeta, John, Jr., Kriz, Jiri, and Berdan, J. M., 1976, Silurian-Devonian pelecypods and Paleozoic stratigraphy of subsurface rocks in Florida and Georgia and related Silurian pelecypods from Bolivia and Turkey: U.S. Geological Survey Professional Paper 879, 32 p.

Popenoe, Peter, and Zietz, Isidore, 1977, The nature of the geophysical basement beneath the Coastal Plain of South Carolina and northeastern Georgia, *in* Rankin, D. W., ed., Studies related to the Charleston, South Carolina, earthquake of 1886–A preliminary report: U.S. Geological Survey Professional Paper 1028, p. 119–137.

Pressler, E. D., 1947, Geology and occurrence of oil in Florida: American Association of Petroleum Geologists Bulletin, v. 31, no. 10, p. 1851–1862.

Privett, D. R., 1974, Widespread laumontization in the central Piedmont of North Carolina and southern Virginia [abs.]: Geological Society of America Abstracts with Programs, v. 6, no. 4, p. 389–390.

Puffer, J. H., Hurtubise, D. O., Geiger, F. J., and Lechler, Paul, 1981, Chemical composition and stratigraphic correlation of Mesozoic basalt units of the Newark Basin, New Jersey, and the Hartford Basin, Connecticut; summary: Geological Society of America Bulletin, pt. 1, v. 92, no. 4, p. 155–159.

Puri, H. S., and Vernon, R. O., 1964, Summary of the geology of Florida and a guidebook to the classic exposures (revised): Florida Geological Survey Special Publication 5, 312 p.

Ramspott, L. D., 1967, Zeolites in the Georgia Piedmont: Georgia Academy of Science Bulletin, v. 25, no. 1, p. 18–24.

Reinemund, J. A., 1955, Geology of the Deep River coal field, North Carolina: U.S. Geological Survey Professional Paper 246, 159 p.

Richards, H. G., 1948, Studies on the subsurface geology and paleontology of the Atlantic Coastal Plain: Philadelphia Academy of Natural Science Proceedings, v. 100, p. 39–76.

Rodgers, John, 1970, The tectonics of the Appalachians: New York, Wiley Interscience, 271 p.

———1972, Latest Precambrian (post-Grenville) rocks of the Appalachian region: American Journal of Science, v. 272, no. 6, p. 507–520.

Rona, P. A., 1980, The central north Atlantic ocean basin and continental margins; geology, geophysics, geochemistry, and resources, including the Trans-Atlantic Geotraverse (TAG): National Oceanic and Atmospheric Administration Atlas 3.

Ross, C. S., 1958, Welded tuff from deep-well cores from Clinch County, Georgia: American Mineralogist, v. 43, nos. 5–6, p. 537–545.

St. Jean, Joseph, 1973, A new Cambrian trilobite from the Piedmont of North Carolina: American Journal of Science, v. 273–A, p. 196–216.

Scholle, P. A., ed., 1979, Geological studies of the COST GE-1 well, United States South Atlantic Outer Continental Shelf area: U.S. Geological Survey Circular 800, 114 p.

Schuchert, Charles, 1935, Historical geology of the Antillean-Caribbean region, or the lands bordering the Gulf of Mexico and the Caribbean Sea: New York, John Wiley and Sons, 811 p.

———1943, Stratigraphy of the eastern and central United States: New York, John Wiley and Sons, 1013 p.

Scott, K. R., Hayes, W. E., and Fietz, R. P., 1961, Geology of the Eagle Mills Formation: Gulf Coast Association of Geological Societies Transactions, v. 11, p. 1–14.

Siple, G. E., 1959, Guidebook for the South Carolina Coastal Plain field trip of the Carolina Geological Society: South Carolina State Development Board, Division of Geology Bulletin 24, 27 p.

Smith, R. C., II, Rose, A. W., and Lanning, R. M., 1975, Geology and geochemistry of Triassic diabase in Pennsylvania: Geological Society of America Bulletin, v. 86, no. 7, 943–955.

Sougy, Jean, 1962, West African fold belt: Geological Society of America Bulletin, v. 73, no. 7, p. 871–876.

Swanson, D. E., and Gernazian, Andrea, 1979, Petroleum exploration wells in Georgia: Georgia Geologic Survey Information Circular 51, 67 p.

Swartz, F. M., 1949, Muscle marks, hinge and overlap features, and classification of some Leperditiidae: Journal of Paleontology, v. 23, no. 3, p. 306–327.

Talwani, Pradeep, Long, L. T., and Bridges, S. R., 1976, Simple Bouguer gravity map of South Carolina: South Carolina Development Board Division of Geology, MS 21, scale 1:500,000.

Taylor, Patrick, Zietz, Isidore, and Dennis, L. S., 1968, Geologic implications of aeromagnetic data for the eastern continental margin of the United States: Geophysics, v. 33, no. 5, p. 755–780.

Templeton, R. S. M., 1971, The geology of the continental margin between Dakar and Cape Palmas, *in* Delany, F. M., ed., The geology of the east Atlantic continental margin, [Pt.] 4, Africa: Institute of Geological Sciences Report no. 70/16, p. 43–60.

Toewe, E. C., 1966, Geology of the Leesburg quadrangle, Virginia: Virginia Division of Mineral Resources Report of Investigations 11, 52 p.

Toulmin, L. D., 1955, Cenozoic geology of southeastern Alabama, Florida, and Georgia: American Association of Petroleum Geologists Bulletin, v. 39, no. 2, p. 207–235.

Uchupi, Elazar, Emery, K. O., Bowin, C. O., and Phillips, J. D., 1976, Continental margin of western Africa–Senegal to Portugal: American Association of Petroleum Geologists Bulletin, v. 60, p. 809–878.

Van der Voo, R., Mauk, F. J., and French, R. B., 1976, Permian-Triassic continental configurations and the origin of the Gulf of Mexico: Geology, v. 4, no. 3, p. 177–180.

Van Houten, F. B., 1969, Late Triassic Newark Group, north-central New Jersey and adjacent Pennsylvania and New York, *in* Subitzky, Seymour, ed., Geology of selected areas in New Jersey and eastern Pennsylvania: New Brunswick, New Jersey, Rutgers University Press, p. 314–347.

———1977, Triassic-Liassic deposits of Morocco and eastern North America; Comparison: American Association of Petroleum Geologists Bulletin, v. 61, p. 79–99.

Vorhis, R. C., 1974, Some structural patterns in sediments of the Georgia Coastal Plain, *in* Stafford, L. P., ed., Symposium on the petroleum geology of the Georgia Coastal Plain: Georgia Geologic Survey Bulletin 87, p. 87–97.

Weigand, P. W., and Ragland, P. C., 1970, Geochemistry of Mesozoic dolerite dikes from eastern North America: Contributions to Mineralogy and Petrology, v. 29, no. 3, p. 195–214.

Whittington, H. B., 1953, A new Ordovician trilobite from Florida: Harvard Museum Comparative Zoology Breviora, no. 17, p. 6.

Whittington, H. B., and Hughes, C. P., 1972, Ordovician geography and faunal provinces deduced from trilobite distribution: Royal Society of London, Philosophical Transactions, ser. B, v. 263, no. 850, p. 235–278.

Wicker, R. A., and Smith, D. L., 1978, Reevaluating the Florida basement: Gulf Coast Association of Geological Societies Transactions, v. 28, pt. 2, p. 681–687.

Wilson, J. T., 1966, Did the Atlantic close and then re-open?: Nature, v. 211, no. 5050, p. 676–681.

Winkler, H. G. F., 1974, Petrogenesis of metamorphic rocks (3d ed.): New York, Springer-Verlag, 320 p.

Zapp, A. D., 1965, Bauxite deposits of the Andersonville district, Georgia: U.S. Geological Survey Bulletin 1199-G, 37 p.

Zietz, Isidore, and Gilbert, F. P., 1980, Aeromagnetic map of part of the Southeastern United States; in color: U.S. Geological Survey Geophysical Investigation Map GP-936.

Potassium-Argon Relations in Diabase Dikes of Georgia—The Influence of Excess ^{40}Ar on the Geochronology of Early Mesozoic Igneous and Tectonic Events

By ROBERT E. DOOLEY and J. M. WAMPLER

STUDIES RELATED TO THE CHARLESTON, SOUTH CAROLINA, EARTHQUAKE OF 1886—TECTONICS AND SEISMICITY

GEOLOGICAL SURVEY PROFESSIONAL PAPER 1313-M

UNITED STATES GOVERNMENT PRINTING OFFICE, WASHINGTON: 1983

CONTENTS

ILLUSTRATIONS

TABLES

STUDIES RELATED TO THE CHARLESTON, SOUTH CAROLINA, EARTHQUAKE OF 1886—
TECTONICS AND SEISMICITY

POTASSIUM-ARGON RELATIONS IN DIABASE DIKES OF GEORGIA—THE INFLUENCE OF EXCESS ^{40}Ar ON THE GEOCHRONOLOGY OF EARLY MESOZOIC IGNEOUS AND TECTONIC EVENTS

By ROBERT E. DOOLEY[1,2] and J. M. WAMPLER[1]

ABSTRACT

Conventional K-Ar ages for 20 diabase dikes from the Piedmont and Blue Ridge provinces of Georgia are highly variable (190–1,628 m.y.) and discordant, in a pattern similar to the K-Ar ages of Liberian diabase dikes. We interpret the large range in conventional K-Ar ages of diabase dikes in Georgia as having been caused by the presence of excess ^{40}Ar in most, if not all, of the dikes. The dikes in Georgia are probably not more than 195 m.y. old and may be contemporaneous with structurally similar dikes in the Northeastern United States that are about 180 m.y. old. Structural relationships indicate that these dikes are part of a system of dikes that formed in the continents around the central Atlantic Ocean as the ocean began to open. The amounts of excess ^{40}Ar in the diabase samples have been calculated by assuming a 180-m.y. age for the dikes in Georgia. Most diabase dikes in the northern part of the Piedmont and in the Blue Ridge contain large and variable amounts of excess ^{40}Ar (as much as 1.6 nmol/g). Samples from diabase dikes in the southern part of the Piedmont of Georgia contain small amounts of excess ^{40}Ar (less than 0.04 nmol/g). This distinct regional variation in excess ^{40}Ar content of diabase does not appear to be related to the argon content of the country rocks at the sampling sites. Locally, the pattern of discordance in K-Ar ages within dikes suggests that excess ^{40}Ar is concentrated in the later crystallizing parts of a dike. This concept is supported by evidence that some of the excess ^{40}Ar is concentrated in microstructural irregularities in the rock. These observations indicate that the excess ^{40}Ar in the diabase is argon that arrived at the site of emplacement as part of the magma. Some of the argon in the magma must have originated at the site of partial melting in the asthenosphere, but the regional pattern of excess ^{40}Ar in the diabase dikes appears to have been influenced by the thickness of the crust through which the magma ascended. Where the crust is thicker, most of the crust is presumably Precambrian basement. Rocks at intermediate or lower levels of the crust are probably the most important source of the excess ^{40}Ar found in the diabase dikes of the northern part of the Piedmont and Blue Ridge. Samples from the southern part of the Piedmont have little excess ^{40}Ar, either because the magma was not contaminated with argon from the crust or because these samples formed close enough to the surface for argon to escape from the magma.

[1]School of Geophysical Sciences, Georgia Institute of Technology, Atlanta, GA 30332.
[2]Now at Department of Physical Sciences, Florida International University, Miami, FL 33199.

INTRODUCTION

A circum-Atlantic system of diabase dikes and sills (fig. 1) has been related to graben formation, continental rifting, and opening of the central Atlantic Ocean early in the Mesozoic Era (May, 1971). In a reconstruction of the continents to their predrift positions, the dikes in eastern North America, northwestern Africa, and northeastern South America form a radial pattern within a broad elliptical area. May suggested that the dikes outline a pattern of tensional fractures that were filled by material from the upper mantle immediately before separation of the continents. Paleomagnetic and geochronologic investigations of lower Mesozoic rocks from these continental areas have made significant contributions to the development of the concept of plate tectonics and have helped establish the time of opening of the central Atlantic Ocean. Some of the more recent investigations (Dalrymple and others, 1975; Smith and Noltimier, 1979; Sutter and Smith, 1979) have shown that steady spreading in the central Atlantic probably began between 175 and 185 million years (m.y.) ago[3] and

[3]Values for the decay constants and isotopic abundance of ^{40}K recommended by the IUGS Subcommission on Geochronology in 1976 (Steiger and Jäger, 1977) differ from those that were in general use until recently. The difference is such that K-Ar apparent ages near 200 m.y. are 2.3 percent greater when the newly recommended values are used in the age calculation than they are when the values in most common use earlier (Dalrymple and Lanphere, 1969, p. 243) are used. Thus, for example, an age reported as 175 m.y. on the basis of the earlier values would now be calculated to be 179 m.y. The IUGS Subcommission also recommended values for decay constants and isotopic abundances used in geochronometric work with ^{87}Rb, ^{232}Th, ^{235}U, and ^{238}U.

In referring to earlier work in which the newly recommended values were not used, we have recalculated the radiometric ages using the new values. If values for the decay constants or isotopic abundance of ^{40}K are not given in the literature, we have assumed that the values in common use at the time of publication were employed. Where we mention specific apparent ages or averages of apparent ages, we have rounded the recalculated values to the nearest million years, but in more general statements about sets of apparent ages or about the dates of events we have used multiples of 5 m.y. Since most of our review in this paper of the chronology of early Mesozoic events is based on recalculated K-Ar ages, the dates in our paper are typically 5 m.y. earlier than those in the original literature.

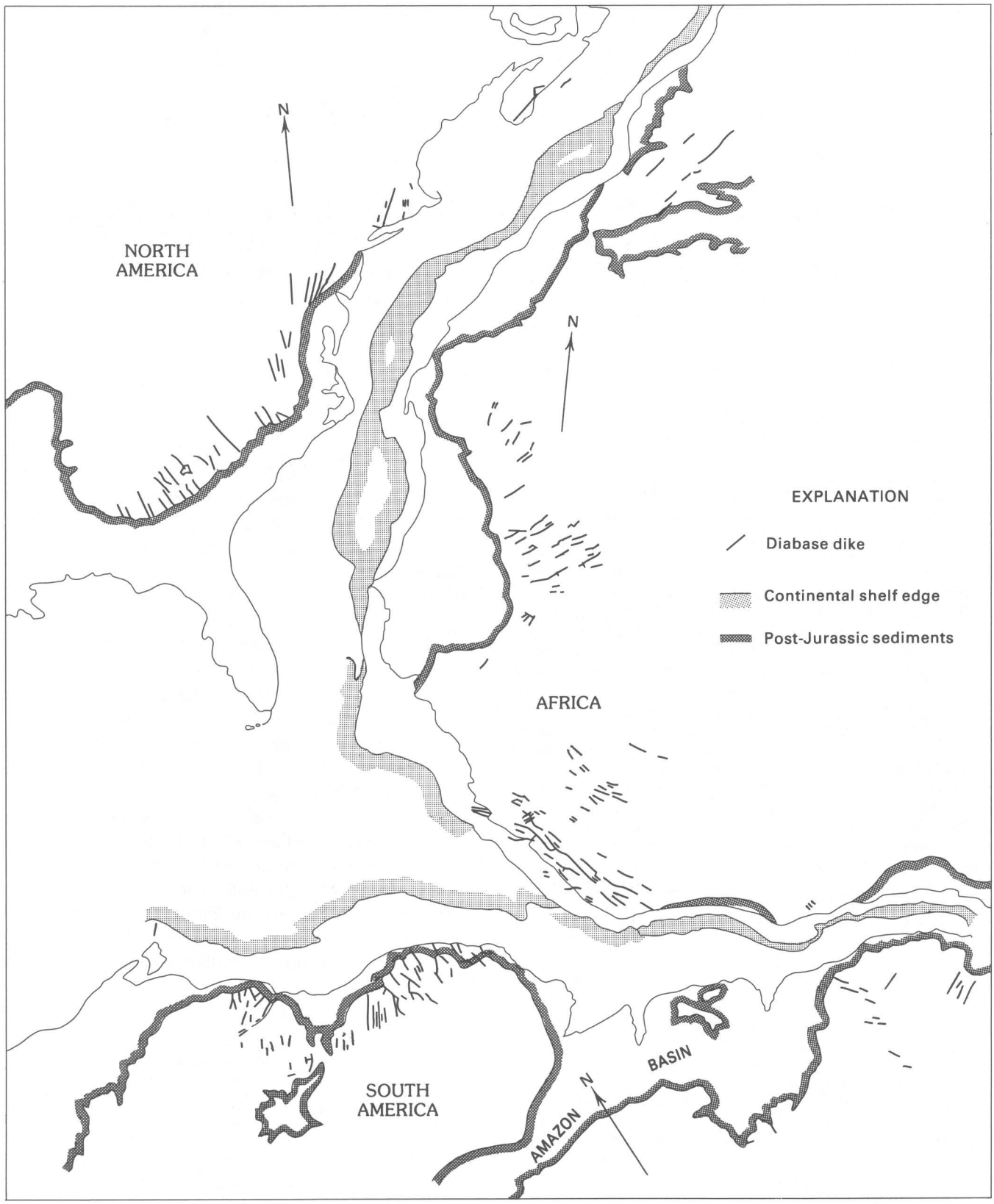

FIGURE 1.—Map of diabase dikes in eastern North America, northwestern Africa, and northeastern South America, showing the continents restored to their relative positions in the Triassic (after May, 1971). The north arrows represent the present-day direction of geographic north relative to each of the restored continents.

that some of the dikes were emplaced during this interval. It is clear, however, that sedimentation and igneous activity within early Mesozoic basins[4] began well before the actual opening of the ocean.

Rift systems are exceedingly complex. Any study of the timing of structural and magmatic events in rift systems will be important to our understanding of global tectonics (Şengör and Burke, 1978). De Boer and Snider (1979) recently summarized the geological, geophysical, and geochemical data pertinent to the early Mesozoic rifting and magmatic activity in eastern North America and interpreted the history of the related events from the Triassic to the Middle Jurassic. The tectonic and magmatic processes that affected the continental crust of the Eastern United States as it separated from Africa and South America must have been active over a long period of time, perhaps continuing for some time after the initial appearance of new sea floor. Accurate determination of the ages of the lower Mesozoic dikes would show the distribution of magmatic activity in time and space and thus would contribute to understanding the role of magmatism in the separation of continents.

We have determined conventional K-Ar ages[5] of samples from 20 lower Mesozoic diabase dikes in Georgia. Although preliminary work had indicated that some of the dikes in Georgia contain extraneous ^{40}Ar,[6] we began our study expecting that such argon might be limited to certain geographic areas and that conventional K-Ar ages would correctly indicate the age of some dikes in Georgia. Our goals were to address the following questions:

1. Can conventional K-Ar ages of diabase dikes in Georgia, for which no radiometric ages have yet been published, contribute to our knowledge of the timing of the magmatic activity that accompanied the opening of the central Atlantic Ocean?
2. How extensive is the problem of extraneous ^{40}Ar in Georgia diabase dikes, and is there any systematic pattern in regional or local distribution of such Ar?
3. What sort of detailed study would most likely be successful in establishing accurately the times when the dikes were emplaced?

Acknowledgments.—Acknowledgment is made to the Donors of the Petroleum Research Fund, administered by the American Chemical Society, for partial support of this research. The remainder of the support was provided by the State of Georgia. Preliminary K-Ar work by George Rothe indicated anomalous apparent ages for two diabase dikes in Georgia. Bruce O'Connor provided valuable information about sample localities. William McLemore, Marvin Lanphere, and Gary Byerly provided helpful reviews of the manuscript.

NORTH AMERICAN GEOLOGIC SETTING

The diabase dikes of Georgia are part of a set of steeply-dipping tholeiitic diabase dikes that are exposed in the Appalachian orogenic belt from Alabama to Nova Scotia (fig. 2). In the southern Appalachian area, the average trend of the dikes is northwest, transecting the Appalachian structures. Around Virginia, the trend of the dikes changes to become more or less parallel to northeast-trending regional structures in the Northeastern United States (King, 1971). Many of the dikes, particularly in the Northeastern States, are wholly or partly within early Mesozoic basins where tholeiitic flows and sills are commonly found within the Newark Group.

Until recently, all of the Newark Group was considered to be Late Triassic in age, and the diabase dikes in the Appalachian belt were associated with the Triassic System even where the dikes are far from any sedimentary basin (Lester and Allen, 1950; King, 1971). In recent years, however, new information has indicated that sedimentation and volcanism in some of the early Mesozoic basins continued into the Jurassic Period (Cornet and others, 1973; Dallmeyer, 1975a; Sutter and Smith, 1979). Structural and paleomagnetic evidence implies that many of the dikes postdate Lower Jurassic formations (see de Boer and Snider, 1979; Smith and Noltimier, 1979). Although K-Ar dating had indicated that some of the eastern North American diabase dikes are Triassic in age, recognition of excess ^{40}Ar in some of these rocks (Dooley and Wampler, 1977a; Sutter and Smith, 1979) has cast doubt on the validity of many of the conventional K-Ar ages for the dikes of eastern North America. The earlier concept that all the tholeiitic rocks are Triassic in age has been replaced by the notion that many of the dikes, sills, and flows formed early in the Jurassic Period.

Because others (de Boer and Snider, 1979; Smith and Noltimier, 1979; Sutter and Smith, 1979) recently have summarized important stratigraphic, structural, geochemical, and geophysical information that relates to

[4]The phrase "early Mesozoic basins" is used for what commonly have been called "Triassic basins," because the uppermost rocks in some of these basins are of Early Jurassic age (Cornet and others, 1973).

[5]Conventional K-Ar ages are age values calculated from analytical data obtained by conventional K-Ar techniques. Dalrymple and Lanphere (1969, p. 43–98) described the conventional K-Ar techniques and specified the fundamental assumptions required to interpret such a calculated age as the actual age of a geological sample. Unless it is certain that the assumptions are correct, a conventional K-Ar age must be viewed as an "apparent age." We shall use the terms interchangeably in this paper.

[6]A fundamental assumption of the conventional K-Ar dating method is that a sample contains *radiogenic* Ar formed in place by radioactive decay of ^{40}K since the event being dated and that any extraneous Ar present in the sample is *atmospheric* Ar (that is, Ar having an isotopic composition like that of Ar in the modern atmosphere). If this assumption is not correct, then the amount of "radiogenic Ar" calculated by the conventional formula will not be consistent with the strict genetic connotation of the term *radiogenic* Ar implied by the assumption. The calculated amount of the "radiogenic Ar" may include some *extraneous* ^{40}Ar (Dalrymple and Lanphere, 1969, p. 121–122). Extraneous ^{40}Ar in an igneous rock is called *excess* ^{40}Ar unless it specifically associated with contaminating mineral grains (for example, in xenoliths or xenocrysts).

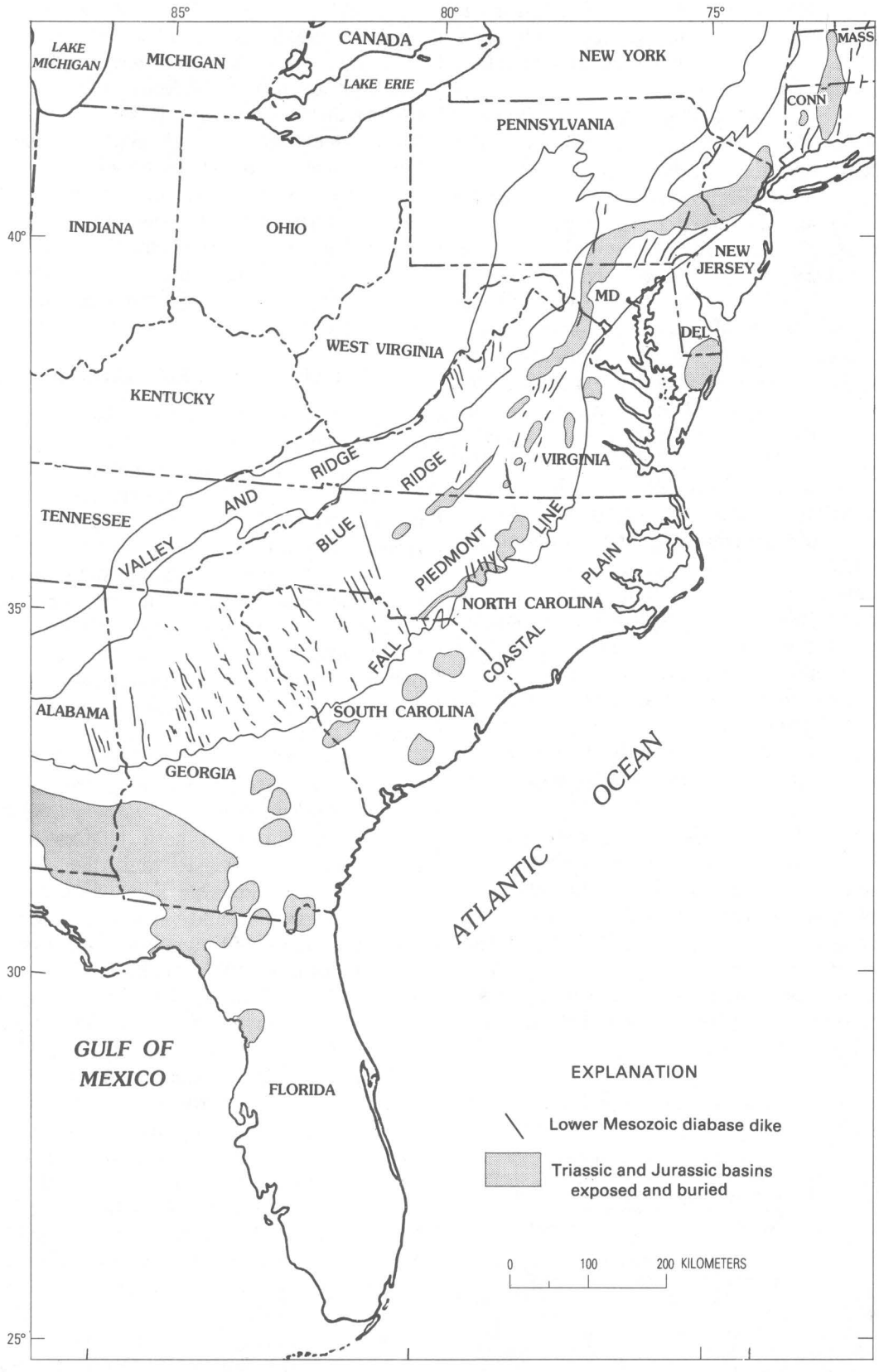

FIGURE 2.—Occurrence of diabase dikes and sills in Eastern United States (after King, 1971, and Marine and Siple, 1974).

the history of early Mesozoic rifting and magmatism in eastern North America and the relationship of these to global tectonics, it is unnecessary to review all of this information here. However, the previous radiometric dating work and some of the paleomagnetic studies are particularly important to the interpretation of our work; therefore we shall review the earlier work in these areas.

RADIOMETRIC GEOCHRONOLOGY AND PALEOMAGNETISM

Early radiometric dating of Mesozoic diabase intrusive rocks and basalt flows from the Northeastern United States and Nova Scotia (Erickson and Kulp, 1961; Fanale and Kulp, 1962; Larochelle and Wanless, 1966; Carmichael and Palmer, 1968; de Boer, 1968) produced apparent ages from less than 100 m.y. to more than 300 m.y., but the age values (individual apparent ages or averages) that these authors considered to be most reliable are near 200 m.y. (As originally reported, these age values were all within 6 m.y. of 196 m.y.; recalculated values are within 7 m.y. of 200 m.y.) With the geochronometric scales in use at that time, the early results were consistent with the idea that these igneous rocks formed late in the Triassic Period.

K-Ar analyses by Armstrong and Besancon (1970) of sills and volcanic rocks from early Mesozoic basins in eastern North America give apparent ages in the range 164–206 m.y.; most are near 200 m.y. Their analyses of diabase dike samples, however, give apparent ages in the range 197–253 m.y. and indicate a concentration (four samples) near 230 m.y. Recognizing evidence that early geochronometric scales had placed the Triassic-Jurassic boundary too far forward in time, and influenced by some new data that suggested the boundary date is about 210 m.y. ago, Armstrong and Besancon proposed that the cluster of K-Ar ages near 200 m.y. may not correctly represent the age of igneous rocks in the Newark Group. They suggested that Ar loss caused by low-grade metamorphism might be responsible for the apparent ages near 200 m.y. and that the apparent ages of some dikes near 230 m.y. might be closer (albeit fortuitously) to the age of the Newark rocks. The dilemma suggested by Armstrong and Besancon has been resolved by later work, which shows that the uppermost sedimentary rocks of the Newark Group are Jurassic (Cornet and others, 1973) and confirms by means of the $^{40}Ar/^{39}Ar$ method that some of the associated igneous rocks are about 195 m.y. old (Dallmeyer, 1975a; Sutter and Smith, 1979).

Many additional reports of conventional K-Ar dating of lower Mesozoic diabase and basalt from eastern North America have given an overall range of apparent ages from less than 100 m.y. to more than one billion years (Milton and Grasty, 1969; Poole and others, 1970; Baldwin and Adams, 1971; Larochelle, 1971; Corrigan, 1972; Reesman and others, 1973; Watts and Noltimier, 1974; Barnett, 1975; Deininger and others, 1975; Wampler and Dooley, 1975; Gottfried and others, 1977; Houlik and Laird, 1977; Dooley and Wampler, 1977a, 1978; Gohn and others, 1978; McHone, 1978; Dooley and Smith, 1982). Although many of the apparent ages are within the geochronometric range of the first half of the Mesozoic Era, many of these studies have not been published as full papers, a fact that perhaps reflects growing awareness of the general unreliability of conventional K-Ar dating for this type of rock.

Conventional K-Ar dating of Mesozoic diabase from other continental areas that originally were close to eastern North America (fig. 1) followed soon after the early research on North America. The K-Ar data of Hailwood and Mitchell (1971) give apparent ages for samples collected from several sills and the Foum Zguid dike in Morocco that are in close agreement (184–191 m.y.) However, other conventional K-Ar studies of Mesozoic diabase and basalt in northwestern Africa have produced results that are less internally consistent (Briden and others, 1971; Leblanc, 1973; Dalrymple and others, 1975; Cousminer and Manspeizer, 1976; Michard, 1976; Thuizat, 1976; Westphal and others, 1979). Apparent ages are as low as 156 m.y. and as high as 1,131 m.y. for whole-rock samples of diabase dikes and sills in northwestern Africa; however, most of the K-Ar apparent ages cluster broadly around 200 m.y.

The Messejana fault-dike system in Portugal and Spain (not shown in fig. 1) is similar in size and trend to the large Foum Zguid dike in Morocco and has been associated with the circum-Atlantic system of early Mesozoic rifting and magmatism by Schermerhorn and others (1978). They used K-Ar data obtained in their study (apparent ages in the range 150–190 m.y.), and some data from earlier studies, to infer that the Messejana dike system was formed by multiple episodes of magmatic activity over a period extending from the latest Triassic or earliest Jurassic through the Middle Jurassic.

The pattern of dikes belonging to the early Mesozoic circum-Atlantic system is not well defined in northeastern South America, because of the occurrence of many older mafic bodies that have intruded the Precambrian Guiana Shield (May, 1971). Many of these intrusive bodies are known to be Precambrian in age on the basis of K-Ar and Rb-Sr dating, but radiometric dating has also indicated a period of basaltic magmatism about 230 m.y. ago during which a set of dikes was formed (Hebeda and others, 1973). Many of the Precambrian mafic intrusive rocks in this region have anomalously great K-Ar ages (apparent ages greater than the age of the Precambrian rocks that they intrude).

In the early K-Ar studies of Mesozoic diabase in the circum-Atlantic system, some samples were found to have anomalously great K-Ar apparent ages, but the number of such samples was small enough that these results were not given much consideration. On the other hand, extensive contamination of Precambrian diabase with excess ^{40}Ar was observed by Evans and Tarney (1964) and by Hebeda and others (1973).

The first report of widespread high levels of excess ^{40}Ar contamination in diabase of the Mesozoic circum-Atlantic system was by Dalrymple and others (1975) in a study of diabase dikes and sills in Liberia. Conventional K-Ar ages for these dikes and sills range from 177 to 1,221 m.y.; two-thirds of the apparent ages are greater than 300 m.y. Large and variable amounts of Ar were found in dikes intruding Precambrian basement rocks. Samples from dikes and sills intruding a Paleozoic sandstone (which contains very little K and hence would have contained almost no radiogenic Ar) have K-Ar ages in the range 177–197 m.y. Paleomagnetic pole positions indicate that the dikes in the Precambrian basement are approximately contemporaneous with the dikes and sills in the Paleozoic terrane.

Using the $^{40}Ar/^{39}Ar$ method, Dalrymple and others (1975) showed that diabase samples with anomalously great apparent ages have ^{40}Ar that is not associated with neutron-produced ^{39}Ar. Such samples have distinctive "saddle-shaped" $^{40}Ar/^{39}Ar$ incremental release spectra. However, $^{40}Ar/^{39}Ar$ studies of a diabase within the Paleozoic sandstone showed no evidence of excess ^{40}Ar contamination, and both the $^{40}Ar/^{39}Ar$ age spectra and the $^{40}Ar/^{36}Ar$ versus $^{39}Ar/^{36}Ar$ isochrons indicated ages within the range of the conventional K-Ar ages. Dalrymple and others (1975) inferred that the dikes intruding Precambrian basement contain extraneous ^{40}Ar that was probably absorbed from the surrounding rocks (at the site of emplacement) during crystallization. Finally, they showed that the mean paleomagnetic pole for these and other intrusive rocks having similar radiometric ages in Morocco and Sierra Leone (Briden and others, 1971; Hailwood and Mitchell, 1971) is nearly coincident with a mean paleomagnetic pole for igneous rocks of latest Triassic to earliest Jurassic age in eastern North America, if the continents are restored to a predrift configuration as proposed by Bullard and others (1965) or by Le Pichon and Fox (1971).

The paleomagnetic data used by Dalrymple and others (1975) to calculate a mean pole for North American diabase and basalt were taken from a number of earlier paleomagnetic studies. In addition to those cited by Dalrymple and others, an earlier paleomagnetic study by de Boer (1967) of diabase dikes from along the length of the Appalachians is of particular significance because he used his data to infer that the dikes are Jurassic rather than Triassic in age. Additional paleomagnetic data from the dikes in the southern Appalachians obtained by Watts (1975), Bell and others (1980), and Dooley and Smith (1982) support this interpretation.

In recent reports, Smith and Noltimier (1979) and Sutter and Smith (1979) presented new paleomagnetic and radiometric data for lower Mesozoic igneous rocks of the north-central Appalachians. Smith and Noltimier (1979) showed that there are two clusters of paleomagnetic poles for the lower Mesozoic igneous rocks in Connecticut and suggested that the two clusters represent two periods of igneous activity. Paleopoles from samples in other areas of the north-central Appalachians fall into the same two clusters, which suggests that the two periods of igneous activity are of regional extent, not limited to Connecticut. Sutter and Smith (1979) established that there are two distinct age-groups of diabase, by using a combination of $^{40}Ar/^{39}Ar$ and conventional K-Ar techniques. They determined that four narrow dikes in Connecticut are about 180 m.y. old, on the basis of isochrons ($^{40}Ar/^{36}Ar$ versus $^{39}Ar/^{36}Ar$), and presented evidence that a diabase dike in Maryland also belongs to the 180-m.y. age-group. Drawing on earlier studies (de Boer, 1968; Cornet and others, 1973; Dallmeyer, 1975a; Smith, 1976), Smith and Noltimier (1979) and Sutter and Smith (1979) used a combination of biostratigraphic, paleomagnetic, and radiometric ($^{40}Ar/^{39}Ar$) data to show that the other period of igneous activity occurred about 195 m.y. ago. Some of the conventional K-Ar ages given in the literature are inconsistent (generally higher and discordant) with their two age-groups. Sutter and Smith (1979) attributed these inconsistencies to the presence of small, variable amounts of excess ^{40}Ar.

The earlier period of igneous activity (195 m.y. ago) identified by Smith and Noltimier (1979) and Sutter and Smith (1979) involved primarily flows, sills, and dikes within the early Mesozoic basins. The later period (180 m.y. ago) is especially well defined in the Connecticut Valley where the narrow dikes cut across the basin and extend tens of kilometers into the surrounding metamorphic terrane. The mean paleomagnetic pole position of the cluster corresponding to the younger age-group (180 m.y.) agrees closely with the mean paleomagnetic pole position for diabase samples from Liberia and Morocco (but not Sierra Leone), if the continents are reassembled to predrift positions. Smith and Noltimier (1979) therefore suggested that the dikes of this 180-m.y. age-group formed just before the onset of active spreading of the central Atlantic Ocean.

De Boer and Snider (1979) have used thermoremanent magnetization inclinations to suggest that there were three periods of diabase dike intrusion in eastern North America in the early part of the Mesozoic Era. The age

ranges that they assigned to these three periods were based largely on conventional K-Ar ages, some of which probably have been inflated by the presence of small amounts of excess ^{40}Ar in the samples.

Hayatsu (1979) and Hodych and Hayatsu (1980) have reported $^{40}Ar/^{36}Ar$ versus $^{40}K/^{36}Ar$ isochrons for lower Mesozoic rocks in Nova Scotia, Newfoundland, and Connecticut that suggest ages of 191 and 201 m.y. Ages inferred by a conventional interpretation of their data would not differ significantly from the isochron interpretation, but the uncertainties in the ages would be greater.

Recent paleomagnetic and radiometric studies indicate an Early Jurassic age for diabase dikes and subsurface basalt in South Carolina (Dooley and Smith, 1982; Phillips, 1983; Lanphere, 1983). The data of Dooley and Smith indicate the presence of a 195-m.y. age-group of diabase dikes in the Piedmont of South Carolina. Their study also tentatively suggests the presence of a 180-m.y. age-group of dikes. Lanphere's $^{40}Ar/^{39}Ar$ study establishes an age of 184 m.y. for one sample of the subsurface basalt at Clubhouse Crossroads, which is a series of flows partially interbedded with sedimentary red-bed units.

In summary, paleomagnetic and radiometric studies show a close relationship among the lower Mesozoic basaltic rocks of eastern North America and northwestern Africa, and $^{40}Ar/^{39}Ar$ methods have produced reliable age values for a number of diabase samples that range from about 175 m.y. to 195 m.y. Two main periods of igneous activity are indicated, at about 180 and 195 m.y. ago. The presence of large amounts of excess ^{40}Ar in diabase samples from Liberia and small amounts in diabase samples from the northern Appalachian region has been established. It seems probable that many of the conventional K-Ar ages that have been reported for diabase from the circum-Atlantic system of dikes have been influenced by the presence of excess ^{40}Ar. Perhaps none of the apparent ages greater than 200 m.y. are valid. These considerations suggest that most of the diabase dikes belonging to the Mesozoic circum-Atlantic system (including those in northeastern South America) were formed in the Jurassic Period.

DIABASE DIKES IN GEORGIA

Within the Piedmont and the Blue Ridge Mountains of Georgia are more than one hundred diabase dikes (fig. 3), which are northwest-trending, nearly vertical, and generally narrow (ranging in width from several centimeters to about one hundred meters). The structural belts of this part of Georgia are products of Paleozoic orogenic activity and are composed largely of Proterozoic Z and Paleozoic metamorphic and igneous rocks. The tholeiitic diabase dikes cut across regional trends of metamorphic rocks (Lester and Allen, 1950), including major faults and fault zones such as the Towaliga and Goat Rock faults and the Brevard zone. The dikes have not been deformed or metamorphosed by Appalachian orogenic activity, and some of them intrude upper Paleozoic granitic plutons. The Sparta granite complex of Fullagar and Butler (1976) and the Stone Mountain Granite (Whitney and others, 1976), both about 300 m.y. old, are each cut by several diabase dikes. At least one dike cuts the 264-m.y.-old Siloam Granite of Jones and Walker (1973).

No diabase dikes have been observed within the Cretaceous and younger sedimentary rocks of the Coastal Plain of Georgia. Many oil test wells have been drilled through these Coastal Plain sediments into a complex basin filled by red-bed sediments similar to those of the Newark Group (Chowns and Williams, 1983). Diabase has been encountered in many of the test wells, and the diabase intrusions of the subsurface have been interpreted to be associated with the diabase dikes that are exposed in the Piedmont and Blue Ridge of Georgia (Milton and Hurst, 1965).

The geologic relationships of the diabase dikes to other rocks in Georgia may be used to establish a time interval during which the system of dikes must have formed. Specific cross-cutting relationships show that a number of the dikes are less than 300 m.y. old, but the system of dikes, as a whole, appears to postdate the late Paleozoic orogenic activity of the southern Appalachian region. Since the influence of compressional tectonics is known to have continued until near the end of the Permian Period, we can be certain that the dikes, which are associated with extensional tectonics, did not begin to form earlier than the beginning of the Mesozoic Era, about 235 m.y. ago. No specific relationship establishes a minimum age for any of the dikes exposed north of the Fall Line, but the absence of dikes in the Coastal Plain sedimentary cover and the common occurrence of diabase below it suggest that the system of dikes was emplaced before the first of these sedimentary formations was deposited about 100 m.y. ago.

Except for some of our work in abstract form, cited above, no reports of radiometric ages for the dikes exposed north of the Fall Line in Georgia have been published. Deininger and others (1975) reported conventional K-Ar ages for two dikes, which represent two different compositional groups, in nearby east-central Alabama. The average K-Ar age for three samples of an olivine-normative dike is 192 m.y., but for a quartz-normative dike the average for three samples is only 168 m.y. Conventional K-Ar ages of diabase from the subsurface in Georgia and Florida are mostly near 190 m.y. (Milton and Grasty, 1969; Barnett, 1975), but the values for subsurface basalt in Florida and South Carolina are

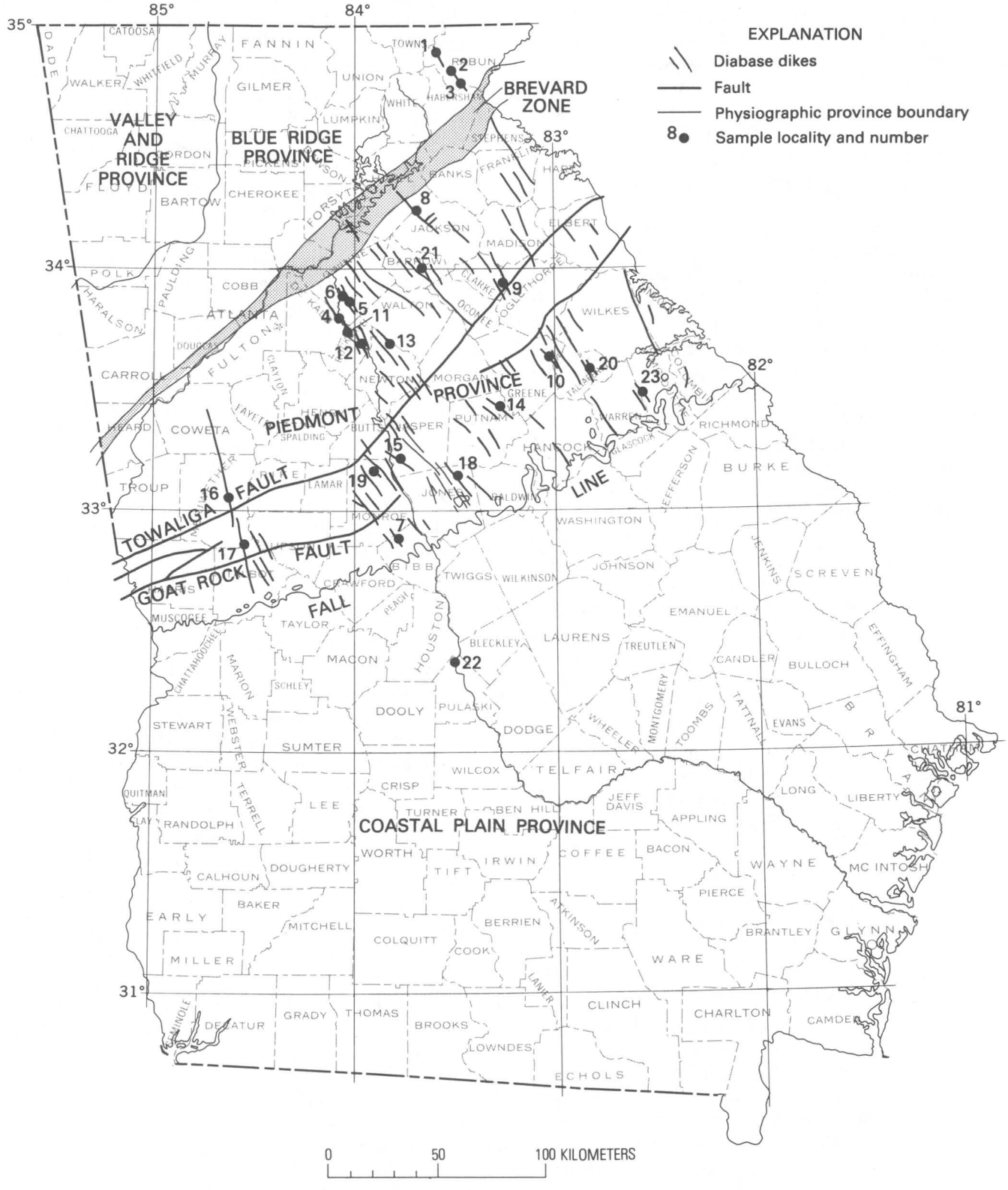

FIGURE 3.—The distribution (diagrammatic) of diabase dikes in Georgia (after Lester and Allen, 1950); sample localities are shown.

much more variable (Barnett, 1975; Gohn and others, 1978; Lanphere, 1983). As noted above, Lanphere has established an age of 184 m.y. by $^{40}Ar/^{39}Ar$ work for the basalt at Clubhouse Crossroads, a quartz-normative tholeiite (Gottfried and others, 1977, 1983) from the subsurface of South Carolina. Conventional K-Ar ages for diabase dikes in North Carolina are 173 m.y. (Watts and Noltimier, 1974) and 253 m.y. (Armstrong and Besancon, 1970), but Armstrong and Besancon recognized that excess ^{40}Ar was probably present in the sample having the 253-m.y. apparent age. The data available from the Southeastern United States indicate that early Mesozoic igneous activity began at the same time in this region as in the Northeastern United States, about 195 m.y. ago, and that emplacement of dikes occurred during a period of at least 25 m.y.

ANALYTICAL METHODS

Samples were collected for this study over a broad area within the Piedmont and Blue Ridge of Georgia (fig. 3). Three samples of diabase well cuttings from below the Coastal Plain sediments in Pulaski County were obtained from the Georgia Geologic Survey (GGS well 3137).

Fresh diabase samples were used for preparation of thin sections, and the rock chips from which the thin sections had been cut were then crushed (to less than 0.5 mm) to provide samples for K and Ar analysis. (The well cuttings, which appeared to be slightly altered, were similarly crushed.) The crushed rock was rinsed with distilled water, fine powder (less than about 0.05 mm) was decanted away, and the remaining material was dried in an oven at about 100°C. Separate portions, for the potassium analysis and the argon isotopic analysis, were taken from each sample with a sample splitter. The portion to be used for the argon analysis was weighed into a copper-foil capsule, dried overnight at 110°C, and then reweighed. The portion to be used for K analysis was not dried after weighing, but the dry mass of this portion was calculated by assuming that the percentage of mass lost upon drying would have been the same for both portions of the sample.

Samples to be analyzed for K were dissolved in a mixture of hydrofluoric and perchloric acids. After low heating overnight in covered Teflon[7] beakers, excess acids were removed by stronger heating in open beakers, leaving perchlorate salts. These were taken up in aqueous solution for measurement of potassium by atomic absorption spectrophotometry.[8] For most samples, two or more separate analyses for K were carried out. The data indicate that the coefficent of variation for repeated analyses is typically about one percent.

Sets of 6 to 12 samples in copper foil capsules were loaded into an apparatus for extraction and mass spectrometric analysis of Ar. Dooley (1977) has written a detailed description of the system. After evacuation of the system, each set of samples was baked overnight at about 200°C to reduce the amount of contaminating atmospheric Ar. The 200°C temperature was established by experiments in which the Ar released from diabase samples (collected from Virginia and Georgia) was examined after the samples were heated for three to four hours at each of several successively higher temperatures in the range 100°C to 400°C. Figure 4 shows the results of our experiments for a sample of diabase from Rockingham County, Va. On the basis of these observations and of procedures used in other laboratories, we chose 200°C as an appropriate temperature for overnight baking of the diabase samples. Unexpectedly, we found that at 200°C some Georgia diabase samples release Ar that has more ^{40}Ar than does atmospheric argon. We have interpreted this phenomenon (see below) as a release of extraneous ^{40}Ar rather than of radiogenic argon formed in place.

After an aliquant portion of argon from a reservoir of virtually pure ^{38}Ar had been admitted into the extraction system, Ar was released from a sample by melting it in a resistance-heated furnace. Water was removed from the gas mixture by a cold trap at −112°C (melting ethanol). A second cold trap in series with the first removed CO_2 and any other volatiles that condense at −196°C (liquid N_2). Reactive gases that pass the cold traps were removed by reaction with hot Ti, in two stages.

For isotopic analysis, a portion of the remaining gas was transferred by expansion (allowing enough time for Ar pressure equilibration) into a MS–10 mass spectrometer, similar to but slightly modified from that described by Farrar and others (1964). A small correction for mass discrimination (usually about 2 percent for the ratio of ^{36}Ar to ^{40}Ar) was applied to the measured ion beam currents; the magnitude of the correction was based on measurements of atmospheric Ar as the standard for Ar isotopic abundances. A slight memory effect was noticeable, since the mass spectrometer was operated in the static mode, but the magnitude of the memory effect and of other background signals usually was negligible.

[7]Any use of trade names is for descriptive purposes only and does not imply endorsement by the U.S. Geological Survey.

[8]The aqueous solution used to take up the samples and to dilute both sample and standard solutions to the appropriate range for potassium measurement (less than 5 mg/kg) was prepared in advance to contain 40 g HNO_3 and 1.0 g NaCl per kilogram of solution. The purpose of the NaCl was to minimize any differences in ionization interference between the sample solutions and the standard solutions. The standard solutions were prepared from KCl (ACS Reagent Grade). Seven solutions prepared from diabase were analyzed by the method of standard additions. These analyses confirmed that there are no systematic errors due to interference when sample and standard solutions are prepared in the way we have described.

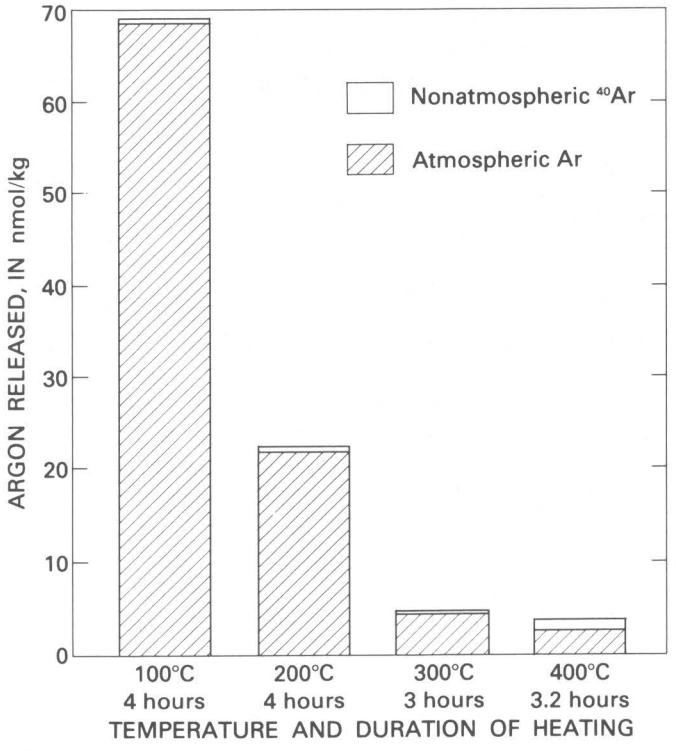

FIGURE 4.—Argon released from a Virginia diabase dike sample (MWD-21) at low temperatures.

After correction for mass discrimination (and, when necessary, for background or memory effects), the Ar isotope ratios were used to calculate the amounts of "radiogenic Ar" and "atmospheric Ar" by a conventional formula[9] (Dalrymple and Lanphere, 1969, p. 56–57). The coefficient of variation of the "radiogenic Ar" measurements, estimated from the observed differences between duplicate analyses, is typically about 1.5 percent. No "blank" correction has been applied to the measured amounts of "atmospheric Ar", but we know that most of the "atmospheric Ar" observed in the analyses of diabase came from the samples, not from the analytical system.

[9]The muscovite P–207 (a reference sample distributed by the U.S. Geological Survey) was used as a standard to calibrate the addition of ^{38}Ar. The radiogenic Ar content of P–207 was assumed to be 1.259×10^{-9} mol/g, the mean value of analyses in many laboratories reported by Lanphere and Dalrymple (1976a).

In the conventional procedure it is assumed that all ^{36}Ar measured is of atmospheric origin, that atmospheric ^{40}Ar is present in an amount 295.5 times the amount of ^{36}Ar, and that the remainder of the ^{40}Ar is *radiogenic*. Many of the diabase samples from Georgia contain extraneous Ar that is not of atmospheric composition, a circumstance that is not recognized in the derivation of the conventional formulas. The calculated amount of "radiogenic Ar" often included extraneous ^{40}Ar (excess ^{40}Ar) as well as radiogenic Ar formed from ^{40}K in place. To emphasize that the "radiogenic Ar" in diabase may include extraneous ^{40}Ar as well as radiogenic Ar formed in place, we shall often refer to such argon as "nonatmospheric Ar."

If extraneous Ar other than Ar from the atmosphere contains an appreciable amount of ^{36}Ar, then the amount of "atmospheric Ar" calculated will be greater than the amount of Ar actually derived from the atmosphere. Study of the Ar released at low temperature from some of our diabase samples suggests that the extraneous Ar (other than contamination from the modern atmosphere) in these samples has very little, if any, ^{36}Ar. If this is true for all samples, then the calculated amount of "atmospheric argon" represents correctly the amount of atmospheric contamination.

K-Ar APPARENT AGES

Table 1 is a compilation of the K and Ar measurements on diabase samples, apparent ages calculated from these data, and an estimate of the amount of excess ^{40}Ar in each sample. Site numbers are shown on figure 3. At sites where more than one sample is listed, samples have been collected from different positions across the width of a dike. (At site 1, samples were collected along strike as well as across the width.) The K and Ar contents listed in table 1 represent analyses of separate portions of each sample. Apparent ages have been calculated from the averages of the K and "radiogenic Ar" values for each sample. The uncertainties given for the apparent ages are based on an estimate of the analytical precision (at the 68 percent confidence level).

In addition to the diabase samples, we analyzed a number of related materials and interlaboratory reference samples (table 2). Three samples of quartz separated from country rock adjacent to dikes and three samples (amphibolites or separated hornblende) of country rock taken some distance from each of the three dikes are from Rabun County, Ga. Two samples are biotite separated from country rock near a dike in Warren County, Ga. The interlaboratory reference samples analyzed during this study of diabase are the LP–6 biotite (Ingamells and Engels, 1976) and the Arvonia Slate (Harper and others, 1973).

Figure 5 is a histogram of the K-Ar apparent ages produced in this study for diabase samples from Georgia. A large proportion (about one-half) of the samples have apparent ages greater than 235 m.y., and a few have apparent ages in excess of one billion years. The number of values observed within a class interval generally decreases as apparent age increases, in a pattern similar to that observed by Dalrymple and others (1975) for diabase in Liberia. As in Liberia, the K-Ar apparent ages of some dikes in Georgia are discordant at all levels of sampling; different whole-rock samples from the same dike have different apparent ages and different minerals from the same specimen have different apparent ages. The data show that many samples of diabase in Georgia contain extraneous ^{40}Ar and that the problem is of similar magnitude to that in Liberia where many of the dikes intrude ancient Precambrian rocks. There is no indication that the extraneous ^{40}Ar in the diabase samples is *inherited* ^{40}Ar (Dalrymple and Lanphere, 1969, p. 121–122), so we shall interpret this argon to be *excess* ^{40}Ar. Sutter and Smith (1979) used the $^{40}Ar/^{39}Ar$ method to show that small amounts of excess ^{40}Ar are present in diabase dikes in Connecticut and suggested that excess ^{40}Ar is the probable cause of discordance that has been observed among conventional K-Ar ages for diabase dikes of eastern North America.

TABLE 1.—*K-Ar results for diabase samples*

County	Site no.[1]		Sample[2]	K[3] (percent)	"Radiogenic Ar"[4] (percent)	"Radiogenic Ar"[4] (10^{-10} mol/g)	Apparent age[5] (m.y.)	Excess ^{40}Ar[6] (10^{-10} mol/g)
Rabun	1	(O)	TRD5	0.429	91.3	7.31	784±16	5.9
			TRD6	.255	88.9	5.20	905±18	4.4
			pyx-ol	.115	89.0	3.189	1,145±25	2.7
			plagioclase	.396	79.8	6.87	796±18	5.6
			TRD7	.483	94.0	5.90	595±12	4.3
			TRD8	405	91.0	5.93	693±14	4.6
			TRD12	.428	94.7	17.36	1,500±30	16.0
	2	(O)	TRD16	.443 .494	45.6 91.3	7.13 6.83	703±12	5.4
	3	(O)	TRD24A	.392, .418	89.7	6.31	729±12	5.0
			pyx-ol	.170	82.6	2.235	633±14	1.7
			plagioclase	.553	92.2	7.90	679±14	6.1
			TRD25	.471	95.7	5.62	583±12	4.1
			TRD27	.365	80.6	3.510	484±11	2.3
			TRD28	.368	75.3	4.345	578±13	3.1
DeKalb	4	(Q)	D4	.456, .462	81.4	2.632	304±7	1.1
			D5	.406 .418	68.8 82.0	2.161 2.236	284±5	.8
			D6	.387	58.3	1.777	247±6	.5
			D9	.371	65.2	1.767	256±6	.5
Gwinnett	5	(O)	G2	.451, .460	85.7	1.582	190±4	.1
			G3	.467 .481	88.1 87.0	1.824 1.855	211±3	.3
	6	(O)	G8	.173 .177	62.5 64.3	.977 1.010	301±5	.4
Bibb	7	(O)	Bi4	.144 .167	54.8 24.6	.605 .563	205±6	.1
Jackson-Hall	8	(O)	JH3	.226 .230	61.9 69.5	1.929 1.961	435±7	1.2
Clarke	9	(O)	C3	.253, .244 .245	95.3 95.0	11.28 11.40	1,628±25	10.5
Greene	10	(O)	Gr7	.109 .110	55.8 47.5	.456 .440	222±5	.1
Rockdale	11	(Q)	R9	.469, .470 .468	77.2 61.8	1.667 1.668	194±3	.1
	12	(Q)	R18	.503, .522 .505	83.8 75.7	2.424 2.365	252±4	.7
Newton	13	(Q)	N3	.655, .663 .645	85.9	2.346	196±4	.2
Putnam	14	(O)	P2	.202, .206	75.6	.946	249±5	.3
Jasper	15	(O)	Ja9	.211, .235 .217	45.4	.926	227±5	.2
Meriwether	16	(Q)	Me13	.377, .367 .361, .370	85.0 88.6	1.288 1.331	194±3	.1
Talbot	17	(Q)	T8	.438 .456	83.5 88.1	1.858 1.808	222±4	.4
Jones	18	(Q)	Jo7	.519	82.5	1.827	192±4	.1
Monroe	19	(O)	M8	.285 .281	75.0 71.4	1.192 1.214	230±4	.2
Taliaferro	20	(O)	Ta12	.185 .185 .190	74.1 66.4 47.0	.669 .650 .649	192±2	.1

See footnotes at end of table, p. M12.

TABLE 1.—*K-Ar results for diabase samples*—Continued

County	Site no.[1]		Sample[2]	K[3] (percent)	"Radiogenic Ar"[4] (percent)	"Radiogenic Ar"[4] (10^{-10} mol/g)	Apparent age[5] (m.y.)	Excess ^{40}Ar[6] (10^{-10} mol/g)
Barrow	21	(O)	B11	.387	90.9 88.6	3.956 3.937	509±7	2.7
Pulaski	22		GGS4780	.239	16.9	.812	186±12	.1
			GGS4820	.208	14.8	.772	202±15	.1
			GGS4850	.299	15.6	1.151	209±14	.2

[1] The letter in parentheses following a site number indicates the chemical class of the diabase at the site: O, olivine-normative diabase; Q, quartz-normative diabase.

[2] Whole-rock diabase samples are indicated by alphanumeric symbols. Minerals separates from two rocks are listed, in each case immediately following the rock sample from which they were separated. Pyx-ol, pyroxene-olivine.

[3] Potassium content is the mass fraction of potassium in the sample, expressed as a percentage.

[4] The percentage of "radiogenic Ar" is the fraction of the measured ^{40}Ar that is not "atmospheric Ar". In computing the fraction of ^{40}Ar that is "atmospheric Ar" we have assumed that all ^{36}Ar in these samples is from the atmosphere.

[5] Constants used to calculate apparent ages: $\lambda_e = 0.581 \times 10^{-10}$/yr, $\lambda_\beta = 4.962 \times 10^{-10}$/yr, n (^{40}K)/n (K) = 0.0001167. The range of uncertainty is based on an estimate of the analytical precision at the 68 percent confidence level.

[6] The amount of excess ^{40}Ar is an estimate based on an assumed age of 180 m.y. for each of the diabase dikes of Georgia.

The results of our study support the idea that excess ^{40}Ar is commonly present in diabase dikes.

Many of our diabase samples (about one-half) have apparent ages less than 235 m.y., and for these we cannot use geologic relationships to show if excess ^{40}Ar is present. In only one of these cases did we analyze more than one sample per dike, so we do not know if discordant K-Ar relationships exist in most of the dikes with apparent ages less than 235 m.y. Apparent ages of two samples from site 5 are discordant. If excess ^{40}Ar causes this discordance (as we suspect), then even sample G2, apparent age 190 m.y. (less than that of any other dike in this study), must be suspected of containing a small amount of excess ^{40}Ar. We consider it likely that none of the diabase dikes in Georgia is entirely free of contamination by excess ^{40}Ar.

Because of uncertainty about the amount of excess ^{40}Ar that may be present in a diabase sample, the K-Ar apparent age can be used only for setting an earlier limit on the date of formation of a dike, and differences in apparent age cannot be related to real differences in the ages of the diabase dikes in Georgia. In spite of these limitations, our K-Ar data may be interpreted as providing direct evidence that these dikes formed early in the Jurassic Period. Samples from six different dikes in the Georgia Piedmont (nearly one-third of the dikes studied) have apparent ages in the range 190–196 m.y. That the apparent ages of these six samples are quite closely clustered, relative to the other data from Georgia, may be significant. The apparent ages for these samples may be closely clustered because these samples have been affected only minimally by excess ^{40}Ar. This interpretation of our K-Ar data leads to the conclusion that these six dikes are Early Jurassic in age. (The im-

TABLE 2.—*K-Ar results from country rocks and reference samples*

[Quartz samples were separated from country rock collected immediately adjacent to dikes; whole-rock amphibolite samples were collected 3 km north of site 1 in Blue Ridge province; hornblende was separated from amphibolite collected about 0.5 km south of site 1. The biotite samples from site 23 were collected by James W. Smith and analyzed by J. M. Wampler for the Georgia Geologic Survey in 1972. JWS-1M was separated from country rock immediately adjacent to a dike in Warren County. JWS-3CHLW was separated from country rock 15 m from the dike.]

Site no.	Sample	Material	K[1] (percent)	"Radiogenic Ar"[1] (percent)	"Radiogenic Ar"[1] (10^{-10} mol/g)	Apparent age[1] (m.y.)
		Samples from country rock				
1	TRD10-CR	quartz	0.048	63.9	0.452	-------
	TRD20-CR	quartz	.036	76.2	.311	-------
	TRD2A	amphibolite	.137	66.6	1.038	391±10
	TRD1A	amphibolite	.128	61.3	1.026	412±10
	WRG-1HH	hornblende	.246	95.6	1.289	279±6
2	TRD21-CR	quartz	.013	26.3	3.715	-------
23	JWS-1M	biotite	6.86	92.1	27.35	216±4
	JWS-3CHLW	biotite	7.84	98.4	39.53	270±5
		Interlaboratory reference samples				
	LP-6	biotite 40–60 mesh[2]	8.37, 8.26, 8.31	93.6 97.1	18.92 19.35	128±2
	Arvonia Slate	A.2	3.35, 3.33, 3.35	95.8 98.8	18.41 18.57	294±4

[1] See table 1 for information about column headings.
[2] Subsamples of portion 7-II-A-8 were analyzed.

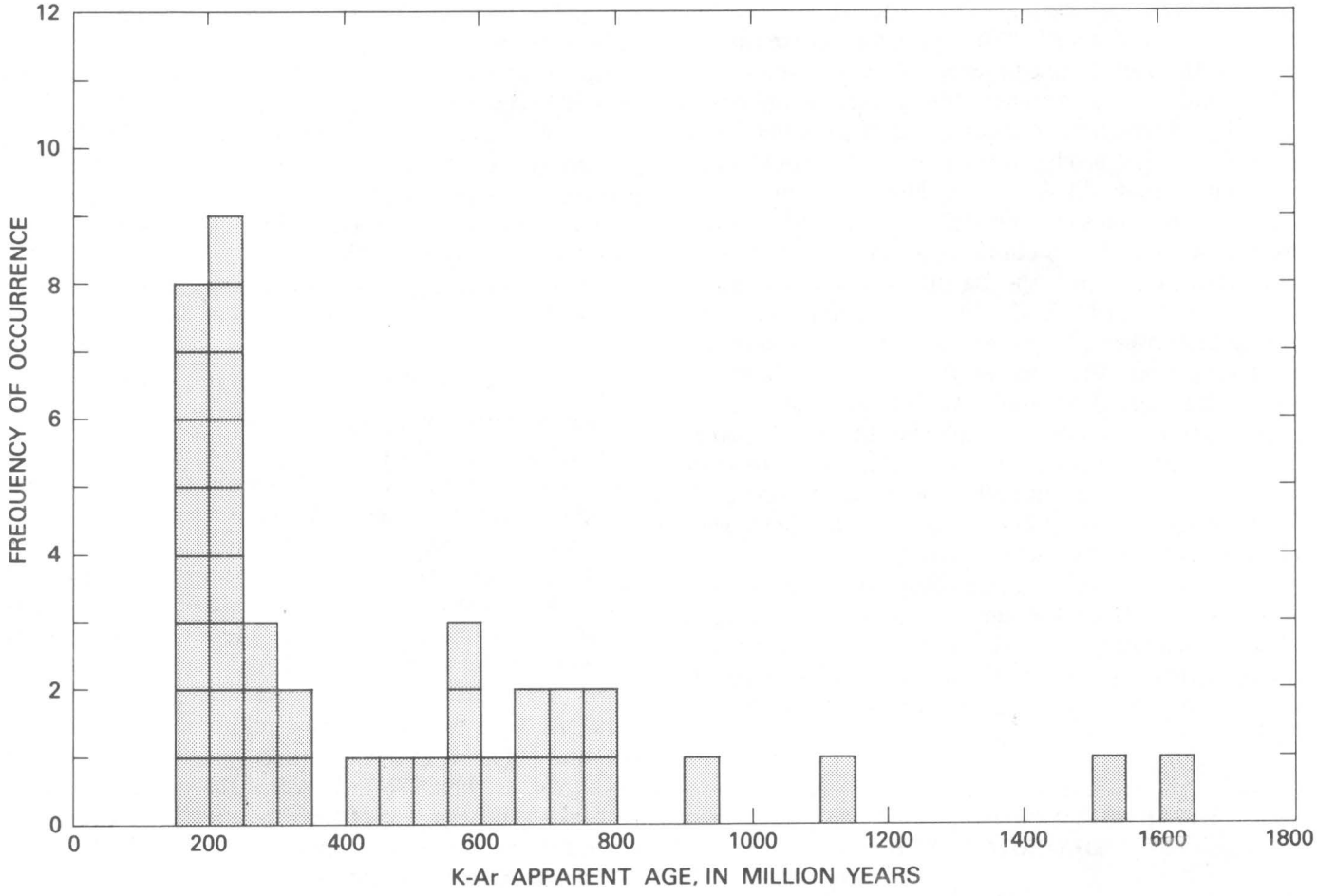

FIGURE 5.—Graph of K-Ar apparent ages of diabase dike samples from the Georgia Piedmont and Blue Ridge.

precise K-Ar ages that we obtained on well cuttings of a subsurface diabase sill in Pulaski County indicate that the sill is of similar age.)

Dooley (1977) used modal and chemical analyses as a basis for determining the chemical classification of the dikes in this study to test for correlations with age; these determinations have since been confirmed by additional chemical analyses (Meadows, 1979). All four types of tholeiite (as classified by Weigand and Ragland, 1970, and Smith and others, 1975) were found in Georgia. The samples that have apparent ages greater than 400 m.y. are from five olivine-normative dikes. Of the six samples having apparent ages in the 190–196 m.y. range, four are from quartz-normative dikes and two are from olivine-normative dikes. Because of the general problem with excess Ar, our data cannot be used to evaluate the idea that there is a difference in age between the dikes of the two main chemical classes, olivine- and quartz-normative tholeiites. It is important to note that the time involved within a single period of intrusion and differentiation of a basaltic magma is relatively short compared to the time intervals that K-Ar dating or paleomagnetic methods can resolve.

The paleomagnetic data of Watts (1975) and the structural similarities among the dikes in Georgia and those in neighboring States indicate that the postorogenic tholeiitic dikes of the southern Appalachian region are broadly contemporaneous. The pattern of dike trends in the circum-Atlantic system and the paleomagnetic and radiometric data discussed above suggest that the entire system formed during a period of time that corresponds approximately to the Early Jurassic Epoch. [The geochronometric range of the Early Jurassic is approximately from 195 m.y. ago to 175 m.y. ago, according to van Hinte's (1976) time scale adjusted to reflect the new values for the decay constants and isotopic abundance of ^{40}K.] Although samples from two-thirds of the dikes we studied have apparent ages greater than 200 m.y., there is no reason to believe that any of the dikes are more than 200 m.y. old.

May (1971) suggested that the stress field the produced the circum-Atlantic system of dikes developed

immediately before breakup of the continents. According to Smith and Noltimier (1979), rifting and magmatism in the early Mesozoic basins preceded the actual separation of the continents by at least 15 m.y. Sutter and Smith (1979) found evidence of a period of magmatism about 180 m.y. ago that produced the narrow dikes of Connecticut (and other dikes in the Northeastern United States). These dikes cut the Hartford basin and extend into the surrounding metamorphic terrane for tens of kilometers away from the basins. The dikes exposed north of the Fall Line in Georgia are similarly intrusive into metamorphic terrane and extend a few hundred kilometers from the nearest (buried) early Mesozoic basin. This structural similarity between the dikes in Georgia and the 180-m.y.-old dikes in the Northeastern United States, and consideration of the overall tectonic regime that produced the dikes of the circum-Atlantic system, might be used to infer that the dikes in Georgia are most likely about 180 m.y. old.

The radiometric data of this study do not allow us to put narrow limits on the ages of the dikes in Georgia, but they do indicate that some of the dikes are Early Jurassic in age. On the basis of other considerations, we infer that all the dikes formed between about 195 and 170 m.y. ago.

DISTRIBUTION OF EXCESS ^{40}Ar IN GEORGIA DIKES

General

The information obtained in this K-Ar study of diabase dikes in Georgia shows that excess ^{40}Ar contamination is a major problem in determining ages. Many of the diabase samples of this study were formed not under the ideal conditions assumed for conventional K-Ar calculations (Damon, 1970) but rather in environments that could maintain a significant Ar partial pressure. The wide range in apparent ages indicates a quite variable distribution of excess ^{40}Ar in the diabase dikes.

To examine the distribution of excess ^{40}Ar in the diabase dikes of Georgia, we have estimated the amount of excess ^{40}Ar in each diabase sample by assuming that all of the dikes are 180 m.y. old. The estimated amount of excess ^{40}Ar, in the last column of table 1, is the difference between the measured "radiogenic Ar" and the amount of radiogenic Ar that would have been formed by decay of ^{40}K in place during the past 180 m.y. If a dike is actually older than 180 m.y., then the estimate of excess ^{40}Ar will be too high, but the uncertainty is of little consequence except for those samples having only a small amount of excess ^{40}Ar. For example, the estimated amount of excess ^{40}Ar in a dike having 0.3 percent K would be too high by only 0.1×10^{-10} mol/g if the age were really 195 m.y. instead of 180 m.y. as we have assumed.

Figure 6 presents graphically the estimates of excess ^{40}Ar for diabase samples from Georgia dikes. The diagram is a plot of the total nonatmospheric Ar in each diabase sample against its K content. A 180-m.y. reference isochron is plotted to show the radiogenic Ar that would have been produced (for a given K content) by radioactive decay of ^{40}K during the past 180 m.y. The distance each sample lies above this isochron represents our estimate of its excess ^{40}Ar content.

Regional Distribution of Excess ^{40}Ar

Diabase dikes having apparent ages greater than 235 m.y. are mostly in the northern part of the Georgia Piedmont and in the Blue Ridge Mountains (Rabun County). Samples from the dikes in Rabun County consistently have large amounts of excess ^{40}Ar (table 1), more than 2×10^{-10} mol/g. One sample has 16×10^{-10} mol/g of excess ^{40}Ar, more than any other diabase sample in this study. Large amounts of excess ^{40}Ar also were found in diabase samples from the northeastern part of the Piedmont ($1.2\text{–}10.5\times10^{-10}$ mol/g). Smaller amounts of excess ^{40}Ar were found in diabase dike samples from near Atlanta, but some of these samples have calculated K-Ar ages greater than 235 m.y. All of the diabase samples from the southern half of the Piedmont have estimated excess ^{40}Ar contents less than 0.4×10^{-10} mol/g.

A regional trend in the distribution of excess ^{40}Ar is evident in the diabase dikes of Georgia, even though the amount of excess ^{40}Ar can vary greatly in different samples of one dike (see below) and even though we did not obtain strictly comparable samples from each of the different dikes. When only one sample from a dike was analyzed, we usually chose a sample from near one contact, on the assumption that such a sample would be more representative of the whole dike composition than would a sample from near the center (which might be more strongly differentiated). In spite of the uncertainty about how closely one sample represents the composition of an entire dike, there are enough samples overall to show a clear trend from large amounts of excess ^{40}Ar in dikes of the northern Piedmont and Blue Ridge to little or no excess ^{40}Ar in dikes of the southern Piedmont.

Local Distribution of Excess ^{40}Ar

The distribution of excess ^{40}Ar within an individual diabase dike can be quite variable, showing large differences among whole-rock samples taken from different parts of a dike and also large differences on the microscopic scale among different minerals. The latter variation is generally understandable in terms of differences in atomic structure of the minerals, but the

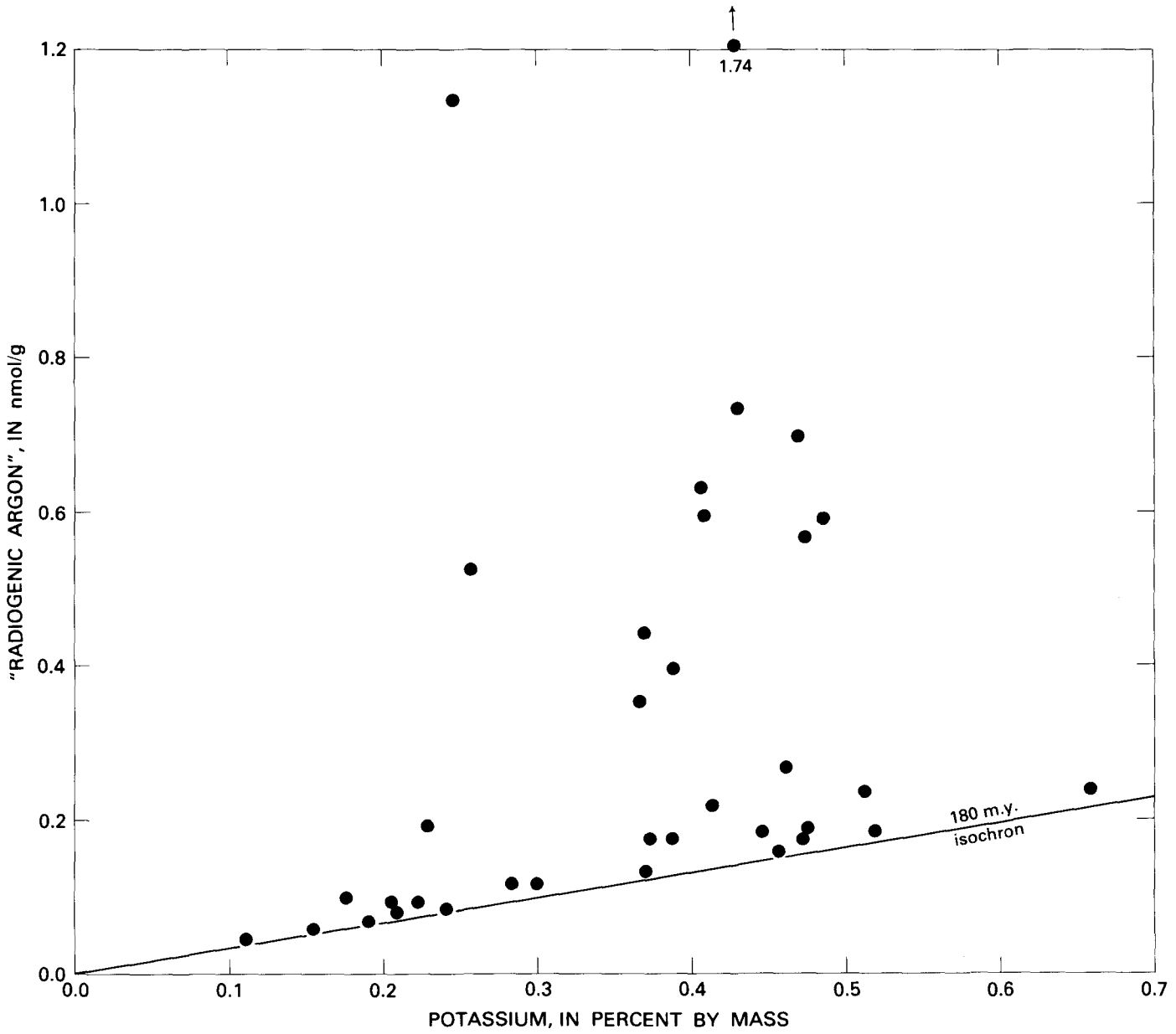

FIGURE 6.—"Radiogenic Ar" content plotted against K content for diabase samples from Georgia. The 180-m.y. isochron is shown for reference.

variation among different whole-rock samples (within the same dike) may be influenced by many factors. Studies of the distribution of excess ^{40}Ar in relation to the position and petrographic character of diabase samples should help one to define the behavior of argon in the environment of crystallization and cooling of diabase.

In a previously reported study of a narrow (1-m-wide) dike in Gwinnett County, Ga. (Dooley and Wampler, 1978), we found the excess ^{40}Ar content of the rock to be uniform in samples from the chilled margin but more than ten times as great in a sample from the center. Multiple samples from sites 1, 3, 4, and 5 (see fig. 3 and table 1) were analyzed in this study; although some samples were taken from near dike margins, none was considered to be part of a chilled margin. The dikes at these locations were 3–30 m wide, and excess ^{40}Ar content does not vary greatly among samples taken across the width of any of these dikes. (Sample TRD12 at site 1 has a much higher excess ^{40}Ar content than do other samples at this location. This sample was taken from the center of the 3-m-wide dike about 70 m along strike from the other samples at site 1.) At sites 3 and 4 the most excess ^{40}Ar is in a sample from near the center of each

dike; however, at sites 1 and 5, samples from near the centers have less excess ^{40}Ar than do those from near the margins of the dikes. In these rather wide dikes (3–30 m), it appears that the excess ^{40}Ar content is not highly variable across the width of the dikes. Except at site 5, where the amount of excess ^{40}Ar in the diabase is small, the greatest apparent ages observed in sets of samples from across the widths of dikes are for samples taken at or near the center.

That excess ^{40}Ar is more concentrated in feldspar than in the ferromagnesian minerals has been established by earlier work (for example, see Dalrymple and others, 1975). Although our mineral separates were not completely pure, the amounts of excess ^{40}Ar are larger in the plagioclase fractions than in the pyroxene-olivine fractions (table 1). However, the ratio of excess ^{40}Ar to K (which is directly related to the apparent age) is not as variable as is the amount of excess ^{40}Ar and is not consistently greater in one fraction than in another. Similar results were obtained by Dalrymple and others (1975) for Liberian diabase dikes.

We examined a few country-rock samples associated with the dikes in Rabun County, where the largest amounts of excess ^{40}Ar in diabase were observed, to see if high ^{40}Ar content is characteristic of the country rock there (table 2). Only one of three quartz samples, separated from gneiss very near contacts with diabase (within 1 or 2 cm), had an ^{40}Ar content comparable to the level of excess ^{40}Ar in the dikes. Some of the ^{40}Ar in the quartz separates is associated with K (impurities within the quartz), but most of it may be viewed as excess ^{40}Ar. It is not known whether this Ar was assimilated during intrusion of diabase or during prior regional metamorphism.

Three samples of country-rock material from the vicinity of the Rabun County dikes, but not close enough to the dikes to have been appreciably influenced by the thermal effects of the intrusions, were examined to see if the country rock has an unusually high ^{40}Ar content. The K-Ar apparent ages correspond to middle to late Paleozoic time. The discordance among these samples of low K content may be a product of incomplete outgassing before late Paleozoic cooling of this region (Rabun County). In any case, the ^{40}Ar content of these rocks is small relative to that of the dikes.

Low-Temperature Release of Nonatmospheric Ar

In a study intended to establish how contaminating atmospheric Ar is released during heating of diabase, we discovered that some Georgia diabase samples release nonatmospheric Ar at unusually low temperatures and that the amount of nonatmospheric Ar released at these temperatures is related to the amount of excess ^{40}Ar in a diabase sample (Dooley and Wampler, 1977b). Figure 4 shows what we interpret to be a normal pattern of release of contaminating atmospheric argon. This pattern is typical of the Ar released, at low temperatures, from several diabase samples from Rockingham County, Va., an area where we have no evidence of excess ^{40}Ar in diabase. Only atmospheric Ar was released during periods (3 to 4 hours each) of heating at temperatures as high as 300°C. At 400°C a small amount of radiogenic argon was released.

In contrast to the samples from Virginia, relatively large amounts of nonatmospheric Ar were released from some Georgia samples, beginning even at 200°C. Figure 7 shows the $^{40}Ar/^{36}Ar$ ratio as a function of release temperature for two samples, one of which (C3) contains a large amount of excess ^{40}Ar (about 10.5×10^{-10} mol/g) whereas the other (Me13) has little excess ^{40}Ar (about 0.1×10^{-10} mol/g). Note that a sawed block of each diabase sample (C3 and Me13), as well as crushed samples, was studied. There is little difference in the character of the Ar released from the samples in the two different forms, so the anomalous release of nonatmospheric Ar at low temperature is not an artifact of the crushing.

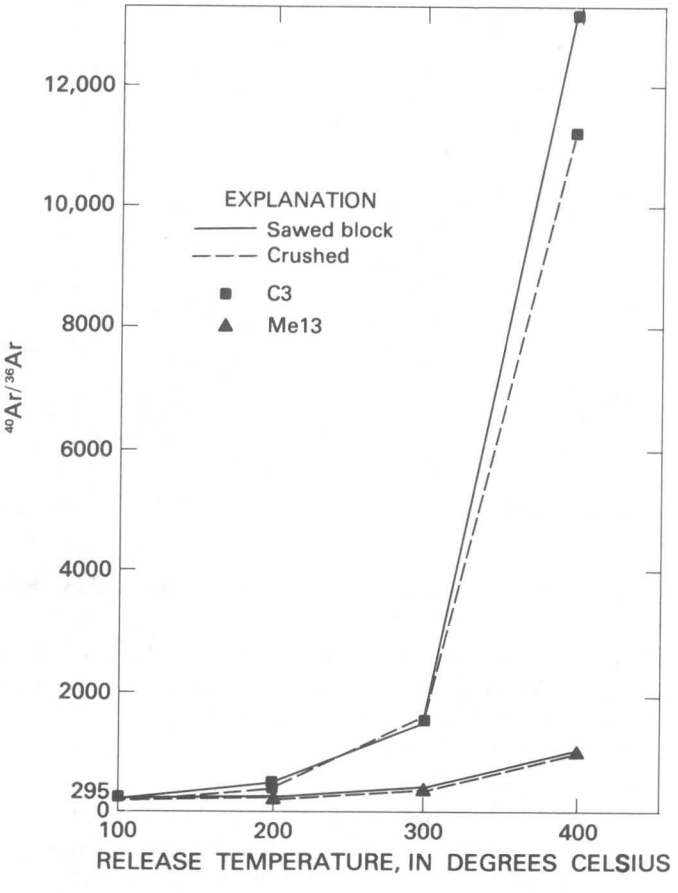

FIGURE 7.—$^{40}Ar/^{36}Ar$ ratios of argon released from samples C3 and Me13, plotted against temperature.

Figures 8, 9, and 10 show the amount of Ar released during each heating step from samples C3 and Me13 and from another sample (D4) that has an excess ^{40}Ar content intermediate between those of C3 and Me13. The shaded and unshaded portion of each bar together represent the total Ar released at each temperature. The ratio of nonatmospheric ^{40}Ar to atmospheric Ar is based on the isotopic composition of the Ar released. (As before, we have assumed that all ^{36}Ar measured is of atmospheric origin and that atmospheric ^{40}Ar is present in an amount 295.5 times the amount of ^{36}Ar.)

Sample Me13 (fig. 8) was heated for about 20 hours at each of the successively higher temperatures. The pattern of atmospheric Ar release from Me13 (shaded portions of bars) is quite similar to that for the Virginia diabase sample (fig. 4), although the amounts are smaller. The $^{40}Ar/^{36}Ar$ ratio of the argon released from Me13 at 100°C and at 200°C indicates that the argon is entirely atmospheric, but a small amount of nonatmospheric ^{40}Ar appeared at 300°C. At 400°C, two-thirds of the Ar released is apparently nonatmospheric ($^{40}Ar/^{36}Ar = 986$).

Three different mechanisms might contribute to the high $^{40}Ar/^{36}Ar$ ratio of the Ar released from Me13 at 400°C. These mechanisms are:

1. Release of a small residual fraction of atmospheric argon that has been enriched in ^{40}Ar by isotopic fractionation;
2. Release of radiogenic argon formed by decay of ^{40}Ar in place;
3. Release of excess ^{40}Ar.

A consideration of the amount and isotopic composition of argon released from Me13 at each different temperature indicates that isotopic fractionation cannot be a significant contributor to the high $^{40}Ar/^{36}Ar$ ratio. The nonatmospheric Ar released at 400°C might be largely radiogenic Ar formed by decay of ^{40}K in place, but, if so, this Georgia diabase sample must contain materials that release radiogenic argon more readily than do any in the Virginia diabase samples. The importance of the third mechanism, release of excess ^{40}Ar, is shown by the release of argon from two other Georgia diabase samples, which contain larger amounts of excess ^{40}Ar.

Nearly half of the Ar released from sample D4 (fig. 9) at 200°C is nonatmospheric, and at 300°C and 400°C most of the Ar released is nonatmospheric. The quantity of nonatmospheric Ar released from D4 is considerably greater than that released from Me13 (fig. 8). Even larger amounts of nonatmospheric Ar were released from sample C3 (fig. 10) when heated in the range 200–400°C. In contrast to the Virginia diabase samples, from which not more than one percent of the radiogenic Ar was released during heating at 400°C (and below),

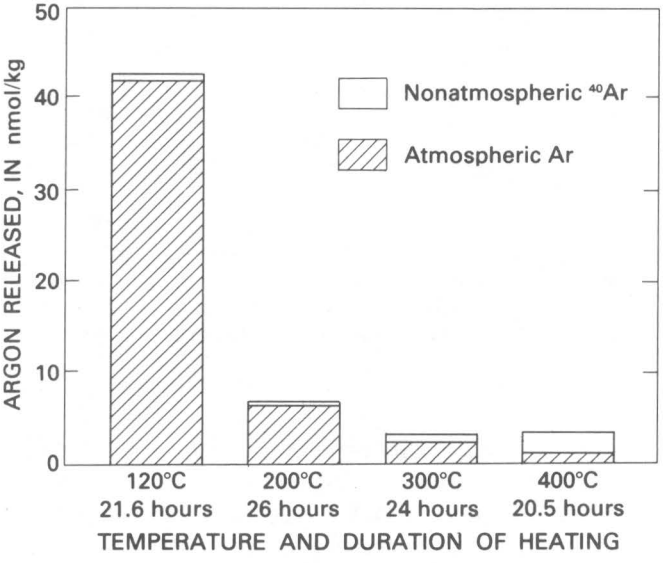

FIGURE 8.—Argon released from sample Me13 at low temperatures.

these samples lost significant fractions of their nonatmospheric Ar during heating in the range 200–400°C. Nearly 8 percent of the nonatmospheric Ar in D4 and 13 percent of the nonatmospheric Ar in C3 had been released by the end of the 400°C heating interval. The amount of nonatmospheric Ar released at low temperatures is related to the amount of excess ^{40}Ar present in a sample.

In addition to the data presented here, we have obtained information on the kinetics of the low temperature release of ^{40}Ar and ^{36}Ar from Georgia diabase samples. The kinetic data indicate that the nonatmospheric Ar released at 400°C and below does not diffuse out of minerals but rather is Ar that has somehow been trapped between mineral grains or in structural irregularities such as microfractures or fluid inclusions. An example of the kinetic data which led to this conclusion has been presented in a short paper (Dooley and Wampler, 1978). A pulse of Ar, almost entirely nonatmospheric, was released from a portion of sample C3 almost immediately (within the first ten minutes) upon heating to 400°C. We have interpreted the rapid release of Ar at low temperatures to be a result of differential thermal expansion which allows previously isolated structural irregularities to become open.

The procedures were not entirely the same for the low-temperature release experiments on different samples. Samples D4 and MWD-21 were heated for about four hours at each temperature, whereas samples C3 and Me13 were heated overnight at each temperature. However, the kinetic data show that most of the Ar released at any temperature comes out rapidly enough that there is not a great difference in the results

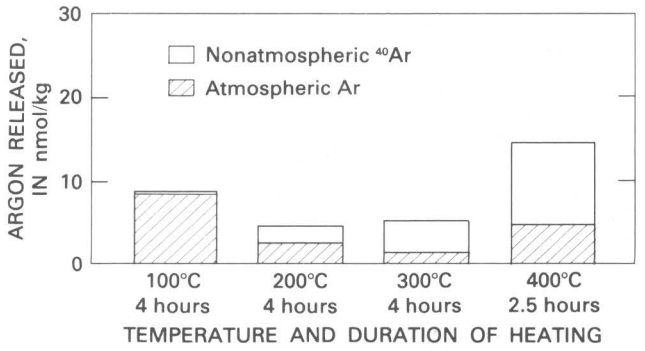

FIGURE 9.—Argon released from sample D4 at low temperatures.

whether the heating interval is four hours or overnight at each temperature. A considerable percentage of the excess ^{40}Ar, up to about 15 percent for the samples shown above, can be released from diabase in a short time by heating to 400°C.

Low-temperature release of nonatmospheric Ar is related to the earlier observation that diabase samples with excess ^{40}Ar tend to show high ^{40}Ar/^{39}Ar ratios in the lowest temperature portions of the age spectra obtained by stepwise heating (Lanphere and Dalrymple, 1976b). Ar released at these low temperatures is not correlated with K within the rock. Thus the anomalous release of nonatmospheric Ar at 400°C and below should be a good indicator of the presence of excess ^{40}Ar in diabase. Sample Me13 released 2.7 percent of its total nonatmospheric Ar during the low-temperature heating experiments. We believe that Me13 contains a small amount of excess ^{40}Ar, even though Me13 has one of the lowest K-Ar apparent ages, 194 m.y., observed for Georgia diabase in this study. This has contributed to our conclusion (see above) that none of the diabase dikes in Georgia is likely to be entirely free of contamination by excess ^{40}Ar.

DISCUSSION

Systematic variations in the occurrence of excess ^{40}Ar within the diabase dikes of Georgia are seen at the regional scale, the local outcrop scale, and the microscopic scale. We shall consider the possible sources of excess ^{40}Ar and the mechanisms by which it may become trapped in diabase.

On a regional scale, variability in excess ^{40}Ar in diabase could represent (1) differences in the environment at the source of magma, (2) differences in the evolution of magma before emplacement, or (3) differences in the environment of emplacement. Although each of these factors may contribute to observed variations in the amount of excess ^{40}Ar in diabase dikes, we may be able to judge which factor is most important.

The K content of mantle rock, the history of previous degassing, and the degree of partial melting during

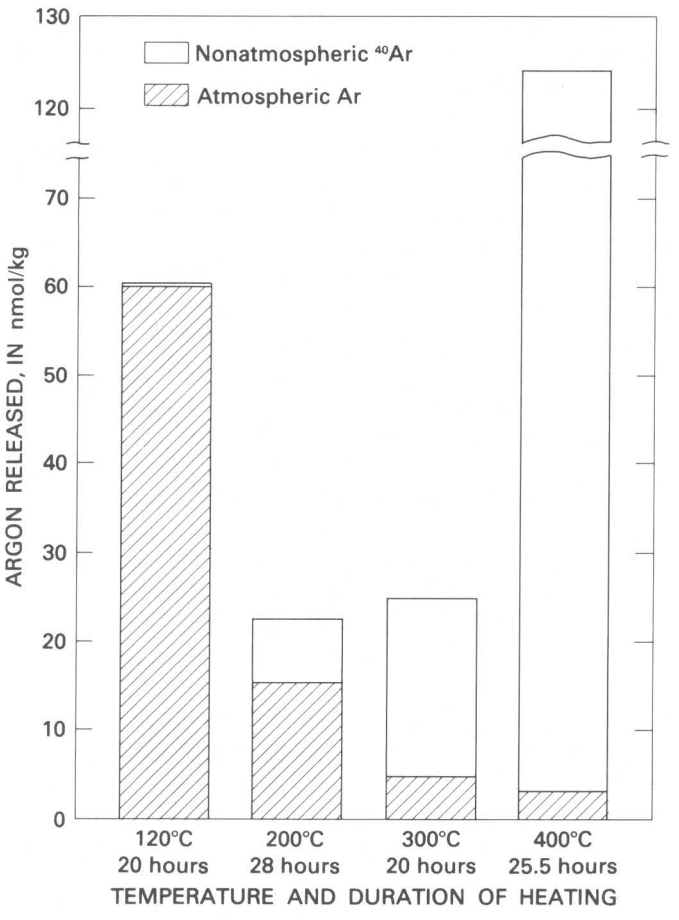

FIGURE 10.—Argon released from sample C3 at low temperatures.

magma formation are factors that would influence the amount and isotopic composition of argon incorporated into a magma at its source (Dymond and Hogan, 1978). In addition to probable lateral variations in the Ar content of mantle rock, there are likely to be variations in Ar content and degree of partial melting that depend on the depth of the magma source. The depth at which basaltic magma forms (Green and Ringwood, 1967; Yoder, 1976, p. 44–56) is largely dependent on temperature, pressure, and volatile content. Temperature and pressure are strongly influenced by the tectonic regime in the overlying crust and by tectonic movements of the crust relative to the mantle. Early Mesozoic tectonic activities, particularly crustal thinning associated with rifting (Ross and Schlee, 1973), must have been important in determining the depth at which basaltic magma formed in the mantle.

Although there are many factors that might cause variation in the amount and isotopic composition of Ar in a basaltic magma as it is formed by partial melting in the asthenosphere, we do not yet have evidence that large or variable amounts of Ar are associated with basaltic magma at its source in the mantle. On the con-

trary, Dymond and Hogan (1978) presented evidence for a rather striking consistency in the distribution of ^{40}Ar in deep-sea basaltic magma. A number of modern, deep-sea basalt glasses studied by Dymond and Hogan (1978) and Fisher (1975) contain about 1×10^{-10} mol/g of nonatmospheric ^{40}Ar mixed with varying amounts of atmospheric argon. The diabase dikes in the southern portion of the Piedmont of Georgia have less than 1×10^{-10} mol/g excess ^{40}Ar, so a mantle origin for any excess ^{40}Ar in these dikes should not be ruled out.

Many diabase dike samples from the northern Piedmont and Blue Ridge of Georgia contain excess ^{40}Ar in amounts greater than 1×10^{-10} mol/g (as much as 16×10^{-10} mol/g). If the amount of mantle-derived ^{40}Ar were only about 1×10^{-10} mol/g, then most of the excess ^{40}Ar in these dikes would have been derived from the crust. Whatever the mechanism of contamination by crustal argon, the degree of contamination should depend, to a large degree, on the K content and effective age (the time elapsed since last degassing) of the crust and temperatures within the crust. If contamination occurs primarily during ascent of the magma, then the character of the deep crust should be important. If the contamination occurs at the site of emplacement, then the character of the rock at that level in the crust will determine the amount of excess ^{40}Ar.

Dalrymple and others (1975) inferred that extraneous ^{40}Ar in the diabase dikes in Liberia probably was not contained in the magma but was derived from the country rocks at the site of emplacement. In support of this idea, they noted that excess ^{40}Ar was abundant in dikes emplaced within the Precambrian basement rocks but absent from diabase dikes emplaced in Paleozoic sandstone. They observed that excess ^{40}Ar was particularly abundant in late-forming materials in the diabase dikes and suggested that this association indicated progressively greater contamination of the system with Ar derived locally from the country rocks by heating.

In Georgia, we see no clear relationship between the character of the country rocks at the site of dike emplacement and the amount of excess ^{40}Ar present in diabase. The diabase dikes intrude rocks that were formed or metamorphosed in the Paleozoic Era. K-Ar ages of micas and hornblendes from the Piedmont of Georgia are nearly all in the range 250–400 m.y. (Smith and others, 1969; Stonebraker, 1973; Dallmeyer, 1978). It is unlikely that the metamorphic rocks as a whole would have retained Ar more effectively than did the hornblende, so the time period for Ar to accumulate in the country rocks, before the dikes were emplaced early in the Mesozoic Era, was not more than a few hundred million years. Our data on country rocks in Rabun County (see table 2) indicate that the same is true for this part of the Blue Ridge, although Dallmeyer (1975b) found Proterozoic Z K-Ar cooling ages for Grenville-age basement rocks farther to the west (more than 50 km from the location of any of the diabase samples in this study). Of particular importance is our observation that the amounts of radiogenic argon in samples of country rock in Rabun County (table 2) are less than the amounts of excess ^{40}Ar in the Rabun County dikes (table 1).

Although there is no clear relationship in Georgia between the amount of excess ^{40}Ar in diabase and the character of the country rock at the site of emplacement, the regional pattern of excess ^{40}Ar does relate to variations in the character of the crust on a larger scale. Figure 11 is a map on which a straight line separates a southern region, where the amount of excess ^{40}Ar is less than 0.5×10^{-10} mol/g in all diabase samples, from a northern region, where most samples have more than 0.5×10^{-10} mol/g excess ^{40}Ar. This line coincides approximately with the Piedmont gravity gradient, which marks the boundary between a region of relatively thick crust to the northwest and a region of relatively thin crust to the southeast (Long, 1979). The dikes that have significant quantities of excess ^{40}Ar are in a region where the crust is relatively thick but where the surface rocks represent thin (less than 8 km) allochthonous sheets (Cook and others, 1979). A distinct gravity low in Rabun County suggests that the crust may be particularly thick there.

Most of the crust (from a depth of about 10 km to about 40 km) underlying the region where the diabase dikes have significant amounts of excess ^{40}Ar is thought to be Precambrian basement rock, presumably of Grenville age. Possibly a considerable portion of the lower crust in this region was not degassed by Paleozoic metamorphism and has retained Ar for as long as a billion years. The excess ^{40}Ar in the diabase dikes of this region may result from ascent of magma through such ancient basement rocks. It seems reasonable that Ar should be more easily derived from deep crustal rocks, during the ascent of magma, than from rocks at the site of emplacement. Ponding of magma in the deep crust (Weigand and Ragland, 1970) for a significant time is one mechanism that would promote contamination of magma by argon. But even if the magma moved upward continuously through the crust until it was emplaced, the higher temperature of the crust at depth, and the fact that more magma must have moved through lower levels than through higher levels, should have facilitated movement of Ar from crustal rock into the magma at depth.

Our studies of local distributions of excess ^{40}Ar in the dikes of Georgia have suggested to us that the Ar arrived at the site of emplacement as a part of the magma (Dooley and Wampler, 1978), and the additional data on local distributions reported herein are consistent with

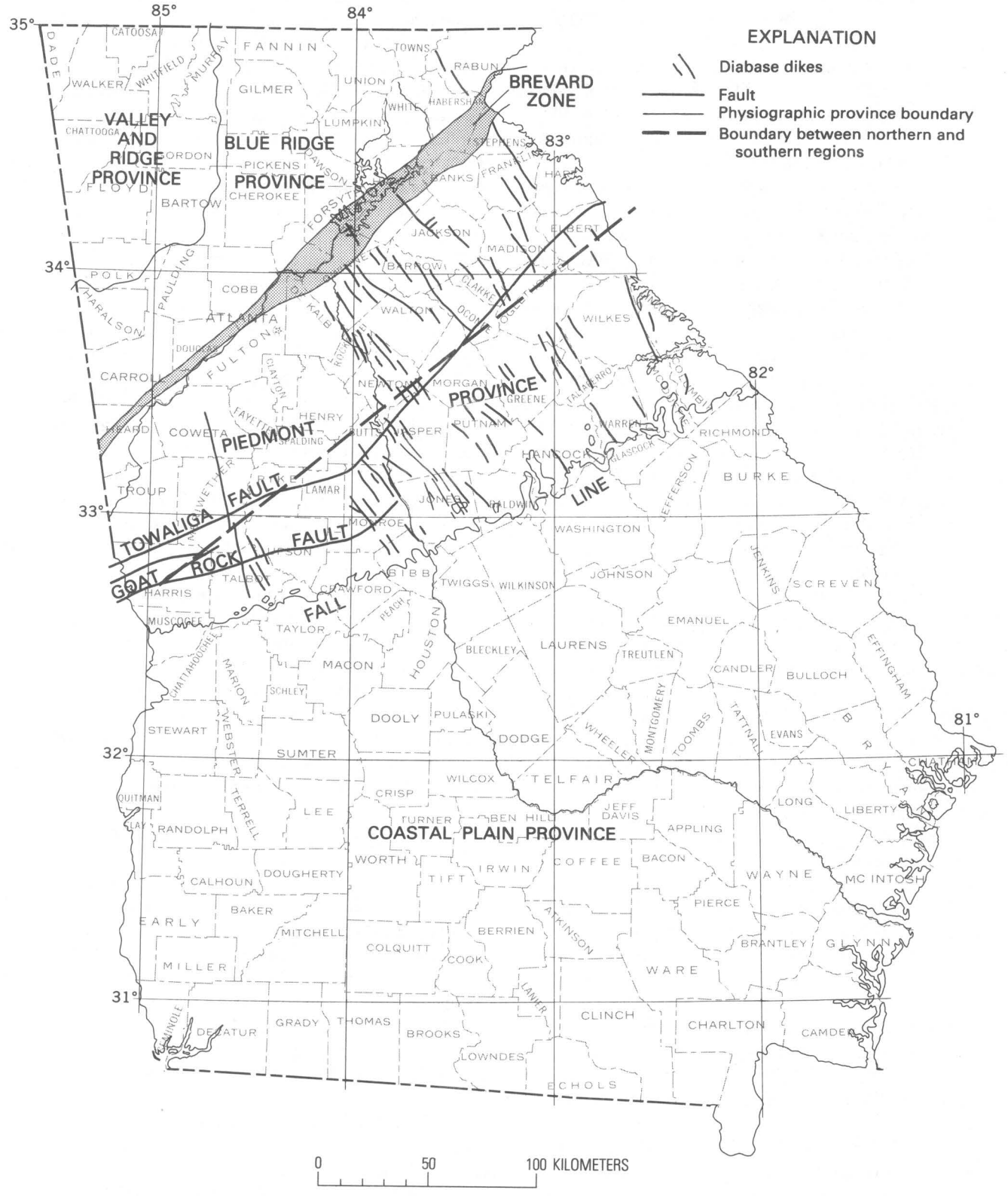

FIGURE 11. – Map of the Piedmont in Georgia. Diabase in southern region (below dashed line) shows little excess ^{40}Ar; diabase in northern region shows relatively large amounts of excess ^{40}Ar.

that view. The concentration of excess ^{40}Ar toward the later crystallizing phases of diabase can be explained by differentiation in an essentially closed system. If the rock now exposed at the surface were at least a kilometer below the surface at the time of intrusion, then the intrusion of magma into nearly impermeable metamorphic terrane should have provided conditions that closely approximated a closed system during crystallization.

There is one characteristic of country rock at the site of emplacement that is likely to be quite important with respect to the incorporation of excess ^{40}Ar in diabase – the permeability (Evans and Tarney, 1964). Intrusion of magma into permeable rocks, such as the Paleozoic sandstone in Liberia, could reasonably allow most of the Ar in the magma to escape during intrusion. We suspect that it is the permeability of sedimentary rocks rather than their low Ar content that accounts for the absence of excess ^{40}Ar in Mesozoic tholeiitic bodies within sedimentary rocks (Dalrymple and others, 1975).

Another aspect of the environment of crystallization of diabase that may be important in explaining the distribution of excess ^{40}Ar in diabase dikes is the depth below the surface at which crystallization occurred. This depth will be the most important factor governing the pressure on the magma, and studies of modern oceanic basalts have established that external pressure is a major factor in determining the ability of basalt to retain Ar during solidification. Even if country rock is relatively impermeable, magma probably will not retain much Ar as it comes close to the surface. The regional variation of excess ^{40}Ar in diabase dikes in Georgia might be partially explained in terms of depth of crystallization if there has been considerable uplift (and subsequent erosion) in the northern part of the study region, since the time when the dikes formed, but little uplift in the southern part of the Georgia Piedmont. There are indications that such differential uplift has occurred in Georgia. Zimmerman (1979) has used apatite fission-track ages to chronicle the post-Triassic uplift in the central and southern Appalachians, and his results indicate progressively greater erosion northwestward across the Piedmont since 180 m.y. ago. These observations, along with more general consideration of the development of the continental margin since rifting began, leave little doubt that the diabase now exposed in the northern part of the Piedmont formed at greater depth and thus at higher pressure than did diabase in the southern part of the Piedmont near the Fall Line. Since the dikes near the Fall Line have less excess ^{40}Ar than do modern deep-ocean basalts, it appears that Ar may have been lost from the crystallizing magma in this part of Georgia.

If our interpretation is correct, that the excess ^{40}Ar in diabase samples from Georgia is Ar that arrived at the site of emplacement as a part of the magma, then it is possible that K-Ar isochron studies can accurately date the intrusion of diabase having considerable amounts of excess ^{40}Ar. But this will be possible only if modern atmospheric Ar contamination can be eliminated and if there is a significant amount of ^{36}Ar in the initial Ar in the rock. Low-temperature Ar-release experiments on some diabase samples from northeastern Georgia, highly contaminated with excess ^{40}Ar, indicate that the contaminating Ar is nearly pure ^{40}Ar. In these cases it is doubtful that any portion of the primary diabase can be dated by K-Ar relationships. The ^{36}Ar content of the initial argon in dikes that do not have large amounts of excess ^{40}Ar (in the southern part of the Piedmont) may be sufficent for successful K-Ar isochron work. The $^{40}Ar/^{36}Ar$ versus $^{39}Ar/^{36}Ar$ isochron method should be applied to samples from these dikes, so that their ages might be established accurately and so that we might have accurate knowledge of the amount and isotopic composition of the argon incorporated in these dikes when they formed.

K-rich materials from the country rock adjacent to dikes (at least the wider ones) might have lost enough Ar in response to thermal effects of intrusion to be useful in dating. The rather coarse-grained biotite from a dike contact in Warren County (sample JWS-1M, table 2) apparently was not completely reset during the formation of the adjacent dike, since we expect that the dike is younger than 216 m.y. Study of materials of differing composition and grain size in the contact zone of a dike might be sufficient to pinpoint the date of intrusion, particularly where there might have been enough fluid movement after crystallization for Ar to escape from the contact zone.

SUMMARY

Conventional K-Ar ages for 20 diabase dikes from the Georgia Piedmont and Blue Ridge are widely variable (190–1,628 m.y.) and discordant, as are the K-Ar ages found for Liberian diabase dikes by Dalrymple and others (1975). The dikes in Georgia and Liberia belong to an early Mesozoic system of dikes in North America, South America, and Africa that appear to have formed just before the opening of the central Atlantic Ocean. As in Liberia, the high and variable K-Ar apparent ages for dikes in Georgia are a consequence of excess ^{40}Ar in the diabase. Our results show that the problem of excess ^{40}Ar in diabase is as large in Georgia as in Liberia, and we suspect that excess ^{40}Ar in at least small amounts is likely to be present in most of the diabase dikes of the circum-Atlantic system.

Samples from about one-third of the dikes that we studied have apparent ages in the range 190–196 m.y. Since these samples may contain a little excess ^{40}Ar, and since structural relationships indicate that all of the postorogenic diabase dikes in Georgia are broadly con-

temporaneous, we have concluded that none of the dikes is likely to be older than about 195 m.y. The paleomagnetic data of Smith and Noltimier (1979) suggest that the dikes in the north-central Appalachians that are about 180 m.y. old formed just before the onset of active spreading of the central Atlantic Ocean. The dikes in Georgia are structurally similar to the 180-m.y. age-group of dikes in the Northeastern United States. Therefore we suspect that the dikes in Georgia are about 180 m.y. old; however, our radiometric data are sufficient only to indicate that the dikes are Early Jurassic in age.

By arbitrarily assuming that all the diabase samples from Georgia are 180 m.y. old, we have been able to estimate the amount of excess ^{40}Ar in each of our samples. Some of the samples have an excess ^{40}Ar content greater than the radiogenic Ar content of nearby country rocks. This observation and the local distribution of excess ^{40}Ar in several dikes suggest that the Ar arrived at the site of emplacement as part of the magma. Crystal-liquid fractionation caused Ar to be concentrated in the later crystallizing portions of the diabase. Some of the excess ^{40}Ar can be released rapidly from diabase samples by heating at temperatures as low as 200°C, which indicates that some of the excess ^{40}Ar is concentrated in intergranular sites or in structural irregularities such as microfractures, microtubes, or fluid inclusions.

A regional pattern in the distribution of excess ^{40}Ar in the diabase dikes of Georgia provides evidence concerning the origin of the excess ^{40}Ar. Diabase samples from the northern portion of the study area contain much more excess ^{40}Ar than do modern deep-sea basalts. Some contain excess ^{40}Ar in amounts considerably greater than the Ar content of the country rock at the sites where the samples were taken. These diabase samples occur in thick crust, much of which may have been accumulating Ar for as long as a billion years. These observations suggest that most of the excess ^{40}Ar in these samples was derived from the lower and intermediate levels of the crust and was transported as part of the magma.

Dikes in the southern part of the Georgia Piedmont have little excess ^{40}Ar, less than that observed in modern deep-sea basalts. Magmas that rose through the relatively thin, young crust in this area may not have been significantly contaminated by Ar from the crust. Alternatively, the samples from this area may have been emplaced so near the surface that most of the Ar in the magma was able to escape. If excess ^{40}Ar is present in *very* small amounts in some of the samples from this area of Georgia, then the apparent ages are close to the geologic ages of these dikes.

REFERENCES CITED

Armstrong, R. L., and Besancon, James, 1970, A Triassic time scale dilemma: K-Ar dating of Upper Triassic mafic igneous rocks, eastern U.S.A. and Canada and post-Upper Triassic plutons, western Idaho, U.S.A.: Eclogae Geologicae Helvetiae, v. 63, no. 1, p. 15–28.

Baldwin, O. D., and Adams, J. A. S., 1971, K^{40}/Ar^{40} ages of the alkalic igneous rocks of the Balcones fault trend of Texas: Texas Journal of Science, v. 22, nos. 2 and 3, p. 223–231.

Barnett, R. S., 1975, Basement structure of Florida and its tectonic implications: Gulf Coast Association of Geological Societies Transactions, v. 25, p. 122–142.

Bell, Henry, III, Books, K. G., Daniels, D. L., Huff, W. E., Jr., and Popenoe, Peter, 1980, Diabase dikes in the Haile-Brewer area, South Carolina, and their magnetic properties, *in* Shorter contributions to geophysics, 1979: U.S. Geological Survey Professional Paper 1123, p. C1–C18.

Briden, J. C., Henthorn, D. I., and Rex, D. C., 1971, Palaeomagnetic and radiometric evidence for the age of the Freetown igneous complex, Sierra Leone: Earth and Planetary Science Letters, v. 12, no. 4, p. 385–391.

Bullard, E. C., Everett, J. E., and Smith, A. G., 1965, The fit of the continents around the Atlantic, *in* Symposium on continental drift: Royal Society of London Philosophical Transactions, ser. A, v. 258, no. 1088, p. 41–51.

Carmichael, C. M., and Palmer, H. C., 1968, Paleomagnetism of the Late Triassic, North Mountain basalt of Nova Scotia: Journal of Geophysical Research, v. 73, no. 8, p. 2811–2822.

Chowns, T. M., and Williams, C. T., 1983, Pre-Cretaceous rocks beneath the Georgia Coastal Plain–Regional implications, *in* Gohn, G. S., ed., Studies related to the Charleston, South Carolina, earthquake of 1886–Tectonics and seismicity: U.S. Geological Survey Professional Paper 1313, p. L1–L42.

Cook, F. A., Albaugh, D. S., Brown, L. D., Kaufman, Sidney, Oliver, J. E., and Hatcher, R. D., Jr., 1979, Thin-skinned tectonics in the crystalline southern Appalachians; COCORP seismic-reflection profiling of the Blue Ridge and Piedmont: Geology, v. 7, no. 12, p. 563–567.

Cornet, Bruce, Traverse, Alfred, and McDonald, N. G., 1973, Fossil spores, pollen, and fishes from Connecticut indicate Early Jurassic age for part of the Newark Group: Science, v. 182, no. 4118, p. 1243–1247.

Corrigan, Donald, 1973, The paleomagnetism and magnetic mineralogy of the Medford diabase dike (Medford area of Boston, Massachusetts): Kingston, Rhode Island University, M.S. thesis.

Cousminer, H. L., and Manspeizer, Warren, 1976, Triassic pollen date Moroccan High Atlas and the incipient rifting of Pangea as middle Carnian: Science, v. 191, no. 4230, p. 943–945.

Dallmeyer, R. D., 1975a, The Palisades sill: A Jurassic intrusion? Evidence from $^{40}Ar/^{39}Ar$ incremental release ages: Geology, v. 3, no. 5, p. 243–245.

———1975b, $^{40}Ar/^{39}Ar$ age spectra of biotite from Grenville basement gneisses in northwest Georgia: Geological Society of America Bulletin, v. 86, no. 12, p. 1740–1744.

———1978, $^{40}Ar/^{39}Ar$ incremental-release ages of hornblende and biotite across the Georgia Inner Piedmont: their bearing on late Paleozoic–early Mesozoic tectonothermal history: American Journal of Science, v. 278, no. 2, p. 124–149.

Dalrymple, G. B., Grommé, C. S., and White, R. W., 1975, Potassium-argon age and paleomagnetism of diabase dikes in Liberia: Initiation of central Atlantic rifting: Geological Society of America Bulletin, v. 86, no. 3, p. 399–411.

Dalrymple, G. B., and Lanphere, M. A., 1969, Potassium-argon dating–Principles, techniques, and applications to geochronology: San Francisco, W. H. Freeman and Company, 258 p.

Damon, P. E., 1970, A theory of "real" K-Ar clocks: Eclogae Geologicae Helvetiae, v. 63, no. 1, p. 69–76.

de Boer, Jelle, 1967, Paleomagnetic-tectonic study of Mesozoic dike swarms in the Appalachians: Journal of Geophysical Research, v. 72, no. 8, p. 2237–2250.

———1968, Paleomagnetic differentiation and correlation of the Late Triassic volcanic rocks in the central Appalachians (with special reference to the Connecticut Valley): Geological Society of America Bulletin, v. 79, no. 5, p. 609–626.

de Boer, Jelle, and Snider, F. G., 1979, Magnetic and chemical variations of Mesozoic diabase dikes from eastern North America: Evidence for a hotspot in the Carolinas?: Geological Society of America Bulletin, Part I, v. 90, no. 2, p. 185–198.

Deininger, R. W., Dallmeyer, R. D., and Neathery, T. L., 1975, Chemical variations and K-Ar ages of diabase dikes in east-central Alabama [abs.]: Geological Society of America Abstracts with Programs, v. 7, no. 4, p. 482.

Dooley, R. E., 1977, K-Ar relationships in dolerite dikes of Georgia: Atlanta, Georgia Institute of Technology, M.S. thesis, 185 p.

Dooley, R. E., and Smith, W. A. 1982, Age and magnetism of diabase dikes and tilting of the Piedmont: Tectonophysics, v. 89, in press.

Dooley, R. E., and Wampler, J. M., 1977a, K-Ar relationships in dolerite dikes of Georgia [abs.]: Geological Society of America Abstracts with Programs, v. 9, no. 2, p. 134.

———1977b, Location of environmental excess ^{40}Ar in dolerites [abs.]: Georgia Journal of Science, v. 35, no. 2, p. 88–89.

———1978, Low temperature release of excess ^{40}Ar from Georgia dolerites, *in* Zartman, R. E., ed., Short papers of the fourth international conference on geochronology, cosmochronology, isotope geology: U.S. Geological Survey Open-File Report 78–701, p. 94–96.

Dymond, J., and Hogan, L., 1978, Factors controlling the noble gas abundance patterns of deep-sea basalts: Earth and Planetary Science Letters, v. 38, no. 1, p. 117–128.

Erickson, G. P., and Kulp, J. L., 1961, Potassium-argon measurements on the Palisades sill, New Jersey: Geological Society of America Bulletin, v. 72, no. 4, p. 649–652.

Evans, C. R., and Tarney, J., 1964, Isotopic ages of Assynt dykes: Nature, v. 204, no. 4959, p. 638–641.

Fanale, F. P., and Kulp, J. L., 1962, The helium method and the age of the Cornwall, Pennsylvania magnetite ore: Economic Geology, v. 57, no. 5, p. 735–746.

Farrar, E., MacIntyre, R. M., York, Derek, and Kenyon, W. J., 1964, A simple mass spectrometer for the analysis of argon at ultra-high vacuum: Nature, v. 204, no. 4958, p. 531–533.

Fisher, D. E., 1975, Trapped helium and argon and the formation of the atmosphere by degassing: Nature, v. 256, no. 5513, p. 113–114.

Fullagar, P. D., and Butler, J. R., 1976, Petrochemical and geochronologic studies of plutonic rocks in the southern Appalachians: II, the Sparta granite complex, Georgia: Geological Society of America Bulletin, v. 87, no. 1, p. 53–56.

Gohn, G. S., Gottfried, David, Lanphere, M. A., and Higgins, B. B., 1978, Regional implications of Triassic or Jurassic age for basalt and sedimentary red beds in the South Carolina Coastal Plain: Science, v. 202, no. 4370, p. 887–890.

Gottfried, David, Annell, C. S., and Byerly, G. R., 1983, Geochemistry and tectonic significance of subsurface basalts near Charleston, South Carolina; Clubhouse Crossroads test holes #2 and #3, *in* Gohn, G. S., ed., Studies related to the Charleston, South Carolina, earthquake of 1886–Tectonics and seismicity: U.S. Geological Survey Professional Paper 1313, p. A1–A19.

Gottfried, David, Annell, C. S., and Schwarz, L. J., 1977, Geochemistry of subsurface basalt from the deep corehole (Clubhouse Crossroads corehole 1) near Charleston, South Carolina–Magma type and tectonic implications, *in* Rankin, D. W., ed., Studies related to the Charleston, South Carolina, earthquake of 1886–A preliminary report: U.S. Geological Survey Professional Paper 1028, p. 91–113.

Green, D. H., and Ringwood, A. E., 1967, The genesis of basaltic magmas: Contributions to Mineralogy and Petrology, v. 15, no. 2, p. 103–190.

Hailwood, E. A., and Mitchell, J. G., 1971, Palaeomagnetic and radiometric dating results from Jurassic intrusions in South Morocco: Royal Astronomical Society Geophysical Journal, v. 24, no. 4, p. 351–364.

Harper, C. T., Russell, C. W., Sherrer, G., Stonebraker, J. D., and Kish, S., 1973, The Arvonia slate: A useful standard for K-Ar dating [abs.]: Geological Society of America Abstracts with Programs, v. 5, no. 5, p. 402.

Hayatsu, A., 1979, K-Ar isochron age of the North Mountain basalt, Nova Scotia: Canadian Journal of Earth Sciences, v. 16, no. 4, p. 973–975.

Hebeda, E. H., Boelrijk, N. A. I. M., Priem, H. N. A., Verdurmen, E. A. T., and Verschure, R. H., 1973, Excess radiogenic argon in the Precambrian Avanavero dolerite in western Suriname (South America): Earth and Planetary Science Letters, v. 20, no. 2, p. 189–200.

Hodych, J. P., and Hayatsu, A., 1980, K-Ar isochron age and paleomagnetism of diabase along the trans-Avalon aeromagnetic lineament–Evidence of Late Triassic rifting in Newfoundland: Canadian Journal of Earth Sciences, v. 17, no. 4, p. 491–499.

Houlik, C. W., Jr., and Laird, H. S., 1977, Mesozoic wrench tectonics and the development of the northern Newark Basin [abs.]: Geological Society of America Abstracts with Programs, v. 9, no. 3, p. 275.

Ingamells, C. O., and Engels, J. C., 1976, Preparation, analysis, and sampling constants for a biotite, *in* Accuracy in trace analysis: Sampling, sample handling, and analysis, Proceedings of the 7th IMR Symposium: National Bureau of Standards Special Publication 422, p. 401–419.

Jones, L. M., and Walker, R. L., 1973, Rb-Sr whole-rock age of the Siloam granite, Georgia: A Permian intrusive in the southern Appalachians: Geological Society of America Bulletin, v. 84, no. 11, p. 3653–3658.

King, P. B., 1971, Systematic pattern of Triassic dikes in the Appalachian region–Second report, *in* Geological Survey Research 1971: U.S. Geological Survey Professional Paper 750–D, p. D84–D88.

Lanphere, M. A., 1983, $^{40}Ar/^{39}Ar$ ages of basalt from Clubhouse Crossroads test hole #2, near Charleston, South Carolina, *in* Gohn, G. S., ed., Studies related to the Charleston, South Carolina, earthquake of 1886–Tectonics and seismicity: U.S. Geological Survey Professional Paper 1313, p. B1–B8.

Lanphere, M. A., and Dalrymple, G. B., 1976a, Final compilation of K-Ar and Rb-Sr measurements on P-207, the USGS interlaboratory standard muscovite, *in* Flanagan, F. J., ed., Descriptions and analyses of eight new USGS rock standards: U.S. Geological Survey Professional Paper 840, p. 127–130.

———1976b, Identification of excess ^{40}Ar by the $^{40}Ar/^{39}Ar$ age spectrum technique: Earth and Planetary Science Letters, v. 32, no. 2, p. 141–148.

Larochelle, A., 1971, Note on the paleomagnetism of two diabase dykes, Anticosti Island, Quebec: Geological Association of Canada Proceedings, v. 23, p. 73–76.

Larochelle, A., and Wanless, R. K., 1966, The paleomagnetism of a Triassic diabase dike in Nova Scotia: Journal of Geophysical Research, v. 71, no. 20, p. 4949–4953.

Leblanc, Marc, 1973, Le grande dyke de dolérite de l'Anti-Atlas et le magmatisme jurassique du Sud marocain [The great dolerite dike of the Anti-Atlas and the Jurassic magmatism of southern Morocco]: Comptes Rendus de l'Académie des Sciences, Paris, v. 276, ser. D, p. 2943–2946.

Le Pichon, Xavier, and Fox, P. J., 1971, Marginal offsets, fracture zones, and the early opening of the North Atlantic: Journal of Geophysical Research, v. 76, no. 26, p. 6294–6308.

Lester, J. G., and Allen, A. T., 1950, Diabase of the Georgia Piedmont: Geological Society of America Bulletin, v. 61, no. 11, p. 1217–1224.

Long, L. T., 1979, The Carolina slate belt–Evidence of a continental rift zone: Geology, v. 7, no. 4, p. 180–184.

Marine, I. W., and Siple, G. E., 1974, Buried Triassic basin in the central Savannah River area, South Carolina and Georgia: Geological Society of America Bulletin, v. 85, no. 2, p. 311–320.

May, P. R., 1971, Pattern of Triassic-Jurassic diabase dikes around the North Atlantic in the context of predrift position of the continents: Geological Society of America Bulletin, v. 82, no. 5, p. 1285–1292.

McHone, J. G., 1978, Distribution, orientations, and ages of mafic dikes in central New England: Geological Society of America Bulletin, v. 89, no. 11, p. 1645–1655.

Meadows, G. R., 1979, Petrology of Mesozoic age diabase dikes in the Georgia Piedmont: Atlanta, Emory University, M.S. thesis, 70 p.

Michard, André, 1976, Eléments de géologie marocaine [Elements of Moroccan geology]: Notes et Mémoires du Service Géologique du Maroc, no. 252, 408 p.

Milton, Charles, and Grasty, Robert, 1969, "Basement" rocks of Florida and Georgia: American Association of Petroleum Geologists Bulletin, v. 53, no. 12, p. 2483–2493.

Milton, Charles and Hurst, V. J., 1965, Subsurface "basement" rocks of Georgia: Georgia Geologic Survey Bulletin 76, 56 p.

Phillips, J. D., 1983, Paleomagnetic investigations of the Clubhouse Crossroads basalt, *in* Gohn, G. S., ed., Studies related to the Charleston, South Carolina, earthquake of 1886–Tectonics and seismicity: U.S. Geological Survey Professional Paper 1313, p. C1–C18.

Poole, W. H., Sanford, B. V., Williams, H., and Kelley, D. G., 1970, Geology of southeastern Canada, *in* Geology and economic minerals of Canada: Geological Survey of Canada Economic Geology Report 1 (5th ed.), p. 227–304.

Reesman, R. H., Filbert, C. R., and Krueger, H. W., 1973, Potassium-argon dating of the Upper Triassic lavas of the Connecticut Valley, New England [abs.]: Geological Society of America Abstracts with Programs, v. 5, no. 2, p. 211.

Ross, D. A., and Schlee, John, 1973, Shallow structure and geologic development of the southern Red Sea: Geological Society of America Bulletin, v. 84, no. 12, p. 3827–3848.

Schermerhorn, L. J. G., Priem, H. N. A., Boelrijk, N. A. I. M., Hebeda, E. H., Verdurmen, E. A. T., and Verschure, R. H., 1978, Age and origin of the Messejana dolerite fault-dike system (Portugal and Spain) in the light of the opening of the North Atlantic Ocean: Journal of Geology, v. 86, no. 3, p. 299–309.

Şengör, A. M. C., and Burke, Kevin, 1978, Relative timing of rifting and volcanism on earth and its tectonic implications: Geophysical Research Letters, v. 5, no. 6, p. 419–421.

Smith, J. W., Wampler, J. M., and Green, M. A., 1969, Isotopic dating and metamorphic isograds of the crystalline rocks of Georgia, *in* Precambrian-Paleozoic Appalachian problems: Georgia Geologic Survey Bulletin 80, p. 121–139.

Smith, R. C., II, Rose, A. W., and Lanning, R. M., 1975, Geology and geochemistry of Triassic diabase in Pennsylvania: Geological Society of America Bulletin, v. 86, no. 7, p. 943–955.

Smith, T. E., 1976, Paleomagnetic study of lower Mesozoic diabase dikes and sills of Connecticut and Maryland: Canadian Journal of Earth Sciences, v. 13, no. 4, p. 597–609.

Smith, T. E., and Noltimier, H. C., 1979, Paleomagnetism of the Newark trend igneous rocks of the north central Appalachians and the opening of the central Atlantic Ocean: American Journal of Science, v. 279, no. 7, p. 778–807.

Steiger, R. H., and Jäger, E., compilers, 1977, Subcommission on geochronology: Convention on the use of decay constants in geo- and cosmochronology: Earth and Planetary Science Letters, v. 36, no. 3, p. 359–362.

Stonebraker, J. D., 1973, Potassium-argon geochronology of the Brevard fault zone, southern Appalachians: Tallahassee, Florida State University, Ph. D. thesis, 187 p.

Sutter, J. F., and Smith, T. E., 1979, $^{40}Ar/^{39}Ar$ ages of diabase intrusions from Newark trend basins in Connecticut and Maryland: Initiation of central Atlantic rifting: American Journal of Science, v. 279, no. 7, p. 808–831.

Thuizat, R., 1976, Ages potassium-argon de dolerites mésozoïques du Maroc [Potassium-argon ages of Mesozoic dolerites of Morocco] [abs.]: Réunion annuelle des sciences de la terre, no. 4, p. 379.

van Hinte, J. E., 1976, A Jurassic time scale: American Association of Petroleum Geologists Bulletin, v. 60, no. 4, p. 489–497.

Wampler, J. M., and Dooley, R. E., 1975, Potassium-argon determination of Triassic and Eocene igneous activity in Rockingham County, Virginia [abs.]: Geological Society of America Abstracts with Programs, v. 7, no. 4, p. 547.

Watts, Doyle, 1975, A paleomagnetic study of four Mesozoic diabase dike swarms of the southern Appalachian Mountains: Columbus, Ohio State University, M.S. thesis, 113 p.

Watts, Doyle, and Noltimier, H. C., 1974, Paleomagnetic study of diabase dikes in the Inner Piedmont of N. Carolina and Georgia [abs.]: EOS, American Geophysical Union Transactions, v. 55, no. 7, p. 675.

Weigand, P. W., and Ragland, P. C., 1970, Geochemistry of Mesozoic dolerite dikes from eastern North America: Contributions to Mineralogy and Petrology, v. 29, no 3, p. 195–214.

Westphal, M., Montigny, R., Thuizat, R., Bardon, C., Bossert, A., Hamzeh, R., and Rolley, J. P., 1979, Paléomagnétisme et datation du volcanisme permien, triasique et crétacé du Maroc [Paleomagnetism and dating of Permian, Triassic, and Cretaceous volcanism in Morocco]: Canadian Journal of Earth Sciences, v. 16, no. 11, p. 2150–2164.

Whitney, J. A., Jones, L. M., and Walker, R. L., 1976, Age and origin of the Stone Mountain Granite, Lithonia district, Georgia: Geological Society of America Bulletin, v. 87, no. 7, p. 1067–1077.

Yoder, H. S., Jr., 1976, Generation of basaltic magma: Washington, D.C., National Academy of Sciences, 265 p.

Zimmerman, R. A., 1979, Apatite fission track age evidence of post-Triassic uplift in the central and southern Appalachians [abs.]: Geological Society of America Abstracts with Programs, v. 11, no. 4, p. 219.

Mesozoic Development and Structure of the Continental Margin off South Carolina

By WILLIAM P. DILLON, KIM D. KLITGORD, and CHARLES K. PAULL

STUDIES RELATED TO THE CHARLESTON, SOUTH CAROLINA, EARTHQUAKE OF 1886—TECTONICS AND SEISMICITY

GEOLOGICAL SURVEY PROFESSIONAL PAPER 1313-N

UNITED STATES GOVERNMENT PRINTING OFFICE, WASHINGTON: 1983

CONTENTS

ILLUSTRATIONS

STUDIES RELATED TO THE CHARLESTON, SOUTH CAROLINA, EARTHQUAKE OF 1886—
TECTONICS AND SEISMICITY

MESOZOIC DEVELOPMENT AND STRUCTURE OF THE CONTINENTAL MARGIN OFF SOUTH CAROLINA

By WILLIAM P. DILLON, KIM D. KLITGORD, and CHARLES K. PAULL

ABSTRACT

A nearly undeformed wedge of Mesozoic and Cenozoic strata forms the Continental Shelf and Blake Plateau off South Carolina. The wedge is built on an unconformity, known as the postrift unconformity, at the top of beveled Triassic and Lower Jurassic sedimentary deposits, Paleozoic crystalline basement rocks, Paleozoic sedimentary rocks of various stages of metamorphism, and Mesozoic volcanic and plutonic mafic igneous rocks. The postrift unconformity generally forms both seismic basement and magnetic basement. This unconformity is marked by two zones of major subsidence off South Carolina, separated by the apparent landward continuation of the deep-sea Blake Spur fracture zone. South of that fracture zone, beneath the Blake Plateau, is the broad Blake Plateau basin, reaching depths of 14 km. North of the fracture zone and parallel to the continental margin is the narrow Carolina trough, which is as much as 11 km deep. The postrift unconformity is formed by a strongly reflecting layer beneath the Continental Shelf off South Carolina that probably represents a seaward extension of the lower Mesozoic volcanic flows penetrated by drilling near Charleston. During Jurassic time, the Blake Plateau basin and Carolina trough subsided rapidly and were filled with sediment to a depth of more than 7 km. In contrast, Cretaceous subsidence of the continental margin was widespread and relatively uniform and resulted in the accumulation of a blanket of sediment 1 to 4 km thick.

INTRODUCTION

During the Mesozoic, the continental margin off South Carolina was the site of rapidly subsiding sedimentary basins. The present shapes of sedimentary bodies in the region reflect both the sedimentation pattern and the subsidence pattern. The pattern of subsidence was controlled by the organization of initial rifting of the continental margin as the North Atlantic Ocean began to open, and the subsidence subsequently was driven by cooling and loading on this passive or trailing-edge continental margin.

The general structure and development of the continental margin in this region has been studied by means of a grid of multichannel common-depth-point (CDP) seismic-reflection profiles (Buffler and others, 1979; Dillon and Paull, 1978; Dillon and others, 1979a) and a detailed aeromagnetic survey (Klitgord and Behrendt, 1977, 1979). The values of depth to basement derived from the magnetic data and from the determination of depths to seismic basement and other selected seismic horizons allow mapping of the structure of the basement and of the overlying sediments. Interpretations of three of the CDP seismic-reflection profiles extending offshore from South Carolina (fig. 1) are included to illustrate the margin structure.

Acknowledgments.—Discussions with John Grow, Peter Popenoe, C. Wylie Poag, Page Valentine, John Schlee, Kathleen Kent, and Mahlon Ball have been especially productive in developing our ideas on the geology of this region. We are very grateful for the help of Peggy Mons-Wengler and Patricia Forrestel. The paper was reviewed and improved by John Behrendt and Harley Knebel.

GENERAL STRUCTURE

The topography of the sea floor off South Carolina (fig. 1) is characterized by a shallow Continental Shelf. Seaward of the Continental Shelf lies the Florida-Hatteras Slope that descends to about 400 m, succeeded to seaward by the broad, flat or gently sloping Blake Plateau. Beyond the Blake Plateau is the more steeply dipping Continental Slope and Blake Escarpment.

The general structure of the margin consists of an onlapping and nearly undeformed wedge of strata interpreted to be mostly of Jurassic and Cretaceous age, as shown in the three profile interpretations (figs. 2, 3, 4). The Cretaceous strata extend beyond the northwest end of the profiles, beneath the emerged Coastal Plain, to a

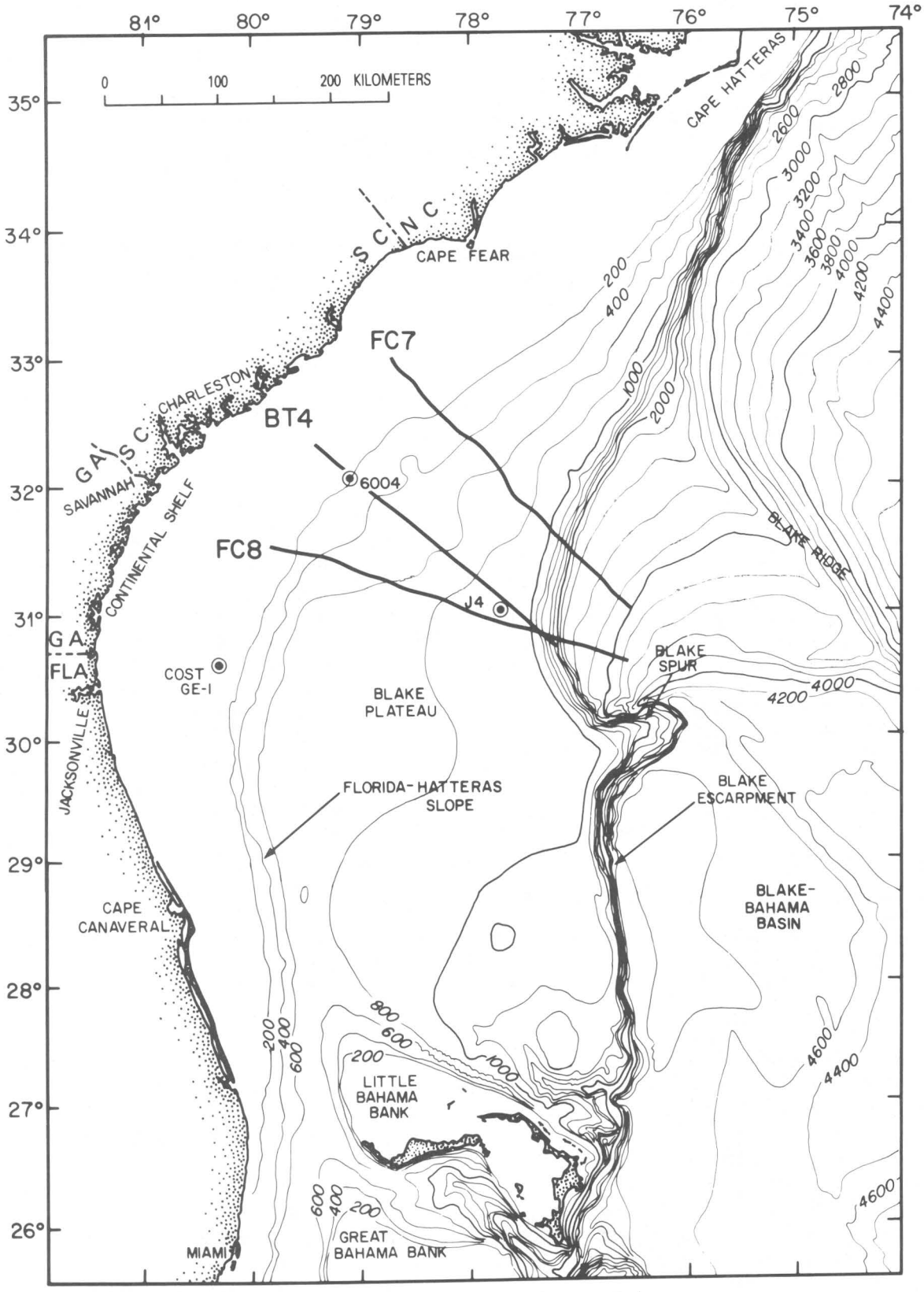

FIGURE 1.—Physiography of the continental margin off the Southeastern United States, locations of profiles discussed in this paper, and locations of stratigraphic drillsites used to estimate age of seismic horizons. Depths in meters adapted from U.S. Naval Oceanographic Office charts N.O. 805 and N.O. 806.

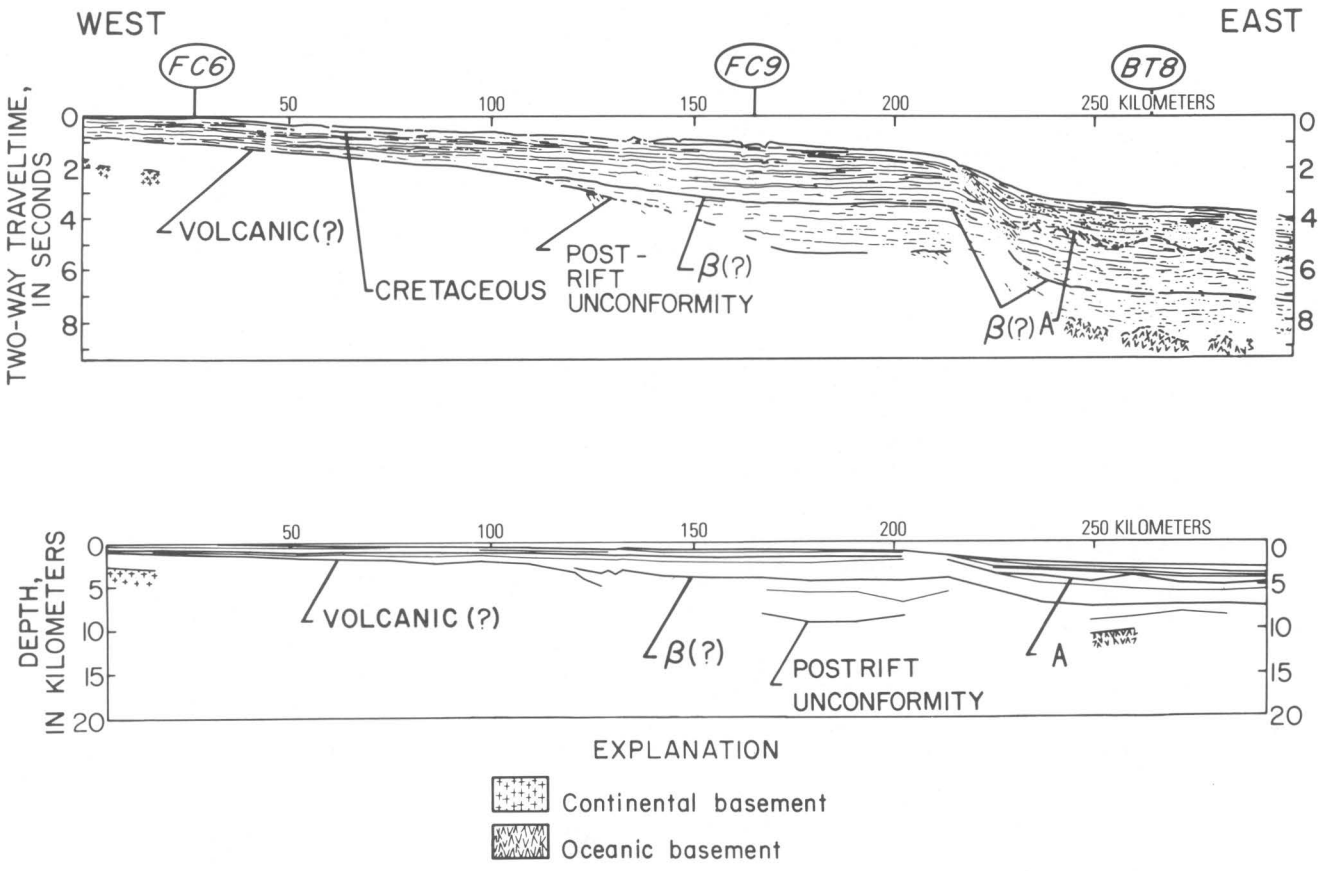

FIGURE 2.—Line-drawing interpretation (above) and calculated depth section (calculated by the method of Taner and Koehler, 1969) of common-depth-point seismic-reflection profile FC7. Vertical exaggeration of calculated depth section is approximately ×2. The 24-channel profile was collected by the Institut français du Pétrole in cooperation with the U.S. Geological Survey (USGS) and was processed by Compagnie Générale du Géophysique to provide 2400 percent stack. Horizon A here represents an unconformity cut down to Cretaceous rocks probably during Oligocene time. Horizon β probably represents the top of Neocomian units. Other horizons are discussed in the text. The numbers enclosed in ovals represent crossing points of other profiles in the USGS grid of common-depth-point seismic profiles.

feather edge near the Fall Line (Cramer, 1974). The Mesozoic wedge is covered by a thin layer of Cenozoic deposits on the Blake Plateau and, to the northwest, by a somewhat thicker Cenozoic buildup that forms the present Continental Shelf. The sedimentary wedge was constructed atop an unconformity that was cut into rocks of varying ages during the earliest stages of formation of the North Atlantic Ocean basin after the completion of rifting.

"BASEMENT" DEVELOPMENT AND STRUCTURE

Nature of the "Basement"

When Africa and North America began to separate, in Triassic time, a broad swath of the continental crust began to be thinned by fracturing resulting from extension. This fractured basement probably was intruded pervasively by mafic, mantle-derived magma, and basaltic volcanism was active. The rough, fractured basement surface eroded rapidly, and floods of terrigenous, clastic continental sediments quickly filled depressions. Eventually a fairly smooth unconformity, known as the postrift unconformity, developed over beveled Triassic and Lower Jurassic sedimentary deposits, Paleozoic or older volcanic and plutonic basement rocks, Paleozoic sedimentary rocks of various stages of metamorphism, and volcanic and plutonic mafic igneous rocks associated with rifting. The igneous and metamorphic material below this postrift uncomformity commonly is referred to as "basement" or, where it is believed to be extensively thinned and intruded, as "transitional basement." It commonly forms both magnetic and seismic basement, although weak deeper reflectors sometimes appear on seismic profiles. A good example of the postrift unconformity in the form of an angular unconformity above possibly Triassic and Lower Jurassic sedimentary rocks or Paleozoic low-grade metamorphic rocks appears in the middle of pro-

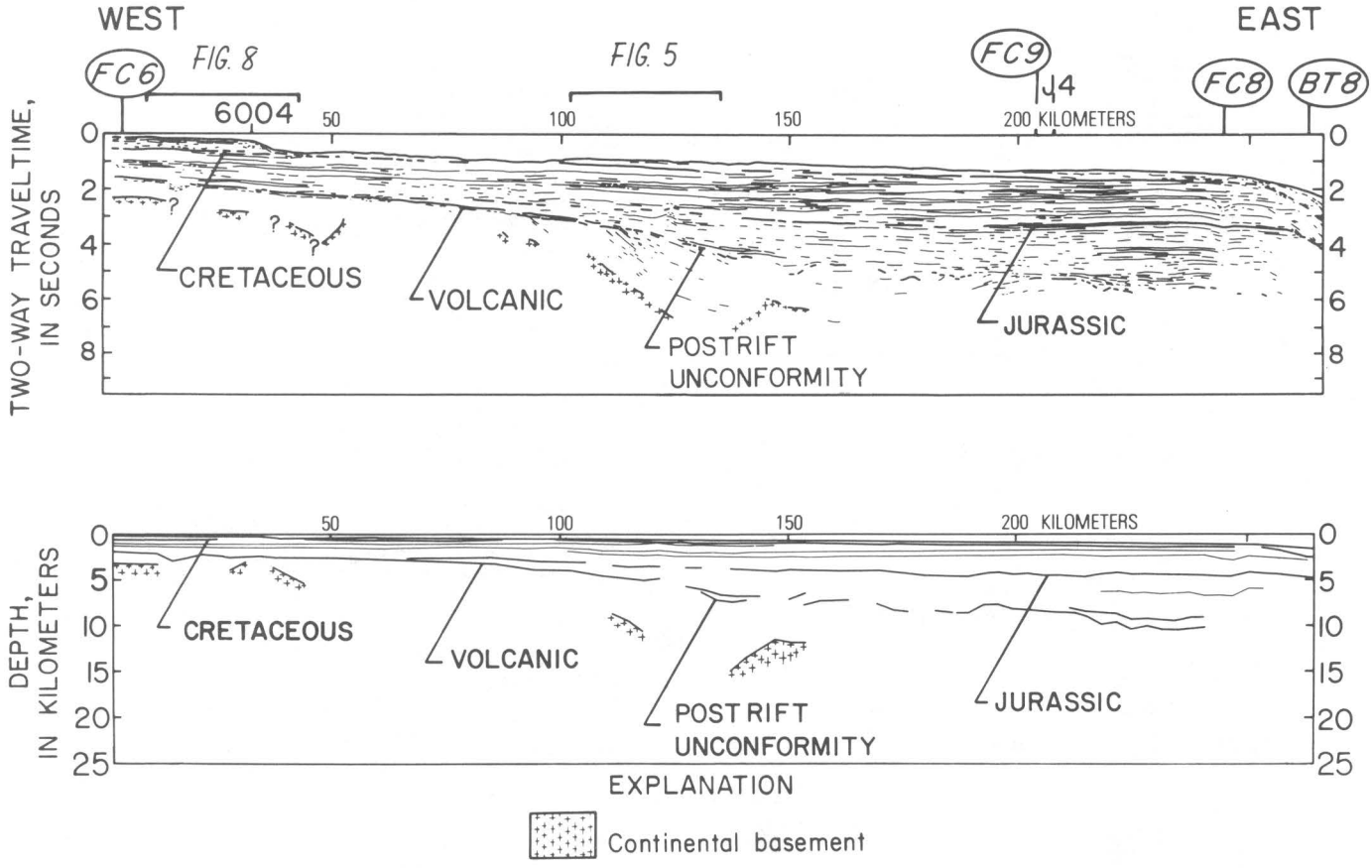

FIGURE 3.—Line-drawing interpretation and calculated depth section of common-depth-point seismic-reflection profile BT4. The profile was collected with a 48-channel streamer and was processed to provide 3600 percent stack by GSI (Geophysical Services Incorporated). The notations "6004" and "J4" above the profile indicate locations of stratigraphic drillsites.

file BT4 (fig. 3). A photograph of this portion of the seismic profile is shown in figure 5; the unconformity appears clearly at about 3 seconds (s) depth. A deeper horizon, possibly crystalline basement, was identified on figure 3; however, as is obvious from the record photograph (fig. 5), this is not a clearly-defined seismic horizon, and the interpretation of continental crystalline basement in this and the other profiles (figs. 2, 4) should be considered tentative.

Magnetic basement in this region (Klitgord and Behrendt, 1979) corresponds reasonably well to the seismically determined postrift unconformity. This would be expected if the unconformity marks the boundary between the overlying, flat-lying sediments and the tops of old continental crust (the Paleozoic igneous and metamorphic rocks) and mafic intrusive and extrusive rocks associated with rifting. The character of the magnetic anomalies and estimates of the depth to magnetic basement enable us to speculate on the type of crust underlying different areas and to divide the region into shallower platform areas and deeper sedimentary basins. The Carolina platform (fig. 6) displays high-amplitude short-wavelength magnetic anomalies that are characteristic of continental crust (Taylor and others, 1968; Kane and others, 1972; Behrendt and Klitgord, 1979). Areas underlain by transitional crust are characterized by long-wavelength, low-gradient, irregular magnetic anomalies. The anomalies over oceanic crust are also long wavelength and low gradient, but they are distinctly linear in pattern.

The general distribution of basement types, as determined from the magnetic and seismic data, indicates that deep sedimentary basins are underlain by transitional crust and are bounded on the landward side by shallow platforms of continental crust and on the seaward side by oceanic crust. Gravity models are consistent with this interpretation and suggest crustal thickness for the transitional basement of 15–20 km (Kent and others, 1979).

Structure of Seismic Basement

The postrift unconformity was judged to be the deepest mappable horizon and to represent the top of transitional basement where that exists; it therefore

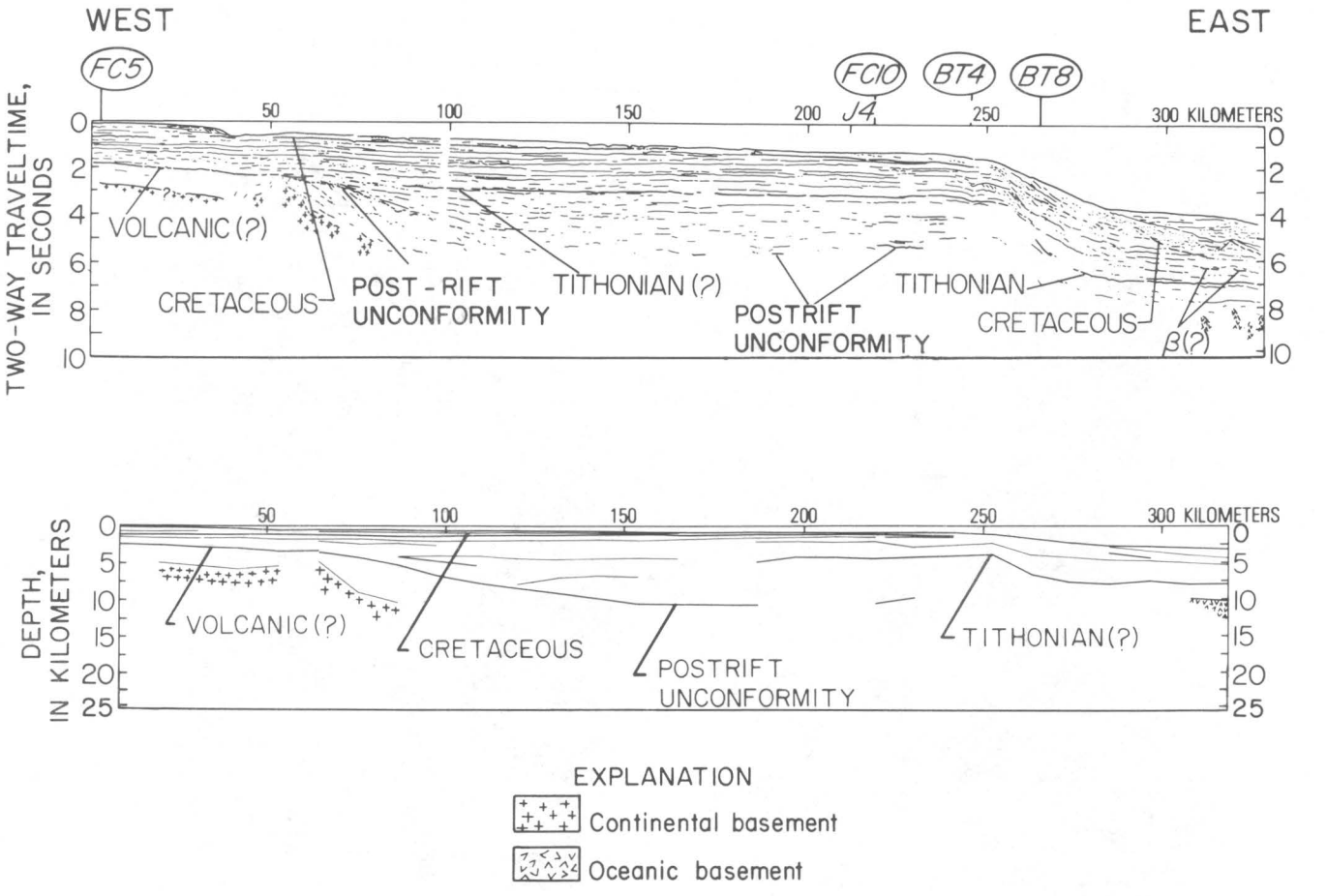

FIGURE 4.—Line-drawing interpretation and calculated depth section of common-depth-point seismic-reflection profile FC8. The profile was collected and processed in the same manner as used for profile FC7 (fig. 2).

was contoured as seismic "basement." The structure of this horizon off South Carolina is dominated by two major basins and a platform area to their northwest (fig. 6). The basins are the Blake Plateau basin and Carolina trough (fig. 6), and the platform has been called the Carolina platform by Klitgord and Behrendt (1979). The shallow ridge that separates the Carolina trough from the Blake Plateau basin (fig. 6) lies on the extension of an oceanic fracture zone, the Blake Spur fracture zone (Schouten and Klitgord, 1977), and probably was the location of transform fault activity during the earliest opening of the Atlantic Ocean basin. Presence of a group of salt diapirs along the seaward side of the Carolina trough (Grow and others, 1977) shows that evaporite deposits accumulated during the early history of the trough.

Structure of Magnetic Basement

The structure map of magnetic basement (fig. 7) is very similar to that determined for the postrift unconformity (fig. 6); it shows the two major basins, separated by the shallow zone, and the platform to the northwest. The increased complexity of the magnetic basement surface may be due in part to the much greater density of magnetic data (lines 3 to 5 km apart) compared to seismic profiles (lines about 60 km apart). However, the postrift unconformity is fairly smooth in the individual seismic profiles (figs. 2, 3, 4), so some of the irregularity of magnetic basement probably results from depth solutions to bodies that lie below or above the unconformity, such as crystalline basement or intrusions, as well as from the variability inherent in the method of magnetic-source depth calculation. The basic agreement in depths and general structures indicated by the two methods is much more notable than are the disagreements, however.

A small basin in magnetic basement, more than 6 km deep, occurs beneath the shelf off Georgia, just west of the COST GE–1 well (fig. 7). A multichannel seismic profile (Dillon and others, 1979b) suggests that this is a graben that subsided mostly in Triassic and Early Jurassic time and that the postrift unconformity crosses it without major effect (fig. 6). However, higher resolu-

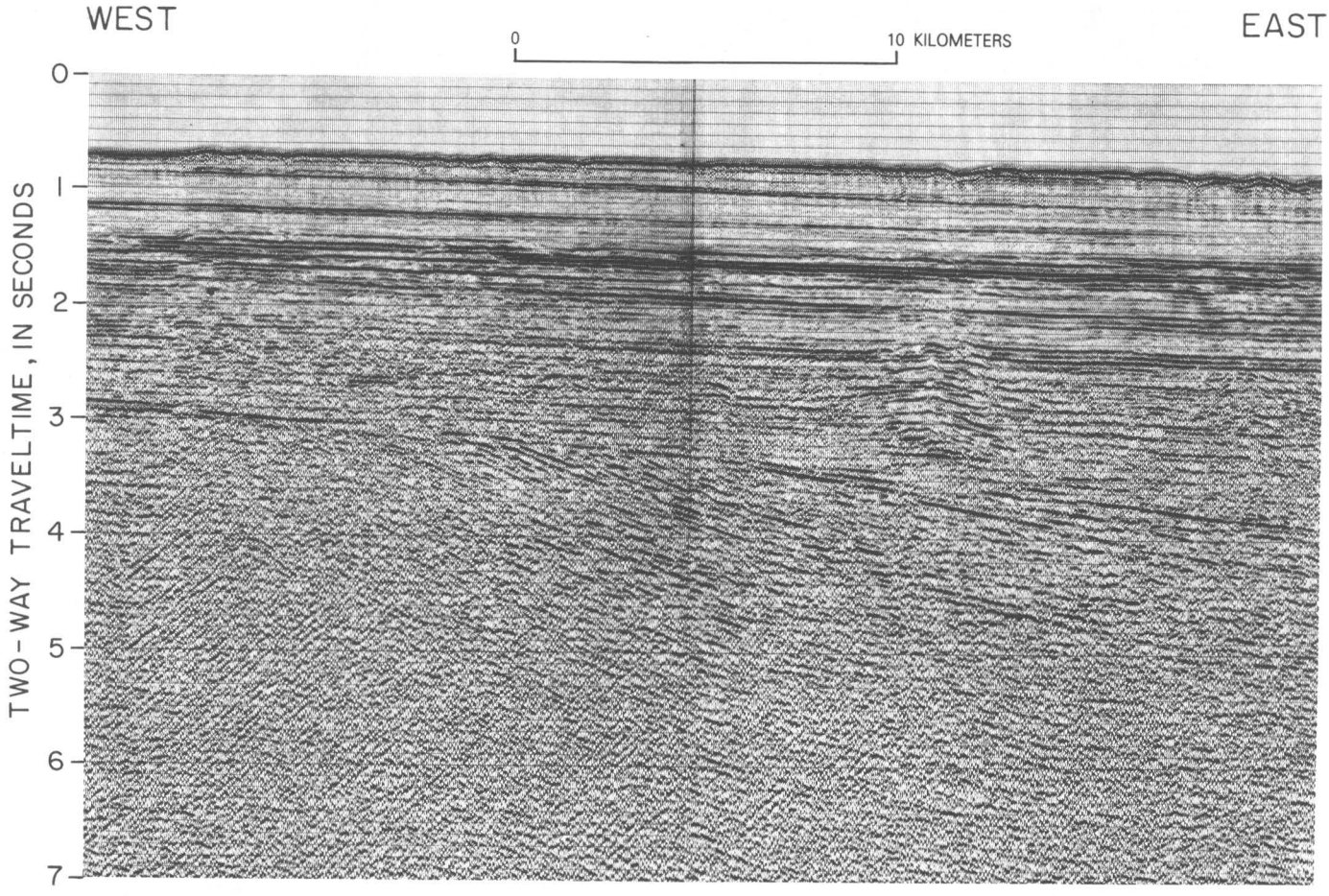

FIGURE 5.—Photograph of part of record for seismic profile BT4 (fig. 3) showing an angular unconformity at about 3 seconds depth. Location shown on figure 3. The unconformity probably is overlain by Upper Jurassic rocks and may be underlain by Triassic or Paleozoic rocks. It is considered to be the postrift unconformity.

tion profiles (Paull and Dillon, 1979, 1980) show that this was a site of continued subsidence into the Tertiary, and it was a location of considerable petroleum leasing interest during Outer Continental Shelf Lease Sale 43.

The boundary between transitional and continental crust undoubtedly is gradational, but we have chosen it at about the 6-km contour on both figures 6 and 7 on the basis of the criteria discussed above. The deepest parts of the basins (>10 km deep) probably are floored by transitional crust that is more mafic and thinner than the crust in areas of shallow basement.

VOLCANIC(?) LAYER

A very strong, smooth reflector, interpreted to be a layer of volcanic rock, occurs just above the postrift unconformity on the landward ends of the profiles off South Carolina (figs. 2, 3, 4). Figure 8 is a photograph of the landward end of profile BT4, showing the volcanic(?) layer (marked V). An interpretation of the entire profile is shown in figure 3. The approximate lateral extent and depth of the very strong reflector are shown in figure 9. Although the reflector is quite continuous, breaks occur, as, for example, near the left side of figure 8.

The strong reflector corresponds in depth to a high-velocity refracting horizon that appears in our refraction profiles and those of other workers (Woollard and others, 1957; Hersey and other, 1959; Dillon and McGinnis, 1983). Refraction compressional-wave velocities in this layer beneath the Continental Shelf range from 5.5 to 6.3 km/s (kilometers/second); 9 of 12 measurements indicate velocities between 5.8 and 6.1 km/s. Ackermann (1977, 1983) has reported a maximum velocity of 5.8 km/s for the basalt horizon drilled in South Carolina in the U.S. Geological Survey Clubhouse Crossroads drill holes; his values range from 4.3 to 5.8 km/s. The range in velocity on land might be due to spotty distribution of flows from localized vents, to variations in amounts of volcanic flow deposits removed by subsequent erosion (Ackermann, 1983), or to variations in weathering. Greater weathering tends to produce slower velocities. Increased amounts of erosion and

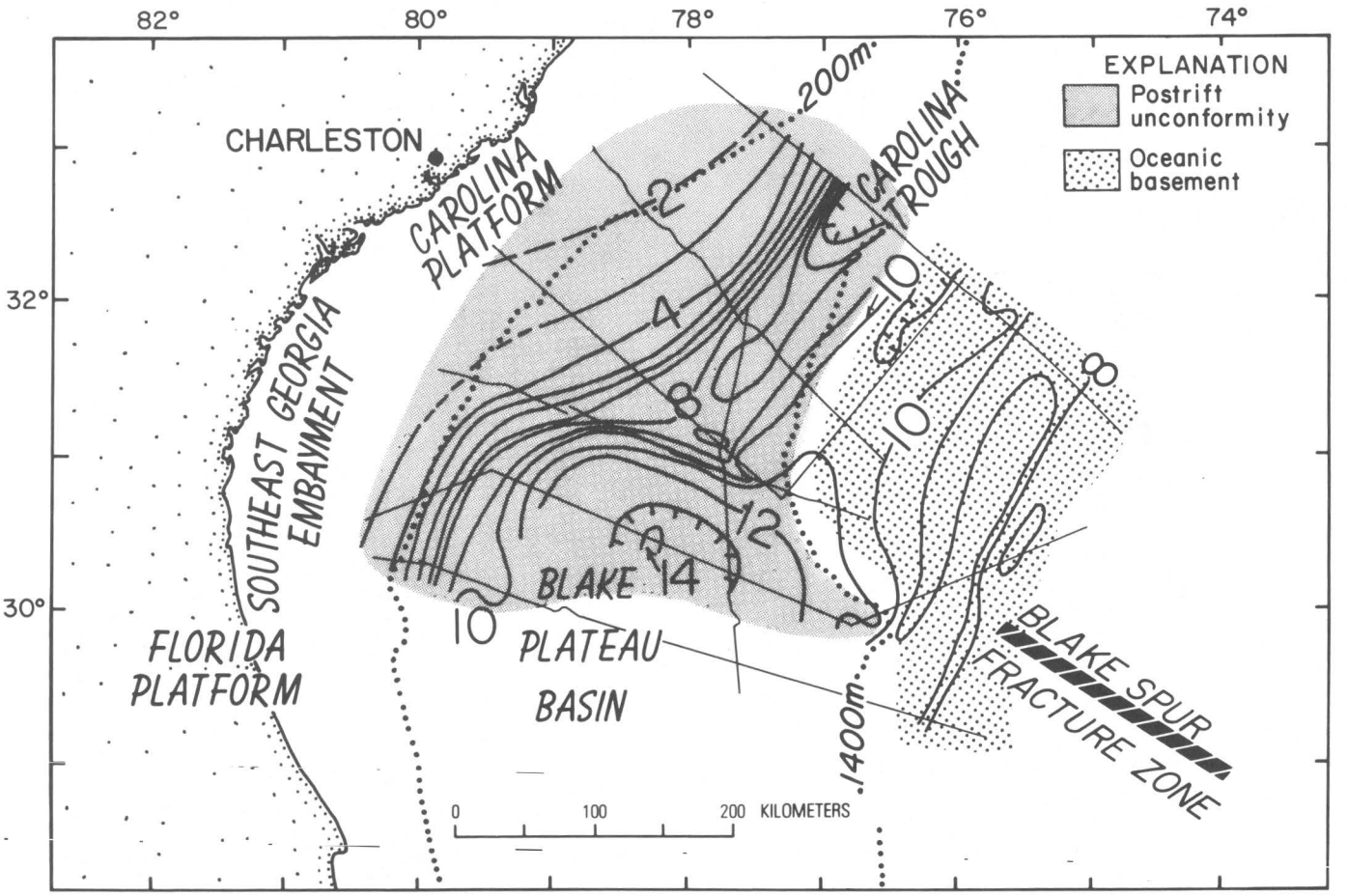

FIGURE 6.—Depth, in kilometers, to a surface considered to be the postrift unconformity beneath the Continental Shelf and Blake Plateau. Light lines show seismic profiles used to construct map.

weathering would be anticipated onshore compared to offshore because the basalt offshore would have been covered much earlier by the onlapping wedge of continental margin sediments.

We have correlated the horizon that displays strong reflections and high refraction velocities offshore with the basalt onshore. We did this (1) because of the general correspondence of high refraction velocities onshore to the basalt (Ackermann, 1977, 1983), (2) because of a general correspondence in depth of the layer offshore to the basalt onshore (see fig. 9, and Ackermann, 1983), and (3) because the offshore layer is smooth and overlies the postrift unconformity (figs. 2, 3, 4) and, therefore, cannot be crystalline basement.

The inferred volcanic layer is slightly younger than the postrift unconformity and apparently indicates a significant episode of volcanic activity. Therefore we speculate that it may be related to a minor tectonic episode associated with an abrupt change in spreading center location and an attendant readjustment in plate movements that occurred about 175 million years ago (Dillon and others, 1979a). This is discussed more fully in Klitgord and others (1983).

INFERRED JURASSIC STRATA

Jurassic deposits (fig. 10) have never been drilled in the continental margin off the Southeastern United States and probably do not exist on land south of Cape Lookout, N. C. Jurassic deposits probably were drilled in the Blake-Bahama basin at DSDP drillsite 391 (Benson and others, 1978).

Reflectors in CDP seismic-reflection profiles that cross the southeastern continental margin were identified as Jurassic on the basis of indirect evidence given by Buffler and others (1978), Shipley and others (1978), and Dillon and others (1979a, b). The profile of Shipley and others (1978) and Buffler and others (1978) crosses profile FC8 (fig. 4) 14 km from FC8's seaward end, and the top of the Jurassic (Tithonian) shown in figure 4 was transferred from their profile (R. T. Buffler, oral commun., 1978). They picked this reflector on the basis of

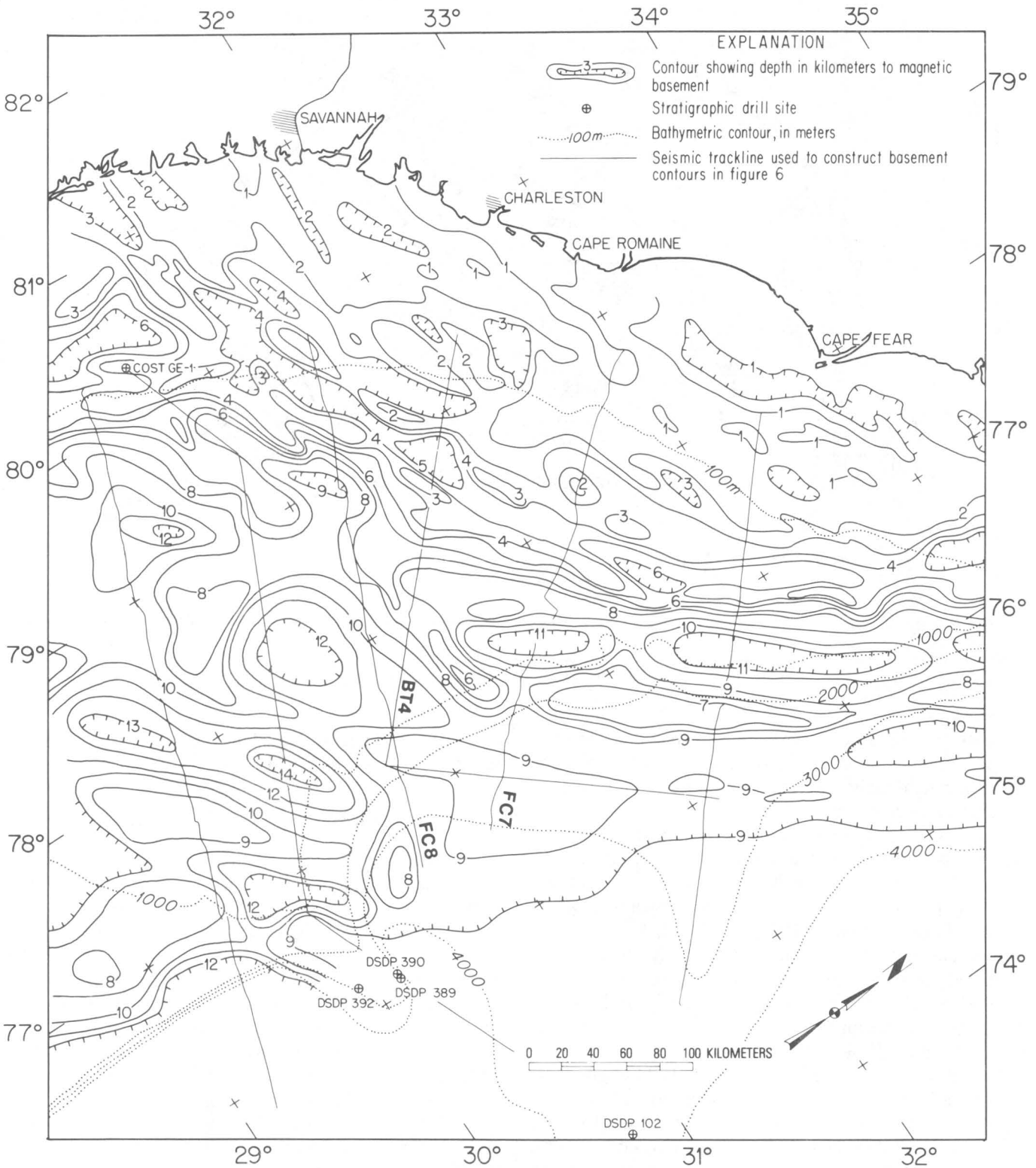

FIGURE 7.—Depth, in kilometers, to magnetic basement. Modified from Klitgord and Behrendt (1979).

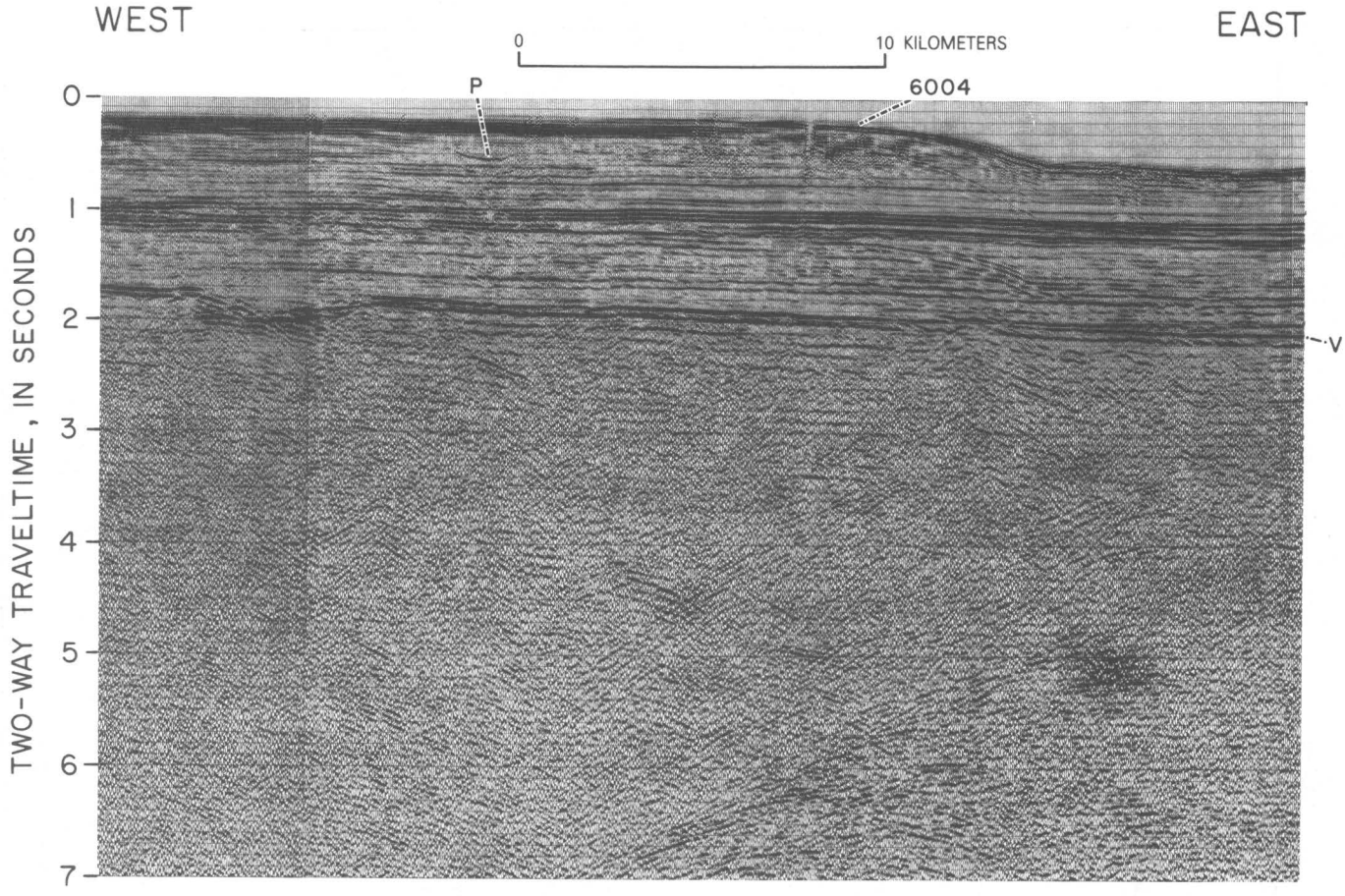

FIGURE 8.—Photograph of part of record for seismic profile BT4 (fig. 3) showing the strong reflector at about 2 seconds depth (V) that is thought to represent an offshore extension of volcanic rocks sampled on land. Location shown on figure 3. Stratigraphic drillsite 6004 (Hathaway and others, 1976) is on this profile. The well penetrated a Paleocene unconformity identified by P.

the probable age of oceanic basement where the reflector pinches out; the basement age was estimated by examining magnetic reversal patterns of the sea floor. We traced the assumed Tithonian top across the Continental Rise to the Blake Plateau with difficulty on profile FC8 and have mapped the reflector so identified as the Jurassic top (fig. 11). Although the choice is reasonable, it is far from dependable.

Thickness of the strata between the assumed Jurassic top and the postrift unconformity is shown in figure 10. Clearly, continental margin subsidence and deposition were irregular and concentrated in the Blake Plateau basin and Carolina trough during Jurassic time. Jurassic deposits pinch out against the postrift unconformity or the volcanic layer beneath the western Blake Plateau.

In contrast to the strong differential subsidence indicated by the Jurassic isopach map, the structure of the Jurassic top (fig. 11) shows almost no reflection of the two major basins. The main center of subsidence, as indicated by the 5-km contour, trends northeastward across the western Blake Plateau. Some effect of the Blake Spur fracture zone beneath the Blake Plateau still appears in the eastward swing of the 4-km contour.

CRETACEOUS STRATA

The top of Cretaceous strata was drilled at a U.S. Geological Survey stratigraphic drill site off South Carolina on profile BT4 (Hathaway and others, 1976). The location of this site (no. 6004) is shown in figure 1 and on the profile in figure 3. The Cretaceous also has been drilled on the Continental Shelf off Jacksonville, Fla. (COST GE–1 well, fig. 7; Scholle, 1979) and on the Blake Spur (DSDP 390 well, fig. 7; Benson and others, 1978) and has been traced from these sites through our grid of profiles (Dillon and others, 1979a). Therefore, the identification of the top of Cretaceous rocks in the seismic profiles is much more dependable than the identification for the Jurassic.

The Cretaceous rocks are thickest, exceeding 4 km, in a northeast-trending zone of subsidence on the inner Blake Plateau (fig. 12). This is the zone of subsidence

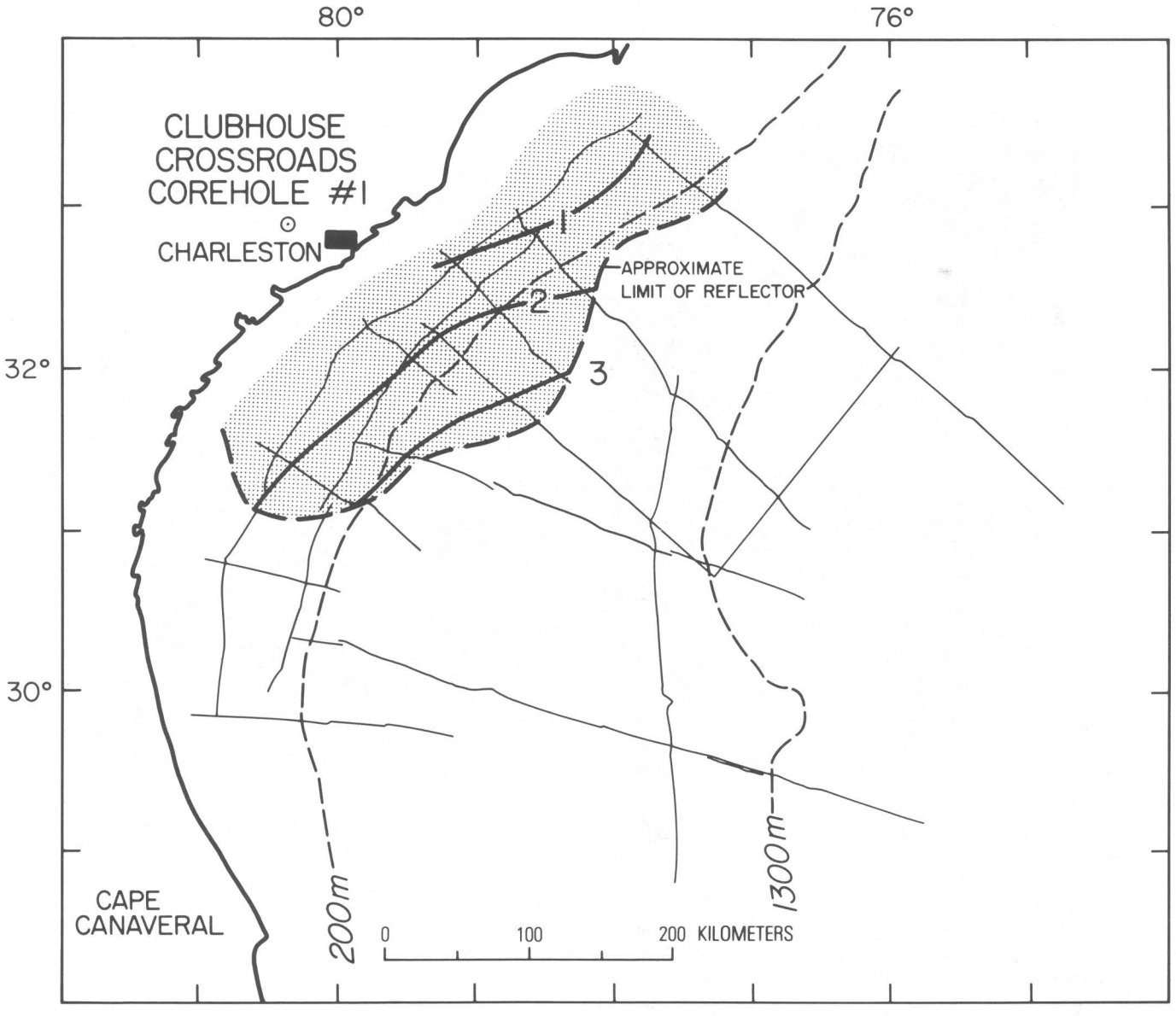

FIGURE 9.—Depth, in kilometers, to the strong reflector and high-velocity refractor that is thought to represent a volcanic layer (shaded). Light lines represent seismic tracklines.

that was identified on the structure map of the top of Jurassic (fig. 11). However, the Cretaceous deposits, unlike the Jurassic ones, form a fairly uniform blanket across the continental margin.

In general, the top of Cretaceous rocks (fig. 13) forms a smooth seaward-dipping planar surface beneath the Continental Shelf and Blake Plateau. The surface is disturbed only by the small basin beneath the Continental Shelf at about 30.5° to 31.5° N. shown by a northwestward reentrant in the contours. This is the Southeast Georgia embayment (restricted sense), which was active into the Tertiary and may be underlain by a relatively small pod of transitional crust (Paull and Dillon, 1979, 1980). A significant basement depression lies beneath this embayment, as indicated in the map of configuration of the top of magnetic basement (fig. 7).

SUMMARY AND CONCLUSIONS

1. The horizon observed as the top of seismic and magnetic basement is believed to be the postrift unconformity. We infer that the unconformity was cut early in the evolution of the continental margin when the block-faulted continental basement and early deposits in grabens were leveled to form a fairly smooth surface (fig. 14). The

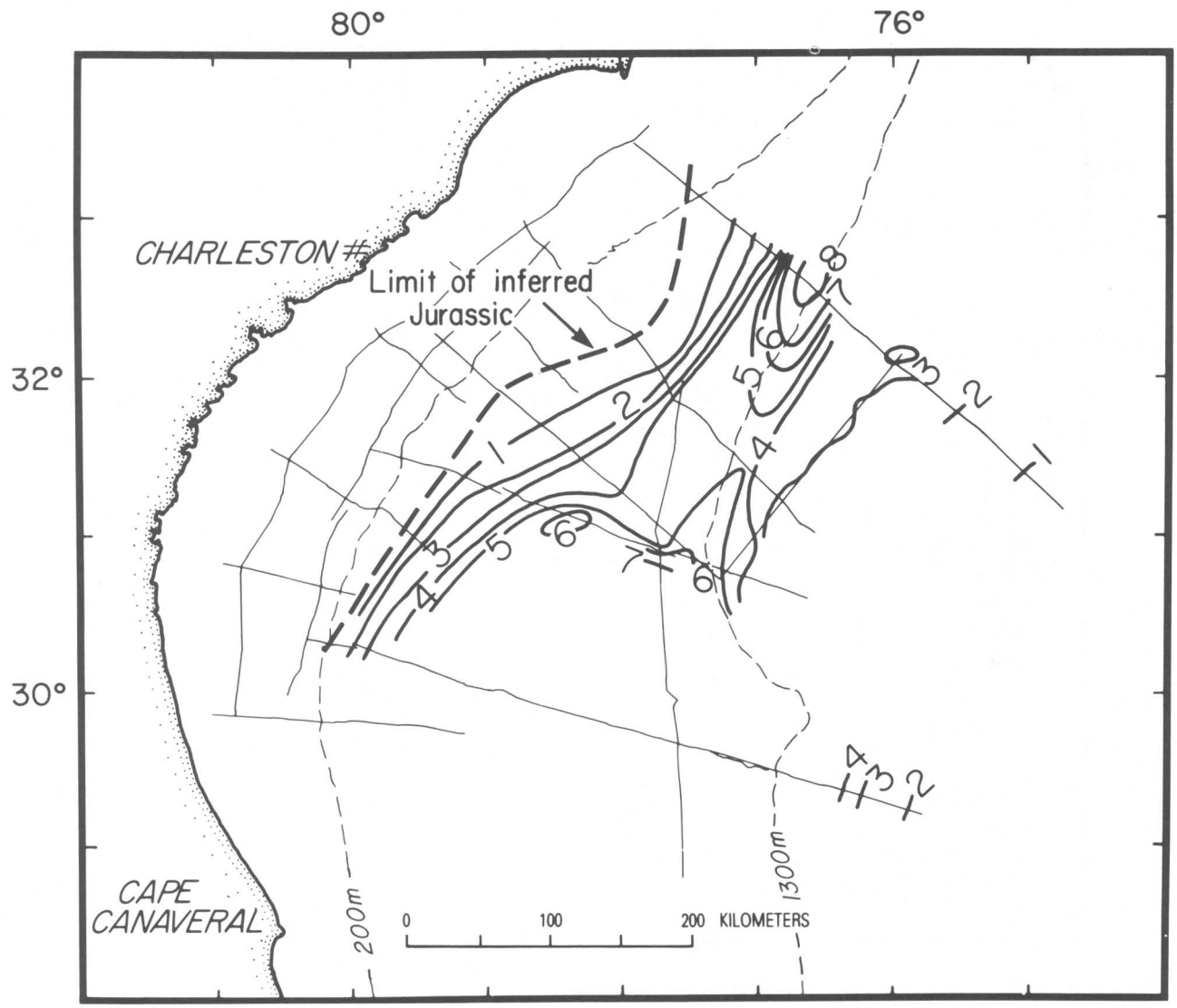

FIGURE 10.—Thickness, in kilometers, of rocks considered to be of Jurassic age. Light lines represent seismic tracklines.

postrift unconformity probably is underlain by Triassic and Lower Jurassic sedimentary strata, Paleozoic igneous, metamorphic, and sedimentary rocks, and volcanic and plutonic mafic igneous rocks emplaced during the rifting. The crust underlying the postrift unconformity is continental beneath a platform to the northwest but becomes transitional in nature beneath the Carolina Trough and Blake Plateau Basin. (Transitional crust is considered to be intermediate in composition and thickness between continental and oceanic crust.)

2. Covering the postrift unconformity beneath the shelf and inner Blake Plateau off South Carolina is a strong reflector, high-velocity refractor that is correlated with basaltic flows on land. These flows may have been erupted about 175 million years ago at the time of an inferred spreading-center jump and possibly a reorganization of plate movements in the North Atlantic (fig. 14).
3. Inferred Jurassic rocks form a wedge that pinches out seaward of the shelf edge and thickens markedly to the eastward into the Blake Plateau basin and Carolina trough (fig. 14).
4. Cretaceous strata extend across the entire continental margin and landward beneath the present Coastal Plain. They form a fairly uniform blanket, compared to Jurassic deposits, and thicken somewhat across the inner Blake Plateau basin (fig. 14).
5. Structure of the continental margin off South Carolina is dominated by two major basins, the Blake Plateau basin to the south and the Carolina

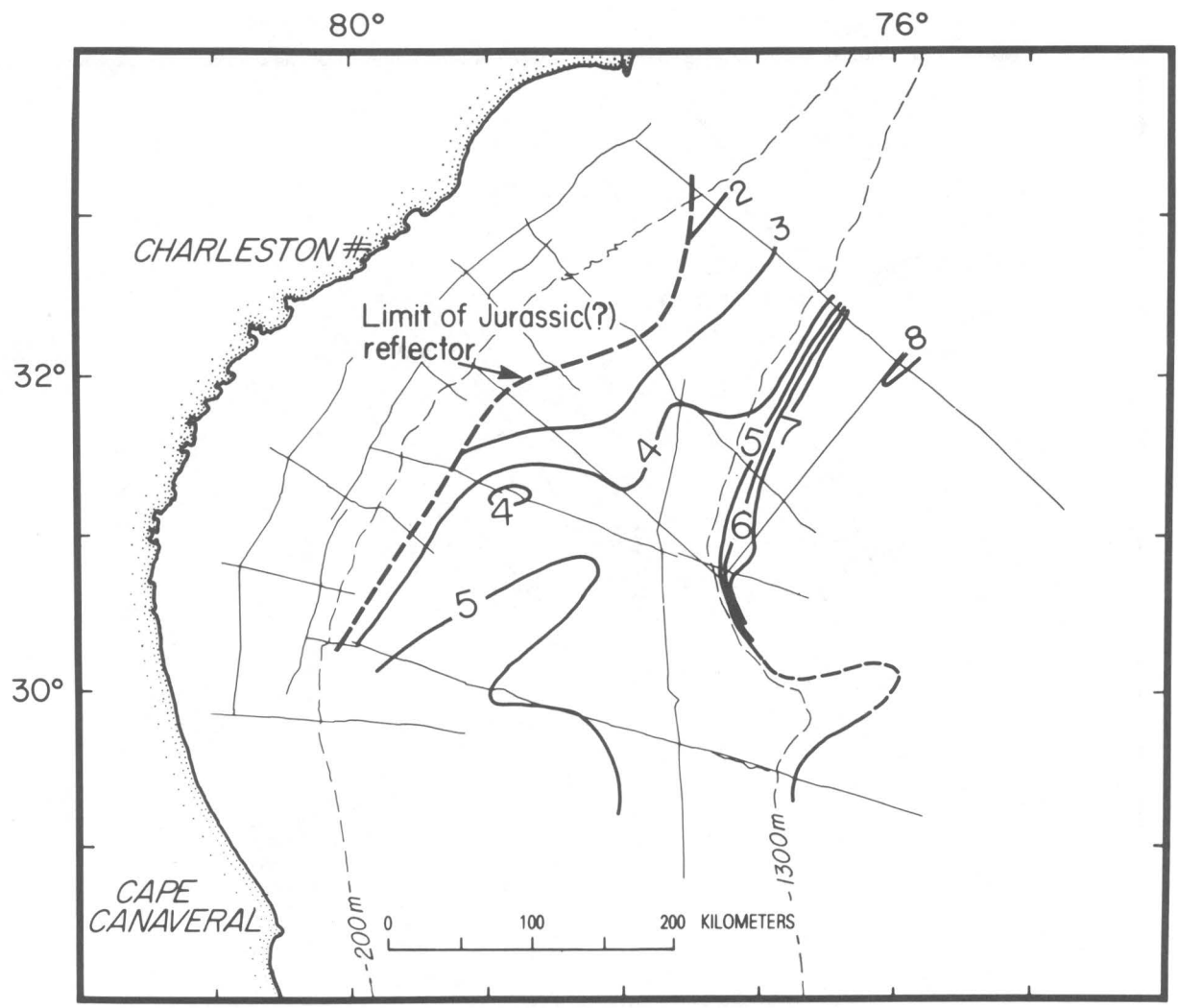

FIGURE 11.—Depth, in kilometers, to the reflector considered to represent the top of rocks of Jurassic age. Light lines represent seismic tracklines.

trough to the north. The basins are seaward of the Carolina platform, a region of shallow continental basement that extends offshore beyond the present shelf edge. Between the broad Blake Plateau basin and the narrow, elongate Carolina trough is a zone of a relatively shallow basement that occurs on the landward (northwestward) extension of the oceanic Blake Spur fracture zone. Beneath the Continental Shelf off Georgia is a small basin, the Southeast Georgia embayment, that subsided early in development of the continental margin and continued to do so into the Tertiary. It also may be underlain by transitional crust.

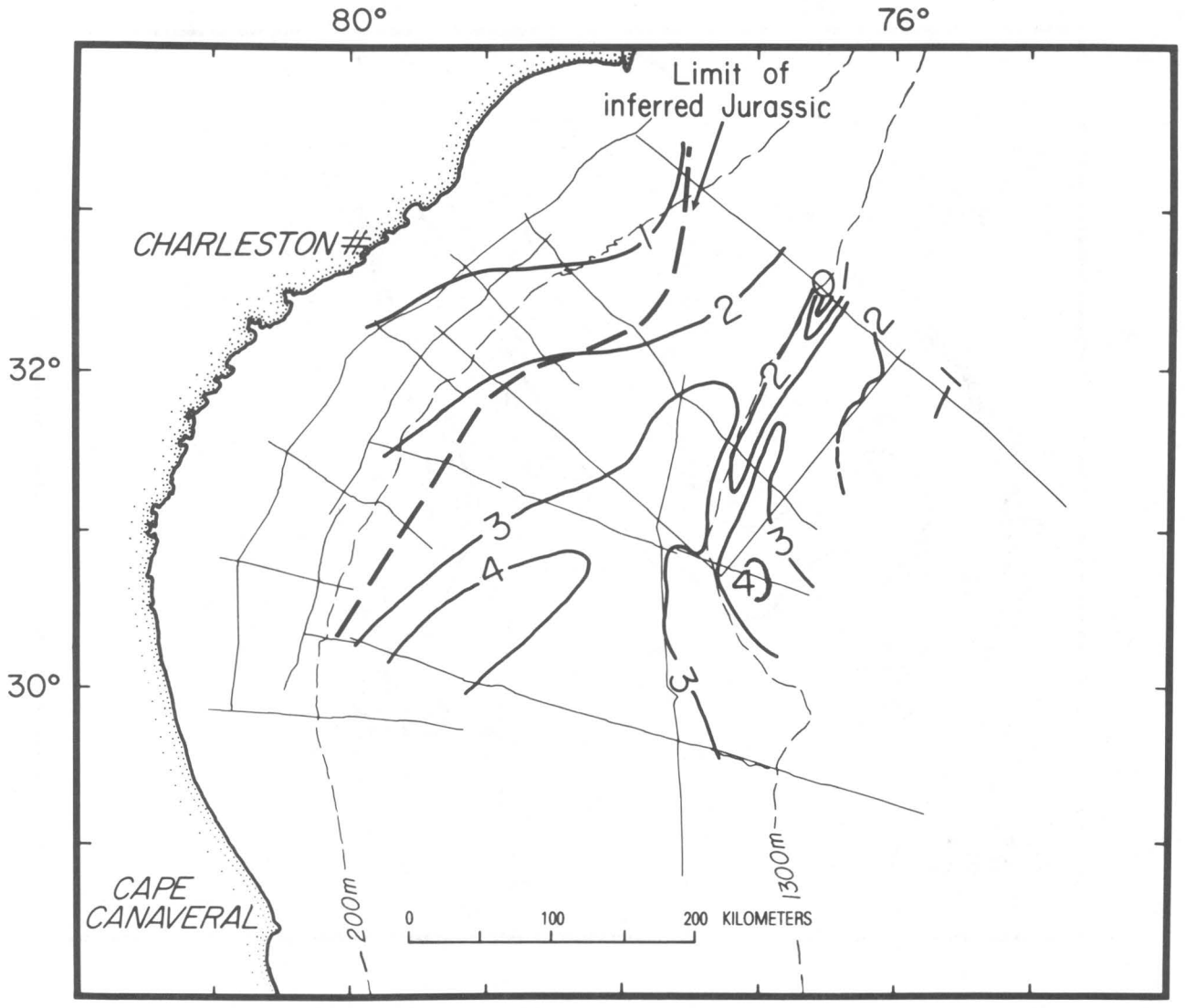

FIGURE 12. – Thickness, in kilometers, of rocks considered to be of Cretaceous age.

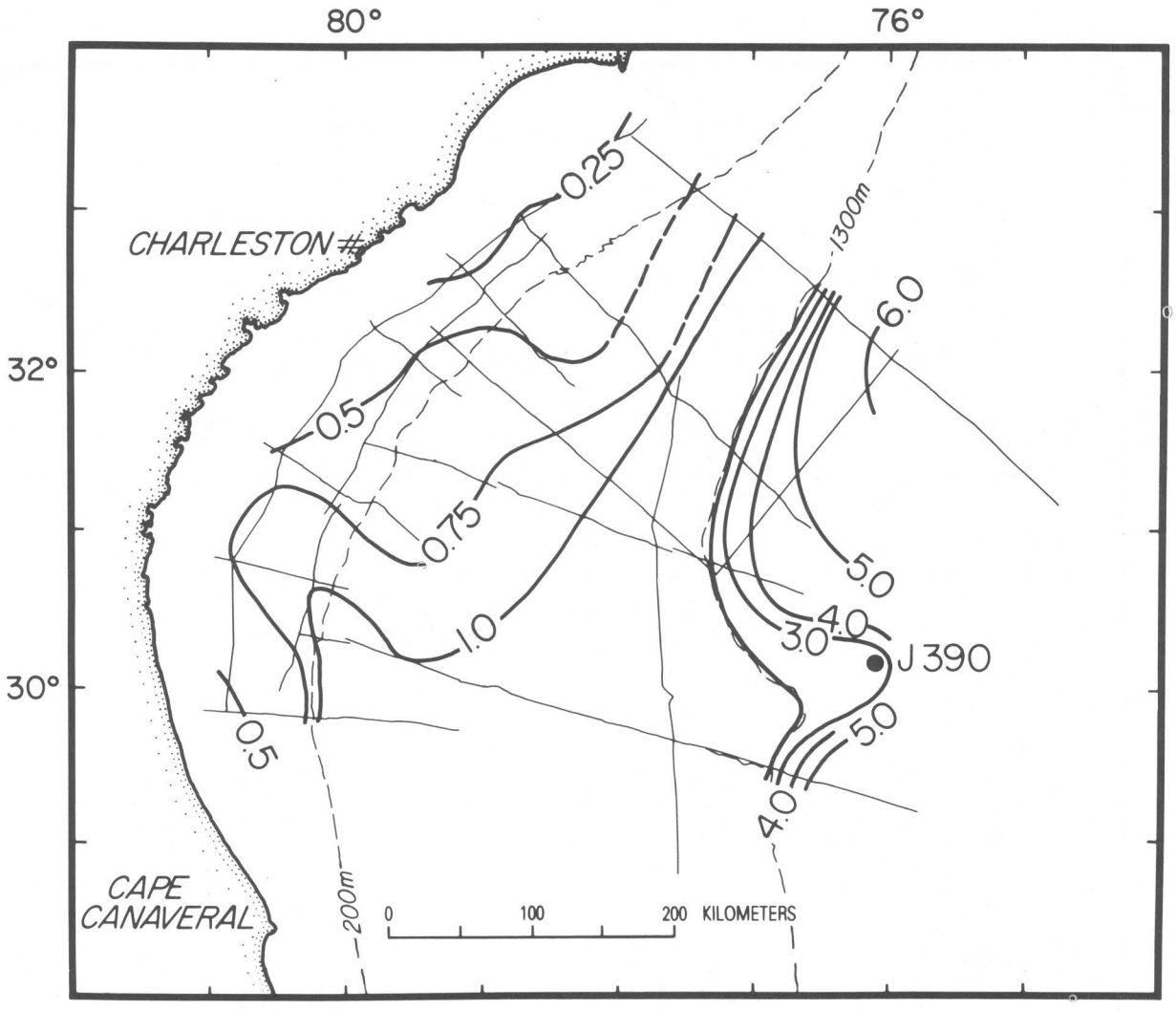

FIGURE 13.—Depth, in kilometers, to the reflector considered to represent the top of rocks of Cretaceous age.

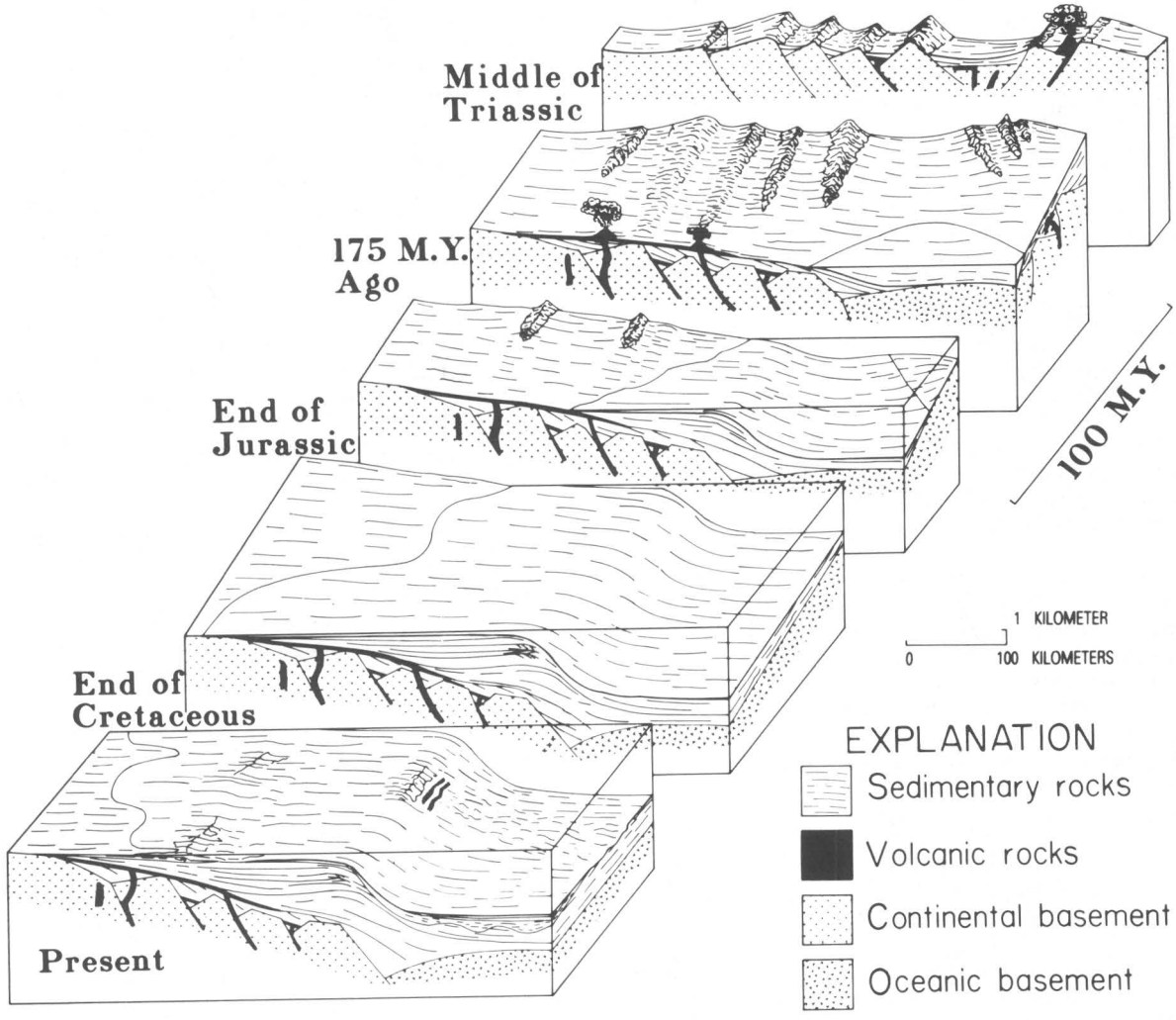

FIGURE 14.—Conceptual block diagram of the development of the continental margin off South Carolina from initial rifting to present. Note that one axis represents time and that the diagram represents the changes at one idealized profile section across the margin since the Triassic. Because the idealized section was chosen off Charleston, S. C., it represents margin development between major subsiding basins (see fig. 6). At this location, the "transitional" or mixed basement, considered to underlie the basins, is probably very slightly developed.

REFERENCES

Ackermann, H. D., 1977, Exploring the Charleston, South Carolina, earthquake area with seismic refraction–A preliminary study, *in* Rankin, D. W., ed., Studies related to the Charleston, South Carolina, earthquake of 1886–A preliminary report: U.S. Geological Survey Professional Paper 1028, p. 167–175.

———1983, Seismic-refraction study in the area of the Charleston, South Carolina, 1886 earthquake, *in* Gohn, G. S., ed., Studies related to the Charleston, South Carolina, earthquake of 1886–Tectonics and seismicity: U.S. Geological Survey Professional Paper 1313, p. F1–F20.

Behrendt, J. C., and Klitgord, K. D., 1979, High resolution aeromagnetic anomaly map of the U.S. Atlantic Continental Margin: U.S. Geological Survey Geophysical Investigations Map GP–931, scale 1:1,000,000.

Benson, W. E., Sheridan, R. E., and others, 1978, Site 391; Blake-Bahama Basin, *in* California University, Scripps Institution of Oceanography, La Jolla, Initial Reports of the Deep Sea Drilling Project, Volume 44: Washington, D.C., National Science Foundation, p. 153–336.

Buffler, R. T., Shipley, T. H., and Watkins, J. S., 1978, Seismic section no. 2; Blake continental margin seismic section: American Association of Petroleum Geologists, catalog no. 701, 1 sheet.

Buffler, R. T., Watkins, J. S., and Dillon, W. P., 1979, Geology of the offshore Southeast Georgia Embayment, U.S. Atlantic Continental Margin, based on multichannel seismic-reflection profiles, *in* Watkins, J. S., Montadert, Lucien, and Dickerson, P. W., eds., Geological and geophysical investigations of continental margins: American Association of Petroleum Geologists Memoir 29, p. 11–25.

Cramer, H. R., 1974, Isopach and lithofacies interpretations of the Cretaceous and Cenozoic rocks of the Coastal Plain of Georgia, *in* Stafford, L. P., ed., Petroleum geology of the Georgia Coastal Plain: Georgia Geologic Survey Bulletin 87, p. 21–43.

Dillon, W. P., and McGinnis, L. D., 1983, Basement structure indicated by seismic-refraction measurements offshore from South Carolina and adjacent areas, *in* Gohn, G. S., ed., Studies related to the Charleston, South Carolina, earthquake of 1886–Tectonics and seismicity: U.S. Geological Survey Professional Paper 1313, p. O1–O7.

Dillon, W. P., and Paull, C. K., 1978, Interpretation of multichannel seismic-reflection profiles of the Atlantic Continental Margin off coasts of South Carolina and Georgia: U.S Geological Survey Miscellaneous Field Studies Map MF–936, 1 sheet.

Dillon, W. P., Paull, C. K., Buffler, R. T., and Fail, J. P., 1979a, Structure and development of the Southeast Georgia Embayment and northern Blake Plateau–Preliminary analysis, *in* Watkins, J. S., Montadert, Lucien, and Dickerson, P. W., eds., Geological and geophysical investigations of continental margins: American Association of Petroleum Geologists Memoir 29, p. 27–41.

Dillon, W. P., Paull, C. K., Dahl, A. G., and Patterson, W. C., 1979b, Structure of the continental margin near the COST GE–1 drill site from a common-depth-point seismic-reflection profile, *in* Scholle, P. A., ed., Geological studies of the COST GE–1 well, United States South Atlantic Outer Continental Shelf area: U.S. Geological Survey Circular 800, p. 97–107.

Grow, J. A., Dillon, W. P., and Sheridan, R. E., 1977, Diapirs along the continental slope off Cape Hatteras [abs.]: Geophysics, v. 42, no. 7, p. 1507.

Hathaway, J. C., and others, editors, 1976, Preliminary summary of the 1976 Atlantic margin coring project of the U.S. Geological Survey: U.S. Geological Survey Open-File Report 76–844, 217 p.

Hersey, J. B., Bunce, E. T., Wyrick, R. F., and Dietz, F. T., 1959, Geophysical investigation of the continental margin between Cape Henry, Virginia and Jacksonville, Florida: Geological Society of America Bulletin, v. 70, no. 4, p. 437–465.

Kane, M. F., Yellin, M. J., Bell, K. G., and Zietz, Isidore, 1972, Gravity and magnetic evidence of lithology and structure in the Gulf of Maine region: U.S. Geological Survey Professional Paper 726–B, 22 p.

Kent, K. M., Grow, J. A., and Dillon, W. P., 1979, Gravity studies of the continental margin off northern Florida [abs.]: Geological Society of America Abstracts with Programs, v. 11, no. 4, p. 184.

Klitgord, K. D., and Behrendt, J. C., 1977 [1978], Aeromagnetic anomaly map of the United States Atlantic continental margin: U.S. Geological Survey Miscellaneous Field Studies Map MF–913, 2 sheets.

———1979, Basin structure of the U.S. Atlantic margin, *in* Watkins, J. S., Montadert, Lucien, and Dickerson, P. W., eds., Geological and geophysical investigations of continental margins: American Association of Petroleum Geologists Memoir 29, p. 85–112.

Klitgord, K. D., Dillon, W. P., and Popenoe, Peter, 1983, Mesozoic tectonics of the Southeastern United States Coastal Plain and continental margin, *in* Gohn, G. S., ed., Studies related to the Charleston, South Carolina, earthquake of 1886–Tectonics and seismicity: U.S. Geological Survey Professional Paper 1313, p. P1–P15.

Paull, C. K., and Dillon, W. P., 1979, The subsurface geology of the Florida-Hatteras shelf, slope, and inner Blake Plateau: U.S. Geological Survey Open-File Report 79–448, 96 p.

———1980, Structure, stratigraphy, and geologic history of Florida-Hatteras Shelf and inner Blake Plateau: American Association of Petroleum Geologists Bulletin, v. 64, no. 3, p. 339–358.

Scholle, P. A., editor, 1979, Geological studies of the COST GE–1 well, United States South Atlantic Outer Continental Shelf area: U.S. Geological Survey Circular 800, 114 p.

Schouten, Hans, and Klitgord, K. D., 1977 [1978], Map showing Mesozoic magnetic anomalies, western North Atlantic: U.S. Geological Survey Miscellaneous Field Studies Map MF–915, scale 1:2,000,000.

Shipley, T. H., Buffler, R. T., and Watkins, J. S., 1978, Seismic stratigraphy and geologic history of Blake Plateau and adjacent western Atlantic continental margin: American Association of Petroleum Geologists Bulletin, v. 62, no. 5, p. 792–812.

Taner, M. T., and Koehler, Fulton, 1969, Velocity spectra–digital computer derivation and applications of velocity functions: Geophysics, v. 34, no. 6, p. 859–881.

Taylor, P. T., Zietz, Isidore, and Dennis, L. S., 1968, Geologic implications of aeromagnetic data for the eastern continental margin of the United States: Geophysics, v. 33, no. 5, p. 755–780.

Woollard, G. P., Bonini, W. E., and Meyer, R. P., 1957, A seismic refraction study of the sub-surface geology of the Atlantic Coastal Plain and Continental Shelf between Virginia and Florida: Madison, University of Wisconsin, Department of Geology, Geophysics Section, Technical Report Contract No. N7onr–28512, 128 p.

Basement Structure Indicated by Seismic-Refraction Measurements Offshore From South Carolina and Adjacent Areas

By WILLIAM P. DILLON and LYLE D. McGINNIS

STUDIES RELATED TO THE CHARLESTON, SOUTH CAROLINA, EARTHQUAKE OF 1886—TECTONICS AND SEISMICITY

GEOLOGICAL SURVEY PROFESSIONAL PAPER 1313-O

UNITED STATES GOVERNMENT PRINTING OFFICE, WASHINGTON: 1983

CONTENTS

ILLUSTRATIONS

STUDIES RELATED TO THE CHARLESTON, SOUTH CAROLINA, EARTHQUAKE OF 1886—
TECTONICS AND SEISMICITY

BASEMENT STRUCTURE INDICATED BY SEISMIC-REFRACTION MEASUREMENTS OFFSHORE FROM SOUTH CAROLINA AND ADJACENT AREAS

By WILLIAM P. DILLON and LYLE D. McGINNIS[1]

ABSTRACT

Seismic-refraction profiling data collected by the U.S. Geological Survey (USGS) and other researchers have been projected to two lines extending parallel to the strike of regional structure on the continental margin of the Southeastern United States. One line extends along the Continental Shelf from northern Florida to southern North Carolina; the other is parallel to it along the inner Blake Plateau. Data from the shelf show a very strong refracting horizon having compressional wave velocities of about 5.8–6.3 km/s. This horizon dips gently away from the Cape Fear arch and appears to terminate near the Georgia-Florida boundary. This seismic horizon is inferred to represent basalt layers comparable with the basalt drilled by the USGS near Charleston. High refraction velocities south of the Georgia-Florida boundary probably represent Paleozoic basement. The set of refraction profiles on the Blake Plateau show only one compressional wave value that probably is related to basement. Other very high refraction velocities (about 7 km/s) beneath the western Blake Plateau might result from mafic or ultramafic plutons.

INTRODUCTION

Refraction profiles taken at sea, although generally not reversed, can be valuable for determining the approximate depths and velocities of high-velocity layers. We use such data from the area offshore from South Carolina, Georgia, and northern Florida (fig. 1) to describe the extent of an inferred basalt layer along the Continental Shelf and to estimate the layer's seismic velocity. The extent of the inferred basalt layer has been mapped more completely by means of multichannel seismic-reflection data (Dillon and others, 1983); however, reflection data do not provide velocity information for the basalt. The refraction data also are interpreted to indicate basement structure where the inferred basalt layer is absent.

Seismic-refraction studies for this region have been reported by Woollard and others (1957), Hersey and others (1959), Antoine and Henry (1965), Sheridan and others (1966), and Dowling (1968); compilations of refraction data have been published by Drake and others (1968), Mayhew (1974), and Grim and others (1980).

Refraction profiles collected by the U.S. Geological Survey (USGS) were obtained by means of airgun sound sources. Profiles labeled "FC SB" in the Continental Shelf section (fig. 2) were collected using the Institut français du Pétrole Flexichoc[2] source, a large, low-pressure airgun (about 50 psi or 345 kPa). This source produces a relatively simple pulse approximately equivalent to a 1,000-in^3 (16,390 cm^3) array of airguns. All profiles in the Blake Plateau Section were obtained by using a 300-in^3 (4,917 cm^3) airgun array fired at approximately 2,000 psi (13,790 kPa). Disposable sonobuoys were used to receive refracted arrivals, and these arrivals were radioed back to the ship to be recorded. Methods for other previously published profiles are reviewed in the articles from which they were obtained.

RESULTS AND DISCUSSION

Refraction data were projected to one of two lines: one along the midshelf for shelf data and one along the inner Blake Plateau for USGS profiles 2 through 13. Locations of these lines of projection are shown in figure 2 (inset). The depth to a picked refractor is shown by a dot (fig. 2), and the velocity of the refractor is shown adjacent to the dot. Additional values in parentheses are dip-corrected velocities. Dip corrections are based on simultaneous seismic-reflection profiles. Although seismic-refraction data represent discrete boundaries formed by abrupt changes in compressional-wave veloci-

[1]Department of Geology, Northern Illinois University, DeKalb, Ill.

[2]Any use of trade names is for identification purposes only and does not imply endorsement by the U.S. Geological Survey.

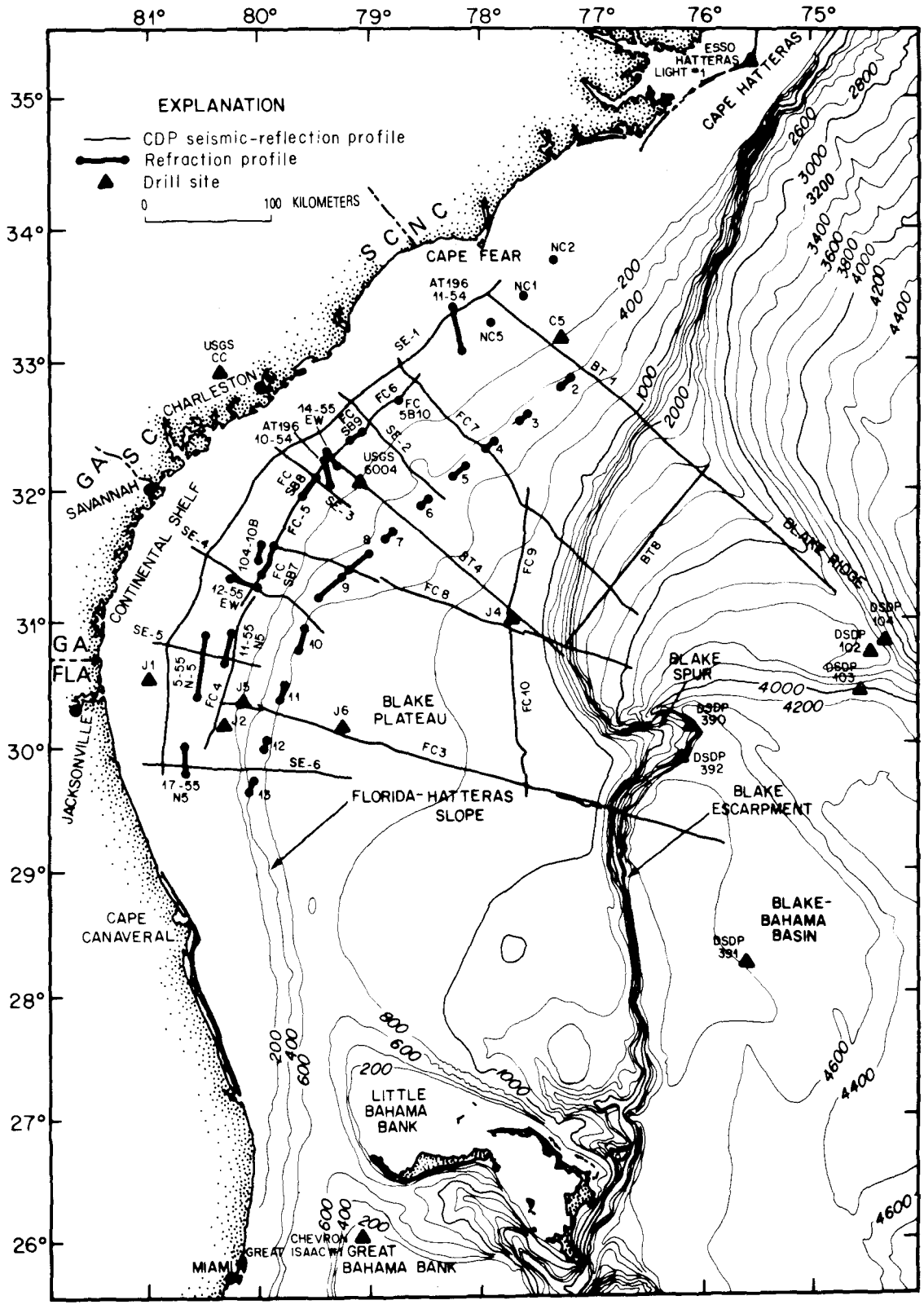

FIGURE 1.—Map showing locations of seismic-refraction and seismic reflection profiles and selected drillsites from northern Florida to southern North Carolina. Refraction profiles identified only by number were collected by the USGS using Flexichoc seismic source. Those identified by hyphenated numbers (for example, 71–55 NA or AT 196 11–54) were reported by Hersey and others (1959). Those identified by "NX" were reported by Woollard and others (1957).

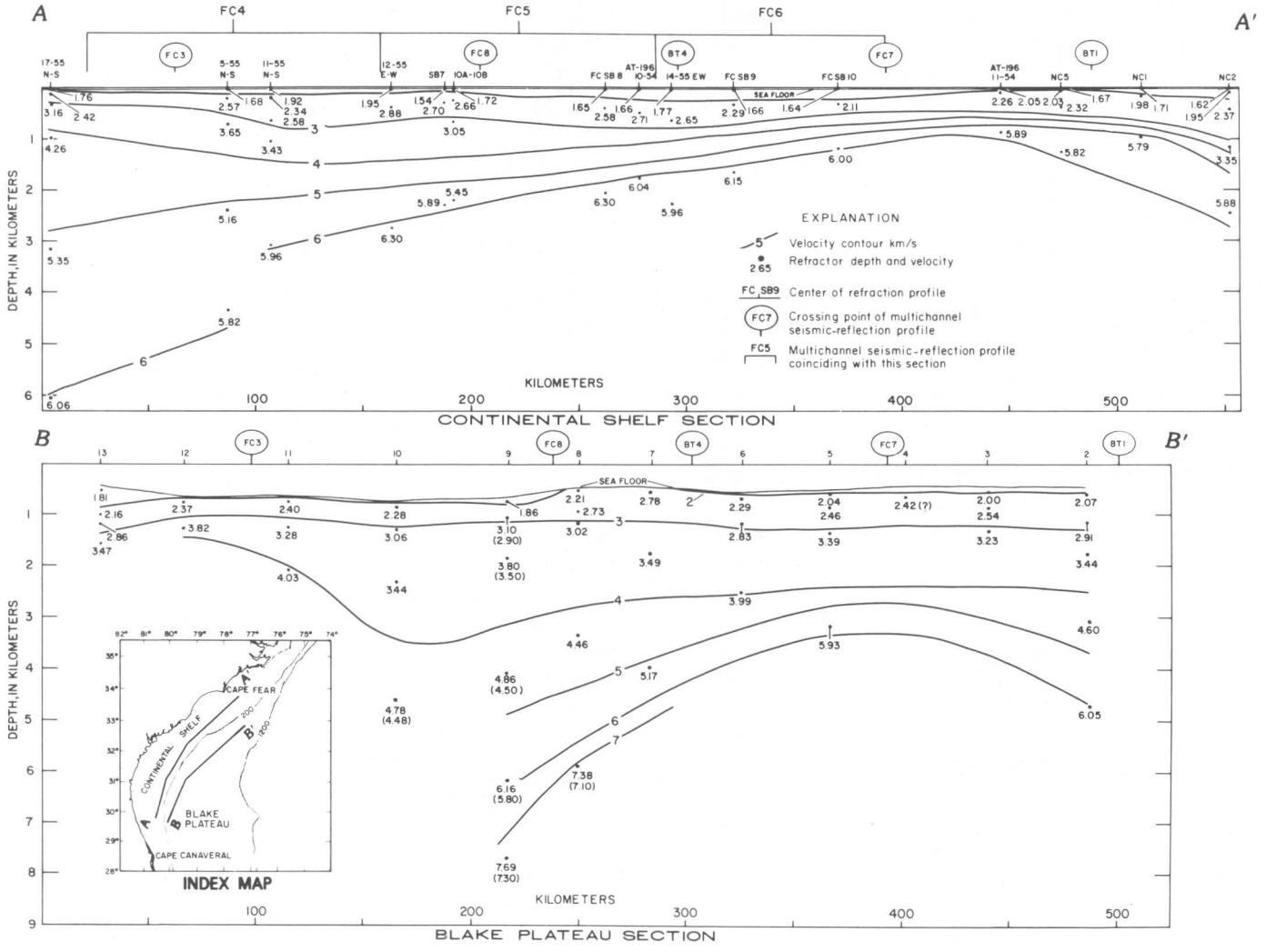

FIGURE 2.—Refraction data projected to lines shown in inset map. Depth of refraction measurement is shown by a dot; the adjacent number indicates the calculated velocity in kilometers per second. Numbers in parentheses indicate dip-corrected values; dips were obtained from simultaneously taken seismic-reflection profiles. Vertical exaggeration is ×24.

ty, the data have been contoured as though velocities increased in a continuous manner. This technique permits the general pattern of velocities to be observed, by focusing attention away from the particular style of velocity change.

Continental Shelf Section

The great majority of compressional-wave refraction velocities in the Continental Shelf section (fig. 2) fall in two groups. In the upper ½ km, values are in the range 1.6–2.7 km/s (kilometer/second); at considerably greater depths, values between 5.8 and 6.3 km/s are found. Apparently, sharp changes in velocity between the two levels, which would produce refractions, are rare. The 3-km/s contour, which defines the base of the group of low-velocity values, is essentially horizontal at a depth of about 0.7 km, although its depth varies by several tenths of a kilometer along the 550-km section.

The 6-km/s contour indicates the pattern of the higher velocity group of refraction events. It shows a minimum depth off northern South Carolina, south of Cape Fear (kilometer 420, fig. 2), and presumably represents the Cape Fear arch. To the southwestward, the depths to refraction velocities near 6 km/s become uniformly greater to a point off southern Georgia (about kilometer 100, fig. 2). The 6-km/s contour then seems to step down abruptly by about 1.5 km. This apparent step is controlled by only two measurements, but they probably are dependable.

Over the northern part of the shelf profile (kilometers 100 to 500), velocities near 6 km/s probably represent refraction returns from an extension of the basalt layer that has been identified on land in South Carolina (Gohn

and others, 1978) and is discussed in several papers in this volume. Depths calculated from refraction data compare well with the depths to inferred basalt mapped in multichannel seismic profiles by Dillon and others (1983) and with the "J" layer of Behrendt and others (1983). For comparison, we have included seismic-reflection profiles FC4 and FC5–6 (fig. 3). These lines are located on the Continental Shelf line of projection; their locations are shown in figure 1, and their extent along the Continental Shelf line of projection is indicated by brackets in figure 2. The depth of the inferred basalt layer in the profile (fig. 3) corresponds closely to that of the 6-km/s refraction velocity contour (fig. 2). The inferred basalt reflector rises gently and smoothly from the northern (right) end of profile FC4 throughout profile FC5–6, as also suggested by the refraction data, interrupted only by some small irregularities at about kilometers 210–230. These irregularities (fig. 4) are located at large positive magnetic and gravity anomalies (Klitgord and Behrendt, 1977; Grow and others, 1979) and may represent the eroded remnants of feeder stocks that supplied the basalt flows.

We believe that the termination of the 6-km/s contour of compressional-wave velocity at kilometer 100 (fig. 2) probably denotes the southern limit of the basalt. Southwest of this location, the high-velocity refractions probably were obtained from Paleozoic crystalline basement. The inferred basalt reflector disappears in the northern part of profile FC4 as well (fig. 3), and penetration increases to more than 4 s (two-way) south of the inferred basalt in that profile.

Blake Plateau Section

On the inner Blake Plateau, the shallow refraction events indicate rather high velocities near the sea floor, generally greater than 2 km/s (fig. 2). We attribute these velocities to exposure of older, lithified strata, due to removal or nondeposition of most Cenozoic sediments beneath the Gulf stream (Paull and Dillon, 1980). The profiles were run essentially along the axis of the stream, where Cretaceous deposits commonly crop out on the sea floor. A uniform increase in compressional-wave velocity with increasing depth is observed everywhere north of the Georgia-Florida boundary (kilometer 150). South of this point, velocity gradients are much higher, possibly due to increased carbonate content in the stratigraphic section.

Only three of the refraction profiles of the Blake Plateau section are near the region of the inferred basalt reflector (Dillon and others, 1983, fig. 9), and these (profiles 5, 6, and 7) are at the edge of the reflector identified as basalt, where this identification becomes questionable. Only one of these three refraction profiles, profile 5, shows a compressional-wave velocity, 5.93 km/s at 3.2 km depth, that apparently should be attributed to the basalt.

Very high refraction velocities of 7.1 and 7.3 km/s at refraction profiles 8 and 9 probably represent intrabasement refractors. These occur at a magnetic and gravity high (Klitgord and Behrendt, 1977; Grow and others, 1979) on the eastward extension of the Brunswick magnetic anomaly. These velocities were measured at the northern boundary of the Blake Plateau basin, presumably the location of an active fracture zone during early rifting (Klitgord and Behrendt, 1977). Shallow high-velocity, high-density bodies are characteristic of oceanic fracture zones and probably result from intrusion of ultramafic material after partial serpentinization (Robb and Kane, 1975; Detrick and Purdy, 1980). Two similar high-velocity refraction values that probably represent intrabasement refractors have been reported east of refraction profiles 8 and 9 on the northern boundary of the basin (Hersey and others, 1959, profiles 2–56 and 36–55). Such values have not been reported elsewhere in the region, so they may be associated with intrusions emplaced during movement at the fracture zone during the early phase of separation of the continents.

SUMMARY AND CONCLUSIONS

1. Beneath the Continental Shelf, most compressional-wave refraction velocities measured are either relatively low (1.6–2.7 km/s) or relatively high (5.8–6.3 km/s). The low velocities generally occur in the upper 500 m of section, and it is presumed that velocities increase gradually below that depth to the depth at which a high-velocity refracting horizon is encountered.
2. The high compressional-wave velocities in the Continental Shelf section probably originate from the basalt layer drilled near Charleston and discussed by other authors in this volume (Gohn, 1983). This refracting horizon clearly corresponds to the strong reflecting layer correlated with the basalt by Dillon and others (1979, 1983) and called the "J" layer by Behrendt and others (1983). The discrepancy between our refraction velocities for this layer and the slightly lower refraction velocities reported by Ackermann (1983) is discussed by Dillon and others (1983).
3. The abrupt increase in depth to high-velocity refractions beneath the shelf off southern Georgia probably occurs at the termination of the inferred basalt layer. High velocities farther south probably represent Paleozoic crystalline basement.

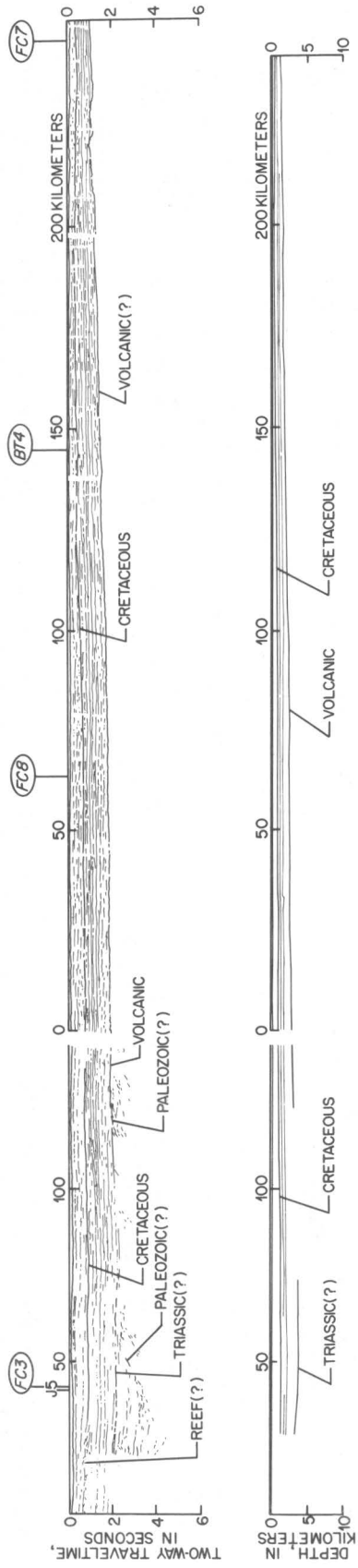

FIGURE 3.—Line drawing (above) and calculated depth section (below) for profiles FC4 and FC5–6. Locations of profiles shown in figure 1.

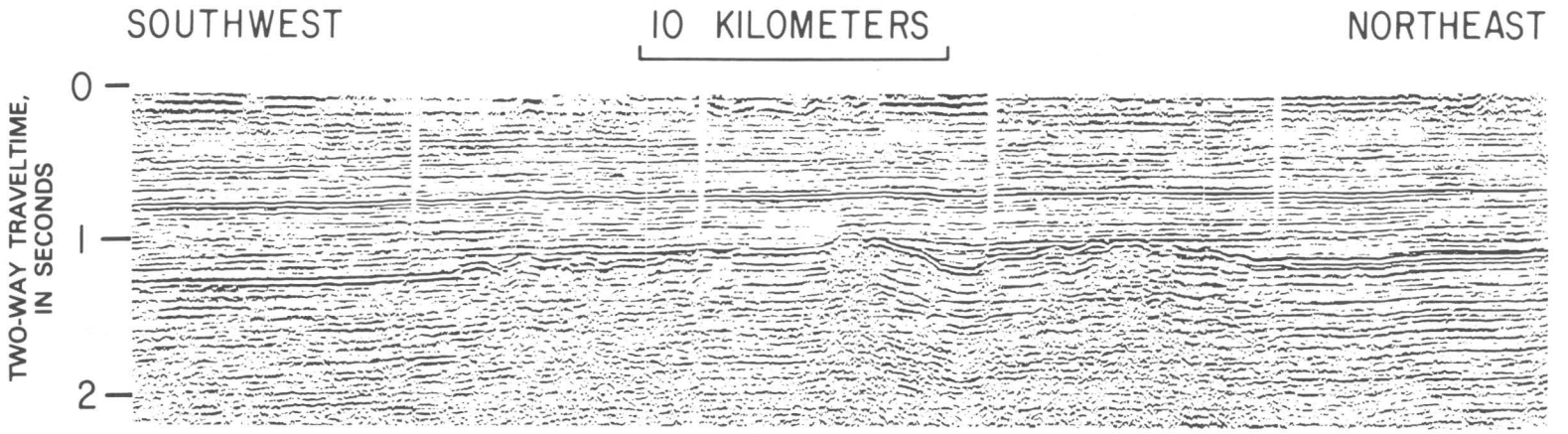

FIGURE 4. – Part of seismic record for profile FC5–6 from kilometers 196 to 243. The strong reflector that intersects the left side of this section of the profile at 1.28 s may be a reflection from a volcanic layer. It is interrupted by an irregular strong reflector in the middle of this figure that may represent basement.

4. Beneath the inner Blake Plateau, high compressional-wave velocities inferred to represent basalt refractions occur at only one station. Other very-high-velocity refraction values, exceeding 7 km/s, might represent refractions from mafic or ultramafic plutons.

REFERENCES CITED

Ackermann, H. D., 1983, Seismic-refraction study in the area of the Charleston, South Carolina, 1886 earthquake, *in* Gohn, G. S., ed., Studies related to the Charleston, South Carolina, earthquake of 1886–Tectonics and seismicity: U.S. Geological Survey Professional Paper 1313, p. F1–F20.

Antoine, J. W., and Henry, V. J., Jr., 1965, Seismic refraction study of shallow part of Continental Shelf off Georgia coast: American Association of Petroleum Geologists Bulletin, v. 49, p. 601–609.

Behrendt, J. C., Hamilton, R. M., Ackermann, H. D., Henry, V. J., and Bayer, K. C., 1983, Marine multichannel seismic-reflection evidence for Cenozoic faulting and deep crustal structure near Charleston, South Carolina, *in* Gohn, G. S., ed., Studies related to the Charleston, South Carolina, earthquake of 1886–Tectonics and seismicity: U.S. Geological Survey Professional Paper 1313, p. J1–J29.

Detrick, R. S., Jr., and Purdy, G. M., 1980, The crustal structure of the Kane fracture zone from seismic refraction studies: Journal of Geophysical Research, v. 85. no. B7, p. 3759–3777.

Dillon, W. P., Klitgord, K. D., and Paull, C. K., 1983, Mesozoic development and structure of the continental margin off South Carolina, *in* Gohn, G. S., ed., Studies related to the Charleston, South Carolina, earthquake of 1886–Tectonics and seismicity: U.S. Geological Survey Professional Paper 1313, p. N1–N16.

Dillon, W. P., Paull, C. K., Buffler, R. T., and Fail, J. P., 1979, Structure and development of the Southeast Georgia Embayment and northern Blake Plateau–Preliminary analysis, *in* Watkins, J. S., Montadert, Lucien, and Dickerson, P. W., eds., Geological and geophysical investigations of continental margins: American Association of Petroleum Geologists Memoir 29, p. 27–41.

Dowling, J. J., 1968, The East Coast onshore-offshore experiment, II. Seismic refraction measurements on the continental shelf between Cape Hatteras and Cape Fear: Seismological Society of America Bulletin, v. 58, no. 3, p. 821–834.

Drake, C. L., Ewing, J. I., and Stockard, Henry, 1968, The continental margin of the eastern United States: Canadian Journal of Earth Sciences, v. 5, no. 4, p. 993–1010.

Gohn, G. S., editor, 1983, Studies related to the Charleston, South Carolina, earthquake of 1886–Tectonics and seismicity: U.S. Geological Survey Professional Paper 1313, 375 p.

Gohn, G. S., Gottfried, David, Lanphere, M. A., and Higgins, B. B., 1978, Regional implications of Triassic or Jurassic age for basalt and sedimentary red beds in the South Carolina Coastal Plain: Science, v. 202, no. 4370, p. 887–890.

Grim, M. S., Dillon, W. P., and Mattick, R. E., 1980, Seismic reflection, refraction and gravity measurements from the Continental Shelf offshore from North and South Carolina: Southeastern Geology, v. 21, no. 4, p. 239–249.

Grow, J. A., Bowin, C. O., and Hutchinson, D. R., 1979, The gravity field of the U.S. Atlantic continental margin: Tectonophysics, v. 59, p. 27–52.

Hersey, J. B., Bunce, E. T., Wyrick, R. F., and Dietz, F. T., 1959, Geophysical investigation of the continental margin between Cape Henry, Virginia and Jacksonville, Florida: Geological Society of America Bulletin, v. 70, no. 4, p. 437–465.

Klitgord, K. D., and Behrendt, J. C., 1977, Aeromagnetic anomaly map of the United States Atlantic continental margin: U.S. Geological Survey Miscellaneous Field Studies Map MF-913, 2 sheets, scale 1:1,000,000.

Mayhew, M. A., 1974, "Basement" to east coast continental margin of North America: American Association of Petroleum Geologists Bulletin, v. 58, no. 6, p. 1069–1088.

Paull, C. K., and Dillon, W. P., 1980, Structure, stratigraphy, and geologic history of Florida-Hatteras Shelf and inner Blake Plateau: American Association of Petroleum Geologists Bulletin, v. 64, no. 3, p. 339–358.

Robb, J. M., and Kane, M. F., 1975, Structure of the Vema fracture zone from gravity and magnetic intensity profiles: Journal of Geophysical Research, v. 80, no. 32, p. 4441–4445.

Sheridan, R. E., Drake, C. L., Nafe, J. E., and Hennion, John, 1966, Seismic refraction study of continental margin east of Florida: American Association of Petroleum Geologists Bulletin, v. 50, no. 9, p. 1972–1991.

Woollard, G. P., Bonini, W. E., and Meyer, R. P., 1957, A seismic refraction study of the sub-surface geology of the Atlantic Coastal Plain and Continental Shelf between Virginia and Florida: Madison, Wisconsin, University of Wisconsin, Department of Geology, Geophysics Section, Technical Report, Contract No. N7onr-28512, 128 p.

Mesozoic Tectonics of the Southeastern United States Coastal Plain and Continental Margin

By KIM D. KLITGORD, WILLIAM P. DILLON, and PETER POPENOE

STUDIES RELATED TO THE CHARLESTON, SOUTH CAROLINA, EARTHQUAKE OF 1886—TECTONICS AND SEISMICITY

GEOLOGICAL SURVEY PROFESSIONAL PAPER 1313-P

UNITED STATES GOVERNMENT PRINTING OFFICE, WASHINGTON: 1983

CONTENTS

ILLUSTRATIONS

STUDIES RELATED TO THE CHARLESTON, SOUTH CAROLINA, EARTHQUAKE OF 1886—
TECTONICS AND SEISMICITY

MESOZOIC TECTONICS OF THE SOUTHEASTERN UNITED STATES COASTAL PLAIN AND CONTINENTAL MARGIN

By KIM D. KLITGORD, WILLIAM P. DILLON, and PETER POPENOE

ABSTRACT

Many of the major structures associated with Paleozoic and Mesozoic tectonic events along the Southeastern U.S. Coastal Plain and continental margin have distinctive geophysical and geological properties, which are described in this integrated study of magnetic, gravity, seismic-reflection, and drill-hole data. These data are used to identify three major tectonic boundaries that separate terranes of Paleozoic, Triassic, and Jurassic tectonic activity and to map sedimentary basins that were formed by Triassic and Jurassic rifting events. The major tectonic boundaries are: (1) An offshore hinge zone in basement that separates an area of crustal subsidence associated with the Jurassic-age marginal basins from an area of significantly less subsidence associated with Triassic and older basement structures to the west; (2) a line of narrow grabens, associated with the magnetic low in the Brunswick magnetic anomaly, that separates a Paleozoic basin underlying northeastern Florida, which was not greatly affected by late Paleozoic or Triassic tectonic activity, from a broad zone of considerable Triassic tectonic activity and sediment accumulation in the Charleston, S. C., region; and (3) a narrow east-west zone near 33°N. that separates the geophysically distinctive northeast-trending Piedmont to the north from the Charleston region. The Triassic sedimentary basins are of two types: (1) narrow basins or grabens within the Piedmont and along the major tectonic boundaries and (2) broad zones of sediment accumulation over a block-faulted Paleozoic basin in northwestern Florida and in areas delineated by low-gradient magnetic and gravity fields in parts of the Charleston region. Deep continental margin basins, containing sedimentary rock as much as 14 km thick, formed at sites of Jurassic rifting and subsequent ocean opening seaward of the basement hinge zone. Reconstruction of the positions of the North American, South American, and African continents during the Early Jurassic provides a framework for relating the Mesozoic tectonic events and structures to major Paleozoic orogenic events and lithotectonic units.

INTRODUCTION

Tectonic activity along plate boundaries characterizes the Paleozoic and early Mesozoic geologic history of the onshore and offshore Southeastern United States. During the Paleozoic, boundaries between plates or platelets were collisional in nature (Hatcher, 1978; Cook and others, 1979), and major offsets of orogenic zones were produced along large transform faults (Thomas, 1976; Cebull and others, 1976). The early Mesozoic tectonic history was dominated by the breakup of Pangea and the subsequent movement of North America away from Africa and South America. During the Triassic, a rift-zone plate boundary, which was offset along several large transform faults, extended the length of the North American Atlantic margin. The subsequent change to sea-floor spreading (drift phase) in the Early Jurassic caused the locus of oceanic-crust generation (the mid-ocean ridge spreading center) to move relatively eastward, ending the most recent period of major plate-margin tectonic activity in the Southeastern United States. Thus, the resultant geologic record in the Southeast is formed in large part by the superposition of early Mesozoic geologic and tectonic structures over Paleozoic and older structures.

Geologic and geophysical mapping have different relative importance east and west of the Fall Line. West of the Fall Line, where basement is not covered by Jurassic and younger strata, geologic mapping, supplemented by geophysical mapping, has delineated major Paleozoic geologic and tectonic units such as the Valley and Ridge province, the Blue Ridge province, the Inner Piedmont belt, the Charlotte belt, and the Carolina slate belt (Rodgers, 1970, pl. 1; Hatcher, 1978; Williams, 1978; Hatcher and Zietz, 1979) and has indicated possible relict plate boundaries (Hatcher, 1978; Cook and others, 1979). East of the Fall Line, drill-hole and geophysical data for the pre-Cretaceous rocks beneath the Atlantic Coastal Plain and continental margin have begun to reveal the geologic and tectonic structure of that region and to characterize it as a primary site of early Mesozoic tectonic activity (Gohn and others, 1978; Daniels and others, 1983).

The early Mesozoic geologic record can be distinguished from the Paleozoic record because of the significantly different tectonic structures and resulting geophysical signatures associated with compressional

(Paleozoic) and extensional (Mesozoic) tectonic events. Compressional tectonics formed orogenic belts characterized by metamorphism, major thrust sheets, and other allochthonous rock units (Rodgers, 1970, p. 219–224; Hatcher, 1978; Cook and others, 1979, 1981). The emplacement of granitic plutons and batholiths accompanied or followed the collision events (Hatcher, 1978; Fullagar and Butler, 1979; Harper and Fullagar, 1981). In contrast, tensional fields associated with continental rifting and drifting resulted in the formation of block-faulted narrow grabens and broad basins (Sanders, 1963; Sheridan, 1974; Van Houten, 1977; Popenoe and Zietz, 1977; Klitgord and Behrendt, 1979). Diabase dikes and sills that were intruded after the block-faulting (May, 1971; Popenoe and Zietz, 1977; Daniels and Zietz, 1978; de Boer and Snider, 1979) clearly mark the extent of the tensional stress field (May, 1971; de Boer and Snider, 1979).

Integration of magnetic-anomaly, gravity-anomaly, and seismic data with data from a sparse suite of samples from drill holes that penetrated pre-Cretaceous sedimentary rock and crystalline basement provides the most comprehensive information to date concerning basement structures and tectonics of the Atlantic Coastal Plain and continental margin. We have attempted to summarize briefly some of these integrated geophysical studies for the Southeastern United States onshore and offshore region (fig. 1). The works of Popenoe and Zietz (1977), Daniels and Zietz (1978), Hatcher and Zietz (1979), Chowns and Williams (1983), and Daniels and others (1983) for South Carolina and Georgia, of Klitgord and others (1983) for onshore and offshore Florida, and of Klitgord and Behrendt (1979) and Dillon and others (1979, 1983) for offshore South Carolina and Georgia have been incorporated into this study. A summary of the COCORP (Consortium for Continental Reflection Profiling) seismic work is presented by Cook and others (1979, 1981). The results from numerous other geological and geophysical studies in the Charleston region are found in this volume (Gohn, 1983a) and a companion volume (Rankin, 1977a). While the details of these studies have not been specifically included in our summary, most of their major conclusions are compatible with the generalized tectonic history presented here.

The overprinting of the Mesozoic tectonic record on the Paleozoic tectonic record and the Mesozoic breakup of the continents, which spatially separated large parts of this record, hinder understanding of the tectonic history of the Southeast. We shall attempt to reduce the effects of these two factors by first examining the record going backwards through time, stripping off the more recent layers and placing the older events in their proper regional framework. We shall then focus on the Charleston region and the relationship of its various tectonic features to the regional tectonic patterns, going forward through time.

Acknowledgments.—Discussions with G. Gohn, D. Daniels, D. Hutchinson, H. Schouten, and I. Zietz are gratefully acknowledged.

TECTONIC MAP

A general tectonic map for the Southeastern United States (fig. 1, from Klitgord and others, 1983) provides a framework within which to discuss the tectonic history of the area. This map, a composite of several studies, shows locations of major tectonic contacts and lithotectonic units, distinctive magnetic anomalies, and sea-floor-spreading isochrons. The tectonic features northwest of the Fall Line are taken directly from Williams (1978). Locations of sedimentary basins, of buried blocks of crystalline rock, and of fracture zones in the Florida region and the Atlantic offshore are from Klitgord and Behrendt (1979), Klitgord and others (1983), and Dillon and others (1979, 1983a). The pattern of sea-floor-spreading magnetic lineations and fracture zones northeast of the Bahamas fracture zone is based on the work of Schouten and Klitgord (1977, 1982), Vogt and Einwich (1979), and Klitgord and Schouten (1980; unpub. data, 1982). The sea-floor-spreading magnetic lineations in the eastern Atlantic (Hayes and Rabinowitz, 1975) have been reidentified (Klitgord and Schouten, 1980; unpub. data, 1982), and the data points, rotated to the western Atlantic, are shown in figure 1. Figure 1 includes some of the more important magnetic anomalies and zones of low-gradient magnetic and gravity fields between the Fall Line and the large Jurassic sedimentary basins of the continental margin, in order to allow a discussion of the Coastal Plain studies of Popenoe and Zietz (1977), Daniels and Zietz (1978), and Daniels and others (1983).

A closer examination of the Atlantic Coastal Plain and continental margin is provided in figure 2. The use of observed magnetic and gravity anomalies, rather than petrologic or lithotectonic map units, between the Fall Line and offshore basement hinge zone north of Florida is meant to emphasize the lower level of understanding of the tectonic structure of this region relative to the surrounding areas. The Charleston region, as the term is used in this paper, lies between the boundary *A–A′* (after Popenoe and Zietz, 1977; Daniels and others, 1983) and the Brunswick magnetic anomaly (BMA). Outcrop geology northwest of the Fall Line (Hatcher, 1978; Williams, 1978), a large suite of drill holes in Florida that penetrate pre-Cretaceous rocks (Barnett, 1975), and a dense grid of multichannel seismic-reflection profiles along the U.S. Atlantic margin (Dillon and others,

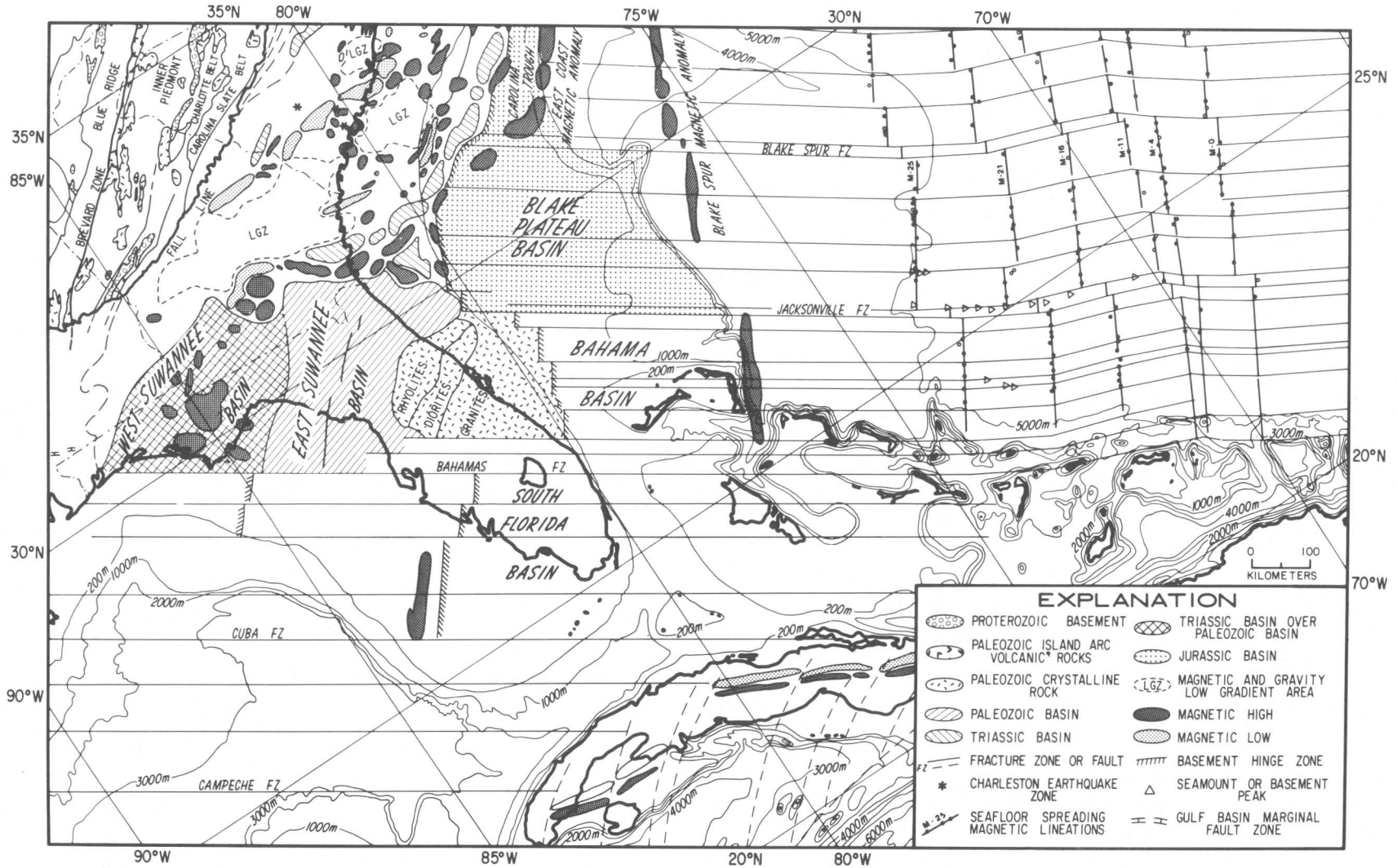

FIGURE 1.—Tectonic map of the southeastern U. S. Appalachians, Coastal Plain, and continental margin (from fig. 9, Klitgord and others, 1983). Major lithotectonic units north of the Fall Line, major sedimentary basins east of the Atlantic coastline, and the pattern of sea-floor-spreading magnetic lineations and fracture zones in the Atlantic Ocean basin and Gulf of Mexico are derived from numerous studies discussed in the text. The locations of sea-floor-spreading magnetic-anomaly data points in the western Atlantic, used to map the magnetic lineations, are shown as solid circles; the data points from the eastern Atlantic, which have been rotated to the west by the appropriate reconstructions, are shown as open circles. The three earthquake zones just landward of the coastline near 80° W. represent the clusters of earthquake epicenters mapped in the Charleston region by Tarr and Rhea (1983).

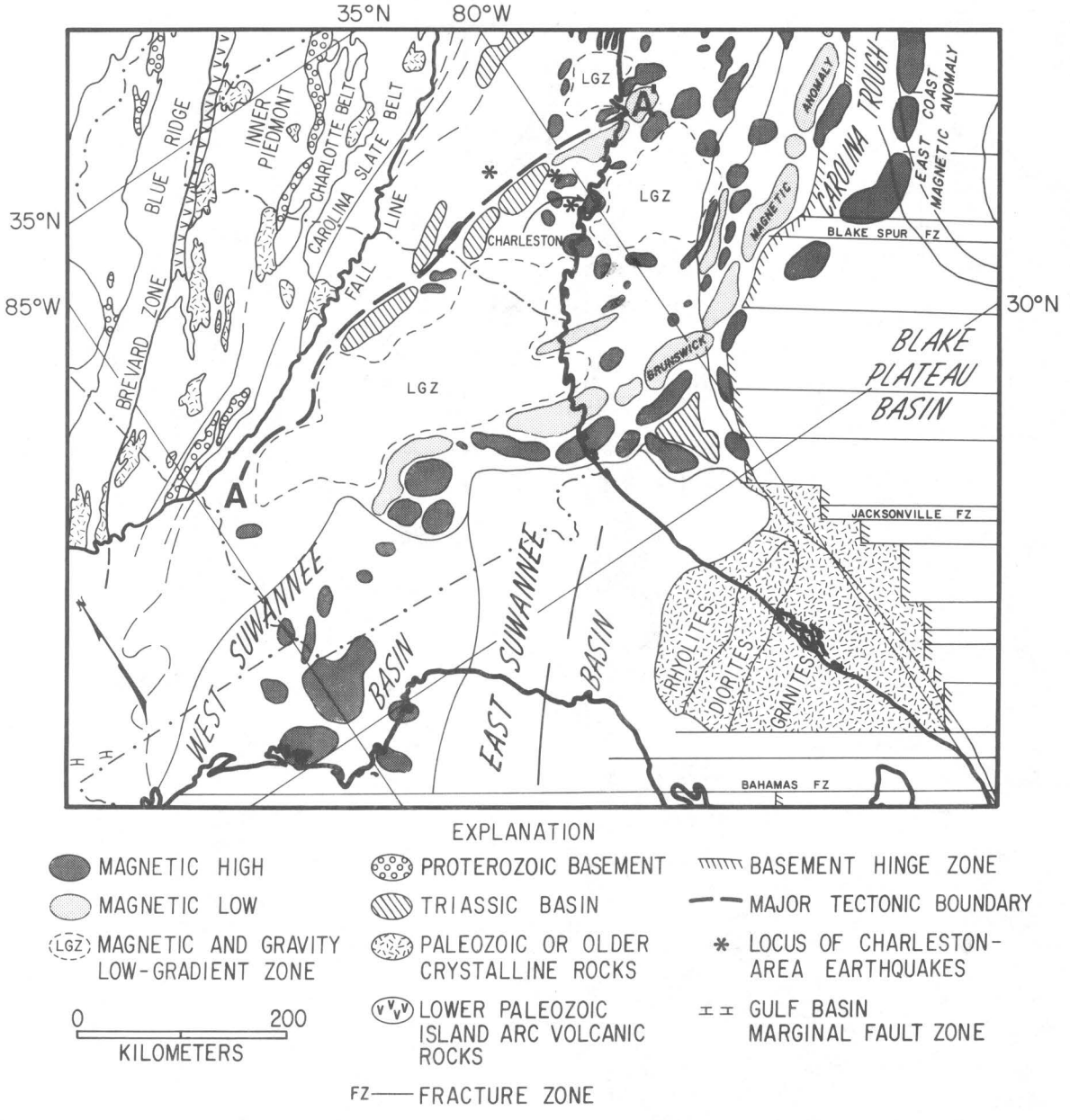

FIGURE 2.—Tectonic map of the Charleston region. The heavy dashed line *A*–*A'* marks the tectonic boundary along the northern edge of the Charleston region (modified from Popenoe and Zietz, 1977) and corresponds to the northern edge of the South Georgia rift (Daniels and others, 1983). The Brunswick magnetic anomaly and the offshore basement hinge zone mark the other two major tectonic boundaries discussed in the text.

1979, 1983; Folger and others, 1979), combined with magnetic and gravity data (Hatcher and Zietz, 1979; Klitgord and Behrendt, 1979; Klitgord and others, 1983), provide a reasonable picture of the tectonic structures in these areas. North of Florida between the Fall Line and the offshore basement hinge zone, the paucity of drill holes penetrating the pre-Cretaceous surface (Chowns and Williams, 1983) requires that our knowledge of this area be derived from geophysical data—primarily magnetic and gravity data (Popenoe and Zietz, 1977; Daniels and Zietz, 1978; Daniels and others, 1983) and a few seismic surveys (Woollard and

others, 1957; Ackermann, 1977, 1983; Behrendt and others, 1981; Cook and others, 1981; Dillon and McGinnis, 1983; Schilt and others, 1983; Hamilton and others, 1983).

JURASSIC TECTONIC ACTIVITY AND STRUCTURE

The North American plate slowly drifted away from the African and South American plates (Bullard and others, 1965) during the Jurassic, as sea-floor spreading generated the Atlantic Ocean basin. At that time, the eastern boundary of the North American plate was a spreading center. As new oceanic crust was generated, the boundary moved relatively eastward; its path is recorded in the pattern of fracture zones and sea-floor-spreading magnetic lineations observed in the western Atlantic (fig. 1). The set of Mesozoic sea-floor-spreading magnetic lineations (magnetic anomalies M–0 through M–25 of Larson and Hilde, 1975) provides isochrons for dating the sea floor and for reconstructing the paleopositions of the continents. These magnetic lineations on both sides of the Atlantic have been compared with model magnetic anomaly profiles generated by using the Mesozoic geomagnetic time scale (Larson and Hilde, 1975; Schouten and Klitgord, 1977, 1982) to accurately identify isochrons on both sides of the Atlantic. The data points from the African side of the Atlantic, rotated to the western Atlantic about the appropriate reconstruction centers of rotation, are compared with the western Atlantic data-point locations (fig. 1) to illustrate the reliability of these centers of rotation for reconstructing paleopositions. The reconstruction of the Early Jurassic and Late Jurassic continental positions around the Atlantic (fig. 3) is based on these isochron identifications and on determination of fracture zones and flow lines between magnetic anomaly M–25 and the East Coast magnetic anomaly (ECMA) (Schouten and Klitgord, 1982).

The fracture-zone pattern on the U.S Atlantic continental margin provides the most useful record, in the absence of sea-floor-spreading magnetic lineations, of the Early Jurassic rift boundary and subsequent spreading center boundary between North America and Africa. Offsets in this rift boundary (fig. 1), now buried beneath younger sedimentary basins, can be located by tracing the offshore fracture-zone pattern into the margin. The fracture-zone pattern within the zone of Mesozoic sea-floor-spreading magnetic lineations is recorded as discontinuities in magnetic anomalies (Schouten and Klitgord, 1982) and in basement lineaments (Klitgord and Grow, 1980; Tucholke and others, 1982). These discontinuities and basement lineaments are used to trace the fracture zones westward to the continental margin. A fairly large number of fracture zones can be traced to the margin, although only the Bahamas, Jacksonville, and Blake Spur fracture zones had large horizontal transform offsets during the early development of the margin (figs. 1, 3). These fracture zones do not extend into continental crust landward of the marginal basins because they record only differential movement in the ocean basin produced by the spreading center, which was initially located within the continental breakup rift zone (Sykes, 1978). The Bahamas fracture zone extended a long distance into the old continental block of Pangea (Bullard and others, 1965) and connected rifting in the Atlantic with rifting in the Gulf of Mexico (Klitgord and Schouten, 1980). All these fracture zones probably were initiated at older zones of weakness in the continental crust (Sykes, 1978), but the older zones are not necessarily alined with the younger fracture-zone trends. As discussed by Sykes (1978), many fracture zones may be traced away from a margin, but only the large-offset fracture zones will have a significant influence on the subsequent tectonic activity along the margin.

Deep sedimentary basins developed along the continental margin on crust formed during rifting and the early phase of drifting. Tectonic activity in the vicinity of these marginal basins changed from extensional tectonics related to rifting and drifting in the Early Jurassic to more passive crustal subsidence for the remainder of the Mesozoic. Uplift, block-faulting, and intrusion of mantle-derived magma along the margin in the early Mesozoic (Sheridan, 1974) gave way to cooling and subsidence of the margin (Steckler and Watts, 1978) as the spreading center moved away. As the basement along the margin subsided, it developed a marginal sediment trap (Falvey, 1974), which controlled the locus of sediment deposition through the early Mesozoic. The continental crust just landward of this zone of block-faulting and extensive heating subsided more slowly than did the crust beneath the marginal basins, which resulted in the formation of a distinctive hinge zone in basement along the landward edge of the marginal basins. As the Atlantic Ocean basin grew, a paleoshelf edge formed at the seaward edge of these marginal basins (Schlee and others, 1979), helping to constrain depositional patterns through the middle and late Mesozoic. The Carolina trough (Klitgord and Behrendt, 1979; Dillon and others, 1983b; Hutchinson and others, 1983), the Blake Plateau basin (Sheridan, 1974; Dillon and others, 1979, 1983a), and the northern and western rim of the Gulf of Mexico basin (Woods and Addington, 1973; Wood and Walper, 1974) were the main Jurassic marginal basins in this area. During the Jurassic, basement of the northern Bahamas, between the Jacksonville and Bahamas fracture zones, did not sink as rapidly as did that of the Blake Plateau (Dillon and others,

1983a), and much less sediment was deposited in the northern Bahamas than in the Blake Plateau basin. During the Cretaceous, sediment was deposited more uniformly in a broad zone that included the South Florida basin (Barnett, 1975), the northern Bahamas (Tator and Hatfield, 1975a, b; Meyerhoff and Hatten, 1974; Sheridan and others, 1981), and the Blake Plateau basin (Dillon and others, 1979, 1983a).

Little is known of the deep structure off eastern Florida underlying the straits of Florida or the Bahamas. Lower Jurassic or Upper Triassic(?) sedimentary rocks were drilled at a depth of about 5.5 km at the Great Isaac well in the northern Bahamas (Tator and Hatfield, 1975a, b), and a deep basin has been postulated to lie beneath these Jurassic rocks (Meyerhoff and Hatten, 1974). Analyses of magnetic anomaly gradients, however, suggests a shallow crystalline basement at a depth of approximately 5–6 km (Klitgord and others, 1983). In southern Florida, crystalline basement deepens abruptly to over 4 km at the Bahamas fracture zone and is overlain by a southward-thickening wedge of Cretaceous and younger sedimentary rocks. South of the Bahamas fracture zone, numerous wells to "basement" have encountered Jurassic igneous rocks beneath the Cretaceous and younger sediments (Barnett, 1975).

Formation of Atlantic marginal basins produced distinctive geophysical markers. The ECMA (fig. 1) marks the seaward edge of the Carolina trough and the landward edge of oceanic crust (Klitgord and Behrendt, 1979; Klitgord and Grow, 1980; Hutchinson and others, 1983). Although the actual source of the ECMA is subject to discussion (Taylor and other, 1968; Rabinowitz, 1974), the edge of the Jurassic paleoshelf lies along its landward edge, and a string of Lower Jurassic salt diapirs lies beneath its axis (Dillon and others, 1983b; Hutchinson and others, 1983). These Lower Jurassic sedimentary features are probably controlled by basement structure, which suggests that the source of the ECMA is related to the Jurassic basement structure (Hutchinson and others, 1983). The basement hinge zone at the landward edge of the Carolina trough is marked by the positive part of the BMA (fig. 1). This magnetic anomaly is characterized by a large magnetic low having a small magnetic high along its seaward flank (Klitgord and Behrendt, 1979). The anomaly high becomes much larger as the BMA swings westward across the coastline near Brunswick, Ga. (Popenoe and Zietz, 1977; Pickering and others, 1977; Daniels and others, 1983). Seismic profiles and estimates of depth to magnetic basement indicate that there is a narrow basement graben beneath the magnetic low and that the hinge zone is directly beneath the anomaly peak for the offshore part of the BMA (Klitgord and Behrendt, 1979; Hutchinson and others, 1983). This hinge zone in basement diverges from the BMA near 31°N.; it can be traced southward along the landward edge of the Blake Plateau basin by means of seismic and magnetic data (Dillon and others, 1979, 1983a; Klitgord and Behrendt, 1979).

The zone of Early Jurassic rifting and subsequent drifting apart of the North American plate from the South American–African plate was located just east of the basement hinge zone on the U.S. Atlantic continental margin and just west of a similar hinge zone on the African margin (fig. 3*A*). The rift zone continued southward between central Florida and the Bafata basin, was offset westward along the Bahamas fracture zone to southern Florida, and finally was connected by the Cuba fracture zone to a zone of extension in the Gulf of Mexico (Klitgord and others, 1983). The large blocks of continental crust (Krivoy and Pyle, 1972; Woods and Addington, 1973) stranded between the Cuba fracture zone and the Bahamas fracture zone–Gulf basin marginal fault zone (fig. 3*A*) indicate that there may have been some Early Jurassic or Late Triassic tectonic activity in that region. The swarms of Lower Jurassic diabase dikes that are located to the west of this rift zone in North America and to the east in Africa (May, 1971; de Boer and Snider, 1979; Daniels and others, 1983) may reflect the extent of influence of the stress field associated with Early Jurassic rifting (de Boer and Snider, 1979).

TRIASSIC TECTONIC ACTIVITY AND STRUCTURE

The extensional tectonic regime that eventually generated the Atlantic Ocean basin began as a rifting event in the Late Triassic (Sanders, 1963; Vogt, 1973;

FIGURE 3.—Reconstructions of the Atlantic during the Early Jurassic and Late Jurassic (from fig. 10, Klitgord and others, 1983). *A*, The Early Jurassic reconstruction shows the inferred continental positions for the closure of the Atlantic. *B*, The Late Jurassic reconstruction shows the inferred continental positions after the separation of North America but before the separation of South America from Africa. The Appalachian and Ouachita Paleozoic fold belts on North America and the Mauritanides Paleozoic fold belt on Africa are indicated. Paleozoic basins that were not affected significantly by the Paleozoic orogenies include the Bafata or Bové basin in West Africa, the East Suwannee and West Suwannee basins in northern Florida, and the Black Warrior basin just west of southern Appalachians. Also shown are the East Coast magnetic anomaly (ECMA), the Blake Spur magnetic anomaly (BSMA) and the spreading center marked by the sea-floor-spreading magnetic lineation M–25. The present-day location of Cuba is shown as dashed lines.

A. EARLY JURASSIC RECONSTRUCTION

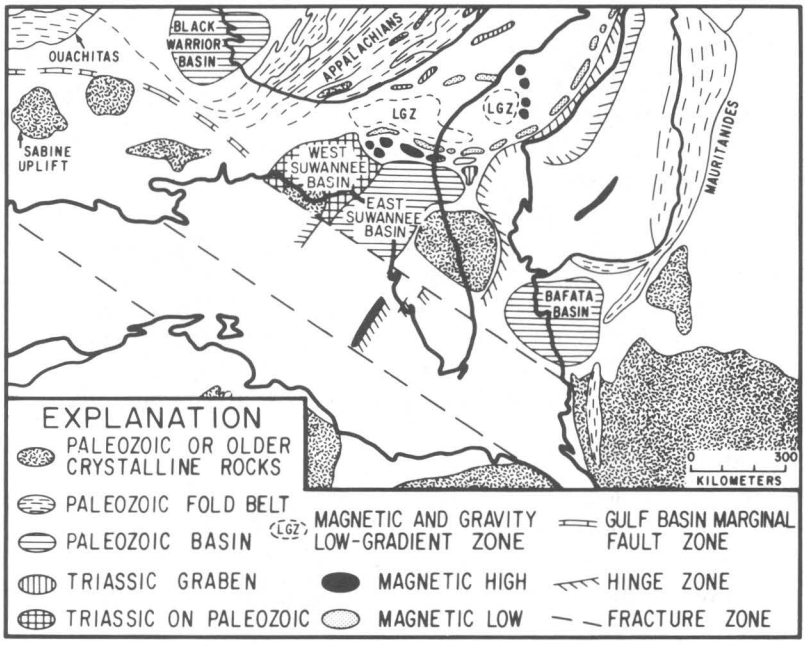

B. LATE JURASSIC RECONSTRUCTION

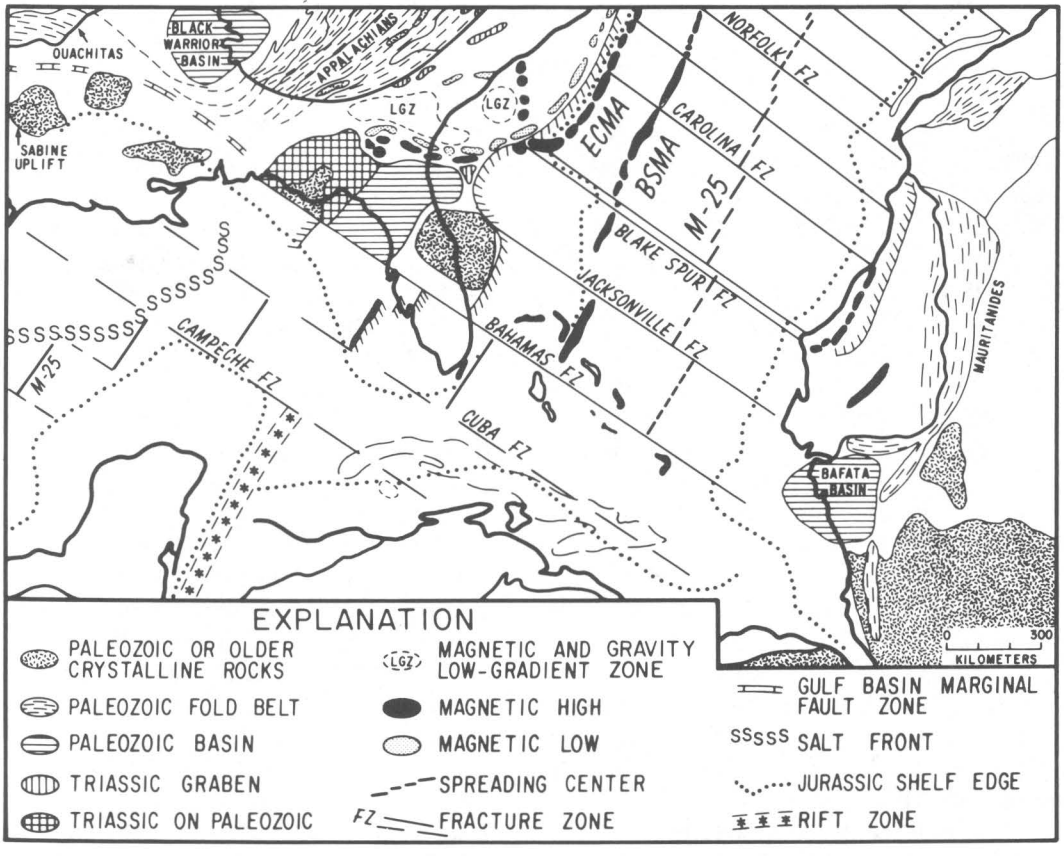

Van Houten, 1977; Cornet, 1977; Manspeizer and others, 1978). At this time the North American, South American, and African continents were part of a single large continental plate (fig. 3*A*) called Pangea (Bullard and others, 1965). South of New England, this Late Triassic rifting was confined between the Appalachian and Mauritanide orogenic belts and formed the South Georgia rift (Daniels and others, 1983) in the Southeastern United States. Triassic rifting did not continue southward of Florida into South America; rather, it was connected to the rifting in the northern Gulf of Mexico basin (Woods and Addington, 1973) by a transform fault that was reactivated in the Jurassic as the Bahamas fracture zone (Klitgord and others, 1983). Peninsular Florida and most of west Africa, south of the South Atlas Fault, were east of the Triassic tectonic activity (Van Houten, 1977; Manspeizer and others, 1978).

Late Triassic rifting is characterized by the development of grabens along older fault zones on the U.S. Atlantic margin and by a lack of significant amounts of horizontal separation. These sedimentary basins or grabens have been mapped from outcrop geology west of the Fall Line (Williams, 1978) and have been inferred from magnetic, gravity, and drill-hole data on the Atlantic Coastal Plain (Marine and Siple, 1974; Popenoe and Zietz, 1977; Daniels and Zietz, 1978). A parallel set of grabens has been postulated to lie just offshore from Georgia to Long Island, on the basis of magnetic and seismic-reflection data (Klitgord and Behrendt, 1979; Hutchinson and others, 1983), although these grabens have never been drilled. Off the Carolinas, the magnetic low of the BMA (fig. 1) is located over these grabens; a series of less continuous magnetic lows along the landward edge of the Baltimore Canyon trough mark these grabens farther north. These magnetic lows continue northward across Long Island and connect with the magnetic low over the early Mesozoic Connecticut Valley graben (Klitgord and Behrendt, 1979).

Upper Triassic to Lower Jurassic red beds and diabase intrusions fill the grabens and basins formed by the Triassic rifting (Sanders, 1963; Barnett, 1975; Van Houten, 1977; Cornet, 1977). These rocks are found within the broad Salisbury embayment (Maher, 1971; Brown and others, 1972) and South Georgia rift (Gohn and others, 1978; Daniels and others, 1983) as well as within narrow Triassic grabens exposed in the Appalachians (Sanders, 1963; Cornet, 1977). This record of Late Triassic to Early Jurassic tectonic activity can be traced as far south as the Florida panhandle where the West Suwannee basin (Klitgord and others, 1983), the western part of a Paleozoic basin that covers all of northern Florida, was block-faulted and subsided (Arden, 1974); diabase intrusive rocks and red beds, like those of the Triassic Eagle Mills Formation of the central Gulf Coast, are quite prevalent in the West Suwannee basin (Barnett, 1975; Daniels and others, 1983).

PALEOZOIC TECTONIC ACTIVITY AND STRUCTURE

Paleozoic tectonic activity was dominated by collision of continental plates and smaller platelets, suturing together the megacontinent of Pangea by the end of the Paleozoic. Assuming that Late Triassic to Early Jurassic rifting had little effect on the relative positions of North America, South America, and Africa, then their positions at the end of the late Paleozoic should be the same as they were in the Early Jurassic (fig. 3*A*). This reconstruction is only appropriate after the end of the late Paleozoic Alleghenian orogeny, because there was a large (about 2,000 km) sinistral shear movement between North America–Greenland–western British Isles and eastern New England–Canadian Maritimes–Europe (Kent and Opdyke, 1978, 1979; Van der Voo and Scotese, 1981) prior to or during the Alleghenian orogeny.

The distribution of Paleozoic orogenic belts and relatively undeformed sedimentary basins at the end of the Paleozoic (fig. 3*A*) indicates that major transform plate boundaries connected the southern ends of the Mauritanide and Appalachian orogenic belts with the Ouachita orogenic belt (Thomas, 1976). The Suwannee basin in northern Florida and the Bafata basin in west Africa lay to the south of one of these major transform boundaries (Klitgord and others, 1983), a zone of weakness that was rejuvenated in the Early Jurassic to form the Jacksonville fracture zone (fig. 3*B*). The Paleozoic rocks in northern Florida and in the Bafata basin are marine sedimentary rocks, Ordovician quartzitic sandstones, and Devonian black shales (Barnett, 1975) that formed in a large sedimentary basin along the continental margin of the South American–African continent. Although a branch of the Mauritanide orogenic belt extends along the east side of the Bafata basin, most of the late Paleozoic orogenic activity continued southward between the Black Warrior and Suwannee basins to where another large transform fault connected it to the Ouachita orogenic belt (Thomas, 1976). This transform fault plate boundary was rejuvenated as part of the Gulf basin marginal fault zone (Woods and Addington, 1973) and the Bahamas fracture zone (Klitgord and others, 1983).

The Southeastern United States contains a variety of Paleozoic structural zones—Valley and Ridge province, Blue Ridge province, Inner Piedmont belt, Kings Mountain belt, Charlotte belt, and Carolina slate belt—that were involved in three Paleozoic collision events—the Taconic, Acadian, and Alleghenian orogenies (Rodgers,

1970, p. 216; Hatcher, 1978; Williams, 1978). The Kings Mountain belt has been postulated to be a suture zone between the Inner Piedmont crystalline block and the Charlotte belt–Carolina slate belt island-arc block (Hatcher, 1978; Cook and others, 1979). The suture zone and magmatic arc associated with the late Paleozoic collision between the South American–African plate and the North American plate, which includes the Inner Piedmont and Charlotte belt–Carolina slate belt blocks, have not been identified but probably are located beneath the Coastal Plain east of the Carolina slate belt (Hatcher, 1978) and may be within the Charleston region (Nishenko and Sykes, 1979; Daniels and others, 1983.)

CHARLESTON REGION TECTONIC STRUCTURE

The Charleston region (fig. 2) is bounded by or close to three important tectonic boundaries. The first of these boundaries is a hinge zone in crystalline basement that separates the Jurassic marginal basins from areas of lesser subsidence in Triassic and older crystalline rocks on the continental platform to the west. The second boundary is a series of narrow grabens, associated with the BMA, which parallel the hinge zone as far south as 31°N., where they swing westward across southern Georgia, separating the East Suwannee Paleozoic basin from an area of low-gradient magnetic field characteristic of the Charleston region. The third boundary (line *A–A'*, fig. 2) is a line of several inferred Triassic grabens that separate the Charleston region from the area beneath the Coastal Plain to the north that has the distinctive geophysical character of the highly deformed Piedmont rocks (Popenoe and Zietz, 1977; Daniels and others, 1983).

The change in geophysical character at these three boundaries is best displayed in the magnetic-anomaly data (pl. 1). We shall use the magnetic data as our base for discussing the Charleston-region tectonic structures. The broad-wavelength magnetic anomalies east of the hinge zone overlie crystalline basement that, near the center of the offshore basins, is at a depth of more than 10 km. The thick section of sedimentary rocks in the Blake Plateau basin and the Carolina trough (fig. 1) is clearly displayed in the multichannel seismic-reflection data (Sheridan, 1974; Dillon and others, 1979, 1983a, 1983b). Estimates of depth to magnetic basement are consistent with the mapped seismic basement in these basins (Klitgord and Behrendt, 1979); the great depth (>10 km) to the magnetic source layer is clearly a significant factor in suppressing shorter wavelength anomalies in the magnetic field. The magnetic-anomaly pattern south of the BMA and west of the hinge zone contains shorter wavelength features than are seen in the field east of the hinge zone and has a northeast grain (Klitgord and others, 1983). Crystalline basement at the eastern edge of the Suwannee basin is at a depth of only 1 km (Klitgord and others, 1983). Although no drill holes near the middle of the East Suwannee basin reached crystalline basement, seismic-reflection data across the West Suwannee basin indicate that depth to basement there exceeds 4 km (Arden, 1974). There are shallower magnetic sources in the western part of Florida where diabase dikes and sills intrude the relatively nonmagnetic sedimentary rock (Daniels and Zietz, 1978; Daniels and others, 1983), causing some isolated short-wavelength magnetic anomalies. North of boundary *A–A'* there are even shorter wavelength (<3 km) anomalies having amplitudes of several hundred nanoteslas (1 nT = 1 gamma). The shallow crystalline basement in this region is composed of Piedmont-type rocks (Popenoe and Zietz, 1977; Daniels and Zietz, 1978; Daniels and others, 1983) that were remagnetized by metamorphic events in the Paleozoic.

The magnetic-anomaly pattern within the Charleston region includes large-amplitude, roughly circular anomalies associated with gravity highs. There is a cluster of magnetic highs near the coastline north of 32° N. (MH1, pl. 1), a cluster around the city of Charleston (MH2, pl. 1), and a string of circular magnetic highs just east of 79° W. between 32° N. and 33° N. (MH3, pl. 1). Many of these features are thought to be mafic intrusive bodies (Popenoe and Zietz, 1977; Long and Champion, 1977; Kane, 1977; Grow and others, 1979; Daniels and others, 1983). MH1 and MH2 sit within a broad complex of magnetic highs, a zone having a magnetic level that is higher than the magnetic level of the surrounding area, which has been referred to as the Charleston Block (Rankin, 1977b). This block is bounded on the south and east by the low-gradient zones LGZ1 and LGZ2 and to the north by the magnetic lows (for example ML3) just south of boundary *A–A'* (pl. 1). A group of magnetic highs (MH4, pl. 1) just south and east of the Riddleville basin has been interpreted as a block of mafic bodies (Daniels and Zietz, 1978) that is bounded by fault *B–B'* (pl. 1) and may be a block of Piedmont rocks (Daniels and others, 1983).

There are three zones of low-gradient magnetic and gravity fields (LGZ) in the Charleston region (Daniels and Zietz, 1978; Long, 1979) (fig. 2). The largest (LGZ1, pl. 1), which lies just north of the BMA, corresponds to the main rift basin of Daniels and others (1983). Estimates of depth to magnetic basement indicate sedimentary rock thicknesses in excess of 4.5 km in the western part of LGZ1 (Daniels and others, 1983) whereas in the eastern part, near the coastline, samples of granitic and rhyolitic rocks have been recovered at a subsurface depth of about 1.5 km (Swanson and Gernazian, 1979). The second-largest zone (LGZ2, pl. 1) is just

offshore from Charleston between 32° N. and 33° N. LGZ2 is bounded by the Helena Banks fault (Behrendt and others, 1981) to the northwest, the string of circular mafic bodies MH3 to the east, the narrow graben beneath anomaly ML1 to the southeast, and the group of mafic(?) bodies MH1 to the west. The smallest low-gradient zone (LGZ3), just north of boundary *A–A'* near the coast, may be associated with a granitic pluton (Popenoe and Zietz, 1977). The character of the magnetic field in these LGZ's most closely resembles that of the Blake Plateau basin. This broad-wavelength geophysical character could indicate either a deep basement or a shallow basement of nonmafic rock like granite (Daniels and Zietz, 1978; Daniels and others, 1983; Gohn, 1983b). As only thin sections of Triassic sedimentary rocks have been encountered just north of Florida, these LGZ's are more likely to reflect a shallow nonmafic crystalline basement than a deep Triassic sedimentary basin. This interpretation is consistent with the shallow samples of rhyolite and granite recovered in southeastern Georgia (Chowns and Williams, 1983) and with the interpretation that LGZ3 is caused by a large granitic pluton (Popenoe and Zietz, 1977).

Large-amplitude, narrow magnetic lows are an important feature of the magnetic field in the Charleston region. Some of these lows have been associated with Triassic grabens (Marine and Siple, 1974; Popenoe and Zietz, 1977; Daniels and others, 1983), and it is possible that nearly all of them are located over grabens of Triassic(?) age. For example, the Dunbarton and Riddleville basins (pl. 1), as well as other Triassic grabens to the north, have been shown to contain Triassic sedimentary rock and are characterized by large-amplitude magnetic lows (Marine and Siple, 1974; Popenoe and Zietz, 1977; Sumner, 1977; Daniels and Zietz, 1978; Daniels and others, 1983). Seismic-reflection profiles and estimates of depth to magnetic basement across the offshore BMA indicate a narrow graben associated with the magnetic low (Klitgord and Behrendt, 1979; Dillon and others, 1983a; Hutchinson and others, 1983). The narrow magnetic low (ML1) that crosses 32° N., 79° W. reflects a trough in basement identified from seismic-reflection data, and the narrow magnetic low (ML2) that crosses the coastline near 31.9° N. may originate from a similar feature. Along the southern side of boundary *A–A'*, in the northern part of the Charleston region, there are magnetic lows over the Riddleville basin, between 80° W. and 81° W. (ML3), and near the coastline.

Seismic data provide significant insight into the nature of the various geophysical anomalies. COCORP seismic-reflection profiles across Georgia (Cook and others, 1981) indicate that several large thrust planes break the surface at well-mapped faults. The Augusta and Modoc faults (pl. 1), which are clearly delineated with the magnetic data (Hatcher and others, 1977), are the best examples. Two additional northeast-trending narrow magnetic lineations between the Augusta fault and the Riddleville basin coincide with possible thrust planes seen in the COCORP data (Cook and others, 1981), as does the fault *B–B'* (pl. 1). At the intersection of COCORP lines 8 and 9, there is a seismic basement high associated with the magnetic high. The COCORP lines near Charleston (Schilt and others, 1983) cross the large magnetic high beneath the Clubhouse Crossroads test holes and the magnetic high just to the east near the locus of numerous earthquakes (pl. 1). Beneath a set of flat-lying shallow reflections related to the Jurassic and younger sedimentary rocks, a basalt layer, and a possible basement reflector, a series of northward- and westward-dipping reflectors (Schilt and others, 1983, figs. 3, 5) are on the gradient that separates the Clubhouse Crossroads magnetic high from a large magnetic low (ML3) to the north and west. ML3, which lies between boundary *A–A'* and 33° N. and between 80° W. and 81° W., corresponds to a basin mapped with seismic-refraction data (Ackermann, 1983).

Many basement structures in the offshore region have been identified by means of seismic data (Dillon and others, 1979, 1983a; Behrendt and others, 1981). The offshore hinge zone in seismic basement is the most distinctive feature; it is beneath a narrow magnetic high. The grabens beneath the BMA low and the magnetic low at 32° N., 79° W. (ML1, pl. 1) were mentioned previously. Near the coastline, the Helena Banks fault (Behrendt and others, 1981), downthrown to the south, is along the northern edge of the low-gradient zone LGZ2. Other features identified in offshore seismic-reflection data include a small basement high along 31° N. between 80° W. and 81° W., coincident with the large magnetic high of the BMA, and a basin of Triassic or older sedimentary rocks just west of the hinge zone between 30° N. and 31° N. that correlates with a triangular magnetic low (Dillon and others, 1979, 1983a; Klitgord and Behrendt, 1979). Seismic-refraction data on the shelf also indicate the greater depth to basement in this triangular area (Dillon and McGinnis, 1983).

The Lower Jurassic basalt layer drilled at the Clubhouse Crossroads wells (Gottfried and others, 1977, 1983) has been traced on seismic-reflection and seismic-refraction data throughout most of the Charleston region southeast of the wells (Ackermann, 1977, 1983; Dillon and others, 1979, 1983a; Behrendt and others, 1981; Hamilton and others, 1983; Schilt and others, 1983). The seaward limit of this layer (pl. 1) is marked by the termination of a very strong, continuous acoustic reflector (Dillon and others, 1979, 1983a). If the layer extends further seaward, it must be a more broken unit.

The termination of this basalt unit corresponds with the magnetic-anomaly peak in the BMA. At 31° N. this termination coincides with the small basement high identified in seismic-reflection data beneath the BMA magnetic high. Northeast of 31° N., 80° W., this termination is at the seaward edge of the graben beneath the BMA magnetic low and coincides with the hinge zone.

CHARLESTON REGION TECTONIC ACTIVITY

The tectonic history developed here for the Charleston region incorporates the major tectonic structures in the area into the general tectonic history discussed previously. We have assumed that the late Paleozoic continent positions, just after the Alleghenian orogeny, were the same as shown in the Early Jurassic reconstruction (fig. 3*A*).

The late Paleozoic collision of North America with South America–Africa generated a magmatic arc and suture zone flanked by large crystalline thrust sheets. The Inner Piedmont belt, Charlotte belt, and Carolina slate belt were part of the North American plate; they were incorporated in large thrust sheets and transported westward (Hatcher, 1978; Cook and others, 1979, 1981). Similar thrust sheets, transported eastward on the South American–African plate, formed part of the Mauritanides (Dillon and Sougy, 1974). This magmatic arc and suture zone lay east of the Piedmont (Hatcher, 1978) and most likely passed through the Charleston region. The magnetic data over the Coastal Plain of North Carolina and southern Virginia are typical of folded Piedmont basement rocks (Daniels and Zietz, 1978) and indicate that the magmatic arc–suture zone probably was located further east, perhaps offshore in the vicinity of the BMA. The Suwannee-Bafata Paleozoic basin was on the South American–African continental margin and must have been just south of this magmatic arc–suture zone. The zone of orogenic activity shifts westward at the northern edge of the Suwannee-Bafata basin and passes between it and the Black Warrior basin (fig. 3*A*) before shifting westward again to the Ouachita orogenic belt (Thomas, 1976). As can be seen in figure 3*A*, the magmatic arc–suture zone must have passed through the Charleston region; the onshore part of the BMA would mark the late Paleozoic transform boundary that was similar to the present-day southern transform boundary of the Caribbean subduction zone (Bowin, 1976).

Large sialic batholiths form the upper crust of a magmatic arc (Hamilton, 1981) and should be expected in the Charleston region. The low-gradient zones in the Charleston region are interpreted here to reflect such batholiths that were exposed in the early Mesozoic, when the overlying sedimentary and volcanic rocks of the magmatic arc were completely eroded. The numerous mafic bodies in the area may be part of this magmatic arc or may have been emplaced later during the early Mesozoic rifting.

Late Triassic rifting elevated the Charleston region and produced the narrow grabens. The grabens formed along old zones of weakness, and some are bounded by the late Paleozoic thrust planes (Cook and others, 1981). The edges of the large batholiths would also have been zones of weakness along which faulting might have occurred, which would account for the narrow grabens that formed around the edges of the Charleston region low-gradient zones. It may have been during this period of uplift that the shallowest part of the magmatic zone was removed, exposing the granitic batholiths. During the period between the Late Triassic and Early Jurassic rifting, the Lower Triassic–Upper Jurassic red beds were deposited in the grabens and in broad zones over the subsiding granitic batholiths. The South Georgia rift was also formed in this period (Daniels and others, 1983).

The Early Jurassic rifting culminated the early Mesozoic rifting episode and evolved into the sea-floor-spreading phase of the breakup of Pangea. The age of the Lower Jurassic diabase dikes that surrounded the opening Atlantic Ocean (May, 1971) and were intruded into rocks of the Charleston region (Popenoe and Zietz, 1977; Daniels and others, 1983) provides a reasonable marker for the actual start of continental drift. The zone of Early Jurassic rifting was narrower than that of Late Triassic rifting and was located just east of the BMA as far south as the Blake Plateau. Instead of swinging westward, along the onshore part of the BMA, the Early Jurassic rifting continued southward offshore from Florida as far as the Bahamas fracture zone. The only major tectonic activity in the Charleston region was the volcanic activity that produced the widespread basalt flow extending as far east as the BMA. Crustal uplift at the western edge of the rift zone probably generated a basement high against which the basalt flow terminated.

Tectonic activity in the Charleston region for the remainder of the Mesozoic was related to the passive subsidence of the area as the crust cooled. The development of Jurassic marginal basins, which have a basement hinge zone along their landward edge and large discontinuities at the Jacksonville and Blake Spur fracture zones, was the last major structural alteration to the Charleston region. Subsequent tectonic activity has been dominated by the minor reactivation of old zones of weakness in response to stress fields generated at a distance (Sykes, 1978).

SUMMARY

Geophysical and drill-hole data in the Southeastern U.S. Coastal Plain and continental margin enable us to

delineate zones of Jurassic, Triassic, and Paleozoic tectonic activity, separated by three distinctive geophysical boundaries that enclose the Charleston region. A major, east-west-oriented tectonic boundary (*A–A'*, fig. 2) separates the Charleston region from a zone of Piedmont rocks to the north (Popenoe and Zietz, 1977; Daniels and others, 1983). The BMA separates the Charleston region from fairly undeformed Paleozoic sedimentary rocks in northern Florida. Finally, an offshore basement hinge zone separates the Paleozoic and Triassic tectonic structures from the Jurassic marginal basins.

Triassic extensional tectonics formed narrow grabens and broad sedimentary basins along the eastern edge of North America. The existence of two sets of Triassic grabens, one chiefly onshore and one offshore, suggests that south of New England there were at least two zones of Triassic rifting, as in the present East African rift system (Girdler and others, 1969). Broad zones of sediment accumulation formed at several locations along the margin between these two rift zones; for example, the South Georgia rift (Daniels and others, 1983) and the Salisbury embayment (Maher, 1971). Part of the eastern (offshore) Triassic rift later served as the locus for the Early Jurassic rifting that evolved into the Atlantic Ocean basin.

As North America pulled away from Africa and South America during the Jurassic, the influx of sediments into the newly formed ocean basin filled marginal basins along the locus of Early Jurassic rifting. The sinuous trace of this early spreading center included many offsets, which were recorded as fracture zones in the oceanic and rift-stage crust. The large-offset transform faults, trending perpendicular to the rifted margin, segmented the marginal basin development; the Jacksonville and Blake Spur fracture zones delimited the Blake Plateau basin, and the Blake Spur and Norfolk fracture zones bounded the Carolina trough. Southward along the Jurassic extensional boundary (for example the lineation M–25, fig. 3*B*), southern Florida was the site of a short segment of spreading center that was connected by transform faults to the Atlantic and the Gulf of Mexico spreading-center systems (Klitgord and others, 1983). The region of transform faulting south of the Bahamas fracture zone and northwest of southern Florida was another site of major early Mesozoic tectonic activity. The Bahamas fracture zone, which connects the Gulf of Mexico spreading center to the Atlantic spreading center, is probably part of the marginal fault zone that forms the northeastern boundary of the Gulf of Mexico basin. These large-offset fracture zones along the Atlantic margin represent major zones of weakness (Sykes, 1978) that would act as stress guides for stress generated by late Mesozoic and Cenozoic tectonic activity.

REFERENCES CITED

Ackermann, H. D., 1977, Exploring the Charleston, South Carolina, earthquake area with seismic refraction–A preliminary study, *in* Rankin, D. W., ed., Studies related to the Charleston, South Carolina, earthquake of 1886–A preliminary report: U.S. Geological Survey Professional Paper 1028, p. 167–175.

———1983, Seismic-refraction study in the area of the Charleston, South Carolina, 1886 earthquake, *in* Gohn, G. S., ed., Studies related to the Charleston, South Carolina, earthquake of 1886–Tectonics and seismicity: U.S. Geological Survey Professional Paper 1313, p. F1–F20.

Arden, D. D., 1974, Geology of the Suwannee Basin interpreted from geophysical profiles: Gulf Coast Association of Geological Societies Transactions, v. 24, p. 223–230.

Barnett, R. S., 1975, Basement structure of Florida and its tectonic implications: Gulf Coast Association of Geological Societies Transactions, v. 25, p. 122–142.

Behrendt, J. C., Hamilton, R. M., Ackermann, H. D., and Henry, V. J., 1981, Cenozoic faulting in the vicinity of the Charleston, South Carolina, 1886 earthquake: Geology, v. 9, no. 3, p. 117–122.

Bollinger, G. A., 1973, Seismicity and crustal uplift in the southeastern United States: American Journal of Science, v. 273–A, p. 396–408.

———1983, Speculations on the nature of seismicity at Charleston, South Carolina, *in* Gohn, G. S., ed., Studies related to the Charleston, South Carolina, earthquake of 1886–Tectonics and seismicity: U.S. Geological Survey Professional Paper 1313, p. T1–T11.

Bowin, Carl, 1976, Caribbean gravity field and plate tectonics: Geological Society of America Special Paper 169, 79 p.

Brown, P. M., Miller, J. A., and Swain, F. M., 1972, Structure and stratigraphic frame work, and spatial distribution of permeability of the Atlantic Coastal Plain, North Carolina to New York: U.S. Geological Survey Professional Paper 796, 79 p.

Bullard, E. C., Everett, J. E., and Smith, A. G., 1965, The fit of continents around the Atlantic, *in* Blackett, P. M. S., Bullard, E. C., and Runcorn, K. S., eds., A symposium on continental drift: Royal Society of London Philosophical Transactions, ser. A, v. 258, p. 41–51.

Cebull, S. E., Shurbet, D. H., Keller, G. R., and Russell, L. R., 1976, Possible role of transform faults in the development of apparent offsets in the Ouachita–southern Appalachian tectonic belt: Journal of Geology, v. 84, no. 1, p. 107–114.

Chowns, T. M., and Williams, C. T., 1983, Pre-Cretaceous rocks beneath the Georgia Coastal Plain–Regional implications, *in* Gohn, G. S., ed., Studies related to the Charleston, South Carolina, earthquake of 1886–Tectonics and seismicity: U.S. Geological Survey Professional Paper 1313, p. L1–L42.

Cook, F. A., Albaugh, D. S., Brown, L. D., Kaufman, Sidney, Oliver, J. E., and Hatcher, R. D., Jr., 1979, Thin-skinned tectonics in the crystalline southern Appalachians: COCORP seismic-reflection profiling of the Blue Ridge and Piedmont: Geology, v. 7, no. 12, p. 563–567.

Cook, F. A., Brown, L. D., Kaufman, Sidney, Oliver, J. E., and Petersen, T. A., 1981, COCORP seismic profiling of the Appalachian orogen beneath the Coastal Plain of Georgia: Geological Society of America Bulletin, v. 92, no. 10, p. 738–748.

Cornet, Bruce, 1977, The palynostratigraphy and age of the Newark Supergroup: State College, Pennsylvania State University, unpub. Ph.D. thesis, 527 p.

Daniels, D. L., and Zietz, Isidore, 1978, Geologic interpretation of aeromagnetic maps of the Coastal Plain region of South Carolina and parts of North Carolina and Georgia: U.S. Geological Survey Open-File Report 78–261, 62 p., 11 pl.

Daniels, D. L., Zietz, Isidore, and Popenoe, Peter, 1983, Distribution of subsurface lower Mesozoic rocks in the Southeastern

United States as interpreted from regional aeromagnetic and gravity maps, *in* Gohn, G. S., ed., Studies related to the Charleston, South Carolina, earthquake of 1886–Tectonics and seismicity: U.S. Geological Survey Professional Paper 1313, p. K1–K24.

de Boer, Jelle, and Snider, F. G., 1979, Magnetic and chemical variations of Mesozoic diabase dikes from eastern North America: evidence for a hotspot in the Carolinas?: Geological Society of America Bulletin, v. 90, no. 2, p. 185–198.

Dillon, W. P., Klitgord, K. D., and Paull, C. K., 1983a, Mesozoic development and structure of the continental margin off South Carolina, *in* Gohn, G. S., ed., Studies related to the Charleston, South Carolina, earthquake of 1886–Tectonics and seismicity: U.S. Geological Survey Professional Paper 1313, p. N1–N16.

Dillon, W. P., and McGinnis, L. D., 1983, Basement structure indicated by seismic-refraction measurements offshore from South Carolina and adjacent areas, *in* Gohn, G. S., ed., Studies related to the Charleston, South Carolina, earthquake of 1886–Tectonics and seismicity: U.S. Geological Survey Professional Paper 1313, p. O1–O7.

Dillon, W. P., Paull, C. K., Dahl, A. G., and Patterson, W. C., 1979, Structure of the continental margin near the COST No. GE-1 drill site from a common-depth-point seismic-reflection profile, *in* Scholle, P. A., ed., Geological studies of the COST GE-1 well, United States South Atlantic Outer Continental Shelf area: U.S. Geological Survey Circular 800, p. 97–114.

Dillon, W. P., Popenoe, Peter, Grow, J. A., Klitgord, K. D., Swift, B. A., Paull, C. K., and Cashman, K. V., 1983b, Growth faulting and salt diapirism; Their relationship and control in the Carolina Trough, eastern North America: American Association of Petroleum Geologists Memoir 34, in press.

Dillon, W. P., and Sougy, J. M. A., 1974, Geology of West Africa and the Canary and Cape Verde Islands, *in* Nairn, A. E. M., and Stehli, F. G., eds., The ocean basins and margins; vol. 2, The North Atlantic: New York, Plenum Press, p. 315–390.

Falvey, D. A., 1974, The development of continental margins in plate tectonic theory: Australian Petroleum Exploration Association Journal, v. 14, no. 1, p. 95–106.

Folger, D. W., Dillon, W. P., Grow, J. A., Klitgord, K. D., and Schlee, J. S., 1979, Evolution of the Atlantic continental margin of the United States, *in* Talwani, M., Hay, W., and Ryan, W. B. F., eds., Deep drilling results in the Atlantic Ocean; Continental margins and paleoenvironment: Maurice Ewing Series 3, American Geophysical Union, p. 87–108.

Fullagar, P. D., and Butler, J. R., 1979, 325 to 265 m.y.-old granitic plutons in the Piedmont of the southeastern Appalachians: American Journal of Science, v. 279, p. 161–185.

Girdler, R. W., Fairhead, J. D., Searle, R. C., and Sowerbutts, W. T. C., 1969, The evolution of rifting in Africa: Nature, v. 224, no. 5224, p. 1178–1182.

Gohn, G. S., editor, 1983a, Studies related to the Charleston, South Carolina earthquake of 1886–Tectonics and seismicity: U.S. Geological Survey Professional Paper 1313, 375 p.

———1983b, Geology of the basement rocks near Charleston, South Carolina–Data from detrital rock fragments in lower Mesozoic(?) rocks, Clubhouse Crossroads test hole #3, *in* Gohn, G. S., ed., Studies related to the Charleston, South Carolina, earthquake of 1886–Tectonics and seismicity: U.S. Geological Survey Professional Paper 1313, p. E1–E22.

Gohn, G. S., Gottfried, David, Lanphere, M. A., and Higgins, B. B., 1978, Regional implications of Triassic or Jurassic age for basalt and sedimentary red beds in the South Carolina Coastal Plain: Science, v. 202, no. 4370, p. 887–890.

Gottfried, David, Annell, C. S., and Byerly, G. R., 1983, Geochemistry and tectonic significance of subsurface basalts near Charleston, South Carolina: Clubhouse Crossroads test holes #2 and #3, *in* Gohn, G. S., ed., Studies related to the Charleston, South Carolina, earthquake of 1886–Tectonics and seismicity: U.S. Geological Survey Professional Paper 1313, p. A1–A19.

Gottfried, David, Annell, C. S., and Schwarz, L. J., 1977, Geochemistry of subsurface basalt from the deep corehole (Clubhouse Crossroads corehole 1) near Charleston, South Carolina–magma type and tectonic implications, *in* Rankin, D. W., ed., Studies related to the Charleston, South Carolina, earthquake of 1886–A preliminary report: U.S. Geological Survey Professional Paper 1028, p. 91–113.

Grow, J. A., Bowin, C. O., and Hutchinson, D. R., 1979, The gravity field of the U.S. Atlantic continental margin: Tectonophysics, v. 59, no. 1–4, p. 27–52.

Hamilton, R. M., Behrendt, J. C., and Ackermann, H. D., 1983, Land multichannel seismic-reflection evidence for tectonic features near Charleston, South Carolina, *in* Gohn, G. S., ed., Studies related to the Charleston, South Carolina, earthquake of 1886–Tectonics and seismicity: U.S. Geological Survey Professional Paper 1313, p. I1–I18.

Hamilton, Warren, 1981, Crustal evolution by arc magmatism: Royal Society of London Philosophical Transactions, ser. A, v. 301, p. 279–291.

Harper, S. B., and Fullagar, P. D., 1981, Rb-Sr ages of granitic gneisses of the Inner Piedmont belt of northwestern North Carolina and southwestern South Carolina: Geological Society of America Bulletin, v. 92, no. 11, p. 864–872.

Hatcher, R. D., Jr., 1978, Tectonics of the western Piedmont and Blue Ridge, Southern Appalachians; review and speculation: American Journal of Science, v. 278, no. 3, p. 276–304.

Hatcher, R. D., Jr., Howell, D. E., and Talwani, Pradeep, 1977, Eastern Piedmont fault system–Speculations on its extent: Geology, v. 5, no. 10, p. 636–640.

Hatcher, R. D., Jr., and Zietz, Isidore, 1979, Tectonic implications of regional aeromagnetic data from the southern Appalachians, *in* Wones, D. R., ed., The Caledonides in the U.S.A., Proceedings of the second symposium of the International Geological Correlation Program, Caledonide Orogen Project: Virginia Polytechnic Institute and State University Memoir 2, p. 235–244.

Hayes, D. E., and Rabinowitz, R. D., 1975, Mesozoic magnetic lineations and the magnetic quiet zone off northwest Africa: Earth and Planetary Science Letters, v. 28, no. 2, p. 105–115.

Hutchinson, D. R., Grow, J. A., Klitgord, K. D., and Swift, B. A., 1983, Deep structure and evolution of the Carolina Trough: American Association of Petroleum Geologists Memoir 34, in press.

Kane, M. F., 1977, Correlation of major eastern earthquake centers with mafic/ultramafic basement masses, *in* Rankin, D. W., ed., Studies related to the Charleston, South Carolina, earthquake of 1886–A preliminary report: U.S. Geological Survey Professional Paper 1028, p. 199–204.

Kent, D. V., and Opdyke, N. D., 1978, Paleomagnetism of the Devonian Catskill red beds: Evidence for motion of the coastal New England-Canadian Maritime region relative to North America: Journal of Geophysical Research, v. 83, no. B9, p. 4441–4450.

———1979, The Early Carboniferous paleomagnetic field of North America and its bearing on the tectonics of the northern Appalachians: Earth and Planetary Science Letters, v. 44, no. 2, p. 365–372.

Klitgord, K. D., and Behrendt, J. C., 1977, Aeromagnetic anomaly map of the U.S. Atlantic continental margin: U.S. Geological Survey Miscellaneous Field Studies Map MF–913, 2 sheets, scale 1:1,000,000.

———1979, Basin structure of the U.S. Atlantic Margin, *in* Watkins, J. S., Montadert, Lucien, and Dickerson, P. W., eds., Geological

and geophysical investigations of continental margins: American Association of Petroleum Geologists Memoir 29, p. 85–112.

Klitgord, K. D., and Grow, J. A., 1980, Jurassic seismic stratigraphy and basement structure of western Atlantic magnetic quiet zone: American Association of Petroleum Geologists Bulletin, v. 64, no. 10, p. 1658–1680.

Klitgord, K. D., and Schouten, H., 1980, Mesozoic evolution of the Atlantic, Caribbean and Gulf of Mexico, *in* Pilger, R. H., Jr., ed., The origin of the Gulf of Mexico and the early opening of the central North Atlantic; Proceedings of a symposium March 3–5, 1980: Baton Rouge, Louisiana State University, p. 100–101.

Klitgord, K. D., Popenoe, Peter, and Schouten, Hans, 1983, Florida: A Jurassic transform plate boundary: Journal of Geophysical Research, in press.

Krivoy, H. L., and Pyle, T. E., 1972, Anomalous crust beneath West Florida Shelf: American Association of Petroleum Geologists Bulletin, v. 56, no. 1, p. 107–113.

Larson, R. L., and Hilde, T. W. C., 1975, A revised time scale of magnetic reversals for the Early Cretaceous and Late Jurassic: Journal of Geophysical Research, v. 80, no. 17, p. 2586–2594.

Long, L. T., 1979, The Carolina Slate belt–Evidence of a continental rift zone: Geology, v. 7, no. 4, 180–184.

Long, L. T., and Champion, J. W., Jr., 1977, Bouguer gravity map of the Summerville-Charleston, South Carolina, epicentral zone and tectonic implications, *in* Rankin, D. W., ed., Studies related to the Charleston, South Carolina, earthquake of 1886–A preliminary report: U.S. Geological Survey Professional Paper 1028, p. 151–166.

Maher, J. C., 1971, Geologic framework and petroleum potential of the Atlantic Coastal Plain and Continental Shelf: U.S. Geological Survey Professional Paper 659, 98 p.

Manspeizer, W., Puffer, J. H., and Cousminer, H. L., 1978, Separation of Morocco and eastern North America: a Triassic-Liassic stratigraphic record: Geological Society of America Bulletin, v. 89, no. 6, p. 901–920.

Marine, I. W., and Siple, G. E., 1974, Buried Triassic basin in the central Savannah River area, South Carolina and Georgia: Geological Society of America Bulletin, v. 85, no. 2, p. 311–320.

May, P. R., 1971, Pattern of Triassic-Jurassic dikes around the North Atlantic in the context of predrift positions of the continents: Geological Society of America Bulletin, v. 82, no. 5, p. 1285–1292.

Meyerhoff, A. A., and Hatten, C. W., 1974, Bahamas salient of North America: Tectonic framework, stratigraphy and petroleum potential: American Association of Petroleum Geologists Bulletin, v. 58, no. 6, p. 1201–1239.

Nishenko, S. P., and Sykes, L. R., 1979, Fracture zones, Mesozoic rifts and the tectonic setting of the Charleston, South Carolina earthquake of 1886 [abs.]: EOS, American Geophysical Union Transactions, v. 60, no. 18, p. 310.

Pickering, S. M., Jr., Higgins, M. W., and Zietz, Isidore, 1977, Relationship between the Southeast Georgia Embayment and the onshore extent of the Brunswick Magnetic Anomaly [abs.]: EOS, American Geophysical Union Transactions, v. 58, no. 6, p. 432.

Popenoe, Peter, and Zietz, Isidore, 1977, The nature of the geophysical basement beneath the Coastal Plain of South Carolina and northeastern Georgia, *in* Rankin, D. W., ed., Studies related to the Charleston, South Carolina, earthquake of 1886–A preliminary report: U.S. Geological Survey Professional Paper 1028, p. 119–137.

Rankin, D. W., editor, 1977a, Studies related to the Charleston, South Carolina, earthquake of 1886–A preliminary report: U.S. Geological Survey Professional Paper 1028, 204 p.

Rankin, D. W., 1977b, Studies related to the Charleston, South Carolina, earthquake of 1886–Introduction and discussion, *in* Rankin, D. W., ed., Studies related to the Charleston, South Carolina, earthquake of 1886–A preliminary report: U.S. Geological Survey Professional Paper 1028, p. 1–15.

Rodgers, John, 1970, The tectonics of the Appalachians: New York, Wiley-Interscience, 271 p.

Sanders, J. E., 1963, Late Triassic tectonic history of northeastern United States: American Journal of Science, v. 261, no. 6, p. 501–524.

Schilt, F. S., Brown, L. D., Oliver, J. E., and Kaufman, Sidney, 1983, Subsurface structure near Charleston, South Carolina–Results of COCORP reflection profiling in the Atlantic Coastal Plain, *in* Gohn, G. S., ed., Studies related to the Charleston, South Carolina, earthquake of 1886–Tectonics and seismcity: U.S. Geological Survey Professional Paper 1313, p. H1–H19.

Schlee, J. S., Dillon, W. P., and Grow, J. A., 1979, Structure of the continental slope off the eastern United States: Society of Economic Paleontologists and Mineralogists Special Publication no. 27, p. 95–117.

Schouten, Hans, and Klitgord, K. D., 1977, Map showing Mesozoic magnetic anomalies, western North Atlantic: U.S. Geological Survey Miscellaneous Field Studies Map MF-915, scale 1:2,000,000.

———1982, The memory of the accreting plate boundary and the continuity of fracture zones: Earth and Planetary Science Letters, v. 59, no. 2, p. 255–266.

Sheridan, R. E., 1974, Atlantic continental margin of North America, *in* Burke, C. A., and Drake, C. L., eds., Geology of continental margins: New York, Springer-Verlag, p. 391–407.

Sheridan, R. E., Crosby, J. T., Bryan, G. M., and Stoffa, P. L., 1981, Stratigraphy and structure of southern Blake Plateau, northern Florida Straits, and northern Bahama Platform from multichannel seismic reflection data: American Association of Petroleum Geologists Bulletin, v. 65, no. 12, p. 2572–2593.

Steckler, M. S., and Watts, A. B., 1978, Subsidence of the Atlantic-type continental margin off New York: Earth and Planetary Science Letters, v. 41, no. 1, p. 1–13.

Sumner, J. R., 1977, Geophysical investigation of the structural framework of the Newark-Gettysburg Triassic basin, Pennsylvania: Geological Society of America Bulletin, v. 88, no. 7, p. 935–942.

Swanson, D. E., and Gernazian, Andrea, 1979, Petroleum exploration wells in Georgia: Georgia Geologic Survey Information Circular IC–51, 67 p.

Sykes, L. R., 1978, Intraplate seismicity, reactivation of preexisting zones of weakness, alkaline magmatism, and other tectonism postdating continental fragmentation: Reviews of Geophysics and Space Physics, v. 16, no. 4, p. 621–688.

Tarr, A. C., and Rhea, Susan, 1983, Seismicity near Charleston, South Carolina, March 1973 to December 1979, *in* Gohn, G. S., ed., Studies related to the Charleston, South Carolina, earthquake of 1886–Tectonics and seismicity: U.S. Geological Survey Professional Paper 1313, p. R1–R17.

Tator, B. A., and Hatfield, L. E., 1975a, Bahamas present complex geology, pt. 1: Oil and Gas Journal, v. 73, no. 43, p. 172–176.

———1975b, Bahamas present complex geology, pt. 2: Oil and Gas Journal, v. 73, no. 44, p. 120–122.

Taylor, P. T., Zietz, Isidore, and Dennis, L. S., 1968, Geologic implications of aeromagnetic data for the eastern continental margin of the United States: Geophysics, v. 33, no. 4, p. 755–780.

Thomas, W. A., 1976, Evolution of Ouachita-Appalachian continental margin: Journal of Geology, v. 84, no. 3, p. 323–342.

Tucholke, B. E., Houtz, R. E., and Ludwig, W. J., 1982, Maps of sediment thickness and depth to basement in the Western North Atlantic Ocean Basin: American Association of Petroleum Geologists Bulletin, v. 66, no. 9, p. 1384–1395.

Van der Voo, Rob, and Scotese, Chris, 1981, Paleomagnetic evidence for a large (~ 2,000 km) sinistral offset along the Great Glen fault during Carboniferous time: Geology, v. 9, no. 12, p. 583–589.

Van Houten, F. B., 1977, Triassic-Liassic deposits of Morocco and eastern North America: Comparison: American Association of Petroleum Geologists Bulletin, v. 61, no. 1, p. 79–99.

Vogt, P. R., 1973, Early events in the opening of the North Atlantic, *in* Tarling, D. H., and Runcorn, S. K., eds., Implications of continental drift to the Earth sciences; Vol. 2, Part 6, Rift margins and continental edge structures: London, Academic Press, p. 693–712.

Vogt, P. R., and Einwich, A. M., 1979, Magnetic anomalies and seafloor spreading in the western North Atlantic, and a revised calibration of the Keathley (M) geomagnetic reversal chronology, *in* California University, Scripps Institution of Oceanography, La Jolla, Initial reports of the Deep Sea Drilling Project, vol. 43: Washington, D. C., National Science Foundation, p. 857–876.

Wentworth, C. M., and Mergner-Keefer, Marcia, 1983, Regenerate faults of small Cenozoic offset–Probable earthquake sources in the Southeastern United States, *in* Gohn, G. S., ed., Studies related to the Charleston, South Carolina, earthquake of 1886–Tectonics and seismicity: U.S. Geological Survey Professional Paper 1313, p. S1–S20.

Williams, H. R., 1978, Tectonic lithofacies map of the Appalachian orogen: Memorial University of Newfoundland Map no. 1, scale 1:1,000,000.

Wood, M. L., and Walper, J. L., 1974, The evolution of the interior Mesozoic basin and the Gulf of Mexico: Gulf Coast Association of Geological Societies Transactions, v. 24, p. 31–41.

Woods, R. D., and Addington, J. W., 1973, Pre-Jurassic geologic framework, northern Gulf Basin: Gulf Coast Association of Geological Societies Transactions, v. 23, p. 92–108.

Woollard, G. P., Bonini, W. E., and Meyer, R. P., 1957, A seismic refraction study of the subsurface geology of the Atlantic Coastal Plain and continental shelf between Virginia and Florida: Madison, University of Wisconsin Department of Geology and Geophysics Technical Report, Contract No. 57onr-28512, 128 p.

Relocation of Instrumentally Recorded pre-1974 Earthquakes in the South Carolina Region

By JAMES W. DEWEY

STUDIES RELATED TO THE CHARLESTON, SOUTH CAROLINA, EARTHQUAKE OF 1886—TECTONICS AND SEISMICITY

GEOLOGICAL SURVEY PROFESSIONAL PAPER 1313-Q

UNITED STATES GOVERNMENT PRINTING OFFICE, WASHINGTON:1983

CONTENTS

ILLUSTRATIONS

TABLES

RELOCATION OF INSTRUMENTALLY RECORDED PRE-1974 EARTHQUAKES IN THE SOUTH CAROLINA REGION

By JAMES W. DEWEY

ABSTRACT

Regionally and teleseismically recorded earthquakes from South Carolina and vicinity have been relocated by using a regional velocity model and station traveltime adjustments determined by the method of Joint Epicenter Determination. The revised hypocenters are accompanied by confidence ellipsoids so that a user can evaluate the likelihood that an earthquake took place on a particular tectonic structure defined by geological or geophysical methods. The revised hypocenters of all nine pre-1974 earthquakes within 100 km of Charleston are consistent with the occurrence of these earthquakes in the Middleton Place–Summerville zone or the Bowman cluster, two source regions identified on the basis of microearthquakes recorded by the South Carolina network since 1974. The confidence ellipsoid on one of the hypocenters indicates that the shock could instead have taken place at the Adams Run cluster, a microearthquake source 20 km south of the Middleton Place–Summerville zone. The previously determined epicenters of several earthquakes had been mislocated by 50 km or more. In the Piedmont of South Carolina and northeast Georgia, shocks tend to occur in the vicinity of several manmade reservoirs. However, the earthquake of July 26, 1945, previously thought to be at Lake Murray, has been relocated away from the lake. The region of Lake Jocassee experienced a regionally recorded earthquake in 1969 prior to the filling of the reservoir.

INTRODUCTION

Prior to 1974, hypocenters of South Carolina earthquakes were often poorly determined by means of instrumental data. The installation, in May 1974, of a regional seismographic network in South Carolina finally enabled precise determination of local hypocenters. However, the source regions defined by earthquakes recorded since 1974 cover a much more limited area than do the routinely determined epicenters of pre-1974 earthquakes (fig. 1). This situation seemed to require regional tectonic models that would account for earthquakes at the source regions identified since 1974 and at the previously determined locations of the pre-1974 earthquakes. The principal conclusion of this study is that pre-1974 instrumentally recorded earthquakes from the region of Charleston, S. C., did not occur over the broad area suggested by figure 1. Instead, they were within or very near two source regions identified from microearthquakes recorded since 1974: the Bowman cluster and the Middleton Place–Summerville zone (fig. 2).

In relocating a pre-1974 earthquake, one now has tools that were not available to those who originally determined the epicenters of the earthquakes. The most important of these tools is undoubtedly the hindsight provided by the accurately located, teleseismically or regionally recorded earthquakes that occurred after the installation of the South Carolina network. As discussed below, these earthquakes are formally used to calibrate the procedure used to locate the prenetwork earthquakes. A second tool is the electronic computer, which was not used in locating earthquakes until the early 1960's. A third tool is a velocity model appropriate to the South Carolina region: many of the original epicenters were determined by means of a global-average traveltime curve (Jeffreys and Bullen, 1958) based on upper mantle velocities significantly lower than those beneath South Carolina.

An important problem that cannot be corrected retroactively is the formerly unfavorable distribution of seismographic stations with respect to South Carolina. The stations that recorded the pre-1974 earthquakes were mostly in North America and at azimuths west to north-northeast of the earthquakes. This unfavorable distribution of stations played a large role in the mislocation of the pre-1974 earthquakes. Although the effect of unfavorable station distribution can be minimized, it cannot be eliminated; relocated epicenters will still tend to be most severely mislocated in a direction approximately perpendicular to the coastline, which is the direction least well resolved by the North American stations as they were distributed prior to 1974. The unfavorable distribution of stations also makes more difficult the already difficult task of determining precise focal depths from regional and teleseismic traveltime data.

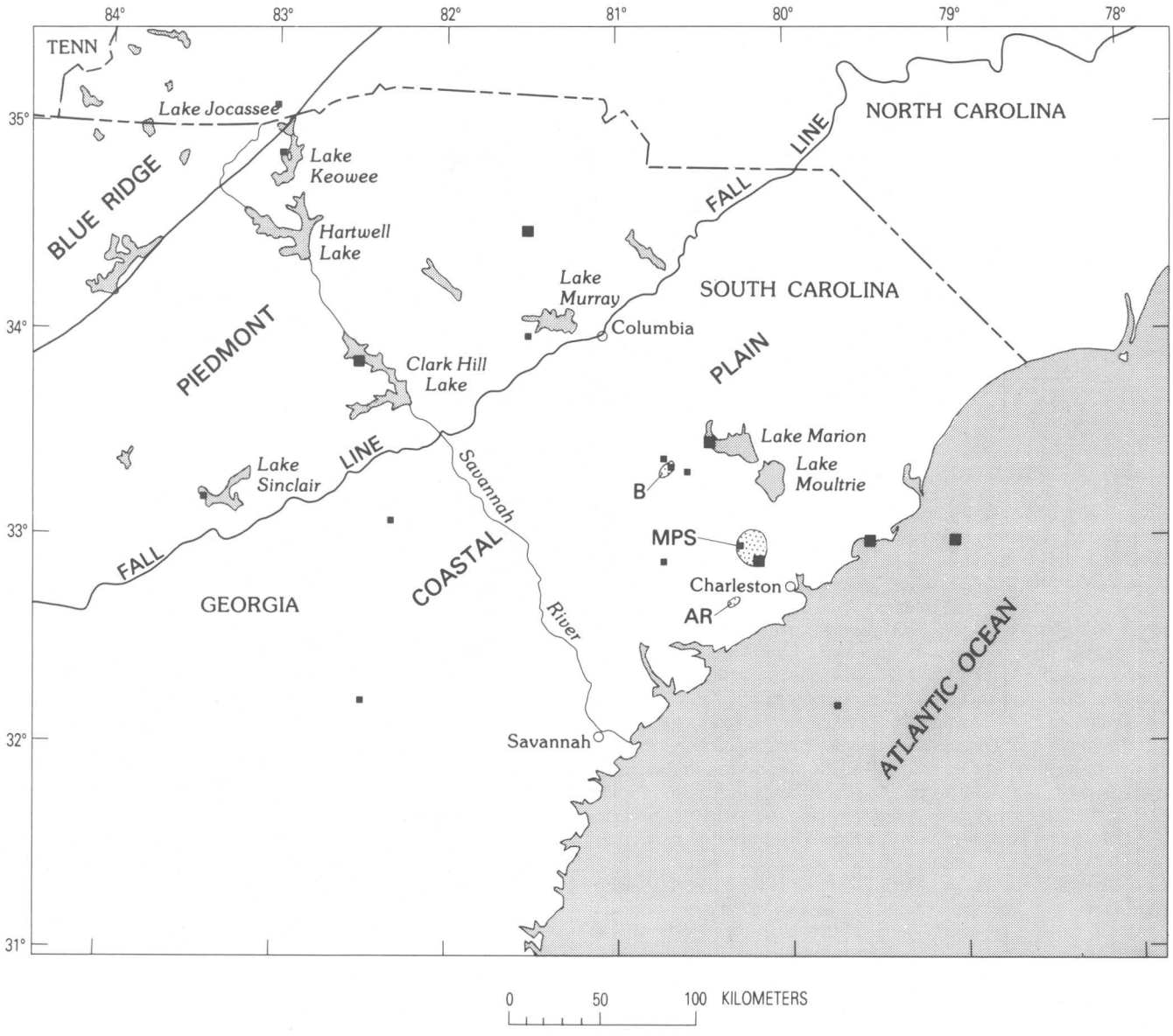

FIGURE 1.—Epicenters of earthquakes studied in this report as previously assigned by the U.S. Geological Survey, the National Oceanic and Atmospheric Administration, the U.S. Coast and Geodetic Survey, or (for two events not located by the U.S. Coast and Geodetic Survey) the International Seismological Centre. B, MPS, and AR are, respectively, the Bowman cluster, the Middleton Place–Summerville seismic zone, and the Adams Run cluster of Tarr and Rhea (1983). Large manmade lakes are plotted. Large squares correspond to earthquakes of magnitude 4.0 and greater; small squares correspond to shocks of magnitude less than 4.0.

LOCATION PROCEDURE

The first step in recomputing hypocenters was to apply the method of Joint Epicenter Determination (JED) to estimate simultaneously the epicenters of a group of earthquakes and the traveltime anomalies that, if not taken into account, would bias the locations of the epicenters. The method as applied to the South Carolina data makes two assumptions about the Earth:

Assumption 1.—Traveltimes from an earthquake in the South Carolina region in the distance range of 0° to 3° (333.6 km) are predicted by the velocity model given in table 1. Stations within 3° are considered to be calibration stations because times from these stations are used to calibrate the location process. Most calibration stations have been installed since 1974; our method of relocating pre-1974 epicenters is based on the fact that several earthquakes that took place in 1974 and later were well recorded by both the South Carolina network and the more distant stations that had also recorded the pre-1974 shocks.

Assumption 2.—Traveltimes of a phase at a particular station more than 3° from an earthquake are determined from the times predicted by the velocity

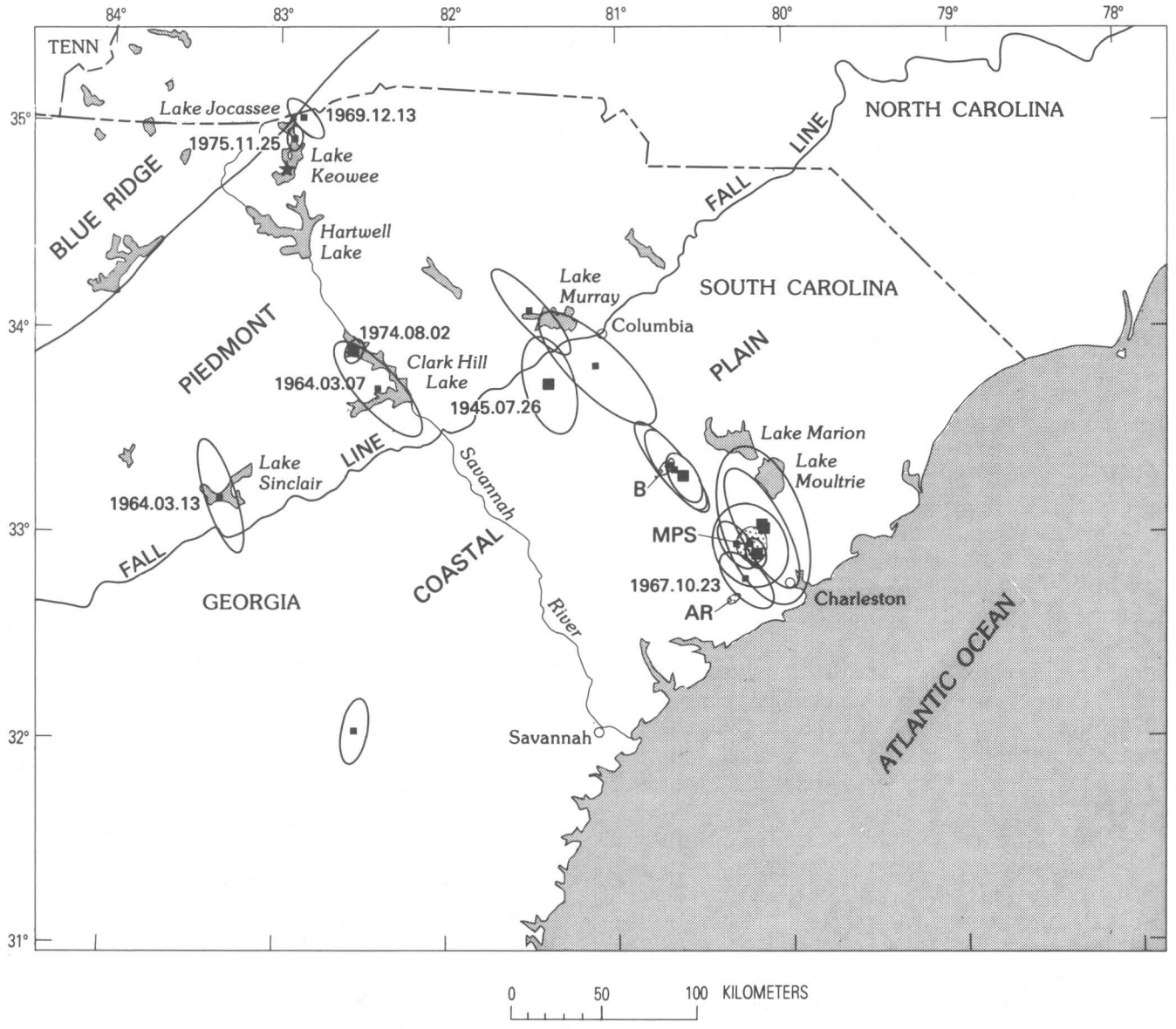

FIGURE 2. – Revised epicenters of regionally recorded earthquakes that occurred between 1945 and 1976. The ellipse around each epicenter is the projection on the earth's surface of the 90-percent confidence ellipsoid on the hypocenter (see text). Star denotes epicenter inferred by Talwani and others (1979) for earthquake of 1971.07.13 (year. month. day). Other symbols as in figure 1.

model (table 1) minus a constant that is the same for all South Carolina earthquakes. This constant is associated with that particular phase at that particular station and is called the station-phase adjustment.

Some stations in the Eastern United States recorded certain phases from only one earthquake out of the group being located. The corresponding station-phase adjustments were then assumed to be equal to the adjustments computed for neighboring stations, and special weighting functions were computed for the station-phases that had only one observation (see discussion of weighting, below).

The hypocenters of South Carolina earthquakes were fixed at 5-km focal depth in the JED computation. Fixing the focal depth is necessary to obtain a stable hypocenter computation for less well recorded earthquakes. The 5-km figure, rather than 10 or 20 km, was chosen because several of the large shocks that have occurred since 1974 are thought, on the basis of local studies, to have had focal depths less than 10 km (Talwani and others, 1975; Talwani, 1977; Tarr, 1977; Tarr and Rhea, 1983).

After the station-phase adjustments for stations at distances greater than 3° were estimated, the fixed-depth assumption was dropped, and the hypocenters

TABLE 1.—*Crust and upper mantle velocity model used to recompute hypocenters of South Carolina earthquakes*

[At depths greater than 246 km, the velocity model is assumed to be model QM2 of Hart and others (1977). Velocities are tabulated for discrete depths, and velocities at other depths are interpolated from the velocities at the tabulated depths]

Depth below surface (km)	*P*-wave velocity (km/s)	*S*-wave velocity (km/s)
0	6.15	3.50
19.99	6.15	3.50
20.01	6.70	3.67
29.99	6.70	3.67
30.01	8.10	4.53
96.99	8.10	4.53
97.01	8.37	4.68
246.00	8.37	4.67

were estimated for each earthquake using the JED-computed station-phase adjustments. The hypocenters computed at this stage are the recomputed hypocenters shown in figure 2 and listed in table 2.

For several events, the computed focal depth became negative or the hypocenter computation became unstable, and the earthquakes' focal depths had to be fixed. Any shock significantly deeper than average should have been identifiable when the hypocenter was computed without fixing focal depth. However, the absolute values of many of the focal depths are dependent on the assumption of 5 km as a typical focal depth for a South Carolina earthquake. If the JED-computed station-phase adjustments had been computed assuming 10-km focal depths, the unfixed focal depths of most of the hypocenters would tend to be greater by about 5 km, but the earthquakes' epicenters would have changed much less.

The JED program used has been modified from Dewey (1971) to use secondary *P*-waves, *S*-waves, and surface waves in the location process (Dewey, 1976) and to use calibration stations (Assumption 1, above), rather than calibration events, to make the set of normal equations for the hypocenters and station adjustments well determined (Dewey, 1978). The following phases were used to relocate South Carolina earthquakes: first-arriving *P*, P_g at regional distance, first-arriving *S*, and L_g at regional distance.

Table 1 gives the velocity model used to determine theoretical times of first-arriving *P*- and *S*-waves for relocating the South Carolina earthquakes. The features of the model that are most important in locating earthquakes are the 30-km-thick crust, the P_n velocity of 8.1 km/s, and the rapid increase of *P*-wave velocity in the uppermost mantle, at a depth of 97 km. Velocities in the crust and upper mantle to a depth of 246 km are based on Nuttli and others (1969); however, the crust is thinned and the P_n velocity is decreased slightly on the basis of traveltime studies done in regions of the eastern seaboard north of South Carolina (for example, as summarized by Healy and Warren, 1969). Amick (1979) has recently derived a velocity model for the crust and uppermost mantle beneath the South Carolina Coastal Plain that differs from the model of table 1 by having a lower average crustal *P*-wave velocity and a slightly higher P_n velocity. For shallow earthquakes, the model of Amick predicts slower traveltimes than does the model of table 1. To illustrate the effect of using the model of table 1 instead of Amick's model, consider traveltimes from a 5-km-deep earthquake recorded at stations at epicentral distances between 0° and 3°. It is this distance range for which the present study assumes that the model of table 1 predicts unbiased traveltimes. The difference between the times predicted by Amick's velocity model and those predicted from table 1 increases from a negligible difference, at zero epicentral distance, to about +1.0 s, at an epicentral distance of 1°, and then decreases to about +0.4 s, at an epicentral distance of 3°. Traveltime differences this large could introduce differences of as much as several kilometers (for the station distribution used in this study) between an epicenter computed from Amick's model and the epicenter of the same earthquake computed from the model of table 1.

In table 1, the rapid increase in *P*-wave velocity at a depth of 97 km is similar to rapid increases at depths of 70 to 130 km inferred in traveltime studies of the Eastern and Central United States (for example, Green and Hales, 1968; Lewis and Meyer, 1968, 1977; Julian, 1970; Massé, 1973). The velocities at depths below 246 km are those of model QM2 of Hart and others (1977). Systematic errors in the part of the model below 246 km depth would tend to be nearly constant for all South Carolina sources recorded at a particular station and would be largely compensated for by the station adjustments computed by JED.

Velocities of the P_g and L_g phases are those derived by Bollinger (1970) for the Central Appalachians, 6.24 km/s and 3.67 km/s, respectively. These velocities, though derived for a different tectonic regime than that in coastal South Carolina, are consistent with data from South Carolina. It should be emphasized that the phases herein called P_g and L_g are secondary phases recorded after the first-arriving *P*- and *S*-waves at distances of more than 250 km from the earthquake epicenters. The notation used herein for these phases is that of Bollinger (1970). P_g is similar to the phase $\bar{P}$ identified in the Western United States (Pakiser, 1963).

Earthquakes relocated in this study were those recorded between 1945 and 1976 at regional or teleseismic distances and reported in the seismological bulletins of the U.S. Geological Survey, the National Oceanic and Atmospheric Administration, the U.S. Coast and Geodetic Survey, the International Seismological Centre, the Bureau Central International Seismologique, and the International Seismological Summary. The earliest shock for which traveltime data

TABLE 2.—*Revised hypocenters of regionally recorded earthquakes*

[SL, length of semiaxis, in kilometers; Tr, trend of axis, measured clockwise from North, in degrees; Pl, plunge of axis, in degrees]

Date (year.month.day)	Time (GMT) (hour	minute	second)	Latitude (°N)	Longitude (°W)	Depth (km)	Magnitude[1]	90-percent confidence ellipsoid Axis	SL	Tr	Pl
1945.07.26	10	32	16.4	33.750	81.376	4.8	4.4(F)	Major	28.8	−14.2	22.8
								Intermediate	20.8	120.0	58.9
								Minor	13.3	−112.9	19.9
1959.08.03	06	08	36.8	33.054	80.126	[2]1.0	4.4(F)	Major	35.0	151.5	.0
								Minor	13.3	61.5	.0
1960.03.12	12	47	44.0	33.072	80.121	9.1	4.0(F)	Major	52.6	−27.5	43.8
								Intermediate	32.0	−167.5	38.6
								Minor	18.5	84.4	21.3
1963.05.04	21	01	50.3	32.972	80.193	[2]5.0	3.3(F)	Major	23.5	148.6	.0
								Minor	20.2	58.6	.0
1964.03.07	18	02	58.6	33.724	82.391	5.4	3.3(J)	Major	38.2	131.9	36.1
								Intermediate	24.7	−22.6	51.1
								Minor	10.3	−128.7	12.6
1964.03.13	01	20	17.5	33.193	83.309	[2]1.0	3.9(J)	Major	32.0	161.5	.0
								Minor	9.2	71.5	.0
1964.04.20	19	04	44.1	33.842	81.096	3.0	3.5(J)	Major	43.4	133.0	2.1
								Intermediate	22.0	38.6	63.7
								Minor	10.6	−136.0	26.2
1967.10.23	09	04	2.5	32.802	80.221	19.1	3.4(B)	Major	22.3	−41.0	41.3
								Intermediate	16.0	132.7	48.5
								Minor	10.1	−133.7	3.1
1968.09.22	21	41	18.2	34.111	81.484	[2]1.0	3.5(J)	Major	31.7	137.1	.0
								Minor	8.4	47.1	.0
1969.12.13	10	19	29.7	35.036	82.846	5.9	3.7(J)	Major	14.8	131.2	55.1
								Intermediate	13.5	−38.5	34.5
								Minor	5.8	−131.8	4.8
1971.05.19	12	54	3.6	33.359	80.655	[2]1.0	3.7(B)	Major	30.5	140.7	.0
								Minor	9.0	50.7	.0
1971.07.31	20	16	55.0	33.341	80.631	3.9	3.8(B)	Major	29.4	−34.4	34.0
								Intermediate	14.1	134.8	55.5
								Minor	9.0	−127.8	5.1
1972.02.03	23	11	9.7	33.306	80.582	1.8	4.5(B)	Major	21.9	−32.5	55.6
								Intermediate	11.8	156.6	34.1
								Minor	7.4	63.7	4.2
1973.12.19	10	16	8.7	32.974	80.274	6.0	3.0(J)	Major	16.2	147.5	18.9
								Intermediate	8.5	−96.4	52.1
								Minor	7.1	45.4	31.4
1974.08.02	08	52	11.1	33.908	82.534	3.7	4.1(B)	Major	14.7	21.8	81.8
								Intermediate	7.8	−152.9	1.7
								Minor	5.2	−62.7	8.0
1974.11.22	05	25	56.7	32.926	80.159	5.7	4.3(B)	Major	9.5	158.2	4.1
								Intermediate	6.2	−116.6	49.8
								Minor	5.2	71.7	39.9
1975.11.25	15	17	34.8	34.943	82.896	9.9	3.2(SLM)	Major	19.9	−179.5	80.1
								Intermediate	6.9	27.0	8.9
								Minor	4.5	−63.7	4.3
1976.12.27	06	57	15.2	32.060	82.504	13.7	3.7(BLA)	Major	20.7	2.5	64.7
								Intermediate	17.5	−167.6	24.9
								Minor	7.6	100.6	3.8

[1] For convenience, only one magnitude is listed, although several earthquakes have had more than one magnitude computed for them. The sources of the magnitudes, and the precedence given to the sources, are as follows: B, Bollinger (1979); J, Jones and others (1977); BLA, Seismographic station at Blacksburg, Va.; SLM, Seismographic station at St. Louis, Mo.; F, computed from the felt area using the formula of Nuttli and Zollweg (1974).

[2] Indicates depth was fixed in computation. Depths were fixed at 1.0 km if the hypocenter computation without fixed focal depth yielded a negative depth. Depths were fixed at 5.0 km if the computation without fixed focal depth was unstable.

are sufficient for instrumental location was that of 1945.07.26; shocks occurring later than 1976 were not considered. Shocks not recorded in the above-cited bulletins were not studied.

Shocks of magnitude 3.5 or less listed in table 2 that took place in 1964–73 were not too well recorded. Bollinger (1972) discussed a magnitude-3.5 earthquake that took place on 1971.08.01, which was not reported in the bulletins listed above, and it would not be surprising if several other shocks of magnitude about 3.5 have not been reported. The Seneca earthquake of 1971.07.13 (Bollinger, 1972; Talwani and others, 1979) is unusual in that it was larger than magnitude 3.5 but was not instrumentally located by the National Oceanic and Atmospheric Administration or the International Seismological Centre, apparently because its *P*-arrival times were obscured by a foreshock (Bollinger, 1972). This earthquake has not been considered in this study. Talwani and others (1979) have made a strong case that the earthquake of 1971.07.13 occurred near lat 34.80° N., long 82.93° W. (fig. 2). Bollinger (1972) estimated a magnitude of 3.8 for 1971.07.13; Jones and others (1977) estimated a magnitude of 4.4. South Carolina earthquakes of magnitude 3.8 and greater normally were well recorded after 1964 and should generally have been listed in the above-cited seismological bulletins. In 1945–60, South Carolina earthquakes below magnitude 4.3, approximately, would not usually have been sufficiently well recorded to be located by means of instrumental data.

Phase arrival times used in locating the South Carolina earthquakes were those reported in the seismological bulletins listed previously. After 1962, bulletin data on shocks were extensively supplemented by arrival times read on seismograms of the World-Wide Standard Seismograph Network (WWSSN). When the seismogram was not available for inspection, I sometimes changed the phase identification of an arrival from the phase type listed in the bulletin to a phase type that was consistent with experience and with the observed arrival times from other South Carolina earthquakes. For example, less sensitive stations at regional distances sometimes identified an arrival as *S* whose time was much later (by 20 to 60 s) than the predicted *S*-time but consistent (within several seconds) with the predicted L_g times. On WWNSS stations having high sensitivity, L_g phases had amplitudes greater than the *S* phase by a factor of four or more at regional distances. It therefore seemed reasonable to identify the apparent late *S*-waves as the L_g phase.

Observations were weighted inversely proportional to their estimated variance. However, it was impractical to estimate a different variance for each individual station-phase; there were usually too few observations of a particular phase at a particular station to estimate the variance reliably. I therefore assumed that observations of a particular phase at all stations within a certain distance range would have the same variance; observations of the phase at these stations were pooled, and a single variance was estimated from the pooled observations. Groups of station-phases known to be reliable were given very high weights during the first two iterations of the JED process. After two iterations, variances were reestimated from the data set itself, and these variances formed the basis for subsequent weighting. The weighting process is summarized in table 3.

Initially, local and regional *P*-waves were presumed to have the smallest errors and were given the highest weights. Local *S*-waves (distance less than 3°) were weighted at 0.1 the weight of local and regional *P*-waves, and regional *S*-waves recorded at distances between 3° and 5° were weighted at 0.01 the weight of local and regional *P*-waves. It turned out, however, that observations of the regional *S*-waves were mutually more consistent than were observations of the local *S*-waves. In the last six iterations, the observations of regional *S*-waves received higher weight than those of the local *S*-waves, a weight of 0.20 that of the local *P*-waves. Because the *S*-wave velocity is substantially less than the *P*-wave velocity, the observations suggest that a single *S*-wave reading from a distance between 3° and 5° is about 70 percent as effective as a locally recorded *P*-wave in estimating the distance of a source from the station (table 3, column SED).

TABLE 3.—*Summary of major features of weighting scheme used in relocating South Carolina earthquakes*

[WT_i, initial weight used in first two iterations. N, number of observations of phase type. VAR, sample variance computed after two iterations. WT_f, weight used in final six iterations, normalized to weight of local *P*-waves. V, velocity used to express VAR as SED, the estimated standard error of distance corresponding to one observation. Δ, epicentral distance]

Phase Type	WT_i	N	VAR (s^2)	WT_f	V (km/s)	SED (km)
P recorded in 0°<Δ<3°, adjustments not computed	1.000	51	0.640	1.00	6.70	5.4
P recorded in 3°<Δ<5°, adjustments computed	1.000	30	.595	1.08	8.10	6.3
P recorded in Δ>5°, adjustments computed	.1	57	2.917	.22	12.00	20.5
P recorded in Δ>5°, adjustments not explicitly computed but set equal to adjustments of neighboring stations	.01	17	1.775	.36	12.00	16.0
P_n recorded in 3°<Δ<5°, adjustments computed	.1	18	2.443	.26	6.24	9.8
S recorded in 0°<Δ<3°, adjustments not computed	.1	8	6.580	.10	3.67	9.4
S recorded in 3°<Δ<5°, adjustments computed	.01	11	3.166	.20	4.53	8.1
S recorded at Δ>5°, adjustments computed	.01	10	8.305	.08	4.68	13.5
S recorded at Δ>5°, adjustments not computed	.01	13	11.322	.06	4.68	15.7
L_g recorded in 3°<Δ<5°, adjustments computed	.1	19	5.505	.12	3.67	8.6
L_g recorded in Δ>5°, adjustments not computed	.01	12	24.993	.03	3.67	18.3

Extreme residuals were weighted out by the method of uniform reduction (Jeffreys, 1948, p. 191) under the assumption that the statistical population of any particular phase type, when free of gross errors, would be a normal distribution, with variance as given in table 3.

Each recomputed hypocenter has associated with it a 90-percent-confidence ellipsoid on the hypocentral coordinates. These ellipsoids are three-dimensional analogues to the 90-percent-confidence ellipses on epicentral coordinates discussed by Flinn (1965) and Evernden (1969). If the assumptions about the Earth used in JED are valid, and if statistical assumptions used in constructing the ellipsoid are valid, then 90 percent of the ellipsoids in table 2, when centered on the computed hypocenters, will cover the true hypocenters.

However, tests of the hypocenter-determination method on seismic events in eastern North America whose locations are known independently of traveltime data seem to indicate that the various assumptions used in computing hypocenters and constructing the confidence ellipsoids are not strictly valid. For eastern North America as a whole, approximately 70 percent of the nominally 90-percent-confidence ellipsoids cover the independently known hypocenters (Dewey and D. W. Gordon, unpub. data, 1980). In places elsewhere in eastern North America in which the confidence ellipsoid does not cover the independently known hypocenter, the computed hypocenters are generally mislocated in the direction of the longest axis of the confidence ellipsoid but are just outside the confidence ellipsoid.

RESULTS OF RELOCATING EARTHQUAKES IN THE SOUTH CAROLINA COASTAL PLAIN

The most important result of relocating hypocenters in South Carolina and vicinity is that the nine regionally or teleseismically recorded shocks from within 100 km of Charleston (eight of them before 1974) have been determined to have occurred at or within tens of kilometers of two source regions identified from microearthquakes recorded since 1974—the Bowman cluster and the Middleton Place–Summerville seismic zone (fig. 2). The confidence ellipsoid of the shock of 1967.10.23 is also consistent with that shock having occurred in the Adams Run cluster identified by Tarr and Rhea (1983). The concentration of pre-1974 epicenters near the source regions identified from microearthquakes is significantly different from that suggested by previously accepted epicenters of these earthquakes (fig. 1), which implied seismically active structures offshore from Charleston.

One cannot rule out the possibility of major shocks elsewhere in the South Carolina Coastal Plain, but recognition of other possible locations for major earthquakes probably depends on understanding why earthquakes occur near Middleton Place, Summerville, and Bowman. The redetermined pre-1974 hypocenters, however, are not well enough located to resolve small clusters of seismicity within the seismically active regions near Middleton Place, Summerville, and Bowman. Similarly these results do not permit us to state that the instrumentally recorded pre-1974 earthquakes originated from precisely the source regions outlined by microearthquake activity since 1974. In fact some of the relocated hypocenters, such as 1967.10.23, are outside the source regions outlined by microearthquake activity, but their confidence ellipsoids extend to the active regions.

The computed focal depths for eight of the nine earthquakes in the South Carolina Coastal Plain are in the upper crust. The focal depths are not well enough determined, however, that the hypocenters can be confidently placed with respect to the décollement surface postulated by Behrendt and others (1983) at a depth of about 11 km. The inaccuracy of the focal-depth determinations is due to noise, from various sources, in the arrival-time data, which is reflected in the size of the confidence ellipsoids, and to possible bias introduced by fixing focal depths to 5 km at the first stage of the location procedure (see section entitled "Location procedure"). Bias in focal-depth determination is not reflected in the size of the confidence ellipsoids.

RESERVOIR-INDUCED SEISMICITY

Several of the regionally or teleseismically recorded earthquakes of the Piedmont of South Carolina and Georgia took place near artificial lakes (fig. 2). Long (1974) and Talwani and others (1975) have postulated the association of earthquakes with the Clark Hill Reservoir, which was impounded in 1952. This reservoir was the site of two of the regionally recorded shocks (1974.08.02 and 1964.03.07), and Long (1974) has suggested that other shocks recorded at the seismographic station ATL originated from the region of the reservoir. We cannot conclude from the relocated hypocenters whether these shocks all originated from a single small source region defined by the aftershocks of 1974.08.02 (Talwani and others, 1975) or whether they took place at more than one location around Clark Hill Reservoir. The confidence ellipsoid of the poorly located earthquake of 1964.03.07 indicates that it might have originated at the same small source as that of 1974.08.02. The epicenter computed for 1964.03.07 by Jones and others (1977), who also used original data, is quite close to the epicenter of 1974.08.02. Long (1974) has noted that the general region of Clark Hill Reservoir had an intensity-VI shock in 1875, before the reservoir was built.

Talwani (1977) has made a strong case for the association of the earthquake of 1975.11.25 with the filling of

Lake Jocassee. Again, however, the vicinity of the earthquake-triggering reservoir had had an earthquake before the construction of the reservoir; the shock of 1969.12.13 took place a short distance northeast of the site of Lake Jocassee before the lake's impoundment. Talwani and others (1979) have suggested that 1969.12.13 may have occurred at Lake Keowee, another impoundment. However, the confidence ellipsoid of 1969.12.13 does not cover Lake Keowee, and the ellipsoid is not within 20 km of the source region identified by Talwani and others for earthquakes in early 1978 at Lake Keowee (fig. 2). The revised hypocenters of both 1975.11.25 and 1969.12.13 were not determined by using the traveltime tables and station adjustments used for the rest of South Carolina. Instead, they were determined jointly with hypocenters from Tennessee, North Carolina, Virginia, West Virginia, and Kentucky, by using a velocity model having a 45-km-thick crust that is more appropriate to the Appalachian Mountain region.

Three teleseismically or regionally recorded earthquakes took place in the region of Lake Murray, which was impounded in 1930. The largest shock was that of 1945.07.26, which was assigned by Coffman and von Hake (1973) to Lake Murray; however, the epicentral coordinates they listed are well north of the lake. The redetermined epicenter of 1945.07.26 is significantly south of the lake. As in the regions of Clark Hill Reservoir and Lake Jocassee, an earthquake (May 20, 1853) had been reported for the Lake Murray region before construction of the reservoir (Bollinger and Visvanathan, 1977).

One teleseismically recorded earthquake (1964.03.13) occurred in the region of Lake Sinclair in the Georgia Piedmont. Lake Sinclair was impounded in 1953.

CONCLUSIONS

The main result of this study is that earthquakes whose epicenters were formerly assigned to the region seaward of Charleston, S. C., are relocated to the region near the Middleton Place–Summerville seismic zone, defined since 1974 by the South Carolina network (Tarr, 1977; Tarr and Rhea, 1983). The new hypocenters of all nine regionally recorded shocks in the South Carolina Coastal Plain are consistent with locations in either the Middleton Place–Summerville zone, the Bowman cluster, or the Adams Run cluster, as defined by the microearthquake epicenters determined through 1978 and reported by Tarr and Rhea (1983). Quite possibly, however, future recording by the South Carolina network will identify sources of microearthquakes beyond the boundaries of the presently identified regions. In addition, other geologic or geophysical studies may reveal possible seismogenic structures outside those boundaries. To test whether some of the pre-1974 instrumentally recorded earthquakes could have occurred on a particular structure outside the principal post-1974 microearthquake source regions, the position of the structure can be plotted on figure 2. If the structure is within the projection of the confidence ellipsoid of an earthquake, the instrumentally measured traveltimes for that earthquake, besides being consistent with the earthquake source being at Middleton Place or Bowman, are also consistent with the source being on the alternate structure.

Of eight shocks in or immediately adjacent to the Piedmont of South Carolina and northeast Georgia, six might be postulated to have been triggered by artificial lakes. The 90-percent-confidence ellipsoids of their hypocenters indicate that these six earthquakes could have taken place beneath artificial lakes and that the earthquakes took place after impoundment of the nearby reservoirs. The other two earthquakes were in the general vicinity of preexisting impoundments, but their hypocenters and confidence ellipsoids indicate that they did not occur directly beneath the lakes.

REFERENCES CITED

Amick, David, 1979, Crustal structure studies in South Carolina coastal plain: Columbia, University of South Carolina, M.S. thesis, 81 p.

Behrendt, J. C., Hamilton, R. M., Ackermann, H. D., Henry, V. J., and Bayer, K. C., 1983, Marine multichannel seismic-reflection evidence for Cenozoic faulting and deep crustal structure near Charleston, South Carolina, *in* Gohn, G. S., ed., Studies related to the Charleston, South Carolina, earthquake of 1886–Tectonics and seismicity: U.S. Geological Survey Professional Paper 1313, p. J1–J29.

Bollinger, G. A., 1970, Travel-time study of six central Appalachian earthquakes 1962–1968: Seismological Society of America Bulletin, v. 60, no. 2, p. 629–637.

———1972, Historical and recent seismic activity in South Carolina: Seismological Society of America Bulletin, v. 62, no. 3, p. 851–864.

———1979, Attenuation of the Lg phase and the determination of m_b in the southeastern United States: Seismological Society of America Bulletin, v. 69, no. 1, p. 45–63.

Bollinger, G. A., and Visvanathan, T. R., 1977, The seismicity of South Carolina prior to 1886, *in* Rankin, D. W., ed., Studies related to the Charleston, South Carolina, earthquake of 1886–A preliminary report: U.S. Geological Survey Professional Paper 1028, p. 33–42.

Coffman, J. L., and von Hake, C. A., eds., 1973, Earthquake history of the United States: U.S. Department of Commerce Publication 41-1 (revised ed., through 1970), 208 p.

Dewey, J. W., 1971, Seismicity studies with the method of joint hypocenter determination: Berkeley, University of California, Ph.D. dissertation, 164 p.

———1976, Use of secondary P-waves, S-waves, and surface waves in joint hypocenter determination [abs.]: Earthquake Notes, v. 47, no. 2, p. 11.

———1978, Joint hypocenter determination using calibration stations–application to eastern North America [abs.]: Earthquake Notes, v. 49, no. 1, p. 35.

Evernden, J. F., 1969, Precision of epicenters obtained by small numbers of world-wide stations: Seismological Society of America Bulletin, v. 59, p. 1365–1398.

Flinn, E. A., 1965, Confidence regions and error determinations for seismic event location: Reviews of Geophysics, v. 3, no. 1, p. 157–185.

Green, R. W. E., and Hales, A. L., 1968, The travel time of *P* waves to 30° in the central United States and upper mantle structure: Seismological Society of America Bulletin, v. 58, no. 1, p. 267–289.

Hart, R. S., Anderson, D. L., and Kanamori, H., 1977, The effect of attenuation on gross earth models: Journal of Geophysical Research, v. 82, no. 11, p. 1647–1654.

Healy, J. H., and Warren, D. H., 1969, Explosion seismic studies in North America: American Geophysical Union Geophysical Monograph 13, p. 208–220.

Jeffreys, Harold, 1948, Theory of probability (2d ed): Oxford, Clarendon Press, 411 p.

Jeffreys, Harold, and Bullen, K. E., 1958, Seismological tables: London, British Association for the Advancement of Science, 50 p.

Jones, F. B., Long, L. T., and McKee, J. H., 1977, Study of the attenuation and azimuthal dependence of seismic-wave propagation in the southeastern United States: Seismological Society of America Bulletin, v. 67, no. 6, p. 1503–1513.

Julian, B. R., 1970, Regional variations in upper mantle structure beneath North America: Pasadena, California Institute of Technology, Ph.D. dissertation, 216 p.

Lewis, B. T. R., and Meyer, R. P., 1968, A seismic investigation of the upper mantle to the west of Lake Superior: Seismological Society of America Bulletin, v. 58, no. 2, p. 565–596.

———1977, Upper mantle velocities under the east coast margin of the U.S.: Geophysical Research Letters, v. 4, no. 8, p. 341–344.

Long, L. T., 1974, Earthquake sequences and b values in the southeast United States: Seismological Society of America Bulletin, v. 64, no. 1, p. 267–273.

Massé, R. P., 1973, Compressional velocity distribution beneath central and eastern North America: Seismological Society of America Bulletin, v. 63, no. 3, p. 911–935.

Nuttli, O. W., Stauder, William, and Kisslinger, Carl, 1969, Travel-time tables for earthquakes in the central United States: Earthquake Notes, v. 40, no. 4, p. 19–28.

Nuttli, O. W., and Zollweg, J. E., 1974, The relation between felt area and magnitude for central United States earthquakes: Seismological Society of America Bulletin, v. 64, no. 1, p. 73–85.

Pakiser, L. C., 1963, Structure of the crust and upper mantle in the western United States: Journal of Geophysical Research, v. 68, no. 20, p. 5747–5756.

Talwani, Pradeep, 1977, Stress distribution near Lake Jocassee, South Carolina: Pure and Applied Geophysics, v. 115, p. 275–281.

Talwani, Pradeep, Secor, D. T., and Scheffler, P., 1975, Preliminary results of aftershock studies following the 2 August 1974 South Carolina earthquake: Earthquake Notes, v. 46, no. 4, p. 21–28.

Talwani, Pradeep, Stevenson, Don, Amick, David, and Chiang, J., 1979, An earthquake swarm at Lake Keowee, South Carolina: Seismological Society of America Bulletin, v. 69, no. 3, p. 825–841.

Tarr, A. C., 1977, Recent seismicity near Charleston, South Carolina, and its relationship to the August 31, 1886, earthquake, *in* Rankin, D. W., ed., Studies related to the Charleston, South Carolina, earthquake of 1886 – A preliminary report: U.S. Geological Survey Professional Paper 1028, p. 43–57.

Tarr, A. C., and Rhea, Susan, 1983, Seismicity near Charleston, South Carolina, March 1973 to December 1979, *in* Gohn, G. S., ed., Studies related to the Charleston, South Carolina, earthquake of 1886 – Tectonics and seismicity: U.S. Geological Survey Professional Paper 1313, p. R1–R17.

Seismicity Near Charleston, South Carolina, March 1973 to December 1979

By ARTHUR C. TARR and SUSAN RHEA

STUDIES RELATED TO THE CHARLESTON, SOUTH CAROLINA, EARTHQUAKE OF 1886—TECTONICS AND SEISMICITY

GEOLOGICAL SURVEY PROFESSIONAL PAPER 1313-R

UNITED STATES GOVERNMENT PRINTING OFFICE, WASHINGTON: 1983

CONTENTS

ILLUSTRATIONS

TABLES

STUDIES RELATED TO THE CHARLESTON, SOUTH CAROLINA, EARTHQUAKE OF 1886—
TECTONICS AND SEISMICITY

SEISMICITY NEAR CHARLESTON, SOUTH CAROLINA, MARCH 1973 TO DECEMBER 1979

By ARTHUR C. TARR and SUSAN RHEA

ABSTRACT

Newly completed seismological studies provide additional insight into the source area of the Charleston, S. C., earthquake of August 31, 1886, its relationship to other seismically active areas nearby, and differences between the patterns of Charleston-area activity and seismicity in the Piedmont province of South Carolina. These studies include refinements to the South Carolina earthquake catalog, relocation of earthquakes recorded instrumentally before installation of the South Carolina seismic network, improved hypocenter determinations from 7 years (1973–79) of seismic-network data, and composite focal mechanisms.

We suggest that current activity in the Middleton Place–Summerville seismic zone is in the fault zone of the August 31, 1886, main shock. The newly determined hypocenters define a three-segmented seismic zone composed of two en-echelon segments that strike northwest and dip about 80° to 90° southwest and a third segment that strikes east-northeast. A composite focal mechanism of 16 earthquakes suggests reverse dip-slip motion, on a northwesterly trending plane, in response to a generally northeasterly trending greatest principal compressive stress.

Two other important clusters of epicenters were located instrumentally near Bowman and Adams Run. They are spatially distinct from the Middleton Place–Summerville seismic zone. No earthquakes have been located in the gap between the Bowman cluster and the Middleton Place–Summerville zone in the 9 years since the Bowman cluster became active in 1971.

All three active areas near Charleston are on the flanks of positive gravity and aeromagnetic anomalies from which others have inferred the presence of relatively dense magnetic bodies that are probably mafic or ultramafic intrusives. In broad areas of flat or negative gravity and aeromagnetic anomalies, seismicity seems to be lacking. Positive traveltime anomalies suggest that these broad areas may be deep basins filled with low-velocity sediments.

Although earthquakes in the Piedmont tend to be scattered, those in the Coastal Plain tend to cluster. We interpret this clustering pattern to result from many localized stressed regions on or near intersecting faults or in zones of weakness between blocklike crustal units, originating from early Mesozoic tectonic processes. We postulate that the broad, flat gravity and magnetic lows between Bowman and Summerville may be aseismic either because no major crustal fractures or zones of weakness cross this area or because strain is being released aseismically.

INTRODUCTION

In March 1973, an earthquake-monitoring program was initiated in South Carolina to determine the characteristics of contemporary seismicity near Charleston and to relate it to the destructive earthquake of August 31, 1886 (Tarr and King, 1974). Preliminary results of analyses of seismic network data recorded between March 1973 and December 1975 were reported by Tarr (1977) in a collection of seismological, geological, and geophysical papers related to the Charleston earthquake of 1886 (Rankin, 1977).

This study reports on results of analyses of four additional years of South Carolina seismic data, as well as a reevaluation of the earlier data and refinements to the South Carolina earthquake catalog.

Support for this study was provided by the Nuclear Regulatory Commission, Office of Nuclear Research, under Agreement No. AT(49–25)–1000.

SUMMARY OF RESULTS

Three topical studies, completed after the work reported by Tarr (1977), contributed significantly to the improved understanding of the seismicity of South Carolina near Charleston. These studies were: (1) An improved catalog of earthquakes that occurred prior to the installation of the South Carolina seismic network; (2) seismograph station corrections accurately determined from the analysis of numerous high-quality network data from 1976 through 1979; and (3) determination of composite focal-mechanism solutions for well-located earthquakes in the Middleton Place–Summerville seismic zone. The catalog was refined with the addition of newly discovered historical shocks (Bollinger and Visvanathan, 1977), the relocation of instrumentally recorded earthquakes (Dewey, 1983), and the correction of errors discovered in older catalogs. The station cor-

rections permitted adjustment for lateral variability of crustal velocity near Charleston and resulted in more precise hypocenter determinations for small-magnitude earthquakes, including all the published events of 1973–75.

The seismological studies reported by Dewey (1983), Bollinger (1983), and in this paper convey a remarkably consistent picture of the seismicity of South Carolina, especially near Charleston (fig. 1). The seismic activity in the Coastal Plain tends to occur in clusters, whereas a more diffuse, scattered pattern seems to be characteristic of Piedmont earthquakes. The most significant concentration of Coastal Plain earthquakes is the Middleton Place–Summerville zone, which may define the fault zone of the 1886 earthquake and represent the latter stages of a rather long aftershock sequence. Furthermore, the size and orientation of the zone are sufficient to explain the intensity pattern of the 1886 shock and to estimate values of source parameters. Quite reasonable values of stress drop (100 bars) and seismic slip (1 m) (Bollinger, 1983) are consistent with these source dimensions. Finally, a composite focal mechanism for the larger earthquakes in the zone indicates vertical faulting in reponse to generally northeast-trending regional maximum compressive stress.

The clustering pattern of epicenters in the South Carolina Coastal Plain may require modification of the hypothesis that the seismicity occurs along an old but unhealed zone of crustal weakness (Sbar and Sykes, 1973; Sykes, 1978). The persistence of seismic activity in spatially limited clusters, the absence of activity between clusters, and the diffuse pattern of seismicity in the Piedmont argues against a continuous, northwest-trending active fault or fault zone crossing South Carolina from the continental margin to the Appalachians.

If the recent seismicity is assumed to be closely related to the historic seismicity of South Carolina, all geological models that seek to explain the Charleston earthquake of August 31, 1886, must also account for the spatial and temporal characteristics of the contemporary earthquake activity.

REVISED SOUTH CAROLINA EARTHQUAKE CATALOG

Most of the essential information about the long seismic history of South Carolina (1698–1979) is con-

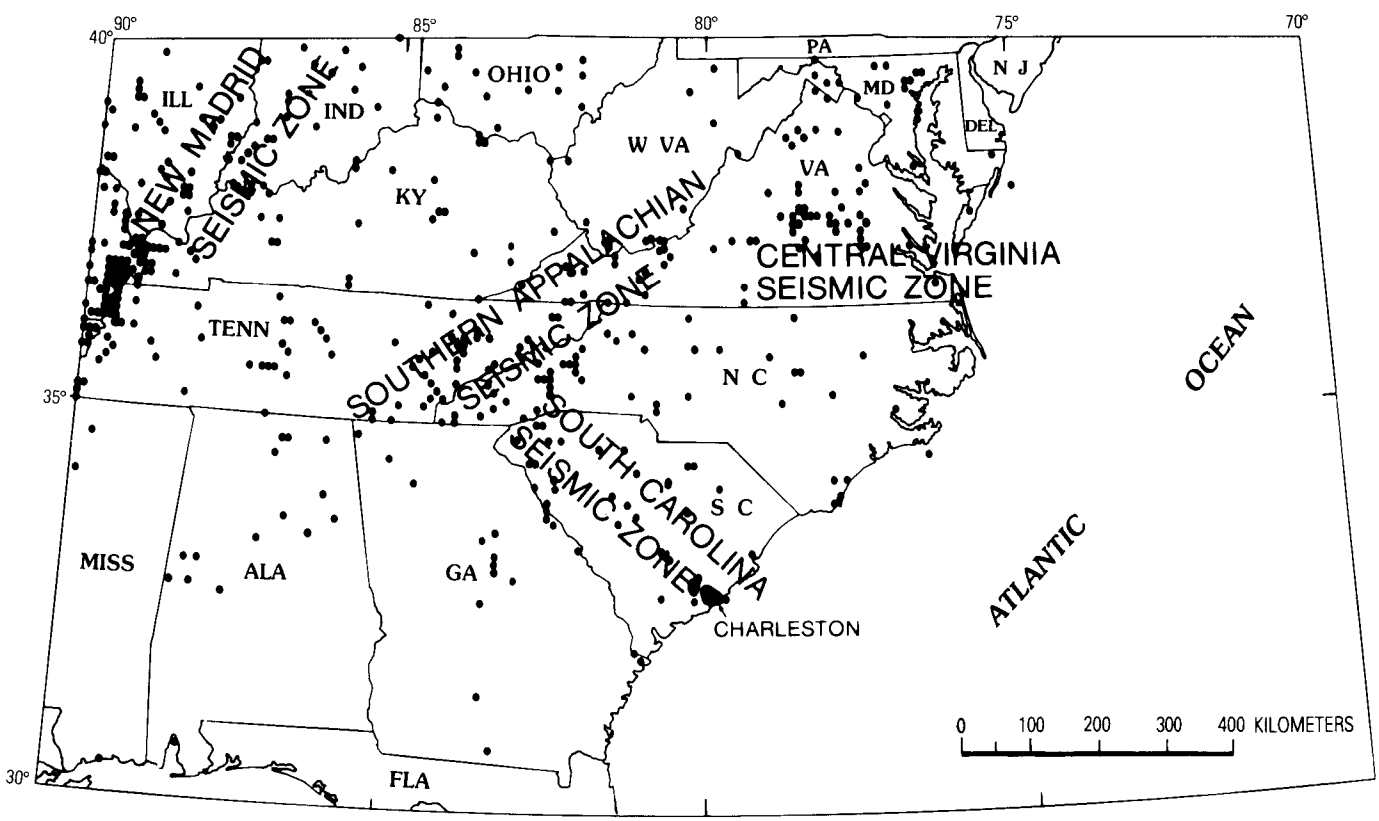

FIGURE 1.—Seismicity of Southeastern United States, 1698–1979. Epicenters are plotted without regard to magnitude or intensity.

tained within its earthquake catalog. The catalog forms the foundation upon which research studies (Bollinger, 1972; Tarr, 1977; Tarr and others, 1981) have been based, and any improvement in the contents of the catalog should result in more sound conclusions from later studies.

The catalog and seismicity map used by Tarr (1977) in his discussion of recent seismicity near Charleston covered the time interval 1754 through 1975. An improved and updated catalog and seismicity map, covering the interval 1698 through 1979, have been compiled for this report. The catalog contains newly discovered and reevaluated shocks (Bollinger and Visvanathan, 1977), results from seismic networks operating in the Southeastern United States (Bollinger and Murphy, 1978; Bollinger and Mathena, 1978, 1979), and revisions and corrections to older catalogs.

In addition, the new catalog contains the results of relocation by the joint-epicenter-determination (JED) method (Dewey, 1972, 1983) of 3 Georgia, 1 North Carolina, and 10 South Carolina earthquakes that occurred before the installation of the South Carolina seismic network. The magnitudes of these shocks were large enough to be recorded well at regional and teleseismic distances. Thus, these events are important because they are generally located more accurately than any epicenters inferred from intensity data alone. Furthermore, associated with each relocated hypocenter are reliable estimates of the precision of each determination, quantities which are not usually available in older catalogs.

The hypocenters near Charleston from the data of the South Carolina seismic network (Tarr and others, 1981) are the most precise and accurate hypocenters in the catalog (table 1). Tarr (1977) has reported on the localization of two seismic sources, a zone between Middleton Place and Summerville and a zone near the town of Bowman, on the basis of the preliminary location of earthquakes recorded by the network between 1973 and 1975. Refined hypocenters of these earthquakes and other events recorded by an expanded seismic network between 1976 and 1979 (Tarr and others, 1981) constitute a much-improved data set for the South Carolina earthquake catalog. In addition, the new catalog contains the estimated uncertainties associated with these hypocenter determinations.

SOUTH CAROLINA SEISMIC NETWORK

A set of preliminary hypocenters, determined from the seismic data recorded by a temporary reconnaissance network (March 1973 through December 1973) and a ten-station permanent network (May 1974 through December 1975), defined the Middleton Place–Summerville seismic zone reported by Tarr (1977). Several earthquakes located near Bowman were presumed to be associated with the seismic activity that had begun in 1971 (Bollinger, 1972) and continued into 1973 (Long, 1972; McKee, 1973). The need to locate earthquakes more precisely in these two areas led to the relocation of three stations and the expansion of the USGS (U.S. Geological Survey) network to its 21-station configuration (fig. 2). The most significant network changes were the installations of a six-station subnetwork centered at Middleton Place and a four-station subnetwork near Bowman.

The capability to detect small-magnitude earthquakes in South Carolina and to locate them accurately improved greatly between 1970 and 1979. This was a direct consequence of the establishment of the USGS South Carolina seismic network and the availability of data from stations deployed in adjacent areas by the University of South Carolina, Savannah River Plant, Georgia Institute of Technology, and several electric power companies.

Assuming that data from the South Carolina network and all the other regional stations were available, we calculated five-station threshold magnitudes for *P*-waves and 90-percent confidence ellipses for hypothetical earthquakes evenly distributed in a grid over South Carolina and parts of adjacent States. The detection-threshold magnitudes and confidence ellipses for Middleton Place and Bowman are summarized for three dates between January 1, 1970, and December 31, 1979, in table 2, and are drawn for the entire State in figures 3 and 4. We conclude from figure 4 that on December 31, 1979, five or more stations would have detected (at a 90-percent confidence level) an earthquake of body-wave magnitude (m_b) 2.7 anywhere in South Carolina.

HYPOCENTER DETERMINATION

Hypocenters determined by the HYPOELLIPSE computer program (Lahr, 1979) are summarized in table 1 and included on figure 5, which shows seismicity for the seven-year interval January 1, 1973, through December 31, 1979. Figure 6 shows the epicenters and associated confidence ellipses in the Charleston area for the same time interval, and figures 7 and 8 show the seismicity superimposed on a map of gravity and aeromagnetic anomalies.

The crustal velocity model (table 3) used in the hypocenter programs was a modification of one determined by Talwani (1977a) and Amick (1979) from seismic-refraction data recorded from explosions in quarries and from shots in drill holes. The refraction lines included several reversed profiles that crossed the Middleton Place–Summerville seismic zone. The resultant model should be a substantial improvement over

TABLE 1.—*Catalog of South Carolina earthquakes, 1973–79*

[UTC, Coordinated Universal Time; negative latitudes and longitudes are south and west, respectively; M, coda length magnitude; *a*, *b*, and *c*, principal semi-axes of confidence ellipsoid; Tr, trend of semi-axis in degrees; Pl, plunge of semi-axis in degrees; Percent, confidence level; Rms, root mean square of residuals; No. ob, number of observations used in hypocenter computation; Gap, largest azimuthal separation between seismograph stations; DM, distance to third nearest station, in kilometers; Q, quality index; E, after origin time, designates known or suspected explosion; leaders (. . . .) designate instances when data values are unknown or not computed]

Catalog		Origin time (UTC)						North latitude (deg)	East longitude (deg)	Focal depth (km)	M	Error ellipsoid axes										Rms	No.			
Name	Index	yr	mo	d	h	min	s					*a* (km)	Tr	Pl	*b* (km)	Tr	Pl	*c* (km)	Tr	Pl	Percent	(*s*)	ob	Gap	DM	Q[1]
Reconnaissance study earthquakes																										
MIDSC	1	1973	3	25	4	29	32.870	32.989	−80.105	5.0	. . .	2.8	229	2	8.9	320	13	>99.9	130	76	68	. . .	3	241	44	D
	2	1973	4	23	21	32	39.300	33.004	−80.239	5.9	. . .	1.9	55	1	5.0	325	10	32.3	151	79	68	. . .	4	197	33	D
	3	1973	6	9	19	23	50.570	33.103	−80.434	15.0	. . .	18.1	254	0	53.6	344	8	>99.9	163	82	68	1.72	6	189	40	D
	4	1973	6	12	20	45	22.530	33.283	−80.417	5.0	. . .	2.1	259	3	8.1	349	3	>99.9	123	85	68	.68	4	239	54	D
	5	1973	8	25	9	17	30.910	32.950	−80.189	1.3	. . .	2.0	239	0	4.1	329	4	>99.9	148	86	68	.10	5	156	30	D
	6	1973	11	13	15	10	3.420	32.923	−80.189	.7	1.4	2.2	237	0	7.5	326	33	12.6	146	56	68	.11	5	248	42	D
	7	1973	12	19	10	16	18.460	32.997	−80.267	12.4	. . .	2.2	57	3	4.8	326	18	17.6	157	71	68	. . .	4	191	32	D
Middleton Place—Summerville earthquakes																										
	8	1974	7	7	4	3	36.640	33.004	−80.223	3.7	.9	1.9	73	6	3.9	342	7	90.1	203	80	68	.04	4	162	44	D
	9	1974	11	22	5	25	56.240	32.921	−80.144	7.6	3.8	1.0	258	1	2.0	348	11	2.9	162	78	68	.13	10	202	41	B
	10	1974	11	22	6	22	44.440	32.892	−80.145	9.6	2.7	.6	87	5	2.0	355	21	6.0	189	68	68	.09	9	208	44	C
	11	1975	4	28	5	46	52.630	33.002	−80.216	10.2	3.1	.8	251	0	1.1	341	8	2.0	160	82	68	.10	10	163	35	A
	12	1976	4	6	21	42	35.910	33.307	−79.728	8.4	2.2	1.2	332	19	3.1	74	32	6.2	217	51	68	.18	11	223	74	C
	13	1976	4	28	6	15	54.110	33.751	−81.668	.3	1.8	.8	92	3	1.1	182	3	4.5	317	85	68	.21	14	105	70	B
	14	1976	7	3	9	28	42.550	32.994	−80.241	13.7	1.1	.7	64	11	1.2	331	13	2.2	192	72	68	.05	6	163	34	A
	15	1976	8	28	23	15	39.560	33.095	−80.182	2.5	.6	3.2	77	2	7.1	347	2	>99.9	211	87	68	. . .	4	164	40	D
	16	1976	9	15	5	15	35.440	33.144	−81.413	4.5	2.4	1.2	323	5	2.7	232	7	4.9	89	81	68	.35	17	189	70	B
	17	1976	11	14	21	12	12.010	32.961	−80.188	4.4	1.2	.8	279	6	1.1	10	11	5.3	160	77	68	.16	12	123	17	C
	18	1977	1	18	18	29	14.220	33.042	−80.214	7.0	2.7	.8	52	29	.4	304	30	1.6	178	46	68	.09	17	136	17	A
	19	1977	1	20	4	5	45.750	32.928	−80.163	6.6	1.9	.6	239	16	.7	335	21	1.6	114	63	68	.15	19	94	10	A
	20	1977	2	26	10	9	56.140	32.923	−80.178	4.9	1.6	.3	21	7	.2	290	8	.6	152	79	68	.05	13	103	12	A
	21	1977	3	18	7	36	8.630	32.934	−80.175	4.2	1.2	.4	268	1	.6	359	7	1.4	169	82	68	.07	9	122	11	A
	22	1977	3	30	8	27	47.780	32.952	−80.184	7.9	2.9	.6	298	18	.8	34	18	1.5	166	64	68	.12	16	91	11	A
	23	1977	5	31	23	50	13.400	32.942	−80.226	12.1	2.5	1.2	300	13	1.7	35	22	4.2	182	64	68	.18	11	89	14	B
	24	1977	6	5	00	42	29.730	33.052	−81.412	3.5	2.7	1.0	121	1	3.7	211	27	2.9	29	62	68	.22	15	213	76	B
	25	1977	6	22	20	43	40.060	32.995	−80.155	1.3	2.1	1.1	293	3	1.3	24	4	15.0	166	84	68	.17	10	123	11	D
	26	1977	8	23	13	45	.030	32.938	−80.163	7.6	2.3	.7	29	5	.5	296	27	1.4	129	62	68	.07	11	104	10	A
	27	1977	12	15	7	15	55.160	32.983	−80.264	13.1	2.0	1.0	25	6	.6	294	14	2.0	138	74	68	.14	17	106	15	A
	28	1977	12	15	19	16	43.630	32.944	−80.167	7.5	2.6	.7	27	12	.5	294	16	1.6	153	69	68	.11	17	85	10	A
	29	1977	12	16	11	14	34.410	32.737	−80.317	8.1	2.1	.8	280	13	1.8	186	18	2.6	45	67	68	.16	25	213	24	A
	30	1977	12	16	11	25	31.800	32.725	−80.318	7.1	2.3	1.4	188	9	.6	275	10	2.6	51	76	68	.15	25	217	25	B
	31	1977	12	18	1	58	37.790	32.739	−80.292	6.6	1.7	2.0	183	9	1.1	275	11	3.3	54	75	68	.14	15	291	23	B
	32	1977	12	20	23	41	23.300	33.064	−80.232	12.0	1.8	1.9	129	5	1.4	220	11	5.3	14	77	68	.14	10	115	18	C
	33	1978	9	7	22	53	22.960	33.063	−80.210	10.0	2.6	.3	313	21	.5	212	25	.8	78	56	68	.12	28	56	16	A
	34	1978	10	30	9	15	6.460	33.045	−80.152	6.8	. . .	.3	159	4	.4	250	10	.9	47	79	68	.06	13	93	16	A
	35	1978	10	30	9	15	13.000	33.045	−80.151	7.3	1.9	.6	186	9	.9	94	10	1.9	317	76	68	.10	10	95	16	A
	36	1978	10	30	9	16	2.780	33.043	−80.154	7.1	. . .	.8	82	6	.5	173	9	1.6	319	79	68	.07	9	96	16	A
	37	1978	10	30	9	16	14.920	33.039	−80.150	3.0	2.4	.7	325	4	1.1	235	6	3.9	89	82	68	.17	13	93	16	B
	38	1978	10	30	10	4	22.000	33.062	−80.187	17.5	1.3	2.9	64	6	4.8	157	24	11.5	321	65	68	. . .	4	153	23	D
	39	1979	1	27	23	55	15.650	33.051	−80.182	6.2	2.8	.9	235	2	.6	325	8	2.3	131	81	68	.14	16	71	13	A
	40	1979	8	11	2	11	56.590	32.989	−80.227	10.4	2.5	.4	317	17	.9	57	30	1.3	202	54	68	.09	14	100	15	A
	41	1979	10	5	23	5	54.740	32.782	−80.281	13.1	2.1	1.5	295	17	3.2	40	40	2.4	188	45	68	.18	13	278	21	B
	42	1979	10	21	7	10	28.650	32.920	−80.186	10.7	1.6	.9	44	4	.5	313	23	2.7	144	66	68	.05	8	154	21	A
	43	1979	12	7	5	43	34.970	33.007	−80.168	4.6	2.9	.3	325	10	.6	233	12	1.5	94	74	68	.12	24	105	11	A
Bowman earthquakes																										
BOWSC	1	1974	5	28	5	1	34.540	33.366	−80.711	5.7	1.7	.4	139	3	1.7	49	5	3.7	259	84	68	.07	8	184	43	B
	2	1976	9	22	8	44	34.680	33.378	−80.703	4.2	1.7	.4	140	2	.9	230	12	6.4	40	77	68	.06	9	132	42	C
	3	1976	9	22	8	52	21.600	33.407	−80.675	1.2	.8	1.8	139	1	11.1	49	1	>99.9	274	88	68	.63	6	164	41	D
	4	1976	9	22	9	14	14.480	33.378	−80.702	.6	1.1	.8	232	0	.2	142	1	8.7	321	88	68	.05	11	110	42	C
	5	1976	9	23	5	40	10.630	33.387	−80.700	9.6	1.1	.8	142	6	5.4	235	24	7.2	38	65	68	.16	9	146	42	C
	6	1976	11	21	13	31	46.800	33.385	−80.696	.1	1.3	.2	315	0	.5	225	2	11.5	45	88	68	.06	9	141	42	D
	7	1976	11	22	00	30	51.750	33.383	−80.709	.9	1.9	.6	321	0	1.1	231	4	32.7	51	86	68	.12	11	166	59	D
	8	1976	11	28	9	38	50.090	33.386	−80.706	3.7	.9	2.8	231	1	.5	140	3	8.6	339	86	68	.08	7	146	43	C
	9	1977	8	25	4	20	7.540	33.369	−80.698	3.4	2.8	2.4	131	3	4.0	221	3	37.5	356	85	68	.37	13	139	42	D
	10	1977	9	1	21	5	32.460	33.408	−80.663	6.2	1.8	1.5	226	3	.4	136	6	4.5	342	83	68	.07	10	159	40	B
	11	1977	11	10	11	25	.090	33.394	−80.685	.3	.8	.6	304	0	1.2	34	2	13.0	214	88	68	.14	10	162	6	D
	12	1979	12	17	17	34	56.970	33.511	−80.647	.0	1.1	2.1	255	0	2.8	345	0	>99.9	90	90	68	.09	6	316	15	D

[1] Quality of hypocenter determination: D, marginal; C, better than marginal; B, good; A, best.

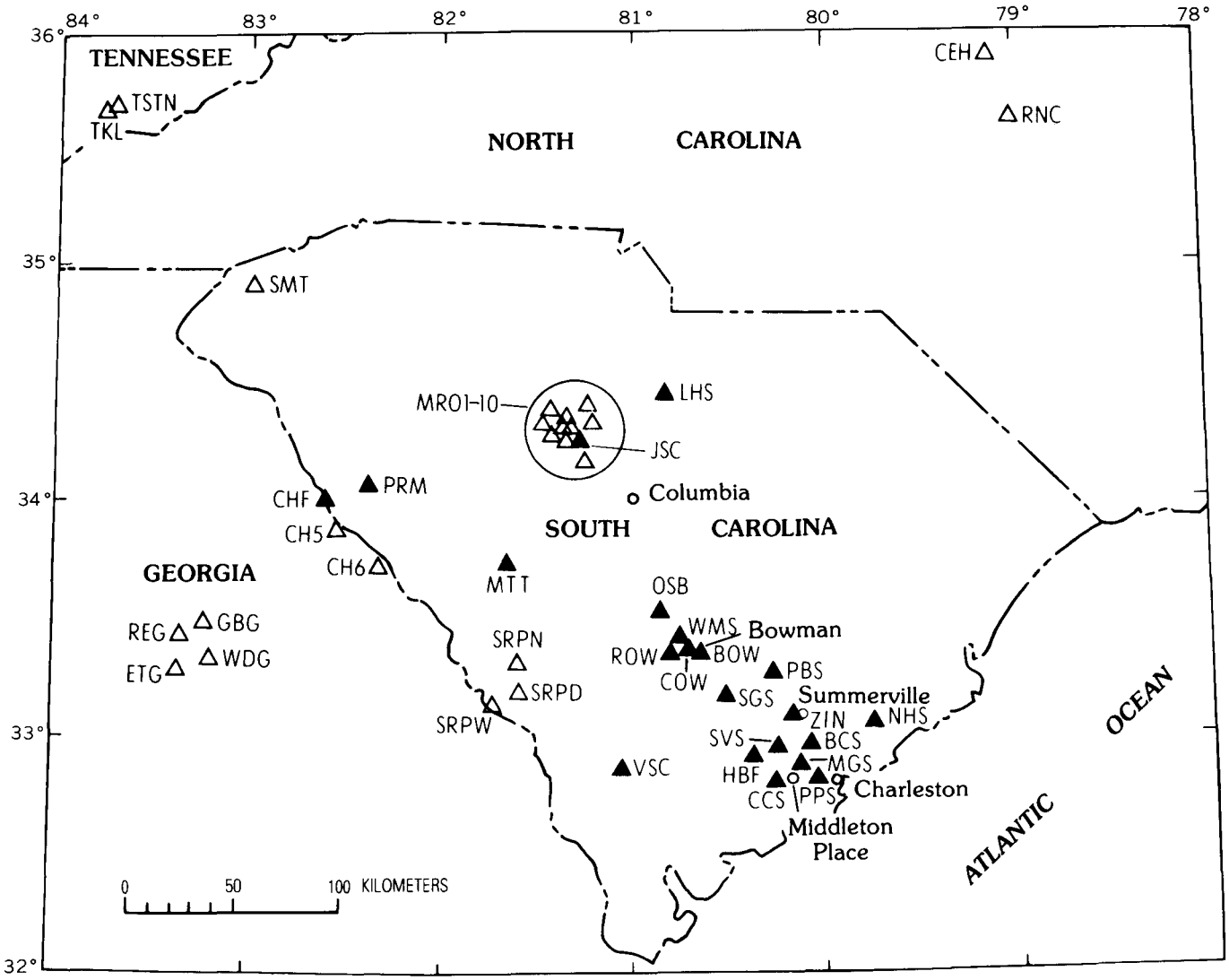

FIGURE 2.—Cooperative network of seismic stations in South Carolina and Georgia, March 1973 through December 1979. Solid triangles designate stations operated by USGS; open triangles designate stations operated by other institutions; letters are abbreviations of station names.

earlier ones and should contribute to improved hypocenter determinations within the zone.

Traveltime adjustments (station delays) were used in the computation of hypocenters to compensate for the departure of actual traveltimes from the traveltimes calculated from the general velocity model. Results from previous geophysical studies (Bonini and Woollard, 1960; Ackermann, 1977, 1983; Popenoe and Zietz, 1977; Phillips, 1977) indicate large lateral variations in physical properties of the upper crust of the study area. Therefore, separate sets of traveltime adjustments were determined for the Middleton Place–Summerville zone and the Bowman cluster (table 4). The traveltime adjustment, δt_{ij}, is the correction added to the traveltime calculated from the model for the ith source area and the jth station. A positive adjustment corresponds to a slow traveltime along the ray path, and a negative adjustment corresponds to a fast traveltime, relative to times computed from the model.

We assume that at a given station the traveltime adjustment is the same for each event in the source zone, even if the zone is extended spatially as it is between Middleton Place and Summerville. This amounts to saying that the average velocity structure is the same along all ray paths from a source area to a given station but is different for all ray paths from another source area to the same station.

We employed an iterative process to determine the δt_{ij}. The initial estimate of δt_{ij} was the mean residual $\bar{r}_{ij}$ taken from the hypocenter computations of a selected

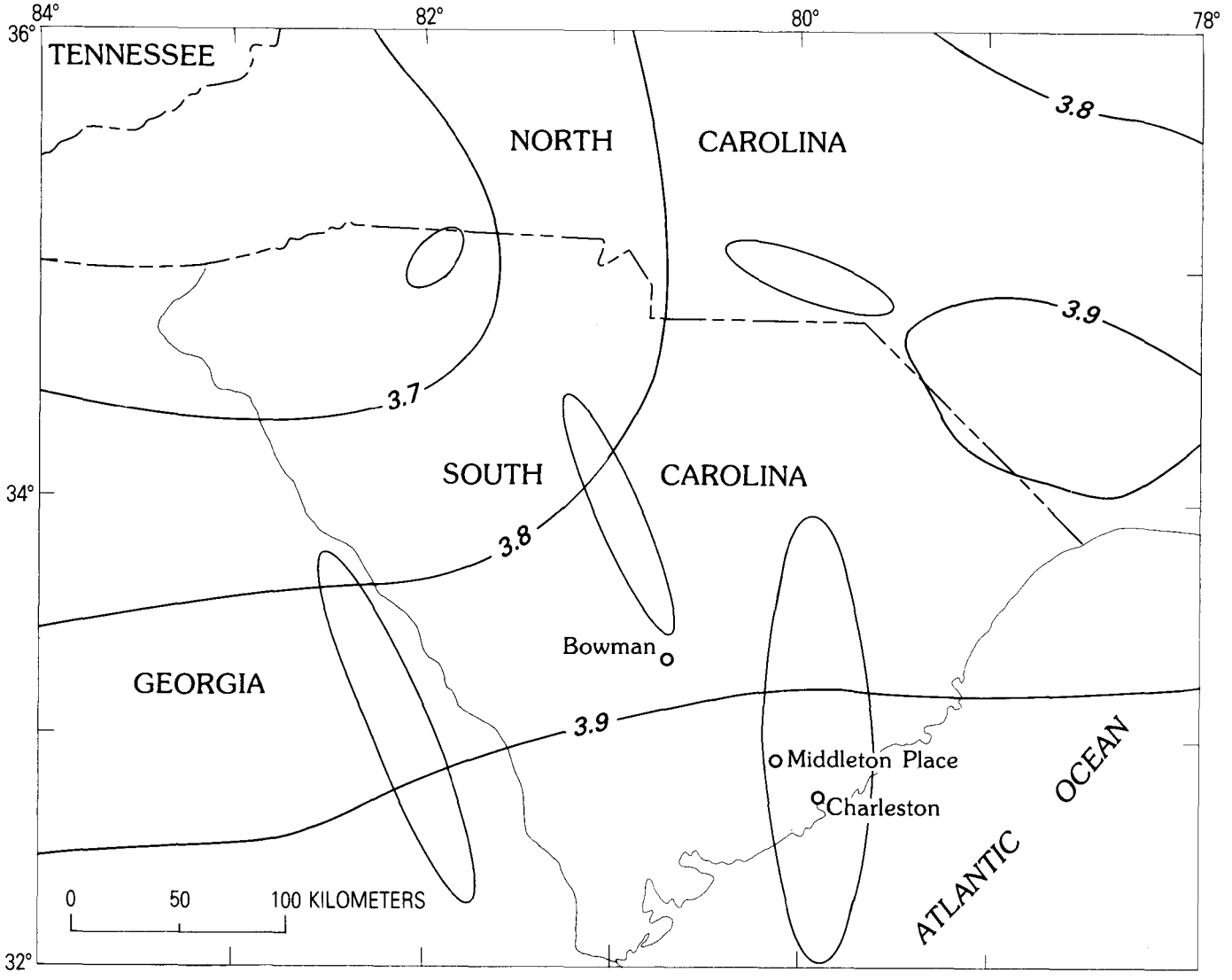

FIGURE 3.—Theoretical detection threshold magnitudes (contours) for five-station detection of *P*-waves and error ellipses in South Carolina on January 1, 1970.

TABLE 2.—*Summary of 90-percent detection threshold magnitudes and associated error ellipses for five-station detections and signal-to-noise ratio of 2.0*

[Mag, magnitude; Az, azimuth, measured clockwise from north; *a* and *b*, semi-major and semi-minor axis lengths, respectively]

	Middleton Place error ellipse					Bowman error ellipse				
Date	Mag	Az (deg)	*a* (km)	*b* (km)	Area (km²)	Mag	Az (deg)	*a* (km)	*b* (km)	Area (km²)
January 1, 1970	3.88	179	90	28	7821	3.84	154	28	23	1997
July 1, 1974	2.63	176	8.3	3.2	84	2.50	43	9.2	2.5	71
December 31, 1979	1.46	40	2.4	1.5	11	1.55	3	2.2	1.2	9

set of well-recorded earthquakes. The hypocenters were redetermined after the δt_{ij} were applied. The resulting $\bar{r}_{ij}$ then were used to adjust the δt_{ij}, and a new computation was performed. We found that only two iterations were required to reduce most of the $\bar{r}_{ij}$ to less than the value of the standard deviation of the mean. We have tabulated the traveltime adjustment, the mean residual for all events, and the corresponding standard deviation in table 4.

The table shows that there are systematic differences between observed traveltimes and theoretical traveltimes computed from the model. Lateral (and possibly even vertical) variations between the actual velocity structure and that of the model are almost certainly the explanation for the relatively large values for some of the δt_{ij}. A large negative or positive adjustment implies a faster or slower *average* velocity, relative to the model, along ray paths connecting source and station. How-

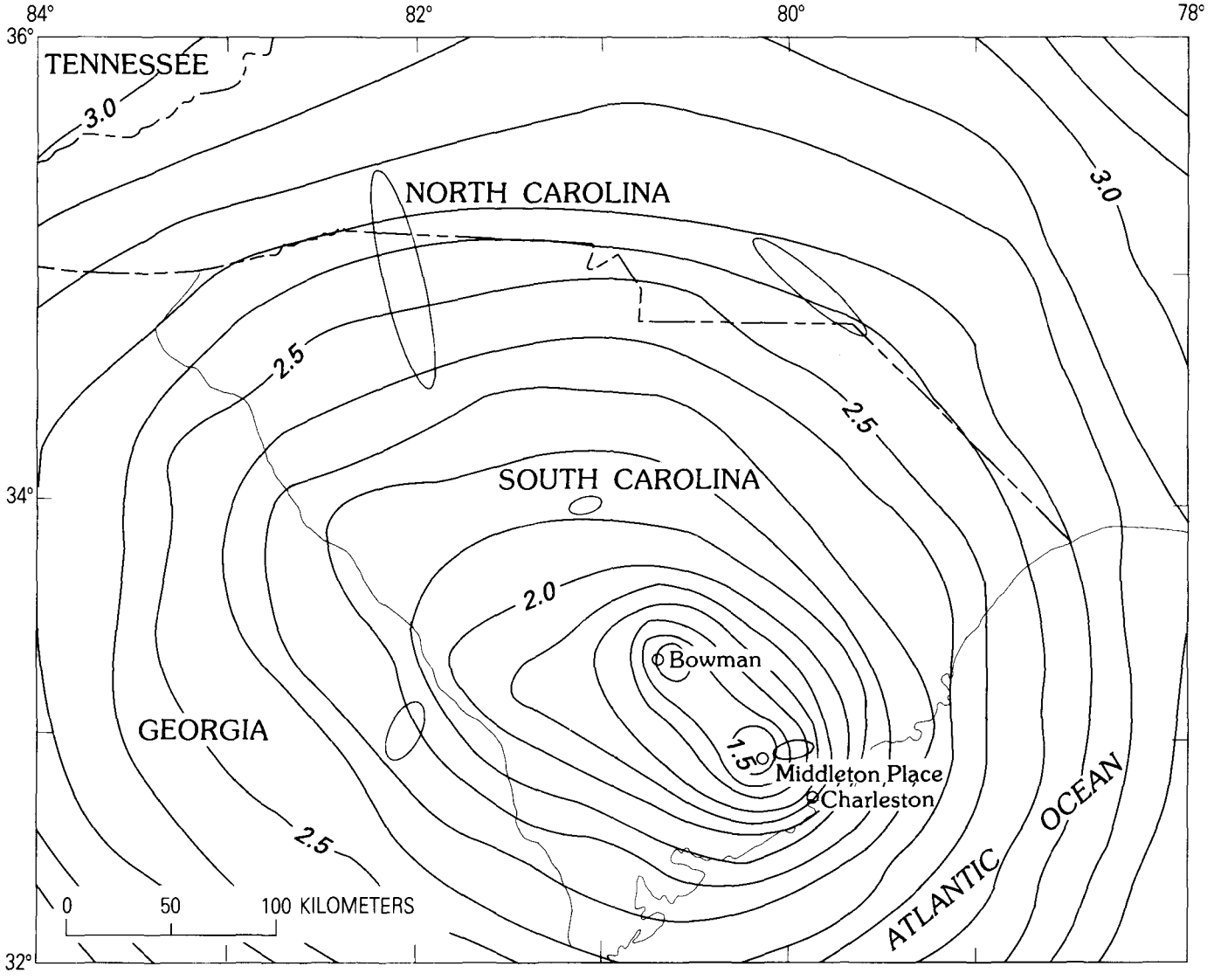

FIGURE 4.—Theoretical detection threshold magnitudes (contours) for five-station detection of *P*-waves and error ellipses in South Carolina on December 31, 1979.

ever, a small adjustment does not necessarily imply the absence of a large anomalous velocity anywhere along the ray path; that is, certain combinations of low- and high-velocity ray-path segments can result in a traveltime close to that predicted by the model.

SOUTH CAROLINA SEISMICITY 1973–79

Middleton Place–Summerville Seismic Zone

The Middleton Place–Summerville seismic zone is an irregular pattern of 29 epicenters, approximately 25–40 km northwest of Charleston. On the basis of 13 preliminary hypocenter determinations, Tarr (1977) had concluded that the zone was nearly vertical and trended approximately northwest-southeast. The distribution of new and relocated hypocenters defined in the present study and the similarity in first-motion patterns indicate that the zone is composed of three groups of epicenters (fig. 9).

Eighteen well-located earthquakes were divided into the Middleton Place (I), Summerville (II), and Slandsville (III) groups, named for the town nearest each association. Within each group, the individual first-motion patterns were similar, except for two earthquakes that had inexplicably scattered first motions; these two earthquakes were not used in the composite focal-mechanism solutions. The composite focal-mechanism solutions are shown in figure 10, and the parameters are summarized in table 5.

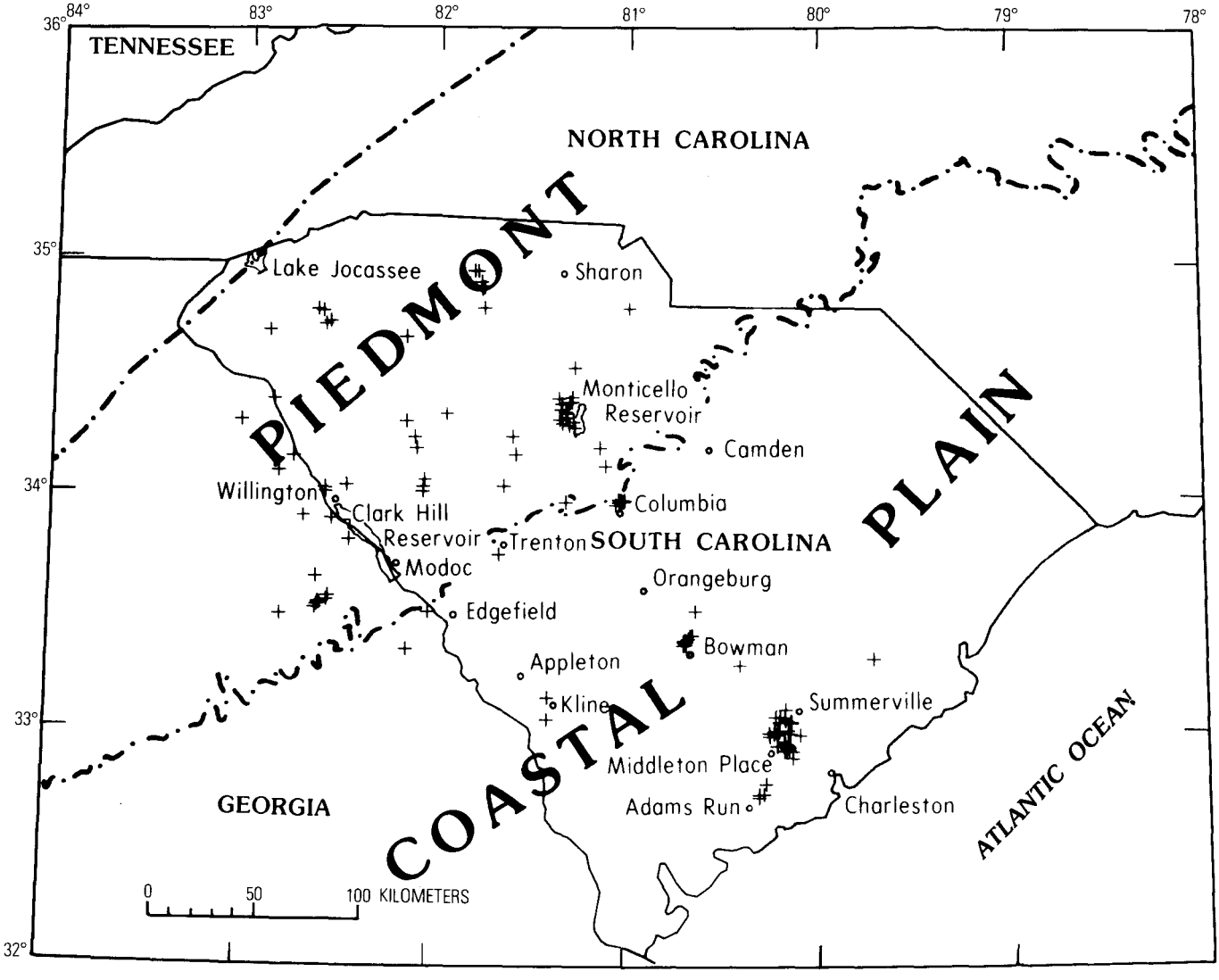

FIGURE 5.—Seismicity of South Carolina, 1973–79. Epicenters are plotted without regard to magnitude or intensity.

TABLE 3.—*Crustal velocity models employed in hypocenter determination*

Layer	Thickness (km)	Compressional velocity (km/sec)
Middleton Place–Summerville:		
1	29.91	[1]6.00–6.39
Half-space	∞	8.23
Bowman:		
1	1.18	2.20
2	28.73	5.98
Half-space	∞	8.15

[1] Velocity gradient 0.013 (km/sec)/km.

The orientation of the nodal planes and first-motion quadrants implies nearly vertical faulting with little or no strike-slip component for all three composite focal mechanisms. Composite focal mechanisms I and II are very similar to the focal mechanism determined earlier by Tarr (1977) for the November 22, 1974, Middleton Place earthquake; the observations from that event are used in composite focal mechanism I. The nearly vertical nodal planes are assumed to be the fault planes because the depth profiles (fig. 9) perpendicular to the strikes of the nodal planes show a nearly vertical distribution of hypocenters. The direction of greatest principal compressive stress as inferred from the fault-plane solution is northeast-southwest in I, II, and IV.

Composite focal mechanism III is similar to mechanisms I and II but rotated approximately 130° clockwise about the vertical axis. The strike of the steeply dipping plane, assumed to be the fault plane, is the same as the trend of the Slandsville group (III). The direction of the pressure axis is north-northwest.

The maximum permissible angular variation of the nodal planes from the preferred solution (while maintaining

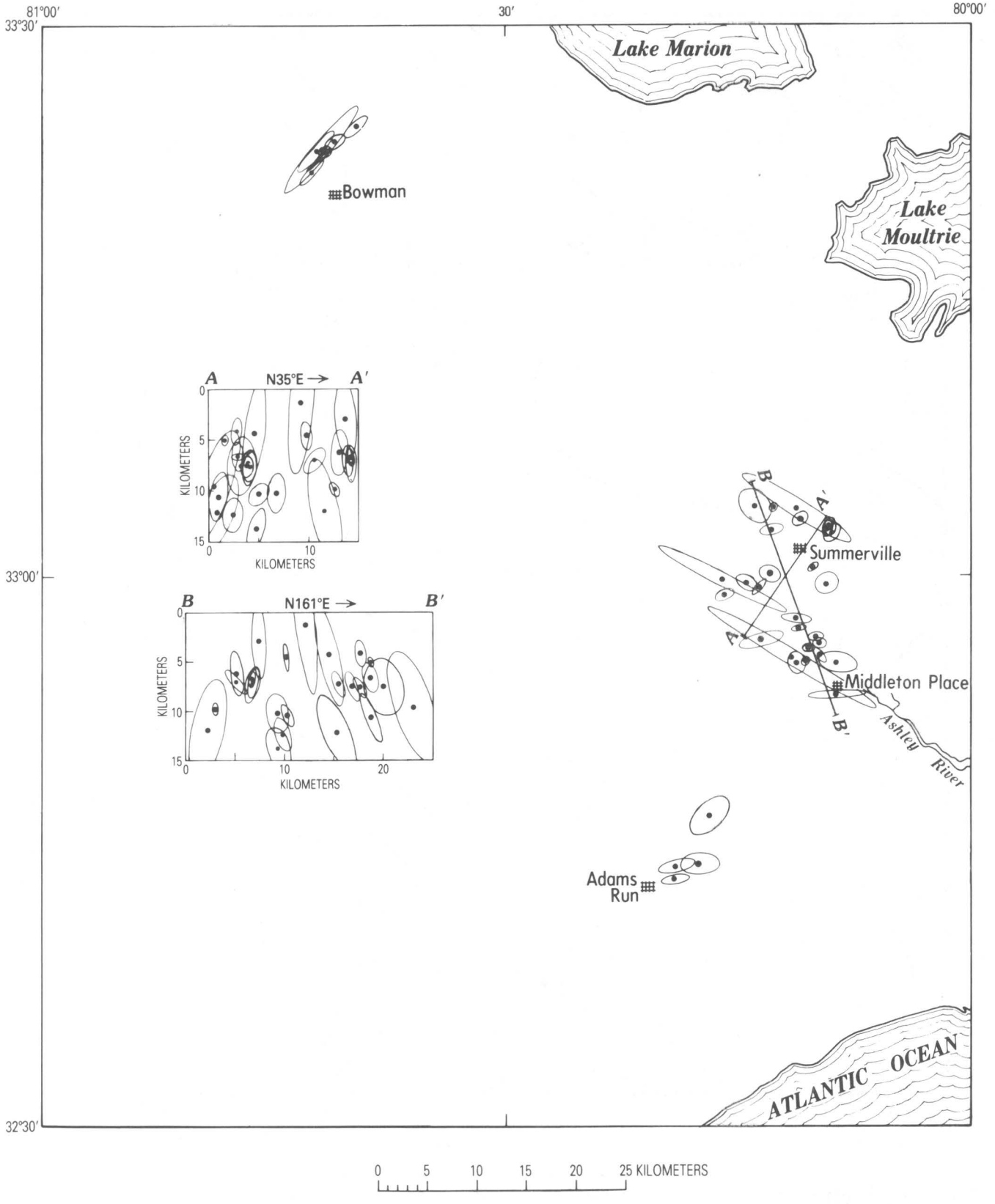

FIGURE 6. – Hypocenters near Charleston, 1973–79. The plotted ellipses are the principal planes (those having the largest projected area) of the standard-error ellipsoid. Depth profiles A–A' and B–B' are also shown.

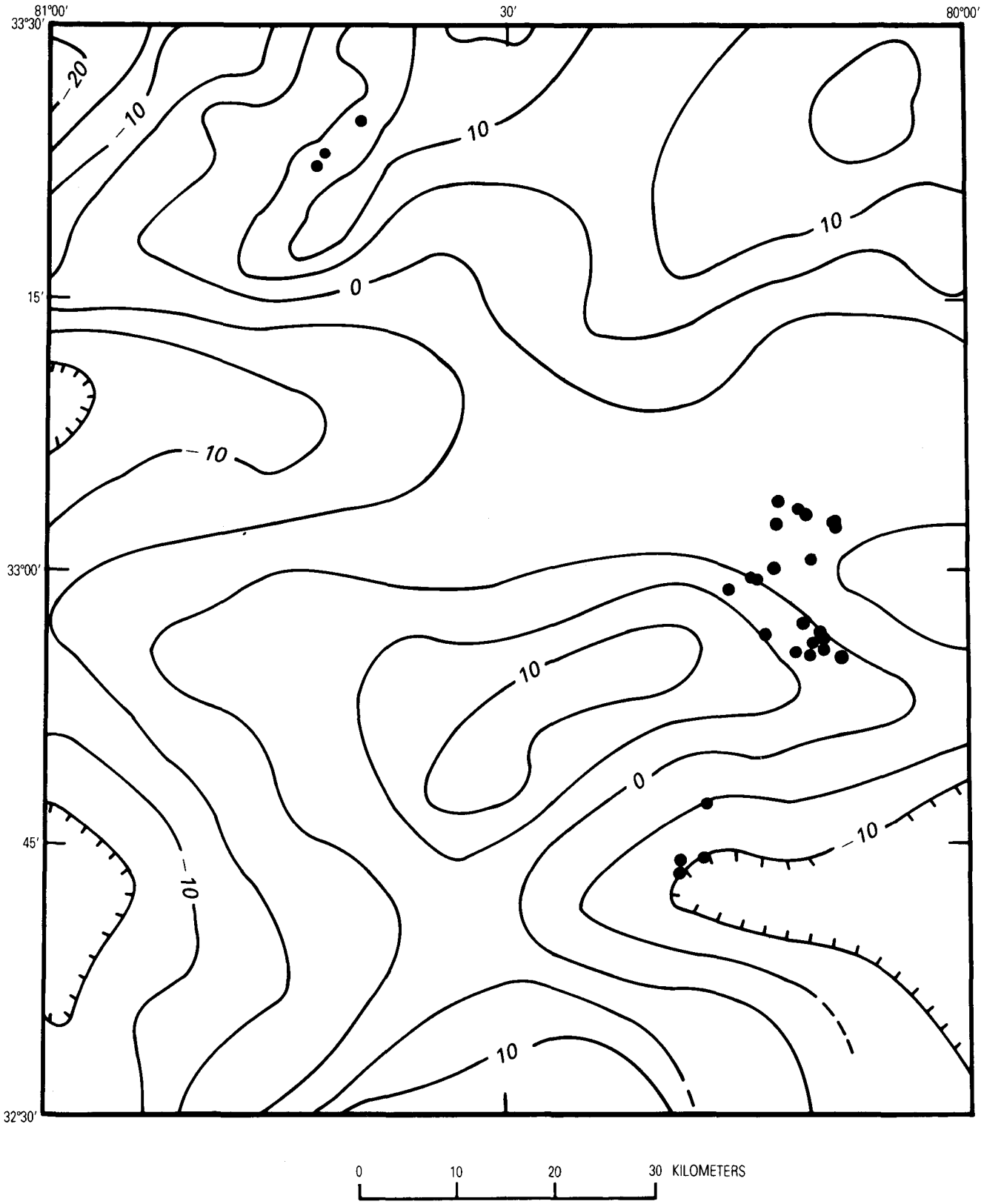

FIGURE 7.—Earthquake epicenters in southeastern South Carolina, 1973–79, superimposed upon Bouguer gravity anomaly map (Long and Champion, 1977). Contour interval, 5 mGal.

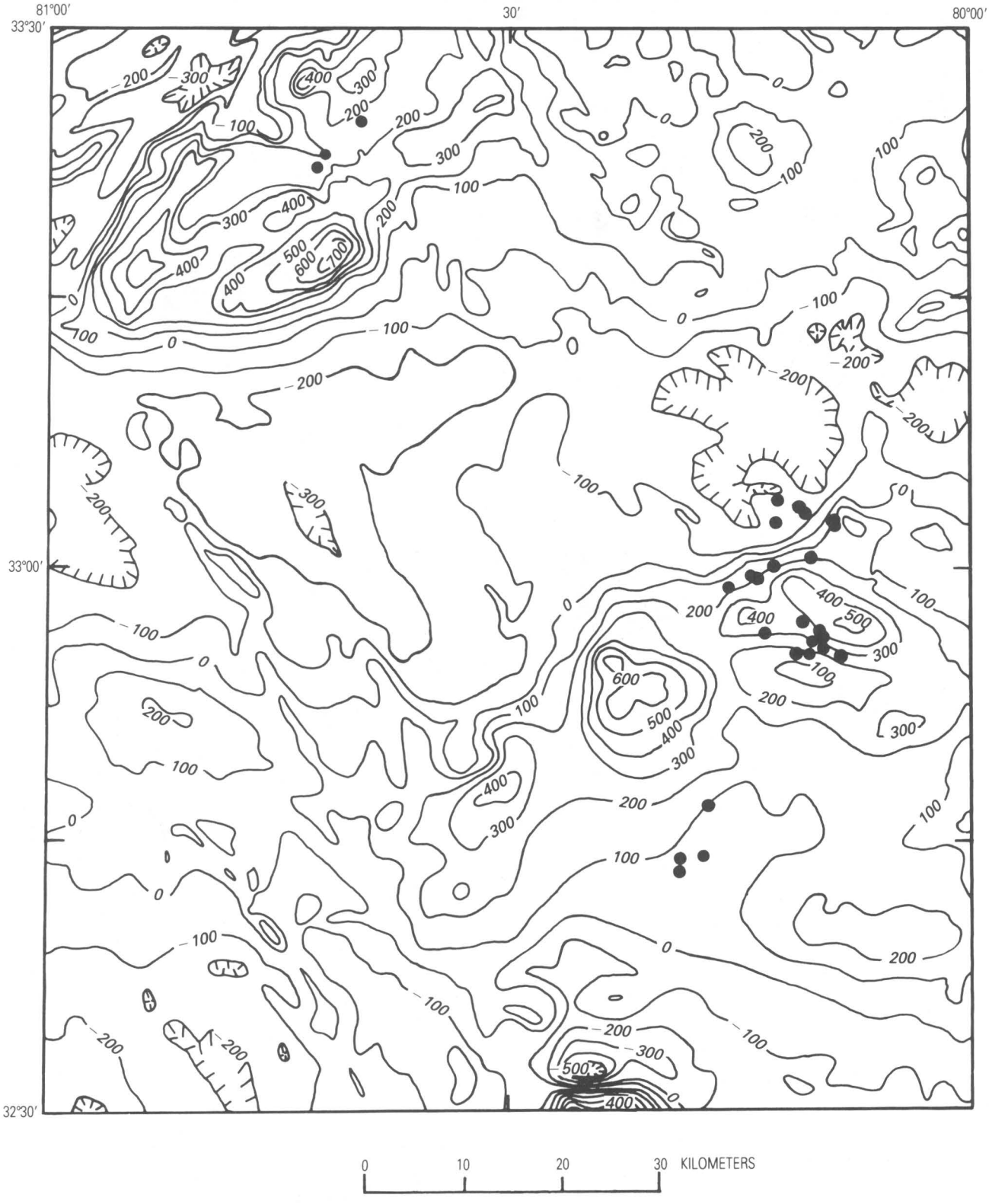

FIGURE 8.—Earthquake epicenters in southeastern South Carolina, 1973–79, superimposed upon aeromagnetic anomaly map (Popenoe and Zietz, 1977). Contour interval, 100 nT (nanotesla).

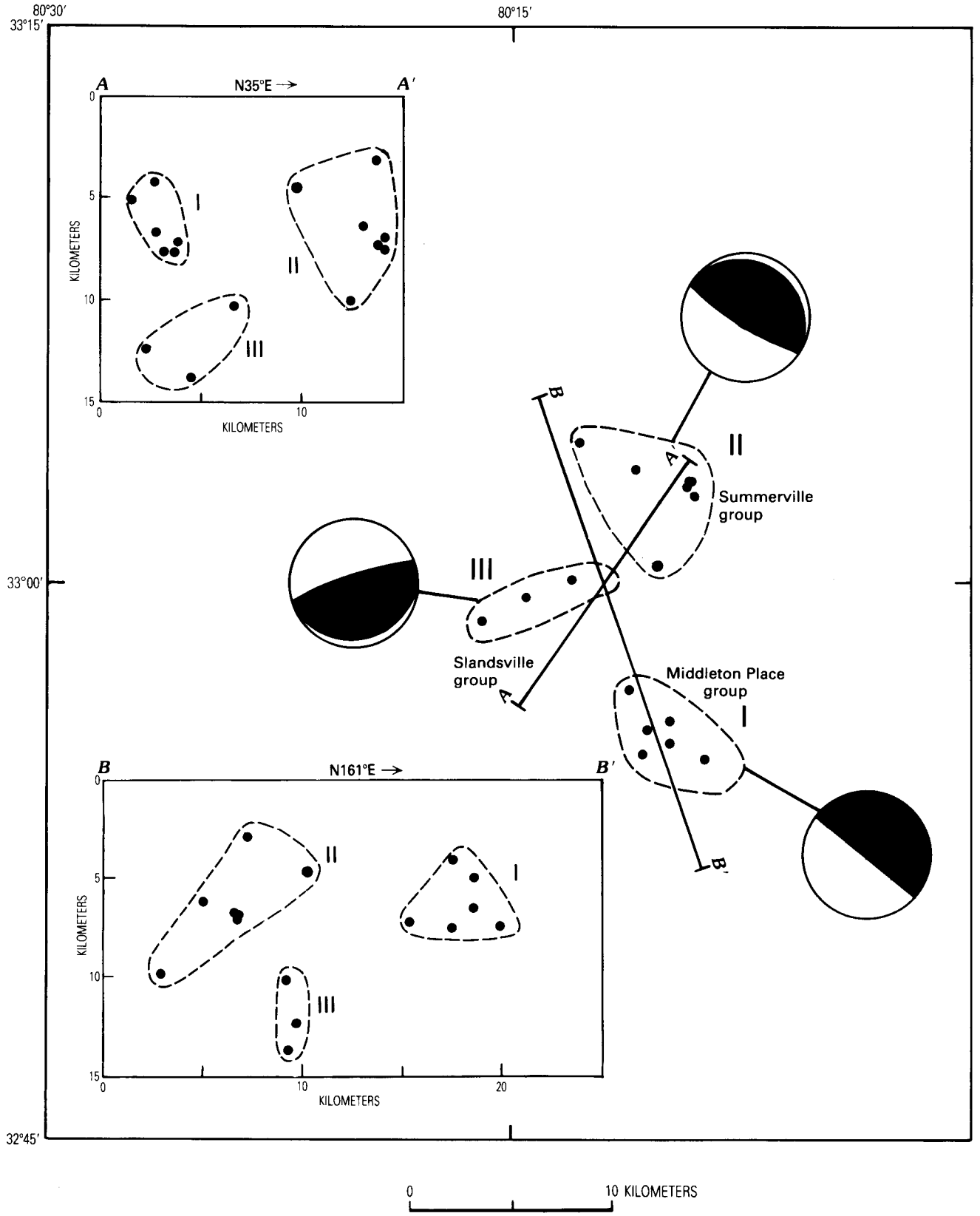

FIGURE 9.—Map of seismicity near Charleston (1973–79) and depth profiles *A–A'* and *B–B'* of the Middleton Place–Summerville seismic zone. Only the best hypocenters are plotted. Dashed lines enclose groups of hypocenters from which composite focal mechanisms were determined.

TABLE 4.—*Traveltime adjustments (in seconds) for southeastern South Carolina earthquakes*

Station	Traveltime adjustments	Mean residual	Standard deviation	Number of observations
Middleton Place–Summerville seismic zone				
HBF	−0.35	−0.02	±0.16	14
OSC	−.31	.06	±.14	6
CCS	−.00	−.03	±.47	12
MGS	.02	.00	±.19	12
PPS	.04	−.01	±.09	6
OSB	.05	.10	±.22	6
BCS	.06	.06	±.10	12
NHS	.08	.06	±.14	14
PBS	.09	.13	±.16	6
VSC	.09	.04	±.11	11
COW	.30	.15	±.17	3
ROW	.30	.14	±.14	3
SVS	.31	.06	±.11	11
WMS	.41	.14	±.03	2
SGS	.47	.06	±.41	16
BOW	.50	.16	±.17	3
Bowman cluster				
SGS	−.18	−.04	±.08	11
CCS	−.16	.08	±.03	2
NHS	−.11	.01	±.19	4
MGS	−.08	.05	±.06	2
HBF	−.01	−.03	±.12	10
SVS	.03	.02	±.09	2
OSB	.07	−.02	±.01	2
PBS	.16	.05	±.11	8
MTT	.17	.14	±.21	6
SRPN	.19	.12	±.12	5
OSC	.44	.25	±.08	8

the minimum number of inconsistent first motions) is about 5° in the strikes and about 10° in the dips (see fig. 10). The preferred solutions are relatively well determined, considering the assumptions that had to be made. These assumptions are, first, that the crustal velocities do not vary significantly across the source region and, second, that the individual focal mechanisms must be similar for all events within each group.

The first assumption is difficult to justify because it is known that the shallow crust in the region is quite heterogeneous (Ackermann, 1983), and some distortion of the angle of departure at the focal sphere and along the ray path to each station must be expected. However, the confidence-ellipse information suggests that the hypocenters are very precisely determined, probably because most of the anomalies in traveltimes caused by crustal heterogeneity have been removed by means of traveltime adjustments.

The second assumption is justified on the internal consistency of the first-motion patterns of spatially associated groups of earthquakes. For example, the consistency of the first-motion patterns of the Slandsville events clearly identifies them as having a distinctly different focal mechanism from those of the Middleton Place and Summerville events. Furthermore, depth profile *A–A'* (fig. 9), oriented approximately perpendicular to the strike direction of the nodal planes, shows two distinct but similar vertical distributions of hypocenters, consistent with one of the nodal planes suggested by the composite focal mechanisms I and II.

Bowman Cluster

The concentration of earthquakes near Bowman stands in remarkable contrast to the Middleton Place–Summerville seismic activity. Whereas the Charleston area has a seismic history that extends back to 1698 (Bollinger and Visvanathan, 1977) and is well documented from 1886 to the present, the Bowman seismic activity has been observed only within the last decade. The Middleton Place–Summerville earthquakes occur within an elongate zone, whereas the Bowman activity is confined to a short segment that appears to trend northeast (fig. 6), in the direction of the long axes of the confidence ellipses.

Two widely felt shocks in 1971 and 1972 signalled the abrupt onset of seismicity near Bowman, which had been previously aseismic (Bollinger, 1972, 1975). Although earlier determinations had placed these epicenters at distances up to 20 km from Bowman, Dewey (1983) has shown that the error ellipses for the relocated epicenters cover the Bowman cluster as it is now defined by the South Carolina seismic network. A depth profile through the Bowman cluster and a composite focal-mechanism solution are not possible at present because of insufficient data from the subnetwork.

Adams Run Cluster

The most recent seismic source to be discovered in southeastern South Carolina is in the vicinity of Adams Run. The cluster of four small but well-located earthquakes is about 30 km southwest of Middleton Place (fig. 6). The South Carolina seismic network data were supplemented for two of the events by recordings from temporary stations deployed for a seismic-refraction experiment by the University of South Carolina. The confidence ellipses of the Adams Run earthquakes (fig. 6) demonstrate that the Adams Run cluster is separate and distinct from the main Middleton Place–Summerville zone. At higher levels of confidence, it is not possible to distinguish the Adams Run cluster from a point source.

DISCUSSION

Perhaps the most striking characteristics of the improved view of the seismicity of South Carolina are the pronounced spatial and temporal discontinuities apparent in the seismicity map and earthquake history (Tarr and others, 1981). Spatially, the South Carolina seismic zone (Bollinger, 1975; Tarr, 1977) seems to be composed of two distinct parts divided approximately by the Coastal Plain–Piedmont boundary; this distinction is

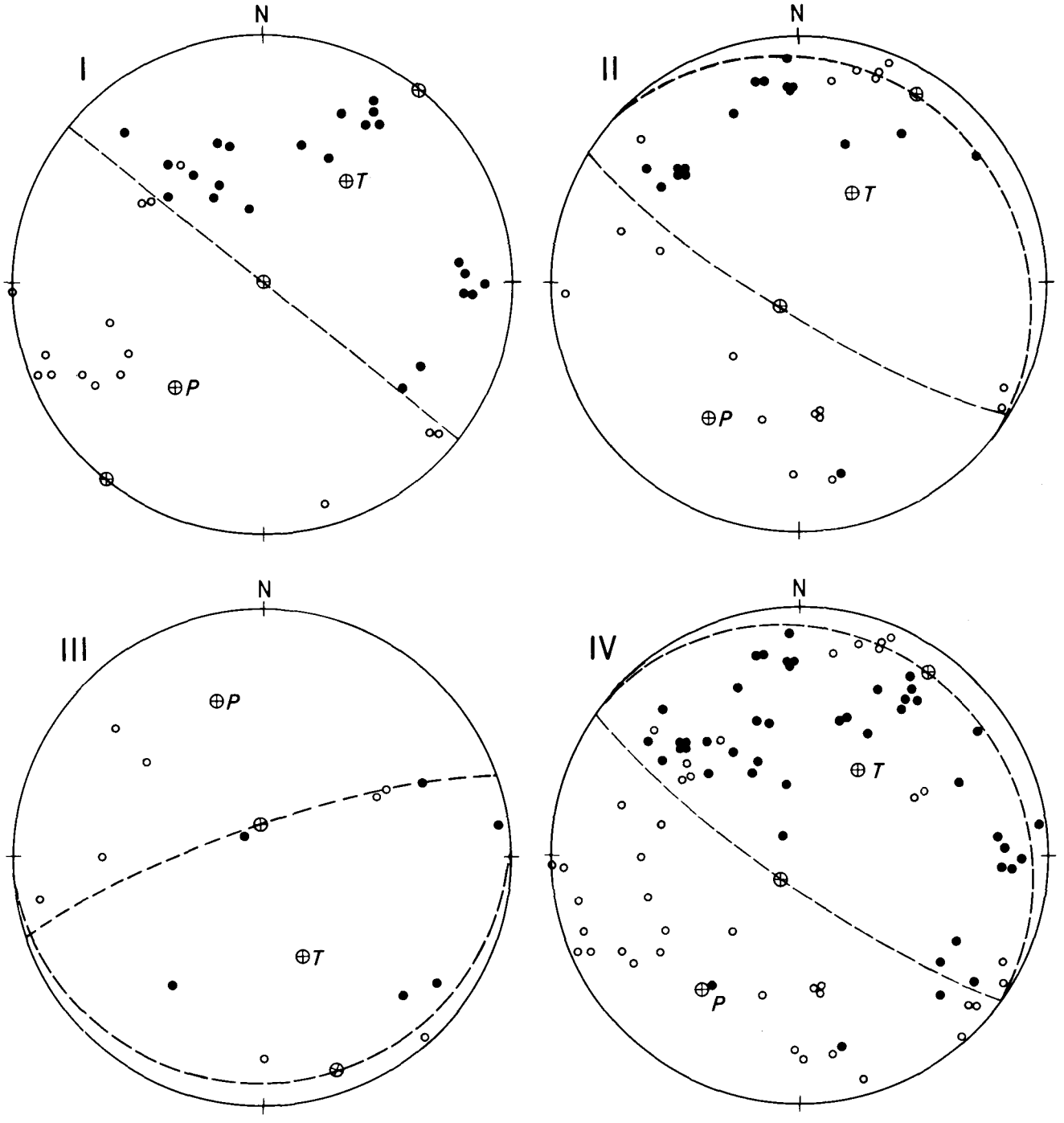

FIGURE 10.–Composite focal mechanisms (lower-hemisphere, equal-area projection) of six (I), seven (II), and three (III) well-recorded earthquakes in the Middleton Place–Summerville seismic zone. Solid symbols are compressions; open symbols are dilatations. *P* and *T* designate axes of inferred maximum and minimum compressive stress. Composite focal mechanism IV was determined from the combined data of I, II, and III.

maintained over the entire period covered by the South Carolina catalog. The seismicity southeast of the boundary shows a predominant clustering habit under the Coastal Plain. In contrast, the seismicity of the Piedmont, excepting "induced" reservoir earthquakes (Talwani, 1976, 1977b), has been characterized variously as scattered or diffuse (Bollinger, 1983; Tarr, 1977) or as alined with boundaries between major Piedmont

TABLE 5.—*Composite focal mechanisms of Middleton Place–Summerville seismic-zone earthquakes*

[I uses 6 earthquakes, II uses 7, III uses 3, and IV uses 16]

Composite mechanism	1st plane		2nd plane		*P* axis		*T* axis		Number of observations	Number of inconsistencies
	Strike	Dip	Strike	Dip	Trend	Plunge	Trend	Plunge		
I	309° (N. 51° W.)	90°	---	0°	219° (S. 39° W.)	45°	39° (N. 39° E.)	45°	38	1
II	302° (N. 58° W.)	80° S.	310° (N. 50° W.)	10° N.	212° (S. 32° W.)	35°	32° (N. 32° E.)	55°	35	7 (3 on planes)
III	71° (N. 71° E.)	80° N.	85° (N. 85° E.)	10° S.	344° (N. 16° W.)	35°	159° (S. 21°E.)	55°	14	1
IV	305° (N. 55° W.)	80° S.	305° (N. 55° W.)	10° N.	215° (S. 35° W.)	35°	35° (N. 35° E.)	55°	87	14 (3 on planes)

lithotectonic zones or with shear zones such as the Eastern Piedmont fault system (Hatcher and others, 1977).

We have identified three distinct concentrations of earthquakes near Charleston: Middleton Place–Summerville, Bowman, and Adams Run. As previously discussed by Tarr (1977), the Middleton Place–Summerville zone is the most probable source of the 1886 Charleston earthquake. The zone has been persistently active since the 1886 main shock and was more active than had been previously suspected (Dewey, 1983). In addition, it had been previously supposed by some that the earthquakes felt in and near Charleston were part of a long linear zone which extended from the Appalachians to far offshore. The results of Dewey's relocation study (1983), our analysis of South Carolina network data (Tarr and others, 1981), and the discovery that several historical shocks that had catalog locations near- or offshore actually had maximum intensities near Summerville support the hypothesis that most seismicity is confined to the zone between Middleton Place and Summerville.

Bollinger (1983) and Bollinger and Visvanathan (1977) have concluded that no long-term increase in South Carolina seismicity is apparent in the historical record prior to the onset of major activity in 1886. Only some of the foreshocks in the days immediately before the August 31 earthquake (Dutton, 1889; Taber, 1914) might be regarded as short-term "precursory" activity. Bollinger (1972) called attention to the similarly abrupt onset in 1971 of seismic activity near Bowman. In both cases, the seismicity has persisted since the principal onsets in 1886 and 1971, although short-term fluctuations are apparent in the seismic history. For example, the Middleton Place–Summerville seismic zone was notably active from 1974 through 1977, nearly quiescent during 1978, and more active again in 1979.

Thus, any tectonic model which seeks to explain specifically the contemporary seismicity of the Charleston area or, more generally, the differences between seismicity in the Coastal Plain and in the Piedmont must account for the contrasting spatial and temporal characteristics of the two provinces, the focal mechanisms, and the inferred directions of greatest compressive stress. The model must also be consistent with the findings of more recent geophysical and geological studies presented in this volume (Gohn, 1983).

One such model, requiring very few assumptions, has been proposed by Tarr and others (1981). The model assumes crustal fractures, faults, or contact zones that are weak enough and suitably oriented to allow shear failure in the presence of a regional stress field. Earlier studies (Rankin, 1977) and ones described in this volume have shown the presence of Mesozoic structures (border faults and cross faults of grabens, dike swarms, and mafic plutons) that are candidates for shear failure in the basement buried under the Coastal Plain sediments. In the Piedmont, boundaries between lithotectonic provinces, incompletely healed faults, dike swarms, and other intrusive bodies are possible seismogenic structures (Kane, 1977; McKeown, 1978). Although not invoked in this model, the zone of weakness proposed by Sykes (1978) to extend onshore from the Blake Spur fracture zone may localize some seismic activity.

Thus, the diffuse seismicity of the Piedmont is plausibly explained by this model, given the presence of a regional stress field. Except in areas where pore-pressure diffusion from reservoirs unloads slightly weak zones, the types of observed preexisting zones of weakness that are available to localize strain release are sparse and (or) areally restricted. These types include zones of brittle deformation in pre-Mesozoic shear zones, contacts of plutons, and a few known faults of Mesozoic and (or) Cenozoic age. The nearly random pattern of Piedmont seismicity may map slightly weaker spots, perhaps at the intersections of lithotectonic belt boundaries, the flanks of intrusive bodies, or faults.

The situation is quite different in the Coastal Plain. Earlier studies of aeromagnetic (Popenoe and Zietz, 1977) and gravity (Long and Champion, 1977) survey data, as well as contributions in this volume (Gohn, 1983), have inferred the presence of grabens and horsts

and mafic plutons and dikes formed in a major zone of early Mesozoic crustal extension related to the separation of the North American and African continents. Graben border faults and contacts of igneous bodies in the basement are good candidates for seismic activity. We believe that contemporary seismicity in the Charleston area occurs in clusters because the weakest places in the crust are located at the intersections of unhealed border and cross faults and contact zones in the basement.

In this context, the Slandsville group suggests activation of an unhealed east-northeast-trending border fault bounding a horst on the southeast and a graben of Triassic or Jurassic age to the northwest. The Slandsville group in fact coincides with a 900-m offset in the top of pre-Cretaceous "basement" inferred from refraction data (Ackermann, 1983). The Middleton Place and Summerville groups indicate activation of nearly vertical, northwest-trending faults or contacts, possibly at the edges of diabase dikes, crossing the Triassic or Jurassic border (Slandsville) fault. It is uncertain if the Adams Run cluster is on the southeast border of the horst, on a cross fault, or at the intersection of the two types of structures.

REFERENCES CITED

Ackermann, H. D., 1977, Exploring the Charleston, South Carolina, earthquake area with seismic refraction–A preliminary study, *in* Rankin, D. W., ed., Studies related to the Charleston, South Carolina, earthquake of 1886–A preliminary report: U.S. Geological Survey Professional Paper 1028, p. 167–175.

———1983, Seismic-refraction study in the area of the Charleston, South Carolina, 1886 earthquake, *in* Gohn, G. S., ed., Studies related to the Charleston, South Carolina, earthquake of 1886–Tectonics and seismicity: U.S. Geological Survey Professional Paper 1313, p. F1–F20.

Amick, David, 1979, Crustal structure studies in South Carolina coastal plain: Columbia, University of South Carolina, M.S. thesis, 81 p.

Bollinger, G. A., 1972, Historical and recent seismic activity in South Carolina: Seismological Society of America Bulletin, v. 62, no. 3, p. 851–864.

———1975, A catalog of southeastern United States earthquakes, 1754 through 1974: Virginia Polytechnic Institute and State University Research Division Bulletin 101, 68 p.

———1983, Speculations on the nature of seismicity at Charleston, South Carolina, *in* Gohn, G. S., ed., Studies related to the Charleston, South Carolina, earthquake of 1886–Tectonics and seismicity: U.S. Geological Survey Professional Paper 1313, p. T1–T11.

Bollinger, G. A., and Mathena, Ellen, compilers, 1978, Seismicity of the Southeastern United States, January 1, 1978–June 30, 1978: Southeastern United States Seismic Network Bulletin No. 2, Virginia Polytechnic Institute and State University, 78 p.

———compilers, 1979, Seismicity of the Southeastern United States, July 1, 1978–December 31, 1978: Southeastern United States Seismic Network Bulletin No. 3, Virginia Polytechnic Institute and State University, 66 p.

Bollinger, G. A., and Murphy, C. A., compilers, 1978, Seismicity of the Southeastern United States, July 1, 1977–December 31, 1977: Southeastern United States Seismic Network Bulletin No. 1, Virginia Polytechnic Institute and State University, 56 p.

Bollinger, G. A., and Visvanathan, T. R., 1977, The seismicity of South Carolina prior to 1886, *in* Rankin, D. W., ed., Studies related to the Charleston, South Carolina, earthquake of 1886–A preliminary report: U.S. Geological Survey Professional Paper 1028, p. 33–42.

Bonini, W. E., and Woollard, G. P., 1960, Subsurface geology of North Carolina–South Carolina coastal plain from seismic data: American Association of Petroleum Geologists Bulletin, v. 44, no. 3, p. 298–315.

Dewey, J. W., 1972, Seismicity and tectonics of western Venezuela: Seismological Society of America Bulletin, v. 62, no. 6, p. 1711–1751.

———1983, Relocation of instrumentally recorded pre-1974 earthquakes in the South Carolina region, *in* Gohn, G. S., ed., Studies related to the Charleston, South Carolina, earthquake of 1886–Tectonics and seismicity: U.S. Geological Survey Professional Paper 1313, p. Q1–Q9.

Dutton, C. E., 1889, The Charleston earthquake of August 31, 1886: U.S. Geological Survey Ninth Annual Report, 1887–1888, p. 203–528.

Gohn, G. S., editor, 1983, Studies related to the Charleston, South Carolina, earthquake of 1886–Tectonics and seismicity: U.S. Geological Survey Professional Paper 1313, 375 p.

Hatcher, R. D., Jr., Howell, D. E., and Talwani, Pradeep, 1977, Eastern Piedmont fault system; Speculations on its extent: Geology, v. 5, no. 10, p. 636–640.

Kane, M. F., 1977, Correlation of major eastern earthquake centers with mafic/ultramafic basement masses, *in* Rankin, D. W., ed., Studies related to the Charleston, South Carolina, earthquake of 1886–A preliminary report: U.S. Geological Survey Professional Paper 1028, p. 199–204.

Lahr, J. C., 1979, HYPOELLIPSE; A computer program for determining local earthquake hypocentral parameters, magnitude, and first motion pattern: U.S. Geological Survey Open-File Report 79–431, 313 p.

Long, L. T., 1972, The Carolina earthquake of February 3, 1972: Earthquake Notes, v. 43, no. 2, p. 13–17.

Long, L. T., and Champion, J. W., Jr., 1977, Bouguer gravity map of the Summerville-Charleston, South Carolina, epicentral zone and tectonic implications, *in* Rankin, D. W., ed., Studies related to the Charleston, South Carolina, earthquake of 1886–A preliminary report: U.S. Geological Survey Professional Paper 1028, p. 151–166.

McKee, J. H., 1973, A geophysical study of microearthquake activity near Bowman, South Carolina: Atlanta, Georgia Institute of Technology, M.S. thesis.

McKeown, F. A., 1978, Hypothesis; Many earthquakes in the central and southeastern United States are causally related to mafic intrusive bodies: U.S. Geological Survey Journal of Research, v. 6, no. 1, p. 41–50.

Phillips, J. D., 1977, Magnetic basement near Charleston, South Carolina–A preliminary report, *in* Rankin, D. W., ed., Studies related to the Charleston, South Carolina, earthquake of 1886–A preliminary report: U.S. Geological Survey Professional Paper 1028, p. 139–149.

Popenoe, Peter, and Zietz, Isidore, 1977, The nature of the geophysical basement beneath the Coastal Plain of South Carolina and northeastern Georgia, *in* Rankin, D. W., ed., Studies related to the Charleston, South Carolina, earthquake of 1886–A preliminary report: U.S. Geological Survey Professional Paper 1028, p. 119–137.

Rankin, D. W., editor, 1977, Studies related to the Charleston, South Carolina, earthquake of 1886–A preliminary report: U.S. Geological Survey Professional Paper 1028, 204 p.

Sbar, M. L., and Sykes, L. R., 1973, Contemporary compressive stress and seismicity in eastern North America: An example of intra-plate tectonics: Geological Society of America Bulletin, v. 84, no. 6, p. 1861–1881.

Sykes, L. R., 1978, Intra-plate seismicity, reactivation of preexisting zones of weakness, alkaline magmatism, and other tectonism postdating continental fragmentation: Reviews of Geophysics and Space Physics, v. 16, no. 4, p. 621–688.

Taber, Steven, 1914, Seismic activity in the Atlantic Coastal Plain near Charleston, South Carolina: Seismological Society of America Bulletin, v. 4, p. 108–160.

Talwani, Pradeep, 1976, Earthquakes associated with the Clark Hill Reservoir, South Carolina–A case of induced seismicity: Engineering Geology, v. 10, no. 2–4, p. 239–253.

———1977a, A preliminary shallow crustal model between Columbia and Charleston, South Carolina, determined from quarry blast monitoring and other geophysical data, *in* Rankin, D. W., ed., Studies related to the Charleston, South Carolina, earthquake of 1886–A preliminary report: U.S. Geological Survey Professional Paper 1028, p. 177–187.

———1977b, Stress distribution near Lake Jocassee, South Carolina: Pure and Applied Geophysics, v. 115, p. 275–281.

Tarr, A. C., 1977, Recent seismicity near Charleston, South Carolina, and its relationship to the August 31, 1886, earthquake, *in* Rankin, D. W., ed., Studies related to the Charleston, South Carolina, earthquake of 1886–A preliminary report: U.S. Geological Survey Professional Paper 1028, p. 43–57.

Tarr, A. C., and King, K. W., 1974, South Carolina seismic program: U.S. Geological Survey Open-File Report 74-58, 15 p.

Tarr, A. C., Talwani, Pradeep, Rhea, Susan, Carver, David, and Amick, David, 1981, Results of recent South Carolina seismological studies: Seismological Society of America Bulletin, v. 71, no. 6, p. 1883–1902.

Regenerate Faults of Small Cenozoic Offset—Probable Earthquake Sources in the Southeastern United States

By CARL M. WENTWORTH and MARCIA MERGNER-KEEFER

STUDIES RELATED TO THE CHARLESTON, SOUTH CAROLINA, EARTHQUAKE OF 1886—TECTONICS AND SEISMICITY

GEOLOGICAL SURVEY PROFESSIONAL PAPER 1313-S

UNITED STATES GOVERNMENT PRINTING OFFICE, WASHINGTON: 1983

CONTENTS

ILLUSTRATIONS

TABLE

STUDIES RELATED TO THE CHARLESTON, SOUTH CAROLINA, EARTHQUAKE OF 1886—TECTONICS AND SEISMICITY

REGENERATE FAULTS OF SMALL CENOZOIC OFFSET—PROBABLE EARTHQUAKE SOURCES IN THE SOUTHEASTERN UNITED STATES

By CARL M. WENTWORTH and MARCIA MERGNER-KEEFER

ABSTRACT

The principal style of Cenozoic faults and earthquake focal-mechanism solutions known along the eastern seaboard suggests that a domain undergoing northwest-southeast compression extends along the eastern seaboard between the continental margin and the front of the Appalachian Mountains. In the Southeast, several mapped northeast-trending zones of high-angle reverse faulting and many faults in isolated exposures offset Coastal Plain deposits as much as 100 m; the youngest recognized offset is 0.35 m in probable Pliocene or Pleistocene surficial gravels in the Stafford fault zone in Virginia. Movement has been progressive from at least Early Cretaceous into the Cenozoic, average offset rates being about 1 m/m.y. (million years). Northeast-striking reverse source mechanisms of various recent earthquakes indicate that reverse faulting is still active and that such faults can be seismogenic.

The extent of the domain is inferred from (1) reverse faults known in South Carolina and along the Fall Line from Georgia to New Jersey; (2) earthquake source mechanisms, particularly in coastal New England; and (3) the broad distribution of early Mesozoic normal faults in the exposed Piedmont terrain and beneath the Coastal Plain and offshore. We suggest that, to a large extent, the reverse faults reuse parts of these early Mesozoic faults. We characterize the domain from the known fault histories, the existence of geometrically compatible earthquakes, and our expectation that seismogenic reverse faults are scattered essentially throughout the region no more than a few tens of kilometers apart. If correct, this expectation implies that the historic seismic pattern is not stationary over the long term.

The intensity-X Charleston earthquake of 1886 occurred within the best documented part of the Atlantic Coast domain, close to a Cretaceous-Cenozoic reverse fault and an inferred early Mesozoic fault zone, both trending east-northeast. Some recent small aftershocks near these faults suggest similar reverse faulting, and the 1886 intensity pattern suggests a northeast strike for the main-shock source. We thus conclude that northeast-trending reverse faulting produced the 1886 earthquake. Many of the recent aftershocks seem to be on northwest-trending structures, however, probably in response to temporary changes in the local stress field resulting from the strain release of the 1886 main shock. If this conclusion and our concept of the Atlantic Coast domain are correct, then earthquakes at least as large as 1886 Charleston should be possible in most parts of the domain.

The Atlantic margin was placed in compression approximately normal to its length sometime after successful rifting; certainly by latest Early Cretaceous, probably in the Jurassic, and possibly soon after extrusion of the 184-m.y. basalt at Charleston. The compression is presumed to be related to some process associated with the continental margin and, on the basis of generally declining rates of reverse faulting, may be inversely related to the duration of Atlantic spreading.

INTRODUCTION

The generation of crustal earthquakes involves rupture and fault offset. Unless each seismic event is spatially unique, geologically recognizable fault offsets should develop through time as deformation proceeds. This argument must be qualified with considerations of rates of faulting, adequacy of the stratigraphic record, depths of activity and levels of exposure. It represents the geologic view, however, that seismicity represents deformation; to some degree, the history of this deformation should be evident in the rock record. It should be worthwhile then, in considering the sources of earthquakes along the eastern seaboard, to examine the recent geologic history of the region.

In the western third of the United States, many large historic earthquakes can be attributed to movement on particular faults, especially where there is accompanying surface faulting or where detailed earthquake locations and focal mechanisms are obtained. Large Cenozoic offsets and convincing evidence in the topography and surficial geology of late Quaternary fault movement support the conclusion that continuing movement of the faults is reasonable. It does not necessarily follow, however, that all seismogenic faults exhibit these traits. In considering seismicity along the eastern seaboard, it may be important to avoid drawing too close a parallel with such impressive western stereotypes as the strike-slip San Andreas fault, the normal faults of the Basin and Range province, or the reverse faults of the California Transverse Ranges. The intraplate structures involved in the generation of earthquakes along the eastern seaboard may be much more modest features, at least in their Cenozoic incarnations. The fact that major

fault scarps and other fault-generated topographic features have not been found suggests that this is true, although the role of Cenozoic tectonics in shaping the topography has yet to be resolved.

The intensity-X (Modified Mercalli) earthquake of 1886 at Charleston, S. C., and the scattering of historic events along the Atlantic seaboard have not been accompanied by recognition of direct geologic evidence of the causative faults. The documented earthquakes along the eastern seaboard have been as shallow as those expressed by surface faulting in the Western United States, so the apparent absence of Quaternary indications of cumulative surface deformation may well result from low deformation rates. Despite recent progress, sufficient information is not available to demonstrate the tectonic regime now in force along the eastern seaboard. Faults having modest Cretaceous and Cenozoic offsets do exist in the Southeast, however, and it is important to examine their implications concerning the pattern of deformation and the generation of earthquakes, there and throughout the Atlantic seaboard. From this viewpoint, we propose and explain a hypothesis involving a consistent pattern of deformation and associated seismicity along the Atlantic seaboard and discuss the relation of the 1886 Charleston earthquake to this hypothesis.

This paper, originally written in 1980, is a synthesis of data from many sources; it is based on a conviction founded on western experience that crustal earthquakes are related to specific geologic faults. It replaces an open-file version (Wentworth and Mergner-Keefer, 1981a) and is complemented by a discussion that expands on northeastern evidence and earthquake recurrence implications (Wentworth and Mergner-Keefer, 1981b). We acknowledge a major debt to W. L. Newell, R. B. Mixon, and D. C. Prowell of the U.S. Geological Survey for their fundamental work on the Stafford and Belair fault zones and for many stimulating discussions.

THE HYPOTHESIS

The available geologic and seismologic evidence leads us to the following hypothesis. An Atlantic Coast domain of northwest-southeast compression extends from Georgia to Canada between the Appalachian Mountains and the edge of the continent. Within this domain, movement on scattered northeast-trending reverse faults has been underway for at least 100 m.y. but in that time has accumulated offsets on individual faults of no more than about 100 m. Movement on these faults is a reasonable source of seismicity in the domain. Such faults exist in the Charleston meizoseismal area and are a reasonable source of the 1886 earthquake. The reverse faults tend to reuse preexisting faults and other discontinuities, particularly the normal faults formed during early Mesozoic rifting. This association and earthquake focal-mechanism solutions permit extrapolation of the domain beyond the presently recognized extent of Cenozoic reverse faulting in the Southeast. Given the inferred extent of the domain and the occurrence of the 1886 earthquake on a northeast-trending reverse fault near Charleston, large, damaging earthquakes should be possible in most parts of the Atlantic seaboard.

With the exception of some Cretaceous-Cenozoic reverse faults and earthquake focal-mechanism solutions indicating northeast-trending reverse faulting, none of the components of this hypothesis are strictly provable with present information. Together, however, they form a coherent and reasonable whole that incorporates the principal style of Cenozoic faulting known to have occurred in the region.

CENOZOIC REVERSE FAULTS IN THE SOUTHEAST

Recent work in the Southeastern United States has demonstrated that northeast-trending reverse faults having modest Late Cretaceous and Cenozoic displacements exist in the Atlantic Coastal Plain and Piedmont. In the most carefully studied examples, the Stafford fault zone in Virginia (Mixon and Newell, 1977) and the Belair fault zone in Georgia (Prowell and O'Connor, 1978), it has been demonstrated that Late Cretaceous and Cenozoic sediments of the Coastal Plain are offset by faults that can be mapped for many kilometers. Compilations and field checks of isolated fault exposures (York and Oliver, 1976; Prowell, 1982) and recent work near Charleston, S. C. (Behrendt and others, 1981) suggest that such faults are widespread in the Southeast and indicate that fault geometries and movement histories are generally consistent throughout the region.

The geology of the Southeast is not ideally suited to the recognition of Cenozoic faults. In the Piedmont the Paleozoic crystalline rocks of the Appalachian orogen and the inset lower Mesozoic red beds and basalts of the initial phase of Atlantic rifting are too old to record the timing of Cenozoic faulting. Recognition of Cenozoic age from the ruptures themselves may be impossible; even the early Mesozoic extensional faults are generally recognized only where red beds and basalts record their presence. Geomorphology has not yet proved fruitful in recognizing Cenozoic faulting, and outliers of Coastal Plain sediment and scattered patches of alluvium and colluvium of uncertain age are of only limited value. In contrast, the nearly flat-lying Upper Cretaceous and Cenozoic sediments of the Coastal Plain that unconformably overlap the crystalline rocks, and especially the unconformity at the base of the sedimentary section,

provide excellent control on postunconformity offsets.[1] However, the poor exposure and subtle stratigraphic differences within the Coastal Plain require careful and deliberate search to find and map those offsets. Where the Coastal Plain section is thick, faulting at its base may degenerate upward into folding, so that no abrupt offset may exist near the surface.

Distribution and Geometry

Isolated exposures of faults that cut Coastal Plain and surficial sediments are scattered within the Piedmont and Coastal Plain, particularly near the Fall Line (pl. 1; Prowell, 1982). In the past, these postunconformity faults were largely encountered and reported in the course of other investigations. They were almost always found exposed in cross section in isolated steep cuts that had been excavated by streams or man. Some of these exposures have since been obliterated by continued excavation, for example, a small graben found in a clay pit in South Carolina (Inden and Zupan, 1975), or concealed by subsequent construction, for example, a fault near the Calvert Street Bridge in Washington, D. C. (Carr, 1950).

These isolated faults are probably parts of more extensive faults and fault zones, as indicated by the careful mapping of two zones of postunconformity faults near the Fall Line. In Virginia, a narrow, anomalously steep gradient of northeast trend on the unconformity beneath sediments of the Potomac Formation, which was discovered by R. B. Mixon during mapping of the Quantico quadrangle (Mixon and others, 1972), led to recognition of the Stafford fault zone (pl. 1). Surface mapping and shallow drilling documented the existence of several northeast-trending faults as long as 35 km, having vertical offsets on the unconformity of 15 to 100 m, down to the east. Together these faults form a northeast-trending zone at least 67 km long that passes through Fredericksburg, Va., and reaches within 30 km of, and possibly through, Washington, D. C. (Mixon and Newell, 1976, 1977, 1978; Seiders and Mixon, 1981; Carr, 1950). Natural exposures of crystalline rock faulted against Coastal Plain sediments found in the course of field mapping, and relations in a trench excavated across the trace of the Dumfries fault demonstrate that the faults have reverse offsets (Newell and others, 1976; Mixon and Newell, 1978).

Seven hundred kilometers to the southwest, near Augusta, Ga., a claypit exposure of saprolitized phyllite faulted against the basal Coastal Plain sediments (Middendorf Formation) was discovered during work on the State geologic map (O'Connor and others, 1974). This stimulated regional mapping, shallow drilling, and trenching that documented the Belair fault zone (O'Connor and Prowell, 1976; U.S. Geological Survey, 1977; Prowell and O'Connor, 1978; pl. 1). The unconformity was shown to be cut by several northeast-trending reverse faults having lengths of 2–5 km and offsets on the unconformity of 5–30 m, down to the west. Together these faults form a northeast-trending zone at least 24 km long.

The work on these two widely separated fault zones shows that faults of significant length and modest Late Cretaceous and Cenozoic displacement do exist in the Southeast. Even for these well-mapped examples, however, the full lengths of the fault zones remain unknown. The Stafford and Belair fault zones have been mapped principally in the vicinity of the Fall Line, which they cross obliquely, because there they involve a thin Coastal Plain section. Along strike in both directions, the limitations of the Piedmont and the thicker Coastal Plain section make recognizing and mapping the faults more difficult.

In a thicker Coastal Plain section about 25 km southeast of the Stafford zone in Maryland, Jacobeen (1972) has mapped the Brandywine fault zone by means of seismic profiling (pl. 1). During exploration for a gas-storage site, reflection profiling across a local 30-m structural high on the Paleocene Aquia Formation revealed two en-enchelon reverse faults. These trend northeastward and offset the unconformity, west side down, along a mapped length of 17 km. The vertical offsets across the two faults are 30 m and 50–60 m at the unconformity. These offsets decrease upward through the lower part of the Coastal Plain section and are expressed largely as folding in the overlying Eocene and Miocene sediments.

Seismic profiling designed to search for this kind of structure has also revealed reverse faults of modest Cretaceous and Cenozoic offset in the Charleston meizoseismal area and off the South Carolina coast (pl. 1). Onshore, the east-northeast-trending Cooke fault offsets the base of the Coastal Plain section 50 m, down to the southeast, and shows decreasing offset upward into the lower Tertiary section (Behrendt and others, 1981). Offshore, the Helena Banks fault has been traced for at least 35 km, and probably 70 km, on an east-northeast trend (Behrendt and others, 1983). It offsets the base of the sedimentary section about 20 m, down to the southeast, and shows decreasing offset upward; the shallowest recognized horizons are warped rather than sharply faulted.

[1]The Coastal Plain section is everywhere underlain by a major unconformity. For brevity, we refer to this, and to the surface of crystalline rocks in the Piedmont, as *the unconformity*, and refer to faults that postdate it as *postunconformity* faults. In a general way this unconformity is equivalent to the postrift unconformity offshore (Dillon and others, 1983); however, the postrift unconformity lies below the basalt at Charleston and offshore, rather than above it (table 1).

The mapped faults and isolated fault exposures throughout the Coastal Plain and Piedmont have generally similar geometries (Prowell, 1976, 1982, written commun., 1979; Howard and others, 1978). The fault zones are probably complex in detail (Mixon and Newell, 1978, p. 19; Prowell, written commun., 1979), and isolated parts may not be representative of the geometry of the zone as a whole. In a chance exposure it is impossible to determine whether a main or a subordinate fault is involved; only where the fault zone is mapped for some length can the overall geometry be confidently established. Nevertheless, presently recognized faults are generally northeast-trending, high-angle reverse faults of small displacement. The dominant strike of individual faults is northeastward, as is the trend of the mapped zones, although the strikes range from northwest through east (fig. 1). Dips are generally high, ranging from 34° to 90°, and are inclined to the northwest or southeast; no regular areal pattern of dip direction is evident. Vertical separations across individual faults are small, ranging from 0.2 to 100 m; the amount of separation depends in part on the age of the offset horizon.

Faults having upthrown hanging walls are considered to be reverse faults, although some may have strike-slip components as well. Evidence that the vertical separations represent actual displacement, or at least the principal component of fault slip, is of two kinds. Almost all the known northeast-trending faults show reverse separation (fig. 1), which is not likely for the dip components of strike-slip faults. Secondly, the well-studied faults show local evidence of dip-slip. Slickensides on both the Belair fault (Prowell and O'Connor, 1978) and the Dumfries fault of the Stafford zone (Mixon and Newell, 1978) indicate primarily dip-slip. Faults of both the Stafford and Belair zones show drag of Coastal Plain sediments up against the upthrown block (Newell and others, 1976; U.S. Geological Survey, 1977).

At least a minor component of strike-slip exists on some of the faults. On the Belair fault, Prowell and O'Connor (1978) report slickensides at about 26° to the dip direction and slight left-lateral offset of kaolin clasts in the Tuscalosa Formation across subsidiary splay faults. In the Stafford zone, some slickensides rake steeply southwest in the fault plane, and structural

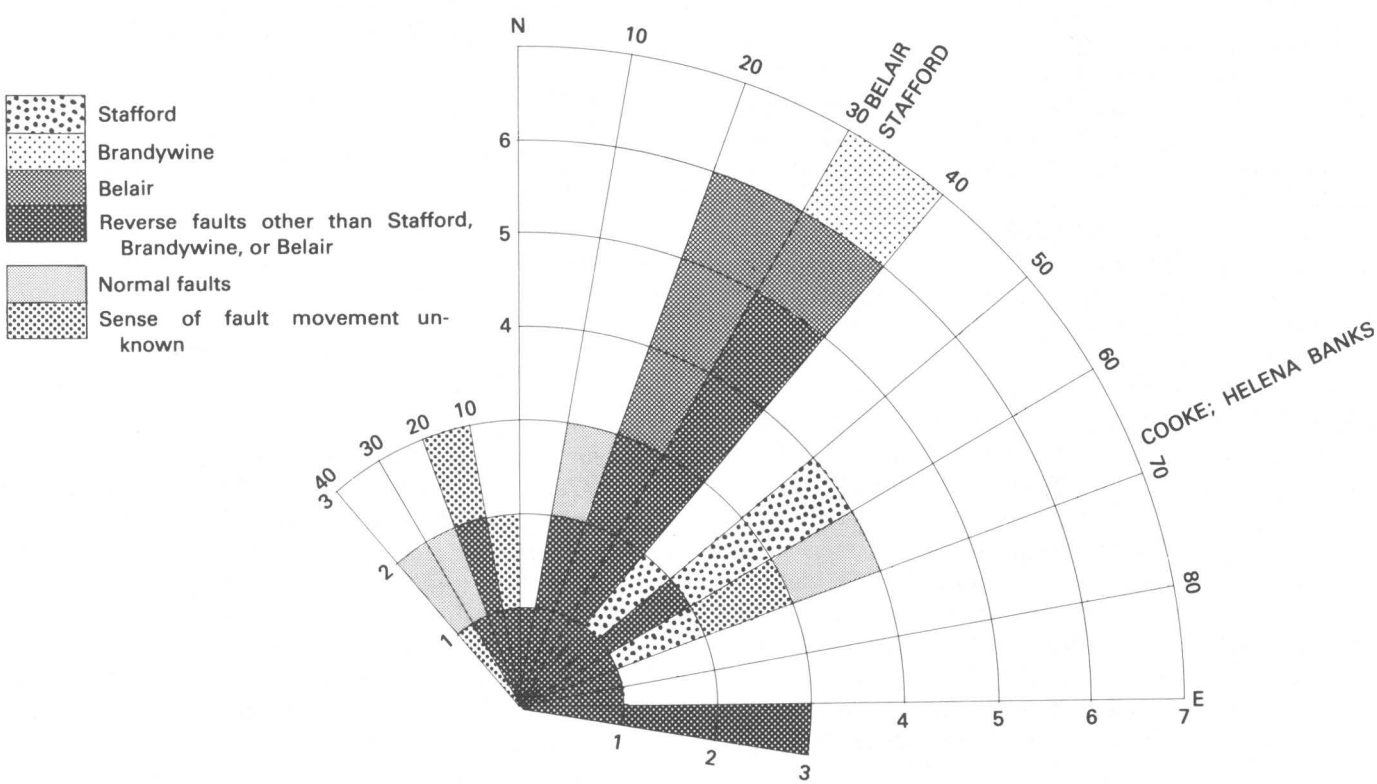

FIGURE 1.—Strikes of postunconformity faults in the southeastern Piedmont and Coastal Plain between eastern Georgia and Washington, D.C. Compiled from Prowell (1982), Behrendt and others (1981), Mixon and Newell (1977), and Prowell and O'Connor (1978). The strikes of 41 individual faults, including those in the Stafford and Belair zones, are plotted; the strikes of the zones are separately shown by location of the zone names.

analysis of a trench exposure indicates that reverse and normal faults subordinate to the Dumfries fault are rotated progressively clockwise with increasing relative age (Newell and others, 1976). In contrast to the findings for the Belair fault, these imply a right-lateral component of slip across the Dumfries fault, at least in Potomac Formation time (latest Early Cretaceous).

Dominant strike-slip seems unreasonable, however, although evidence is elusive because of the small displacements and the lack of piercing points or steeply dipping planes in the Coastal Plain section to use as control. Lateral offsets in the older Piedmont crystalline rocks, such as the 23-km left-lateral offset of the Augusta fault across the Belair fault described by Prowell and O'Connor (1978), do not necessarily bear on the Cretaceous-Cenozoic faulting. The Cretaceous-Cenozoic faults in the Belair and Stafford zones do not show the branching and anastomosing pattern characteristic of strike-slip faults but instead form an open-spaced, en-echelon pattern of parallel faults.

The known distribution of Cretaceous and Cenozoic reverse faults extends along the Fall Line from Georgia to Virginia and about 200 km southeast of the Fall Line on- and offshore near Charleston, S. C. (pl. 1). The principal concentration near the Fall Line, however, is probably apparent rather than real, a result of the geologic opportunity provided by the thin Coastal Plain section there. The discovery of reverse faults where looked for onshore and offshore near Charleston and their existence well east of the Fall Line in Virginia suggest that more will be found elsewhere on the Coastal Plain and Continental Shelf as the search proceeds.

History of Fault Movement

Offsets of the several postunconformity faults shown in figure 1 are recorded by sediments that range in age from latest Early Cretaceous to Pliocene or Quaternary (Prowell, 1982), a period of 100 million years. The Stafford zone displaces sediments that record much of this time range, but at most of the fault localities the sediments probably represent only a very limited age range. Most of the ages are uncertain, however, because of the difficulties in determining the age of isolated patches of sediment, particularly unfossiliferous alluvium and colluvium.

In the more complete and well-studied records, the offsets across particular faults decrease with decreasing age of correlative horizons, which indicates progressive movement through time (fig. 2): the Stafford zone records movement from late Early Cretaceous through probably Pliocene or Pleistocene, the Brandywine zone from Late Cretaceous through Miocene or younger, the Belair zone from Late Cretaceous through at least Eocene, and the Cooke fault from pre-Late Cretaceous through at least Paleocene. The Helena Banks fault also shows progressive movement, but the identities of the offset sedimentary horizons are less certain. Present knowledge of the movement on the isolated faults is not inconsistent with a pattern of progressive movement through time, particularly considering the uncertainties of age assignments and the likelihood that both main and subordinate faults are involved. There is no good indication of geographic variation in the timing of faulting, although the data are much too limited to prove uniformity.

The greatest detail about the history of fault movement is provided by stratigraphic relations across the Stafford fault zone. As indicated by detailed structures exposed in a trench across the Dumfries fault (Newell and others, 1976), offset was underway during accumulation of the uppermost Lower Cretaceous Potomac Formation. Later movement progressively offset the Paleocene Aquia Formation, the Paleocene and Eocene Marlboro Clay, possibly the Miocene Calvert Formation, and, in one gutter exposure on the Fall Hill fault, upland gravel of probable Pliocene or Pleistocene age (Mixon and Newell, 1978, fig. 7).

More specifically, for vertical separations across the Brooke structure (Mixon and Newell, 1978, fig. 4, p. 9), the movement history required to produce a cumulative 105 m of offset (including drag) is approximately 83 m in the 55 million years (m.y.) represented from the base of the Cretaceous Potomac Formation to the base of the Paleocene Aquia Formation (1.5 m/m.y.), 13.5 m in the 3.5 m.y. represented from there to the base of the latest Paleocene and Eocene Marlboro Clay (3.9 m/m.y.), and 8.5 m in the 54 m.y. since then (0.2 m/m.y.), assuming that movement continued to the present (fig. 2). Present data are insufficient to determine the exact configuration of the Miocene Calvert Formation, so that any offset is unrecognized. If the Fall Hill gravel is considered representative of Brooke offset as well, then 0.35 m of offset can be added in perhaps the past 2 m.y. The average offset rate through the whole of the Late Cretaceous and Cenozoic is 0.9 m/m.y., but the data indicate that the rate has generally decreased over time.

Expectable Quaternary offset across an individual fault is so small, perhaps 0.5 to 1 m at most, that it would be difficult to resolve in most situations where Quaternary control is actually available and essentially impossible elsewhere. The youngest displacement reported in the Stafford zone, 0.35 m on the base of a gravel of probable Pliocene or Pleistocene age, is of this general amount. The 0.6 m of reverse offset at the base of high-level terrace gravels over the Brandywine zone (Prowell, 1982) may represent recent fault movement of similar amount there. The tectonic origin of even smaller offsets that have been seen in gravels along the

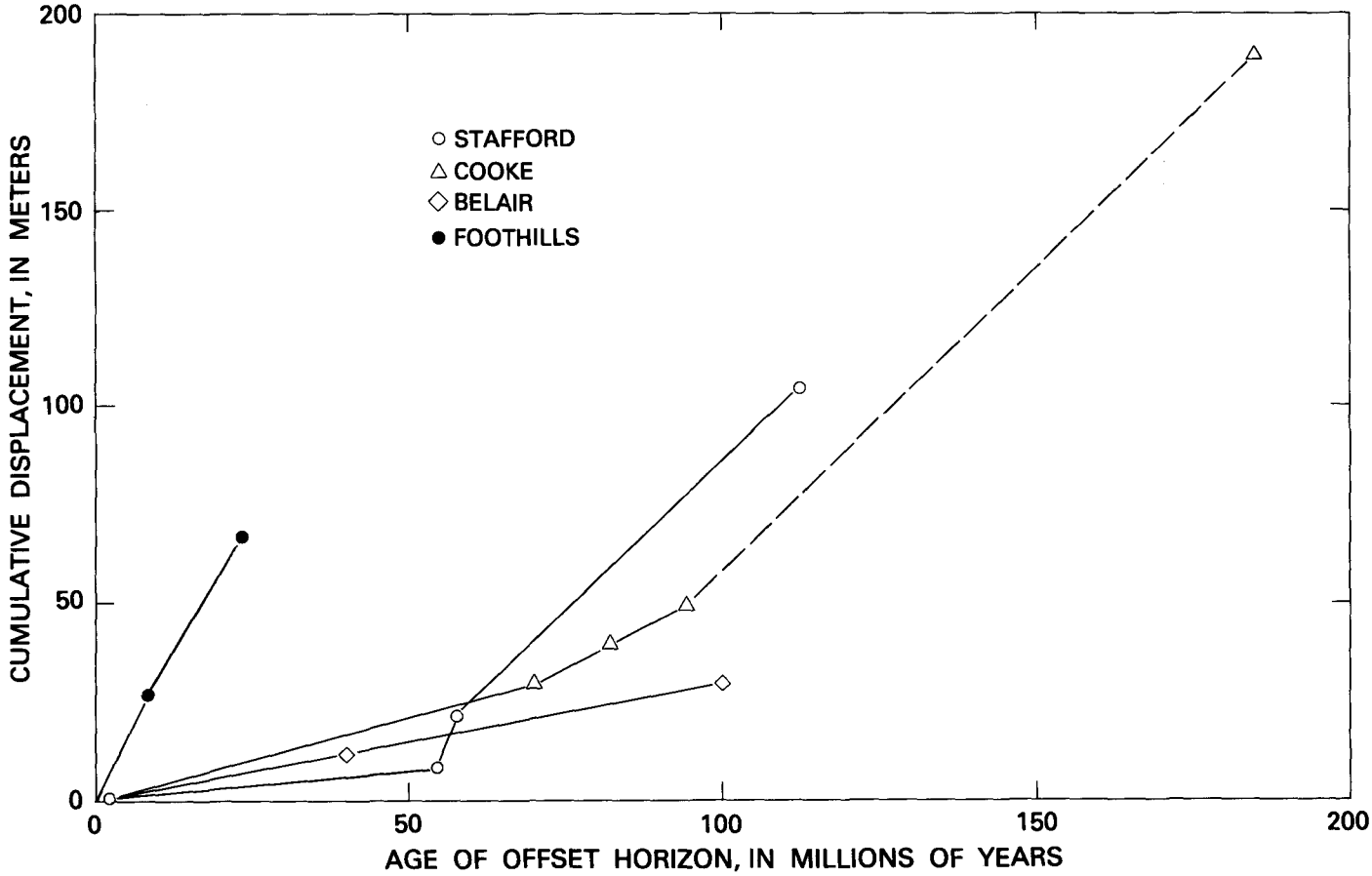

FIGURE 2.—Fault offset histories, showing age and displacement of marker horizons. Brooke structure of Stafford zone from Mixon and Newell (1978), Belair fault zone from Prowell and O'Connor (1978), Poorman Gulch fault in the Foothills fault system from Woodward-Clyde Consultants (1977), Cooke fault from Behrendt and others (1981), Hamilton and others (1983), and see text discussion; dashed line shows minimum pre-Late Cretaceous rate of offset.

Stafford zone is uncertain, simply because the offsets are so small. It is thus very difficult to test directly whether or not any movement has occurred across individual faults in the past several hundred thousand years.

Seismicity

Available seismologic information indicates that some reverse faults are moving and that reverse faults are capable of generating at least moderate earthquakes. Although the presence and geometry of earthquakes can indicate that a fault is moving, an absence of historic earthquakes does not mean that a fault is geologically inactive, only that it lacks historic movement. This fact, the relatively low frequency of earthquakes along the eastern seaboard, the scarcity of detailed studies, and inconsistencies in the data greatly limit application of seismologic evidence to the hypothesis.

The most compelling relation is presented by earthquakes along the Ramapo fault system, located west of New York City and about 400 km northeast of the Stafford fault zone. This 100-km-long fault system borders the early Mesozoic Newark basin on the northwest, strikes northeastward, and dips 60° to the southeast (Ratcliffe, 1980). No Cretaceous or Tertiary sediments are present to record its behavior during the past 100 m.y., and the Quaternary sediment that is present is very young. The current behavior of the fault system is indicated by the source mechanisms of numerous small earthquakes in the area and by the pattern of their hypocenters (Aggarwal and Sykes, 1978; Yang and Aggarwal, 1981). The focal-mechanism solutions show subhorizontal to gently plunging pressure axes and at least one north- to northeast-striking reverse focal plane, and the hypocenters define a southeast-dipping zone. Thus, contrary to its extensional movement in the early Mesozoic, the fault system is now moving in reverse fashion and is generating earthquakes at least as large as magnitude 3.3. Aggarwal and Sykes (1978) suggest that three intensity-VI and three intensity-VII

earthquakes reported in the greater New York area in the past 250 years may well have occurred on the same system, although the rather broad distribution of recent earthquakes recorded in the area (Chiburis and others, 1979) raises the possibility that other structures may be involved as well.

A magnitude-3.8, intensity-V to -VI earthquake occurred in 1973 near Wilmington, Del., in an area of previous earthquakes, including one of intensity VII (Sbar and others, 1975). The earthquake occurred at shallow depth beneath the northeast-trending lower reach of the Delaware River and produced an isoseismal pattern elongate northeastward along the Fall Line. A composite focal-mechanism solution determined from the main shock and five aftershocks indicates northwest-southeast compression, although the computed pressure axis plunges about 40°. One nodal plane indicates reverse dip-slip on a nearly vertical plane striking north-northeast, northwest side up. This plane (pl. 1) was preferred by Sbar and others over the alternate nearly horizontal plane because it is consistent with the northeast-trending Fall Line and other similar geologic trends and with the implied uplift of the Piedmont relative to the Coastal Plain.

In South Carolina, a small, shallow earthquake near Trenton in 1976 suggests northeasterly striking reverse faulting at a site 40 km northeast of the Belair fault zone (Talwani, 1977; Talwani and Tarr, written commun., 1979). A focal-mechanism solution yields a subhorizontal pressure axis and northeasterly striking reverse focal planes (pl. 1).

Recent work in the epicentral area of the 1886 Charleston earthquake (Tarr, 1977; Tarr and Rhea, 1983) has produced focal-mechanism solutions that suggest reverse faulting on both northwest and northeast trends (pl. 1). A magnitude-3.8 earthquake occurred there on November 22, 1974, the largest event since the South Carolina seismic network began operating in 1973. This yielded a focal-mechanism solution indicating northeast-southwest compression and a pressure axis plunging 40–50° (Tarr, 1977). The focal planes are both northwest-striking; one is subhorizontal and the other steeply southwest dipping. Tarr and Rhea (1983) have divided the well-located earthquakes that have been recorded through October 1979 into three groups (fig. 6) having internally consistent first-motion patterns. Composite focal-mechanism solutions for two of the groups (I and II) are similar to the 1974 solution. The steep, west-dipping focal planes are preferred by Tarr and Rhea because of the vertical pattern of hypocenters in northeast-southwest section. In contrast, the third focal mechanism (group III) has a pressure axis plunging 35° to the north and a subhorizontal and a steep north-northwest-dipping focal plane.

Microseismicity has been observed at four large reservoirs in the Southeast: North Anna reservoir, Virginia (Dames and Moore, 1976), and, in South Carolina, Monticello (Talwani and others, 1980), Clark Hill (Talwani and others, 1975; Guinn, 1980), and Jocassee (Talwani and others, 1980). For the most part, however, this seismicity is exceedingly shallow or geometrically inconsistent. The microseismicity at North Anna (Dames and Moore, 1976) extends to depths of at least 4 km and indicates compression oriented east-west to northwest-southeast. Composite focal-mechanism solutions have in common subhorizontal pressure axes and one focal plane orientation, which is northeast-striking and northwest-dipping (an average of N. 25° E., 60° NW.). If only one fault orientation is involved, this geometry is consistent with that of the westernmost strand of the Stafford fault zone (Dumfries fault), which is 35 km along strike to the northeast.

The coastal New England region southeast of the Appalachian Mountain highland also experiences small earthquakes that indicate generally northeast-trending reverse faulting. Of the 18 earthquakes in the area from eastern Connecticut to Maine studied by Graham and Chiburis (1980), 5 of the 7 that have reasonably good focal-mechanism solutions have subhorizontal pressure axes and north- to northeast-striking reverse focal mechanisms. For the two exceptions, in Rhode Island and southern New Hampshire, Yang and Aggarwal (1981) present focal-mechanism solutions with subhorizontal pressure axes and northeast-striking reverse focal mechanisms.

REUSE OF OLD DISCONTINUITIES

The Cretaceous-Cenozoic reverse faults may well reuse preexisting discontinuities in the crust. This possibility is raised by the general alinement of the reverse faults with the structural grain of the Appalachian orogen and the early Mesozoic basins. The early Mesozoic normal faults offer the best opportunity for reuse: they are properly oriented, abundant, and the most recent major faults in the region, and, as they are products of crustal extension during Atlantic rifting, they probably extend well into the crust.

The strongest evidence for reuse of early Mesozoic faults is the reverse movement associated with the Ramapo fault system indicated by recent earthquakes, because there the existence of the older faults is well documented (Ratcliffe, 1971, 1980). The corollary demonstration from field relations that these faults have moved during the Cretaceous and Cenozoic is prevented by the absence of stratigraphic control.

The Cretaceous-Cenozoic reverse faulting of the Brandywine zone in Virginia also seems to reuse an early Mesozoic border-fault system, as discussed by Mixon

and Newell (1977). The Brandywine zone is alined with faults of the Richmond basin (pl. 1), and continuity of faults across the intervening 80 km is suggested by an alined east-dipping gravity gradient. Red beds of the Richmond basin probably extend northeastward beneath the Coastal Plain cover, as indicated by drill-hole and geophysical evidence (Mixon and Newell, 1977); they were encountered in several holes near the Brandywine faults. There, the faults separate largely granitic basement on the northwest from largely red beds on the southeast (Jacobeen, 1972). This suggests local presence of an early Mesozoic border-fault system with offset down to the southeast, as well as continuity with the western boundary of the Richmond basin. The Stafford zone is similarly alined with the Farmville basin (pl. 1; Mixon and Newell, 1977), but local evidence for the presence and dip direction of an early Mesozoic fault along the Stafford zone is lacking.

About 30 km southeast of the Brandywine trend, Newell (written commun., 1979) reports another northeast-trending structure between the North Anna and Potomac Rivers, across which the shallow Coastal Plain section is monoclinally folded, down to the southeast. This structure lies close to the buried southeastern margin of the Richmond-Brandywine tongue of lower Mesozoic sedimentary rocks inferred from aeromagnetic data (Klitgord and Behrendt, 1979; Zietz and others, 1977; pl. 1). This relation could also reflect reuse of an early Mesozoic border-fault system. Similarly, the Cooke fault is adjacent to a northeast-trending early Mesozoic fault inferred principally from geophysical data, as discussed below.

The possibility of two other similar associations between buried early Mesozoic border faults and Coastal Plain faults has been raised by Daniels and others (1983) as an adjunct to their considerations of basement structure. Daniels and others (1983) suggest the presence beneath the Coastal Plain in western Georgia of a major west-trending boundary between Piedmont rocks and lower Mesozoic rocks and point out its possible association with the nearby Andersonville fault (pl. 1). This fault and nearby possible faults also trend westward and vertically offset lower Tertiary sediments as much as about 30 m, south side up (Owen, 1963; Zapp, 1965).

Daniels and Zietz (1978) had earlier suggested that faults reported in Coastal Plain sediments near Kinston, N. C., were related to the nearby northwest boundary of a buried early Mesozoic basin inferred from aeromagnetic data (pl. 1). These faults, proposed by Brown and others (1977), have vertical separations in Upper Cretaceous and lower Tertiary rocks that are largely up on the west, and they form a northeast-trending en-echelon pattern (the Graingers fault zone) having an inferred aggregate left slip of about 6.4 km.

A crude test of the significance of these spatial associations between Cretaceous-Cenozoic faults and early Mesozoic normal faults can be made by comparing the sense of vertical separation across the younger structures with the dip direction predicted from the older normal-fault relations. The early Mesozoic normal faults should dip toward the adjacent red-bed basins, so that subsequent reverse movement on the same structures should be up on the basin side, the relation demonstrated along the Ramapo fault. This is the case for the Brandywine, Cooke, and Andersonville faults and the monocline in Virginia, for all of which there is a local basis for inferring the direction of dip of the early Mesozoic faults. Brown and others (1977) do not consider the Graingers zone to be dip-slip, so perhaps it should not be included. Although the Stafford zone lies on strike with faults at the northwest end of the Farmville basin, there is no local control on the dip direction of any early Mesozoic faulting.

It is not necessary that reuse of old discontinuities be limited to early Mesozoic faults, nor have all early Mesozoic faults necessarily undergone reverse faulting. None of the exposed border faults can be demonstrated with available evidence to have undergone displacement similar to that of the Stafford zone, and many of the isolated fault exposures lack evidence concerning older faulting. Although the early Mesozoic faults may be preferred for reuse by the reverse faulting, other structural elements of the Appalachian orogen are also properly oriented and may be used as well.

If reuse of early Mesozoic normal faults is assumed to be common, the general abundance of Cretaceous-Cenozoic reverse faults can be estimated. Early Mesozoic faults are known along the borders of the exposed red-bed basins, and similar faults presumably occur in association with the buried basins as well (pl. 1). On the basis of magnetic depth estimates, Klitgord and Behrendt (1979) find northeast-trending horst and graben structure to characterize the whole of the offshore continental margin beneath the Jurassic postrift unconformity. These faults and basin boundaries, together with the locations of known Cretaceous-Cenozoic faults, typically have a lateral spacing of about 25 to 50 km and show few longitudinal gaps larger than 100 km. Early Mesozoic faults may also exist in areas now devoid of red beds. We would therefore expect the distribution of Cretaceous-Cenozoic faults to be approximated by a system of northeast-trending lines spaced 25 to 50 km apart, each line containing scattered gaps, some of which may be as long as 100 km.

SIERRAN FOOTHILL ANALOGY

The western foothills of the Sierra Nevada in California (fig. 3) show similarities to the southeastern Pied-

mont in framework geology and Cenozoic tectonics that, by analogy, reinforce parts of the reverse-fault hypothesis. Recent attention has been drawn to the foothills largely by the magnitude-5.7 Oroville earthquake in 1975, which involved normal faulting of several centimeters along a surface trace 3.8 km long, and concurrent plans for a major thin-arch dam in the region. In contrast to the recognized tectonic activity around the Sierran structural block (fig. 3), no active faults or seismic hazard had been anticipated in the foothills. The result of the recent interest has been much new work, both on the earthquakes and on the late Cenozoic tectonics of the region, on which the present discussion is based (Akers and McQuilkin, 1975; Bartow, 1980; Bufe and others, 1976; Cloud, 1976; Harwood and others, 1981; Lahr and others, 1976; Langston and Butler, 1976; U.S. Geological Survey Staff, 1978; Woodward-Clyde Consultants, 1977).

Like the Piedmont, the Sierran foothills consist of old metamorphic and intrusive rocks cut by Mesozoic faults, in this case thrusts of the Foothills fault system. In contrast to the situation in the Piedmont, however, Eocene and younger sedimentary and volcanic rocks in the foothills are locally preserved along old, west-draining valleys. Evidence of Cenozoic faulting is retained by these younger rocks, whereas in the rest of the crystalline terrain it has been obliterated by erosion. Offsets in the younger rocks indicate that normal faulting along preexisting faults has been underway since the Miocene but has accumulated relatively small offsets. The Cenozoic offsets occur across thin gouge and shear zones that follow the older faults in the crystalline rocks. This implies that such zones elsewhere in the crystalline terrain may also represent Cenozoic faults. Not all the older faults have been reused as normal faults, however, nor is the whole of any one older fault necessarily involved in the younger faulting.

The late Cenozoic offsets along the Foothills system range from 1 to 200 meters, but, away from the edge of the Basin and Range on the north, the offsets do not exceed several tens of meters. Evidence that offset has been cumulative since the Miocene exists locally, but in some places movement seems to have begun later. Locally preserved buried soils in colluvium record fault movements within the past 100,000 years. These paleo B soils, exposed in many exploratory trenches in various parts of the foothills, show offsets that range from barely perceptible to as much as 0.6 m. As an example of fault history in the Foothills system, offsets across the Poorman Gulch fault are shown in figure 2: 60–75 m in the past 23 m.y., 27 m in the past 4–12 m.y., and, in addition, apparent truncation of a paleo B soil.

The Foothills fault system has been marked by a scattering of small earthquakes and perhaps seven intensity-VI and three intensity-VII events in the past 125 years, including the intensity-VII Oroville earthquake (Cloud, 1976; Woodward-Clyde Consultants, 1977). In the context of the design and safety of the thin-arch Auburn dam, the fault system is considered capable of generating an earthquake as large as magnitude 6.5–7 (U.S. Geological Survey Staff, 1978).

The Sierran foothills and southeastern Piedmont are far from identical, but there is enough similarity to warrant drawing instructive analogies about regenerate fault behavior, recognition of Cenozoic faults, and seismogenic potential. The Foothills example suggests that much more evidence of Cenozoic faulting may be found in the scattered surficial deposits in the Piedmont but that trenching probably will be necessary. Little other direct evidence of Cenozoic faulting may exist, because scarps cannot be expected to survive, and Cenozoic and early Mesozoic shear and gouge zones in the Piedmont may be indistinguishable. In the Foothills, and probably in the Piedmont as well, regenerate faulting occurs selectively along preexisting faults and, despite relatively low average rates of offset, can be seismogenic.

COMPRESSIONAL DOMAIN ALONG THE ATLANTIC MARGIN

The Cretaceous-Cenozoic reverse faults indicate that parts of the Southeast have been undergoing northwest-southeast compression for at least 100 m.y. The youngest stratigraphic evidence indicates probably Pliocene or Quaternary movement, and earthquakes indicative of similarly oriented compression show that this regime is still in force. The dip of the faults to both the northwest and southeast requires that on a regional scale this compression be horizontal.

The extent of the domain subject to northwest-southeast compression, from the evidence of the reverse faults themselves, includes at least South Carolina and a band along the Fall Line from Georgia to Virginia. Earthquakes, together with the inferred reuse of early Mesozoic faults, suggest that much of the Atlantic margin from Georgia northeast through coastal New England is involved. Zoback and Zoback (1980), using in-situ stress measurements as well as earthquake focal mechanisms and Cenozoic faults, define an Atlantic Coast stress province under northwest-southeast compression that has a similar extent. The apparent axis of compression is approximately perpendicular to the continental margin and to Appalachian structure and topography (Diment and Urban, 1981) and approximately parallel to the early Atlantic spreading direction represented by the near-shore oceanic fracture zones (pl. 1). Thus there is a geometric coherence along the

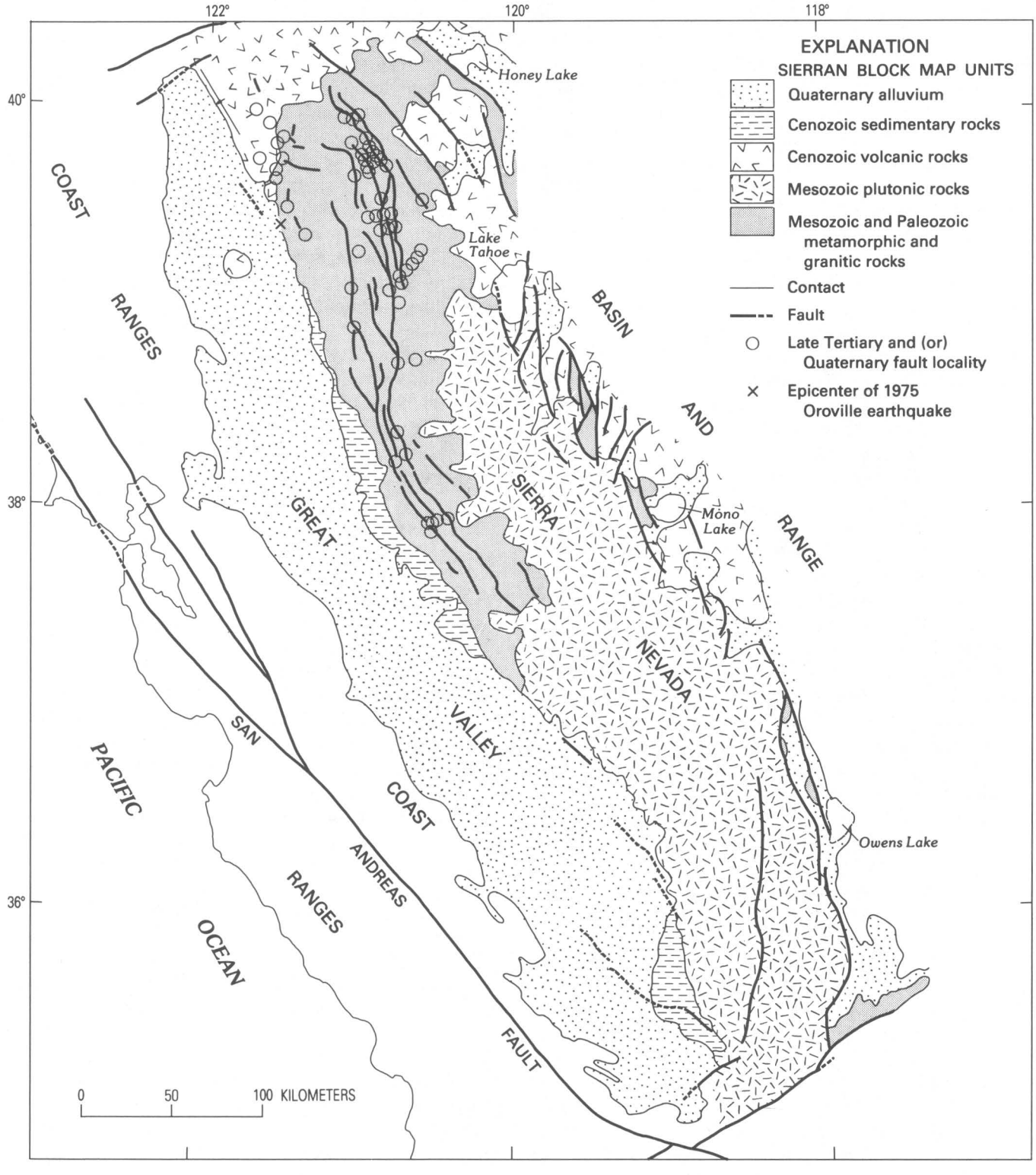

FIGURE 3.—Foothills fault system, points of known late Cenozoic offset, and setting within the westward tilted Sierran block. Details in Sierra Nevada foothills from Woodward-Clyde Consultants (1977, v. 1, fig. 34) and Jennings (1977); eastern Sierran front and general setting from King and Beikman (1974).

whole of the passive U.S. continental margin that implies a single tectonic system.

The lateral extent of the domain is difficult to estimate. Given the early Mesozoic horst-and-graben structure (Klitgord and Behrendt, 1979) that characterizes the offshore continental margin and the recent demonstration that reverse faults can be found offshore, we postulate that most or all of the offshore continental margin is involved. Northwest of the Fall Line, the distribution of the exposed early Mesozoic basins suggests that the domain extends at least as far as the eastern front of the Appalachian Mountains. West of the Appalachian front (and the Hudson-Champlain lowland in the northeast), Zoback and Zoback (1980) find east-west to southwest-northeast compression, although control on the location of the boundary between the two provinces is poor.

To characterize the Atlantic Coast domain of northwest-southeast compression, we combine the history of reverse faulting in the southeast, the source geometries of some modern earthquakes there and in the northeast, and the expectation that reverse faults are scattered diffusely throughout the domain. This yields a domain of scattered faults that have been moving in principally reverse fashion for at least 100 m.y. At least a modest strike-slip component is present on some faults as well, probably depending on fault orientation; this makes inference of the trend of the compression axis only approximate. The Cretaceous-Cenozoic faulting probably follows early Mesozoic faults to a considerable extent. As suggested by analogy with the Foothills fault system, however, the regenerate faulting is probably selective, involving only some of the preexisting faults, and probably only parts of those. The faulting has proceeded at low average rates of only about 1 m/m.y., which over 100 m.y. has produced cumulative vertical offsets on individual faults of only about 100 m or less. Evidence from the Stafford zone and from the Cooke fault (discussed below) suggests a generally decreasing rate of offset with time, so that Quaternary rates may be even lower.

REVERSE FAULTS AS EARTHQUAKE SOURCES

The reverse faults in the Atlantic Coast domain can be seismogenic, as indicated by the Ramapo activity and the existence of other earthquakes with northeast-striking, reverse source mechanisms. The numerous earthquakes of intensity V to VII and greater that have occurred in the Atlantic Coast domain (Coffman and von Hake, 1973) need structural explanation, although sources other than the northeast-trending reverse faulting could be involved as well. How large the earthquakes from the reverse faults can be is unknown. The faults are small, almost inconsequential by Western U.S. standards, although no larger faults with a history of Cenozoic movement have been found. Analogy with the Foothills fault system in California suggests, however, that relatively small faults can generate earthquakes at least as large as intensity VII. Aggarwal and Sykes (1978) suggest that the Ramapo system is capable of generating at least intensity-VII earthquakes, and we suggest that the intensity-X Charleston earthquake occurred on a northeast-trending reverse fault, as discussed below.

Not all early Mesozoic faults need be potential earthquake sources. The probable abundance of such faults, however, and the relatively close spacing of reverse faults demonstrated by recent work in Virginia suggest that seismogenic reverse faults occur in most parts of the Atlantic Coast domain. The historic absence of earthquakes in some parts of the domain may simply indicate that 200 to 300 years is too short a period to sample the long-term seismic behavior of the domain. The occurrence of Cretaceous-Cenozoic faults in some areas lacking historic seismicity, such as North Carolina, suggests this.

Of the alternative sources of earthquakes that have been proposed, the Appalachian décollement has the most direct relation to the reverse-fault hypothesis (Behrendt and others, 1981; Seeber and Armbruster, 1981). If the implication of recent proposals (Cook and others, 1979; Harris and Bayer, 1979) is carried to the limit, such a décollement could extend throughout the Atlantic Coast domain. Although there is no geologic evidence that such a décollement has moved at all since the Paleozoic, some of the early Mesozoic extension could have reused such a décollement as a sole, and the reverse faulting might be a shallow expression of more recent décollement movement in a compressional regime. It is also possible, however, that the early Mesozoic faulting and (or) the reverse faulting cut across and extended below any such décollement. Regardless, the existence of Cenozoic reverse faults and earthquakes with similar reverse source mechanisms and subhorizontal pressure axes indicates that reverse faults are producing earthquakes along the eastern seaboard.

1886 CHARLESTON EARTHQUAKE

The origin of the Charleston earthquake of 1886 is still uncertain. Despite its relatively large size (Bollinger, 1977, 1983), the careful field investigation following the earthquake found no surface offset on the low swampy ground of the meizoseismal area (Dutton, 1889). The shallowest rocks in which the earthquake could have originated are buried beneath a kilometer-thick layer of Cretaceous and Cenozoic Coastal Plain sediments, which are nearly flat-lying and lack major faults or other

conspicuous local structure. As a result, information bearing on the specific structural origin of the earthquake must come largely from drilling and geophysics, interpreted in the context of the regional geologic setting.

Various origins have been proposed for the earthquake. The relative isolation of Charleston seismicity on the Coastal Plain has tempted consideration of some unique, but unspecified, tectonic source. Charleston seismicity can be viewed as part of a northwest-trending zone of earthquakes that extends from Charleston to the Blue Ridge (Bollinger, 1973). Sykes (1978) argues that the earthquake was related to an old northwest-trending crustal feature that had localized the development of the Blake Spur fracture zone when Atlantic spreading began, although no such feature is known. The Charleston earthquake has been attributed to stress concentration around or within mafic or high-density rock masses, which are inferred from gravity and magnetic data to occur beneath the Coastal Plain near Charleston (Kane, 1977; Long and Champion, 1977; McKeown, 1978). Taber (1914) proposes a buried northeast-trending fault on the basis of 1886 intensity data, and Bollinger (1983) reaches a similar conclusion. Northeast-trending Paleozoic and early Mesozoic faults in the exposed Piedmont 150 km to the northwest have led to suggestions that similar faults beneath the Charleston epicentral area may have been responsible. The recently proposed décollement beneath the Appalachian orogen has been suggested to be the earthquake source (Behrendt and others, 1981; Seeber and Armbruster, 1981). Tarr (1977) and Tarr and Rhea (1983), on the basis of focal-mechanism solutions for recent small earthquakes in the 1886 meizoseismal area, suggest that the Charleston earthquake resulted from reverse faulting in a regional stress field with maximum horizontal compressive stress oriented northeast-southwest.

Most of these hypotheses involve little or no information about local structure and the Cenozoic geologic history of the region. The presence of the 1886 epicenter within the best documented part of the Atlantic Coast domain suggests northeast-trending reverse faulting as the source of the 1886 earthquake. Evidence in the meizoseismal area for an early Mesozoic fault system and the recent discovery there of Cretaceous-Cenozoic reverse faulting reinforce this view.

Meizoseismal Area

The meizoseismal area of the 1886 earthquake lies immediately northwest of the city of Charleston, S. C., and is bisected by the Ashley River (fig. 4). Bollinger (1977) draws a simple egg-shaped figure around the intensity-X effects that is about 50 km long and 30 km wide and elongate northeast-southwest. The original isoseismal patterns of Dutton and of Sloan, although more intricate, are also elongate along a northeast-trending axis that is approximately coincident with a line connecting the two points of highest intensity (epicentrums of Dutton, 1889). The principal difference between Dutton's and Sloan's patterns—the reentrant at the northern end—results from their differing conclusions on whether the general absence of higher intensity indicators there was real or simply due to having few objects available to express the intensity (Dutton, 1889). Much of the meizoseismal area is low swampy ground, whereas a Pleistocene barrier beach in the northwest part causes that area to stand about 15 m higher. Because much of the intensity evidence consisted of sand boils and damage related to liquefaction, local ground conditions may have distorted the intensity pattern.

Bollinger (1983) sought indications of the orientation of the causative fault for the 1886 earthquake from the intensity data. He concluded that the northeast elongation of the inner 1886 isoseismals suggests a northeast fault strike, inasmuch as the elongation of at least the innermost isoseismals for an earthquake tends to mimic the fault trend. Comparison of the broader 1886 isoseismal pattern with those of the 1954 Fairview Peak and 1971 San Fernando earthquakes led him to the same conclusion.

Structure

The Charleston meizoseismal area lies within a region that is distinct from exposed Piedmont to the northwest and that is considered to represent a lower Mesozoic extensional terrain (Gohn and others, 1978; Popenoe and Zietz, 1977; Daniels and Zietz, 1978). Some local basins within this buried lower Mesozoic terrain (Daniels and others, 1983), the exposed early Mesozoic basins in the Piedmont (King and Beikman, 1974), and similar structures offshore (Klitgord and Behrendt, 1979) are characterized by northeast-trending boundaries between the basin fill and adjacent basement.

Northeast-trending basement structure is also present in the meizoseismal area, as shown by the refraction results of Ackermann (1983). The surface of crystalline basement in the Charleston area (figs. 4, 5; table 1) defines a northeast-trending high that has a moderately sloping southeast flank and an abrupt, 900-m downward step along its northwest margin. A red-bed section is inferred to fill the deep on the northwest; its upper part extends across the high to be encountered in Clubhouse Crossroads test hole 3 (CC#3). The steep northwest margin of the basement high would thus represent an early Mesozoic normal fault or fault system displaced down to the northwest.

Above the lower Mesozoic red beds and basalt, both refraction and reflection seismic profiling show the J horizon (table 1) in the area of figure 4 to be a nearly featureless surface that slopes seaward at about 7.5 m/km (Ackermann, 1983; Behrendt and others, 1981). However, this surface is slightly offset, down to the east, in several places within the meizoseismal area (fig. 4), as demonstrated by a reflection survey designed to achieve high resolution in the upper few kilometers of section (Behrendt and others, 1981). Three principal reflectors are involved, B, J, and K (table 1). The offsets are expressed in the seismic records largely as irregular monoclinal bends as wide as a kilometer or more, but these probably represent faulting, at least at greater depth. Some of the offsets extend with decreasing magnitude up into the overlying Coastal Plain section, indicating continued movement at least into the early Tertiary (fig. 4).

The east-northeast-striking Cooke fault (fig. 4) appears in the seismic records as a steep reverse fault, down to the southeast, within a wider zone of associated deformation (Behrendt and others, 1981; Hamilton and others, 1983). The zone offsets B about 190 m, J about 50 m, K about 40 m, and a younger horizon about 30 m. This younger horizon probably lies in the uppermost Peedee Formation (about 70 m.y.), on the basis of data from Yantis and others (1983) and its position relative to K (Hazel and others, 1977). The movement history to achieve a cumulative offset of 50 m at the top of the basalt is 10 m in the 12 m.y. between J and K (0.8 m/m.y.), 10 m in the 13 m.y. between K and the younger reflector (0.8 m/m.y.), and 30 m in the 70 m.y. since latest Peedee time (0.4 m/m.y.), if movement has continued to the present (fig. 2). There is no documented stratigraphic evidence of offset in the Eocene and younger section, where irregular unconformities and near absence of post-Oligocene sediments complicate the record.

The 190-m offset of the B horizon poses an apparent contradiction, because 140 m of offset preceding extrusion of the 184-m.y.-old basalt places reverse faulting within the early Mesozoic extensional regime. A hiatus of about 90 m.y. separates the top of the basalt from the base of the overlying Coastal Plain section, during which time extensive erosion should have occurred. It is reasonable that the 140 m of fault displacement occurred during this hiatus but that the resultant offset at the top of the basalt was planed off by erosion. The offset and 140-m difference in basalt thickness would then be evident only at the base of the basalt. Of the 50 m of offset now evident at the top of the basalt, 10 m predated the K horizon. This must largely or entirely postdate initiation of Coastal Plain sedimentation or it, too, should have been destroyed by erosion.

We can thus add to the movement history of the Cooke fault 140 m of reverse movement in the 90-m.y. hiatus above the basalt, which represents a minimum rate of 1.6 m/m.y. The long-term average rate of offset for the fault is approximately 1 m/m.y., but, as for the Stafford fault, offsets across the several stratigraphic intervals indicate that the rate has decreased with time (fig. 2).

This structure in the Charleston meizoseismal area is the same kind as that characterizing the Atlantic Coast domain. The Cooke fault strikes east-northeastward, as indicated by Behrendt and others (1981), lies close to an early Mesozoic fault of similar trend, and has a sense of offset consistent with reuse of the older structure. The offset is small but has been cumulative through the Late Cretaceous and early Tertiary.

The interpretation that the 140-m offset of the B horizon across the Cooke fault postdates the basalt provides the closest control yet available on the timing of the reversal from extension in the early Mesozoic to the compression of the Atlantic Coast domain. The reverse faulting began between 184 and 95 m.y. ago. Unless the early rate of movement was four times higher than that in the Late Cretaceous, however, the shift must have occurred in the Jurassic and possibly soon after extrusion of the basalt.

The spatial correlation between reverse faulting and the step in the basement surface in the meizoseismal area is only approximate (figs. 4, 5). The two isolated fault localities having Cenozoic offset seem to lie directly above the basement step, rather than up-dip from it, and the Cooke fault and the pre-Cenozoic fault lie southeast of any reasonable up-dip extension of a simple steep border fault. If early Mesozoic faults are controlling the specific locations of the reverse faulting, then they must be present off the main basement boundary as well as along it. This is not unreasonable, as the border fault system may involve splays and subordinate faults that either are masked by the smoothing inherent in refraction work or involve post-red-bed offsets too small to be resolved.

The documented basement fault and the Cenozoic faults lie in the northwest third of the meizoseismal area, rather than near its center (fig. 4). Ground conditions could have caused this eccentricity by localizing the damage away from the source, either the Cooke fault or another nearby fault. Alternatively, the source of the 1886 earthquake could be about 10 km southeast of the Cooke fault. In this central part of the meizoseismal area, Ackermann's refraction work (1983) shows the basement surface to be smoothly inclined to the southeast at about 10 m/km, and no significant vertical offsets are evident in COCORP line 2, although reflections in the vicinity of 1 second are irregular and discontinuous (Schilt and others, 1983).

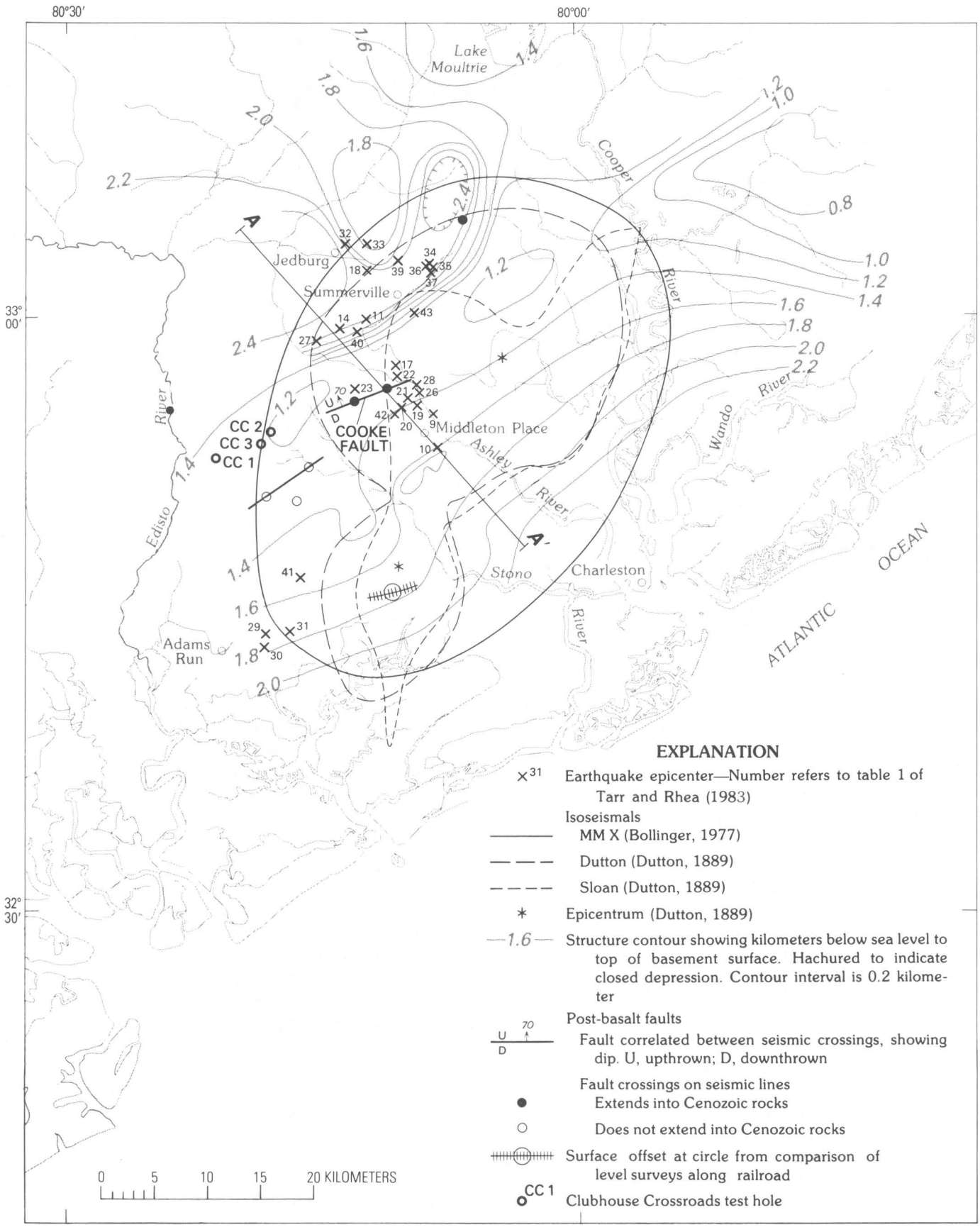
80°30′
80°00′
33° 00′
32° 30′
Lake Moultrie
Cooper River
Jedburg
Summerville
Middleton Place
COOKE FAULT
CC 2
CC 3
CC 1
Ashley River
Wando River
Edisto River
Stono River
Charleston
Adams Run
OCEAN
ATLANTIC
A
A′
0 5 10 15 20 KILOMETERS
EXPLANATION
Earthquake epicenter—Number refers to table 1 of Tarr and Rhea (1983)
Isoseismals
MM X (Bollinger, 1977)
Dutton (Dutton, 1889)
Sloan (Dutton, 1889)
Epicentrum (Dutton, 1889)
Structure contour showing kilometers below sea level to top of basement surface. Hachured to indicate closed depression. Contour interval is 0.2 kilometer
Post-basalt faults
Fault correlated between seismic crossings, showing dip. U, upthrown; D, downthrown
Fault crossings on seismic lines
Extends into Cenozoic rocks
Does not extend into Cenozoic rocks
Surface offset at circle from comparison of level surveys along railroad
Clubhouse Crossroads test hole

TABLE 1.—*Major stratigraphic horizons and intervals near Charleston*

[K, J, and B are principal seismic reflectors; J and B mark the tops of refraction intervals characterized by the velocities shown. Compiled from Behrendt and others, 1981; Gohn and others, 1977; Hazel and others, 1977; Ackermann, 1983; Lanphere, 1983; Schilt and others, 1983; Yantis and others, 1983]

Horizon	Interval velocity	Description
Surface	2.0 km/s	Coastal Plain section, ½–1 km thick, principally Oligocene to Late Cretaceous in age, base at CC#1 is Cenomanian. K is correlated in CC#1 with a velocity contrast near the Campanian-Santonian boundary (approximately 82 m.y. old).
K		
Base of Cretaceous section		Approximate age 94 m.y. old.
Top of basalt (J)	4.2–5.8 km/s	Major hiatus and unconformity. Basalt over red beds; at CC#3 basalt is 257 m thick, underlain by at least 120 m of red beds, which in places may reach J where basalt seems to be missing. Age of basalt determined by $^{40}Ar/^{39}Ar$ method is 184±3.3 m.y. (Lanphere, 1983).
Top of basement (B)	6.0–6.4 km/s	Presumed crystalline basement predating Atlantic rifting; identity somewhat ambiguous, at least in places, as basalt within red-bed section might produce similar reflections and velocities, and layered reflections are locally observed below B.

It is intriguing that 20 mm of differential vertical offset of the ground surface, east side down, reported by Lyttle and others (1979) from comparison of 1963 and 1974 first-order level surveys, occurs along the railroad just south of the southern 1886 epicentrum (fig. 4). This raises the possibility that surface deformation has been occurring along the axis of the 1886 meizoseismal area, perhaps from some form of afterslip or slow upward propagation of the main-shock offset through the Coastal Plain section.

Recent Seismicity

Recent small earthquakes in the Charleston meizoseismal area, as relocated by Tarr and Rhea (1983), form a diffuse north-trending zone about 20 km long and 10 km wide and range in depth from near surface to about 15 km (figs. 4, 5, 6). No single, simple source zone is evident in the three-dimensional pattern of hypocenters (fig. 6), although errors in location may have dispersed a tighter pattern of sources.

The earthquakes are considered to be aftershocks of the 1886 main shock (Tarr, 1977; Bollinger, 1983) and may indicate the depth of the main shock. Bollinger (1983) suggests that the 1886 intensity pattern permits a shallow focus, and there is no evidence requiring a deeper one. It is not necessary, however, that the recent earthquakes represent either the geometry or the specific location of the 1886 source. Like the basement step and Cenozoic faults, the recent earthquakes are eccentric to the center of the meizoseismal area (fig. 4), and there is no means of tying them with certainty to the specific 1886 source.

The three composite focal-mechanism solutions determined by Tarr and Rhea (1983) yield conflicting source geometries, which prevent direct inference of a regional stress orientation. Two of the solutions yield pressure axes plunging 35° and 45° to the south-southwest, and one yields a pressure axis plunging 35° to the north. Combining the focal mechanisms and the three-dimensional pattern of hypocenters, Tarr and Rhea (1983) conclude that northwest-striking reverse faulting has occurred on two steeply-dipping planes represented by hypocenter groups I and II (fig. 6). Group III, in contrast, represents east-northeast-striking reverse faulting, down to the south, if the steep focal plane is selected. The latter is consistent with the geometry of the Cooke fault.

In order to further test the possible relation of these earthquakes to the northeast-trending basement step and the younger faults, a cross section (fig. 5) was drawn approximately normal to the structures and the axis of the meizoseismal zone. The group-III source (earthquakes 11, 14, and 27), in addition to yielding a source geometry consistent with the Cooke fault, lies about 15 km down-dip from it. Behrendt and others (1981) find a 70° dip for the Cooke fault above about 3 km; correlation of the group-III source with the Cooke fault yields a similar 60° dip.

Inspection of figure 5 and the stereographic presentation of hypocenters in figure 6 demonstrates that, within their location uncertainties, all the earthquakes except those in the southern group can lie on two northeast-

FIGURE 4.—Meizoseismal area of the 1886 Charleston earthquake. Isoseismals from Bollinger (1977), Dutton (1889, pl. 26) and Sloan (*in* Dutton, 1889, pl. 27): isoseismals shown for Dutton and Sloan are their outermost complete lines, for which no values were given. Plotting on the modern base map is only approximate and depends principally on distances along railroads and rivers. Basement surface from Ackermann (1983). Faults from Behrendt and others (1981). Earthquakes through December 1979 of location quality A to C from Tarr and Rhea (1983). Surface offset indicated by level surveys from Lyttle and others (1979).

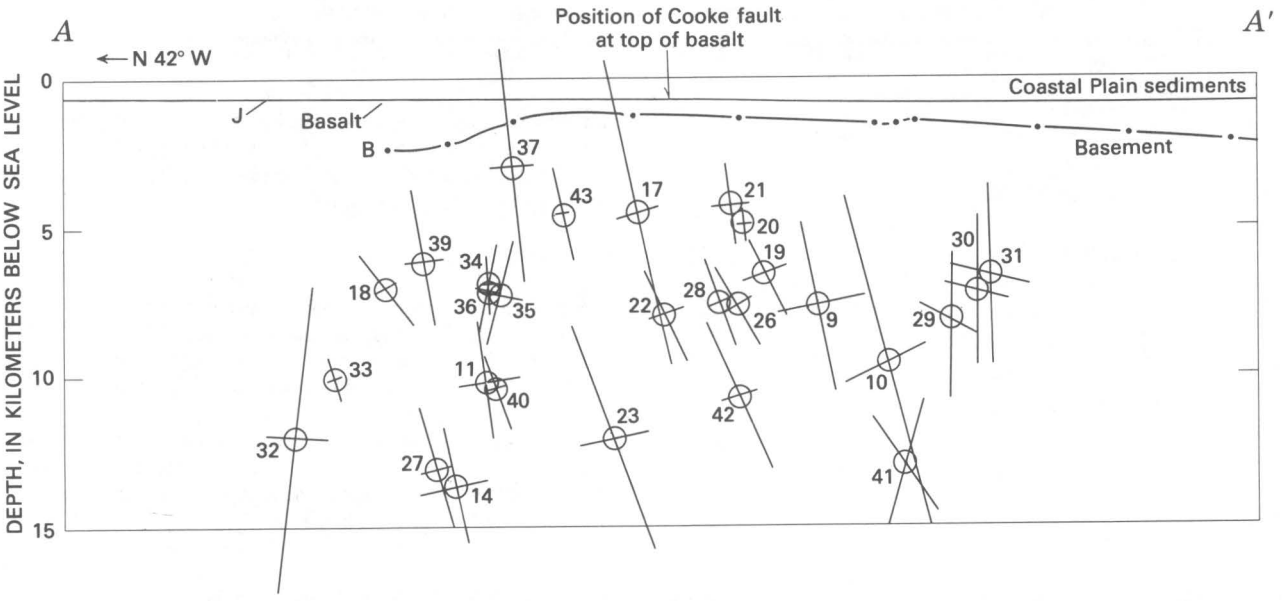

FIGURE 5.—Northwest-southeast cross section through 1886 Charleston meizoseismal area. See figure 4 for section line; scale is 2× scale of figure 4. Basalt and basement surfaces from Ackermann (1983). Cooke fault from Behrendt and others (1981); J and B as in table 1. Earthquake hypocenters from Tarr and Rhea (1983); numbers are keyed to their table 1. Bars represent axes of location-error ellipses projected into section.

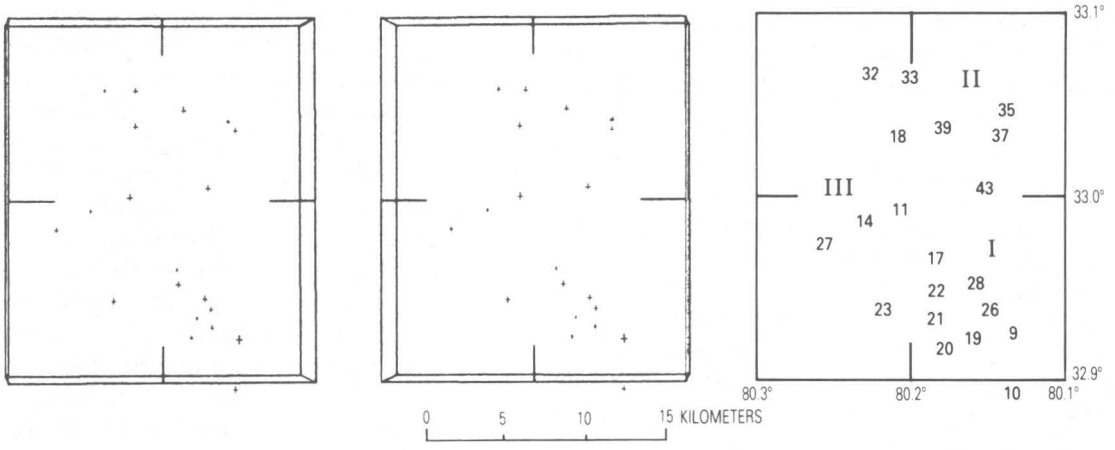

FIGURE 6.—Stereogram of recent earthquake hypocenters (1974–79) in the Middleton Place–Summerville zone, Charleston area, South Carolina. Shows hypocenters of earthquakes of location quality A to C through January 1979 and magnitude 2.9 event of December 7, 1979, from Tarr and Rhea (1983); numbers are keyed to their table 1; roman numerals identify their three groups of hypocenters. Vertical view from altitude of 250 km; top of box at ground surface, bottom at depth of 10 km. Stereogram prepared by C. E. Johnson and P. T. German.

striking, northwest-dipping surfaces, one passing through group III and the Cooke fault and one about 5 km above that surface. Although this organization would be consistent with northeast-trending structure, it would require ignoring the focal-mechanism results for group II.

The focal-mechanism solutions for earthquake groups I and II suggest that northwest-trending structures are present in the meizoseismal area. The hypocenters in these groups can be viewed as forming very steep west-northwest-trending zones (fig. 6). Northwest-trending mafic dikes are present in the region (Daniels and Zietz, 1978), and Schilt and others (1983) found a suggestion of possibly northwest-striking basement structure where COCORP reflection line 3 crosses the Ashley River.

One means of resolving the conflict in source mechanisms is to infer that the horizontal stresses are approximately equal (Zoback and Zoback, 1980) in the

area in which the regional stress field has been perturbed by the strain release of the 1886 main shock. The northwest-southeast compression typical of the Atlantic Coast domain would not yet have been restored, and the geometries of continuing aftershock adjustments would be sensitive both to existing structures and to the effects of preceding adjustments.

Source of the Main Shock

The Cenozoic regional setting of the Charleston earthquake is one of scattered northeast-trending reverse faults. Faults of this style have been documented west of Charleston near the Fall Line and to the southeast offshore, as well as in the 1886 meizoseismal area itself. This kind of fault in the Atlantic Coast domain can be seismogenic and probably has produced earthquakes at least as large as intensity VII. No other faults having a record of Cenozoic movement have been found in the area. Analysis of some of the recent small earthquakes in the meizoseismal area suggests that movement on east-northeast-trending reverse faults is occurring, at least as part of the aftershock adjustments, and the 1886 intensity pattern suggests a northeast strike to the main-shock source. We thus conclude, in a fashion similar to that suggested by Bollinger (1983), that northeast-trending reverse faulting produced the 1886 earthquake, but that many of the recent aftershocks seem to be occurring on northwest-trending structure, probably in response to temporary changes in the local stress field resulting from the strain released in the main shock.[2]

Exploration is still incomplete in the meizoseismal area, and the Cooke fault may only be representative of the structure there. The facts that the Stafford and Belair fault zones consist of several faults and that other Cenozoic offsets exist in the meizoseismal area make it reasonable that a system of northeast-trending reverse faults exists in the meizoseismal area. If the Cooke fault was not the 1886 source, a possibility raised by its position eccentric to the meizoseismal area, some similar nearby fault (or faults) probably was.

DISCUSSION

Beginning with geologic structure and history, we conceive a tectonic behavior for the whole of the eastern seaboard on the basis of the principal mode of Cenozoic faulting known in the region. We argue that an Atlantic Coast domain of northwest-southeast compression and resulting reverse faulting has existed since at least the early Cretaceous and that reverse-fault movements in the domain can account for much of its seismicity, including the 1886 Charleston earthquake, although other mechanisms may be at work as well. In constructing the hypothesis, we have been guided by the expectations that geologic history is not capricious and that the history of the passive Atlantic margin has been generally consistent in its details as well as in outline. Thus, for example, we have combined fault histories in Virginia and South Carolina with earthquakes in New Jersey and New England to determine a coherent tectonic style and history for the whole domain.

The most important implication of the hypothesis is the possibility that earthquakes as large as the 1886 event are not limited to Charleston. If that earthquake did occur on a northeast-trending reverse fault, then similar earthquakes should be possible wherever such faults are present and still active. We infer that the reverse faults have a common history of movement extending from the Mesozoic through the present and argue that they are scattered essentially throughout the region no more than a few tens of kilometers apart. The result is that large damaging earthquakes should be possible in most parts of the Atlantic Coast domain.

The potential for surface faulting in the domain is not clear, although the record along the Stafford zone, in particular, indicates that offset near or at the surface has occurred in the past. The thickness of sediment overlying hard rock is probably a key factor in determining whether or how the faulting will be expressed at the surface. Monoclinal folding rather than discrete faulting in the thick Coastal Plain section, for example, might account for the lack of surface faulting in the meizoseismal area at the time of the 1886 earthquake. Because the displacement expectable in a million years or less across a single fault is very small, it is unlikely that evidence of offset will be found along most faults that have moved in the late Quaternary. Furthermore, the absence of such evidence, except where the late Quaternary record is exceedingly clear, cannot demonstrate that offset has not occurred.

The northwest-southeast compression of the Atlantic Coast domain is an important element in the postrift

---

[2]Talwani (1982, written commun., 1982) has developed an internally consistent interpretation of the recent earthquakes in the Charleston meizoseismal area that involves strike-slip faulting. By simultaneously inverting phase data for the better located earthquakes and several explosions, he computed a new crustal-velocity model and new hypocentral locations and then reexamined focal mechanisms. Like Tarr and Rhea (1983), he obtained composite solutions consistent with northwest-trending reverse faulting for the shallower earthquakes, but for earthquakes deeper than 8 km, which form a north-northeast-striking map trend 25 km long, he obtained a composite strike-slip solution with a right-lateral focal plane that also strikes north-northeast. The pressure axes for both strike-slip and reverse solutions are similar, subhorizontal and trending N. 60°E.

This interpretation would remove the modest support from the northeast-trending focal-mechanism solution of Tarr and Rhea (1983) for a northeast-trending reverse fault origin of the 1886 earthquake. A strike-slip origin involving northeast-southwest compression suffers, however, from inconsistency with the northwest-southeast compression inferred from the regional Cenozoic deformation pattern. A continuing problem is the difficulty of demonstrating a direct relation between the recent earthquakes and the specific structure(s) responsible for the 1886 earthquake. We reiterate our suggestion that post-1886 earthquakes in the Charleston area may be occurring in a stress field not yet recovered from the perturbation of the 1886 strain release, we continue to expect the source of the 1886 earthquake to be consistent with regional geological relations, which in the Cretaceous and Cenozoic are characterized by northeast-trending reverse faulting.

history of the Atlantic margin. Following the extension that resulted in Atlantic rifting about 190 m.y. ago, the trailing continental margin has sagged and accumulated a mantling wedge of sediment upon the depressed postrift unconformity. In addition, at some time between rifting and the beginning of the Coastal Plain record about 100 m.y. ago, the continental margin was placed in compression approximately perpendicular to its length. Our interpretation of Cooke fault offsets indicates that the transition from extension to compression may have occurred soon after rifting was accomplished. Ever since, the compression has driven small reverse faults, which we suggest are scattered throughout the Atlantic Coast domain.

The source of the compression is unknown, although the perpendicular relation between the compression axis and the Appalachian orogen, the continental margin, and the Jurassic axis of Atlantic spreading suggests that one or more of these is involved. A causal relation between the compression and something associated with the continental margin is implicit in our argument. The possibility that the compression began soon after rifting, and the decrease in rates of reverse faulting through time indicated by Stafford and Cooke fault offsets, suggests an inverse relation between the general rate of faulting and the duration of Atlantic spreading.

REFERENCES CITED

Ackermann, H. D., 1983, Seismic-refraction study in the area of the Charleston, South Carolina, 1886 earthquake, *in* Gohn, G. S., ed., Studies related to the Charleston, South Carolina, earthquake of 1886–Tectonics and seismicity: U.S. Geological Survey Professional Paper 1313, p. F1–F20.

Aggarwal, Y. P., and Sykes, L. R., 1978, Earthquakes, faults, and nuclear power plants in southern New York and northern New Jersey: Science, v. 200, no. 4340, p. 425–429.

Akers, R. J., and McQuilkin, M. J., 1975, Geologic investigation of the Oroville earthquake, *in* Oroville, California earthquake 1 August 1975: California Division of Mines and Geology Special Report 124, p. 45–52.

Bartow, J. A., 1980, Constraints on the latest movements on the Melones fault zone, Sierra Nevada foothills, California: U.S. Geological Survey Professional Paper 1126–J, p. J1–J4.

Behrendt, J. C., Hamilton, R. M., Ackermann, H. D., and Henry, V. J., 1981, Cenozoic faulting in the vicinity of the Charleston, South Carolina, 1886 earthquake: Geology, v. 9, no. 3, p. 117–122.

Behrendt, J. C., Hamilton, R. M., Ackermann, H. D., Henry, V. J., and Bayer, K. C., 1983, Marine multichannel seismic-reflection evidence for Cenozoic faulting and deep crustal structure near Charleston, South Carolina, *in* Gohn, G. S., ed., Studies related to the Charleston, South Carolina, earthquake of 1886–Tectonics and seismicity: U.S. Geological Survey Professional Paper 1313, p. J1–J29.

Bollinger, G. A., 1973, Seismicity and crustal uplift in the southeastern United States: American Journal of Science, v. 273–A, p. 396–408.

———1977, Reinterpretation of the intensity data for the 1886 Charleston, South Carolina, earthquake, *in* Rankin, D. W., ed., Studies related to the Charleston, South Carolina, earthquake of 1886–A preliminary report: U.S. Geological Survey Professional Paper 1028, p. 17–32.

———1983, Speculations on the nature of seismicity at Charleston, South Carolina, *in* Gohn, G. S., ed., Studies related to the Charleston, South Carolina, earthquake of 1886–Tectonics and seismicity: U.S. Geological Survey Professional Paper 1313, p. T1–T11.

Brown, P. M., Brown, D. L., Shufflebarger, T. E., Jr., and Sampair, J. L., 1977, Wrench-style deformation in rocks of Cretaceous and Paleocene age, North Carolina Coastal Plain: North Carolina Division of Earth Resources Special Publication 5, 47 p.

Bufe, C. G., Lester, F. W., Lahr, K. M., Lahr, J. C., Seekins, L. C., and Hanks, T. C., 1976, Oroville earthquakes: normal faulting in the Sierra Nevada foothills: Science, v. 192, no. 4234, p. 72–74.

Carr, M. S., 1950, The District of Columbia, its rocks and their geologic history: U.S. Geological Survey Bulletin 967, 59 p.

Chiburis, E. F., Ahner, R. O., and Graham, Timothy, 1979, Seismicity of the northeastern United States, January-March, 1979: Weston Observatory, Boston College, Northeastern U.S. Seismic Bulletin No. 14, fig. 3, Earthquake epicenters during the period October 1975-March 1979.

Cloud, W. K., 1976, Report on evaluation of seismic data in the Auburn Dam area: U.S. Bureau of Reclamation, Order 6–01–DP–01220, 23 p.

Coffman, J. L., and von Hake, C. A., editors, 1973, Earthquake history of the United States, revised edition (through 1970): National Oceanic and Atmospheric Administration Publication 41–1, 208 p.

Cook, F. A., Albaugh, D. S., Brown, L. D., Kaufman, Sidney, Oliver, J. E., and Hatcher, R. D., Jr., 1979, Thin-skinned tectonics in the crystalline southern Appalachians; COCORP seismic-reflection profiling of the Blue Ridge and Piedmont: Geology, v. 7, no. 12, p. 563–567.

Dames and Moore, 1976, Summary report on the in-progress seismic monitoring program at the North Anna site, January 21, 1974, through May 1, 1976: report submitted to Virginia Electric and Power Company (Vepco), representing results of the seismographic study required of Vepco by the Nuclear Regulatory Commission (then Atomic Energy Commission) in 1973 as Question 2.28 to the Preliminary Safety Analysis Report for North Anna 3 and 4 power reactors, 117 p.

Daniels, D. L., and Zietz, Isidore, 1978, Geologic interpretation of aeromagnetic maps of the Coastal Plain region of South Carolina and parts of North Carolina and Georgia: U.S. Geological Survey Open-File Report 78–261.

Daniels, D. L., Zietz, Isidore, and Popenoe, Peter, 1983, Distribution of subsurface lower Mesozoic rocks in the Southeastern United States as interpreted from regional aeromagnetic and gravity maps, *in* Gohn, G. S., ed., Studies related to the Charleston, South Carolina, earthquake of 1886–Tectonics and seismicity: U.S. Geological Survey Professional Paper 1313, p. K1–K24.

Dillon, W. P., Klitgord, K. D., and Paull, C. K., 1983, Mesozoic development and structure of the continental margin off South Carolina, *in* Gohn, G. S., ed., Studies related to the Charleston, South Carolina, earthquake of 1886–Tectonics and seismicity: U.S. Geological Survey Professional Paper 1313, p. N1–N16.

Diment, W. H., and Urban, T. C., 1981, An average elevation map of the conterminous United States: U.S. Geological Survey Geophysical Investigations Map GP–933, scale 1:2,500,000.

Dutton, C. E., 1889, The Charleston earthquake of August 31, 1886: U.S. Geological Survey Ninth Annual Report, 1887–88, p. 203–528.

Godson, R. H., 1981, Digital terrain map of the United States: U.S. Geological Survey Miscellaneous Investigations Map I–1318, scale 1:7,500,000.

Gohn, G. S., Gottfried, David, Lanphere, M. A., and Higgins, B. B., 1978, Regional implications of Triassic or Jurassic age for basalt and sedimentary red beds in the South Carolina Coastal Plain: Science, v. 202, no. 4370, p. 887–890.

Gohn, G. S., Higgins, B. B., Smith, C. C., and Owens, J. P., 1977, Lithostratigraphy of the deep corehole (Clubhouse Crossroads corehole 1) near Charleston, South Carolina, *in* Rankin, D. W., ed., Studies related to the Charleston, South Carolina, earthquake of 1886–A preliminary report: U.S. Geological Survey Professional Paper 1028, p. 59–70.

Graham, Timothy, and Chiburis, E. F., 1980, Fault plane solutions and the state of stress in New England: Earthquake Notes, v. 51, no. 2, p. 3–12.

Guinn, S. A., 1980, Earthquake focal mechanisms in the southeastern United States: U.S. Nuclear Regulatory Commission, NUREG/CR-1503, 164 p.

Hamilton, R. M., Behrendt, J. C., and Ackermann, H. D., 1983, Land multichannel seismic-reflection evidence for tectonic features near Charleston, South Carolina, *in* Gohn, G. S. ed., Studies related to the Charleston, South Carolina, earthquake of 1886–Tectonics and seismicity: U.S. Geological Survey Professional Paper 1313, p. I1–I18.

Harris, L. D., and Bayer, K. C., 1979, Sequential development of the Appalachian orogen above a master decollement–a hypothesis: Geology, v. 7, no. 12, p. 568–572.

Harwood, D. S., Helley, E. J., and Doukas, M. P., 1981, Geologic map of the Chico monocline and the northeastern part of the Sacramento Valley, California: U.S. Geological Survey Miscellaneous Investigations Map I–1238, scale 1:62,500.

Hazel, J. E., Bybell, L. M., Christopher, R. A., Frederiksen, N. O., May, F. E., McLean, D. M., Poore, R. Z., Smith, C. C., Sohl, N. F., Valentine, P. C., and Witmer, R. J., 1977, Biostratigraphy of the deep corehole (Clubhouse Crossroads corehole 1) near Charleston, South Carolina, *in* Rankin, D. W., ed., Studies related to the Charleston, South Carolina, earthquake of 1886–A preliminary report: U.S. Geological Survey Professional Paper 1028, p. 71–89.

Howard, K. A., and others, 1978, Preliminary map of young faults in the United States as a guide to possible fault activity: U.S. Geological Survey Miscellaneous Field Studies Map MF–916, scale 1:5,000,000.

Inden, R. F., and Zupan, A. W., 1975, Normal faulting of upper Coastal Plain sediments, Ideal Kaolin Mine, Langley, South Carolina: South Carolina Development Board, Division of Geology, Geologic Notes, v. 19, no. 4, p. 161–165.

Jacobeen, F. H., Jr., 1972, Seismic evidence for high-angle reverse faulting in the Coastal Plain of Prince Georges and Charles Counties, Maryland: Maryland Geological Survey Information Circular 13, 21 p.

Jennings, C. W., 1977, Geologic map of California: California Division of Mines and Geology, scale 1:750,000.

Kane, M. F., 1977, Correlation of major eastern earthquake centers with mafic/ultramafic basement masses, *in* Rankin, D. W., ed., Studies related to the Charleston, South Carolina, earthquake of 1886–A preliminary report: U.S. Geological Survey Professional Paper 1028, p. 199–204.

King, P. B., and Beikman, H. M., compilers, 1974 [1975], Geologic map of the United States: U.S. Geological Survey, scale 1:2,500,000.

Klitgord, K. D., and Behrendt, J. C., 1979, Basin structure of the U.S. Atlantic margin, *in* Watkins, J. S., Montadert, Lucien, and Dickerson, P. W., eds., Geological and geophysical investigations of continental margins: American Association of Petroleum Geologists Memoir 29, p. 85–112.

Lahr, K. M., Lahr, J. C., Lindh, A. G., Bufe, C. G., and Lester, F. W., 1976, The August 1975 Oroville earthquakes: Seismological Society of America Bulletin, v. 66, no. 4, p. 1085–1099.

Langston, C. A., and Butler, Rhett, 1976, Focal mechanism of the August 1, 1975 Oroville earthquake: Seismological Society of America Bulletin, v. 66, no. 4, p. 1111–1120.

Lanphere, M. A., 1983, $^{40}Ar/^{39}Ar$ ages of basalt from Clubhouse Crossroads test hole #2 near Charleston, South Carolina, *in* Gohn, G. S., ed., Studies related to the Charleston, South Carolina, earthquake of 1886–Tectonics and seismicity: U.S. Geological Survey Professional Paper 1313, p. B1–B8.

Long, L. T., and Champion, J. W., Jr., 1977, Bouguer gravity map of the Summerville-Charleston, South Carolina, epicentral zone and tectonic implications, *in* Rankin, D. W., ed., Studies related to the Charleston, South Carolina, earthquake of 1886–A preliminary report: U.S. Geological Survey Professional Paper 1028, p. 151–166.

Lyttle, P. T., Gohn, G. S., Higgins, B. B., and Wright, D. S., 1979, Vertical crustal movements in the Charleston, South Carolina–Savannah, Georgia area: Tectonophysics, v. 52, p. 183–189.

McKeown, F. A., 1978, Hypothesis: many earthquakes in the central and southeastern United States are causally related to mafic intrusive bodies: U.S. Geological Survey Journal of Research, v. 6, no. 1, p. 41–50.

Mixon, R. B., and Newell, W. L., 1976, Preliminary investigation of faults and folds along the inner edge of the Coastal Plain in northeastern Virginia: U.S. Geological Survey Open-File Report 76–330, scale 1:24,000.

———1977, Stafford fault system: structures documenting Cretaceous and Tertiary deformation along the Fall Line in northeastern Virginia: Geology, v. 5, no. 7, p. 437–440.

———1978, The faulted Coastal Plain margin at Fredericksburg, Virginia–Guidebook for Tenth Annual Virginia Geology Field Conference, October 13–14, 1978: Reston, Va., 50 p.

Mixon, R. B., Southwick, D. L., and Reed, J. C., Jr., 1972 [1973], Geologic map of the Quantico quadrangle, Prince William and Stafford Counties, Va., and Charles County, Md: U.S. Geological Survey Geologic Quadrangle Map GQ–1044, scale 1:24,000.

Newell, W. L., Prowell, D. C., and Mixon, R. B., 1976, Detailed investigation of a Coastal Plain–Piedmont fault contact in northeastern Virginia: U.S. Geological Survey Open-File Report no. 76–329, 14 p.

O'Connor, B. J., Carpenter, R. H., Paris, T. A., Hartley, M. E., and Denman, H. E., 1974, Recently discovered faults in the central Savannah River area [abs.]: Georgia Academy of Science Bulletin, v. 32, no. 1–2, p. 15.

O'Connor, B. J., and Prowell, D. C., 1976, The geology of the Belair fault zone and basement rocks of the Augusta, Georgia area: Georgia Geologic Society Guidebook 16, p. 21–32.

Owen, Vaux, Jr., 1963, Geology and ground-water resources of Lee and Sumter Counties, southwest Georgia: U.S. Geological Survey Water-Supply Paper 1666, 70 p.

Popenoe, Peter, and Zietz, Isidore, 1977, The nature of the geophysical basement beneath the Coastal Plain of South Carolina and northeastern Georgia, *in* Rankin, D. W., ed., Studies related to the Charleston, South Carolina, earthquake of 1886–A preliminary report: U.S. Geological Survey Professional Paper 1028, p. 119–137.

Prowell, D. C., 1976, Implications of Cretaceous and post-Cretaceous faults in the eastern United States [abs.]: Geological Society of America Abstracts with Programs, v. 8, no. 1, p. 249–250.

———1982, Index of Cretaceous and Cenozoic faults in the Eastern United States: U.S. Geological Survey Miscellaneous Field Studies Map MF–1269.

Prowell, D. C., and O'Connor, B. J., 1978, Belair fault zone: evidence of Tertiary fault displacement in eastern Georgia: Geology, v. 6, no. 11, p. 681–684.

Ratcliffe, N. M., 1971, The Ramapo fault system in New York and adjacent northern New Jersey; a case of tectonic heredity: Geological Society of America Bulletin, v. 82, no. 1, p. 125–142.

——1980, Progress report on northeastern U.S. seismicity and tectonics, *in* Turner, M. L., compiler, Summaries of technical reports, volume IX, prepared by participants in National Earthquake Hazards Reduction Program: U.S. Geological Survey Open-File Report No. 80–6, p. 83.

Sbar, M. L., Jordan, R. R., Stephens, C. D., Pickett, T. E., Woodruff, K. D., and Sammis, C. G., 1975, The Delaware–New Jersey earthquake of February 28, 1973: Seismological Society of America Bulletin, v. 65, no. 1, p. 85–92.

Schilt, F. S., Brown, L. D., Oliver, J. E., and Kaufman, Sidney, 1983, Subsurface structure near Charleston, South Carolina–Results of COCORP reflection profiling in the Atlantic Coastal Plain, *in* Gohn, G. S., ed., Studies related to the Charleston, South Carolina, earthquake of 1886–Tectonics and seismicity: U.S. Geological Survey Professional Paper 1313, p. H1–H19.

Seeber, Leonardo, and Armbruster, J. G., 1981, The 1886 Charleston, South Carolina earthquake and the Appalachian decollement: Journal of Geophysical Research, v. 86, no. B9, p. 7874–7894.

Seiders, V. M., and Mixon, R. B., 1981, Geologic map of the Occoquan quadrangle and part of the Fort Belvoir quadrangle, Prince William and Fairfax Counties, Virginia: U.S. Geological Survey Miscellaneous Investigations Map I–1175, scale 1:24,000.

Sykes, L. R., 1978, Intraplate seismicity, reactivation of preexisting zones of weakness, alkaline magmatism, and other tectonism postdating continental fragmentation: Reviews of Geophysics and Space Physics, v. 16, no. 4, p. 621–688.

Taber, Steven, 1914, Seismic activity in the Atlantic Coastal Plain near Charleston, South Carolina: Seismological Society of America Bulletin, v. 4, p. 108–160.

Talwani, Pradeep, 1977, Recent earthquakes in the South Carolina Coastal Plain and their tectonic significance [abs.]: Geological Society of America Abstracts with Programs, v. 9, no. 2, p. 189.

——1982, The Woodstock fault is alive and ticking near Charleston, S. C.: EOS, American Geophysical Union Transactions, v. 63, no. 6, p. 155.

Talwani, Pradeep, Rastogi, B. K., and Stevenson, Don, 1980, Induced seismicity and earthquake prediction studies in South Carolina: Tenth Technical Report to U.S. Geological Survey, Contract No. 14–08–0001–17670, 212 p.

Talwani, Pradeep, Secor, D. T., and Scheffler, P., 1975, Preliminary results of aftershock studies following the 2 August 1974 South Carolina earthquake: Earthquake Notes, v. 46, no. 4, p. 21–28.

Tarr, A. C., 1977, Recent seismicity near Charleston, South Carolina, and its relationship to the August 31, 1886, earthquake, *in* Rankin, D. W., ed., Studies related to the Charleston, South Carolina, earthquake of 1886 –A preliminary report: U.S. Geological Survey Professional Paper 1028, p. 43–57.

Tarr, A. C., and Rhea, Susan, 1983, Seismicity near Charleston, South Carolina, March 1973 to December 1979, *in* Gohn, G. S., ed., Studies related to the Charleston, South Carolina, earthquake of 1886 Tectonics and seismicity: U.S. Geological Survey Professional Paper 1313, p. R1–R17.

U.S. Geological Survey, 1977, Preliminary report on Belair Exploratory Trench No. 10–76 near Augusta, Georgia: U.S. Geological Survey Open-File Report no. 77–411, 20 p.

U.S. Geological Survey Staff, 1978, Technical review of earthquake evaluation studies of the Auburn Dam area (Woodward-Clyde Consultants, 1977) –a report to the U.S. Bureau of Reclamation: U.S. Geological Survey Administrative Report, July 1978, 143 p.

Wentworth, C. M., and Mergner-Keefer, Marcia, 1981a, Regenerate faults of small Cenozoic offset—Probable earthquake sources in the southeastern United States: U.S. Geological Survey Open-File Report 81–356, 37 p.

———1981b, Reverse faulting and potential for large earthquakes along the eastern seaboard, *in* Beavers, J. M., ed., Earthquakes and earthquake engineering: the eastern United States: Ann Arbor Science Publishers, Earthquake Engineering Research Institute and others, proceedings of conference, September 14–16, 1981, Knoxville, Tenn., v. 1, p. 109–128.

Woodward-Clyde Consultants, 1977, Earthquake evaluation studies of the Auburn Dam area: Contract Number 6/07/D5/72090, Auburn-Folsom South Unit, Central Valley Project, California, for the U.S. Bureau of Reclamation, 8 volumes.

Yang, Jih-Ping, and Aggarwal, Y. P., 1981, Seismotectonics of northeastern United States and adjacent Canada: Journal of Geophysical Research, v. 86, no. B6, p. 4981–4998.

Yantis, B. R., Costain, J. K., and Ackermann, H. D., 1983, A reflection seismic study near Charleston, South Carolina, *in* Gohn, G. S., ed., Studies related to the Charleston, South Carolina, earthquake of 1886–Tectonics and seismicity: U.S. Geological Survey Professional Paper 1313, p. G1–G20.

York, J. E., and Oliver, J. B., 1976, Cretaceous and Cenozoic faulting in eastern North America: Geological Society of America Bulletin, v. 87, no. 8, p. 1105–1114.

Zapp, A. D., 1965, Bauxite deposits of the Andersonville district, Georgia: U.S. Geological Survey Bulletin 1199–G, 37 p.

Zietz, Isidore, Calver, J. L., Johnson, S. S., and Kirby, J. R., 1977 [1978], Aeromagnetic map of Virginia, in color: U.S. Geological Survey Geophysical Investigations Map GP–916, scale 1:1,000,000.

Zoback, M. L., and Zoback, Mark, 1980, State of stress in the conterminous United States: Journal of Geophysical Research, v. 85, no. B11, p. 6113–6156.

Speculations on the Nature of Seismicity at Charleston, South Carolina

By G. A. BOLLINGER

STUDIES RELATED TO THE CHARLESTON, SOUTH CAROLINA, EARTHQUAKE OF 1886—TECTONICS AND SEISMICITY

GEOLOGICAL SURVEY PROFESSIONAL PAPER 1313-T

UNITED STATES GOVERNMENT PRINTING OFFICE, WASHINGTON: 1983

CONTENTS

ILLUSTRATIONS

TABLE

STUDIES RELATED TO THE CHARLESTON, SOUTH CAROLINA, EARTHQUAKE OF 1886—
TECTONICS AND SEISMICITY

SPECULATIONS ON THE NATURE OF SEISMICITY AT CHARLESTON, SOUTH CAROLINA

By G. A. BOLLINGER[1]

ABSTRACT

The data base for the Charleston, S. C., seismicity consists of Dutton's study (1889) of the 1886 earthquake, information on historical and recent earthquakes from many sources, and the results of 6 years of instrumental monitoring by a statewide network. These data are considered in conjunction with results from seismic studies in other areas in an attempt to infer source information for the 1886 shock.

The Charleston area is an unusual locale in the Southeastern United States. What is known concerning pre-1886 South Carolina seismicity suggests that most of the activity may have been concentrated in the Charleston vicinity. The post-1886 activity does show a concentration there. Additionally, this area is the only such seismically active locale in the Atlantic Coastal Plain province. The temporal characteristics of the post-1886 seismicity suggest that the aftershock process is probably not over. Focal-mechanism studies of recent events show steeply dipping nodal planes that have a northwest strike. Statewide, the seismicity changes from a clustering habit in nonmetamorphic "basement" terrane to a diffuse habit in metamorphic basement terrane.

Given a body-wave magnitude (m_b) estimate of 6.7 for the 1886 earthquake (derived from intensity studies), published scaling relations allow order-of-magnitude estimation of the parameters for the event: fault length = 25 km, fault width = 12 km, average slip = 1 m. (A surface-wave magnitude of 7 and a stress drop of 100 bars are assumed in the above estimates.)

Relationships between the strike of surface ruptures and (or) focal-mechanism nodal planes and the trend of the innermost isoseismal contour for selected earthquakes are interpreted to favor, although not conclusively, a northeast-trending causal fault for the 1886 shock. The strong vertical motions reported in the 1886 meizoseismal area indicate dip-slip fault movement.

A single source zone localized by intersecting structures is suggested as the cause of both the current Charleston-area seismicity and the 1886 earthquake. The faulting in 1886 was probably on a northeast-trending structure, whereas the current activity is on a northwest-trending structure. The geological-geophysical data base to date gives evidence for structures along both trends but does not allow selection among them.

INTRODUCTION

The purpose of this study is to bring the results of studies in other seismic regions to bear on the interpretation of the data base available for the 1886 Charleston, S. C., earthquake. This is effected primarily by means of published scaling relations for earthquake source parameters and by a detailed consideration of the relationships between the strike of an active fault and (or) focal-mechanism nodal planes and the orientation of intensity patterns. The data base for South Carolina seismicity consists of intensity maps for the 1886 and subsequent shocks, some information on the aftershock sequence, data on the spatial distribution of seismic energy release throughout the State, the results from recent geophysical and geological studies, and the data from several years of monitoring by a statewide seismic network.

Acknowledgments.—The author extends his sincere appreciation to the reviewers of this paper: James W. Dewey, W. H. Diment, Marcia Mergner-Keefer, Susan Rhea, Carl M. Wentworth, and an anonymous referee. Their efforts caused me to rethink and, in some instances, to revise my original interpretations. Moreover, they markedly improved the clarity of exposition and brought several omissions to my attention. This research was funded in part by the Earth Sciences Section, National Science Foundation, NSF Grant DES75-14691-AO1 and in part by the Nuclear Regulatory Commission, Grant NRC-04-077-134.

PRE-1886 SEISMICITY

An extensive archival study of the pre-1886 seismicity of South Carolina was made by Bollinger and Visvanathan (1977). They found that the State was not aseismic before the 1886 intensity-X shock, and they divided the 18 possible events noted between 1698 and 1886 into two groups, one clustered around Charleston and one scattered in the northwestern (Piedmont) half of the State. If the assumption is made that those pre-1886 shocks reported only from Charleston (or for

[1]U.S. Geological Survey and Virginia Polytechnic Institute and State University, Blacksburg, VA 24061.

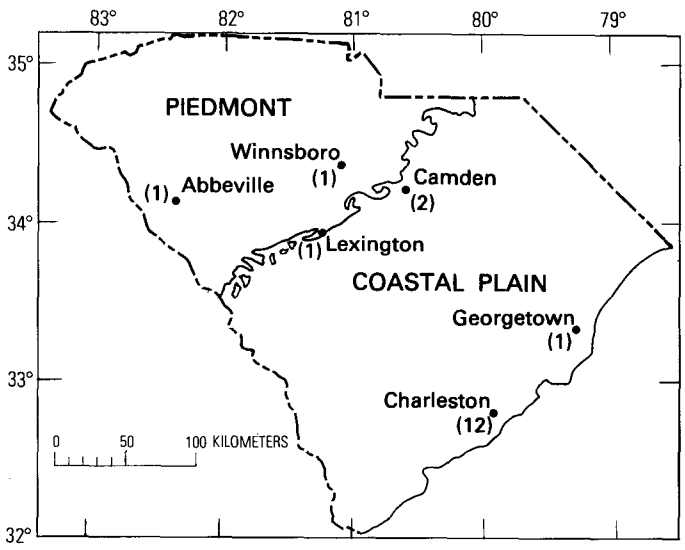

FIGURE 1.—Pre-1886 seismicity of South Carolina (Bollinger and Visvanathan, 1977). Numbers in parentheses indicate the number of events that may have taken place near the indicated town or city.

which Charleston had among the highest reported intensities) were indeed centered nearby, then the distribution shown in figure 1 results. This distribution is obviously speculative, as the epicenters of the pre-1886 "Charleston" shocks can probably not be estimated to within a hundred kilometers. Too, the early development of a large population center at Charleston could bias the earliest portions of the written record. However, subsequent to the 1886 event, similar distributions (clustering in the Charleston area) are shown in the seismic frequency contours on Hadley and Devine's (1974) seismotectonic map of the Eastern United States (1800–1972) and on Bollinger's (1973) seismicity map of the Southeastern United States (1920–1970).

Thus, the Charleston area appears to be a seismically unique locale in the Coastal Plain province of the Southeastern United States. That is, it is the only locale in that province to have experienced an earthquake large enough to perturb the stress regime for nearly a century. The pre-1886 South Carolina seismicity also could have been concentrated in the Charleston-Summerville area. Clearly, such a concentration would be an insufficient basis on which to predict an imminent large earthquake, but it could suggest that the locale was atypical before the 1886 shock.

THE 1886 EVENT

Fortunately, the effects of the 1886 shock were well studied and reported by Dutton (1889). Recently, Dutton's intensity data were reinterpreted by Bollinger (1977). In the absence of seismographic recordings, these data, on the distribution of intensity in the source area and throughout the Eastern United States, constitute virtually all the available source information.

Source Parameters

From the attenuation with distance of the 1886 shock's intensity, Nuttli and others (1978) have derived a body-wave magnitude (m_b) estimate of 6.6. They also studied the area encompassed by the intensity-IV isoseismal and obtained an m_b of 6.9. Thus, from the Modified Mercalli intensity distribution, some measure of the size of the 1886 shock can be determined. This is an important parameter, from which others can be derived by means of published scaling relations (Geller, 1976; Kanamori and Anderson, 1975). Before these scaling relations can be applied, an estimate of the surface-wave magnitude (M_s) is required. Given an m_b of, say, 6.7 for the 1886 event, published conversion formulas give M_s values of 6.3 (Geller, 1976), 6.7 (Gutenberg and Richter, 1956), 6.9 (Gupta and Rastogi, 1972), 7.1 (O. W. Nuttli, oral commun., 1978), 7.4 (Basham, 1969), and 8.0 (Nagamune, 1972, given in Geller, 1976). The average value is 7.1, and I choose $M_s = 7 \pm 0.5$ as representative.

Kanamori and Anderson (1975) used M_s, seismic moment (M_o), and fault area (S) data from 41 worldwide earthquakes ($5.8 \leq M_s \leq 8.5$) in conjunction with crack theory and dynamic dislocation theory to relate magnitude to other source parameters. In particular, they developed relationships between M_s, M_o, S, and stress drop ($\Delta\sigma$). Also, they suggested that a stress drop of 100 bars is appropriate for intraplate earthquakes (defined as shocks whose fault planes were not along plate boundaries, even though they may have occurred near a boundary). There is a scatter of about half an order of magnitude (a factor of 3) in the intraplate stress-drop data about the 100-bar value.

Given estimates of M_s and $\Delta\sigma$, the values of M_o, S, and average fault slip ($\bar{D}$) can be inferred. However, to specify the scatter present in the basic data sets involved, all calculations will be made for $M_s = 6.5$, 7.0, and 7.5 and for $\Delta\sigma = 30$, 100, and 300 bars. In the following paragraphs, the preferred results—for $M_s = 7$, $\Delta\sigma = 100$—will be given first. Following these preferred values, the extremes of the values resulting from all the other determinations will be given in parentheses.

The scaling relations of Kanamori and Anderson (1975) imply a preferred M_o of $10^{25.7}$ dyne-cm ($10^{24.4}$, $10^{27.1}$). These M_o and $\Delta\sigma$ values in turn imply a fault area of 100 km^2 (10 km^2, 1000 km^2). Dip-slip crack theory (Starr, 1928) assumes length (l) equal to width (w), which yields a 10 km × 10 km fault plane (3 × 3 km, 30 × 30 km) in this case. Results from circular fault theory (Starr, 1928) give a fault diameter of 11 km (6 km, 36 km). Use of the relationship $M_o = \mu S \bar{D}$, in which the seismic moment (M_o) is expressed as a function of the

average fault slip ($\bar{D}$) and where μ is the rigidity (3×10^{11} dyne/cm^2), gives an average slip of 1.7 m (0.01 m, 420 m) for both extremes.

Geller (1976) also studied the scaling relations between earthquake source parameters and magnitude. He used the same 41-earthquake data base and interplate-intraplate classification as did Kanamori and Anderson (1975). There is some overlap between the two studies, but the main objective of Geller's study was to develop empirical relations between m_b, M_s, l, w, and other parameters. His basic approach was to consider logarithmic fault parameters and to develop trends, not exact correlations. Geller (1976) found empirically that fault length l (parallel to strike) and fault width w (perpendicular to strike) were related by $l = 2w$; there is scatter in the data of about a factor of 2. He also found that $\log S = M_s - 4.53$ (for $6.76 \leq M_s \leq 8.12$), which gives a fault area of 300 km^2 (90 km^2, 900 km^2) for $M_s = 7$ (6.5, 7.5). Because $l = 2w$, those values yield a fault length of about 24 km (14 km, 44 km) and width of about 12 km (7 km, 22 km). When these values are used in the calculation, $M_o = \mu S\bar{D}$ gives an average slip of 1 m (0.01 m, 45 m).

I chose a fault length of 24 km, a fault width of 12 km, and a fault slip of 1 m as reasonable approximations for the 1886 South Carolina shock. Clearly, these estimates are not tightly controlled. However, the long dimension of the intensity-X isoseismal was some 50 km (Bollinger, 1977), which allows the 24-km fault length selected. The strong, predominantly vertical ground motions in the meizoseismal area (primarily at Summerville, S. C.; Dutton, 1889) would allow, but not require, 1 m of dip-slip fault movement.

Type of Faulting

Slemmons (1977) has reviewed and updated the relations between magnitude and surface faulting parameters. However, given the uncertainty in the m_b-to-M_s conversion and the scatter present in Slemmons's data base, it is not possible to use those relations to infer a preferred faulting mode for the 1886 event.

Intraplate shocks whose measured or estimated source parameters (Geller, 1976) correspond approximately to those inferred for the 1886 South Carolina earthquake are given in table 1. These earthquakes occurred in tectonic environments that are almost certainly very different from that at Charleston. The table includes cases of strike-slip, reverse, and mixed fault motions but no observed case of normal or predominately normal faulting. Within the list, there is no preference for a particular mode of faulting versus source parameters. Thus this type of comparison also provides no insight into the type of faulting that occurred in 1886 at Charleston.

Orientation of Faults

Intensity patterns have been used in some instances to infer the approximate length and strike of earthquake faults. The qualitative nature of intensity data necessarily makes such approximations also qualitative. There are exceptions to the fault strike–isoseismal trend correspondence (Richter, 1958, p. 143), and certainly the effects of local soils, water-table levels, surficial geology, and tectonic fabric are very important.

Isoseismal elongation in the direction of faulting is most clearly seen in cases of strike-slip fault movement. A recent, well-documented example for a different mode of faulting (predominately thrust) is the 1971 San Fernando, Calif., earthquake. For that event, there was excellent agreement between the observations of surface faulting, the strike of the focal-mechanism nodal planes, and the trend of the innermost isoseismals (VIII–X and VII) (Allen and others, 1973; Dillinger, 1973; Scott, 1973; Yerkes, 1973).

Less well controlled examples of fault strike–isoseismal trend agreement for cases of mixed normal–strike-slip faulting are the 1954 Nevada earthquakes (July 6, August 23, December 16). For those shocks, both the

TABLE 1.—*List of intraplate earthquakes whose measured or estimated source parameters (Geller, 1976) correspond approximately to those inferred for the 1886 South Carolina earthquake*

[--, data not given in Geller (1976)]

Date	Place	Body-wave magnitude	Surface-wave magnitude	Seismic moment ($\times 10^{26}$)	Stress drop (bars)	Length of fault plane (km)	Width of fault plane (km)	Average fault slip (m)	Type of faulting
1886	South Carolina	6.7	7.0	1.0	100	25	12	1.0	Unknown
1933	Japan	--	6.75	.7	59	20	10	1.0	Predominately strike-slip
1943	Do.	--	7.4	3.6	99	33	13	2.5	Strike-slip
1945	Do.	--	7.1	.9	140	12	11	2.5	Predominately reverse
1948	Do.	--	7.3	3.3	100	30	13	2.0	Strike-slip
1954	Nevada	--	7.1	1.3	100	36	6	2.0	Mixed
1961	Japan	--	7.0	.9	170	12	10	2.5	Do.
1964	Spain	7.1	6.2	1.3	11	95	10	.4	Reverse
1969	Japan	6.6	5.5	.4	35	18	10	.6	Strike-slip
1971	California	6.2	6.6	1.2	62	20	14	1.4	Predominately reverse

surface ruptures and the innermost isoseismal (VII or VII–VIII) had northerly trends (Murphy and Cloud, 1956). However, due to the sparse population of the region, those isoseismals are not well determined. This points up other qualitative factors in the determination of intensity: the population density of the region and the subjectivity of the interpreter. In the case of the Nevada earthquakes, it would be difficult not to define a meizoseismal area trending in the direction of the spectacular surface breaks. However, given dense data (for example, for the San Fernando earthquake), we can find instances of innermost isoseismals trending in agreement with the strike of a causal fault that is not strike-slip.

An example of the complexity that can arise between isoseismal elongation and major geologic structural trends is the Kern County, Calif., earthquake of July 21, 1952 (M_s = 7.7). For that shock, the lower level isoseismals (V and less) are elliptical in a northwest-southeast direction, parallel to the trend of the San Andreas system (Murphy and Cloud, 1954), whereas the causal White Wolf fault trends northeast-southwest. However, the two innermost isoseismals (VIII–IX and VII) have a north-south trend that is not too different from the northeast-trending White Wolf fault. Therefore, in this instance, the innermost isoseismals are somewhat similar in trend to the strike of the fault, whereas the shape of the lower level isoseismals is more influenced by the regional tectonic fabric.

Although there was extensive craterlet development in the epicentral area of the 1886 shock, no surface faulting as such was identified by Dutton (1889) and his co-workers. The greatest horizontal extent of these craterlets, plus railroad track and building damage (intensity-X effects), was approximately 50 km (Bollinger, 1977), in a northeast-southwest direction. A northeast-trending causal fault for the 1886 earthquake could, therefore, be inferred. However, this would place the 1886 fault strike and the apparent northwesterly trend of modern seismicity (network results, Tarr and Rhea, 1983) at right angles to each other. It is possible to explain this by cross-faulting or modern activity on a secondary fault, but the possibility of a northwest-striking causal fault should also be considered. Cases for and against a parallel relationship between fault orientation and isoseismal orientation are considered below.

Case 1.—It is known from source theory (for example, Haskell, 1963) that the Rayleigh wave radiation patterns can be two-lobed and, in the case of dip-slip faulting, oriented perpendicular or oblique to the fault. That is, a line joining the centers of the radiation lobes is normal or oblique to the strike of the fault (see fig. 2). If we assume a dip-slip fault [focal mechanisms for the Middleton Place shock indicate dip-slip (Tarr and Rhea, 1983)] and assume that the Rayleigh waves are the principal contributing influence to the intensity effects, then it would be possible to have a meizoseismal area whose long dimension is normal to the causal fault.

An example of this type of situation (a focal-mechanism nodal plane perpendicular to the meizoseismal area) is the November 9, 1968, southern Illinois earthquake (m_b = 5.5, M_s = 5.2, depth = 25 km; Stauder and Nuttli, 1970). Figure 3 presents the focal-mechanism solution (Stauder and Nuttli, 1970), the isoseismal map (Coffman and Cloud, 1970), and a map showing contours of theoretical maximum vertical and horizontal ground-motion velocities for Rayleigh and Love waves (Herrmann, 1973) for this event. As indicated in the figure, the nodal planes of the focal-mechanism solution are dip-slip and have a north-south strike. The long dimension of the innermost isoseismal (VII) is oriented east-west. The theoretical surface-wave amplitude calculations show that the maximum vertical motion (vertical component of the Rayleigh waves) is greater than the maximum horizontal motion (Love waves plus radial component of the Rayleigh waves). Furthermore, the long dimensions of the vertical motion radiation ellipses are oriented east-west. This correlation between the orientation of the VI and VII isoseismals and the shape of the velocity contours for the vertical motion was noted by Herrmann (1973) in his study of the event. It should be mentioned here that no north-trending fault was observed and that major faults with easterly strike are well known (for example, Cottage Grove fault system) from surface geologic studies in the area. However, the focal depth of 25 km is expected to be too great to produce surface rupturing.

Case 2.—Any comparison of the intensity pattern of the 1886 shock with those from other regions is complicated by the low attenuation in the Eastern United States. Allowing for this, we can compare the 1886 event with the following intraplate earthquakes [except Guatemala; Kanamori and Anderson's classification (1975)] whose source parameters are within the scatter of the scaling data used for estimation of the 1886 parameters: 1954, Nevada (Murphy and Cloud, 1956); 1964, Spain (Udias and Arroyo, 1970); 1971, San Fernando (Allen and others, 1973); and 1976, Guatemala (Espinosa and others, 1977). Figure 4 shows this comparison. In each case, the individual intensity maps have been subjectively reoriented so that the VI and higher isoseismals have an orientation that is similar to those of the 1886 shock. In this reorientation, the faulting (too small to be shown at the scale of fig. 4) associated with the Nevada (1954) and San Fernando (1971) isoseismal patterns had easterly and northeasterly trends, respec-

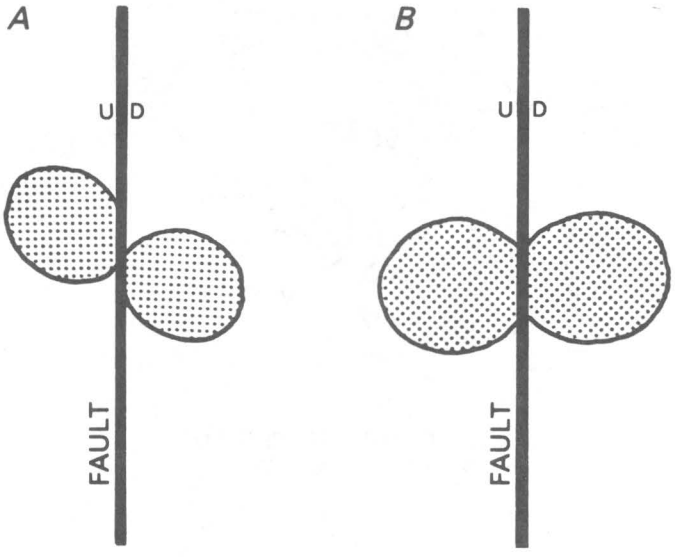

FIGURE 2.—Rayleigh wave radiation patterns after Haskell (1963). Double-couple source model. *A*, Right-oblique slip, normal motion on a fault of 45° dip. *B*, Dip-slip, normal motion on a fault of 45° dip.

tively. In a minor way, then, a northeasterly fault trend for the 1886 earthquake is suggested by this comparison of isoseismal patterns.

The reason for including the interplate Guatemala earthquake in this comparison is its unusual intensity pattern. Because of an apparent Doppler effect due to fault propagation, the isoseismals broaden markedly about the western terminus of faulting (Espinosa and others, 1977). Secondary faulting at the terminus of the causal Motagua fault (Langer and Bollinger, 1979) was probably also a contributor to the isoseismal broadening, particularly on the south side of the main fault. It might be hypothesized that a Doppler effect and (or) terminal secondary faulting occurred in 1886. That is, rupture along an offshore strike-slip fault (the Blake Spur fracture?) might have propagated from east to west and stopped near the coast, thereby causing enhanced effects onshore. The 1886 foreshock activity in the Charleston-Summerville area in June and in the days immediately preceding the main shock (August 27 and 28; Dutton, 1889, p. 230–231) argues against an epicenter far offshore. Too, while Sykes (1978) interprets the onshore activity in South Carolina to be associated with an onshore extension of the Blake Spur fracture zone, the offshore portion of the zone is known to be currently aseismic (Tarr and Rhea, 1983).

Case 3.—As a final case, the intensity results from recent shocks in the Charleston area should be considered. It is necessary for the sake of completeness to consider these smaller shocks (magnitude ≤ 4.5, intensity $\leq$ VI). However, it should be emphasized that the effects of local surficial conditions and population distribution are

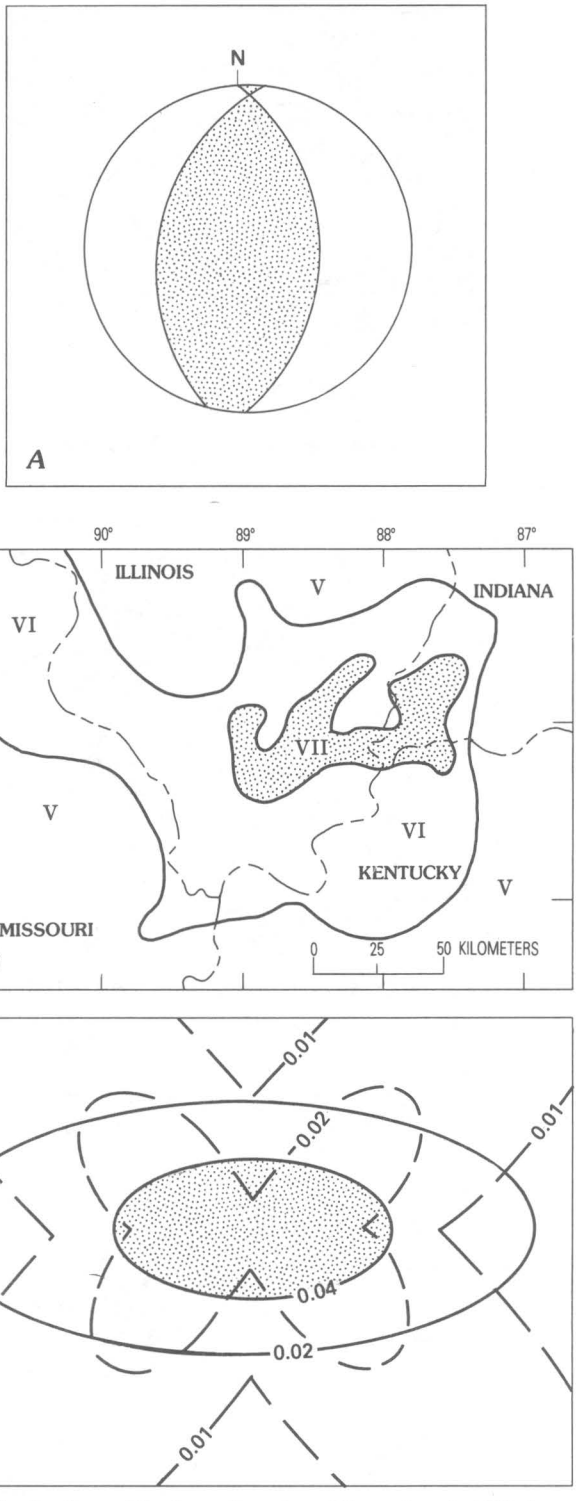

FIGURE 3.—Southern Illinois earthquake of November 9, 1968 (m_b = 5.5, M_s = 5.2, depth = 25 km). *A*, Focal mechanism (lower hemisphere); compressional quadrants shaded (Stauder and Nuttli, 1970). *B*, Isoseismal map; maximum-intensity area shaded (Coffman and Cloud, 1970). *C*, Contours of theoretical maximum vertical (solid curves; area of maximum level shaded) and horizontal (dashed curves) ground-motion velocities (Herrmann, 1973). Units are in cm/s. The area shown is slightly greater than that shown in *B*.

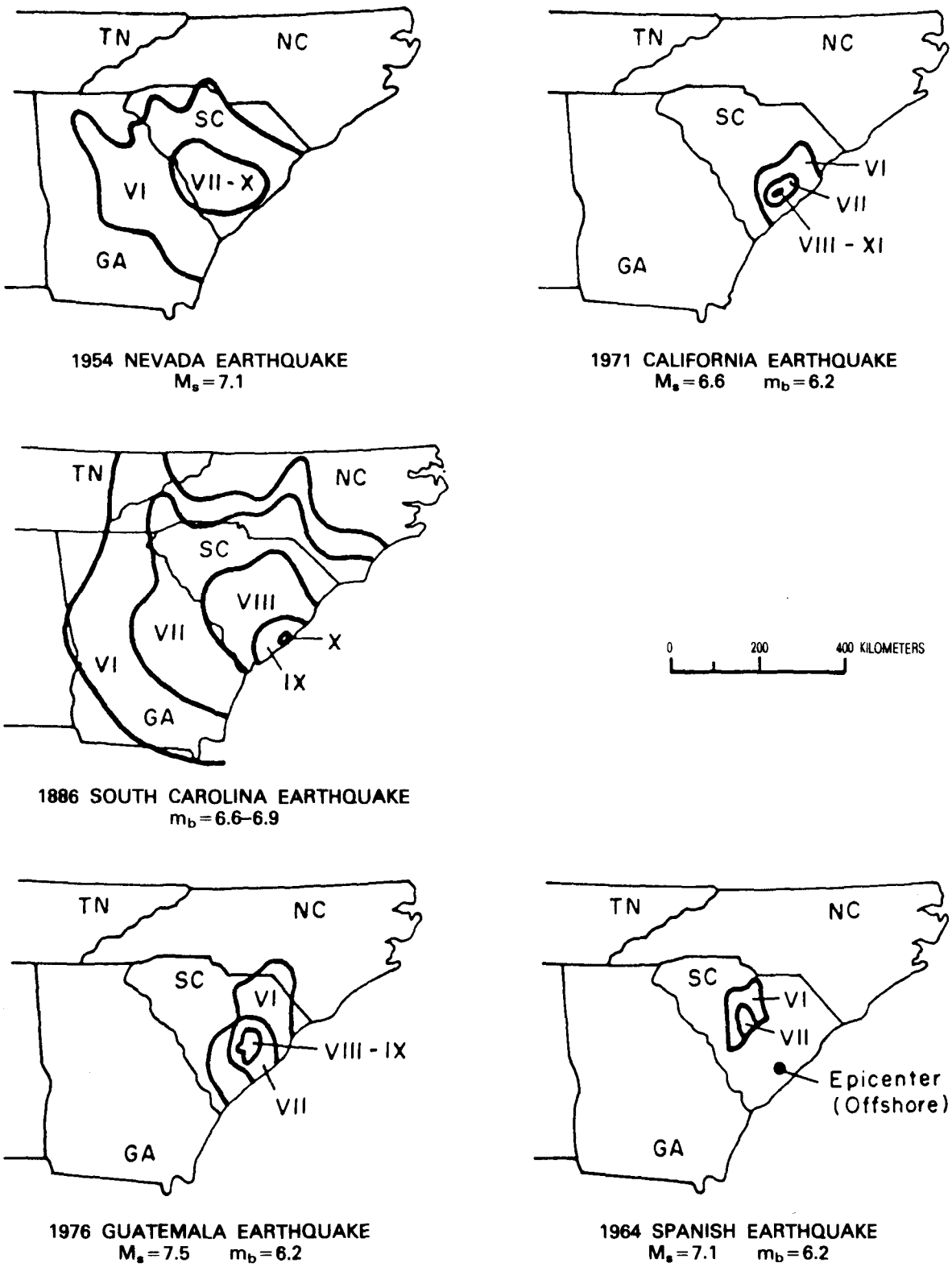

FIGURE 4.—Intensity distribution (VI and greater) for the Charleston, S. C., 1886 earthquake and for four other shocks whose source parameters are similar to those inferred for the 1886 event. The isoseismal contours for these latter four earthquakes have been subjectively reoriented so that the contours for the VI and higher levels have a trend similar to those of the 1886 shock.

likely to be dominant. Bollinger (1973) showed that the generalized shapes of the innermost isoseismals for three Charleston-area events that occurred prior to 1973 were not consistent: elongated east-west, circular, and elongated northwest-southeast. Bagwell (1979) reported that the isoseismal trends for three of four small shocks (III to V) in the Charleston area during 1977–78 had a northwest-southeast orientation.

The most recent example of intensity pattern–nodal plane orientation is the November 22, 1974, Charleston earthquake (m_b = 4.7). Stover and others (1976) show a northwest-trending innermost isoseismal (VI), on the basis of five intensity-VI data points, surrounded closely by six IV values and one III value. Tarr (1977) gave a focal mechanism for the shock that showed reverse faulting on a northwest-striking nodal plane. Subsequently, that focal mechanism has been corroborated by two of the three most recent composite focal mechanisms for the locale (Tarr and Rhea, 1983). Thus, we have, in this instance, agreement between isoseismal trend and focal-mechanism nodal-plane trend.

A possible solution to the problem of choosing, by means of intensity patterns, a northeast or a northwest fault orientation in the Charleston area is suggested by the 1974 earthquake's isoseismal map (Stover and others, 1976). The innermost isoseismal has a definite northwest trend, but the surrounding isoseismals, a II–IV and a II–V, are elongated in a northeast-southwest direction. Those isoseismals are separated by a well-defined (by more than 40 data points) not-felt zone that also has a northeast-southwest orientation. This suggests the possibility that the representative intensity response of the South Carolina Coastal Plain favors a northeasterly trend and that it is only with very dense data coverage in the epicentral locale that a northwesterly trend (if present) can be discerned.

Summary

The preceding arguments are an effort to glean as much information as possible from intensity-distribution data. In particular, some preference for the strike of the causal fault was sought. That effort has produced mixed results. Because determination of intensity depends on a multiplicity of factors (seismic, geologic, engineering, human), that is probably expectable. However, comparison with similar-size shocks indicates that the intensity data from the 1886 earthquake can be interpreted to favor a northeast fault trend at Charleston. On the other hand, the modern intensity data (especially the 1974 event with a focal-mechanism solution) and the P-wave first-motion data of the South Carolina seismic network indicate a northwesterly trend.

Perhaps these mixed results indicate a dual cause. That is, the 1886 shock had a northeast-striking fault, whereas the modern activity is occurring on northwest-striking faults. Both original interpreters of the 1886 intensity data, Dutton and Sloan (Dutton, 1889), presented a definite northeast trend to the high-intensity isoseismals. Modern studies (1971 San Fernando, M_s = 6.6; 1954 Nevada, M_s = 7.1; 1962 Kern County, M_s = 7.7) indicate that, if a shock is large enough, the trend of the causal fault can indeed be reflected in the trend of the higher intensity isoseismals. With an m_b of about 6.7 (the San Fernando earthquake had an m_b = 6.2), the 1886 shock should be in that class. There are locally poor ground conditions in the 1886 intensity-X meizoseismal area, but the northeast elongation of surficial effects is also present in the intensity-IX contour. Those effects extend to distances (from the presumed epicenter near Middleton Place) of some 35 km to the northwest and some 80 km to the southwest (Bollinger, 1977).

POST-1886 SEISMICITY

Aftershocks of the 1886 Earthquake

Statistical studies (Utsu, 1961; Page, 1968) of primarily interplate sequences have shown that the frequency of occurrence of aftershocks, $n(t)$, decays with time, t, after the main shock according to the inverse power law,

$$n(t) = At^{-p}.$$

Page (1968) found that p did not vary significantly from one aftershock sequence to another or from one tectonic region to another. The stationary value of the exponent p was determined to be somewhat greater than 1.0.

The aftershock process of the 1886 event is rather poorly documented, especially during the first few years following the main shock. However, Taber (1914) compiled an extensive listing of events that occurred between 1886 and 1914. Those data, plus what can be obtained from other sources (Bollinger, 1972, 1975), provide some insight into the aftershock sequence.

Figure 5 shows the average number of felt aftershocks per year occurring in logarithmically uniform time intervals starting seven years (1893) after the 1886 earthquake. A curve fitted by eye to the data of that figure has a slope of about 1.4.

In studying the frequency of occurrence of aftershocks, it is necessary to count only those events above some specified size. The 1886 data base is primarily noninstrumental (felt events), and thus we have virtually no size control of the type needed. Considering this lack of uniformity and completeness, the value of 1.4 is surprisingly close to Page's (1968) value of unity. It is also well within the range (0.9–1.8) reported by other investigators (Utsu, 1961; Mogi, 1962). Finally, there is the fact that we are comparing an intraplate sequence with results derived primarily from interplate sequences.

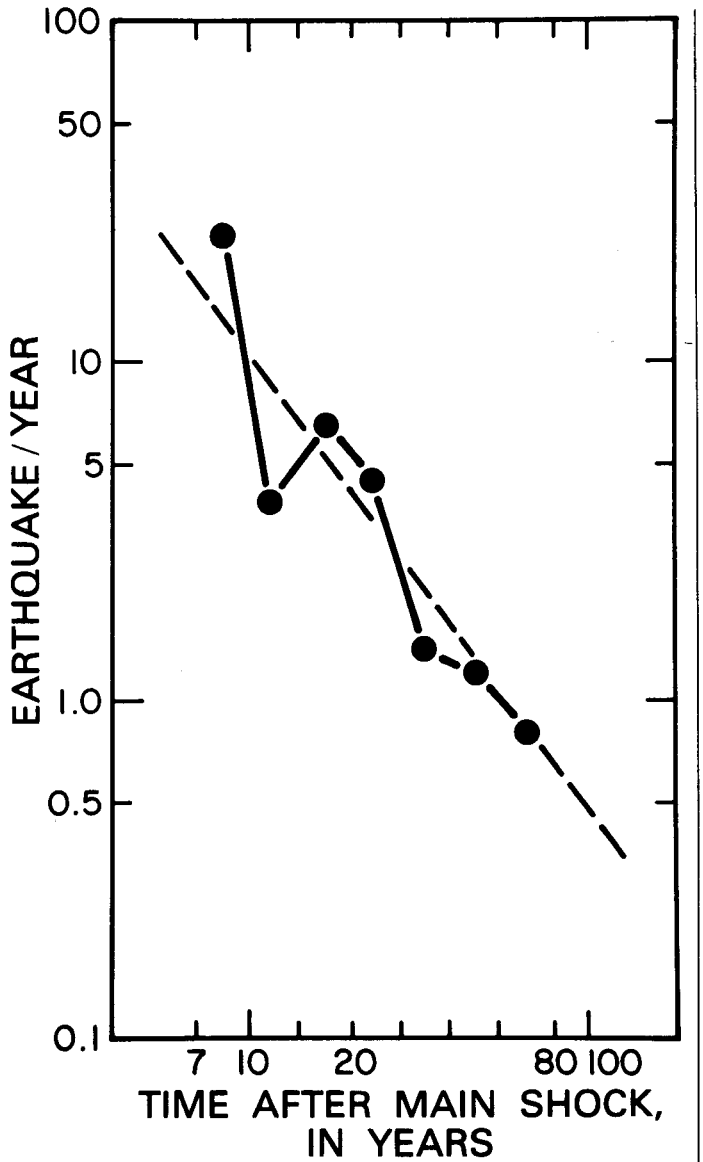

FIGURE 5.—Frequency of occurrence of aftershocks of the 1886 Charleston, S. C., earthquake as a function of time for the period 1893–1964. The number of felt earthquakes per year is plotted against time (t), in years, after the main shock beginning at $T_1 = 7$ for 1893. The ordinate of a point represents the number of shocks occurring in the time interval (T_i, T_{i+1}) divided by the length of the interval; the abscissa is given by $t_i = (T_i, T_{i+1})^{1/2}$ where $T_{i+1} = 1.4\ T_i$. The dashed line, fitted by eye to the data, has a slope of 1.4.

The data of figure 5 show no departure from an inverse-power-law decay and, therefore, do not show that the process is over. The frequency for the next time interval in the sequence (1964–1995) cannot be computed. However, extrapolation of the dashed-line curve on figure 5 would give a rate of about one earthquake every two years. We do know that there were approximately 90 felt aftershocks during the first year following the intensity-X event (Bollinger, 1975). If $p = 1$, that rate would imply about one event per year 90 years later (1976). The Charleston area had one felt event in 1975, no felt events in 1976, five felt events in 1977 (Coffman and Stover, 1977, 1978, 1979), and one felt event in 1978 (J. Bagwell, oral commun., 1980). Thus, the activity is at nearly the expected rate.

Spatial Distribution of Post-1886 Seismicity in South Carolina

Apart from the clustering of events in the 1886 epicentral area, the general pattern of earthquake activity has been minor clusters in the Bowman and Adams Run locales and a broad, diffuse scattering of events in the northwestern half of South Carolina (Tarr and Rhea, 1983). That scattered activity is primarily, but not completely, contained within the Piedmont province. The Middleton Place, Bowman, and Adams Run clusters are in the Coastal Plain province.

Thus, a regional view of the seismicity of South Carolina shows a change from a clustering habit in the Coastal Plain to a diffuse habit in the Piedmont portion of the State. As previously mentioned, that pattern is independent of time: 1800–1972 (Hadley and Devine, 1974), 1920–70 (Bollinger, 1973), and 1973–78 (Tarr and Rhea, 1983; exclusive of reservoir-associated activity). The South Carolina part of the Coastal Plain is the only portion of that province in the Southeastern United States to exhibit seismic activity. However, this change in spatial habit from clustering to scattering would appear to be most closely associated with the two distinctive shallow crustal provinces beneath the South Carolina Coastal Plain as defined by gravity and magnetic data (Popenoe and Zietz, 1977; Daniels and others, 1983). Those provinces juxtapose metamorphic and nonmetamorphic terranes, and it appears that the clustering habit occurs in the latter.

Results from the South Carolina Seismic Network

Tarr and Rhea (1983) present improved hypocenter determinations and composite focal mechanisms from six years (1973–78) of monitoring by the South Carolina seismic network. They interpret the hypocenter distribution in the Middleton Place–Summerville area as defining a three-segmented seismic zone having two en-echelon segments, each about 8 km long, striking northwest and dipping about 80° to 90° to the southwest. The third segment is about 5 km in length and trends east-northeast (no dip given) between the en-echelon pair.

The epicentral distribution at Middleton Place–Summerville, rather than being subdivided, could be enclosed by a rectangle having dimensions of 13 km (east-west) by 20 km (north-south) or by a rhomboid having side lengths of 17 km (north-south and northwest-southeast). A rather tight clustering, rather than separate zonations, would be the result. In this model, a

composite focal-mechanism solution of all the events in the cluster would yield a nearly vertical, northwest-striking nodal plane, down on the northeast. The companion plane would, of course, be horizontal or nearly so. Such a composite would have approximately the same level of inconsistent P-wave first-motion readings (~20%) as do two of the three separate composites by Tarr and Rhea (1983). In the overall composite, the equal-area plot is definitely compressional over approximately 1½ quadrants from northwest clockwise to east. It is dilatational from the southwest clockwise to the northwest. That first-motion pattern requires a nearly vertical, northwest-striking nodal plane. Thus, two of the three composites or the total distribution of P-wave first motions, in conjunction with focal depths ranging from 3 to 12 km, indicate a nearly vertical source zone, some 15 to 20 km long, in which failure occurs on one or more planes that strike northwest-southeast.

SUMMARY

The seismological data base available to be brought to bear on the question of the nature of the Charleston, S. C., seismicity consists of Dutton's study (1889) of the 1886 earthquake, historical and recent seismicity information from numerous sources, and the results of instrumental monitoring, including some six years by an instate network. Consideration of these data in the light of results from studies in other seismic areas leads to the following speculations:

1. With respect to strain energy release, the Charleston, S. C., area is unique in the Southeastern United States. The earthquake activity there has persisted for some three centuries and has been more abundant than anywhere else in the region. Charleston is the only such seismically active locale in the Coastal Plain province.
2. Prior to 1886, South Carolina was not aseismic, and pre-1886 seismicity could have been concentrated in the Charleston-Summerville area.
3. Given an m_b estimate of 6.7, the parameters of the 1886 shock as inferred from published scaling relations are

   magnitude: $m_b \cong 6.7$, $M_s \cong 7 \pm 0.5$
   fault parameters: length $\cong$ 25 km (3 km, 44 km)
   width $\cong$ 12 km (3 km, 36 km)
   average slip $\cong$ 1 m (0.01 m, 420 m).

   The values in parentheses are the extreme values allowed by the range in M_s (6.5 to 7.5) and by the scatter of the stress-drop estimates (30 bars to 300 bars) in the log M_o versus M_s data (Kanamori and Anderson, 1975).
4. The agreement between causal fault strike and trend of the innermost isoseismals for events which are assumed to be similar in size to the 1886 shock and for which surface faulting was observed was investigated. Also, recent South Carolina events were considered, one of which had a focal-mechanism solution. Those studies suggest that, if an event is large enough (m_b greater than approximately 6), the innermost isoseismal(s) probably will reflect the general trend of the fault. Under this assumption, the strike of the causal fault for the 1886 Charleston earthquake would be northeasterly.
5. Published scaling and fault length–magnitude relations give no insight into the mode of faulting for the 1886 shock. The reported dominance of strong vertical ground motions at Summerville (Dutton, 1889) would allow a dip-slip component in the faulting motion.
6. The temporal characteristics of the post-1886 seismicity indicate that the aftershock process is probably not over. The number of earthquakes per year (1893–1964) decreases at an inverse power law rate of about 1.4 and exhibits no departure from that rate. Additionally, the current activity rate is at or near an expectable level.
7. Statewide, the seismicity of South Carolina exhibits a change from a clustering habit (Charleston and Bowman areas) in the nonmetamorphic "basement" terrane [the "Charleston block" as defined by gravity and magnetic data (Rankin, 1977, p. 10)] portion of the State to a diffuse habit in the remaining metamorphic basement portion. Additionally, the South Carolina portions of the Coastal Plain and Piedmont provinces are the only places in the Southeastern United States where appreciable seismicity occurs in those provinces (except for the Virginia Piedmont). Thus, not only is the seismicity pattern in South Carolina distinctive but the fact that it is there at all is atypical. To explain the presence of the South Carolina seismicity, Sykes (1978) suggested that there is a major lineation extending from the Blake Spur fracture zone that includes the epicenter of the Charleston earthquake and the South Carolina–Georgia seismic zone. It trends northwesterly through South Carolina and western North Carolina and into eastern Tennessee.
8. Concerning the relation between the location and geometry of the current seismicity and the 1886 earthquake:

Spatial factors.—The pre-1886 seismicity could have been concentrated in the Charleston locale. Subsequently, during the aftershock sequence, both the pre-instrumental events and the instrumentally located shocks also occurred there. Population bias is probably not severe in this case, as earthquake reports from other localities in the State date back to 1799 (Bollinger and Visvanathan, 1977).

The current seismicity has shallow focal depths. No focal-depth estimate is available for the 1886 earthquake. However, the widespread surficial effects would allow a shallow focus, even with allowance for exaggeration due to ground and water table conditions.

Geological-geophysical factors.—The instrumentally located earthquakes define a cluster or zone whose long dimension is about 20 km. That dimension is compatible with a fault-length estimate made herein for the 1886 shock (25 km) and would fit easily inside the 35 × 50 km dimensions of the 1886 intensity-X isoseismal.

The modern seismicity indicates strain release on a steeply-dipping fault(s) having northwest strike and reverse dip-slip movement. A study of the 1886 intensity distribution with respect to the intensity patterns of other, similar-size earthquakes suggests a northeast-striking fault plane. The intense vertical ground motions at Summerville during the 1886 shock allow a dip-slip component to the causal fault's motion.

Seismic-reflection data (Hamilton and others, 1983; Schilt and others, 1983) show shallow normal and reverse faults. These faults appear to have been active in the Tertiary; they have displacements of a few tens of meters. Their trends and linear extent could not be determined accurately. Their location at levels shallower than the current seismicity's focal depths allows the possibility that they are not part of the seismogenic zone. However, a zone of inferred faulting (sense of basement relief: southwest side up) beneath the Ashley River may be part of the active zone.

Gravity and magnetic data in the Charleston area show anomaly patterns that have been interpreted to indicate the presence of northwest-trending dikes and faults, northeast-trending faults, and mafic plutons (that could serve as possible stress concentrators).

Hypothesis.—The source zone for the 1886 Charleston earthquake is localized by the intersection of at least two seismogenic structures, one trending northwest and the other trending northeast. The faulting in 1886 was on the northeast structure. Ninety years later, the aftershock activity has shifted to the northwest element. The variable trends in the few isoseismal maps that are available for the intervening period could reflect activity on one or the other of these two structures.

REFERENCES

Allen, C. R., Hanks, T. C., and Whitcomb, J. H., 1973, San Fernando earthquake: Seismological studies and their tectonic implications, *in* Murphy, L. M., ed., San Fernando, California, earthquake of February 9, 1971, v. 3: Washington, D.C., National Oceanic and Atmospheric Administration, p. 13–21.

Bagwell, J. B., 1979, Isoseismal intensity studies of 1977–1978 Charleston-Summerville earthquakes [abs.]: Earthquake Notes, v. 50, no. 3, p. 12.

Basham, P. W., 1969, Canadian magnitudes of earthquakes and nuclear explosions in southwestern North America: Royal Astronomical Society Geophysical Journal, v. 17, no. 1, p. 1–13.

Bollinger, G. A., 1972, Historical and recent seismic activity in South Carolina: Seismological Society of America Bulletin, v. 62, no. 3, p. 851–864.

———1973, Seismicity and crustal uplift in the southeastern United States: American Journal of Science, v. 273–A, p. 396–408.

———1975, A catalog of southeastern United States earthquakes, 1754 through 1974: Virginia Polytechnic Institute and State University Research Division Bulletin 101, 68 p.

———1977, Reinterpretation of the intensity data for the 1886 Charleston, South Carolina, earthquake, *in* Rankin, D. W., ed., Studies related to the Charleston, South Carolina, earthquake of 1886–A preliminary report: U.S. Geological Survey Professional Paper 1028, p. 17–32.

Bollinger, G. A., and Visvanathan, T. R., 1977, The seismicity of South Carolina prior to 1886, *in* Rankin, D. W., ed., Studies related to the Charleston, South Carolina, earthquake of 1886–A preliminary report: U.S. Geological Survey Professional Paper 1028, p. 33–42.

Coffman, J. L., and Cloud, W. K., 1970, United States earthquakes 1968: Washington, D.C., U.S. Department of Commerce, 111 p.

Coffman, J. L., and Stover, C. W., editors, 1977, United States earthquakes, 1975: U.S. Department of Commerce and U.S. Department of Interior, National Technical Information Service PB-278261/AS, 136 p.

———1978, United States earthquakes, 1976: U.S. Department of Commerce and U.S. Department of Interior, National Technical Information Service PB-288937/AS, 94 p.

———1979, United States earthquakes, 1977: U.S. Department of Commerce and U.S. Department of Interior, National Technical Information Service PB-300863, 81 p.

Daniels, D. L., Zietz, Isidore, and Popenoe, Peter, 1983, Distribution of subsurface lower Mesozoic rocks in the Southeastern United States as interpreted from regional aeromagnetic and gravity maps, *in* Gohn, G. S., ed., Studies related to the Charleston, South Carolina, earthquake of 1886–Tectonics and seismicity: U.S. Geological Survey Professional Paper 1313, p. K1–K24.

Dillinger, W. H., 1973, Focal mechanism of San Fernando earthquake, *in* Murphy, L. M., ed., San Fernando, California, earthquake of February 9, 1971, v. 3: Washington, D.C., National Oceanic and Atmospheric Administration, p. 49–67.

Dutton, C. E., 1889, The Charleston earthquake of August 31, 1886: U.S. Geological Survey Ninth Annual Report 1887–88, p. 203–528.

Espinosa, A. F., Husid, Raul, and Quesada, Antonio, 1977, Intensity distribution and source parameters from field observations, *in* Espinosa, A. F., ed., The Guatemala earthquake of February 4, 1976, a preliminary report: U.S. Geological Survey Professional Paper 1002, p. 52–66.

Geller, R. J., 1976, Scaling relations for earthquake source parameters and magnitudes: Seismological Society of America Bulletin, v. 66, no. 5, p. 1501–1523.

Gupta, H. K., and Rastogi, B. K., 1972, Earthquake *mb* vs. *Ms* relations and source multiplicity: Royal Astronomical Society Geophysical Journal, v. 28, no. 1, p. 65–89.

Gutenberg, Beno, and Richter, C. F., 1956, Magnitude and energy of earthquakes: Annali di Geofisica, v. 9, no. 1, p. 1–15.

Hadley, J. B., and Devine, J. F., 1974, Seismotectonic map of the Eastern United States: U.S. Geological Survey Miscellaneous Field Studies Map MF–620; scale 1:5,000,000.

Hamilton, R. M., Behrendt, J. C., and Ackermann, H. D., 1983, Land multichannel seismic-reflection evidence for tectonic features near Charleston, South Carolina, *in* Gohn, G. S., ed., Studies related to the Charleston, South Carolina, earthquake of 1886–Tectonics and seismicity: U.S. Geological Survey Professional Paper 1313, p. I1–I18.

Haskell, N. A., 1963, Radiation pattern of Rayleigh waves from a fault of arbitrary dip and direction of motion in a homogeneous medium: Seismological Society of America Bulletin, v. 53, no. 3, p. 619–642.

Herrmann, R. B., 1973, Surface-wave generation by the south central Illinois earthquake of November 9, 1968: Seismological Society of America Bulletin, v. 63, no. 6, p. 2121–2134.

Kanamori, Hiroo, and Anderson, D. L., 1975, Theoretical basis of some empirical relations in seismology: Seismological Society of America Bulletin, v. 65, no. 5, p. 1073–1095.

Langer, C. J., and Bollinger, G. A., 1979, Secondary faulting near the terminus of a seismogenic strike-slip fault: Aftershocks of the 1976 Guatemala earthquake: Seismological Society of America Bulletin, v. 69, no. 2, p. 427–444.

Mogi, Kiyoo, 1962, On the time distribution of aftershocks accompanying the recent major earthquakes in and near Japan: Tokyo University Earthquake Research Institute Bulletin, v. 40, pt. 1, p. 107–124.

Murphy, L. M., and Cloud, W. K., 1954, United States earthquakes 1952: U.S. Department of Commerce Serial no. 773, 112 p.

Murphy, L. M., and Cloud, W. K., 1956, United States earthquakes 1954: U.S. Coast and Geodetic Survey Serial no. 793, 110 p.

Nagamune, Tomeo, 1972, Magnitudes estimated from body waves for great earthquakes [in Japanese]: Quarterly Journal of Seismology, v. 37, p. 1–8.

Nuttli, O. W., Bollinger, G. A., and Griffiths, D. W., 1978, On the relation between Modified Mercalli intensity and body-wave magnitude: Seismological Society of America Bulletin, v. 69, no. 3, p. 893–909.

Page, Robert, 1968, Aftershocks and microaftershocks of the great Alaska earthquake of 1964: Seismological Society of America Bulletin, v. 58, no. 3, p. 1131–1168.

Popenoe, Peter, and Zietz, Isidore, 1977, The nature of the geophysical basement beneath the Coastal Plain of South Carolina and northeastern Georgia, *in* Rankin, D. W., ed., Studies related to the Charleston, South Carolina, earthquake of 1886–A preliminary report: U.S. Geological Survey Professional Paper 1028, p. 119–138.

Rankin, D. W., editor, 1977, Studies related to the Charleston, South Carolina, earthquake of 1886–A preliminary report: U.S. Geological Survey Professional Paper 1028, 204 p.

Richter, C. F., 1958, Elementary seismology: San Francisco, W. H. Freeman, 768 p.

Schilt, F. S., Brown, L. D., Oliver, J. E., and Kaufman, Sidney, 1983, Subsurface structure near Charleston, South Carolina; Results of COCORP reflection profiling in the Atlantic Coastal Plain, *in* Gohn, G. S., ed., Studies related to the Charleston, South Carolina, earthquake of 1886–Tectonics and seismicity: U.S. Geological Survey Professional Paper 1313, p. H1–H19.

Scott, N. H., 1973, Felt area and intensity of San Fernando earthquake, *in* Murphy, L. M., ed., San Fernando, California, earthquake of February 9, 1971, v. 3: Washington, D.C., National Oceanic and Atmospheric Administration, p. 23–48.

Slemmons, D. B., 1977, Faults and earthquake magnitude, Report 6, *in* State-of-the-art for assessing earthquake hazards in the United States: U.S. Army Engineer Waterways Experiment Station Miscellaneous Paper S–73–1, 129 p.

Starr, A. T., 1928, Slip in a crystal and rupture in a solid due to shear: Cambridge Philosophical Society Proceedings, v. 24, p. 489–500.

Stauder, William, and Nuttli, O. W., 1970, Seismic studies; South central Illinois earthquake of November 9, 1968: Seismological Society of America Bulletin, v. 60, no. 3, p. 973–981.

Stover, C. W., Simon, R. B., and Person, W. J., 1976, Earthquakes in the United States, October-December 1974: U.S. Geological Survey Circular 723–D, p. D1–D27.

Sykes, L. R., 1978, Intraplate seismicity, reactivation of preexisting zones of weakness, alkaline magmatism and other tectonism postdating continental fragmentation: Reviews of Geophysics and Space Physics, v. 16, no. 4, p. 621–688.

Taber, Stephen, 1914, Seismic activity in the Atlantic Coastal Plain near Charleston, South Carolina: Seismological Society of America Bulletin, v. 4, p. 108–160.

Tarr, A. C., 1977, Recent seismicity near Charleston, South Carolina and its relationship to the August 31, 1886, earthquake, *in* Rankin, D. W., ed., Studies related to the Charleston, South Carolina, earthquake of 1886–A preliminary report: U.S. Geological Survey Professional Paper 1028, p. 43–57.

Tarr, A. C., and Rhea, Susan, 1983, Seismicity near Charleston, South Carolina, March 1973 to December 1979, *in* Gohn, G. S., ed., Studies related to the Charleston, South Carolina, earthquake of 1886–Tectonics and seismicity: U.S. Geological Survey Professional Paper 1313, p. R1–R17.

Udias, A., and Arroyo, A. L., 1970, Body and surface wave study of source parameters of the March 15, 1964, Spanish earthquake: Tectonophysics, v. 9, no. 4, p. 323–346.

Utsu, T., 1961, A statistical study of the occurrence of aftershocks: Geophysical Magazine, v. 30, no. 4, p. 521–605.

Yerkes, R. F., 1973, Effects of San Fernando earthquake as related to geology, *in* Murphy, L. M., ed., San Fernando, California, earthquake of Feburary 9, 1971, v. 3: Washington, D.C., National Oceanic and Atmospheric Administration, p. 137–154.


U.S. DEPARTMENT OF THE INTERIOR
March 3, 1849